QC
851
.G73
V. 8

Air Ministry
Meteorological Research Committee
MRP 841-901 (non-inclusive)

MRP No.	Title	Author
841 AD 063908	The Electronic Computation of Two Series of 500 mb., 1000 mb., and 500-1000 mb. Thickness Forecast Charts by Application of the Sawyer-Bushby 2 Parameter Baroclinic Model.	F.H. Bushby M.K. Hinds
842 AD 059063	The Airflow Over Mountains - a Report on the State of Current Knowledge.	G.A. Corby
843 AD 223069	The Rainfall of Depressions Which Move Eastward Across Scotland.	J.S. Sawyer
854	Artificial Production of Precipitation.	H.W.L. Absalom
858 AD 223071	A Total Radiation Fluxmeter.	J. MacDowall
859	A Method of Increasing the Range of the Dobson Brewer Aircraft Frost Point Hygrometer.	P. Goldsmith
860	Variation of Temperature in the Lower Stratosphere Above Larkhill and Lerwick (Addendum to M.R.P. 819).	J.K. Bannon
861 AD 065159	Diurnal and Semi-diurnal Oscillations of the Lower Stratosphere.	D.H. Johnson
862 AD 223079	Report on the Automatic Integration of Solar Radiation at Kew Observatory.	M.J. Blackwell
863 AD 063984	A Preliminary Report on Ten Computed Sets of Forecasts Based on the Sawyer and Bushby Two-parameter Atmospheric Model.	F.H. Bushby M.K. Hinds
867 AD 083296	A Remote Recording Electrical Anemograph.	G.E.W. Hartley
868 AD 223078	Note on Exceptionally Severe Clear-air Turbulence and Other Phenomena on 14th April, 1954.	D.C.E. Jones
869 AD 083291	The Relationship Between Standard Deviation of Contour Height and Standard Vector Deviation of Wind, With Practical Applications.	A.F. Jenkinson
872 AD 063983	An Investigation into the Speed and Direction of Motion of Simple Warm Sector Depressions.	H.D. Hoyle

MRP No.	Title	Author
873 AD 223077	On the Determination of the Vertical Convective Heat Flux by Observations of Wind and Temperature Near the Ground.	A.J. Lander G.D. Robinson
874 AD 063981	Average Pressure and Temperature of the Tropopause.	J.G. Moore
875 AD 063982	Fine Scale Characteristics of the Lowest 5,000 ft. of the Atmosphere as Observed From an Aircraft.	D.G. James
877 AD 063910	An Interim Report on Measurements of Humidity From Aircraft to Heights of About 50,000 Feet Over Southern England.	R.J. Murgatroyd P. Goldsmith W.E.H. Hollings
878 AD 223076	Assessment of Maximum Concentration at Ground Level of Gas From a Heated Elevated Source.	A.C. Best
883	A Note on an Instrument for the Continuous Recording of Soil Temperatures.	N.E. Rider
888 AD 079756	Diurnal and Interdiurnal Variations of the Measured Heights of Pressure Surfaces.	D.H. Johnson
889 AD 223075	The Application of Radiation and Lag Corrections to Radio-sonde Temperatures.	F.J. Scrase
894 AD 223021	Estimation of the Reflection and Absorption of Solar Radiation by a Cloudless Atmosphere From Recordings at the Ground, With Results for Kew Observatory.	R.H. Eldridge G.D. Robinson
895 AD 223084	Five Years Continuous Recording of Total and Diffuse Solar Radiation at Kew Observatory.	M.J. Blackwell
896 AD 079755	Some Characteristics of Fronts and Their Relation to Frontogenesis.	J.S. Sawyer
901	Index of M.R.P.'s Approved for General Distribution.	

At the time of issue this report has not been published. Any author desiring to quote this paper should refer to it as "A paper of the Meteorological Research Committee (London).
M.R.P. No. ..... by Mr. .....
A copy is available in the Library of the Meteorological Office."

R 5544

M.R.P. 901
6th April, 1955.

AIR MINISTRY

METEOROLOGICAL RESEARCH COMMITTEE

INDEX OF M.R.Ps. APPROVED FOR GENERAL DISTRIBUTION
Appendix 14 of M.R.P. 200

M.R.P.	Title	Author
841	The electronic computation of two series of 500 mb., 1000 mb., and 500-1000 mb. thickness forecast charts by application of the Sawyer-Bushby 2 parameter baroclinic model.	F.H. Bushby and Mavis K. Hinds
842	The airflow over mountains - A report on the state of current knowledge.	G.A. Corby
843	Rainfall of Depressions which move E across Scotland	Sawyer
853	Index of M.R.Ps. approved for general distribution (Appendix No. 13 of M.R.P. 200).	
854	Artificial Production of Precipitation	Absalom
858	A total radiation fluxmeter.	J. MacDowall
859	A method of increasing the range of the Dobson Brewer Aircraft Frost Point Hygrometer.	P. Goldsmith
860	Variation of temperature in the lower stratosphere above Larkhill and Lerwick (Addendum to M.R.P. 819).	J.K. Bannon
861	Diurnal and semi-diurnal oscillations of the lower stratosphere.	D.H. Johnson
862	Report on the automatic integration of solar radiation at Kew Observatory.	M.J. Blackwell
863	A preliminary report on ten computed sets of forecasts based on the Sawyer and Bushby two-parameter atmospheric model.	F.H. Bushby and Mavis K. Hinds
867	A remote recording electrical anemograph.	G.E.W. Hartley
868	Note on exceptionally severe clear-air turbulence and other phenomena on 14th April, 1954.	D.C.E. Jones
869	The relationship between standard deviation of contour height and standard vector deviation of wind, with practical applications.	A.F. Jenkinson
872	An investigation into the speed and direction of motion of simple warm sector depressions.	H.D. Hoyle
873	On the determination of the vertical convective heat flux by observations of wind and temperature near the ground.	A.J. Lander and G.D. Robinson

/874

M.R.P.	Title	Author
874	Average pressure and temperature of the tropopause.	J.G. Moore
875	Fine scale characteristics of the lowest 5,000 ft. of the atmosphere as observed from an aircraft.	D.G. James
877	An interim report on measurements of humidity from aircraft to heights of about 50,000 feet over Southern England.	R.J. Murgatroyd, P. Goldsmith and W.E.H. Hollings
878	Assessment of maximum concentration at ground level of gas from a heated elevated source.	A.C. Best
883 888	A note on an instrument for the continuous recording of soil temperatures.	N.E. Rider
889	The application of radiation and lag corrections to radio sonde temperatures.	F.J. Scrase
894	Estimation of the reflection and absorption of solar radiation by a cloudless atmosphere from recordings at the ground, with results for Kew Observatory.	R.H. Eldridge and G.D. Robinson
895	Five years continuous recording of total and diffuse solar radiation at Kew Observatory.	M.J. Blackwell
896	Some characteristics of fronts and their relation to frontogenesis.	J.S. Sawyer

At the time of issue this report has not been published. Any author desiring to quote this paper should refer to it as "A paper of the Meteorological Research Committee (London), M.R.P. No. 841 by Mr. F.H. Bushby and Miss M.K. Hinds. A copy is available in the Library of the Meteorological Office".

M.R.P. 841

S.C.II/162

31st December, 1953.

AD 63908

AIR MINISTRY

METEOROLOGICAL RESEARCH COMMITTEE

The electronic computation of two series of 500 mb., 1000 mb., and 500-1000 mb. thickness forecast charts by application of the Sawyer-Bushby 2 parameter baroclinic model

by

F.H. Bushby and Mavis K. Hinds (Meteorological Office)

1. Introduction.

Several authors have recently suggested that the large-scale atmospheric motions could be predicted by the application of numerical methods of mathematical analysis to equations which represent the motion in various simplified models of the atmosphere. Charney and his colleagues at Princeton University have investigated the barotropic model atmosphere and Charney, Fjörtoft and von Neumann (1950) give the results of some 12 and 24 hour forecasts of the 500 mb. contour surface based on this model. More recently Charney and Phillips (1953) have given the results of some 12 and 24 hour forecasts based on the two-layer barotropic model. Alternatively, some of the baroclinic features of the atmosphere can be incorporated in a 2 parameter baroclinic model by assuming that the variation of the horizontal and vertical components of velocity with height is the same along all verticals. Eady (1952), Eliassen (1952), Sawyer and Bushby (1953) and Thompson (1953) have derived sets of equations which describe the motions in particular versions of this model.

The model of the atmosphere adopted by Sawyer and Bushby consists of a baroclinic fluid in which the thermal wind is constant in direction in any vertical column but not necessarily parallel to the wind direction at any level, and the thermal wind speed is assumed proportional to the pressure difference through the layer concerned. The atmosphere is considered bounded by two pressure surfaces across which the movement of the air is assumed to be negligible; one pressure surface $p = p_1$, corresponding to a level near the tropopause and one, $p = p_0$, corresponding to a level near the ground. The variation of the vertical motion with respect to pressure is assumed to be parabolic, and the geostrophic approximation is made after the horizontal divergence has been eliminated from the equations.

The present paper gives the result of 6, 12, 18 and 24 hour forecasts based on the Sawyer-Bushby model for two synoptic situations. The forecast charts are compared with the actual charts and an attempt is made to estimate the effect of computational instability and arbitrarily chosen boundary conditions on the answers.

/2.

fuel #3

2. The equations.

The state of motion in the Sawyer-Bushby model atmosphere is specified by the two parameters h_m, the height of the central pressure level of the layer (at $p = p_m$) and h', the thickness of the layer from p_0 to p_m. The method is one in which the instantaneous rates of change of h_m and h' are computed for time t and from these the values of h_m and h' for time $t + \delta t$. The process is then repeated n times and forecast charts are produced for time $t + n\delta t$.

Eliminating Π_m ($\Pi = dp/dt$, a measure of vertical motion) from the equations derived by Sawyer and Bushby, and neglecting the term representing the vertical advection of vorticity, the following equations can be derived for $\partial h_m/\partial t$ and $\partial h'/\partial t$:-

$$\nabla^2 \partial h_m/\partial t + J(h_m, \beta^2 g l^{-1} \nabla^2 h_m + l) + \tfrac{1}{3} J(h', \beta^2 g l^{-1} \nabla^2 h') = 0 \quad \ldots (1)$$

$$\nabla^2 \partial h'/\partial t + \frac{4g(\nabla^2 h_m + l^2/\beta^2 g)\{\beta^2 g l^{-1} J(h_m, h') + \partial h'/\partial t\}}{R A \Gamma (p_0 - p_1)}$$

$$+ J(h_m, \beta^2 g l^{-1} \nabla^2 h') + J(h', \beta^2 g l^{-1} \nabla^2 h_m + l) = 0 \quad \ldots (2)$$

where $A \equiv \frac{1}{2} \frac{p_0 + 3p_1}{p_0 - p_1} - \frac{4 p_0 p_1}{(p_0 - p_1)^2} \log_e \frac{2p_0}{p_0 + p_1}$,

∇^2 and J are the two dimensional Laplacian and Jacobian operators referred to rectangular Cartesian co-ordinates in the stereographic projection of the northern hemisphere on to a plane perpendicular to the earth's axis passing through the north pole; β is the magnification factor $\sec^2(\pi/4 - \theta/2)$, θ being the geographical latitude; g is the acceleration due to gravity; l is the Coriolis parameter; R is the universal gas constant and Γ_p a measure of the departure of the lapse rate from the adiabatic given by $\Gamma_p = \frac{\partial T}{\partial p} - \gamma/gl$, γ being the appropriate wet or dry adiabatic lapse rate, l the density and T the absolute temperature. Neglect of the terms involving the vertical advection of vorticity is justified by the small values of this term obtained in M.R.P. 790.

The following system of equations was used for the time integration process:-

$$H_{n+1} = h_{n-1} + 2(\partial H/\partial t)_n \, \delta t \quad \ldots (3)$$

$$h_{n+1} = h_n + \tfrac{1}{2}\left[(\partial H/\partial t)_n + (\partial H/\partial t)_{n+1}\right] \delta t \quad \ldots (4)$$

/where

where H_n represents the first approximation and h_n the second approximation to either h_m or h' at time $t + n\delta t$. Initially, as only values of h_m and h' are known at one instant of time, it was necessary to replace the centred difference of Equation (3) by the forward difference formula

$$H_1 = h_0 + \left(\partial h/\partial t\right)_0 \delta t \qquad \ldots\ldots\ldots\ldots (5)$$

It was decided to use Equations (3) and (4) instead of Equation (3) alone for the time integration procedure in an attempt to reduce the effect of computational instability.

The computations were carried out on LEO, an electronic computing machine owned by Messrs. J. Lyons and Co. The finite difference approximations to Equations (1) and (2) were solved for $\partial h_m/\partial t$ and $\partial h'/\partial t$ using the technique described by Bushby and Hinds (1953a and b). A grid of 18 x 14 points was used, but as two rings of points are lost in computing the finite difference approximations to the vorticity advection terms, Equations (1) and (2) are solved for a grid of 16 x 12 points including boundary points.

Due to limitations of storage space in LEO, it was impossible to keep the complete programme in the machine, and this slowed down the computation. The new values of h_m and h' were printed after each time step. The time spent in completing one cycle of the computations was 20 minutes: of this 5 minutes were spent in input, 5 minutes in output and 10 minutes in actual computation. To produce a forecast at time $t + n\delta t$ from initial data at time t would thus take $n/3$ hours if the intermediate results were printed, and $(n/4 + 1/12)$ hours if only the final results were printed.

In the present work the values of p_0 and p_1 were taken to be 1000 mb. and 200 mb. respectively. This would give p_m = 600 mb., a level for which charts are not normally available. h_m was therefore identified with the height of the 500 mb. surface and h' with the thickness of the 1000-500 mb. layer.

After consideration of previous computational results a constant value, 38°F. per 500 mb., was taken for Γ_p.

3. The space and time increments.

In order that the solution of the finite difference approximations to Equations (1) and (2) should closely approximate to the continuous solution, it is necessary that the space and time increments δs and δt must be small in comparison with the space and time scales of the large scale atmospheric systems. However, the smaller δs, the more grid points are necessary to cover a given area, and the computation time is increased. After some experimenting it was decided to use a value of δs which approximates to 162 statute miles in middle latitudes.

Apart from the aforementioned considerations it is also necessary to ensure that the small-scale irregularities in the field of h_m and h', of which there is inevitably a large distortion, do not amplify during the integration process. The computation is said to be unstable when such amplification takes place. Due to the complex nature of the equations involved it is extremely difficult to derive rigorously the conditions necessary for stability, but it is apparent that the ratio $\delta s/\delta t$ has to lie within certain limits.

/From

From general considerations, it was decided to commence the computations with δt equal to 2 hours. It can be seen from inspections of the results (Figs. 1-5) that the integration based on the initial data of 1500 G.M.T. 27.1.1952 was unstable after 18 hours. The distortions increased in amplitude by 24 hours but did not affect the region of the British Isles, for which a reasonable 24 hour forecast was computed.

During the integration based on the initial data of 1500 G.M.T. 14.3.1949 instability became apparent after 10 hours and considerable amplification and distortion over most of the chart had taken place by 12 hours. The computation was stopped and re-started from the 8 hour stage, using δt equal to 1 hour. The calculations then remained stable over the whole of the chart for the 24 hours (Figs. 6-10).

Charney et al (1950), when solving the barotropic equation using a centred difference formula for the time integration, derived the following approximate relationship

$$\frac{\delta s}{\delta t} \geqslant \sqrt{2}\beta - v \qquad \text{(6)},$$

where v is the maximum particle speed in the forecast region, as giving a lower bound to the stability criterion. If the same relationship applied to the present set of equations, then with δt = 2 hours, the computations would become unstable if v were greater than 60 knots in middle latitudes. It is thought that the present method of time integration is more stable than the simple centred difference formula used by Charney et al (1950), but the problem of computational instability is at present being further investigated in the Forecast Research Division at Dunstable.

4. The boundary conditions.

A sufficient boundary condition for the solution of Equations (1) - (5) in a given region is that h_m, h', $\nabla^2 h_m$ and $\nabla^2 h'$ should be given along the boundary of that region. Thus when the finite difference approximations to Equations (1) - (5) are being solved, it is necessary to specify the values of h_m, h', $\nabla^2 h_m$ and $\nabla^2 h'$ at all grid points on the boundary (except corner points) or alternatively to specify the values of h_m and h' at all grid points on the boundary and at all grid points immediately exterior to the boundary. The second of these two alternatives was used in the present computations.

It was considered that the arbitrary boundary values would not affect the centre of the forecast region by the end of the forecast period. The actual boundary values assigned to h_m and h' have to be chosen quite arbitrarily, because unless one considers the whole of the northern hemisphere in order to make use of the observed fact that h_m and h' show little variation near the equator, there are no conclusive reasons for pre-determining the values of h_m and h' along the boundary. The following boundary values were chosen as they are quite simple and tend to smooth the field of h_m and h' in a direction normal to the boundary in the vicinity of the boundary.

The initial data used in the computations were the values of h_m and h' at the points of an 18 x 14 grid. This enabled the Poisson and Helmholtz Equations (1) and (2) to be solved for $\partial h_m/\partial t$ and $\partial h'/\partial t$ at 16 x 12 points including the boundary points at which values of $\partial h_m/\partial t$ and $\partial h'/\partial t$ were assumed zero. However in using Equations (3), (4) and (5)

/for

for the time integration, $\partial h_m/\partial t$ and $\partial h'/\partial t$ were taken as zero at the boundary points of the 18 x 14 grid but at the boundary points of the inner 16 x 12 grid $\partial h_m/\partial t$ and $\partial h'/\partial t$ were now taken equal to half the value at the immediate interior point except at the four corner points where a value of one quarter of the nearest interior point was used. The area covered by this 16 x 12 grid of points is that inside the curved boundary shown in Fig. 2b.

5. The results.

(a) Time-integration based on initial data for 1500 G.M.T. 27th January, 1952.

The initial charts on which this computation is based are shown in Figs. 1a and 1b. The situation was one in which there was a broad westerly flow across the North Atlantic at 500 mb., with large-amplitude troughs over eastern Canada and western Europe and an intermediate shallower trough south-east of Greenland. Surface and thickness patterns were also largely westerly over the Atlantic, but over western Europe the surface pressure gradient was flat and mainly cyclonic, there being a tongue of deep cold air down the North Sea into northern France.

During the ensuing twenty-four hours the cold trough over the North Sea moved slowly eastwards to Scandinavia and eastern Germany, the associated surface trough also moving away eastwards. The movements of this feature were well forecast, the axis of the 500 mb. trough being in almost the correct position on each of the forecast charts. The surface low pressure area was not, however, forecast to move far enough eastwards. Behind the base of the cold trough the ridge originally over the Bay of Biscay was forecast to intensify considerably and move eastwards to reach a position over northern Italy after twenty-four hours. The ridge moved as forecast for the first twelve hours but thereafter, possibly owing to the close proximity of the Alps, moved more north-eastwards than forecast. This is a particularly marked example of a circumstance in which an experienced forecaster would almost certainly use his knowledge of the topography to modify a forecast produced by numerical methods. The elongated frontal trough to the west of Ireland intensified and moved eastward over the British Isles slightly faster than forecast, but the axis of the warm ridge was correctly forecast to be over Great Britain after twenty-four hours. The separate low pressure centre forecast to develop in the lower end of the trough did in fact form at the point of occlusion shortly after the end of the forecast period.

The part of the forecast charts to the west of the British Isles has been considerably affected by computational instability and arbitrary choice of boundary values, the difficulties discussed in sections 3 and 4. During the forecast period the deep cold trough over eastern Canada moved eastwards across the boundary of the area involved in the computations. Since, however, the values of h_m and h' along this boundary were assumed to remain constant, the cold trough was assumed to remain back over America and an intense warm ridge was forecast to be thrown up ahead of it. This gave rise to very tight gradients just south of Greenland on the forecast charts and small, intense irregularities appear downstream on the forecast charts due to computational instability.

(b) Time-integration based on initial data for 1500 G.M.T. 14th March, 1949.

Figs. 6a and 6b show the initial charts used in this forecast. A large stationary depression is situated over the Baltic in a very slack

/thermal

thermal gradient, whilst a vigorous depression is approaching the southern tip of Greenland from the south-west. Between the two a considerable ridge extends northwards from the Azores high pressure area. There is a small wave-depression over southern England and a shallow low pressure area with an almost concentric cold pool south-west of Spain.

In this situation the movements of various pressure systems were quite well forecast, but the predictions of their development and intensity were considerably in error. It is particularly noticeable how similar the forecast and actual patterns are at 500 mb., the main errors in the forecast being the intensification of the 500 mb. ridge north of the Azores and the small trough west of Iceland.

During the twenty-four hours for which the forecast was made the wave depression moved rapidly away into Russia and was followed by a mobile ridge which spread down into southern England and France and was absorbed into the considerably enlarged Azores High. On the forecast charts the oscillation in the thickness pattern was predicted to intensify too much giving a very strong westerly thermal gradient over Iceland and northerly thermal gradient over the British Isles. This oscillation gave a very marked anticyclonic development area over the British Isles and in consequence the mobile ridge was forecast to develop into an extremely intense high pressure area with the Azores High as a ridge extension.

The depression approaching the tip of Greenland at the beginning of the period was forecast to split into two parts, a shallow low pressure area in the Davis Strait and a more intense depression moving north-eastward to Iceland. This movement actually occurred but the depression over Iceland was less deep than it was forecast to be.

Reducing the time-step to one hour appears to have removed most of the effects of computational instability and the western halves of the twenty-four hour forecast charts in this case are very much more in agreement with actuality than in the other case where two-hour time-steps were used throughout. It is possible that if one-hour time-steps had been used throughout all the effects of computational instability would have been removed.

(c) Correlation and regression coefficients.

Correlation coefficients have been calculated comparing computed changes with actual changes over 6, 12, 18 and 24 hour periods starting from the initial data. Regression coefficients were calculated for the best fitting straight lines giving the actual change (Y tens of feet) in terms of the computed change (X tens of feet) in the form

$$Y = bX + c \qquad \ldots\ldots(7)$$

In order to gain an indication of the adverse effects of computational instability and wrong boundary conditions on the western part of the forecast charts, correlation and regression coefficients were calculated both for the 16 x 12 grid of points over which the contour heights and thickness were forecast to change and also over the same area without the six westernmost columns of points.

/Table I.

Table I.

Correlation and regression coefficients of actual and computed height and thickness changes for forecast period beginning 1500 G.M.T. 27.1.52.

Forecast period ending	grid size	500 mb.			1000 mb.			1000-500 mb.		
		r	b	c	r	b	c	r	b	c
2100 G.M.T. 27.1.52	16x12	0.53	0.64	0.2	0.68	0.68	0.9	0.68	0.64	-0.5
	10x12	0.71	0.94	1.1	0.80	0.80	3.4	0.71	0.80	-0.5
0300 G.M.T. 28.1.52	16x12	0.41	0.43	3.6	0.35	0.47	-0.3	0.55	0.46	2.4
	10x12	0.82	0.98	9.2	0.71	0.67	6.0	0.77	0.78	-0.4
0900 G.M.T. 28.1.52	16x12	0.29	0.24	-0.9	0.33	0.46	-1.4	0.55	0.34	-0.4
	10x12	0.78	0.76	7.6	0.81	0.78	9.0	0.77	0.59	-0.5
1500 G.M.T. 28.1.52	16x12	0.05	0.04	3.0	0.22	0.29	-1.5	0.45	0.22	2.9
	10x12	0.83	0.78	12.7	0.78	0.81	11.0	0.77	0.56	2.6

r = correlation coefficient.

Table II.

Correlation and regression coefficients of actual and computed height and thickness changes for forecast period beginning 1500 G.M.T. 14.3.49.

Forecast period ending	grid size	500 mb.			1000 mb.			1000-500 mb.		
		r	b	c	r	b	c	r	b	c
2100 G.M.T. 14.3.49	16x12	0.79	0.94	-3.1	0.79	0.56	0.6	0.53	0.57	-1.8
	10x12	0.85	0.89	5.0	0.77	0.56	0.5	0.73	0.66	0.4
0300 G.M.T. 15.3.49	16x12	0.66	0.58	-3.0	0.81	0.59	0.7	0.78	0.82	-5.1
	10x12	0.84	0.83	-4.7	0.90	0.70	-2.2	0.85	0.80	-0.8
0900 G.M.T. 15.3.49	16x12	0.74	0.66	-7.5	0.77	0.54	-1.4	0.72	0.69	-5.1
	10x12	0.86	0.79	-9.0	0.89	0.61	-3.5	0.88	0.75	1.4
1500 G.M.T. 15.3.49	16x12	0.69	0.59	-9.7	0.76	0.47	-3.3	0.81	0.64	-4.4
	10x12	0.76	0.71	-13.3	0.83	0.52	-6.8	0.94	0.68	-0.1

The figures given in Tables I and II confirm what has been said in sections 5a and 5b. The most striking feature of Table I is the very high correlations obtained if the six westernmost columns of the grid are ignored. In Table II the correlations are fairly high even when these columns are included, but it will be noticed that the values of b are almost invariably lower than the corresponding correlation coefficients owing to the fact that many features on the charts were forecast to intensify too much.

/6.

6. Conclusions.

Although one must not generalise from two examples, in the two situations so far considered the equations describing the motion in the Sawyer-Bushby 2 parameter baroclinic model atmosphere give a fair representation of the motion in the real atmosphere for a 24 hour period in the regions not affected by computational instability and the arbitrary choice of boundary conditions.

References:

Bushby, F.H. and Hinds, M.K.	1953	(a) Air Ministry, Met. Res. Ctee., M.R.P. 790.
		(b) Air Ministry, Met. Res. Ctee., M.R.P. 794.
Charney, J.G., Fjörtoft, R. and von Neumann, J.	1950	Tellus, 2, p.237.
Charney, J.G. and Phillips, N.A.	1953	J. Met., 10, p.71.
Eady, E.T.	1952	Tellus, 4, p.157.
Eliassen, A.	1952	Tellus, 4, p.145.
Sawyer, J.S. and Bushby, F.H.	1953	J. Met., 10, p.54.
Thompson, P.D.	1953	Quart. J. R. Met. Soc., 79, p.51.

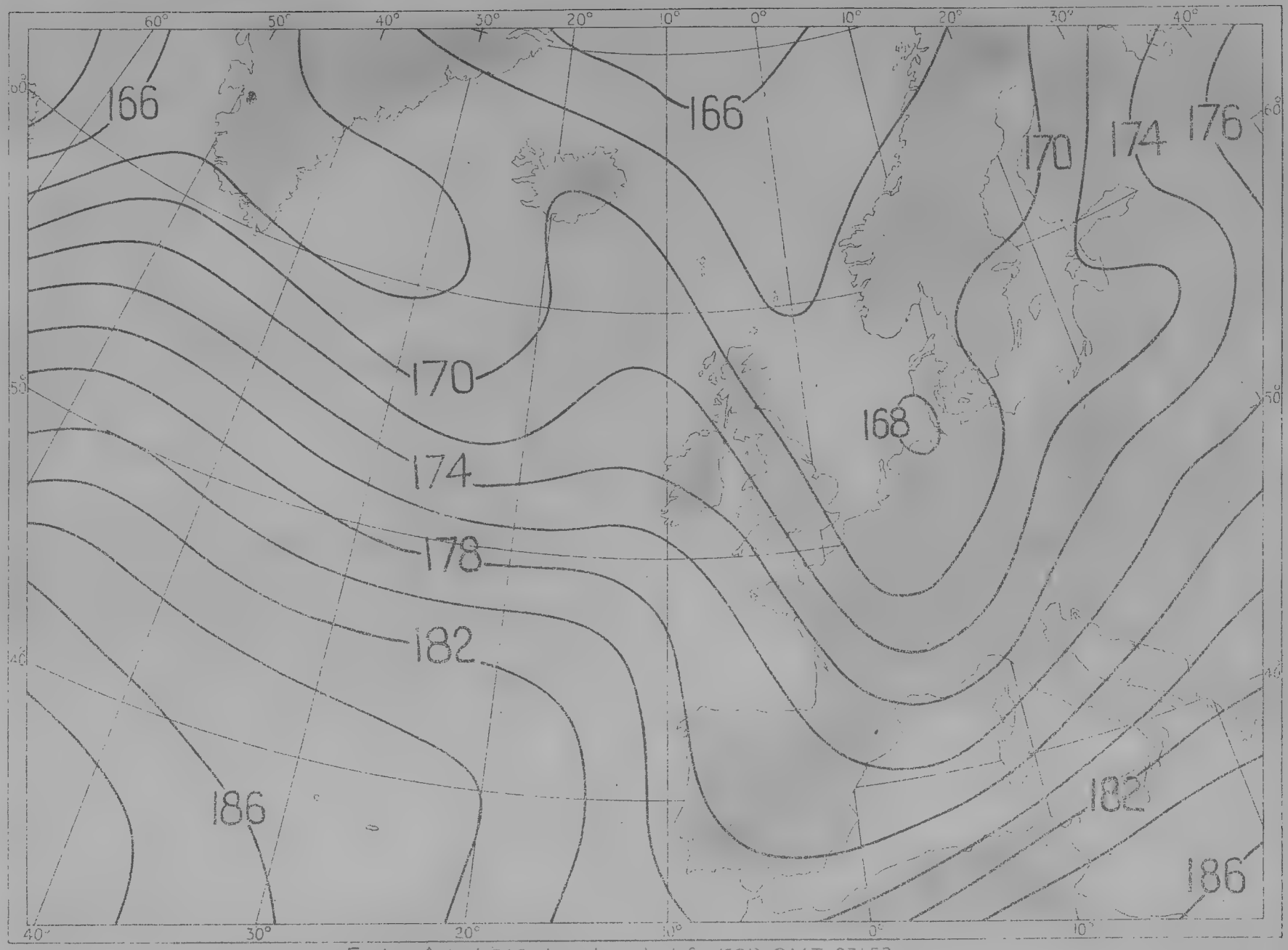

Fig. 1(a) Actual 500mb. contour chart for 1500 G.M.T. 27.1.52

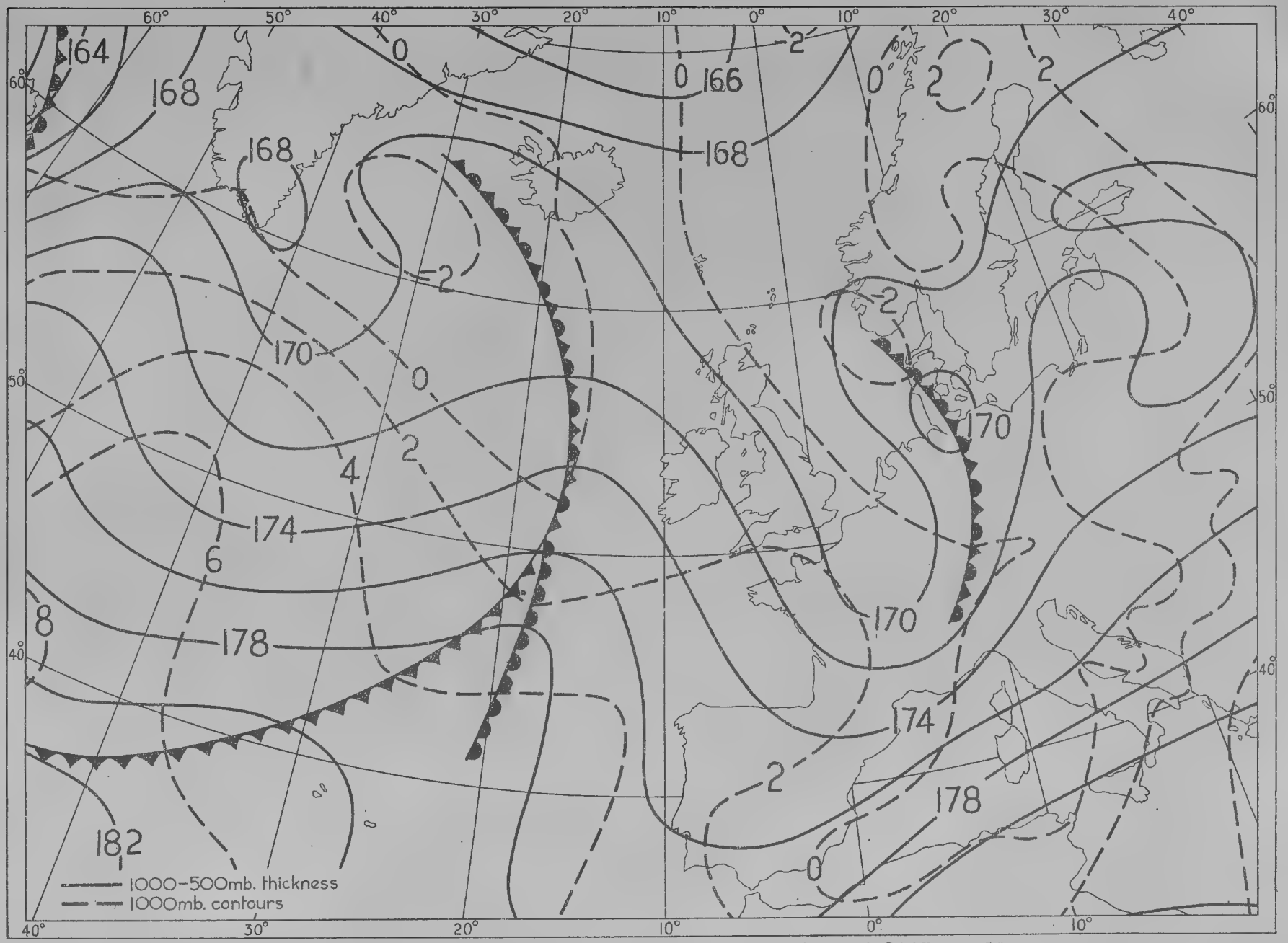

Fig. 1(b) Actual 1000–500mb. thickness and 1000mb. contours for 1500 G.M.T. 27.1.52

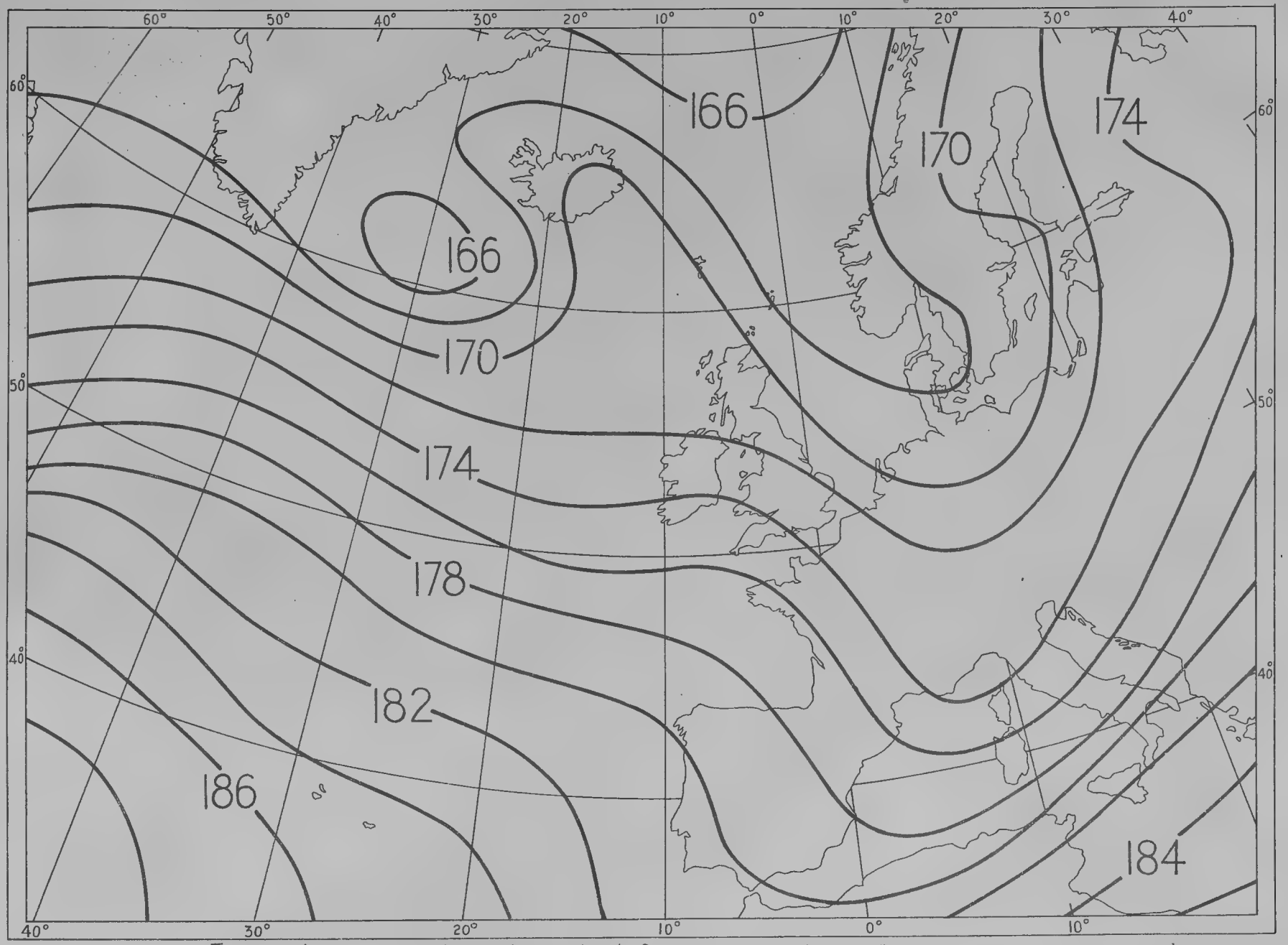

Fig. 2(a) Actual 500mb. contour chart for 2100 G.M.T. 27.1.52

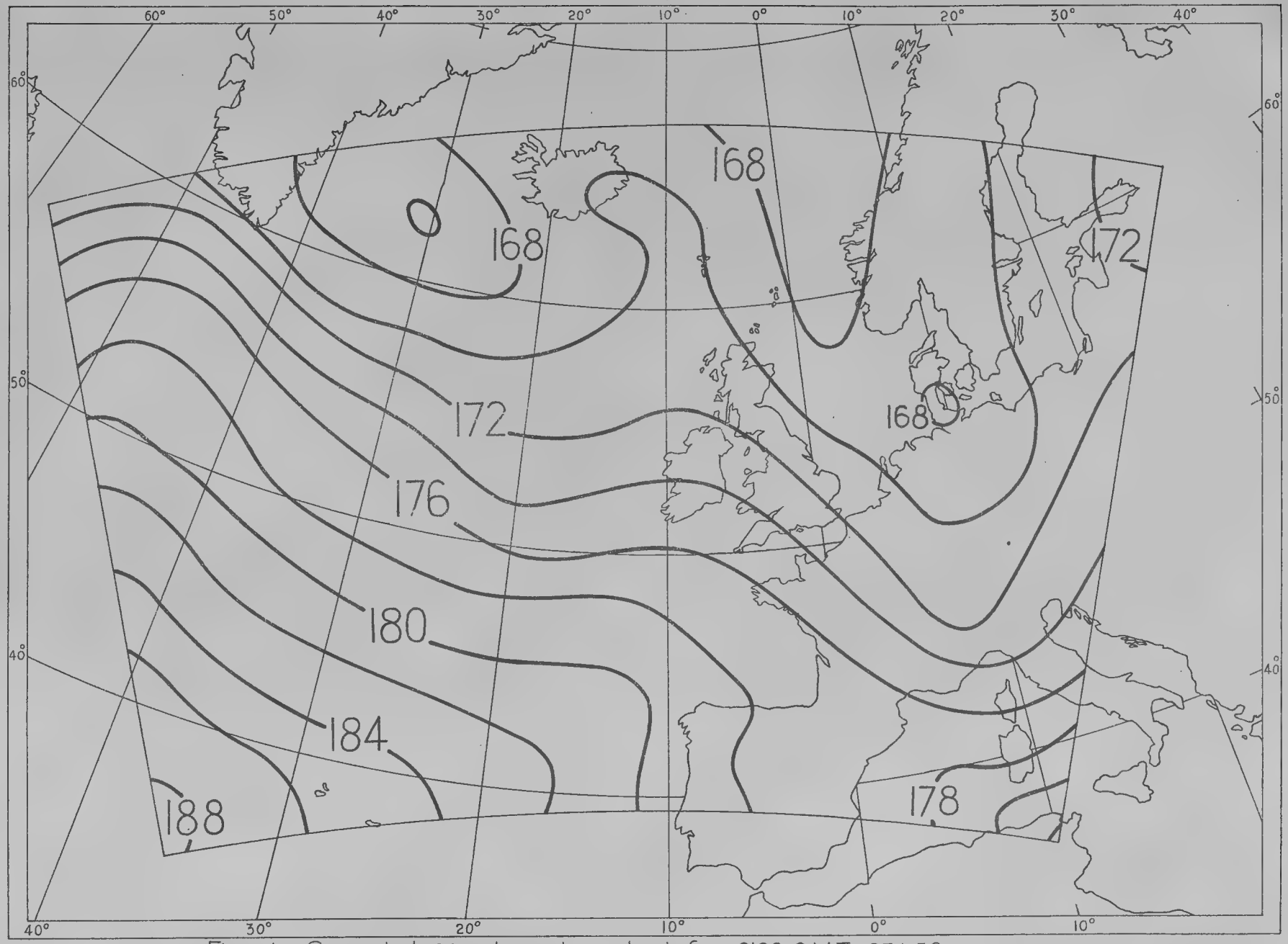

Fig. 2(b) Computed 500mb. contour chart for 2100 G.M.T. 27.1.52

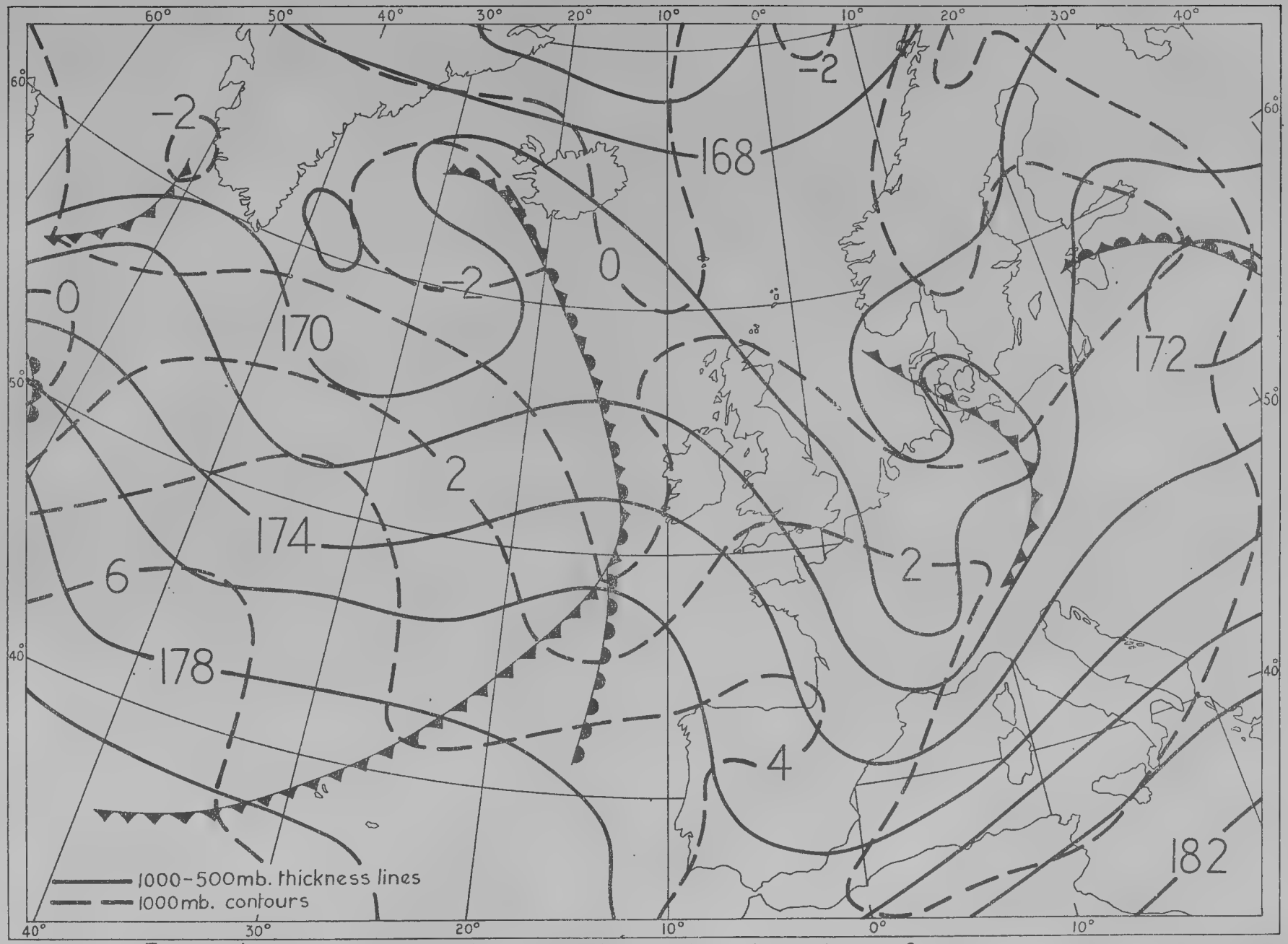

Fig. 2(c) Actual 1000-500mb. thickness and 1000mb. contour charts for 2100 G.M.T. 27.1.52

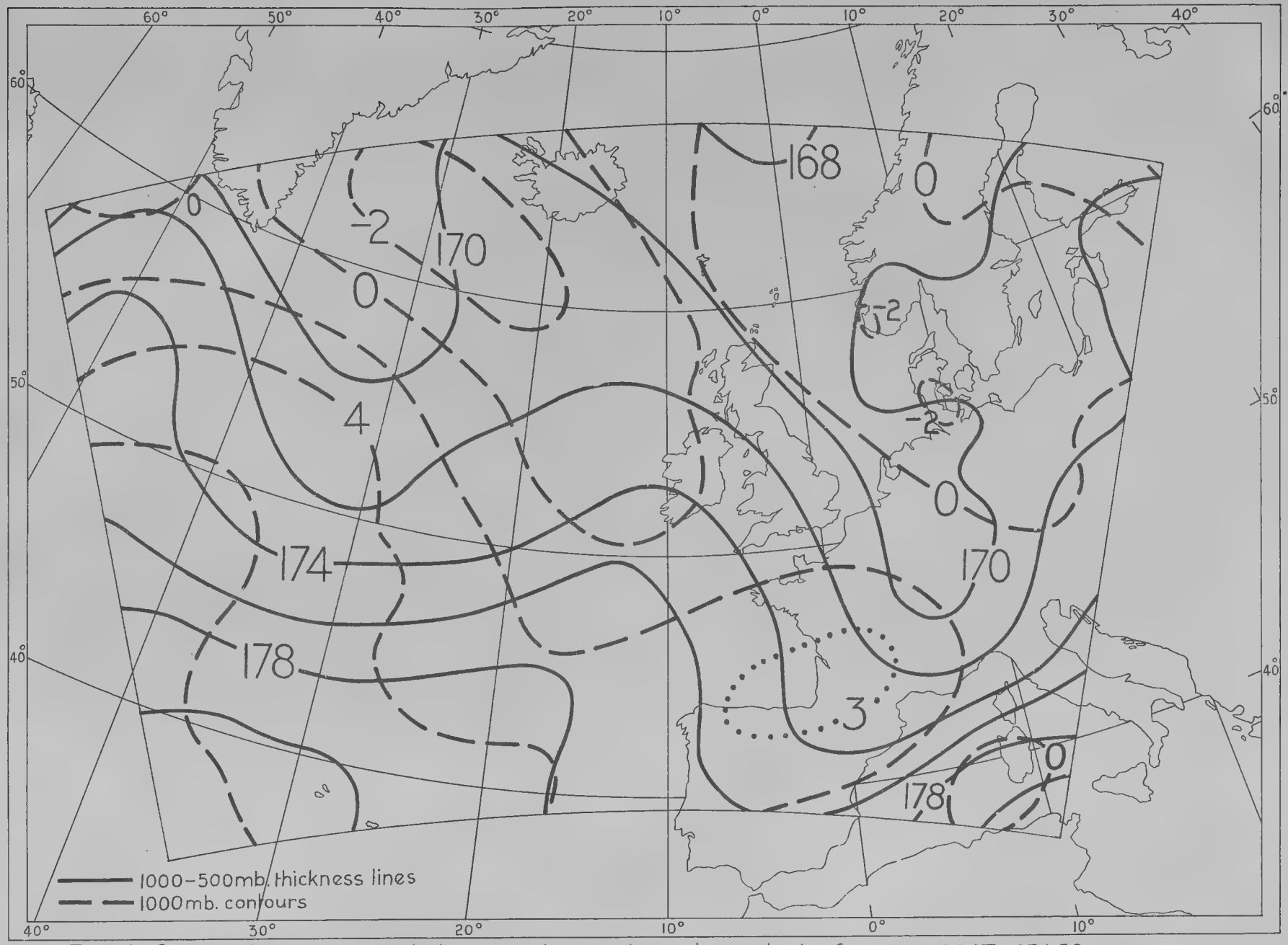

Fig. 2(d) Computed 1000-500mb. thickness and 1000mb. contour charts for 2100 G.M.T. 27.1.52

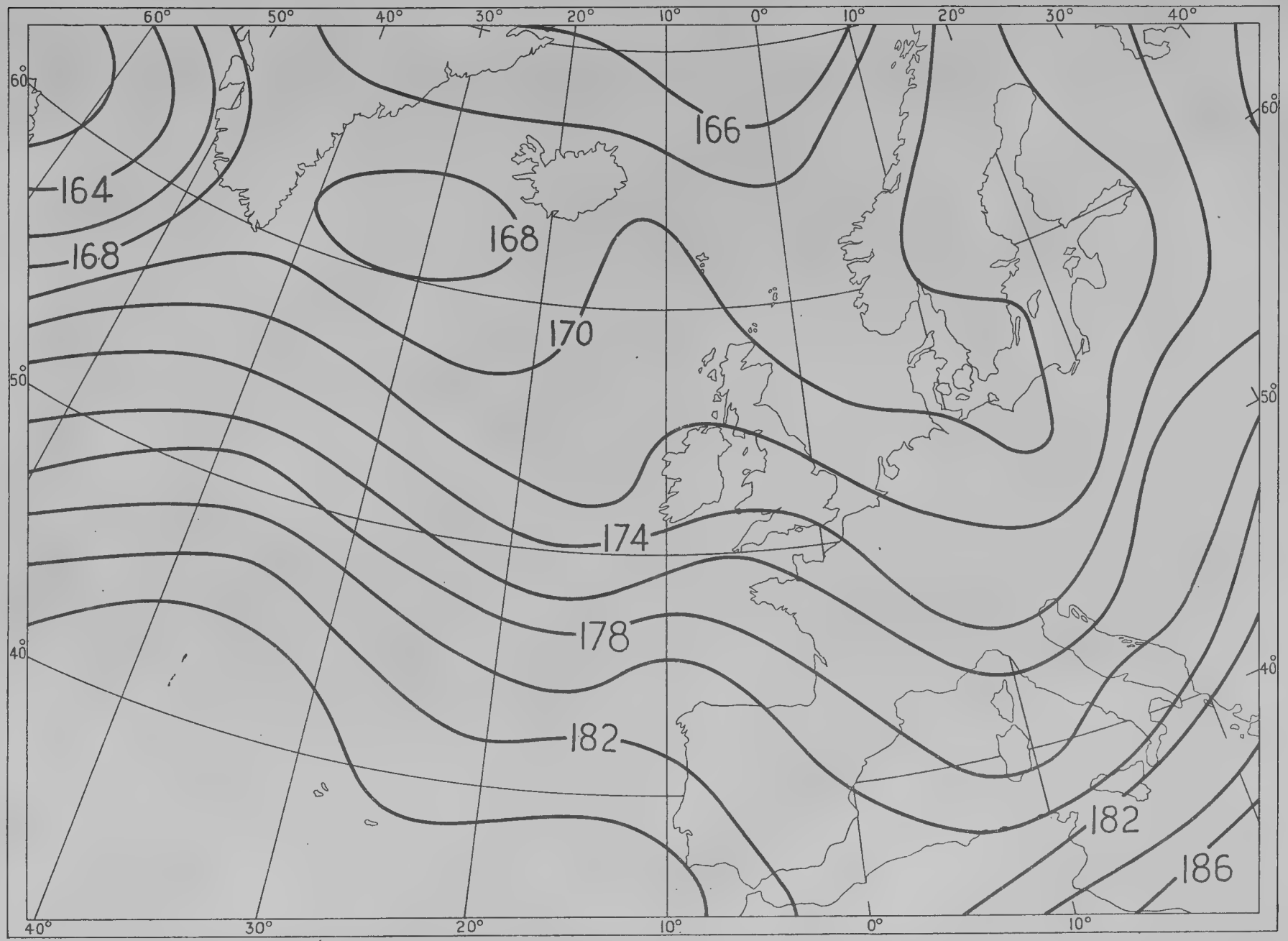

Fig. 3(a) Actual 500mb. contours for 0300 G.M.T. 28.1.52

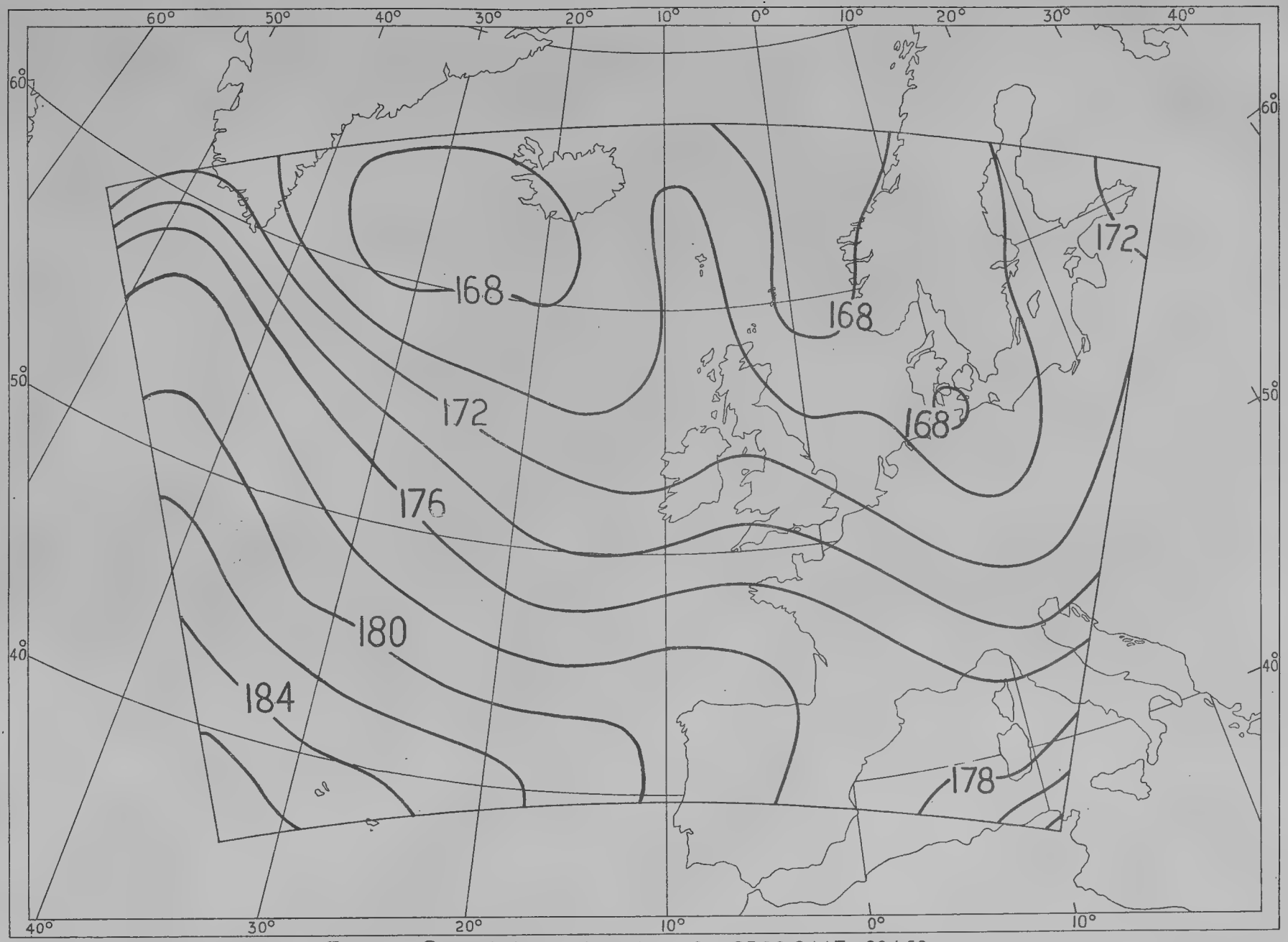

Fig. 3(b) Computed 500mb. contours for 0300 G.M.T. 28.1.52

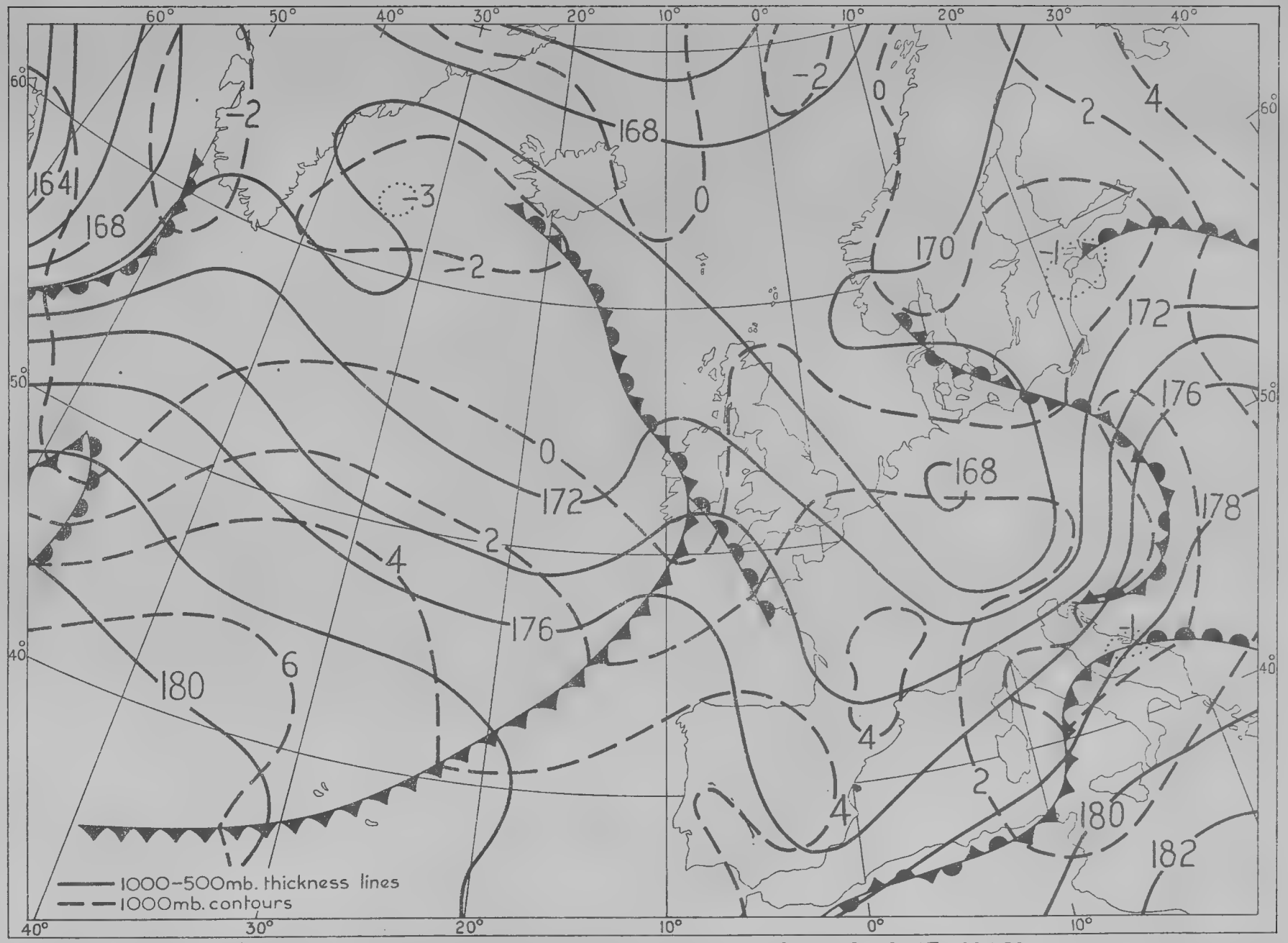

Fig. 3(c) Actual 1000–500mb. thickness and 1000mb. contours for 0300 G.M.T. 28.1.52

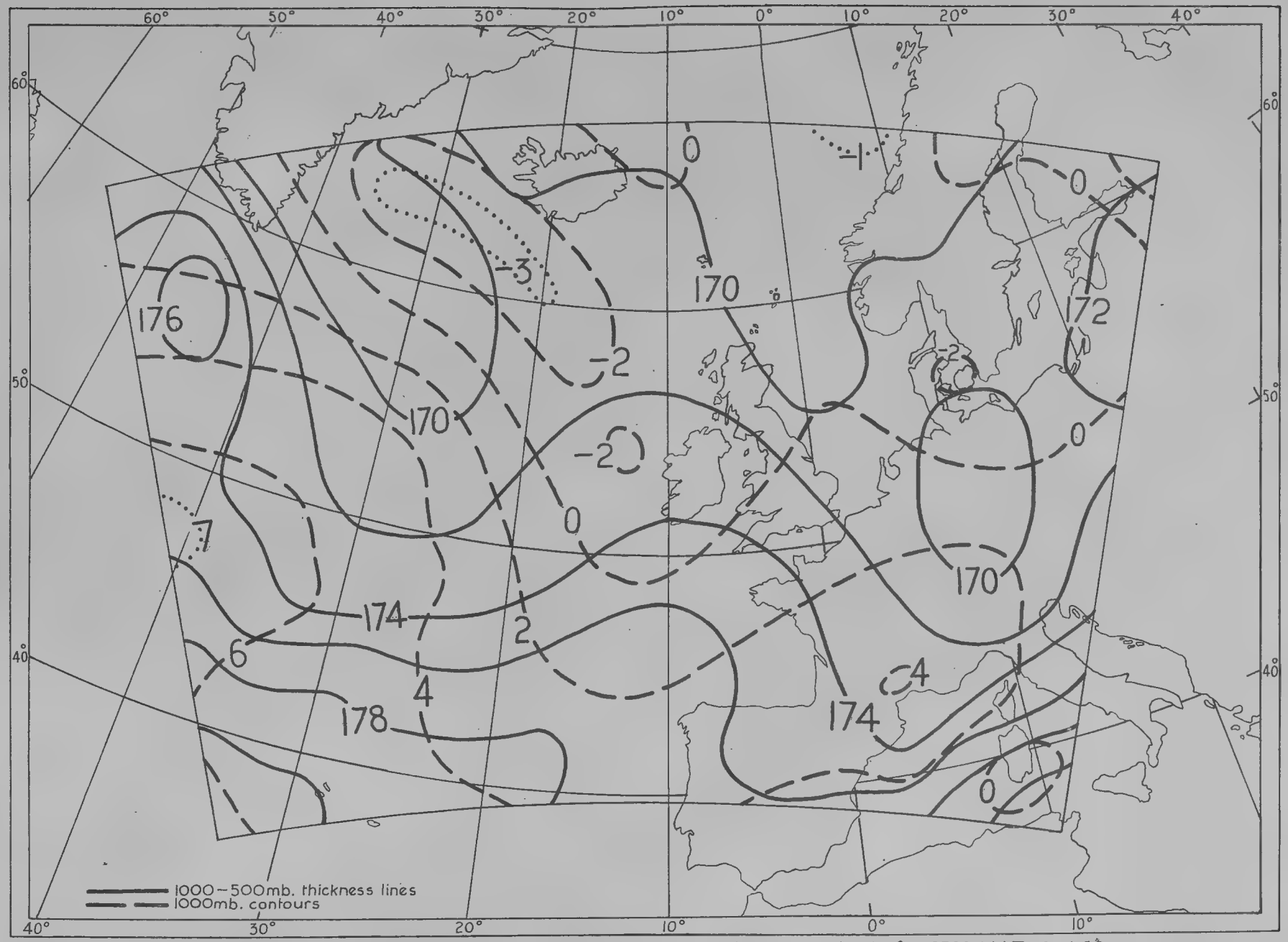

Fig. 3(d) Computed 1000–500mb. thickness and 1000mb. contour charts for 0300 G.M.T. 28.1.52

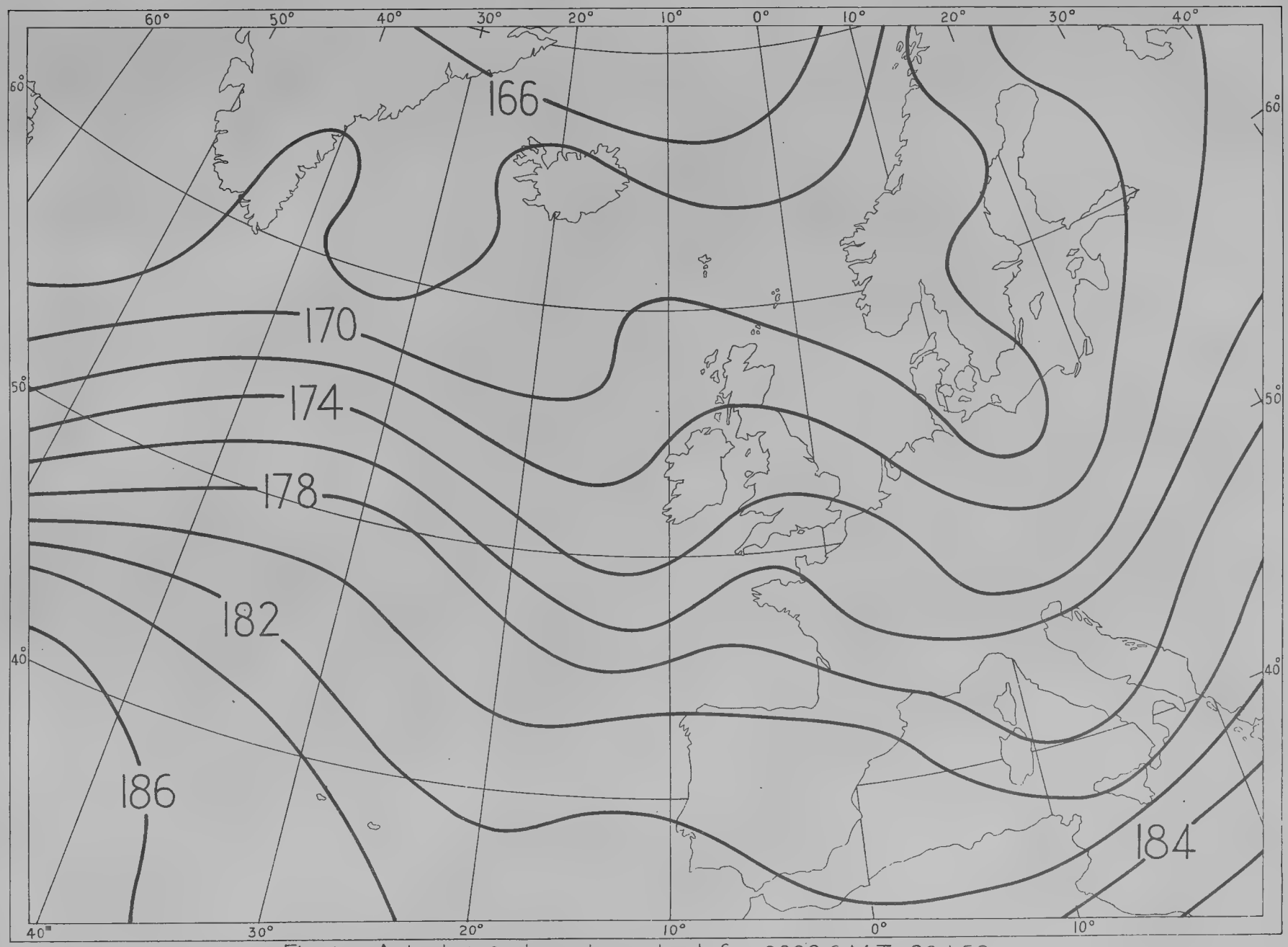

Fig. 4(a) Actual 500mb. contour chart for 0900 G.M.T. 28.1.52

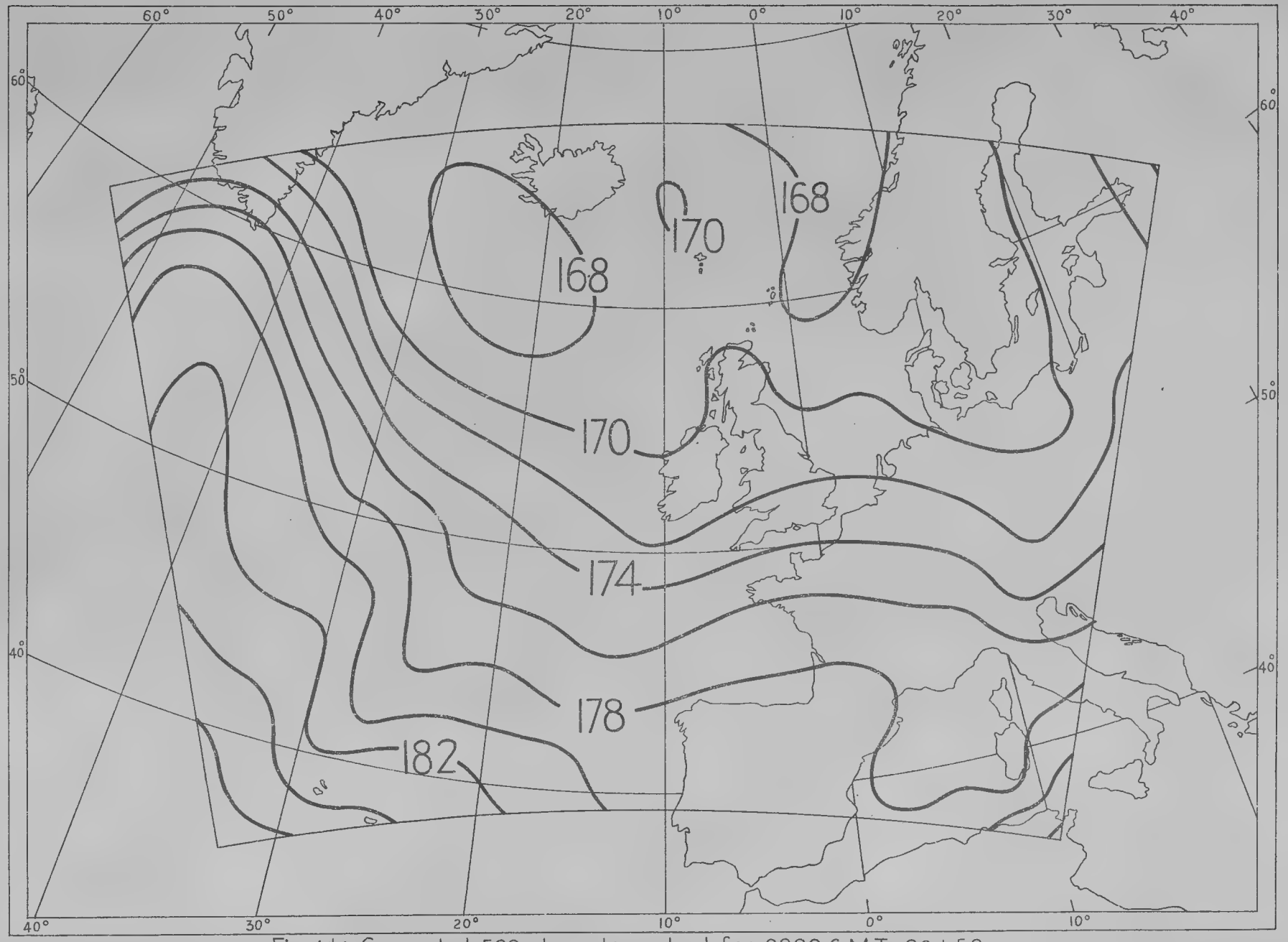

Fig. 4(b) Computed 500mb. contour chart for 0900 G.M.T. 28.1.52

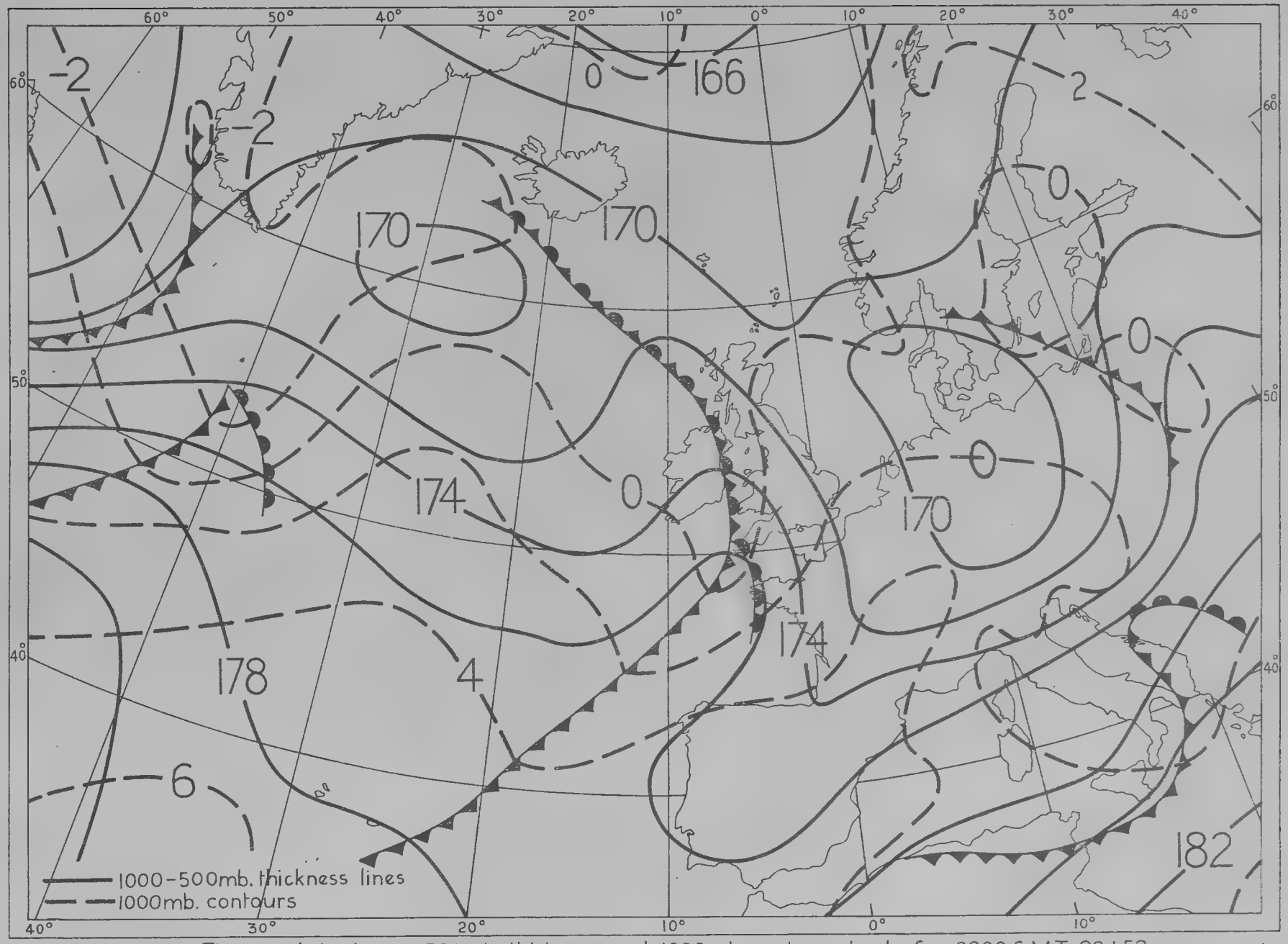

Fig. 4(c) Actual 1000-500mb. thickness and 1000mb. contour charts for 0900 G.M.T. 28.1.52

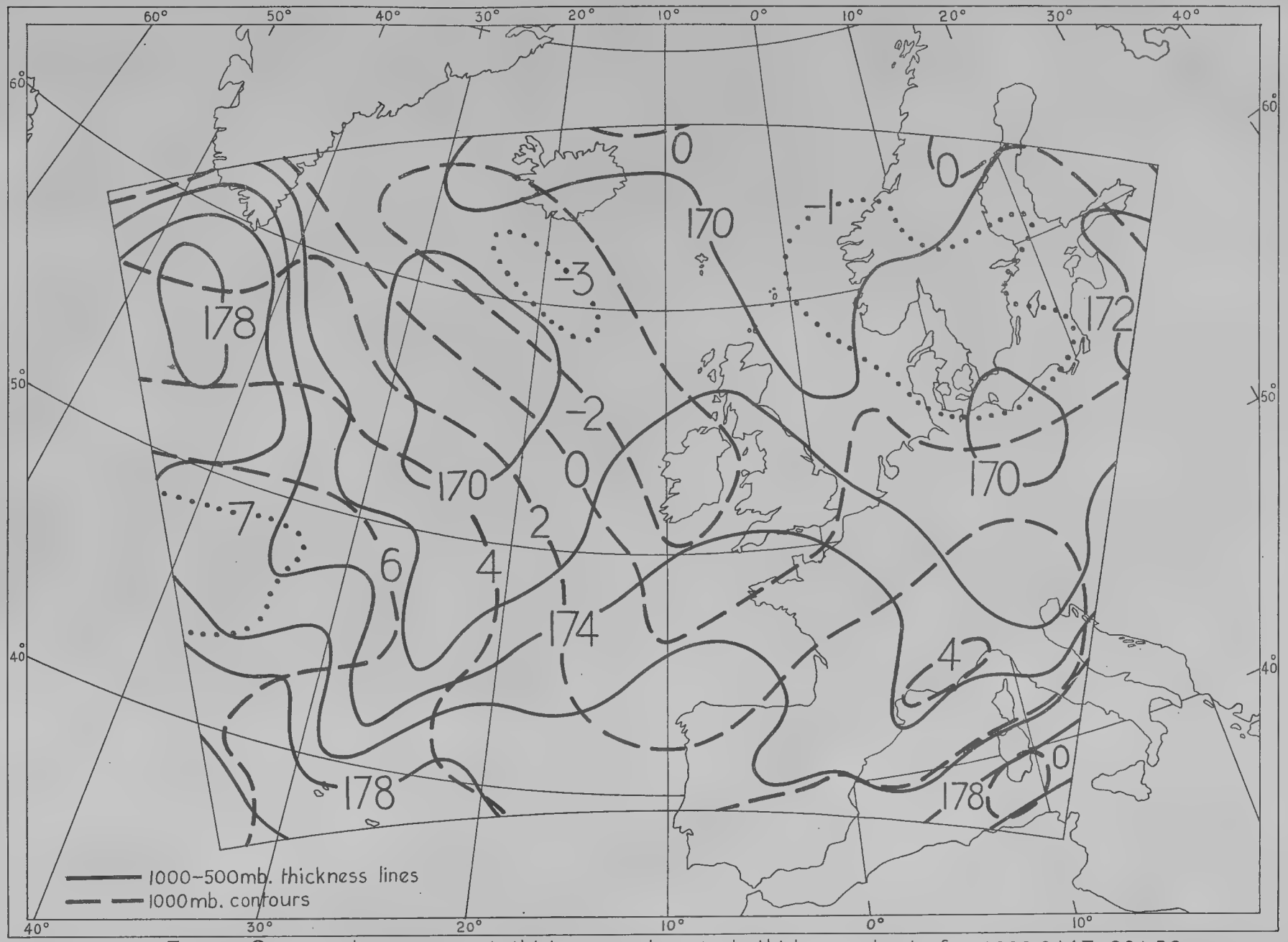

Fig.4(d) Computed 1000-500mb. thickness and 1000mb. thickness charts for 0900 G.M.T. 28.1.52

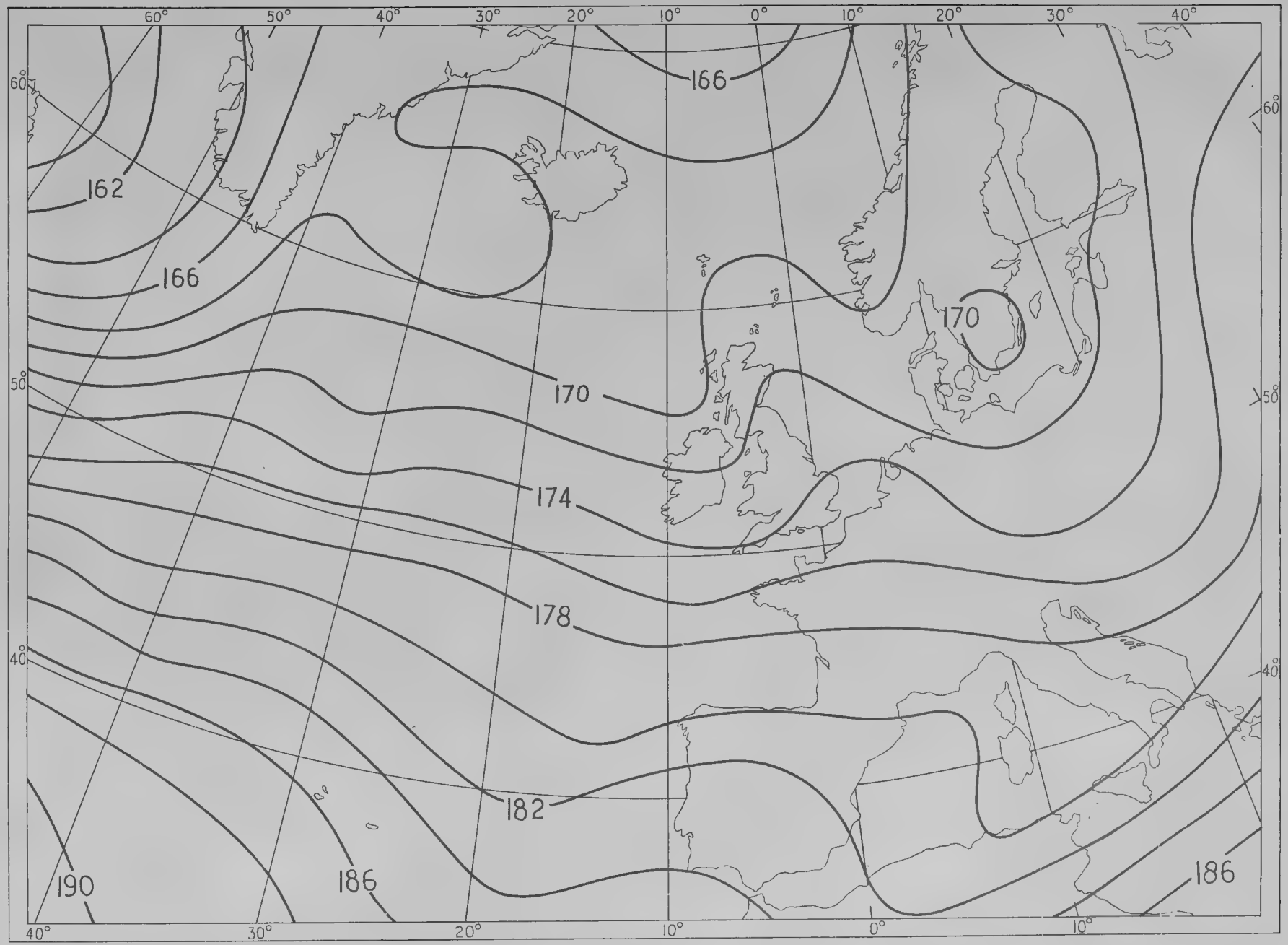

Fig. 5(a) Actual 500mb. chart for 1500 G.M.T. 28.1.52

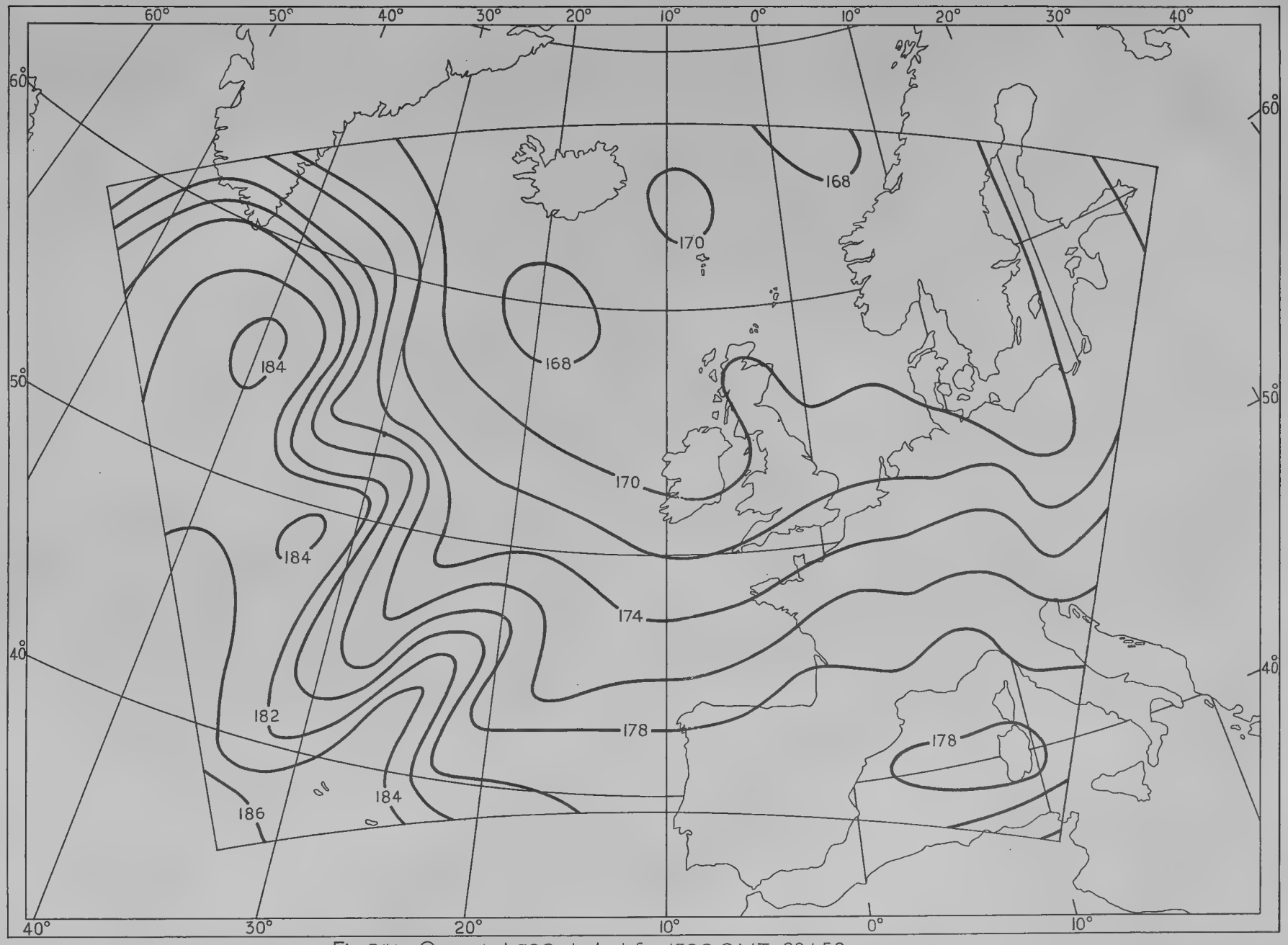

Fig. 5(b) Computed 500mb. chart for 1500 G.M.T. 28.1.52

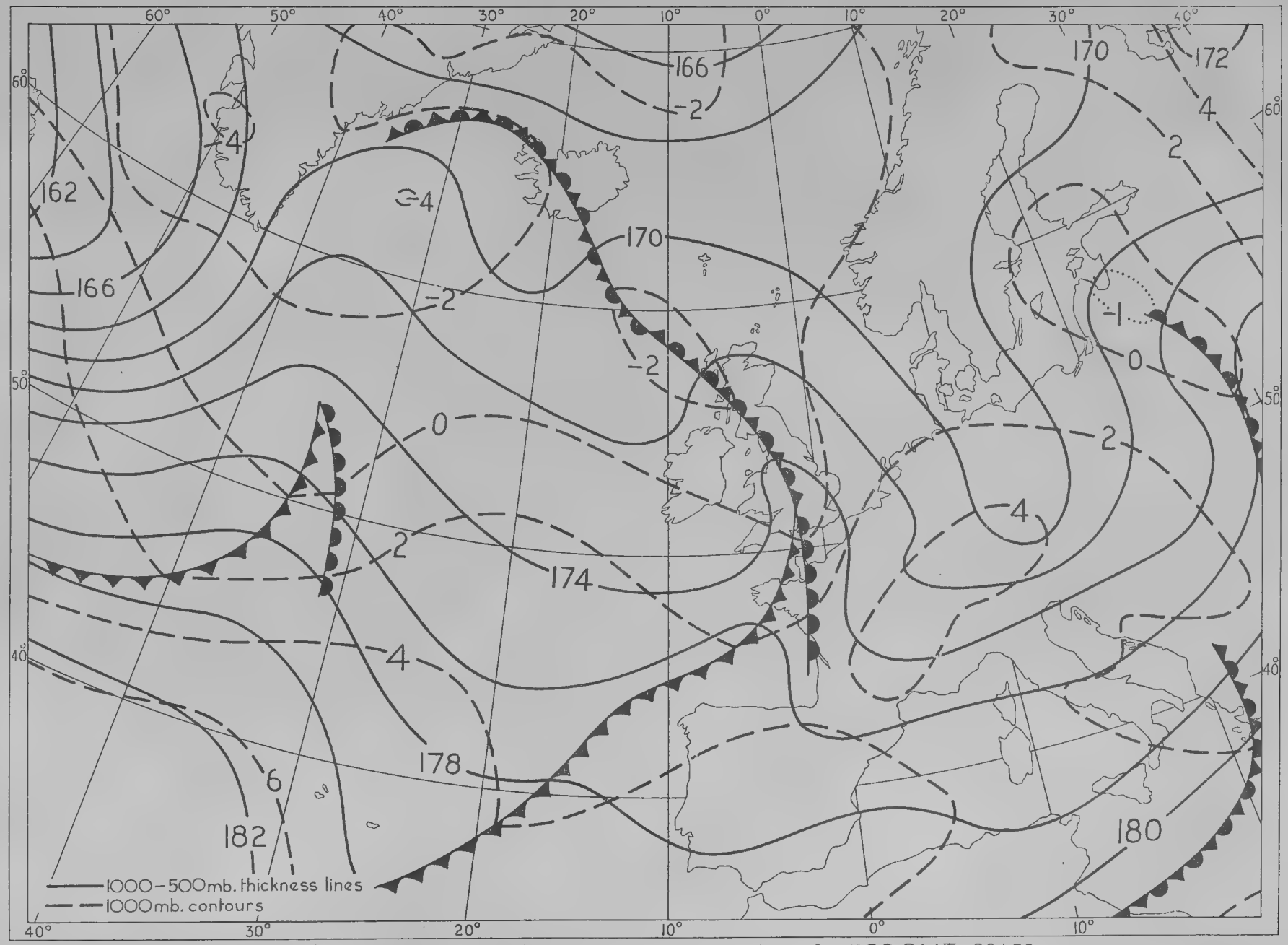

Fig. 5(c) Actual 1000–500mb. thickness and 1000mb. contours for 1500 G.M.T. 28.1.52

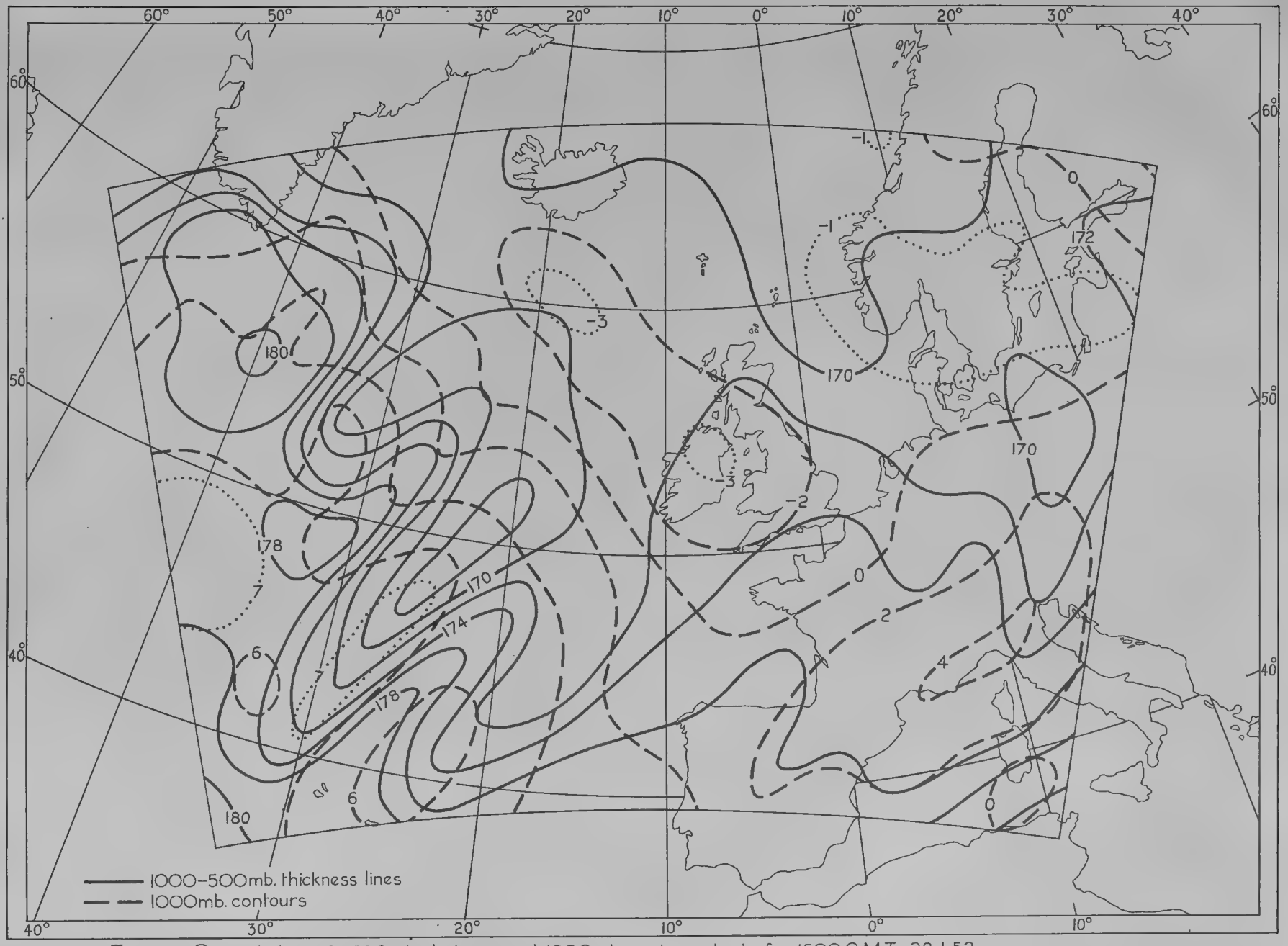

Fig. 5(d) Computed 1000–500mb. thickness and 1000mb. contour charts for 1500 G.M.T. 28.1.52

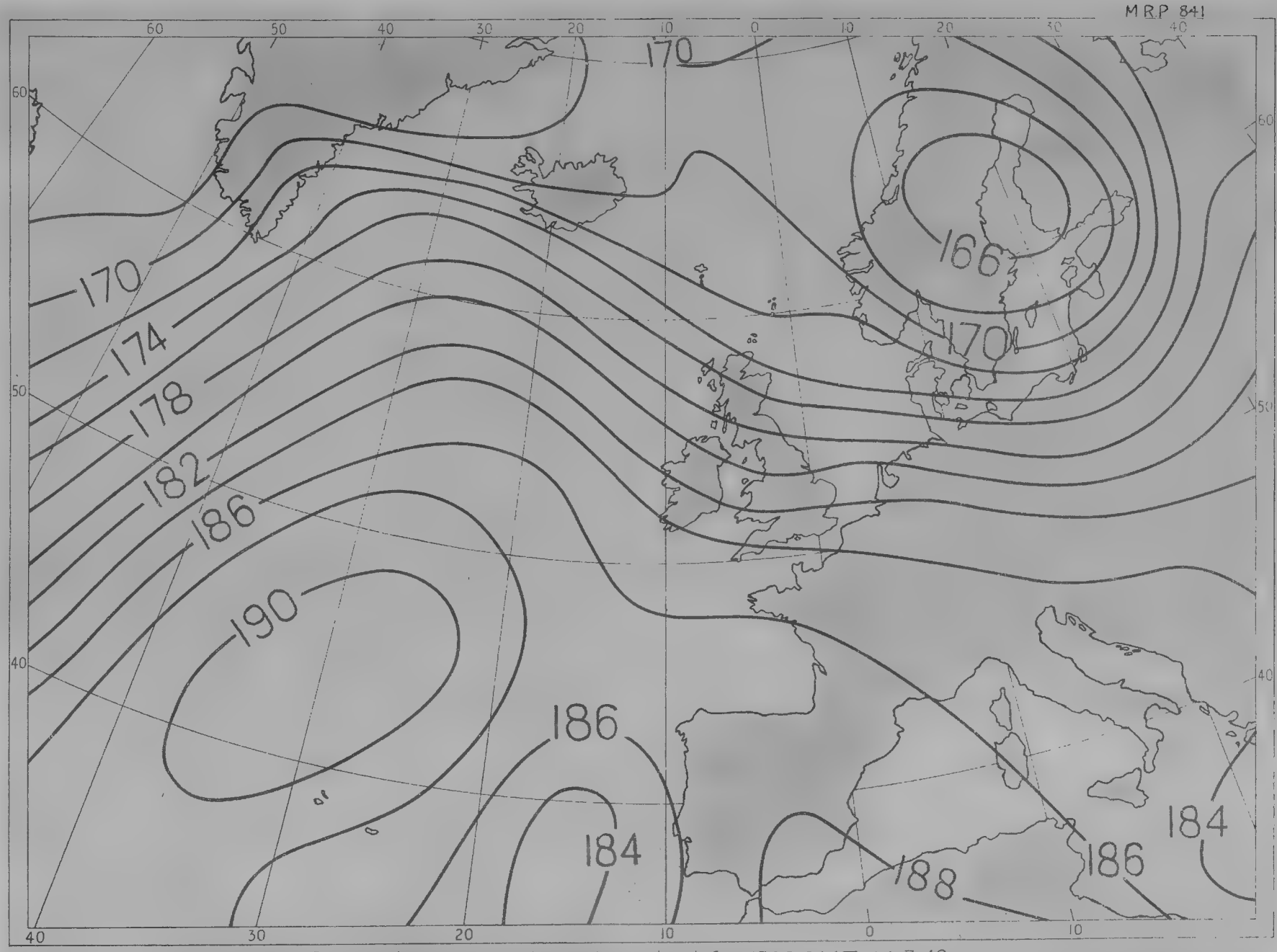

Fig. 6(a) Actual 500mb. contour chart for 1500 G.M.T. 14.3.49

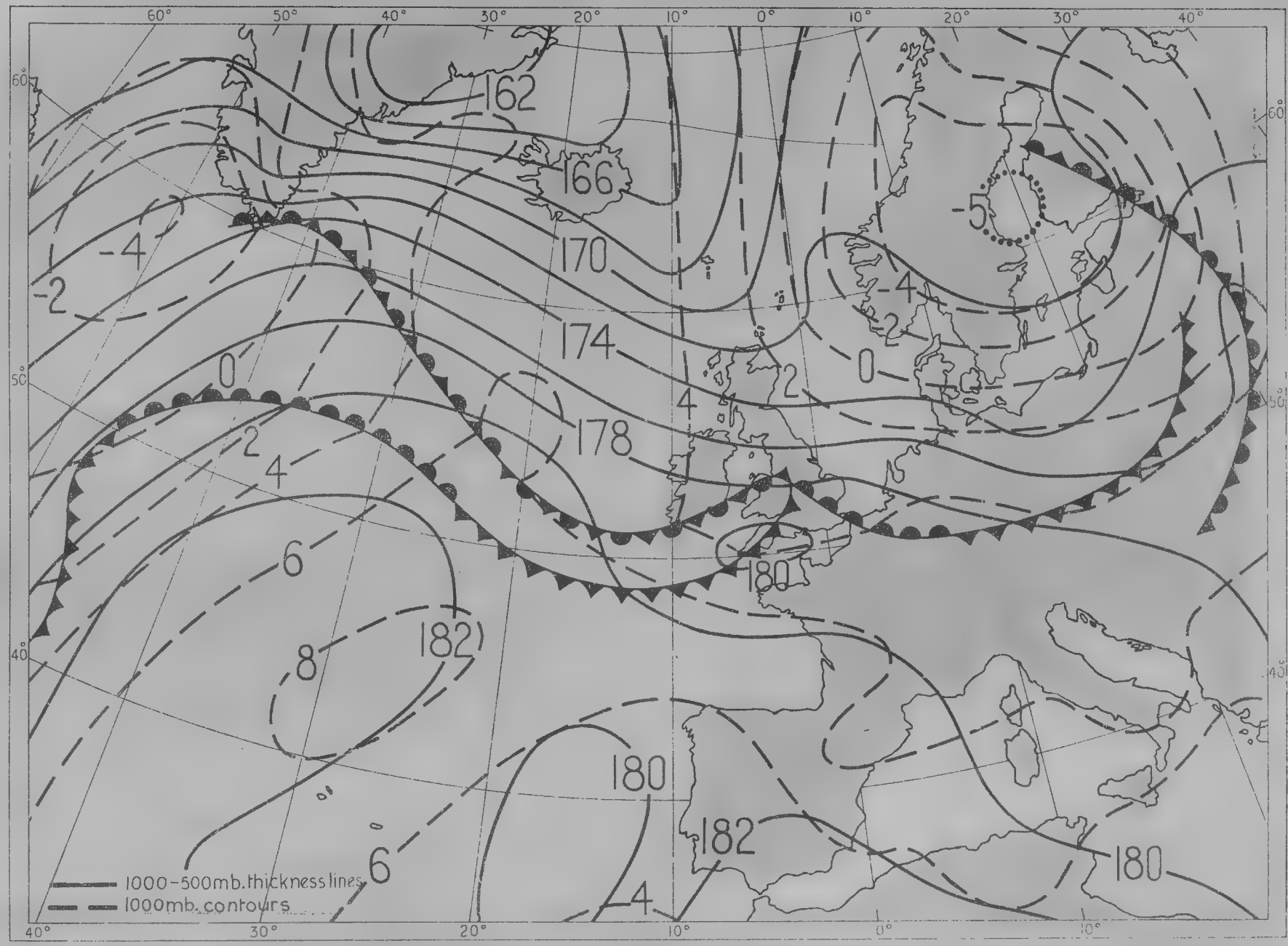

Fig. 6(b) Actual 1000-500mb. thickness and 1000mb. contour charts for 1500G M.T. 14.3.49

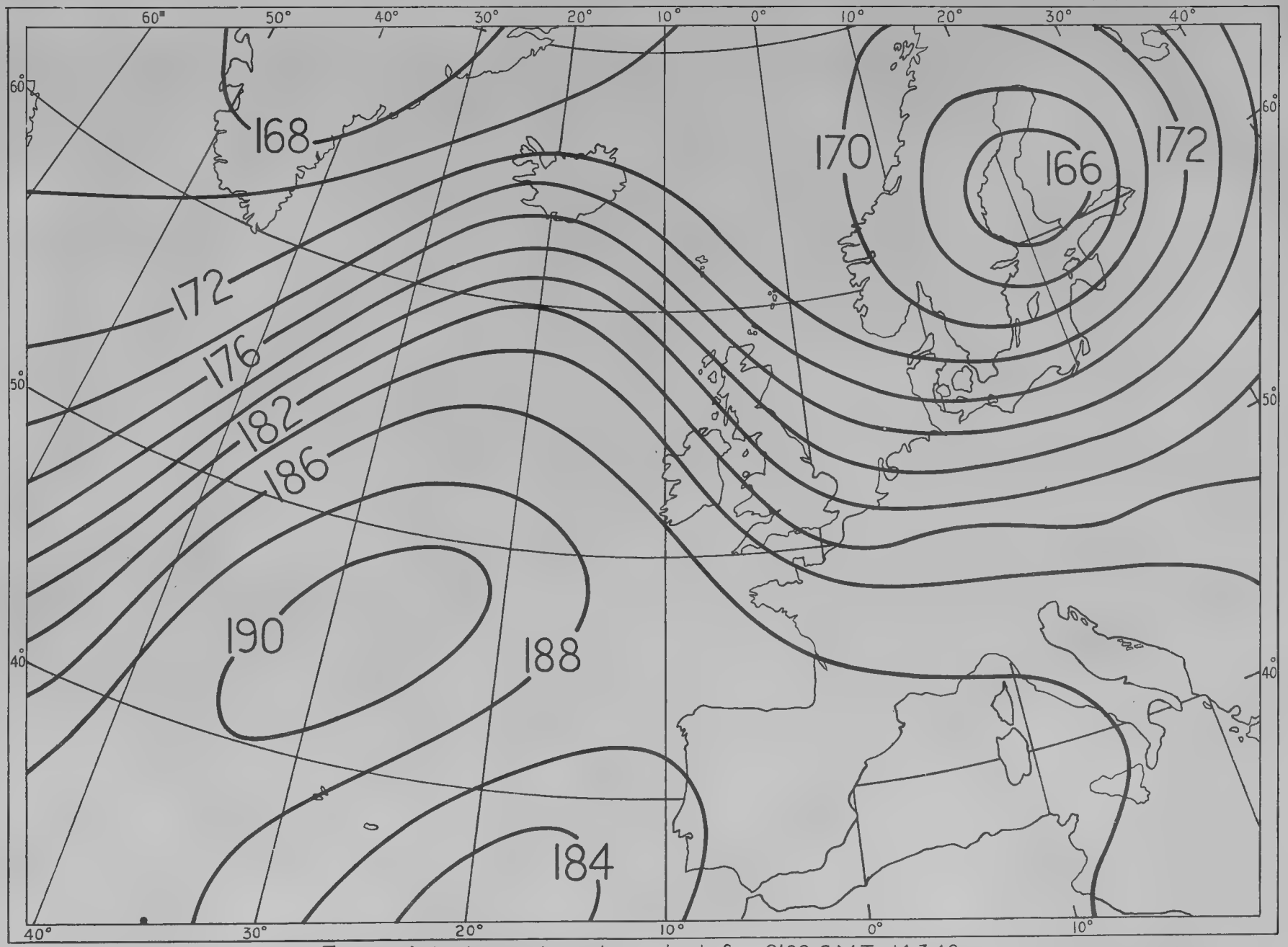

Fig. 7(a) Actual 500mb. contour chart for 2100 G.M.T. 14.3.49

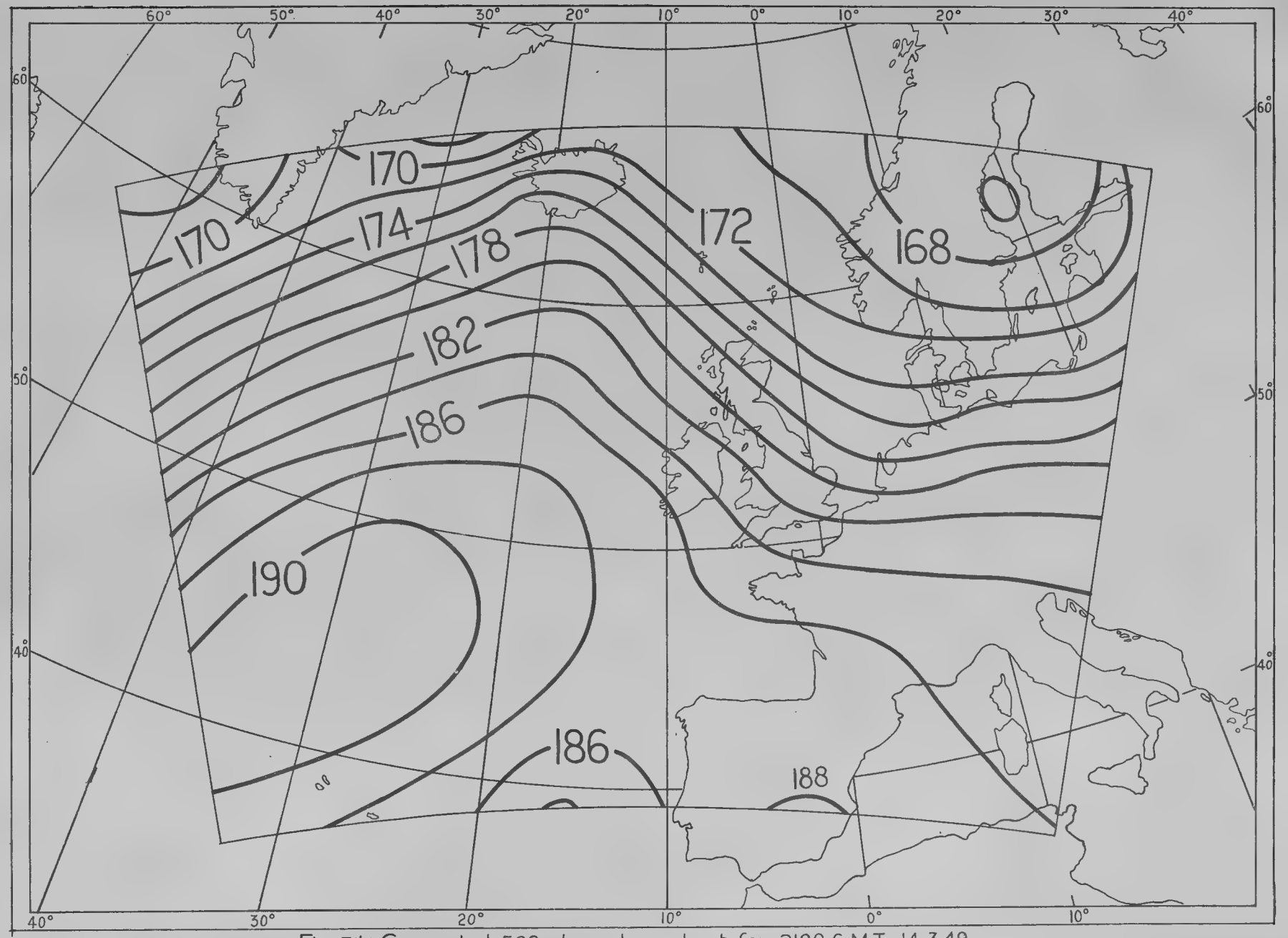

Fig. 7(b) Computed 500mb. contour chart for 2100 G.M.T. 14.3.49

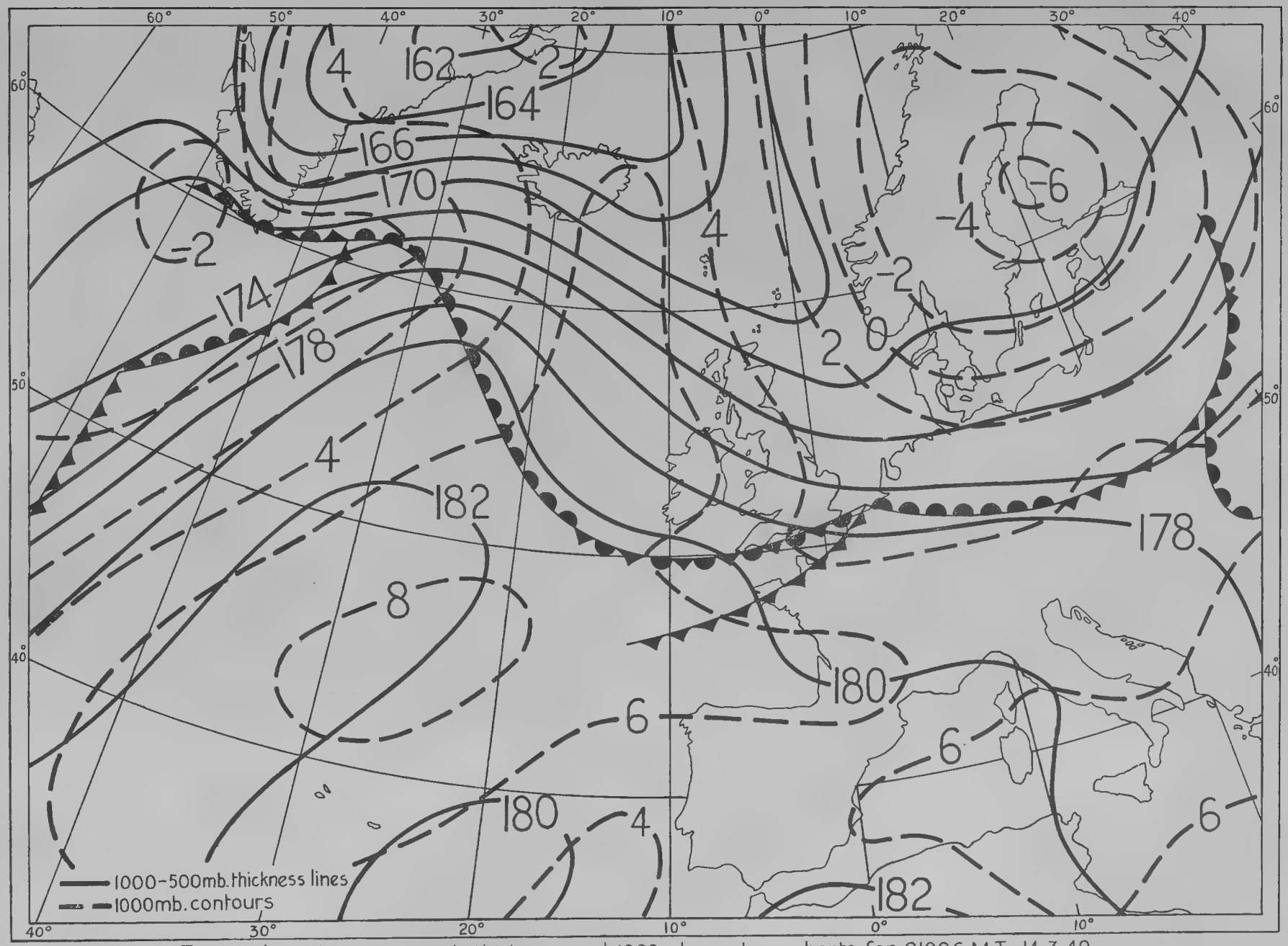

Fig. 7(c) Actual 1000-500mb. thickness and 1000mb. contour charts for 2100 G.M.T. 14.3.49

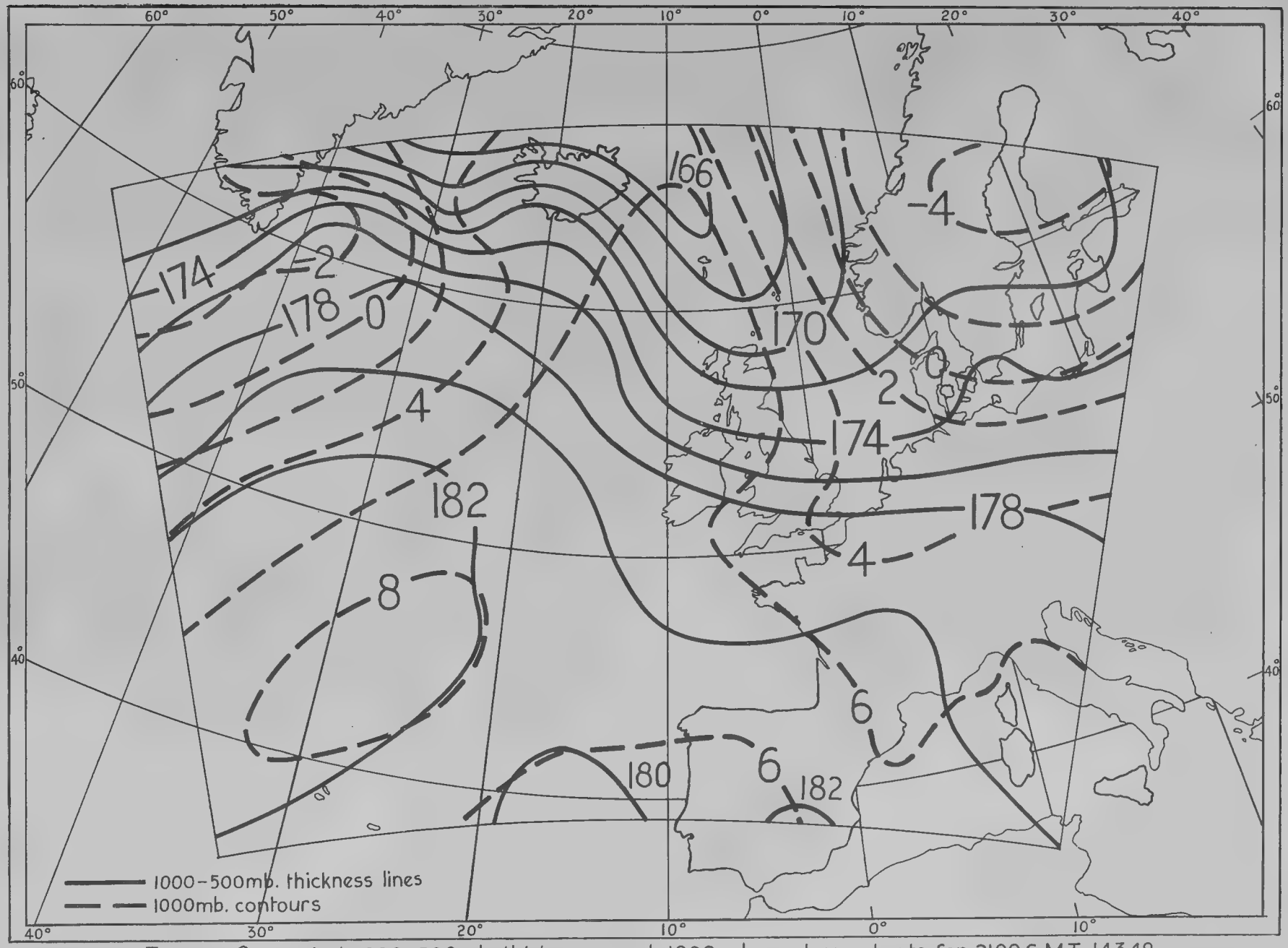

Fig. 7(d) Computed 1000-500mb. thickness and 1000mb. contour charts for 2100 G.M.T. 14.3.49

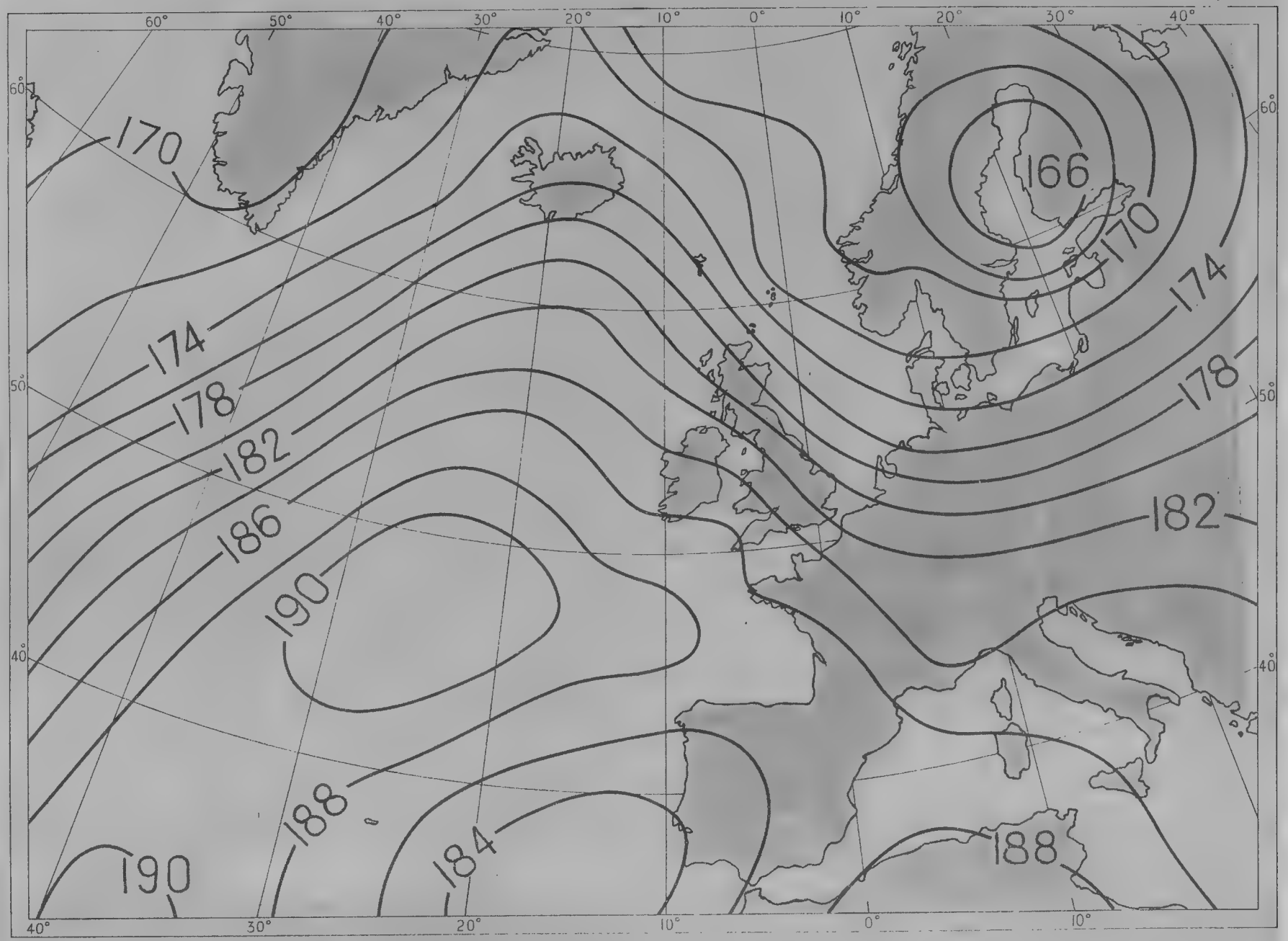

Fig. 8(a) Actual 500mb. contour chart for 0300 G.M.T. 15.3.49

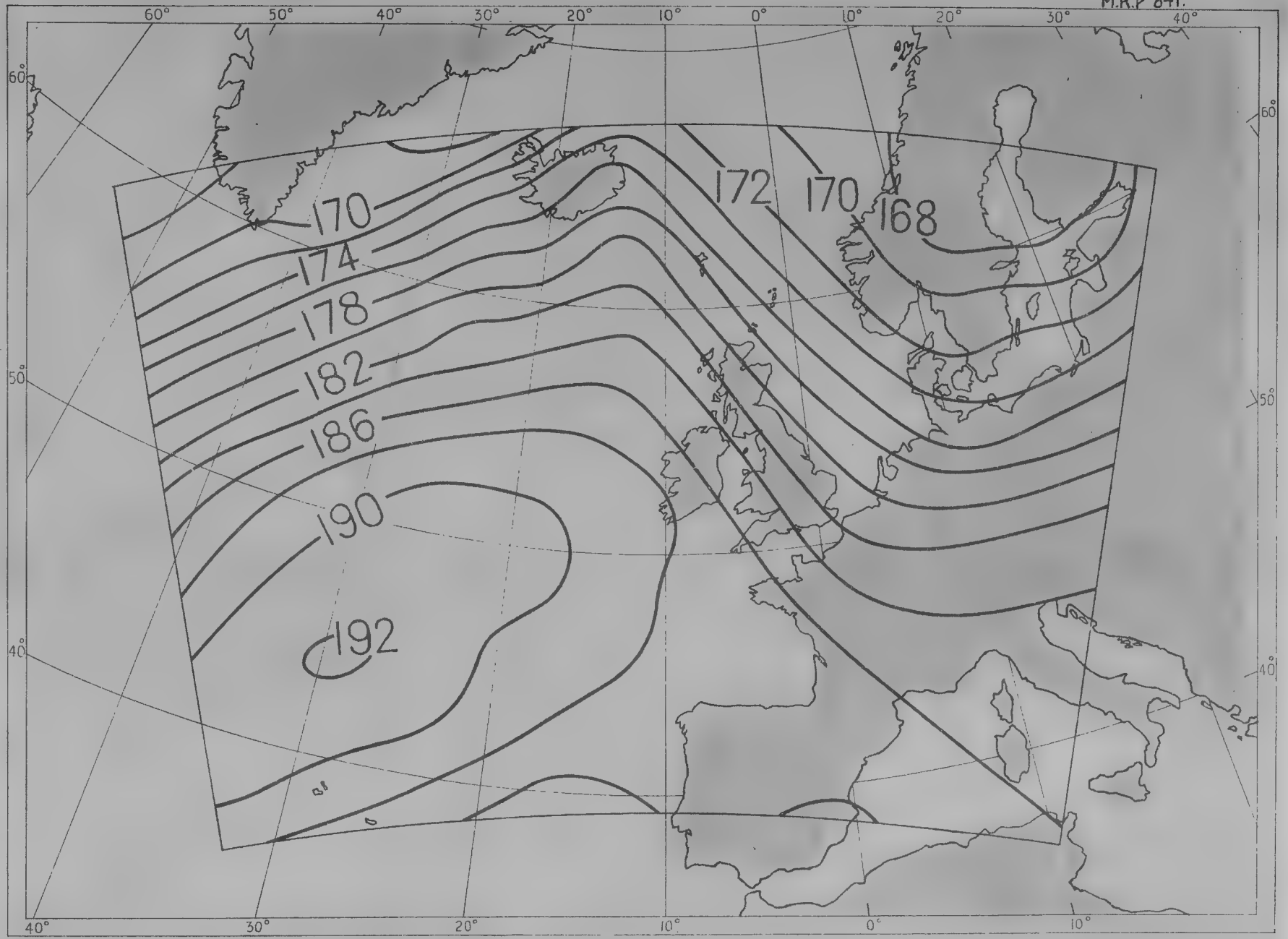

Fig. 8(b) Computed 500mb. contour chart for 0300 G.M.T. 15.3.49

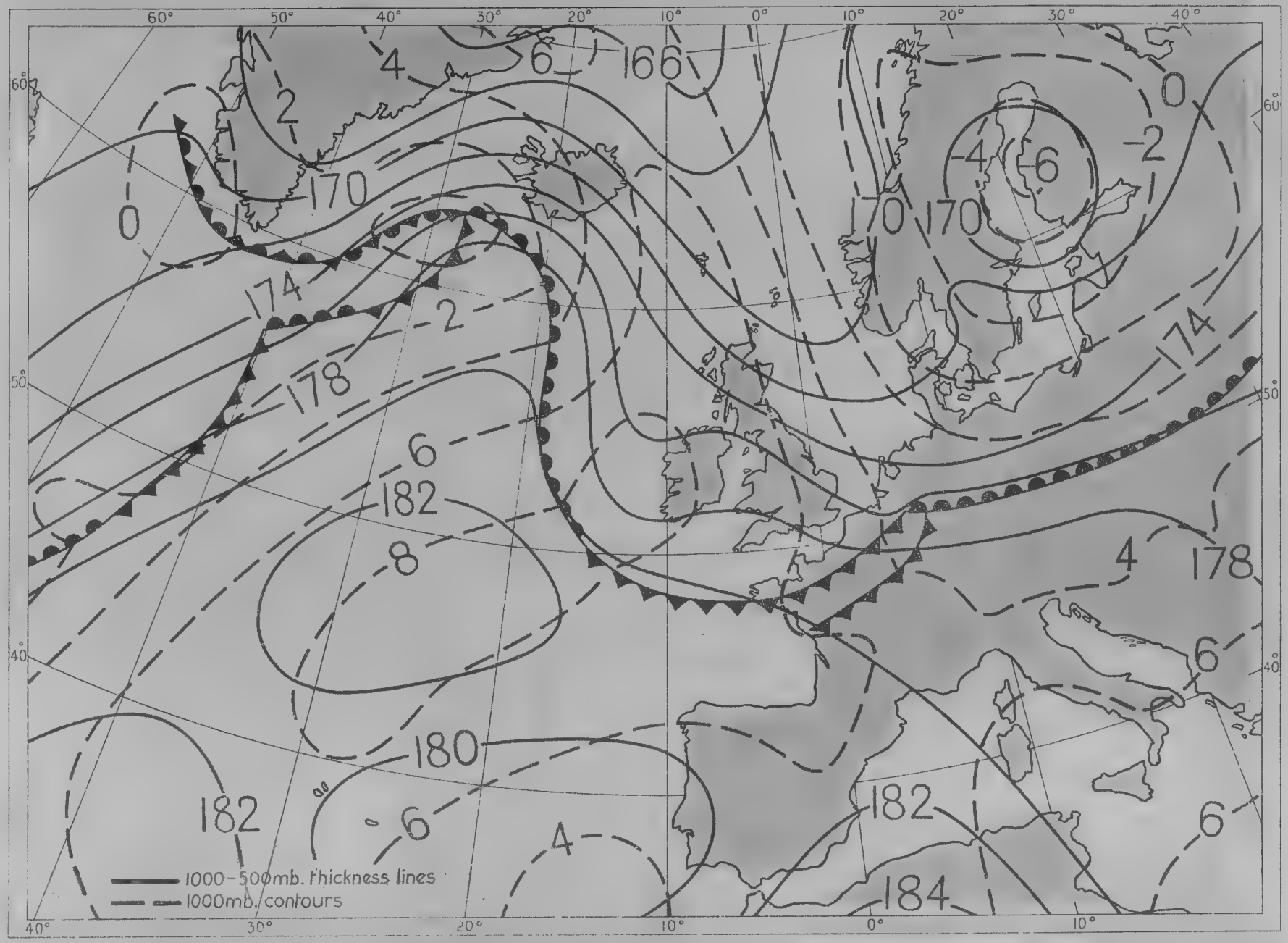

Fig. 8(c) Actual 1000-500mb. thickness and 1000mb. contour charts for 0300 G.M.T. 15.3.49

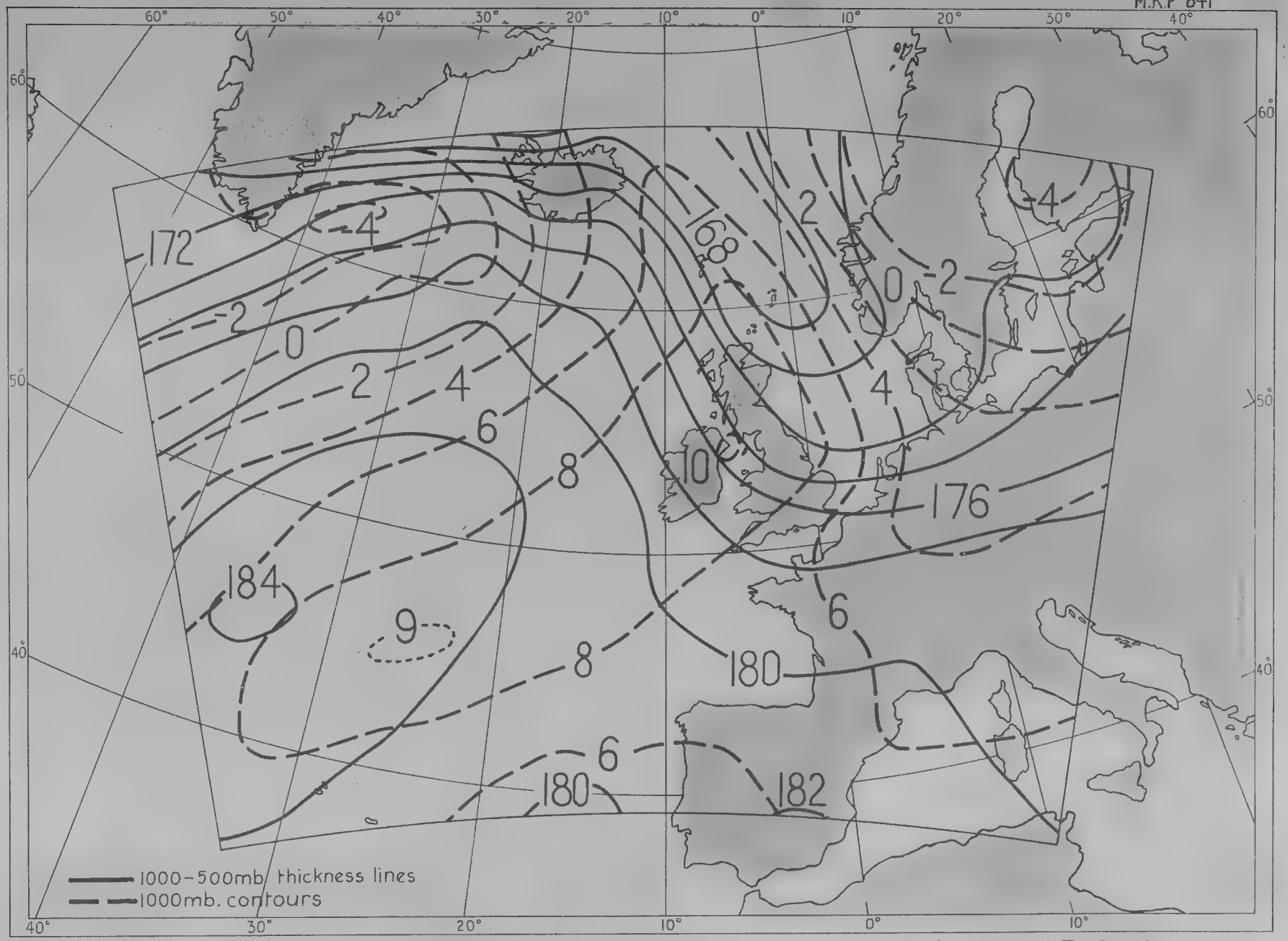

Fig. 8(d) Computed 1000–500mb. thickness and 1000mb. contour charts for 0300 G.M.T. 15.3.49

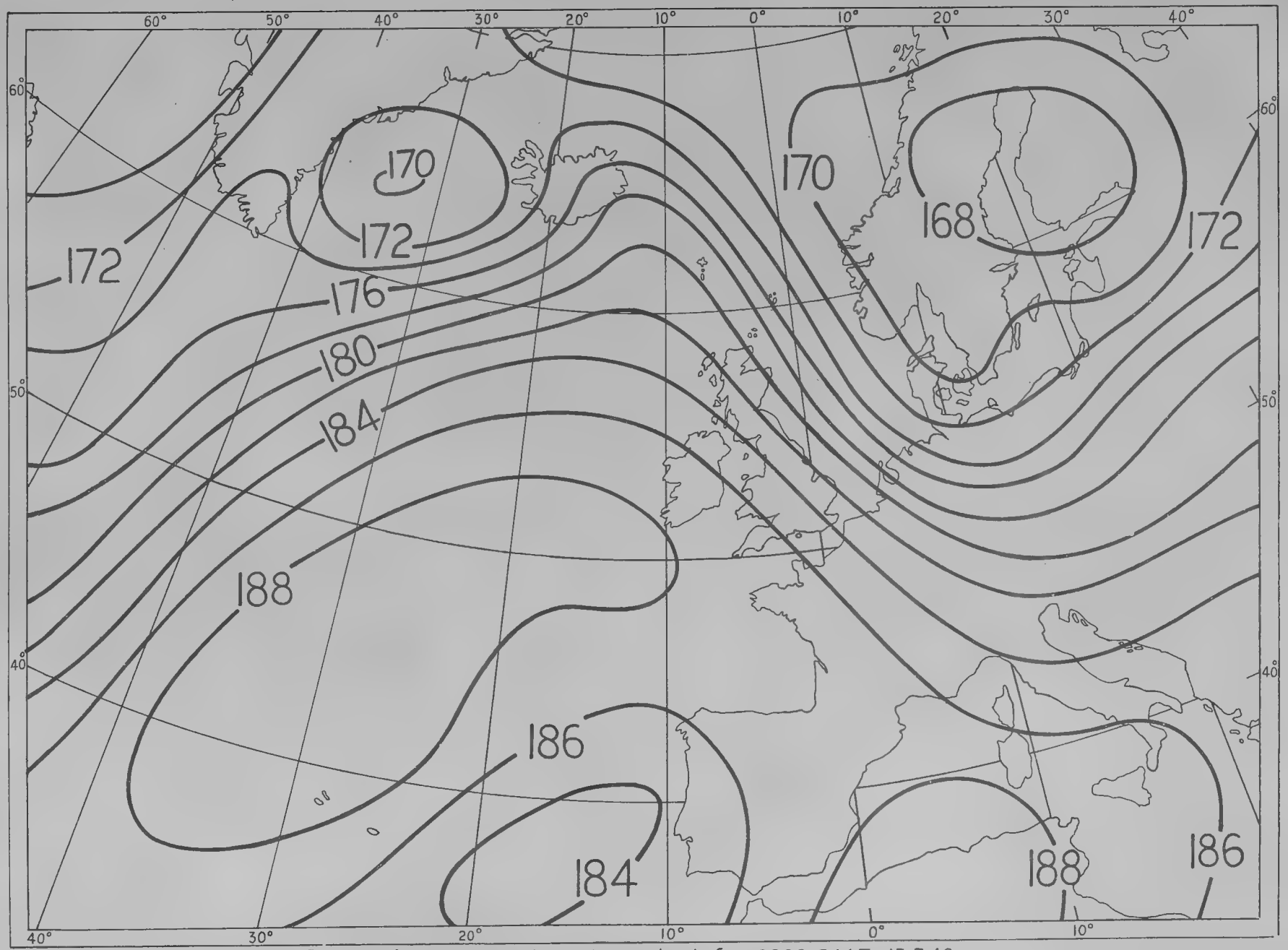

Fig.9(a) Actual 500mb. contour chart for 0900 G.M.T. 15.3.49

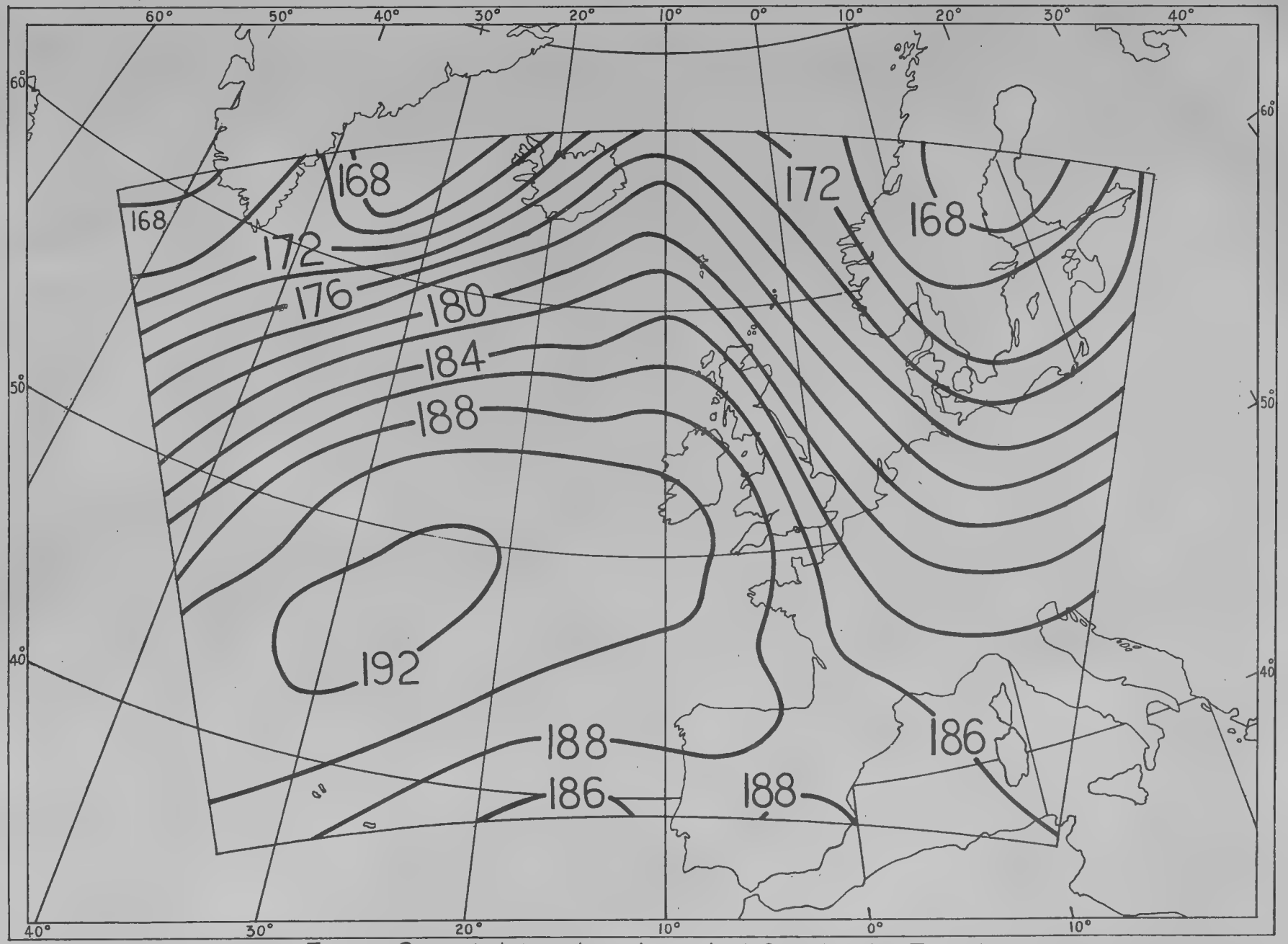

Fig. 9(b) Computed 500mb. contour chart for 0900 G.M.T. 15.3.49

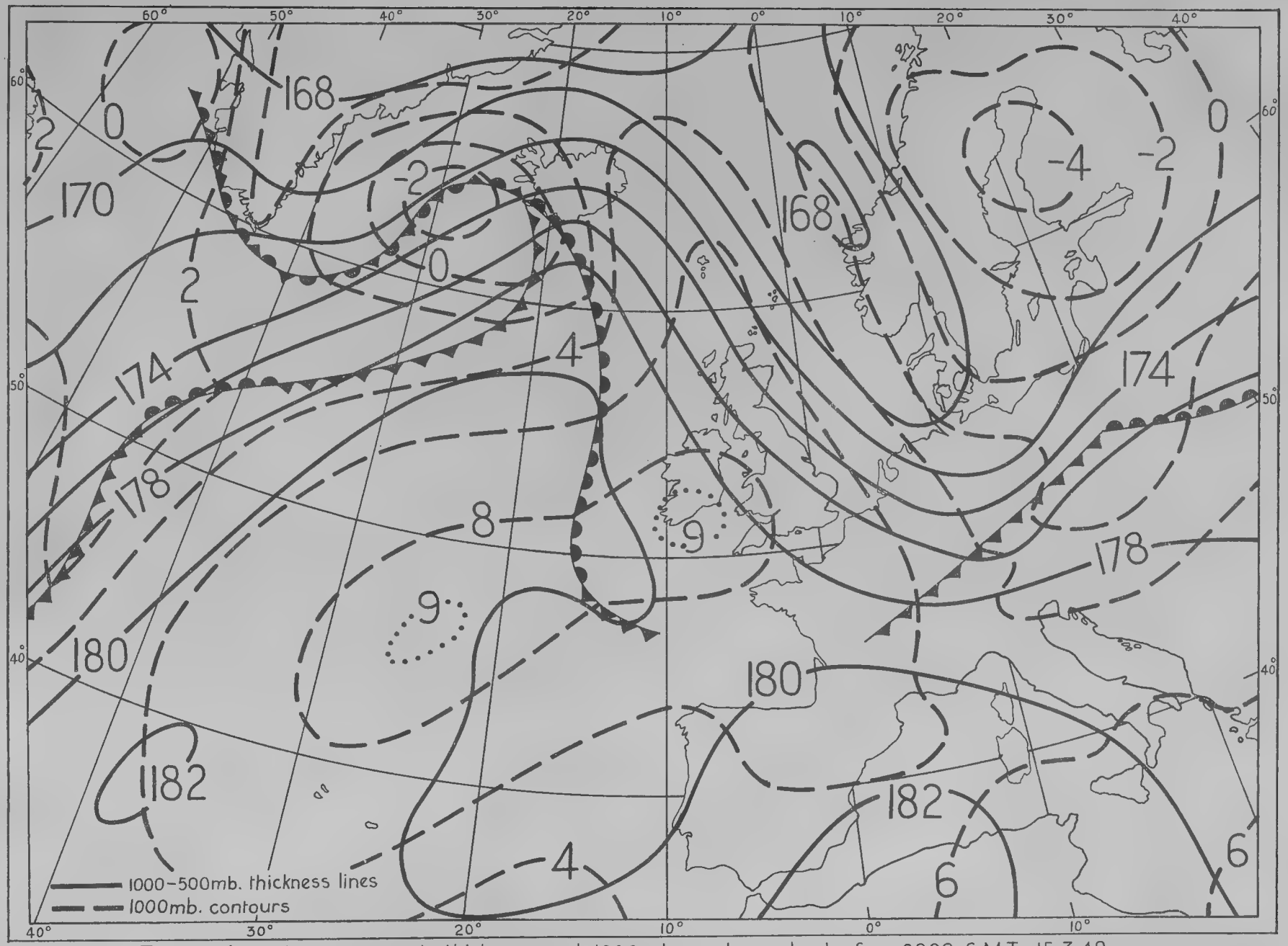

Fig. 9(c) Actual 1000–500mb. thickness and 1000mb. contour charts for 0900 G.M.T. 15.3.49

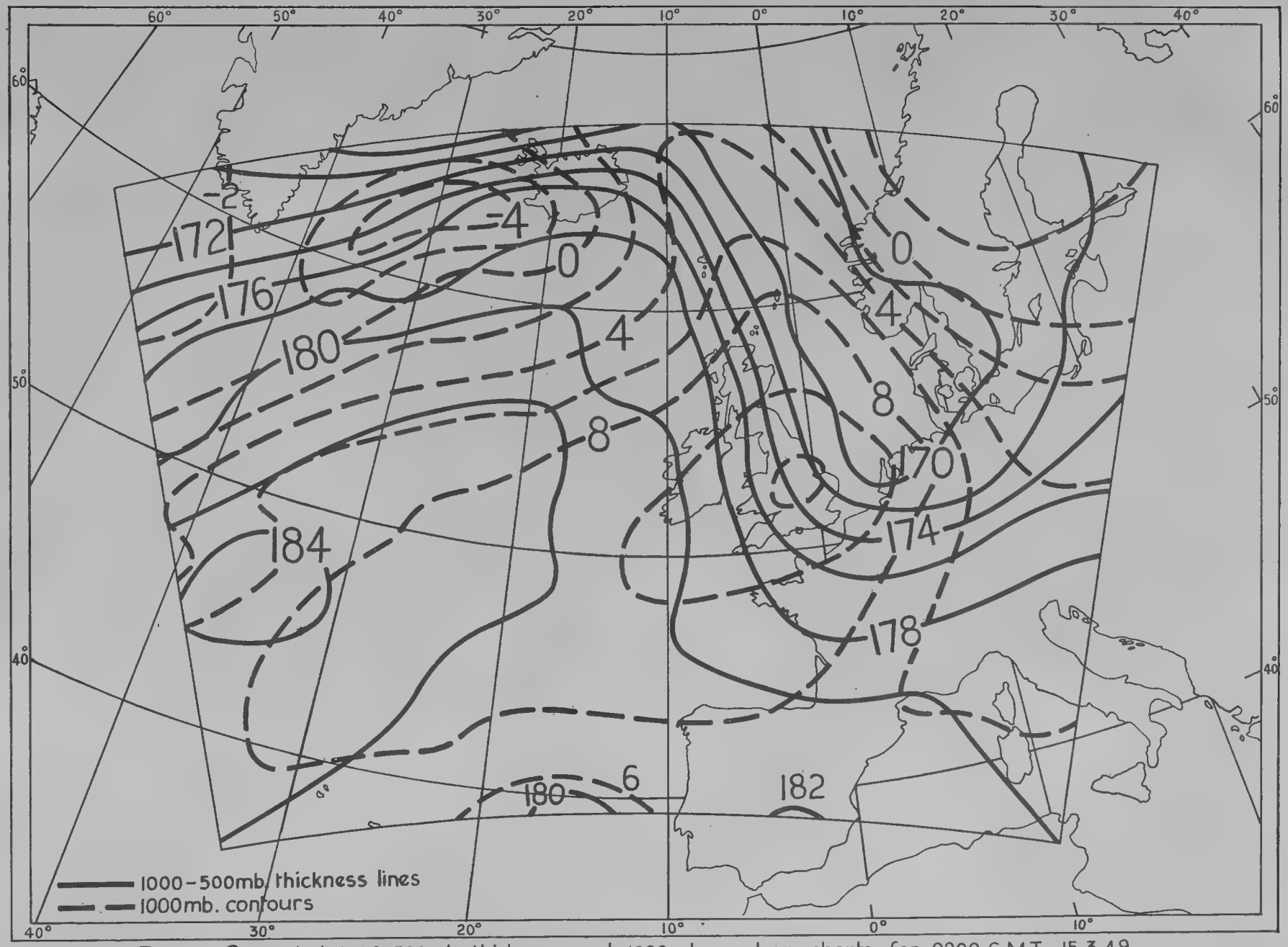

Fig. 9(d) Computed 1000-500mb. thickness and 1000mb. contour charts for 0900 G.M.T. 15.3.49

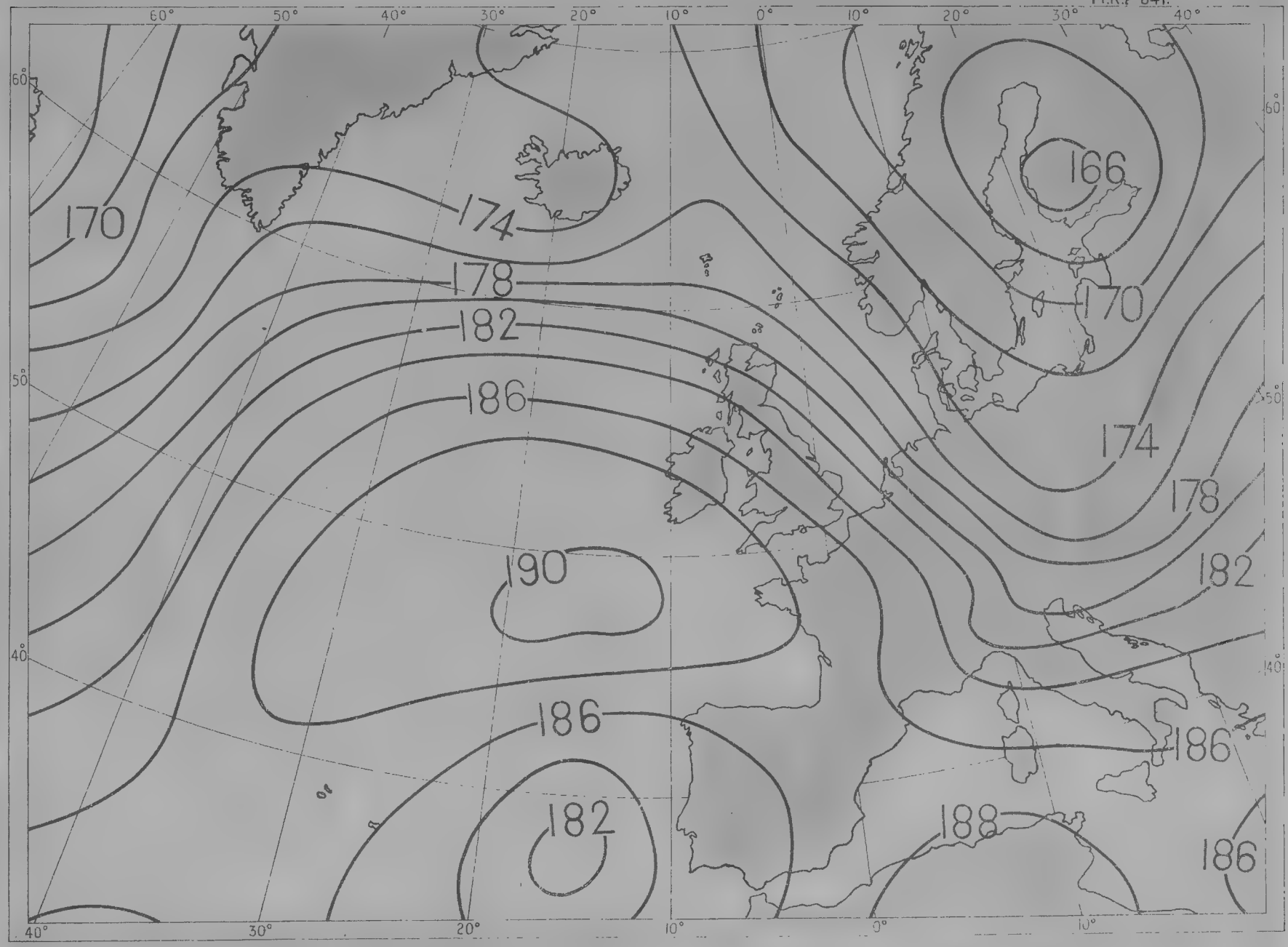

Fig. 10(a) Actual 500mb. contour chart for 1500 G.M.T. 15.3.49

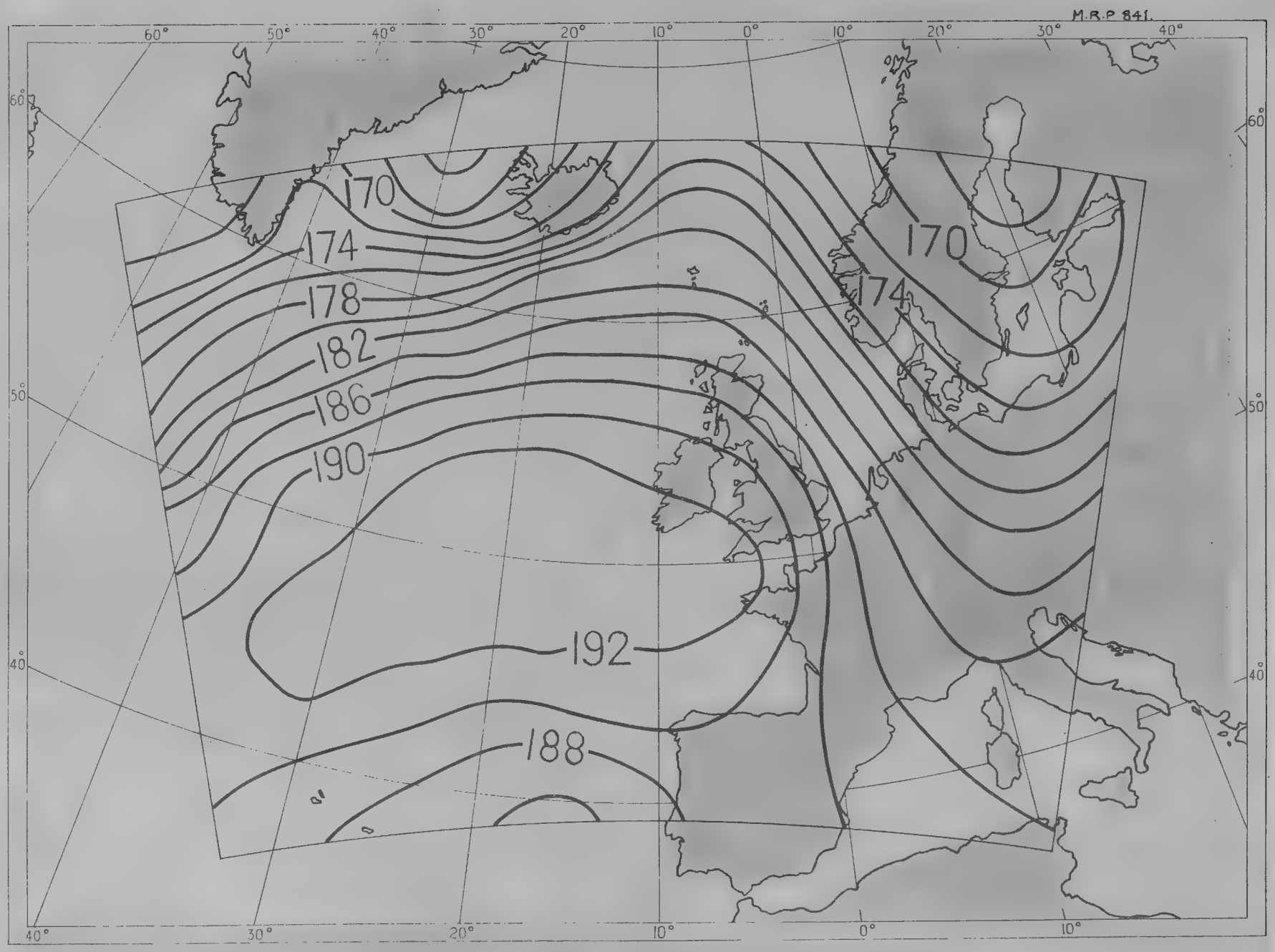

Fig.10(b) Computed 500mb. contour chart for 1500 G.M.T. 15.3.49

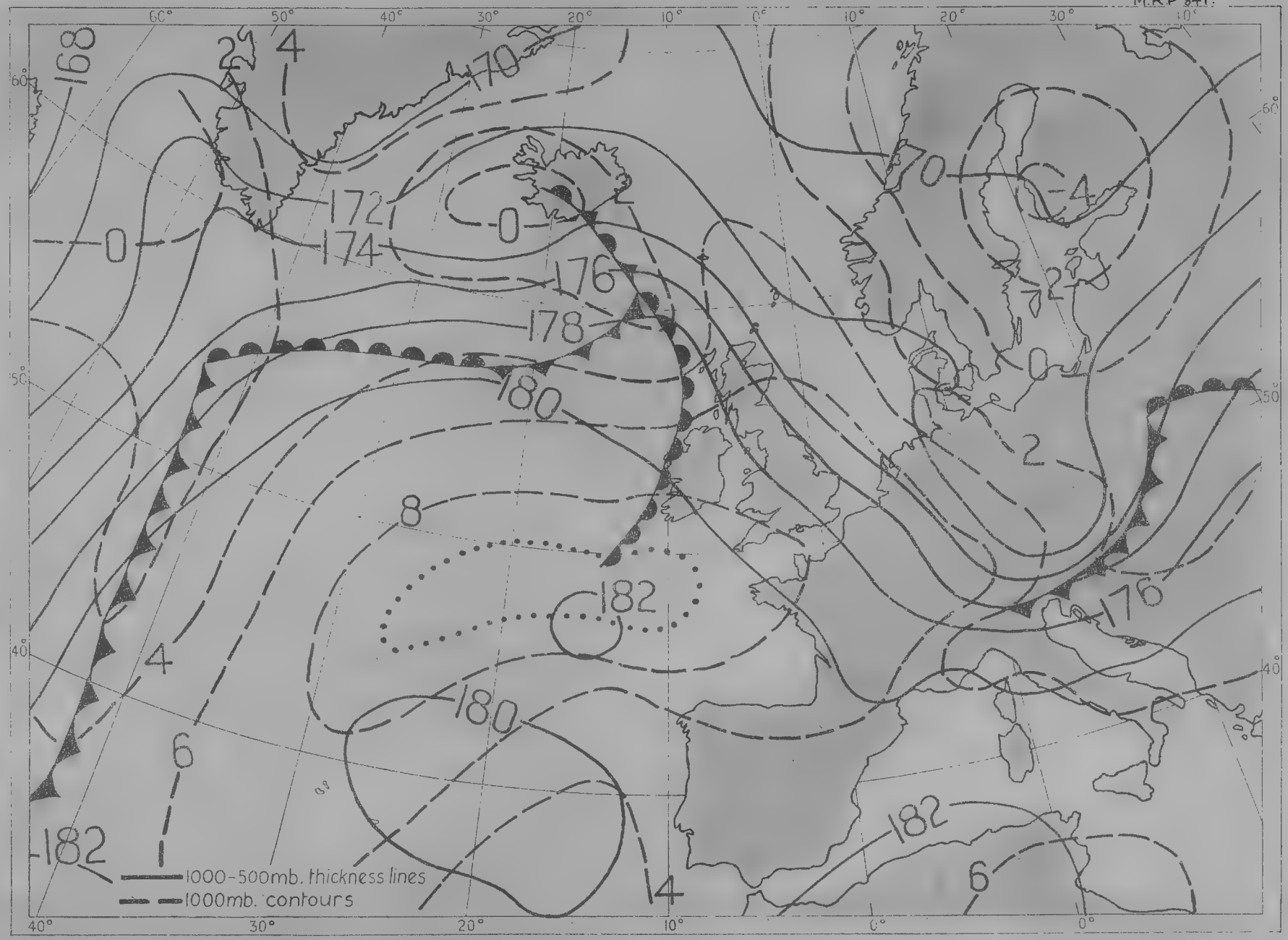

Fig. 10(c) Actual 1000-500mb. thickness and 1000mb. contour charts for 1500 G.M.T. 15.3.49

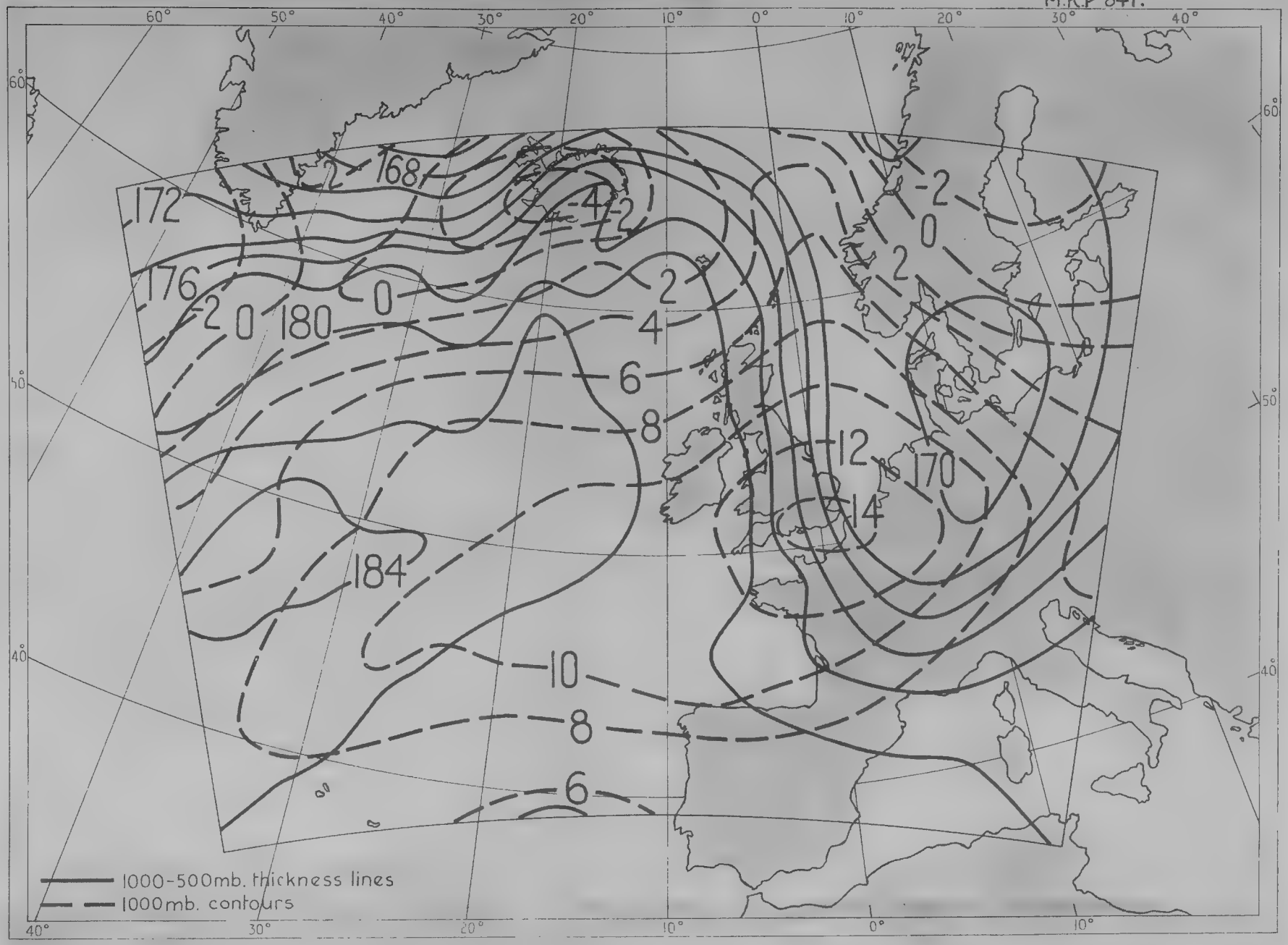

Fig. 10(d) Computed 1000–500mb. thickness and 1000mb. contour charts for 1500 G.M.T. 15.3.49

At the time of issue this report has not been published. Any author desiring to quote this paper should refer to it as "A paper of the Meteorological Research Committee (London). M.R.P. No. 842 by Mr. G.A. Corby. A copy is available in the Library of the Meteorological Office"

M.R.P. 842

S.C.II/163

31st December, 1953.

A.D. 17463

AIR MINISTRY

METEOROLOGICAL RESEARCH COMMITTEE

THE AIRFLOW OVER MOUNTAINS

A REPORT ON THE STATE OF CURRENT KNOWLEDGE

BY

G.A. CORBY (METEOROLOGICAL OFFICE)

SUMMARY

INTRODUCTION

PART I Summary and Examples of Observational Evidence.

PART II Theoretical Studies.

PART III Model Experiments.

PART IV The Work of Förchtgott.

PART V Aviation Applications.

SUMMARY

A brief survey is first given of the observational evidence regarding special airflow effects in the neighbourhood of mountains, as provided by the visual evidence of clouds, the experiences of glider pilots and effects noted by the pilots of powered aircraft. This serves to indicate the phenomena requiring explanation. The review of theoretical studies is confined mainly to the work of Queney and Scorer. Both these authors apply the perturbation method to laminar, isentropic and inviscid flow over an ideal ridge. Queney deals with a uniform airstream (constant velocity and constant stability) and derives streamlines showing wave motions, both vertical and horizontal. Queney's waves are dependent partly on the stability and partly on geostrophic forces, and the order of the wavelength is several hundred km. In his treatment, Scorer deals with smaller scale phenomena, so enabling geostrophic forces to be neglected, and provides for variations of stability and wind shear in the vertical. He finds that realistic wave effects, of the type observed in nature, are predicted by the theory provided the variation of stability and wind shear with height is in accord with certain criteria. The criteria have some practical value for forecasting purposes. Past.

/experimental

experimental work with models in wind tunnels is briefly considered in the light of what can be deduced from theoretical treatments regarding the conditions for dynamical similarity. More recent work by Long, using a tank containing several layers of immiscible liquid to simulate a density gradient is referred to briefly; this technique appears to have promise. A comprehensive field study by Förchtgött, who used teams of gliders, is summarised. From his observations, Förchtgott has built up a theory of the flow patterns which occur in the lee of mountains. The main value of Förchtgott's work lies in the practical support it provides for some of the results deduced by perturbation theory and in throwing light on the nature of non-laminar flow patterns which cannot be dealt with by existing theoretical treatments. In a concluding section, aviation applications of existing knowledge on this subject are discussed. These concern forecasting and the determination of safety heights over mountains.

INTRODUCTION

It has long been known that the airflow over mountainous terrain is commonly more disturbed than over level country. In the past, information on the subject in meteorological textbooks has usually been scanty and generally confined to the statement that disturbances to the airstream above a given mountain can be expected to extend to about three times its height. This gives no clue as to the nature of the disturbances or the meteorological factors which have a bearing on them. From its very incompleteness, therefore, the information is quite unsatisfactory especially now, in view of the increasing demand for more detailed advice on the subject and the better understanding of such problems which has developed recently.

It might be supposed that the effect of a mountain range on an airstream would be merely to bring about a change in the extent, scale and degree of turbulence experienced by an aircraft flying above. Turbulence, however, is essentially a disorganised type of flow whilst often the airstream over a mountain is deformed in a fully organised manner which is highly significant but not necessarily turbulent. In this report we shall be much concerned with such organised deformations and the circumstances in which they occur.

During the last few years, there has grown a considerable body of experimental data on the subject from various sources and notable theoretical researches into the problem have been carried out, so much so that over at least an important part of the subject a logical system of ideas has developed and can now be presented. As glider pilots rely on vertical currents to support their sail-planes, it is natural that they should have learnt a great deal of the special airflow effects which occur in the neighbourhood of mountains; accordingly, much of the practical evidence has come from glider pilots. Förchtgott has exploited the potentialities of gliders in a valuable and illuminating programme of field research. More recently the experiences of the pilots of powered aircraft have been receiving attention and have been reported by Austin, Turner and others. As regards other specific experimental work, mention must be made of the investigation by Field and Warden (1929-30) into the air currents in the Bay of Gibraltar, the work of Abe in Japan who studied mountain cloud formations and supplemented this by wind tunnel experiments, and Küttner's studies of the airflow over the Alps. Currently, the powerful mountain wave phenomena at Bishop, California, are the subject of an elaborate investigation as part of the U.S. Research project on this subject.

The challenge to the mathematician offered by the problem of mountain airflow has been taken up, and major contributions in the form of theoretical treatments have been made by Lyra, Queney, Scorer and others. The hydrodynamical theory solves the problem of the flow pattern successfully if the flow is laminar and steady, but when this is not the case we must draw what

/conclusions

conclusions we can from the observational data. The theory indicates the great limitations of wind tunnel experiments and makes it clear that the problem of ensuring dynamical similarity in the general case poses almost insuperable laboratory difficulties; any past results obtained in this way, therefore, must be interpreted with great caution.

It is the purpose of this report to summarise existing knowledge on the subject of mountain airflow. The literature is very extensive and we shall confine ourselves to those aspects which appear to have a bearing, real or potential, on the aviation problems arising from the subject.

PART I - SUMMARY AND EXAMPLES OF OBSERVATIONAL EVIDENCE

The observational evidence of special airflow effects in the neighbourhood of mountains, notably the phenomenon of stationary lee waves, falls roughly into three categories, viz. the visual evidence provided by clouds, the experiences of glider pilots, and effects observed from powered aircraft. It will be convenient, before discussing theoretical and other studies, to summarise this evidence and give a few examples, in order to make clear the nature of the phenomena requiring explanation.

(a) The Evidence of Mountain Clouds

Lenticular clouds are frequently seen over hilly or mountainous terrain in all parts of the world. As observed from the ground they have smooth lens-shaped outlines and remain stationary relative to the ground or nearly so. The wind blows through them and this can be verified when the movement of an identifiable fragment of the cloud can be followed visually. This has been confirmed by time lapse photography of mountain clouds, for example by Abe (1). The inference that such clouds form where the airstream executes a vertical undulation initiated by the terrain below is almost inescapable. On many occasions, especially to the lee of long ridges, a succession of lenticular clouds, parallel to each other and to the ridge, may be seen; the suggestion that they constitute visible signs of systems of atmospheric lee waves is very strong. Over irregular hilly terrain, the lenticulars too are irregularly distributed; such skies are frequent in Scotland and many examples are to be found in the Clarke collection of cloud photographs.

A similar phenomenon which can sometimes be observed occurs when an airstream containing a layer of stratocumulus crosses a mountainous area. Organised stationary clearances of the cloud in the form of holes or parallel zones to the lee of hills or ridges can be seen. The inference is that the clearances are located where the airstream executes downward undulations associated with the topography.

A number of field studies have been carried out aimed at elucidating the mechanism of formation of particular cloud formations which are characteristic of given hills or mountains. Amongst these are Manley's exhaustive study (2) of the Crossfell Helm wind, and its associated clouds, and Küttner's study (3) of the so-called Moazagotl clouds which form over the Reisengebirge in the Alps. Although on a different scale, both these phenomena have much in common and in particular at both locations rotor clouds are commonly observed at levels similar to those of the hilltops, whilst lenticular clouds may also be seen high above the rotors.

/Recently

Recently Ludlam (4) has discussed the formation of orographic cirrus over the hills of U.K. and has put forward evidence which strongly supports his suggestion that a great deal of cirrus forms in atmospheric waves initiated by topographical features. He is satisfied from his observations that hills in U.K. can produce waves having sufficient amplitude at 20,000 feet or more to produce cirrus cloud. This comes as no surprise to those who have accepted that 'mother of pearl' clouds seen high above the Norwegian mountains at 70,000-80,000 feet and described by Störmer (5) also owe their origin to topography. 'Mother of pearl' clouds have been observed in other parts of the world besides Norway, even it seems over Scotland on rare occasions.

(b) The Experiences of Glider Pilots

In the early days of gliding, the sources of vertical motion made use of were first the upslope motion to be found on the windward side of hills and ridges and later thermal up-currents. During the 1930's, the possibilities of soaring in atmospheric waves began to be exploited, especially on the continent. Numerous ascents were made on the North side of the Alps in Föhn wind conditions and by 1939 several glider ascents to beyond 30,000 feet had been made in the air rising on the upwind side of wave clouds. The significant aspect was that many of these ascents were made well to the lee of the highest ground and could not, therefore, have been simple cases of flights in the airstream ascending the windward slopes. The first important ascent by a glider in a standing wave in U.K. was made in 1939 by McLean who reached 11,000 feet on the Helm phenomenon. On this first occasion, McLean had difficulty in getting down and was only able to do so by locating the downdraught of the wave. The occurrence was described graphically by Horsley (6).

Since the war, wave soaring has become commonplace and the various Gliding journals literally abound with articles by glider pilots describing experiences in standing waves. Some of these accounts are merely descriptive but many others are based on careful and detailed observation. The sinking speed of a glider for a given forward speed is a quantity which is known fairly exactly, especially if the machine has been calibrated, and therefore gliders are able to explore waves and determine the vertical component of the wind. It is by such means that a fairly complete picture of the characteristics of standing lee waves has emerged.

From large numbers of reports of this sort has grown the conception of standing waves as vertical undulations in the airstream to the lee of hills and ridges. It is found that over the lee ground, waves, if any, increase in amplitude upwards to some level above which the waves decrease and eventually die out. They die away downstream but a succession of several observable waves has often been noted in U.K. The order of magnitude of the wavelength is usually in the range 1 to 10 miles, but wavelengths up to 20 miles or so are sometimes observed.

We can scarcely leave this reference to gliders without mentioning the spectacular 'Bishop' wave which is characteristic of the airstream over the Sierra Nevada range in California during winter time. Many ascents to well above 40,000 feet have been made by gliders in this wave system and there seems no reason why a pressurised glider, which is planned, should not reach far greater heights. If the wave develops at all, vertical components of 2,000 ft./min. are common, whilst 4,000 ft./min. has been recorded and it is believed that components up to 5,000 ft./min. may occur on occasions. The field

/work

work for the U.S. Mountain Wave Project was carried out at this location, but reports published so far have been confined to descriptions of the organisation of the project and of the techniques used for tracking gliders, etc. A reasoned discussion of the results obtained has yet to appear.

(c) Effects Observed from Powered Aircraft

During the last 3-4 years there has been a steadily increasing number of reports of mountain airflow effects from the pilots of powered aircraft. This may be because aircraft are now flying over mountain ranges which lie across air routes, with increasing regularity and frequency. The reports confirm that areas of lift and sink are commonly to be found over and to the lee of mountains. To date most of these reports have been made by pilots who have for some reason a special interest in the subject as, for example, because they are also glider pilots, or because a specific experience was sufficiently notable to arouse a special interest. Mild standing lee waves may easily pass unnoticed in a powered aircraft because they are not necessarily accompanied by any turbulence effects and in fact many reports mention the remarkably smooth flying conditions in waves. In addition, a pilot ignorant of wave effects might well ascribe gentle height fluctuations, having a period of a minute or two, to oscillations of the aircraft due to instability of trim or to the movement of passengers about the cabin.

Austin and Turner have reported in references (7), (8), (9) cases of standing waves encountered by pilots. Furthermore, the Aviation journals contain several contributions by pilots describing their experiences. One pilot, Capt. Neilan of Skyways, whose work amongst other things involves the flight testing of aircraft over Scotland, has reported details of several experiences in standing waves. On many occasions Capt. Neilan has encountered alternate areas of up and down currents exceeding 1,000 ft./min.; such currents force themselves upon his attention because they are a hindrance to flight testing.

Capt. Mason of B.E.A. in an article in Shell Aviation News (10) gave a detailed description of an incident over the mountains of Northern Spain on 18th December 1952, when he was flying a Viking aircraft from Madrid to London. He approached the mountains north of Madrid at 11,000 feet and the aircraft subsequently fell to 8,800 feet and then rose to 14,000 feet. This was repeated three times in what were undoubtedly powerful standing waves. The height changes took place in spite of his using maximum power in the areas of sink and almost closing the throttles in the areas of rising air. It can be inferred from this that the vertical components exceeded 2,500 ft./min.

Some fifty or so reports of mountain airflow effects have now been collected at Northolt from British European Airways pilots and a record of these has been assembled by Turner in an unpublished report. Three cases from this record are now quoted by way of example.

(i) 18th December 1952
2000 G.M.T.

Mean flying height 8,500 feet. Location: midway between Nice and Montelimar. After slight vertical motion two powerful waves were encountered giving lift of 1,000 ft. per minute with aircraft in descending attitude and sink of 1,000 ft. per minute with full climbing power on. Wave crests about 8 minutes apart. Wind 340 deg. 30 kt. Sky cloudless.

/(ii)

(ii) 21st March 1952
1210-1310 G.M.T.

Mean flying height 10,500 feet. Location: Maritime Alps into Rhone Valley. Successive up and down draughts of 1,500 feet per minute resulting in 2,000 feet displacement of aircraft. There were 3/8 Cu below aircraft, otherwise no cloud. Wind NW. 40 kt.

(iii) 11th March 1953
1030 G.M.T.

Mean flying height 5,500 feet. Location: Barrow-in-Furness to Solway. Smooth waves encountered giving up and down currents of 700 feet per minute. Pilot made no attempt to counteract vertical motion, and therefore there were only small fluctuations of airspeed. About six separate waves were distinguished but beyond Solway the waves became negligible. Cloud: 6/8 Sc below aircraft and 7/8 Ac above. Wind 350 deg. 35-40 kt.

One feature worth noting is that in many cases the pilot records a marked drop in airspeed on entering an area of sink and an increase in airspeed in the areas of lift. This, of course, would be expected if the pilot uses his controls in an attempt to maintain constant height, but it is a little unexpected to find similar (although smaller) variations of airspeed when no such correcting action is taken. This aspect has been discussed from the aerodynamical standpoint by Yates (11).

Turner examined the distribution of lapse-rate and wind in the vertical in the cases reported at Northolt, with a view to ascertaining whether the airstreams possessed any special characteristics common to all cases. His conclusions were used to carry out a forecasting test which was reported in M.R.P. 815. Briefly, he found that when pilots noted special airflow effects over hilly terrain, there was always a markedly stable layer (commonly at least isothermal) at middle levels, with usually a layer of steep lapse rate below. The type of effect depended upon the wind shear. When standing waves were found, the vertical wind shear was in the direction of the general wind (i.e. the wind increased with height). In the cases of marked turbulence the vertical wind shear was opposed to the general wind, i.e. there was reversed wind shear. In some intermediate cases both turbulence and standing waves, sometimes at different levels, occurred. It cannot be held, of course, that this kind of empirical approach yields conclusive evidence of necessary conditions for given effects, but it is interesting to note that although based on few observations Turner's conclusions are broadly consistent with some of the results obtained by Scorer and Förchtgott and described later in this report. With regard to the lower layer of steep lapse rate, found by Turner, one might expect this to be a normal attribute of a fast-moving airstream over rough hilly terrain. However, he found the layer to be at least 5,000 feet thick and it may, therefore, have real significance; in addition, there are other grounds against thinking this factor to be merely incidental and some notes by Corby on this point were added to M.R.P. 815. Turner's views developed from his own personal enquiries of pilots in the course of aviation forecasting, and his results showed that useful information may be obtained in this way. In the hope of securing further information more suitable for investigation purposes, arrangements have now been made at Northolt for a regularised scheme of detailed reporting by Northolt-based B.E.A. pilots.

/PART II

PART II - THEORETICAL STUDIES

(Note: For convenience in this section a common notation is used throughout which is not necessarily that of the particular author being quoted. After Queney we shall use $\rightleftharpoons$ to denote "is equal to the real part of".)

(a) General

The problem of the flow of an incompressible, homogeneous and inviscid current over an obstacle at the bottom was first solved by Kelvin in 1886. Lamb extended this work in 1916 to cover the case of a stratified, but still incompressible, fluid. In their solutions a system of stationary gravity waves appears downstream of the obstacle, provided the speed of the flow is less than a critical value depending on the depth of the fluid. These waves are analagous to those which constitute the wash of a ship.

The corresponding atmospheric problem is a great deal more complex. Firstly, apart from shallow adiabatic layers, e.g. near the ground on hot days, the atmosphere has continuous stable stratification. Secondly, the atmosphere, being compressible, has no definite upper boundary; as we shall see later the formulation of a satisfactory upper boundary condition in the atmospheric problem is difficult and has given rise to some controversy. Finally, for phenomena on the scale of, say, the airflow over the Alps, the earth's rotation must be taken into account, whilst on an even larger scale the variation of Coriolis parameter with latitude must be introduced.

So far, all theoretical treatments have made use of the perturbation method since no other mathematical method yet exists which can be applied successfully to this problem. In this method, the motion is considered as a disturbance superimposed on a given basic flow which is assumed to be laminar, frictionless and isentropic in the first instance. The hydro-dynamical equations of motion are set up and are used with the equation of continuity and the equation expressing the isentropic nature of the flow. It is assumed that the disturbance quantities are small compared with the values in the basic motion and this justifies neglect of the squares and products of the disturbance quantities and enables the equations to be linearised. Elimination of all but one of the unknowns yields a partial second order differential equation which is used to determine the nature of the perturbation.

(b) The work of Queney

We shall first consider the work of Queney who commenced studying the subject in 1936. After several contributions he published in 1947 a completely general theory of adiabatic perturbations in a stratified rotating atmosphere (12). The problem of the flow of an airstream over a mountain is a particular application of his generalized theory. Queney found that the degree of stability and the vertical component of the earth's rotation made the important contributions to the terms in the wave equation and he was able to justify neglect of several other terms. The detail of Queney's mathematics is elaborate and lengthy. For brevity in this report and for convenience in comparing subsequently Queney's results with Scorer's we may regard Queney's treatment as equivalent to the derivation of the wave equation represented by:

$$\left(1-\frac{f^2}{k^2U^2}\right)\frac{\partial^2\psi}{\partial z^2}-\left(\frac{g}{c^2}+\beta\right)\frac{\partial\psi}{\partial z}+\left(\frac{g\beta}{U^2}-k^2\right)\psi=0 \quad \ldots(1)$$

/where

where U = horizontal velocity of the undisturbed current (assumed constant and uniform in space)

ψ = stream function of the disturbance

f = 2 x vertical component of the earth's angular velocity

g = acceleration due to gravity

β = coefficient of stability defined as $\frac{1}{\theta}\frac{\partial \theta}{\partial z}$ where θ is potential temperature

K = wave number of the disturbance in the x direction (the direction of U) i.e. a harmonic variation of the disturbance is assumed in the x direction of wavelength $2\pi/K$

c = velocity of sound

z = height measured vertically upwards.

This equation expresses the variation of the disturbance with height assuming that the variation in the horizontal is harmonic. The nature of the source of the perturbation is as yet unspecified. Queney introduces a further simplification by taking the stability as constant with height and is then able to treat the coefficients of Eq.(1) as sensibly constant (for a given value of K) provided the magnitude of the perturbation is not of the order of thousands of km.

$\sqrt{\frac{g\beta}{U}}$ is denoted by l_s and $\frac{f}{U}$ by l_f

and we put $$\mu = +K\sqrt{\frac{l_s^2 - K^2}{l_f^2 - K^2}}$$

The solution of Eq. (1) may then be written

$$\psi = A e^{\lambda_1 z} + B e^{\lambda_2 z}$$

where $$\lambda_1, \lambda_2 = \frac{1}{2}\left\{\frac{K^2(g/c^2+\beta)}{K^2 - l_f^2} \pm \sqrt{\left(\frac{K^2(g/c^2+\beta)}{K^2 - l_f^2}\right)^2 + 4\mu^2}\right\}$$

$$\doteq \frac{1}{2}\left(g/c^2 + \beta\right) \pm \mu$$

if K is not in the vicinity of

l_f or l_s.

/Also

Also if ρ = density, $\left(g/c^2 + \beta\right) = -\frac{1}{\rho}\frac{\partial \rho}{\partial z}$

$= 2S$, say

(Queney calls S the heterogeneity)

Thus the solution may be expressed as

$$\psi = e^{Sz}\left(Ae^{\mu z} + Be^{-\mu z}\right) \text{ - - - - - - (2)}$$

Queney shows that with typical atmospheric values, e^{Sz} is closely equal to $\sqrt{\frac{\rho_0}{\rho}}$.

The vertical displacement of the streamlines from their undisturbed level will then be given by

$$\zeta = \frac{\psi}{U} = \frac{1}{U}\sqrt{\rho_0/\rho}\left(Ae^{\mu z} + Be^{-\mu z}\right) \text{ - - (3)}$$

We have the two cases:

(i) If μ is real, i.e. if $\kappa > \ell_s$ or $\kappa < \ell_f$ we must have A = 0, otherwise the disturbance would increase exponentially upwards indefinitely (clearly an unacceptable solution because such a result is impractical).

(ii) If μ is imaginary, i.e. if $\ell_s > \kappa > \ell_f$ the solution becomes

$$\zeta = \frac{1}{U}\sqrt{\rho_0/\rho}\left(Ae^{i\nu z} + Be^{-i\nu z}\right) \text{ where } \mu = i\nu.$$

This represents sinusoidal variation in the vertical. Relative to the airstream there is a downward progressing wave component $e^{i\nu z}$ and an upward component $e^{-i\nu z}$. Both are indeterminate for $Z = \infty$ and so there is some difficulty about the upper boundary condition. Queney overcomes the difficulty by temporarily introducing small viscosity (an artifice used by Rayleigh and others in problems of fluid motion). He does this by applying a factor $e^{-\epsilon z}$ to the term in $e^{i\nu z}$ and $e^{+\epsilon z}$ to the term in $e^{-i\nu z}$ where ϵ is small and positive. He is then, of course, able to reject the upward progressing wave and takes as his solution for imaginary μ :

$$\zeta = \frac{A}{U}\sqrt{\rho_0/\rho}\, e^{i\nu z}.$$

/The

The second boundary condition at the ground causes no difficulty. If the ground profile is the sinusoidal corrugation represented by the real part of $e^{i\kappa x}$ then we must have $\zeta = e^{i\kappa x}$ for $z = 0$. Thus the appropriate solutions for such a ground profile are:

For $\kappa > \ell_s$ or $\kappa < \ell_f$,

$$\zeta = \sqrt{\ell_0/\ell}\, e^{i\kappa x - \mu z}$$

$$= \sqrt{\ell_0/\ell}\, e^{-\mu z} \cos \kappa x \quad \text{---------- (4)}$$

For $\ell_s > \kappa > \ell_f$,

$$\zeta = \sqrt{\ell_0/\ell}\, e^{i(\kappa x + \nu z)}$$

$$= \sqrt{\ell_0/\ell}\, \cos(\kappa x + \nu z) \quad \text{---------- (5)}$$

Similarly, expressions could be deduced for the horizontal disturbance and the variation of pressure or density. The concept of a sinusoidal ground profile extending to infinity does not in itself provide a solution of direct practical value but it is derived in anticipation of subsequent generalisation by the Fourier integral method. Before doing so it is worth examining the elementary solutions given by (4) and (5) and in Fig. 1 are illustrated the streamlines corresponding to steady flow over an infinite sinusoidal ground profile for the three cases $\kappa > \ell_s$, $\ell_s > \kappa > \ell_f$ and $\kappa < \ell_f$.

For $\kappa > \ell_s$, (Fig. 1a), the order of the wavelength of the ground profile, with typical atmospheric values, is up to about 2π km. We see that on this scale, the solution gives wavy streamlines whose amplitude decreases exponentially upwards. The critical wavelength up to which this solution applies is determined by the value of ℓ_s i.e. by the stability and speed of the airstream. In the atmosphere $\ell_s \gg \ell_f$ and on this scale ℓ_f may be ignored, which is equivalent to saying that geostrophic forces have no opportunity to affect the result. There is thus negligible horizontal deformation in this case. The restoring force which makes the wave motion in the vertical possible arises solely from the stratification of stability, represented by ℓ_s.

/For

For $l_s \geq \kappa > l_f$, (Fig. 1b), the order of the wavelength of the ground profile is in the approximate range 2π to 200π km. On this scale geostrophic forces as well as stability play a part and there is both vertical and horizontal deformation of the streamlines. The vertical deformation is not now subject to an exponential decrease upwards; the amplitude remains nearly constant but there is a retardation of phase with increasing height.

For $\kappa < l_f$, (Fig. 1(c)), the order of the wavelength is $> 200\pi$ km. and the scale is such that geostrophic forces predominate in determining the deformation which is therefore almost entirely horizontal. Queney studied this further and found it necessary to introduce on this scale the latitudinal variation of the Coriolis parameter but he has not published a full acount of this study.

(c) Generalisation of Queney's results

As the differential equation of the wave is linear we are at liberty to superpose solutions to achieve a practical result. For a realistic two-dimensional mountain ridge, Queney used the profile presented by the Fourier integral

$$\zeta = ab\int_0^\infty e^{i\kappa x - \kappa a}\, d\kappa$$

$$= ab\int_0^\infty e^{-\kappa a}\cos \kappa x . d\kappa$$

$$= a^2 b/(a^2+x^2) \quad \text{----------(6)}$$

This is a synthesis of sinusoidal ground corrugations for all values of the wave number κ, with the exponential factor $e^{-\kappa a}$ applied to each of them. The result is a single corrugation of bell-shaped cross-section. We see that its height is b and the half width is a (the half width is the value of x, for which the height is half the maximum). We must ensure that $b \ll a$ otherwise the assumption that the disturbance quantities are small relative to their undisturbed values would be invalidated.

The displacement of the streamlines for flow over the ridge represented by Eq.(6) will be given by

$$\zeta = ab\sqrt{\frac{l_0}{l}}\int_0^\infty e^{i\left(\kappa x + \kappa\sqrt{\frac{l_s^2-\kappa^2}{\kappa^2-l_f^2}}\, z\right) - \kappa a}\, d\kappa \quad \text{----(7)}$$

The problem therefore reduces to the evaluation of this integral for the various cases with which it is desired to deal. The integral cannot be evaluated exactly in the general case but approximate solutions can be obtained. Queney found that the nature of the result depended very much on

/the

the scale of the ground deformation, represented by a , in relation to the critical values $1/l_s$ and $1/l_f$. The most significant of his results can be summarised as follows.

(i) $a \ll 1/l_s$.

This corresponds to the flow over a very small hill of width up to about 100 metres. The effects of stability and the earth's rotation (represented by l_s and l_f in the integral) both prove to be negligible and the streamlines are given by

$$\zeta \simeq ab\sqrt{l_0/l}\int_0^\infty e^{ikx - kz - ka}\,dk$$

$$= ab\sqrt{l_0/l}\,\frac{a+z}{(a+z)^2+x^2} \qquad \text{------(8)}$$

The streamlines are given in Fig. 2 and it is seen that there is a single symmetrical wave over the hill. The displacement decreases both vertically and horizontally away from the hill and there is no train of lee waves.

(ii) $1/l_s \ll a \ll 1/l_f$

In this case the width of the ground obstruction is of the order of a few km. Queney found that on this scale the effect of the earth's rotation was still negligible but that the stability became important. The form of the integral applicable in this case is

$$\zeta \simeq ab\sqrt{l_0/l}\int_0^\infty e^{ikx + il_s z - ka}\,dk$$

$$= ab\sqrt{l_0/l}\,\frac{a\cos l_s z - x\sin l_s z}{a^2+x^2} \qquad \text{----(9)}$$

The streamlines are illustrated in Fig. 3. There is a single wave above the hill having sinusoidal variation in the vertical, but no lee wave train. The important characteristic is that with the entry of stability into the result (represented by l_s) the airstream is disturbed throughout its depth as distinct from the last case in which the disturbance decreased rapidly upwards. Geostrophic forces play no part and, accordingly, there is no horizontal deformation of the streamlines.

/(iii)

(iii) $1/\ell_s \ll a \doteqdot 1/\ell_f$

This is the case of a still broader ground obstruction whose width is of the order of 100 km. Both stability and geostrophic forces are significant on this scale and we have

$$\zeta \doteqdot ab\sqrt{\ell_0/\ell}\int_0^\infty e^{i\left(\kappa x + \kappa\sqrt{\frac{\ell_s^2-\kappa^2}{\kappa^2-\ell_f^2}}\,z\right)-\kappa a}\,d\kappa \quad \cdots (10).$$

After a transformation of co-ordinates Queney derived an approximate value for this integral in terms of Bessel functions and the associated Struve functions. His streamlines for this case are given in Fig. 4. There is a lee wave system with horizontal as well as vertical displacement of the streamlines. The horizontal disturbance is much larger than that in the vertical and the horizontal wavelength is of the order of several hundred km. (actually the horizontal wave length tends to $2\pi/\ell_f$ for large x .) As regards the vertical deformation of the streamlines, there is a retardation of phase with height, the vertical wavelength being $2\pi/\ell_s$, i.e. dependent on stability. The lee waves increase in amplitude upwards and persist further downstream with greater height. In many respects, therefore, these "Queney" waves are unlike those responsible for ordinary lenticular clouds and exploited by glider pilots. We shall return to this later.

(iv) Queney also studied the case of a westerly airstream blowing across a very broad mountain range having a width of the order of 1000 km. i.e. the case of $a \gg 1/\ell_f$. On this scale the variation of Coriolis parameter with latitude also figures in the result and a system of stationary lee waves, mainly horizontal, was obtained, the wavelength being several thousand km. These waves have the nature of stationary Rossby waves and although of great interest from the synoptic viewpoint need not be discussed further in this report.

(d) The work of Lyra

This author published theoretical studies in 1940 and 1943 which at that time appeared highly significant and suggestive (13), (14). Lyra, too, employed the perturbation method but for the profile of his mountain ridge he used a narrow rectangular section developed from the Fourier integral $\int_0^\infty \cos \kappa x \, d\kappa$; the resulting profile has steep vertical sides. In his solutions he obtained a type of lee wave system in which the waves increase in amplitude with height and decrease downstream. Queney (and Scorer) used the mountain profile $z = a^2 b/(a^2+x^2)$ which with $b \ll a$ has a smooth shallow section with gently sloping and symmetrical sides. It is clear from the work of both latter writers that Lyra's waves are dependent upon the steepness of the mountain slopes in the profile used by him and that they disappear when a smooth mountain replaces the rectangular one. Furthermore, it is unrealistic to adopt a rectangular mountain section as a model for study whilst at the same time assuming laminar flow. Thus although of considerable importance when published, Lyra's theory is largely superseded by the work of Queney and Scorer and will not be discussed further here.

/(e)

(e) The work of Scorer

Scorer recognised the inadequacies of the solutions obtained by Queney and Lyra. In both, the waves are almost negligible at low levels and die away rapidly downstream. In addition, Lyra's waves are somewhat artificial in that they depend on the choice of an unrealistic ground profile, whilst Queney's waves given in Fig. 4 are of very long wavelength and are mainly a horizontal oscillation about the geostrophic wind. Scorer realised that the observational evidence of mountain wave clouds and the experiences of glider pilots etc. suggested lee waves of a different character, viz. waves which increased in amplitude upwards to some level and then decreased to die away at great height, which had a wave length of a few km. and which in the absence of friction would continue indefinitely downstream over level ground to the lee of the obstacle.

Scorer (15), (16) considered frictionless, steady, laminar and isentropic flow but set out to provide for variations of lapse rate and wind shear in the vertical. He derives a second order partial differential equation for the stream function of the disturbance and simplifies this on similar grounds to Queney. The earth's rotation is then neglected, as his subsequent study relates to small wavelengths (up to 50 km. say). The simplified equation is:

$$\frac{\partial^2\psi}{\partial z^2} - \left(\frac{g}{c^2} + \beta\right)\frac{\partial\psi}{\partial z} + \left(\frac{g\beta}{U^2} - \frac{1}{U}\frac{\partial^2 U}{\partial z^2} - \kappa^2\right)\psi = 0 \quad \text{--- (11)}$$

The notation is as used for Eq. (1) applicable to Queney's work and we see, in fact, that the equation is the same except that the earth's rotation term in f does not appear, owing to the smaller scale of the problem to be studied, and there is the additional term in $\partial^2 U/\partial z^2$ representing the vertical rate of change of shear (U now varies with z).

Scorer neglects the second term in $\partial\psi/\partial z$ on the grounds that its effect is small and quantitative only. In the expressions for the displacement of the streamlines subsequently obtained, the result of this approximation is that the factor $\sqrt{\rho_0/\rho}$ which figures in Queney's results does not appear. The simplified equation used is thus

$$\frac{\partial^2\psi}{\partial z^2} + \left(\ell^2 - \kappa^2\right)\psi = 0 \quad \text{- - - - - - - - - - - - (12)}$$

where $$\ell^2 = \frac{g\beta}{U^2} - \frac{1}{U}\frac{\partial^2 U}{\partial z^2}$$

Considering first an airstream in which ℓ^2 is constant, we may use solutions of (12) for constant coefficients. The restriction ℓ^2 = constant does not imply the uniform airstream considered by Queney and Lyra since both β and U can vary with height within this limitation. The vertical displacement will be given by

$$\zeta = \frac{\psi}{U} = \frac{1}{U}\left(Ae^{\mu z} + Be^{-\mu z}\right) \text{ ------ (13)}$$

where $\mu = +\sqrt{k^2 - l^2}$

Once again we have the two cases

(i) If μ is real, i.e. if $k > l$, we must have A = 0 otherwise the disturbance increases indefinitely upwards.

(ii) If μ is imaginary, i.e. if $k < l$ then

$$\zeta = \frac{1}{U}\left(Ae^{i\nu z} + Be^{-i\nu z}\right)$$

where $\nu = +\sqrt{l^2 - k^2}$

We have again the difficulty that both components $e^{i\nu z}$ and $e^{-i\nu z}$ are indeterminate as $z \to \infty$. Scorer does not accept the application of the Rayleigh method of limits in this case and rejects Queney's (and Lyra's) choice of the downward component $e^{i\nu z}$. He argues instead that since the source of disturbance in the present context is at the ground, and there is no relevant energy source at high levels, the only realistic choice is the upward progressing wave. He therefore uses the solution:

$$\zeta = \frac{B}{U} e^{-i\nu z}$$

For an infinite sinusoidal ground profile of wavelength $2\pi/k$, the streamlines of Scorer's elementary solutions are thus:

(i) $k > l$:

$$\zeta = \frac{U_0}{U_z} e^{ikx - \mu z}$$

$$= \frac{U_0}{U_z} e^{-\mu z} \cos kx$$

where $\mu = +\sqrt{k^2 - l^2}$

(ii) $k < l$:

$$\zeta = \frac{U_0}{U_z} e^{i(kx - \nu z)}$$

$$= \frac{U_0}{U_z} \cos(kx - \nu z)$$

where $\nu = +\sqrt{l^2 - k^2}$

These solutions are similar to those of Queney illustrated in Figs. 1(a) and (b) except that there is no horizontal deformation (the effect of the earth's rotation being neglected) and in the case of imaginary μ Scorer adopts the wave progressing upwards relative to the moving airstream (i.e. the loci of the crests slope forward instead of backward).

(f) Generalisation of Scorer's Results

Scorer uses the ground profile represented by the Fourier integral

$$\zeta = ab\int_0^\infty e^{ikx - ka}\,dk = a^2b/(a^2+x^2)$$

For an airstream in which l^2 is constant, the streamlines for the perpendicular flow across this ridge are given by

$$\zeta = \frac{U_0}{U_z}\,ab\int_0^\infty e^{ikx - \mu z - ka}\,dk \qquad \text{------(14)}$$

If $l = 0$, the integral can readily be evaluated to obtain

$$\zeta = \frac{ab(a+z)}{(a+z)^2 + x^2} \qquad \text{- - - - - - (15)}$$

This solution applies to an airstream having neither static stability nor shear (i.e. $\beta = 0$, U = constant) for this would be a particular case of $l = 0$. The flow is seen to be similar to that obtained by Queney for a very small obstacle and illustrated in Fig. 2. We have therefore the interesting result that the flow over a very small hillock or obstacle (up to about 100 m. in width) is dynamically similar to that of an airstream with no stability in the full scale mountain problem. As we shall see later this is the only case in which wind tunnel experiments might be carried out easily and with a good prospect of success. Scorer describes this type of flow as "aerodynamic" since gravity, stability and the earth's rotation play no part.

In order to emphasise the very important role played by stability, Scorer contrasts "aerodynamic" flow with the results obtained for an airstream with constant stability (or more precisely with constant l). The approximate value obtained for the integral of Eq. (14) becomes

$$\zeta = \frac{U_0}{U_z}\,ab\,\frac{a\cos lz + x\sin lz}{(a^2+x^2)} \qquad \text{- - - - (16)}$$

/This

This is the same as Queney's solution for $1/\ell_s \ll a \ll 1/\ell_f$ except that the sign before the term $x \sin \ell z$ is reversed. This reversal occurs because of the different interpretation of the upper boundary condition; the streamlines have the same shape but their direction is reversed. However, as stated before, the important thing to note is that with the introduction of stability there is a complete change in the flow - the airstream is now disturbed throughout its whole depth. Scorer calls this "barostromatic" flow because of the vital part played by stability, i.e. by the stratification of potential density. It is to be noted that so far no trains of lee waves have appeared in these solutions of Scorer's, and this is now examined further.

The vertical velocity $w = \frac{\partial \psi}{\partial x} = ik\psi$, and thus we may write the wave Eq. (12) as follows

$$\frac{\partial^2 w}{\partial z^2} + (\ell^2 - k^2) w = 0 \quad \text{- - - - - - - - (17)}$$

Considering the application of this equation to flow over level ground to the lee of an obstacle, we require that $w = 0$ at the ground and $w \longrightarrow 0$ as $z \rightarrow \infty$. It is clear that if these boundary conditions are imposed with constant ℓ, w will be everywhere zero and therefore we can have no lee waves with such an airstream. For realistic lee waves we must have w finite at some level(s) and also zero at $z = 0$ and tending to zero as z becomes very large. Thus $\frac{\partial^2 w}{\partial z^2}$ must change sign at least once; in fact it can be inferred that we must have ℓ^2 less in some fairly deep upper layer than in a layer below. This notion led Scorer to introduce, for purposes of theoretical study, the concept of an interface in the airstream, dividing it into two layers in each of which ℓ^2 has a constant but different value. There is then a different solution of the wave equation for each layer, corresponding to the two different values of ℓ^2, and accordingly four arbitrary constants. For the four boundary conditions required we have those at the ground and at infinite height, whilst continuity considerations at the interface supply the remainder.

If for such an airstream suffixes 1 and 2 refer to the lower and upper layers respectively and for convenience we take the interface at $z = 0$ and the ground at $z = -h$, then the vertical displacement will be given by

Upper layer: $(z > 0)$

$$\zeta_2(z) = \frac{A}{U_z} e^{-\mu_2 z} \quad \text{- - - - - - - (18)}$$

Lower layer: $(0 > z > -h)$

$$\zeta_1(z) = \frac{A}{U_z}\left(\cosh \mu_1 z - \frac{\mu_2}{\mu_1} \sinh \mu_1 z\right) \text{- - (19)}$$

/Here

Here the boundary conditions at the interface and at infinite height have already been introduced whilst A awaits the ground boundary condition. For the flow over level ground to the lee of the (so far) unspecified disturbance of wave number K, waves may only occur if $Z_1(-h) = 0$, i.e. if

$$\mu_1 \cosh \mu_1 h + \mu_2 \sinh \mu_1 h = 0 \quad \text{-----(20)}$$

As $\mu_1 = \sqrt{K^2 - l_1^2}$ and $\mu_2 = \sqrt{K^2 - l_2^2}$, Scorer regards Eq. (20) as an equation in K determining the wave number of those waves which could persist in the airstream over level ground when once initiated by a disturbance upwind. He shows that Eq.(20) only has solutions if $l_1^2 - l_2^2 > \pi^2/4h^2$ and in that event there may be more than one value of K. However, it is also shown that the lee waves corresponding to the smallest root, denoted by K_0, will be amplified to a much greater extent than the others which in practice may be ignored.

Allocating the value of A for flow over the sinusoidal ground profile e^{iKx} (real part) the streamlines in the lower layer become

$$Z(z) = \frac{e^{iKx} f_z(K)}{f_{-h}(K)}$$

where $$f_z(K) = \frac{1}{U_z}\left(\cosh \mu_1 z - \frac{\mu_2}{\mu_1} \sinh \mu_1 z\right)$$

Generalising, we have that the streamlines for the flow over the ridge represented by

$$Z(-h) = ab \int_0^{\infty} e^{ikx - ka}\, dk = a^2 b/(a^2 + x^2)$$

will be given by

$$Z(z) = ab \int_0^{\infty} \frac{f_z(K)}{f_{-h}(K)} e^{ikx - ka}\, dk$$

/This

This may be evaluated by contour integration but as $f_{-h}(K_0) = 0$, the integrand is infinite for $K = K_0$. Scorer invokes the stationary phase principle to overcome this difficulty and derives as a close approximation for the streamlines in the lower layer:

$$\zeta(z) \rightleftharpoons ab\frac{f_2(0)}{f_{-h}(0)}\frac{(a+ix)}{(a^2+x^2)} + 2i\pi ab\frac{f_2(K_0)}{\frac{\partial f_{-h}(K_0)}{\partial K_0}} \quad \text{for } x>0 \quad \text{--(21)}$$

$$\zeta(z) \rightleftharpoons ab\frac{f_2(0)}{f_{-h}(0)}\frac{(a+ix)}{(a^2+x^2)} \quad \text{for } x<0 \quad \text{----------(22)}$$

In the upper layer the lee waves, represented by the second term in the expression for $x>0$, die away exponentially being proportional to $e^{-\mu_2 z}$

Scorer has exploited this result for a simple two-layer model to calculate the streamlines in selected cases. One of his examples is reproduced at Fig. 5. Since $l^2 = g\beta/U^2 - \frac{1}{U}\frac{\partial^2 U}{\partial z^2}$, there is considerable latitude in the choice of the wind and temperature profiles whilst still ensuring that l^2 is constant within each of the two layers. In fact in the example illustrated, there are effectively three layers but the value of l^2 in two of them is the same. The characteristics of the wind and temperature profiles used by Scorer for this example are shown on the left of Fig. 5; they are similar to those commonly found in nature when waves are observed, viz. marked forward wind shear through a stable layer at fairly low levels. The lee waves predicted by the theory also accord well with what is commonly observed. By avoiding the artificiality of the uniform airstream case studied by Lyra and Queney, and dealing with more realistic model airstreams, Scorer has revealed the significance of variations of lapse rate and wind speed in the development of lee waves.

Multilayer models, with several different values of l^2 could in theory be set up and examined in similar fashion. However, the mathematics would become inordinately complex and no new general principle could emerge. In practice where l^2 may vary continuously it would remain true that for lee waves to occur l^2 must assume lower values through some fairly deep upper layer than in some layer below (but see qualifying comments below re inversions).

We have led up to this result in some detail because it is of fundamental importance and it seems likely that it may prove useful for practical forecasting. Scorer has, however, deduced a number of other conclusions which it is now proposed to summarise without giving the derivation in full detail.

Two-Layer Models

(i) In the case of the simple two-layer model, Eq. (20), which determines the wavelength, only has solutions if $l_1^2 - l_2^2 > \pi^2/4h^2$. Thus the magnitude of the decrease in l^2 must exceed a limit depending on the depth of the lower layer.

If $l_1^2 - l_2^2 > \frac{9\pi^2}{4h^2}$ there will be one nodal surface within the lower layer, where the wave has zero amplitude and the phases above and below are opposite.

If $l_1^2 - l_2^2 > 25\pi^2/4h^2$ there will be two nodal surfaces, etc.

(ii) Distinguishing for a moment between the disturbance over the hill itself (the so-called hill-lift) and the lee wave train, if any, the hill-lift disturbance will be greater and will extend to greater heights if l^2 decreases upwards i.e. the condition for a large disturbance over the hill itself is the same as for lee waves.

(iii) We have noted that the amplitude of the lee waves increases upwards to some level above which it decreases to die out in the upper levels. For a given simple two-layer model the level of maximum amplitude can be obtained from Eq. (21) but in the general case we may say that the maximum amplitude will occur roughly where l^2 is greatest.

Adiabatic Layers

(iv) In the atmosphere adiabatic layers in the lower levels are common. In such layers $l^2 = 0$ (neglecting shear) and it might appear that Scorer's condition for lee waves could not be satisfied. However, the condition for lee waves is that l^2 should be greater in some lower layer than in the layers above; the largest values of l^2 do not necessarily have to occur in the surface layer. Scorer has studied this further and finds that waves are still possible with an adiabatic ground layer, provided his criterion is satisfied above, but the magnitude of the disturbance aloft will then be less than with stable stratification down to the surface. He has in fact published the streamlines calculated for a three-layer model in which the bottom layer is adiabatic (Fig. 7 in ref. (16)) and obtained lee waves in such a case.

(v) If there is an adiabatic layer (or more generally a layer in which $l^2 = 0$) in middle levels, and one starts from the assumption that steady laminar flow with lee waves is possible, it is found that the boundary conditions at the top and bottom of the adiabatic layer are related. Since these conditions are necessarily independent it is concluded that the kind of flow assumed cannot occur, i.e. that steady laminar flow over a mountain must break down if there is an adiabatic layer in middle levels. Perturbation theory cannot assist in determining the type of flow in such a case.

/Inversions

Inversions

(vi) The development of stationary lee waves on flowing water is closely connected with the large density discontinuity at the surface. Several writers, notably Küttner, have recognised that an inversion in the atmosphere might possibly act in the same way and thus have a bearing on the occurrence of atmospheric lee waves. However, the work of Queney and Scorer indicates that one need not introduce an inversion in the model airstream considered in order to obtain lee waves. Scorer, in fact, has been at great pains to emphasise in many papers that an inversion is not a dynamical requirement for lee waves. It is true that an inversion is commonly found in airstreams in which waves are observed, but as has been pointed out an inversion would commonly be associated with a distribution of humidity favouring wave clouds, i.e. conditions in which any waves become visibly revealed. Scorer has now agreed, however, (Weather, July 1953) that although not a dynamical necessity for waves, an inversion could make them possible when his criterion regarding the variation of l^2 with height did not appear to be otherwise fulfilled. An ideal inversion would be a layer of no depth and infinite l^2, but in practice we can regard an inversion as a very shallow layer through which the value of l^2 is very large. The occurrence of waves in airstreams containing inversions is therefore quite consistent with the general criteria regarding the variation of l^2 with height. However, further theoretical study of the role played by inversions (and by shallow but very stable layers) would probably be profitable.

Diurnal Variation

(vii) In the lower layers of the atmosphere, the lapse rate, wind speed and wind shear (and therefore the value of l^2) are subject to large diurnal variations especially near sunrise and sunset.

Generally speaking the net result is a reduction in the value of l^2 after sunrise and an increase around dusk. In theory this would mean an increase after sunrise in the wavelength of any waves until perhaps the waves ceased owing to infringement of the condition $l_1^2 - l_2^2 > \pi^2/4h^2$, whilst around dusk the waves might reform if and when the condition was again satisfied. Both these effects have been observed and reported by other writers (2), (17). It is appropriate to mention here that on similar grounds, one would expect a greater frequency of wave effects in winter than in summer; this too is in accord with observation.

Oblique Flow and other Mountain Shapes

(viii) So far discussion has been limited to the airflow perpendicularly across an infinite symmetrical ridge. This lends itself to theoretical study because the problem is then essentially only two-dimensional. In theory one can deal with more complicated two-dimensional profiles by superposing the solutions for different ridges. In this way the streamlines for the flow across an asymmetrical ridge and various plateaux have been obtained.

For oblique flow across a ridge, the component along the ridge remains undisturbed whilst the component across the ridge is disturbed as in the case of perpendicular flow. Scorer has shown (16) that if

/the

the undisturbed stream contains a component of shear parallel to the ridge, the total shear in the disturbed stream may assume almost any direction. This conclusion has a bearing on the formation of billow clouds and also may be significant in connection with the navigation of aircraft over mountain ranges.

Theoretical study of the flow over an isolated hill (as distinct from an infinite ridge) is complicated since the problem becomes fully three-dimensional. One can exploit the result for oblique flow over a ridge, by synthesising the flow patterns for an infinity of ridges whose axes are inclined in all horizontal directions through a point. In this way Scorer was able to obtain the distribution of vertical displacement for the flow over a single hill (18) and his results are consistent with the bow-shaped orographic cloud which has been observed in such a case and discussed by Abe (1). As regards the development of waves to the lee of a single hill, the general conclusions are that any waves will be of smaller amplitude than those to the lee of an infinite ridge of similar section and that the waves will decrease in amplitude rapidly downstream. This is in contrast to the infinite ridge case when the lee waves (in the absence of viscosity) persist indefinitely downstream. For a ridge of finite length lying across the airstream the results are intermediate, viz. the persistence of any lee waves downstream is greater the greater the length of the ridge.

A Layer of Calm Air

(ix) If an airstream has a layer of calm air between some levels the difficulties about the flow at great heights, and in particular about the boundary condition at infinite height, disappear. Scorer studied such a case and found that lee waves, confined to the airstream below the calm layer, were possible provided certain conditions were satisfied. This case appeared to be of academic interest only, but recently a case of lee waves has been reported (19) in circumstances which were possibly of this type.

(g) The Validity and Limitations of the Results of Perturbation Theory

In order to assess the practical value of the theoretical results deduced from the applications of the perturbation method, it is necessary to review the initial assumptions. The main assumptions involved are commented on below.

(i) Viscosity. The effect of the assumption of frictionless flow was examined by Queney, who concluded that viscosity would merely exert a damping effect on the disturbances. The damping effect would be small and would not alter the results qualitatively.

(ii) Isentropic Flow. The assumption that the potential temperature is constant along the streamlines involves neglect of radiation and condensation effects. Radiative effects would in general be too slow to affect the results on the scale considered by Scorer, but on the synoptic scale (e.g. for the long waves of the stationary Rossby type) they would probably be important. However, the latter question has not been fully studied and is irrelevant in the present report.

As regards condensation, the results could easily be applied to a completely cloudy airstream by using wet bulb potential temperature in the coefficient of stability β. One could similarly allow for an 8/8 layer of cloud but not readily for broken clouds. In the case of an airstream containing, say, well broken cumulus, most of the atmosphere (i.e. that between the clouds) would be stably

/stratified

stratified and the conclusions from perturbation theory would be closely applicable. This means that convection is not necessarily inconsistent with the simultaneous occurrence of orographic waves, although it must at least complicate the flow to some extent by mutilating the laminar flow.

(iii) Steady Laminar Flow. The restriction to steady laminar flow is serious because there is ample evidence that the flow over mountains is commonly otherwise. No mathematical treatment of unsteady or non-laminar flow has yet been put forward and it is unlikely that much progress could be made by such a theoretical study until some completely new and superior mathematical approach is forthcoming. In the meantime, we must be content with what has been learnt of the flow in such cases from observational evidence. Here the work of Förchtgott, although in many respects inconclusive, is valuable and illuminating and it is probable that extended field studies on similar lines would be profitable. (Förchtgott's work is discussed in Part IV of this report.)

(iv) Displacements Small. The displacements, and indeed all the disturbance quantities, are taken to be small compared with the corresponding undisturbed values. This enables the equations to be linearised since the products and squares of the disturbance quantities are then justifiably neglected. The condition is satisfactorily fulfilled if the height of the mountain is small compared with its width. It is reasonable to accept the results as qualitatively correct (and very nearly quantitatively also) provided the mountain height is no more than about 10% of the width, although Queney claims rough validity if the ratio "height to width" is up to 1/4 or even 1/2 in special cases. We must bear in mind, however, that with increasing steepness of the mountain ridge, separation of the flow from the surface becomes increasingly probable. This would be manifest in the form of lee eddies or some other form of motion and would constitute, in effect, violation of the assumption of laminar flow.

(v) The Earth's Rotation. For Queney's waves, the earth's rotation provides one of the essential restoring forces, the scale of the phenomena considered being large enough for this to be possible. For Scorer's lee waves, the scale is too small for the earth's rotation to have any significant effect since he confines his study to cases when the mountain ridge and the régime considered are traversed by the airstream in an hour or two at the most. With this restriction, neglect of the earth's rotation in Scorer's examples is quite justified, but his results would not be applicable to large scale phenomena.

PART III - MODEL EXPERIMENTS

The hope that model experiments could be used to advance our understanding of the difficult problem of mountain airflow has been cherished by many writers on the subject in the past and a number of attempts has been made to exploit model techniques. These attempts have met with little or only partial success. In some cases no consideration at all was given to the need for achieving dynamical similarity between the model and the full scale problem, whilst in other cases the only precaution taken was to obtain a reasonable Reynolds number in the model on the assumption that molecular viscosity in the model would correspond to eddy viscosity on the full scale. In defence of these past attempts, however, it must be mentioned that the

/theoretical

theoretical studies described in the last section were not available at the time most of the model experiments were carried out; furthermore no general study of the conditions for dynamical similarity of atmospheric motions, such as that published recently by Batchelor (30), had then been made. It is probable therefore that the very great importance of, and the criteria for, dynamical similarity were not appreciated by model experimenters in the past.

The differential equation used by Scorer to determine the wave motion, in cases when the scale of the problem permits the earth's rotation to be neglected, is:

$$\frac{\partial^2\psi}{\partial z^2} + \left(\frac{g\beta}{U^2} - \frac{1}{U}\frac{\partial^2 U}{\partial z^2} - K^2\right)\psi = 0$$

(Part II, Eq. (12), notation as before).

Here $g\beta/U^2$ represents the effect of stability or the stratification of potential density and $\frac{1}{U}\frac{\partial^2 U}{\partial z^2}$ represents the effect of the vertical rate of change of shear. K is the wave number having the units $(\text{length})^{-1}$, and figures instead of a representative length. Scorer argues that if a model experiment is to reveal accurately the motion in the full scale problem, the conditions in the model experiment must be so arranged that the relationship between the terms of the equation is the same both for model and full scale. That is, the non-dimensional number:

$$S = \frac{1}{K^2}\left(\frac{g\beta}{U^2} - \frac{1}{U}\frac{\partial^2 U}{\partial z^2}\right) \qquad (23)$$

must have the same value on both scales. We must bear in mind, however, that Eq. (12) is not exact, several assumptions and approximations being involved in its derivation. It is not, therefore, immediately apparent that the conditions for dynamical similarity can be deduced in such a manner from the approximate wave equation. The conditions so obtained depend on the assumptions and approximations being justified on the model, as well as on the full scale, and a separate examination of the relative magnitude of the terms of the full equation as applicable to the model problem would seem to be first necessary. Alternatively, one could avoid this difficulty by deducing the conditions from the basic equations or motion, i.e. before linearization and approximation. For inviscid, isentropic flow, such that Coriolis forces can be neglected, Batchelor (30) deduced in this way the criteria to be equality of the non-dimensional numbers:

$$\frac{gL}{U^2}, \quad \frac{p}{\rho U^2}, \text{ and } \gamma$$

where L is a representative length (equivalent to $1/K$ in Eq. (23)). He found also that if the flow field is assumed to be such that the departures of pressure and density from values in an equivalent isentropic atmosphere are small and that the vertical scale of the motion is small, the second and third non-dimensional numbers disappeared from the dimensionless

/equations

equations of motion. He was left with a single condition, viz. equality of a special form of Richardson number which proves to be equivalent to the "Scorer number" $S = g\beta L^2/U^2$. His special assumptions regarding the flow field are satisfied in the atmosphere if the perturbation is small, so that it does in fact appear that Scorer's condition for similarity is adequate to a degree. The important limitations are that equality of the "Scorer number" would not justify conclusions from model experiments regarding turbulent flows or flows in which the perturbation was not a first order quantity. The more rigorous conditions of Batchelor would need to be satisfied for this higher degree of similarity.

Assuming that the limited degree of similarity achieved by equating the "Scorer number" were acceptable for a particular experiment, the model flow conditions can be calculated for a typical case. For a model 3×10^{-5} times full size, with $U = 10^3$ cm./sec. and $\beta = 2 \times 10^{-7}$ cm.$^{-1}$ (a lapse rate of about 4°C/km.) on the full scale, then even with the very large temperature gradient of 1°C/cm. in the model, the wind tunnel flow speed would have to be as low as 4 cm./sec. For faster flow speeds very much greater temperature gradients would be required. It is clear that Scorer regarded it as impracticable to obtain such experimental control and abandoned pursuit of the possibility of wind tunnel experiments.

It is interesting to consider for which full scale cases wind tunnel experiments could legitimately be regarded as valid, if no control at all is exercised over the temperature gradient in the model. If in the wind tunnel the temperature and flow speed are constant, then the "Scorer number" for the model is zero. Thus the experiment should reproduce the full scale flow only in the special case when $l^2 = 0$ on the full scale. Such experiments might, therefore, be of limited value if one wished to investigate the flow over hills in, say, Northern India in the pre-monsoon period when the lapse rate is nearly dry adiabatic up to 10,000 feet or more, i.e. a case when the static stability is zero or very small for a considerable depth. In addition, and this might be more useful, the experiments could be applied to examine the flow of a completely cloudy airstream over a mountain for then the static stability (and thus l^2) would be approximately zero in the full scale case as well as in the model. The type of case in mind for this is one in which the airstream contains 8/8 nimbostratus and has a wet adiabatic lapse rate throughout a great depth. Apart from the special full scale case in which $l^2 = 0$, we may infer from the theory of the last section that a wind tunnel experiment without control of temperature would reproduce the flow over a small obstacle or hill up to about 100 m. in width since, as we saw, the full scale flow in such a case is practically independent of the stability effect, i.e. of the variation of l^2.

If we wished to devise model experiments to investigate larger scale phenomena in which the earth's rotation is concerned, e.g. Queney waves, it would be necessary for the non-dimensional number

$$Q = \frac{f^2}{k^2 U^2} \qquad \text{(24)}$$

to be equated in both model and full scale. This condition is effectively the same as equality of the Rossby number and must be satisfied in addition to equality of the Scorer number. The condition follows from consideration of Eq. (1) and it would ensure the proper representation of geostrophic forces in the model experiment. In a typical case, the condition would require rotation of the model at about 1 revolution per 2/3 minute to

/simulate

simulate the earth's rotation. It seems unnecessary to pursue this further here since mountain airflow on the large scale implied is not of direct concern to aviation.

In connection with the Gibraltar investigation of 1929/30 (20), Field and Warden supplemented their field work by wind tunnel experiments on a 1 in 5,000 model of the Rock. As they made no arrangements to simulate stability, the flow obtained in the model should have corresponded to the flow in the full scale case of an airstream with zero static stability. In spite of this, what they described as remarkable agreement between the flow in the experiment and the flow on the site was obtained. We must remember, however, that the flow on the site was in no sense fully mapped out; it was only possible to determine some of the characteristics of the flow to a limited extent from the programme of balloon work. Furthermore they were dealing with a constantly changing turbulent flow pattern which made specific comparison between the model experiment and the site work much more difficult than would have been the case had the flow been steady and laminar.

Abe studied the mountain clouds around Mount Fuji in Japan from 1920 onwards and from time to time supplemented his site study with wind tunnel experiments (21). He used a 1 in 50,000 model and selected a tunnel flow speed so as to equate the Reynolds number to that applicable on the full scale; this was, of course, on the usual assumption that molecular viscosity in the model corresponded to eddy viscosity on the full scale. The tunnel flow speeds required for this were of the order of 2 m.p.h. In an attempt to achieve greater realism, Abe arranged wind shear and a temperature gradient in the model experiments. For wind shear, he introduced an extra blower or used partial interruption of the flow, and for a temperature gradient he introduced dry ice smoke at the bottom of the tunnel. He also reproduced a change of wind direction with height by introducing blowers at the side of the tunnel. So far as is known, this has been the only attempt to simulate shear and stability in wind tunnel experiments. Unfortunately Abe did not arrange these effects quantitatively to ensure that strict dynamical similarity was achieved, and we must assume that if there was complete similarity it was accidental. He photographed the model flow and found approximate qualitative agreement with some properties of the flow on the site, insofar as he had deduced them from observations of the mountain clouds. In particular in both cases many vortices were observed with vertical, horizontal or inclined axes. Abe's work tells us a good deal about the characteristics of the flow over and around Mount Fuji; it assists very little towards a more complete understanding of the problem of mountain airflow in general.

Rouse (22) has discussed the potentialities of model experiments and refers, without giving details, to the value of experiments on large models of mountains in hangars using blowers or airscrews to provide the flow. We have seen that a model experiment in a wind tunnel without control of stability will with certain restrictions give dynamical similarity with cases of the flow over obstacles and small hills up to about 100 m. in width (and in addition with a full scale mountain problem in the special case of $l' = 0$). To proceed, therefore, from the wind tunnel scale to the scale of hangar experiments does not avoid the awkward problem of controlling the temperature gradient to simulate stability. Some advantage might derive from the increase of scale, however, insofar as much smaller temperature gradients would be required on the hangar scale than in the case of the wind tunnel.

So far, we have not discussed viscosity. If viscosity is introduced into the equations of motion by means of the usual terms, it is found that for dynamical similarity the Reynolds number must be equated on both scales

/in

in addition to the other dimensionless numbers already discussed. It has usually been suggested that if this equality is achieved by using molecular viscosity in the model and eddy viscosity in the full scale, the simulation of this feature will be satisfactory. On the face of it, this idea seems of dubious validity and although doubt has been expressed by some writers, it does not appear to have been thoroughly examined in the literature. Possibly the similarity hypotheses and other ideas of Kolmogoroff and Batchelor recently discussed by the latter (31) would be of value here.

In the course of a study of the flow of stratified liquids, Long has commenced experiments using a three-layer system of immiscible fluids in a long glass-sided tank. Long has recently given a preliminary account (23) of his first experimental results. In this case the obstacle, which filled the space between the front and back glass walls, was steadily drawn at various speeds along the bottom of the tank by mechanical means. The deformations of the three layers of fluid were studied and photographed. Long applied a rough dimensional analysis to the obvious parameters of his model arrangement and considered that his experimental conditions roughly reproduced the effect of stability and in fact suggested that the two interfaces might approximately correspond to an inversion at mid-tropospheric levels and the tropopause. The flow obtained in the three-layer system exhibited broadly some of the characteristics of the "Bishop" wave. In some of Long's photographs there is some sign of the fluid ascending towards the obstacle at low levels and descending at higher levels above the same position. This is interesting since the streamlines calculated by perturbation theory for many atmospheric cases show the same feature and the validity of this aspect of the theoretical results has not in the past been readily accepted. The use of layers of liquid of different densities for the simulation of stability appears to have much to recommend it as, presumably, the adjustment of densities in such an arrangement poses a far simpler laboratory problem than the production of a very large temperature gradient in a wind tunnel. Admittedly the compressibility of the atmosphere is not reproduced, but as was seen from Batchelor's work this can be ignored if first order perturbations only are to be studied. Even in a wind tunnel dynamical similarity for large amplitude perturbations requires what seem to be impossibly rigorous conditions, so that in this respect the stratified liquid model is on at least an equal footing. Long was quite conscious of the limitations of his experiment and in future work intends to simulate more closely a continuous density gradient by using a large number of layers of liquid and also to use a scale model of the Sierra range instead of an arbitrary obstacle. Long's future results are awaited with interest.

PART IV - THE WORK OF FÖRCHTGOTT

Förchtgott has carried out intensive investigations of the airflow over ridges during the post war years (24), (25). He is, amongst other things, a gliding instructor who has specialised in soaring in mountainous areas and in view of his wide experience his ideas on the subject must command respect. His work has comprised a series of field studies at various mountain locations in Bohemia using light aircraft and groups of gliders fitted with instruments. The flights were supplemented by the study of mountain clouds (both visually and by time lapse photography), of smoke and of the flight of birds. In all, during the period 1946-1950, he gathered about 35 different sets of observations spread over 5 different mountain locations. By studying the observational data gathered and drawing on his own considerable gliding experience, Förchtgott has built up a fairly comprehensive theory which is presumably

/consistent

consistent with both the data and his experience. His classification of mountain airflow into four main types is attractive and plausible but is deduced mainly by a process of subjective interpretation. It is not clear to what extent we can regard his conclusions as being of general validity.

Förchtgott has been severely critical of the conclusions deduced from perturbation theory on the grounds that by neglecting the turbulent layer and treating the flow as wholly laminar and steady, theorists have ignored a vital feature of mountain airflow. However, it must be stated that the significance of the restriction to steady laminar flow has been most fully acknowledged in all theoretical treatments, and in point of fact there is little or no conflict between Förchtgott's results and those of perturbation theory.

Förchtgott found that no organised flow patterns could be discerned unless the airstream had stable or neutral stratification, the wind was roughly normal to the mountain ridge and the wind direction varied little with height. Accordingly his studies were confined to situations when these conditions were satisfied. He found that mountain ridges with steep lee slopes were most favourable for lee wave effects and that the topography of the upwind slope had no evident importance. Apart from these provisions he concluded that the type of flow depended on the speed of the wind as compared with the height of the ridge above the lee plain and the variation of wind with height. His classification on this basis into four main types of flow is given in Fig. 6, the wind profile which he found to be appropriate to each flow type being indicated at the left of each diagram. With the exception of the first type (Fig. 6(a)) the flow patterns are non-laminar (and possibly unsteady) and we must presume, therefore, that Förchtgott's streamlines are merely symbolic. The flow types are now briefly commented upon.

(a) Undisturbed Streaming

This occurs with very light winds; each streamline executes a single shallow wave and the vertical displacement of the streamlines dies out rapidly with height.

(b) Standing Eddy Streaming

Slightly stronger winds are required for this type. The surface streamline separates from the ground and there is a stationary lee eddy with approximately horizontal axis. The crest in the laminar streaming above the eddy is displaced downwind from the mountain, and we may regard the effective shape of the mountain as being changed by the presence of the eddy. Reverse flow up the lee slope is implied in this type of flow and has been observed frequently in mountain areas. Although not specifically stated by Förchtgott, it is obvious that zero static stability would favour the formation of the lee eddy.

(c) Wave Streaming

With still stronger winds, the stationary lee eddy disappears and a system of lee waves develops in association with a stationary vortex system having both clockwise and counter-clockwise rotations in two horizontal rows. Turbulence is found in the vicinity of the vortices. The waves die out both horizontally and vertically away from the ridge. Thus Förchtgott does not find in practice steady laminar wave streaming down to the surface on the lee side. He always finds some form of turbulent wake to the lee of the ridge even when there are smooth waves above. However the evidence for stationary closed vortices does not seem conclusive and we must remember that an impression of rotation of the bar clouds, or so called "rotors", would be provided by the wind

/shear

shear in the wave system. The turbulence too could be accounted for by shear, which in theory would be intensified in the crests and troughs of the waves.

(d) Rotor Streaming

With very strong winds extending through a restricted vertical depth comparable with the height of the mountain (see wind profile in Fig. 6(d) and (e)), the double vortex system becomes intensified and the spacing closes up towards the mountain. There is in this case no significant wave system above the vortices. Flight investigation of this type of flow was found very difficult owing to heavy turbulence, expecially close to the lee slope. In discussing the conditions for this type of flow, Förchtgott introduces the term "streaming layer" and speaks of critical values of its depth. The streaming layer is not defined, but he appears to have in mind the layer in which there is a definite component across the ridge either increasing or remaining roughly constant with height. A strong component of reverse shear, reducing the component across the ridge to zero or small values at some level, is regarded as providing a streaming layer of limited depth. Förchtgott claims that wave streaming breaks down into rotor streaming when the depth of the streaming layer falls to about $1\frac{1}{2}$ times the height of the ridge. Further decrease in the depth of the streaming layer transforms the flow pattern into a completely chaotic type in which no organised fetures can be recognised.

As regards the limits of wind speed determining which of the types of flow (a), (b), (c) will appear in any given case, Förchtgott's observations indicated that these would depend upon the height of the ridge above the lee ground. He quotes, for example, that for a ridge 900 metres high, a wind of 12 m./sec. is necessary for wave streaming. If the obstacle is a solitary hill, rather than a very long ridge, a much stronger wind speed is necessary for a given type of flow than in the case of a long ridge of a similar height.

Förchtgott has assembled his various deductions in the form of a diagram from which, it is claimed, one could decide which type of flow to expect in any given case. The variables are the height of the hill, the wind speed and the depth of the streaming layer, but there is no provision for the length of the ridge. Something of this sort would be extremely valuable for aviation forecasting but for the time being we cannot regard Förchtgott's diagram as more than a convenient summary of his own ideas. Further intensive field work would be necessary before these results could be exploited with confidence.

There is much in Förchtgott's results to confirm the predictions of perturbation theory as obtained by Scorer. The stable stratification and increase of wind with height implied for wave streaming (Fig. 6(c)) means a decrease of the parameter l^2 with height, as required by perturbation theory. The wind profile for Förchtgott's rotor streaming (Fig. 6(d) (e)) involves a large increase of l^2 with height. In such a case perturbation theory tells us that steady laminar streaming with lee waves is not possible, but is unable to indicate what type of flow occurs in its place. Förchtgott, too, does not find lee waves but has suggested the alternative from his field data.

/PART V

PART V - AVIATION APPLICATIONS

Although the state of knowledge of mountain airflow is far from being complete and satisfactory, sufficient is now known to justify some cautious and tentative applications to aviation problems, including forecasting. Experience in other fields suggests that attempts at the practical application of new work can often assist by throwing fresh light on aspects which are only partially understood, so making possible further advances. A few remarks are, therefore, given below on the possibilities, difficulties and limitations of applying current knowledge on mountain airflow to aviation problems.

(a) Aviation Forecasting

The theoretical studies reviewed in Part III included streamlines calculated for a number of special cases. It should be said at the outset that similar calculations for real cases would be totally impracticable as a normal routine in a forecast office. Firstly it would be necessary to determine a model airstream which approximated to the real airstream and was at the same time suitable for the calculations. Secondly, the computation of the streamlines would be extremely laborious and lengthy, even for the case of the flow over a simple symmetrical ridge.

The most that could be done in practical forecasting would be to exploit, mainly qualitatively, some of the general results which emerge from the perturbation theory studies and in particular to make use of Scorer's deductions regarding the significance of the variations in the vertical of his parameter l^2. There has, of course, been no extended study of reported cases of standing waves aimed at testing the validity of these deductions, but in a few reported cases where there were sufficient details to permit such an examination, e.g. in ref. (26), the l^2 profile has been calculated and the theory verified. Furthermore, if there are no large discontinuities of lapse rate, Scorer's criterion for waves reduces to a requirement for a strong forward wind shear in the air current across the ridge or mountain. This general property of airstreams containing waves is such a common feature in reported cases that there is in effect a good deal of circumstantial support for the theory. In addition it will be remembered that Förchtgott's field studies revealed the same feature.

The reports of wave effects contributed at Northolt by B.E.A. pilots permit a rough check of the theory, and this has been done in 33 cases. It was not possible in all these to select radio sonde and wind ascents representative of the area where the disturbances were found and at the same time sufficiently upwind to be unaffected by the disturbances. The profiles of l^2 cannot, therefore, be regarded as precisely applicable. However, they all showed a pronounced maximum of l^2 through some layer, the mean height of which was centred at about 800 mb., with very much smaller values above. The mean of the ratio "maximum l^2" to "value of l^2 in the upper layer" was 8·8 for the 33 cases, showing the substantial nature of the reduction of l^2 with height in these cases.

One criticism which has been voiced against Scorer's condition for waves is that most airstreams would show some decrease in l^2 with height, whereas one might well have expected some highly selective criterion to apply. In order to examine whether this criticism is

/justified,

justified, the l^2 profiles were calculated for a sample of 50 airstreams. These were chosen so that there was little change of wind direction with height, but in other respects the sample was a random one with cases both day and night and at all times of the year. As expected, it was found that some decrease upwards in the value of l^2 was common but the average value of the ratio "maximum l^2" to "value of l^2 above" for the 50 cases was only 3·3. It will be noted that this is much smaller than that obtained for the occasions when waves were reported at Northolt. In this connection, also, it will be remembered that in the case of the two-layer model airstream, it was found that the reduction in the value of l^2 from the lower to the upper layer had to attain a minimum magnitude (depending on the depth of the lower layer) for a wave solution to be possible. A decrease alone in the value of l^2 was not a sufficient condition. Unfortunately it is not possible for this further condition to be used quantitatively in practical work, since we must deal with airstreams as we find them rather than with ideal two-layer models. It can be inferred that when the profile of l^2 varies continuously, some form of condition regarding the magnitude of the decrease in l^2 is certainly necessary but this cannot yet be formulated. The most that can probably be said at present is that the greater the decrease of l^2 with height, the greater is the likelihood of waves. Here, more detailed reports than those collected in the past may assist towards a better understanding of this aspect of the problem.

In view of the above considerations it now seems that an attempt could be made to indicate to pilots when waves might be expected to operate and give rise to large areas of lift or sink for flights crossing, or passing to the lee of mountain areas. When perturbation theory indicates that steady laminar, wavelike flow to the lee of mountains cannot occur, the forecaster can at present do little more than make guarded use of the results of Forchtgott. Scorer has discussed in a recent report (27) these forecasting aspects and indicated the sort of advice which could be issued to pilots. With regard to the computation of the profile of l^2, a convenient method, in which a celluloid scale is applied to the appropriate tephigram, has now been devised by Wallington (28).

One great difficulty in bridging the gap between the theoretical results and practical forecasting arises from topographical reasons. The theory necessarily deals with simple mountain shapes, mostly infinite ridges; in practice something approaching the ideal obstacle occurs only at a few rare locations. In general the forecaster is concerned with what can only be described as irregular mountainous or hilly terrain. Over such areas on a day favourable for wave motions, the actual airflow must be the complex result of interference between many separate wave trains and for this reason alone the forecaster has little hope of saying much more than that areas of lift and sink will be encountered by a pilot. He cannot indicate the magnitude or horizontal extent of vertical currents on the basis of what is known at present.

(b) Safety Heights

One fact which emerges very clearly is that, because of the vertical motion which may occur in airstreams over and to the lee of mountains, safety heights applicable to air routes crossing mountains should provide for a greater margin of safety than is normal over level terrain. The large number of unexplained or inadequately explained aircraft accidents in mountainous country adds point to this need.

/Tentative

Tentative proposals as to what increases in safety heights should be applied have already been put forward (10), (29), but these are very much in the nature of interim suggestions and have no precise basis. This is an important operational problem but no rigorous solution seems possible on the basis of existing knowledge. Some of the more obvious considerations and difficulties are mentioned below.

(i) On a civil air route, climbing to unnecessary heights over mountains may be expensive (on account of extra fuel), sometimes unwise (due to icing liabilities) and possibly inconvenient (owing to the effect of Air Traffic Control procedures, the quadrantal height system, etc.). Therefore if airline operators are to accept a requirement for increased safety heights, it must be possible to demonstrate beyond question that the proposed increases are essential.

(ii) Consider for a moment the simple case of an airstream flowing perpendicularly across a ridge and let us assume that harmonic waves are operating in the airstream to the lee. If an aircraft is flying into wind it will be subject to harmonic fluctuations of height out of phase with the waves in the airstream. The magnitude of the aircraft's height changes will depend on the speed of the aircraft and the speed of the wind in addition to the amplitude of the atmospheric waves. If the aircraft is flying with the wind, its height changes will be in phase with the waves in the airstream but will be of smaller magnitude than when on the reciprocal course. If the aircraft is flying parallel to the ridge it could be in an area of lift or sink continuously, depending on its track relative to the wave crests. A simple formula could be deduced to give the height fluctuations of the aircraft in terms of the amplitude of the waves in the airstream, the wind speed, aircraft speed and the track being flown, and this could be used as a basis for determining safety heights. For non-laminar or unsteady flow patterns we should need to introduce the horizontal extent and magnitude of the vertical currents in place of tne amplitude of the atmospheric waves.

(iii) It is clear from (ii) that any rigid solution to this problem would require the safety height to be determined for each individual flight. This would only be practicable from the point of view of the airlines if the procedure were very simple. The primary difficulty, however, is that it is not yet possible to predict the amplitude of the waves (or details of the vertical currents in non-laminar flows) except very approximately. In addition, the fact that in practice we must deal with rough irregular terrain, rather than simple ridges, makes the problem even more complicated. It therefore seems that some compromise solution is inevitable. If there were large numbers of detailed aircraft reports giving accurate values of vertical currents and their horizontal extent, it might be possible to develop on a statistical basis a procedure for fixing safety height. The information available, however, is inadequate for such an approach, and could not be obtained without aircraft flying in regions and circumstances which must now be regarded as dangerous.

(iv) There are some grounds for thinking that the worst circumstances that occur (as regards involuntary loss of height by an aircraft) are roughly equivalent to those which would be produced if the airstream exactly followed the topography. Without attempting to substantiate this here we can at least use this assumption as a basis for examining a little further the factors and difficulties involved in the problem. It is a matter of simple algebra to show that on this assumption the maximum loss of height for an aircraft of speed V flying into an airstream of speed v flowing perpendicularly over a ridge of

/height

height h (above the surrounding countryside) would be $vh/(V-v)$. It could then be argued that the usual 1,000 feet adopted as the acceptable clearance over level country should be increased by values for the possible loss of height calculated from this relation. For an aircraft crossing a ridge obliquely, e.g. on a course making an angle θ with the ridge, the maximum involuntary loss of height would be $vh/(V\sin\theta - v)$. The following table gives the result of applying the criterion to a few typical cases of flight perpendicularly across a ridge, assuming an aircraft speed of 150 knots.

Height of Ridge (feet)	Wind Speed at Crest Level (knots)	Required increase in clearance (feet)	Clearance (feet)
1000	30	250	1250
2000	40	730	1730
3000	50	1500	2500
4000	60	2670	3670

The increases in safety height required for slower aircraft or for oblique flight across the ridge would, of course, be greater. It is clear, even from this elementary approach, that it may sometimes be impossible for a slow aircraft with small climbing power to cross a mountain range especially obliquely in strong winds. It is also clear that all of the factors, wind speed, aircraft speed, height of mountain and the direction of flight are significant. It follows that the tentative suggestions made by the Court of Enquiry which investigated the Aer Lingus aircraft accident in January 1952 cannot be regarded as a final solution since the proposed increases of clearance depend on only one of the important factors, viz. wind speed. An acceptable solution must also take account of the height of the mountain range above the surrounding terrain, must provide for the fact that slow aircraft would remain in regions of sink for longer than fast aircraft, and must in addition take account of the course of the aircraft.

REFERENCES

1. ABE, M. — The formation of cloud by the obstruction of Mount Fuji. Geophys. Mag., Tokyo, 6, 1932, p.1.

2. MANLEY, G. — The helm wind of Crossfell, 1937-1939. Quart. J. R. Met. Soc., 71, 1945, pp. 197/215.

3. KÜTTNER, J. — Moazagotl und Föhnwelle. Beit. Phys. Atm., 25, 1938, pp. 79/114.

4. LUDLAM, F.H. — Orographic Cirrus Clouds. Quart. J. R. Met. Soc., 78, 1952, pp. 554/562.

/5.

5. STÖRMER, C. "Mother of Pearl" clouds. Weather, 3, 1948, No. 1, p. 13.

6. HORSLEY, T. New light on the standing wave. Aeronautics, London, 11, No. 6, 1945, pp. 38/41.

7. AUSTIN, A.R.I. Wave clouds over southern England. Weather, 7, 1952, pp. 50/52.

8. TURNER, H.S. Standing waves and powered flight. Met. Mag., 81, 1951, p. 106.

9. TURNER, H.S. Severe turbulence over the Inner Hebrides. Met. Mag., 81, 1952, pp. 239/241.

10. MASON, D. Hill standing waves and safety heights. Shell Aviation News, 179, pp. 14/18.

11. YATES, A.H. Airspeed fluctuations when entering waves. Gliding, 2, 1951, p. 186.

12. QUENEY, P. Theory of perturbations in stratified currents with application to airflow over mountain barriers. Chicago, Univ. Dept., Misc. Rep., No. 23, 1947.

13. LYRA, G. Uber den einfluss von Bodenerhebungen auf die Strömung einer stabil geschichteten Atmosphäre. Beit. Phys. Atm., 26, 1940, pp. 197/206.

14. LYRA, G. Theorie der stationaren Leewellenströmung in freier Atmosphäre. Z.a. Math. Mech., Berlin, 23, 1943, pp. 1/28.

15. SCORER, R.S. Theory of waves in the lee of mountains. Quart. J.R. Met. Soc., 75, 1949, pp. 41/56.

16. SCORER, R.S. Theory of airflow over mountains: II - The flow over a ridge. Quart. J.R. Met. Soc., 79, 1953, pp. 70/83.

17. ROPER, R.D. Evening Waves. Quart. J. R. Met. Soc., 78, 1952, pp. 415/419.

18. SCORER, R.S. Properties of Barostromatic Airflow (unpublished).

19. SCORER, R.S. A second kind of wave. Gliding, 4, No. 2, 1953, pp. 61/62.

20. FIELD, J.H. and WARDEN, R. A survey of the air currents in the Bay of Gibraltar. Met. Off. G.M., 7, No. 59, 1933.

21. ABE, M. An attempt to make visible the mountain air current. J. Met. Soc., Japan, Tokyo, 1942, p. 69.

22. ROUSE, H. Model techniques in meteorological research. Compendium of Meteorology, Boston, Mass., 1951, p. 1249.

23. LONG, R.R. A laboratory model resembling the "Bishop Wave" phenomenon. Bull. Amer. Met. Soc., 34, No. 5, p. 205.

24. FÖRCHTGOTT, J. Wave streaming in the lee of mountain ridges. Bull. met. tchécosl, Praha, 3, No. 3, 1949, pp. 49/51.

/25.

25. FÖRCHTGOTT, J. Mechanical Turbulence. Letecká Met. (Aeron. Met.) Praha, 1952, pp. 114-161.

26. SCORER, R.S. Forecasting the appearance of lee waves. Weather, 6, 1951, pp. 99/103.

27. SCORER, R.S. Forecasting dangerous flying conditions near mountains. Met. Res. Pub. No. 814.

28. WALLINGTON, C.E. A lee wave scale. Quart. J. R. Met. Soc., 79, 1953, pp. 545/547.

29. M.C.A.P. 102 Report of the Court Investigation on the accident to Dakota EI - AFL on 10th January 1952. H.M.S.O., 1952.

30. BATCHELOR, G.K. The conditions for dynamical similarity of motions of a frictionless perfect-gas atmosphere. Quart. J. R. Met. Soc. 79, 1953, pp. 224/235.

31. BATCHELOR, G.K. The application of the similarity theory of turbulence to atmospheric diffusion. Quart. J. R. Met. Soc., 76, 1950, pp. 133/146.

G.381714/DP/12/53/40.

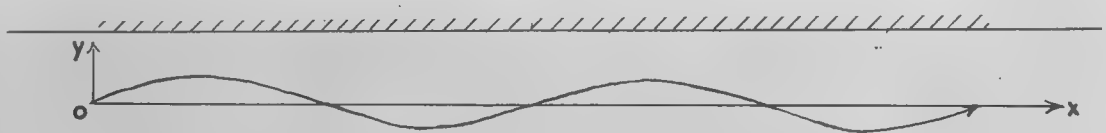

Fig.1(b). $l_s > k > l_f$. Medium scale corrugation (wavelength 2π to 200π km.)

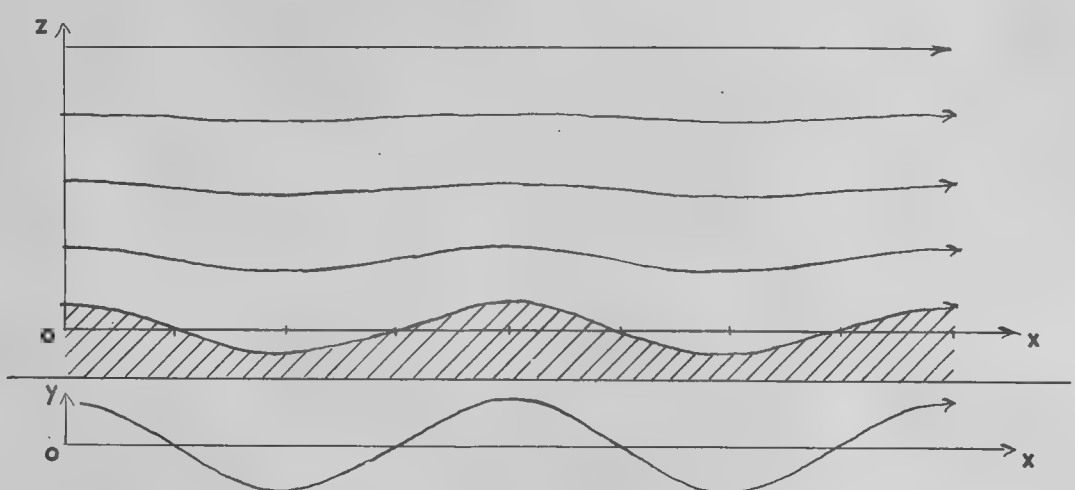

Fig.1(c). $k < l_f$. Large scale corrugation (wavelength $> 200\pi$ km.)

Fig. 1. Streamlines produced by an infinite sinusoidal ground profile.

15. SCORER, R.S. Theory of waves in the lee of mountains. Quart. J.R. Met. Soc., 75, 1949, pp. 41/56.

16. SCORER, R.S. Theory of airflow over mountains: II - The flow over a ridge. Quart. J.R. Met. Soc., 79, 1953, pp. 70/83.

17. ROPER, R.D. Evening Waves. Quart. J. R. Met. Soc., 78, 1952, pp. 415/419.

18. SCORER, R.S. Properties of Barostromatic Airflow (unpublished).

19. SCORER, R.S. A second kind of wave. Gliding, 4, No. 2, 1953, pp. 61/62.

20. FIELD, J.H. and WARDEN, R. A survey of the air currents in the Bay of Gibraltar. Met. Off. G.M., 7, No. 59, 1933.

21. ABE, M. An attempt to make visible the mountain air current. J. Met. Soc., Japan, Tokyo, 1942, p. 69.

22. ROUSE, H. Model techniques in meteorological research. Compendium of Meteorology, Boston, Mass., 1951, p. 1249.

23. LONG, R.R. A laboratory model resembling the "Bishop Wave" phenomenon. Bull. Amer. Met. Soc., 34, No. 5, p. 205.

24. FÖRCHTGOTT, J. Wave streaming in the lee of mountain ridges. Bull. met. tchécosl, Praha, 3, No. 3, 1949, pp. 49/51.

/25.

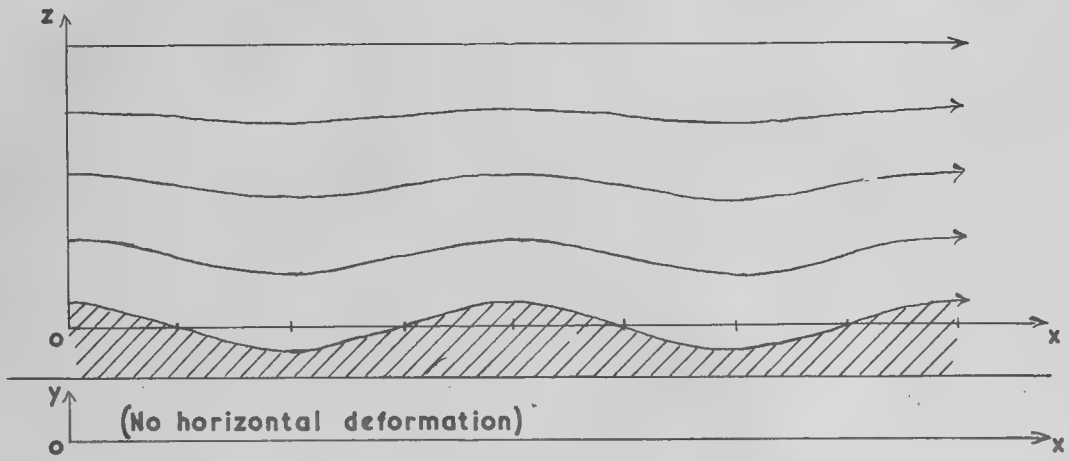

Fig. 1(a). $k > l_s$. Small scale corrugation (wavelength $< 2\pi$ km.)

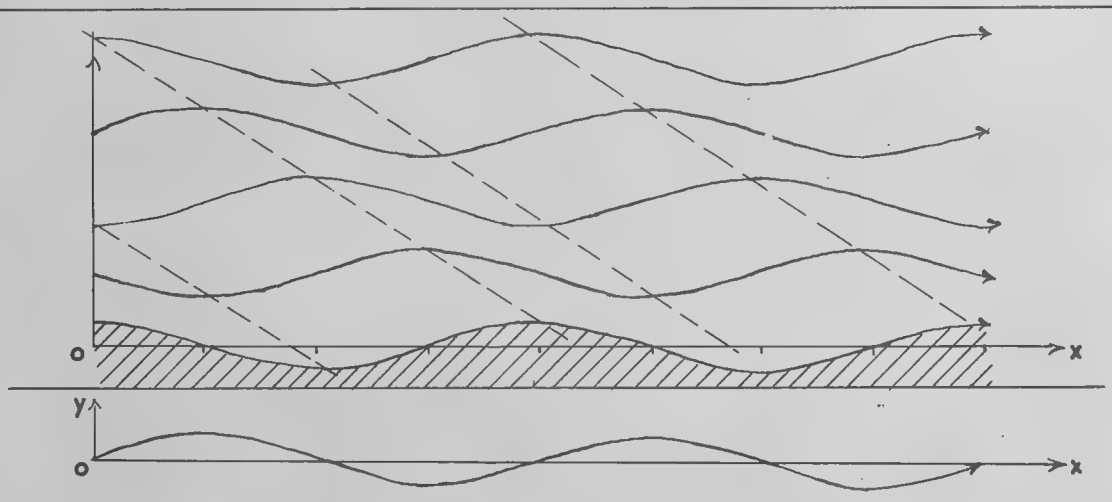

Fig. 1(b). $l_s > k > l_f$. Medium scale corrugation (wavelength 2π to 200π km.)

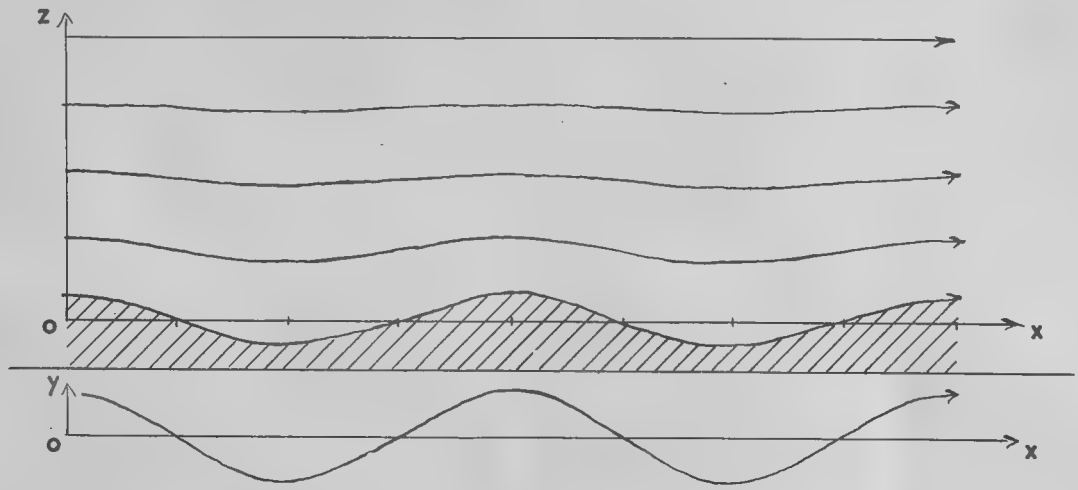

Fig. 1(c). $k < l_f$. Large scale corrugation (wavelength $> 200\pi$ km.)

Fig. 1. Streamlines produced by an infinite sinusoidal ground profile.

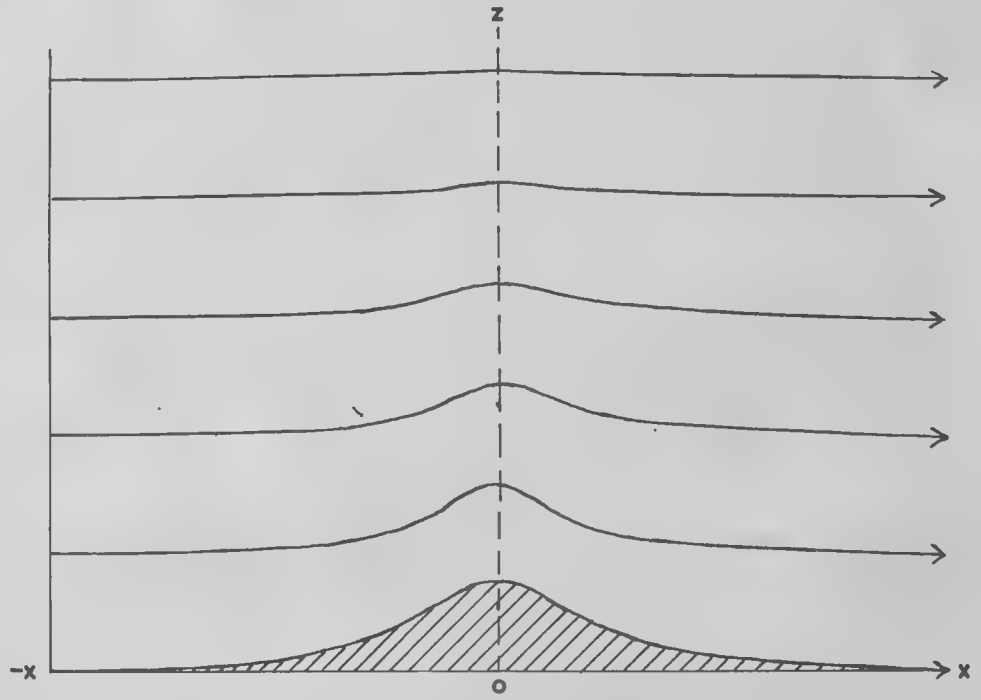

Fig. 2. The flow over a very small ridge of width up to about 100 m.

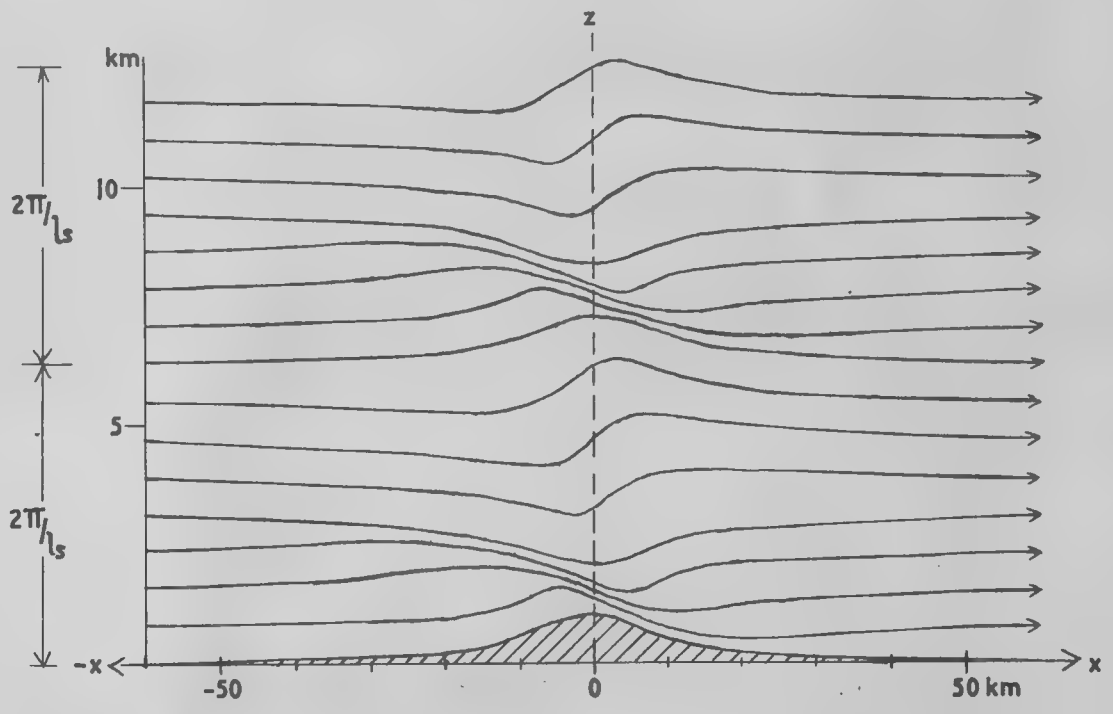

Fig. 3. The flow of a uniform airstream over a ridge having a width up to a few km. (after Queney). In the case illustrated $l_s = 1\ km^{-1}$, $a = 10$ km, $U = 10$ m/s.

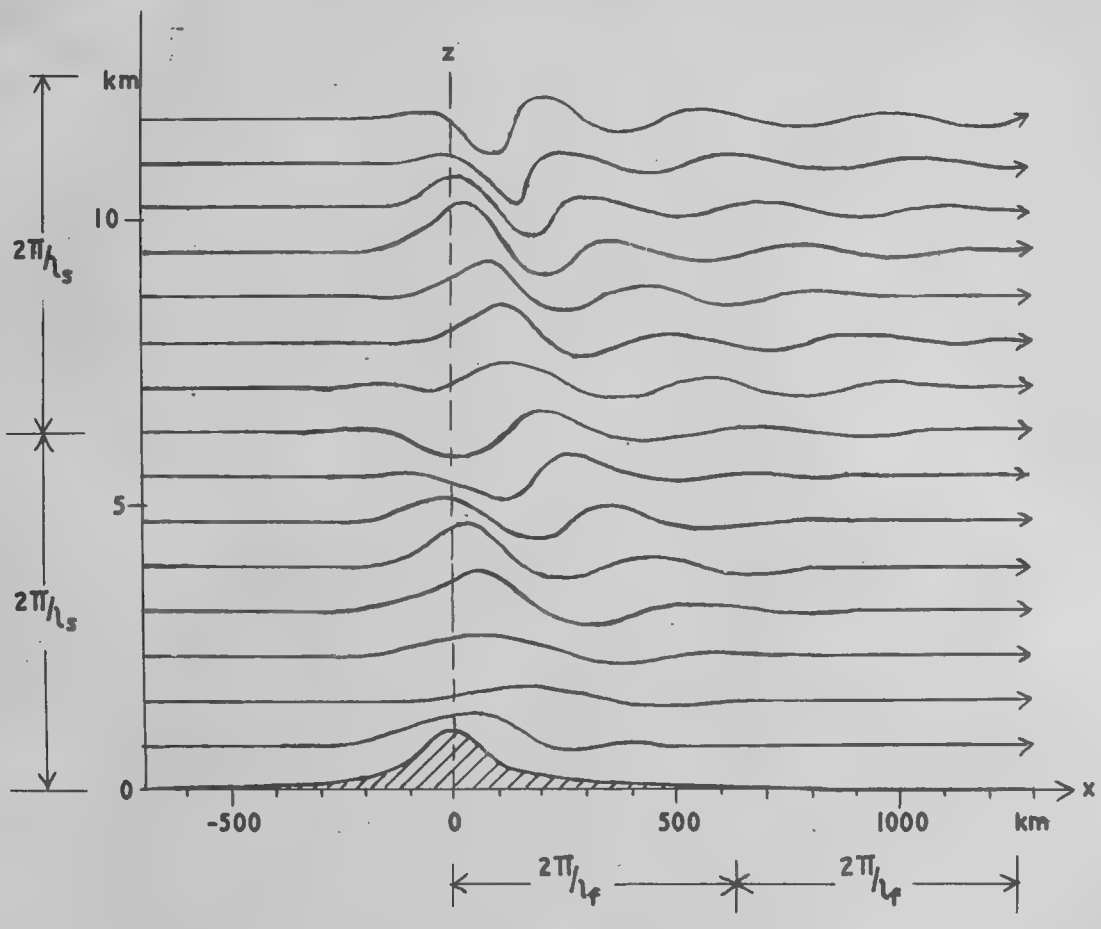

(a) Vertical Projection of Streamlines.

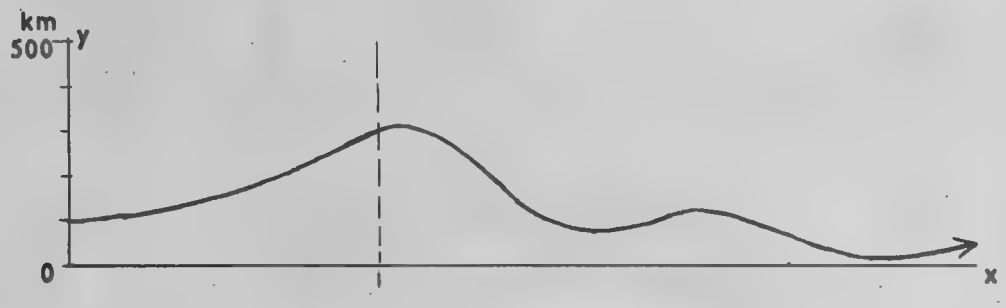

(b) Horizontal Projection of Ground Streamline.

Fig. 4. The flow of a uniform airstream over a ridge having a width of about 100 km. In the case illustrated $l_s = 1\,km^{-1}$, $a = 100$ km., $l_f = \cdot 01\,km^{-1}$, $U = 10$m/s.

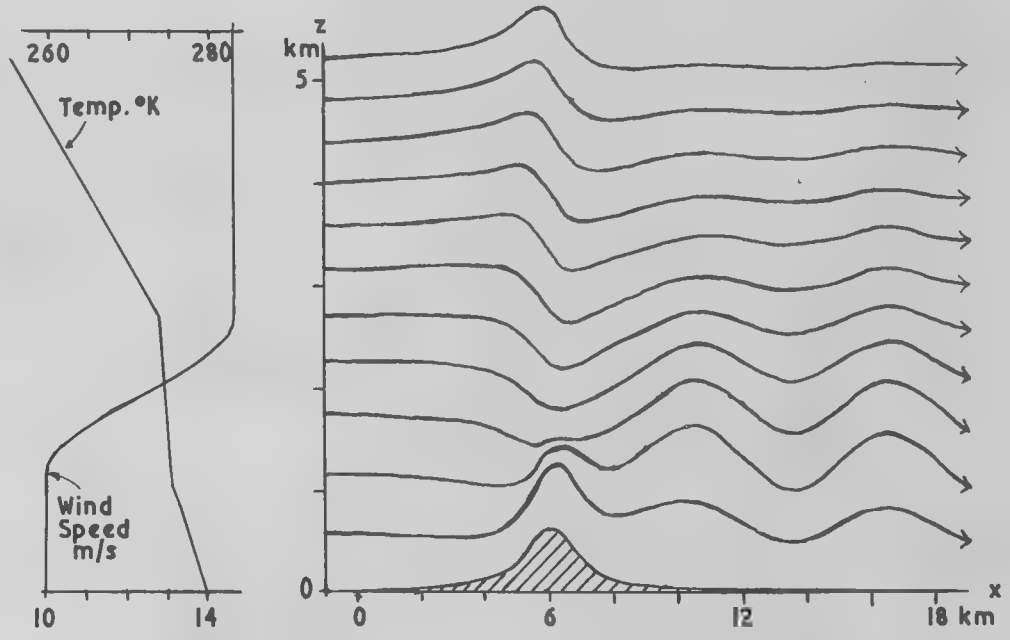

Fig. 5. Airflow over a mountain ridge under conditions favourable for the occurence of lee waves (after Scorer).

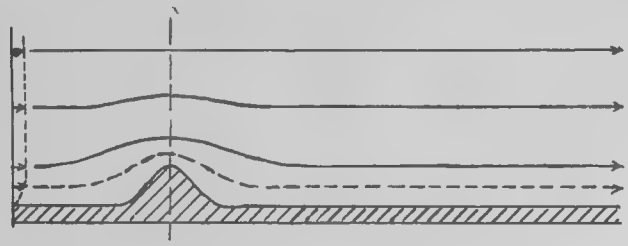

(a) Laminar streaming.

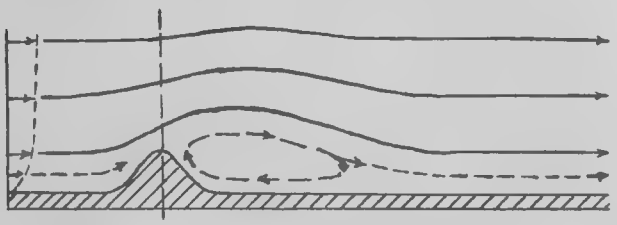

(b) Standing eddy streaming.

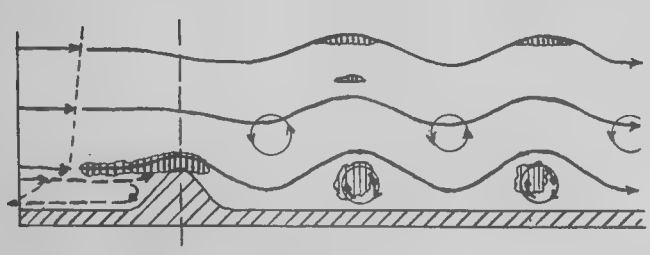

(c) Wave streaming.

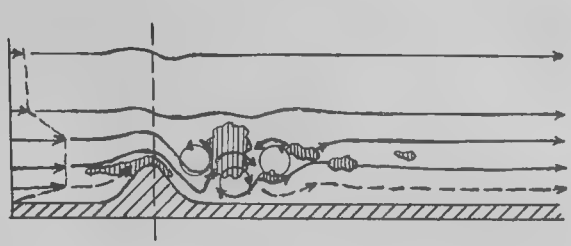

(d) Rotor streaming.

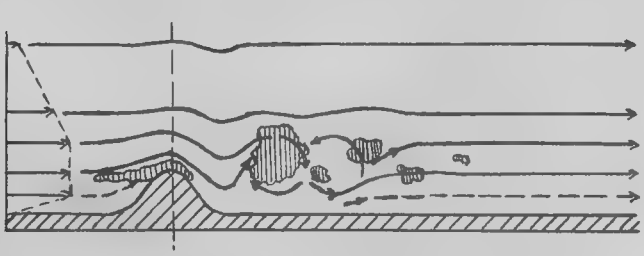

(e) Rotor streaming

Fig. 6. Types of airflow over ridges. (after Förchtgott).

o the British Isles have already been reported in M.P.Ps.

he ten years 1941 - 1950.

ts were drawn for the British Isles on the basis of th
d in the Daily Weather Report. The period covered by

M.R.P. 843
S.C.II/164
31st December, 1953

At the time of issue this report has not been published. Any author desiring to quote this paper should refer to it as "A paper of the Meteorological Research Committee (London),
M R.P. No. 843 by Mr. J. S. Sawyer
A copy is available in the Library of the Meteorological Office."

AD 223069

AIR MINISTRY

METEOROLOGICAL RESEARCH COMMITTEE

The rainfall of depressions which move eastward across Scotland

by
J.S. Sawyer (Meteorological Office)

1. Introduction. Studies of the rainfall of depressions which move eastward over or near to the British Isles have already been reported in M.R.Ps. 748, 762 and 816. These previous investigations have dealt with depressions which passed north of Scotland, crossed England or moved eastward near the English Channel. The present paper is concerned with depressions which crossed Scotland and completes the study of the rainfall of all depressions which moved eastward near or over the British Isles in the ten years 1941 - 1950.

2. Method. The method followed that of the previous investigations. From the Daily and Monthly Weather Reports all occasions were selected from the period 1941 - 50 on which a depression (defined by a closed isobar) crossed Scotland with an eastward component of motion. 49 such depressions were noted.

Rainfall charts were drawn for the British Isles on the basis of the observations printed in the Daily Weather Report. The period covered by the chart was chosen to include all of the frontal rain from the depression; showers in the adjacent air masses were necessarily included and in some cases there was difficulty in separating the rain from that of preceding or following systems. However the main features of the rainfall distribution were rarely in doubt. Two of the rainfall charts covered a 60 hour period but the remainder included 48 hours or less, the majority including only 24 or 36 hours.

For each depression a 1000-500 mb thickness chart was constructed; this was drawn for a time chosen to present the thermal structure of the depression as it crossed the British Isles. Observations from the German Daily Weather Reports were used to extend the British charts for the war-period.

3. The average rainfall distribution. Fig. 1 shows the average rainfall distribution for the periods during which the depressions moved across Scotland. It is based on the average rainfall values shown on it, and in calculating these, values have been interpolated from individual rainfall charts for occasions for which observations were not available in the Daily Weather Report. Since the observations on which Fig. 2 is based were nearly all made on relatively low ground the chart does not adequately represent the rainfall of the hilly areas. However some average values for higher level stations in Scotland, Wales and Devon are given as an inset.

/The

The values for Princetown, Cray Reservoir (Breconshire) and Cwm Dyli near Snowdon are taken from the autographic records; those for Eskdalemuir and Dalwhinnie from the Daily Weather Report.

Fig. 1 shows a maximum of about 15 mm near to the average track of the depressions with rainfall values falling off more or less regularly to south and north. Rainfall in the west of the British Isles is greater than the east; the difference is more marked in the south. Considered in relation to the tracks of the depressions studied the average rainfall amount and pattern is very similar to that shown in M.R.Ps. 762 and 816 for depressions on tracks further south.

As would be expected the rainfall at the high-level stations in Wales and Devon is much greater than that at neighbouring stations on low ground. Eskdalemuir also receives more rain than other stations in South Scotland but the difference here is not so marked. In the previous reports also it was noted that the most marked orographic effect was found some distance to the south of the track of the depression where a deep westerly current was likely to be more persistent.

In order to present a clearer picture of the rainfall in relation to the track of the depression an estimate has been made of the average rainfall over areas centred 50, 150 and 250 miles north and south of the track of the depression. The resulting average profiles of rainfall are given in Fig. 2 for east and west coast districts separately. The curves for east and west coast districts are generally similar but confirm the greater rainfall of the west. The curves also are very similar to the profiles of rainfall for depressions crossing the British Isles further south as given in M.R.Ps. 762 and 816.

Fig. 3 shows the percentage of the 49 depressions which gave less than 0.1 mm of rain at stations in the British Isles.
The main features of the chart are:-

(a) At stations in Southern Scotland (i.e. near to the average track of the depressions) all of the depressions gave measurable rain.

(b) The number of cases without measurable rain increases southeastward and becomes 20% at about 300 miles from the general track of the centres.

(c) The distribution of "dry" cases is very similar to that accompanying depressions which move eastward between Scotland and the Faeroes although the proportion of dry cases is not so high. Over England and Wales the proportion of dry cases is much greater in the east than in the west.

(d) The difference between the frequency of dry cases at the high level stations and neighbouring stations on lower ground is not very great (see inset to Fig. 3).

Fig. 4 contains histograms of rainfall amounts for selected stations and shows the wide range of variation at individual stations among the rainfall of the various depressions which follow the selected track.

4. Characteristics of individual rainfall distributions. The rainfall patterns from individual depressions were very irregular. In the previous investigations a well defined band of heavier rainfall had frequently been noted along the track of the depression. This was less common for depressions crossing Scotland than for depressions following tracks further south and such a rainfall band was noted in association with only 14 out of the 49 depressions which crossed Scotland. Probably the irregular topography of Scotland has an effect in disturbing the regular organisation of the rainfall pattern. In the previous studies also it was found that a clearly defined rainfall band usually occurred with fast moving depressions in a pattern of thickness lines with little distortion. Neither the relation with the speed of the depression nor with the thickness pattern could be demonstrated for the depressions which crossed Scotland.

/5.

5. Variation in rainfall amounts in relation to synoptic parameters. As a measure of the general rainfall in Scotland the average rainfall was calculated for two groups of six stations in and near Scotland. The correlation between the two groups was + 0.86 and it was assumed that the average of all 12 stations would give a reasonably representative measure of the rainfall activity of the depression in Scotland. As a similar measure of the "raininess" of the depressions over England the average rainfall of 6 stations in Wales and the southern half of England was used (viz Holyhead, Spurn Head, Plymouth, Boscombe Down, Mildenhall and Lympne). The correlation between the average rainfall of this group and that of the 12 Scottish stations was only + 0.43 and indicates that the rainfall from these depressions in the south of England is not closely related to that in Scotland.

The relation between the rainfall at both the Scottish and the English groups of stations was compared with various synoptic parameters. The central pressure of the depression was found to have only a small negative correlation (about -0.35) with the rainfall of both groups. The lowest pressure in the pressure trough in latitude 50°N is a much better guide to the rainfall in England and has a correlation of -0.60 with the rainfall at the English group of stations. A similar fairly high correlation is given in M.R.P. 748 in respect of depressions which pass between Scotland and the Faeroes.

There is very little correlation between the direction of motion of the depression or its speed and the rainfall in either Scotland or England. The relations with Scottish rainfall are insignificant but small negative correlations of about -0.25 and -0.4 are obtained with the rainfall at the English group of stations indicating that the depressions with a component of motion towards the south and those moving more quickly tend to give less rain.

Examination of the 1000-500 mb thickness patterns associated with the depressions gives no obvious relation between the rainfall amounts and the distribution of 1000-500 mb thickness. There is a slight tendency for the depressions with a strong thermal wind over the centre in the direction of motion to give less rain but the correlation between rainfall and thickness gradient normal to the direction of motion is numerically less than -0.2. Also there is a positive relation between thermal wind component towards the left of the track and the rainfall amount (correlation coefficient about + 0.35) for the Scottish group of stations indicating that depressions with a strong thermal trough behind the centre tend to give more rain than those with a less marked trough.

6. Conclusions. The average pattern of rainfall from depressions moving eastward across Scotland shows a maximum of about 15 mm near the track of the centres falling off to north and south to about half the central value at a distance of about 300 miles. In relation to the track of the depressions the average rainfall pattern is very similar to that for depressions moving eastward on other tracks near the British Isles, suggesting that orographic features are of only secondary importance in determining the rainfall distribution at stations on low ground. On the other hand there is a very great orographic increase in the rainfall amounts at high level stations south of the depression track compared with neighbouring low level stations.

There is a very great deal of variation between the rainfall patterns resulting from individual depressions and comparison of rainfall amounts with various synoptic parameters fails to bring out any relationships close enough to be of much value in forecasting. The rainfall amounts in Scotland are not closely related to those in England. Rainfall tends to be greater in association with the deeper depressions, but the depth of the pressure trough south of the centre is a better guide to the rainfall over England. The existence of a thermal trough behind the centre also tends to be associated with larger rainfall amounts.

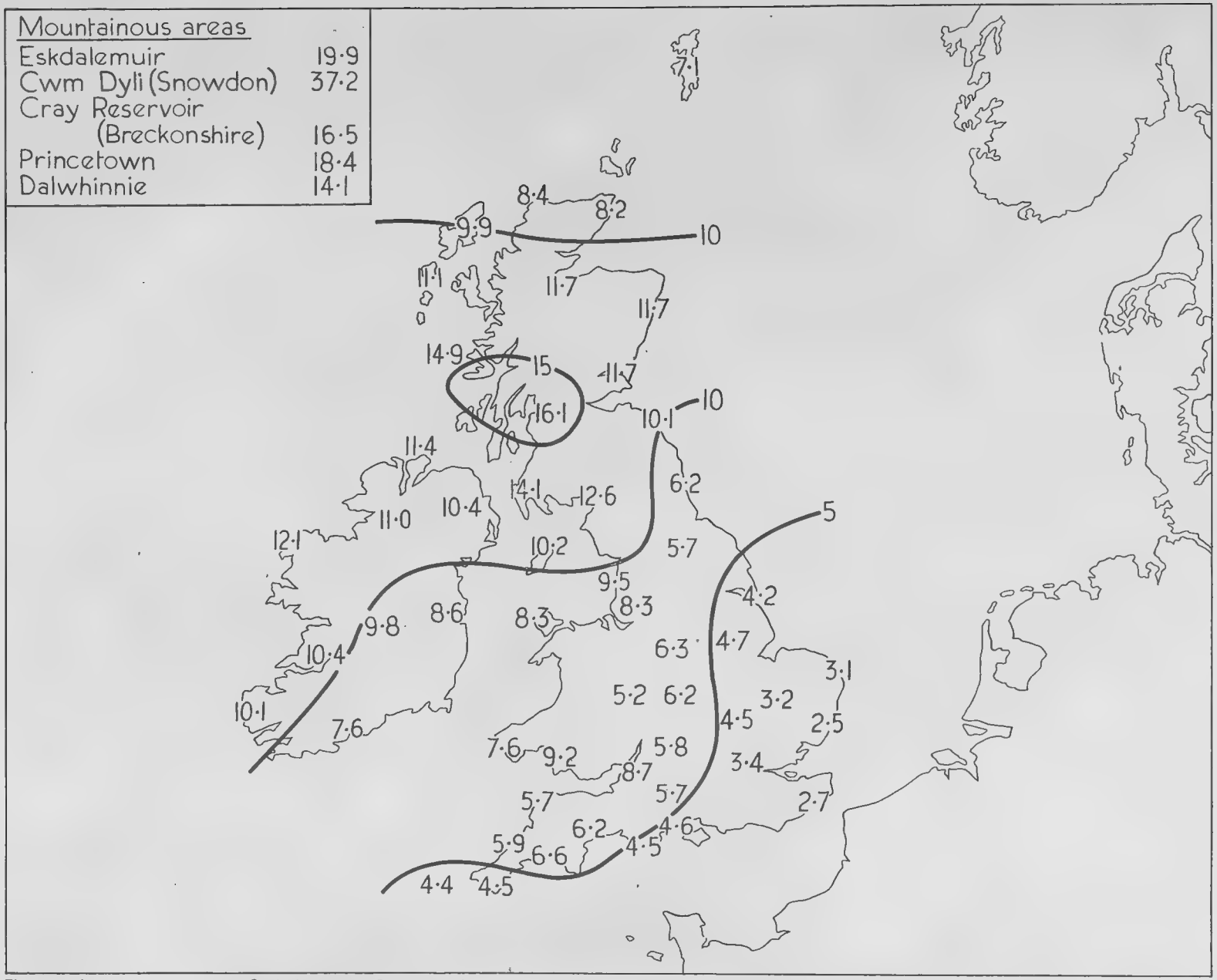

Fig.1 Average rainfall (m.m.) from depressions which moved eastward across Scotland — 49 cases — period 1941-1950

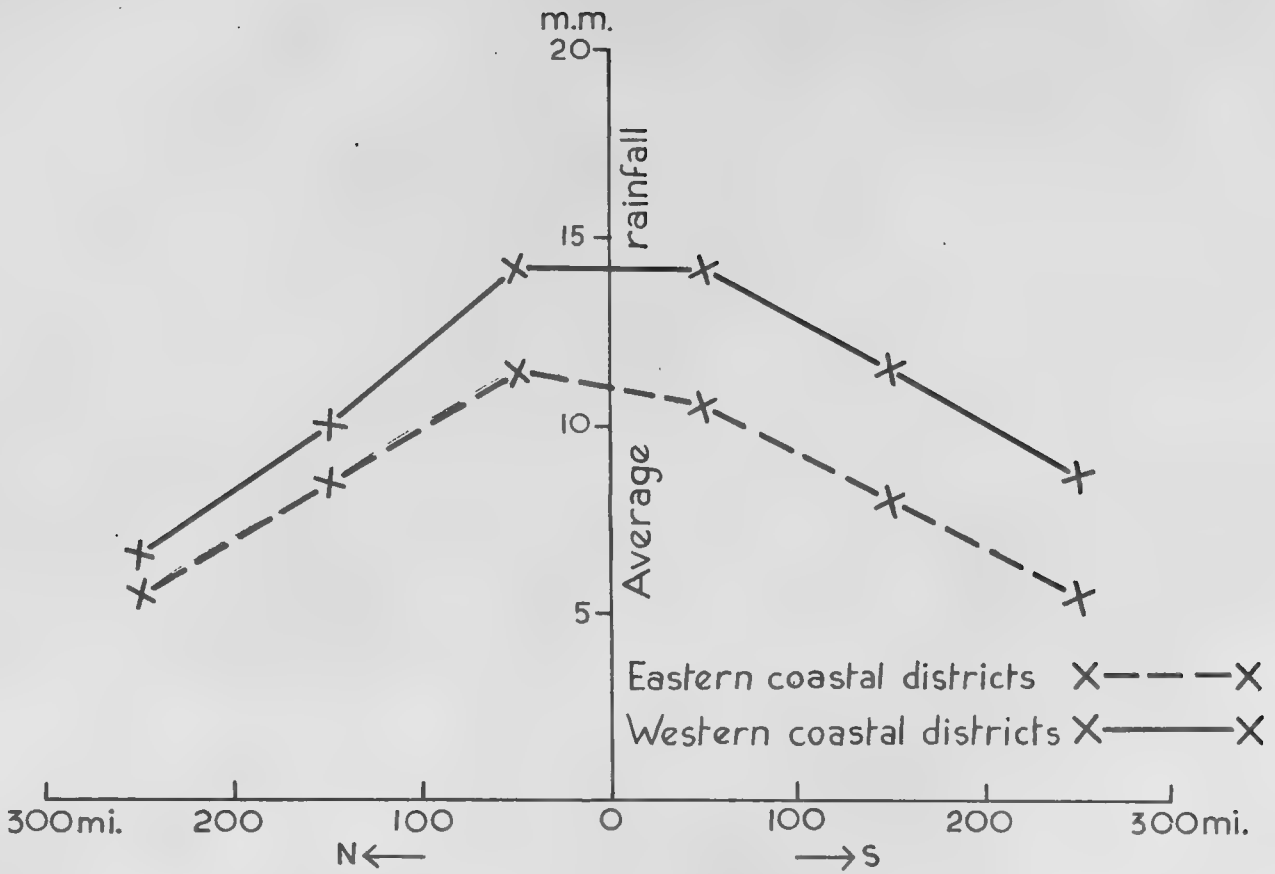

Distance from track of depression

Fig. 2 Average profile of rainfall across the track of a depression moving eastward across Scotland

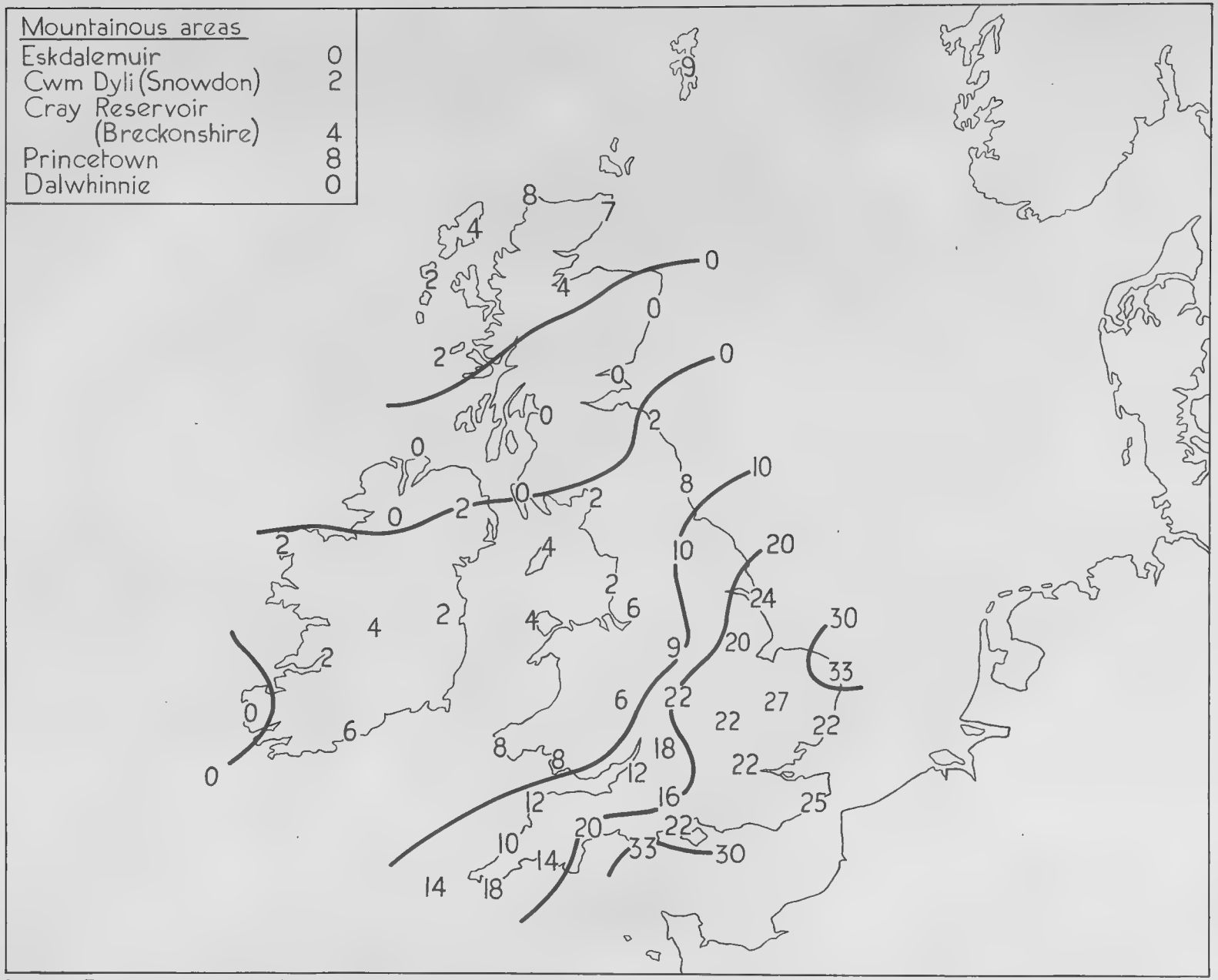

Fig. 3 Percentage of depressions moving eastward across Scotland which gave less than 0·1 m.m. of rain — 49 cases — period 1941–1950

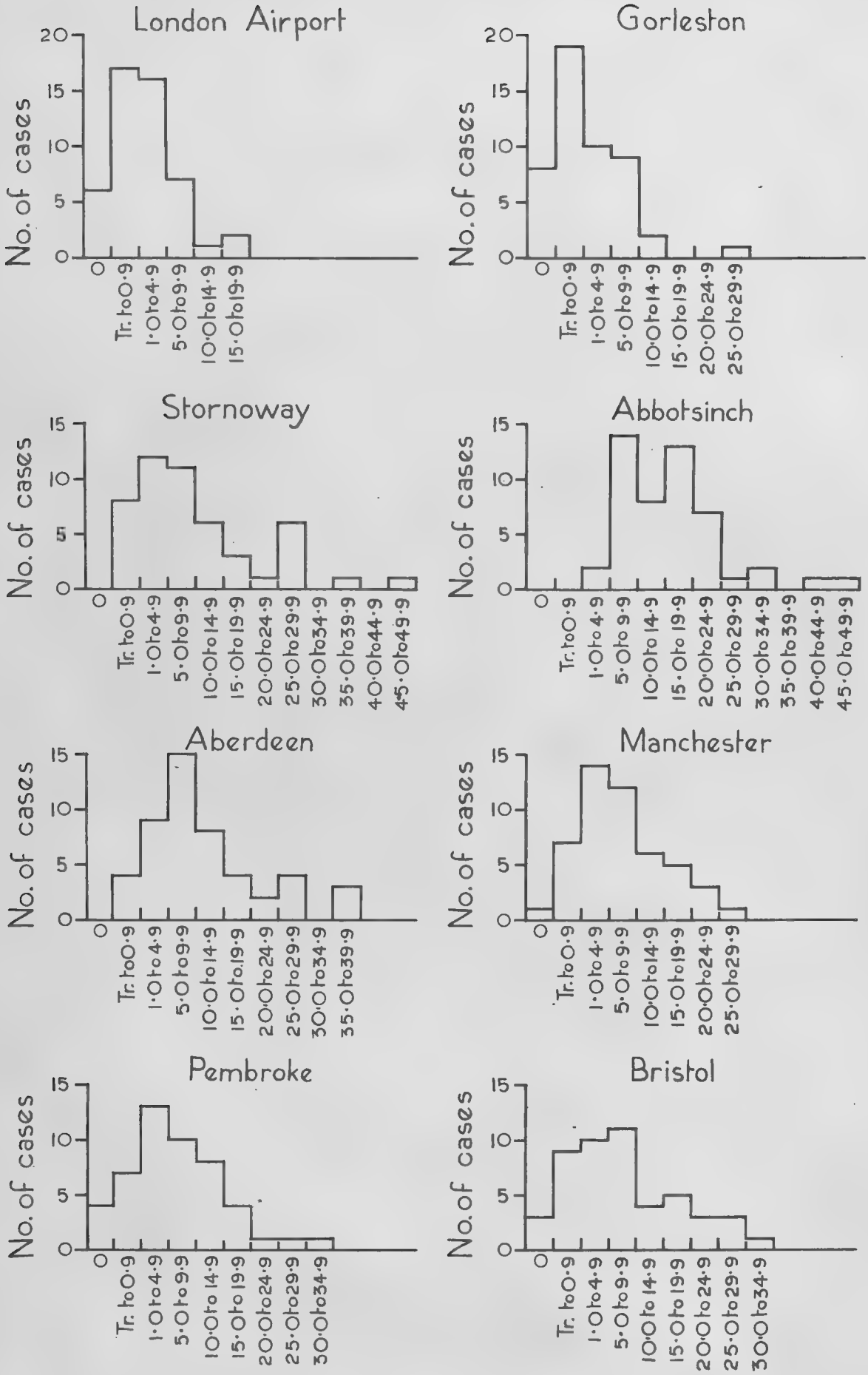

Fig. 4 Depressions which moved eastward across Scotland — 49 cases — period 1941–1950
Frequency diagrams of rainfall totals (m.m.) from individual depressions at selected stations

A copy is available in the Library of

both. It is a matter of observation that cloud droplets can continue to

ypical cloud particles are so minute - much smaller than typical rain- r snowflakes - that they remain in suspension: or, if they fall from

of processes within cloud which result in growth or aggregation icles to drops or snowflakes which, by reason of their size and

several thousands of feet in vertical extent.

(a) Rôle of ice crystals.

In temperate latitudes, at least, the temperature of the upper of the majority of precipitating clouds is as low as -12°C, or

e in size or nish. The optimum temperature for this stage of and -15°C. The larger crystals fall relatively

At the time of issue this report has not been published. Any author desiring to quote this paper should refer to it as "A paper of the Meteorological Research Committee (London), M.R.P. No 854. by Mr H.W.L. Absalom
A copy is available in the Library of the Meteorological Office."

M.R.P. 854

S.C.III/168

27th February, 1954

AIR MINISTRY
METEOROLOGICAL RESEARCH COMMITTEE

Artificial production of precipitation

by
H.W.L. Absalom (Meteorological Office)

Note:- This paper was prepared in connection with an inquiry received by the Meteorological Office.

1. Introduction.

Cloud consists of small water drops or ice crystals, or a mixture of both. It is a matter of observation that cloud droplets can continue to exist in liquid form at temperatures far below 0°C, to -20°C or even lower. Water cloud at temperature lower than 0°C is said to be supercooled.

Typical cloud particles are so minute - much smaller than typical raindrops or snowflakes - that they remain in suspension: or, if they fall from the cloud, evaporate completely before reaching the ground.

The occurrence of rainfall or snowfall, as normally understood, implies the operation of processes within cloud which result in growth or aggregation of cloud particles to drops or snowflakes which, by reason of their size and increased rates of fall, reach the ground before evaporation is complete.

Attempts to produce precipitation by artificial means must aim to assist or stimulate natural processes.

2. Outline of natural precipitation processes.

Most precipitation in substantial amount (other than drizzle) falls from cloud several thousands of feet in vertical extent.

The release of natural precipitation from cloud is attributed to two main processes, one of which depends on the presence of ice crystals in cloud.

(a) Rôle of ice crystals.

In temperate latitudes, at least, the temperature of the upper parts of the majority of precipitating clouds is as low as -12°C, or lower. Natural ice crystals are found to occur in the supercooled parts of cloud, and more probably and more profusely at temperatures of about -10°C and lower.

When ice crystals and supercooled water droplets co-exist the crystals grow at the expense of the neighbouring droplets which therefore decrease in size or vanish. The optimum temperature for this stage of growth is between -10° and -15°C. The larger crystals fall relatively to the smaller liquid or solid cloud particles. Further growth by collision with other crystals and supercooled droplets results in the formation of crystal aggregates, i.e. snowflakes, of sufficient size to reach the ground as snow, or as rain if they melt in the warmer lower parts of cloud or in the air below. It has been suggested that the splintering of ice crystals during the process of growth gives rise to additional crystal elements and so to additional snowflakes (or, eventually, rain drops).

/On

On occasions, well-developed cumulus ('shower') clouds with tops at temperatures below -12°C do not precipitate. It has been claimed that this is due to the lack of natural ice crystals in the upper parts of the clouds.

(b) Coalescence of droplets.

Particularly, though not exclusively, in tropical areas substantial rainfall occurs from well-developed cloud no part of which is at a temperature below 0°C. There is no question of the ice crystal process in such conditions. As the growth of a cloud droplet to a raindrop by condensation alone is a very slow process, the rain must result primarily from the coalescence of water droplets. Cloud droplets are not of uniform size. Droplets larger than normal, when carried upwards and downwards by the air currents within the cloud, grow by sweeping up a proportion of smaller droplets and eventually become large enough in vertically deep cloud to fall out as rain. Some may grow sufficiently to split up into a number of drops large enough to initiate further cycles of growth by coalescence. There is evidence that hygroscopic elements (having affinity for water) such as sea spray are carried up into clouds and constitute the relatively large droplets which are the first stage in the coalescence mechanism.

The coalescence process doubtless operates also in deep clouds which extend upwards to temperatures below 0°C (as in (a) above).

3. Artificial rain-making.

(a) General.

The possibility of producing rain, or snow, by human intervention is by no means a new concept, though it is only since 1946 that rather intensive and widespread effort has been devoted to the problem. In 1946 research staff of the General Electric Company of America demonstrated in the laboratory that an artificially produced cloud of water droplets at a temperature well below 0°C changed very rapidly to a cloud of minute ice crystals after the introduction of a particle or two of solid carbon-dioxide (dry ice) of which the temperature is in the neighbourhood of -70 to -80°C. Ensuing experiments, by the G.E.C. group, in which pellets of dry ice were dropped from aircraft into natural supercooled cloud showed that changes of cloud structure occurred and that snow fell from the cloud in a short time after the 'seeding' operation. These early results aroused much interest and were quickly followed by similar experiments and related investigations in America and several other countries. Much of the subsequent work has been investigational in character and carried out by official or comparable institituions. There has also been considerable commercial exploitation, notably by American agencies.

At an early stage it became evident that it is possible in favourable conditions to induce rain or snow to fall from certain clouds by seeding them with dry ice. As mentioned below, other methods of cloud seeding have been suggested. The effectiveness of present methods of attempting to produce precipitation in conditions which would be unlikely to give rise to natural precipitation, and the significance of the amount of precipitation produced artificially are still controversial topics.

Other proposals or speculations which have emerged relate to the application of cloud seeding to prevent hailstorms and the more intense downpours of rain, and also to the possibility of clearing low cloud e.g. in the vicinity of airfields.

(b) Methods of cloud seeding.

The chief methods which have been used in recent years are outlined briefly below.

/(i)

(i) Dry ice.

Pellets of dry ice are dropped from an aircraft into water-drop cloud of which the top at least is at temperature some degrees below 0°C. The likelihood of success is greater if the cloud-top temperature is lower than -7°C.

Intense local cooling produced in the cloud along the paths of the falling pellets of dry ice results in the formation of numbers of minute ordinary ice crystals, which become diffused by turbulence within the cloud. Subsequent growth of the crystals to the magnitude of precipitation elements may be expected, as outlined in para. 2(a), in favourable conditions.

From the remarks in para. 2(a) on the rôle of naturally occurring ice crystals in water cloud at temperature lower than -12°C, in initiating natural precipitation, it would appear that the utility of seeding with dry ice is restricted mainly to occasions or stages of cloud development where the tops of cloud are at temperatures between -7°C and -12°C. Hence, it is argued, the injection of dry ice at the appropriate stage of growth (judged by temperature at the top) should result in precipitation falling earlier than, and in a different area from, precipitation which would result from further development of the cloud.

Dry ice evaporates quickly in falling to levels of higher temperature.

(ii) Silver iodide.

When introduced into supercooled water cloud at a temperature lower than -3 or -4°C, extremely small crystals of silver iodide lead to the formation of ice crystals. The ice crystals may form, not as a result of intense cooling as is produced by dry ice, but because the crystalline structure of silver iodide and ice are closely alike and the minute silver iodide crystals serve as nuclei for the formation of ice crystals. The effectiveness of silver iodide as a producer of ice crystals appears to increase rapidly as temperature decreases from -3° or -4°C to -15°C but thereafter changes little.

Ice crystals produced in cloud through the agency of silver iodide may be supposed, in favourable circumstances, to grow by natural processes and result in precipitation from the cloud, as indicated in para. 2(a). If the quantity of silver iodide used in seeding results in the production of too numerous elementary ice crystals in relation to the number of water droplets present, the ice crystals will not grow sufficiently to initiate precipitation, but the supercooled water cloud will be transformed to a cloud of small ice crystals.

In seeding operations, the silver iodide in finely divided form is produced by vaporising a solution of silver iodide in acetone containing an alkali iodide. The vapour can be injected directly into cloud at the appropriate temperature by means of apparatus carried on aircraft; or, somewhat less directly, by means of small bombs, containing gunpowder impregnated with silver iodide, carried upward into the cloud by small balloons and arranged to explode sufficiently high above the 0°C level. Much of the cloud seeding with silver iodide has been done with generators suitably deployed at ground level, a procedure less costly than any involving the use of aircraft. The invisible effluent from a generator travels with the wind, diffusing as it goes and, if upward air currents are present, enters cloud and eventually may reach the temperature levels at which silver iodide is effective in ice crystal formation.

/It

It would appear that there must be some uncertainty as to when or whether silver iodide generated at the ground will reach the right part of the cloud, or even the right cloud mass, but advocates of the method claim that proper positioning of generators in relation to the area on which it is desired to produce precipitation can be achieved by making due allowance for changes of wind direction and speed with height (say to 15,000 feet above ground) and other local conditions.

Silver iodide does not dissolve in water, evaporate or melt. It may therefore be long-lived in the atmosphere and might conceivably affect cloud remote from the area of operations. There is however some uncertainty as to the effectiveness of this substance after exposure to sunlight.

(iii) Water drops.

Water drops of diameter about 1/20 to 1/10 millimetre have been sprayed by aircraft into the lower parts of cloud some thousands of feet in vertical extent and in which there is updraft. Drops of the size mentioned are larger than the majority of cloud droplets: the aim of the method is to promote the coalescence mechanism referred to in para. 2(b).

(iv) Hygroscopic material.

Very fine particles of a hygroscopic substance quickly become relatively large liquid droplets when introduced into a cloud of water droplets and, if the cloud conditions are suitable, would be expected to cause precipitation by the coalescence process indicated in para. 2(b).

Trials have been made by dispersing a mixture of finely powdered sea-salt and calcium chloride (hygroscopic substances) in the lower part of suitable clouds. The material and a charge of gunpowder are carried up by a small balloon into the cloud and arrangements made for the charge to explode at an appropriate height above the cloud base.

(c) Discussion.

From the outline of the bases and the methods of attempts to cause precipitation artificially we pass to a review of the evidence on results.

Assessment is by no means a straightforward matter. A particular cloud may be seen to yield rain or snow at from 10 to 40 minutes after it has been treated with dry ice, but it is often difficult or impossible to be certain that precipitation would not have fallen naturally from that cloud at about the same time or somewhat later. In a series of well controlled experiments carried out jointly by the U.S. Air Force, National Advisory Committee for Aeronautics and the U.S. Weather Bureau in March - September 1948 (ref. 1), precipitation fell from 18 cumulus-type clouds after seeding with dry ice when there was no precipitation before seeding, but in all except five of the cases natural precipitation occurred within a radius of 30 miles and even in these five cases natural showers were occurring within 40 to 60 miles. On the other hand, seeding of suitable cumulus-type cloud with dry ice by the Radio Research Division of the Commonwealth Scientific and Industrial Research Organisation (C.S.I.R.O.), Australia, during a three-year period resulted in rain falling from the cloud on about 100 occasions when similar (unseeded) cloud in the immediate neighbourhood produced no rain. Observations of results were made visually and by radar. Information as to the amounts of rain which reached the ground on these occasions is less precise because of absence of rain gauges in the paths of some of the showers, but it is stated that estimated amounts of rainfall ranged from 0 to 0.25 inch.

/At

At this point, in relation to amount of rainfall, it may be noted that even if a cloud 30,000 feet in vertical extent and of average constitution were to deposit its entire content of liquid water the resulting rainfall would be about one-fifth inch in the area affected, unless there were some mechanism for replenishing the cloud. The heavier falls of rain which occur naturally are associated with systems in which natural forces maintain renewal of the cloud as the water is precipitated. There is no evidence that methods of cloud seeding mentioned earlier can induce mechanism which results in the replenishment of a particular precipitating cloud. Indeed many of the operations aimed to produce precipitation for utilitarian purposes have been restricted to occasions on which a suitable cloud system is maintained for sufficiently long periods of time by natural processes.

Although some qualitative estimation of the results, positive or negative, of the seeding of clouds may be obtained by visual and radar observation (and probably more readily when the seeding agent is injected from an aircraft than when silver iodide is diffused from ground generators), information more quantitative in character is required in assessing the efficacy of cloud seeding in causing precipitation. It is not sufficient merely to compare the amount of rainfall measured at places in the 'target' area on a day of seeding operations with the amount of rainfall received on the same day at places in neighbouring similar areas ('control' areas) which could not have been affected by the seeding operations. While it is true that there is normally an 'average' relationship between the natural rainfall received at two places not too far apart and subject to the same general regime of weather there can be on occasions substantial departures from the normal 'average' relationship. This random natural variability is found not only in the rainfall received in the course of a day but also in the rainfall for a month or longer period. Therefore, the difference in rainfall in the target area and a control area on days of seeding operations must be compared with the range of natural variability in the difference between the areas on non-seeding occasions. It is desirable when practicable to determine the natural variability of rainfall difference between the two areas from rainfall measurements made in each during as many years as possible before the advent of seeding. If, from such statistical processes, it is concluded that there is a high probability that the difference between the rainfall amounts in the target and control areas on occasions of seeding is greater than is to be expected from natural variability, the effects of seeding on those particular occasions are regarded as statistically significant. It has been represented that it is not valid, when determining the standard ('average') relationship between natural rainfall in a target and a control area, to group all rainfall amounts together irrespective of the weather situations in which they occurred; in other words, that separate target-control area relationships should be determined for a series of different types of rain-giving weather situations and that the significance of the relationship between target and control area rainfalls on occasions of seeding should be assessed against the standard relationships for the types of weather situation in which seeding was carried out. This proposed refinement, which is an indication of the complications encountered in measures to evaluate the results of cloud-seeding, raises the question of how closely the weather situation on a seeding occasion might resemble any of the types selected as standard.

From this background of generalities we proceed briefly to note some published accounts of rain-making operations and experiments.

Africa

The Overseas Food Corporation in collaboration with the East African Meteorological Department conducted experiments during the rainy season January - April in 1951 and 1952 (2,3). The site of the experiments was a cleared area of some 200 square miles near Kongwa, Tanganyika. There was a network of about 50 raingauges in the cleared area. In the 1951 season the seeding agent used was silver iodide, dispersed either from

/ground

ground generators or from balloon-borne bombs (see para. 3(b)(ii)). There were periods in this season when conditions were unsuitable for successful seeding operations. Considering only days other than these it was concluded that the experiments were probably unsuccessful on 12, inconclusive on 10 and probably successful on 5 days. In the 1952 season ground generators were not used. All seedings were made by balloon-bomb and were conducted in three-day cycles: silver iodide, hygroscopic material (see para. 3(b)(iv)), no seeding, on days 1, 2, 3 and so on. Every care was taken to ensure that the seeding agent should enter cloud above a small region in the central section of the experimental site and be dispersed at the appropriate level in the cloud according to the agent used. Winds were almost entirely easterly. Total amounts of rain for each of the three groups of days, measured in each of the 50 raingauges, were examined. As compared with the distribution of rain on days of no seeding, the rain on days of silver iodide seeding showed an excess in the sector of the site upwind of the central area of seeding, while the central sector showed a definite deficit and the downwind sector no pronounced difference. Rain amounts for the group of days of hygroscopic seeding showed an excess upwind, a marked deficit over the central sector but a pronounced excess in the extreme downwind part of the downwind sector. The report mentions the possibility that the apparent deficit of rain in the central area of seeding with silver iodide and in the downwind sector was due to overseeding with the material, but regards the apparent enhancement of rainfall in the extreme of the downwind sector on days of hygroscopic seeding as consistent with the time interval which would be expected for rain to develop following that method of seeding. Further careful similar experiments are desirable.

America

Results of seeding operations by the California Electric Power Company in the Bishop Creek part of the Sierra Nevada watershed in 1948 (33 days), 1949 (29 days) and 1950 (19 days) are discussed in a joint report by T.J. Henderson and S.A. Cundiff of the Power Company and Ferguson Hall of the U.S. Weather Bureau (4). Deep orographic cloud before and after the passage of storm systems was seeded, mainly with dry ice though silver iodide was dispensed from the aircraft on a few occasions. Seeding was confined to the Bishop Creek area (about 15 by 5 to 10 miles in extent). Numerical data on the river flow in Bishop Creek and in neighbouring creeks in each of the years of seeding were examined in relation to corresponding data for earlier periods of 20 to 30 years, in the general manner mentioned above. Only for one period, October 1948 - September 1949, was the Bishop Creek river flow significantly greater than expectation. A corresponding assessment of the water content of the snowpack in April of each year in the Bishop Creek and nearby unseeded areas suggested somewhat negative effects of seeding on snowpack. The report states that it is not possible to determine by purely statistical process if the rather pronounced departure of the 1948-9 river flow, from the standard relationship, resulted from the seeding operations or was due to natural causes, but comments that the 1948-9 winter was characterised in the Californian area by pronounced meteorological anomalies which possibly may have been at least partly responsible for departures in relationships between the flows of Bishop Creek and adjacent streams.

Cloud-seeding operations were conducted during the months January to April 1951 over a 10,000 square mile area in Central Arizona by the Salt River Valley Water Users' Association. P.B. MacCready, Jr., of the California Institute of Technology, reported (5) that for each of the four months the proportion of rainfall to normal (average) was greater in the seeded region than in the neighbouring comparison regions and that in relation to corresponding measurements in five and nine previous years (of no seeding) the relative increase in rainfall in the seeded region was statistically significant. G.W. Brier and I. Enger, of the U.S. Weather Bureau (6), found that while the 1951 January - April total rainfall in the seeded region was larger than expected when judged in relation to

/the

the data for 30 years in the seeded and the comparison regions, the excess could not be rated as significant. On using rainfall measurements from a larger number of stations in the seeded and comparison regions but for a shorter period of 10 years they found the excess of 1951 (January - April) rainfall in the seeded region to be highly significant. These different results, arising from the use of different lengths of comparison records and different selections of rainfall stations, further illustrate the difficulty of assessing the effect of cloud seeding on rainfall.

Commercial cloud-seeding was carried out in the South Oregon Cascades during the months November to March 1949-50 and 1950-51 with the object of increasing the snow pack, and in the Tri-Counties area of Oregon during the months September to June 1950-51 and 1951-52 with the object of increasing precipitation for the benefit of wheat growers. In the Cascades operation the seeding agents used were dry ice, silver iodide and an unknown material, in the Tri-Counties operation silver iodide from ground generators alone was employed. The results of statistical assessment (on the lines indicated earlier) of both Oregon operations have been reported (7) by R.T. Beaumont of the Oregon Agricultural Experiment Station, Medford. For the winter-months operations in the Cascades the criterion used was the relationship between the accumulated water content in snow pack on April 1 (i.e. at the end of each of the two seeding seasons) in the seeded area and adjacent comparison areas as compared with corresponding data during periods of from nine to nineteen earlier years (no seeding). The analysis showed that during the two seasons of seeding there was significantly less water stored as snow on the target area than might have been expected under normal climatic conditions. In dealing with the Tri-Counties operations, November to June, the monthly and total amounts of rain in the target and control areas were examined statistically in relation to corresponding data for 20 years of no seeding. It was found that the relationship between rainfall in the seeded and control areas in the two periods of seeding did not depart significantly from the regression estimates based on 20 years' data, and hence that departures (positive or negative) in the seeding periods may have been due entirely to chance. It should be mentioned that the control area adopted in assessing the Tri-Counties operation, though up-wind of the target area, is subject to a somewhat different climatological regime. The sensitivity of the statistical tests may therefore have been somewhat reduced, but the selection of the particular area was necessitated by the fact that more appropriate areas nearer to the target area were known or believed to be the scene of other cloud-seeding work.

On behalf of the Bonneville Power Administration the Water Resources Development Corporation, Denver, carried out a cloud-seeding programme in the Pend Oreille River Basin, N.W. Montana during 21-30 September 1951. Other seeding projects in Montana or neighbouring states were in operation in September, and also in August and October. This work is the subject of a published report (8) by an independent committee consisting of the chairman of the Power Administration and representatives of the Bureau of Reclamation, the Geological Survey and the Weather Bureau. Statistical evaluation was made of precipitation and stream-flow measurements in the seeded area and unseeded areas during the months of seeding and in the same months in a series of years in which no seeding occurred. The precipitation in the period of cloud seeding in 1951 was found to be within the limits of natural variation while the excess of run-off (stream-flow) was significant only in September. On the basis of the analyses made, and in view of the possibility of effects from other seeding activities, the committee decided that a definite conclusion could not be reached that the seeding operation was effective in increasing the run-off in the river basin. In any event, even in ideal conditions, one ten-day period of seeding would be insufficient to justify firm conclusions.

/From

From the preceding paragraphs it is a reasonable inference that the American work there discussed yields no clear evidence that cloud-seeding is effective in increasing the amount of rain. This inference is at variance with widely publicised claims from other sources. Very few detailed reports on operations for which unambiguous success is claimed have been available for examination by the present writer and it is possible here to remark only on the results made public and discussed by one commercial organisation. Irving P. Krick, a leading exponent and practitioner of cloud-seeding, in 1949-50 established the American Institute of Aerological Research and the Water Resources Development Corporation, Denver, to undertake work in this field. A 35-page record of a statement by Krick in April 1951 before sub-committees of the U.S. Senate, published in the official report (9), gives much information on the operational organisation and methods of the Corporation and refers to several occasions when cloud-seeding operations in different parts of the United States are considered to have succeeded. Some of these occasions have also been reported separately, and in rather more detail, elsewhere. The Corporation's operations depend on the use of silver iodide emitted from ground generators positioned according to local circumstances and the weather situation at the time. Current weather developments are closely studied and seeding effort is directed specially to weather systems which are most likely to yield rain naturally. One instance presented in reference (9) relates to the seeding of persistent clouds in winter 1950 over the high mountain areas of Colorado with the object to build up snowpack and so to provide storage water for irrigation in the lower plateau region in later months. On December 15, after seedings during six weeks, the water content of the snowpack in the seeded region was 7.6 inches as compared with the normal value of 7.9 inches on February 1: the absolute maximum value at the centre of the operational area is said to have been 250 per cent. of normal as against 25 per cent. of normal in areas to the south and unaffected by seeding. In (10) I.P. Krick and T.B. Smith assess operations conducted between July and December 1950 in northeast New Mexico (2 months), southeast Colorado (two months) and Oregon (3 months). For each of the seven monthly periods the rainfall measured in the seeded region was compared with the amount which would be expected from statistical relationships between rainfall in the seeded and neighbouring control region during periods of from 23 to 37 years. On this basis, the rainfall in the target region was in excess of expectation in six of the seven months, markedly so in two months. The statistical significance of the positive departures in the six months in relation to occurrences of past years was not investigated, on the grounds that reliable techniques were not available. Claims of success in other operations are presented by Krick in (11). Charts are given of the distribution of rainfall (as percentages of the appropriate average amounts for the month) in and up to about 150 miles around a seeded area of about 1,600 square miles in the Horse Heaven Hills district of the state of Washington for the periods June 6 - 8 and June 11 - 12, 1950. A storm system traversed the district during each of the two seeding periods. The normal (average) monthly rainfall for June in the target area is stated to be about 0.5 inch. The distribution chart for each of the two periods shows a compact pattern with rainfall a maximum of about 200 per cent. of the normal monthly amount at or near the target and decreasing outwards from the centre (rapidly, in some directions) to 50 per cent. or less of normal. Elsewhere (in (9)) it is stated that at one station in the area of seeding the rainfall for June 1950 considerably exceeded the largest amount recorded in June during the previous 36 years. The author states that the distribution pattern is so compact and decisive that it eliminates almost entirely the possibility of occurrence by chance. It may be remarked, however, that not dis-similar patterns do occur on some occasions of localized heavy natural rain, though it may be unusual for two occasions to affect a given locality at an interval of four or five days. In the same paper (11) Krick advocates the use of weather analogues in assessing the results of cloud-seeding a storm system. That is, the amount of rainfall measured in the target area in a particular storm system is to be compared with that measured in the same area during a closely similar storm system

/(unseeded)

(unseeded) selected from past records, or possibly with the average rainfall of several such similar storm systems. He applies this to the seeding of a particular type of storm during a 6-day period of June 1951 in southwest Nebraska. The average storm of the type in question is said to give rain about equal to the average of all rainfall (for the season) in the area. An individual type analogue (unseeded) in six days of June 1948 gave about 180 per cent. of the average rain and the seeded storm of June 1951 nearly 400 per cent. The author concludes that a good portion of this increment in the June 1951 storm must be credited to the effectiveness of the cloud-seeding operation. The author recognises that the perfect analogue to a given weather system probably cannot be found, but it must be remarked that this method of assessing the results of cloud-seeding will not inspire confidence unless full information is made available on the variability of rainfall amounts associated with a sufficiently large number of storms classified as closely alike. Krick has published (in (12) and the appendix to (9)) a short account of operations undertaken in the Colorado Rockies in the winter months of 1950-51 with the object of increasing the snowpack in the upper watershed of the Arkansas River and others. As it was not feasible to compare the water content of snowpack in the seeded area at dates in the late winter with corresponding snowpack data in closely neighbouring unseeded areas, comparison was made with the precipitation measured during winter months at a position upwind of and some 2,000 to 3,000 feet lower than the area of seeding. Reasonably close correlation had been found between the winter precipitation at this position and the snowpack data in the upper Arkansas Basin during the 11 preceding winters. According to the figures in the paper, the snowpack content in the seeded area in February, March, April 1951 was greater proportionately to the value of precipitation in the upwind control position than in the majority of the 11 preceding years, while the total precipitation at the control position in the seeding period was greater than in the same group of months in all except very few of the 11 previous years. While one may agree with the author that these relationships are suggestive of the effectiveness of cloud-seeding, one could wish that it had been possible to present information on the natural variability of the precipitation and snowpack data over a longer period of years. Krick has stated in (9) and (11) that his organisation has no evidence that cloud-seeding with silver iodide can exercise effect on weather at great distances from the operational area.

Under Project Cirrus, which was operated by G.E.C. of America under the sponsorship of the U.S. Signal Corps and Office of Naval Research, regular seedings, at intervals of a week, of silver iodide from a generator at a site in New Mexico were initiated early in December 1949 and maintained, with some changes in programme, until early July 1951. Towards the end of 1950 and during 1951 Irving Langmuir of G.E.C. announced, (13), (14), that from the earliest stage of the periodic seedings a seven-day periodicity in rainfall had developed, and had persisted, over a large area many hundreds of miles northeastward of New Mexico: and moreover that a similar periodicity in upper air temperature over large areas and the strength of the south-north component of the air circulation across the head of the Gulf of Mexico had been found. Various meteorologists in America, e.g. in (15) and (16), criticised Langmuir's deductions on periodicity in weather elements on the ground that his periodicity was no more significant in the statistical sense than 7-day periodicities which have occurred naturally from time to time in weather elements in previous years before the introduction of cloud-seeding operations. Although this complicated question of the reality of large-scale effects attributed to seeding has been further and extensively investigated by Langmuir (17) and the U.S. Weather Bureau (18), it is believed that the difference of opinion or interpretation persists. Langmuir does not suggest that long-distance and wide-area effects on weather which he describes were caused by direct action of silver iodide more than a thousand miles from the point of release, but rather that some of the silver iodide perhaps drifted eastwards from New Mexico towards the Mississippi region, caused widespread showers there in moister, cloudier conditions and that the latent heat so released was responsible in some way for promoting the

periodic development of 'storm' circulations which, travelling north or northeast, gave rise to the periodic fluctuations in weather in the north-east of U.S.A. It may be noted that even if the attribution of weather fluctuations of 7-day period in many areas of the country to 7-day seedings in New Mexico were shown to be unwarranted, it would not necessarily follow that seeding with silver iodide is non-effective in causing rainfall in the immediate area of release of the material.

Australia

Mention has been made in the early part of para. 3(c) of the results obtained by C.S.I.R.O., Australia in experiments to seed suitable cloud in the Sydney area with dry ice. It is estimated that suitable opportunities for rain making in that area occur about 30 times a year, though with marked variations from year to year. Suitable meteorological conditions for rain making attempts are discussed in (19). Full quantitative information on the rainfall measured on occasions of seeding appears not to be available. From some 20 or 30 experiments in which silver iodide was dispensed, within cloud, from aircraft it was concluded that this agent, applied in this way, is probably less effective than dry ice (20). The possibilities of rain making by means of silver iodide emitted from a ground generator were examined in July to September 1951 in an area 500 miles west of Sydney in which prevailing winds are very persistent in direction. The rain measured during the period in the downwind quadrant (of a circle of 50 miles radius centred at the generator) slightly exceeded that in the other quadrants but the magnitude of the excess was less than the normal variability between the rainfall measured in the quadrants. C.S.I.R.O. have also experimented (20), (21) with the spraying of suitable cumulus-type clouds with water droplets (see para. 3(b)(iii)). In 10 experiments out of 11, distinct changes in the cloud followed the injection of water spray, while precipitation fell from the treated cloud in eight of the cases but reached the ground in only four. No other clouds in the vicinity produced precipitation for at least two hours after an experiment.

Other countries

Some reports of cloud-seeding in other countries are available (e.g., Canada, France, India, Israel, South Africa and United Kingdom), but are not considered to contain information which adds materially to that given in this memorandum.

4. Conclusions.

Though there may be differences of scientific opinion as to the exact physical mechanism by which dry ice and silver iodide, when introduced into supercooled cloud, lead to the formation of ice crystals in the cloud, it is accepted that dry ice and, perhaps less certainly, silver iodide can initiate precipitation from suitable supercooled cloud in favourable circumstances. With either agent, only the slightest precipitation (if any) is to be expected if the treated cloud is unsubstantial and unlikely to yield precipitation naturally: the main result (if any) would be the dissipation of the cloud.

There is evidence, less extensive, that spraying fine water drops of suitable size into cumulus cloud of sufficient vertical depth will cause showers to fall from the cloud. There is also some published evidence, slighter as yet, that the introduction of finely ground hygroscopic substances into cumulus cloud of sufficient vertical extent may be effective in promoting rain. On current ideas these last two methods, if confirmed, would have special application to cloud at temperatures higher than 0°C and therefore to rain-making attempts in the warmer regions of the world.

/The

The crucial issue is whether the seeding of cloud over or about to traverse a given locality results in more precipitation on that locality than would have occurred in the absence of seeding. A rigorously absolutely certain answer to this question is unlikely. For the present, any considered and unbiased answer must depend on assessment of probability by critical examination of accurate and adequate factual date. The reports of seeding experiments and operations summarised in para. 3 are believed to be reasonably representative of the general situation and indicate some of the difficulties which beset the assessment of the effects of cloud seeding. The statistical comparison method necessary in judging the effects of a sustained series of seeding operations on precipitation, snowpack or riverflow involves consideration of the natural variability of these items as between the area of operations and neighbouring areas of similar climate - and this is a problem in itself. It is noted in para. 3 that the period of years and the density of observational data used in these comparisons can materially affect the answer obtained. It is not unlikely that in some of the investigations quoted the observational data used were insufficient or otherwise inadequate for the purpose, perhaps unavoidably.

The first four paragraphs on American work in para. 3 refer to area seeding operations mainly extending through periods of months and, in two instances, in more than one year. Considered together, the results of the investigations afford little, if any, certain support to the view that the operations were effective in increasing the amount of precipitation. The two seasons' work in East Africa and the three months' trial of area seeding by silver iodide in Australia yielded no clear evidence of the effectiveness of seeding. The fifth paragraph on American work quotes several results reported by Krick and, with one exception, put forward as evidence of clearly positive effects of seeding. Only one of these reports by Krick is presented in the statistical form directly comparable with that adopted in the other four American reports mentioned, and it shows that in six of the seven months of seeding operations considered the amount of rainfall in the area of operations exceeded the probable amount of natural rainfall to be expected on the basis of statistical relationships between rainfall in the operational and comparison areas in past years. It does not appear possible, from the information available, to reach a conclusion as to the reason for the difference between Krick's results and those which emerged from the four other American investigations mentioned. One may speculate as to the relative effectiveness of the techniques of seeding employed by the different operators. It may be that on some occasions seeding inhibits rather than promotes precipitation and that the relative incidence of these opposed effects in different series of operations may explain in part the differences in the results obtained. Some methods used in assessment of the effects of seeding seem less reliable than others. Some claims of successes achieved in rain-making attempts require to be supported by more detailed information before they can be regarded as convincing. There is need for further experiments or operations, carefully planned and controlled; and, not least important, objectively assessed.

The discussion of the reported results considered does not lead to a definite unqualified answer to the main question. This position may be changed as further information becomes available. It seems at present that cloud seeding may result in some increase in precipitation on some occasions, but there is uncertainty as to the magnitude of the effect and as to the dependability of the method on a given occasion.

References

1. R.D. Coons, E.L. Jones and R. Gunn. Second partial report on the artificial production of precipitation - cumuliform clouds - Ohio - 1948. Bull. Amer. Met. Soc. 29: p. 544, Dec. 1948.

2. D.A. Davies, D. Hepburn and H.W. Sansom. Report on experiments at Kongwa on artificial stimulation of rain January - April 1951. East African Meteorological Department Memoirs, Vol. 2, No. 9, 1951.

3. D.A. Davies, D. Hepburn and H.W. Sansom. Report on experiments at Kongwa on artificial stimulation of rain January - April 1952. East African Meteorological Department Memoirs, Vol. 2, No. 10, 1952.

4. Ferguson Hall, T.J. Henderson and S.A. Cundiff. Cloud Seeding Operations in the Bishop Creek, California Watershed. U.S. Weather Bureau Research Paper No. 36, 1953.

5. P.B. MacCready, Jr. Results of Cloud Seeding in Central Arizona, Winter 1951. Bull. Amer. Met. Soc., 33: p. 48, Feb. 1952.

6. G.W. Brier and I. Enger. An analysis of the results of the 1951 cloud seeding operations in Central Arizona. Bull. Amer. Met. Soc., 33: p. 208, May 1952.

7. R.T. Beaumont. Cloud-seeding analysis in Oregon. Bull. Amer. Met. Soc., 34: p. 298, September 1953.

8. Report on Bonneville Power Administration Cloud-Seeding Operations. U.S. Department of Interior, July 1952.

9. Weather Control and Augmented Potable Water Supply. Joint hearings before subcommittees of the Committees on Interior and Insular Affairs, Interstate and Foreign Commerce, and Agriculture and Forestry. U.S. Senate, 82 Congress, 1. U.S. Government Printing Office, 1951.

10. I.P. Krick and T.B. Smith. Some evaluations of sustained cloud-seeding operations. Trans. Amer. Geophys. Un. 33: p.53, Feb. 1952.

11. I.P. Krick. Increasing water resources through weather modification. J. Amer. Water Works Assoc. 44: p. 996, Nov. 1952.

12. I.P. Krick. Snow pack increase in the Colorado Rockies by artificial nucleation. Western Snow Conference at Victoria, B.C., April 1951, p. 108.

13. I. Langmuir. A seven-day periodicity in weather in the United States during April, 1950. Bull. Amer. Met. Soc. 31: p. 386, Dec. 1950.

14. I. Langmuir. Cloud-seeding by means of dry ice, silver iodide and sodium chloride. Trans. N.Y. Acad. Sci. 14: p. 40, Nov. 1951.

15. Wm. Lewis. On a seven-day periodicity. Bull. Amer. Met. Soc. 32: p. 192, May 1951.

16. E. Wahl. On a seven-day periodicity in weather in the United States in April, 1950. Bull. Amer. Met. Soc. 32: p. 193, May 1951.

17. I. Langmuir. Analysis of the effects of periodic seeding of the atmosphere with silver iodide. Final Report - Project Cirrus, Part II, May 1953. G.E.C. Report No. R.L. -785.

18. Ferguson Hall. An evaluation of the technique of cloud seeding to date. Trans. N.Y. Acad. Sci. Ser. II, 14: p. 45, Nov. 1951.

19. E.J. Smith. The influence of meteorological conditions on rain making in the Sydney area. Aust. J. Sci. Res. A5: p. 87, March 1952.

20. E.G. Bowen. Australian experiments in artificial rainmaking. Bull. Amer. Met. Soc. 33: p. 244, June 1952.

21. E.G. Bowen. A new method of stimulating convective clouds to produce rain and hail. Q.J.R. Met. Soc., 78: p. 37, 1952.

Control Number

[illegible] No. 658 by Mr. J. MacDowall
A copy is available in the Library
of the Meteorological Office."

[illegible]

[illegible] is designed to measure the net flow of radiation through [illegible]. In principle the method of doing this is quite [illegible] place a horizontal plate, which is blackened on both [illegible] surface (see appendix I). The problem is [illegible] when a device of this sort is used in the open for [illegible]s, firstly, because of the wide range of wavelength [illegible] found to eliminate the effect of the wind blowing on [illegible] and causing large variations in the energy interchange between the [illegible] of the plate and the air. It is not possible to enclose the plate [illegible]y whilst still satisfying the first requirement, because there is no [illegible] interest, i.e. from about [illegible] [illegible]oming this difficulty is to ensure, by artificial means, that [illegible] equally over the plate, keeps the energy interchange between the [illegible] of the plate and the air at a high level which is not appreciably [illegible]red when the free wind varies. With this radiometer the response is [illegible] Instruments of this type have [illegible]structed by G. Falkenberg (1) and independently by W. Mörikofer [illegible] In G. Falkenberg's "vibration-pyranometer" the effect was [illegible] by rapidly vibrating the horizontal plate in its own plane, so that [illegible] calm conditions it was effectively operating in rapidly moving [illegible] other two instruments used a stationary plate ventilated by a small [illegible] instrument to be described is very similar to J.T. Gier's which [illegible]d commercially in the U.S.A. As the instrument is by no means [illegible]

Ferguson Hall, T.J. Henderson and S.A. Cundiff. [illegible] in the Bishop Creek, California Watershed. U.S. [illegible] Paper No. 36, 1953.

5. P.B. MacCready, Jr. Results of Cloud Seeding in C[illegible]

6. G.T. Drier and I. Enger. An analysis of the results of [illegible] seeding operations in Central Arizona. Bull. Amer. Met. Soc. [illegible] p. 206, May 1952.

Soc., 34: p. 2[illegible], September [illegible].

[illegible]

Before subcommittees of the Committee [illegible]

[illegible]

12. [illegible]

[illegible]

14. [illegible]

[illegible]

April, 1950. Bull. Amer. Met. Soc. 32: p. 193, [illegible]

I. Langmuir. Analysis of the effects of pe[illegible] with silver iodide. Final Report - Project Ci[illegible]

[illegible]

20. E.C. Bowen. [illegible] Amer. Met. Soc. [illegible]

C.P. 8053

At the time of issue this report has not been published. Any author desiring to quote this paper should refer to it as "A paper of the Meteorological Research Committee (London), M.R.P. No. 858 by Mr. J. MacDowall A copy is available in the Library of the Meteorological Office."

M.R.P. 858

S.C.I./85

24th March, 1954

AD22-3071
MATS

AIR MINISTRY

METEOROLOGICAL RESEARCH COMMITTEE

A Total Radiation Fluxmeter

by

J. MacDowall (Meteorological Office)

I. Introduction

This instrument is designed to measure the net flow of radiation through a horizontal surface. In principle the method of doing this is quite simple; one has only to place a horizontal plate, which is blackened on both surfaces, in this radiation field and then to measure the temperature difference between the upper and lower surface (see appendix I). The problem is complicated somewhat when a device of this sort is used in the open for meteorological purposes, firstly, because of the wide range of wavelength to which the instrument must respond with equal sensitivity and secondly, because a means must be found to eliminate the effect of the wind blowing on the plate and causing large variations in the energy interchange between the surfaces of the plate and the air. It is not possible to enclose the plate completely whilst still satisfying the first requirement, because there is no readily available material equally transparent over the wavelength range of meteorological interest, i.e. from about 0.3 μ to beyond 40 μ. The device for overcoming this difficulty is to ensure, by artificial means, that the plate is always operating in a blast of air. This sustained blast, directed equally over the plate, keeps the energy interchange between the surfaces of the plate and the air at a high level which is not appreciably altered when the free wind varies. With this radiometer the response is kept constant to 2% in winds up to 20 m.p.h. Instruments of this type have been constructed by G. Falkenberg (1) and independently by W. Mörikofer (2) and J.T. Gier (3). In G. Falkenberg's "vibration-pyranometer" the effect was obtained by rapidly vibrating the horizontal plate in its own plane, so that even under calm conditions it was effectively operating in rapidly moving air. The other two instruments used a stationary plate ventilated by a small blower. The instrument to be described is very similar to J.T. Gier's which is now produced commercially in the U.S.A. As the instrument is by no means new the emphasis of this paper is on the special problems of calibration and an examination of its behaviour in use.

II. Construction

(a) General

The instrument consists of three parts: the radiation sensitive element in the form of a thin 3 in. square plate, a blower to maintain the steady blast of air, a nozzle which directs the air from the blower symmetrically over the upper and lower surfaces of the element. A photograph of the complete

/radiometer

A-10

radiometer is shown in figure 1 and the radiometer is drawn to scale in figure 2. It will be noticed that the sides of the nozzle are extended alongside the element by two side plates marked D D^1 in figure 2. The function of these is to constrain the air flow over the element and to provide a little protection against deflection of the blast by broadside winds. W. Mörikofer at the 1951 U.G.G.I. meeting maintained that it was essential to use an aerodynamically-shaped nozzle and an element in the form of an aerofoil. This instrument is not aerodynamically designed but it was found most important for the disposition of the element, side plates and nozzle mouth to be symmetrical about a plane through the centre of the element. Any inaccuracy in this arrangement, or any asymmetry in the design of one of these parts, will lead to incomplete wind compensation (see III (a)). Power for the blower was drawn from the mains and regulated with a simple carbon pile voltage regulator to 24±1 volts. A variation in the voltage of this size was found to keep the ventilation velocity constant to 0.7%.

(b) The Sensitive Element

Figure 3 shows the radiometer element in more detail. It has a sandwich-like structure, bakelite in the centre with 1/100 in. sheet aluminium on top and bottom. The aluminium surfaces are separated from the bakelite core by thin sheet polythene. Two slots are cut out of the central bakelite sheet forming a frame for the thermopile. This is made by winding about 60 turns of 46 S.W.G. constantan wire around bakelite strips whose size is slightly smaller than the slots in the bakelite frame. One half of each turn of wire on the strips is copper plated, so that a series of copper-constantan thermojunctions is formed down the centre line of the top and bottom surfaces of each strip. These thermopile strips fit inside the bakelite frame and the connections between the strips and to the external leads are made to the copper plated part of the last turn on each strip. The whole sandwich is stuck together with Everett's wax. When the element is mounted in position at the mouth of the nozzle, Parson's optical black is used to paint the aluminium surfaces.

III. Characteristics of the Radiometer

(a) Effect of wind speed on the sensitivity

The effect of wind was examined in the laboratory by placing the radiometer in a crude wind tunnel formed by the floor, a large horizontal plane and a powerful blower. By altering the distance between the radiometer and this blower different wind speeds could be simulated. A 2000 watt tungsten filament lamp, whose supply was hand regulated, provided a constant source of radiation. In figure 5 is shown the arrangement for this experiment. Two positions of the radiometer were tested:

A. Wind in opposition to radiometer ventilation.
B. Wind at right angles to radiometer ventilation.

In figure 6 the percentage change in the output of the radiometer is plotted against the wind speed for the two positions A and B. The dotted curve shows the result of a similar experiment performed by G. Falkenberg with his "vibration pyranometer", and table I gives J.T. Gier's figures.

TABLE I

Position A		Position B	
Wind speed m.p.h.	% change	Wind speed m.p.h.	% change
5.7	4.8	7.3	-2.5
11.4	0.0	9.8	-3.4
15.0	-2.5	15.3	-4.2
19.8	-16.0	20.5	-6.3
25.0	-11.0	23.6	-8.3
27.6	-11.0		

/During

During the course of this experiment the importance of correctly aligning the position of the element, nozzle and side plates was discovered. More extensive wind tunnel tests were performed with a mark II instrument of larger design and without the protective side plates. This instrument was tested in position B (see above). If the radiometer blast of air is moving south then the wind directions used were east and west. In each run the surface of the radiometer was set horizontal with a small spirit level and the four possible positions for the radiometer, satisfying the general classification B, were tried. For each of these four positions the lamp was moved from above the radiometer to below it. The reasons for all these different positions were:
(a) although it is simple to set the radiometer surface horizontal it was not certain that the flow of air in the wind tunnel was truly horizontal,
(b) to find if a difference existed between effect of an E. and W. wind,
(c) to find if there was an effect depending on the direction of flux through the radiometer. By taking means of experiments done under identical conditions with respect to coordinates fixed on the radiometer, any contribution due to a wind component perpendicular to the element could be eliminated. From these results the effect for an east and west wind was deduced, and little effect due to flux direction was found. Unfortunately it was not possible to estimate the angle between the wind tunnel stream and the horizontal, but its effects were not significant below wind speeds of 16 m.p.h. and even then were only of the order of 1%. In table II are the results of this experiment. Each table is labelled with respect to axes fixed in the radiometer. It is assumed that the wind tunnel flow, which is nominally parallel to the radiometer element, has a component perpendicular to the element. Each experiment is classified X or Y according to whether this component is in the same direction or the opposite direction to the flow of radiation. Then the mean of run 1 and run 3a gives the true effect of an east windwith positive flux. The mean of run 1a and run 3 gives the effect of an east wind with negative flux. Similarly for the west wind runs.

TABLE II

East Wind Runs

Wind Speed	Run 1 East Wind +ve flux Class X	Run 1a East Wind -ve flux Class Y	Run 3a East Wind +ve flux Class Y	Run 3 East Wind -ve flux Class X	Mean of Runs 1, 3a East Wind +ve flux	Mean of Runs 1a, 3 East Wind -ve flux
m.p.h.	%	%	%	%	%	%
00.0	100	100	100	100	100	100
05.0	100.4	99.5	99.4	99.8	99.2	99.7
10.2	99.9	98.9	99.4	99.8	99.2	99.4
16.0	98.5	98.7	99.6	97.2	99.0	98.0
20.5	97.8	98.7	100.3	98.8	99.0	98.8
24.5	96.6	101.5	101.5	99.4	99.0	100.5
29.3	97.7	103.1	102.6	100.5	100.1	101.8
34.5		102.6		100.5		

West Wind Runs

Wind Speed	Run 2 West Wind +ve flux Class Y	Run 2a West Wind -ve flux Class X	Run 4a West Wind +ve flux Class X	Run 4 West Wind -ve flux Class Y	Mean of Runs 2, 4a West Wind +ve flux	Mean of Runs 2a, 4 West Wind -ve flux
m.p.h.	%	%	%	%	%	%
00.0	100	100	100	100	100	100
05.0	99.4	99.8	100.2	99.4	99.8	99.6
10.2	99.0	100.0	99.8	99.2	99.4	99.6
16.0	98.6	98.6	98.6	98.4	98.6	98.5
20.5	96.9	95.8	98.3	98.4	97.6	97.1
24.5	97.6	95.8	97.3	98.7	97.5	97.3
29.3	97.7	96.6	98.1	98.8	97.9	97.7

/(b)

(b) The aperture of the Radiometer

The amount of the sphere that can be "seen" by the element is defined on two sides by the side plates and on the third side by the leading edge of the nozzle; the fourth side is unobstructed. Figure 4 shows how on three sides the sensitive central area of the element will only partly "see" portions of the upper hemisphere between +22° and +6° elevation, similarly for the lower hemisphere. No radiation within 6° above and below the horizon is accepted on these three sides. If the radiometer were placed in a field of radiation isotropic over the upper hemisphere, the calculation in appendix II shows that its effective aperture is 97% of the hemisphere. When used in daytime it is undesirable for the shadow of the side plates to be too near the central sensitive area. This instrument was only required to work for periods of about one hour, so it was orientated according to the sun's position.

(c) The paint

The upper and lower surfaces of the radiometer element were painted with Parson's optical black. As was explained in the introduction, this instrument must respond with equal sensitivity over the wavelength range from about 0.3 μ to beyond 40 μ. The emissivity of this paint was determined by the N.P.L. in the visual range and for black body radiation at 2580°C, 1000°C, 200°C. In paragraph IVa it will be shown (equation 3) how, during the course of the calibration, the emissivity of a piece of tinned copper painted with Parson's optical black is determined. The results of this work are shown in table III:

TABLE III

λ max	0.5 μ	1.1 μ	2.4 μ	6.3 μ	10.0 μ
Black Body Temperature	Visual	2580°C	1000°C	200°C	25°C
Emissivity	0.985	0.985	0.980	0.985	0.98
Work done at:	N.P.L.	N.P.L.	N.P.L.	N.P.L.	Kew

(d) Cosine law for surface of Radiometer

When the radiometer is placed in a parallel beam of radiation, the output should be proportional to the cosine of the angle of incidence. Figure 7 shows that this law is obeyed quite well.

IV. Calibration of the Radiometer

For meteorological work this instrument must be equally sensitive to radiation in the wavelength range from about 0.3 μ to 40 μ. The paint used for the surface of the element did not show any appreciable variation of emissivity with wavelength. It was still considered necessary to determine the sensitivity of the radiometer when used in fields of long wave ($> 3\mu$) and short wave (roughly 0.3 μ to 3 μ) radiation, both in the laboratory and in the open. Four separate methods were used, two of them, (a) and (b), in the laboratory with long and short wave radiation respectively. The other two methods were both done in the field, (c) at night when the radiation is long wave only, and (d) during daytime when the radiation is a mixture of long wave atmospheric and terrestrial radiation with short wave solar and sky radiation. The results of these four methods are tabulated in table IV:

/TABLE IV

TABLE IV

	Laboratory Long Wave	Laboratory Short Wave	Field Long Wave	Field Long and Short Wave
Sensitivity μV/m.watt cm^{-2}	66$\pm$1	71$\pm$1	67.4$\pm$0.6	68$\pm$1

Mean 68$\pm$1

(a) Laboratory calibration with long wave radiation

One of the difficulties in calibrating a radiometer with the radiation of a "low" temperature body is to keep radiation from the surroundings constant, also care must be taken to see that no heat is convected (either forced or natural) from the body to one surface of the radiometer. To these ends a copper calibrating box, shown in figure 8, was constructed. This box was painted black on the inside and covered with felt on the outside. In the top of this box a square aperture B was cut and holes were made at each end; one, C, just large enough to allow the radiometer to be placed directly underneath the aperture, the other hole, D, was made to allow air blown through the radiometer to escape. Flaps E E^1 were fitted to the edges of this latter hole and were adjusted so that there was no flow of air through the aperture B when the radiometer was in position and blowing. This condition was determined by placing a thin sheet of paper over the aperture. The efficiency of the box as a radiation enclosure was tested by placing a shutter over the aperture and measuring the output of the radiometer over 24 hours. If left undisturbed for 2 min. to 3 min. the box was found to be effective in so much that it reduced any flux inside the box to less than 0.01 m.watts cm.$^{-2}$. A large cavity black body, used by W.H. Dines, was placed over the aperture. One junction of a calibrated thermocouple, X, was soldered to the calibrating box directly underneath the radiometer, the other junction, Y, was placed in the water bath which surrounded the black body. The dimensions of the aperture, sensitive element and the distance of the radiometer below the aperture were measured. From these measurements the effective aperture, which L. Bossy and R. Pastiels[4] call the "rapport surface-angle", was calculated in the manner shown in appendix II.

Now if
T_1 = Temperature of the cavity black body
T_2 = Temperature of the calibrating box
D = Output of the radiometer
ε = Emissivity of the inside surface of the box
F = Flux of radiation normal to the radiometer surface
ψ = Effective aperture as defined in appendix II
σ = Stefan's constant

Then neglecting water vapour and carbon dioxide absorption, we have:

$$F = \psi\sigma(T_1^4 - \varepsilon T_2^4) \qquad (1)$$

$$= \lambda D \quad \text{from appendix I} \qquad (2)$$

$$\text{therefore } \frac{D}{T_2^4} = \frac{\psi\sigma}{\lambda}\left[\left(\frac{T_1}{T_2}\right)^4 - \varepsilon\right] \qquad (3)$$

Now in the calibration T_1 was varied from 50°C to 25°C and T_2 varied between 20°C and 21°C.

/By plotting

By plotting

$$\frac{D}{T_2^4} \text{ against } \left(\frac{T_1}{T_2}\right)^4$$

we get a straight line and so determine λ and ε , the calibration constant of the radiometer and the emissivity of the bottom surface of the calibrating box. From the air temperature and humidity these values are corrected for the effect of water vapour and carbon dioxide absorption (5).

(b) Laboratory calibration using short wave radiation

The radiation for this calibration was produced by a 2000 watt lamp, and the intensity of the radiation was measured by means of a Linke-Feussner actinometer carefully set at the same distance from the lamp as was the radiometer. When comparing two instruments of such widely differing apertures care must be taken to see that all contributions to the radiation flux through the radiometer are accounted for by the Linke-Feussner actinometer. For although the major part of the radiation field underneath a 2000 watt tungsten filament lamp consists of the short wave radiation from the incandescent filament, there exists an appreciable field of long wave radiation due in the most part to the large and heated box which surrounds the 2000 watt lamp. To eliminate effects of this sort the radiometer was placed (as is shown in figure 9) in between two large sheets of glass, B B^1 in figure 9, which act as a filter opaque to all radiation whose wavelength is greater than about 3μ . Any contribution to the flux of radiation due to a temperature difference between the glass sheets can be measured by reversing the position of the Linke-Feussner actinometer, pointing it first at the lamp through one glass sheet and then at the other glass sheet. The voltage to the lamp was hand regulated and a time schedule was adhered to throughout the experiment because the laboratory warmed up by 2°C during this experiment. The Linke-Feussner actinometer was itself standardised, both on the sun and in the laboratory, against the Angstrom pyrheliometer. The output of the Linke-Feussner actinometer for a radiation intensity of one $g.cal.cm^{-2}$ $min.^{-1}$ was found by these two methods to be 10.8 ± 0.2 m.V and 10.8 ± 0.1 m.V respectively.

(c) Field method at night (Long Wave)

At night the radiation field is purely long wave radiation of atmospheric and terrestrial origin. It is only on cloudless nights, however, that the radiative flux can be measured. This is done by pointing a Linke-Feussner actinometer first at the sky and then at the ground (5) and the result of this measurement was compared with the output of the radiometer.

(d) Field method during the day (Long and Short Wave)

During the day the radiative flux consists of a mixture of short wave radiation from the sun and sky, mixed with atmospheric and terrestrial long wave radiation. The long wave component can only be measured under cloudless conditions. On these days the output of the radiometer was compared in the field with the radiative flux computed by means of a Moll solarimeter and the Linke-Feussner actinometer. By pointing the solarimeter, first at the sky and then at the ground, the flux of short wave radiation was computed. Each component of the long wave radiation was measured by two readings with the actinometer, one using a glass filter and one without the glass filter.

Conclusion

The radiometer provides a convenient method for the measurement of net radiative flux near the ground, and is particularly adapted for continuous measurement. The instrument will not function correctly in rain, or when fog develops, as the surfaces wetted would act as a "wet bulb". Prolonged exposure to rain would entail repainting and subsequent recalibration, but a few drops of rain will dry very rapidly and not cause any lasting effect.

/An

An instrument of this type has been functioning continuously for some time at Kew Observatory and during the first six months' use the calibration constants determined are ±5%.

Acknowledgments

I should like to thank Dr. G.D. Robinson for suggesting that this work should be done and for his constant advice and encouragement.

I am indebted to M.J. Blackwell and J.C. Gordon for their assistance. Valuable help with the field work was given by various members of the staff of Kew Observatory. The instrument was largely constructed in Kew Observatory workshops.

REFERENCES

1. G. Falkenberg. Zeit. fur Met. 1, 11/12, p. 372, (1947).

2. W. Morikofer. Proc. of U.G.G.I., Brussels (not yet published), 1951.

3. J.T. Gier et alia. University of California, thermal radiation project report, (1949).

4. L. Bossy and R. Pastiels. Met. Inst. Roy. Met. de Belgique. Vol.29, (1948).

5. G.D. Robinson. Quart. J.R. met. Soc., 73. 315-316, (1947).

APPENDIX I (After Gier)

Theory of the instrument (after Gier et alia)

In figure 10 let

ε = emissivity of radiometer surfaces
k = thermal conductivity of bakelite
h = thermal convective conductance of air (see footnote)
T_a = air temperature
T_1 = temperature of surface 1 of radiometer
T_2 = temperature of surface 2 of radiometer

Without loss of generality we can consider the radiometer in a parallel stream of radiation, where the flux of radiation $F = G_1 - G_2$ (4)

E.M.F. produced by the thermopile $D = \mu (T_1 - T_2)$ (5)

At surface 1 we have $\varepsilon G_1 = \varepsilon\sigma T_1^4 + h (T_1 - T_a) + \frac{k}{l}(T_1 - T_2)$

At surface 2 we have $\varepsilon G_2 = \varepsilon\sigma T_2^4 + h (T_2 - T_a) - \frac{k}{l}(T_1 - T_2)$

subtracting and using (4)

$$\varepsilon F = \varepsilon\sigma (T_1^4 - T_2^4) + h (T_1 - T_2) + \frac{2k}{l}(T_1 - T_2) \quad (6)$$

as a first approximation, put $T_1^4 - T_2^4 = 4 T_1^3 (T_1 - T_2)$ (7)

$$\therefore F = \left(4\sigma T_1^3 + \frac{h}{\varepsilon} + \frac{2k}{\varepsilon l}\right)(T_1 - T_2) \quad (8)$$

or $$F = \left(4\sigma T_1^3 + \frac{h}{\varepsilon} + \frac{2k}{\varepsilon l}\right)\frac{D}{\mu} = \lambda D \quad (9)$$

In order to estimate the relative importance of the three terms contained within the instrumental constant in square brackets, equation (9), put

σ = 5.7×10^{-5} erg. cm.$^{-2}$ deg.$^{-4}$ sec.$^{-1}$

ε = 1

k = 16,000 erg. cm.$^{-1}$ sec.$^{-1}$ deg.$^{-1}$

T = 300°A

l = 0.1 cm.

h = 50,000 erg. cm.$^{-2}$ sec.$^{-1}$ deg.$^{-1}$

whence

$4\sigma T_1^3$ = 6,200

$\frac{2k}{\varepsilon l}$ = 320,000

$\frac{h}{\varepsilon}$ = 50,000 (see footnote).

Consequently the temperature dependent term is effectively swamped by the other two terms.

Note

This rather unusual term "the thermal convective conductance of air" is not a property of air but of the system. It is an expression widely used by ventilation engineers and can vary within wide limits. J.T. Gier gives a

/value

value of 50,000 erg. $cm.^{-2}$ $sec.^{-1}$ $deg.^{-1}$. An experiment done comparing the sensitivity of this radiometer when the blower was not in operation with the normal sensitivity gives a value for this system of 140,000 erg. $cm.^{-2}$ $sec.^{-1}$ $deg.^{-1}$

APPENDIX II

Effective aperture of the radiometer (Rapport surface - angle of Bossy & Pastiels)

For the laboratory low temperature calibration which is described in paragraph IVa it is required to find the mean flux through the radiometer. In figure 11 HKLM represents the aperture marked 'B' in figure 6 and ABCD is the sensitive area of the radiometer. Consider only that radiation which comes through the aperture from the black body radiator. The intensity, I, of this radiation is uniform and determined by the temperature of the water bath surrounding the black body. Consequently at P on the surface of the radiometer the flow of energy perpendicular to ABCD through the area dx dy contained in a pencil centred at P and circumscribing the area $d\xi d\eta$ about Q is dE,

where $dE = I.dw.dx.dy.\cos i$

and dw = solid angle of the pencil

which $= \dfrac{d\xi.d\eta\cos i}{d^2}$

Therefore
$$dE = \frac{I.\cos^2 i}{d^2}\, dx.dy.d\xi d\eta$$
$$= I.\frac{l^2}{d^4} dx.dy.d\xi d\eta$$

since $\cos^2 i = (l/d)^2$

or $$dE = I.l^2 \; dx.dy.d\xi d\eta \Big/ \left[(\xi-x)^2+(\eta-y)^2+l^2\right]^2$$

So the mean flux E through ABCD

$$E = I.l^2 \int_{-X}^{X}\int_{-Y}^{Y}\int_{-\xi_1}^{\xi_1}\int_{-\eta_1}^{\eta_1} \frac{dx\,dy\,d\xi\,d\eta}{\left[(\xi-x)^2+(\eta-y)^2+l^2\right]^2}$$

Now for an infinitely large aperture

$$E_H = I.l^2 \int_{-X}^{X}\int_{-Y}^{Y}\int_{-\infty}^{\infty}\int_{-\infty}^{\infty} \frac{dx\,dy\,d\xi\,d\eta}{\left[(\xi-x)^2+(\eta-y)^2+l^2\right]^2}$$

We now define

$$\psi = \frac{E}{E_H}$$

Using ψ we can now write down the flux through the radiometer if

T_1 = temperature of the black body over the aperture

T_2 = temperature of the calibrating box

ε = emissivity of the inside of the calibrating box

F = mean flux through the radiometer

$$F = \psi\sigma T_1^4 + (1-\psi)\varepsilon\sigma T_2^4 - \varepsilon\sigma T_2^4$$
$$= \psi\sigma\left[T_1^4 - \varepsilon T_2^4\right]$$ as in equation (1), paragraph IVa.

/NOTE

NOTE

I would like to draw attention to the following misprints in Bossy and Pastiels

(a) p. 19, line 6. For $2Evw$ read $2Etv$

(b) p. 105, line 6. For $\frac{E\ell^2 dx dY}{2\left[(x-Y)^2+\ell^2\right]^{3/2}}$ read $\frac{E\ell^2 dx dY}{2\left[(y-Y)^2+\ell^2\right]^{3/2}}$

(c) p. 108, line 6. For

$$+(t+v)\log\left[(v-w)^2+(t+v)^2+\ell^2\right]$$

read

$$-(t+v)\log\left[(v-w)^2+(t+v)^2+\ell^2\right]$$

(d) p.108, line 15. For

$$-\sqrt{(t-v)^2+\ell^2} \quad \text{read} \quad +\sqrt{(t-v)^2+\ell^2}$$

(e) p.108, line 18. For

$$+\sqrt{(t-v)^2+\ell^2}\log\left[(v-w)^2+(t-v)^2+\ell^2\right]$$

read

$$-\sqrt{(t-v)^2+\ell^2}\log\left[(v-w)^2+(t-v)^2+\ell^2\right]$$

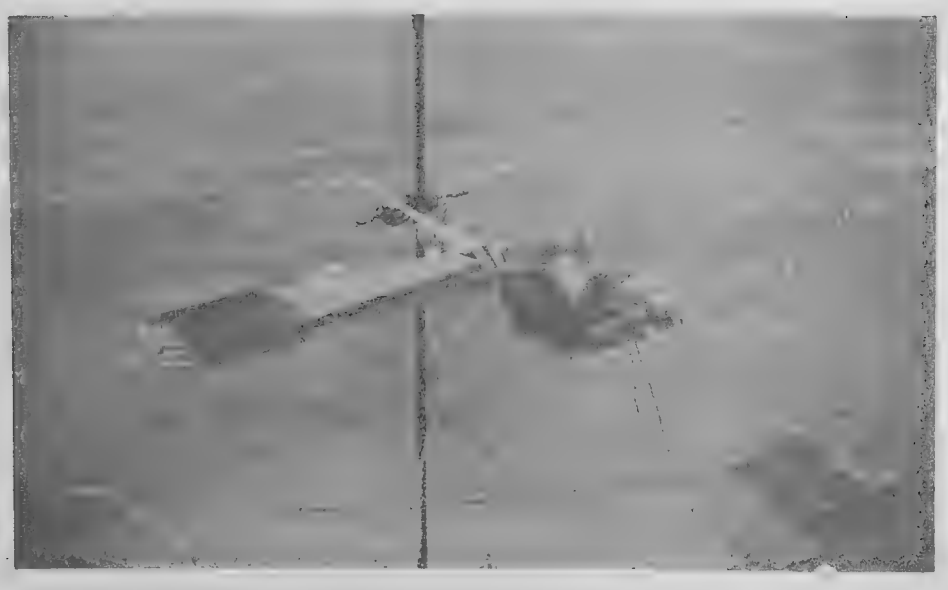

Fig. 1 Complete radiometer.

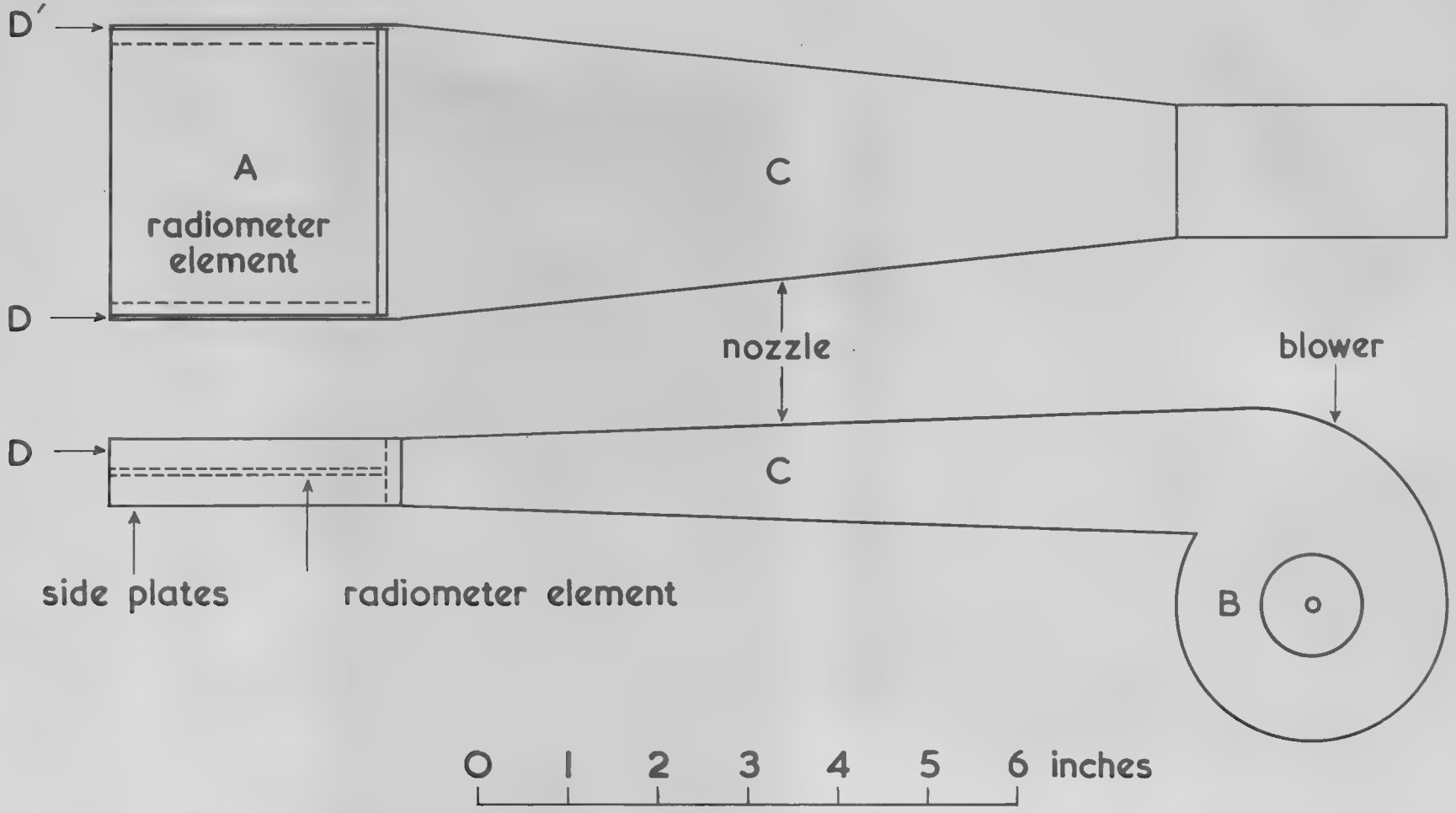

Fig. 2 Complete radiometer

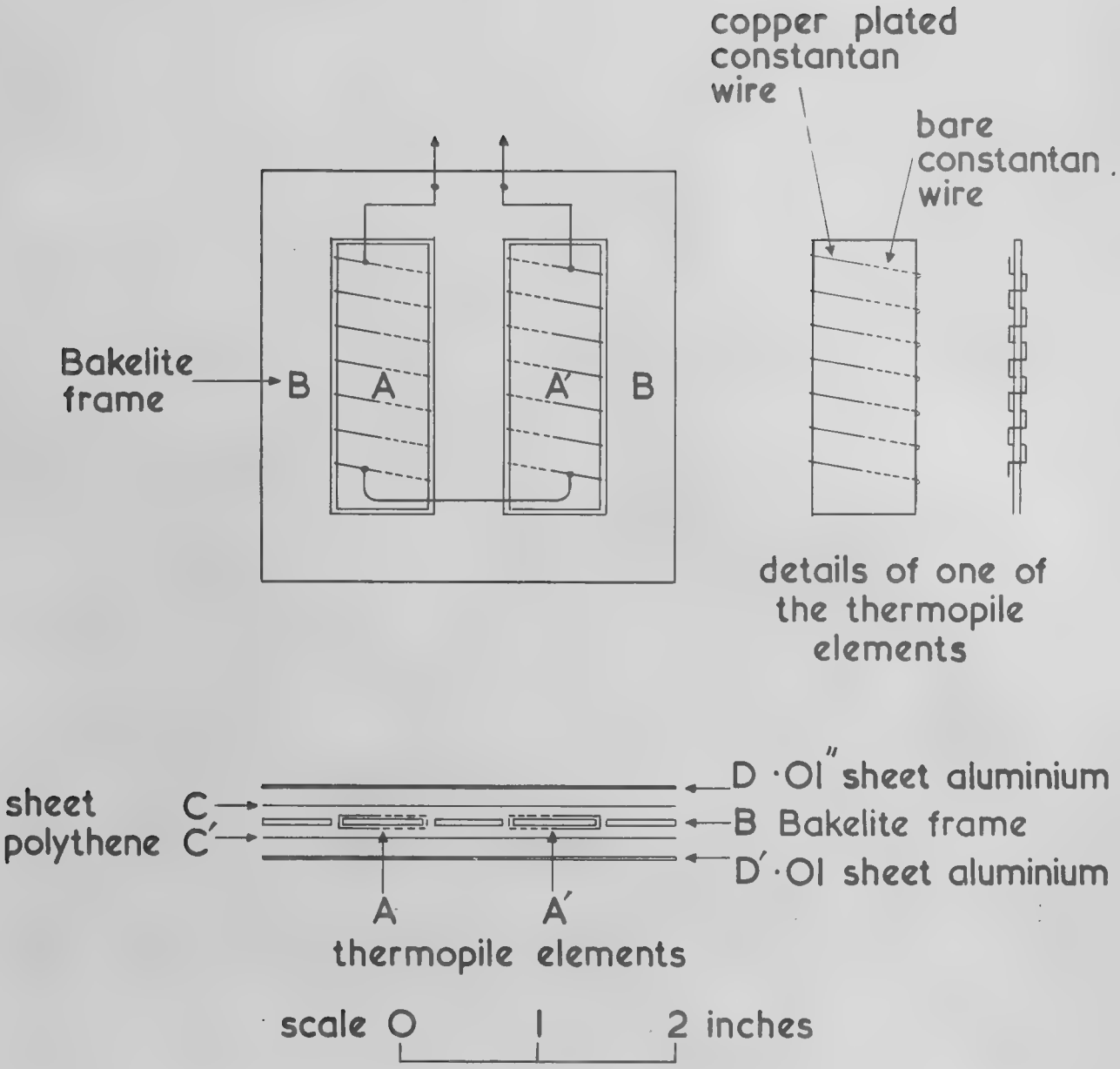

Fig. 3 Radiometer element

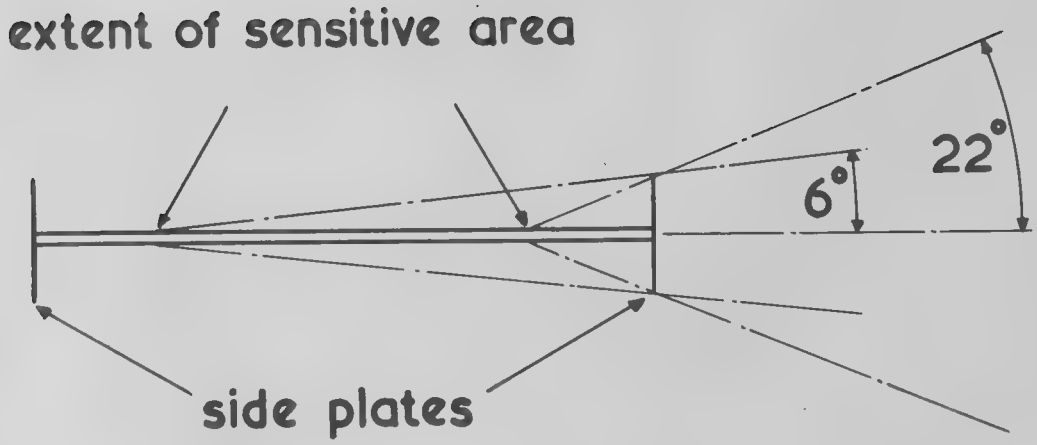

Fig. 4 Aperture of the radiometer

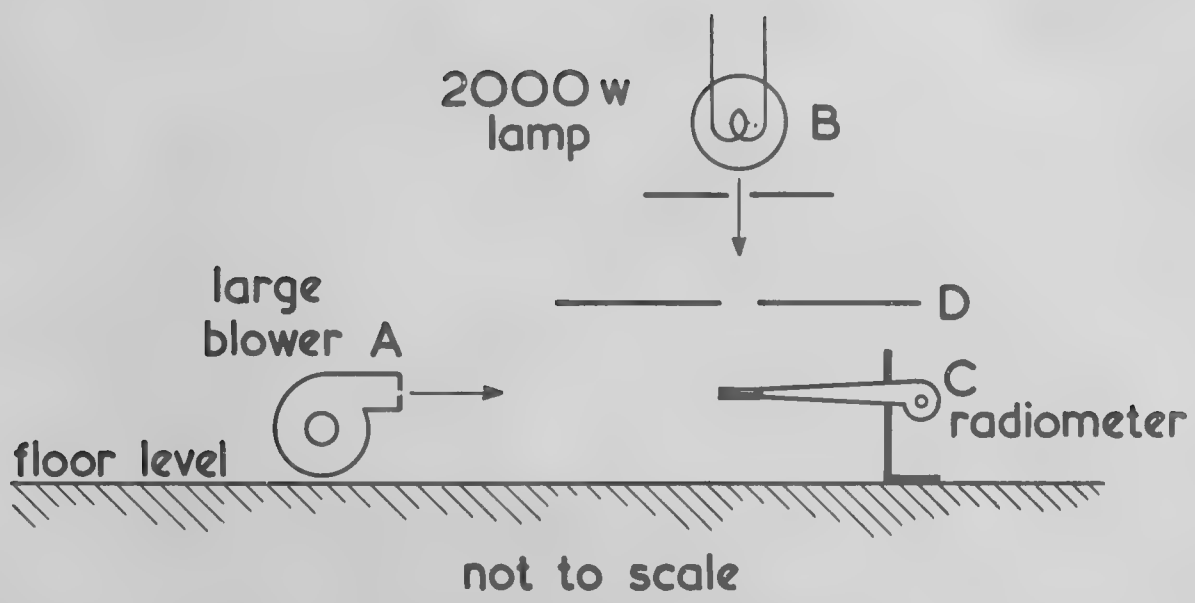

Fig. 5 Experimental arrangement for the determination of wind effect

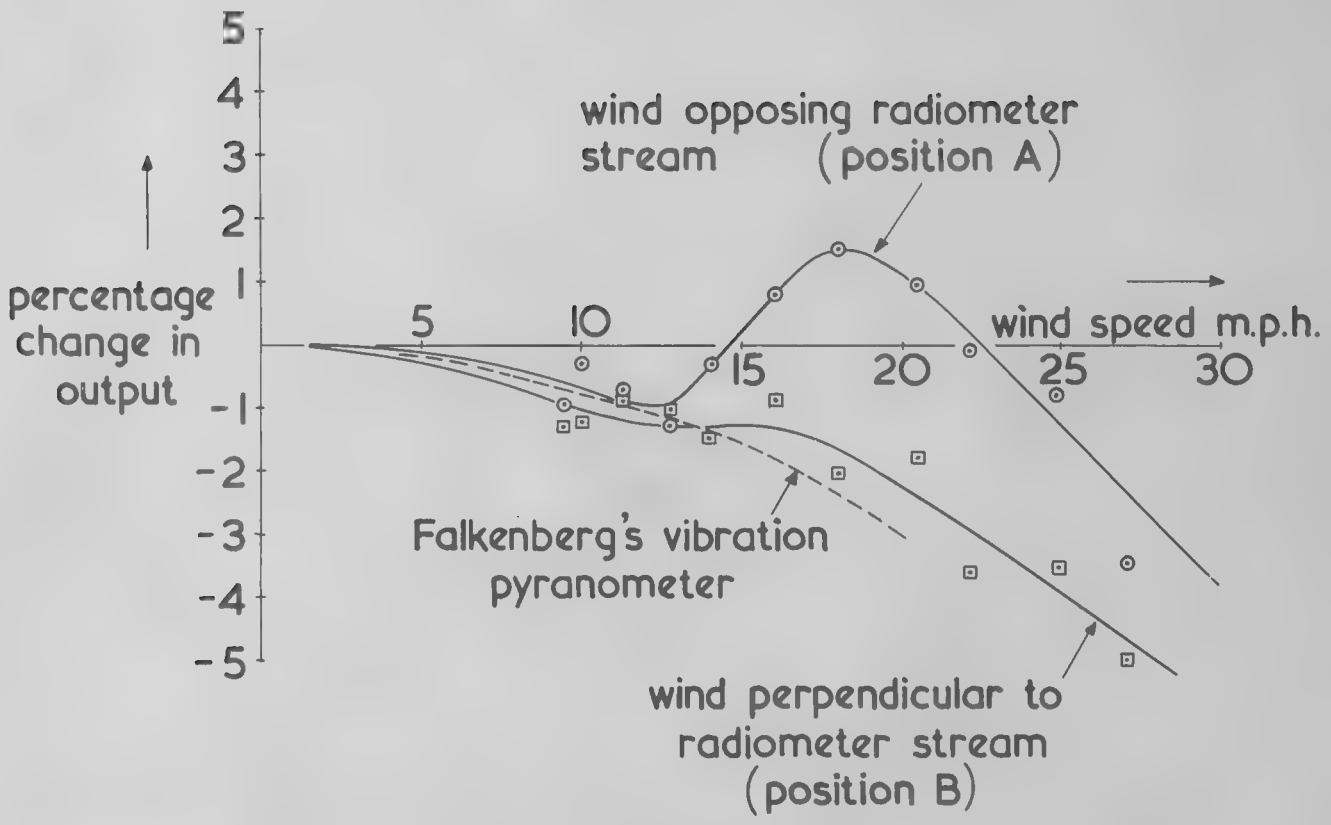

Fig. 6 Effect of wind

position A	
velocity	% change
5·7 m.p.h.	4·8
11·4 ,,	0·0
15·0 ,,	-2·5
19·8 ,,	-16·0
25·0 ,,	-11·0
27·6 ,,	-11·0

position B	
velocity	% change
7·3 m.p.h.	-2·5
9·8 ,,	-3·4
15·3 ,,	-4·2
20·5 ,,	-6·3
23·6 ,,	-8·3

Table I Effect of wind on Gier's radiometer

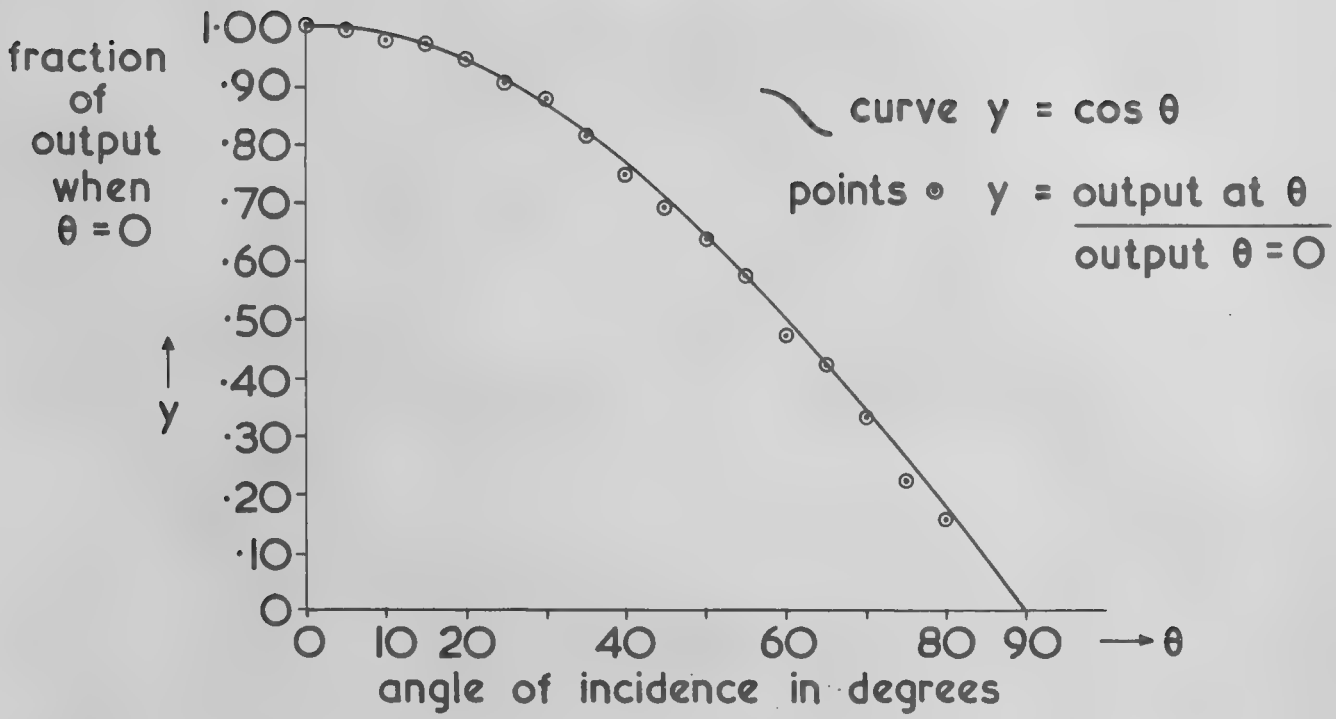

Fig. 7 Cosine characteristic of surface

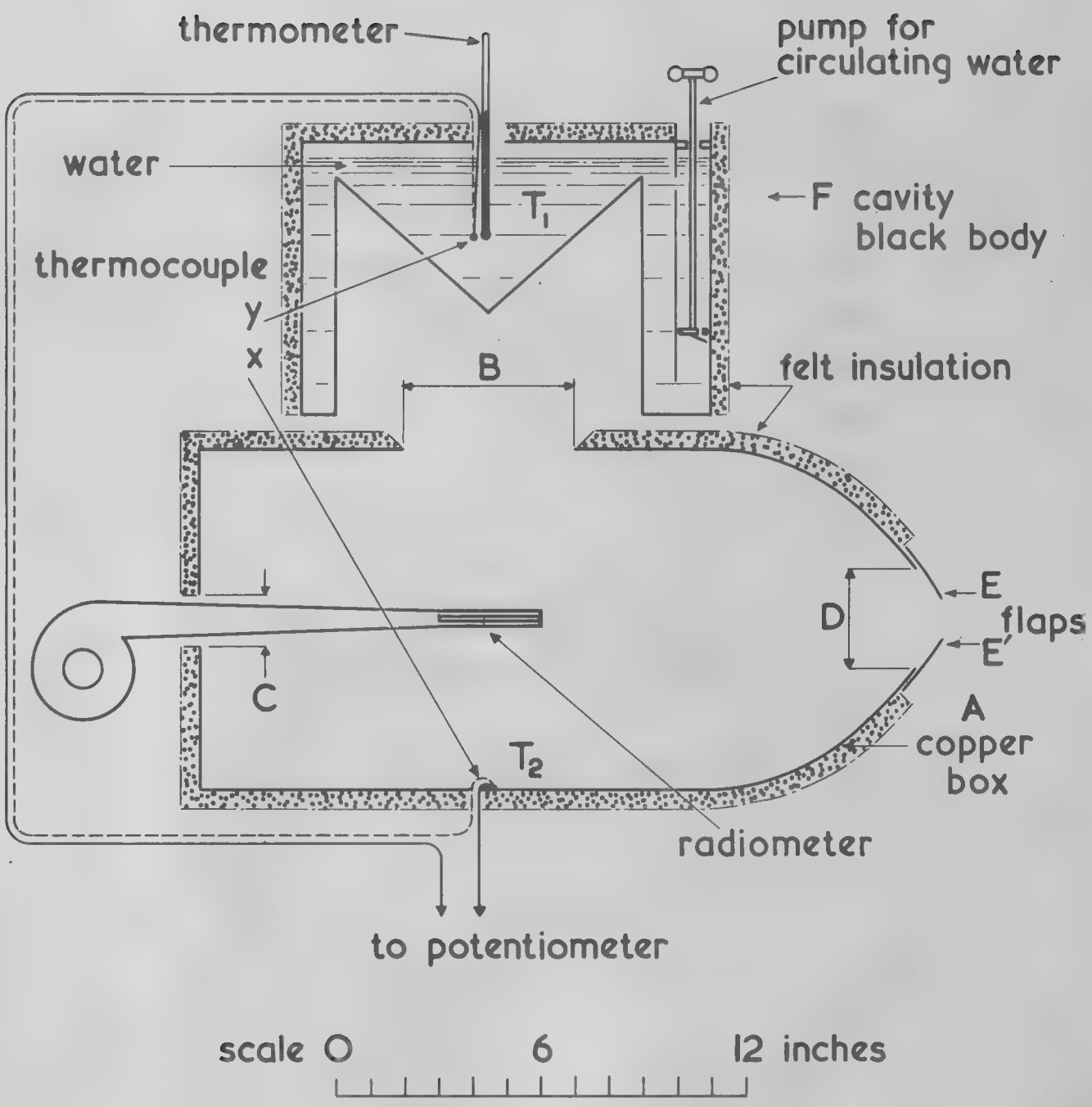

Fig. 8 Radiometer calibration

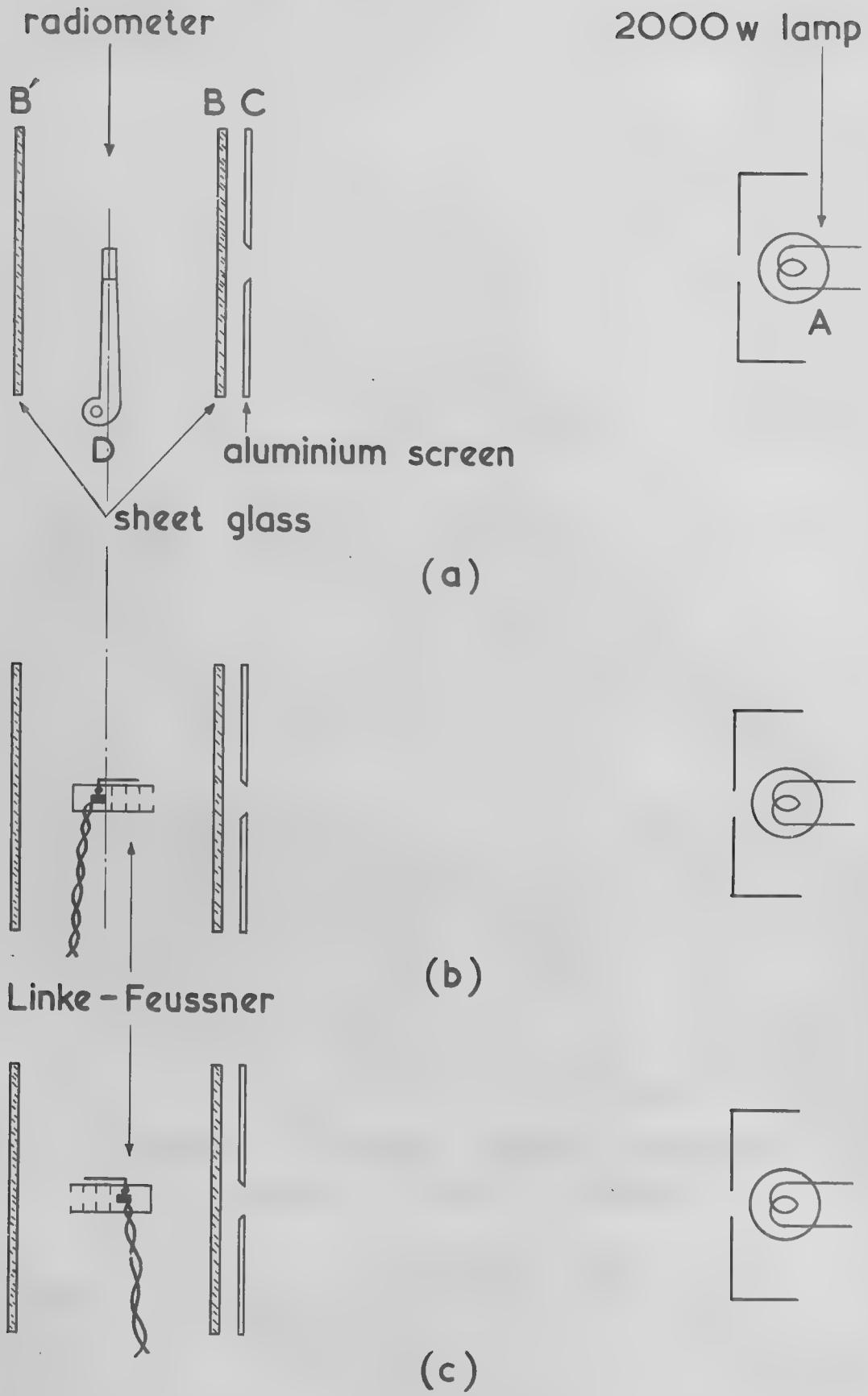

Fig. 9 Radiometer calibration

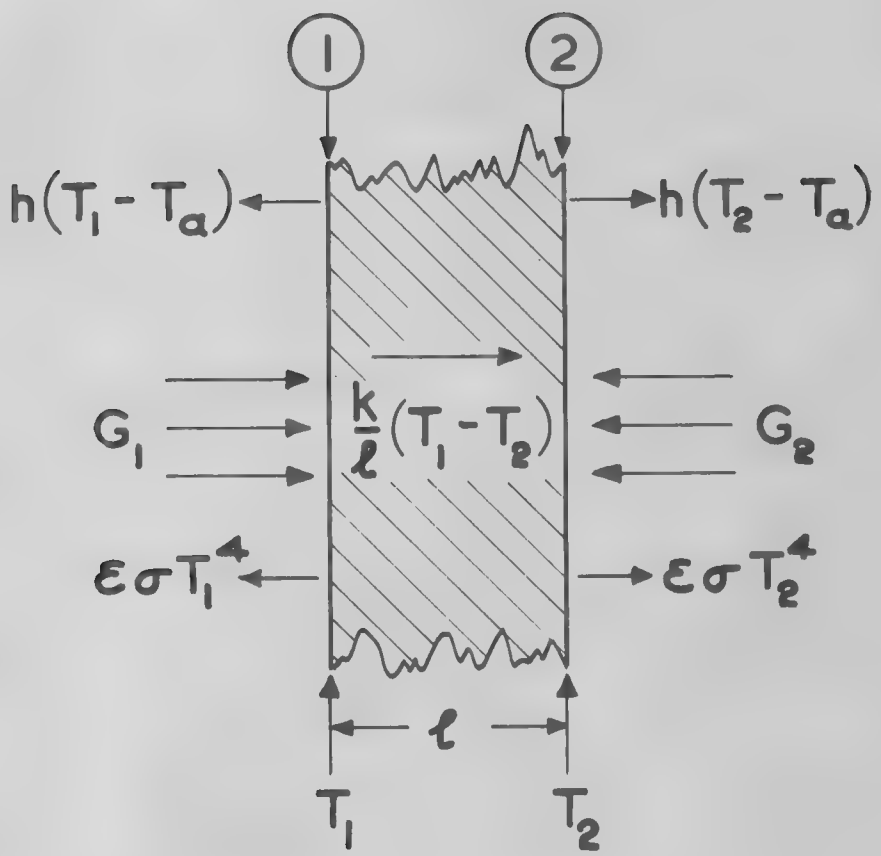

Fig. 10 Enlarged section through radiometer perpendicular to its surface

(see appendix I)

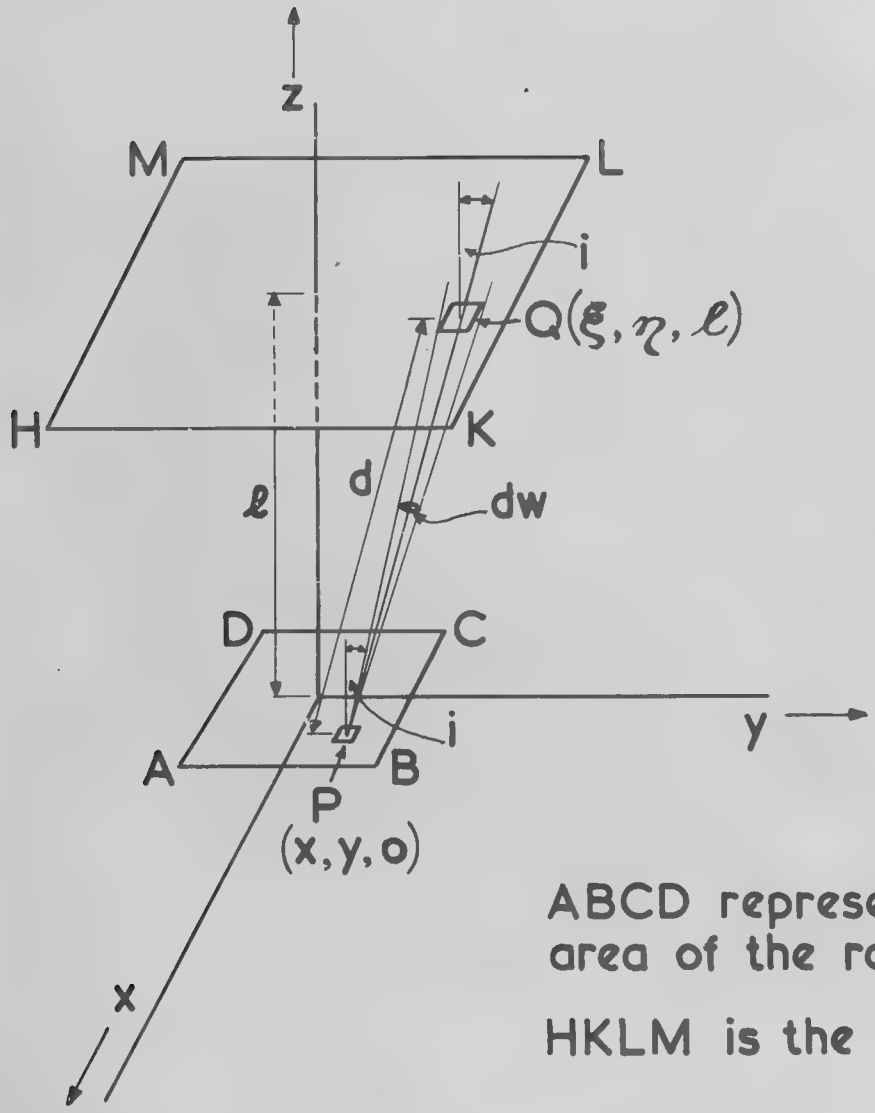

ABCD represents the sensitive area of the radiometer

HKLM is the aperture

Fig. II The aperture – radiometer system (see appendix II)

MRP's 859, 860, 861, 862, 863

At the time of issue this report has not been published. Any author desiring to quote this paper should refer to it as "A paper of the Meteorological Research Committee (London), M.R.P. No. 859. by Mr. P. Goldsmith. A copy is available in the Library of the Meteorological Office."

M.R.P. 859

S.C.I/86

25th March, 1954.

AIR MINISTRY
METEOROLOGICAL RESEARCH COMMITTEE

A method of increasing the range of the Dobson-Brewer Aircraft Frost Point Hygrometer

by
P. Goldsmith (Meteorological Office)

Summary

It has been thought that should there be a requirement to measure frost points below about -130°F the Dobson-Brewer hygrometer would fail as the frost deposit then becomes invisible. This paper describes a method which would increase the range of the hygrometer in jet aircraft by about 20°F by making the measurements in air which has been previously passed through the aircraft compressor.

Introduction

Up to the present the only accurate measurements of humidity at altitude in this country have been made by the Meteorological Research Flight. For the past few years regular flights have been made in Mosquito aircraft to its ceiling of about 40,000 feet for the main purpose of obtaining accurate humidity and temperature soundings at that height. These soundings up to 1951 are summarised and discussed in Reference 1. A study of these ascents will show that the lowest frost points usually measured were about -100°F with occasional readings down to about -120°F.

The method of obtaining these frost points depends upon the recognition of a frost deposit on a cooled metal thimble over which outside air is passing. The instrument is fully described in Reference 2. The operation of the hygrometer requires much experience as the frost deposit becomes more difficult to recognise the lower the frost point becomes. Indeed at a frost point of about -100°F the deposit is only confidently recognised by the most experienced operators. At temperatures below about -130°F any frost deposit may be glassy and so impossible to recognise. Therefore it is seen that the Dobson-Brewer hygrometer in its present form will fail if used to measure a frost point of below about -130°F.

It has been pointed out in a previous paper (Reference 3) that frost points of below -120°F will probably be found at the tropopause in tropical regions and occasionally at moderate altitudes in polar regions.

A study of the Mosquito soundings (Reference 1) will also show that the tendency of the frost points at about 40,000 feet over southern England, that is in the lower stratosphere, is to become lower. Should this tendency persist further into the stratosphere, then the Dobson-Brewer hygrometer may also fail at great heights over England.

The addition of a Canberra, with ceiling of over 50,000 feet, to the strength of the Meteorological Research Flight has made the problem more acute. With this situation in mind, experiments on the hygrometer installation in an Avro Ashton aircraft have been carried out, the details of which are given below.

/The

The method

Figure II is a simplified extended T ∅ gram showing only the isobars, isotherms, the humidity mixing ratio and potential temperature isopleths. If air at 200 mb with a frost point of -92°F (say) is compressed to 1000 mb, the humidity mixing ratio would remain constant, although the temperature would change. The frost point of this air at 1000 mb is then readily seen to be -72°F. Thus the frost point would be made 20°F higher simply by compressing the air. The same procedure applied to air having a frost point of -150°F would similarly give a frost point of about -130°F if compressed to the same degree.

It therefore appears that, as suggested by Dr. A.W. Brewer, if the hygrometer can be supplied with compressed air, then its range will be increased at the lower end by an amount dependent on the degree of compression.

The compression of air to the extent required would be very inconvenient in piston engined aircraft. However an integral part of the jet engine is a fairly high ratio compressor. Indeed in the most modern jets the practice now is to use the engine compressors to supply the cabin pressurisation system instead of using separate "blowers".

It was therefore decided to attempt to supply the hygrometer in the Avro Ashton in a similar manner. The twelfth stage of the compressor on No. 3 engine was tapped and the pipe led through a needle valve to the intake pipe of a pressurised hygrometer. Pressure gauges were fitted in the intake and outlet pipes and gas tight cocks were also provided in these pipes. A diagram of the installation is shown in Figure I.

Operation of the modified hygrometer

By keeping the needle valve closed and opening the two cocks it was possible to measure the frost point of the outside air directly in the normal manner. But by opening the needle valve, to admit compressed air, and closing the cock in the normal intake pipe, the pressure inside the hygrometer could be controlled by partially closing the cock in the outlet pipe. To achieve such sensitive control of the internal hygrometer pressure, it was of course necessary to use an instrument with the liquid oxygen pump outside the pressure seal. The pressure gauges in the intake and outlet pipes enabled the internal hygrometer pressure to be measured. Three flights were made and are described below.

Flights I and II

These flights were made on 4th and 5th January, 1954 at 20,000 feet and 35,000 feet respectively, primarily for other than meteorological purposes. On both flights a series of frost points was measured with the internal hygrometer pressure at various values. Unfortunately on both flights a fault in the hygrometer shutter made it impossible to obtain frost points of the outside air in the orthodox manner.

The results are given below in Tables Ia and Ib. The evaluated true frost point, obtained by reference to an extended T ∅ gram, is also given. On Figure II the frost points are plotted at their appropriate pressure. It is seen that in both cases the readings lie about a line of constant water content. Any deviation from this line is well within the limits of experimental error, especially when it is considered that atmospheric inhomogeneities could also cause some deviation.

/Table Ia

Table Ia (4/1/54)

Time	Height of a/c.	Air Temp.	Internal hygrometer pressure	Frost point at that pressure	Evaluated true frost point
G.M.T.	ICAN	°F	mb	°F	°F
1130	19700	-33	1296	-43	-57
1134	19700	-32	1013	-46	-57
1136	19700	-32	875	-48	-57
1139	19750	-32	758	-53	-59
1143	19700	-32	675	-54	-58
1146	19900	-32	944	-47	-57
1150	19800	-33	1234	-44	-57

Table Ib (5/1/54)

Time	Height of a/c.	Air Temp.	Internal hygrometer pressure	Frost point at that pressure	Evaluated true frost point
G.M.T.	ICAN	°F	mb	°F	°F
1214	34700	-82	585	-86	-97
1217	35000	-83	800	-83	-97
1221	34500	-83	723	-84	-97
1226	34700	-81	854	-79	-95
1230	34600	-81	944	-76	-93
1235	34600	-81	737	-82	-95

Flight III

This flight was carried out on 18th January, 1954 and was made mainly for the testing of the hygrometer system. Having shown on the previous two flights that changes in the internal pressure of the hygrometer caused the measured frost point to vary along a line of constant water content, the purpose of this flight was to compare the frost point measured normally with that found by using the hygrometer at a fairly high internal pressure.

Runs were made at 15, 20, 25, 30 and 35,000 feet during which measurements were taken using the orthodox method and others were taken with the internal hygrometer pressure at atmospheric. These results are presented in Table II and are given on a modified T ∅ gram (Figure III). It is seen that the difference between the frost points arrived at by the orthodox and pressurised methods is again small enough to be accounted for by experimental error or atmospheric inhomogeneities.

Table II

Height	Air Temp.	Internal hygrometer pressure	Frost point at that pressure	Evaluated true frost point	True frost point as measured by orthodox method
ICAN	°F	mb	°F	°F	
15000	+5	1013	+3	-6	-5 and -7
20000	-11	1013	-18	-33	-33 and -32
25000	-31	1013	-45	-59	-63
30000	-55	1013	-59	-75	-77 and -78
35000	-76	1013	-65	-83	-85

/Conclusion

Conclusion

It is seen from Table II and Figure III that the increase of pressure from 238 mb (35,000 feet) to 1013 mb gives an improvement of 20°F in frost point. Therefore, should it be required, the range of the hygrometer can be increased by about 20°F or over depending upon the degree of compression.

Addendum

Whether it will be necessary to use this method to measure humidities above 40,000 feet over England is still not decided.

The first measurements of frost point to 50,000 feet made in the Canberra of the Meteorological Research Flight by the author are plotted on Figure IV. It is seen that on this occasion there was a "tropopause-like" change in the lapse rate of the frost point at about 44,000 feet. It is not proposed to discuss the significance of this result here, but future measurements will show whether this feature is a regular feature of the humidity of the stratosphere. However the hygrometer was nearing its limit on this flight and should lower frost points be encountered the method described above can readily be applied to the Canberra.

Acknowledgment

Acknowledgments are due to M.E. Department R.A.E. for their co-operation in allowing this work to be carried out on their aircraft, at a time when the Meteorological Research Flight did not have a jet aircraft.

References

(1) 1952 Bannon, J.K., Frith, R. and Shellard, H.C. Geophysical Memoirs No.88.

(2) 1948 Brewer, A.W., Cwilong, B.M. and Dobson, G.M.B. Proc. Phys. Soc., London, Vol. 60, (52 - 70).

(3) 1953 Goldsmith, P. M.R.P. 789.

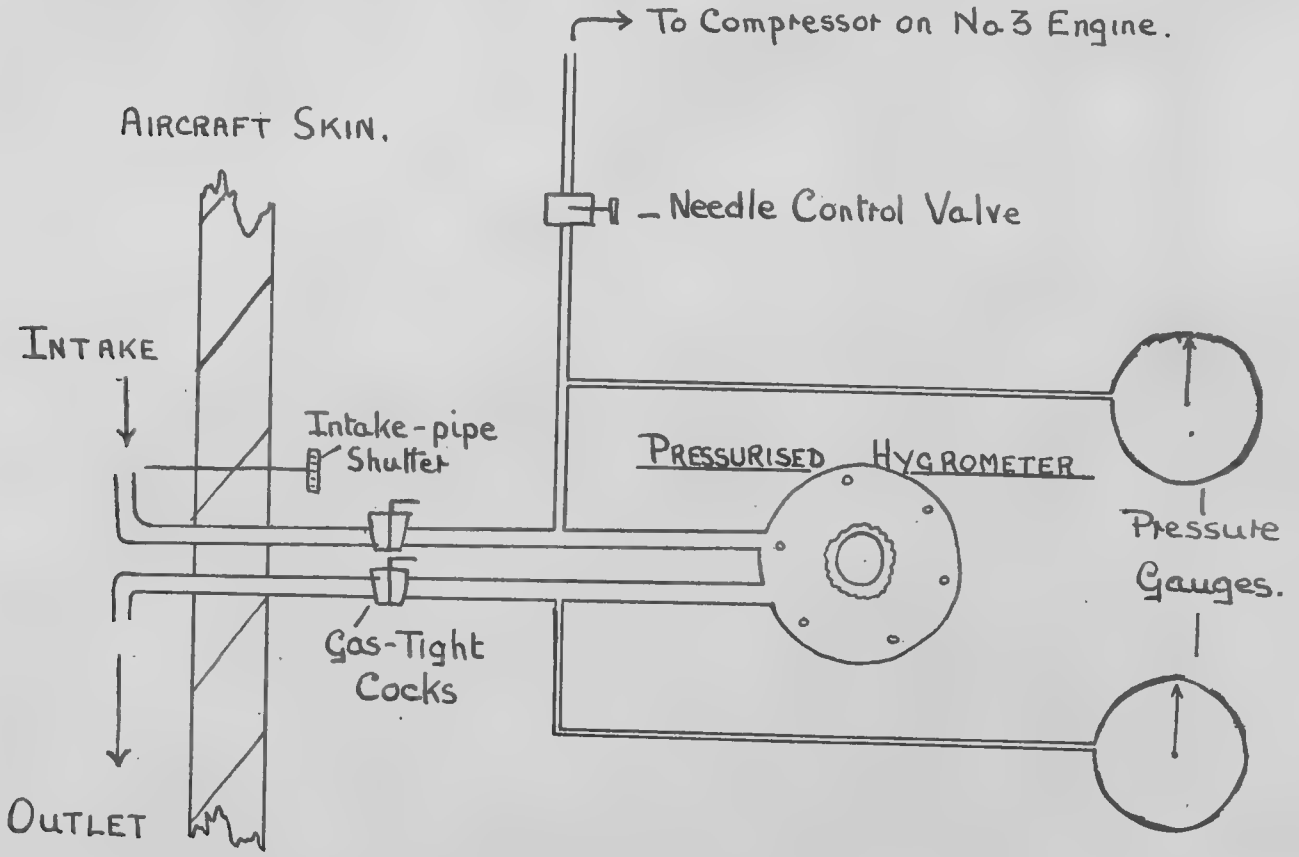

Plan View of the Hygrometer Installation on the Avro-Ashton.

Figure I.

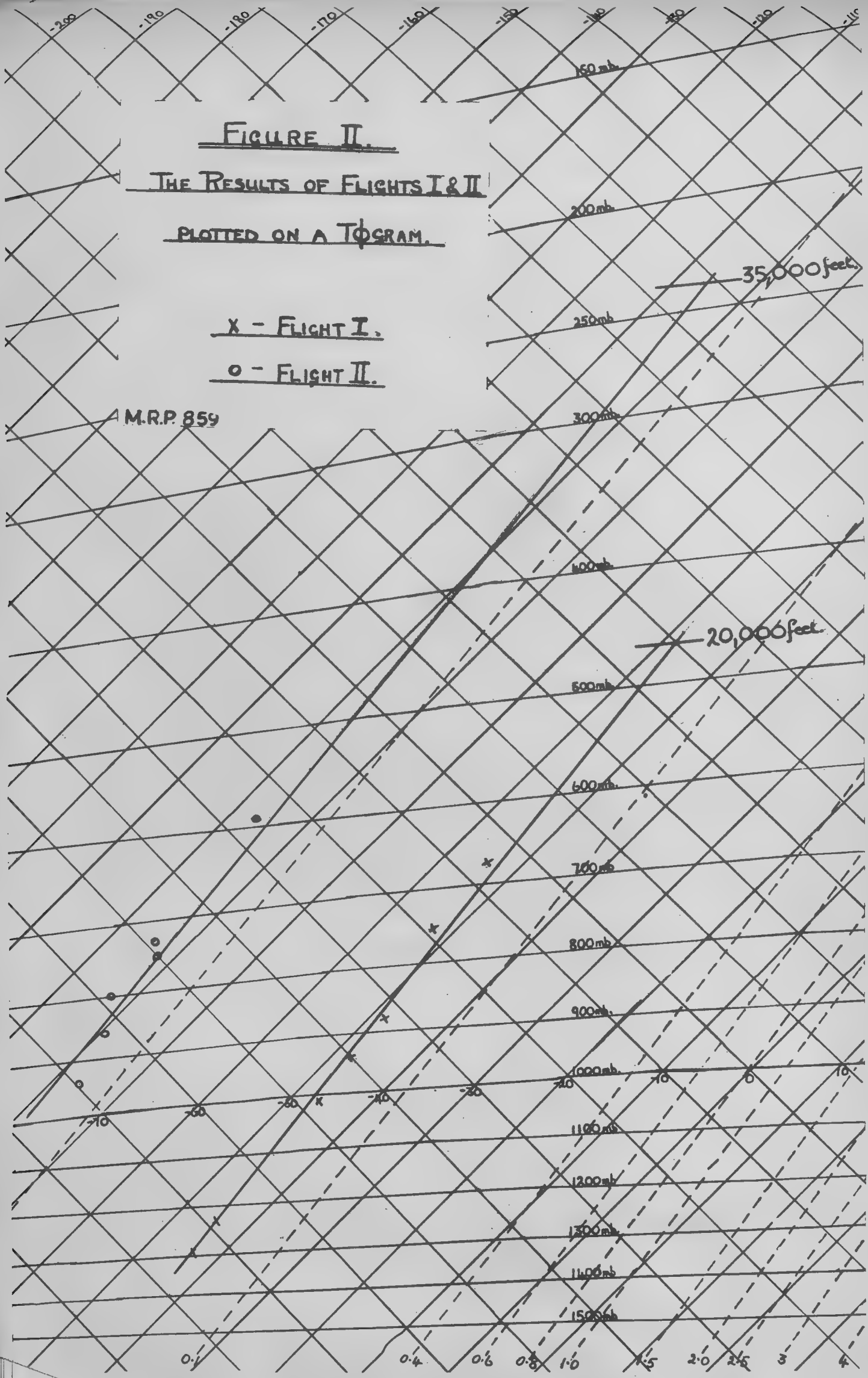

FIGURE II.

THE RESULTS OF FLIGHTS I & II

PLOTTED ON A TΦGRAM.

X - FLIGHT I.

o - FLIGHT II.

M.R.P. 859

M.R.P. 859

FIGURE III

THE RESULTS OF FLIGHT III

PLOTTED ON A TΦGRAM

X - Frost Point measured normally

\+ - Frost Point of air compressed to 1013 mb.

o - Evaluated Frost Point (from +).

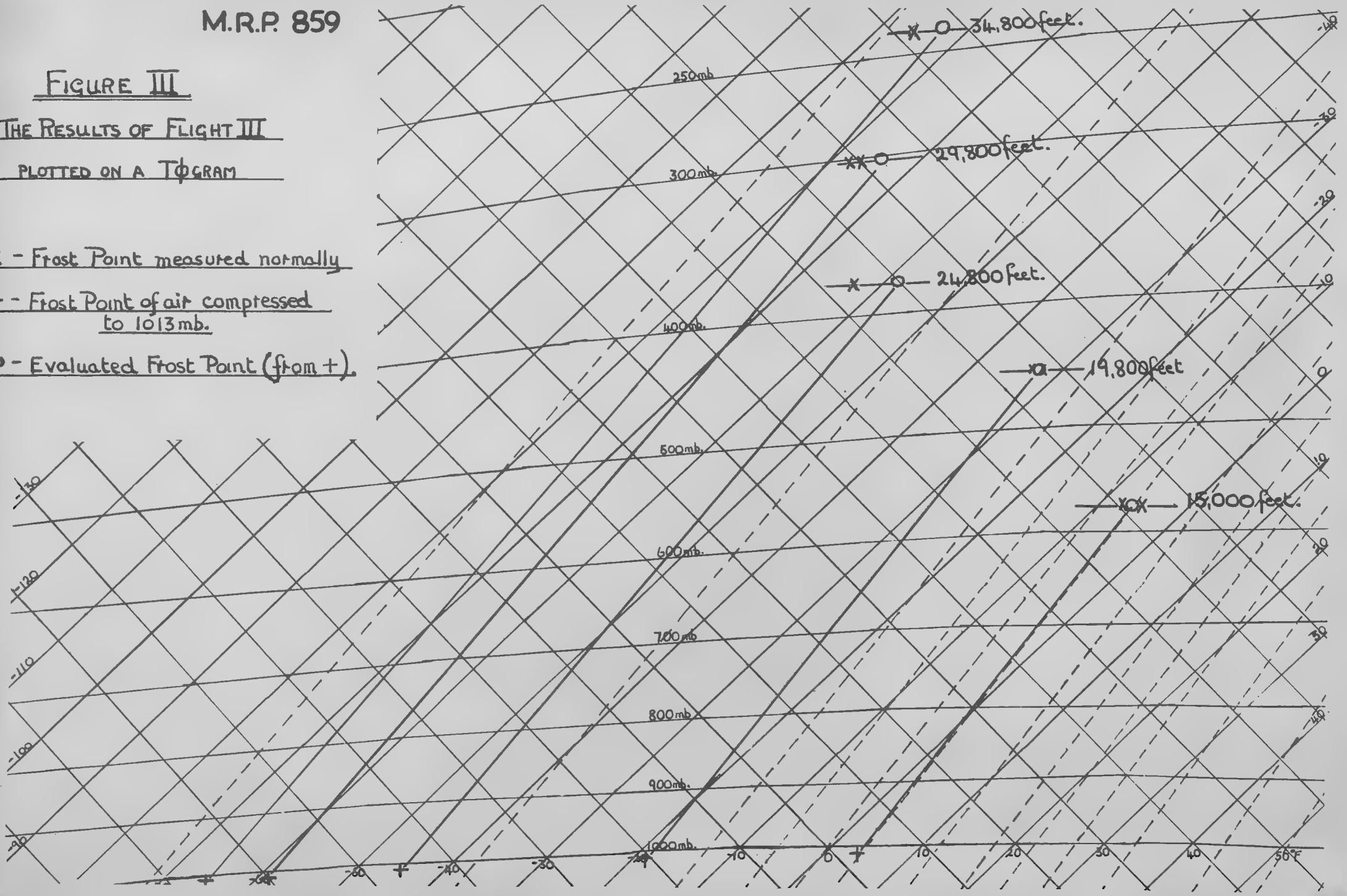

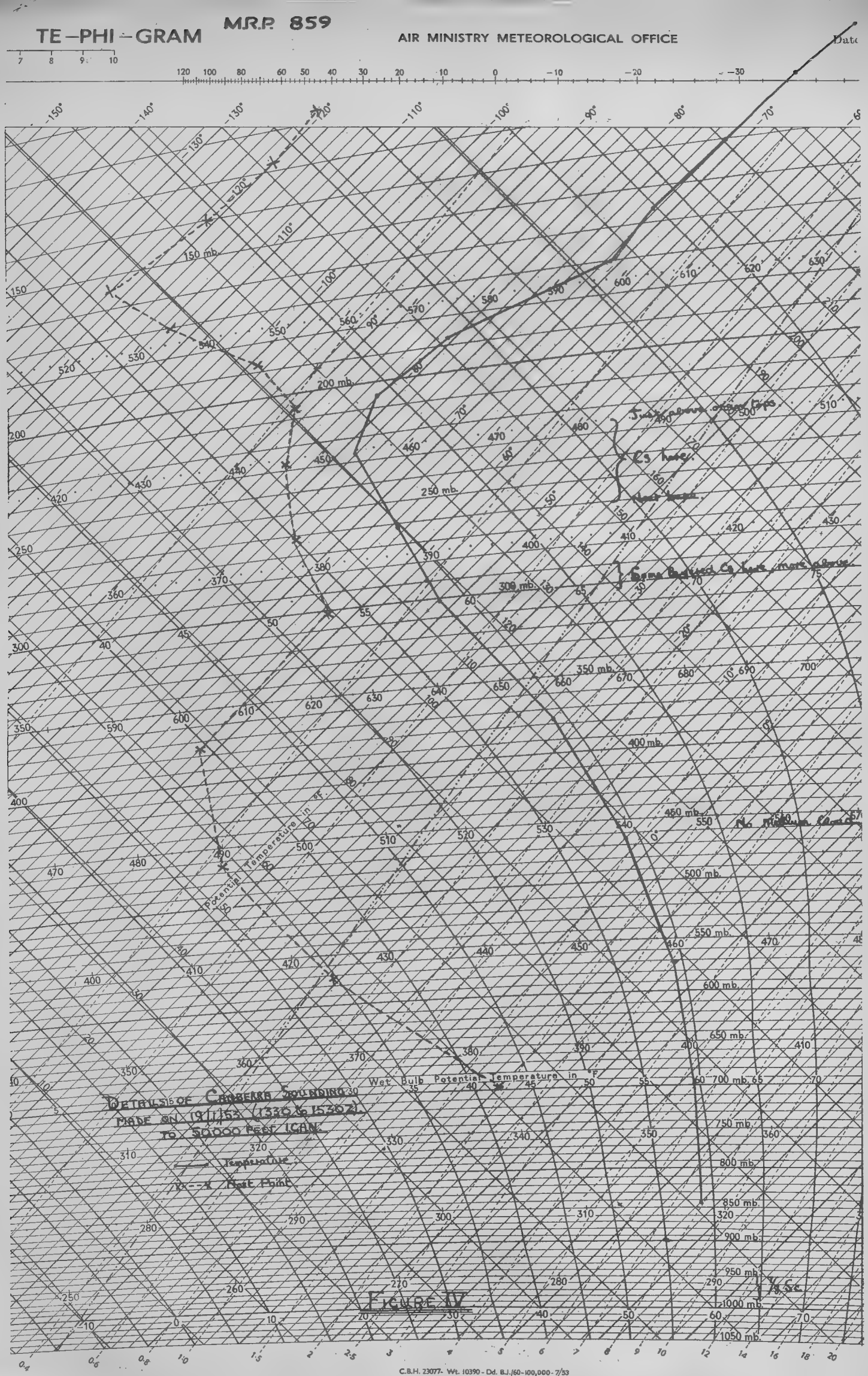
TE-PHI-GRAM
M.R.P. 859
AIR MINISTRY METEOROLOGICAL OFFICE
Date
Potential Temperature in °F
Wet Bulb Potential Temperature in °F
Cs here.
Some layered Cs here, more above.
No Medium Cloud
DETAILS OF CANBERRA SOUNDING MADE ON 19/1/53 (1330 to 1530Z) TO 50000 FEET ICAN.
Temperature
Dew Point
1/8 Sc
C.B.H. 23077- Wt. 10390 - Dd. B.J./60-100,000-7/53

FIGURE IV

At the time of issue this report has not been published. Any author desiring to quote this paper should refer to it as "A paper of the Meteorological Research Committee (London), M.R.P. No. 860 by Mr. J.K. Bannon, A copy is available in the Library of the Meteorological Office".

M.R.P. 860
S.C.II/167
27th March, 1954

MATS

AIR MINISTRY

METEOROLOGICAL RESEARCH COMMITTEE

Variation of temperature in the lower stratosphere above Larkhill and Lerwick

(Addendum to M.R.P. 819)

by
J.K. Bannon (Meteorological Office)

Introduction and Summary

The numbers of observations for 60 mb. used in the analysis described in the previous paper, M.R.P. 819(1), were not large. Moreover, data for all hours of observation, day and night, were used. Because of the comparatively scanty data and the possibility that radiation errors might result in correlation coefficients being erroneously small, the stratospheric correlation coefficients were computed again for Larkhill and Lerwick using all available data for the level of 60 mb. for specified hours of observation, day and night separately. The important result obtained previously, namely that the relation between temperature and the height of the 300 mb. surface and tropopause pressure respectively, falls off rapidly between 150 and 60 mb. was confirmed, but the seasonal variations in these relations appear to be less marked than was indicated in the earlier paper.

1. Data

As in M.R.P. 819 the analysis was restricted to data for the four mid-season months, January, April, July and October. All observations reaching the level of 60 mb. at 00 and 12h. G.M.T. before 1948 and at 03 and 15h. G.M.T. in 1948 and later years at Larkhill and Lerwick were used and values of the height of the 300 mb. surface (H_{300}), the pressure of the tropopause (P_T), and temperatures at levels 150, 100 and 60 mb. (T_{150}, T_{100}, T_{60} respectively) were extracted, the day and night observations being treated separately. For January and April at Lerwick and April at Larkhill so few observations were available for the selected hours that it was necessary to use data for other hours of observation, the data being grouped according to whether the observations were in daylight or darkness. These data provided comparable sets of observations at each of the three levels, 150, 100 and 60 mb. in contrast with the data used in M.R.P. 819 which embraced many more observations at 150 mb. than at 60 mb. whence there was always the possibility that observations at the higher level, through some bias or another, might not be in the same class as the observations from lower levels.

Correlation coefficients between H_{300} and T_{150}, T_{100} and T_{60} respectively and between P_T and the same temperatures were computed. The results are given in Tables I and II for Larkhill and Lerwick respectively. Results for day and

/night

night are given separately although in several months the figures for one or other of day or night have no great significance. They serve, however, as a useful reminder of the limitations of correlation analysis and help in assessing the accuracy of the results.

2. Discussion

(a) Larkhill. Table I.

The day and night sets appear to be consistent and there is no significant difference in the correlation coefficients from those given in Table I of M.R.P. 819 except that values at 60 mb. are generally smaller than in M.R.P. 819.

As a means of judging whether the selected observations used in the preparation of Table I are representative of general conditions in the stratosphere, Table III was prepared comparing some of the statistics in Table I with similar statistics for all observations in the period 1946-1950. In some months the standard deviations differ appreciably but considering the numbers of observations it can be said that the selected sets are representative of general conditions. The majority of the day/night observations used in compiling Table I were separated by more than 24 hours in time. Persistence effects will thus be small and the effective number of observations must be little short of the actual number used. (See discussion in M.R.P. 819).

(b) Lerwick. Table II.

Here there are significant differences between the night and day except in October. In January the day correlation coefficients show weaker relationships than the night at each of the stratospheric levels. Table IV, prepared as Table II to compare the sets of selected observations with the more general observations, shows that for the day observations the pressure of the tropopause was much less variable and the temperature at 150 mb. slightly less variable than in general. The night set with nearly double the number of observations is much more in agreement with the general unselected data. It is deduced that the day coefficients are not representative and that the night coefficients are more likely to represent the general relations. The differences between the day and night correlation coefficients in April and July are also almost certainly not significant as the number of night observations is small in each case; in July there is small variability in P_T and T_{150} for the night observations.

To get a more representative set of correlation coefficients for January and to reduce sampling errors the day and night observations were combined. The resulting statistics are given in Table V. Data are sufficient to make only a rough estimate of diurnal variation of temperature at 60 mb. as observed by radio-sonde at Lerwick in January. The statistics in Table II would suggest a figure of 2-3°F. A comparable figure for Larkhill would be 4-5°F. from the data for 1946-1950(2) but rather less (3-4°F.) from the figures in Table I assuming that diurnal variation at 150 mb. is of the order 1°F. As discussed in M.R.P. 819 such a small variation between day and night observations would have a very small effect on correlation coefficients computed from these observations combined when the standard deviation of temperature is three or four times as large as the semi-diurnal range.

The correlations for January in Table V and for daylight for April, July and October in Table II do not show great differences from those in Table II of M.R.P. 819. The other statistics in Tables II and V compared with the statistics for unselected ascents in Table IV show that these selected data for high altitude are fairly representative of general conditions.

The effective number of observations must, as in Table I, be only a few less than the number of observations.

/3.

3. Variation of the correlation coefficients with height

The correlation coefficients in Tables I, II and V show a marked decrease with decreasing pressure. The direct relationship between two variables varies as the square of their correlation coefficient. Accordingly Table VI was prepared giving the ratio of the squares of the correlation coefficients for T_{60} and T_{150} (compare Table VII, M.R.P. 819). It is a reasonable inference from these figures that the influence of the disturbances of the troposphere in middle latitudes on temperature in the stratosphere is reduced to at least a half between 150 and 60 mb. and for much of the year to one-fifth or one-third.

4. Variation of the correlation coefficients with season

At Larkhill (Table I) the correlation coefficients are lowest in January and highest in July and October. In M.R.P. 819 the coefficients for January are almost as great as those for October. Except at 60 mb. the differences between the seasons are not large. Table VI shows that the decrease with height in the relationship between stratospheric temperatures and H_{300} and P_T respectively is least in October and greatest in January and April.

At Lerwick (Tables II and V) the correlation coefficients are least in January, not very much greater in April and largest in October. January and October have the greatest and least reductions respectively in the coefficients between the 150 and 60 mb. levels (Table VI). The greatest correlation coefficients (October) have similar values at Larkhill and Lerwick but the coefficients at Lerwick are lower than at Larkhill in January and April especially at 60 mb. where the differences between the coefficients for H_{300} are certainly significant. The same types of differences were noted in M.R.P. 819.

It was suggested in M.R.P. 819 that the variability in temperature distribution over Lerwick in January, where two different stratospheric regimes can occur, is the cause of the lower correlations in that month. This argument has some force. It is noted, however, that as for H_{400} at Arctic Bay (M.R.P. 819, Table III), it is the H_{300} correlations which are markedly reduced, the correlations involving P_T being not much less than in summer. Much of the relation between pressure at the tropopause and stratospheric temperature must arise from the close relation between vertical motion at the tropopause and vertical motion within the lower stratosphere; a low tropopause can be partly caused by subsidence and this subsidence would increase the temperature in the lower stratosphere; the reverse would apply for a high tropopause. Presumably the moderate correlation between P_T and temperature in the lower stratosphere in winter and spring arises mainly from this effect of vertical motion. The surprising fact, however, is that although P_T and H_{300} are still moderately correlated in January and April the H_{300} correlations with stratospheric temperatures are lower than the P_T correlations. Table VII shows the correlations between H_{300} and P_T for the data used in preparing Table II and these may be compared with similar coefficients for larger numbers of observations in M.R.P. 819, Table II; it is seen that the correlations are always about -0.7 to -0.8. There is nothing inconsistent in the statistics, however, since a correlation coefficient of 0.7 merely signifies roughly a 50% relation, assuming the relationship to be linear. All the factors resulting in the reduced H_{300} correlations in winter and spring at Lerwick are not obvious from this analysis, and further work is required to throw light on this interesting point.

In M.R.P. 819 the seasonal variation of ozone was compared with the seasonal variation of these correlation coefficients at Lerwick and Larkhill. The more reliable figures given here in Tables I, II and V certainly show that the correlation coefficients for the level 60 mb. (19 km.) which is not far below the ozone levels (20-35 km.) are, in general, least in January and April, and greatest in October. The ozone maximum is in March and the minimum in October (see, for example, reference (3)) and the seasonal variation in the above correlation coefficients may thus well be associated with the variation in ozone, but this is not proved and the mechanism relating to it is obscure.

/Acknowledgment

Acknowledgment

The correlation coefficients used in this analysis were computed by Mr. J.W. Bird.

REFERENCES

1. Bannon, J.K. and Gilchrist, A. — A statistical study of the variation of temperature in the troposphere and lower stratosphere. Air Ministry, M.R.P. No. 819, 1953.

2. - — Upper Air Data, Larkhill, 1946-1950. Met. Off. London, M.O. 555, Part I, 1952.

3. Normand, Sir Charles — Atmospheric Ozone and Upper Air Conditions. Q.J. Roy. Met. Soc., 79, 1953, page 39.

TABLE I

Stratospheric Statistics for Larkhill (51° 12'N, 01° 48' W)

Period 1944-1952 (-1953 for January)

	H_{300} and T			P_T and T						H_{300} and T			P_T and T					
	ρ	$\bar{H}_{300}$ (10's of ft.)	$\sigma_{H_{300}}$ (10's of ft.)	ρ	$\bar{P}_T$ (mb.)	σ_{P_T} (mb.)	$\bar{T}$ (°F.-ve)	σ_T (°F.)	n	ρ	$\bar{H}_{300}$ (10's of ft.)	$\sigma_{H_{300}}$ (10's of ft.)	ρ	$\bar{P}_T$ (mb.)	σ_{P_T} (mb.)	$\bar{T}$ (°F.-ve)	σ_T (°F.)	n
Night 00,03 GMT				**JANUARY**						**Night 00,03 GMT**				**JULY**				
T_{150}	-0.61	2920	63	0.67	220	43	76.3	10.8	52	T_{150}	-0.86	3090	45	0.82	221	45	63.4	7.7	41
T_{100}	-0.53	2920	63	0.50	220	43	78.5	6.9	52	T_{100}	-0.79	3090	45	0.65	221	45	64.3	4.9	41
T_{60}	-0.28	2920	63	0.29	220	43	80.4	7.1	52	T_{60}	-0.55	3090	45	0.41	221	45	61.7	4.0	41
Day 12,15 GMT										**Day 12,15 GMT**									
T_{150}	-0.60	3000	60	0.69	212	43	73.6	10.1	62	T_{150}	-0.71	3100	38	0.72	212	29	58.6	7.6	73
T_{100}	-0.67	3000	60	0.63	212	43	73.4	8.4	62	T_{100}	-0.70	3100	38	0.61	212	29	58.1	6.4	73
T_{60}	-0.27	3000	60	0.35	212	43	74.8	8.7	62	T_{60}	-0.40	3100	38	0.44	212	29	51.4	6.5	73
Night 00,03,21 GMT				**APRIL**						**Night 00,03 GMT**				**OCTOBER**					
T_{150}	-0.77	3000	58	0.80	233	43	67.6	7.2	55	T_{150}	-0.80	3030	70	0.72	222	57	72.4	9.2	56
T_{100}	-0.67	3000	58	0.71	233	43	69.4	5.7	55	T_{100}	-0.73	3030	70	0.61	222	57	74.5	7.6	56
T_{60}	-0.22 *	3000	58	0.37	233	43	69.9	5.0	55	T_{60}	-0.56	3030	70	0.40	222	57	72.8	5.2	56
Day 12,15 GMT										**Day 12,15 GMT**									
T_{150}	-0.69	3010	58	0.74	230	45	63.4	7.2	89	T_{150}	-0.88	3040	62	0.82	219	46	69.0	8.4	79
T_{100}	-0.64	3010	58	0.61	230	45	63.8	5.7	89	T_{100}	-0.79	3040	62	0.69	219	46	69.8	7.0	79
T_{60}	-0.24	3010	58	0.39	230	45	61.5	5.7	89	T_{60}	-0.57	3040	62	0.49	219	46	66.7	5.8	79

H_{300} = height of 300 mb. surface $\sigma_{H_{300}}$ = standard deviation of H_{300} T_{150}, T_{100}, T_{60} = temperature (°F.) at 150, 100, 60 mb. respectively

P_T = pressure at the tropopause σ_T = standard deviation of T ρ = appropriate correlation coefficient

n = No. of observations σ_{P_T} = standard deviation of P_T.

* Not significant at 5% level

TABLE II

Stratospheric Statistics for Lerwick (60° 08'N, 01° 11' W)

Period 1944-1952 (-1953 for January)

	H_{300} and T			P_T and T						H_{300} and T				P_T and T					
	ρ	$\bar{H}_{300}$ (10's of ft.)	$\sigma_{H_{300}}$ (10's of ft.)	ρ	$\bar{P}_T$ (mb.)	σ_{P_T} (mb.)	$\bar{T}$ (°F.-ve)	σ_T (°F.)	n	ρ	$\bar{H}_{300}$ (10's of ft.)	$\sigma_{H_{300}}$ (10's of ft.)	ρ	$\bar{P}_T$ (mb.)	σ_{P_T} (mb.)	$\bar{T}$ (°F.-ve)	σ_T (°F.)	n
Night 00,03,06,18 and 21 GMT			JANUARY							Night 00 GMT			JULY						
T_{150}	-0.58	2910	71	0.74	242	55	72.8	9.3	88	T_{150}	-0.26 *	3040	32	0.49	224	21	57.3	4.9	22
T_{100}	-0.30	2910	71	0.53	242	55	75.9	8.3	88	T_{100}	-0.32 *	3040	32	0.33 *	224	21	57.9	3.6	22
T_{60}	-0.11 *	2910	71	0.32	242	55	81.2	9.1	88	T_{60}	+0.07 *	3040	32	-0.11 *	224	21	55.1	3.2	22
Day 12,15 GMT										Day 12,15 GMT									
T_{150}	-0.19 *	2930	71	0.46	230	39	72.4	8.8	46	T_{150}	-0.79	3050	55	0.77	242	38	50.8	7.6	70
T_{100}	+0.08 *	2930	71	0.19 *	230	39	74.7	7.9	46	T_{100}	-0.71	3050	55	0.61	242	38	49.0	5.4	70
T_{60}	+0.22 *	2930	71	0.03 *	230	39	78.4	10.2	46	T_{60}	-0.39	3050	55	0.27	242	38	44.2	4.4	70
Night 00,03,21 GMT			APRIL							Night 00,03 GMT			OCTOBER						
T_{150}	-0.70	2950	75	0.79	260	53	59.8	7.3	19	T_{150}	-0.81	3010	68	0.72	217	47	71.2	9.5	61
T_{100}	-0.73	2950	75	0.73	260	53	62.1	5.1	19	T_{100}	-0.76	3010	68	0.64	217	47	71.1	7.9	61
T_{60}	-0.40 *	2950	75	0.49	260	53	63.9	4.6	19	T_{60}	-0.57	3010	68	0.50	217	47	71.5	5.8	61
Day 12,15 GMT										Day 12,15 GMT									
T_{150}	-0.54	2940	66	0.58	277	55	55.7	7.8	75	T_{150}	-0.83	3000	75	0.78	232	53	65.8	10.0	91
T_{100}	-0.35	2940	66	0.54	277	55	57.7	6.3	75	T_{100}	-0.82	3000	75	0.76	232	53	65.6	7.7	91
T_{60}	-0.07 *	2940	66	0.28	277	55	57.3	6.0	75	T_{60}	-0.61	3000	75	0.55	232	53	64.5	6.1	91

For explanation of symbols, see Table I

* Not significant at 5% level

TABLE III - Comparison of sets of upper air data: Larkhill

	$\bar{H}_{300}$ (10's of ft.)	σH_{300} (10's of ft.)	$\bar{P}_T$ (mb.)	σP_T (mb.)	$\bar{T}_{150}$ (-°F.)	σT_{150} (°F.)	n
January							
Selected night ascents	2920	63	220	43	76.3	10.8	52
Selected day ascents	3000	60	212	43	73.6	10.1	62
All observations 1946-1950 *	2969	77	236	54	68.9	9.7	528 /
April							
Selected night ascents	3000	58	233	43	67.6	7.2	55
Selected day ascents	3010	58	230	45	63.4	7.2	89
All observations 1946-1950 *	2979	67	243	56	63.3	8.9	467/
July							
Selected night ascents	3090	45	221	45	63.4	7.7	41
Selected day ascents	3100	38	212	29	58.6	7.6	73
All observations 1946-1950 *	3081	44	223	39	60.1	7.7	560 /
October							
Selected night ascents	3030	70	222	57	72.4	9.2	56
Selected day ascents	3040	62	219	46	69.0	8.4	79
All observations 1946-1950 *	3041	66	219	50	73.0	8.8	574 /

For explanation of symbols, see Table I.

/ Number of observations of T_{150}.

* From M.O. 555, Part 1; statistics for H_{300} refer to 1948-1950 only.

TABLE IV - Comparison of sets of upper air data: Lerwick

	$\bar{H}_{300}$ (10's of ft.)	σH_{300} (10's of ft.)	$\bar{P}_T$ (mb.)	σP_T (mb.)	$\bar{T}_{150}$ (-°F.)	σT_{150} (°F.)	n
January							
Selected night ascents	2910	71	242	55	72.8	9.3	88
Selected day ascents	2930	71	230	39	72.4	8.8	46
All observations 1946-1950 *	2895	76	254	57	69.0	9.5	502 /
April							
Selected night ascents	2950	75	260	53	59.8	7.3	19
Selected day ascents	2940	66	277	55	55.7	7.8	75
All observations 1946-1950 *	2912	65	281	57	55.2	9.1	489 /
July							
Selected night ascents	3040	32	224	21	57.3	4.9	22
Selected day ascents	3050	55	242	38	50.8	7.6	70
All observations 1946-1950 *	3033	51	247	37	51.0	7.0	541 /
October							
Selected night ascents	3010	68	217	47	71.2	9.5	61
Selected day ascents	3000	75	232	53	65.8	10.0	91
All observations 1946-1950 *	2967	71	234	53	66.9	9.9	549 /

For explanation of symbols, see Table I.

/ Number of observations of T_{150}.

* From M.O. 555, Part 2; statistics for H_{300} refer to 1948 -1950 only.

TABLE V - Stratospheric statistics for Lerwick in January
Day and night combined: 1944-53

	H_{300} and T				P_T and T					
	ρ	H_{300} (10's of ft.)	$\sigma_{H_{300}}$		ρ	$\bar{P}_T$ (mb.)	σ_{P_T} (mb.)	$\bar{T}$ (-°F.)	σ_T (°F.)	n
T_{150}	-0.45	2920	71		0.66	238	50	72.6	9.1	134
T_{100}	-0.16*	2920	71		0.43	238	50	75.5	8.1	134
T_{60}	+0.03*	2920	71		0.21	238	50	80.2	9.9	134

For explanation of symbols, see Table I.

* Not significant at 5% level.

TABLE VI - Ratio of squares of correlation coefficients for T_{60} and T_{150}

	January		April		July		October		Year //	
	H_{300}	P_T	H_{300}	P_T	H_{300}	P_T	H_{300}	P_T	H_{300}	P_T
Larkhill										
Night	0.21	0.19	0.08*	0.21	0.41	0.25	0.49	0.31		
Day	0.20	0.26	0.12	0.28	0.32	0.37	0.42	0.36	0.25	0.31
Lerwick										
Night	0.03*	0.19	0.33*	0.38	0*	0.05*	0.49	0.48		
Day	0*	0.004*	0.02*	0.23	0.24	0.12	0.54	0.50	0.12	0.21

* Correlation for T_{60} (or T_{150}) not significant at 5% level. If correlation coefficient changes sign from 150 to 60 mb., ratio counted as zero.

// Values here are the squares of the mean ratios of the daylight coefficients for T_{60} and T_{150} for all four months, except for January, Lerwick where the correlation coefficients for all hours combined were used instead of the daylight values.

TABLE VII - Correlation coefficients between H_{300} and P_T
High altitude ascents at Lerwick

	Night		Day	
	Correlation Coefficient	No. of Obs.	Correlation Coefficient	No. of Obs.
January	-0.77	88	-0.87	46
April	-0.85	19	-0.79	75
July	-0.69	22	-0.86	69
October	-0.75	61	-0.83	91

	N_{max}	$\sigma_{H_{max}}$						
	(10's of ft.)							
	2920	71		0.66	238			
	2920	71						
	2920	71						

At the time of issue this report has not been published. Any author desiring to quote this paper should refer to it as "A paper of the Meteorological Research Committee (London), M.R.P. No. 861 by Mr. D.H. Johnson. A copy is available in the Library of the Meteorological Office".

M.R.P. 861
S.C.II/168
11th May, 1954

AD65159

AIR MINISTRY

METEOROLOGICAL RESEARCH COMMITTEE

Diurnal and semi-diurnal oscillations of the lower stratosphere

by
D.H. Johnson (Meteorological Office)

Summary

It is demonstrated that diurnal and semi-diurnal variations of wind occur in the lower stratosphere. These oscillations appear to be associated with the solar tides. The stratospheric semi-diurnal oscillation of wind is in phase with, and of comparable magnitude to, the surface semi-diurnal oscillation of wind. In the stratosphere, the diurnal oscillation is found to be of similar magnitude to the semi-diurnal oscillation.

1. Introduction

Whilst methods of representing the 100 mb wind field were under investigation, a diurnal variation was detected in the winds observed at the 100 mb level. A study of the periodic variations of wind in the lower stratosphere has been made in order to establish their significance, form and magnitude.

2. Reduction of the data

Occasions in 1950-51 were selected when winds were reported at 100 mb from a British upper air station at times t hr and t + 6 hr on the same day. Four sets of data were extracted corresponding to the four six-hour intervals 0900 G.M.T. - 0300 G.M.T., 1500 G.M.T. - 0900 G.M.T., 2100 G.M.T. - 1500 G.M.T. and 0300 G.M.T. - 2100 G.M.T. The observed winds were resolved into south and west components and two-year monthly mean components of the wind change over the 6 hr interval were computed for each period. These are reproduced in Table I.

No very critical statistical test is required to show that at least some of the annual means given in Table I differ significantly from zero e.g. for the 0900 G.M.T. - 0300 G.M.T. west component variation, all the monthly means have the same sign. If the monthly means themselves belonged to a population whose mean was zero, the odds against their having the same sign would be $(2^{11}-1) : 1$, i.e. 2047: 1. The magnitudes of the annual mean six-hour variations are less than the standard error (3 or 4 kt) of the individual wind observations and are also less than the six-hour synoptic variations. To obtain some indication of the general level of accuracy of the individual monthly means, an estimate has been made of the standard errors of 1500 - 0900 G.M.T. variations for four months. The individual values of the 1500 G.M.T. - 0900 G.M.T. variations do not form an independent set because, although the serial correlation for individual stations is negligible, a small but significant correlation does exist between simultaneous values at different stations. If the data were composed of simultaneous values

/from

from K stations and the average correlation coefficient between pairs of stations was $\bar{\rho}$, it can be shown that the standard deviation of the mean of n observations is given by

$$\sigma_M = \sigma \sqrt{\frac{1 + (K-1)\bar{\rho}}{n}} .$$

This replaces the usual relation for independent values of $\sigma_M = \sigma\sqrt{\frac{1}{n}}$. Using the former relation with appropriate values of K and $\bar{\rho}$ the standard errors of the monthly means in June, July, December and January respectively were estimated to be, for the south component, 0.43 kt, 0.53 kt, 1.00 kt and 0.70 kt; and for the west component, 0.39 kt, 0.42 kt, 0.65 kt and 0.54 kt. Evidently, a number of the monthly means themselves differ significantly from zero.

If a_1, a_2, a_3 and a_4 are the four true six-hour variations of wind then, neglecting the seasonal variation of wind, which is small in comparison with the diurnal changes, we can put $a_1 + a_2 + a_3 + a_4 = 0$. This relationship is not obeyed exactly by the variations given in Table I because, on many days, winds are lacking at one or more of the hours of observation. For these days, only one or two of the six-hour variations were obtained. We can thus obtain from Table I two estimates of each of the a_i; one is given directly by a_i, and the other is given by $-(a_j + a_k + a_l)$. The means of the two estimates are given as the "derived" monthly mean six-hour variations in Table II. These derived variations form the basis of the analysis which follows. They are illustrated graphically in Figure 1. Figure 2 shows the implied twelve-hour variations for each wind component.

Inspection of Figures 1 and 2 suggests that any seasonal variations which may occur in the diurnal changes are definitely smaller than the annual means. To test this impression, averages were calculated for the winter (November to March) and summer half years. These are given in Table III. "Student's" t-test applied to this data showed that the differences between the winter and summer means were in no case significant, even at the 10% level.

A test was also made to determine whether any of the differences between the monthly and annual mean six-hour variations was so great as to merit special investigation. The variances of the monthly means about the annual means averaged 0.26 kt for the west components and 0.46 kt for the south components. None of the west component monthly means differs significantly from the annual mean. For the south component, the 0900 G.M.T. - 0300 G.M.T. January monthly mean differs from the appropriate annual mean by an amount, 2.16 kt, equal to 3.19 times the standard deviation. The odds against such a difference occurring by chance on any specified occasion are a little under 999:1 but the odds against such a difference occurring by chance in a sample of 48 values are less than 957:43. The deviation of the January value from the annual mean is therefore of doubtful significance.

Since the data show no clear cut seasonal variation further study has been confined to the annual mean six and twelve-hour changes.

Soon after the first results of this work became known, H.W.L. Absalom generously made available for study by the writer, some further, very valuable, unpublished data. These data consist of six-hourly variations of wind at 150 mb calculated from British wind observations made during the years 1944-47, when upper winds were measured at the hours 0600, 1200, 1800 and 2400 G.M.T. These additional data are contained in Table IV.

3. Analysis of the oscillations

The sum of the four annual mean six-hourly variations should be zero. In order that the annual means given in Table II should satisfy this condition, and so to facilitate further analysis, they have been adjusted slightly. The south

/component

component variations have been increased by 0.01 kt and the west component variations by 0.12 kt. The appropriate deviations, corresponding to the adjusted six-hour variations, of the winds at each hour of observation relative to the overall mean wind are then readily calculated. The difference between the wind at each synoptic hour and the mean wind is given in Table V which, in effect, combines the results given in Table II with those given in Table IV.

The next step was to break down the oscillations represented by the data in Table V by harmonic analysis. For each wind component it is possible from this data to obtain four harmonics. These are given by the equations:

$$100\ S = -54 \cos(\theta + 32^\circ 14') + 67 \cos(2\theta + 44^\circ 24') - 6 \cos(3\theta + 80^\circ 32') + 0.25 \cos 4\theta ; \quad (1)$$

$$100\ W = +51 \cos(\theta + 84^\circ 24') + 51 \cos(2\theta - 29^\circ 3') - 7 \cos(3\theta - 26^\circ 34') + 0.0 \cos 4\theta ; \quad (2)$$

where S and W are the south wind and west wind components in kt, and θ varies from 0 to 2π as time varies through 24 hours from 0300 G.M.T.

Equations (1) and (2) reveal that the oscillation can be accounted for largely by the first two harmonics, i.e. by two component oscillations, one having a period of twenty four hours and the other having a period of twelve hours. A test has been made to determine to what extent the individual harmonics could account for the observed variations. Table VI gives the values of "Student's" t obtained for each of the six-hour variations given in Table II, in order to examine the following possibilities, viz., that the twelve monthly means are drawn from a population whose mean is (a) zero, (b) given by the first harmonic, (c) given by the second harmonic, (d) given by the first and second harmonics combined or (e) given by the sum of the first three harmonics. For each of these tests values of t, corresponding to probabilities of 0.1%, 1%, 5% and 10% that the sample tested is drawn from a population with the postulated mean value, are 4.44, 3.11, 2.20 and 1.80 respectively. From Table VI we deduce that the observed system of variations cannot be accounted for satisfactorily on the assumptions (a) that there is no real variation, (b) that they consist of a diurnal oscillation alone or (c) that they consist entirely of a semi-diurnal oscillation alone. The variations can be explained satisfactorily by a combination of the diurnal and semi-diurnal oscillations: it is not necessary to invoke harmonics of higher order than the second to account for the present data.

4. The diurnal and semi-diurnal oscillations

The diurnal oscillations of the south wind and west wind components are defined by the first terms on the right hand sides of equations (1) and (2). These have been combined in Figure 3, which is a vector diagram giving, for any time, the resultant wind velocity due to the diurnal oscillations. The semi-diurnal variation of wind, given by the second terms on the right hand sides of equations (1) and (2), is represented in a similar fashion in Figure 4.

It was demonstrated above that we can account very largely for the observed six-hour variations by combining the diurnal and semi-diurnal oscillations. Figure 5 shows the result of superimposing one oscillation on the other and also gives, for comparison, the observed variations.

The elliptical paths which would be followed by particles moving with the wind systems defined in Figures 3 and 4 are shown in Figures 6 (a) and 6 (b). Figure 6 (c) depicts the kidney-shaped path followed by particles undergoing the combined oscillation.

/5.

5. Physical nature of the oscillations

In the preceding sections it has been established that the measured changes of wind in the lower stratosphere contain small periodic components. Possible explanations of the periodic variations are: (i) that they are spurious and are due to some systematic error of the wind measurements or (ii) that they are real and are associated with the tidal oscillations which are known to occur in the atmosphere.

It has not been possible to conceive of any direct instrumental effect which could account for the observed variations. The 1944-47 winds were measured for the most part by radio direction-finding techniques, whereas the 1950-51 winds were measured by the use of G.L. III radar equipment. It is difficult to envisage any inherent periodic instrumental effects which could be common to both techniques.

Some diurnal effect could arise as follows. There is an apparent diurnal variation in the measured height of the 100 mb surface. The apparent diurnal 1500 G.M.T. - 0300 G.M.T. change of contour height ranges from about 140 ft at the winter solstice to 380 ft at the summer solstice, for stations in the British Isles.

It is believed that this apparent variation in height is largely false, and that it results from the effect of solar radiation on the radio-sonde itself. It is likely that the 1500 G.M.T. "100 mb" winds refer to a level which is in fact from 140 ft to 380 ft higher than the true 100 mb surface. Consequently the wind observations will contain a false diurnal variation, the magnitude of which depends on the shear of wind at 100 mb. An examination of the shear of the mean wind in the lower stratosphere showed that the shear in the south component is so small as to have a completely negligible effect at all seasons. At the most favourable time of the year (June and July), the shear could give rise to an apparent 1500 G.M.T. - 0300 G.M.T. variation in the west component of about 0.4 kt, but from December to May the effect of shear in the west component is again negligible. Inspection of Figure 3 shows that the annual mean 1500 G.M.T. - 0300 G.M.T. diurnal change of west wind component is, in fact, quite small. The greatest twelve-hour change of west wind takes place between about 0900 G.M.T. and 2100 G.M.T., a period when there is little apparent variation of contour height. It is clear that for the annual means, we can discount the effect of the apparent diurnal variation of height of the 100 mb surface as being small in comparison with the observed diurnal variation of wind.

Atmospheric tides have been extensively studied in terms of the changes of pressure which occur at the earth's surface. The most important solar tides have periods of twelve and twenty four hours (1). Of these two, the semi-diurnal oscillation has attracted greater attention, partly because, at the earth's surface, it has the greater amplitude and shows greater uniformity than the diurnal oscillation. Simpson (2) has given the following expression for the observed semi-diurnal pressure variation;

$$p = 0.937 \cos^3 \theta \sin [2 (\omega t + \lambda) + 154^\circ] \qquad (3)$$

where p is pressure in mm of mercury, θ is latitude, ω is the earth's angular velocity, t is Greenwich mean time and λ is longitude east of Greenwich. Bartels (3) has derived theoretically, the following expressions for the low-level wind components associated with the pressure variation given by equation (3):

$$U = - 54.6 \sin \theta \cos [2 (\omega t + \lambda) + 154^\circ]$$

$$V = - (21.8 + 32.8 \sin^2 \theta) \sin [2 (\omega t + \lambda) + 154^\circ] \qquad (4)$$

where U is the south component and V is the west component of wind in cm/sec.

/It

It follows from expressions (3) and (4) that the pressure and west wind component oscillations are in antiphase at the earth's surface, maximum west wind component occurring at about 0400 and 1600 local time. In the northern hemisphere, the pressure and south wind component oscillations are in quadrature, maximum south wind component occurring at about 0100 and 1300 local time. Reference to Figure 4 shows that the semi-diurnal oscillation in the lower stratosphere is approximately in phase with the surface oscillation. This relationship is to be expected from modern tidal thoery (1).

The amplitudes of the surface tidal wind components as given by expression (4) are in latitude 55°N, 0.87 kt for the south component and 0.85 kt for the west component. These may be compared with the lower stratosphere semi-diurnal amplitudes of 0.67 kt for the south component and 0.51 kt for the west component. It appears that there is no great variation in the amplitude of the tidal winds, at least up to the 100 mb (16 km) level. It is interesting to note however, that recent studies, by Elford and Robertson (4) and others, of the drift of meteor trails, indicate that the semi-diurnal variations in the wind components have magnitudes of the order of 60 kt in the 80 km to 100 km layer.

As previously mentioned, the surface diurnal pressure changes have not been studied to the same extent as the semi-diurnal pressure changes. The present study indicates that the diurnal and semi-diurnal oscillations are of comparable magnitude in the lower stratosphere. Elford and Robertson's data (4) show that the two effects are also of equal importance in the 80 km - 100 km layer.

There appears to be little doubt that the periodic variations of wind discussed in this paper are largely associated with the solar tides. Wind observations made at 100 mb are particularly suitable for study in connection with the tidal oscillations since, at least between latitudes 30°N and 60°N, the synoptic variations of wind are considerably smaller at that level than they are in the upper troposphere. The lower stratosphere is also free from the smaller scale effects which would complicate studies of periodic wind variations occurring in the lower troposphere.

References

(1) Wilkes, M.V. 1949 Oscillations of the Earth's Atmosphere. Camb. Univ. Press.

(2) Simpson, G.C. 1918 Quart. J. Roy. Met.Soc. 44, p.20.

(3) Bartels, J. 1928 Handbuch der Experimentalphysik. 25, p.163.

(4) Elford, W.G. and Robertson, D.S. 1953 J. Atmosph. Terr. Phys. 4, p.271.

TABLE I. THE OBSERVED MONTHLY MEAN SIX-HOUR CHANGES OF WIND AT 100 mb OVER THE BRITISH ISLES FOR 1950-51

Component (kt)	Interval G.M.T.	Jan.	Feb.	Mar.	Apr.	May	June	July	Aug.	Sept.	Oct.	Nov.	Dec.	Annual Mean
West	0900-0300	-0.85	-1.20	-1.25	-1.17	-1.42	-1.42	-2.40	-0.91	-0.73	-0.93	-1.77	-0.36	-1.23
	No. of cases	111	90	106	110	150	151	143	120	121	151	87	90	1430
	1500-0900	0.48	0.85	1.96	1.17	1.51	1.50	2.30	1.93	1.52	1.90	2.00	0.02	1.50
	No. of cases	134	119	169	166	212	200	185	175	146	180	104	107	1897
	2100-1500	0.16	-0.42	0.04	-0.56	0.50	-0.41	-1.09	-0.11	0.07	-0.92	-0.67	-0.44	-0.32
	No. of cases	123	97	121	103	134	141	129	134	120	165	92	120	1479
	0300-2100	0.58	0.13	0.32	0.47	0.15	0.43	1.14	0.46	0.30	0.51	1.17	0.62	0.52
	No. of cases	128	77	100	92	109	141	120	107	116	165	84	101	1340
South	0900-0300	-1.58	-0.81	0.07	-0.10	0.26	-0.07	-0.22	-0.03	-0.90	0.25	-0.33	0.10	-0.24
	No. of cases	111	90	106	110	150	151	143	120	121	151	87	90	1430
	1500-0900	2.38	2.03	1.30	1.42	0.76	0.62	1.64	0.88	2.43	0.83	0.36	-0.16	1.23
	No. of cases	134	119	169	166	212	200	185	175	146	180	104	107	1897
	2100-1500	-0.94	-3.48	-2.04	-1.08	-1.70	-1.65	-2.01	-1.96	-1.99	-1.16	-1.88	-0.23	-1.64
	No. of cases	123	97	121	103	134	141	129	134	120	165	92	120	1479
	0300-2100	1.95	1.33	0.85	1.09	0.32	0.78	0.37	-0.73	0.59	0.71	1.21	0.14	0.72
	No. of cases	128	77	100	92	109	141	120	107	116	165	84	101	1340

/TABLE II.

TABLE II. THE "DERIVED" MONTHLY MEAN SIX-HOUR CHANGES OF WIND AT 100 mb OVER THE BRITISH ISLES FOR 1950-51.

Component (kt)	Interval G.M.T.	Jan.	Feb.	Mar.	Apr.	May	June	July	Aug.	Sept.	Oct.	Nov.	Dec.	Annual Mean
West	0900-0300	-1.03	-0.88	-1.79	-1.12	-1.79	-1.47	-2.37	-1.59	-1.31	-1.21	-2.13	-0.28	-1.47
	1500-0900	0.29	1.17	1.43	1.21	1.14	1.45	2.33	1.24	0.94	1.62	1.63	0.10	1.27
	2100-1500	-0.03	-0.10	-0.49	-0.51	0.13	-0.46	-1.06	-0.79	-0.51	-1.20	-1.03	-0.36	-0.55
	0300-2100	0.39	0.45	-0.21	0.51	-0.22	-0.38	1.16	-0.22	-0.28	0.23	0.80	0.70	0.29
South	0900-0300	-2.43	-0.35	-0.01	-0.76	0.34	0.04	-0.11	0.89	-0.96	-0.06	-0.01	0.17	-0.27
	1500-0900	1.47	2.49	1.21	0.75	0.94	0.78	1.75	1.80	2.37	0.56	0.68	-0.09	1.19
	2100-1500	-1.84	-3.01	-2.13	-1.74	-1.50	-1.49	-1.90	-1.04	-2.05	-1.47	-1.56	-0.15	-1.67
	0300-2100	1.04	1.79	0.76	0.42	0.50	0.94	0.48	0.19	0.52	0.39	1.53	0.21	0.69

/TABLE III.

TABLE III. MEAN SIX-HOUR VARIATIONS OF 100 mb WIND FOR WINTER AND SUMMER HALF YEARS, 1950-51

Interval G.M.T.	West Component (kt)		South Component (kt)	
	Summer	Winter	Summer	Winter
0900 - 0300	-1.61	-1.22	-0.09	-0.45
1500 - 0900	1.39	1.04	1.40	1.05
2100 - 1500	-0.53	-0.53	-1.62	-1.69
0300 - 2100	0.09	0.39	0.51	0.95

/TABLE IV.

TABLE IV. THE OBSERVED MONTHLY MEAN SIX-HOUR CHANGES OF WIND AT 150 mb OVER THE BRITISH ISLES FOR 1944-47 * (DUE TO ABSALOM)

Component (kt)	Interval G.M.T.	Jan.	Feb.	Mar.	Apr.	May	June	July	Aug.	Sept.	Oct.	Nov.	Dec.	Annual Mean
West	0600-0000	00	1.6	0.6	-1.6	0.5	-0.9	-0.5	-1.1	-2.5	0.0	-0.9	2.5	-0.2
	1200-0600	0.4	-0.8	-2.7	1.2	-0.9	0.1	1.3	-0.7	-0.4	-1.5	-0.5	-2.3	-0.6
	1800-1200	1.8	0.8	0.6	1.3	1.5	0.5	0.7	1.7	2.0	1.5	3.0	0.3	1.3
	0000-1800	1.7	-2.1	1.3	-1.7	-0.3	-1.5	-0.3	0.1	-1.1	-0.2	0.3	0.2	-0.3
South	0600-0000	-1.3	0.7	0.6	-0.5	1.0	0.7	-1.9	-1.3	-0.7	0.1	1.3	-2.3	-0.3
	1200-0600	1.7	0.3	0.8	2.2	1.5	1.7	2.5	1.8	0.2	0.6	3.8	3.6	1.7
	1800-1200	-0.2	-1.5	-1.3	-1.3	-1.5	-1.8	-1.4	-1.1	-0.1	-1.9	-2.2	-1.4	- -1.3
	0000-1800	3.1	0.8	-1.1	0.5	0.6	-1.4	0.1	-1.0	1.1	-3.4	4.6	-0.1	0.3

* The 0000-1800 variations were calculated from 2 years data.

/TABLE V.

TABLE V. DEVIATION OF ANNUAL MEAN WIND COMPONENT FOR STATED HOURS FROM THE OVERALL MEANS

Time G.M.T.	0300	0600	0900	1200	1500	1800	2100	2400
South Component (kt)	0.01	-0.54	-0.25	1.03	0.95	-0.40	-0.71	-0.11
West Component (kt)	0.43	-0.05	-0.92	-0.70	0.46	0.55	0.03	0.20

/TABLE VI

TABLE VI. VALUES OF "STUDENT'S" t OBTAINED IN TESTS OF THE SIGNIFICANCE OF THE OBSERVED SYSTEM OF SIX-HOUR VARIATIONS

Component	Period G.M.T.	A	B	C	D	E
South	0900-0300	-1.13	-4.25	2.87	-0.25	-0.04
	1500-0900	5.59	4.82	1.23	0.45	0.18
	2100-1500	8.74	-4.79	-3.68	0.26	-0.05
	0300-2100	4.87	6.00	-1.53	-0.40	0.07
West	0900-0300	-8.29	-5.00	-3.00	0.29	-0.23
	1500-0900	7.12	4.41	1.82	-0.88	-1.06
	2100-1500	-4.42	-9.08	3.08	-1.58	-0.83
	0300-2100	1.60	4.67	-4.40	-1.33	-1.13

Column "A" gives values of t obtained for difference between observed variations and zero variation.
Column "B" gives values of t obtained for difference between observed variations and the first harmonic of the observed variation.
Column "C" gives values of t obtained for difference between observed variations and the second harmonic of the observed variation.
Column "D" gives values of t obtained for difference between observed variations and the first two harmonics of the observed variation.
Column "E" gives values of t obtained for difference between observed variations and the first three harmonics of the observed variation.

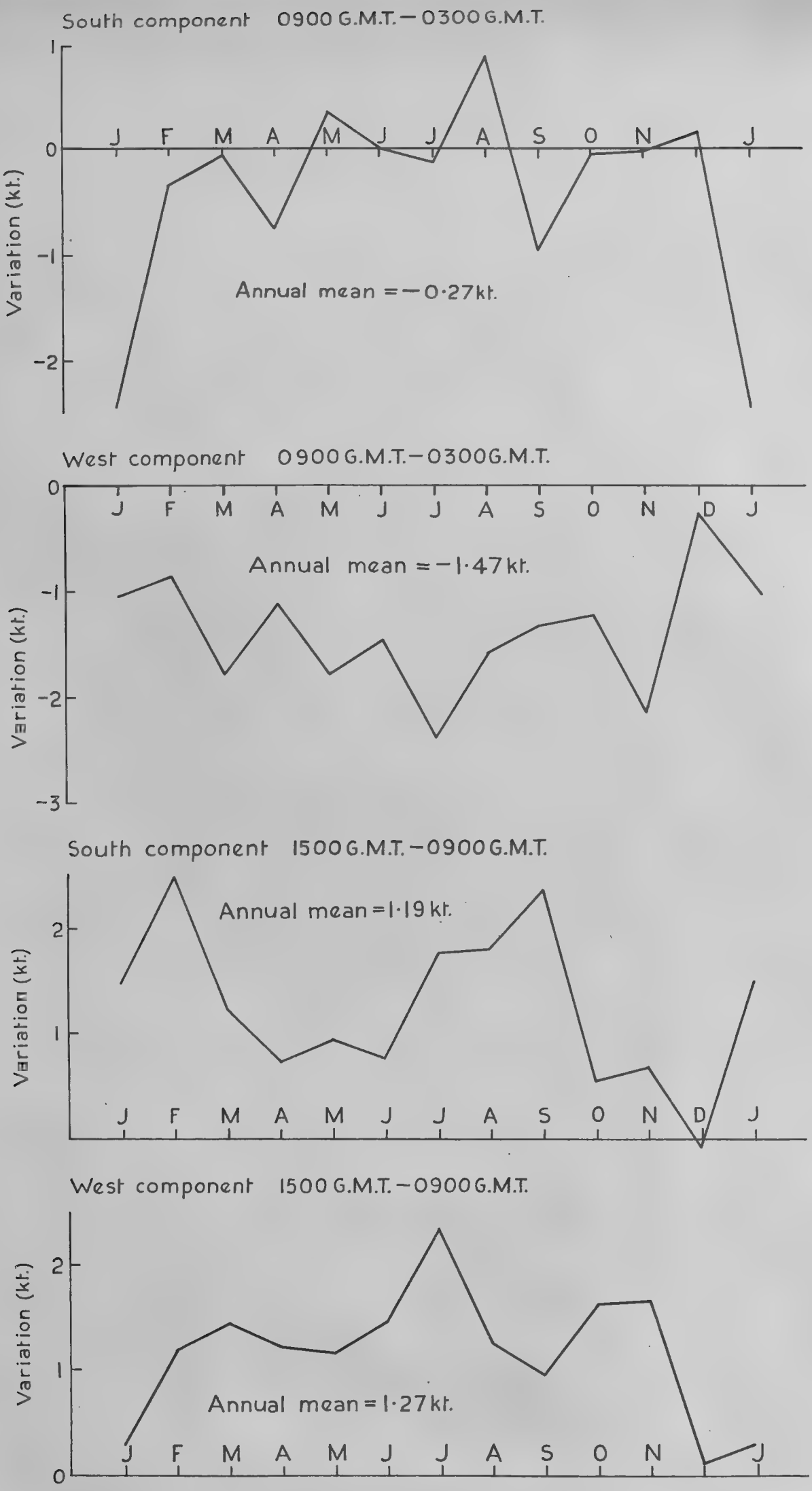

Fig. 1 Monthly mean six-hour variations of wind at the 100mb. level
1950 – 1951

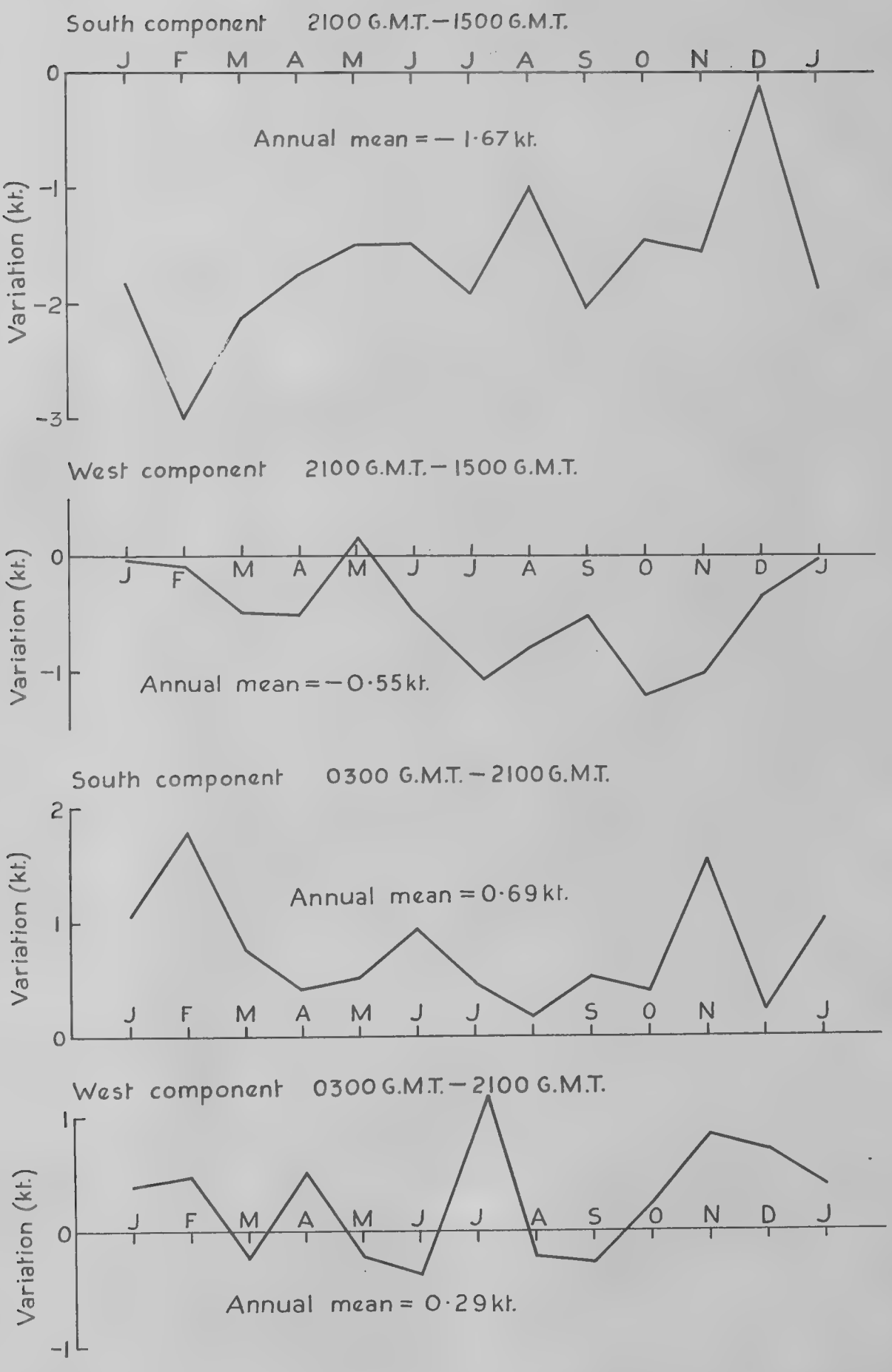

Fig.1 (cont'd.) Monthly mean six-hour variations of wind at the 100mb. level 1950–1951

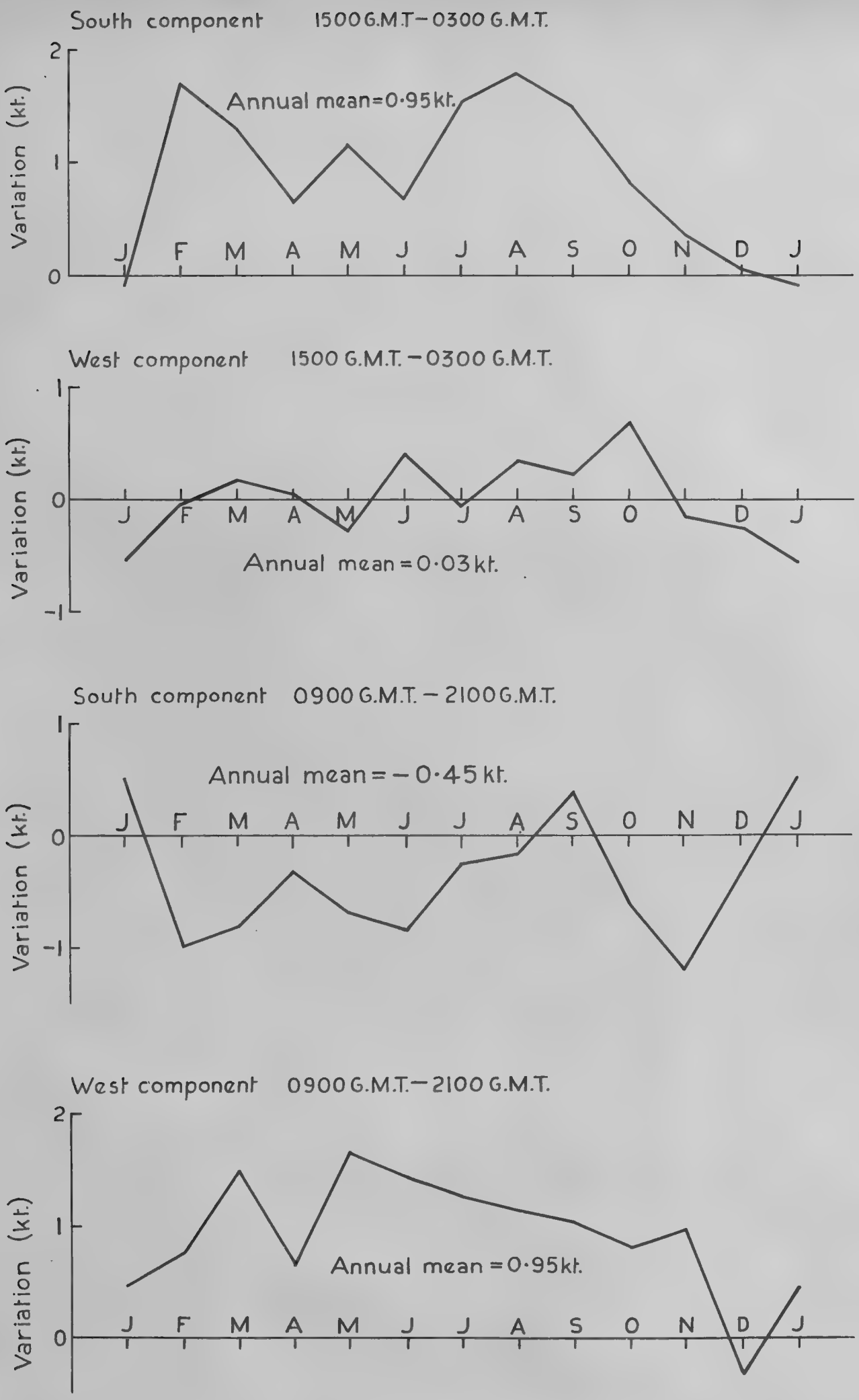

Fig. 2 Monthly mean twelve-hour variations of wind at the 100 mb. level 1950–1951

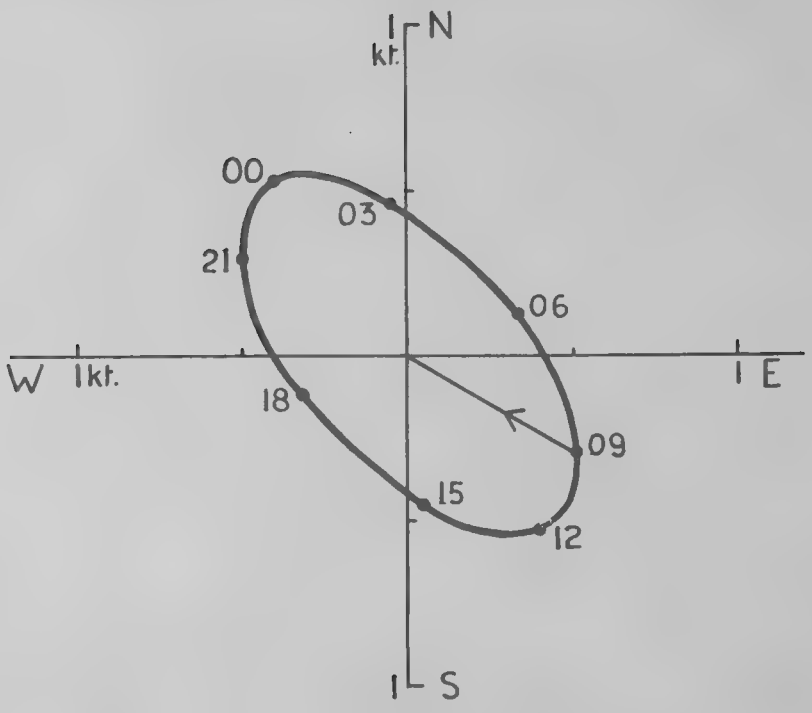

Fig.3 Vector diagram giving the wind velocity due to the diurnal oscillation. The wind velocity at any time is defined by the line joining the appropriate point on the ellipse to the origin

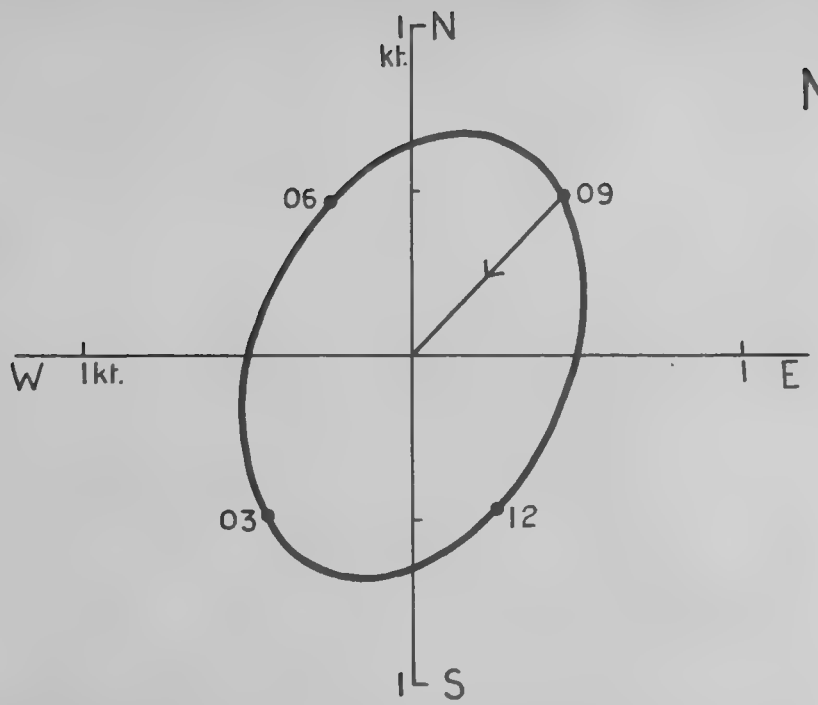

Fig.4 Vector diagram giving the wind velocity due to the semi-diurnal oscillation. The wind velocity at any time is defined by the line joining the appropriate point on the ellipse to the origin

(a) South component (kt.)

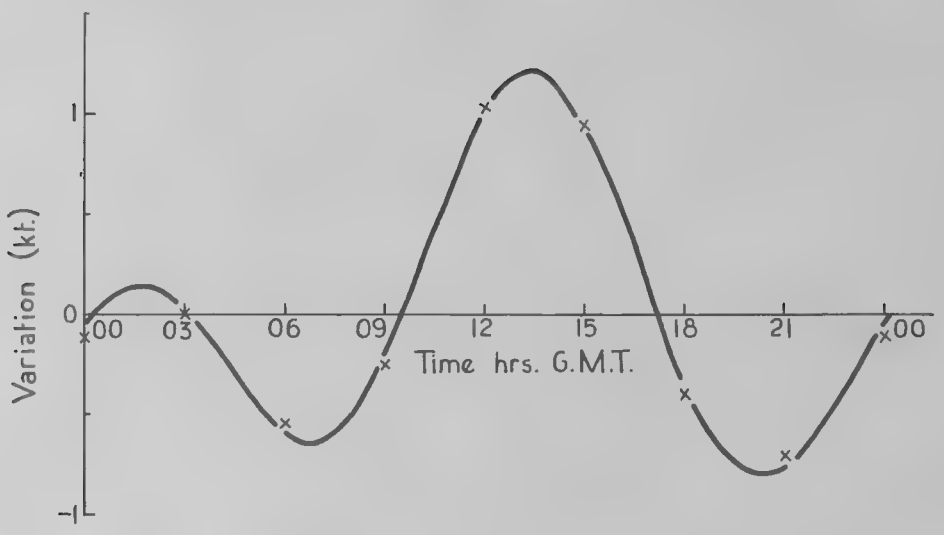

(b) West component (kt.)

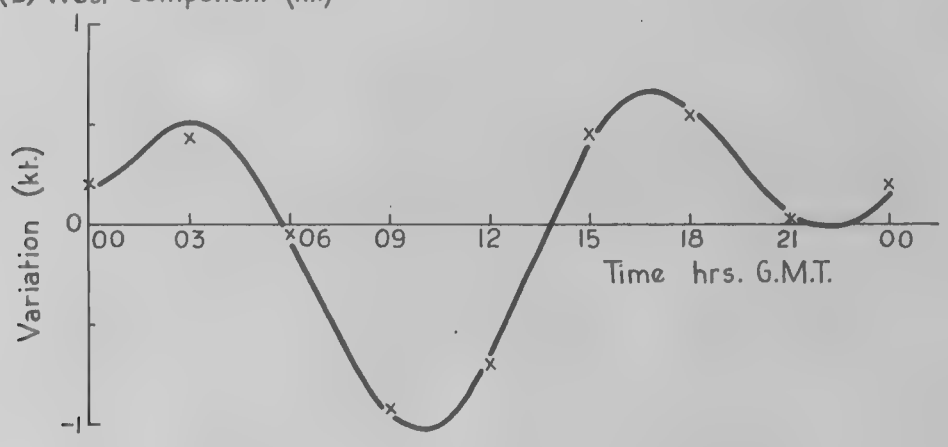

(c) Vector diagram giving the resultant wind velocity due to the combined diurnal and semi-diurnal oscillations. The wind velocity at any time is defined by the line joining the appropriate point on the curve to the origin

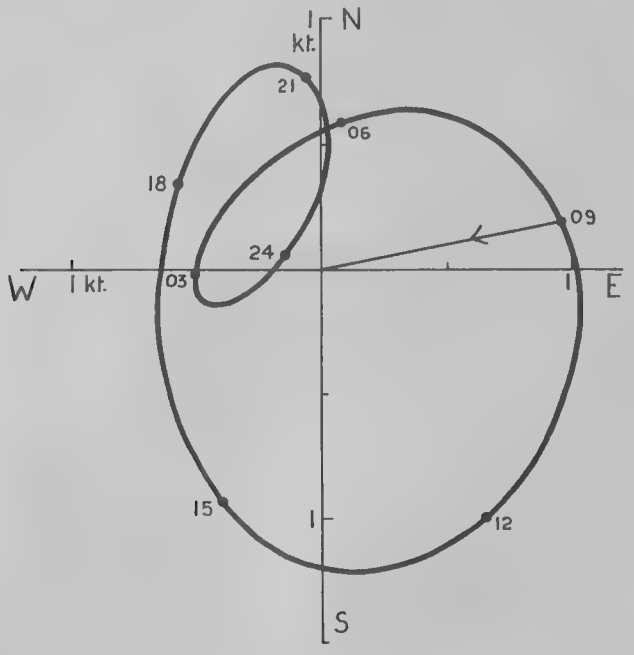

Fig. 5 The combined diurnal and semi-diurnal oscillations

(a) and (b) The crosses represent the observed deviation (given in Table V) of the wind components from the mean. The curves give the sum of the first two harmonics of these observed variations

(a) Diurnal oscillations

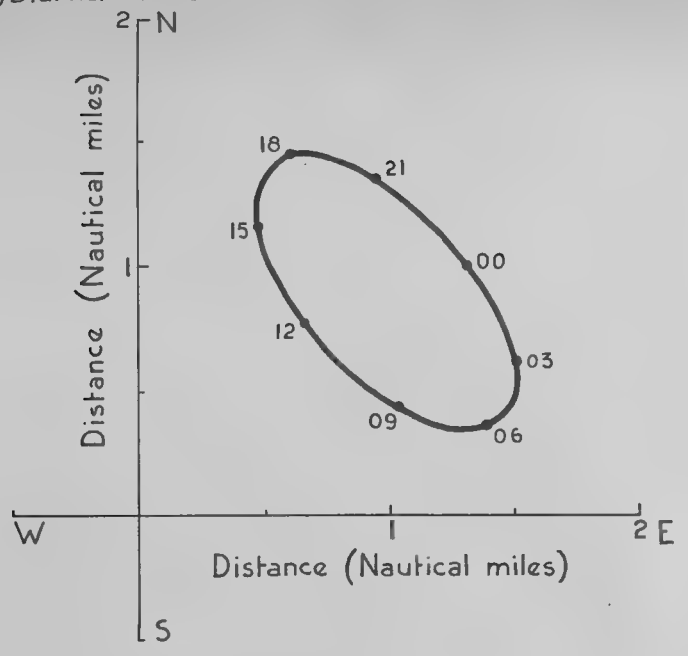

(b) Semi-diurnal oscillations

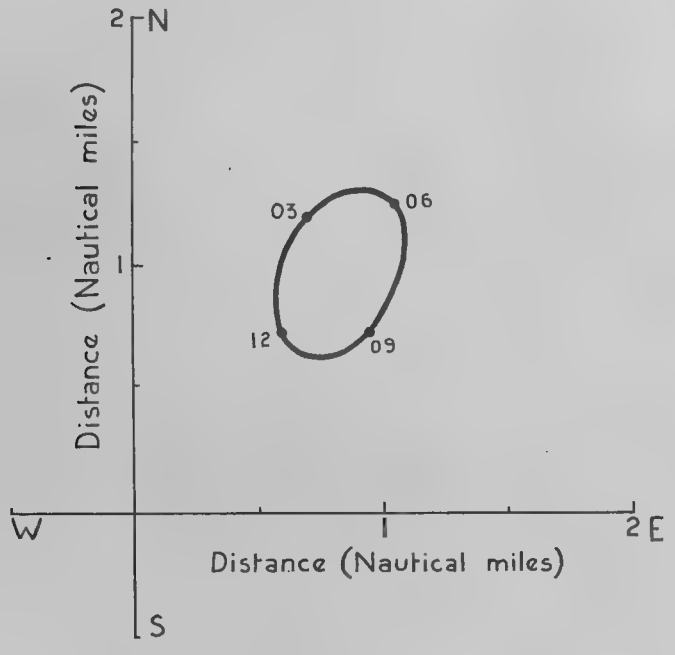

(c) Combined diurnal and semi-diurnal oscillations

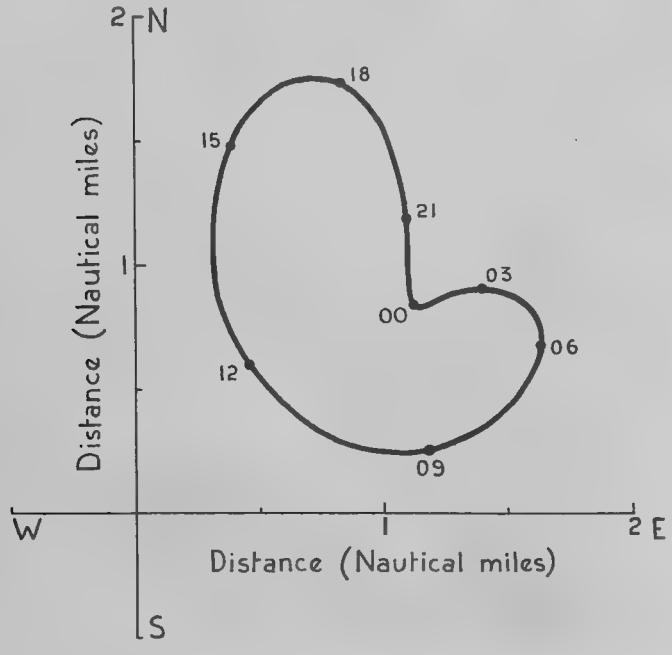

Fig. 6 Paths followed by particles oscillating under the wind systems defined by the diurnal and semi-diurnal variations of 100 mb. wind

Meteorological Office."

At the time of issue this report has not been published. Any author desiring to quote this paper should refer to it as "A paper of the Meteorological Research Committee (London), M.R.P. No. 862 by Mr. M. J. Blackwell
A copy is available in the Library of the Meteorological Office."

M.R.P. 862

S.C.I/87

12th May, 1954

A.J. 223079

AIR MINISTRY

METEOROLOGICAL RESEARCH COMMITTEE

Report on the automatic integration of solar radiation at Kew Observatory

by

M.J. Blackwell (Meteorological Office)

Summary

An account is given of the development and performance trials of an automatic integrating device for giving daily values of total (sun + sky) solar radiation. Circuit details are given, accuracy is assessed, and calibration technique discussed. In conclusion, future developments are outlined.

1. Introduction

Experience in the measurement of solar radiation has shown that reliable instruments and recording equipment, when repeatedly calibrated against suitable standards, may be combined to yield data having an estimated accuracy of the order of ±5% for hourly totals. Because of the very rapid fluctuations of intensity, caused by broken clouds or haze patches, it is found that errors introduced during the subsequent measurement of the charts amount to a further ±(5 - 10)%.

Of the short wave solar radiation measurements made at Kew Observatory, the most generally applicable component is that of total (sun + sky) radiation falling on a horizontal surface, and this was selected for the experiments in automatic integration to be described here.

Recording of total radiation began in 1946 (1) and had continued for three years when integrating methods were first surveyed. The solarimeters are of the Moll-Gorczynski type made by Messrs. Kipp and Zonen; their outputs are measured by Cambridge Instrument Co. thread-recorders. Measurement of the charts is done by estimating the mean intensity, hour by hour, and so summing to give daily totals. The thermopiles give a maximum D.C. output of about 10 mV on a bright summer's day. The problem was to integrate quantities of total radiation over periods of a day or less, and to be able to check the performance under all conditions.

2. The method adopted

Since the first three years' total radiation data had been analysed by estimation of mean hourly intensities with an accuracy of about 5-10%, the required accuracy of any automatic integrating device needed to be within 2-3%. Simplicity of design, stability of performance and ease of maintenance were the prime objectives if the time saved were not to be lost in attention to the equipment. The method adopted was to use a magnetic amplifier (type PDS.2 made by Electro Methods Ltd.) to drive a low inertia, permanent magnet D.C. integrating motor (type 900, 1.5 V nominal voltage, by the same firm) and a suitable counter.

/Amplifiers

Amplifiers of the type chosen have been fully described in a review article by Tweedy (2). Stability and linearity are enhanced by using two amplifier units in push-pull, and by restricting the power gain to 5000. Combined with the linear voltage-speed characteristic of the motor, the unit gives a closely linear performance with a stability of $\pm 2\frac{1}{2}\%$ for mains voltage/frequency variations of +5% and -15% (a 230V constant voltage transformer controls the supply).

Features special to the present unit include an input attenuator control to give a variable voltage amplification from 100 to 400, and a zero-setting control, which alters the effective operating point by varying a D.C. current in a separate bias winding. The result of this is to enable the output to be set at zero for zero input, or at a value close to the starting voltage of the integrating motor. The use of this control is further discussed in later sections. As shown in Fig. 1, the amplifier has been designed to match the impedance of the source.

3. History of the experiment

(i) Preliminary trials

After check calibrations had been made for linearity and suitable gain settings, the magnetic amplifier was connected to a spare solarimetric thermopile, and the motor coupled to a five-digit decade revolution counter (cyclometer type). Recording trials, started in November 1950 with a voltage amplification of 150, soon showed that the power developed at the solarimeter in winter was insufficient to enable the motor to turn the counter from say 4999.9 to 5000.0, thus giving poor correlation with the estimated totals on days of weak solar radiation.

The cyclometer was therefore replaced by a Post Office type relay counter; a suitable cam on the motor output shaft working a sensitive anemometer type of contact which in turn operated a telephone message register. The resulting performance remained satisfactory for the next year, but soon after deteriorated rapidly as the relay contacts wore out, having already far exceeded their rated life. To monitor the performance during each day, a recording voltmeter (Evershed tapping recorder) was placed in parallel with the motor across the output from the amplifier. Tests showed that this did not affect the calibration factor.

(ii) Correlation with estimated totals

Fourteen months' data (June 1951 - July 1952) were examined by plotting tabulated calories/cm^2 against the integrator counts. Superposed on this was the calibration of the integrating device as a whole, which was derived from two calculations. A plot of input voltage against counts gave the slope of the line, and the starting input voltage interpreted in terms of cal/cm^2/hr gave the intercept, as shown in Fig. 2. This question of the equivalent "starting" radiation intensity, and the method of correcting for it, is considered further in section 5(ii).

This period gave a close fit of the estimated values with the theoretical line derived from the integrator calibrations. Four calibrations were carried out during the period, and the conversion equations used were:-

July 1951	Cals = 0.034 Counts + 0.8 h *
Dec. 1951	Cals = 0.035 Counts + 2.5 h
May 1952	Cals = 0.034 Counts + 3.3 h
July 1952	Cals = 0.035 Counts + 3.4 h

These show nothing worse than a gradual increase of starting voltage under load, which was some 5mV at first and about 18mV at the end.

* See sec. 5(ii) for form of these equations.

/4.

4. Details of present apparatus

As a result of the experience outlined above, the final version of the integrating device, now in operation, was assembled in July 1952. Amplifier and integrating motor remain as before, but the relay counter has been replaced by a direct drive, dial type of counter. This is a light gear train meter, formerly incorporated in a Negretti and Zambra fan-anemometer. The torque required to start this counter is only 1/20 that required to work the relay counter.

Apart from routine stripping and cleaning of the motor every six months, the only major attention was the replacement of the gold brushes, which had become severely worn, in June 1953. This was foreshadowed by a rise in starting voltage from 12-18 mV, and erratic movement of the armature. With reasonable attention at six month intervals, the motor will start on load at 4.5 mV immediately after cleaning, and should be re-examined when this has increased to about 12 mV. These values are to be compared with the nominal starting voltage (no load), which is quoted as 4.2 mV.

5. Calibration technique

(i) Method

The impedances of the input side of the amplifier and that of the solarimeter + leads are first measured accurately with a resistance bridge. A circuit is then set up as in Fig. 3. The input voltage is fed in across a fixed resistance equal to that of the solarimeter + leads. The integrating motor and recording voltmeter remain connected to the output side as in normal running. The P.D. across both input and output terminals is measured by potentiometer during the calibration.

The zero setting control is then adjusted, as required, until the motor ceases to move backwards or forwards for zero input voltage. Its precise setting depends to some extent on the values of the input and output impedances. When no movement occurs over say 12 hours, the calibration can be done. The values of the input and output voltages give the voltage amplification factor; the former also enables the radiation not measured (through sticking) to be allowed for; the latter is a routine check on the condition of the motor. Lastly, a series of values of input voltage are plotted against integrator counts, giving the calibration factor and checking the linearity of the response.

(ii) Interpretation and application

The solarimeter, by comparison with an Ångström pyrheliometer, is found to generate a known e.m.f. for an incident radiation intensity of 1 cal/cm^2/hr. The corresponding integrator counts for this intensity can therefore be determined.

Secondly, from the value of the input starting voltage, the corresponding "starting" radiation intensity can be computed in cal/cm^2/hr. Formerly, this figure was multiplied by the length of day in hours to give the total correction for the day. This was then added to the quantity actually registered. Typical conversion equations were given in section 3(ii), e.g.:-

$$\text{Cals} = 0.035\ \text{Counts} + 0.8\ h$$

where h = length of day in hours, and the second term on the R.H.S. corresponds to the intercept in Fig. 2. This method gave good results for days of lowest radiation totals, but over-corrected the summer values. The reason for this is twofold: the full loss in the registered radiation obtains only for the fraction of the day during which the motor has actually stopped and the input is insufficient to restart it; secondly, when the motor is in motion, the value of the sliding friction is somewhat less than the static value which determines the starting voltage.

/It

It was found that the best empirically determined correction is given by adding a constant term (usually about 5-10 calories per day), which corresponds to the winter correction used above. This supports the theory that the reduced sliding friction in summer (due to the larger input signal) is compensated by the longer days. Fig. 4 contains six months' data plotted in this way against the tabulated totals.

A final point of interest lies in the shape of the integrator calibration curve near the zero. Recent experience has shown that this becomes slightly non-linear at high gain settings, and it becomes necessary to decide what is the form of the conversion equation giving the best fit under all conditions. Fig. 5 shows that a straight line can be drawn which is close to the experimental points at all places. This intercepts the axis at the effective starting voltage (less than the measured value in practice). This intercept determines the correction term to be used. The zero setting control can be used to shift the operating zero close to this effective starting voltage, thus reducing the correction term to a minimum. On the other hand, it is inadvisable to do this if the effective and measured starting voltages are nearly coincident, in case the motor moves slightly during periods of zero input.

6. Assessment of present performance

It must be remembered that the tabulated totals have to some extent been used as the reference for comparison in this experiment. This approach is justified as far as errors of estimation (introduced in the process of tabulation) are concerned, since these are found to be nearly randomly distributed about the true values *. Thus, provided a minimum of six months' data is used at one time (as in Fig. 4), with a check calibration of the integrator done at the beginning and end of each period, a valid comparison can be made.

In addition to the long term comparison, it has also been possible to carry out spot checks in the following way. A series of clear days is chosen, and the daily totals of solar radiation are found by planimetering the charts of the recording voltmeter (in parallel with the integrating motor). The totals are compared with the integrator counts for the same days, and hence the calibration of the voltmeter is effected (in terms of integrator counts). The calibration is then repeated (in terms of cal/cm^2/hr) by alternately shading and unshading the solarimeter; the difference in deflection between the two readings on the voltmeter record is then equivalent to $I \sin \theta$, where I is the intensity given by the Ångström pyrheliometer and θ is the sun's elevation at the time.

One further piece of evidence, though somewhat indirect, arose during the development of a bimetallic actinometer (3) which is also designed to give daily values of total (sun + sky) radiation. Its performance was originally checked with reference to the estimated totals since the integrating device was still in the experimental stage (June - November 1951). Even at this stage, however, a much improved correlation was obtained when the automatically integrated values were used as reference.

Finally, some comments on the scatter shown in Fig. 4 are perhaps called for, since this is largely attributed to errors other than those produced by the integrating device. The first point concerns the use of one solarimeter with a thread-recorder for the standard of reference, and a second solarimeter with the integrating device under test. Part of an investigation into errors inherent in radiation data (see Footnote) compared independent tabulations of the same daylight illumination records, which correspond closely in appearance with total radiation records (4). Also considered were tabulations of the records of the two solarimeters used here, when both were used in conjunction with thread-recorders. The correlations of the two sets of data were practically the same ($\sigma \sim 6\%$) and hence, in this respect, the use of a different solarimeter with the integrating device is justified.

* these results, based on trials in which many charts were measured independently by different observers, are due to Mr. R.H. Eldridge.

/The

362

The scatter of individual days is therefore attributed to errors caused by the minute by minute sampling of the thread recorder, the effect of its lag constant, and the random errors of tabulating ($\sigma \sim 2\%$ for daily totals). In conclusion, the estimated accuracy of the present apparatus is considered to be of the order of 2 - 3%.

7. Future developments

This report is presented at this stage of the work because the principle and accuracy of the method have been found satisfactory. Furthermore, the existing equipment requires no further modification for the stated purpose: namely, the integration of solar radiation over periods of a day. Certain extensions of the method, however, are contemplated.

The present amplifier has a continuously variable gain-setting knob. A future version would more conveniently have three or four settings for use at different times of the year. Finally, a time-marking system will be utilised to operate an automatic camera to photograph the counter-dial in order to give hourly totals of solar radiation.

8. Acknowledgments

I wish to acknowledge the help and guidance, during the preparation of this report, of Dr. G.D. Robinson, who planned the experiment from its inception in 1949. Thanks are also due to Mr. A.J. Lander for carrying out subsequent modifications to the original apparatus.

9. References

1. Stagg, J.M. Geophys. Mem., London, 11.86.1950

2. Tweedy, S.E. Electronic Eng., 20th Feb. 1948

3. Blackwell, M.J. M.R.P. 791, 1953

4. Blackwell, M.J. M.R.P. 831, 1953

G.401341/DMP/5/54/40

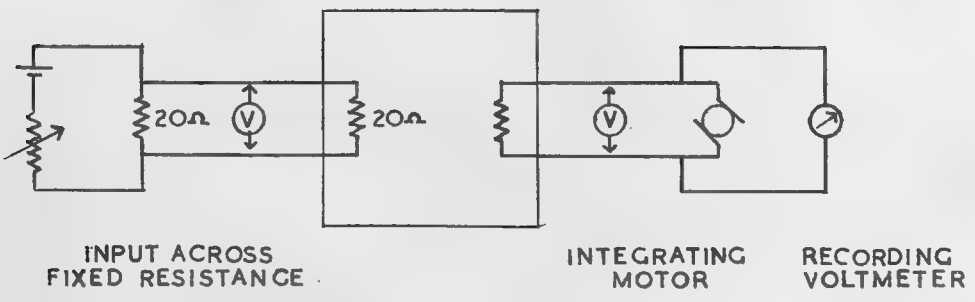

FIG.3 - CALIBRATION CIRCUIT

It
adding a
to the v
sliding
longer
tabulate

A
curve n
non-line
form of
Fig. 5
points
voltage
the cor
the ope
correct
if the
the mot

6. As

It
as the
as far
concern
values
(as in
and end

In
out spo
daily t
recordi
compare
of the
is then
the sol
voltmet
by the

On
develop
values
with re
the exp
much im
were us

Finally, some comments on the scatter shown in Fig. 4 are perhaps called for, since this is largely attributed to errors other than those produced by the integrating device. The first point concerns the use of one solarimeter with a thread-recorder for the standard of reference, and a second solarimeter with the integrating device under test. Part of an investigation into errors inherent in radiation data (see Footnote) compared independent tabulations of the same daylight illumination records, which correspond closely in appearance with total radiation records (4). Also considered were tabulations of the records of the two solarimeters used here, when both were used in conjunction with thread-recorders. The correlations of the two sets of data were practically the same ($\sigma \sim 6\%$) and hence, in this respect, the use of a different solarimeter with the integrating device is justified.

* these results, based on trials in which many charts were measured independently by different observers, are due to Mr. R.H. Eldridge.

/The

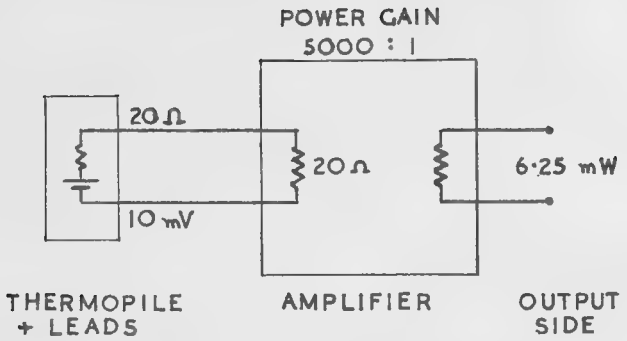

FIG. 1 — CIRCUIT

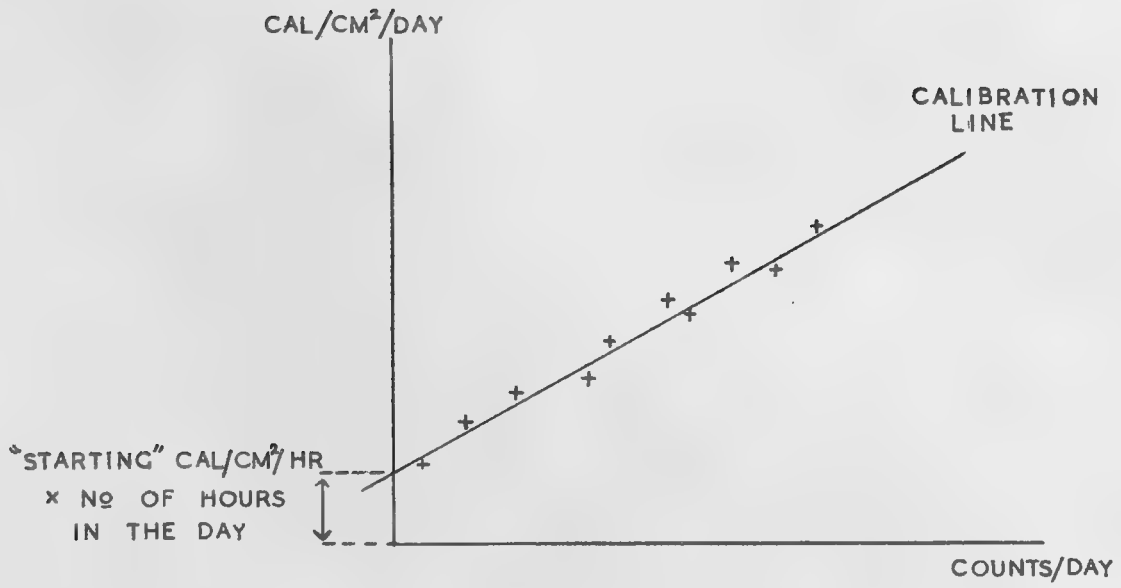

FIG. 2 — PRESENTATION OF DATA

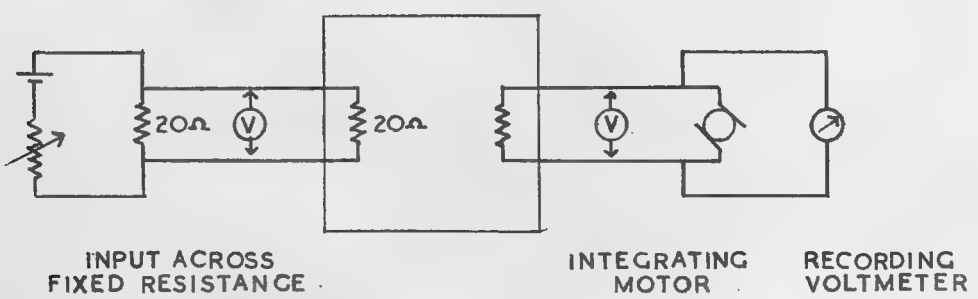

FIG. 3 — CALIBRATION CIRCUIT

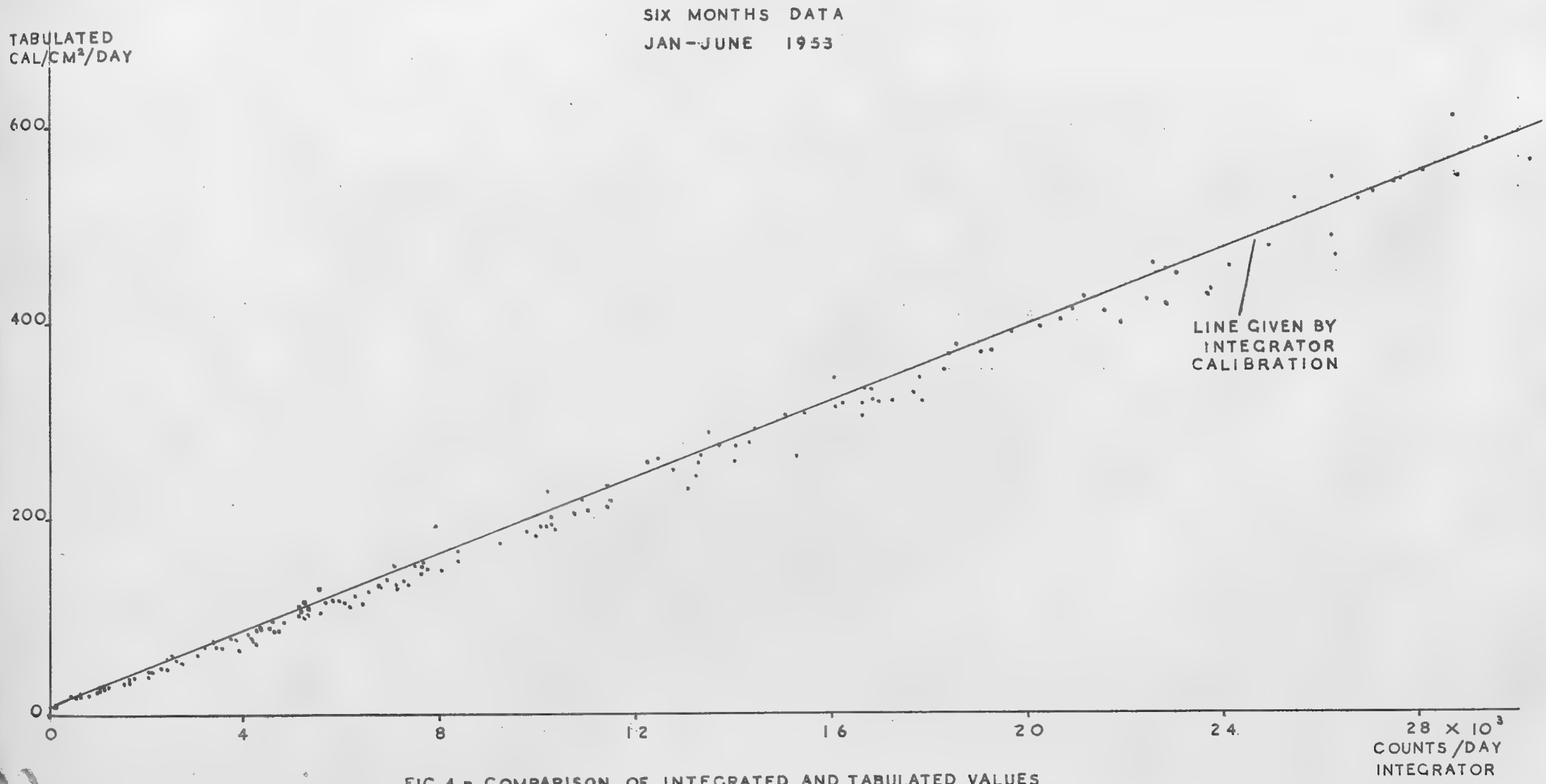

FIG.4 - COMPARISON OF INTEGRATED AND TABULATED VALUES

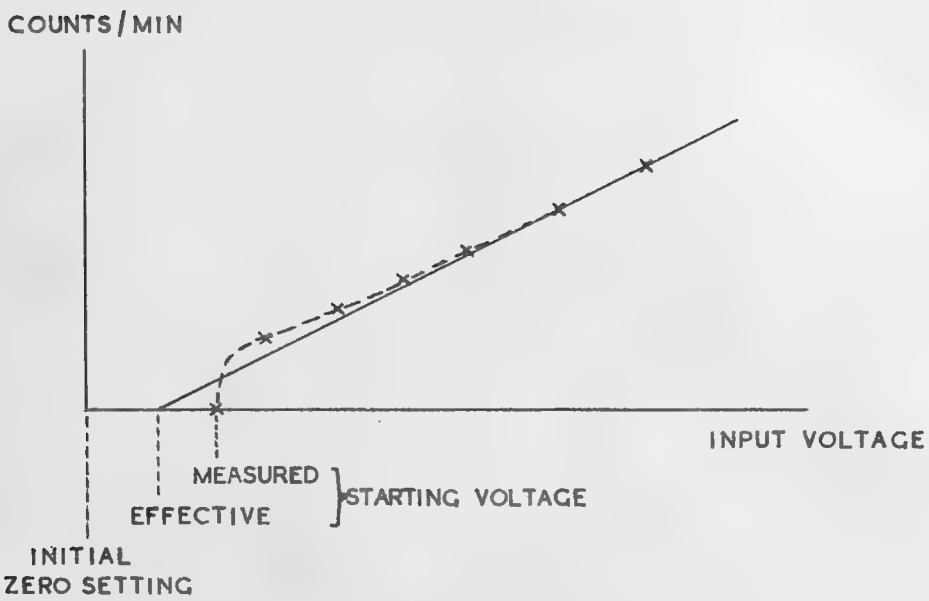

FIG . 5 — EFFECTIVE STARTING VOLTAGE

Miss M.K. Hinds.
copy is available in the Library

At the time of issue this report has not been published. Any author desiring to quote this paper should refer to it as "A paper of the Meteorological Research Committee (London), M.R.P. No. 863 by Mr. F.H. Bushby and Miss M.K. Hinds. A copy is available in the Library of the Meteorological Office"

M.R.P. 863
S.C.II/169
26th May, 1954

AD63784

AIR MINISTRY

METEOROLOGICAL RESEARCH COMMITTEE

A Preliminary Report on Ten Computed Sets of Forecasts Based on the Sawyer and Bushby Two-Parameter Atmospheric Model

by
F.H. Bushby and Mavis K. Hinds (Meteorological Office)

1. Introduction

In a recent paper Bushby and Hinds (1954) have presented the results of the first two sets of 12-hr and 24-hr computed forecasts of the 500 mb and 1000 mb contour charts and the 1000-500 mb thickness charts using the Sawyer-Bushby (1953) two-parameter model atmosphere. The results were sufficiently good to justify performing the elaborate computations for a further ten synoptic situations in order to ascertain the effects of the limitations of the model.

The present paper gives a descriptive account of the results of these ten computations. Suggestions are made of the way in which certain limitations of the two-parameter model could possibly account for some of the discrepancies between the computed and actual charts, but until these limitations have been removed and the calculations repeated, it is not possible to be definite about this matter.

Correlation coefficients have been evaluated between the observed 24-hr changes and the computed 24-hr changes, and regression equations have been worked out. This has been repeated with the 24-hr forecast charts prepared by conventional methods in the Forecasting Branch, Dunstable, in an attempt to compare these two methods of forecasting.

2. The Method

The method of solution is essentially the same as that described by Bushby and Hinds (1954), but 1-hr time-steps were used throughout the computation in order to eliminate the effects of computational instability. In certain of the summer situations a longer time-step might have been satisfactory, but it was thought best to introduce a uniform procedure for this series of calculations. The actual time integration formulae used were:-

$$H_1 = H_0 + \left(\partial H/\partial t\right)_0 \delta t \qquad \text{(1)}$$

$$H_{n+1} = H_{n-1} + 2\left(\partial H/\partial t\right)_n \delta t \qquad \text{(2)}$$

where H_n represents a value of the 500 mb contour height or 1000-500 mb thickness at time $t + n\delta t$, and t is the time to which the initial data of the computation refer.

Nine of the ten computations were performed on LEO, the electronic computing machine owned by J. Lyons and Co., and the tenth by a Ferranti machine at Manchester University. The machine time (including output) per time step was $8\frac{1}{2}$ minutes, irrespective of which machine was used.

The ten situations were chosen so as to cover a wide range of synoptic conditions.

3. Results

(a) 1500 GMT 8 Jan., 1951

The most significant feature of the synoptic situation during the 24 hours commencing 1500 GMT 8 Jan., 1951 was the development of a depression from a small trough associated with a frontal system in mid-Atlantic. This depression became moderately deep and moved to 47°N 12°W by the end of the period. It was associated with a developing thermal trough and a cut-off depression at 500 mb.

This development was not indicated by the computed charts (see Figs. 1a-j). The weak 500 mb trough in existence at the commencement of the period was certainly computed to intensify, but the main vortex was forecast too far NNE. The forecast 1000-500 mb thickness trough was about 5° too far east and the absolute values were much too low, almost certainly due in part to the neglect of the non-adiabatic heating over the warm sea. Thus the computed 1000 mb chart for 1500 GMT 9 Jan., 1951 bore very little resemblance to the actual synoptic situation. During the forecast period a considerable change took place on the northern half of the western boundary and this may have contributed towards the failure of the computed forecast.

The forecasts produced by the conventional methods of the Forecast Division, Dunstable, for this period contained similar errors in the region of the British Isles to those of the computed charts.

(b) 1500 GMT 10 Aug., 1951

This situation was one in which a depression centred at 54°N 24°W associated with a thermal trough moved eastwards to North Wales during the ensuing 24-hr period. This movement was calculated quite well (Figs. 2a-j) although the calculated deepening of the depression was a little too much. The computed 500 mb pattern also agreed closely with the actual pattern, although the 500 mb ridge in mid-Atlantic was computed to be too intense and this was reflected in the intensity of the computed 1000 mb ridge. The over-development of the mid-Atlantic contour ridge is probably partly due to the use of the wrong boundary conditions and partly due to the limitations of the model.

(c) 1500 GMT 19 Sept., 1951

This case was chosen as typical of a slow-moving situation of early autumn (Figs. 3a-j). At 500 mb the ridge to the west of the British Isles moved only 1 or 2 degrees east in 24 hours, but the northwesterly flow over the north-eastern half of the British Isles and the North Sea was decreased to approximately half of its original strength in that time. The computed chart showed the decrease in the northwesterly flow, but moved the axis of the ridge a little too far east. The 500 mb contour height was computed to be about 300 ft higher in the Bay of Biscay than actually occurred.

The anticyclone centred at 49°N 11°W moved to the Straits of Dover in this 24-hr period with only little change of intensity, whereas the centre was computed to be in central France and the anticyclone was

/calculated

calculated to intensify. The ridge over the British Isles was computed to move into Scandinavia, and a moderate SW'ly was computed for the British Isles. In fact, the ridge only moved into the North Sea and most of the British Isles experienced light variable winds.

Since speeds of movement of several features were overestimated the computed forecast would probably be improved if the 600 mb contour heights and the 1000-600 mb thicknesses had been used instead of the 500 mb contour heights and the 1000-500 mb thicknesses.

(d) 1500 GMT 30 Jan., 1952

This situation (Figs.4a-j) was one in which the strong winds over the Atlantic at 500 mb associated with a jet stream at higher levels spread south-eastwards to affect the south-western sea-board of Europe throughout the ensuing 24 hours. The 12-hr computed forecast was quite reasonable, but subsequently the strong winds were computed to extend across the North Sea. The 500 mb vortex was also computed to move in its entirety to the Faroes, but this did not happen. The computed winds were stronger than those that actually occurred, which was partly due to the incorrect treatment of the 500 mb vortex, and partly due to the fact that the height of the 500 mb contour along the 50°N parallel was forecast to increase whereas it actually decreased in the region of the British Isles. The effect of the western boundary may have spread further into the chart than usual as a result of the exceptionally strong winds.

The behaviour of the 1000 mb depression was more accurately dealt with, but the main frontal trough was computed much further east than actually occurred. There are signs of the beginnings of computational instability in the computed charts, especially the thickness and 1000 mb charts. This is not surprising considering the exceptionally strong winds.

The computed thickness chart for 1500 GMT 31 Jan. gave the main thickness trough too far north-east, and most of the absolute values of thickness over the sea were too low. This forecast could probably be improved by taking into account the effect of the warming of cold air masses over the sea, and also by using the flow at 600 mb instead of 500 mb.

(e) 1500 GMT 13 May, 1952

The computed charts for the 24-hr period commencing 1500 GMT 13 May, 1952 agree quite well with the actual charts (Figs. 5a-j). During this period only slight changes occurred. The 500 mb flow over the British Isles was correctly computed to be displaced northwards and intensified, but the absolute values of the computed 500 mb contour height for 1500 GMT 14 May were about 200 ft too high.

The computed 1000 mb charts agrée quite well with actuality in the vicinity of the British Isles, but slight errors in both the computed contour height and thickness in the vicinity of the mid-Atlantic surface depression have caused the computations to indicate the north-northeastwards motion of that depression, whereas it actually drifted slowly eastwards.

(f) 1500 GMT 3 July, 1952

This was another situation in which the computed charts agree quite well with the actual charts in the region of the British Isles. A cut-off depression at 500 mb, together with an associated cold pool, developed during the period. The computed charts indicated this, although in each case the centre was too far east. The absolute values of the highest regions of the computed 500 mb contour chart for 1500 GMT 4 July were again about 200 ft too high, and the area SE of Greenland was incorrectly dealt with due to considerable changes on the boundary which were ignored.

/(g)

(g) 1500 GMT 31 Dec., 1952

At the commencement of this forecast period the flow over Western Europe and the North Atlantic was largely meridional at all levels in the troposphere, there being a deep 500 mb trough over Labrador and another over the western seaboard of Europe with a cut-off low over England and the North Sea. During the ensuing twenty-four hours there was slow progession in fairly high latitudes, the Atlantic ridge moving in towards the British Isles and the cut-off 500 mb low moving southwards over France. The accompanying surface low moved from the North Sea to northern Italy.

These main trends were well forecast by computational methods, but minor surface cyclonic activity moved into the forecast area from south of Labrador and was therefore not forecast. In association with this error the surface anticyclone and warm ridge south of Iceland were computed to develop too strongly.

(h) 1500 GMT 30 Jan., 1953

This was the occasion of the disastrous flooding in the Netherlands and along the east coast of England. At 1500 GMT on the 30th the centre of the depression which caused the floods was over the Faroes, the main warm front over southern Norway and the Kattegat, a secondary warm front over Ireland and the cold front approaching the western coasts of Scotland and Ireland. During the forecast period the depression moved south-eastwards to the Skegerrak, the cold front and secondary warm front amalgamated to give an occlusion over Eastern Germany and a surface trough formed in the cold air over the North Sea. Meanwhile the anticyclone south-east of Greenland developed and moved eastwards to a position south of Iceland.

The depression was computed to move eastwards to the Norwegian coast with troughs in the correct places over Germany and the North Sea. However, the anticyclonic development in the Western Approaches was over-estimated by the computations giving a very strong north-northwesterly gradient over the British Isles at all levels in the troposphere. In association with this very deep cold air was forecast to be advected across the British Isles from the Iceland region. These effects combine to give the forecast charts shown in Figs. 8h and 8j. There is no doubt that if these charts had been correct the floods would have been even more calamitous than they actually were. These errors were due to a number of causes including the considerable surface friction which would be associated with such high winds, the warming of the deep cold air as it passed over the warm sea near the British Isles and the over-estimation of anticyclonic development which appears inherent in the present model. It will be noticed from the table of correlation coefficients that despite these errors the computed forecasts were of a similar standard to those produced by conventional methods.

(i) 1500 GMT 18 July, 1953

During the forecast period a large but shallow low pressure area centred near the Shetlands moved north-eastwards into central Norway and a ridge moved in from the Atlantic over the British Isles. During this time the 500 mb low over the British Isles was also replaced by a ridge and a 1000-500 mb thickness trough moved from Ireland to the North Sea. These considerable changes near the British Isles were well forecast both by conventional and numerical methods. However, the computed forecast was not quite so successful over the Atlantic. A depression which was south-east of Greenland at the beginning of the forecast period moved eastwards and at the end of the twenty-four hours the warm front was approaching south-western Ireland. Although a considerable trough was computed to move eastwards with a similar speed to the actual frontal

/trough

trough, the depression itself was computed to deepen and remain stationary. This error appears to be due to the fact that at present the computational forecast does not allow motion across the western boundary, and in this case, as in several others, such motion actually occurred.

(j) 1500 GMT 15 Oct., 1953

The charts on which the forecast was based show a deep depression south-east of Greenland with a frontal trough at about 15°W. There are anticyclones to the west of the Azores and over Scandinavia and a shallow low pressure area covers most of the rest of Europe. In the 1000-500 mb thickness pattern there is a deep cold trough behind the Atlantic depression, a small ridge to the west of the British Isles and a cut-off cold pool over the Western Mediterranean. Both computed and conventional forecasts correctly brought the frontal trough and thermal gradient in over Ireland but kept the main centre back south-west of Iceland. Over Europe, however, the computed forecasts suffered from an error due to an unusual cause. Both 500 mb contour and 1000-500 mb thickness charts for the beginning of the period show a strong southerly jet-stream in the region of Algeria to the east of a cut-off low. Since this region is close to both the southern and eastern boundaries of the computed charts, this jet-stream was assumed to be maintained and the consequent advection of cyclonic vorticity on its western flank was computed to give rise to a small but intense 500 mb low over Germany and an accompanying surface depression over the Low Countries.

4. Comparison of computed and conventional forecasts

Correlation coefficients between the computed and actual 24-hr changes of contour height and thickness and regression coefficients a and b of the best fitting straight line giving the actual change (Y tens of feet) in terms of the computed change (X tens of feet) in the form

$$Y = a X + b \qquad (3)$$

were calculated for the interior grid of 12 x 8 points.

TABLE I

CORRELATION AND REGRESSION COEFFICIENTS

Starting Date	Method	500 mb			1000-500 mb			1000 mb (A) and Surface Pressure (B)		
		r	a	b	r	a	b	r	a	b
8. 1.51	A	0.68	0.63	13.2	0.59	0.81	19.8	-0.27	-0.18	- 2.2
	B	0.61	0.71	2.3	0.82	1.02	-0.1	0.59	0.75	- 1.5
10. 8.51	A	0.90	0.69	-10.2	0.84	0.75	-5.4	0.85	0.58	- 0.7
	B	0.87	1.23	- 4.2	0.91	1.32	-4.4	0.87	1.15	- 1.5
19. 9.51	A	0.89	0.83	-12.5	0.47	0.43	-3.3	0.72	0.53	- 5.6
	B	0.74	0.89	- 2.9	0.22	0.21	-0.4	0.86	0.81	- 0.6
30. 1.52	A	0.61	0.36	25.3	0.58	0.33	-3.3	0.52	0.51	21.7
	B	0.67	0.62	-16.7	0.86	0.69	-4.6	0.79	0.92	- 1.6
13. 5.52	A	0.87	0.56	- 8.8	0.85	0.62	3.7	0.35	0.15	- 5.3
	B	0.94	0.85	- 2.1	0.92	1.02	1.5	0.67	0.66	- 2.2
3. 7.52	A	0.48	0.87	- 8.3	0.46	0.68	-7.7	0.27	0.19	0.2
	B	0.87	0.99	- 7.0	0.74	1.04	3.9	0.36	0.31	1.7
31.12.52	A	0.46	0.43	- 5.9	0.08	0.06	-2.6	0.55	0.51	- 6.5
	B	0.79	1.00	- 9.0	0.57	0.66	0.2	0.79	1.09	- 5.8
30. 1.53	A	0.96	0.75	-12.3	0.89	0.56	1.2	0.88	0.62	-15.5
	B	0.90	1.10	21.3	0.86	1.03	7.5	0.91	1.09	- 1.2
18. 7.53	A	0.78	0.79	- 3.9	0.93	1.01	0.7	0.67	0.55	- 3.6
	B	0.91	1.04	5.9	0.89	1.14	7.7	0.89	0.79	1.4
15.10.53	A	0.64	0.62	24.1	0.75	0.81	2.1	0.73	0.39	22.4
	B	0.90	1.10	9.1	0.85	1.38	-5.4	0.73	0.59	6.5

r = correlation coefficient, A = computed forecast,
B = conventional forecast, heights in tens of feet, pressures in mb

The conventional forecasts prepared by the Forecast Branch of the Meteorological Office, Dunstable, do not cover exactly the same period as the computed charts, but a similar set of values comparing the conventional forecast changes with the actual changes is also shown in Table I, using the conventional forecast which related as closely as possible to the period covered by the computations.

The grid of 12 x 8 points was used in order to decrease the effect of boundary conditions on the correlation coefficients. However, large pressure changes in mid-Atlantic due to the eastward movement of large atmospheric systems across the western boundary can cause large errors in the computed charts at some of the 12 x 8 grid points. As these changes are often of greater magnitude than those in the vicinity of the British Isles, the correlation between the computed and actual changes is lower than it otherwise would be. This was particularly noticeable for the two situations of 8 Jan., 1951 and 3 May, 1952. The computed and conventional forecast charts were quite similar in the region of the British Isles but there was a considerable difference in the correlation coefficients due to the conventional forecaster correctly estimating large changes in mid-Atlantic. Another limitation of the correlation method of comparing forecasts is the fact that in a situation of little change, a small error in the position of a depression may have a considerable effect on the correlation coefficient. A similar adverse effect is caused by any large forecast change which is correct in magnitude, but in error in position. Nevertheless, Table I does give some indication of the degree of success of the computed forecast compared with that of the conventional forecast for the interior grid of 96 points.

5. Conclusion

The main conclusion for the present series of calculations is that the Sawyer-Bushby two-parameter model has achieved an encouraging amount of success away from the boundary in nine of the ten situations that were examined. In five of these the computed forecasts for the vicinity of the British Isles were of the same standard as those prepared by conventional methods, but in the other four situations conventional methods produced a somewhat better forecast than the computations.

The discrepancies between the actual and computed charts were examined in an attempt to decide if any aspect was common to more than one of the computations. It is immediately apparent that in winter months, the computed thickness over the sea is often much less than it actually was and this is almost certainly due to the neglect of the heating of cold air masses over the sea in the basic equations.

Another common discrepancy is the over-estimation of the absolute value of the contour heights in anticyclonic regions. The reason for this is not immediately apparent, but in the theory of the method the parameters h_m and h' are treated more as stream functions than as contour heights, and as the geostrophic vorticity is an underestimate in anticyclonic regions, the use of the geostrophic approximation to obtain a contour height from the computed vorticity field could give rise to this type of error. The reason why the cyclonic developments are dealt with more accurately could be that in cyclonic regions errors due to the neglect of friction and to the use of the geostrophic approximation tend to cancel out, whereas they do not in anticyclonic regions.

In certain of the situations where the mobility was computed to be more than actually occurred, this may have been due to the use of the 500 mb contour heights and the 1000-500 mb thicknesses instead of the 600 mb contour heights and the 1000-600 mb thicknesses to which the theoretical equations were designed to apply.

Finally, it is quite apparent that the present size of the 18 x 14 grid is a bare minimum if reasonably correct forecasts are to be produced for the British Isles.

/Further

Further investigation will be needed to ascertain how far the standard of the computed charts can be improved by reducing the aforementioned limitations on the model, but the success so far achieved with the crude two-parameter model is sufficient to encourage the belief that further progress forward from this stage can be made.

References

Bushby, F.H. and Hinds, M.K.	1954	Quart. J. R. Met. Soc., 80 (in press).
Sawyer, J.S. and Bushby, F.H.	1953	J. Met., 10, p.54.

G.401483/JWP/5/54/40.

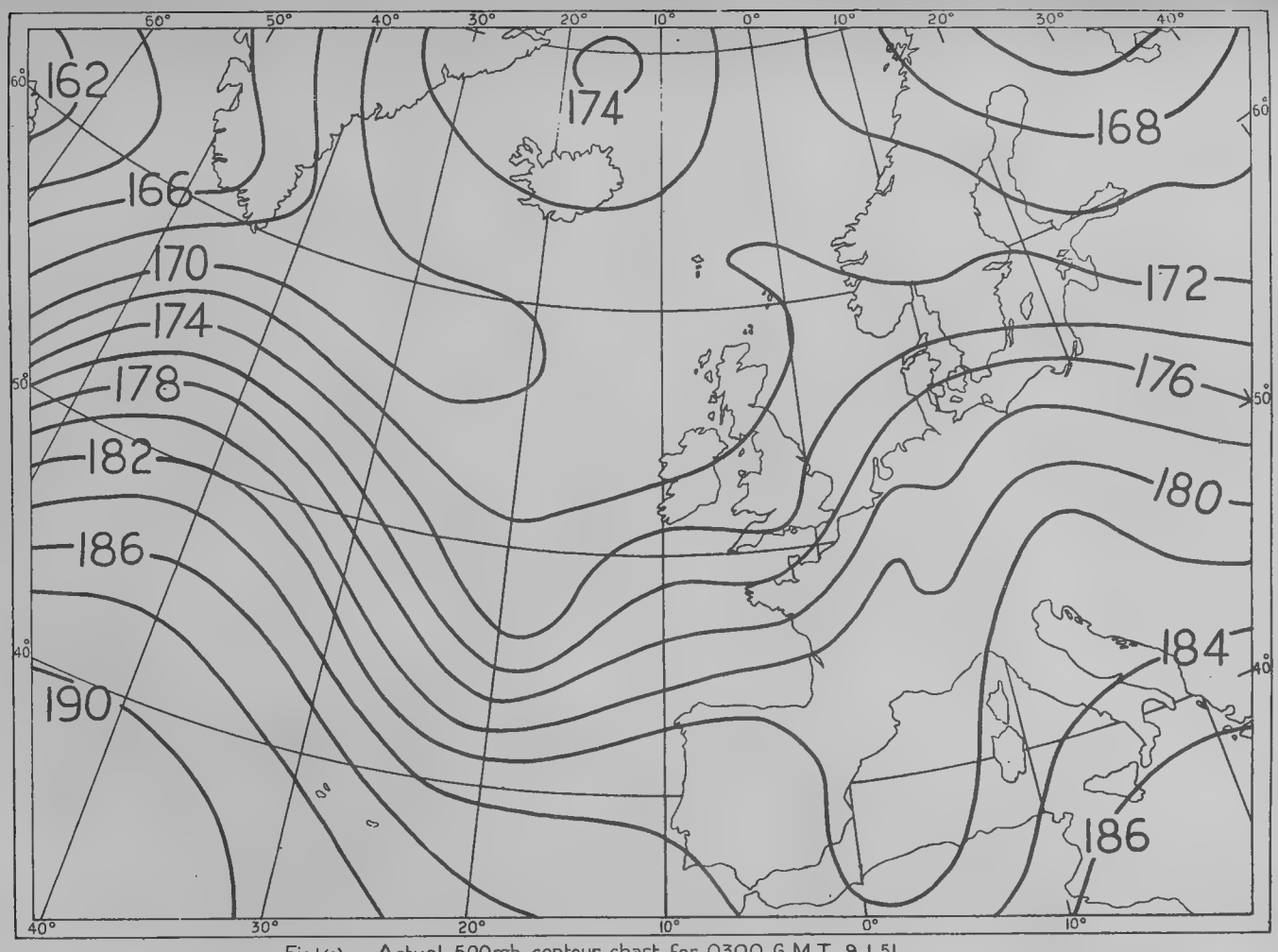

Fig1(c) Actual 500mb. contour chart for 0300 G.M.T. 9.1.51

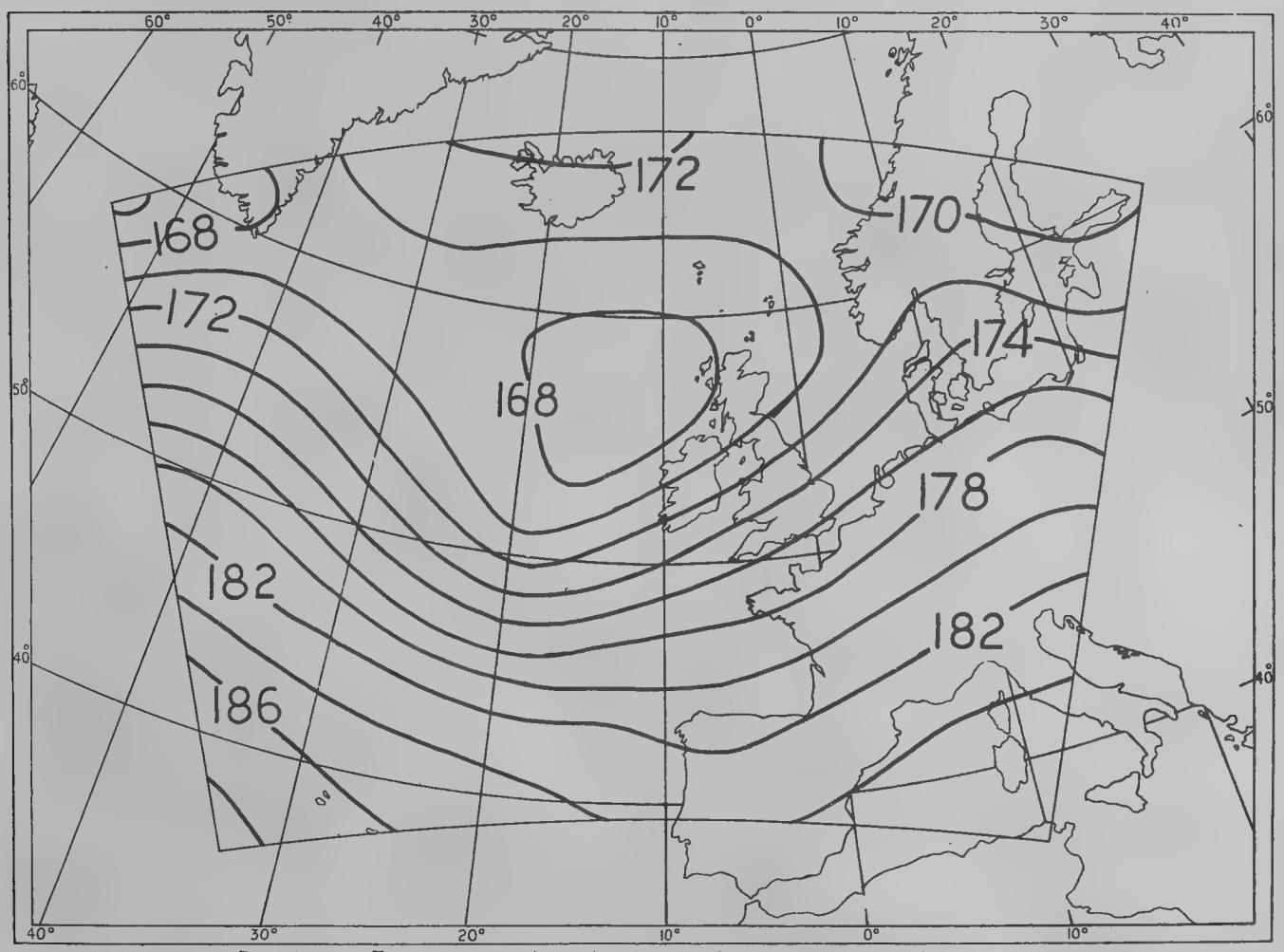

Fig.1(d) Forecast 500mb. contour chart for 0300 G.M.T. 9.1.51

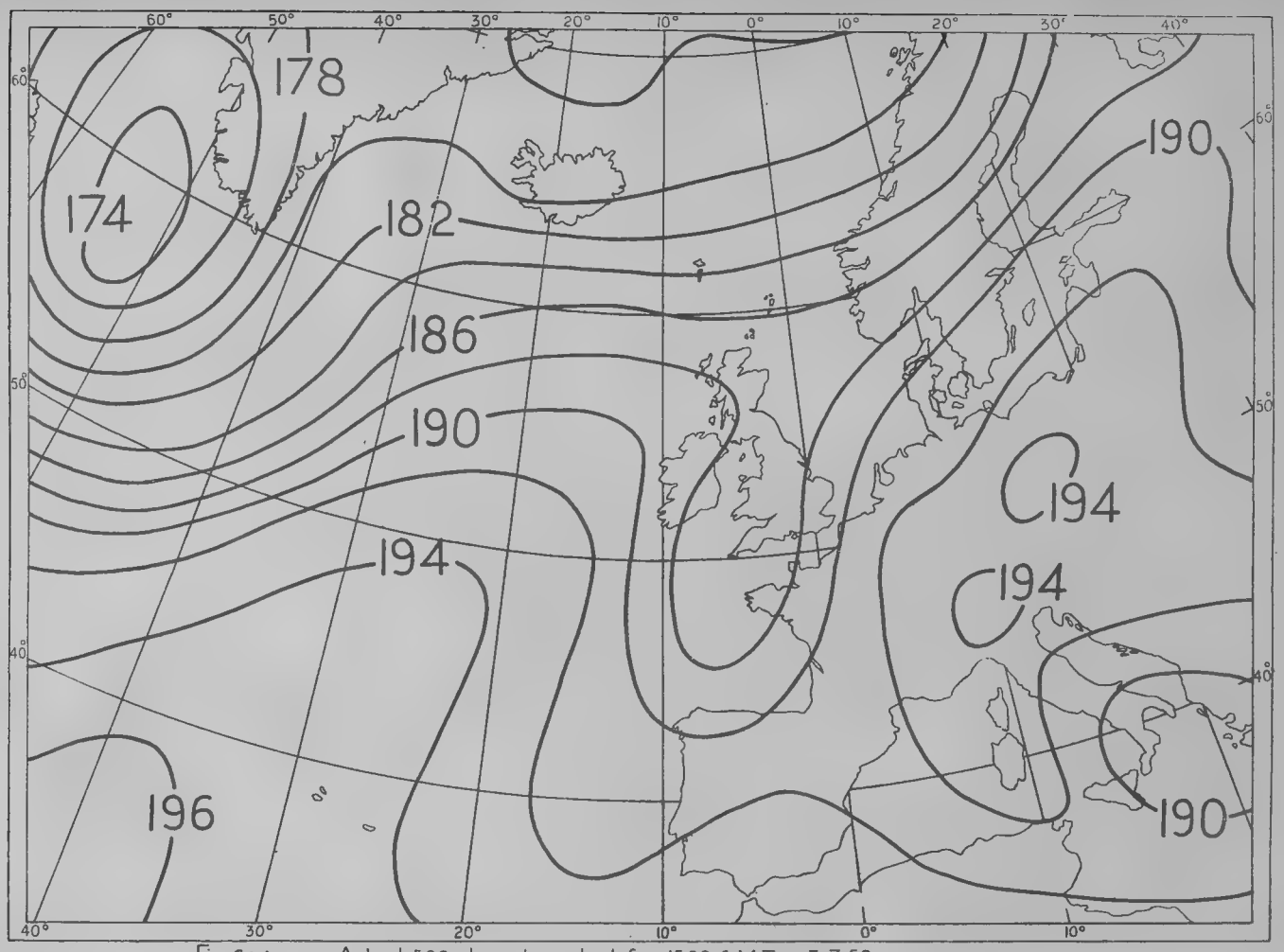

Fig.6(a) Actual 500mb. contour chart for 1500 G.M.T. 3.7.52

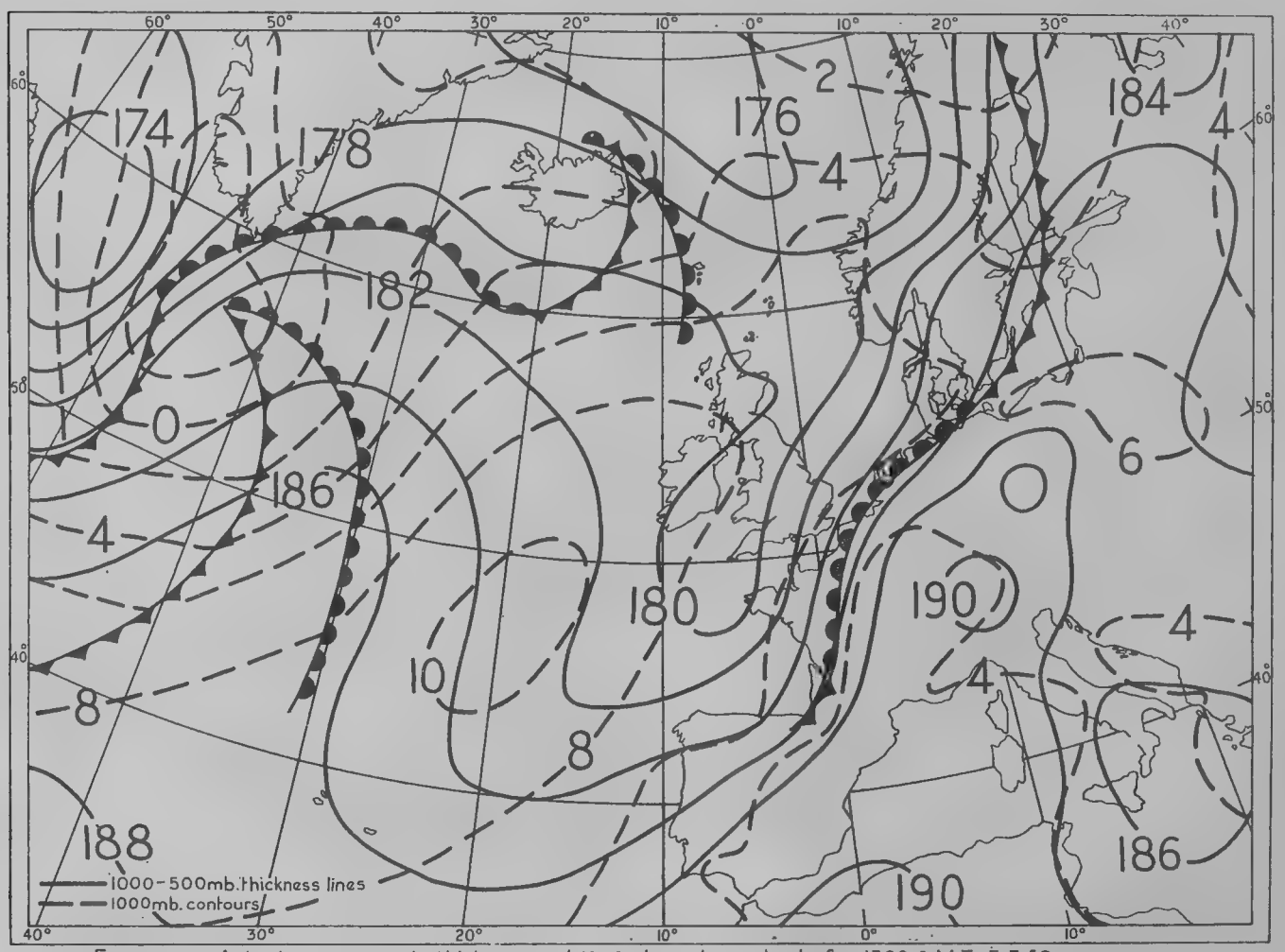

Fig.6(b) Actual 1000-500mb. thickness and 1000mb. contour charts for 1500 G.M.T. 3.7.52

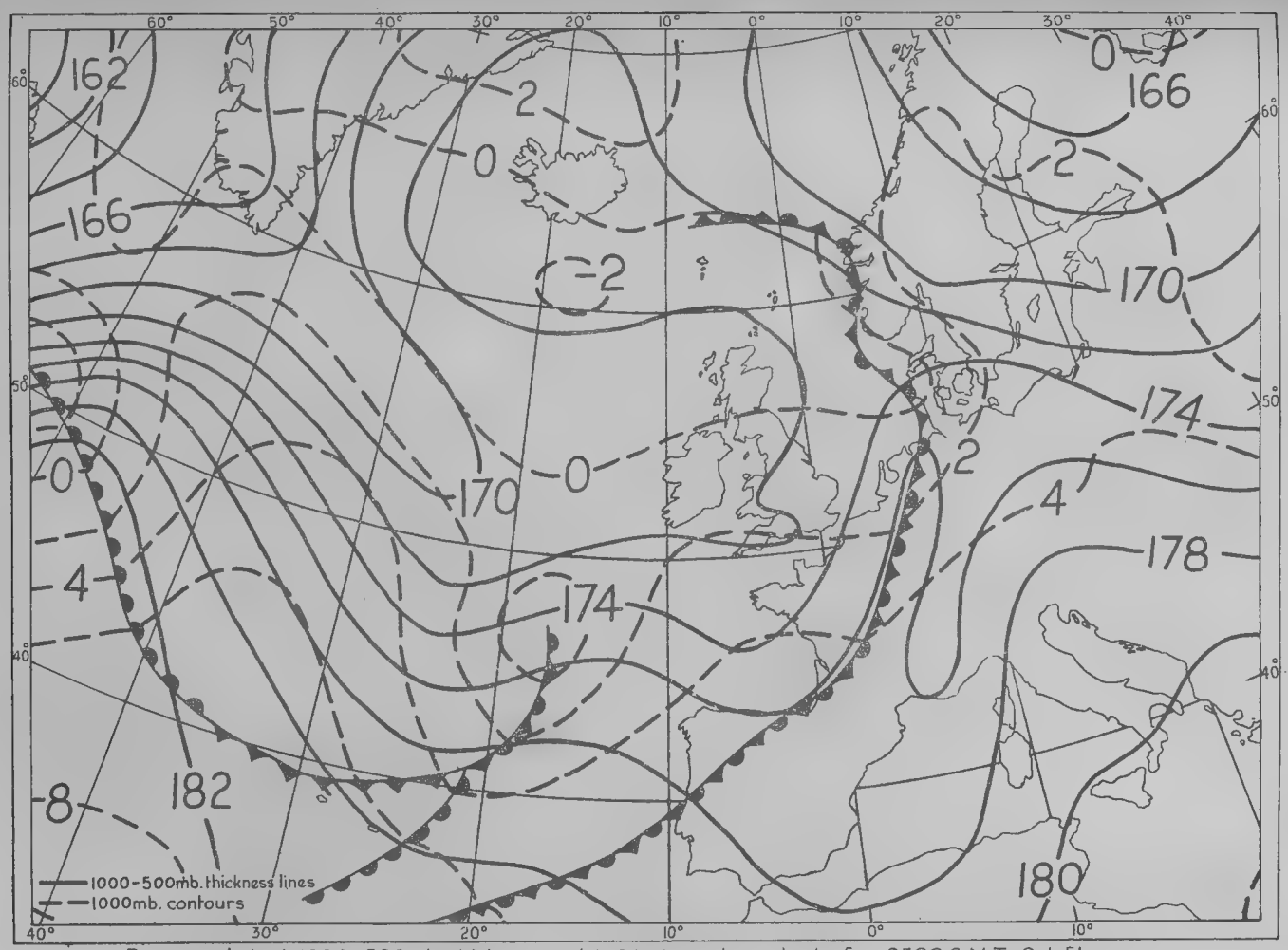

Fig.1(e) Actual 1000-500mb. thickness and 1000mb. contour charts for 0300 G.M.T. 9.1.51

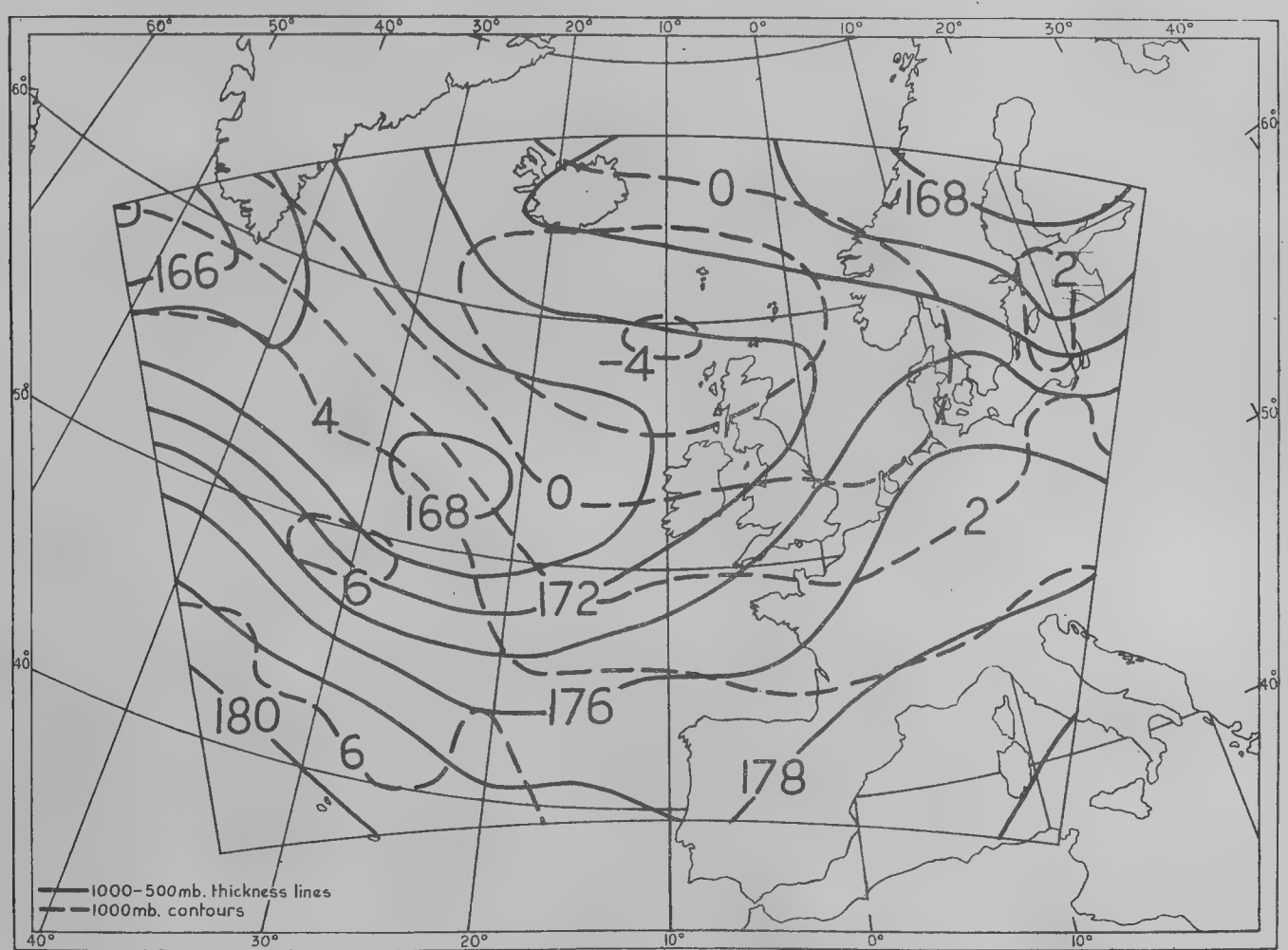

Fig.1(f) Forecast 1000-500mb. thickness and 1000mb. contour charts for 0300 G.M.T 9.1.51

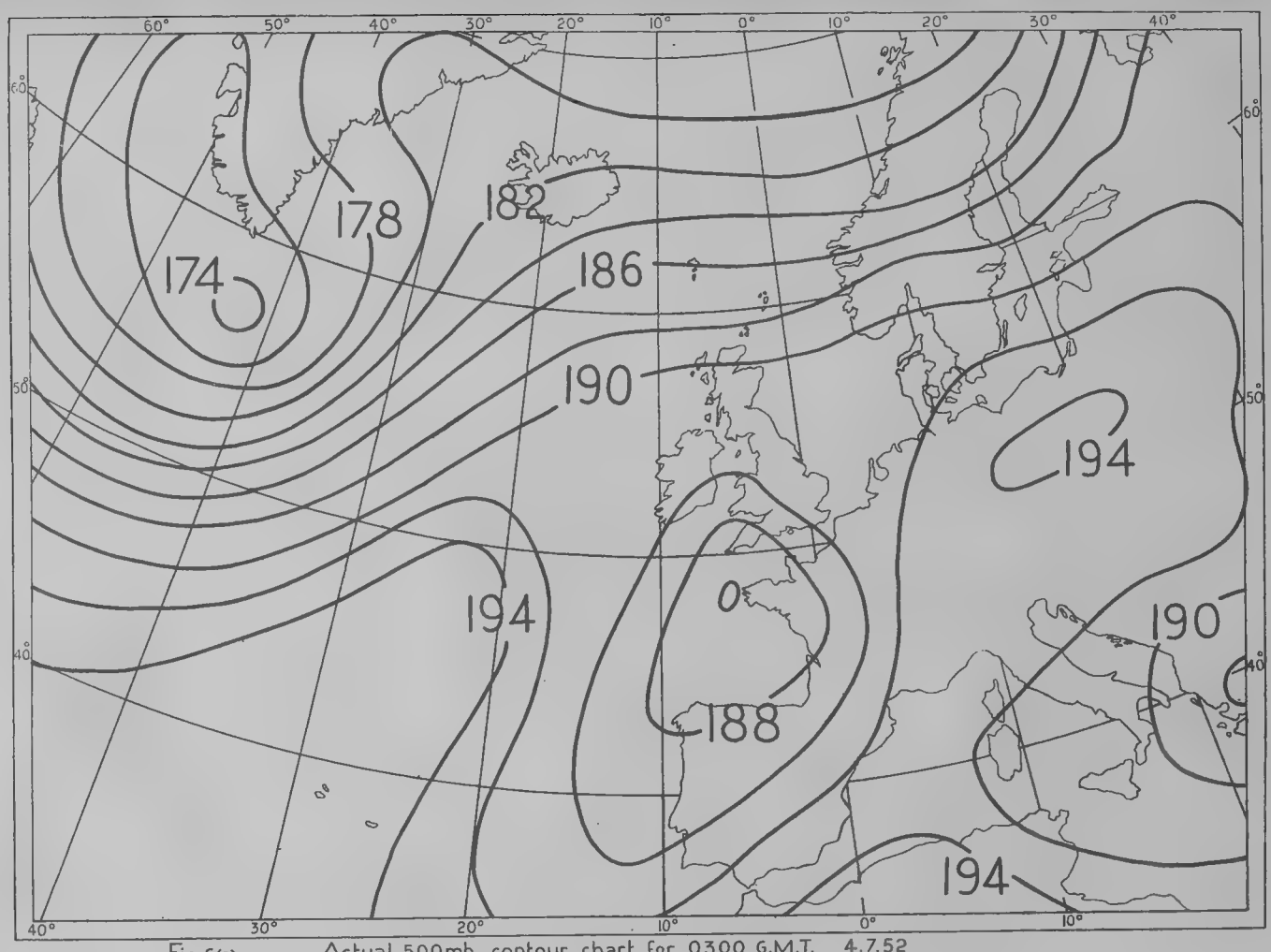

Fig.6(c) Actual 500mb. contour chart for 0300 G.M.T. 4.7.52

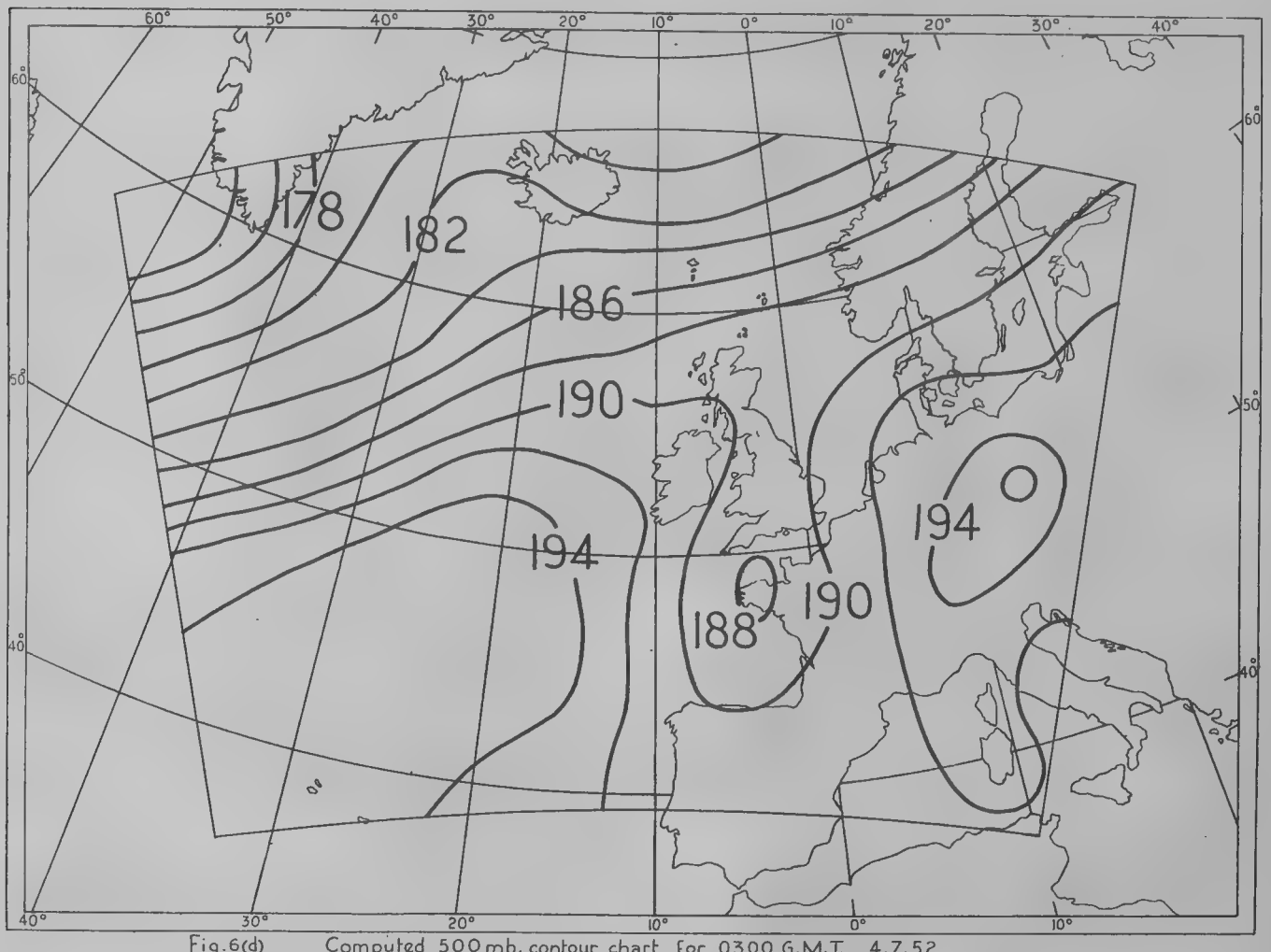

Fig.6(d) Computed 500 mb. contour chart for 0300 G.M.T. 4.7.52

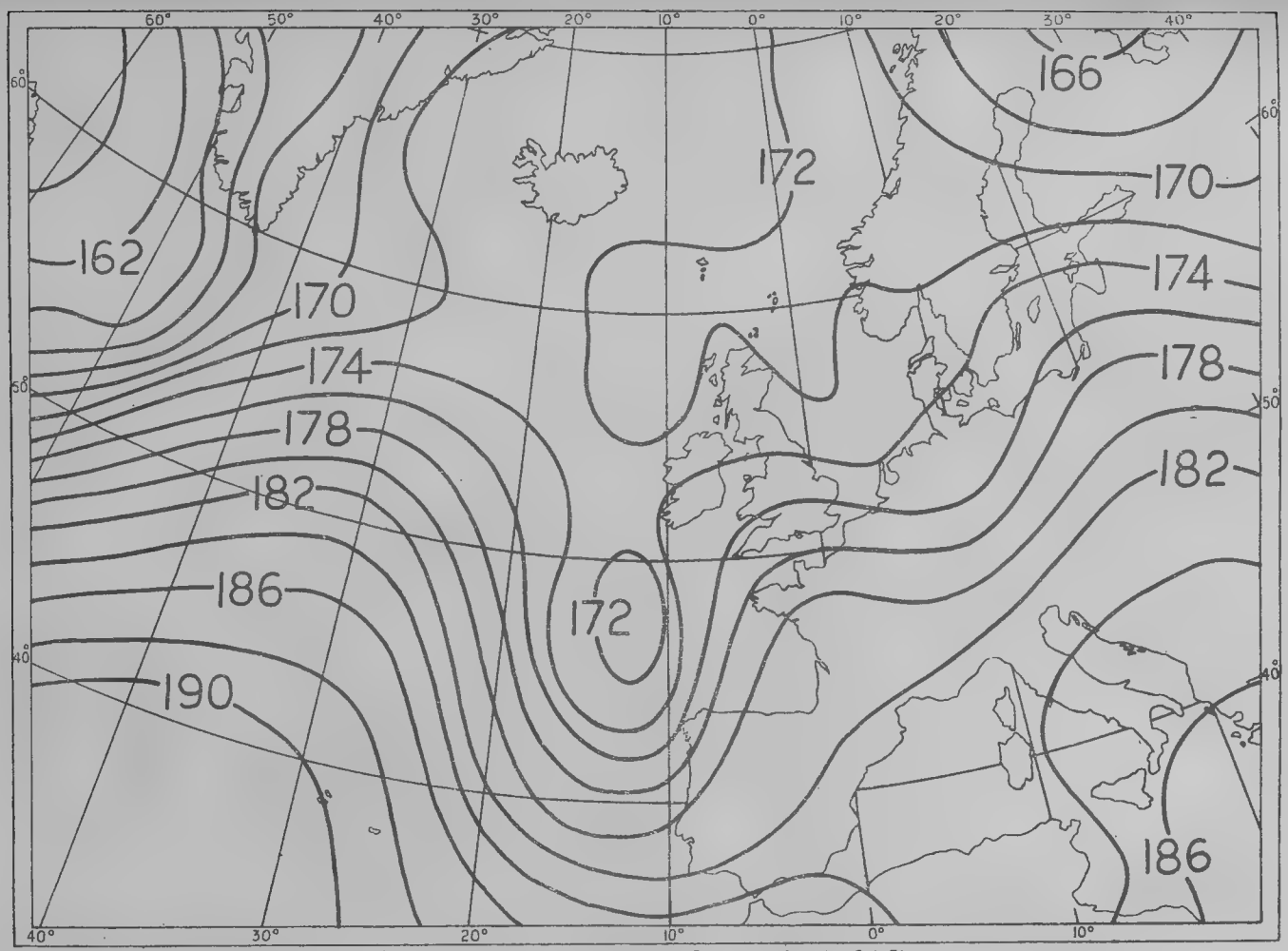

Fig.1(g) Actual 500mb. contour chart for 1500 G.M.T. 9.1.51

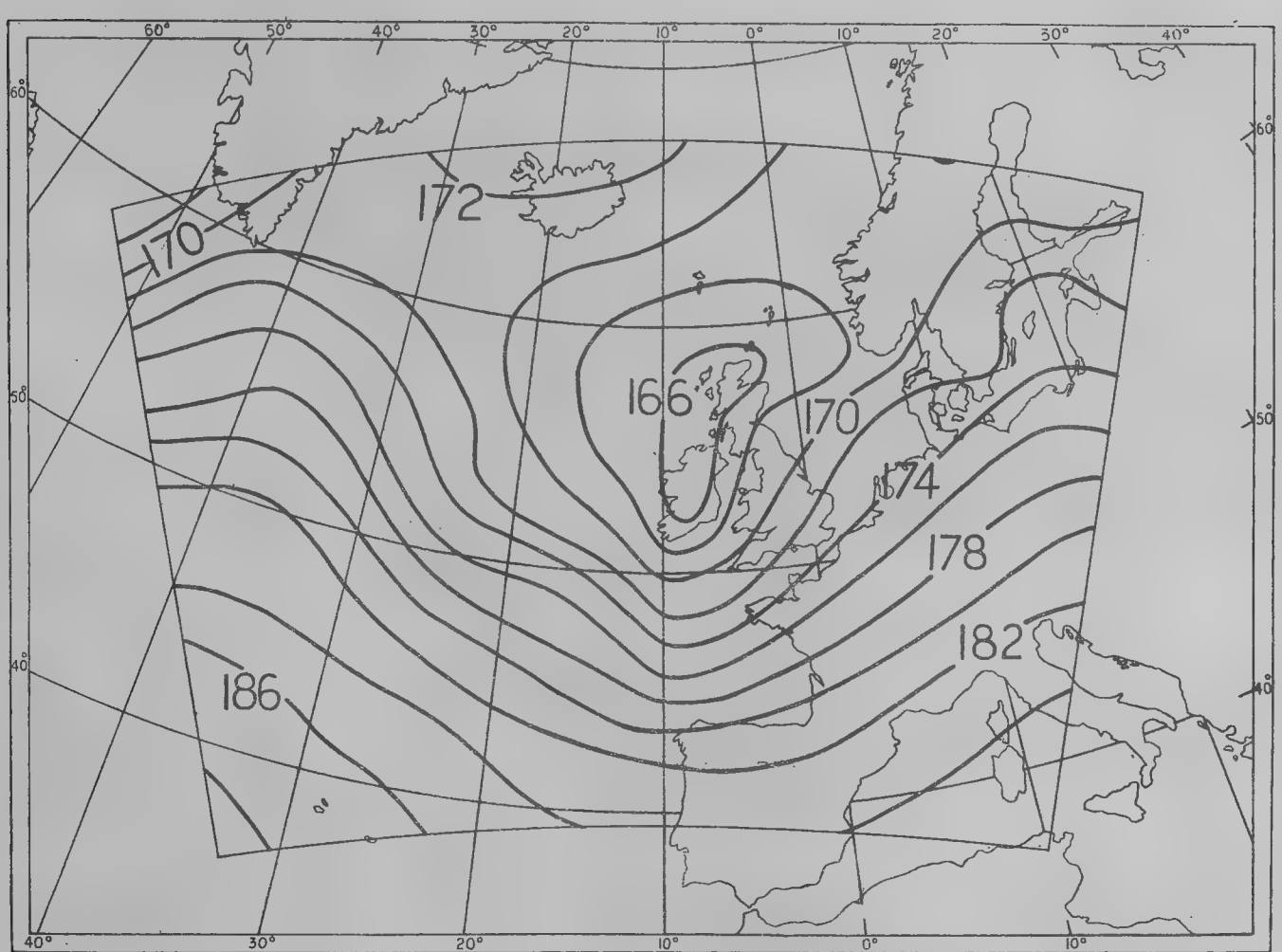

Fig.1(h) Forecast 500mb. contour chart for 1500 G.M.T. 9.1.51

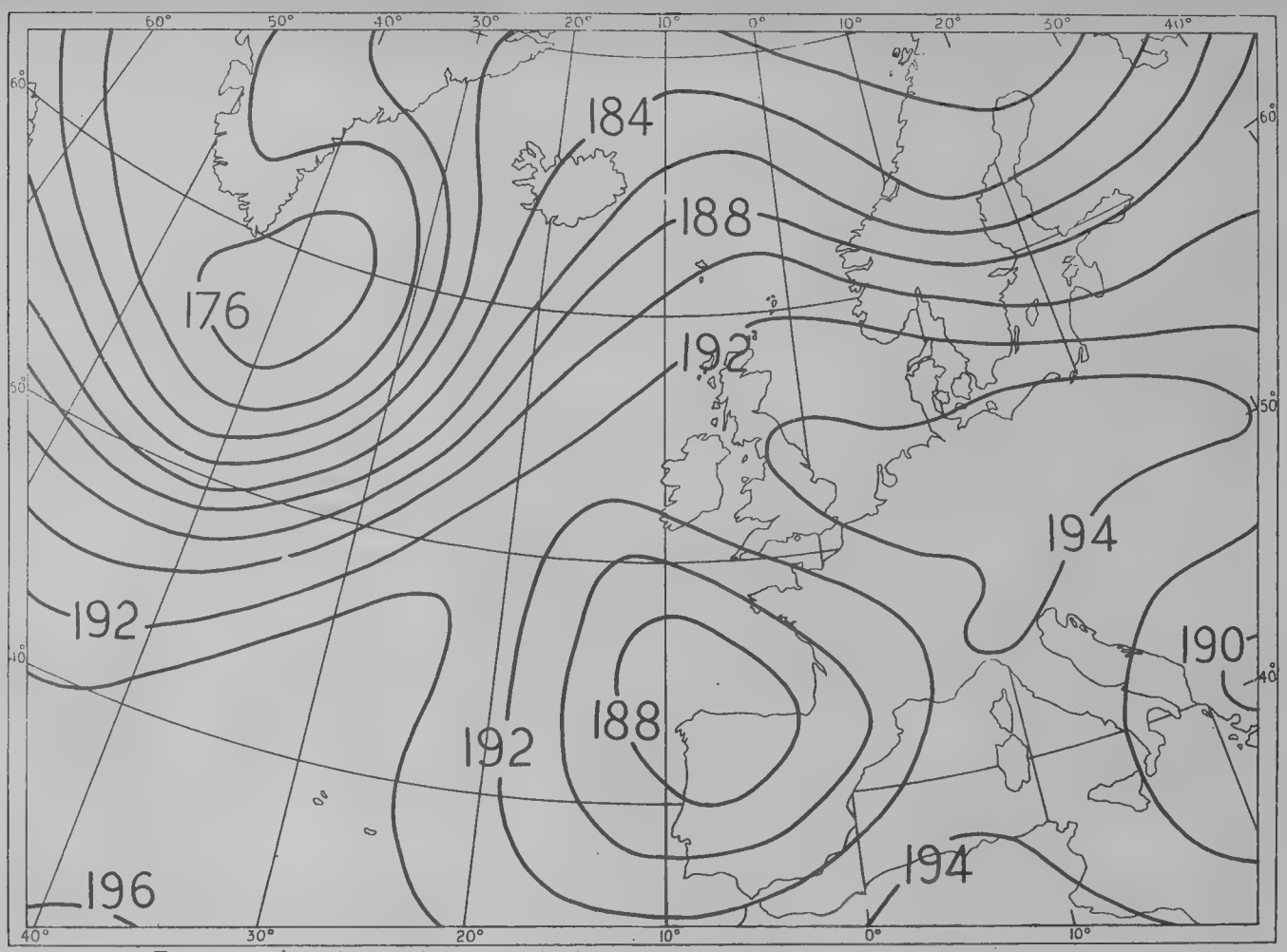

Fig.6(g) Actual 500mb. contour chart for 1500 G.M.T. 4.7.52

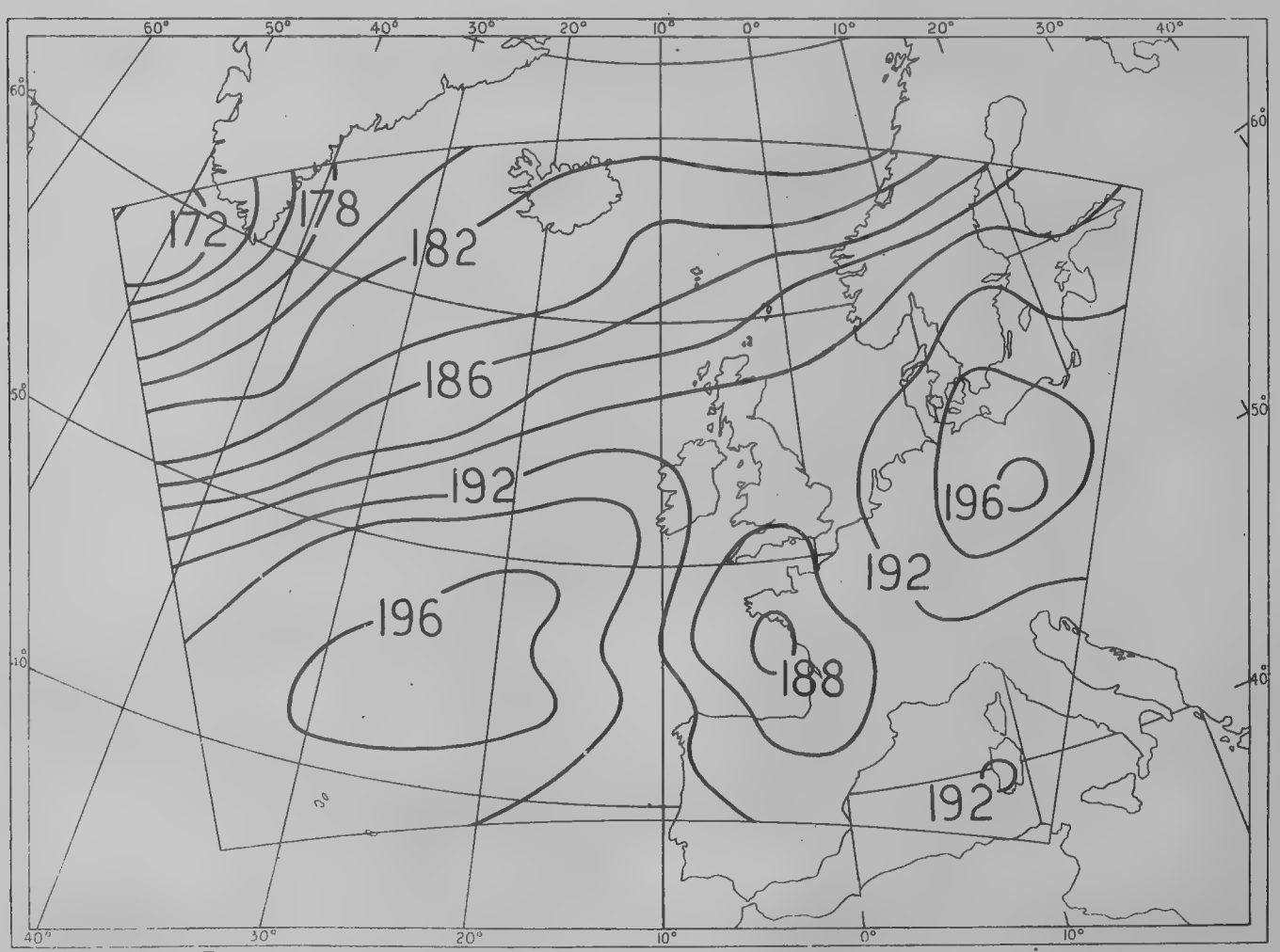

Fig.6(h) Computed 500mb contour chart for 1500 G.M.T. 4.7.52

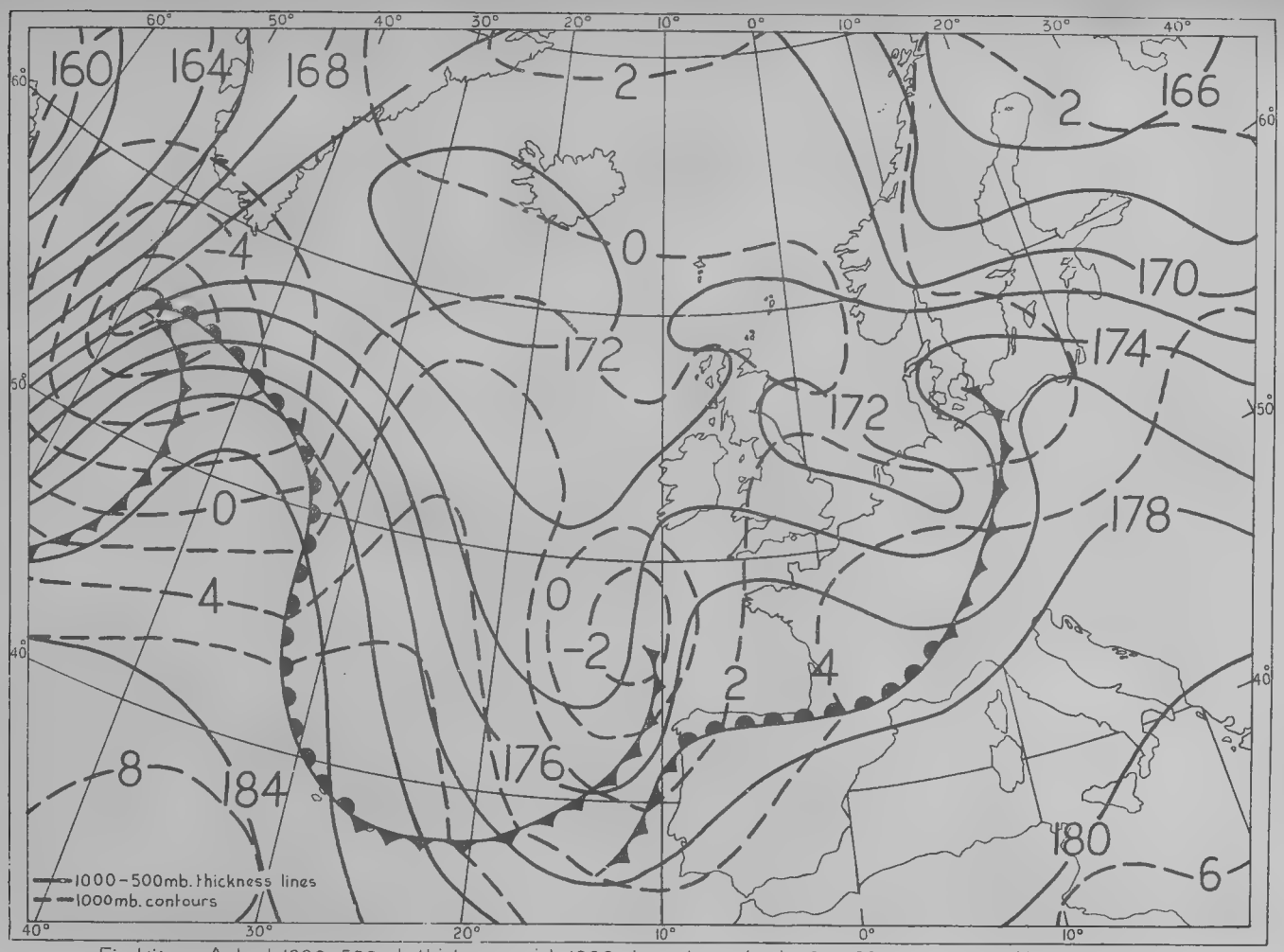

Fig.1(i) Actual 1000-500mb. thickness and 1000mb. contour charts for 1500 G.M.T. 9.1.51

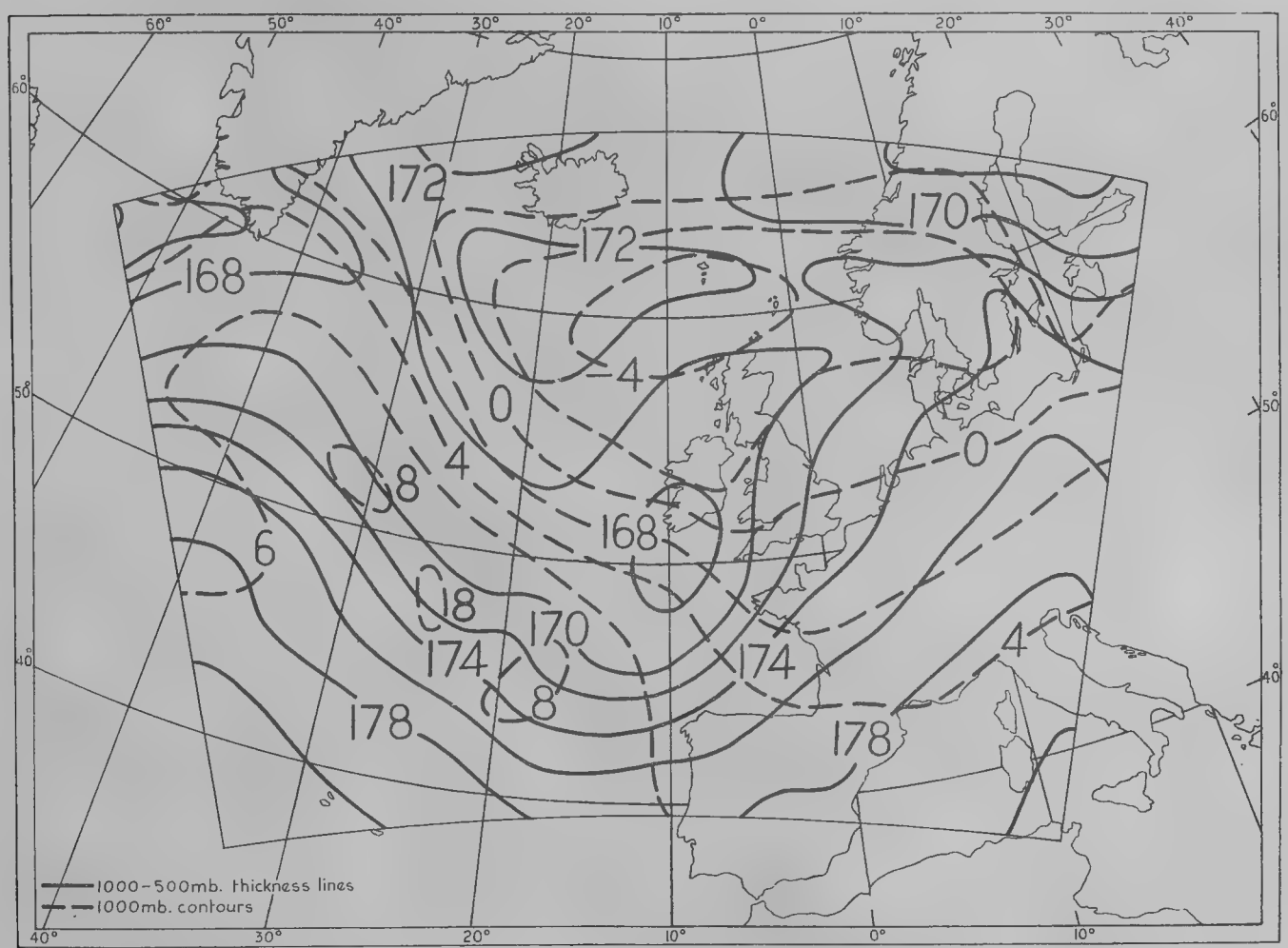

Fig.1(j) Forecast 1000-500mb. thickness and 1000mb. contour charts for 1500 G.M.T. 9.1.51

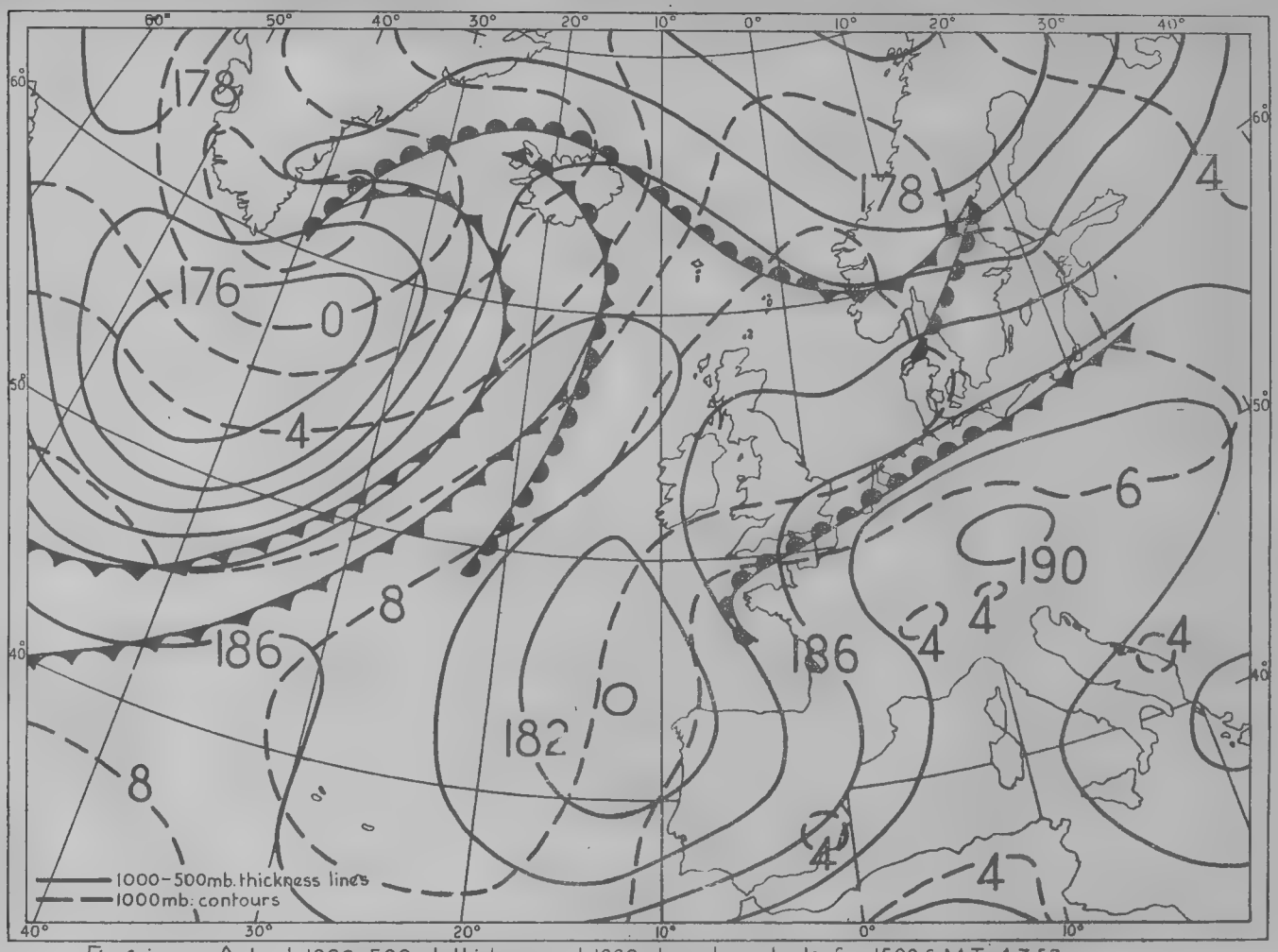

Fig.6(i) Actual 1000-500mb. thickness and 1000mb. contour charts for 1500 G.M.T. 4.7.52

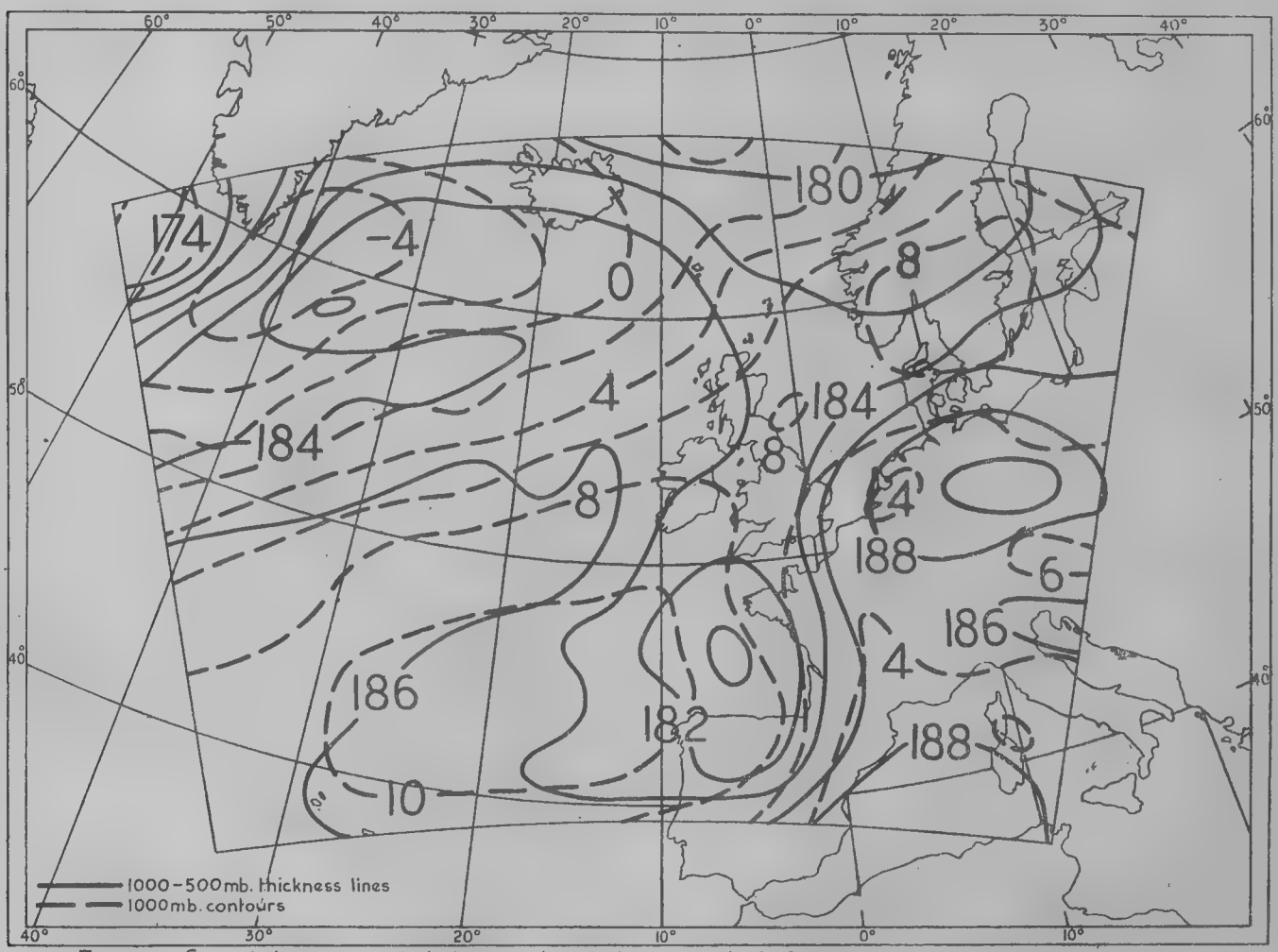

Fig.6(j) Computed 1000-500mb. thickness and 1000mb. contour charts for 1500 G.M.T. 4.7.52

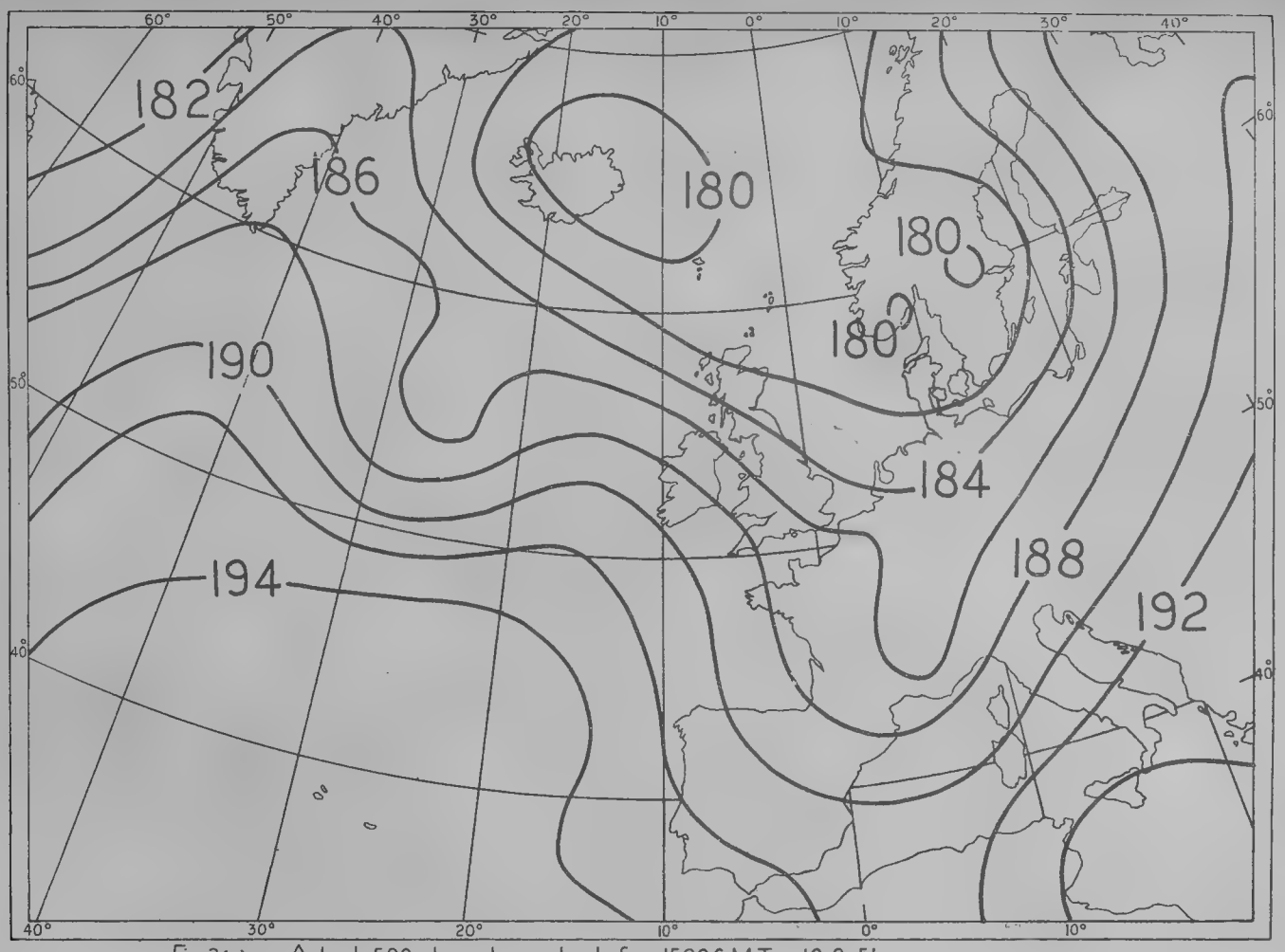

Fig.2(a) Actual 500mb. contour chart for 1500 G.M.T. 10.8.51

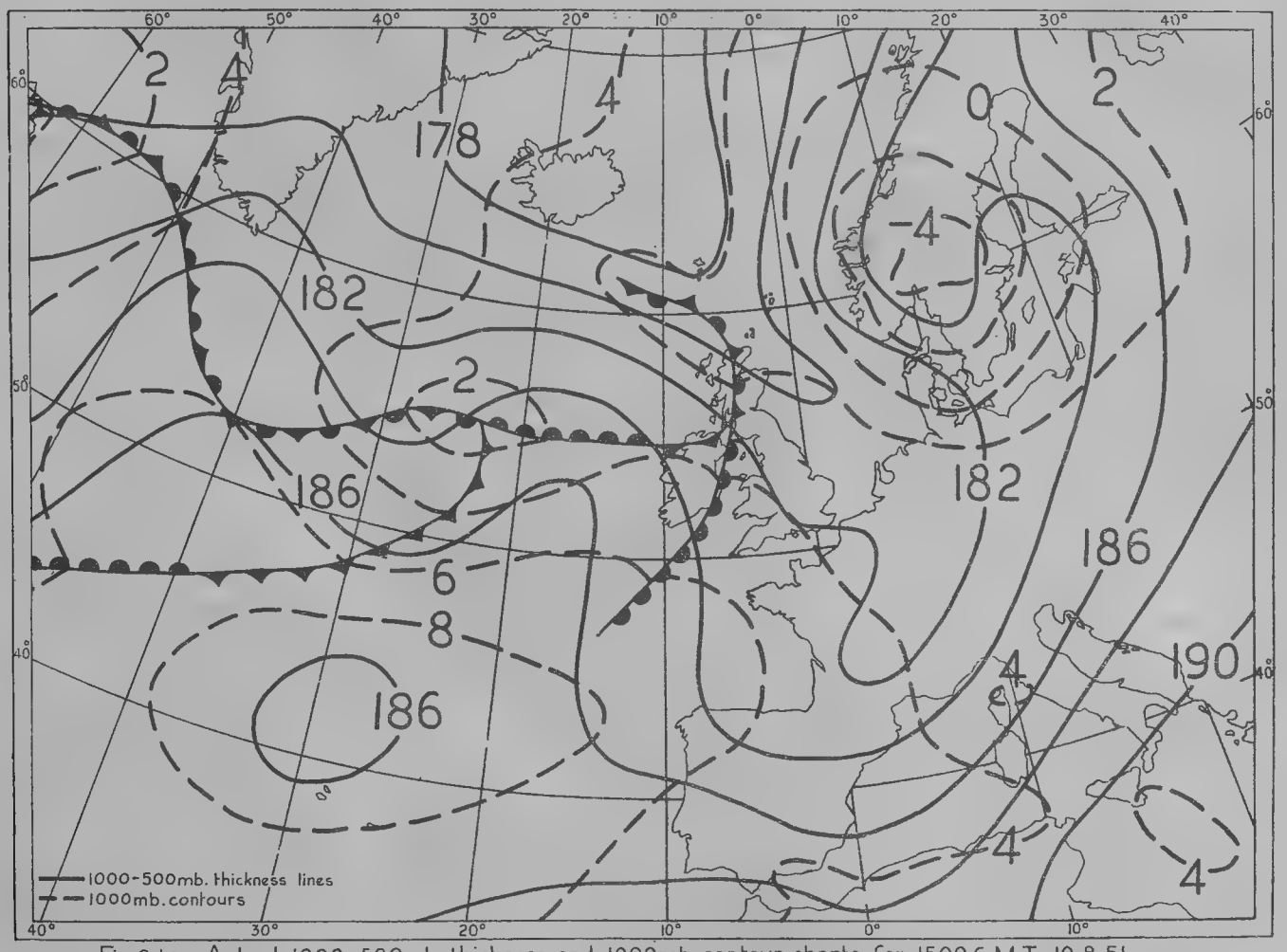

Fig.2(b) Actual 1000-500mb. thickness and 1000mb. contour charts for 1500 G.M.T. 10.8.51

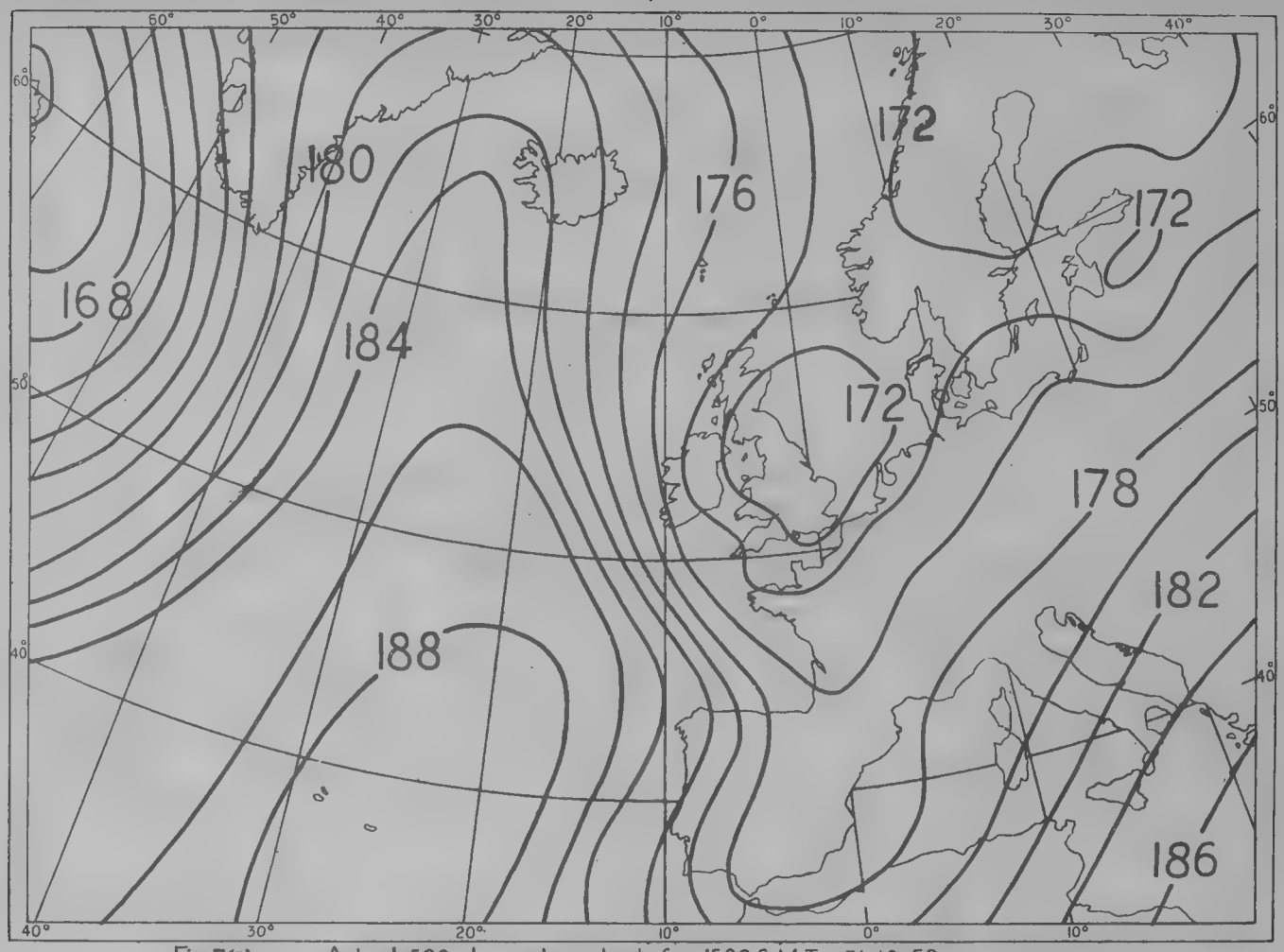

Fig.7(a) Actual 500mb. contour chart for 1500 G.M.T. 31.12.52

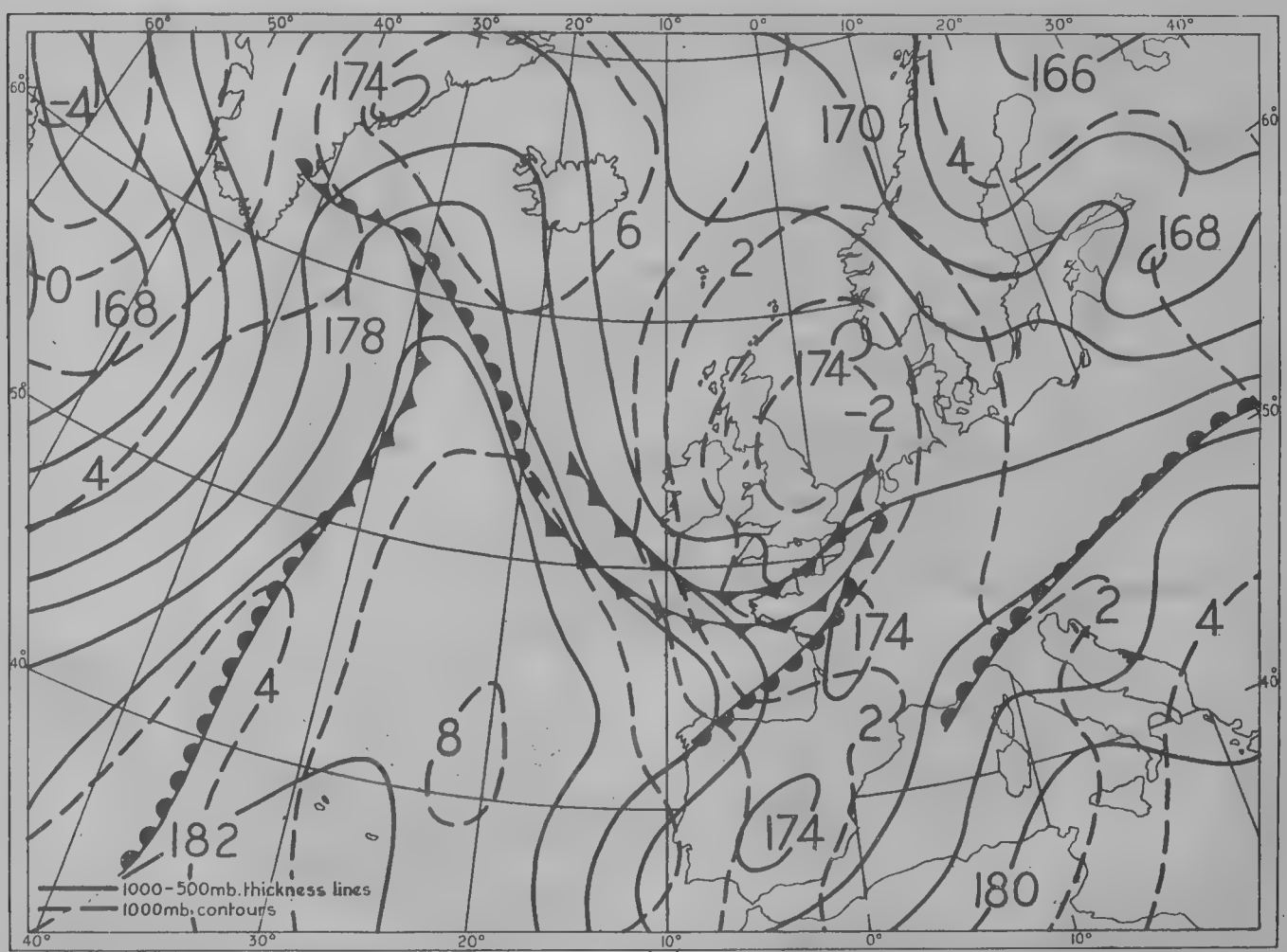

Fig.7(b) Actual 1000-500mb. thickness and 1000mb. contour charts for 1500 G.M.T. 31.12.52

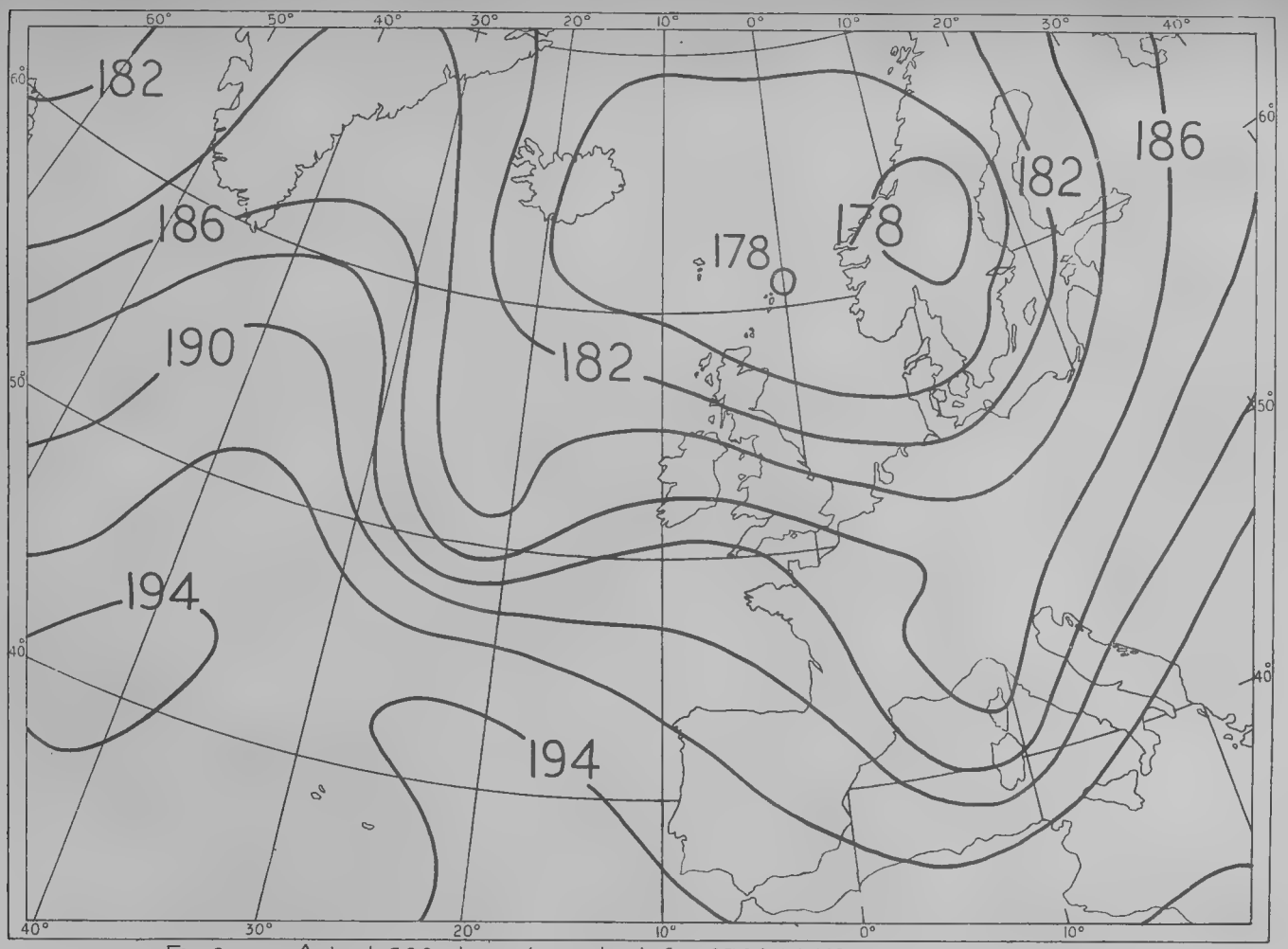

Fig. 2(c) Actual 500mb. contour chart for 0300 G.M.T. 11.8.51

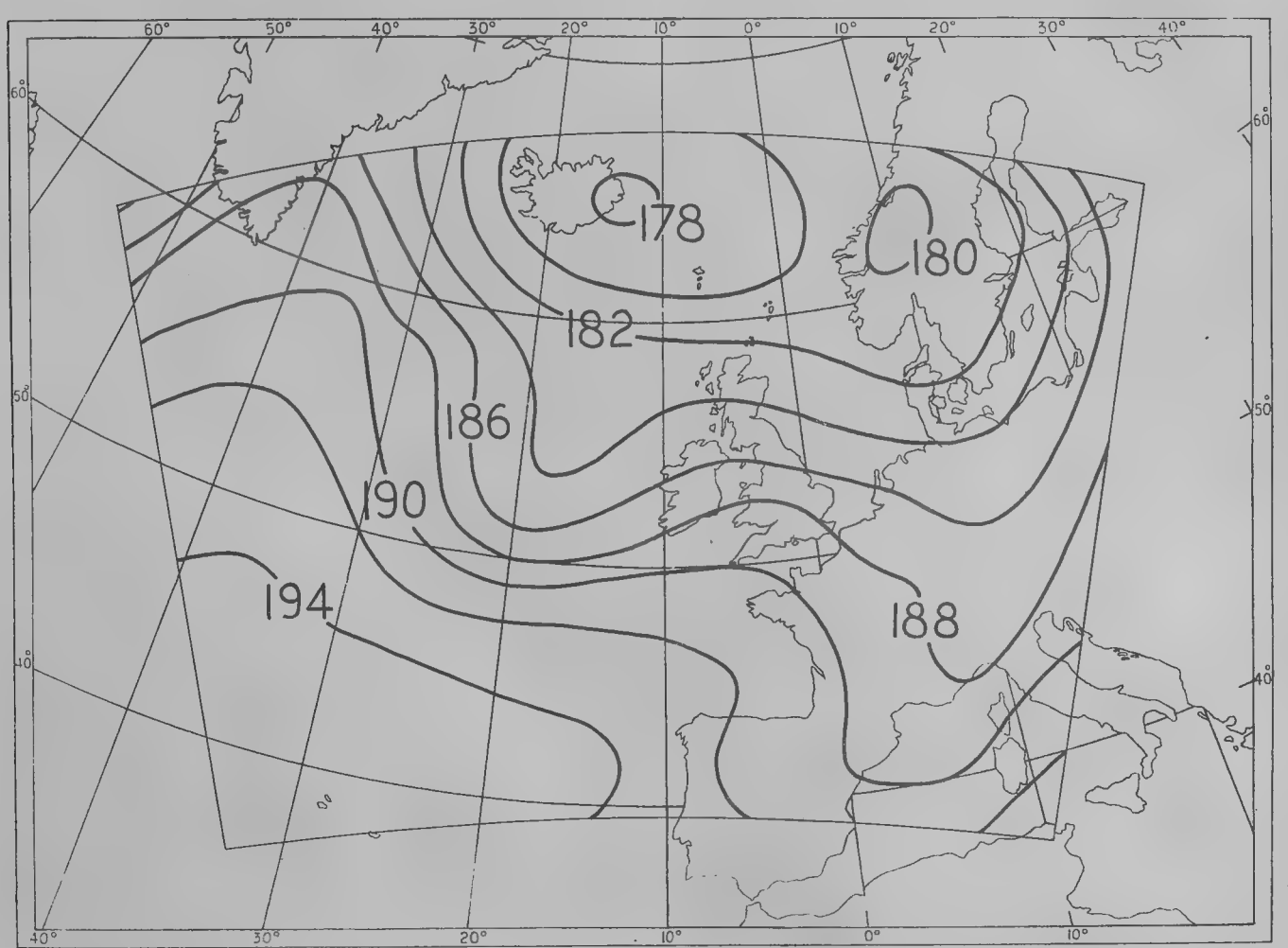

Fig. 2(d) Computed 500mb. contour chart for 0300 G.M.T. 11.8.51

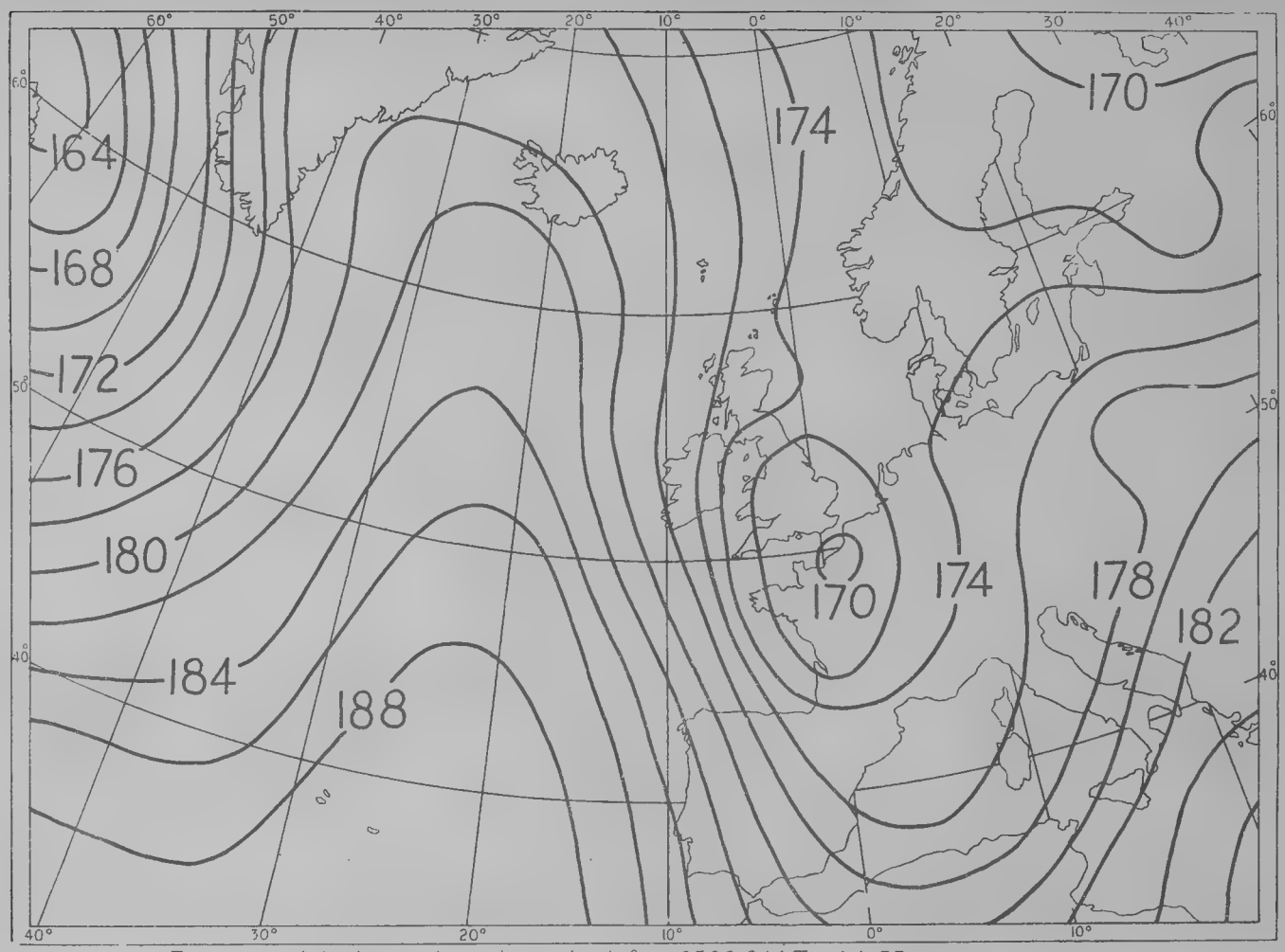

Fig.7(c) Actual 500mb. contour chart for 0300 G.M.T. 1.1.53

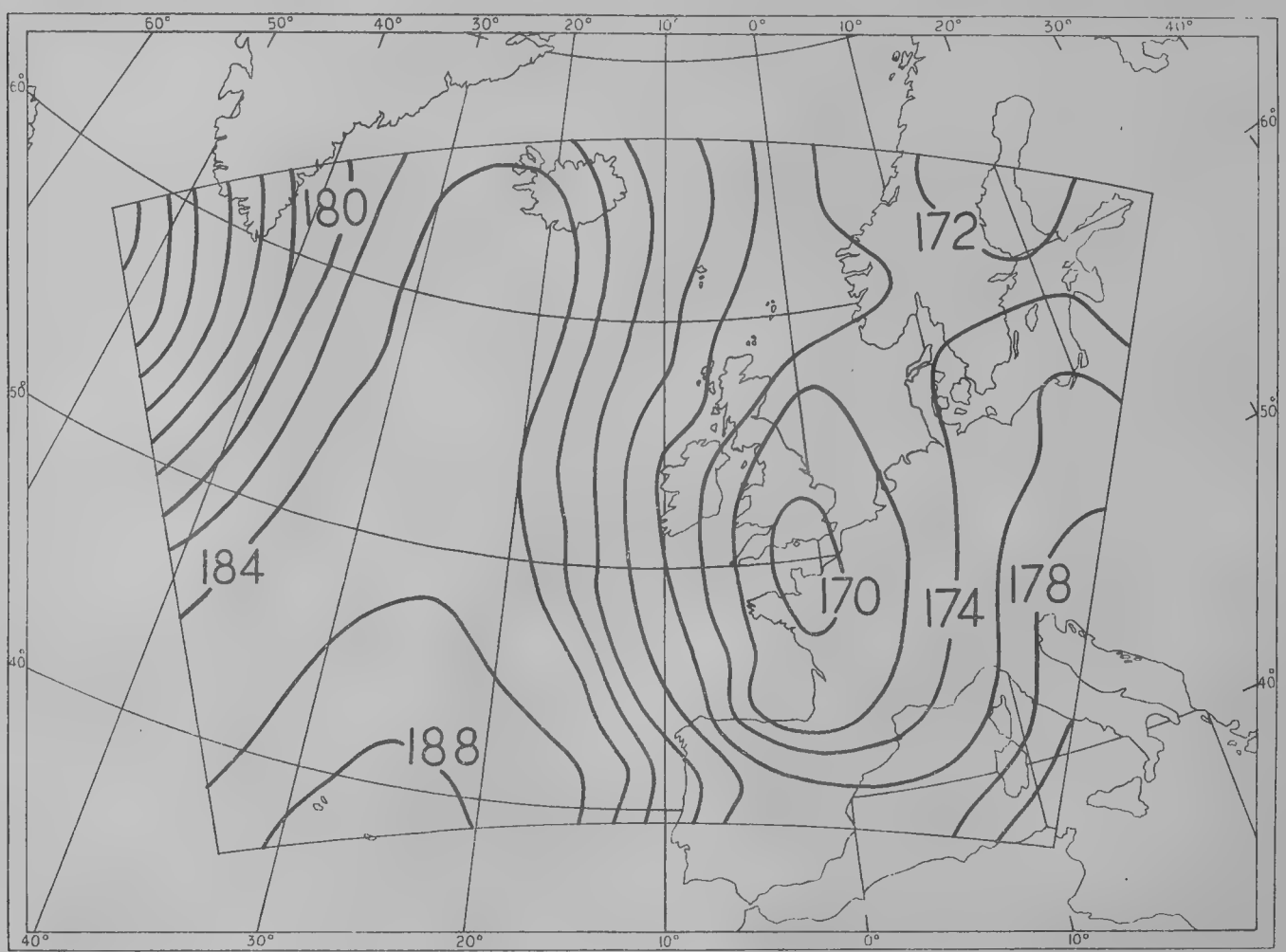

Fig.7(d) Computed 500mb. contour chart for 0300 G.M.T. 1.1.53

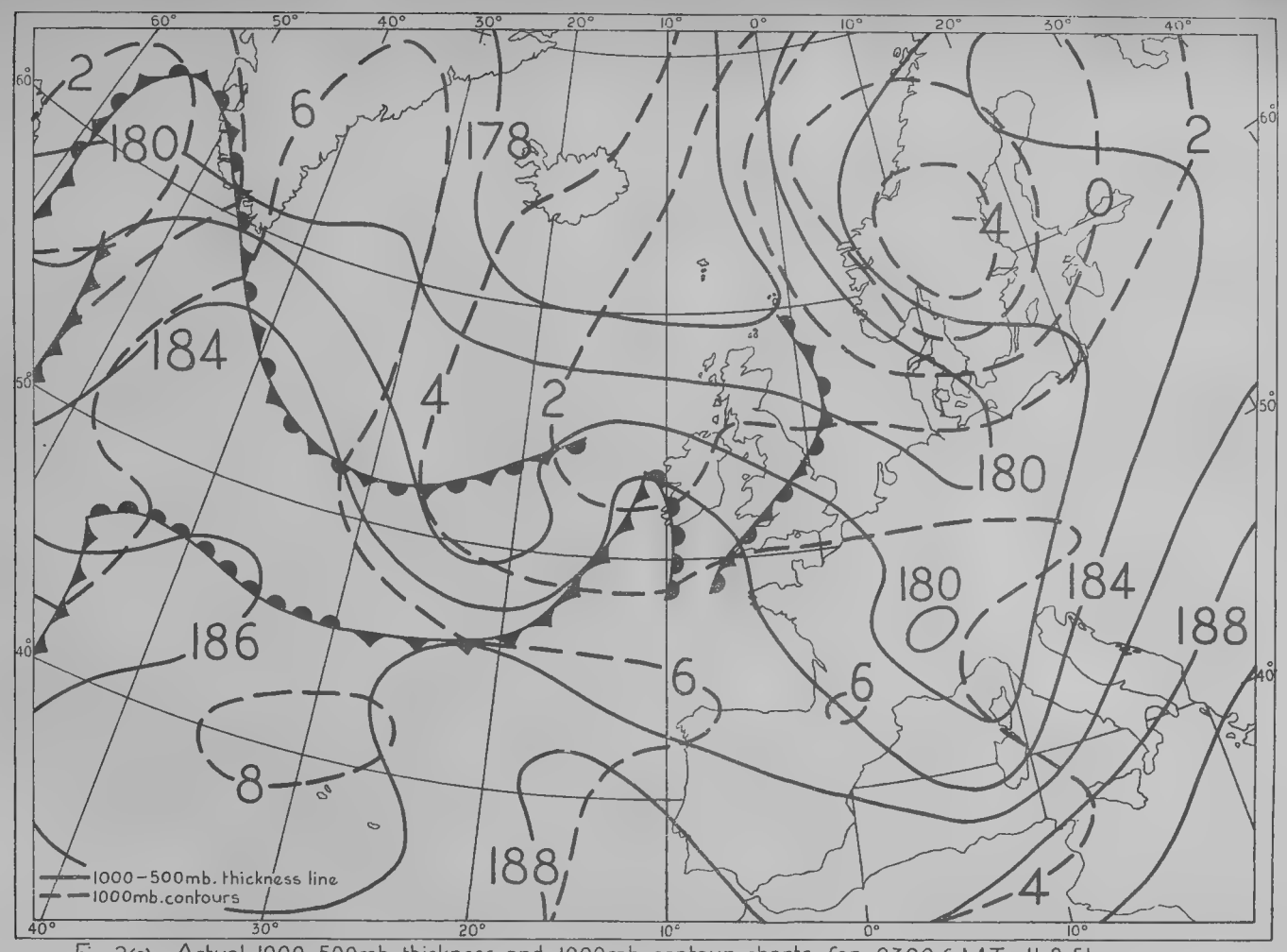

Fig.2(e) Actual 1000–500mb. thickness and 1000mb. contour charts for 0300 G.M.T. 11.8.51

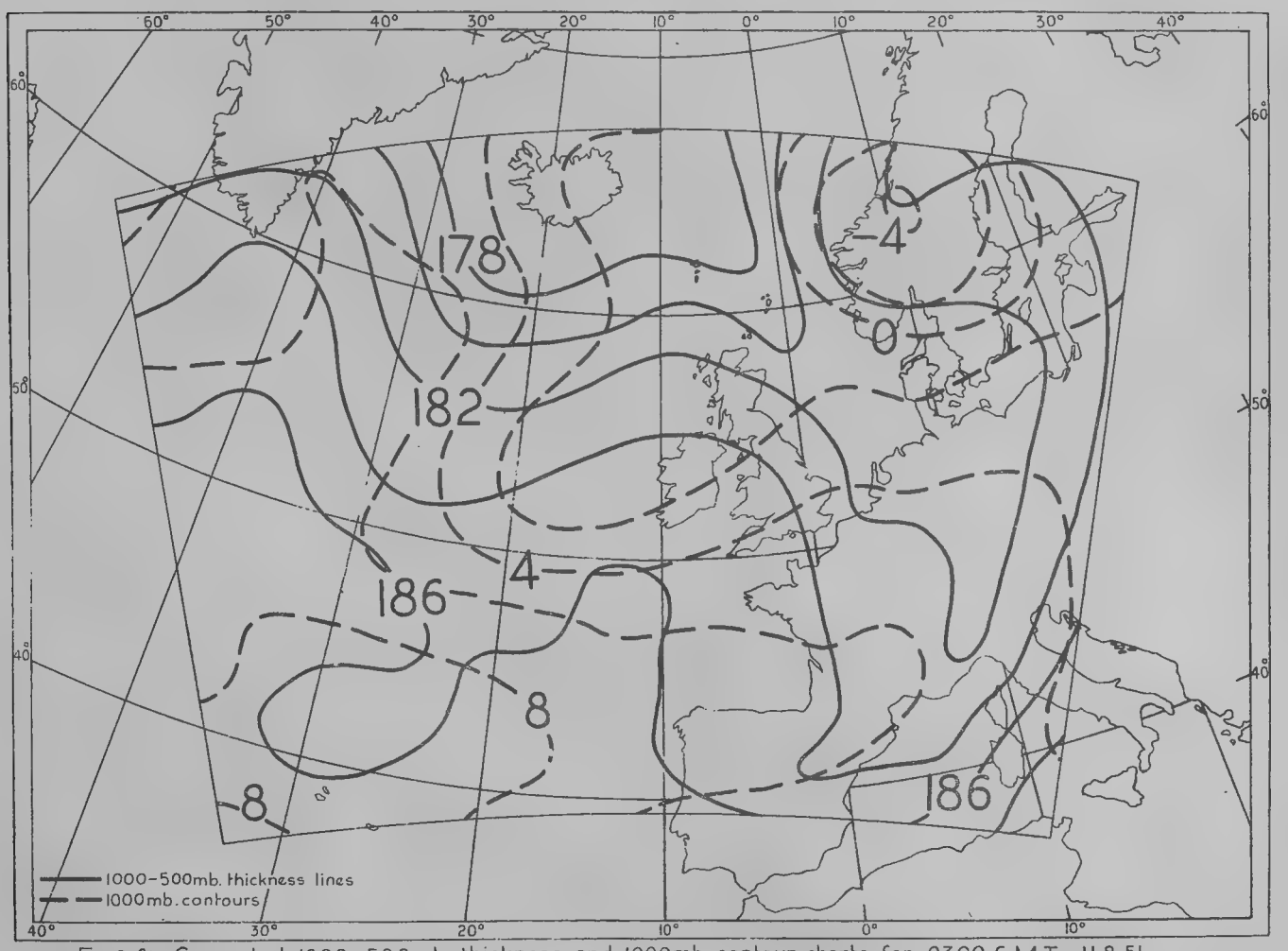

Fig.2(f) Computed 1000–500mb. thickness and 1000mb. contour charts for 0300 G.M.T. 11.8.51

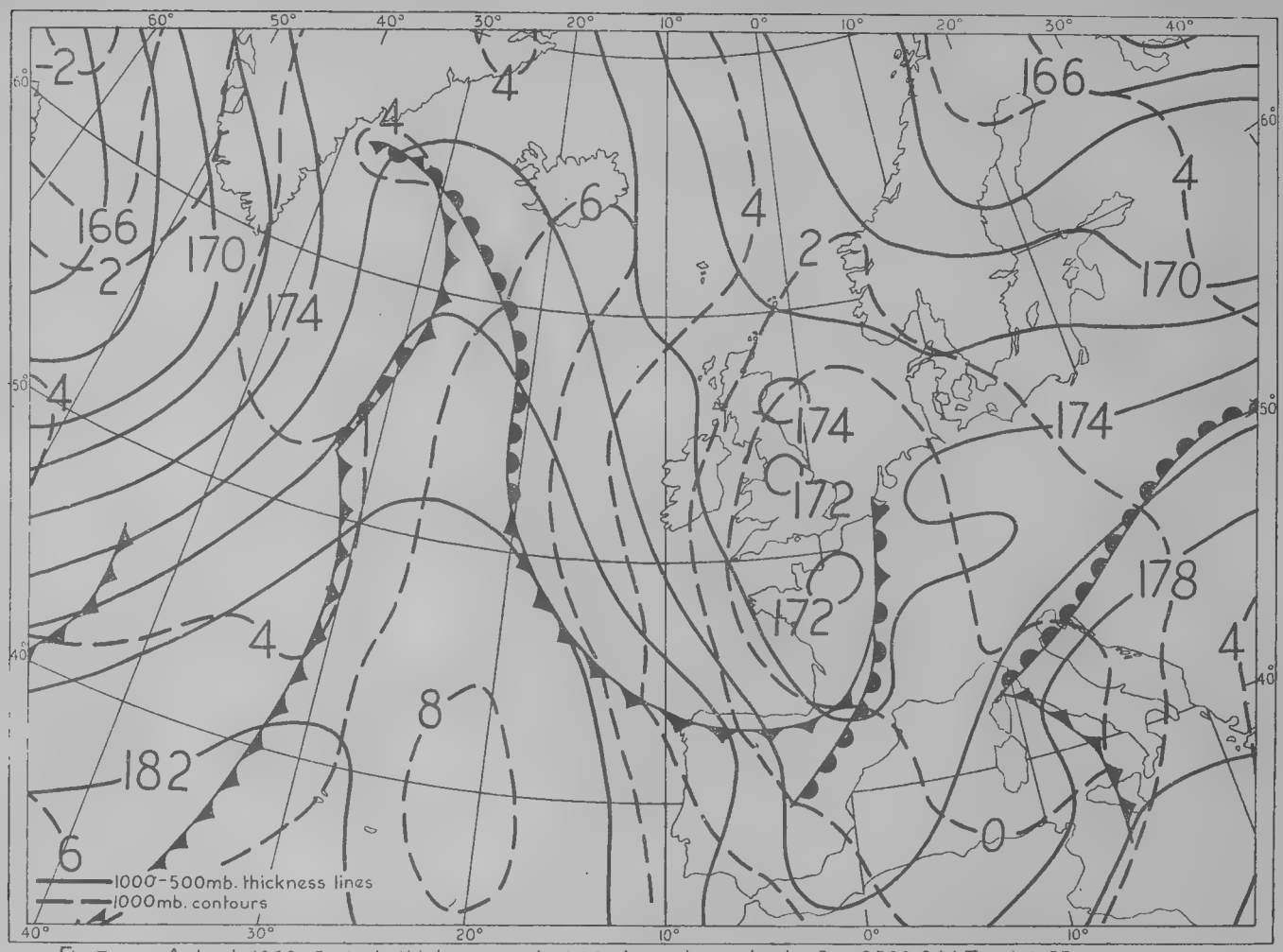

Fig.7(e) Actual. 1000-500mb. thickness and 1000mb. contour charts for 0300 G.M.T. 1.1.53

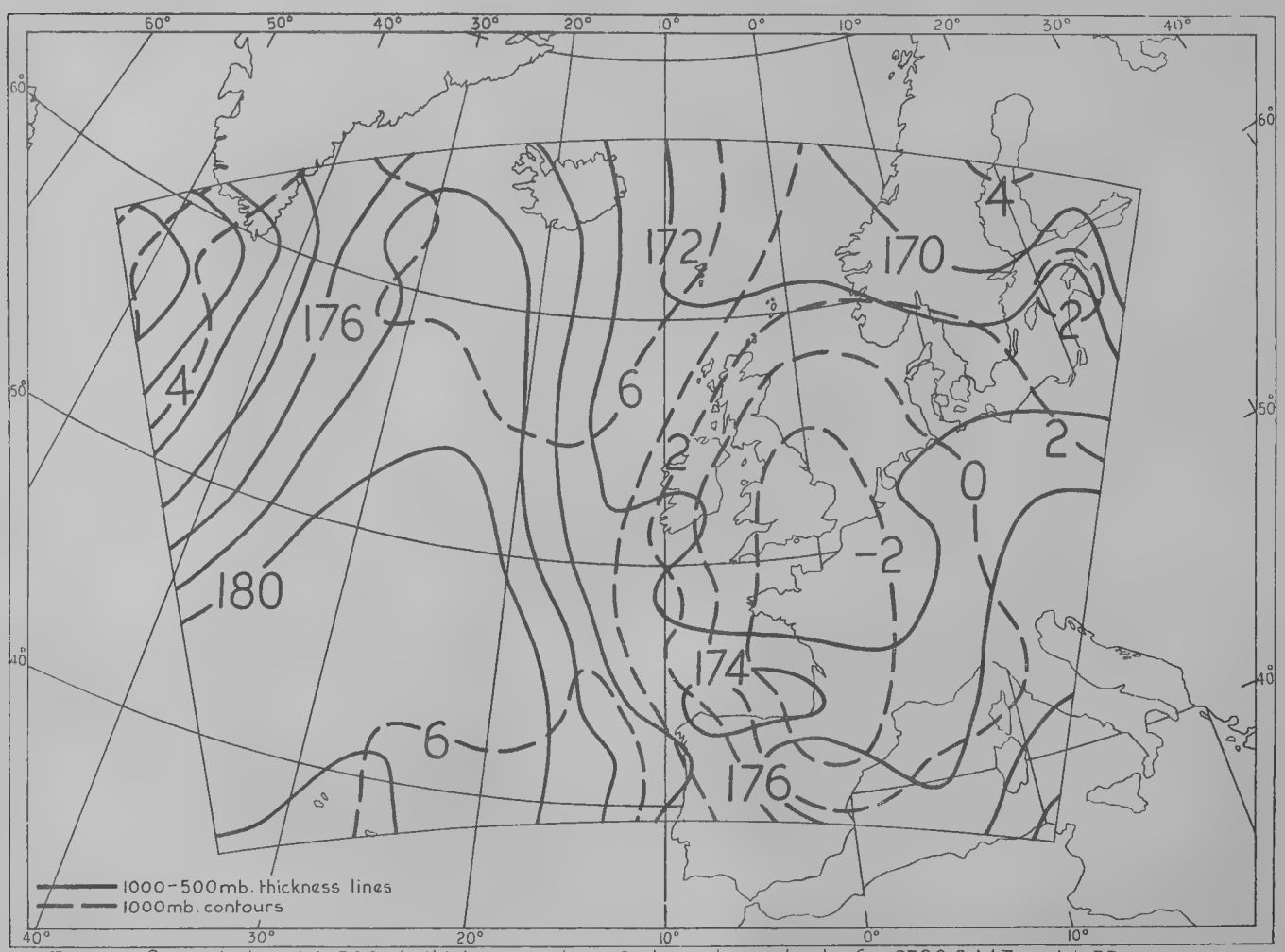

Fig.7(f) Computed 1000-500mb. thickness and 1000mb. contour charts for 0300 G.M.T. 1.1.53.

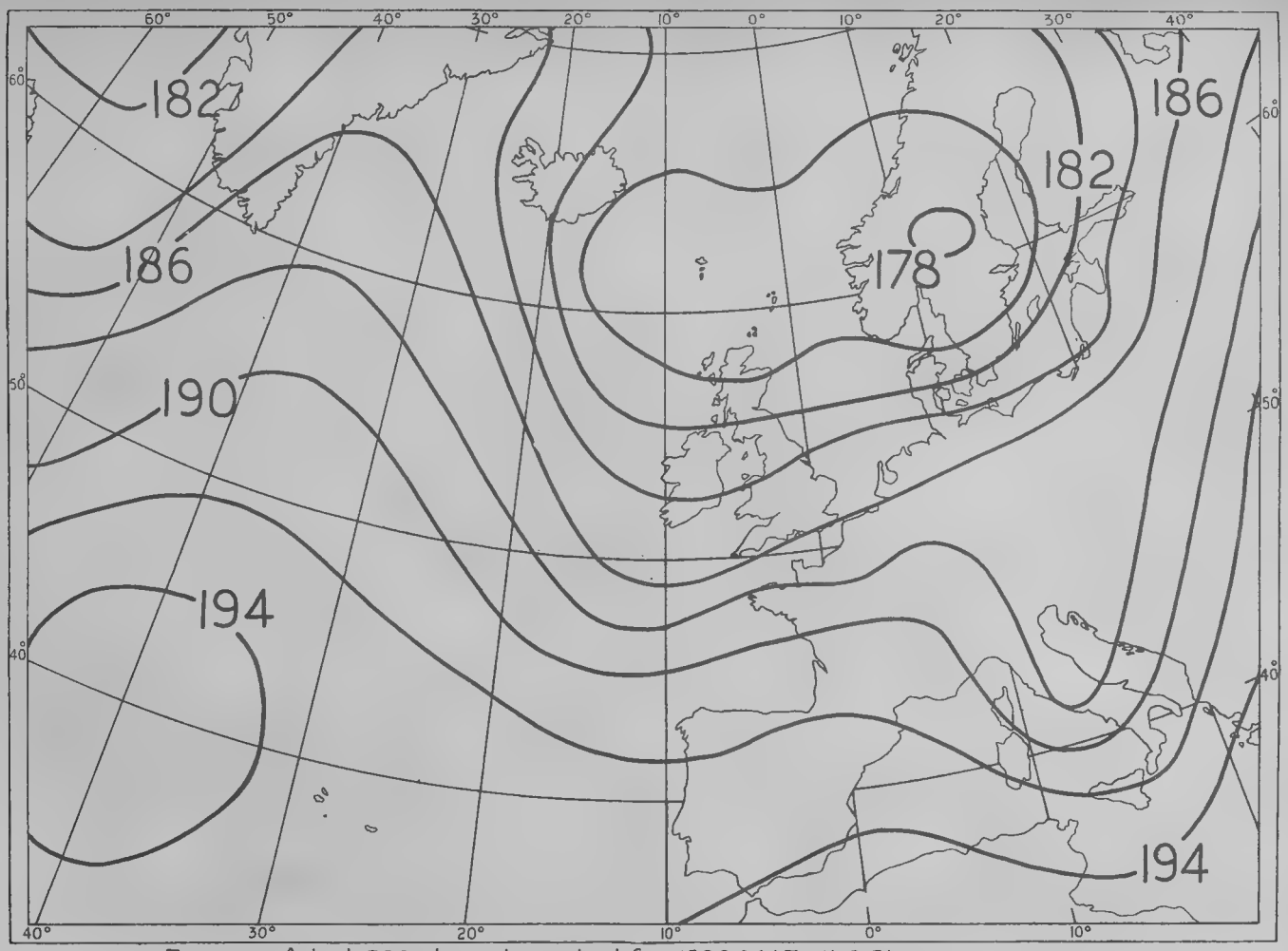

Fig.2(g) Actual 500mb. contour chart for 1500 G.M.T. 11.8.51

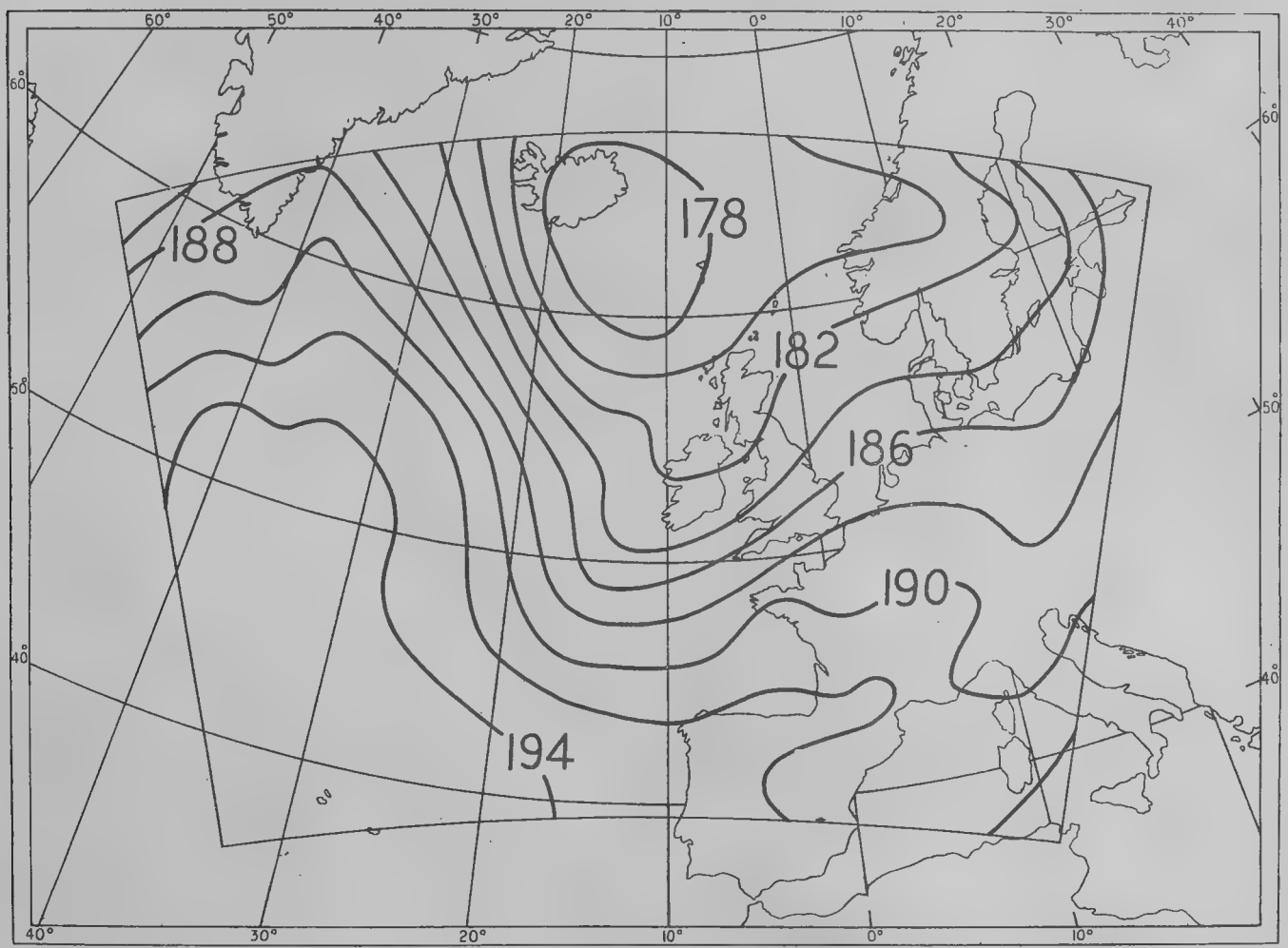

Fig.2(h) Computed 500mb. contour chart for 1500 G.M.T. 11.8.51

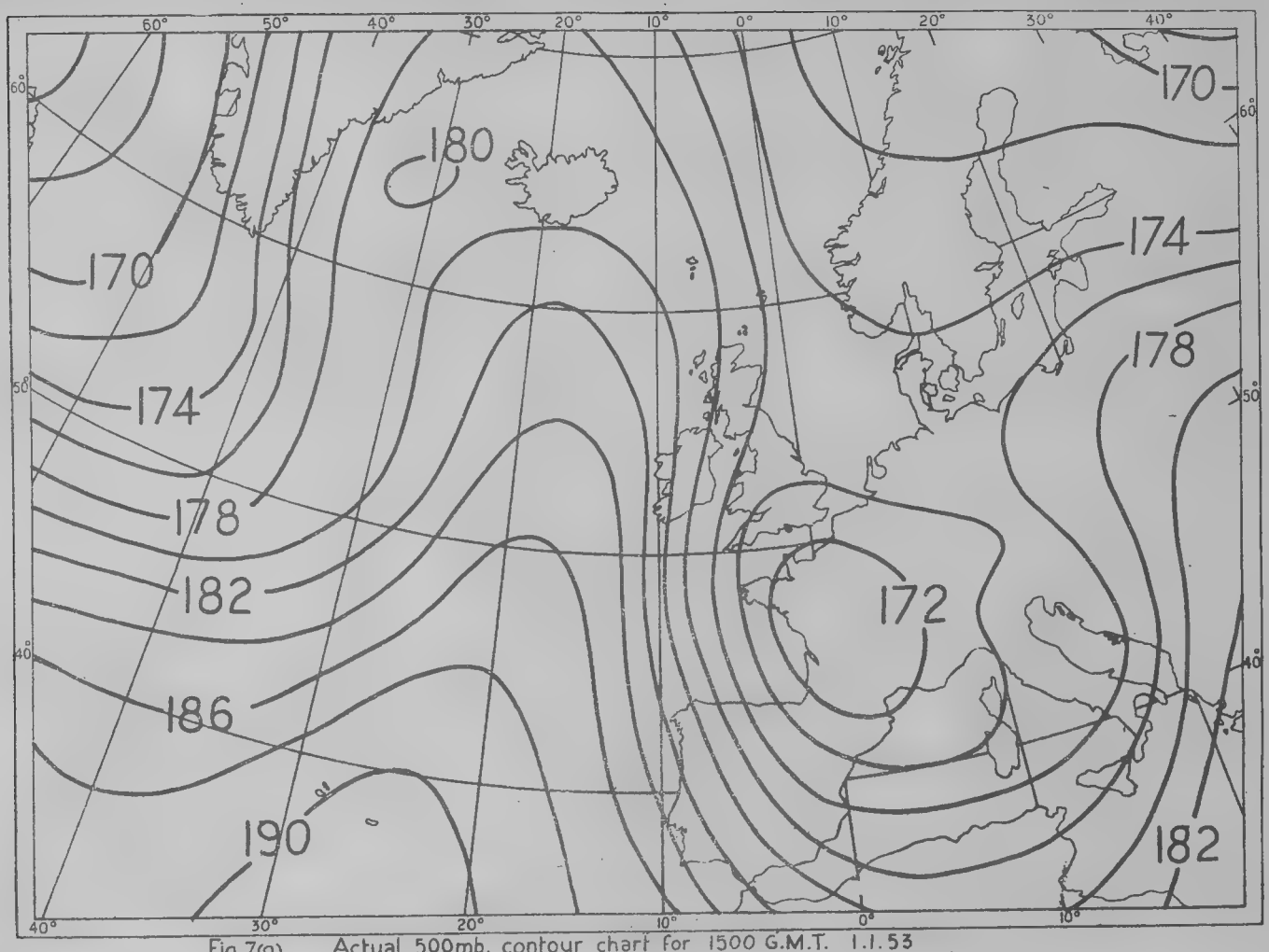

Fig.7(g) Actual 500mb. contour chart for 1500 G.M.T. 1.1.53

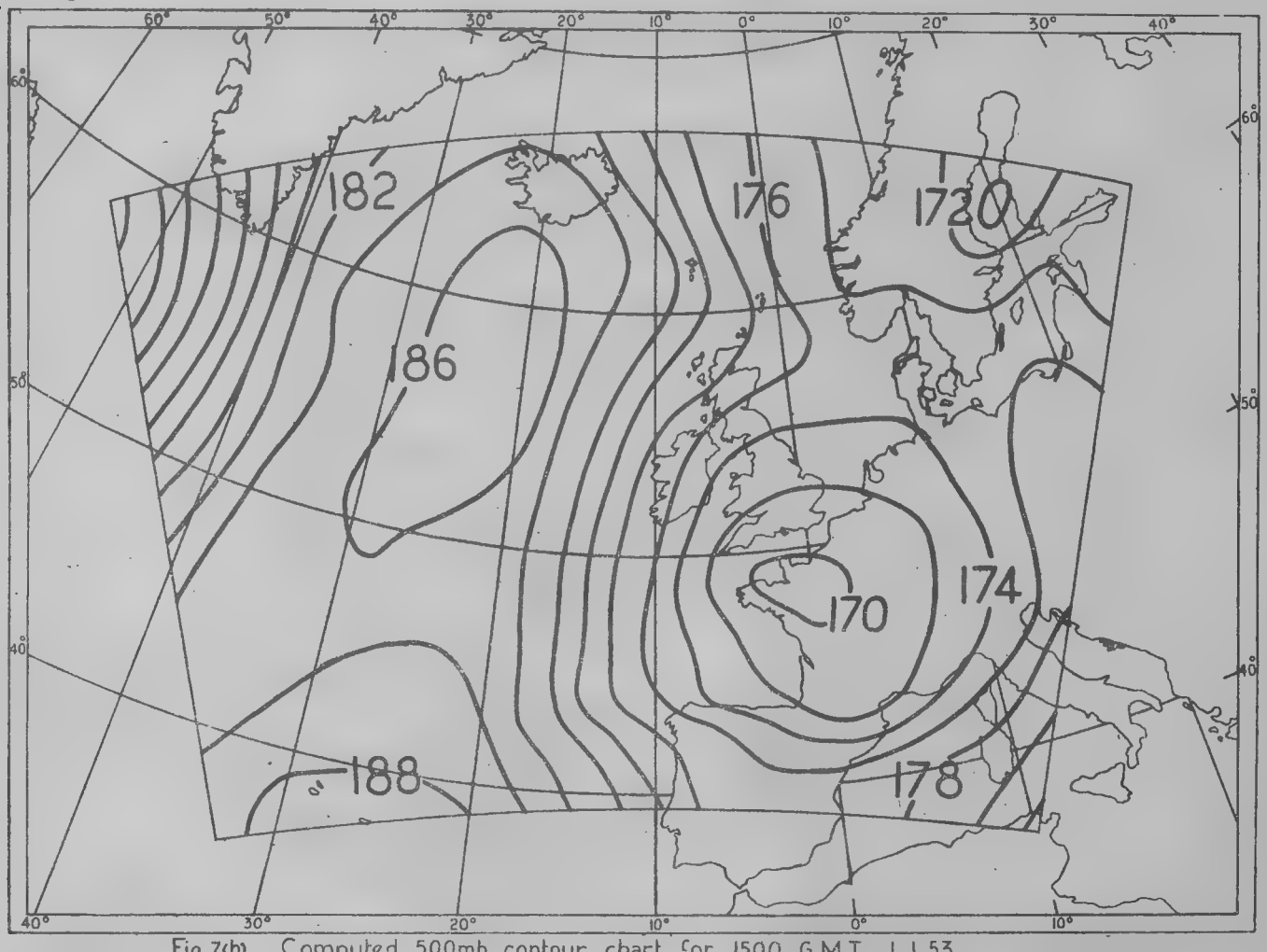

Fig.7(h) Computed 500mb. contour chart for 1500 G.M.T. 1.1.53

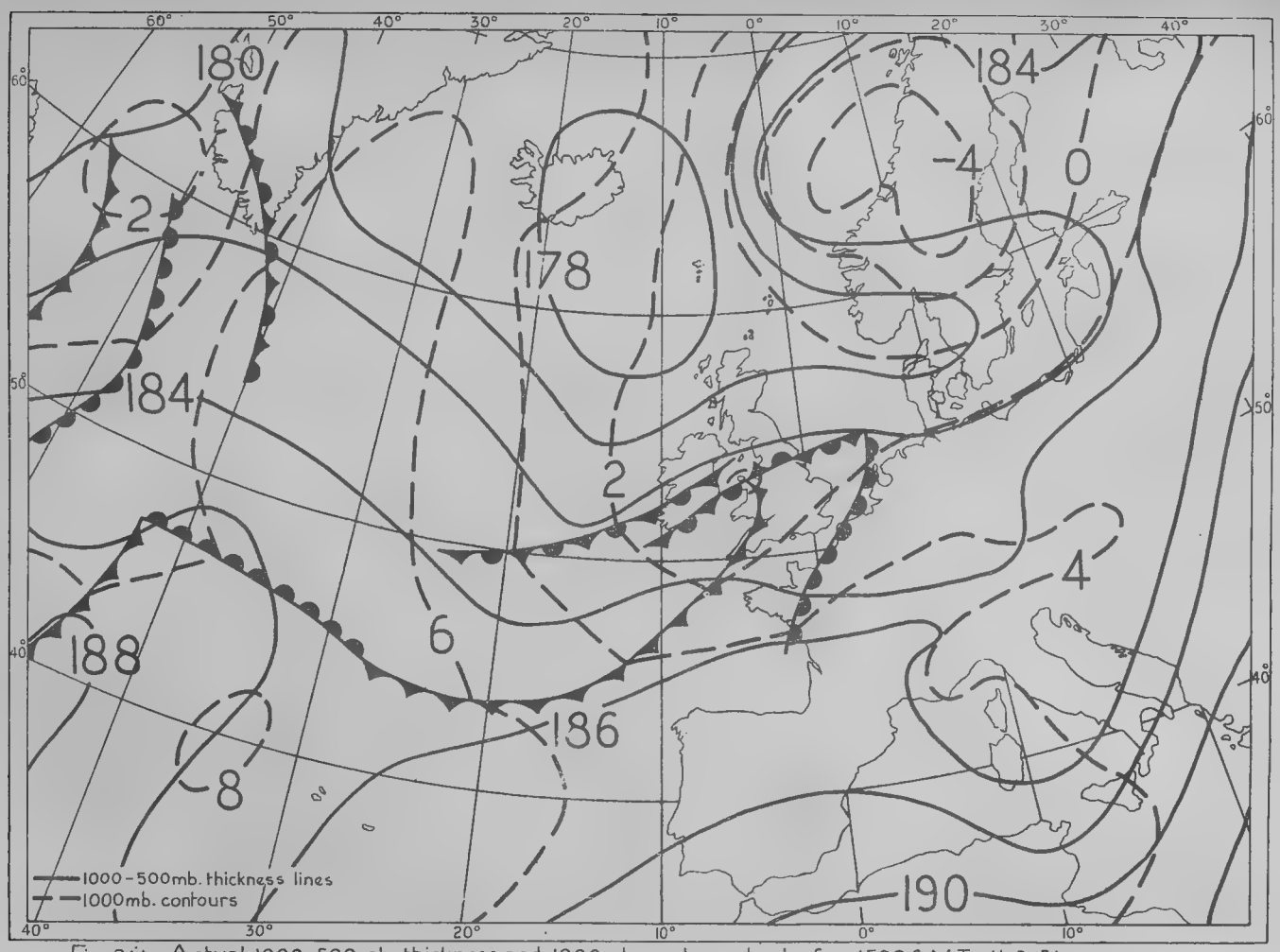

Fig.2(i) Actual 1000-500mb. thickness and 1000mb. contour charts for 1500 G.M.T. 11.8.51

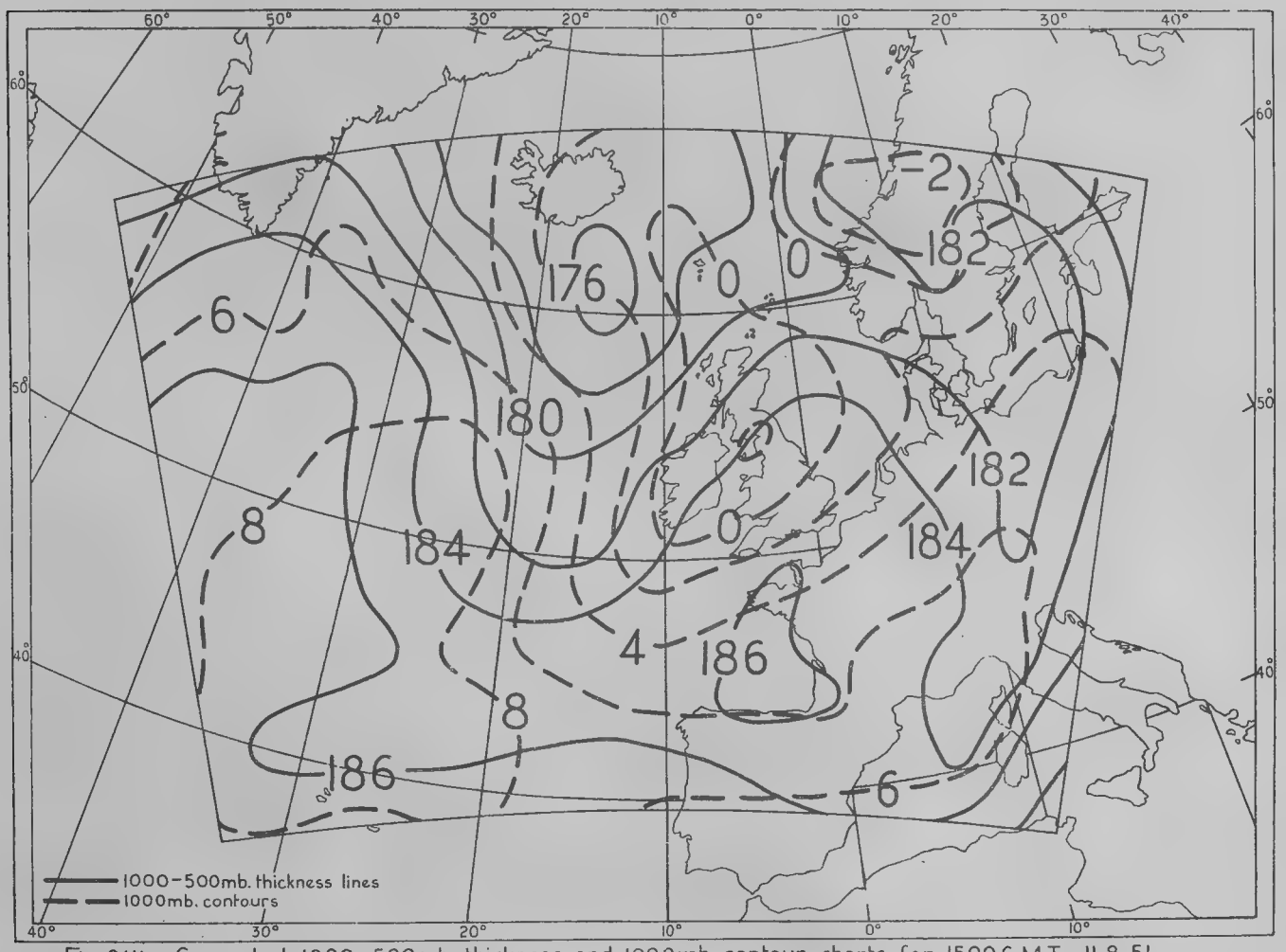

Fig.2(j) Computed 1000-500mb. thickness and 1000mb. contour charts for 1500 G.M.T. 11.8.51

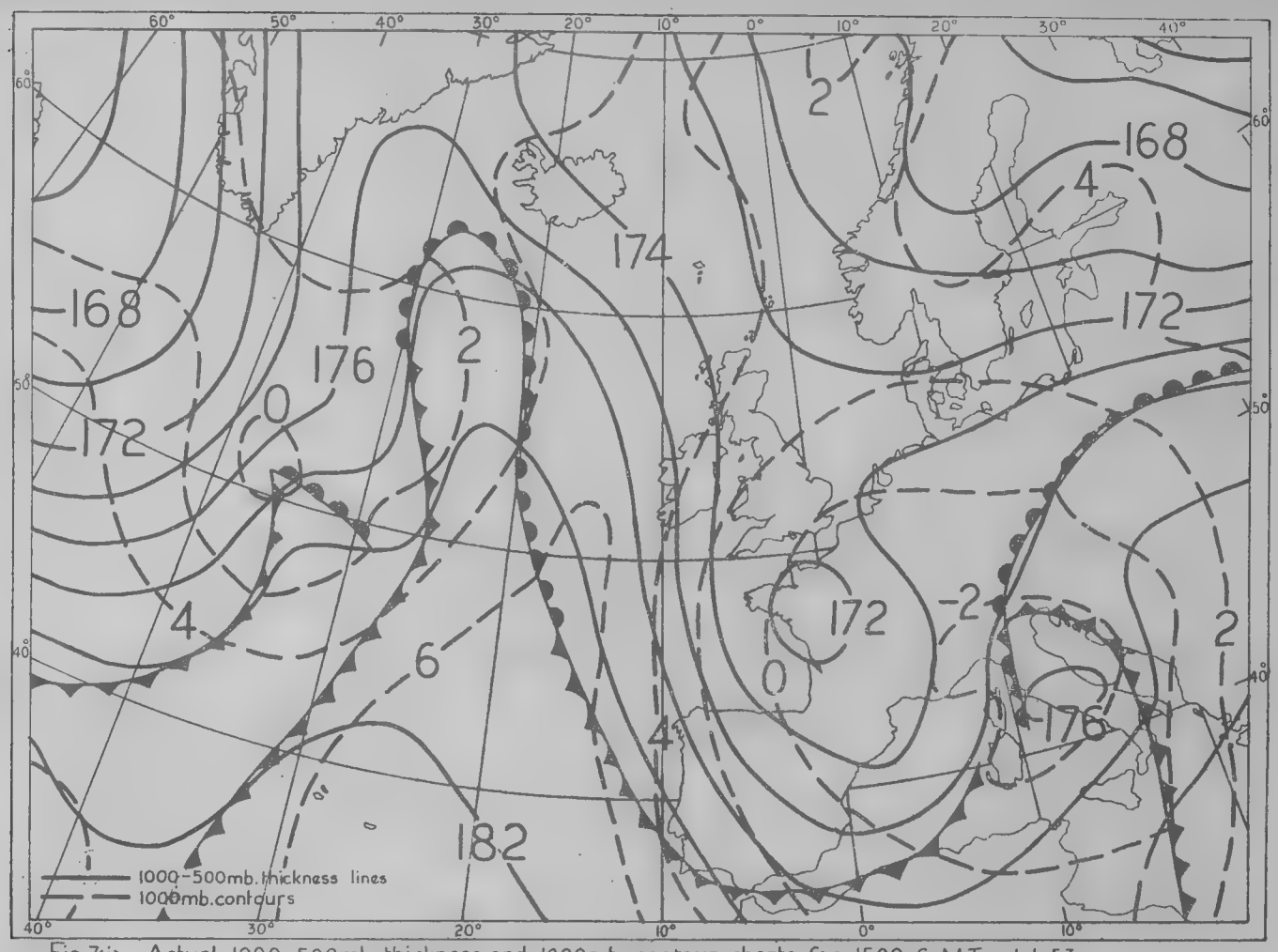

Fig.7(i) Actual 1000-500mb. thickness and 1000mb. contour charts for 1500 G.M.T. 1.1.53

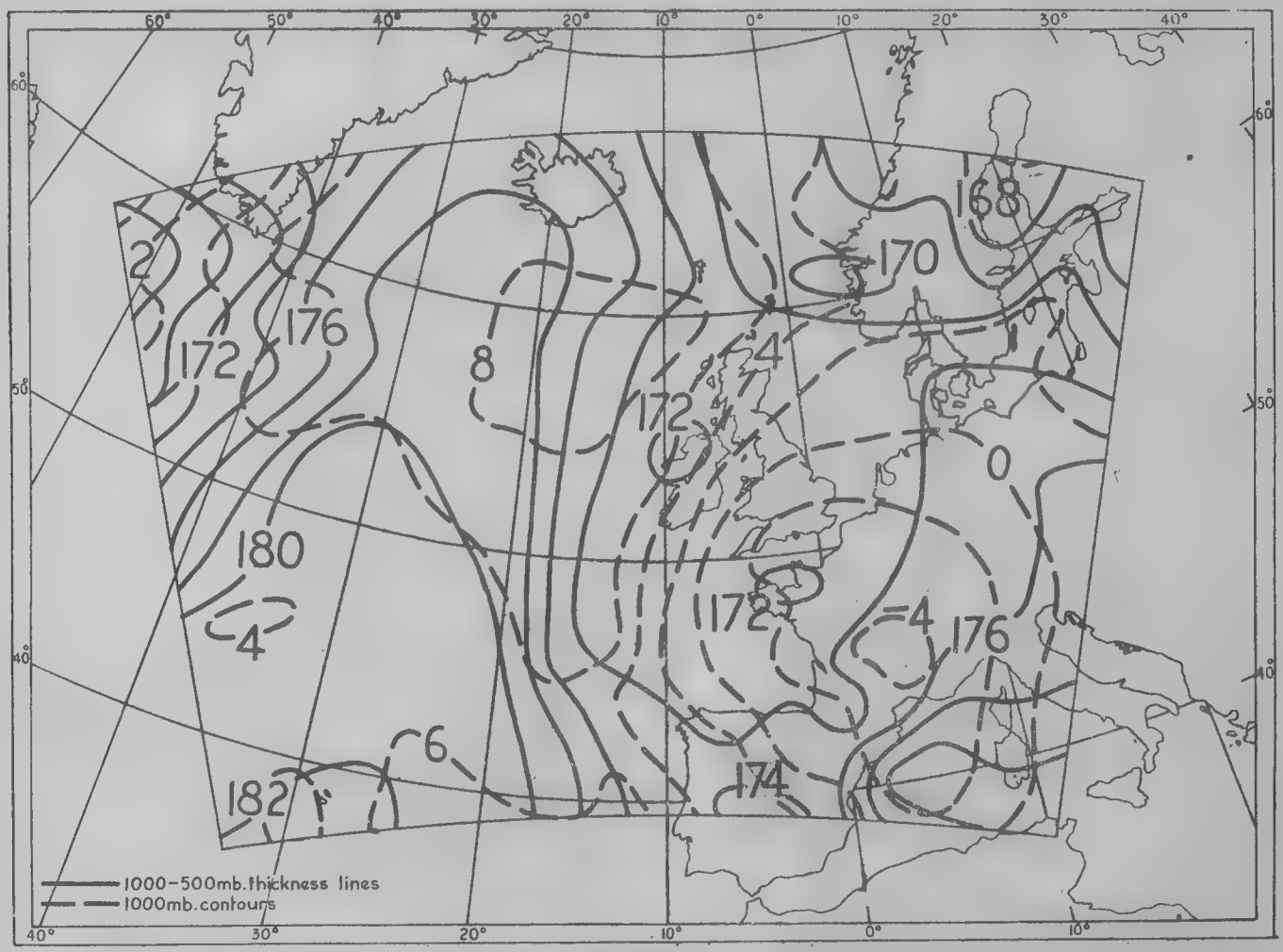

Fig.7(j) Computed 1000-500mb. thickness and 1000mb. contour charts for 1500 G.M.T. 1.1.53

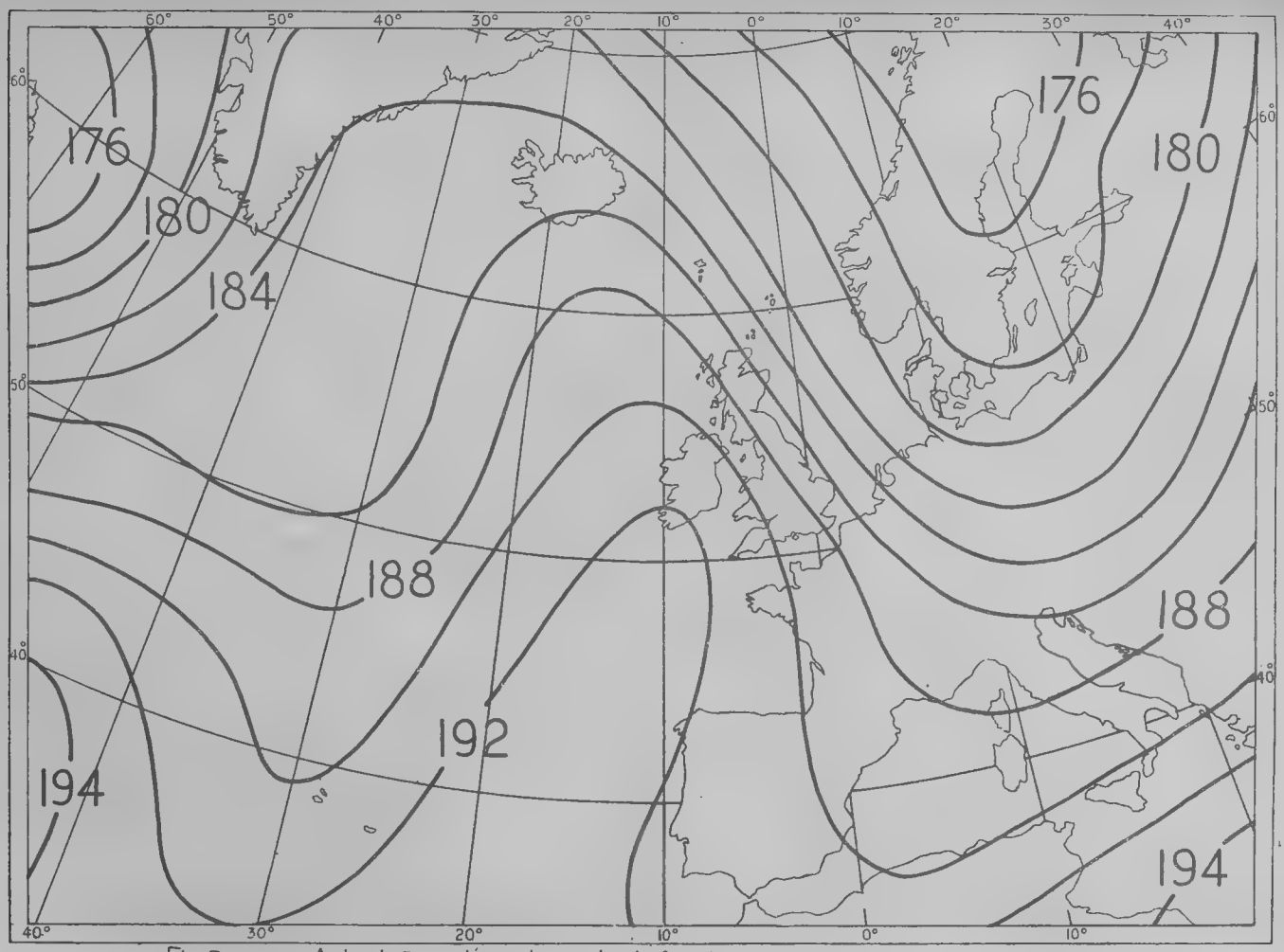

Fig. 3(a) Actual 500mb. contour chart for 1500 G.M.T. 19.9.51

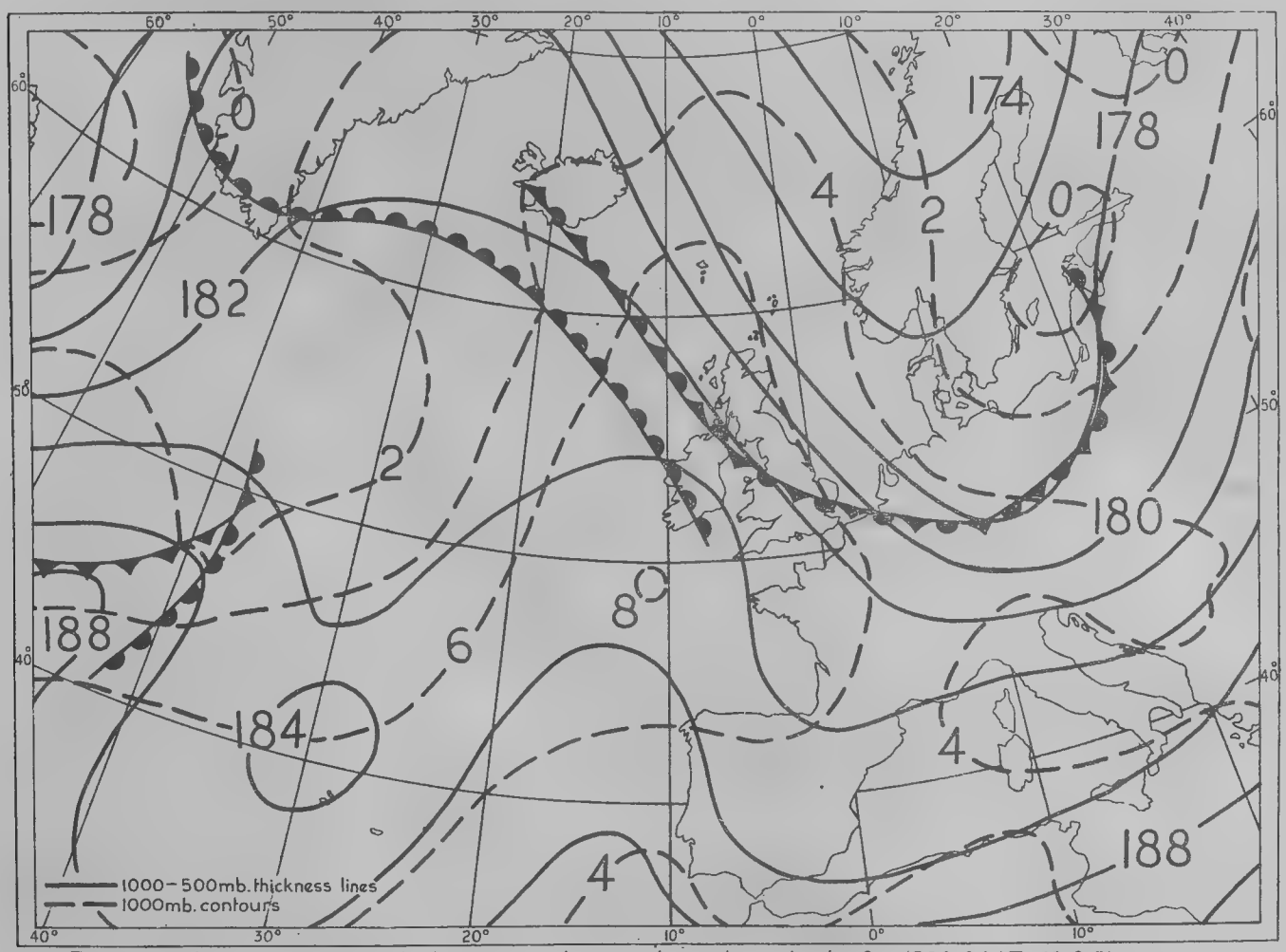

Fig. 3(b) Actual 1000-500mb. thickness and 1000mb. contour charts for 1500 G.M.T. 19.9.51

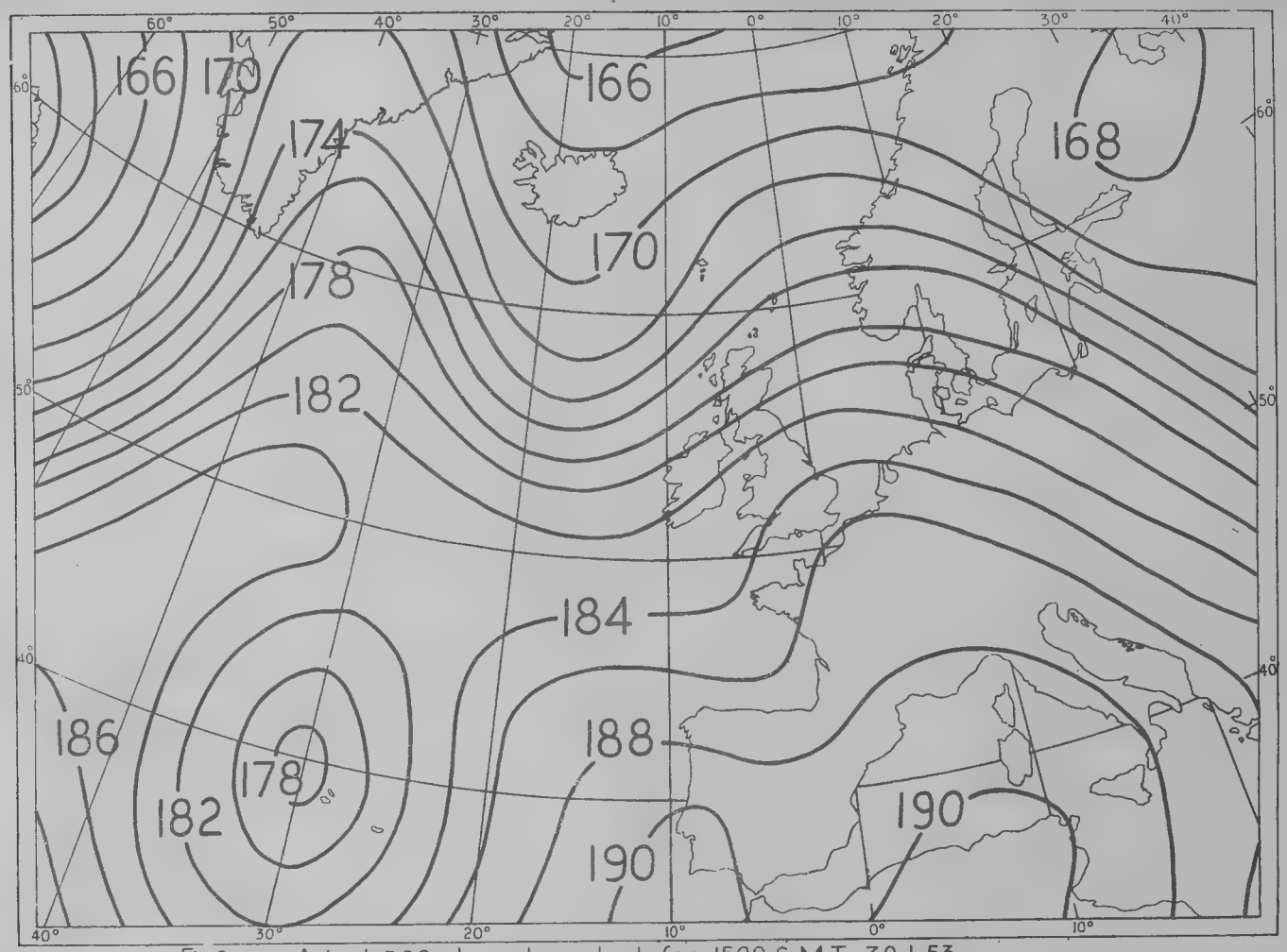

Fig.8(a) Actual 500mb. contour chart for 1500 G.M.T. 30.1.53

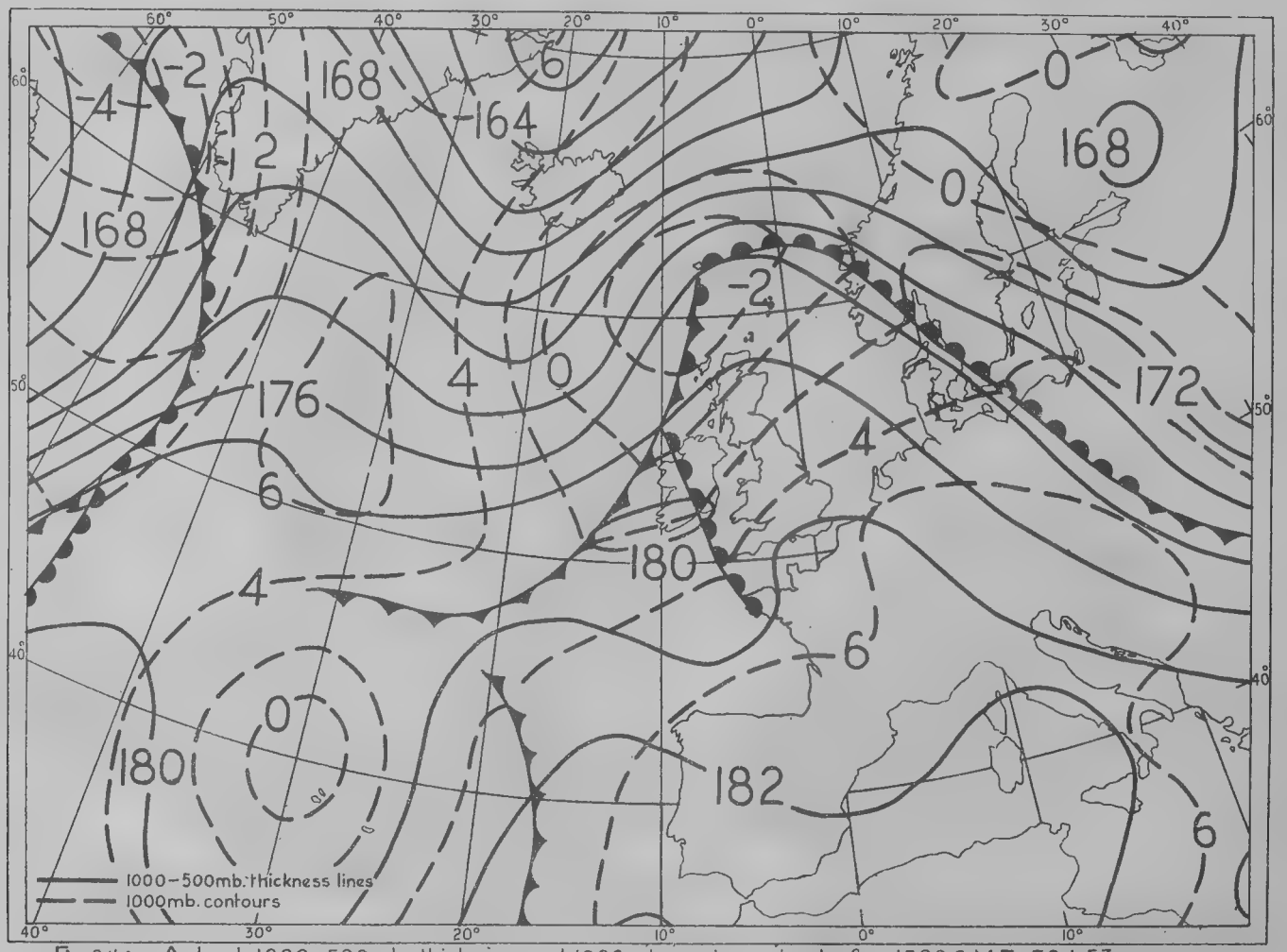

Fig.8(b) Actual 1000–500mb. thickness and 1000mb. contour charts for 1500 G.M.T. 30.1.53

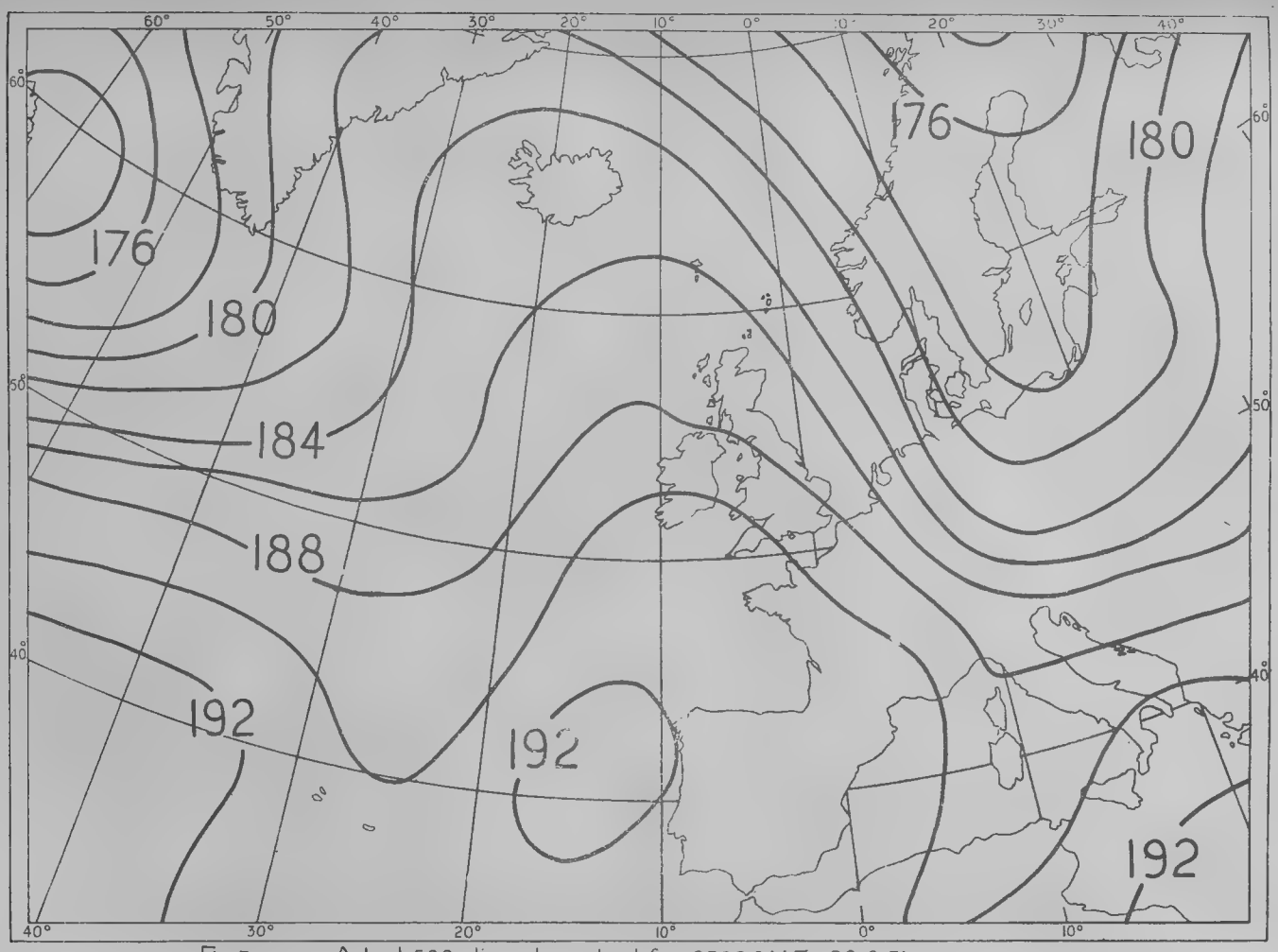

Fig.3(c) Actual 500mb. contour chart for 0300 G.M.T. 20.9.51

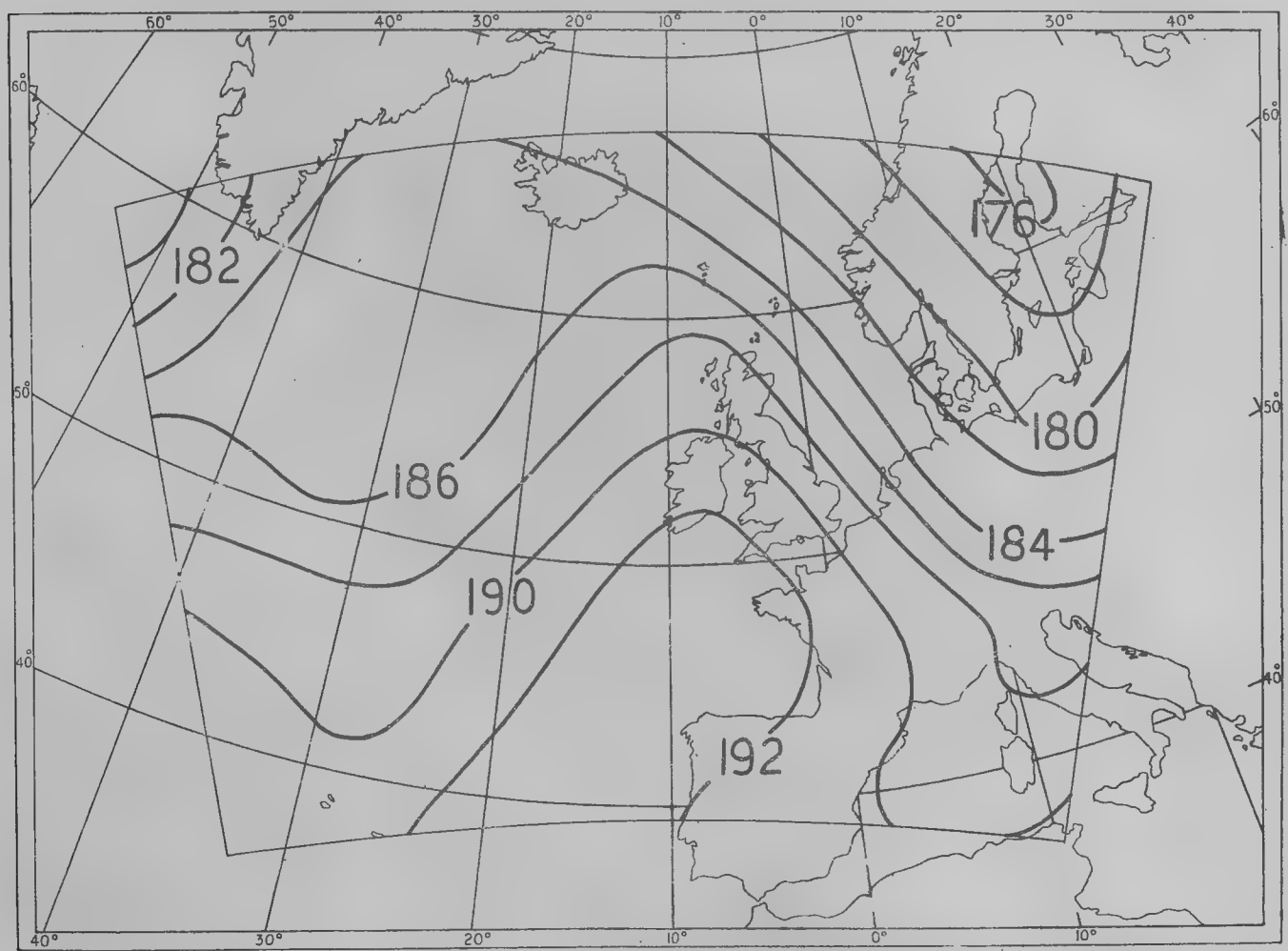

Fig.3(d) Computed 500mb. contour chart for 0300 G.M.T. 20.9.51

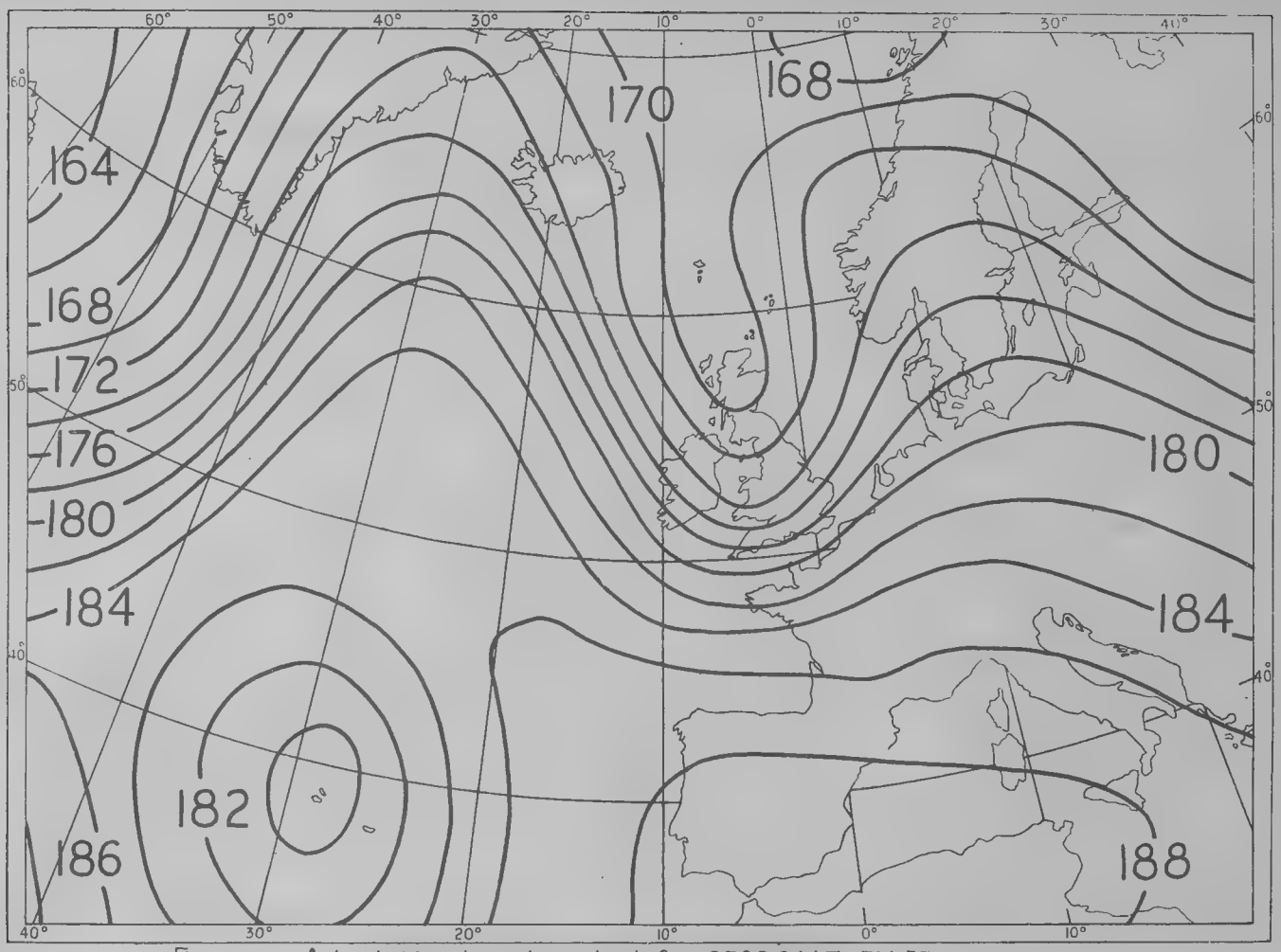

Fig.8(c) Actual 500mb. contour chart for 0300 G.M.T. 31.1.53

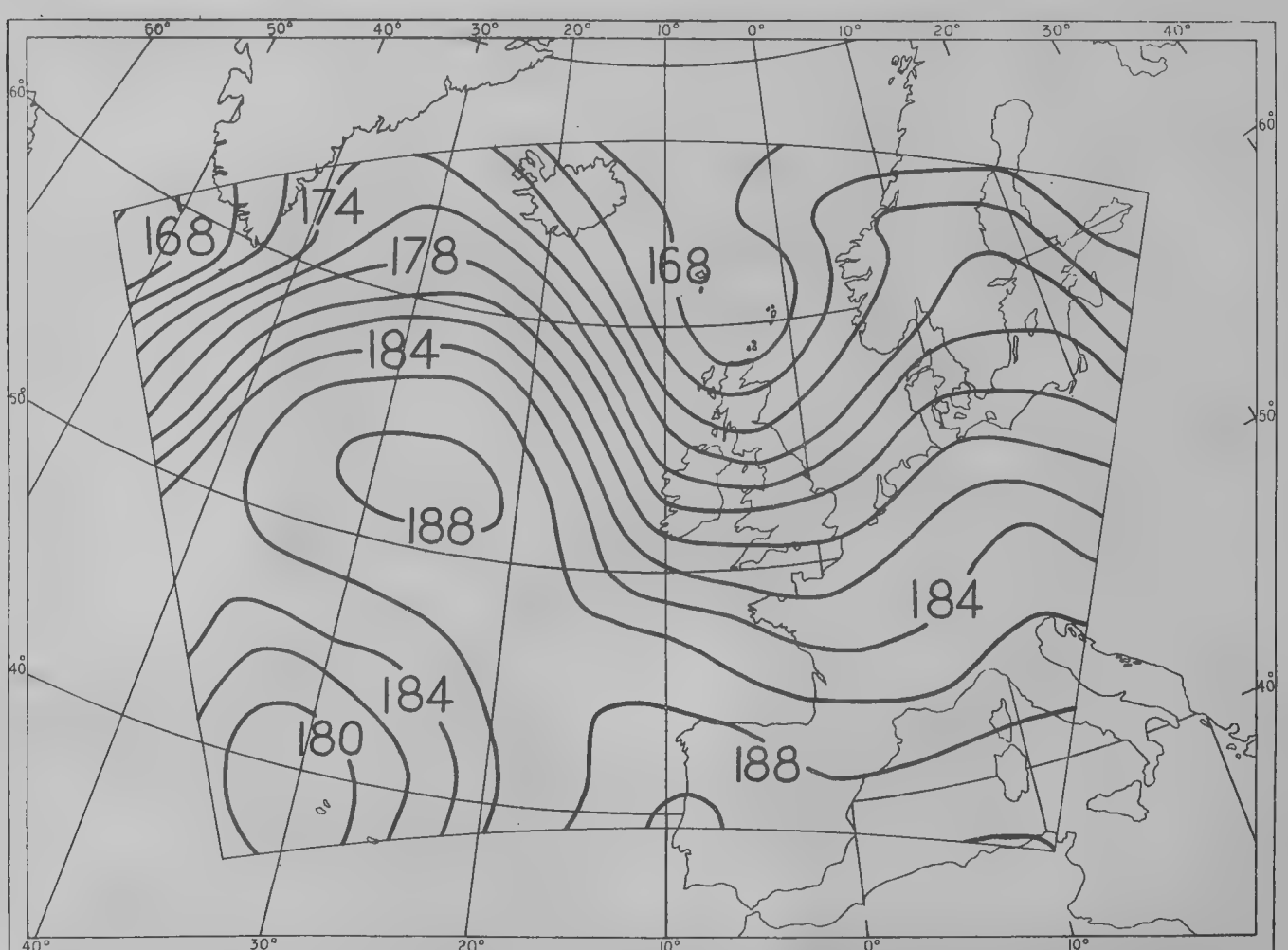

Fig.8(d) Computed 500mb. contour chart for 0300 G.M.T. 31.1.53

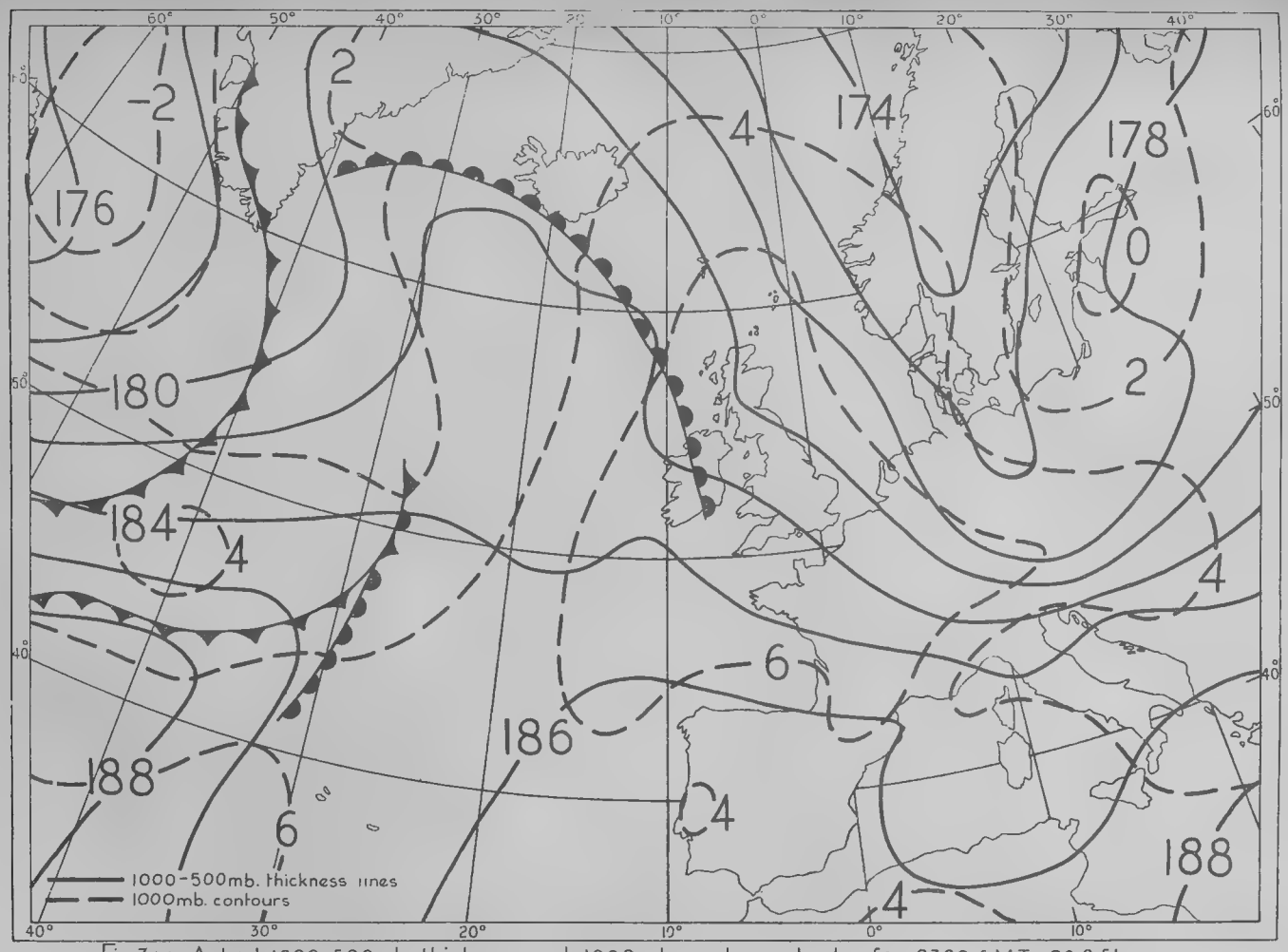

Fig.3(e) Actual 1000-500mb. thickness and 1000mb. contour charts for 0300 G.M.T. 20.9.51

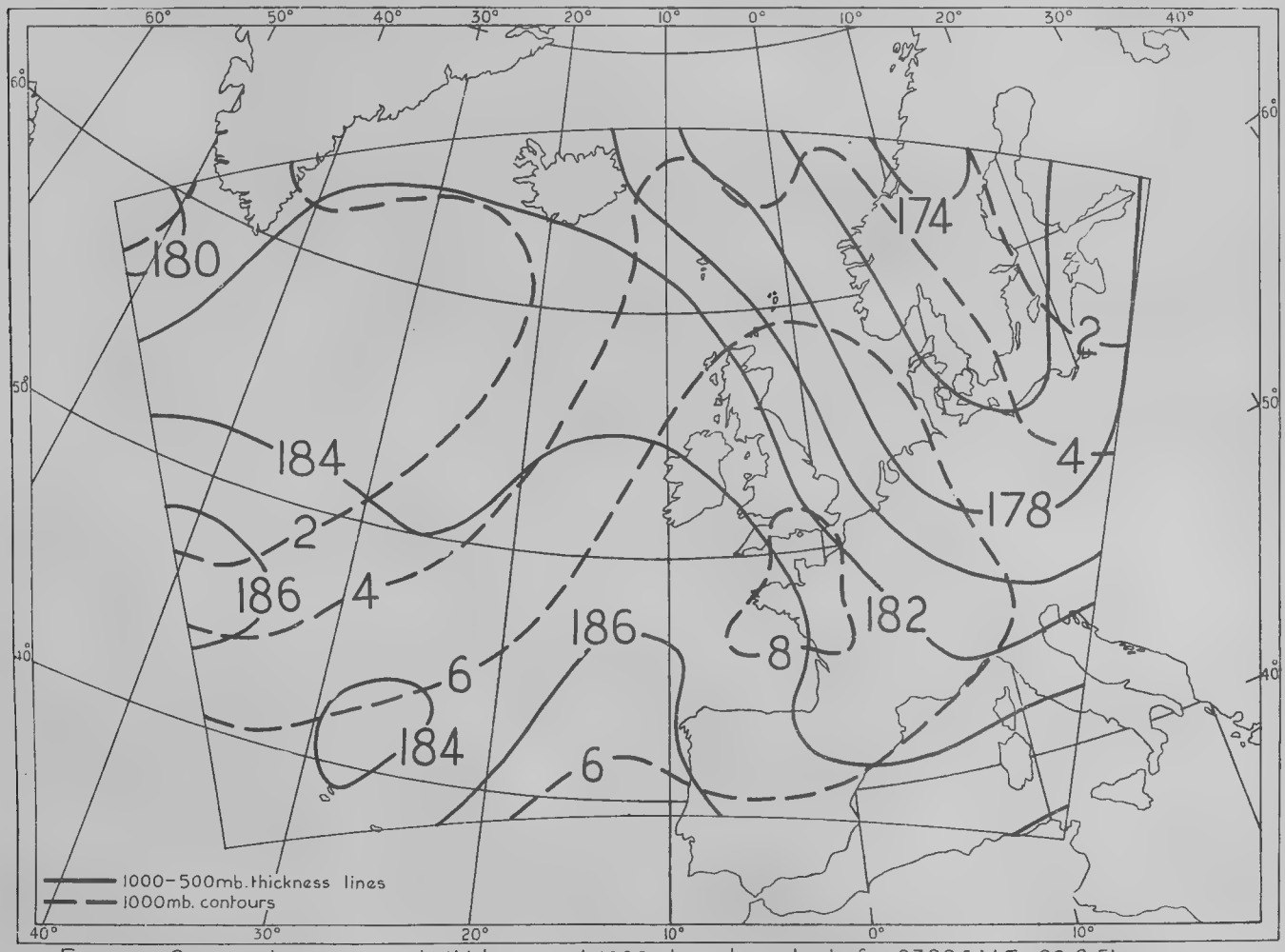

Fig.3(f) Computed 1000-500mb. thickness and 1000mb. contour charts for 0300 G.M.T. 20.9.51

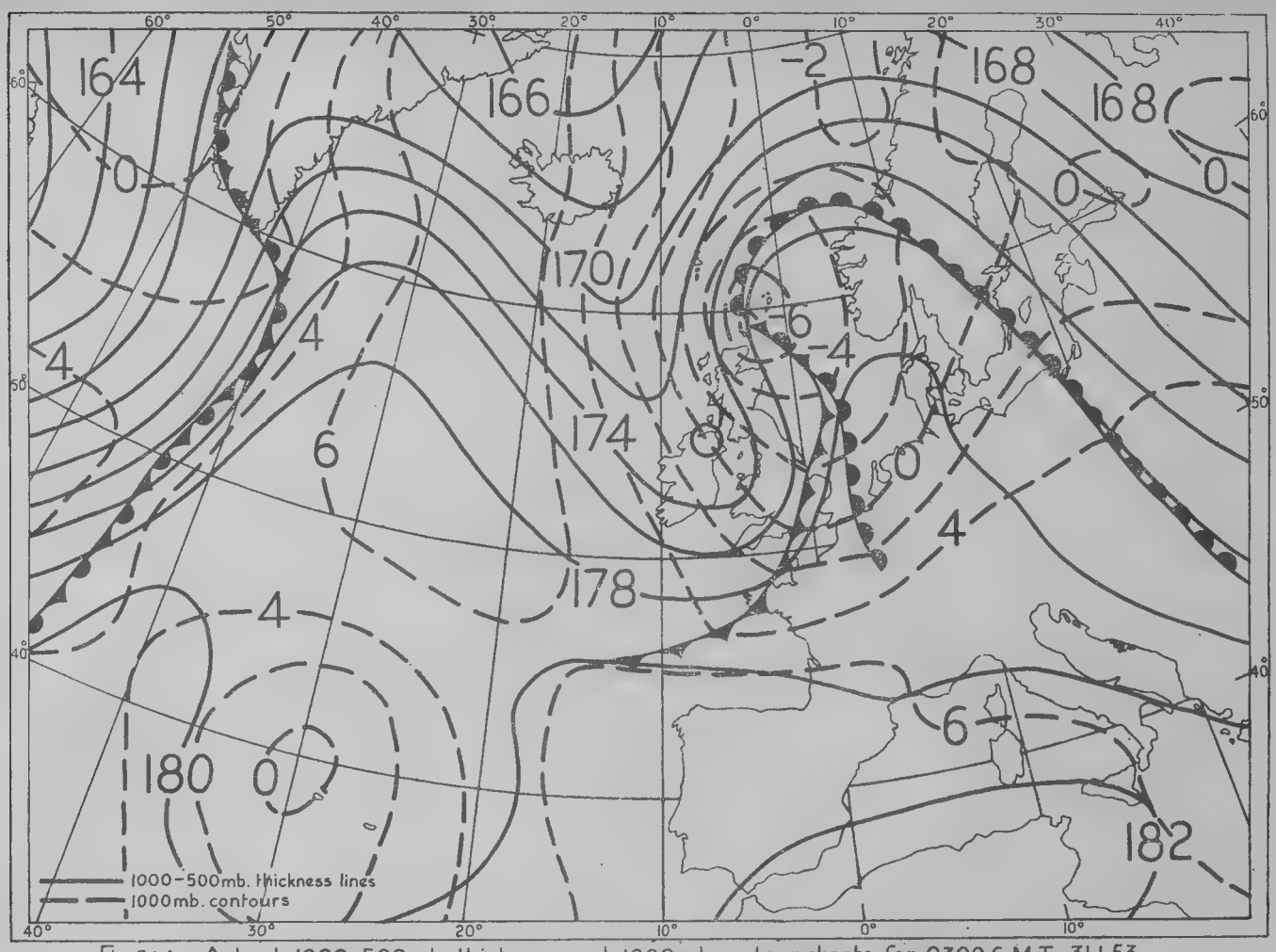

Fig.8(e) Actual 1000-500mb. thickness and 1000mb. contour charts for 0300 G.M.T. 31.1.53

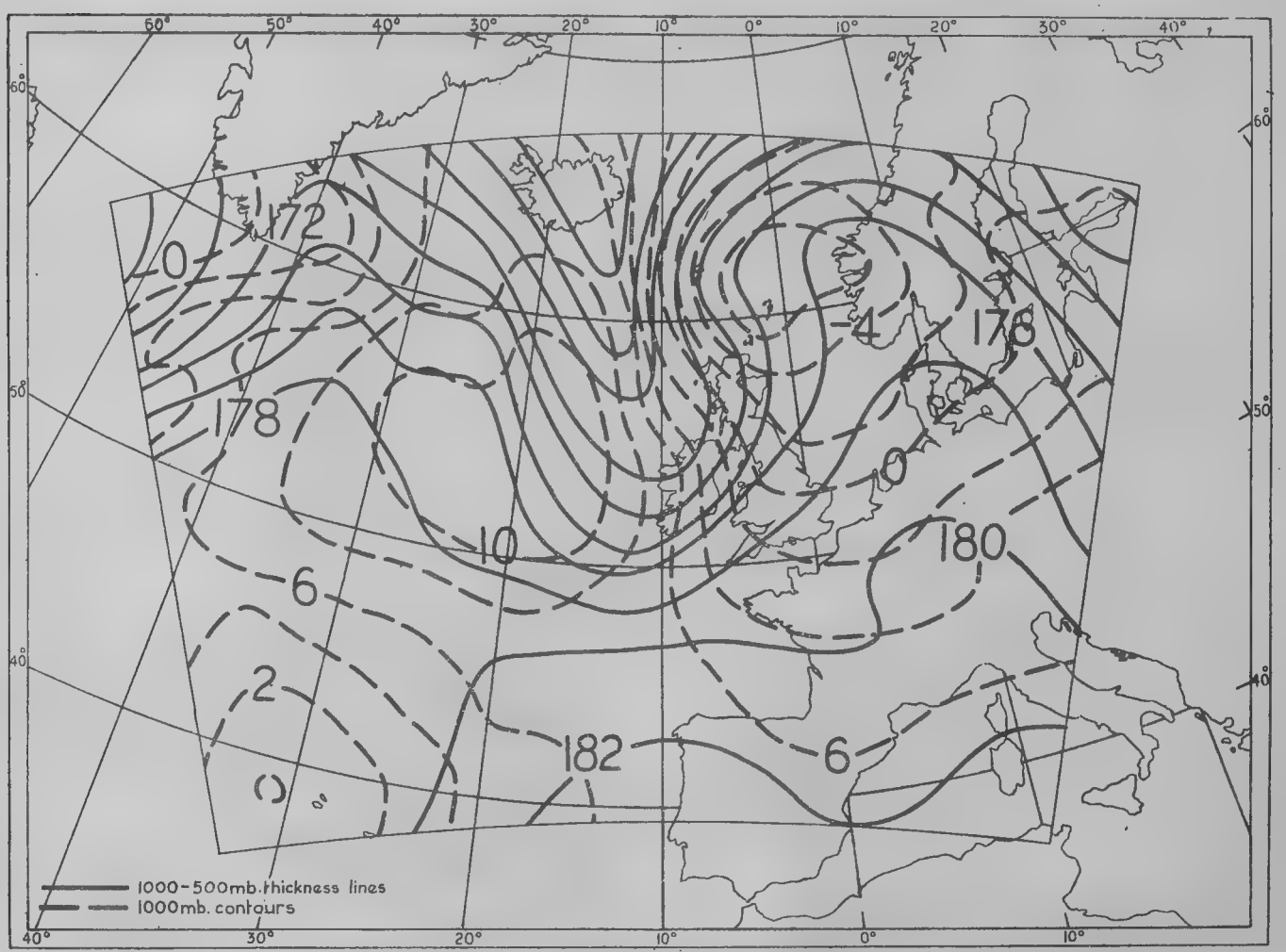

Fig.8(f) Computed 1000-500mb. thickness and 1000mb. contour charts for 0300 G.M.T. 31.1.53

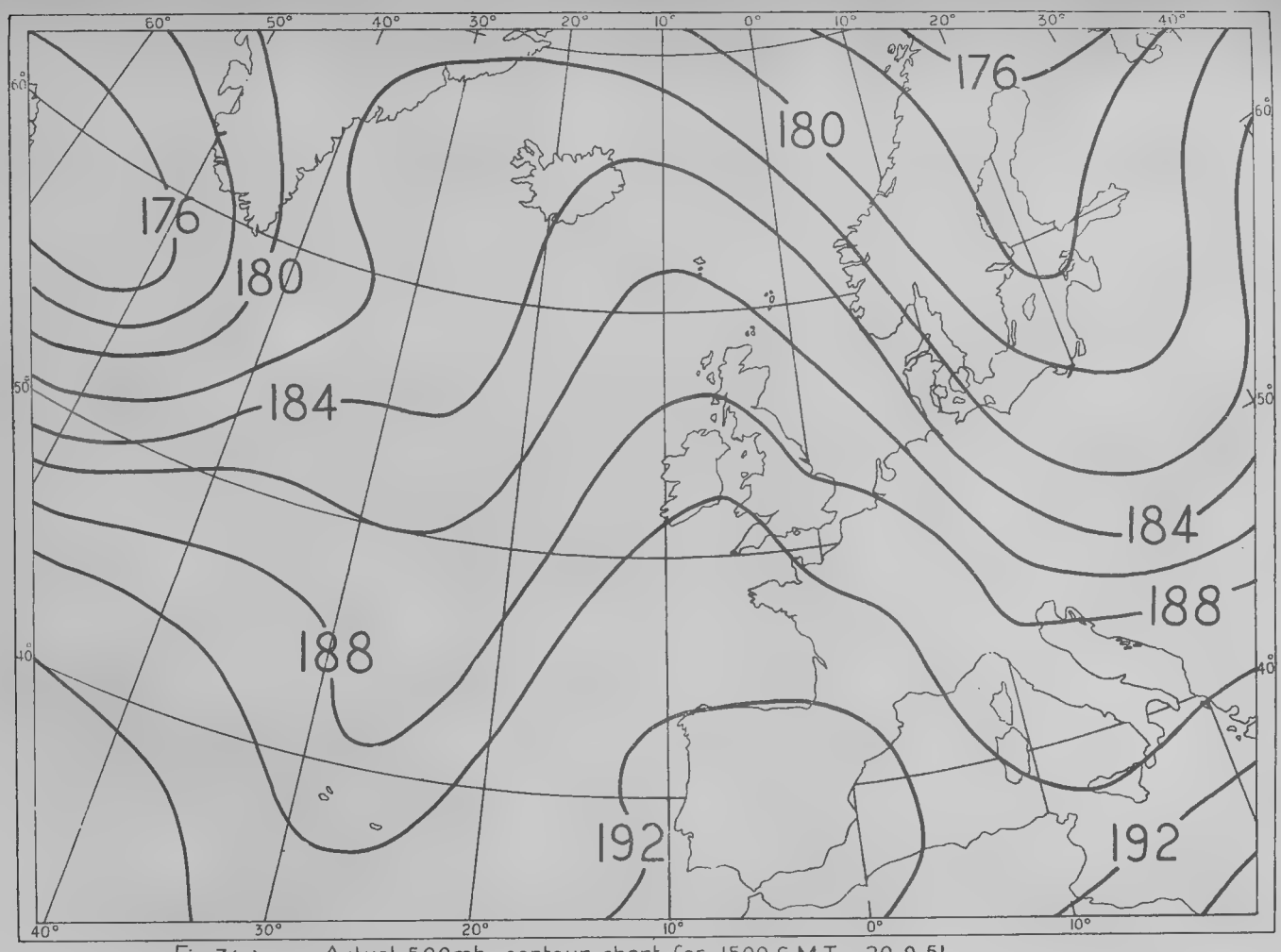

Fig.3(g) Actual 500mb. contour chart for 1500 G.M.T. 20.9.51

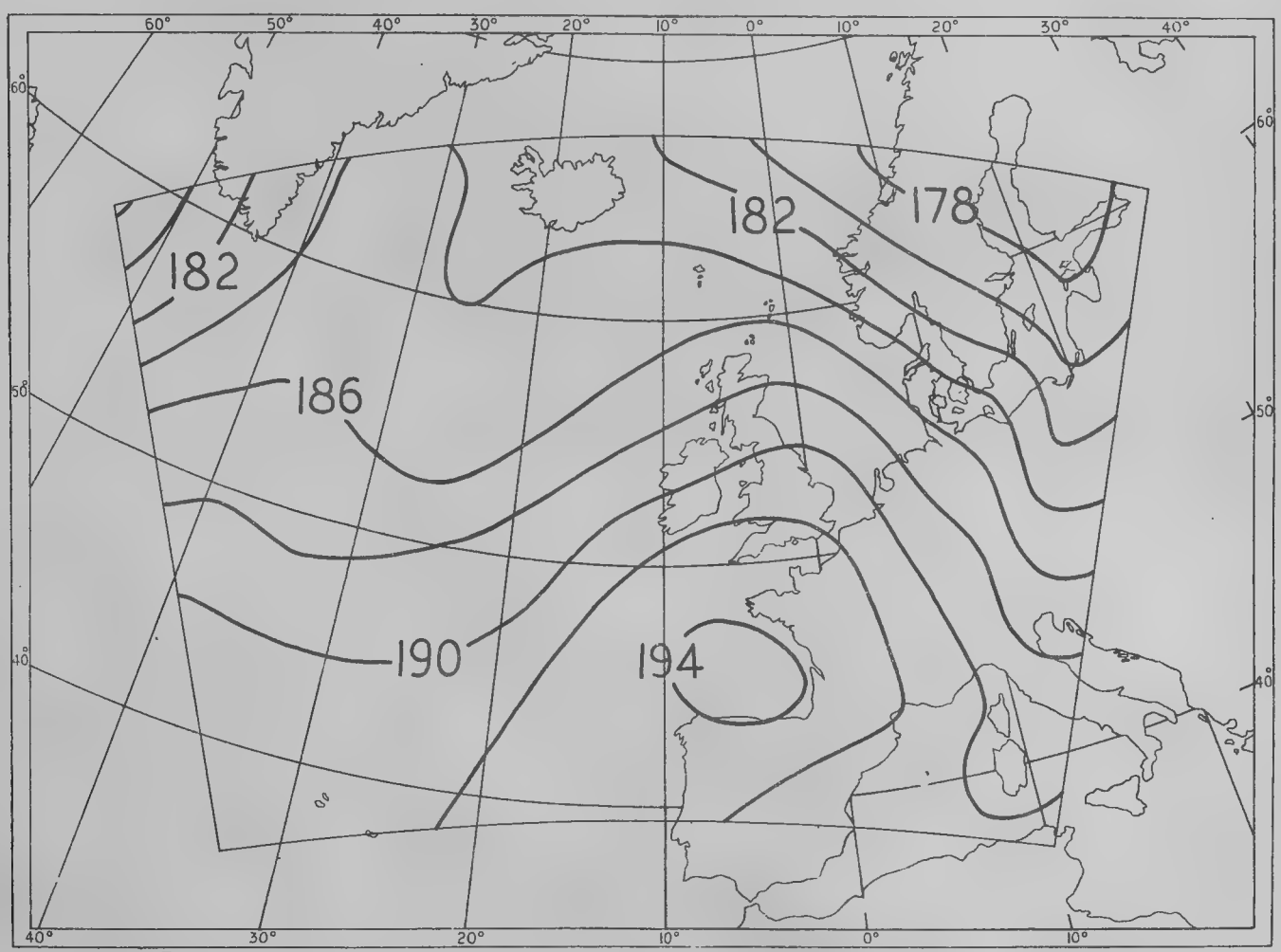

Fig.3(h) Computed 500mb. contour chart for 1500 G.M.T. 20.9.51

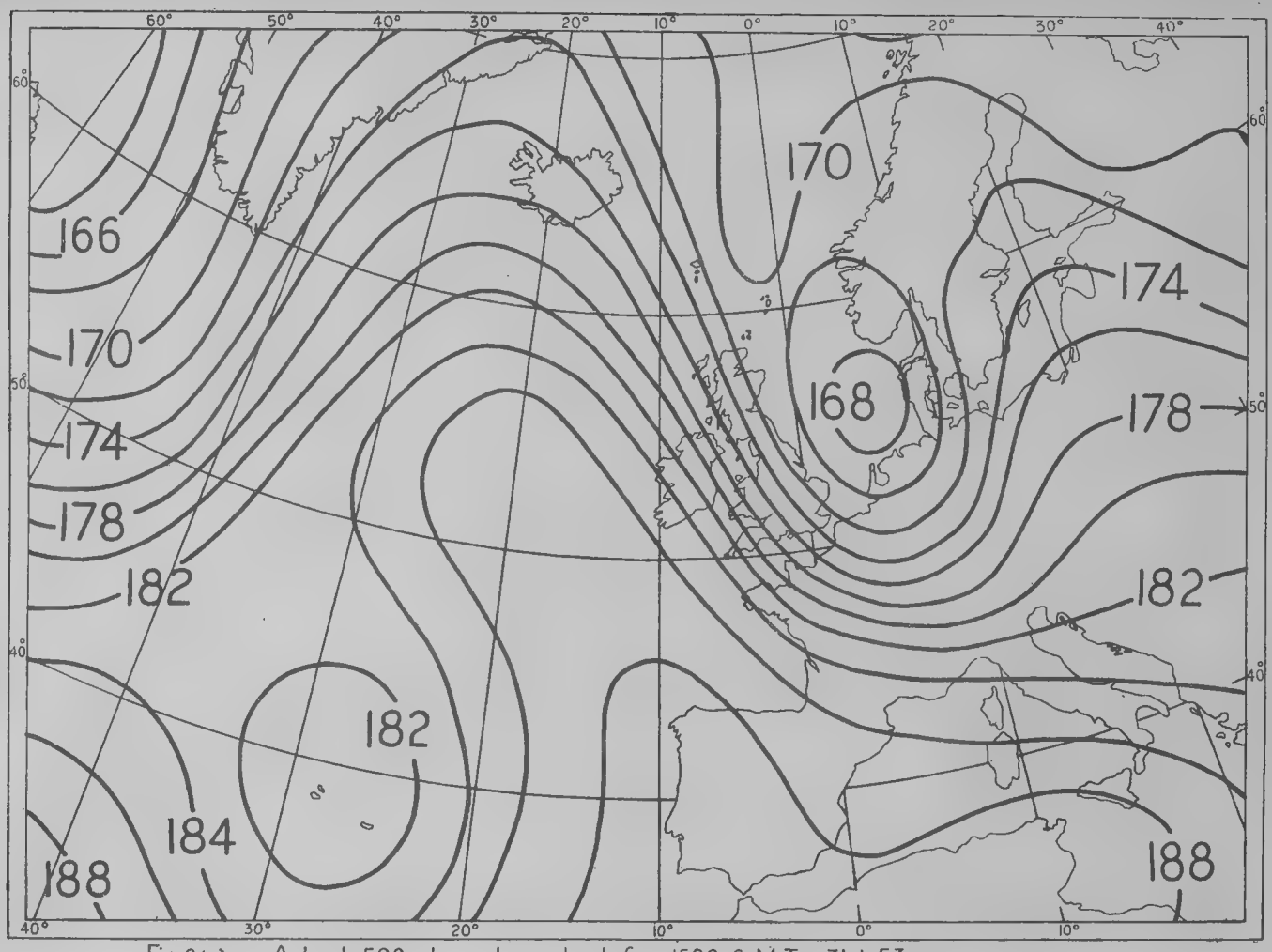

Fig.8(g) Actual 500mb. contour chart for 1500 G.M.T. 31.1.53

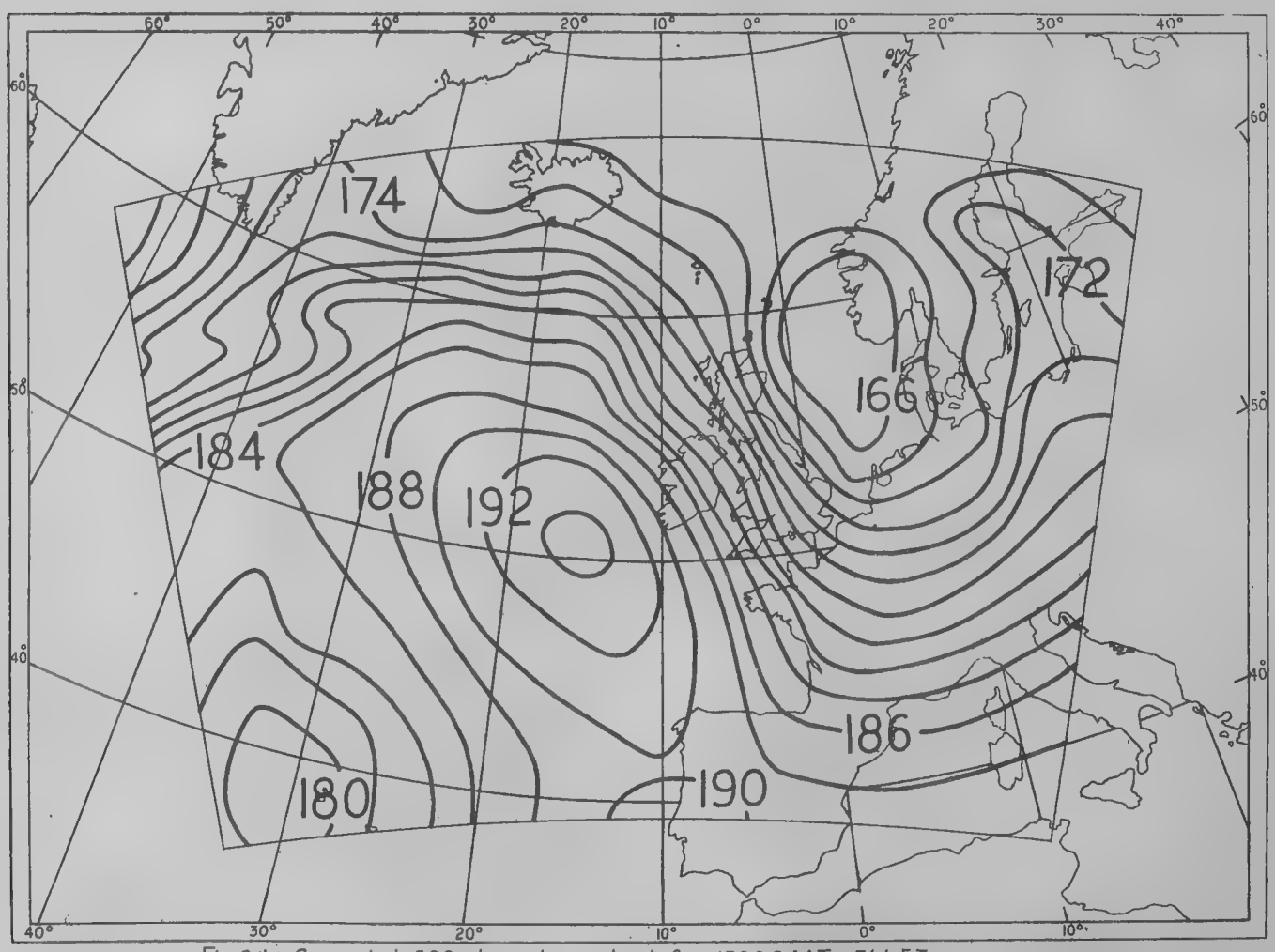

Fig.8(h) Computed 500mb. contour chart for 1500 G.M.T. 31.1.53

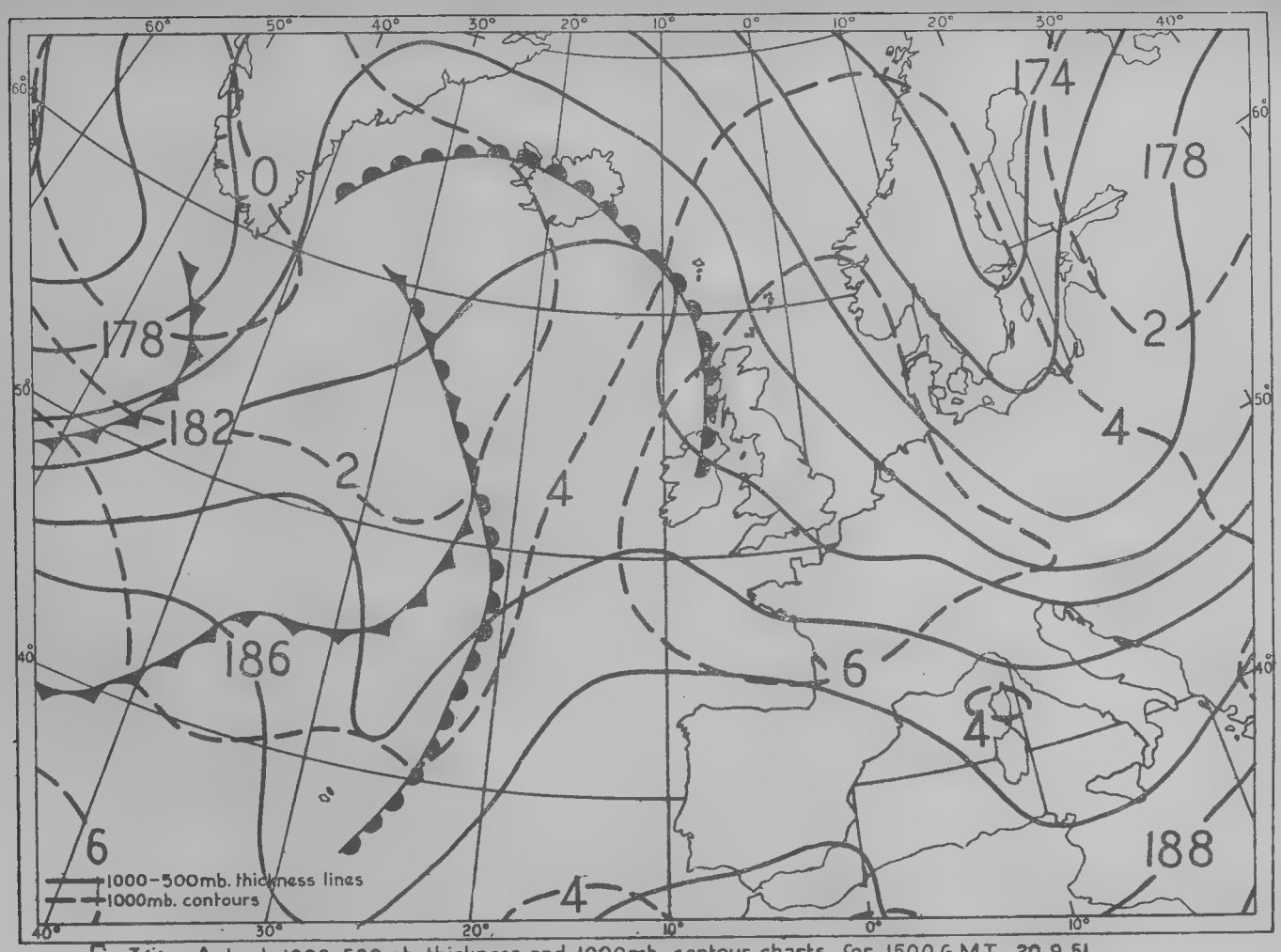

Fig.3(i) Actual 1000–500mb. thickness and 1000mb. contour charts for 1500 G.M.T. 20.9.51

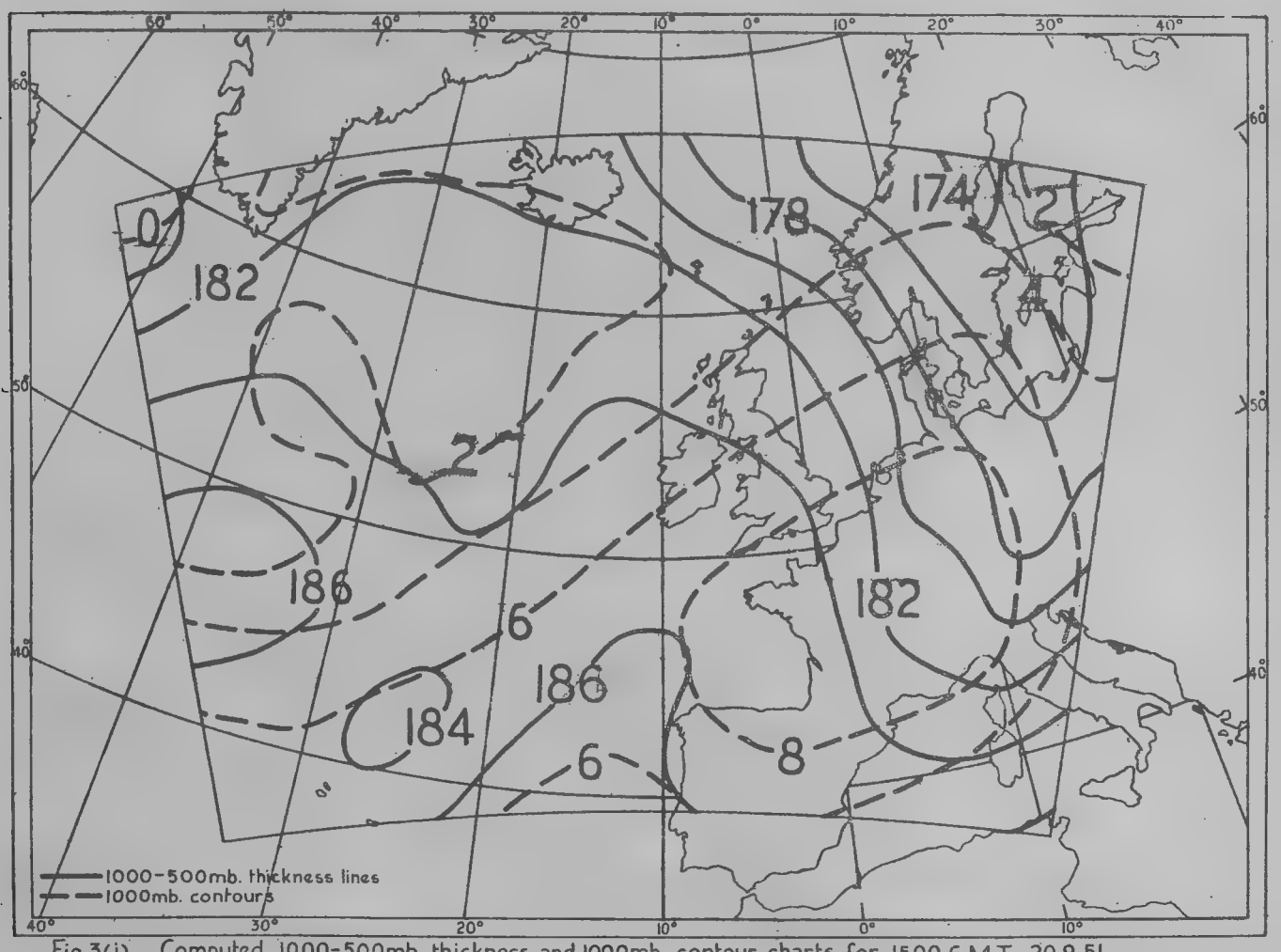

Fig.3(j) Computed 1000–500mb. thickness and 1000mb. contour charts for 1500 G.M.T. 20.9.51

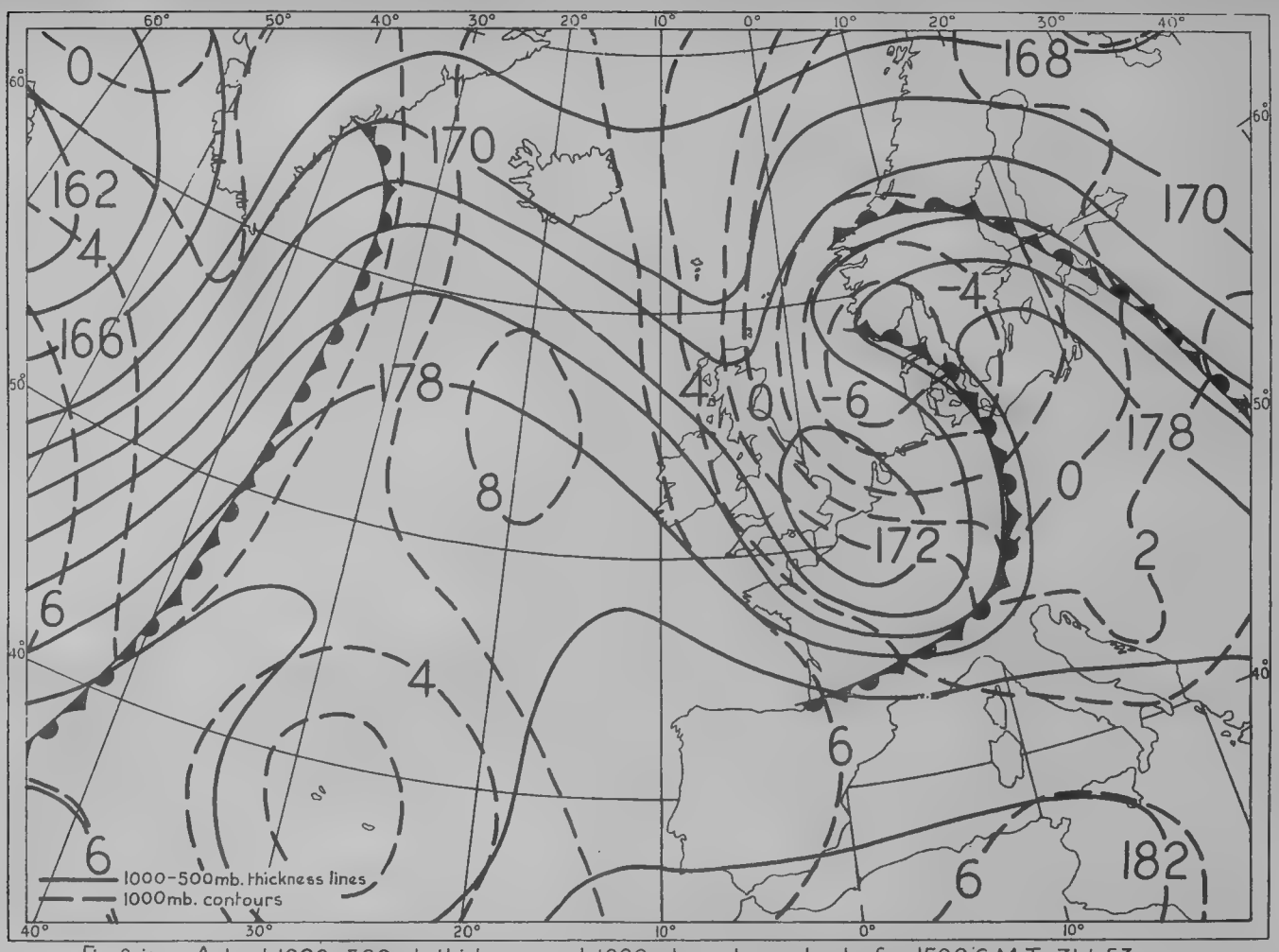

Fig.8(i) Actual 1000-500mb. thickness and 1000mb. contour charts for 1500 G.M.T. 31.1.53

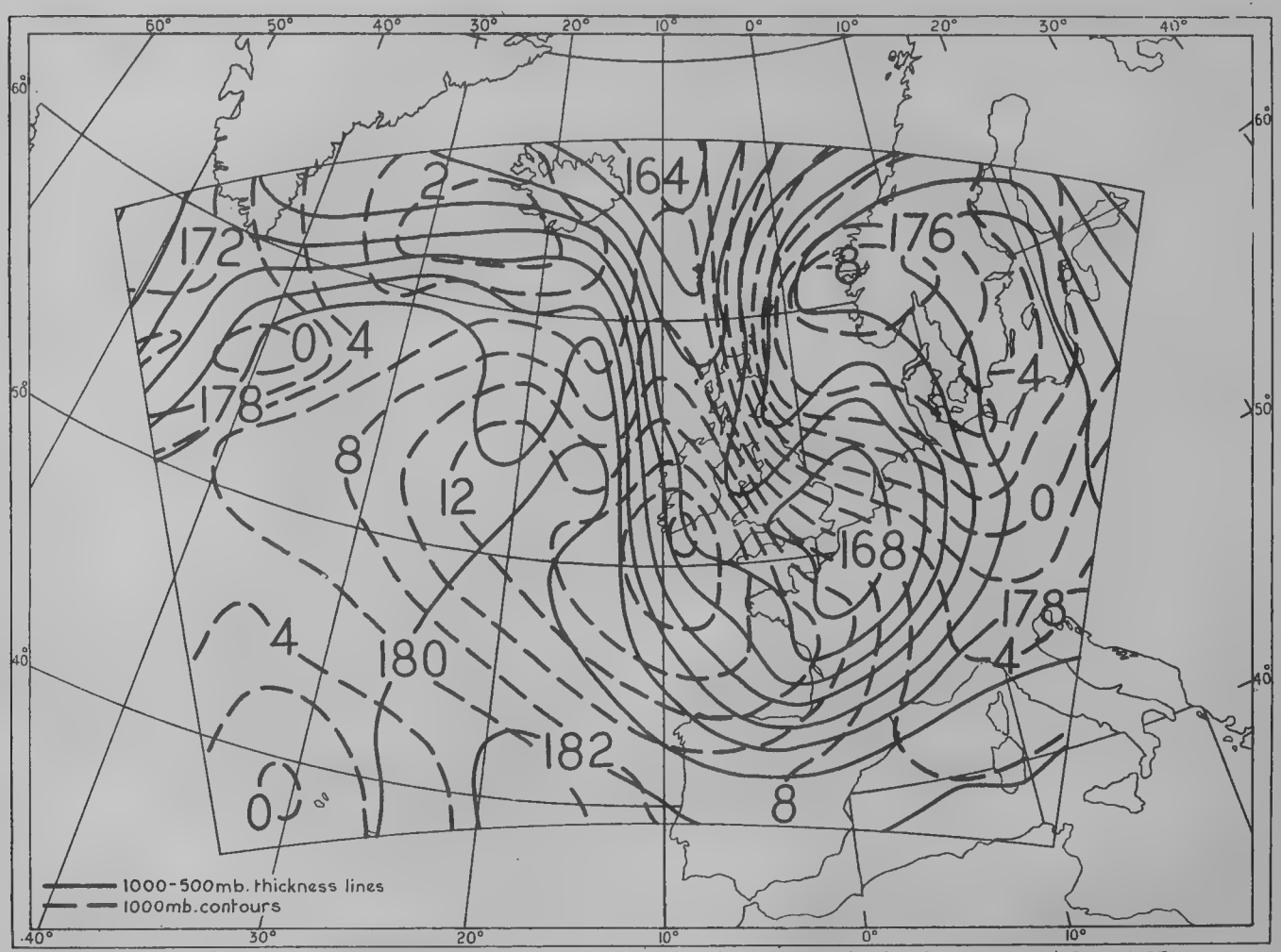

Fig.8(j) Computed 1000-500mb. thickness and 1000mb. contour charts for 1500 G.M.T. 31.1.53

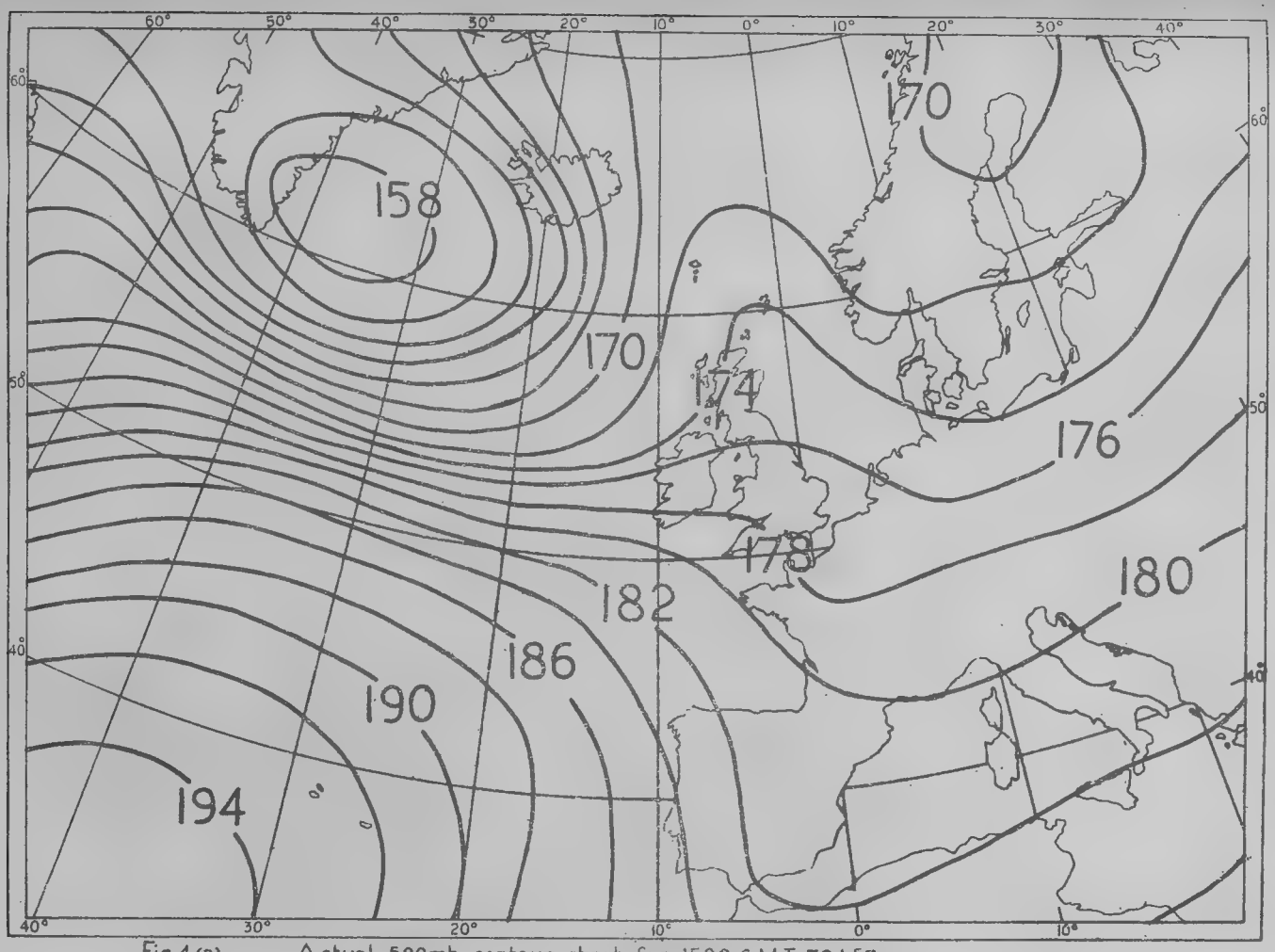

Fig.4(a) Actual 500mb. contour chart for 1500 G.M.T. 30.1.52

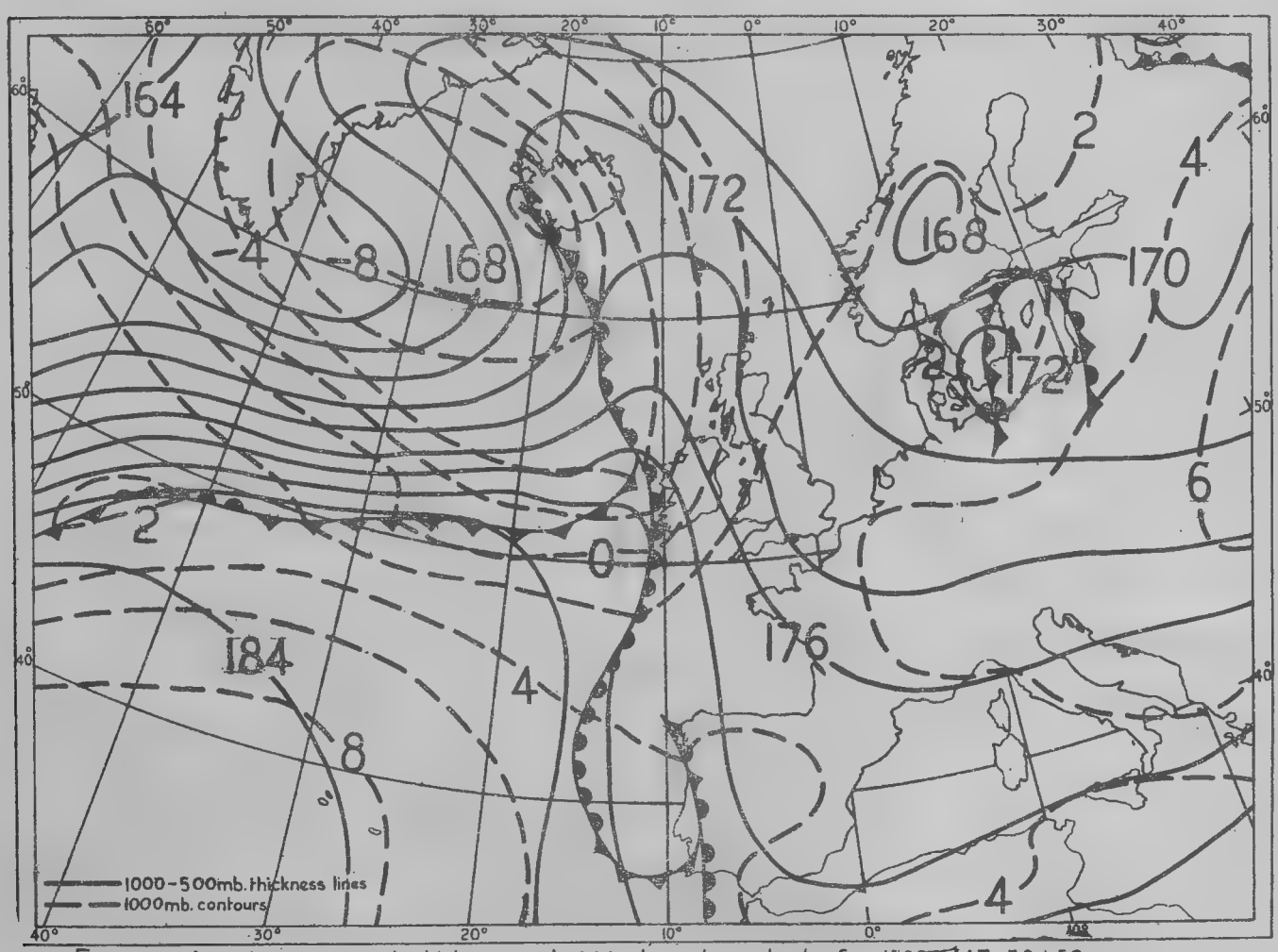

Fig.4(b) Actual 1000-500mb. thickness and 1000 mb. contour charts for 1500 G.M.T. 30.1.52

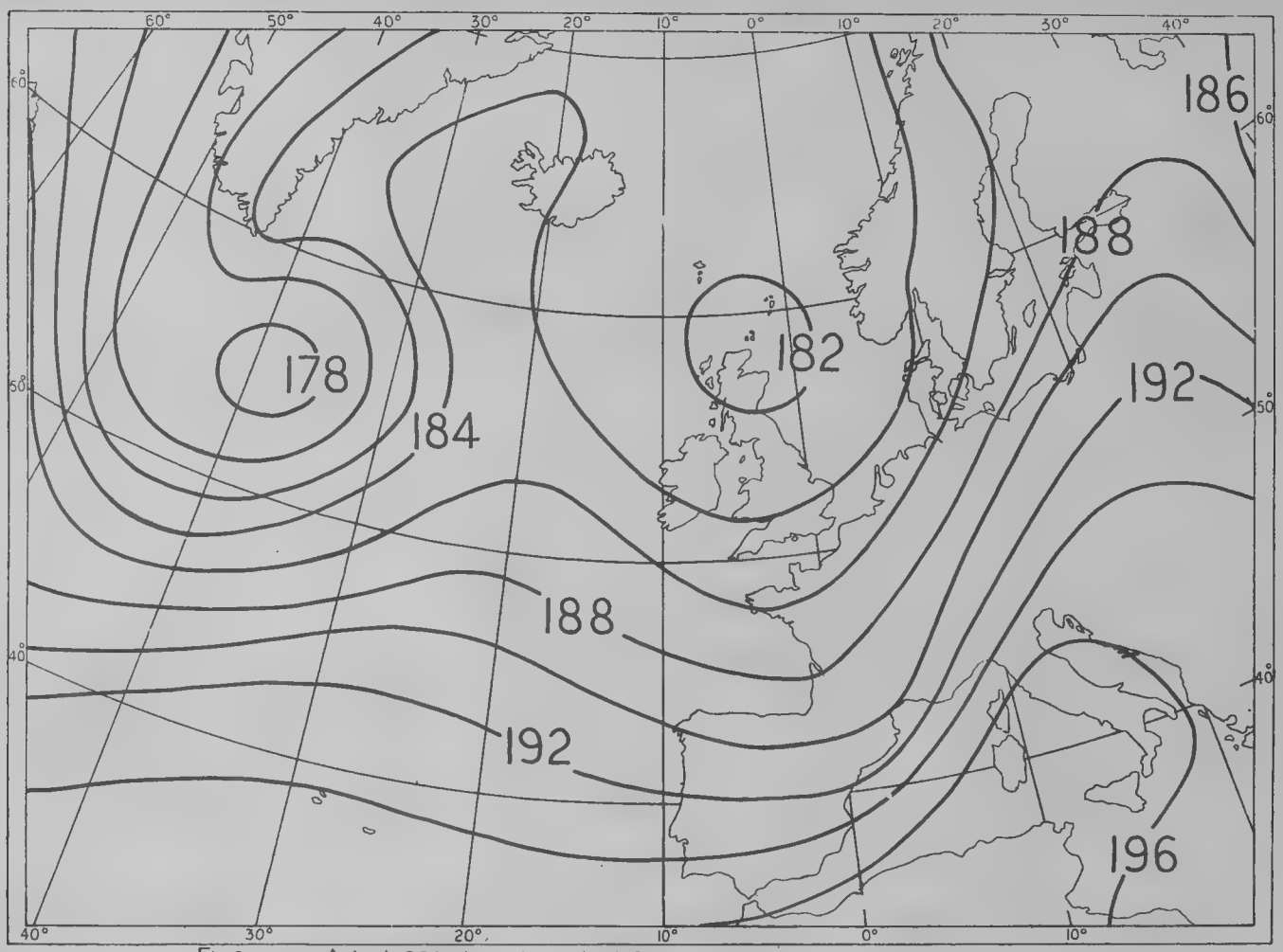

Fig.9(a) Actual 500mb. contour chart for 1500 G.M.T. 18.7.53

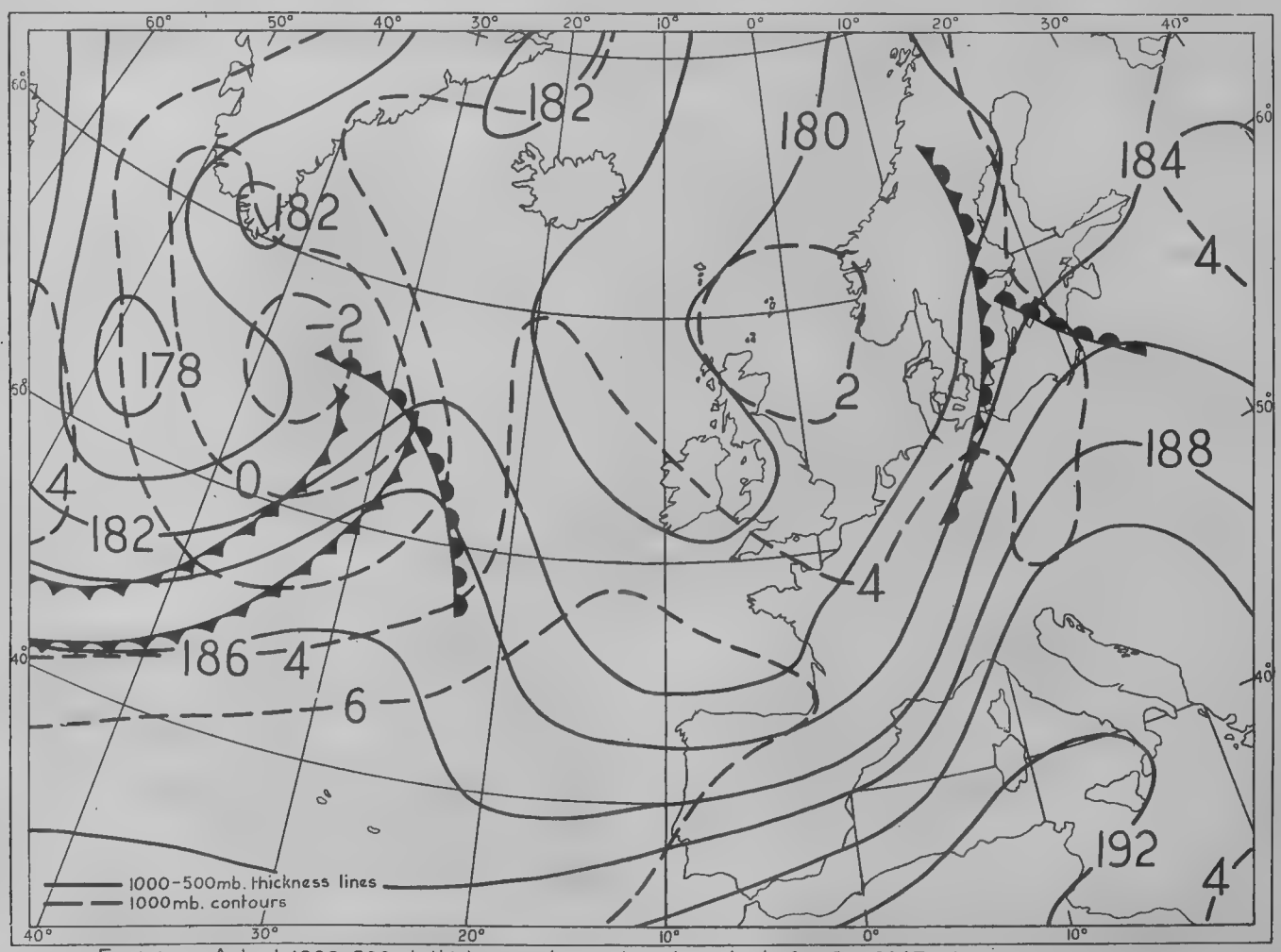

Fig.9(b) Actual 1000-500mb. thickness and 1000mb. contour charts for 1500 G.M.T. 18.7.53

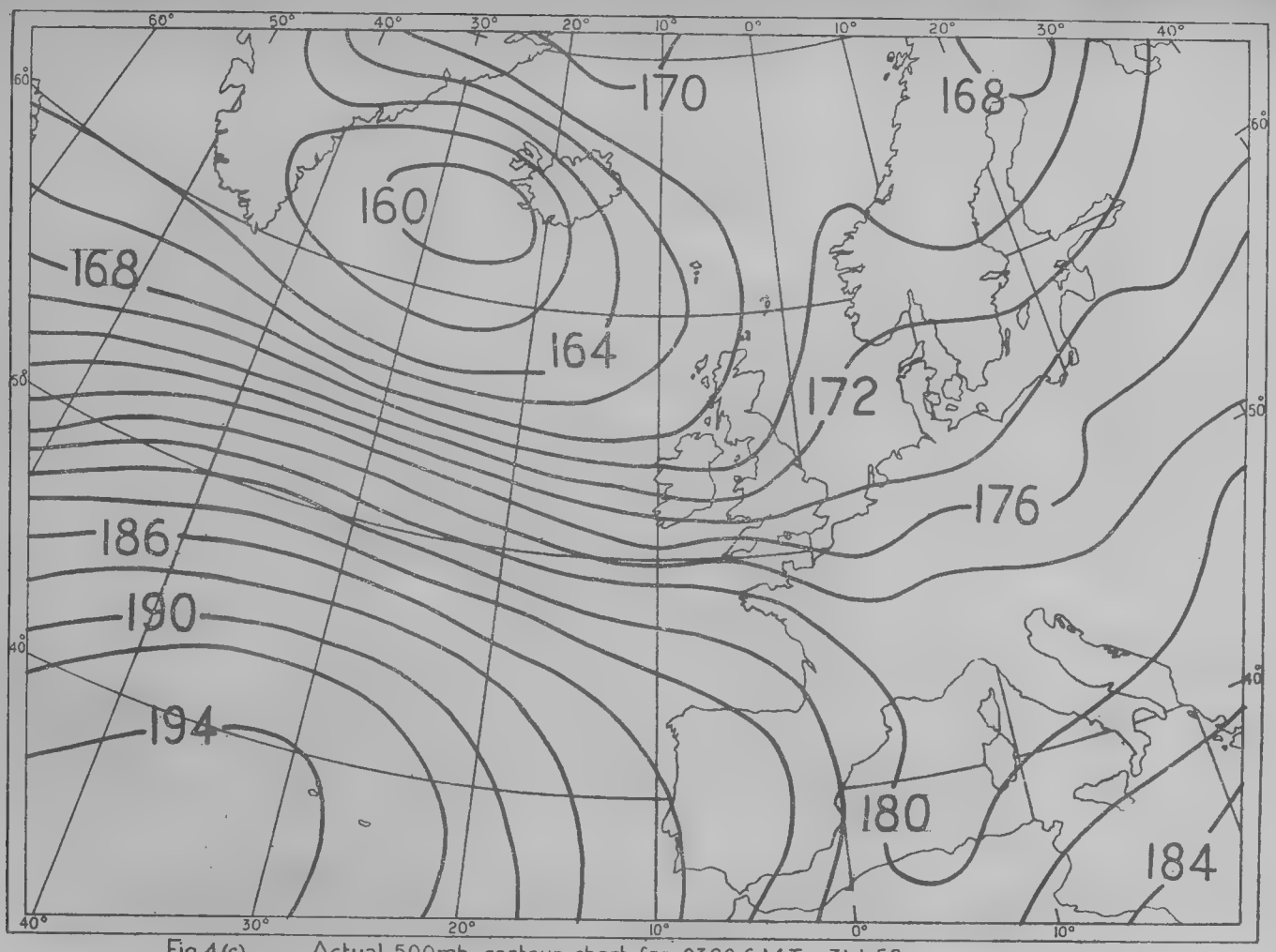

Fig.4(c) Actual 500mb. contour chart for 0300 G.M.T. 31.1.52

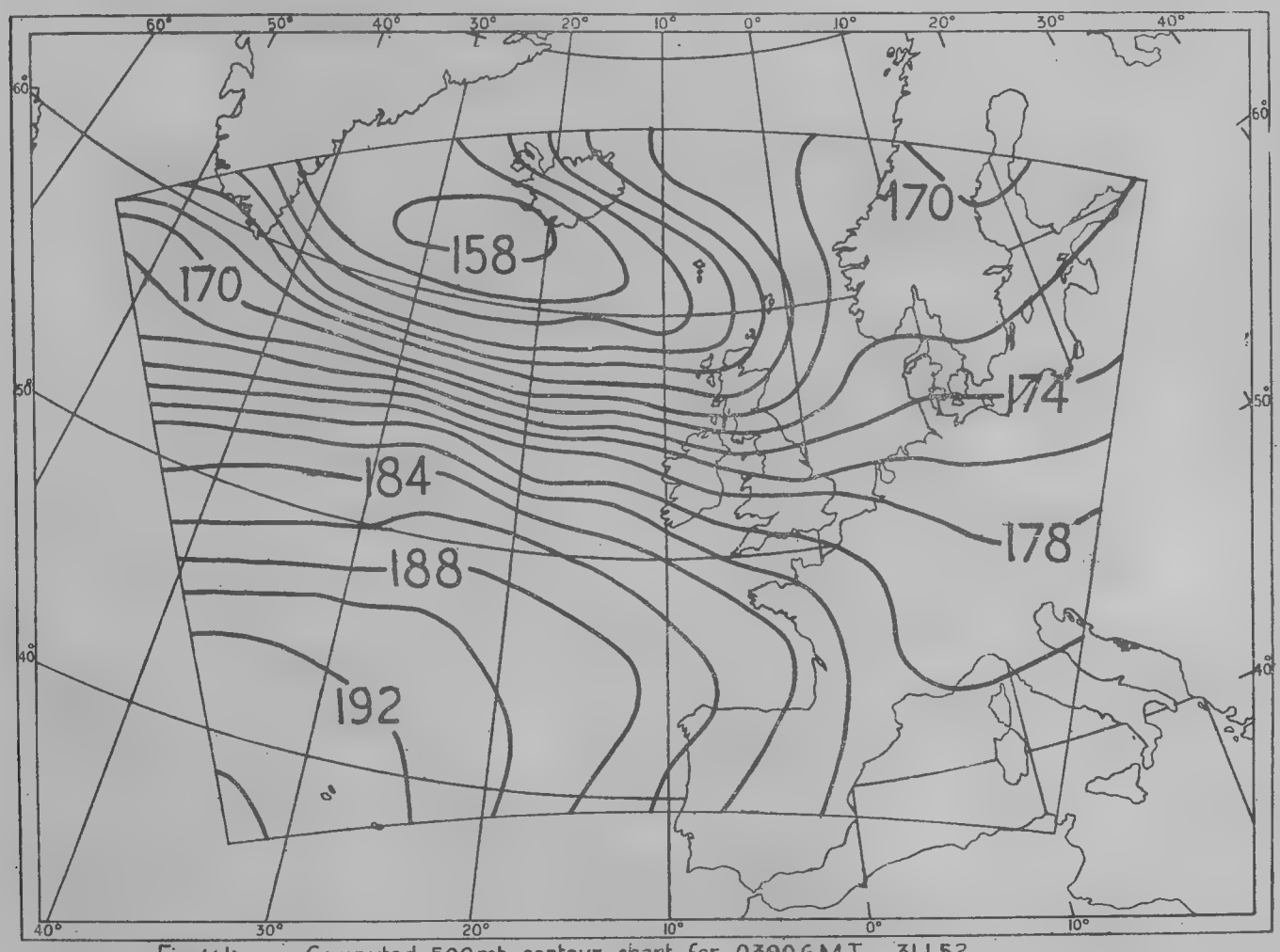

Fig.4(d) Computed 500mb. contour chart for 0300 G.M.T. 31.1.52

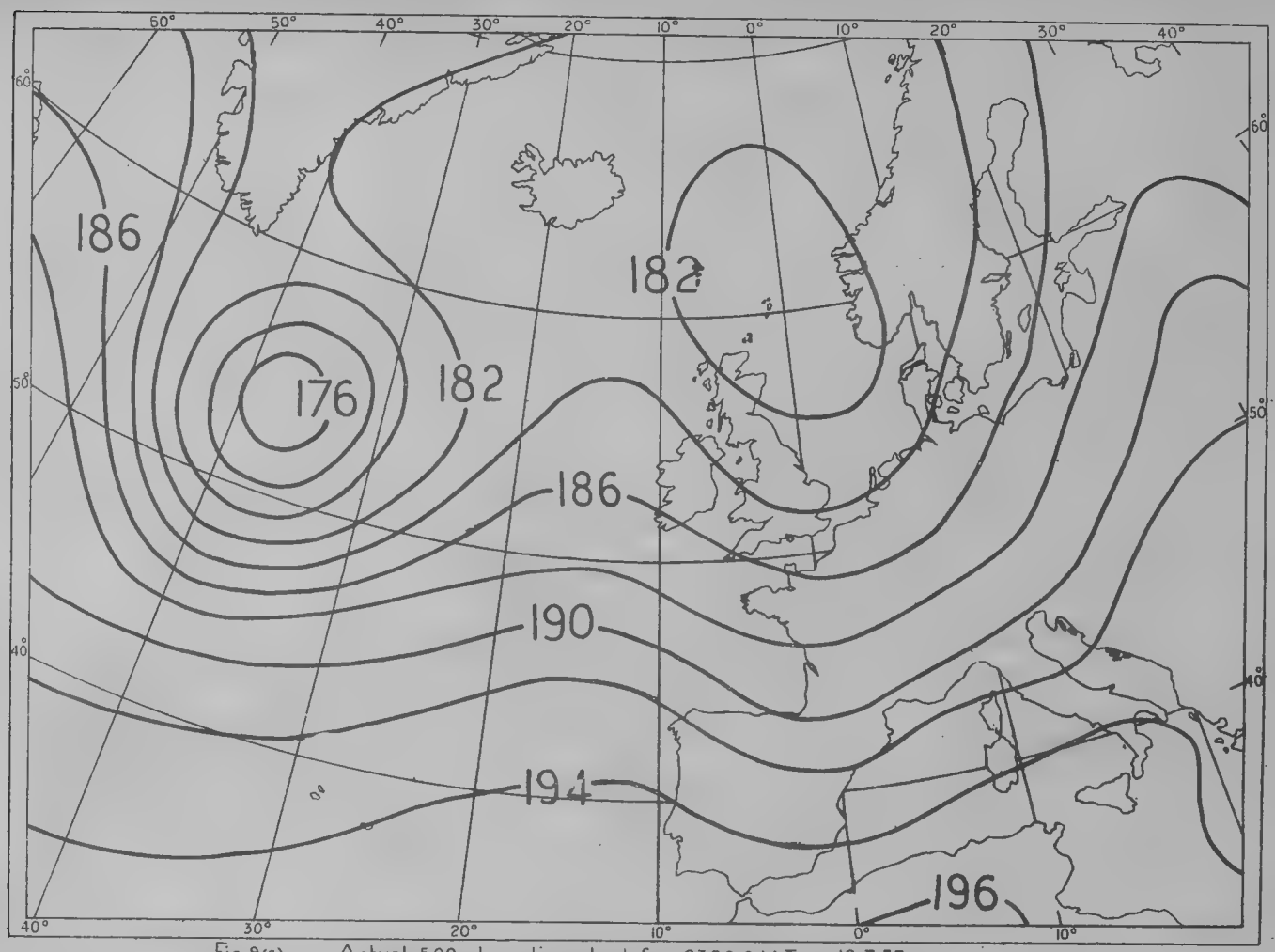

Fig.9(c) Actual 500mb. contour chart for 0300 G.M.T. 19.7.53

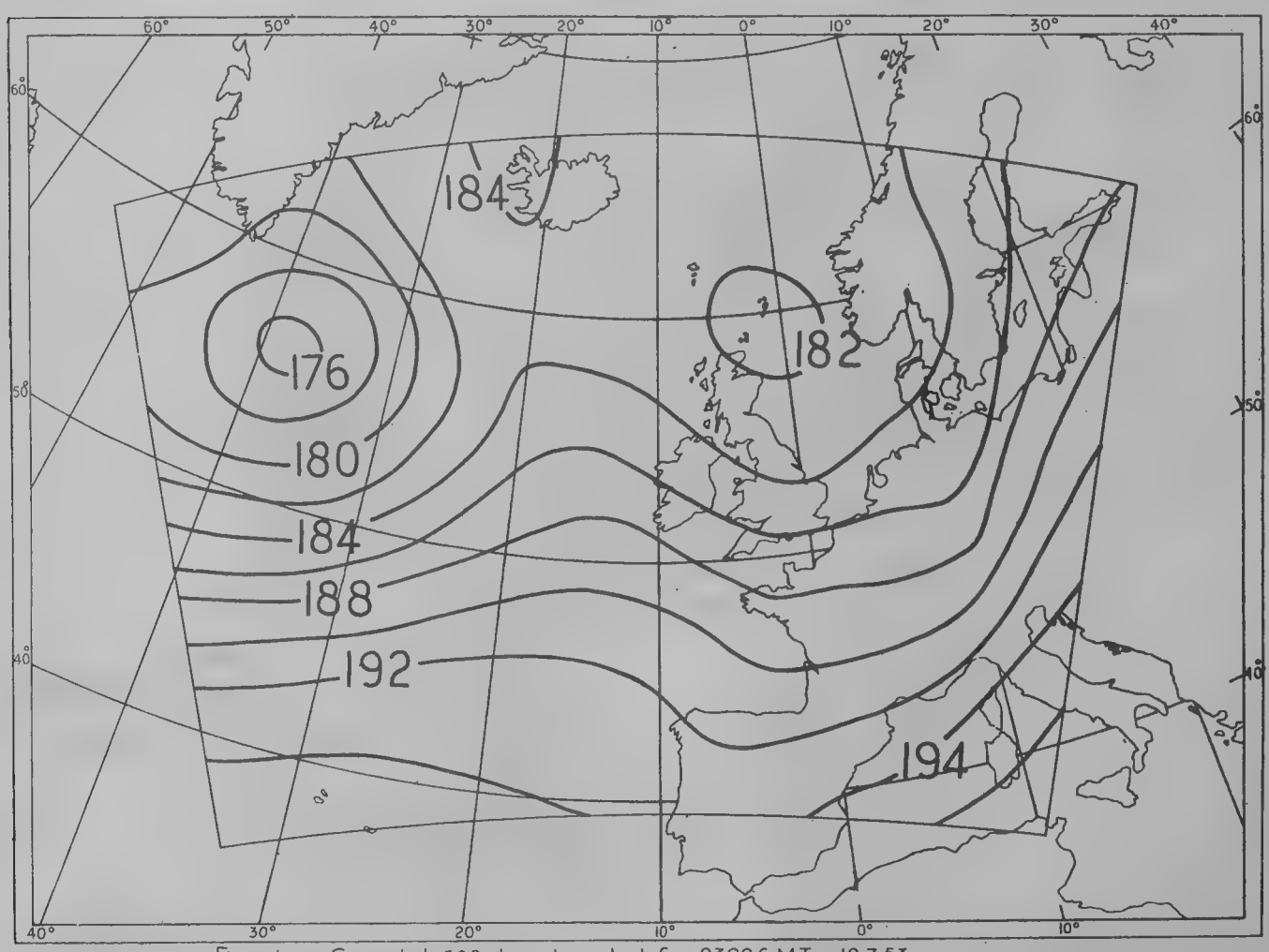

Fig.9(d) Computed 500mb. contour chart for 0300 G.M.T. 19.7.53

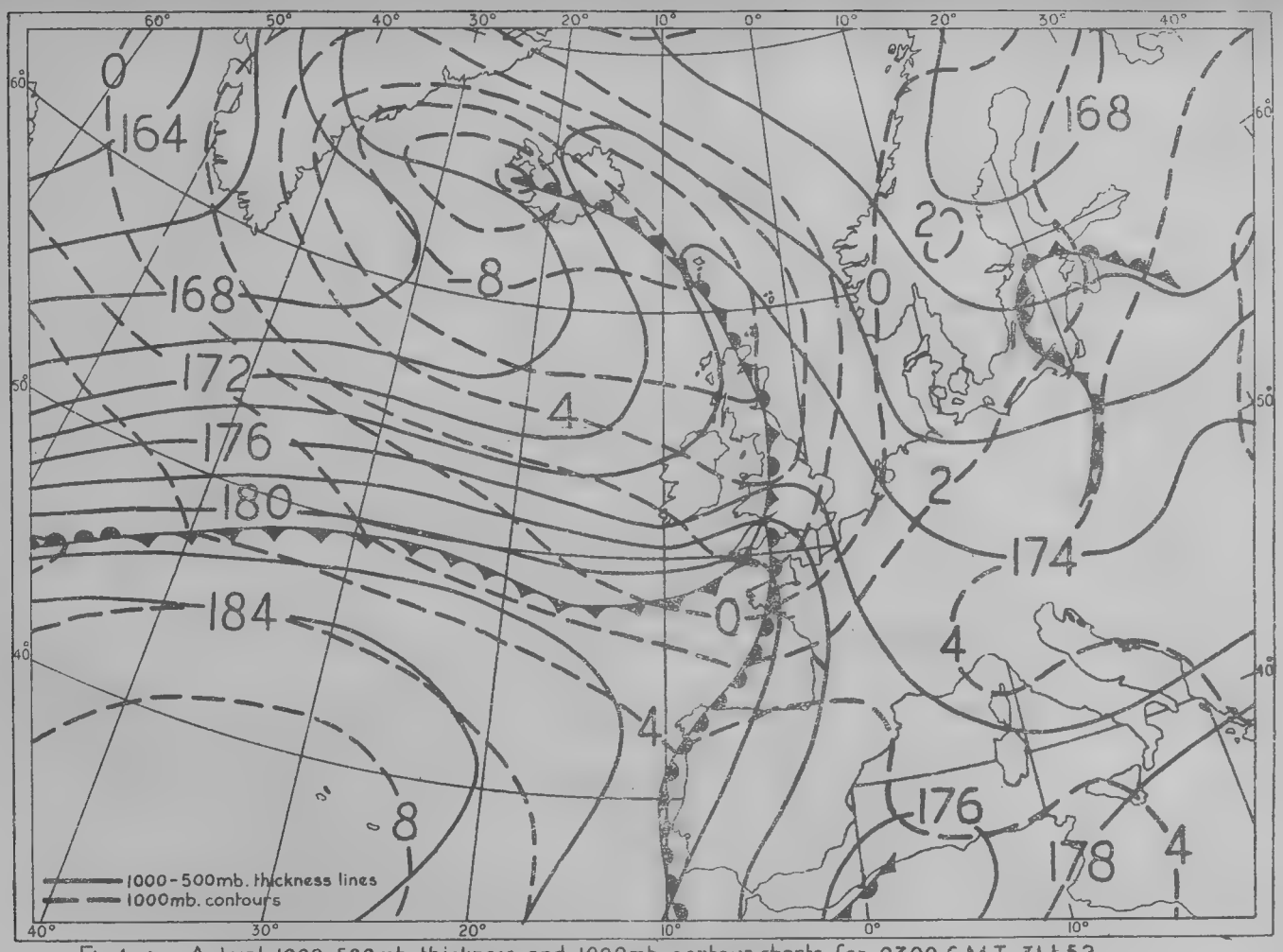

Fig.4(e) Actual 1000-500mb. thickness and 1000mb. contour charts for 0300 G.M.T. 31.1.52

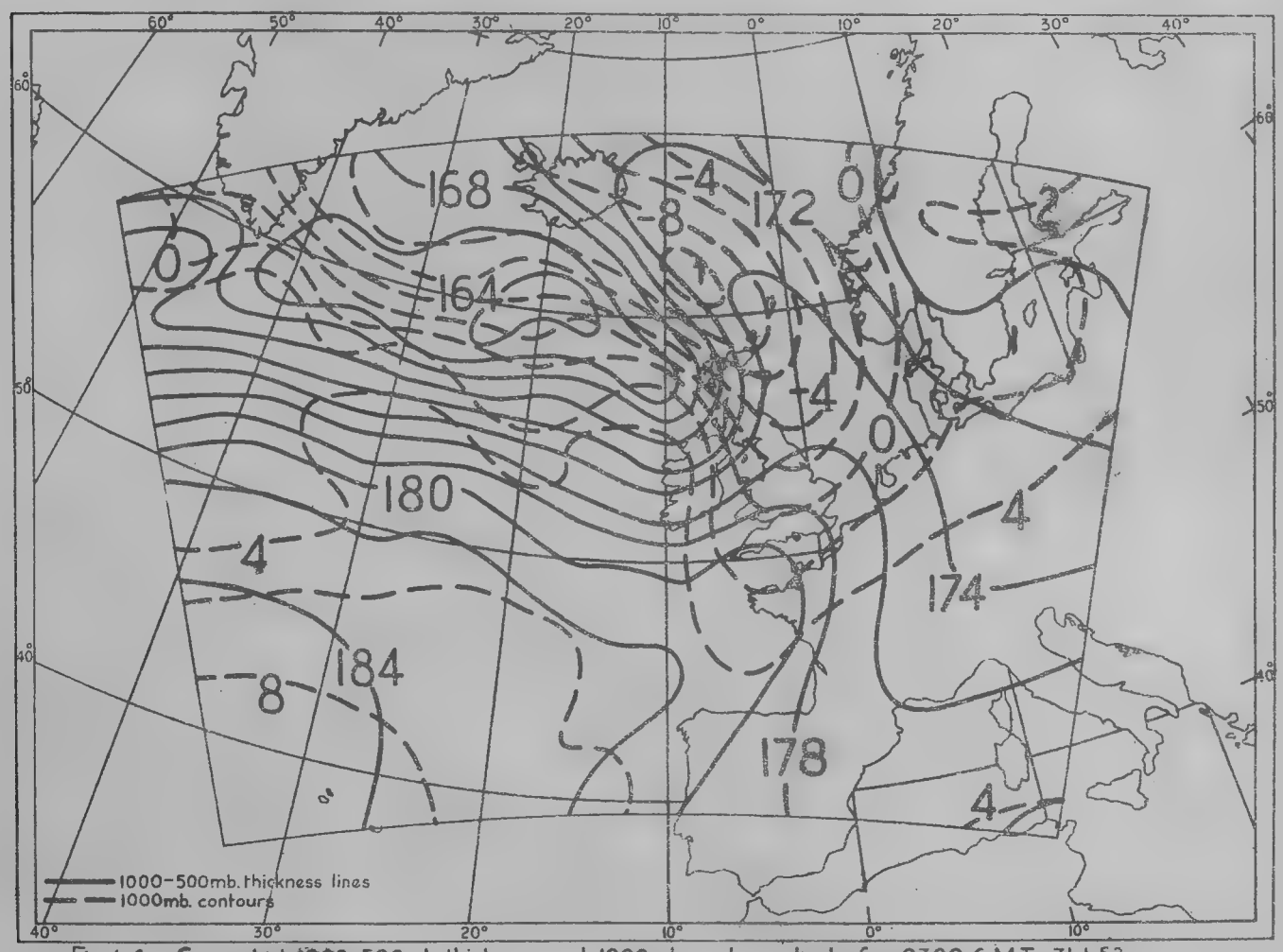

Fig.4(f) Computed 1000-500mb. thickness and 1000mb. contour charts for 0300 G.M.T. 31.1.52

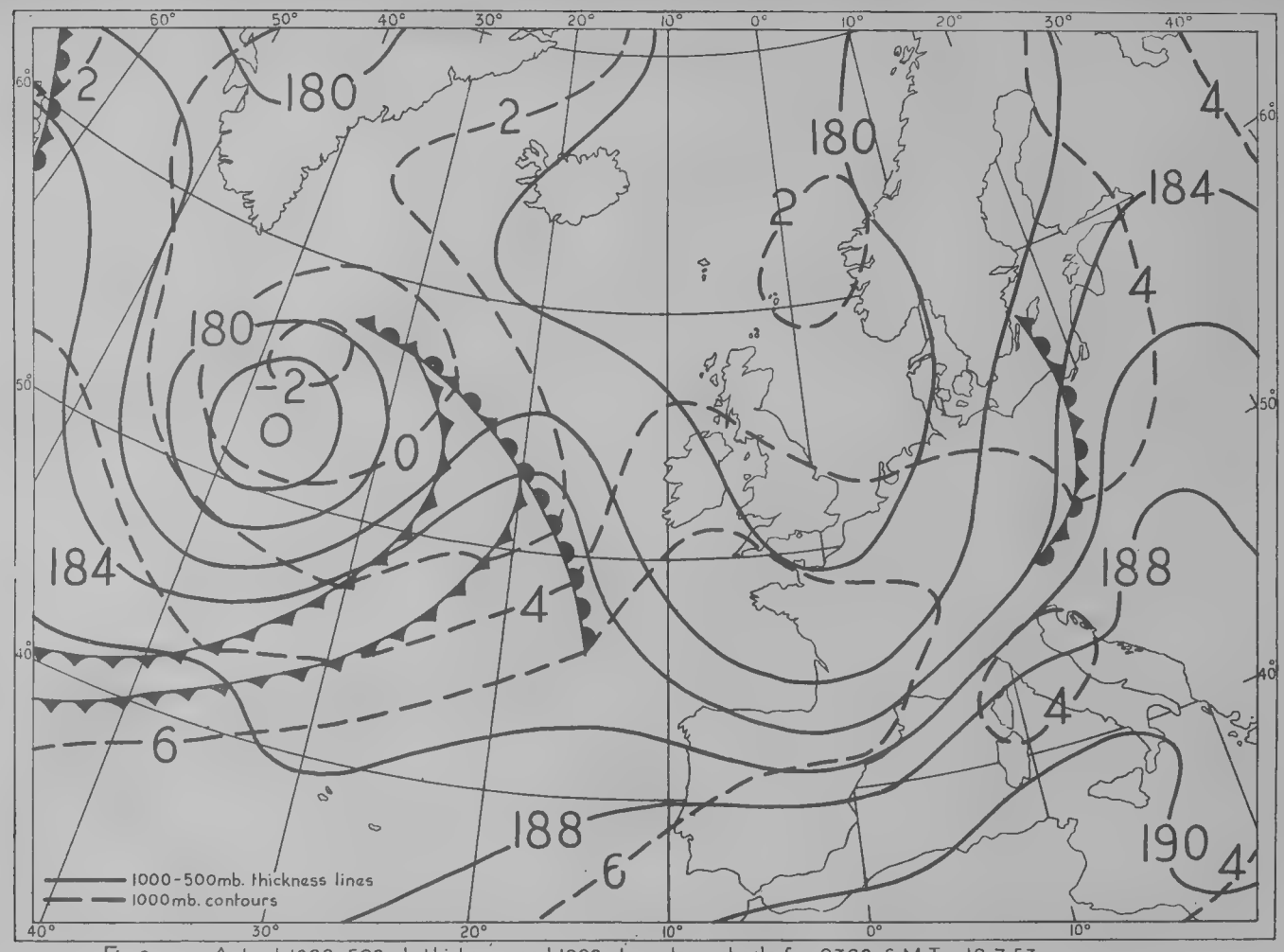

Fig.9(e) Actual 1000-500mb. thickness and 1000mb. contour charts for 0300 G.M.T. 19.7.53

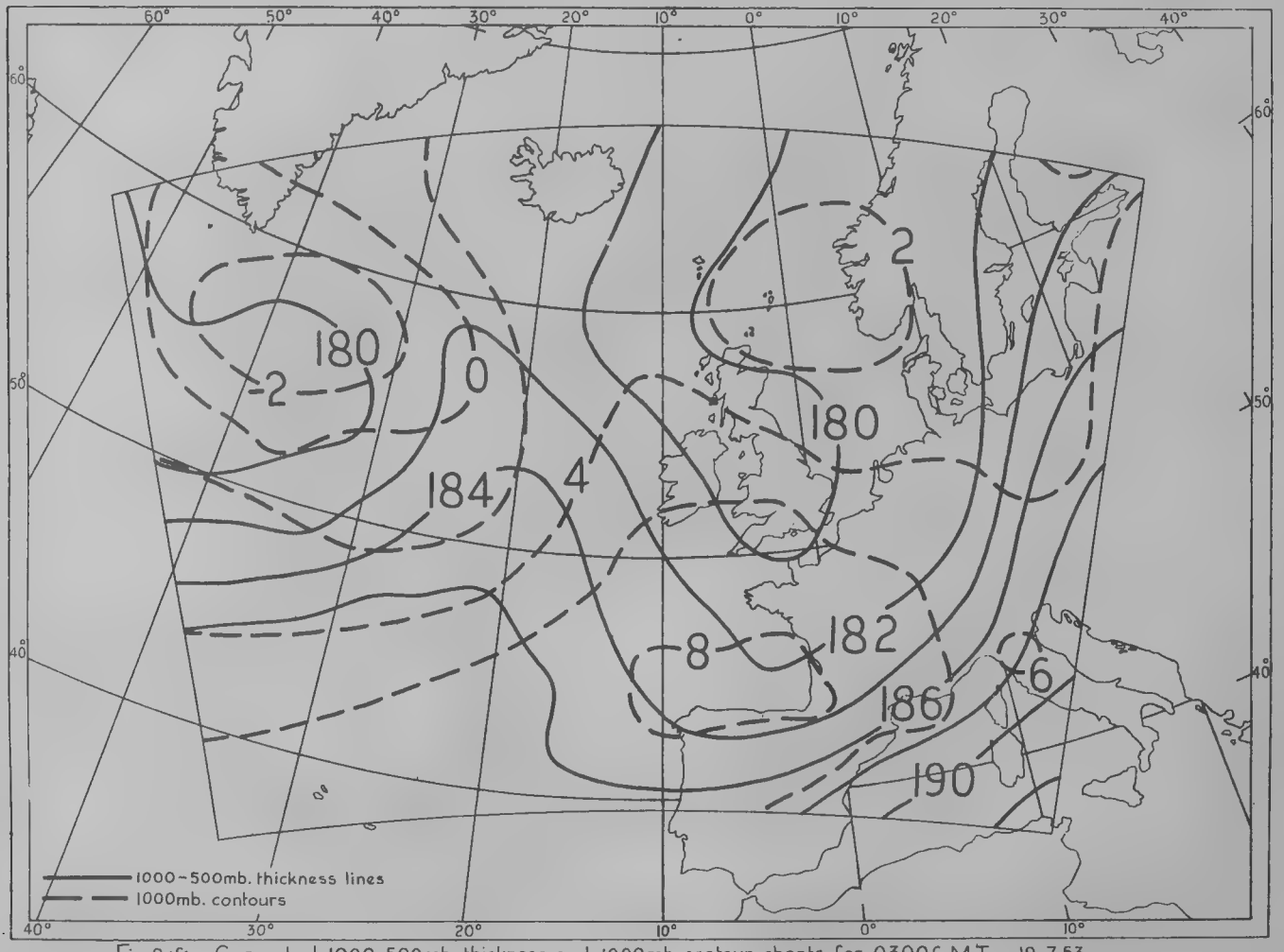

Fig.9(f) Computed 1000-500mb. thickness and 1000mb. contour charts for 0300G.M.T. 19.7.53

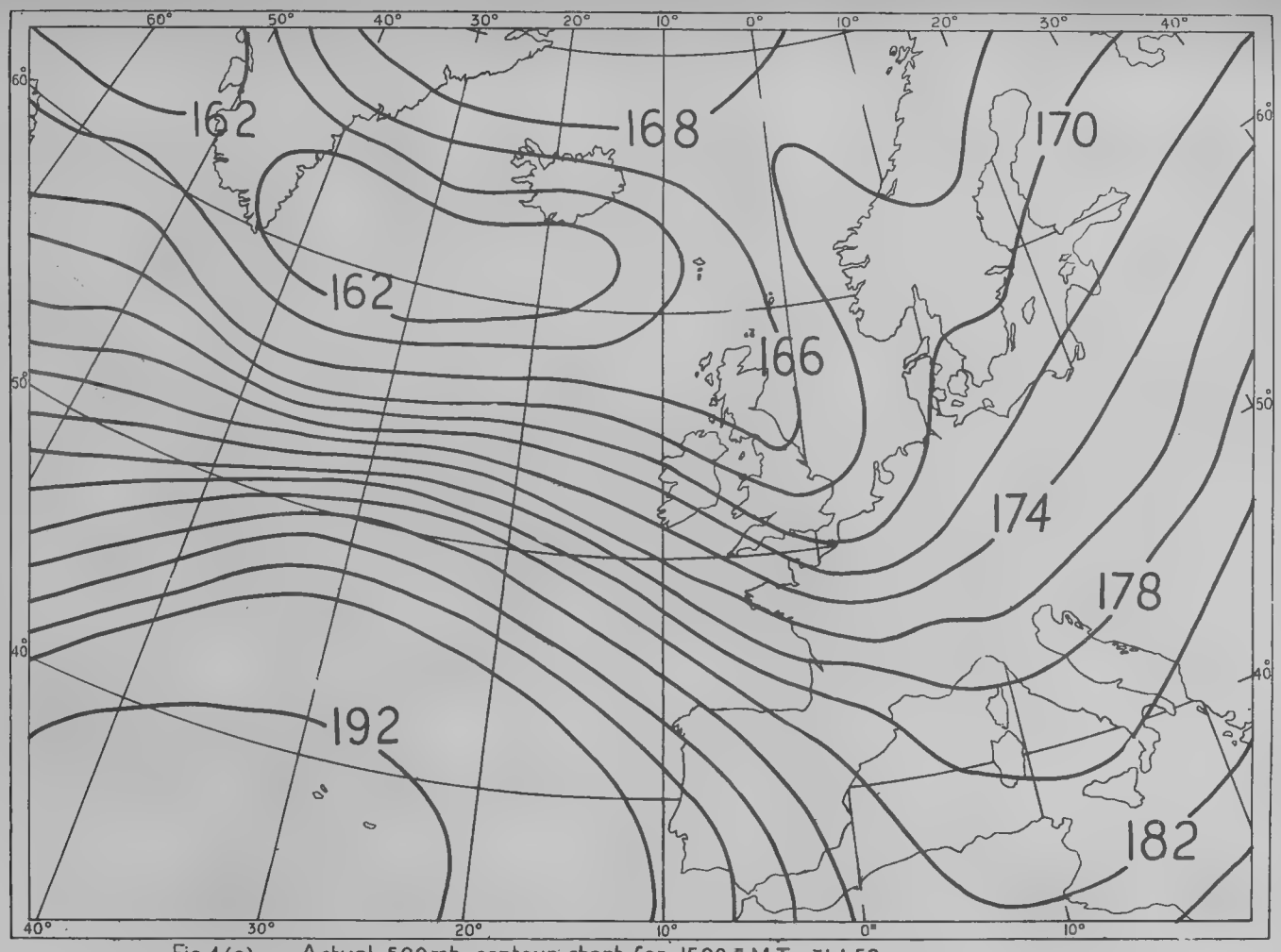

Fig.4(g) Actual 500mb. contour chart for 1500 G.M.T. 31.1.52

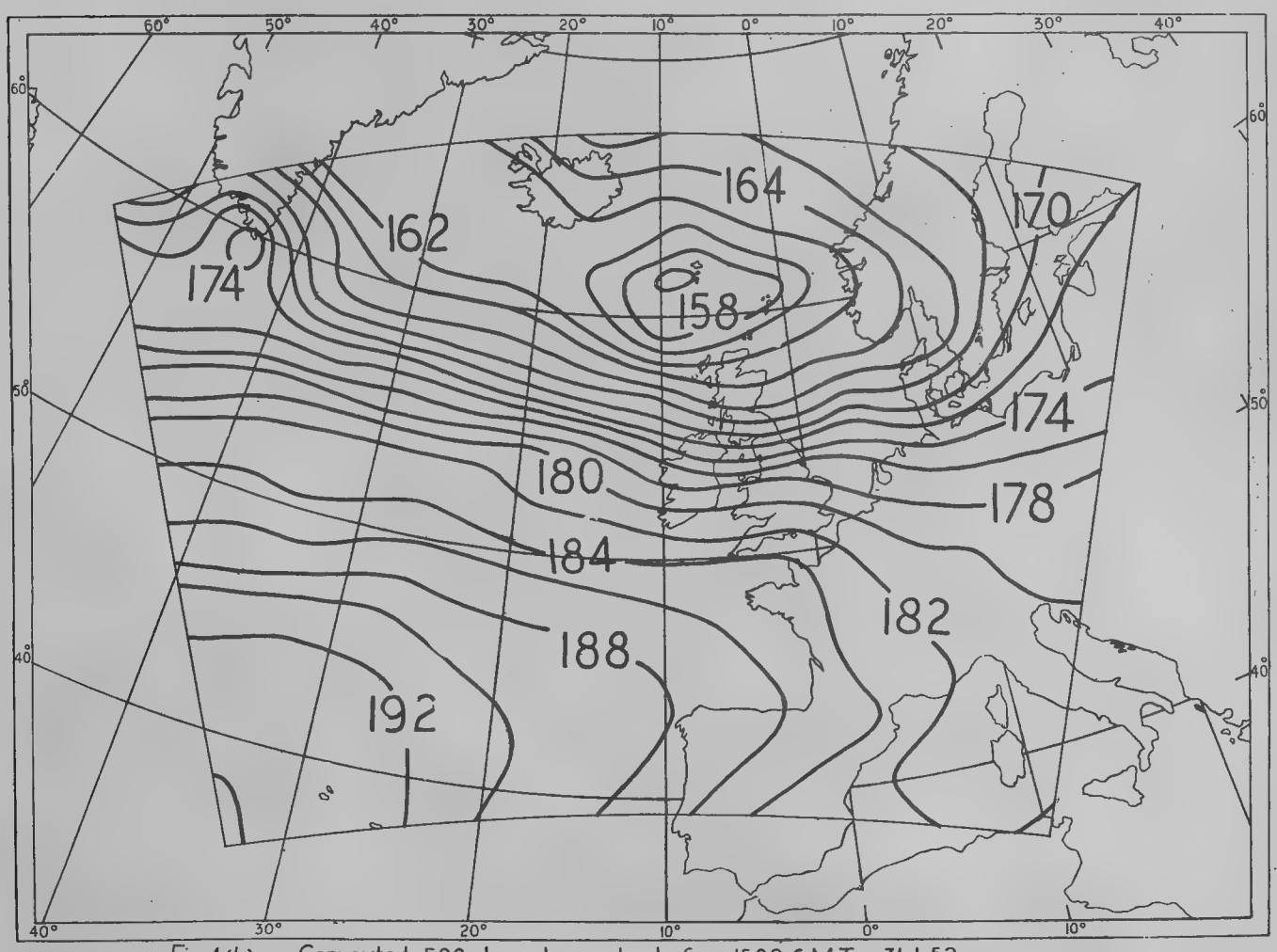

Fig.4(h) Computed 500mb. contour chart for 1500 G.M.T. 31.1.52

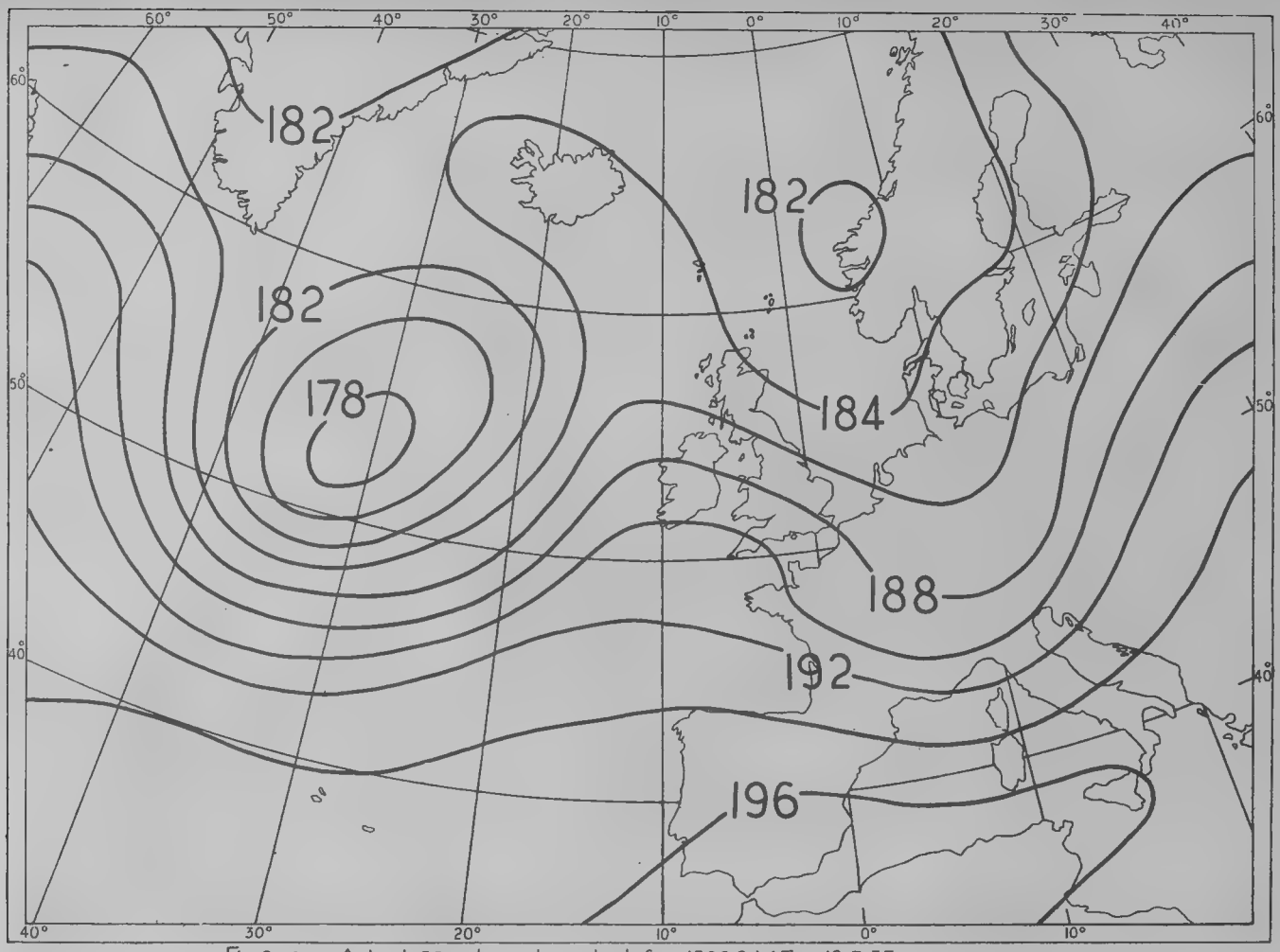

Fig.9(g) Actual 500mb. contour chart for 1500 G.M.T. 19.7.53

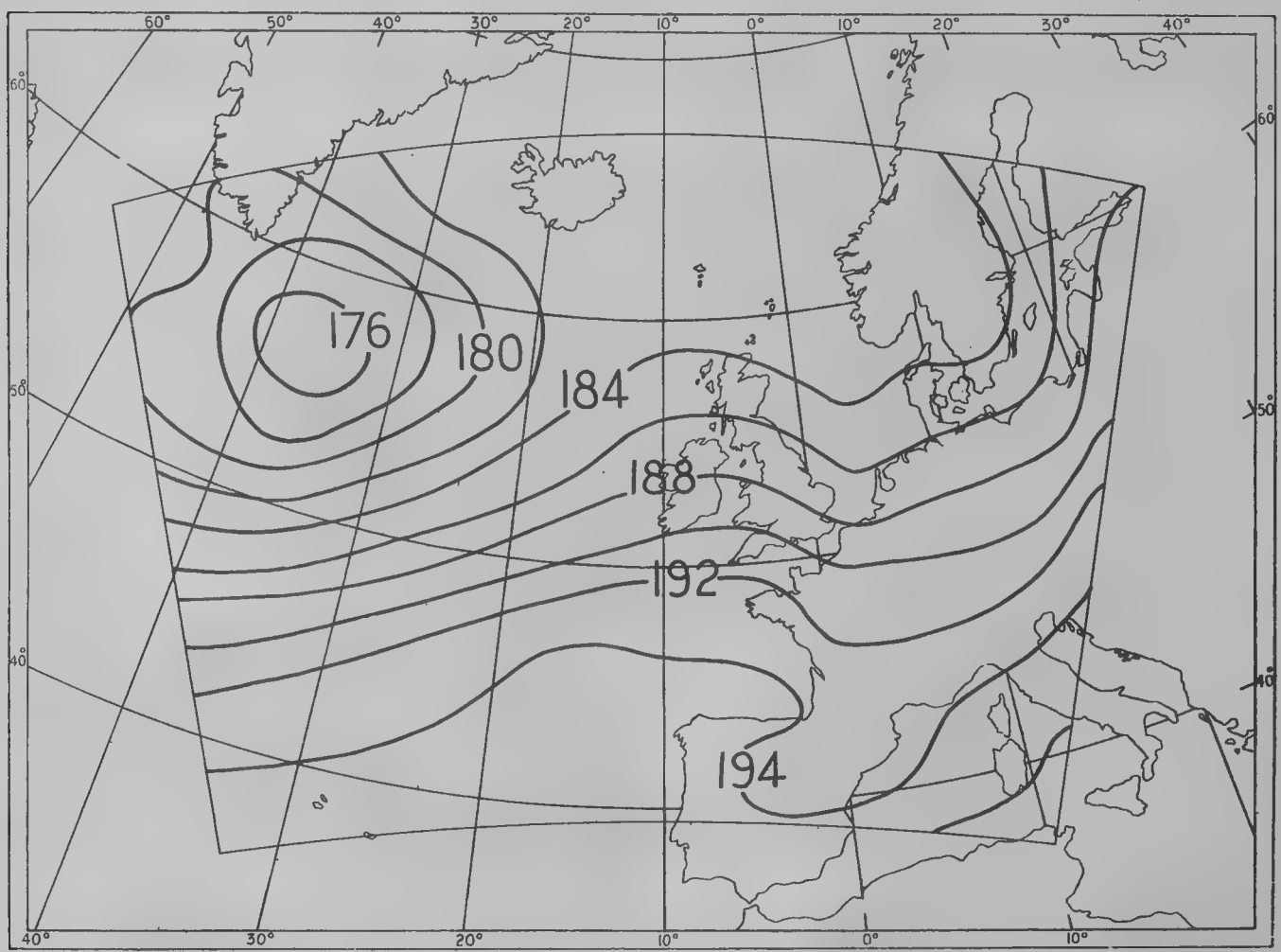

Fig.9(h) Computed 500mb. contour chart for 1500 G.M.T. 19.7.53

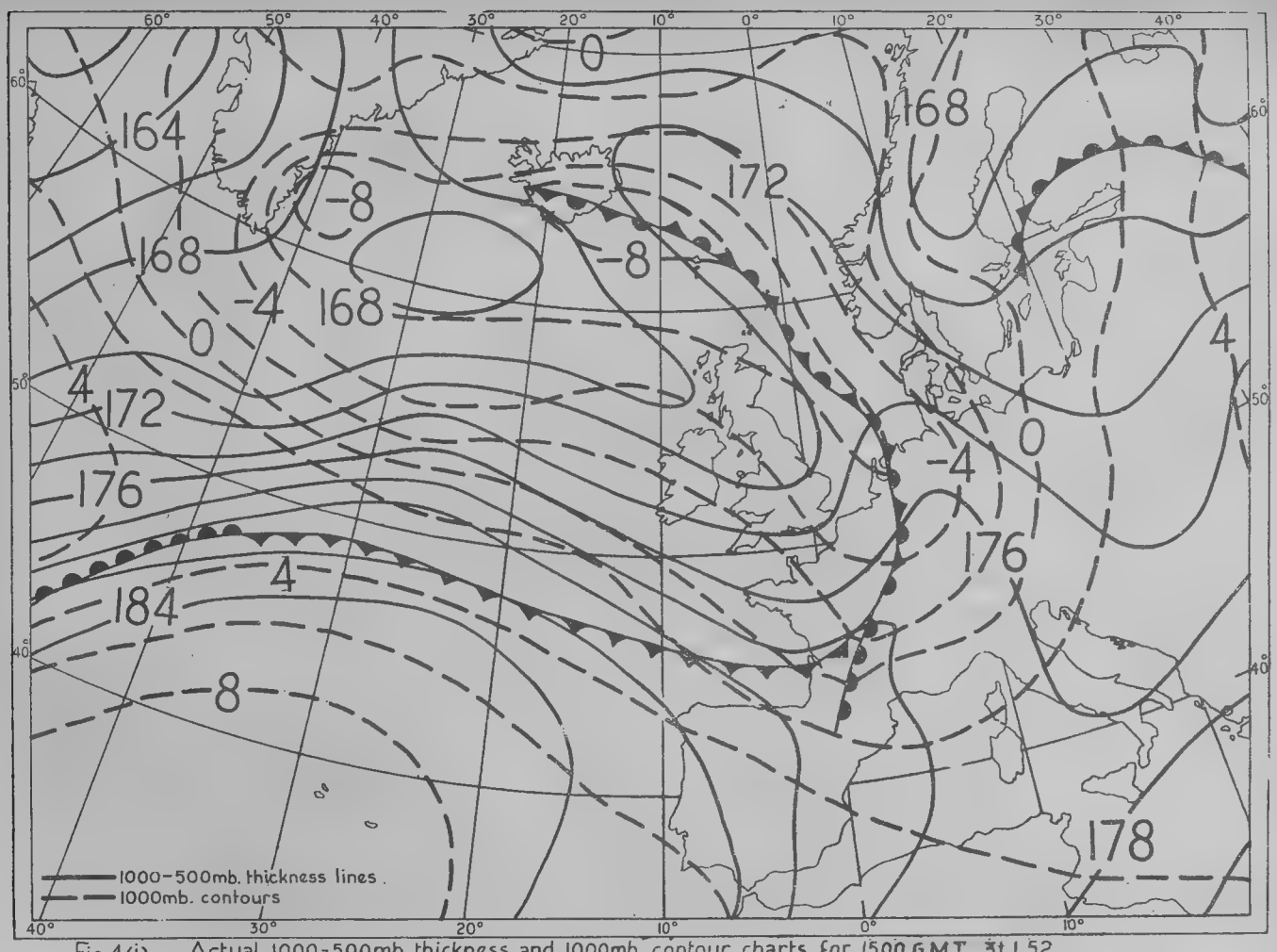

Fig.4(i) Actual 1000-500mb. thickness and 1000mb. contour charts for 1500 G.M.T. 31.1.52

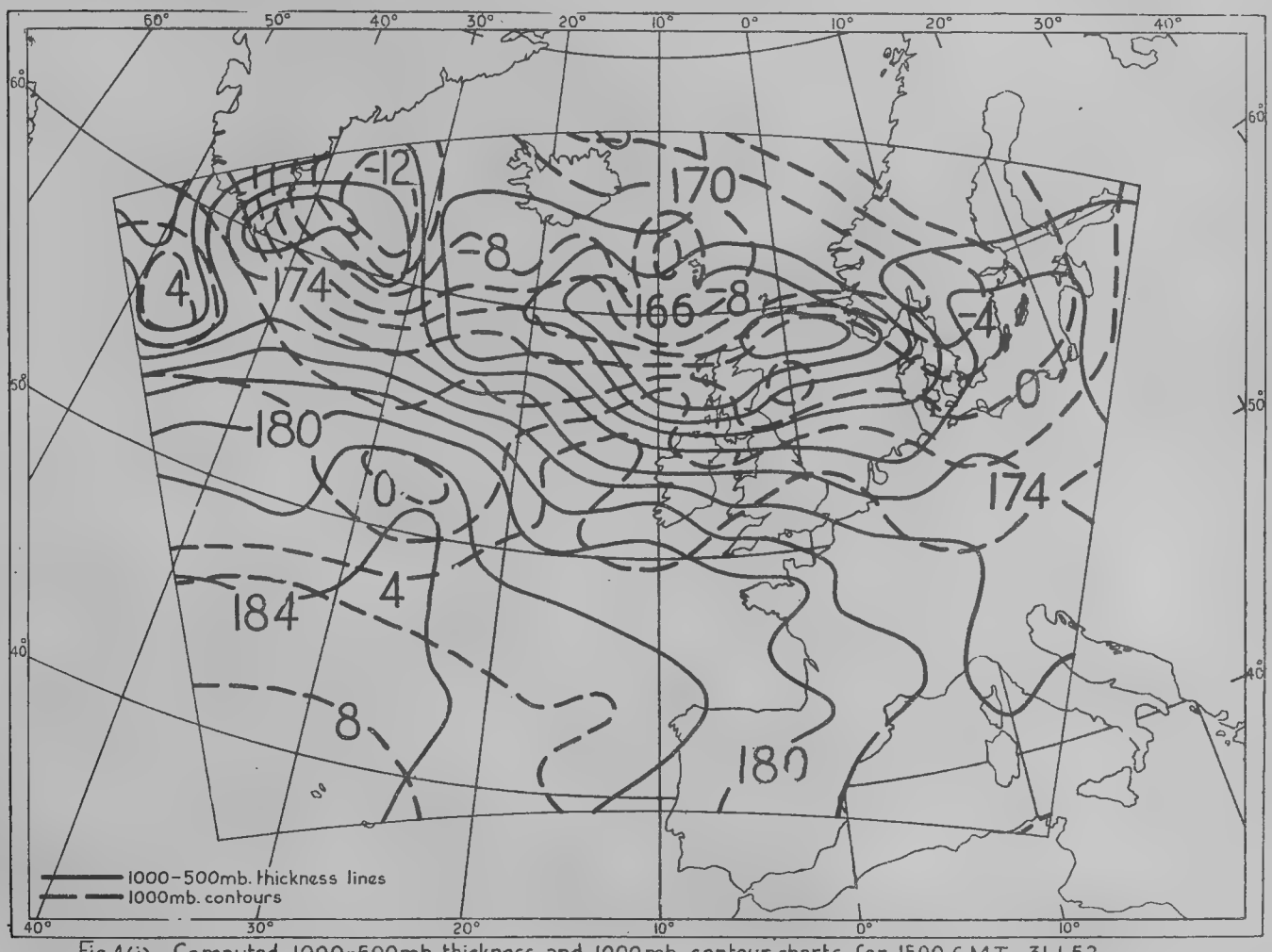

Fig.4(j) Computed 1000-500mb. thickness and 1000mb. contour charts for 1500 G.M.T. 31.1.52

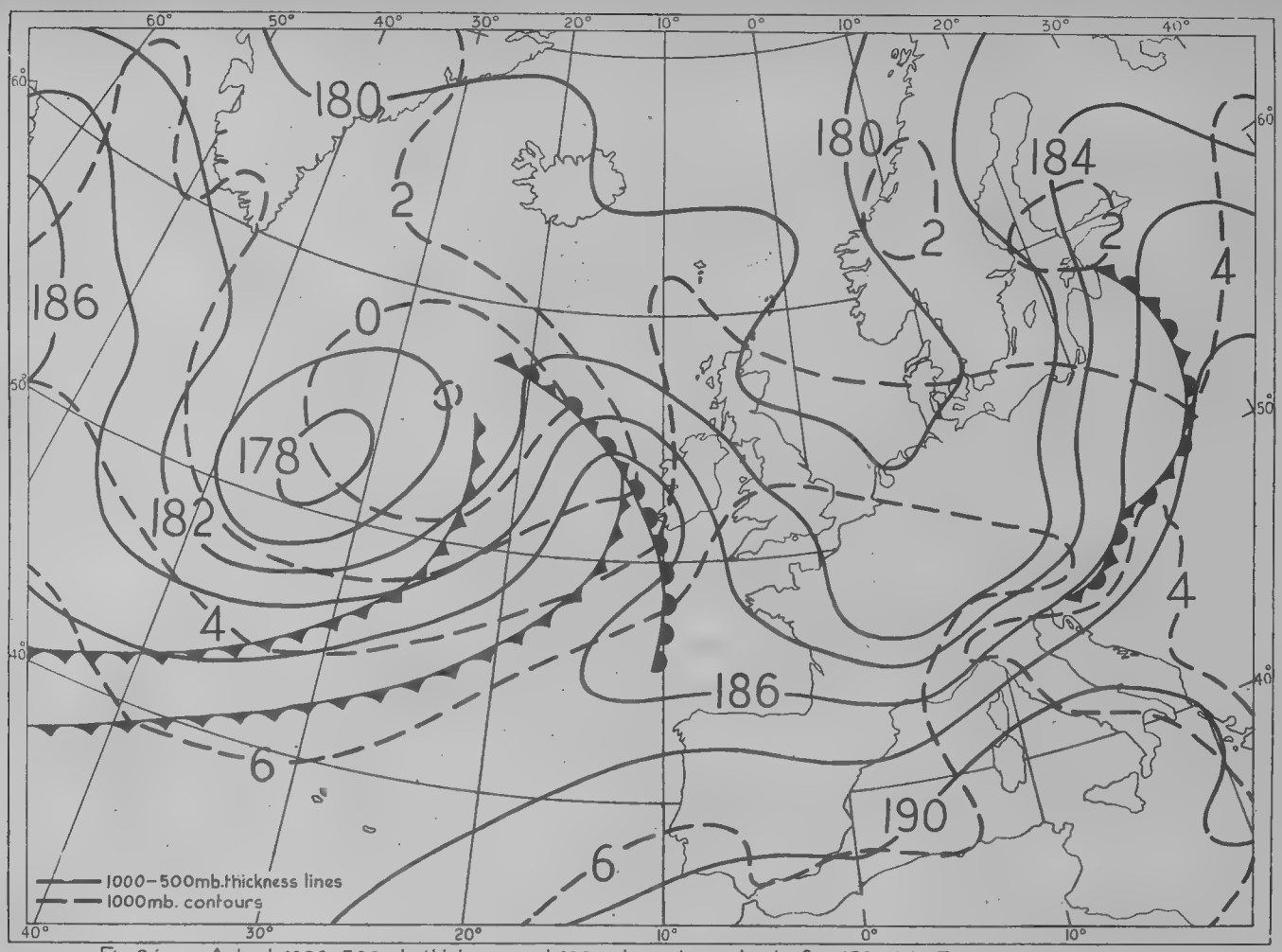

Fig. 9(i) Actual 1000–500mb. thickness and 1000mb. contour charts for 1500 G.M.T. 19.7.53

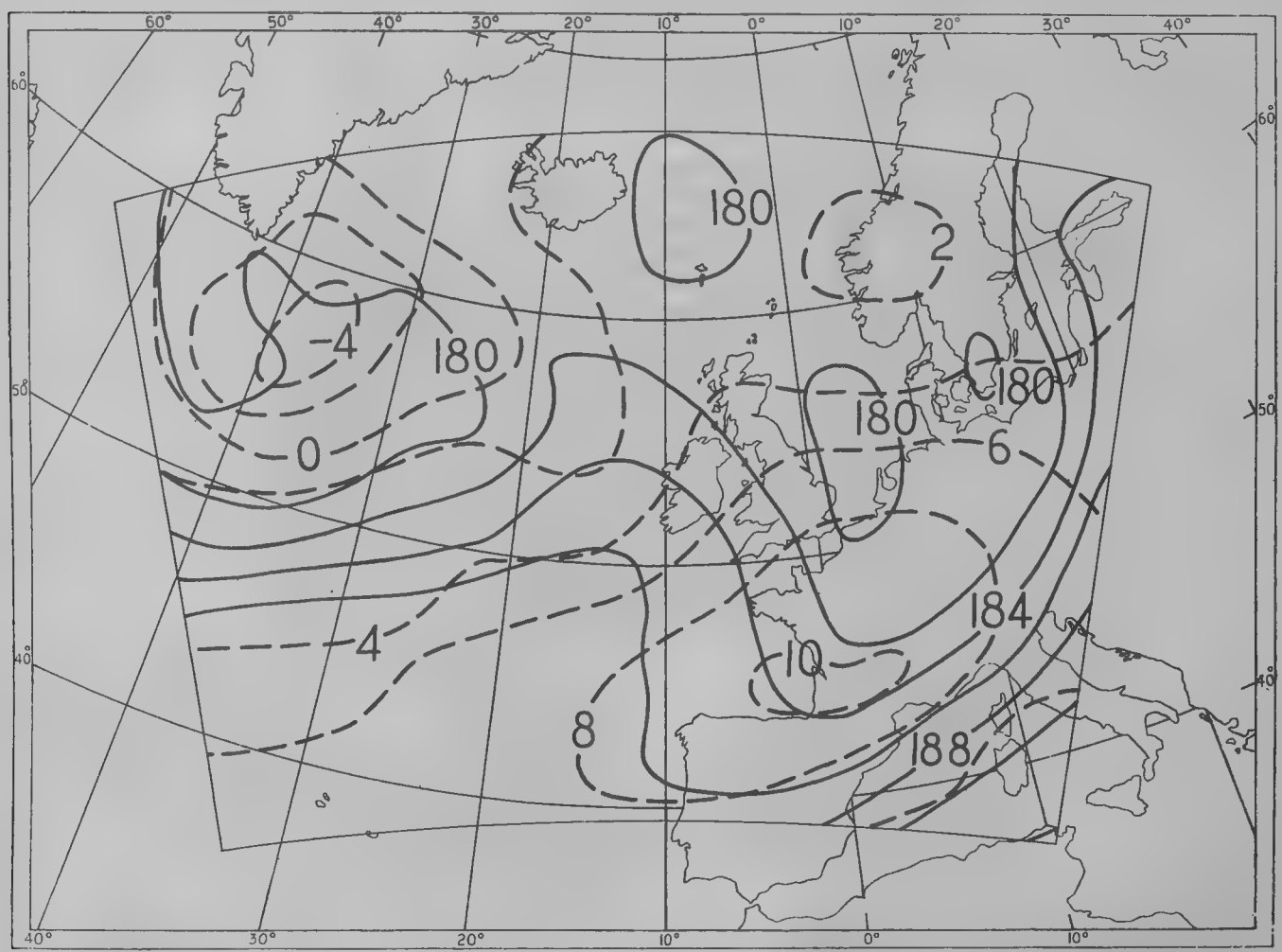

Fig. 9(j) Computed 1000-500mb. thickness and 1000mb. contour chart for 1500 G.M.T. 19.7.53

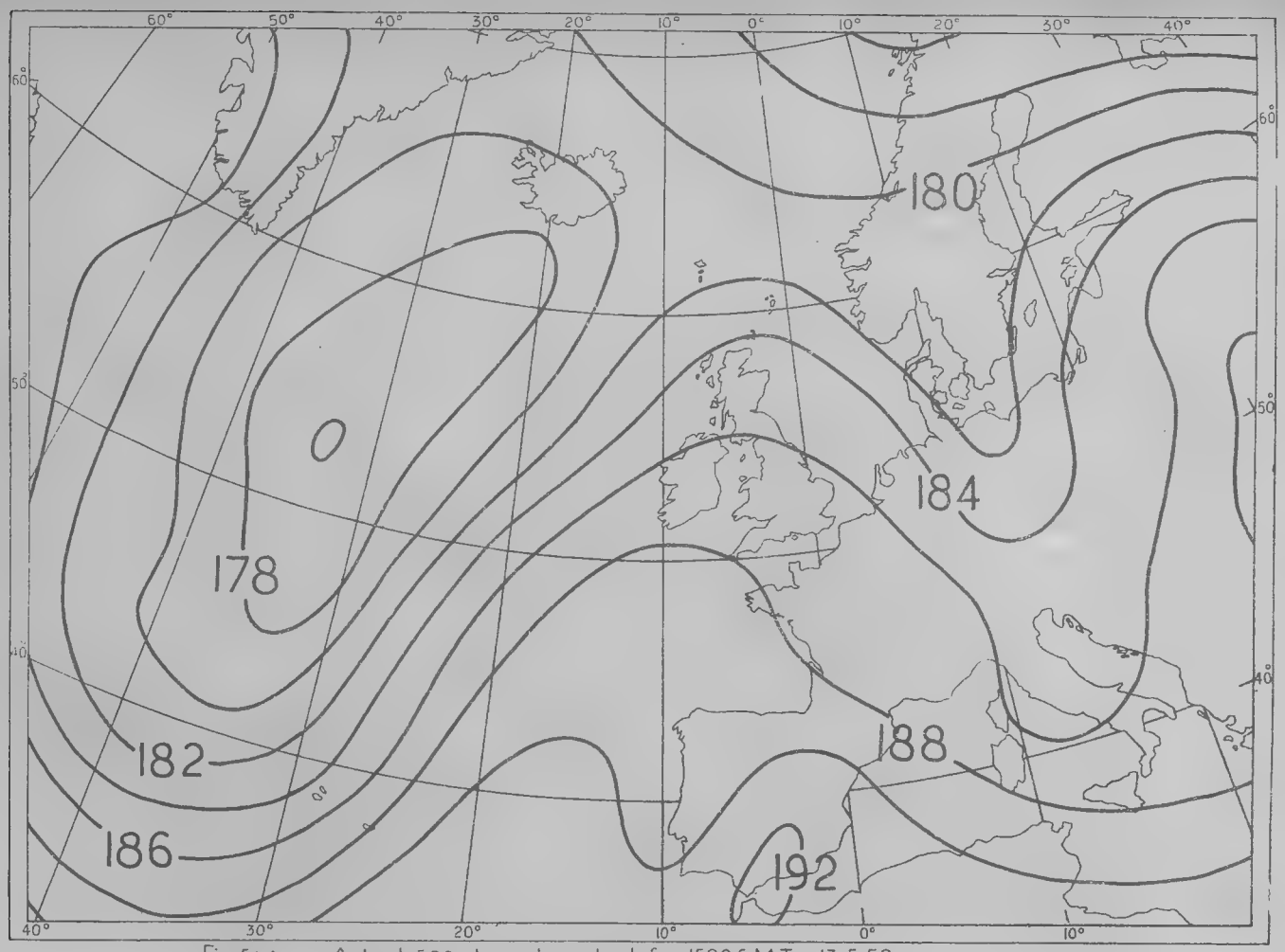

Fig.5(a) Actual 500mb. contour chart for 1500 G.M.T. 13.5.52

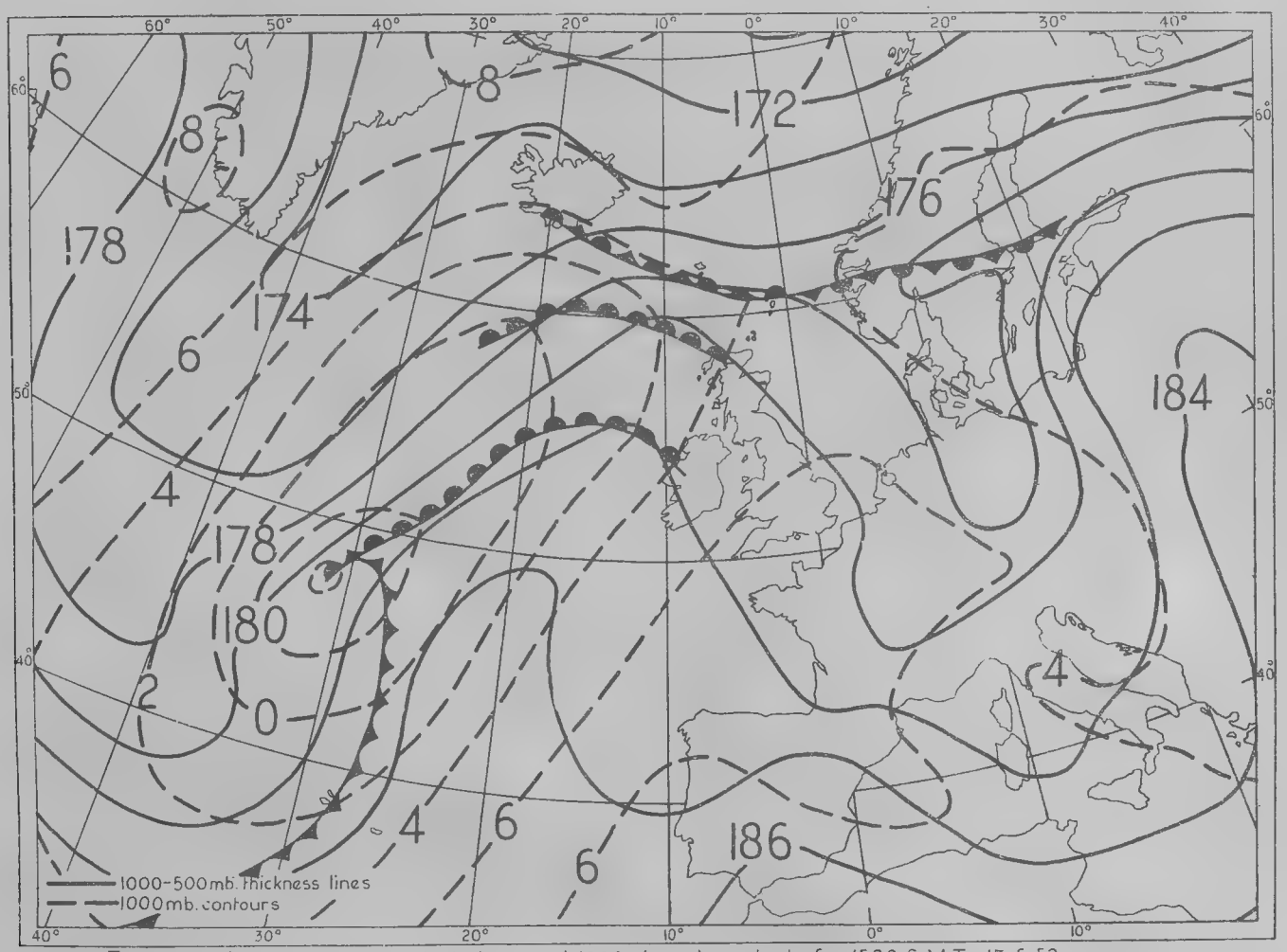

Fig.5(b) Actual 1000-500mb. thickness and 1000mb. contour charts for 1500 G.M.T. 13.5.52

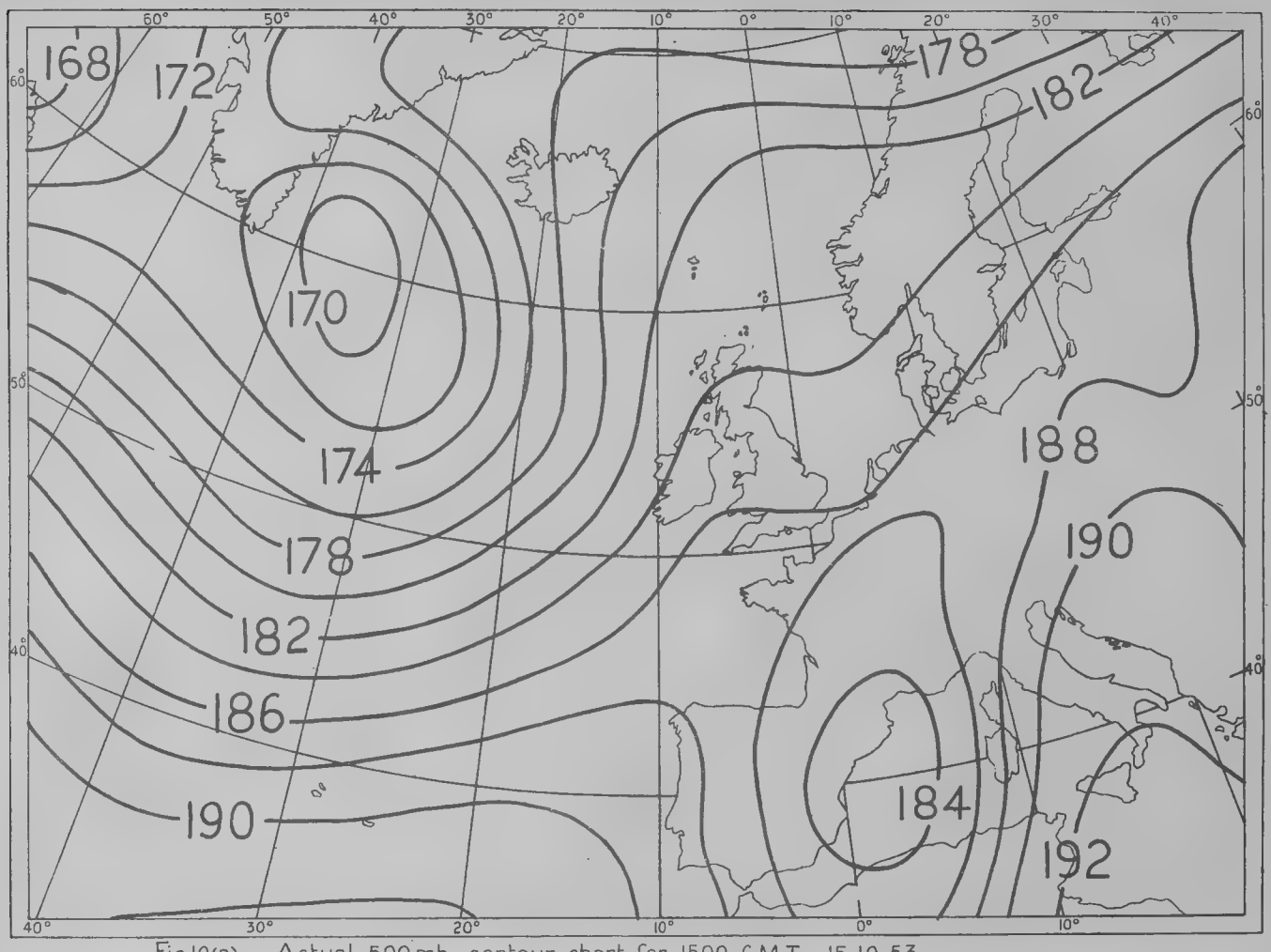

Fig.10(a) Actual 500mb. contour chart for 1500 G.M.T. 15.10.53

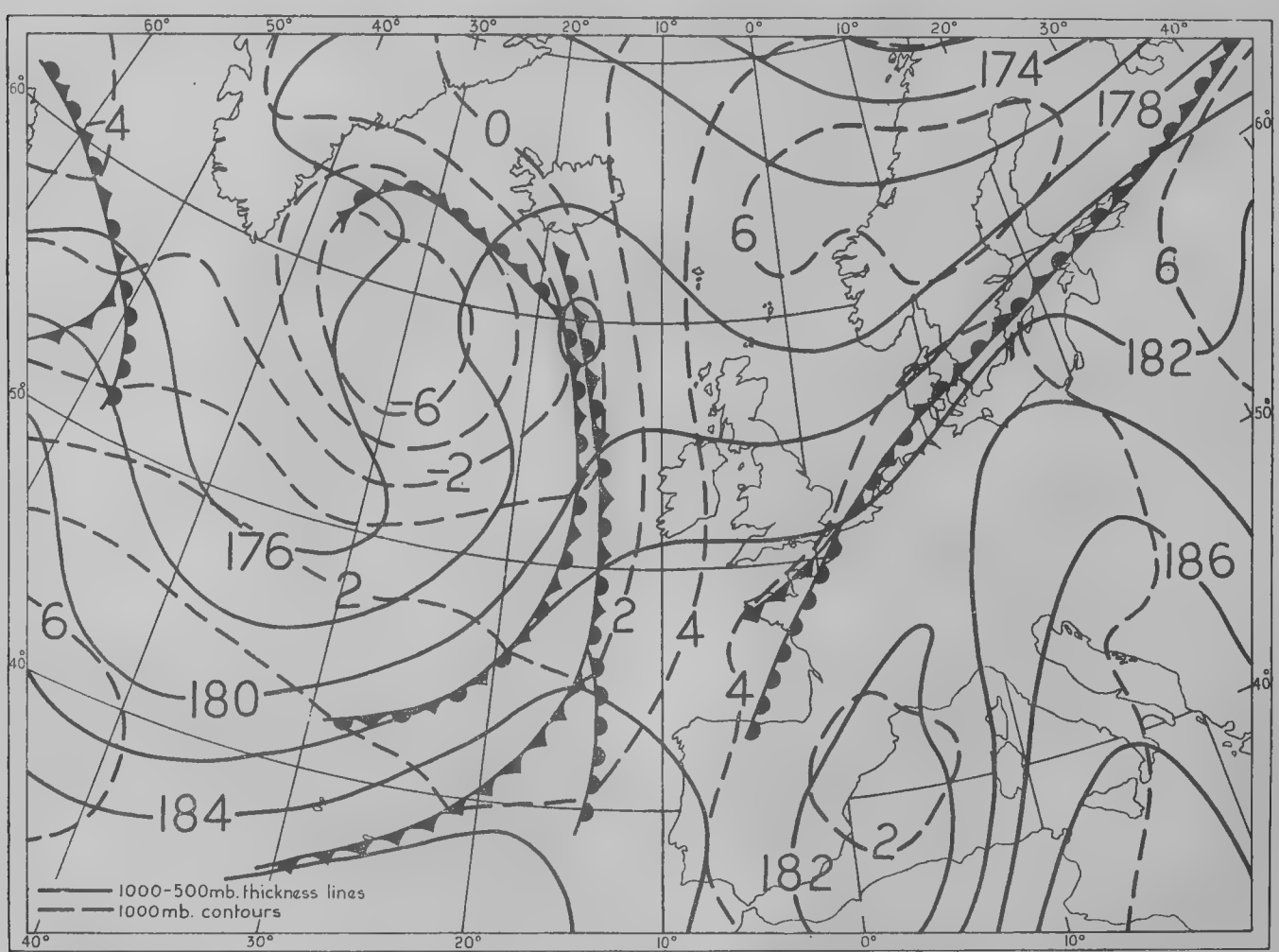

Fig.10(b) Actual 1000-500mb. thickness and 500mb. contours for 1500 G.M.T. 15.10.53

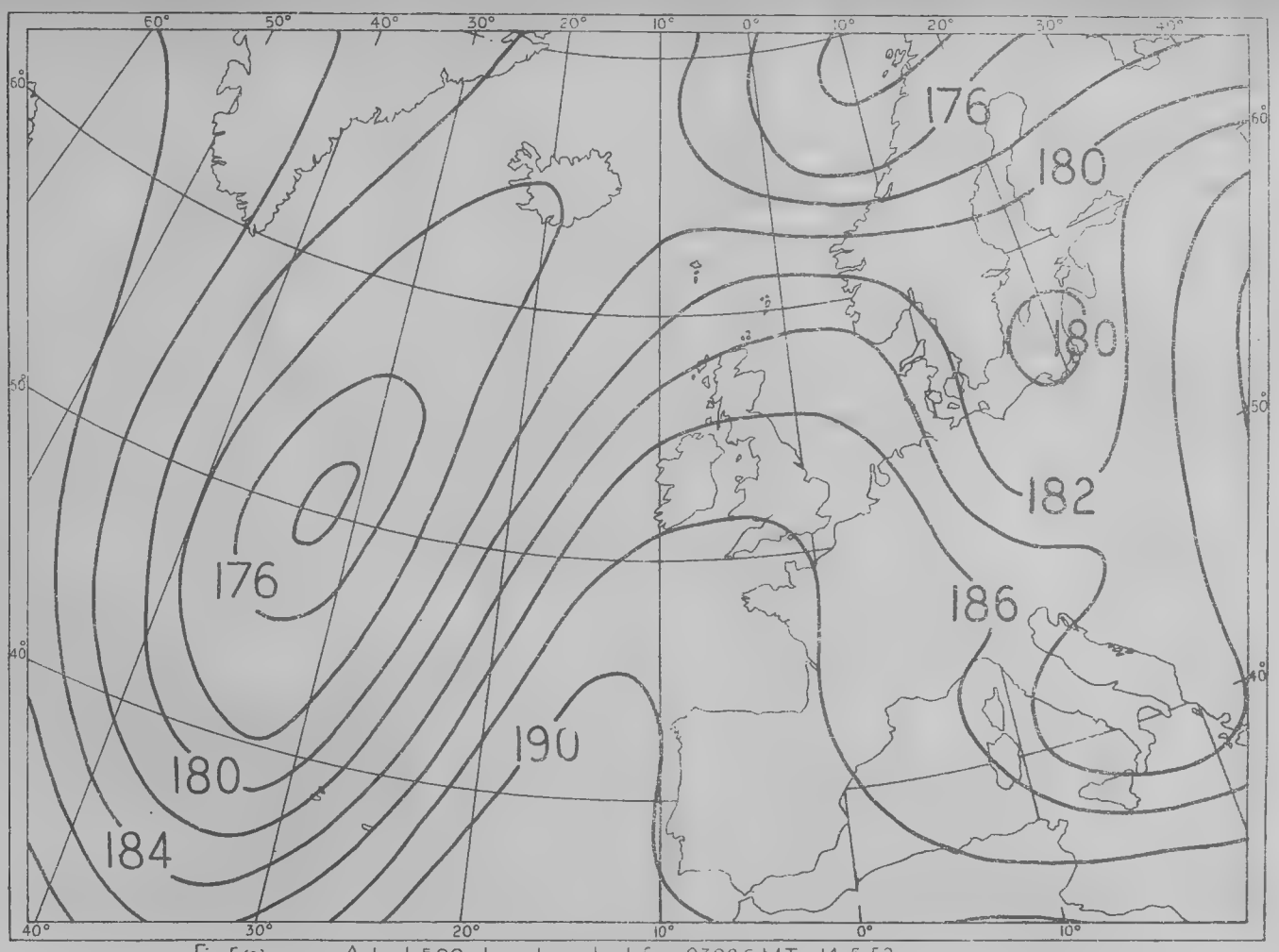

Fig.5(c) Actual 500mb. contour chart for 0300 G.M.T. 14.5.52

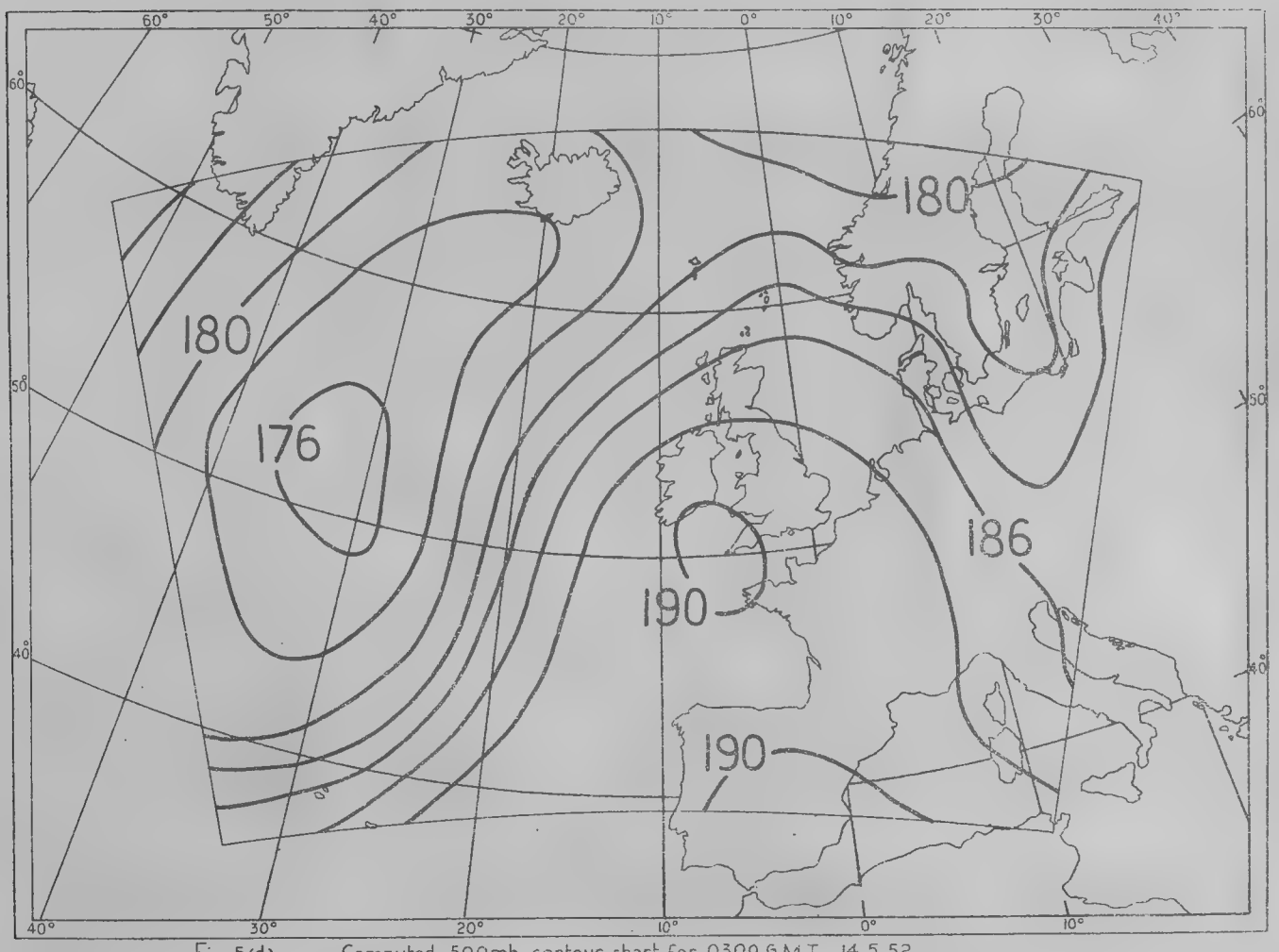

Fig.5(d) Computed 500mb. contour chart for 0300 G.M.T. 14.5.52

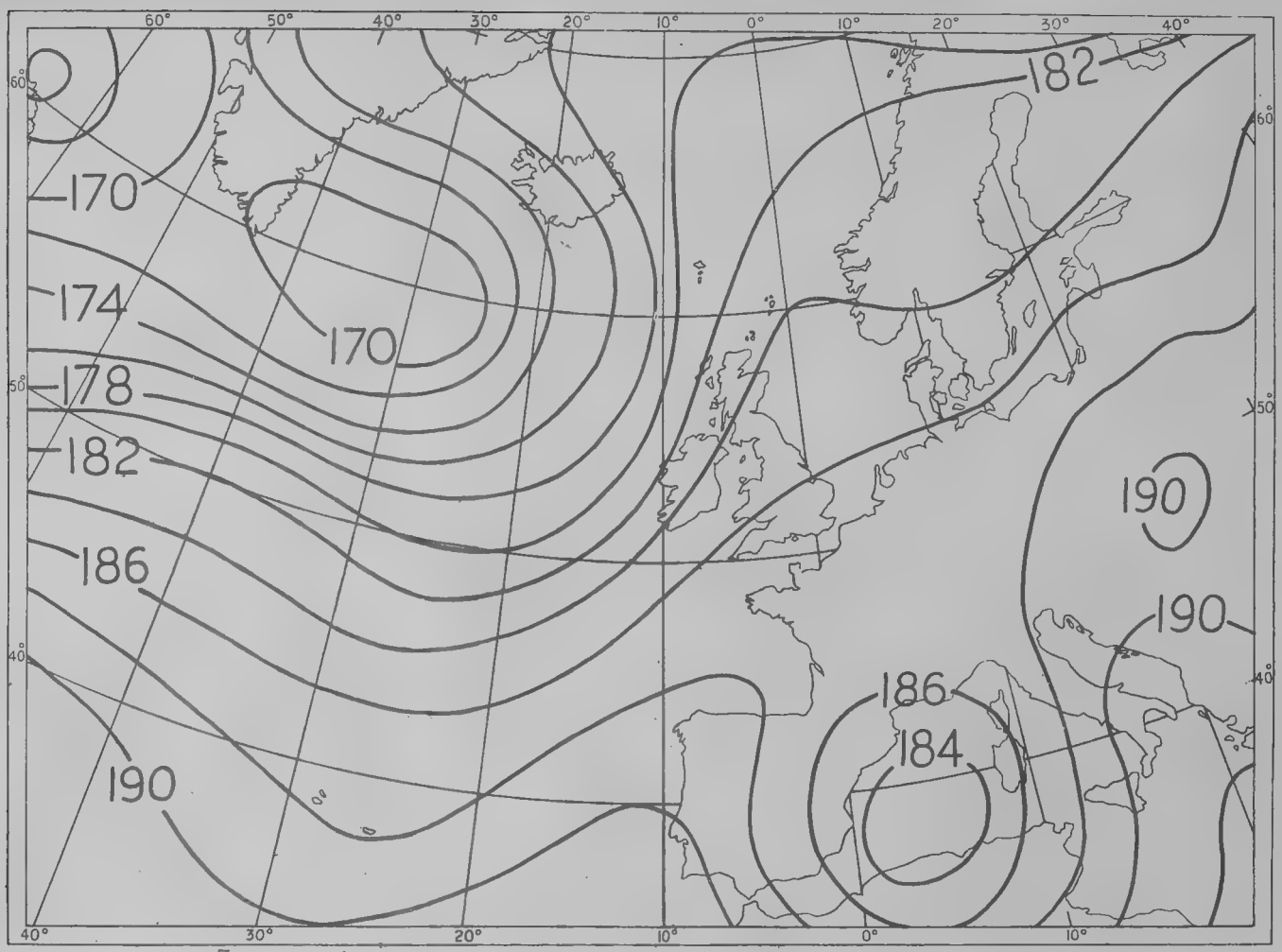

Fig.10(c) Actual 500mb. contour chart for 0300 G.M.T. 16.10.53

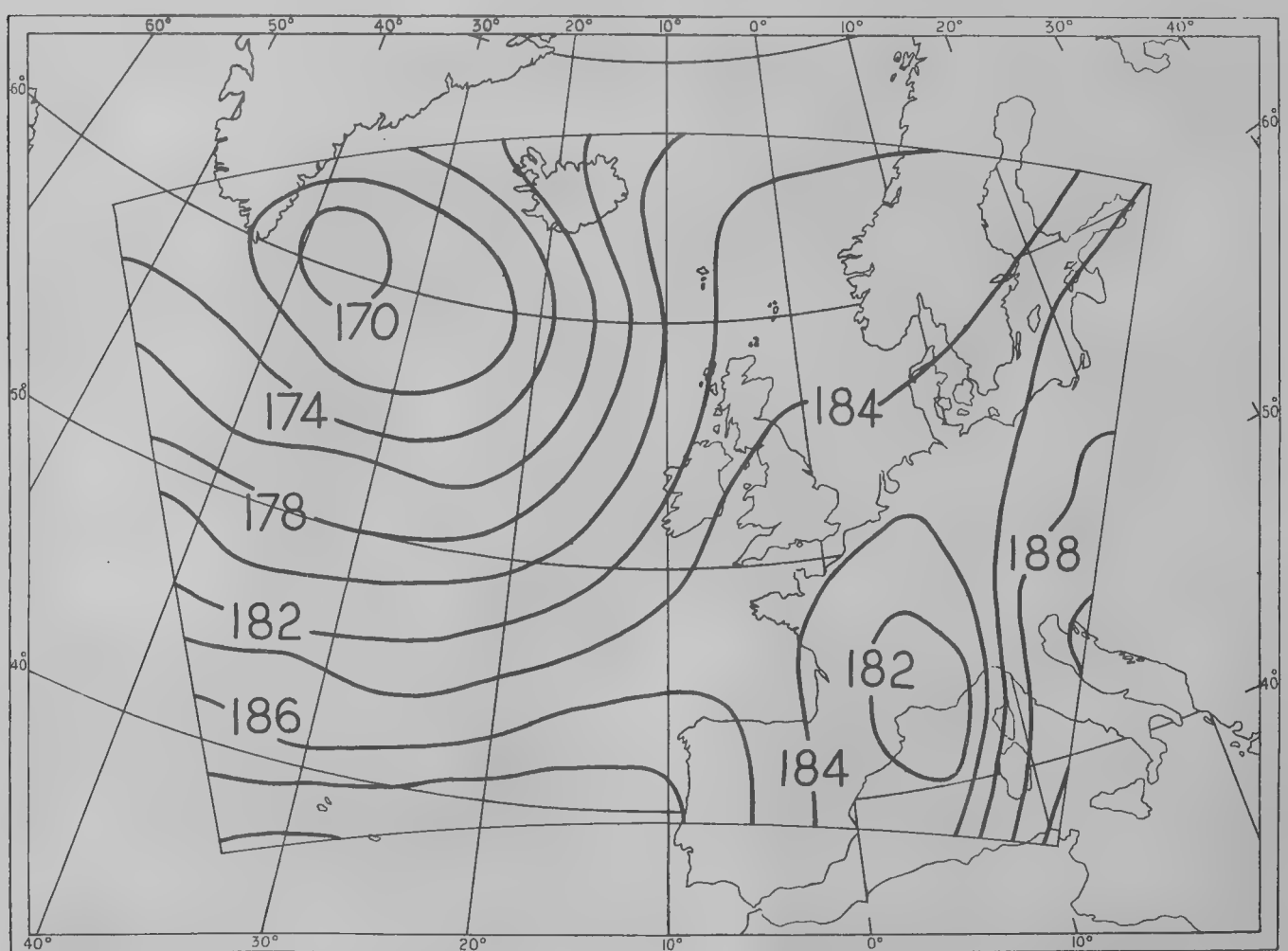

Fig.10(d) Computed 500mb. contour chart for 0300 G.M.T. 16.10.53

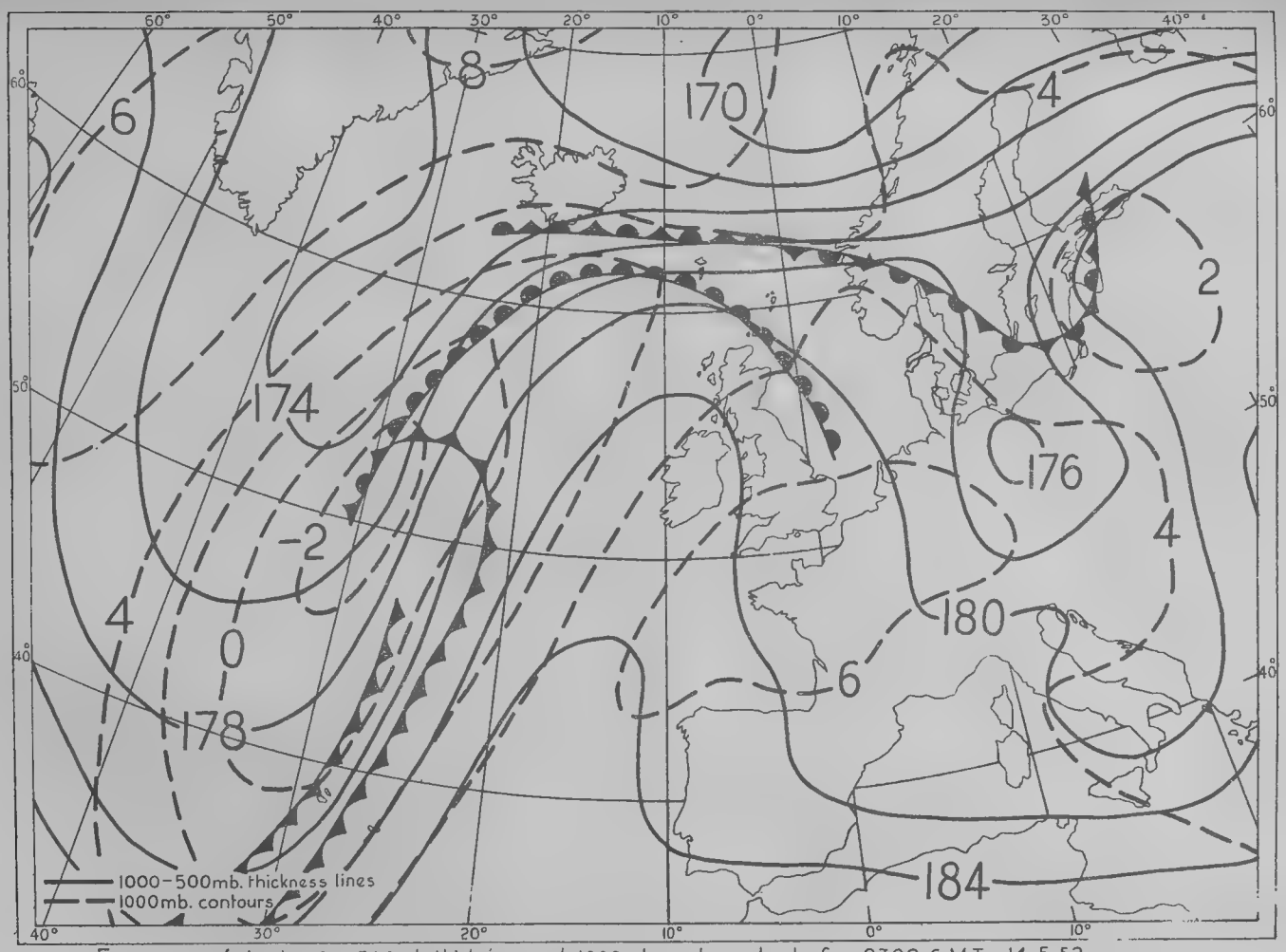

Fig. 5(e) Actual 1000–500mb. thickness and 1000mb. contour charts for 0300 G.M.T. 14.5.52

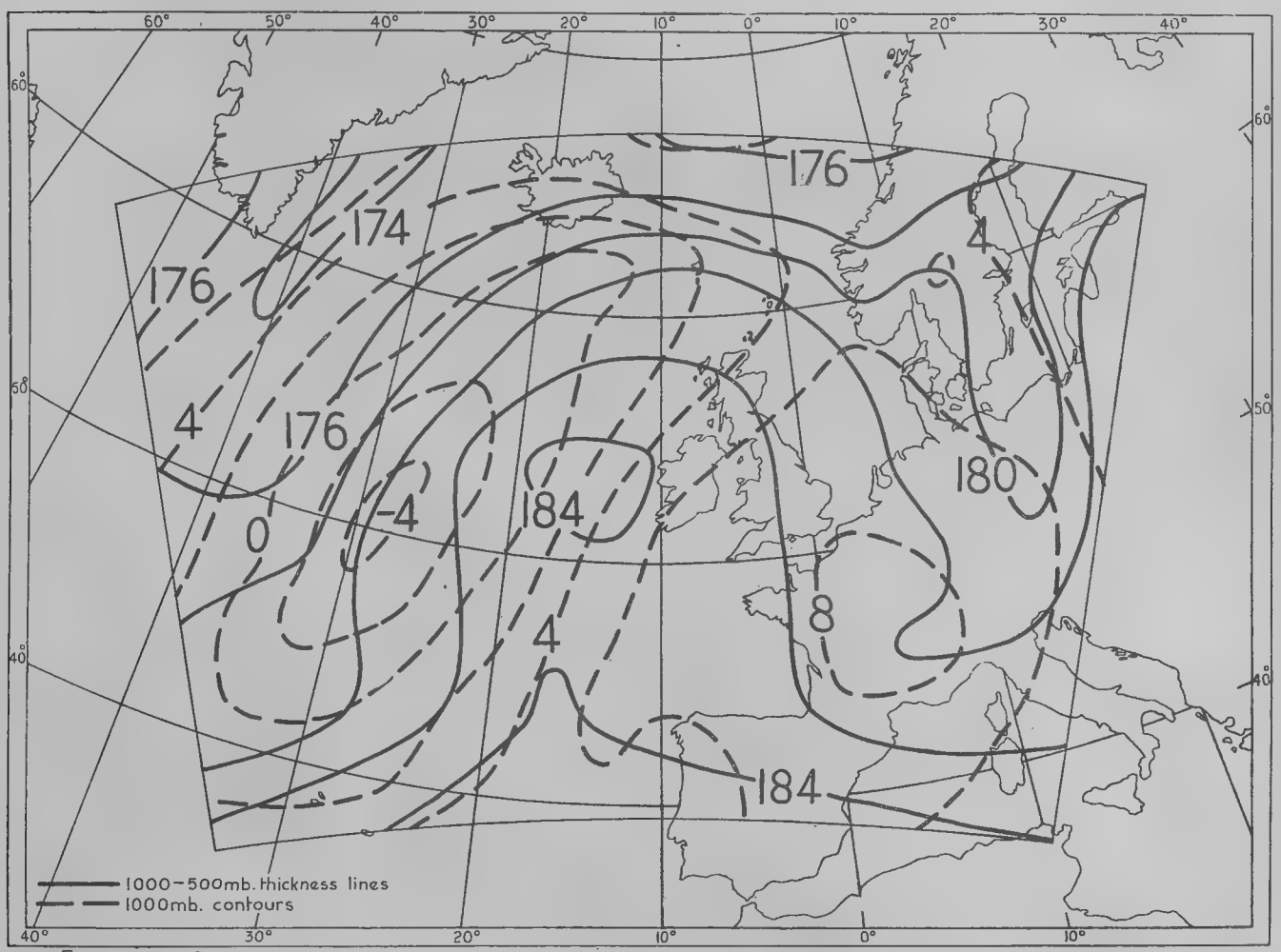

Fig. 5(f) Computed 1000–500mb. thickness and 1000mb. contour charts for 0300 G.M.T. 14.5.52

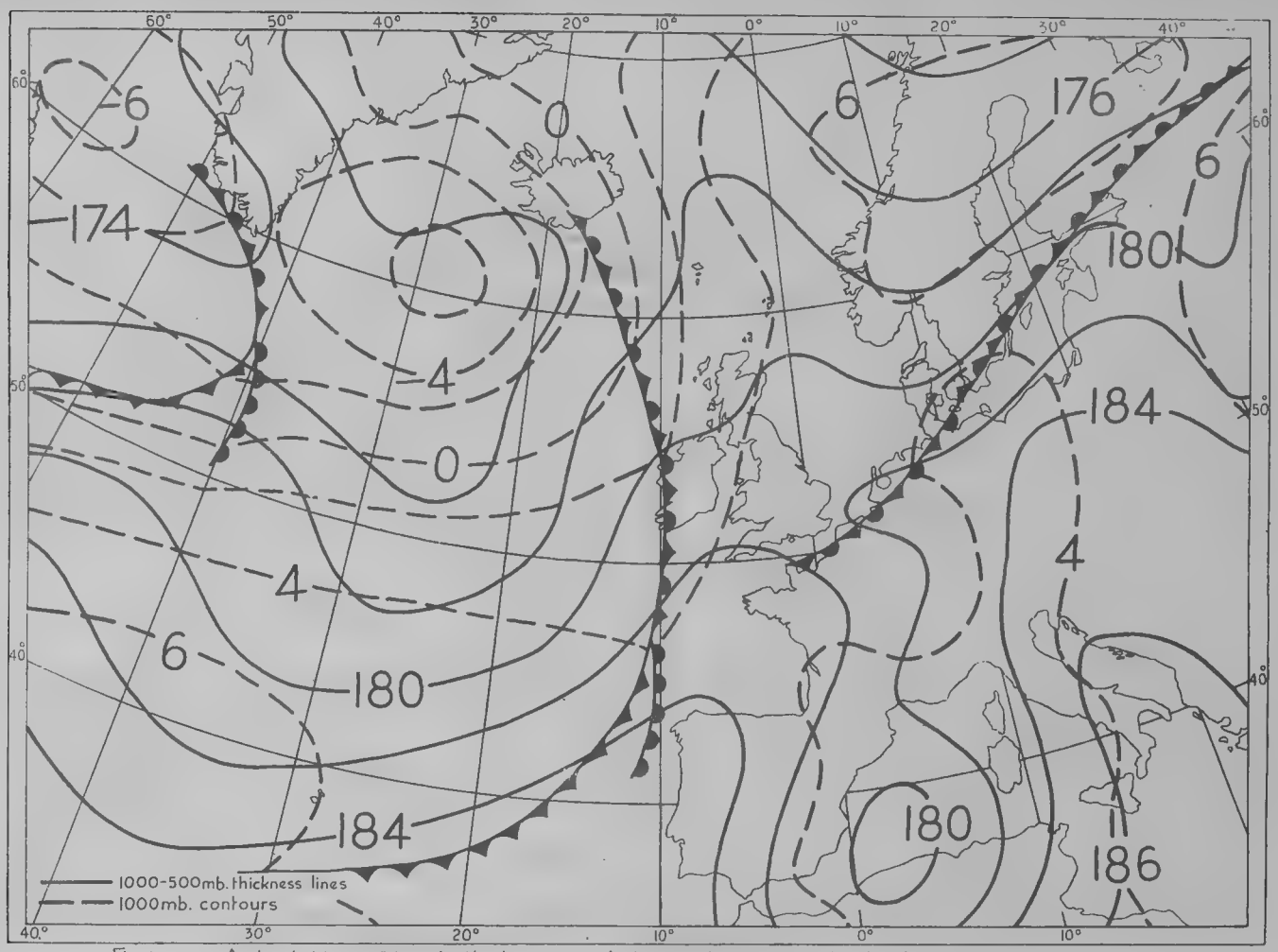

Fig.10(e) Actual 1000-500mb. thickness and 1000mb. contour charts for 0300 G.M.T 16.10.53

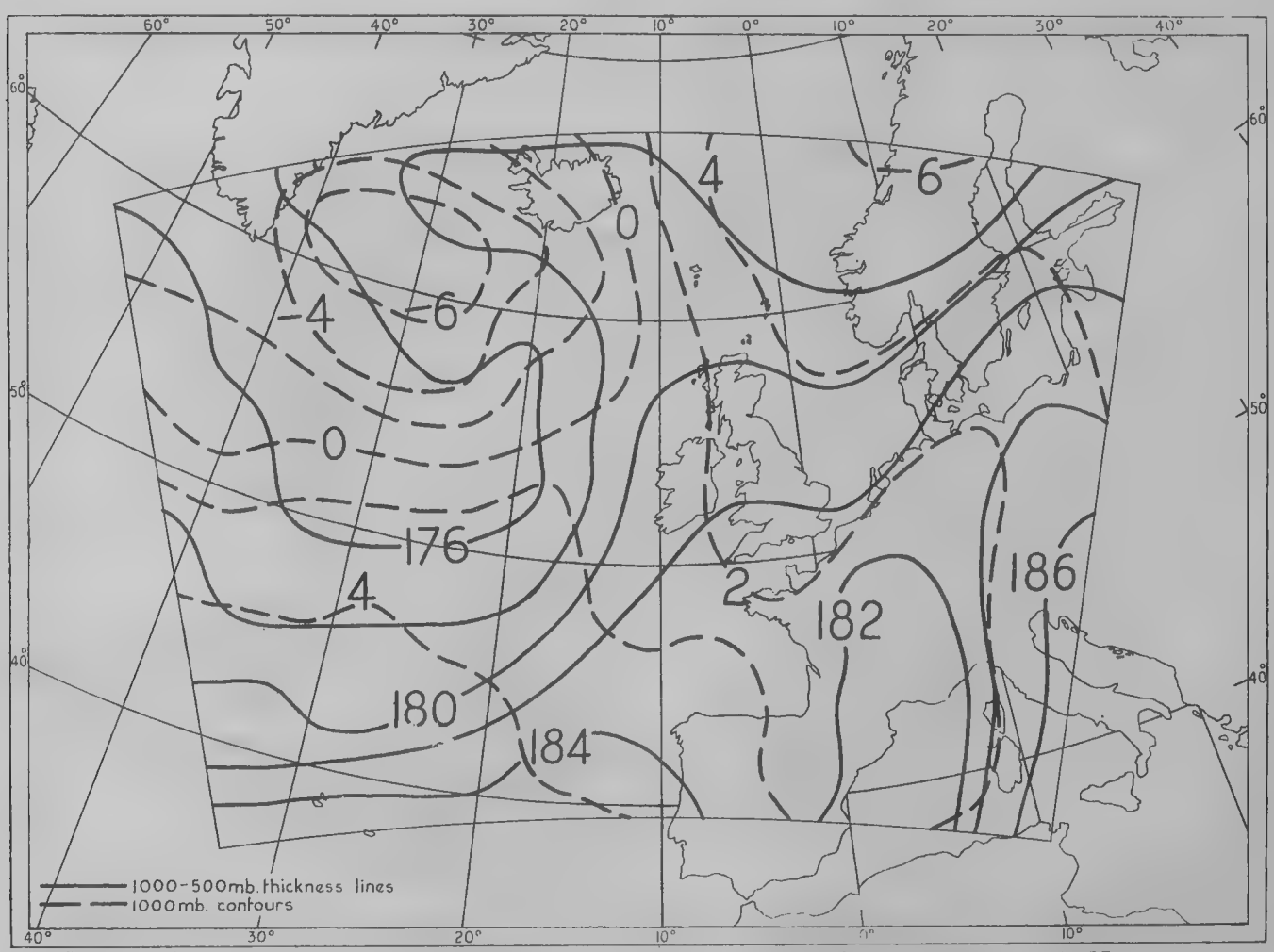

Fig.10(f) Computed 1000-500mb. thickness and 500mb. contour charts for 0300 G.M.T. 16.10.53

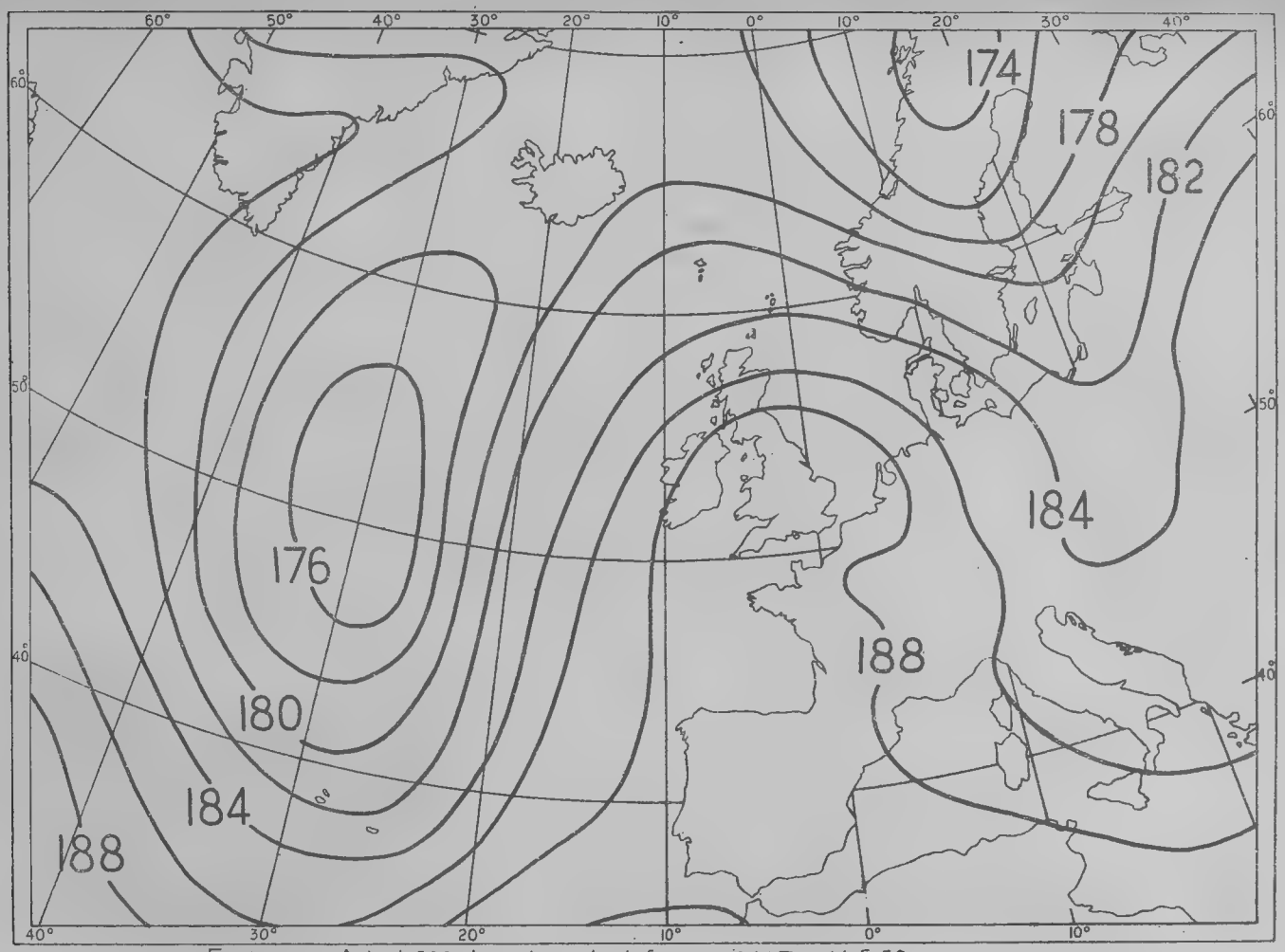

Fig.5(g) Actual 500mb. contour chart for 1500 G.M.T. 14.5.52

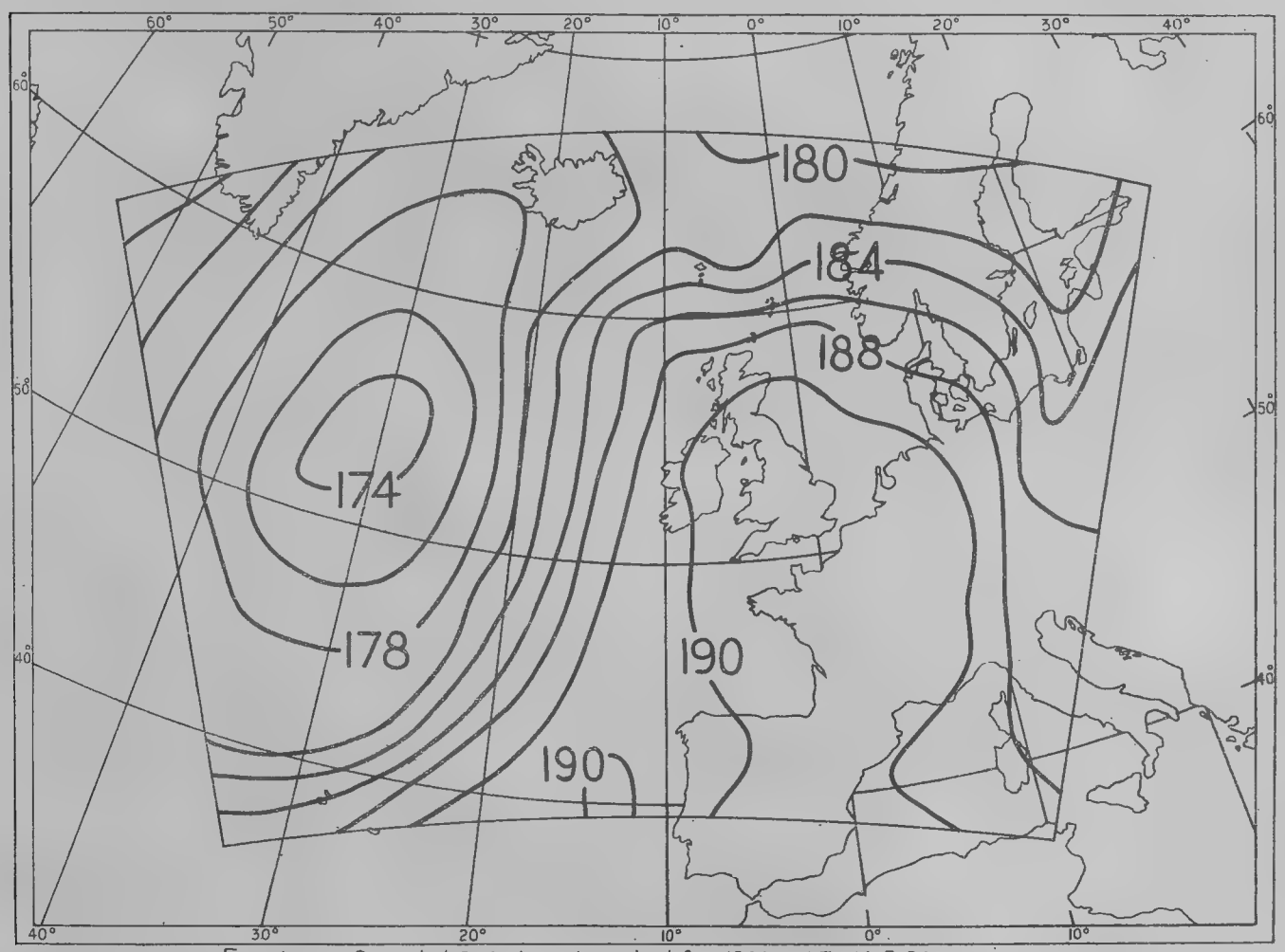

Fig.5(h) Computed 500mb. contour chart for 1500 G.M.T. 14.5.52

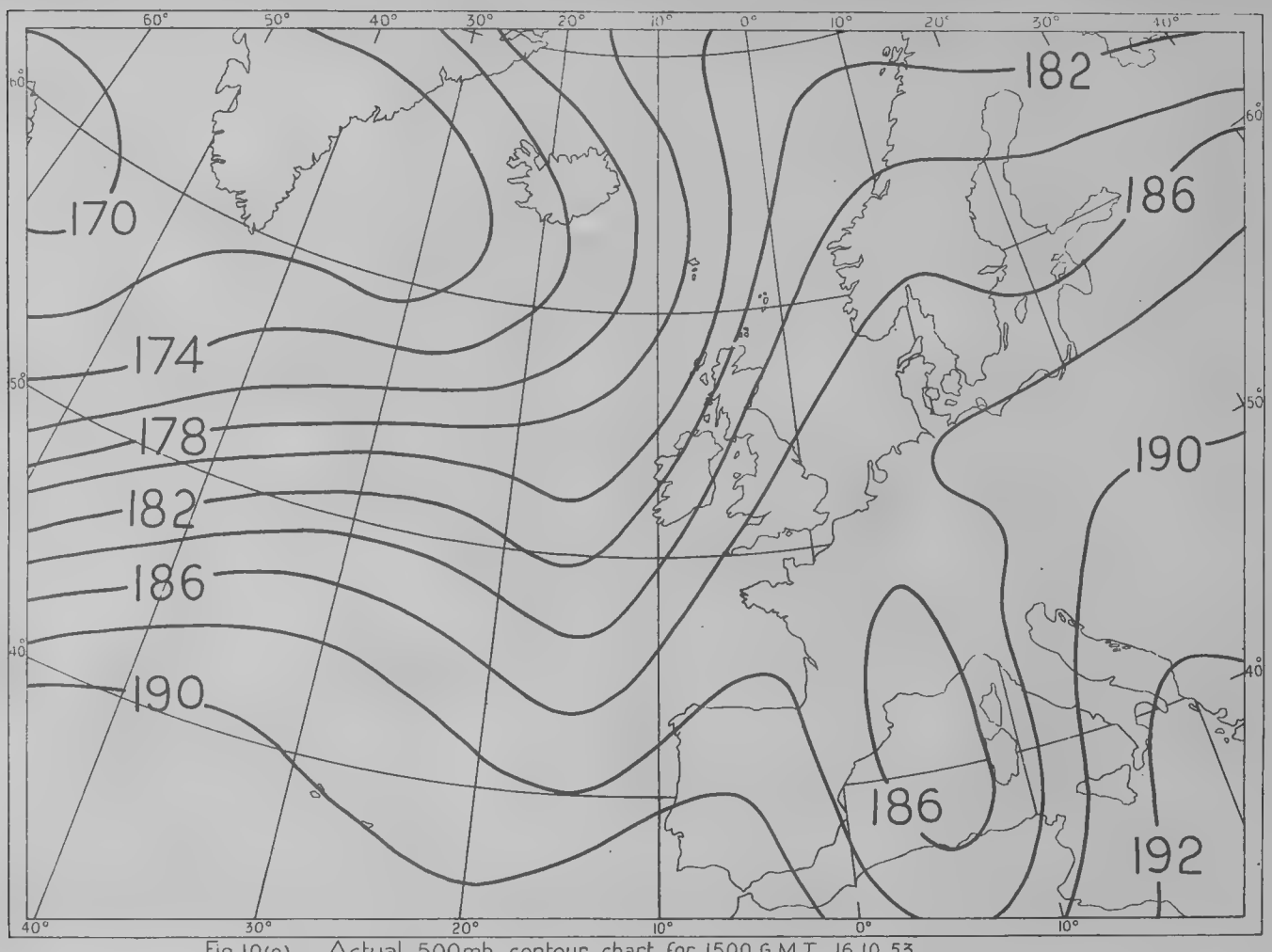

Fig.10(g) Actual 500mb. contour chart for 1500 G.M.T. 16.10.53

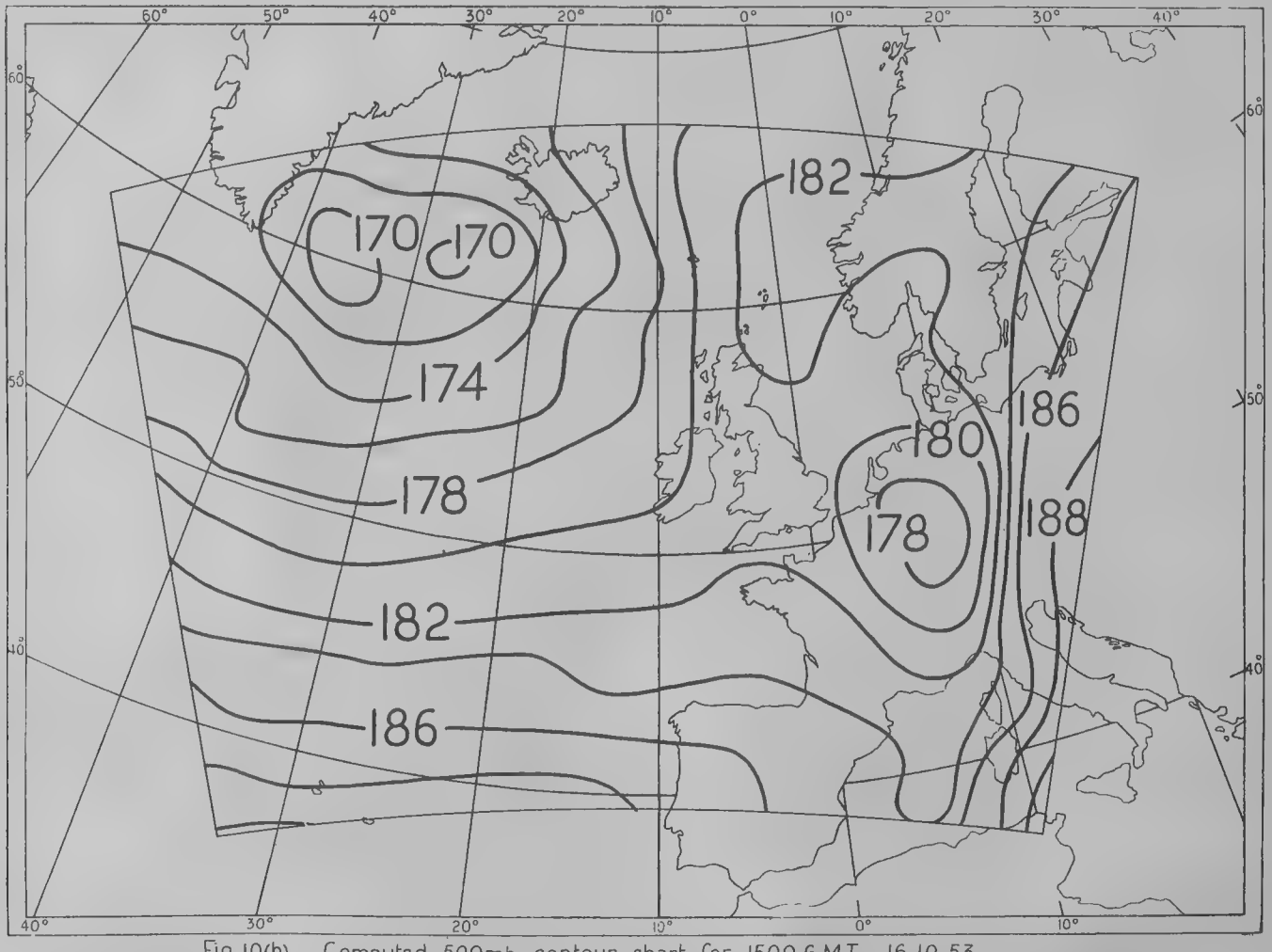

Fig.10(h) Computed 500mb. contour chart for 1500 G.M.T. 16.10.53

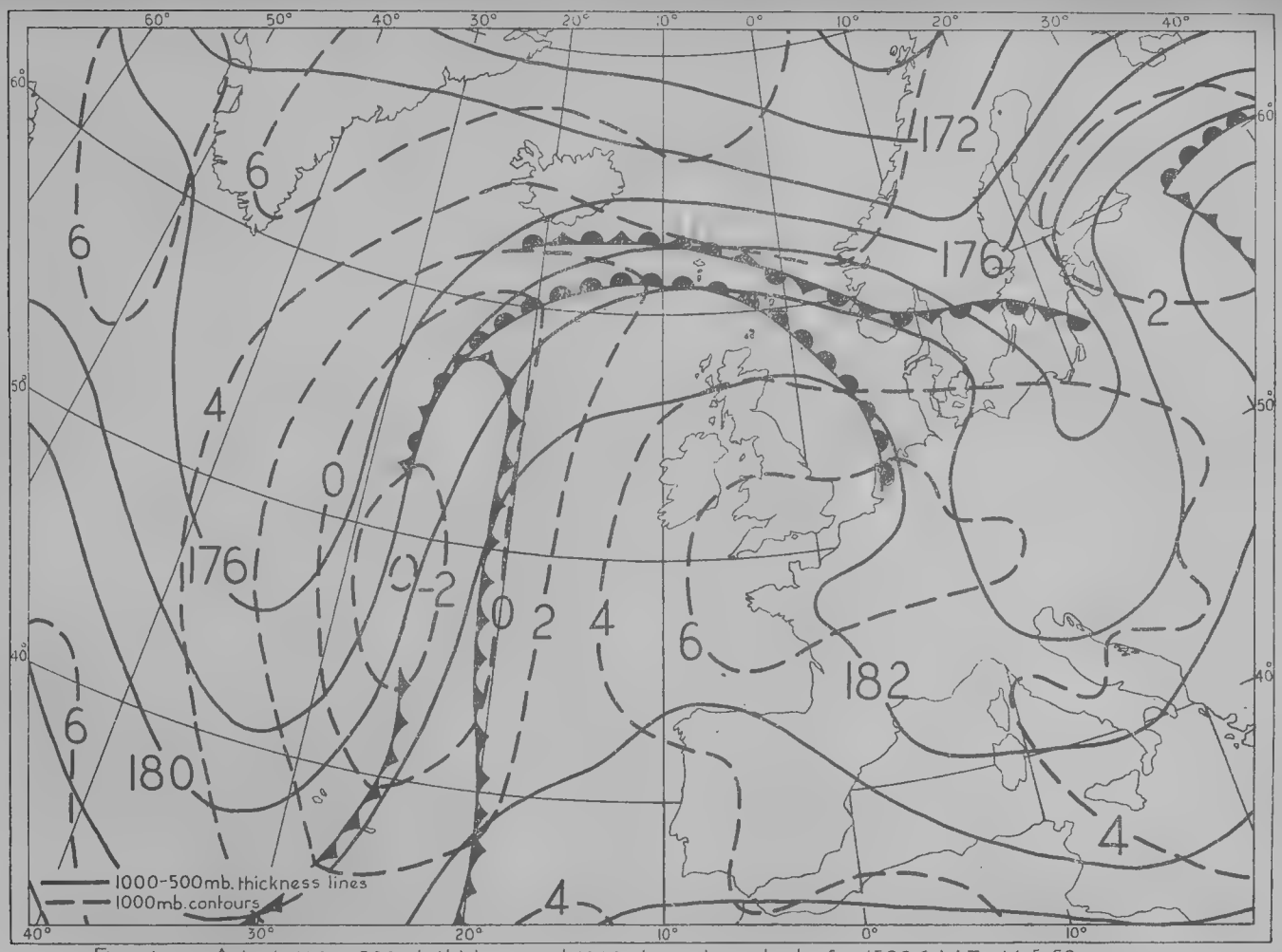

Fig. 5(i) Actual 1000-500mb. thickness and 1000mb. contour charts for 1500 G.M.T. 14.5.52

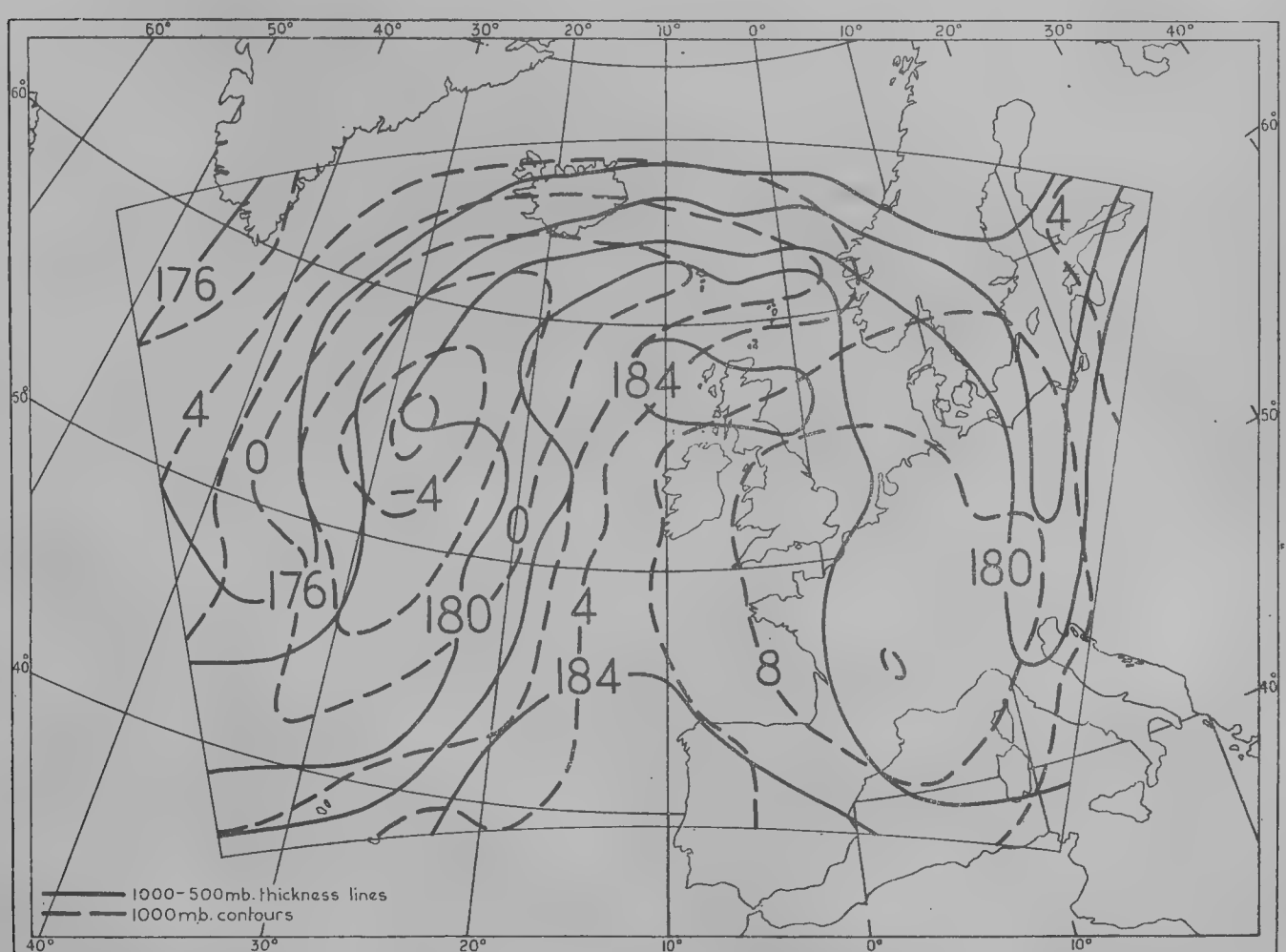

Fig. 5(j) Computed 1000-500mb. thickness and 1000mb. contour charts for 1500 G.M.T. 14.5.52

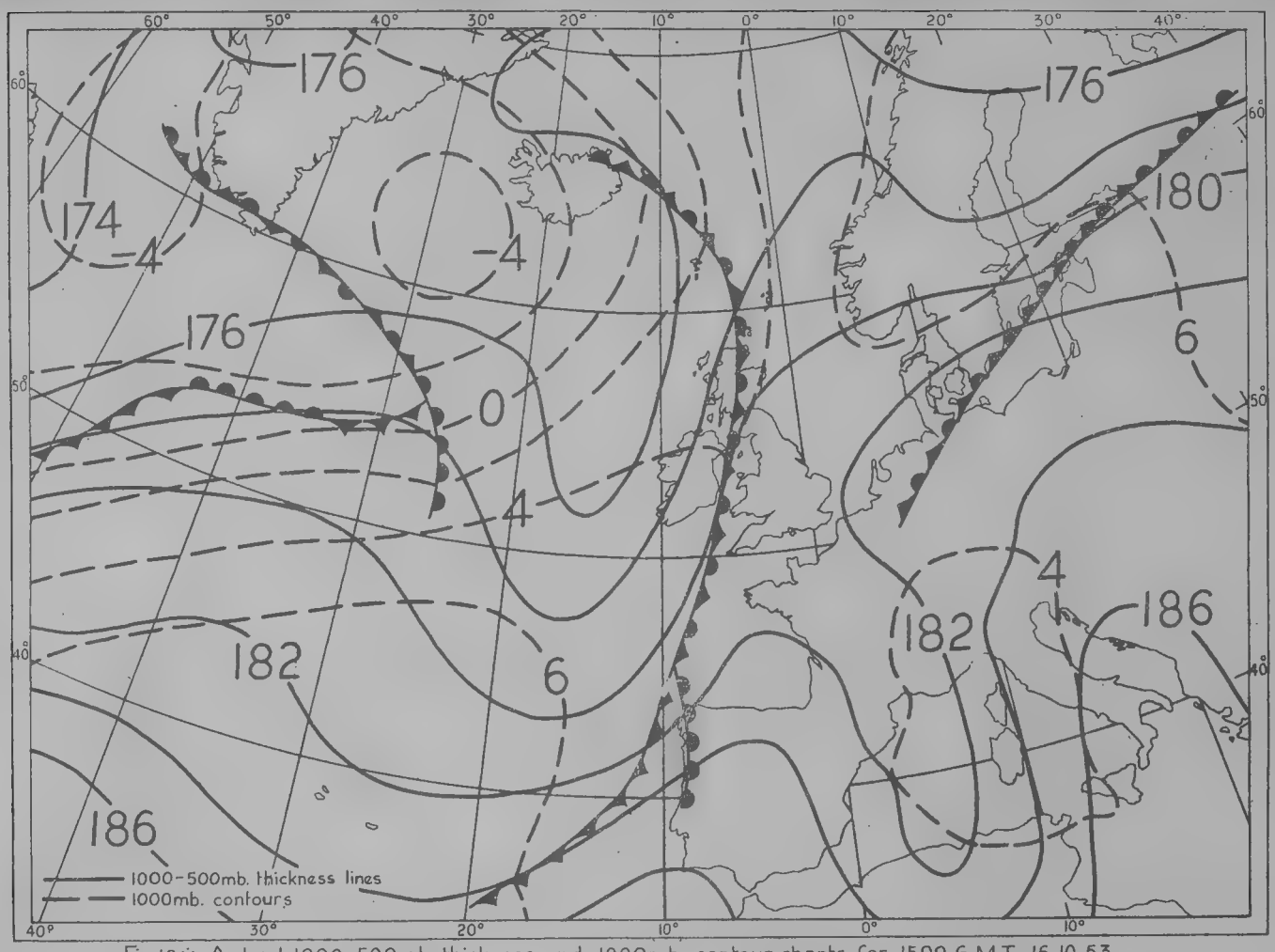

Fig.10(i) Actual 1000-500mb. thickness and 1000mb. contour charts for 1500 G.M.T. 16.10.53

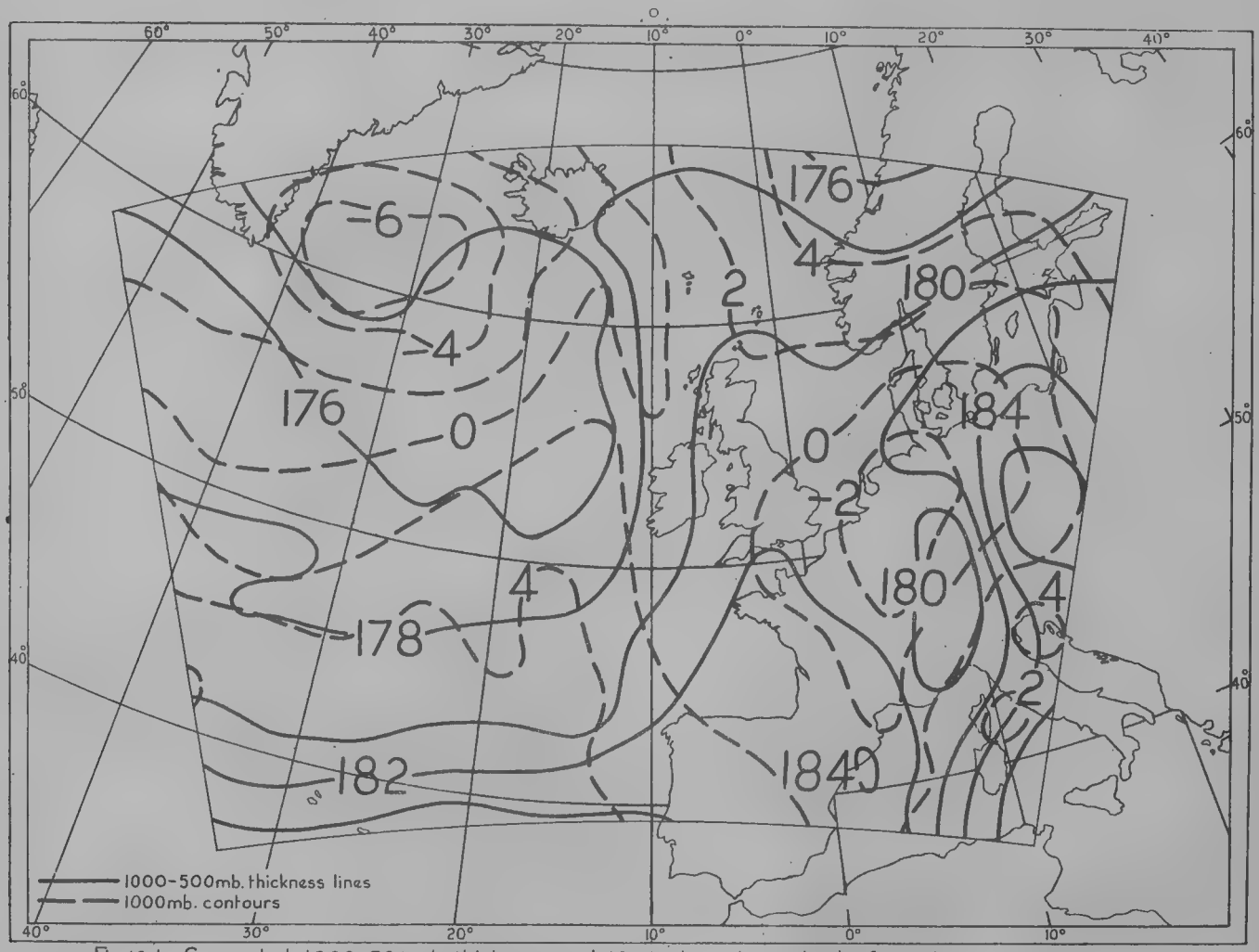

Fig.10(j) Computed 1000-500mb. thickness and 1000mb. contour charts for 1500 G.M.T. 16.10.53

MRP's 867, 868, 869, 872, 873

Control Number
C.D. 5053

At the time of issue this report has not been published. Any author desiring to quote this paper should refer to it as "A paper of the Meteorological Research Committee (London), M.R.P. No. 867 by Mr. G. E. W. Hartley
A copy is available in the Library of the Meteorological Office."

M.R.P. 867
S.C.I/88
9th June, 1954

AD/3296
MATS

AIR MINISTRY

METEOROLOGICAL RESEARCH COMMITTEE

A Remote Recording Electrical Anemograph

by
G.E.W. Hartley (Meteorological Office)

Summary:

This report deals with trials of the Cup Generator Anemometer Mk. Ib with a quick response recording voltmeter to record wind speed and a Magslip transmitting wind vane with a single pen direction recorder developed in M.O.16 to record wind direction. The instruments are described, with notes on their performance, reliability and cost: specimen charts are shown.

1. Wind speed

A recorder to work with the standard M.O. Generator Anemometer Mk. Ib has been described by the writer in Proceedings of the Institution of Electrical Engineers, Vol. 98, Part II, No. 64, August 1951, (2.5.) pp. 434-435. It was subsequently found that if the speed scale on the chart was that derived from wind tunnel tests, isolated gusts were recorded as much as 15% low, because the speed of response of the recorder was not high enough to enable it to follow the generator, although a persisting wind was correctly recorded.

The recorder was therefore modified by changes in the transformer and rectifier, which necessitated their being housed in a separate case instead of inside the recorder, and by altering the coil winding of the recorder so that it took a considerably larger current from the generator, the extra power so obtained enabling stronger hair springs to be used in the recorder. With these modifications the recorder will now follow the generator and gusts are correctly recorded, as well as steady speeds. One small effect of taking a larger current from the generator is to be noted: if an indicating dial is connected in parallel with the recorder, its readings will be about 3% low. In any case the correct indicated speed is shown on the chart, and by the recording pen acting as a pointer against the range strip of the recorder.

Comparisons between this recorder and a Dines Remote Recording P.T.A. were made at S. Farnborough for some months, the generator anemometer being supported on a side bracket from the top of the tower on which the P.T.A. head is mounted. Charts from both were tabulated in M.O.16 and the tabulations showed that, taking daily averages of hourly means, the two types of instrument agreed to within $\frac{1}{2}$ knot; for daily averages of maximum gusts the generator anemometer showed 1-2 knots higher, probably due to the quicker response of the cup generator anemometer at speeds of 30 knots and over.

/Two

H6
G.401604/DOP/5/54/40
55 A-8

Two more recorders of the same type were obtained; wind tunnel tests showed that their scale values were in close agreement with those of the original recorder, so that the same charts could be used for all three with confidence. These two recorders have been connected to two generator anemometers mounted on the 40 ft. tower on the roof at Harrow and have been in operation for some months; their charts show close agreement, though there are sometimes differences due to interference between the two anemometers and other instruments on the tower. The recorder is shown in Fig. 1 and its dimensions in Fig. 2.

Accuracy and consistency of performance are rather difficult to assess; but in the case of the original recorder calibration was carried out in the wind tunnel before and after the S. Farnborough tests, and no change of calibration occurred; and during the wind tunnel tests, the tunnel speed was brought to a given value from several other speeds both higher and lower and the speed was correctly recorded with an error not exceeding $\pm \frac{1}{2}$ knot.

The inking system supplied by the makers of the recorder has proved very satisfactory; it consists of a fine tube suitably shaped, one end of which dips in an inkwell situated at the axis of the pen movement, the other end carrying the writing nozzle and resting lightly on the chart. The spindle of the electrical movement carries a stirrup with V slots; the inking tube is pivoted on knife-edge supports which rest in these slots. The inkwell end of the tube moves only in the ink, not through it; the hole in the top of the inkwell through which the tube enters is only just larger than the tube so that very little dust can get in and clogging of the tube does not occur. The weight of ink in the tube is constant, and the whole pen is balanced so that it will write with very small friction. Ink feed is by capillary, not syphon, action.

The chart is of 4 inches writing width, and has a speed of 3 inches per hour which can be altered to 1, 6 or 12 inches by changing the driving gears. It is 65 feet long, which gives a run of about 10 days with 3 inches per hour time scale. A range of 0-90 knots has been used but it would be easily possible to provide a smaller range and larger scale for normal use, with an extra series resistance which can be switched in to increase the range e.g. to 0-180 knots and reduce the scale.

As will be seen from the blank chart (Fig. 3) the graduations are nearly linear above 10 knots, and closer between 5 and 10 knots. Below 5 knots the readings are not distinguishable; the anemometer cups start to revolve at between 3 and 5 knots. In the specimen records (Figs.4 and 5) the charts used are not correct, and the scale of the blank chart applies to them too. Charts with scales of 1 inch and 3 inches per hour are shown.

No trouble has been experienced with these recorders during M.O.16 trials; the only attention given is to top up the inkwell once a week and fit new charts when needed. The chart mechanisms used are synchronous motor driven but the makers can supply spring-driven mechanisms at a slightly higher cost.

In the case of six recorders used for the Severn Bridge wind measurements over several years, there were three cases of chart motor failure, and two cases where the calibration of the recorder changed; this was found to be due to faulty rectifiers, and when these were changed to another type as now used, no further trouble occurred.

The costs of the various parts are:-

		£. s. d.
Cup Generator Anemometer		18. 10. 0.
Indicating dial (if needed)		9. 0. 0.
Wind speed recorder	about	60. 0. 0.
Charts per dozen		2. 10. 0.

/2.

2. Wind Direction

For remote transmission of wind direction from the vane to the recorder, 2 inch Magslip motors type E2 are used. These operate from 50V. A.C. obtained from mains by a transformer, and form a synchronous link.

At present there is no standard M.O. wind vane embodying 2 inch Magslips, but they are commercially obtainable incorporating a mounting for the generator anemometer above the wind vane and Magslip, so that only one support is needed for both instruments.

Two vanes of this type made in M.O.16 were used in these tests.

The wind direction recorder is of the single pen type developed in M.O.16. In its original form it was shown at the Physical Society's Exhibition in April 1951 and was briefly described in the Met. Magazine, No. 949, Vol. 80, July 1951, page 202 and two illustrations.

In its present form it is shown diagrammatically in Fig. 6. The receiving Magslip (1) is geared down 1:8 to a gear wheel (2) which carries eight evenly spaced pins (3). One of these pins engages with a slot in a specially shaped block (4) pivoted to a moving arm (5) which also carries the recording pen (6). The axes of the gear wheel and moving arm are not coincident, and are so placed that when the gear wheel moves 45° from a central position, the slotted block disengages from the pin and is returned by a centering device (7) to the adjacent pin near to the central position. In the original design, the centering device was a torsion spring; this proved inconsistent in its performance, and was replaced by two pivoted and weighted levers (7) which are set so as to bring the part of the pen arm (8) on which they press, to a central position. This system has proved very reliable.

The movement of the arm from the central to the disengaged position corresponds to 360° of vane movement, and also to the movement of the pen from the centre of the chart to one or other edge.

The chart is marked with 720° of direction; when the pen gets to either edge of the chart, the pin disengages from the slot, and the centering device returns the pen through 360° (chart marking) to near the centre of the chart, and the slotted block engages with the pin nearest to the central position. The recorder is shown in Fig. 7.

There is a slight risk that when the arm is moving back to the centre the block may jump over, or stop short of, the central pin without engaging with it, thereby giving an incorrect record. In practice over several months trial re-centering has taken place many times and the block has only twice failed to engage. Specimen charts showing the appearance of the trace when re-centering occurs are shown in Figs. 8 and 9.

The centering device is adjustable but once set requires no further adjustment.

The chart mechanism and inking system are the same as those used in the wind speed recorder.

There are two theoretical objections to the geometry of the system. One is that as the pins on the gear wheel have a finite thickness, if recording takes place when the pin is on the point of emerging from the slot, the movements of the block and therefore of the pen do not exactly agree with those of the pin. In practice if this occurs, the block is always either released, or goes back fully on to the pin, and no wrong readings persist.

The other is shown in Fig.11. When the pin B moves about the axis O, the link BC (i.e. the arm) moves about the axis C.

/For

For correct recording, for equal angular movements AOD, DOE, EOF, FOB of the link OB, the angles BCE, ECE, ECD, DCA should also be equal to each other.

By calculation, when angles AOD etc. are $11^{\circ}15'$ each, BCF = $5^{\circ}54.5'$, FCE = $5^{\circ}53.5'$, ECD = $5^{\circ}53'$, DCA = $5^{\circ}52'$. The differences between these are so small that they do not show on the chart at all and may be neglected.

A later modification has been to reduce the size of the mechanism to allow it to go inside the same kind of case as the wind speed recorder. This recorder works perfectly satisfactorily, and is shown in Fig. 10.

Wind direction recorders of the type described have been used for some years in the Falkland Islands and at Cardington and have given satisfactory service. The latest design has been undergoing trials at Harrow and has given no trouble.

Costs:-

		£. s. d.	£. s. d.
Commercially obtainable Magslip wind vane, with anemometer mounting platform			42. 10. 0.
Recorder:	Case	8. 0. 0	56. 12. 0.
	Chart Mechanism	20. 0. 0.	
	E.2 Magslip	18. 12. 0.	
	Rest of Mechanism (Est)	10. 0. 0.	
Direction dial if needed			15. 0. 0.
Charts per dozen			2. 10. 0.

FIG. 1

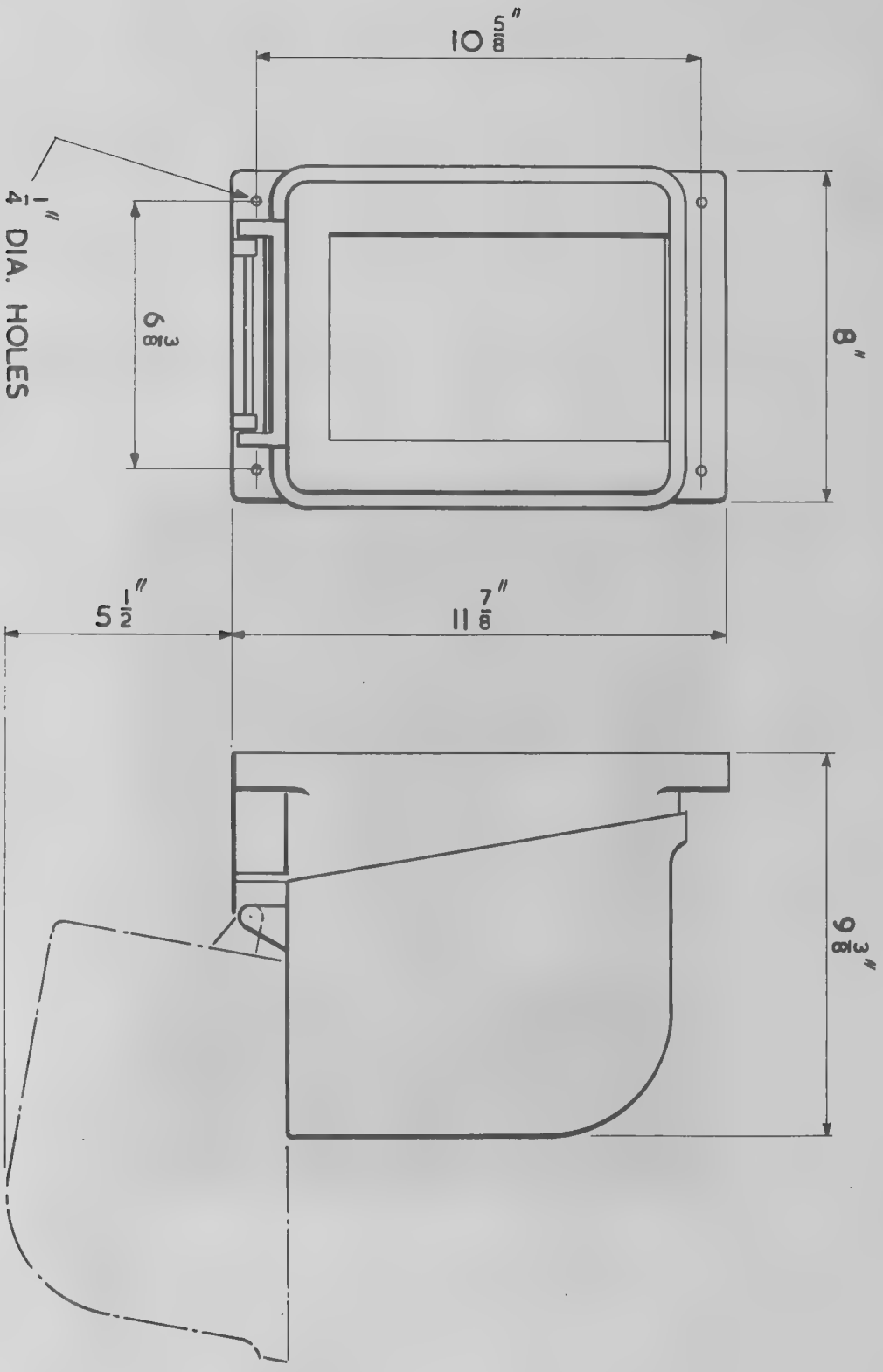

FIG. 2

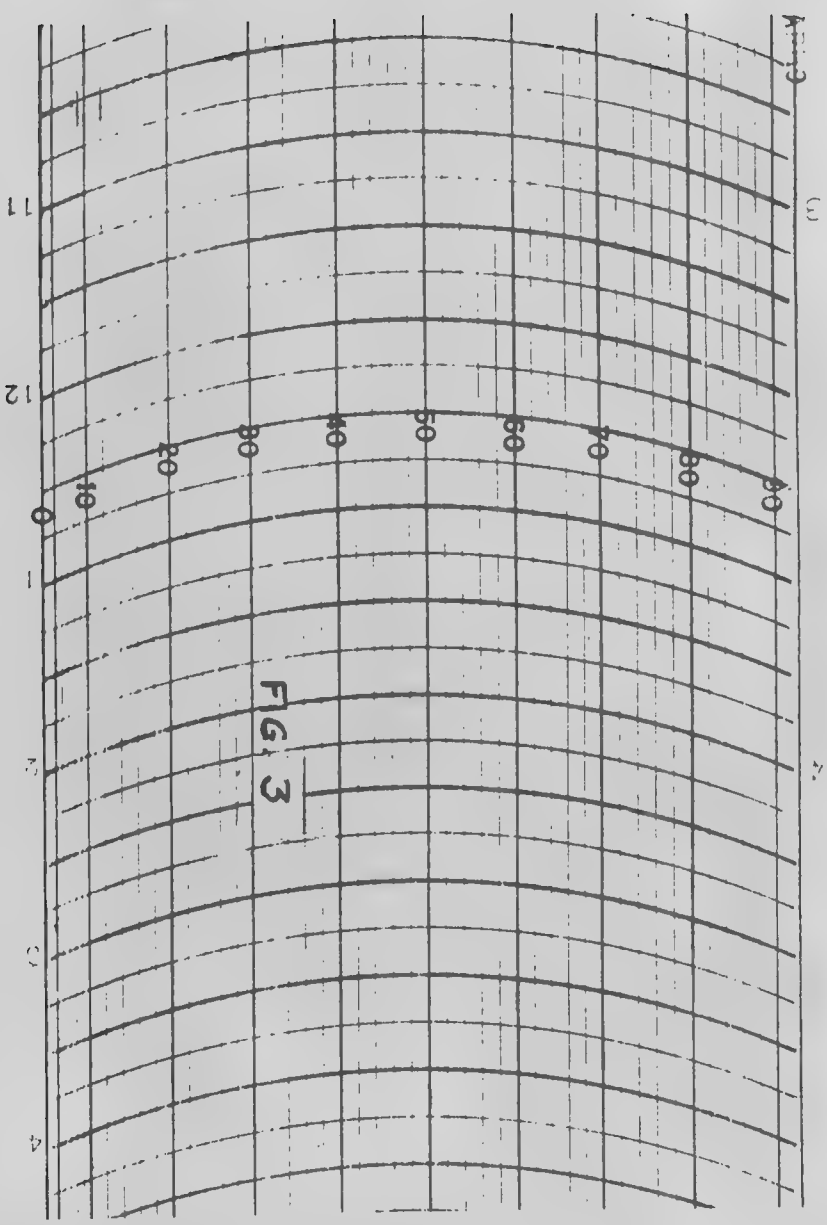

FIG. 3

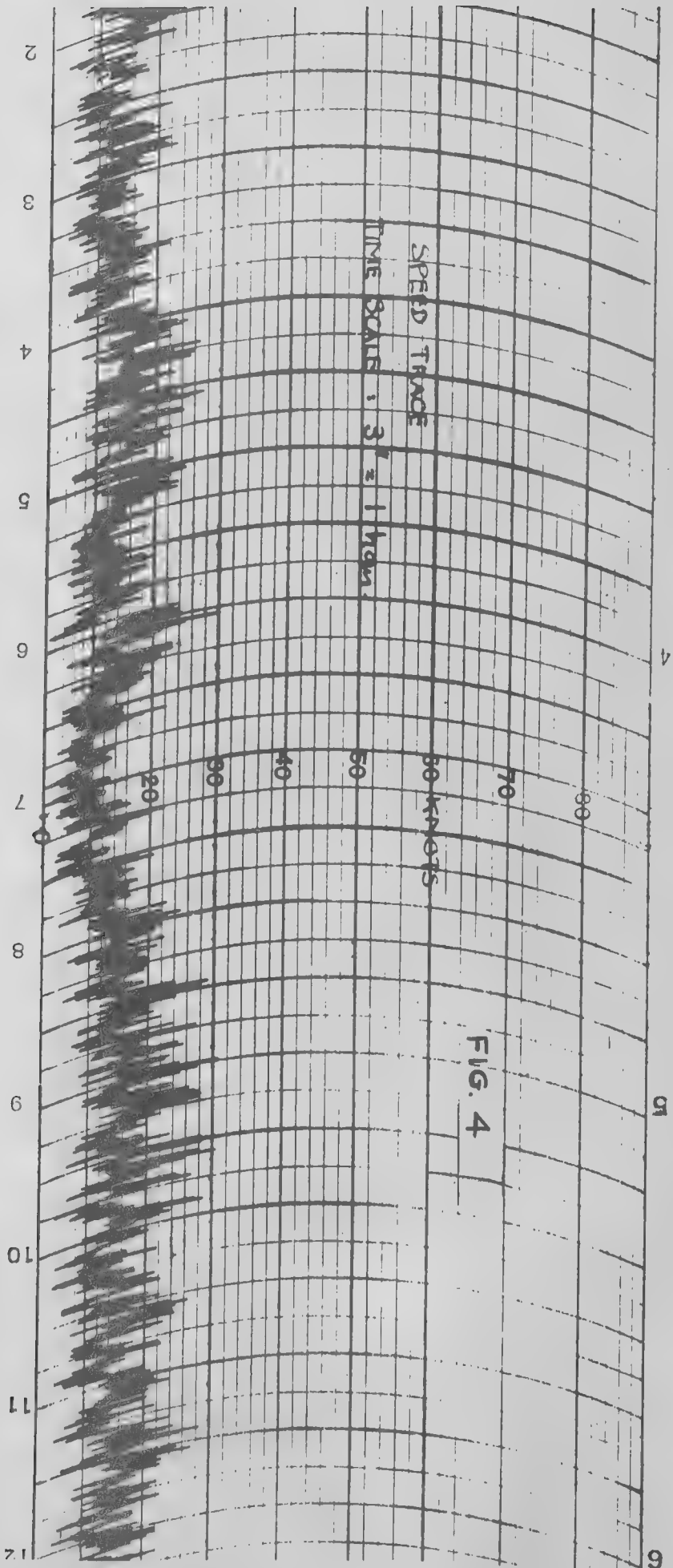
SPEED TRACE
TIME SCALE : 3" = 1 HOUR
20
30
40
50
60
70
80 KNOTS
2
3
4
5
6
7
8
9
10
11
12
1
2
3
4
5
6

FIG. 4

M.R.P. 867

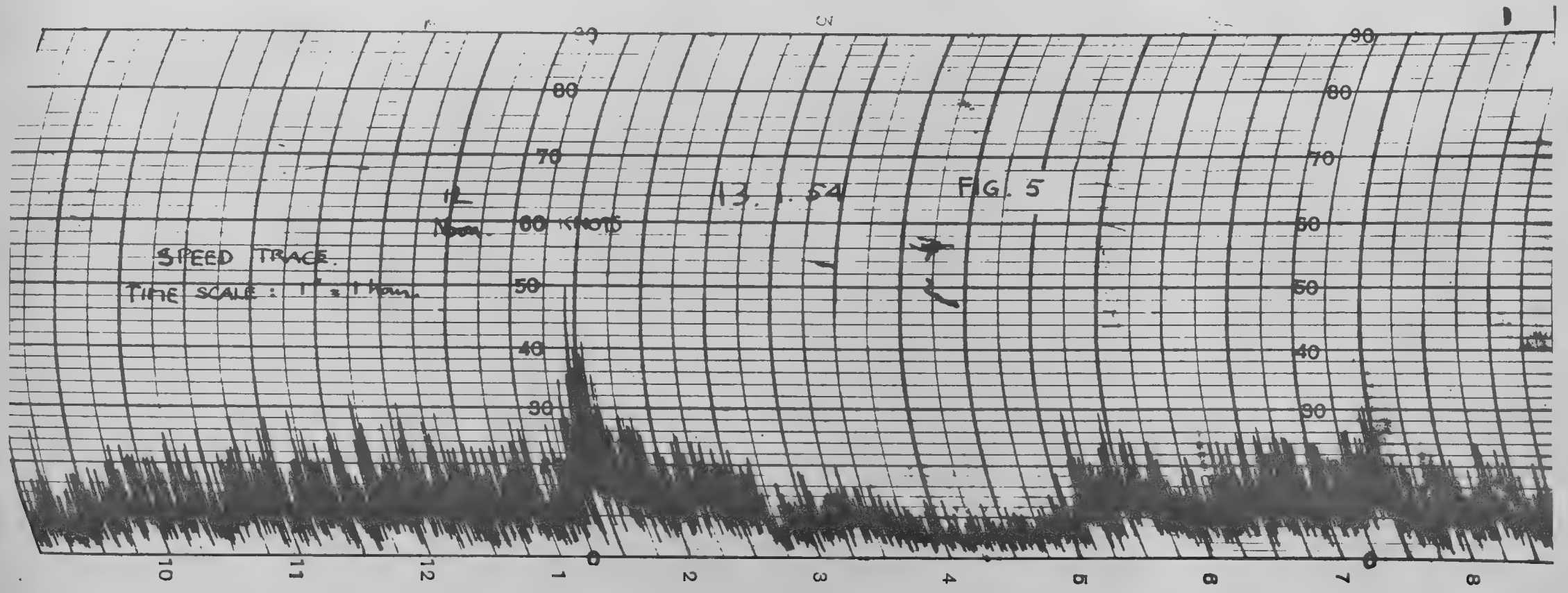
SPEED TRACE.
TIME SCALE : 1" = 1 Hour.
12 Noon.
60 KNOTS
13.1.54
FIG. 5
90
80
70
60
50
40
30
10
11
12
1
2
3
4
5
6
7
8

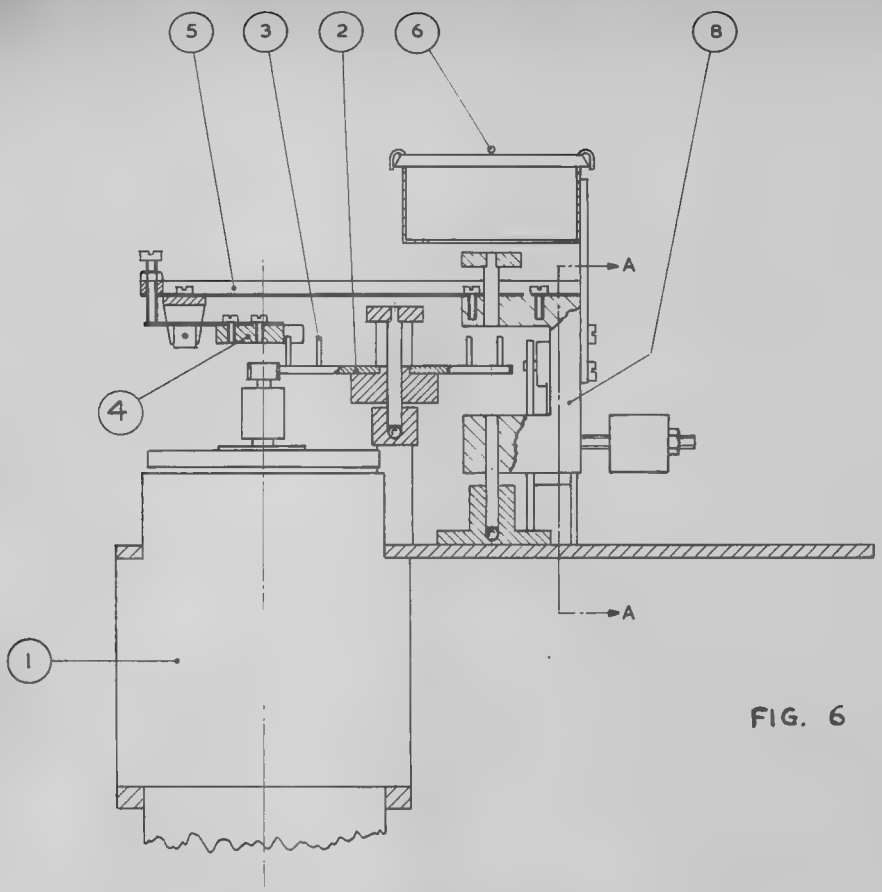

FIG. 6

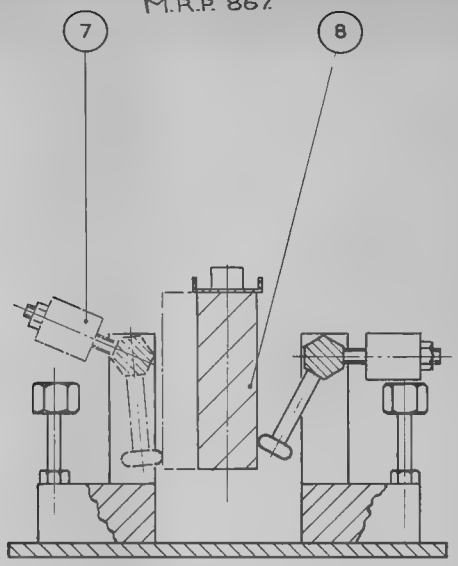

SECTION AT AA

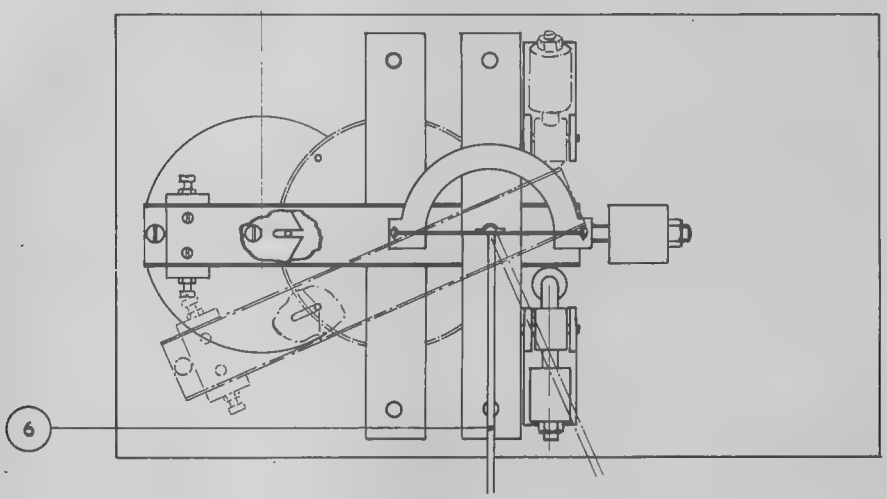

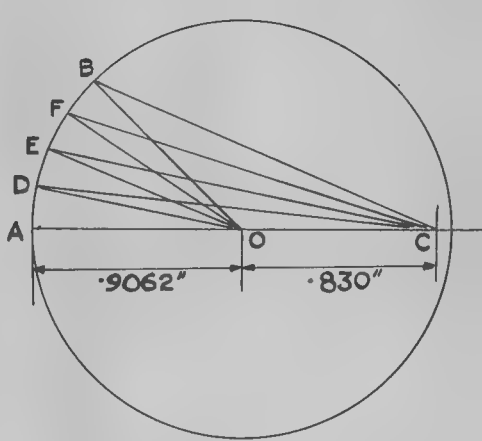

FIG. 11

FIG. 7

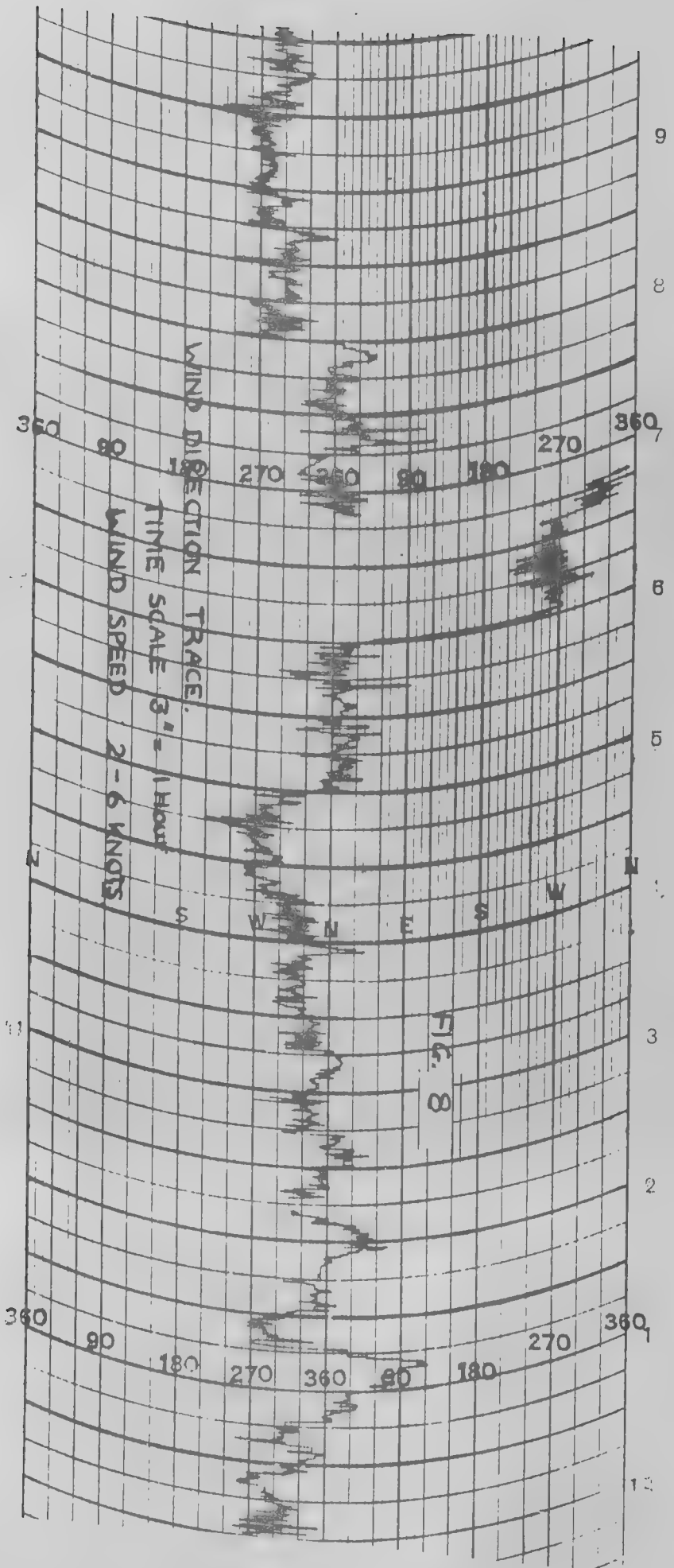
WIND DIRECTION TRACE.
TIME SCALE 3" = 1 HOUR
WIND SPEED 2 - 6 KNOTS
360
90
180
270
360
90
180
270
360
N
S
W
N
E
S
W
N
9
8
7
6
5
4
3
2
1
12

Fig. 8

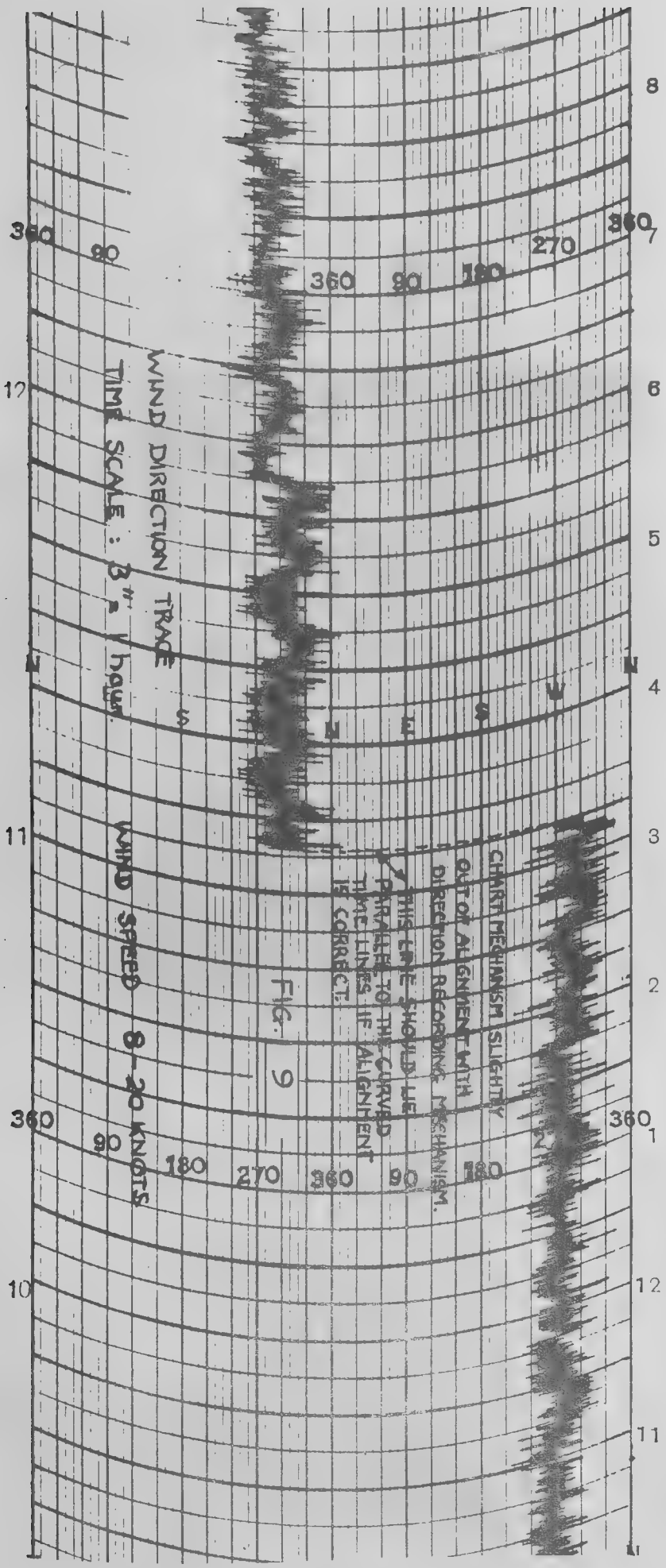
WIND DIRECTION TRACE
TIME SCALE : 3" = 1 hour
WIND SPEED 8-20 KNOTS
CHART MECHANISM SLIGHTLY OUT OF ALIGNMENT WITH DIRECTION RECORDING MECHANISM.
THIS LINE SHOULD LIE PARALLEL TO THE CURVED TIME LINES IF ALIGNMENT IS CORRECT.
360
90
180
270
N
E
S
W
12
1
2
3
4
5
6
7
8
9
10
11

FIG. 9

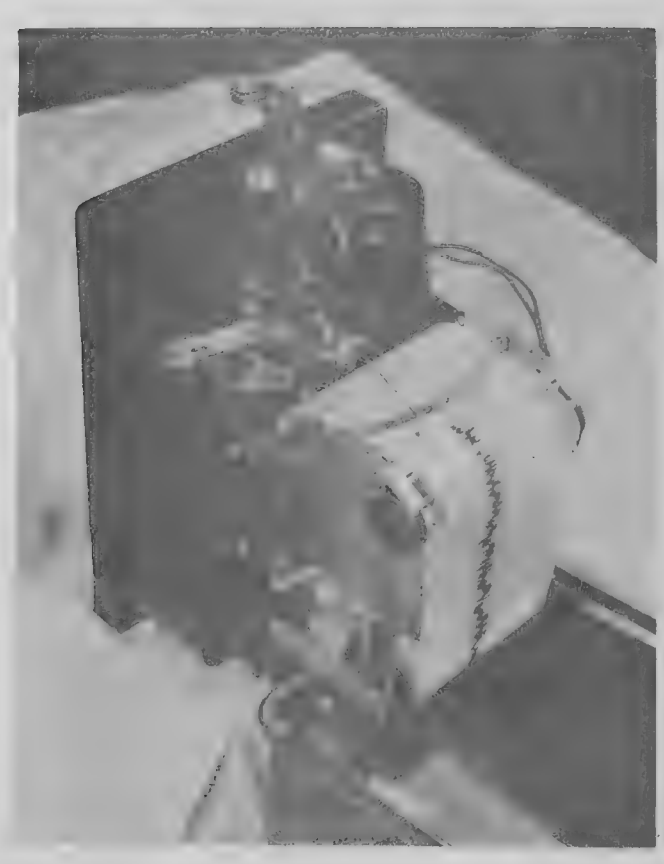

FIG. 10

o (London),
o. 868 by Mr. D.C.E. Jones.
A copy is available in the Library
of the Meteorological Office".

9th June, 1954

assed (1, 2).

At the time of issue this report has not been published. Any author desiring to quote this paper should refer to it as "A paper of the Meteorological Research Committee (London), M.R.P. No. 868 by Mr. D.C.E. Jones. A copy is available in the Library of the Meteorological Office".

M.R.P. 868

S.C.II/172

9th June, 1954

AD223078

AIR MINISTRY

METEOROLOGICAL RESEARCH COMMITTEE

Note on exceptionally severe clear-air turbulence and other phenomena on 14th April, 1954

by

D.C.E. Jones (Meteorological Office)

1. Introduction

Very severe turbulence experienced in clear air at heights between 28,000 and 41,000 ft. have previously been described and the meteorological situations on these occasions discussed (1, 2).

An exceptionally severe patch of turbulence was recently encountered without warning by a Canberra jet bomber flying at 40,000 ft. There were also reports of very strong "Standing Waves" in the same airstream but at different times and several different locations.

2. Description of the turbulence

At about 2130 G.M.T. on April 14th, 1954 a Canberra aircraft was flying at 40,000 ft. on a heading of 084 degrees (true) near Edinburgh. After flying in smooth air conditions at an indicated air speed of 210 kt. (.7 Mach Number) the aircraft suddenly experienced severe turbulence. The pilot began to turn to the right to avoid the region of turbulence but during the turn a severe gust lifted the port wing and rolled the aircraft on to its back. Full aileron control proved ineffective in preventing the roll and while upside down the aircraft gained 500 ft. in altitude. Control was eventually regained and the aileron became effective again. The pilot then descended quickly and found that turbulence ceased below 38,000 ft. The aircraft returned to its base and landed safely. No damage was found to have been suffered by the Canberra.

The only cloud in the vicinity of the incident was about 3/8 cumulus below 20,000 ft.

3. Meteorological situation

Fig. 1 shows the surface chart for 0001 hours and Fig. 2 the 300 mb. chart for 0200 G.M.T. 15th April.

The depression over Southern Scandinavia was moving southeastwards. The associated cold front was moving slowly southwards over Northern England and was being followed by a secondary cold front which was over Northern Scotland.

At high levels the whole of the British Isles and the North Sea were under the influence of a strong northwesterly air current. There are indications of a well marked jet stream with its axis extending from Iceland to the Shetlands to North West Germany. Fig. 3 shows a cross-section from Valentia to Lerwick at 0200 G.M.T. 15th April which is the time nearest to that of the incident under

/discussion

discussion when temperature and wind soundings were made simultaneously. Only upper winds are observed at 2000 hours and those for stations in Scotland, Northern Ireland and Northern England on the evening of 14th April are given in Table I.

Table I

Winds at 2000 hours 14th April, 1954

	Lerwick	Leuchars	Stornoway	Liverpool	Aldergrove
24,000 ft.	315/132 kt.	310/67 kt.	313/75 kt.	322/59 kt.	306/58 kt.
27,000 "	316/118	302/77	302/82	316/65	308/55
30,000 "	316/118	300/80	295/89	313/60	298/49
35,000 "	316/135	303/83	296/88	309/53	289/46
40,000 "	318/138	309/68	312/40	309/50	287/42
45,000 "	318/125* (42,000 ft.)	314/43	293/22	351/32	312/47

* (The wind at 45,000 feet is given in the Daily Aerological Record as 318/144 kt. but this was computed from the last minute of the observation at the extreme range of the radar and the Senior Meteorological Officer, Lerwick advises that this value is probably in error).

It will be seen that when the incident occurred the aircraft was flying in the upper troposphere, in a region of pronounced vertical and horizontal wind shear, on the warm side of the jet stream and above the level of the axis of the jet.

4. Reports of "Standing Waves"

At the debriefing of the pilot involved in the above incident he stated that the only unusual conditions he noticed before the onset of the very severe turbulence were found over the Midlands previously that evening. At a height of 40,000 ft. he noticed up and down currents, and variations in the indicated air speed which he thought were caused by "standing waves".

Another interesting report showing the existence of strong vertical currents was received from the pilot of a jet fighter aircraft who was doing a flight to check his R/T set. While trying to fly straight and level at 35,000 ft. over Norwich at an indicated air speed of 200 kt. at about 1100 hours 14th April he noticed that the vertical Airspeed Indicator and the Altimeter were registering a rate of climb of 3,000 ft. per minute. He then tried to descend and in his report states -

> "I was now at 37,000 ft. I noticed that I was still in cirrus cloud. My rate of climb still showed 3,000 ft. per minute and the Altimeter reading rose quickly to just under 40,000 ft. I was still in cirrus cloud. I then opened the throttles and dived out to the south to carry out further R/T checks at lower altitudes.

/My

My aircraft was heavily laden and should, once I had levelled off, have been unable to climb at anything more than 1,000 ft. per minute at the beginning, and when the nose was down should have lost height at least at 2,000 ft. per minute, probably more.

There was no vestige of turbulence during the climbing incident which took place 10 miles south of Norwich".

The existence of standing waves in the air stream at lower levels has subsequently been confirmed by the large number of reports received at Northolt from civil aircraft. During the period 13th - 15th April about 30 reports of standing waves were received, the heights at which they were reported varied from 4,500 ft. to 18,000 ft. and the rates of lift and sink ranged up to 2,000 ft. per minute. It has been stated that the number of reports in this period was exceptional; the usual rate of receiving such reports is about 2 or 3 per week.

5. Discussion

There were other reports of high level turbulence over the British Isles on the 14th April. The existence also of standing waves at various levels at more or less the same time poses a problem as to whether the turbulence is in some way associated with standing waves which are generated when wind blows over a mountain range. Hislop tentatively suggested in his report on the British European Airways special investigational flights (3) that under certain conditions the waves might break - (like the waves of the sea) - and thus degenerate into turbulent motion. He quotes an occasion when a B.E.A. Mosquito experienced smooth lift of about 1,500 ft. to 2,000 ft. per minute between 35,000 and 37,000 ft. which finally petered out into rather sluggish turbulence. It has also been suggested by Radok (4) that topography can be responsible for localising and rendering severe turbulence within a favourable jet stream region. But on the other hand, Press, Schindler and Thompson (5) reported after a recent investigation that clear air turbulence had been reported in all parts of the United States and there were no indications of geographical variations, which would be the case if there were an association between the two phenomena.

6. Conclusions

The incident of the Canberra which encountered, in clear air, a gust of sufficient violence to turn it upside down while in normal flight focuses attention on the extreme severity of turbulence that may be encountered at high level. So far as is known no such incident has previously been reported. It occurred on the warm side of the jet stream, about 250 miles from the axis and above the level of the axis. The depth of the turbulent layer was about 2,000 ft.

The simultaneous occurrence of high level turbulence and standing waves raises a question as to whether there is any connection between them, but no conclusive evidence one way or the other has been found so far. Further work on this aspect of turbulence might be desirable.

References

1. Hislop, G.S.; Clear air turbulence incident encountered by D-H "Comet" aircraft, 14th November, 1949. British European Airways R.S.D. Note No. 41, London, 1949.

2. Bannon, J.K.; Severe turbulence encountered by aircraft near jet streams. Met. Mag. London, 80, 1951, p. 262.

/3.

3. Hislop, G.S. Clear Air Turbulence over Europe. J.R. Aero Soc. 55, 1951, p. 199.

4. Radok, U; Severe turbulence at high levels over New South Wales. Met. Mag. London,83, 1954, p. 48.

5. Press, Schindler and Thompson; Summary of pilots' reports of clear air turbulence at altitudes above 10,000 ft. N.A.C.A. Report RML52 L30.a.

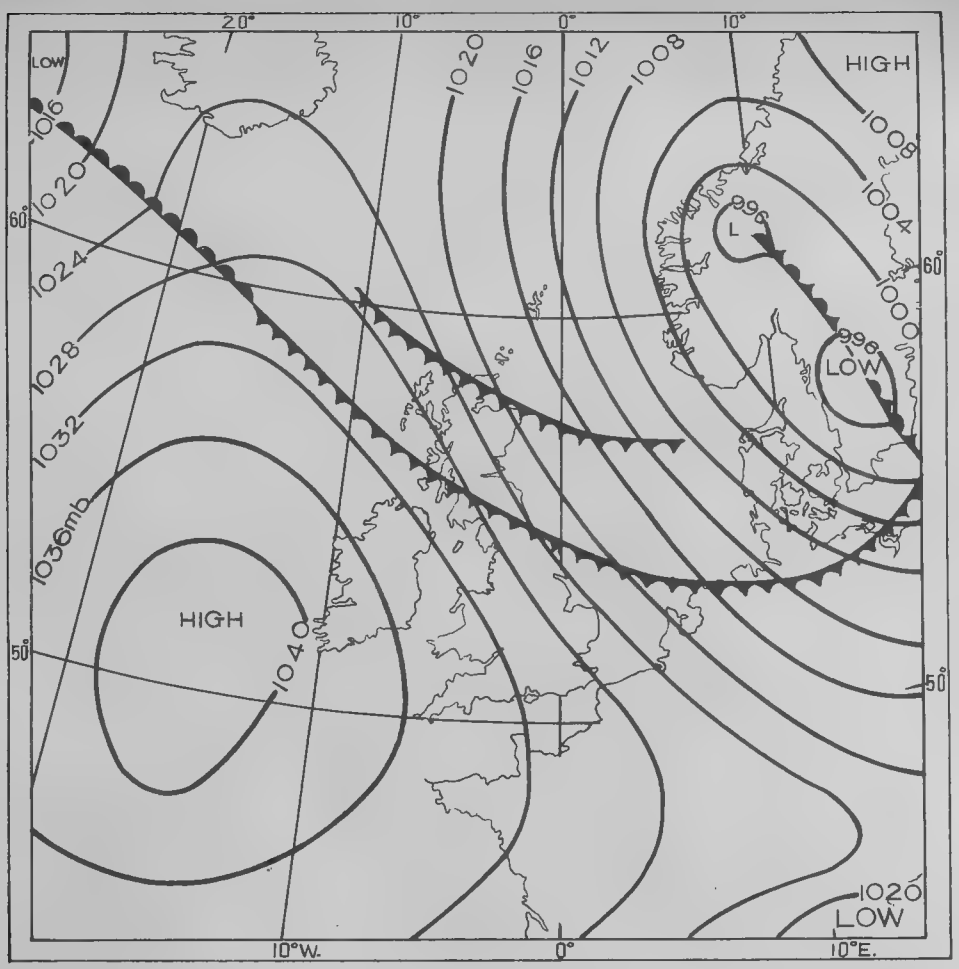

Fig.1 Surface synoptic chart for 0001 G.M.T. 15th April 1954

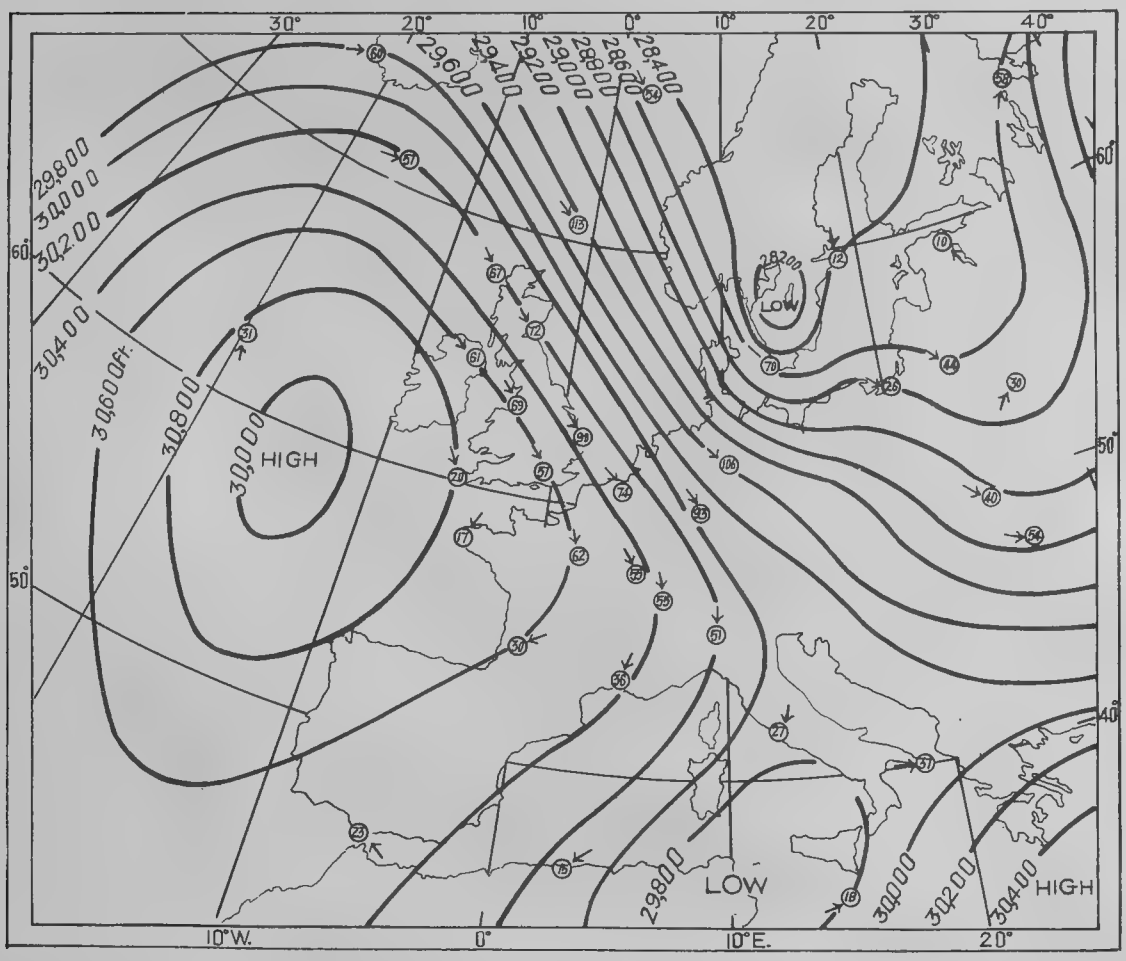

Fig.2 Contours of the 300mb. pressure level at about 0200 G.M.T. 15th April 1954

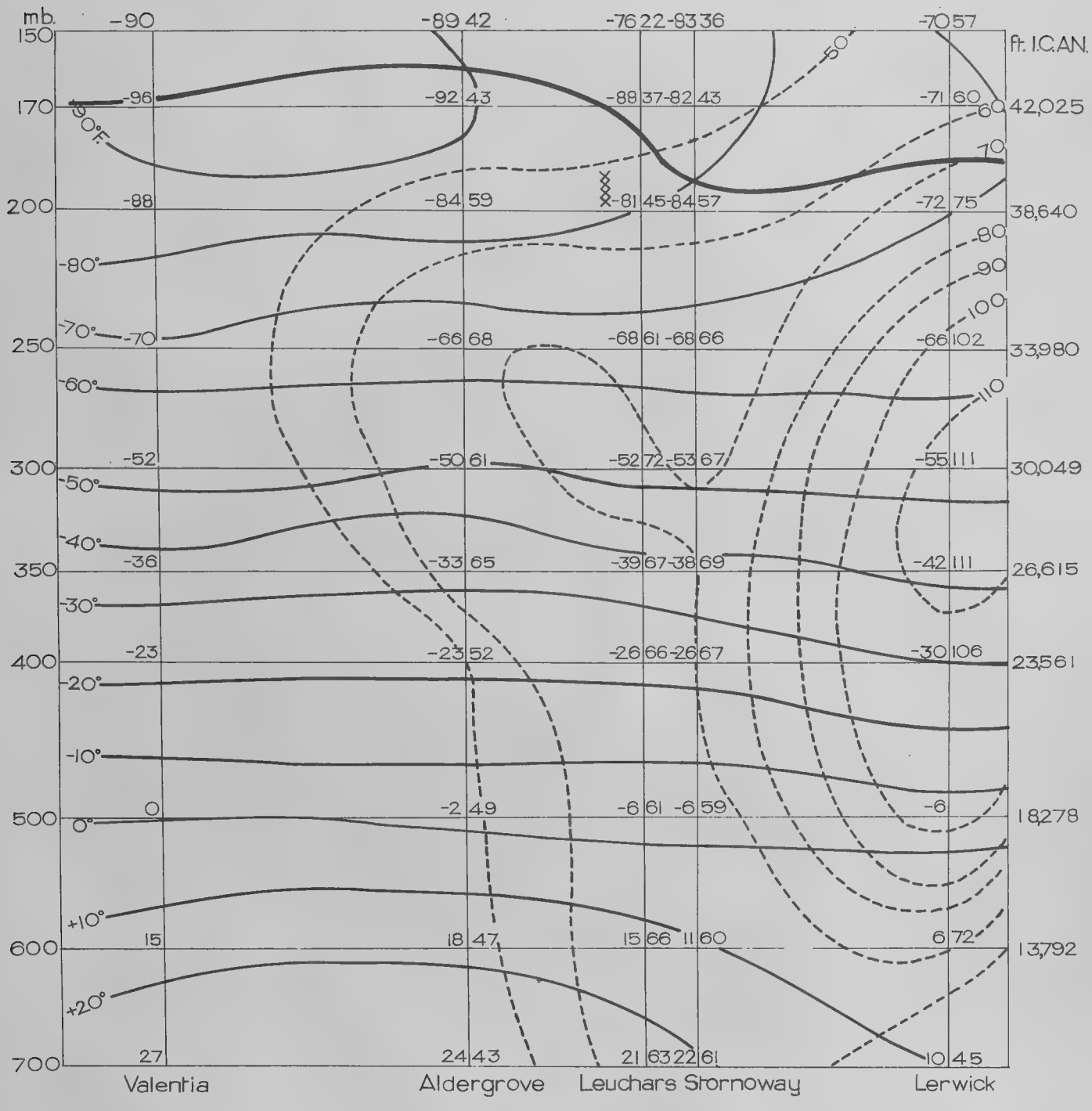

---Isopleths of wind velocity component from 310°(kt)
——Isotherms (°F.)
▬▬Tropopause surface
Exceptionally severe turbulence experienced at 2130 G.M.T. 14th April 1954

For each ascent the temperature °F. is given on the left, and component of the wind velocity from the direction 310° on the right, at the specified levels

Fig. 3 Cross section Valentia to Lerwick 0200 G.M.T. 15th April 1954

[illegible] by Mr. A.F. Jenkinson
[illegible]opy is available in the Library of
[illegible]

[illegible] in two parts. In the first part a formula is derived, [illegible] everywhere outside the tropics and at all levels between [illegible] and as a [illegible] multiplied by the product [illegible]

[illegible] written $\sigma = 0.[illegible] \cos \phi$ where σ is the [illegible] in kt., ϕ is the standard deviation of [illegible] the latitude.

[illegible] 300 mb. to 0.035 at 100 [illegible]

[illegible] to about 300 mb., in terms of [illegible]

At the time of issue this report has not been published. Any author desiring to quote this paper should refer to it as "A paper of the Meteorological Research Committee (London), M.R.P. No.869 by Mr. A.F. Jenkinson
A copy is available in the Library of the Meteorological Office."

M.R.P. 869
S.C.II/173
1st July, 1954.

AD 8329
MET

AIR MINISTRY

METEOROLOGICAL RESEARCH COMMITTEE

The relationship between standard deviation of contour height and standard vector deviation of wind, with practical applications

by
A.F. Jenkinson (Meteorological Office)

Summary

The paper is in two parts. In the first part a formula is derived, believed to be valid everywhere outside the tropics and at all levels between the top of the friction layer and about 300 mb., expressing standard vector deviation of wind as a universal constant multiplied by the product of the standard deviation of contour height and the cosecant of latitude.

The formula may be written $\sigma = 0.064 s \operatorname{cosec} \phi$ where σ is the standard vector deviation of wind in kt., s is the standard deviation of contour height in ft. and ϕ is the latitude.

A similar relationship is derived for levels between 300 mb. and 100 mb. We may write $\sigma = ks \operatorname{cosec} \phi$ where k is constant for different places but decreases uniformly with height from 0.064 at 300 mb. to 0.033 at 100 mb.

In the second part a formula is derived expressing the standard deviation of contour height, at levels up to about 300 mb., in terms of the standard deviation of surface pressure and the mean standard deviation of temperature.

The relationship $\sigma = 0.064 s \operatorname{cosec} \phi$ was then used to compute the standard vector deviation of wind at 300 mb. over the northern hemisphere during the winter season, December to February.

World seasonal maps of the standard vector deviation of wind above the friction layer have been prepared from corresponding maps of the standard deviation of surface pressure; and seasonal maps of standard vector deviation of wind at 500 mb. over part of the North Atlantic were prepared from maps of standard deviation of contour height computed directly from daily values.

Some discussion is given of the variation with height of standard vector deviation of wind.

1. The relationship between standard deviation of contour height and standard vector deviation of wind.

(a) Derivation of the relationship

Let P_1 and P_2 be two points close together on an isobaric surface. Let y be the distance between the points and h_1 and h_2 the contour heights of P_1 and P_2. Then if u is the mean component

/of

55 A-9

of geostrophic wind speed in the direction perpendicular to the line P_1P_2

$$\lambda y u = h_1 - h_2 \qquad (1)$$

where $\lambda = 2(\omega/g)\sin\phi$

ω is the earth's angular velocity, g is the acceleration due to gravity and ϕ is latitude.

Then $$s_{12}^2 = s_1^2 - 2r_{12}s_1s_2 + s_2^2 = \lambda^2y^2\sigma_u^2 \qquad (2)$$

where s_{12} is the standard deviation of the difference, $(h_1 - h_2)$, in contour heights, s_1 and s_2 are standard deviations of contour height at P_1 and P_2, r_{12} is the correlation coefficient between h_1 and h_2, and σ_u is the standard deviation of the velocities u.

Equation (2) may be re-arranged

$$s_{12}^2 = (s_1 - s_2)^2 + 2s_1s_2(1 - r_{12}) = \lambda^2y^2\sigma_u^2 \qquad (3)$$

In the limit, as $y \longrightarrow 0$
$r_{12} \longrightarrow 1$ $\qquad s_1 - s_2 \longrightarrow 0$

So it is not obvious what are the relative contributions of $(s_1 - s_2)^2$ and $2s_1s_2(1 - r_{12})$ to their sum s_{12}^2.

But consideration of actual examples shows that

$$(s_1 - s_2)^2 \ll 2s_1s_2(1 - r_{12})$$

The values of

$$s_{12}^2,\ s_1,\ s_2 \quad \text{and} \quad (s_1 - s_2)^2$$

were computed and are given in Table 1 for the point pairs

(i) Larkhill and Liverpool at 200 mb. for January, 1952.

(ii) Habbaniya and Bahrein at 300 mb. for January, 1950-52.

(iii) Malta and Benina at 300 mb. for January, 1950-52.

(iv) Tateno and Kagoshima at 200 mb. for October, 1951.

(v) Tateno and Kagoshima at 200 mb. for July, 1950-51.

TABLE 1. CORRESPONDING VALUES OF s_1, s_2, $(s_1 - s_2)^2$, s_{12}^2

Units of height	(i)	(ii)	(iii)	(iv)	(v)
	Tens of feet			metres	
s_1	66	31	43	100	90
s_2	68	29	33	76	59
$(s_1 - s_2)^2$	4	4	100	576	961
s_{12}^2	657	1444	1529	5853	10920

Authorities for data:- (i), (ii), (iii), MS. data available in the Upper Air Branch of the Meteorological Office; (iv) and (v), Tokyo, Aerological Data of Japan.

/In

In equation (3) divide throughout by y^2 and take limits as $y \longrightarrow 0$, when P_1 and P_2 approach the point P.

Then $s_1 \rightarrow s$ $s_2 \rightarrow s$ $(s_1 - s_2)^2/y^2 \longrightarrow (\partial s/\partial y)^2$ where s is the standard deviation of contour height at P.

Since in the examples quoted in Table 1 $(s_1 - s_2)^2$ makes only a small contribution to the value of s_{12}^2, it may reasonably be deduced that

$$\lim_{y \rightarrow 0} \frac{2s_1 s_2 (1 - r_{12})}{y^2}$$

exists and is very nearly equal to $\lambda^2 \sigma_u^2$. That is

$$\sigma_u^2 = 2s^2/\lambda^2 \lim_{y \rightarrow 0} (1 - r_{12})/y^2 \qquad (4)$$

Equation (4) at once arouses speculation about

$$\lim_{y \rightarrow 0} (1 - r_{12})/y^2$$

If the limit is the same for any direction of P_1P_2 then σ_u^2 is the same for all directions, since λ and s are dependent only on the position of P. That is, the wind distribution is circular, and

$$\sigma_u^2 = \sigma^2/2 \qquad (5)$$

where σ is the standard vector deviation of wind.

Conversely, if the wind distribution is circular, then

$\lim_{y \rightarrow 0} (1 - r_{12})/y^2$ is independent of direction.

It has been shown by Brooks and others (1950) that wind distributions are very nearly circular. So it follows that

$$\lim_{y \rightarrow 0} (1 - r_{12})/y^2$$

is the same for all directions.

It may then be asked whether the limit is the same for all levels, and whether indeed it is a universal constant. If the limit were a universal constant then equation (4), modified by equation (5), would take the form

$$\sigma = ks \operatorname{cosec} \phi \qquad (6)$$

where k is a universal constant, the same for all places and all levels.

(b) Verification of the relationship for levels up to 300 mb.

The validity of the hypothesis expressed in equation (6) has been tested on corresponding data of standard deviation of contour height and standard vector deviation of wind for eleven stations in the northern hemisphere. The data are given in Table 2. It should be noted that the validity of the hypothesis cannot be tested for stations in the tropics for two reasons: (i) the standard deviation of error in measurement of contour height may be of the same order as the true standard deviation of contour height, and hence the standard deviation of contour height given by the data may be altogether incorrect, (ii) the derivation of equation (6) depends on the geostrophic relationship, which does not apply near the equator.

/TABLE 2.

TABLE 2. CORRESPONDING VALUES OF STANDARD DEVIATION OF CONTOUR HEIGHT (FT./10) AND STANDARD VECTOR DEVIATION OF WIND (KT.)

STATION NAME LATITUDE PERIOD	MONTHS	850mb. s	850mb. σ	700mb. s	700mb. σ	500mb. s	500mb. σ	300mb. s	300mb. σ	200mb. s	200mb. σ	150mb. s	150mb. σ	100mb. s	100mb. σ	Authority
LERWICK * 60°8' 1948-50	Dec. - Feb.	44	29	47	29	57	38	77	51	72	38	68	29	70	26	a
	Mar. - May	35	24	41	26	53	35	69	47	59	33	57	25	60	21	
	June - Aug.	23	19	27	20	36	28	53	42	49	31	40	19	36	12	
	Sept.- Nov.	36	26	38	26	47	35	65	52	61	39	53	27	47	18	
LARKHILL * 51°12' 1948-50	Dec. - Feb.	35	29	40	32	53	42	69	56	65	43	56	31	49	25	a
	Mar. - May	28	22	33	26	43	34	72	49	50	36	43	24	42	18	
	June - Aug.	21	17	25	21	34	29	50	45	49	39	41	26	33	15	
	Sept.- Nov.	27	22	32	24	44	34	61	49	62	43	54	31	42	19	
GIBRALTAR 36°9' 1950-52	Jan.			26	23	35	32	48	45	53	39	50	26	44	20	b
	Apr.			16	19	20	28	30	39	31	33	25	22	27	18	
	July			13	15	16	21	23	29	28	33	30	26	27	19	
	Oct.			15	16	22	20	32	35	34	34	40	27	28	16	
MALTA 35°53' 1950-52	Jan.	19	19	23	21	30	31	43	48	39	37	39	29	31	22	b
	Apr.	15	18	18	18	25	26	38	36	35	32	30	23	29	18	
	July	7	11	8	16	11	18	20	22	29	27	33	22	23	15	
	Oct.	14	14	17	17	23	24	27	34	31	39	30	28	33	18	
NICOSIA 35°12' 1950-52	Jan.			18	18	28	29	39	43	39	39	33	26	31	21	b
	Apr.			20	17	29	24	42	37	41	30	40	24	42	17	
	July			8	9	11	16	21	22	24	24	26	21	28	18	
	Oct.			10	15	14	18	24	27	30	28	33	26	31	16	
HABBANIYA 33°22' 1950-52	Jan.			16	15	24	29	31	40	37	29	37	29	32	17	b
	Apr.			14	17	24	26	35	34	40	34	38	29	35	19	
	July			10	14	13	16	16	19	19	21	24	20	29	15	
	Oct.			9	14	17	15	21	25	28	30	28	24	26	17	
BENINA 32°6' 1950-52	Jan.			15	20	23	28	33	43	36	39	35	24	33	23	b
	Apr.			17	16	23	25	30	35	37	33	34	27	29	18	
	July			9	14	10	14	18	22	24	23	27	22	31	15	
	Oct.			11	18	13	19	22	27	29	29	30	24	29	15	
BAHREIN 26°14' 1950-52	Jan.			13	16	18	23	29	36	30	33	29	22	29	18	b
	Apr.			9	15	13	20	22	30	26	38	27	31	25	21	
	July			8	15	9	13	11	14	16	14	20	15	27	15	
	Oct.			7	13	9	14	18	20	19	21	21	19	26	18	
WAKKANAI 45°25' 1952	Jan. - Feb.	18	14	20	19	27	27									c
	July - Aug.	15	13	18	15	14	19									
TATENO 36°3' 1950-52	Jan.			23	22	32	34	42	48							c
	Apr.			21	25	32	40	47	48							
	July			16	15	19	24	24	34							
	Oct.			19	18	26	27	35	38							
MARCUS I 24°18' 1952	Jan. - Feb.			9	15	10	20	14	27							c
	July - Aug.			7	12	8	15	11	17							

NOTE * Values of s and σ are mean monthly values for each season.

AUTHORITIES (a) Published values of s and σ ; Meteorological Office, M.O.555, Parts 1, 2 and 3.

(b) Values of s and σ were computed from manuscript tabulations of contour height and upper wind available in the Upper Air Branch of the Meteorological Office.

(c) Values of s and σ were computed from published tabulations of contour height and upper winds; Tokyo, Aerological Data of Japan.

Combining together data from all stations, a separate graph for each of the levels 850, 700, 500, 300, 200, 150 and 100 mb. was drawn with σ plotted against s cosec ϕ . These are shown in Fig. 1 (a, b, c, d, e, f, g). The units of speed are kt., and of contour height, ft.

(i) The data for 850, 700, 500 and 300 mb.

Very good fits for the data at each of the levels 850, 700, 500 and 300 mb. are provided by straight lines passing through the origin. These are shown in Fig. 1 (a, b, c, d). The mean error in σ at 300 mb. is only eight per cent., that is $1\frac{1}{2}$ kt. for σ = 20 kt. and 4 kt. for σ = 50 kt. The best fitting straight lines for the individual levels 850, 700, 500 and 300 mb. are:-

850 mb. $\sigma = 0.062\ s\ \text{cosec}\ \phi$

700 mb. $\sigma = 0.063\ s\ \text{cosec}\ \phi$

500 mb. $\sigma = 0.065\ s\ \text{cosec}\ \phi$

300 mb. $\sigma = 0.064\ s\ \text{cosec}\ \phi$

It will thus be seen that the straight line

$$\sigma = 0.064\ s\ \text{cosec}\ \phi$$

gives an excellent fit to corresponding values of σ and s at each of the levels 850, 700, 500 and 300 mb., showing that the relationship between σ and s is well expressed by equation (6), with k = 0.064, for widely different latitudes and at all levels from 850 to 300 mb. The straight line $\sigma = 0.064\ s\ \text{cosec}\ \phi$ also provides an excellent fit for each station separately, with data for the levels 850, 700, 500 and 300 mb. combined.

The data show some slight seasonal variation in the value of k, with k appearing to have a rather higher value in summer than in the other seasons; but this may be partly accounted for by errors in the summer standard deviations of contour height. The variation is least at 300 mb.

The seasonal variations in k; (1) for each station separately, with all levels taken together; (2) for each level separately, with all stations taken together; (3) for all stations combined and all levels taken together, are shown in Table 3.

/TABLE 3.

TABLE 3. SEASONAL AND ANNUAL VARIATIONS IN THE VALUE OF k FOR THE LEVELS OF 850, 700, 500, 300 MB.

		Winter	Spring	Summer	Autumn	Year
(1)	Lerwick	.057	.058	.065	.065	.061
	Larkhill	.063	.064	.066	.062	.064
	Gibraltar	.056	.077	.074	.061	.062
	Malta	.062	.060	.085	.065	.065
	Nicosia	.062	.050	.068	.064	.062
	Habbaniya	.066	.059	.070	.064	.066
	Benina	.068	.062	.071	.076	.068
	Bahrein	.056	.066	.067	.062	.059
	Wakkanai	.065		.070		.068
	Tateno	.064	.066	.073	.062	.065
	Marcus I	.077		.070		.074
(3)		.062	.062	.070	.064	.064
(2)	850 mb.	.060	.059	.070	.062	.062
	700 mb.	.059	.061	.070	.066	.063
	500 mb.	.062	.063	.073	.063	.065
	300 mb.	.064	.062	.068	.065	.064

(1) Each station separately, all levels combined.
(2) All stations combined, each level separately.
(3) All stations combined, all levels combined.

(c) The form of the relationship for levels above 300 mb.

(i) The data for 200, 150 and 100 mb.

Fig. 1 (e, f, g) shows the data for each level separately, with the best fitting straight lines drawn. The fits are good, and for each level separately a relationship between σ and s

$$\sigma = ks \operatorname{cosec} \phi$$

holds good, but with different values for k at each level, and different also from the value k = 0.064 which holds good for every one of the levels 850, 700, 500 and 300 mb.

The best-fitting straight lines for the 200, 150 and 100 mb. levels give values for k equal to 0.054, 0.043 and 0.033 respectively. The seasonal and annual variation of k at each level is shown by the data of Table 4.

TABLE 4. SEASONAL AND ANNUAL VARIATIONS IN THE VALUE OF k FOR THE LEVELS OF 200, 150, 100 MB.

		200 mb.	150 mb.	100 mb.
(1)	Winter	.050	.039	.034
	Spring	.053	.043	.033
	Summer	.057	.044	.032
	Autumn	.057	.045	.033
	Year	.054	.043	.033
(2)	Lerwick	.051	.040	.032
	Larkhill	.056	.045	.036
	Gibraltar	.056	.041	.033
	Malta	.060	.045	.037
	Nicosia	.052	.044	.032
	Habbaniya	.051	.044	.031
	Benina	.053	.041	.031
	Bahrein	.051	.040	.030

(1) Seasonal and annual values, all stations combined.
(2) Annual values, each station separately.

/(ii)

(ii) Variation of k with height

The best fitting values of k were plotted in Fig. 2 as a graph of height (logarithm of pressure) against k.

The variation of k with height is seen to be represented very well by two straight lines, k constant and equal to 0.064 up to 300 mb., and k decreasing thereafter uniformly with height to a value of 0.033 at 100 mb.

Brooks and others (1950) have shown that standard vector deviation usually increases up to a certain level, above which it decreases. This level of discontinuity is associated with the tropopause, but because of variations in tropopause height it is usually below the average level of the tropopause.

The level of 300 mb. may be considered as the mean level of discontinuity for the stations examined.

(d) Conclusion

It may be concluded that at all levels from the top of the friction layer to about 300 mb. there is a universal relationship between the standard vector deviation of wind and the standard deviation of contour height which may be written in the form of equation (6)

$$\sigma = 0.064 \, s \, \operatorname{cosec} \phi \, .$$

It may also be asserted that above 300 mb. a similar relationship is approximately true, $\sigma = ks \operatorname{cosec} \phi$, with k now varying with height and taking values which lie on the straight line of Fig. 2, that is,

$$k = 0.064 - 0.028 \ln (300/p)$$

where p is the pressure in mb.

2. Some practical applications.

(a) Introduction

Sufficient wind data are not available to enable maps of standard vector deviation of wind to be drawn for many areas.

The results obtained in part one may be used to estimate standard vector deviation of wind from standard deviation of contour height. Maps of standard deviation of contour height can be prepared from daily values of contour height read from working charts. This procedure is however rather laborious, and an alternative method of deriving standard deviation of contour height at levels up to 300 mb. is given in the following section.

/(b)

(b) Preliminary - an expression for the standard deviation of contour height at levels up to 300 mb.

If h is the contour height of the pressure surface p
h_o is the height of the 1000 mb. surface
h' is the height from 1000 mb. to pressure p
R is the gas constant
θ is the mean (log p, T) temperature of the column 1000 mb. to p
T_o is the temperature at 1000 mb.
p_o is the pressure in mb. at mean sea level
$\Delta p_o = p_o - 1000$

Then $h = h' + h_o$ and

$$\left.\begin{aligned} h' &= (R/g)\theta \ln (1000/p) \\ h_o &= (R/g)T_o \ln(p_o/1000) = (R/g)T_o(\Delta p_o/1000) \end{aligned}\right\} \quad (7)$$

neglecting in the second of these equations terms of order $(\Delta p_o/1000)^2$.

Now $$s^2 = (s')^2 + 2rs's_o + s_o^2 \quad (8)$$

where s' and s_o are the standard deviations of h' and h_o respectively; and r is the correlation coefficient between h' and h_o. r is small, and is found to have a value of very nearly 0.35.

From equation (7) we derive

$$s' = (R/g)\sigma_\theta \ln(1000/p) \quad (9)$$

where σ_θ is the standard deviation of the mean temperatures θ. Also, since the proportional variation of T_o is very small compared with that of Δp_o we can write, with sufficient accuracy,

$$s_o = (R/g)\overline{T}_o(\sigma_p/1000) \quad (10)$$

where $\overline{T}_o$ is the average temperature at 1000 mb. and σ_p is the standard deviation (mb.) of surface pressure.

Consideration of actual examples shows that the error introduced by ignoring the variation of T_o is about one per cent., and this is less than the error in the computed values of h_o.

If we use the notation $\sigma_T(\pi)$ for the standard deviation of temperature at fixed pressure levels π between 1000 mb. and p, and write σ_T for the root mean square of the quantities $\sigma_T(\pi)$; then by the usual algebra of analysis of variance it can be shown that σ_θ is less than σ_T.

For pressure levels p above about 700 mb., an examination of data for the summer and winter seasons for Larkhill and Malta shows the value of the ratio σ_θ/σ_T to be nearly 0.85. Substituting this value for the ratio in equation (9) we have

$$\begin{aligned} s' &= 0.85(R/g)\ln(1000/p)\,\sigma_T \\ &= 0.85\, s'' \qquad \text{defining } s'' \end{aligned} \quad (11)$$

Substituting the known value 0.35 for r in equation (8)

$$s^2 = (s')^2 + 0.7s's_o + s_o^2 \quad (12)$$

that is, $$s^2 = 0.72(s'')^2 + 0.6s''s_o + s_o^2 \quad (13)$$

Equation (13) was used to compute s at 300 mb. for several places in different seasons. These computed values are compared with actual values in Table 5.

/TABLE 5.

TABLE 5. MEANED MONTHLY VALUES OF σ_T, s_o, s_{300}

		σ_T (°C)	s_o	s_{300} ft./10	computed s_{300}
Lerwick	Dec. - Feb.	5.2	44	77	78
1946-50	Mar. - May	5.1	35	69	71
	June - Aug.	3.9	23	53	51
	Sept. - Nov.	4.9	36	65	69
Larkhill	Dec. - Feb.	5.1	35	69	71
1946-50	Mar. - May	4.4	26	56	58
	June - Aug.	3.8	20	50	48
	Sept. - Nov.	4.3	27	61	58
Malta	Jan.	3.4	20	43	44
1950-52	Apr.	3.0	17	38	39
	July	2.0	8	20	24
	Oct.	2.3	13	27	30
Habbaniya	Dec. - Feb.	3.6	13	38	42
1948-50	Mar. - May	3.6	12	37	41
	June - Aug.	1.9 *	8	20	23
	Sept. - Nov.	2.4	8	24	27

Note * July, 1951-52.

Authorities - Malta, and σ_T for Habbaniya, July, 1951-52: computed from MS. data available in the Upper Air Branch of the Meteorological Office; Lerwick, Larkhill, Habbaniya: Meteorological Office, M.O.555, Parts 1, 2 and 3.

The computed values are very good estimates and it may be concluded that the expression for s in equation (13) gives good estimates for the standard deviation of contour height at levels up to about 300 mb.

(c) Estimation of standard vector deviation of the wind above the friction layer

Equation (6)

$$\sigma = 0.064\ s\ \mathrm{cosec}\ \phi$$

can be used to give σ_o, the standard vector deviation of the wind above the friction layer, by substituting s_o for s.

$$\sigma_o = 0.064\ s_o\ \mathrm{cosec}\ \phi \qquad (14)$$

or, combining this equation with equation (10),

$$\sigma_o = 0.00614\ \bar{T}_o\ \sigma_p\ \mathrm{cosec}\ \phi \qquad (15)$$

where the units are

σ_o in kt., $\bar{T}_o$ in °K., σ_p in mb.

Brockmöller (1911) has published data of average monthly pressure range for many stations all over the world. Schumann and Rooy (1951) have published monthly values for the northern hemisphere of standard deviation of daily pressure at points of a grid of latitude and longitude. The values were computed from pressure readings derived from the daily maps of the United States Weather Bureau, analysed once daily, for the period 1929-38.

/The

The Weather Bureau, South Africa, has published (1952-53) in Notos daily values of mean sea level pressure for the southern hemisphere at points of a grid of latitude and longitude for the period January, 1951 to August, 1952.

Brockmöller's data may readily be converted to monthly standard deviation of daily pressure by dividing by the factor 3.7. The mean range in samples of 30 from a normal population is 4.09 times the standard deviation (Tippett, 1925), but a test with data supplied by the Marine Branch of the Meteorological Office for the weather ships Jig and Item, and with data for stations in Europe, the Mediterranean and Australia gave dividing factors with little variation about a mean of 3.7.

From similar considerations the Notos data were used to give mean seasonal values of standard deviation of daily pressure for the southern hemisphere by dividing mean seasonal values of 10-day pressure ranges by the factor 2.7.

Brockmöller's converted data, the converted Notos data, and the data of Schumann and Rooy were used in equation (15) to give a very large number of values of σ_o for all four seasons over the northern hemisphere between 15°N. and 70°N. and the southern hemisphere between 15°S. and 55°S.

In the tropics use was made of unpublished seasonal maps of the standard vector deviation of surface wind over the oceans, prepared by Mrs. A.H.R. Goldie (Miss N. Carruthers) from data used by the Marine Branch in the construction of charts of surface wind. Since over the oceans the surface wind is approximately two thirds of the wind above the friction layer, the standard vector deviation of the surface wind over the tropical oceans was taken to be approximately two thirds of the standard vector deviation of the wind above the friction layer, with corresponding sets of isopleths forming geometrically similar patterns. This approximate relationship held good in extra-tropical ocean areas, and its use would be expected to give very little error in the tropics, where σ_o is relatively low.

World seasonal maps of σ_o are reproduced in Figs. 3 to 6. The isopleths are given at intervals of 4 kt., but intermediate isopleths, or parts of intermediate isopleths, are drawn as pecked lines in areas where interpolation is thereby made easier.

(d) Estimation of standard vector deviation of wind at 300 mb.

Equations (6) and (13) may be used to give the standard vector deviation of wind at levels up to 300 mb.

Combining them

$$\sigma = 0.064\ (0.72 s''^2 + 0.6 s'' s_o + s_o^2)^{1/2} \operatorname{cosec} \phi \qquad (16)$$

or $$\sigma = (\sigma_o^2 + 0.6 \sigma_o \sigma'' + 0.72 \sigma''^2)^{1/2} \qquad (17)$$

writing σ'' for $0.064\ s''\ \operatorname{cosec} \phi$.

Equation (17) has been used to compute standard vector deviations of wind at 300 mb. in January over the northern hemisphere.

The simplification was introduced of using the standard deviation of temperature at 500 mb., σ_T (500), instead of σ_T , after checking in several areas that this was justifiable during this season. World maps of standard deviations of temperature have been prepared in the Upper Air Branch of the Meteorological Office; and the map for January at 500 mb. was put at my disposal.

/Substituting

Substituting numerical values in the expression for σ'' we obtain

$$\sigma'' = 7.29\ \sigma_T\ \text{cosec}\,\phi \qquad (18)$$

where σ, σ_o, σ'' are in kt. and σ_T or its approximate equivalent $\sigma_T(500)$ is in °C.

From isopleths of $\sigma_T(500)$ values were read off at 30°N., 40°N., 50°N., 60°N. at intervals of 20° longitude. For the points at 30°N. and 40°N. the values of $7.29\ \sigma_T\ (500)\ \text{cosec}\,\phi$ were computed; for 50°N. and 60°N. the values of standard vector deviation at 300 mb. were estimated to have the same value as at 340 mb., since standard vector deviation reaches its maximum value below the tropopause. (Brooks and others, 1950). So at 50°N. and 60°N. values of $6.6\sigma_T(500)\ \text{cosec}\,\phi$ were computed.

At the corresponding points 30° (10°) 60°N., 180°W. (20°) 180°W., values of σ_o were read off. From equation (17) the values of σ_{300}, the standard vector deviation at 300 mb., were computed for the 72 points of this grid. They were plotted, and isopleths of standard vector deviation were drawn. They are shown in Fig. 7.

Some standard vector deviations computed along with vector means for a previous work (Jenkinson, 1954) were added (figures in circles), and standard vector deviations computed from cirrus cloud observations (figures in squares). These were used to draw isopleths south of 30°N.

(e) Estimation of standard deviation of wind at levels above 300 mb.

There appears to be no simple way of deriving standard deviation of contour height, at levels above about 300 mb., from data of standard deviation of surface pressure and standard deviation of temperature at given levels.

And so to use the relationship derived in the first part to estimate standard vector deviation of wind at say 100 mb. we need actual values of s, the standard deviation of contour height, to insert in the formula

$$\sigma = 0.033\ s\ \text{cosec}\,\phi \qquad (19)$$

($k = 0.033$ for the 100 mb. level)

Working charts of contours at this level could be used to obtain frequency distributions of contour height at a network of points; and the standard deviation of contour height could then be computed for this network, making allowance for the standard error in contour heights.

This method could of course be used to derive values of s at levels up to 300 mb. It may perhaps be more accurate to use values of s obtained directly in this way than indirectly from equation (13); but the time taken is very much longer.

(f) An example of the mapping of σ at 500 mb. from maps of s prepared directly from daily values of contour height

As an example of the direct transformation of maps of s to maps of σ, average seasonal maps of standard vector deviation of wind at 500 mb. over the North Atlantic (35-65°N., 70°W.-10°E.) were prepared from the corresponding maps of s. From the 500 mb. working charts of the Central Forecasting Office of the Meteorological Office values of contour height were read off to the nearest hundred feet. Charts for January, April, July and October at 1400 G.M.T.

/for

for the period 1949-53 were used, and readings were made at points of the network 35°N. (5°) 65°N., 80°W. (10°) 30°E.

At a selection of points values of s were computed directly. At the other points of the grid values of s were computed from values of the average ten-day range. The formula $\sigma = 0.064\ s\ \mathrm{cosec}\ \phi$ was then used to compute σ at the grid points.

The maps of standard vector deviation of wind are shown in Fig. 8.

(g) Variation with height of standard vector deviation of wind

Clayton (1896), in his discussion of the cloud observations at Blue Hill, said "The velocity of circulation per unit mass is approximately the same at all heights..... This is what would be expected provided the same mass of air at each cloud level flows through the same vertical section".

The result was confirmed by other writers who worked with the data obtained during the International Cloud Year 1896-97. Egnell (1903) concluded "The mass of air displaced by the wind is constant at all heights. The mean (scalar) speed varies inversely with air density".

Brooks and others (1950) have described the relationship between scalar and vector wind speeds and standard vector deviation, and have enunciated the rule that the product of standard vector deviation with density is constant with height up to a level somewhat below the tropopause; and have suggested that in the tropics the rule holds for levels up to 200 mb. They give the ratios

$$\sigma_{500}/\sigma_{700} = 1.32$$

$$\sigma_{300}/\sigma_{700} = 2.0$$

$$\sigma_{200}/\sigma_{700} = 2.8 \text{ where the rule holds.}$$

Table 6 gives standard vector deviation of wind for representative seasonal months for temperate, sub-tropical and tropical places:

TABLE 6. STANDARD VECTOR DEVIATION (KT.)

Station	LARKHILL				MALTA				HABBANIYA			
Months	Wi.	Sp.	Su.	Au.	Jan.	Apr.	July	Oct.	Jan.	Apr.	July	Oct.
700 mb.	32	26	21	24	21	18	16	17	15	17	14	14
500 mb.	42	34	29	34	31	26	18	24	29	26	16	15
300 mb.	56	49	45	49	48	36	22	34	40	34	19	25

Station	BAHREIN				ADEN				NAIROBI			
Months	Jan.	Apr.	July	Oct.	Jan.	Apr.	July	Oct.	Jan.	Apr.	July	Oct.
700 mb.	16	15	15	13	13	9	9	8	10	8	11	8
500 mb.	23	20	13	14	14	11	10	10	11	7	13	10
300 mb.	36	30	14	20	20	18	8	13	16	11	16	13
200 mb.	33	38	14	21	27	19	10	16	20	15	24	17

Authorities and periods for data - Larkhill, 1948-50: London, Meteorological Office, M.O.555, Parts 1, 2 and 3. Upper Air Data. Values for other stations were computed from manuscript data for the period 1950-52, available in the Upper Air Branch of the Meteorological Office.

/Considering

Considering the validity of the rule up to 300 mb., it will be seen that it fails for Malta and Habbaniya in July; for Bahrein and Aden in July and October; and that it does not work very well in any month for Nairobi.

Considering the validity of the rule up to 200 mb., Bahrein and Aden ought to provide a test in July, and Nairobi throughout the year. The rule fails in each case, although at Nairobi the rule would provide a good estimate of the 200 mb. values given those at 300 mb.

It would appear from Table 6 that in tropical air the standard vector deviation of wind increases more slowly with height than would be indicated by the rule.

From equations (6) and (14) we derive

$$\sigma/\sigma_o = s/s_o \qquad (20)$$

This is certainly true in extra-tropical regions, since equation (6) is valid; but it seems to hold good in the tropics, where in general s varies slowly with height and σ does also.

The slow variation of s with height in the tropics might be expected from equation (13)

$$s^2 = 0.72\, s''^2 + 0.6\, s''s_o + s_o^2$$

since s'' is proportional to the standard deviation of temperature, which becomes very small in the tropics.

REFERENCES

Brockmöller, W.	1911	Aus dem Archiv der Deutschen Seewarte, 34, Nr. 4.
Brooks, C.E.P.; Durst, C.S.; Carruthers, N.; Dewar, D. and Sawyer, J.S.	1950	Geophys. Mem. Met. Off., London, No. 85.
Clayton, H.H.	1896	Annals of the Blue Hill Meteorological Observatory, 30, Part 4.
Egnell, A.	1903	Comptes Rendus, 136, p.358.
Jenkinson, A.F.	1954	Meteorological Research Papers, London. No. 823 (Revised).
Schumann, T.E.W. and van Rooy, M.P.	1951	Union of South Africa, Weather Bureau.
South Africa, Weather Bureau	1952-53	Notos, Vol. 1 and Vol. 2., Nos. 1, 2/3.
Tippett, L.H.C.	1925	Biometrika, 17, p.364.

Graphs to show the relation between
s cosec ø and σ at various levels

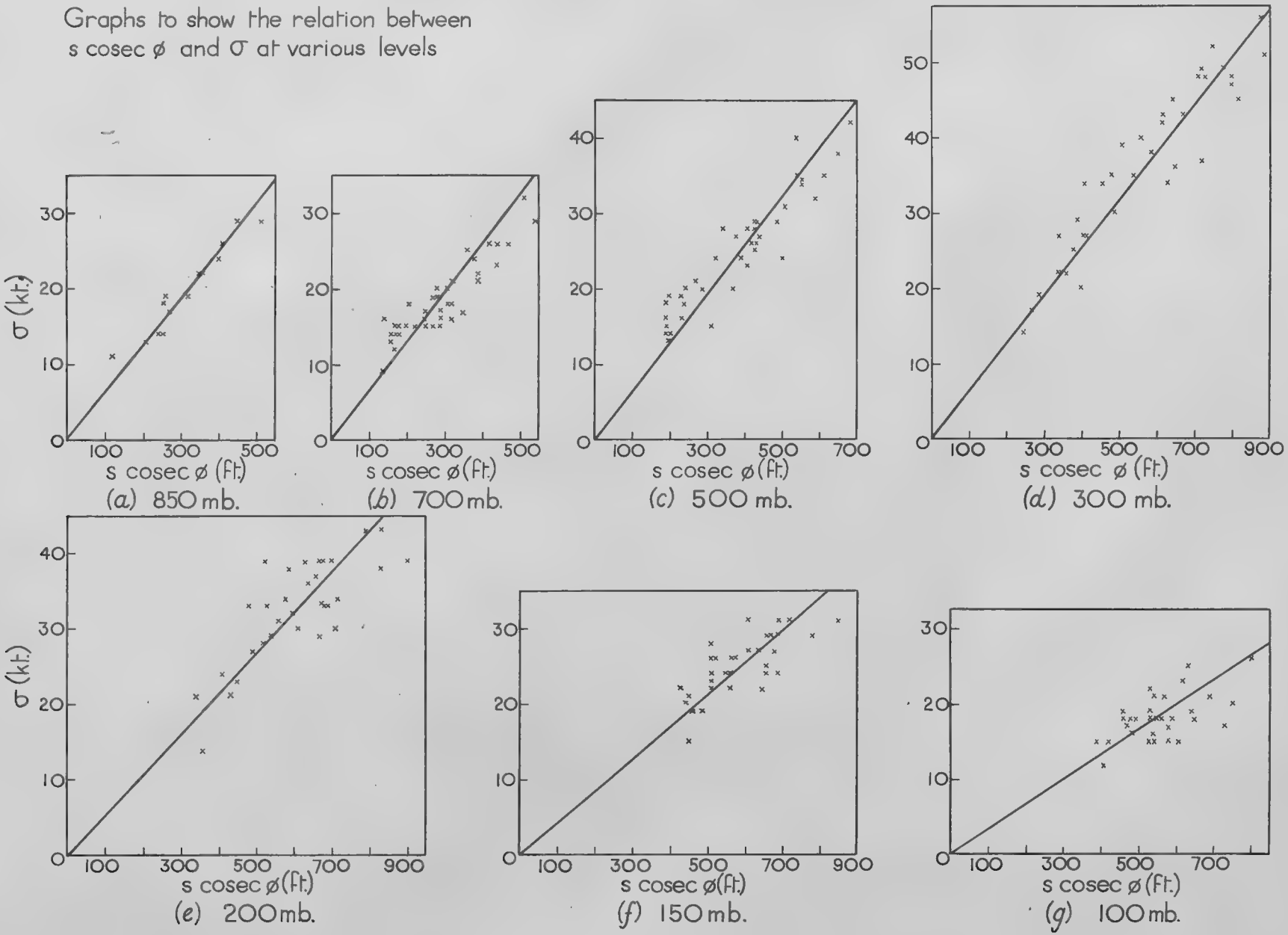

FIG. 1 (*a,b,c,d,e,f,g*)

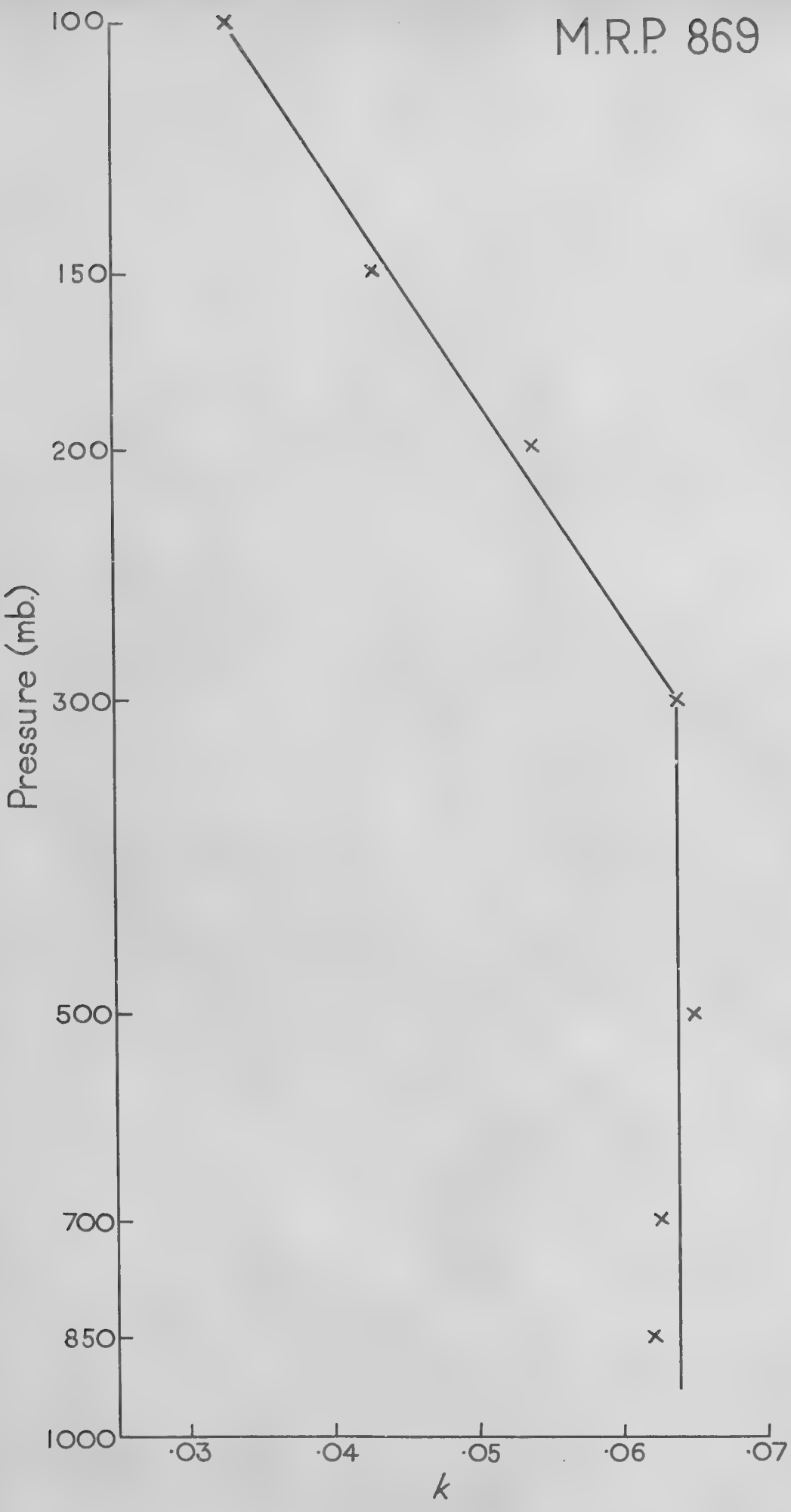

Fig. 2 Variation of k with height

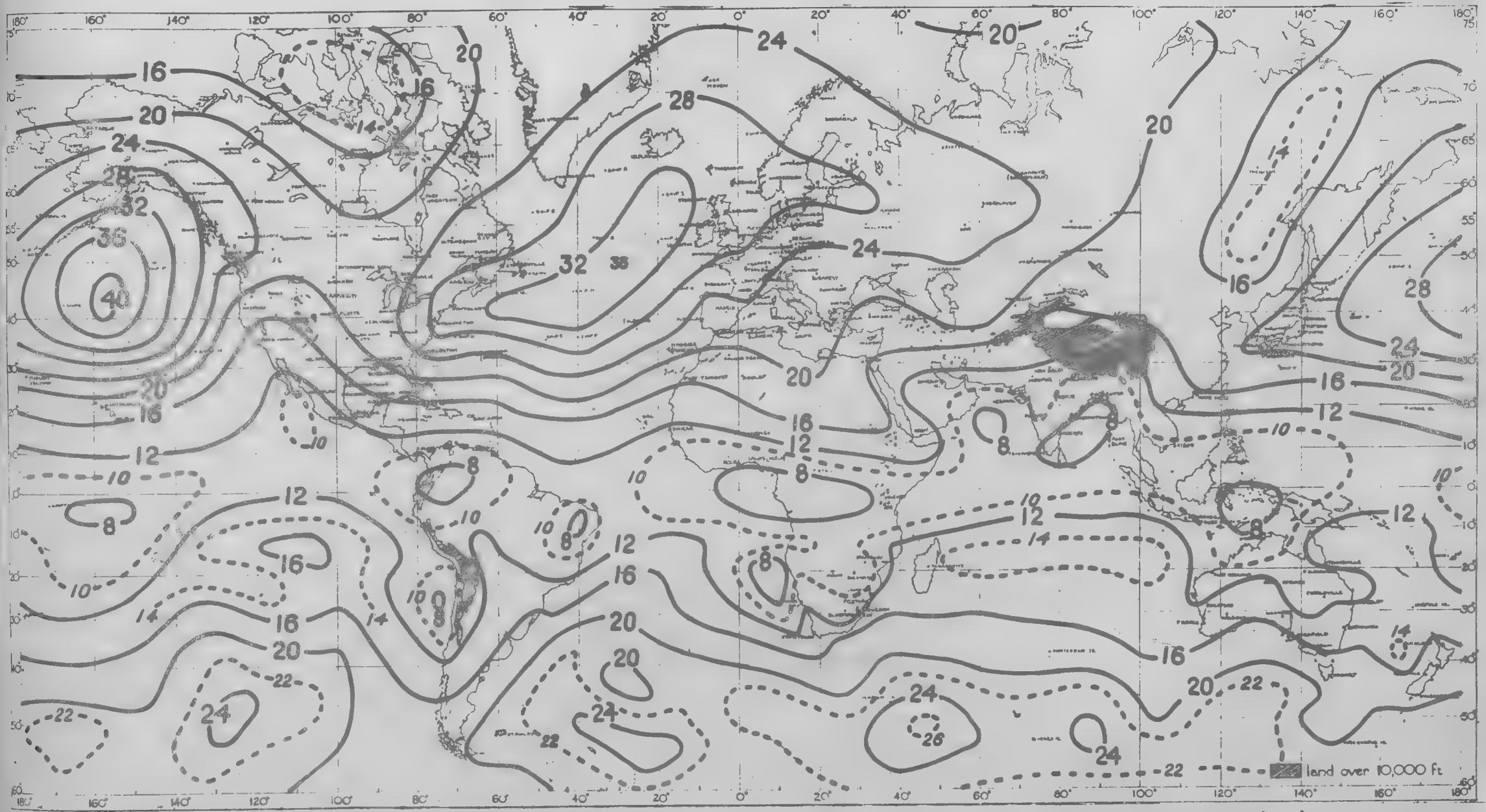

FIG. 3 ESTIMATED STANDARD VECTOR DEVIATION OF THE WIND ABOVE THE FRICTION LAYER (KT.) — JANUARY

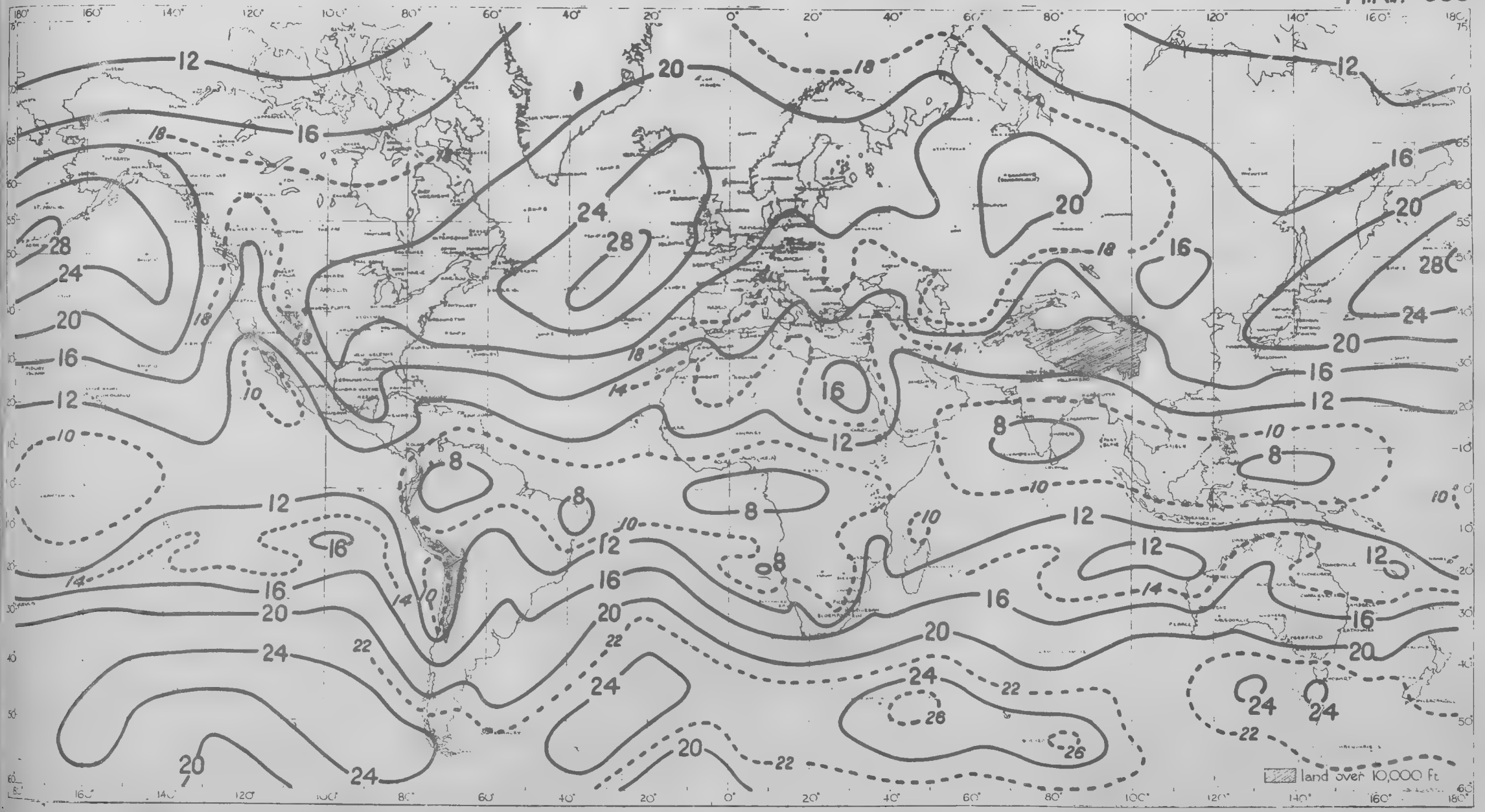

FIG. 4 ESTIMATED STANDARD VECTOR DEVIATION OF THE WIND ABOVE THE FRICTION LAYER (KT.) – APRIL

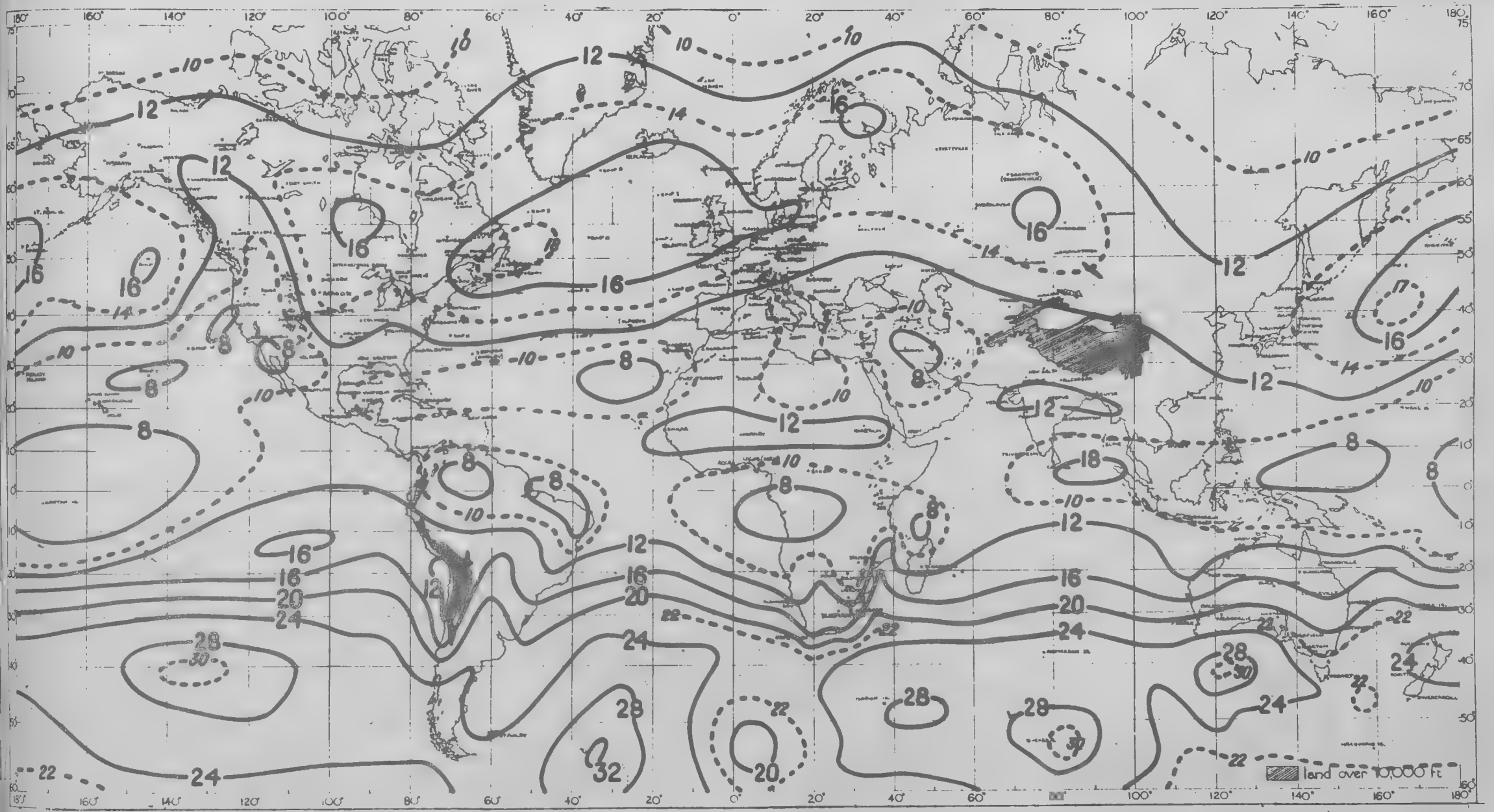

FIG. 5 ESTIMATED STANDARD VECTOR DEVIATION OF THE WIND ABOVE THE FRICTION LAYER (KT.) — JULY

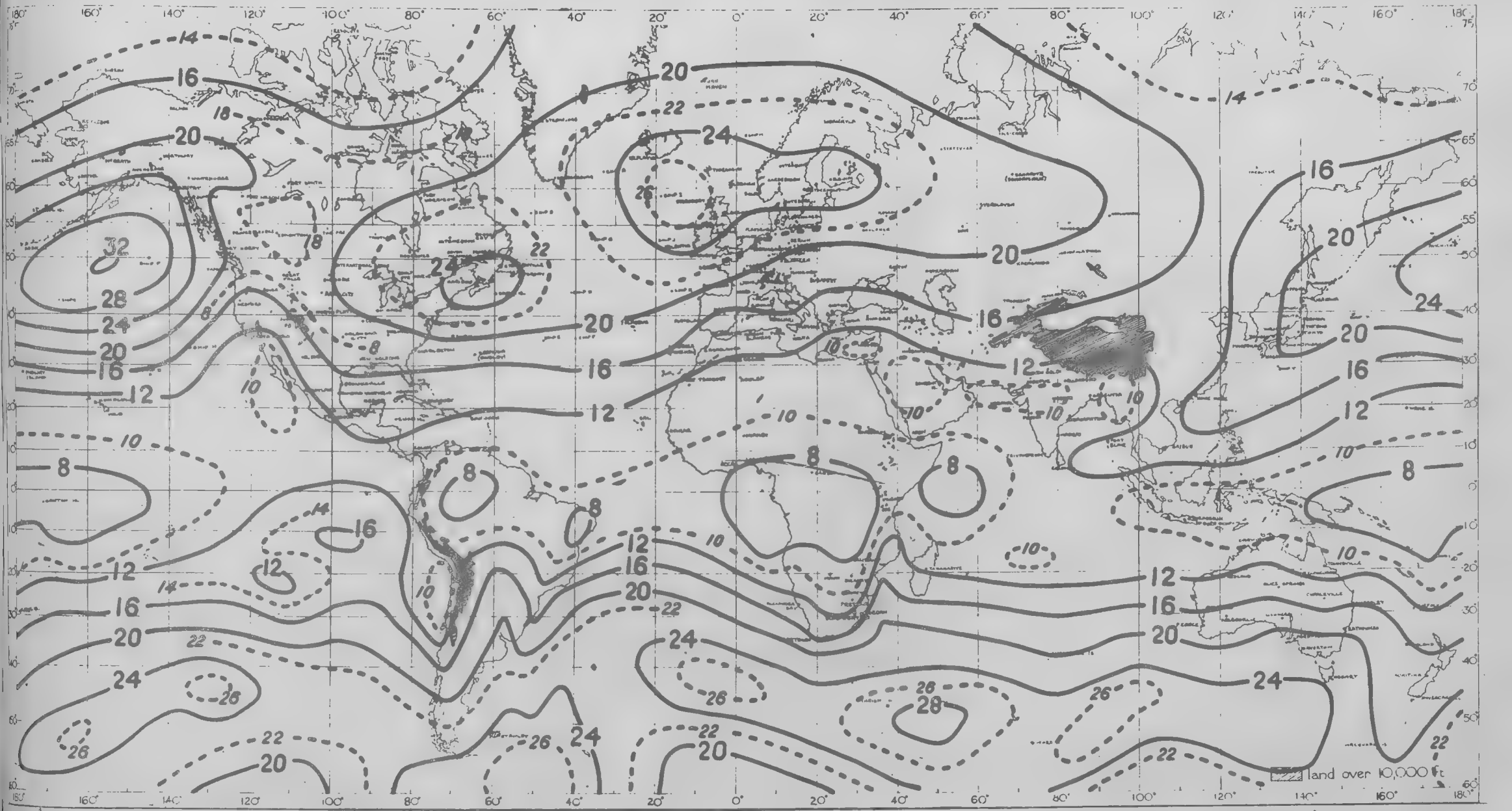

FIG. 6 ESTIMATED STANDARD VECTOR DEVIATION OF THE WIND ABOVE THE FRICTION LAYER (KT.) – OCTOBER

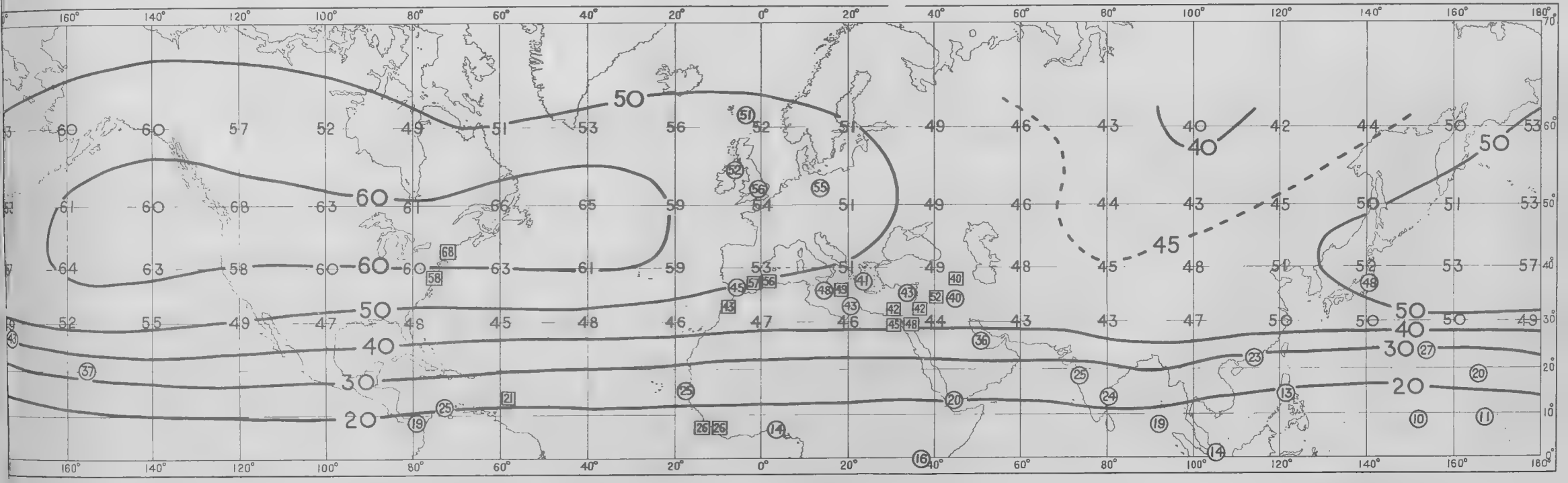

Fig. 7 Estimated standard vector deviation (kt.) at 300 mb. — January

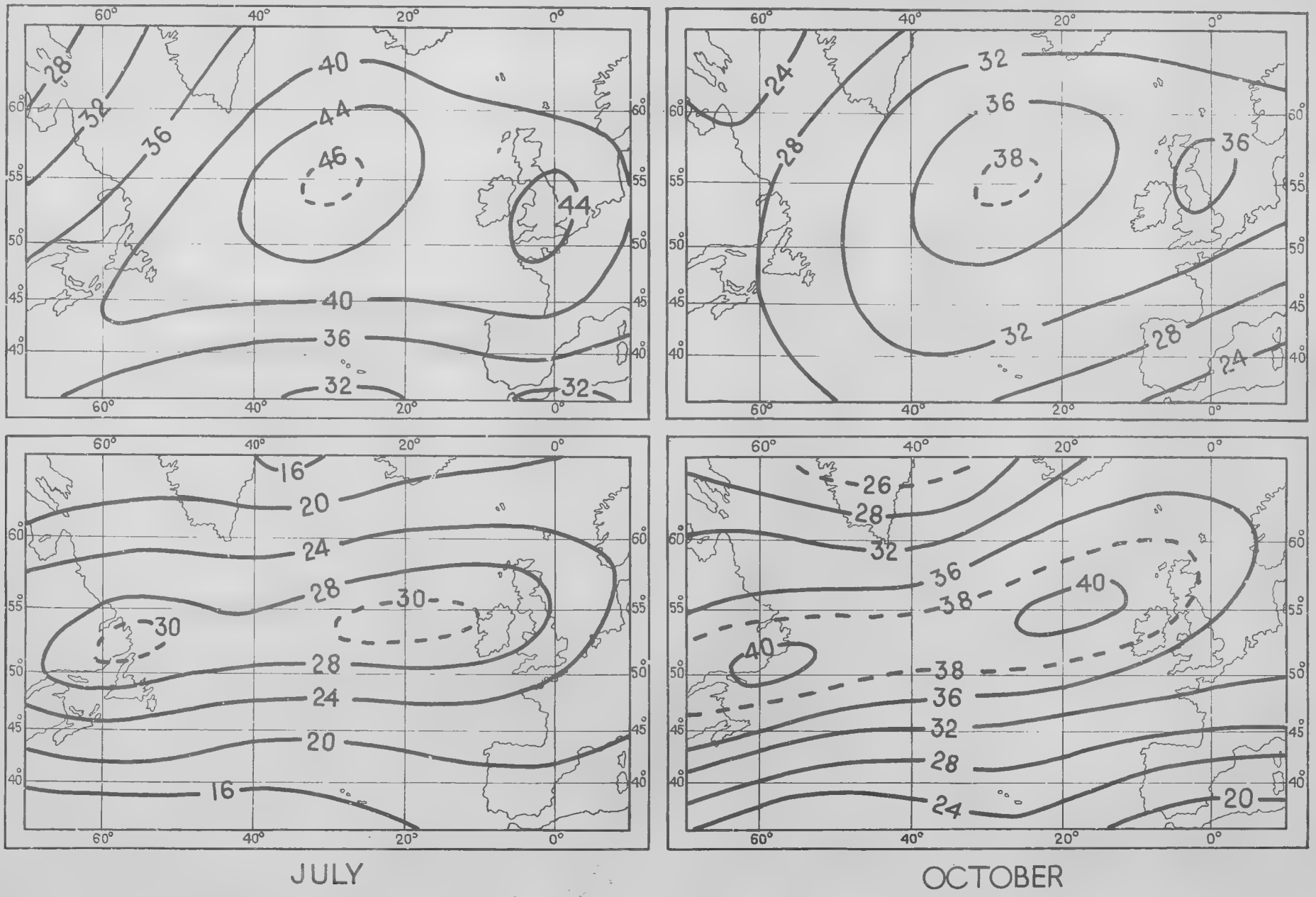

Fig. 8 Estimated standard vector deviation of wind (kt.) at 500 mb.

... M.O. [illegible]
... is available in the Library of
... Meteorological Office."

At the time of issue this report has not been published. Any author desiring to quote this paper should refer to it as "A paper of the Meteorological Research Committee (London), M.R.P. No.872 by Mr. H.D. Hoyle
A copy is available in the Library of the Meteorological Office."

M.R.P. 872

S.C.II/175

9th August, 1954

AD53983

AIR MINISTRY

METEOROLOGICAL RESEARCH COMMITTEE

An investigation into the speed and direction of motion of simple warm sector depressions

by

H.D. Hoyle (Meteorological Office)

Summary. For a limited class of depressions both the direction and the speed of motion are given with good accuracy by the 1000-500 mb. thermal wind. The mean value over an area centred on the depression gives better results than a "spot" value of the thermal wind through this layer. The results suggest that for this type of depression better forecast positions than could be expected by simple extrapolation or by the use of the tendency field might be obtained by using thermal wind as indicating speed as well as direction.

No other empirical rule could be formulated which gave equal success.

There is a suggestion that the relation between thermal wind and motion of depression is affected by thickness patterns showing marked "development" areas (Sutcliffe (1)) in the neighbourhood of the depression.

1. Introduction. A considerable amount has been written, by various authors, on the movement of depressions. Usually all types of depression have been considered together and results have usually been rather unsatisfactory.

Reasonable agreement was found by Hollis (2) using the 1000-500 mb. thermal wind, and by Austin (3) using the 700 mb. and 500 mb. winds, with regard to the direction of motion of depressions, angular deviations usually being within about 30 degrees. Hollis, however, found no correlation between the speed of the depression and the thermal wind speed.

It was therefore decided that better results might well be obtained by considering separately different types of depression - a good result over a narrow field probably being of more use to the forecaster than a somewhat unsatisfactory result over a much wider field.

It was also decided to measure the mean flow over an area centred on the depression rather than to use the usual geostrophic scale to measure the flow at a point over the centre. This was not only in view of the theoretical idea of the barotropic advection of a vortex in a general stream, but also to lessen the effect of the somewhat subjective details of chart drawing.

2. Selection of cases. Depressions in the six months 1/1/51 to 30/6/51 were considered. To avoid complication by orographic and diurnal effects, depressions over the Atlantic alone were considered, and depressions near the western extremity of the charts where the chart drawing might therefore be more erratic were also excluded.

/Depressions

Depressions which were occluded, and depressions with very complex or doubtful analyses (or whose position was in doubt due to lack of observations) were also omitted.

Very great care was taken to see that the upper air flow was typical of unoccluded warm sector depressions. Any cases with a closed cyclonic circulation at 500 mb. in association with the surface centre were excluded. The 1000-500 mb. thickness pattern had to be of conventional type also, cases being excluded if the thermal trough behind was unusually well marked or if there was marked difluence or confluence in the neighbourhood of the depression.

There were 16 satisfactory cases in the period considered. A further 18 cases were similarly obtained from the six-month period 1/7/50 - 31/12/50 and these were used to test the main results found from the original 16 cases.

3. Extraction of data. The motion of the depression was measured by its W to E and S to N components (in knots) over a 12-hour period (H to H + 12). Preliminary work indicated that the original drawing of the charts was somewhat erratic. Consequently all the surface charts, including the ones for several 6-hourly intervals before and after the 12-hour measured period, were completely redrawn, so as to satisfy fully all available observations and at the same time give a track for the depression which was as smooth as possible.

The upper flow over an area centred on the surface depression was estimated by measuring the difference in contour height (or thickness) at points a known distance due N and S, and again due E and W of the centre. This readily gave W to E and S to N speed components. The size of the area used was chosen in order to facilitate conversion into knots, a diameter of about 600 nautical miles being used. A scale was prepared for this purpose (Fig.1) which incorporates a correction for map distortion. The line AB is placed over the depression centre with the lines perpendicular to AB in the required direction (due N say) and such that the latitude figure on the scale conforms to the latitude immediately under it on the chart. The height (or thickness) is then read off on the line XY at the point appropriate to this latitude line on the scale. The height (or thickness) is similarly read in the opposite direction (due S say). For the 1:10^7 charts used, the scale was so drawn that the speed component in knots was given by multiplying the diametrical height difference by 4. It is a simple matter to prepare such a device for use with charts of any scale.

As well as the 1000, 700, 500 and 300 mb. winds and the 1000-500 mb. thermal wind (all of which were meaned over the two upper air charts at H + 3 and H + 9), measurements were made of the warm sector wind speed, the depression size and change of size, and the rate of filling or deepening. 6-hour isallobars were also drawn by gridding the surface charts.

4. Results. Correlation coefficients were calculated between the component velocities of the depressions and the wind components for the various levels and these are given in Table 1 below. There were 32 pairs of numbers (two components for each of the 16 cases) in the correlations. The correlation coefficient between the motion of the depression and the "spot" value of the 1000-500 mb. thermal wind using a geostrophic scale in the usual manner is also given.

TABLE 1

1000 mb. wind	.47	
700 mb. wind	.86	
500 mb. wind	.90	
300 mb. wind	.89	
Warm sector wind	.81	
1000-500 mb. thermal wind	.92	(.94 for the 18 test cases)
"Spot" value of 1000-500 mb. thermal	.80	

/The

The ratio of the depression speed (c) to the 1000-500 mb. thermal wind speed (V') varied between .66 and .98 with a mean value of .80. In the 18 test cases c/V' varied between .71 and 1.20 with a mean value of .97. The variations in c/V' were studied in relation to all the other parameters measured, and also in relation to tropopause height. No worthwhile correlation was evident. There was a slight tendency, however, for the smaller depressions to have a smaller value of c/V', (i.e. to move more slowly) and also for depressions whose size was decreasing to have a larger value of c/V' (i.e. to move quickly).

Previous writers have used angular deviation as a measure of the success of "steering" ideas, and values obtained in this investigation are given in Table 2 below:-

TABLE 2

Track of depression minus direction of:-	Mean	Standard Deviation	Mean ignoring signs
700 mb. wind	-5.5°	7.2°	7.6°
500 mb. wind	-2.9°	8.3°	6.5°
300 mb. wind	-4.1°	8.3°	7.4°
Warm sector wind	-6.1°	11.9°	10.2°
1000-500 mb. thermal	-0.6°	9.8°	6.3°

(the apparently smaller variability of the deviation from the 700 mb. direction is not thought to be significant, as this is based on only 15 cases. The case omitted is one in which lack of observations at 700 mb. made it impossible to give any reliable reading at this level - and it is by far the worst case of the 16 at the other levels, so that the 700 mb. level is doubtless favoured by its omission.)

It is interesting to compare the figures above with those for the angular deviation of the depression's motion from the direction of the isallobaric gradient. This gave a mean deviation of -2.3° (standard deviation 8.3) and, ignoring signs, a mean of 6.3.

It was found impossible to formulate any empirical rule to improve upon the thermal steering results by utilising any of the other parameters measured. It is particularly interesting that no success could be achieved in this way by using the 1000 mb. wind.

5. Errors. A rough check on the magnitude of errors involved in using thermal steering was thought to be worth while. Means and standard deviations were calculated for:-

(a) The difference between the 32 components for c and the corresponding components of $4V'/5$.

(b) The difference between the components for V' and the corresponding components found by subtracting the measured 1000 mb. components from the 500 mb. components.

(c) The difference between the components originally read off the charts for c, and those for c after redrawing the charts.

The values found were:-

	Mean	Standard deviation
a)	-0.5	1.5
b)	+0.5	2.4
c)	+2.4	5.4

/Now

Now a) is a measure of the reliability of using $4V/5$ as an estimate for c, whilst b) is to some extent a measure of the reliability of the charts. As this latter includes only errors of inconsistency in gridding and measurement, whereas there are also other errors (consistent drawing errors, observational errors, errors due to the geostrophic assumption) likely to worsen the reliability of our measurement of upper winds, b) is very probably an under estimate of the errors one might expect to find in the investigation by these methods of even a perfect steering law. Consequently the fact that a) is less than b) suggests that little improvement can be expected on the thermal steering result found, using present charting technique.

The fact that c) is more than twice as large as b) and about four times as large as a) suggests that considerably greater errors can exist in the placing of surface depressions on the Atlantic on the current surface chart than the errors involved in using thermal steering.

The standard deviations listed above are very small and the 18 further test cases gave somewhat higher values, but still gave a probable error of less than 5 kt. in using $4V/5$ as an estimate for c.

6. Conclusions.

(a) Non-occluded warm sector depressions over the Atlantic which have simple, conventional thermal structure, with no closed circulation at 500 mb. move in good agreement with steering by the 1000-500 mb. thermal wind.

(b) Better results are obtained by measuring the mean thermal wind over an area than by reading a "spot" value of the thermal wind at the depression centre. Such a mean value may readily be obtained by using the type of scale shown at Fig. 1.

(c) Simple warm sector depressions on the Atlantic move with the direction of, and slightly over 4/5 the speed of the 1000-500 mb. thermal, (meaned over an area) with a probable error of less than 5 kt. in speed and less than 10 degrees in direction.

(d) The surface pressure distribution in the vicinity of the depression seemed to have little effect so that the barotropic advection of a surface vortex in the surface stream does not seem to be a very helpful theoretical concept, in connection with these depressions.

(e) Although cases of marked "development" in the thermal pattern were excluded from this investigation, during the course of the investigation several cases were noted where there was marked difluence ahead of the surface centre. A cursory check suggested that in all such cases the speed of the depression was greater than would otherwise have been expected. The presence of marked development areas in the thermal pattern in the vicinity of the depression may well have some considerable effect on the motion of the depression, but this is a subject for further investigation and was not undertaken in the present work.

(f) Although the figures quoted throughout this investigation apply to measurements of the thermal wind simultaneous with the measured motion of the depression, and not to the reliability of thermal steering at any instant as a guide to the motion of a depression over the subsequent 24 hours, the technique of forecasting the pre-thickness charts is already sufficiently well developed for them to be used with reasonable confidence for forecasting the subsequent 24-hour motion of a depression if and when thermal steering is known to be the right principle to employ. The figures quoted in para. 7 above suggest that for the limited class of depressions considered, thermal steering by the 1000-500 mb. thermal wind might well give better results than extrapolation of the past track, or the use of isallobars, provided that the mean thermal is estimated over a substantial area centred on the depression.

REFERENCES

1. Sutcliffe, R.C. 1947. Q.J. 73, 317-318.
2. Hollis, R.S. "An investigation into the motion of depressions relative to straight thickness patterns"(unpublished).
3. Austin, J.M. 1947. Journal of Met., Vol. 1, No. 1.

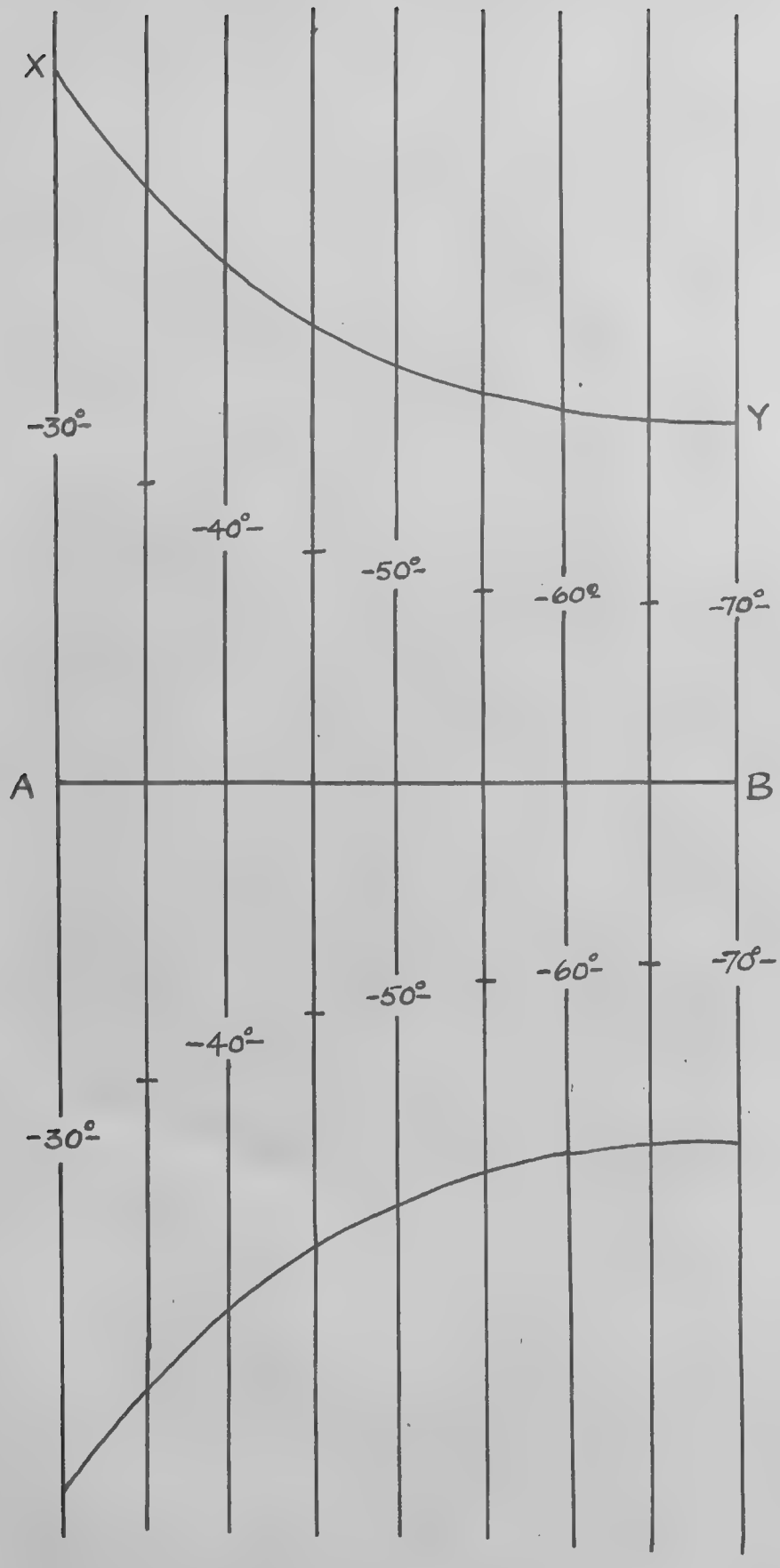

Fig. 1.

Scale for obtaining Mean Flow over an Area.

At the time of issue this report has

At the time of issue this report has not been published. Any author desiring to quote this paper should refer to it as "A paper of the Meteorological Research Committee (London), M.R.P. No.873 by Messrs. A.J. Lander and G.D. Robinson.
A copy is available in the Library of the Meteorological Office."

M.R.P. 873
S.C.III/171
31st August, 1954.

AD 223077

AIR MINISTRY

METEOROLOGICAL RESEARCH COMMITTEE

On the determination of the vertical convective heat flux by observations of wind and temperature near the ground

by
A.J. Lander and G.D. Robinson (Meteorological Office)

Summary

An attempt to measure the vertical convective flux of heat by simultaneous observation at a point of the vertical component of wind and the temperature has been continued, and fluctuations of frequency up to about 50 c/s have been recorded. The results obtained are about half of those of check determinations by the Bowen ratio method.

The evidence for the validity of the Bowen ratio method is reviewed, and considered satisfactory. The basis in theory of the "fluctuations" method is discussed, in particular the consequences of using instrumental means on various scales to replace the velocities and temperatures of fluid elements which figure in the theory. Observed similarities between results on different time scales are discussed. The possible effects of instrumental defects are examined. No firm reason for the discrepancy between the two methods of measuring the heat flux is found.

An appendix describes the apparatus used for recording at the highest frequencies.

I. Introduction

In M.R.P. 740 we reported an attempt to measure the vertical convective flux of heat near the ground by simultaneous observation of temperature and the vertical wind component, and gave reasons for our belief that the results we obtained were systematically low by a factor of about two. We have continued this type of observation, making certain changes in detail. We have now available about twice the amount of material, and we have investigated some of the possible sources of error, but consistently obtain similar results. In the present report we collect together all our observations and discuss known sources of error, mainly in the hope of obtaining advice on our difficulties.

The technique we have used is a popular one (see e.g. Hewson 1952), but few of its users appear to have subjected it to any serious test. Swinbank (1951, 1952) and his co-workers, and McCready (1953), form the only exceptions known to us, and we later compare their experience with our own.

/II.

II. Apparatus and procedure

The apparatus was for the most part the same as that described in M.R.P. 740. The previous work had been carried out at a height of 25 cm, the response of the recording apparatus being controlled by suitably damped galvanometers of free period 1/10 sec. Most of the observations now reported were made at a height of about 150 cm with these galvanometers, the same site being used. In addition observations have been taken at a height of 150 cm with a similar apparatus incorporating galvanometers of period 1/60 sec. Details of this apparatus and its performance are given in Appendix I.

The method of dealing with the charts was unchanged. The records with the 1/60 sec. galvanometers were measured at intervals of 1/30 sec., each record being long enough to give 300 such readings. Only one set (5 records) of observations with this apparatus has been completely reduced.

III. Results

The results of all observations so far reduced, including those previously discussed in M.R.P. 740, are set out in Table I. The last three columns of this table give the heat flux as determined by the fluctuation technique and the heat balance - Bowen ratio method, and the ratio of the two determinations. The discrepancy previously found is repeated in the new results; the mean value of the ratio, weighted to take account of the number of records in each observation, is 0.44. The likely errors of the various results will be discussed in more detail in the following sections of this report, but the position may be summarised by saying that within the accuracy of the measurements the fluctuation technique as we have applied it gives a value for the heat flux which is half that obtained by the Bowen ratio method. In lapse conditions the magnitude of the ratio of the two determinations found at a height of 140 cm is rather greater than that at 25 cm, but this does not hold for the inversion case, observation 12. There is a very high degree of internal consistency in the results, compare for example observations 5, 6 and 13, and particularly 2, 8 and 12. These three inversion cases constitute, as nearly as is possible in work in the field, a repetition of the same experiment, and the results are almost identical (Observation 1, the only other inversion examined, was a very different case, with much higher wind speed).

In view of this consistency we suggest that we have minimized casual errors of observation and that the discrepancy disclosed in Table I must be due to an important systematic error in our methods of measurement, or in our application of the principles of either the Bowen ratio or fluctuation method, or in these principles themselves. We will examine these possibilities in turn.

IV. Discussion of the results

IV.1. The Bowen ratio method

This is a well known method for the separation of the heat exchanges at a surface due to convection of heat and evaporation, when the sum of these is known. Its applicability to a natural cropped surface has been questioned, e.g. by Pasquill (1949). Since we rely on it for a standard of comparison we will recapitulate the evidence for its validity.

It is not a method securely founded in theory since it implies that the transfer of heat and water vapour near the surface can be described by means of eddy diffusion coefficients, and in its practical application these coefficients are assumed equal. Rider and Robinson (1951) working on the site of our present experiments, made observations which could be explained in terms of eddy diffusion coefficients related by a constant but undetermined factor (possibly unity). Rider (1953) working at Cardington has extended this result and shown that this constant factor is normally near unity;

/though

though he reported a number of occasions (about 20%) when the validity of the method was in doubt. Rider's results concerning the ratios of the eddy diffusion coefficients are set out in Table II, where K_W, K_M, and K_H represent respectively the eddy diffusion coefficients for water vapour, momentum and heat. Table II also contains the standard deviations of these ratios estimated from the accuracy of the measurements of the various components as assessed by Rider. It will be seen that only observation No. 35 is exceptional and it has been omitted in the means. Observation No. 48 is doubtful, but has been included. The difference from unity of the observed ratios appears to be significant, but in the case of K_H/K_W with which the Bowen ratio method is concerned, this difference is small, and we have neglected it in the computation of Table I.

Equality of the eddy diffusion coefficients implies similarity of the profiles of wind, humidity, and temperature since, within the accuracy of the gradient measurements, the fluxes of heat and water are known to be constant over the range of heights concerned, and the assumption, which is usually made, that the flux of momentum is constant, leads to a consistent interpretation of observations. This similarity of profiles is always observed on the Kew site up to a height of 200 cm, within the accuracy of the measurements. Rider and Robinson (1951) gave examples; a further one, associated with observation No. 10 of the present series, is shown in Fig. 1. We consider that we are justified in applying the Bowen ratio method to measurements on the Kew site, and in particular that there is no reason in principle for the method systematically to overestimate the vertical convective heat flux at this site by a factor of about 2.

The accuracy of the measurements remains to be considered. The greatest source of random error is probably the measurement of heat flux into or from the soil layers, and we have minimised this by choosing occasions when, for a given radiation field, this term is small. We are satisfied that there is no systematic error in this term sufficient to affect our results. The most likely source of large systematic error is faulty measurement of one or more of the radiation terms, since the required convective heat flux, at least in the lapse conditions investigated, is often of the order of 10% of the incident solar energy, and 5% errors in radiation measurements are not uncommon. In the Bowen ratio method an error in the measurement of radiation is divided between the heat flux and evaporation, but if the evaporation is determined directly, as for example by Pasquill (1949) and Rider (1953), the whole error is included in the heat flux. In these circumstances a systematic error of 10% in solar radiation measurement can lead to an error of order 100% in the ratio K_H/K_W for lapse conditions. The radiometers used at Kew are frequently standardised, the solar radiation being referred to a substandard Ångström pyrheliometer known to be in accord with international standards (Eldridge 1952), and the terrestrial radiation to black body sources (Robinson 1947). The Gier and Dunkle type radiometer used in observation 13 (see Appendix I) had been calibrated against both types of substandard, with satisfactory consistency. We therefore do not believe that there is a large systematic error in the radiation measurements, and in consequence the Bowen ratio heat flux results in Table I are considered to be a satisfactory standard of comparison. We estimate that the casual error of these results does not exceed ± 2 mw cm^{-2} or $\pm$ 20%, whichever is the greater.

IV.2. Theory of the "fluctuations" method

Various ways of defining the heat flux in terms of the instantaneous winds and temperatures were mentioned in M.R.P. 740. Probably the most general is that set out, e.g. by Starr (1952), who considers all the forms of energy entering and leaving a specified domain in the atmosphere.

/His

His expression contains the terms

$$\int_A \int_t (\rho I + p) v_n \, dA \, dt \qquad - (1)$$

which may be written

$$\int_A \int_t \rho c_p T v_n \, dA \, dt \qquad - (2)$$

for an atmosphere of constant composition, where I is the specific internal energy, p the pressure, T the temperature, and v_n the normal component of velocity relative to a surface element dA at time t. If we apply this expression to a system defined by the earth's surface, a vertical wall, and a horizontal surface, and assume that the integral is zero over the wall (i.e. no horizontal advection of enthalpy) we have for the flow of enthalpy through the upper surface

$$\int_A \int_t \rho c_p T w \, dA \, dt \equiv A.t.c_p \overline{\rho w T} \qquad - (3).$$

The assumption underlying the present experiment is that the integration can be performed over a domain for which the flow of mass through the wall and the vertical mass flow are both zero i.e. $\overline{\rho w} = 0$ so that

$$F_H \equiv c_p \overline{\rho w T} = c_p \overline{(\rho w)' T'} \qquad - (4)$$

is now the vertical flux of heat, to be compared with the flux of heat into the domain at the earth's surface.

Three difficulties arise. Firstly we observe at a constant level, whereas the condition $\overline{\rho w} = 0$ defines a constant pressure surface. It is therefore implied that systematic vertical flux of mass through a constant level is not an essential part of the heat transfer mechanism. Secondly we measure w rather than ρw and deduce $\overline{w}$ and w' not $\overline{\rho w}$ and $(\rho w)'$ (see M.R.P. 740). Thirdly we observe only at one point, on the assumption that the time and space integrations are equivalent, as in the corresponding problem of statistical mechanics.

We shall not discuss the first difficulty further. The implication seems reasonable, though we know of no demonstration of its truth. The immediate consequence of the second difficulty is that we must approximate to $\overline{\rho w T}$. Writing $\rho = \overline{\rho} + \rho'$ etc. we find

$$\overline{\rho w T} = \overline{\rho}\,\overline{w}\,\overline{T} + (\overline{\rho}\,\overline{w'T'} + \overline{T}\,\overline{w'\rho'}) + \overline{w}\,\overline{\rho'T'} + \overline{\rho'w'T'} \qquad - (5)$$

or by making immediate use of $\overline{\rho w} = 0$

$$\overline{\rho w T} = \overline{\rho w T'} = \overline{\rho}\,\overline{w'T'} + \overline{w}\,\overline{\rho'T'} + \overline{\rho'w'T'} \qquad - (6).$$

We now neglect the pressure fluctuation p', the term $\overline{\rho'T'}$ so that $T'/\overline{T} = -\rho'/\overline{\rho}$, and the term $\overline{\rho'w'T'}$ so (5) becomes

$$F_H = c_p \overline{\rho w T} \simeq c_p \overline{\rho}\,\overline{w}\,\overline{T} \qquad - (7)$$

Similarly (6) becomes

$$F_H = c_p \overline{\rho w T'} \simeq c_p \overline{\rho}\,\overline{w'T'} \qquad - (8).$$

The neglect of p' and $\rho'T'$ may be justified numerically in cases (such as those we have investigated) where the fluctuations of wind velocity, and hence the Reynolds pressures, are not extremely large. The neglect of the triple correlation term implies no correlation between w' and $|T'|$ which seems reasonable, so that (7) and (8) would be expected to give F_H with an accuracy of a few parts per cent in the cases here considered.

/Of

Of these expressions (7) does not depend on the condition $\overline{\rho w} = 0$, it is therefore valid as an expression for the flow of enthalpy past the instrument during the period of observation; (8) on the other hand contains $\overline{\rho w} = 0$ and should be applied only when this condition holds.

So far we have been concerned with expressions involving the properties of elements* of the fluid; ρ, w, T, in (7) and (8) are instantaneous values for such an element. Instrumental readings are necessarily means over a domain in space and time determined by the size and time constant of the instrument. If we denote such instrumental means by $[\rho]$, $[w]$ and $[T]$ we have from (7)

$$\overline{F_H} \simeq c_p \overline{[\rho][w][T]} \simeq c_p [\rho]\overline{[w]}\overline{[T]} \phi \qquad - (9)$$

to the same degree of approximation as (7). We cannot, however, establish an expression analogous to (8), involving $[w]'$ and $[T]'$. We conclude from this examination, by comparing expressions (7) and (9), that a flux of enthalpy, or flux of heat for a constant mass system, determined in this way from instrumental readings, is independent of the scale of the instrument used. We conclude also that expression (8) is valid only for a constant mass system, and then only if the observations of w' and T' are on the scale of the fluid elements.

We turn now to the results of our observations. The ideal constant mass system is never realised, $[w]$ being found always to be numerically 10^2 to 10^3 times greater than that required to account for the heat flux. (The value of $[w]$ normally fluctuates about a large mean; if exceptionally a mean value of the required magnitude were to be present the individual values of $[w]$ are so large that tens of thousands of consecutive readings would be required to eliminate the statistical fluctuations of $[w]$. Although $\overline{\rho w}$ is not measured, it is obviously not zero, and (9) therefore gives the flux of enthalpy past the instrument, which is not an interesting quantity. We are left with no theoretically sound method of estimating the heat flux from the observations. The values quoted in Table I are the result of computing $\overline{[w]}$, $\overline{[T]}$ and $\overline{[w]}\,\overline{[T]}$ and writing

$$F_H = c_p \bar{\rho} \left(\overline{[w][T]} - \overline{[w]}\,\overline{[T]}\right) = c_p \bar{\rho} \overline{[w]'[T]'} \qquad - (10)$$

which is an expression which we have failed to justify theoretically. (Indeed we have shown $c_p [\rho][w][T]$ to be a good approximation to the total enthalpy flux).

This procedure, of observation and computation, is similar to that adopted by other workers (e.g. Swinbank and McCready whose results are discussed in Section V), although there are differences in interpretation of the observations. We can only conclude from the preceding analysis that there should be no significance in heat fluxes computed from (10) but we see from Table I that they bear a simple relation to the true values. There is a further point of interest. In M.R.P. 740 we made some attempt to determine the periods of the eddies responsible for the heat transport, with rather paradoxical results. We wrote there "The results of filtering out the short period components (Table III (of M.R.P. 740), 14th September, 1950 and 6th June, 1951) suggest indeed that the main effect is due to fluctuations of period less than 2 sec., which is hardly in accord with the results obtained on 2nd July, 1951 using 2 sec. galvanometers". Table I (of the present report) shows that comparable results are obtained on three very different

/scales

* It is of course a fundamental assumption, here and in all dynamical treatment of atmospheric motion, that a scale of motion exists which is sufficiently large compared with the molecular scale, and at the same time sufficiently small compared with the smallest scale on which turbulent mixing occurs, for a volume of fluid to be defined and followed as an entity in its motion. This is the fluid element.

ϕ Here and in the sequel we conveniently ignore the fact that the instrument is not a linear detector so that instrumental means are not the means defined by the integral (2).

scales, and we recall in this connection that Swinbank's work has been done in the main with 2 sec. galvanometers, so that we can be satisfied that our only observation on this scale is not unrepresentative. The independence of scale of observation recalls the similar independence to be expected if the heat flux is determined by (9); again we find a regularity in the results which we cannot justify theoretically but which suggests that they are in fact at least related to the heat fluxes.

These questions can be seen to be related to the third major difficulty of the method which we mentioned above, in that they would not arise if the means could be taken over the postulated domain for which $\overline{\rho w} = 0$. This would involve space as well as time integration, and is in practice impossible. The customary assumption of equivalence of time integrals and space integrals is by no means obviously true in the present connection - it implies that a scale of observation exists on which the mean values of temperature and vertical wind at a point are not correlated. Some aspects of our results can indeed be explained by saying that we have computed only one contribution to the flux and that some form of patterned flow in space is an essential feature of the heat transfer mechanisms but we do not think our method of computation is sufficiently well founded to allow us to press this explanation. Indeed we conclude that the method we have adopted for computation of the heat flux, though the customary one and at first sight reasonable, has not a firm theoretical basis. We hesitate to attribute our anomalous results to this until all other possibilities have been explored, in view of the regularities we have found and cannot explain, and of the success claimed by other users of the method. We are unable to suggest a more satisfactory method for reduction of the results.

IV.3. Duration of the observations

There is no way, a priori, of fixing the length of time over which the observations are to be made. If the integration in expression (2) were possible in practice it would be necessary to carry it out over a time and area such that $\overline{\rho w} = 0$ held to a very close approximation. Experience, our own and others', suggests that this condition would not in general be attained in observations at one point.

In M.R.P. 740 we followed Swinbank in an analysis which we interpreted as showing that we had taken mean values over a sufficiently long period. We had a series of independent observations of vertical velocity w (we now drop the distinction between the instantaneous w and the instrument mean $[w]$), $w_1, w_2, \text{----} w_p$, and corresponding temperature observations $T_1, T_2, \text{----} T_p$. We formed the mean product of the fluctuations $1/p \sum_{q=1}^{p} w'_q T'_q$ proportional to the heat flux as determined from p observations, F_p. We then divided the series of observations into r consecutive sets each of n observations $(rn = p)$ and found for each set the means of w and T and the product of the fluctuations from these means, taking the mean of this over the r sets, i.e.

$$\frac{1}{p} \sum_{a=0}^{r-1} \left[\sum_{q=an+1}^{n(a+1)} w_q T_q - \frac{1}{n} \sum_{q=an+1}^{n(a+1)} w_q \sum_{q=an+1}^{n(a+1)} T_q \right]$$

which is proportional to the heat flux as determined from n observations, F_n. We did this for a series of values of n and formed the ratio F_n/F_p, exhibiting the results in Table III of M.R.P. 740. We argued that since F_n/F_p was effectively unity over a wide range of n/p, the p observations were sufficient to give the heat flux. We have repeated this analysis for a number of occasions, and find that the behaviour of the case studied in detail in M.R.P. 740 (14th September, 1950) is not typical. The behaviour of individual runs of 200 or 300 readings varies widely as may be seen from Table III, which shows the results for the 5 sets of 300 readings

/comprising

comprising observation No. 13 of Table I and the 5 sets of 200 readings comprising observation No. 10 of that Table. The mean values for these two observations are plotted in Fig. 2, in which we have also plotted the mean of the five cases similarly analysed by Swinbank in M.R.P. 429. (Swinbank's series were of 160 observations. He did not form the mean product for the full series, so we have fitted this result for $n = 55$ to the curve determined from our own work). This curve has some curious features which are discussed further in Appendix II; here we consider its implications in regard to the heat flux determinations.

Figure 2 incorporates observations of very different types. Swinbank's series were obtained with 2 sec. galvanometers and comprise 160 equally spaced readings over a duration of 5 minutes. Our series are of 200 readings at intervals of 1/4 sec. (1/10 sec. galvanometers) and 300 readings at intervals of 1/30 sec. (1/60 sec. galvanometers). Thus there is thirty fold range in total time of observation but only a twofold range of p, and we are not justified in extrapolating over a wider range of p. If however the extrapolation is made, the curve suggests that the heat flux is doubled by a tenfold increase of p, or increased by 10% if p is doubled. We cannot therefore be satisfied, by this type of argument, that we have taken sufficient independent consecutive readings of w and T.

IV.4. Instrumental errors

Certain instrumental errors were mentioned in M.R.P. 740, where it was suggested that they were small, though unfortunately most of them tend to reduce the computed heat flux. The main sources of error seem to be poor synchronisation of wind and temperature records, temperature coefficient of the anemometer, and failure to follow the variations in direction of the horizontal component of wind.

We have no further evidence concerning the effect of lack of synchronisation between the wind and temperature traces. This can occur to any serious extent only by distortion of the photographic paper. We have estimated the error as less than 5%, and some confirmation of this is obtained from the results with the high speed galvanometers (observation 13). We see from Fig. 2 that in this observation combination of the measured winds and temperatures in groups of 5 reduced the computed flux by only 10% in spite of the smaller number of independent observations. Combination of observations in this way greatly reduces the possibility of error due to lack of synchronisation.

In M.R.P. 740 we noted that the temperature coefficient of the anemometer was about 1.5% per degree C. This was a rough determination. Analysis of the circuit (by Mr. D.R. Samuel) shows that the coefficient should vary considerably with wind speed, but that 2% /°C is a reasonable value at the speeds encountered in the observations. We had previously checked by trial that a temperature coefficient of this magnitude would have little effect on the computed results for the heat flux. This is easily confirmed. It is assumed that the instrument is calibrated at the mean temperature of the run. If we denote instrumental determinations of vertical wind by W, true values by w, the temperature fluctuations by T', and the temperature coefficient by α we have

$$\begin{aligned}
\text{measured heat flux} &= \bar{\rho}\, c_p \left(\overline{WT} - \overline{W}\,\overline{T}\right) \\
&= \bar{\rho}\, c_p \left[\overline{wT(1+\alpha T')} - \overline{T}\left(\overline{w} + \alpha\overline{wT'}\right)\right] \\
&= \bar{\rho}\, c_p \left[\overline{wT} - \overline{w}\,\overline{T} + \overline{w(\overline{T}+T')\alpha T'} - \overline{T}\alpha\,\overline{wT'}\right] \\
&= F_H + \bar{\rho}\, c_p\, \alpha\overline{wT}^{12}
\end{aligned}$$

i.e. the error is of an order less than that of the terms neglected in deriving (7) and (8).

/The

The most serious instrumental error is probably that caused by the vane not following the most rapid changes in direction of the horizontal wind. This has two consequences. In the first place the angle of yaw may be great enough to carry air from the anemometer wires to the thermometer, giving spurious temperature fluctuations. Trials in the wind tunnel show that these fluctuations are large and have a characteristic appearance. We have detected such effects on a number of traces taken in the field in light winds; they do not occur in a large majority of the traces we have measured and we are confident that they do not noticeably affect our results. The second effect of yaw is to change the calibration of the anemometer in such a way that the indicated total wind increases, the indicated angle to the horizontal decreases rapidly, and the computed vertical component decreases, as the angle of yaw is increased. The effect has been investigated very approximately in the wind tunnel and Fig. 3 gives an indication of the magnitude of the error in the vertical component of wind for various angles of inclination and yaw. Fig. 4 allows an estimate of the effect of this on the computed flux. It shows the frequency of occurrence of various angles of yaw from the mean direction, determined on the site with a fixed horizontal ^{V} anemometer and 1/10 sec. galvanometers, in a mean wind of 450 cm sec.$^{-1}$ on 27th January, 1953, and the distribution of angle of inclination as indicated by the anemometer in normal use in a mean wind of 195 cm sec.$^{-1}$ during part of observation 11, Table I. The occasion used for distribution of yaw is not typical owing to the high wind speed, but is the only one available to us. A wider distribution would be expected with lighter winds, but of course the vane follows all but the most rapid excursions. The distributions of yaw and inclination are not independent but if we base an estimate of error on these curves assuming independence it should not be far wrong. It can be seen that the mean error in the vertical wind should be well below 10%, and we suggest this as a reasonable value for the degree to which the heat flux is underestimated due to all instrumental defects.

V. Results of other investigators

As we mentioned in Section I we know of only two other investigations in which the heat flux determined by the fluctuations method has been compared with a measurement or estimation obtained otherwise. By far the more extensive of these is the work carried out near Melbourne, Australia by a team from the C.S.I.R.O. Section of Meteorological Physics, preliminary reports of which have been published by Swinbank (1951, 1952). We have been informed in conversation that a very considerable amount of material has been collected and reduced, and that the conclusion drawn is that the fluctuations method yields a correct value for the heat flux - a result which we have been unable to obtain at Kew. The only results of which we have any detailed knowledge are however those published by Swinbank in his preliminary account; the relevant parts are reproduced here as Table IV, for the convenience of readers of this report.

Swinbank's method of test differs from ours in that he does not apply the Bowen ratio technique, but measures the flow of both heat and water by the fluctuations method. For those who maintain that the Bowen ratio method is unreliable in principle, Swinbank's test is the more satisfactory - it relies on the technique under test to give the sum of the energies used in evaporation and removed by convection, which sum is measured independently. It has however one weakness of principle - the expression for the flux of water analogous to (8) for heat is valid, but not those analogous to (7) and (9), as may be seen by substituting the water vapour concentration for temperature in the analysis of Section IV.2. The use of instrumental means in place of the elementary velocities and humidities when computing water flux is not analogous to the corresponding procedure for the heat flux and should strictly be justified by experiment e.g. by determining the water flux from means on different time scales. So far as his published work goes Swinbank does not seem to have done this.

/A

A glance at Table IV shows that only those measurements made with large incident solar radiation are of value in comparing Swinbank's results with ours. In his night observations the heat flux unaccounted for is, in all cases but one, much larger than the measured convective heat flux. His daytime observations check very satisfactorily, but it will be noted that the measured gradients of temperature and humidity are such that the Bowen ratio technique would give results for the heat flux differing by almost an order of magnitude from those computed from the fluctuations. If therefore we accept the latter fluxes as the correct values we see that Swinbank's measurements discredit the Bowen ratio method, and are in contradiction to the evidence presented in Section IV.1.

McCready's (1953) measurement of the heat flux was part of an extensive investigation aimed mainly at analysing the velocity fluctuations, and he reports only one run useful for our purpose. His apparatus responded to frequencies up to 50 c/s, but the length of record and details of analysis (except that this was automatic) are not clear from his paper. The observation was made over a desert surface, and the check value for the heat flux obtained from the net radiative flux and the ground conduction, i.e. evaporation could be neglected. He made simultaneous measurements at three heights with the result (approximate, from Fig. 10 of his paper)

$\rho c_p \overline{w'T'}$	at 15 cm	2.5×10^{-3}	cal cm^{-2} $sec.^{-1}$
$\rho c_p \overline{w'T'}$	at 70 cm	5.0×10^{-3}	cal cm^{-2} $sec.^{-1}$
$\rho c_p \overline{w'T'}$	at 240 cm	8.0×10^{-3}	cal cm^{-2} $sec.^{-1}$
	check value	7.1×10^{-3}	cal cm^{-2} $sec.^{-1}$

McCready attributes this height variation to horizontal inhomogeneities at his site, but a single observation does not allow useful discussion of the point. It will be recalled that we have found no significant difference between measurements at 25 cm and 150 cm.

VI. Conclusions. Future work

The discrepancies between our two methods of determining heat flux have not been resolved, and the position is not clarified by appeal to the published results of other workers. Of the possible explanations which we discussed in M.R.P. 740 we have shown by the analysis of Section IV.2 and by the work on different time scales that the arguments concerning the periodicity of eddies mainly concerned in the heat transport were not well founded, and also that the results are not affected by changing the height at which observations are made. We have not settled satisfactorily whether the length of time for which the records are taken has a serious effect on the result.

We propose next to make observations on a site with much more uniform surroundings, and in conjunction with N.E. Rider to have simultaneous measurements of evaporation (by weighing) and of the drag of the surface on the wind. At the same time we will attempt to take longer unbroken series of observations, by modification of the recording mechanism. We propose to do this work with the 1/10 sec. and 2 sec. galvanometers.

Acknowledgements

Several members of the staff of Kew Observatory have helped in the field measurements and the reduction of results particularly Mr. M.J. Blackwell, Mr. J. Gordon, Mr. J. MacDowall and Mr. D.B.B. Powell. We are indebted to Mr. D.R. Samuel for valuable discussion of the instrumental errors and the content of Section IV.2.

/References

References

Dunkle, R.V., Shimazaki, T., Gier, J.T. and Possner, L., 1949.
University of California, Thermal Radiation Project.
NR-015-202 Report No. 9.

Eldridge, R.H. 1952. Q.J.R. Met. S., 78, p.260.

Grant, D.R. 1950. M.R.P. 542.

Hewson, E.W. (Ed.). 1952. Geophys. Res. Paper No. 19, Cambridge, Mass.

Lander, A.J. and Robinson, G.D. 1952. M.R.P. 740.

McCready, P.B. 1953. J. Met., 10, p.434.

Pasquill, F. 1949. P.R.S. A198, p.116.

Rider, N.E. 1953. M.R.P. 809.

Rider, N.E. and Robinson, G.D. 1951. Q.J.R. Met. S., 77, p.375.

Robinson, G.D. 1947. Q.J.R. Met. S., 73, p.127.

Starr, V.P. 1951. Compendium of Met., p. 572.

Swinbank, W.C. 1951. J. Met., 8, p.135.

1952. Geophys. Res. Paper No. 19, p.355, Cambridge, Mass.

Appendix I

The apparatus used in conjunction with the short period galvanometers.

1. The properties of the galvanometers

The four galvanometers used for the high speed recording were a standard model made by Messrs. Pye. They have a nominal "response time" of 1/100 sec., a sensitivity of about 2 mm/μa at 1 metre, an internal resistance of about 50 Ω , and nominally require an external resistance of order 100 Ω for critical damping. It was proposed to operate them at optimum damping (i.e. 0.6-0.7 critical, giving a minimum of amplitude distortion and an approach to linear variation of phase distortion with frequency) so their characteristics were investigated fairly thoroughly. The free period was found to be close to 60 c/s in all cases, the internal resistance was as specified, but the behaviour with change of external resistance was rather different for the different galvanometers, and in one case the critical damping resistance was much less than that specified. The required damping resistance was found in each case by recording the response of the instrument with different parallel resistances to a step voltage. The determination was checked by measuring the response of the instrument with its appropriate damping resistance to a fixed current of varying frequency. Fig. 5 shows the result of one such test, the points being the response of the galvanometer relative to its D.C. response, the full curve being the calculated response for a free period of 60 c/s and damping 0.7 critical. (The wave form used in these tests differed considerably from a pure sine wave).

2. The recording of temperature

It seemed desirable to use the same sensing head and vane as in the previous work, but with the thermometer incorporated in this (4 cm of 0.0005 in. diam. Pt, resistance about 37 Ω) the sensitivity of the high speed galvanometers was not sufficient to give the required resolution on the temperature trace. An amplification of X5 or X10 was needed. A photo-electric method was used as shown in Fig. 6. Light from a 12v. 48 watt projector lamp passed through a metal grid and was focussed on the primary galvanometer mirror (which is about 2 mm x 1 mm) by an achromatic condenser. The divergent beam from the galvanometer mirror was intercepted by a second grid, a suitably enlarged copy of the first, which masked two selenium photocells arranged side by side in parallel opposition, the separation of the cells being variable. The output of the cells was applied to the secondary galvanometer, which gave the temperature record. Both galvanometers were correctly damped, and it was confirmed that the phase lag introduced by the amplifier system was that appropriate to two galvanometers.

The amplification was checked before and after each run by noting the deflections corresponding to variation of R 12, Fig. 6, in steps of 0.1 Ω. The amplification was found to be linear over a range of several degrees C, the central temperature of this range being variable by moving the masking grid and photocells. The degree of amplification was variable by controlling the D.C. voltage on the projector lamp, and so long as this voltage was held constant both gain and zero of the system were sufficiently stable over the half to one hour periods required.

We have not seen a record of the use of this type of amplifier (i.e. without electronic amplification) with high speed galvanometers, but the only difficulty not met with in more orthodox examples is introduced by the small area of the mirror. Our amplifier is mainly distinguished by its small gain, rudimentary optical system, and inelegant construction.

/The

The use of two damped galvanometers in the thermometer circuit introduces a phase lag between the wind and temperature traces; this is calculable from the circuit properties as 90° for a 60 c/s input. The value was checked by recording a 50 c/s voltage simultaneously on a single galvanometer and through the amplifier. With the damping chosen to give linear phase distortion this means that the temperature trace lagged 1/240 sec. behind the wind traces. As readings were taken at 1/30 sec. intervals only, and in view of the measurements on the time constant of the sensing wires (see below), this lag was ignored.

3. The time constant of the sensing wires

It is assumed when computing the heat fluxes that the nature of the traces obtained is controlled entirely by the time constants of the galvanometers and their associated circuit, the effect of the sensing wires being negligible. This was clearly true for the 1/10 sec. and slower galvanometers, but it was thought necessary to investigate the response speed of the wires before using the 60 c/s galvanometers. The device used was that described by Grant (1950). The wire under investigation is used as a resistance thermometer in one arm of an audio frequency bridge, the out of balance voltage being recorded on a C.R.O. A heating current is passed through the wire for a time with the rest of the bridge out of circuit. The heating current is switched off, the bridge switched in, and the decay of the out of balance voltage recorded. This process is repeated cyclically, the C.R.O. being synchronised to it. The only difference between our apparatus and Grant's was that we used an available 1000 c/s fork-controlled oscillator as the bridge voltage source, in place of his 2000 c/s oscillator. Tests were made in the wind tunnel at various wind speeds. Examples of the records obtained are shown in Fig. 7. The variation of lag, i.e. the time for recording of a fraction (1 - 1/e) of a step function disturbance, with ventilation speed is shown in Fig. 8, from which we conclude that the use of the 60 c/s galvanometers is justified in wind speeds of about 100 cm sec.$^{-1}$ and upwards. It is clear that the galvanometer period cannot usefully be further reduced at these wind speeds.

4. Apparatus used to determine the heat flux by the Bowen ratio method

Certain changes were made in this apparatus in connection with observation 13, Table I, but no change of principle was involved. In place of the mast of 7 wet and dry bulb thermocouples previously used to determine the temperature and humidity profiles two electric Assmann psychrometers were used, at heights of about 110 and 160 cm. They were read by eye at about 1 min. intervals. The net radiative flux was measured by a carefully calibrated aspirated plate recording radiometer, of the type described by Dunkle, Shimazaki, Gier and Possner (1949). This allowed the work to be done in long sunny intervals which occur on days with appreciable cumulus cloud cover (up to about 4/10), when the atmospheric radiation cannot be determined by a radiometer of limited aperture, such as the Linke-Feussner previously used.

Appendix II

Determination of the heat flux from the whole and parts of a series of consecutive observations.

In Fig. 2 F_n/F_p is plotted against n/p for three sets of data obtained in very different circumstances (F_n is the mean value of the heat flux determined by applying formula (9) to sets of n consecutive observations in a series of p observations). The fact that these very different experiments should give the same curve was so unexpected that we have examined the procedure to see if the cause is algebraic rather than physical. This does not seem to be the case; the curve is related to certain other similarities which we have noted in observations made on different time scales. The first of these, discussed in this paper, is that the observations made with the 1/60 sec., 1/10 sec., and 2 sec. galvanometers give the same result for the heat flux; the second, for which we hope to produce evidence in a later report, is that the serial correlation functions of sets of observations of vertical velocity taken on these three different scales are similar.

The following crude analysis of the form of F_n/F_p applies when the individual observations in the series of p are used once only in computing F_n, i.e. when the separate series of n observations do not overlap. In Fig. 2 this is true of the points for which $n/p < 0.25$. Dropping for convenience the constant multiplier $\bar{\rho} c_p$ we write

$$F_p = \frac{1}{p} \sum_{p} w'T'$$

and

$$F_n = \frac{1}{p} \sum_{a=0}^{r-1} \left[\sum_{an+1}^{n(a+1)} w'T' - \frac{1}{n} \sum_{an+1}^{n(a+1)} w' \sum_{an+1}^{n(a+1)} T' \right] \quad (p = n-r)$$

$$= F_p - \frac{1}{pn} \sum_{a=0}^{r-1} \left[\sum_{an+1}^{n(a+1)} w' \sum_{an+1}^{n(a+1)} T' \right]$$

$$\equiv F_p - \frac{1}{rn^2} \sum_{a=0}^{r-1} \alpha_a \beta_a \equiv F_p - \frac{1}{n^2} \overline{\alpha_a \beta_a}$$

$$\equiv F_p - F_r^*$$

F_r^* is the heat flux computed from r sets of simultaneous means over n readings. We note in passing that Fig. 2 shows that in general $F \neq F^*$, but the difference between them is not large.

Similarly we have

$$F_{2n} = F_p - \frac{1}{p.2n} \sum_{a=0}^{r/2-1} \left[(\alpha_a + \alpha_{a+1})(\beta_a + \beta_{a+1}) \right]$$

$$= F_p - \frac{1}{2^2 n^2} (2 \overline{\alpha_a \beta_a} + 2 \overline{\alpha_a \beta_{a+1}})$$

/assuming

assuming the series of α and β to be homogeneous, and generally

$$F_{qn} = F_p - \frac{1}{q^2 n^2}\left(q\,\overline{\alpha_a \beta_a} + 2(q-1)\,\overline{\alpha_a \beta_{a+1}} + 2(q-2)\,\overline{\alpha_a \beta_{a+2}} + \text{-----} + 2\,\overline{\alpha_a \beta_{a+q-1}}\right).$$

We now write

$$A_1\,\overline{\alpha_a \beta_a} = \overline{\alpha_a \beta_{a+1}} \quad \text{etc.}$$

so that

$$F_{qn} = F_p - F_r^{*}\left(\frac{1}{q} + \frac{2(q-1)}{q^2}A_1 + \frac{2(q-2)}{q^2}A_2 + \text{-----} + \text{-----}\right)$$

or

$$\frac{F_{qn}}{F_p} = 1 - \frac{(F_p - F_n)}{F_p}\left(\frac{1}{q} + \frac{2(q-1)}{q^2}A_1 + \frac{2(q-2)}{q^2}A_2 + \text{-----} + \text{-----}\right).$$

We see from this that two series of simultaneous values of w' and T' will give the same curve in Fig. 2 if F_n/F_p is the same for one value of n/p, and the coefficients A are the same. For each series these coefficients depend on the correlations between an observation or mean of vertical wind and the simultaneous and subsequent observations or means of temperature. If these correlations are the same whatever the time scale of observation (or number of observations involved in the mean) the results shown in Fig. 2 follow. We have not computed any such correlations; we do however find that the correlations of vertical wind and simultaneous temperature $\overline{\alpha_a \beta_a}/\sigma_\alpha \sigma_\beta$ and the serial correlation function for vertical wind $\overline{\alpha_a \alpha_{a+x}}/\overline{\alpha^2}$ are similar on the three scales of observation we have used, and it seems reasonable to accept this explanation of the facts displayed in Fig. 2. If we do this it seems that we cannot use arguments based on Fig. 2 either to draw conclusions concerning the length of the series of observations necessary to give a satisfactory value for the heat flux, or to indicate the extent to which the observations we have made underestimate the true heat flux.

/TABLE I

TABLE I

Results of the heat flux computation

Observation No.	Date	Type	Height cm	Galvanometer period sec.	Duration of record sec.	Readings per record	No. of records	Heat flux (1) $\bar{\rho}\, c_p\, \overline{w'T'}$ mw cm^{-2}	Heat flux (2) by Bowen ratio mw cm^{-2}	Ratio (1)/(2)
1	25 Oct. 50	Inversion	25	0.1	40	200	7	-4.2±1 [*]	-9.2	0.46
2	11 Dec. 50	Inversion	25	0.1	40	200	5	-1.7±0.3	-5.5	0.31
3	24 Apr. 51	Isothermal	25	0.1	50	200	2	-0.2±1	(0)	-
4	2 June 51	Lapse	25	0.1	50	200	7	+7.1±2	+21	0.34
5	6 June 51	Lapse	25	0.1	50	200	1	+7.1	+13.5	0.53
6	9 June 51	Lapse	25	0.1	50	200	1	+7.1	+12.5	0.57
7	2 July 51	Lapse	25	2	240	48	3	+2.5±0.6	+8	0.32
8	23 Oct. 51	Inversion	25	0.1	50	200	6	-1.7±0.3	-5	0.34
9	30 Apr. 52	Lapse	140	0.1	50	200	7	+4.6±1	+8	0.58
10	22 July 52	Lapse	140	0.1	50	200	5	+12.6±1	+20	0.63
11	28 Aug. 52	Lapse	140	0.1	50	200	5	+3.0±1.5	+6	0.50
12	11 Nov. 52	Inversion	140	0.1	50	200	6	-1.3±0.5	-4.5	0.29
13	9 June 53	Lapse	140	0.017	10	300	5	+6.9±1.8	+11.5	0.60

[*] The mean deviation of the heat fluxes calculated from the individual records is given.

TABLE II

Relation between the eddy conductivity for water (K_W) heat (K_H) and momentum (K_M) (after N.E. Rider)

Rider's Observation No.	K_W / K_M	K_H / K_M	K_H / K_W
29		1.40	
30		1.49	
31	1.07	1.13	1.06
32	1.09		
33	1.34	1.63	1.22
34	1.34		
35			2.80
37	1.23		
38	1.47		
39	1.02		
40	0.83		
43	1.25		
44	1.67	1.96	1.18
45		1.10	
46	1.23	1.35	1.09
48		2.10	
50		1.28	
Mean	1.23	1.48	1.14
Mean Deviation	±0.17	±0.27	±0.06
Estimated S.Ds.	±20%	±26%	±23%

TABLE III

Values of heat flux from complete (F_p) and partial (F_n) series of observations (factor $\overline{\rho}\, c_p$ omitted)

Date	p	Chart No.	F_p	F_n for n = 5	25	50	75	100	150	200
22 July 52	200	2	10.6		4.9	8.0	8.6	8.2	7.8	
		6	9.2		3.2	6.3	8.8	8.0	8.5	
		7	9.8		8.5	9.3	9.9	9.5	9.7	
		8	8.4		4.2	7.5	9.6	9.1	10.3	
		9	9.3		4.9	6.6	8.3	7.1	7.1	
		Mean	9.5		5.1	7.5	9.0	8.0	8.7	
9 June 53	300	2	3.1	0.3	1.5	1.8		2.2	3.4	4.1
		3	7.0	1.6	5.1	6.8		7.6	7.7	6.6
		4	6.0	0.2	0.4	2.0		3.4	3.8	5.2
		5	8.6	0.7	5.7	7.1		5.9	8.8	7.7
		7	3.9	0.3	0.9	0.9		3.3	3.2	3.3
		Mean	5.7	0.6	2.7	3.7		4.4	5.4	5.3

TABLE IV

Swinbank's measured values of heat, water vapour, momentum and radiative heat fluxes, and calculated transfer coefficients. Abridged from W.C. Swinbank (1952)

Date and Time (EST)	$(\frac{\partial T}{\partial z} + \Gamma)$ (°C/cm x 10^4)	Humidity gradient (gm/gm/cm x 10^6)	Gradient of momentum per unit mass per second x10^2	Fluxes of (all positive upwards)				Radiative flux (cal/cm²/sec. x 10^4)			Heat flux into ground (cal/cm²/sec. x 10^4)	Warming of layer of grass (cal/cm²/sec. x10^4) estimated.	Vertical flux of heat unaccounted (cal/cm²/sec. x 10^4)	Transfer coefficient (cm²/sec./x 10^{-2})		
				Sensible heat (cal/cm²/sec. x 10^4)	Water vapour (gm/cm²/sec. x 10^7)	Latent heat (cal/cm²/sec. x 10^4)	Momentum (gm/cm/sec.²)	Net short wave	Long wave from ground	Long wave from atmosphere				K_H	K_W	K_M
5.3.51 1145	-34.3	-18.9	131	+23.4	+82.0	49	-1.94	118	122.4	85	14	3	+6	22.3	3.4	11.6
5.3.51 1200	-38	-19	123	+15.0	+68.9	40.3	-1.19	129	122	86	24	5	8	12.9	2.83	7.5
7.3.51 2035	28.6	-1.23	42	-3.2	-0.28	-0.16	-0.25	-	89.1	70.2	-18	-4	6	3.7	-	4.7
8.3.51 2050	25.0	1.02	-	-1.0	-1.3	0.7	-	-	89.5	72.6	-8.4	3	4	1.35	0.97	-
8.3.51 2135	47.0	1.69	-	-0.9	-0.8	-0.5	-	-	88.6	73.5	-18	-3	7	0.69	0.37	-
14.3.51 2125	110	-1.64	52	-1.2	1.1	0.6	-	-	98	93.0	3.0	1	0.5	0.35	0.52	-
15.3.51 1130	-53	-7.5	59	32	48	29	-0.53	166	131.3	89.7	47	10	6	19.3	5.1	7.0
15.3.51 1240	-71	-	71	28.6	-	-	-0.63	135	129.0	89.1	47	10	-	13.0	-	7.0
15.3.51 2115	17.5	-1.06	-	0.18	1.7	1.0	-	-	-	-	-	-	-	-	-	-

Fig. 1.

Mean Profiles . 22 July 52. 1415 - 1445.

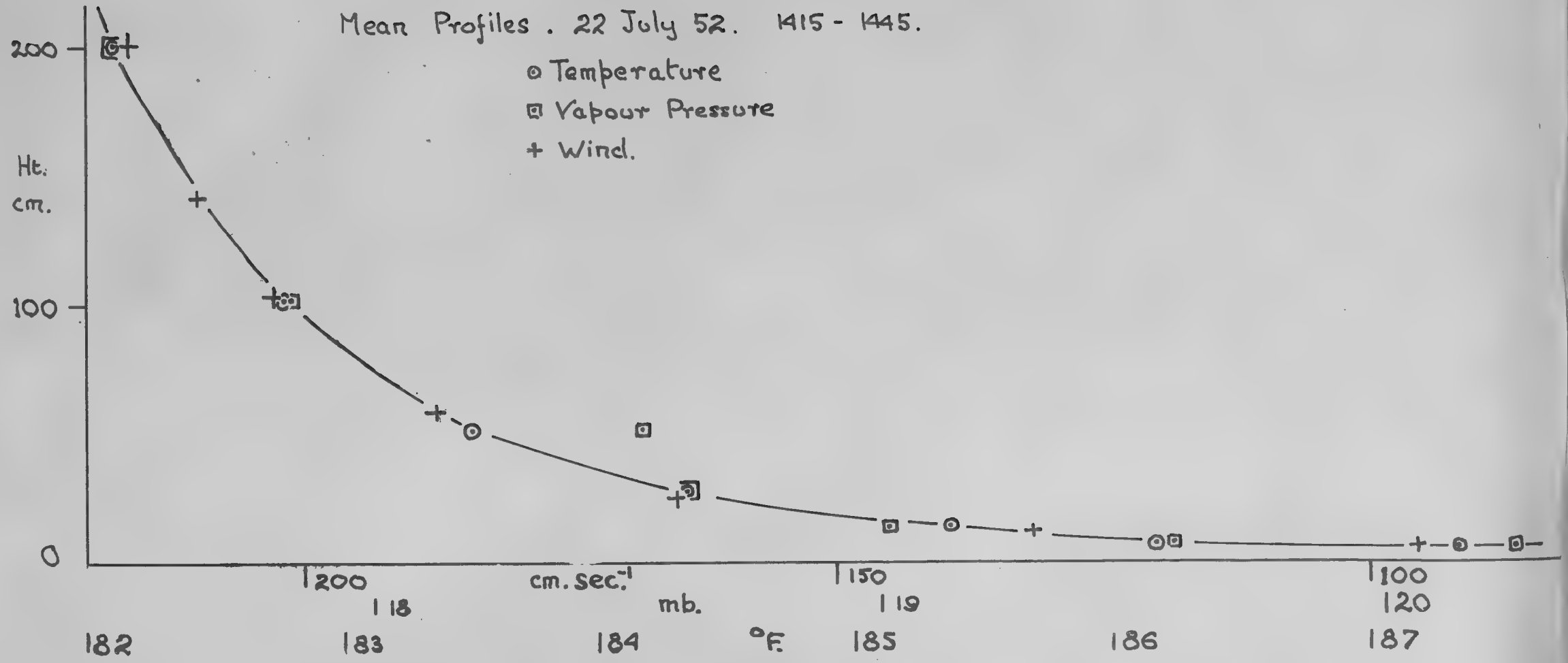

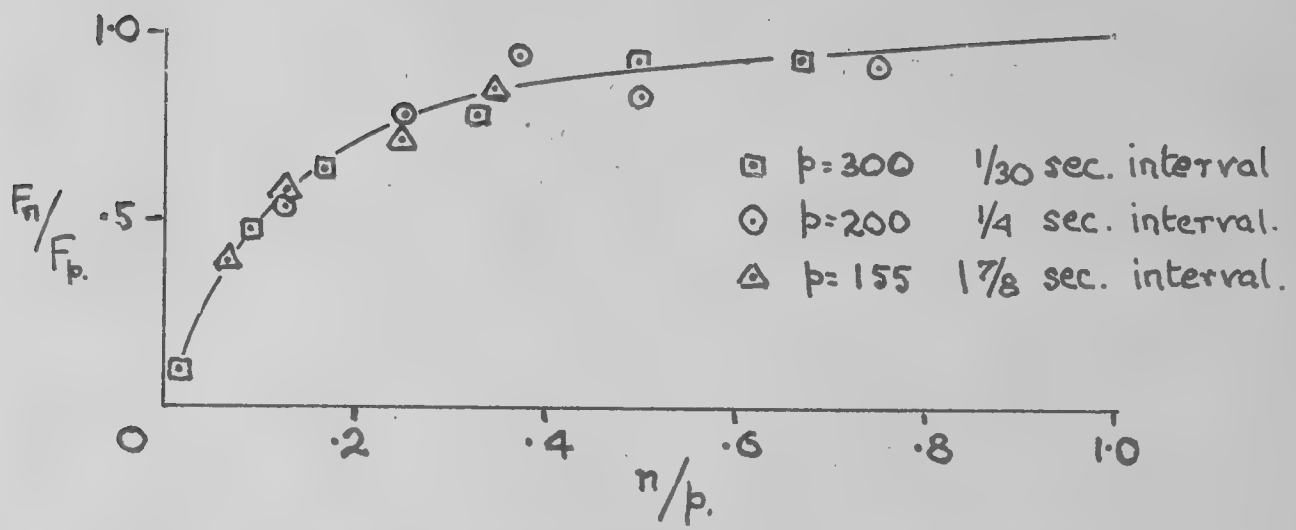

Fig.2. Heat flux from partial and complete series

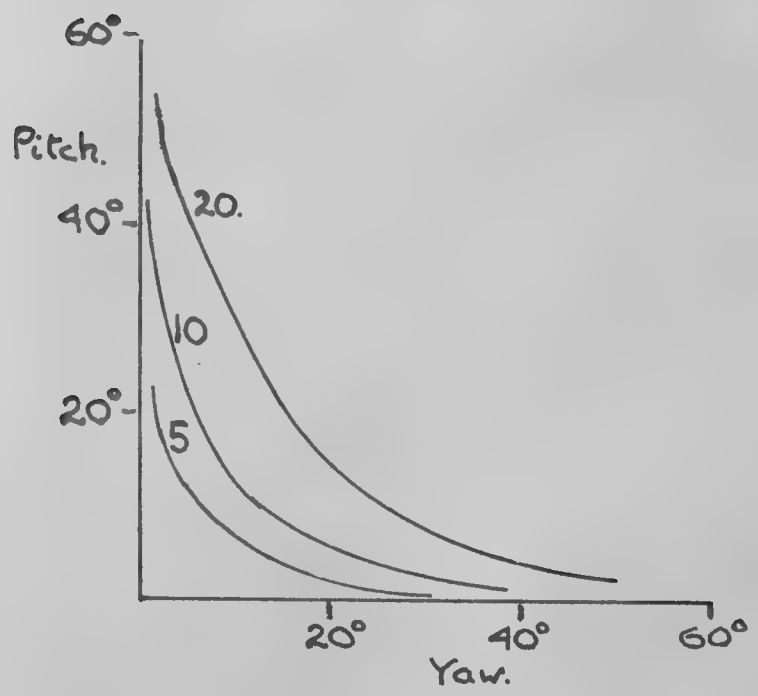

Fig.3 Approximate isopleths of error (per cent) in vertical component of wind at various angles of attack

Fig.4. Examples of frequency of deviations from mean wind direction in 1 min run

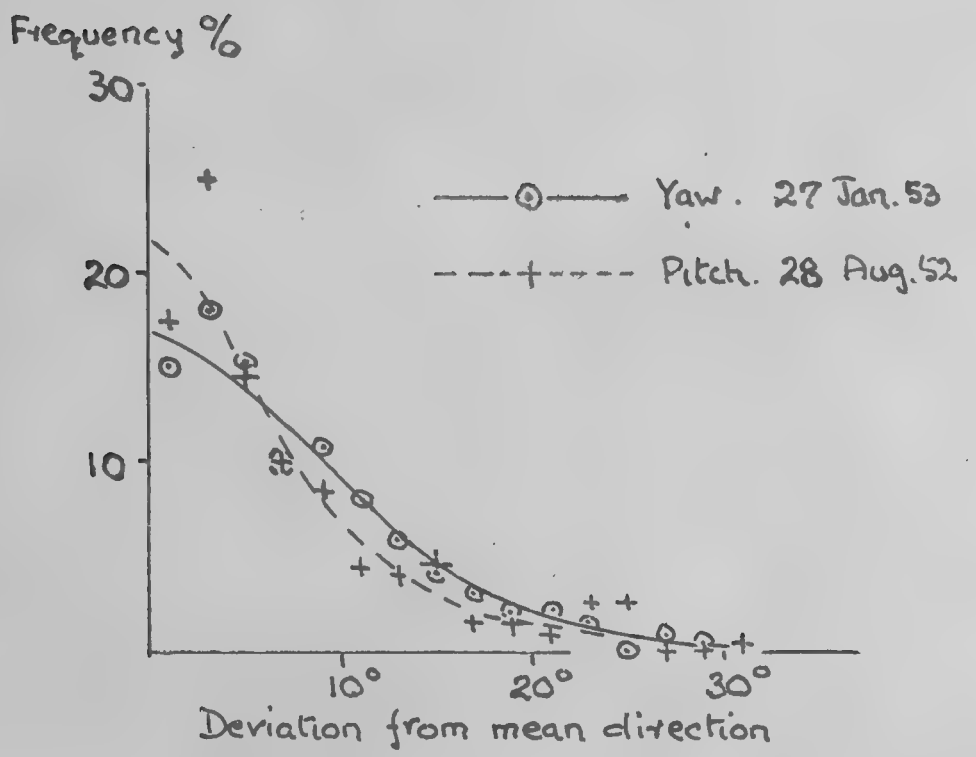

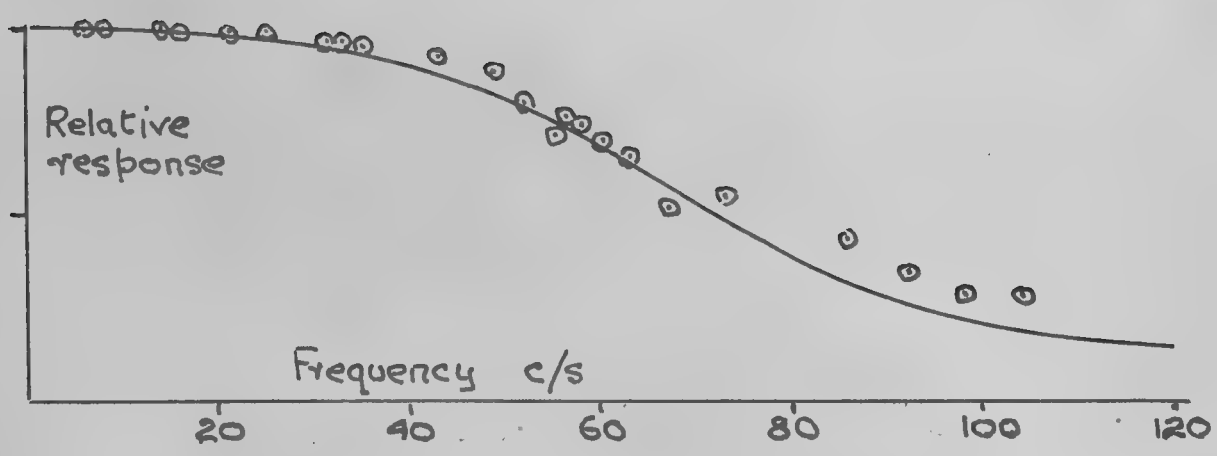

Fig.5. Response of damped galvanometer (Rye 19997). Damping resistance 135 Ω. (Full curve is theoretical response at 0·7 critical damping)

Fig.6. Circuit for high speed galvanometers

Anemometer

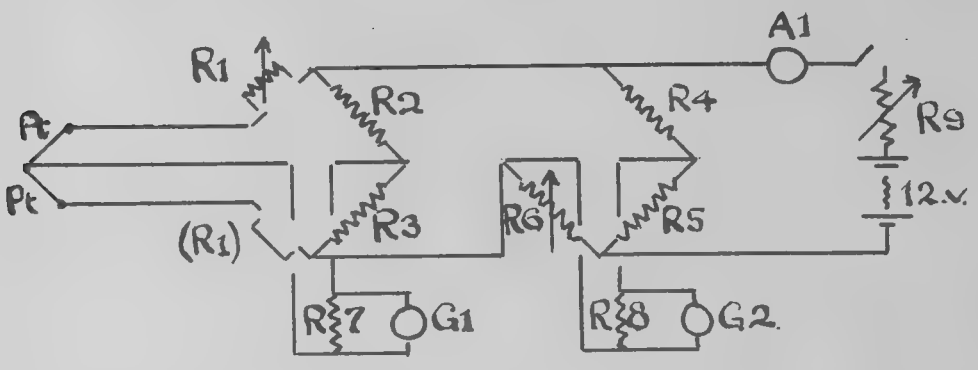

Thermometer

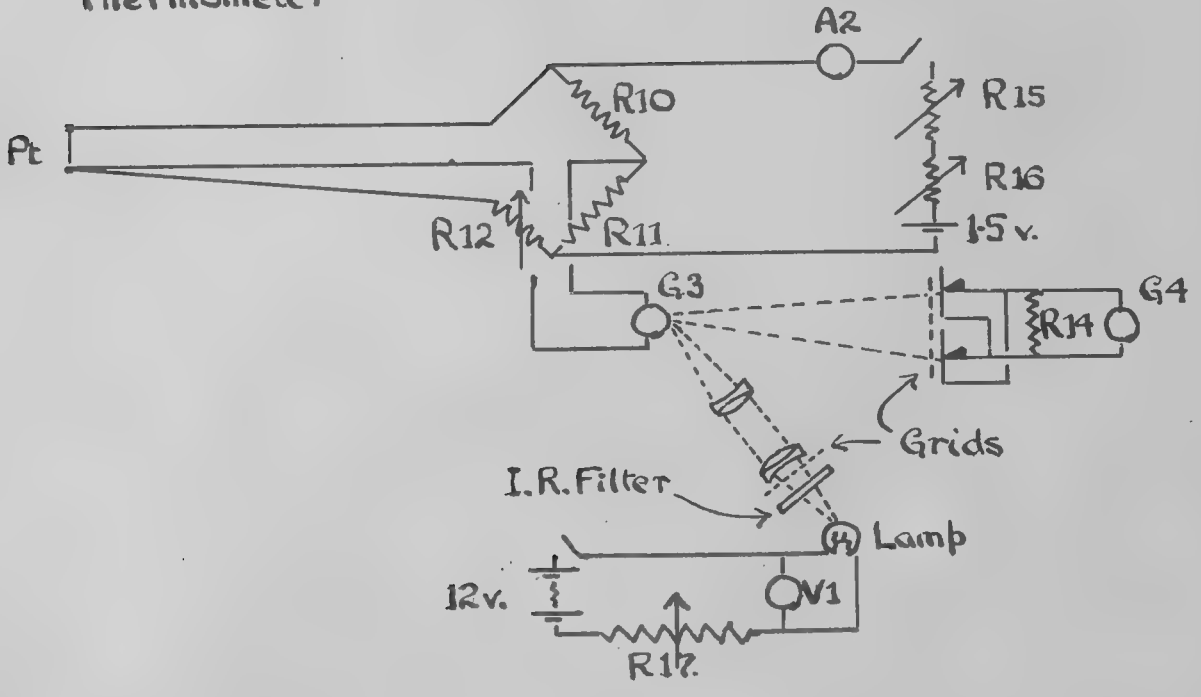

R1	Slide wire	0-1 ohm.		R14		165 "
R2,3,4,5.		500 "		R15		5000 "
R6	Decade	0-111 "		R16		50 "
	Slide wire	0-0·1 "		R17		0-1 "
R7		180 "				
R8		155 "		A1	Ammeter	0-200 mA.
R9		0-115 "		A2	"	0- 5 mA.
R10,11		50 "		V1	Voltmeter	0-15 v.
R12	Decade	0-111 "				

Galvanometers

G1	Inclination of wind	50·9	ohm.
G2	Wind speed	48·0	"
G3	Temperature primary	48·7	"
G4	" secondary	51·3	"

$u = 40\ cm.sec^{-1}$

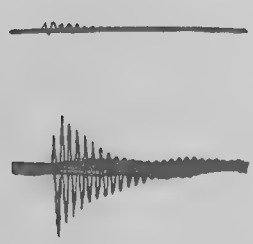

$u = 97\ cm.sec^{-1}$

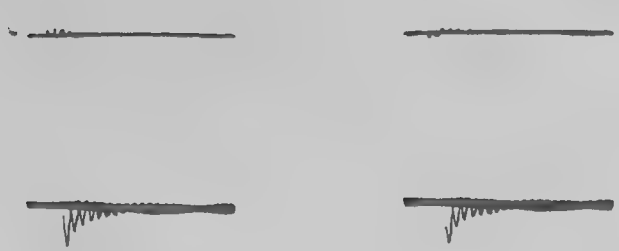

$u = 250\ cm.sec^{-1}$

Fig. 7

Determination of time constant of 0·0005 in. diam. Pt. wire

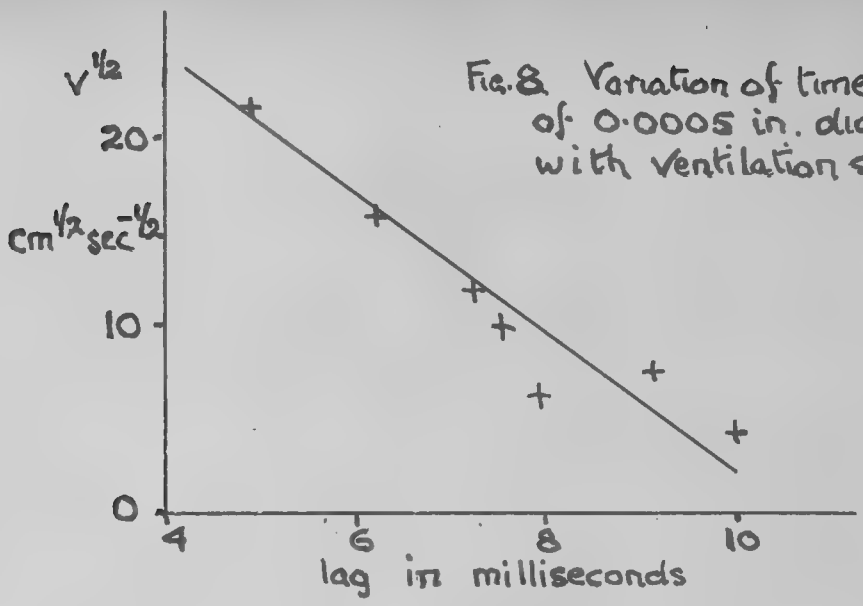

Fig. 8 Variation of time constant of 0·0005 in. diam. Pt. with ventilation speed

MRP's 874, 875, 877, 878, 883

the time of issue this report has not been published. Any author desiring to quote this paper should refer to it as "A paper of the Meteorological Research Committee (London), M.R.P. No. 874 by Mr. J.G. MOORE A copy is available in the Library of the Meteorological Office."

M.R.P.874
S.C.II/176
27th August, 1954.

AD 63981
Tech File

AIR MINISTRY

METEOROLOGICAL RESEARCH COMMITTEE

Average Pressure and Temperature of the Tropopause

by
J. G. Moore (Meteorological Office)

1. Summary

Charts of the world (Figs.1-8) are reproduced showing the average pressure and temperature of the tropopause in the mid-season months, a distinction being made between "polar" and "tropical" tropopauses.

An attempt is made to delineate the region in which both polar and tropical tropopauses are found and to estimate their respective frequencies of occurrence.

The variation through the year of the monthly averages of the pressure and temperature at the tropopause is investigated.

2. Definitions

In general it was not found possible to apply a rigid definition of the tropopause to the available data. Many of the data were taken from publications of other meteorological services or received in manuscript form with the mean values already evaluated. In these doubt often existed as to the methods used in assessing the tropopause pressures and temperatures and the definitions, if any, that had been employed.

When the tropopause pressures and temperatures were extracted from individual ascents, the following tentative definitions were applied. They are those provisionally adopted for M.O.555 (Upper Air Data).

Troposphere

The troposphere is the layer of the atmosphere immediately around the earth's surface in which temperature normally falls with height. The fall must, in general, exceed 2°C. in any Km. of height, but layers of lower lapse rate may occur:

(a) in the lowest 2 Km.

(b) at higher levels in the troposphere provided that the thickness of such a layer is less than 1 Km. and that the fall in the subsequent half Km. is greater than 1°C.

Stratosphere

The stratosphere is the layer of the atmosphere above the troposphere in which temperature either increases or changes little with height. Any fall in temperature must not exceed 2°C. in any Km. of height. There may be shallow layers of lapse rate greater than 2°C. in a Km. of height within the stratosphere provided that the general criterion holds. Such a layer cannot occur at the boundary.

/Tropopause

Tropopause

The tropopause is the boundary between stratosphere and troposphere and may be defined either as the top of the troposphere or as the base of the stratosphere. If the two coincide there is a single tropopause. If the top of the troposphere and base of the stratosphere determined from the above definitions do not coincide two tropopauses are reported.

In the middle and high latitudes the base of the stratosphere and the top of the troposphere normally coincide in a single surface. In the tropics, also, stratosphere and troposphere are normally coterminous. In the sub-tropics, however, two tropopauses are frequently found, an upper, which appears to be a poleward extension of that over the tropics, and a lower which appears as an equatorward extension of the tropopause of middle latitudes. These are referred to as the tropical and polar tropopauses respectively.

3. Data available and methods of computing

The data used were mainly radio-sonde observations made between the years 1940 and 1952 with observations for earlier years at a few stations. The number of years available at the different stations varied considerably and no attempt has been made to adopt a uniform period.

Three classes of data may be distinguished:-

A. Average values taken directly from publications and MS. data of other meteorological services. For these the definitions are for the most part unknown, and for some regions no rigid definition appears to have been used.

B. Average values computed from individual ascents using the definitions set out above.

C. Values obtained by estimation from average temperatures at standard pressure levels.

The regions with data in these different classes and the periods covered are shown below:-

A		B		C	
Africa	1948-53	Alaska	1949-51	Caribbean	1940-43
Australia	1949-52	British Isles	1946-53	Pacific Is.	1950-51
Canada	1942-50	China	1942-44	U.S.S.R.	1949-51
Germany	1948-52	Falklands	1948-53		
Hong Kong	1950-53	Greenland	1949-51		
Hungary	1913-14, 1927-40	Iceland	1949-51		
India	1926-40	Japan	1949-52		
New Zealand	3-9 years	Mediterranean and Middle East (M.O. stations)	1950-51		
Norway	1949-51	Ocean stations	1949-52		
		Switzerland	1948-51		
		U.S.A.	1949-51		
		U.S.S.R.	1949-51		

In computing the averages for class B, mean monthly values of pressure and temperature were evaluated for the individual years and the long period averages were obtained by giving equal weight to each year. When the number of observations in any month was less than ten the monthly mean for that month was weighted: months with 10 or more observations were given unit weight, months with 9 observations .9 and so on.

Data in class C were used only when no data were available in classes A or B. For these the pressure and temperature at the tropopause were assessed by a method due to Flohn(1). In this method the average monthly temperature at the

/station

station was plotted against the logarithm of the pressure. Two straight lines, drawn to fit the curve, one in the upper troposphere and the other in the lower stratosphere, were extended to intersect. Their intersection was taken as giving the average pressure and temperature at the tropopause. This method can of course only be used in regions where a single tropopause is normally reported and even there it is to some extent subjective. The values thus found will normally differ from those obtained by averaging the values for individual ascents (class B) which may be regarded as the true values. In order to test the extent to which the two differ a comparison was made of data obtained by the two methods, with the following result:

In regions of polar tropopause it was found that in January and April the difference of pressure was not systematic. The values in general agreed to within about 15 mb. though occasionally the difference was 20 mb. In July and October, on the other hand, the tropopause pressure obtained from the mean curve was always larger than the true mean, the difference being of the order of 15-20 mb. except in the Arctic where it reached 50 mb. in July and 70 mb. in October. Temperature differences showed greater regularity and throughout the year the temperatures assessed from the mean curves (class C) were some 2 or 3°C. higher than the true values.

In regions of tropical tropopause it was found that assessments of tropopause pressure from the mean curves gave a reasonable approximation to the true values though at some places they appeared to be too high. Values of tropopause temperature obtained from the mean curves were about 3°C. higher than the true values.

In spite of these differences, isopleths of pressure and temperature drawn from values obtained from mean curves showed for the most part the same general pattern as the true isopleths even though the actual values of the isopleths differed. This similarity proved of no small assistance in drawing isopleths over regions such as Russia where data were very sparse.

4. The charts (Figs.1-8)

The average values of pressure and temperature at the tropopause in the mid-season months are set out on eight Mercator charts of the World extending from 75°N. to 60°S. (Figs.1a to 8a) with supplementary charts, on circumpolar projection, for the North Polar region (Figs.1b to 8b). Isopleths are drawn for intervals of 20 mb. of pressure for the polar tropopause, and 10 mb. for the tropical tropopause. Isopleths of temperature are drawn at intervals of 4°C. for both types of tropopause. Temperatures are given in degrees absolute (273° + C). Isopleths for the polar tropopause are shown by full lines, broken lines being used where isopleths for intermediate values of pressure and temperature are drawn, those for the tropical tropopause by lines consisting of alternate dashes and dots.

Method of plotting and of drawing the isopleths

Values of pressure and temperature are plotted for all stations for which they are available. Where there are two tropopauses, the values are plotted one above the other, the figures for the polar tropopause being on the poleward side; the figures for the tropical tropopause are plotted in italics. The reliability of the values is indicated by underlining the figure if it is based on a period of four years or more, and by enclosing it in brackets if it is based on only one year or on less than 20 observations. On the working charts the period of years on which each value was based was also plotted but these figures have not been reproduced in the final charts.

In drawing the isopleths more weight was given to values in classes A and B than to those in class C, and the longer the period of the record the greater was considered the reliability.

As far as possible the isopleths were drawn to fit the plotted values, smoothing where the lines appeared unduly tortuous.

/In

In regions where few data for the polar tropopause were available certain general principles were borne in mind: first, that unless there was strong evidence to the contrary the isopleths should not diverge much from the mean wind flow of the middle troposphere i.e. from the pressure contour lines and secondly, that in temperate latitudes there is a high positive correlation between the height of the tropopause and the temperature of the troposphere(2) and that pressure at the tropopause is therefore likely to be low over regions where the troposphere is relatively warm.

In equatorial regions, if data were insufficient, the isopleths were drawn largely by analogy with the temperature at 100 mb.

Over the greater part of the northern hemisphere the isopleths have been drawn with reasonable confidence in so far as their main features are concerned, except perhaps over Russia where data were very scanty. In the tropics although data were not numerous the values at different stations showed good agreement and errors are not therefore likely to be large. It must be borne in mind, however, that earlier investigations (3,4) indicate that the structure of the tropopause in equatorial regions is more complex than has been envisaged in this work. Over the southern hemisphere except in the region of Australasia, information was available for very few stations and little reliance can be placed on the lines.

5. The region with two tropopauses

In the sub-tropical regions of both hemispheres, roughly between latitudes 35° and 45°, two tropopauses are frequently indicated on the curves of ascent, but on some occasions there may be a polar tropopause only and on others a tropical only. An attempt was therefore made to determine the frequency with which the different types occurred.

In order that the results should not be biased by the loss of records at great heights the data used were as far as possible restricted to those which reached 80 mb., unless below that level an upper tropopause had already been reached or its probable existence had been indicated by the presence of a tropospheric lapse rate above the lower tropopause.

The percentage frequencies of the different types of tropopause are shown in the following table:

/Percentage frequency

Percentage frequency of occurrence of polar and tropical tropopauses and of two tropopauses in the sub-tropics

Station and Period	Position	JANUARY				APRIL				JULY				OCTOBER			
		Polar Trops.	Tropical Trops.	Two Trops.	No. of Ascents	Polar Trops.	Tropical Trops.	Two Trops.	No. of Ascents	Polar Trops.	Tropical Trops.	Two Trops.	No. of Ascents	Polar Trops.	Tropical Trops.	Two Trops.	No. of Ascents
		per cent.				per cent.				per cent.				per cent.			
Wakkanai 1950-52	45°25'N 141°41'E.	100	11	11	119	99	22	21	136	73	81	54	151	91	56	47	158
Ship X Ray 1950-52	39°N. 153°E.	97	74	72	78	88	64	52	97	18	95	12	145	19	98	17	129
Shionomisaki 1950-52	33°27'N. 135°46'E.	43	96	38	136	83	89	72	119	4	100	4	144	2	100	2	161
Ship T July 1950 -Oct. 1952	29°N. 135°E.	11	100	11	72	37	100	37	101	0	100	0	146	0	100	0	159
Gibraltar 1950-51	36°09'N. 05°21'W.	97	51	48	69	98	45	43	58	35	80	15	72	63	62	25	79
Malta 1950-51	35°50'N. 140°27'E.	96	93	89	99	98	92	89	83	10	100	10	113	82	88	70	73
Nicosia 1950-51	35°09'N. 33°17'E.	95	96	91	105	100	95	95	103	2	100	2	111	67	75	42	109
Habbaniya 1950-51	33°22'N. 43°34'E.	72	100	72	110	97	97	94	108	0	100	0	123	48	98	46	112
Benina 1950-51	32°05'N. 20°16'E.	57	98	54	123	78	75	54	106	0	100	0	96	19	93	12	115
Bahrein 1950-51	26°16'N. 50°37'E.	21	100	21	97	41	100	41	102	0	100	0	119	0	100	0	116

The table shows that, in any month, as the latitude increases, the polar tropopause occurs more and more frequently until at a certain latitude it is always present, whereas the tropical tropopause occurs less and less frequently until finally it does not occur at all; similarly as the latitude decreases the tropical tropopause becomes more and more frequent until equatorward of a certain latitude it is always present whereas the polar tropopause becomes less and less frequent and finally ceases to appear at all.

In order to give an indication of the poleward limit of the tropical tropopause and equatorward limit of the polar tropopause, areas on the charts are "hatched" where the frequency of both types is greater than 10 per cent. These limits are largely conjectural especially in the southern hemisphere.

The charts show that the tropical tropopause extends further poleward in summer than in winter, reaching furthest north in July in the northern hemisphere and furthest south in January in the southern. The polar tropopause extends further towards the equator in winter than in summer but it reaches its lowest latitude in April in the northern hemisphere and in October in the southern.

At most stations in the zone of two tropopauses the polar tropopause is most frequent in spring and least frequent in summer, e.g. at Benina where it occurs on 78% of occasions in April but vanishes entirely in July. The tropical tropopause is most frequent in summer and generally least frequent in spring, e.g. at Gibraltar where it occurs on 80% of occasions in July compared with 45% in April.

In the transition regions from two tropopauses to a single tropopause the isopleths of temperature and pressure of the less frequent tropopause should be treated with reserve as the values are valid only for the relatively few occasions on which the tropopause exists.

6. Variation through the year

Averages for all twelve months of the year have been computed for a few stations where the necessary data were available, but for the most part the variation through the year has to be judged from data for the mid-season months only. Diagrams for selected stations are shown in Figs.9 and 10.

Polar tropopause

In the northern hemisphere the charts for the mid-season months show that, in general, the pressure at the tropopause is highest in April and lowest in July. In most parts the difference is of the order of 40-60 mb. but it is greater over the large land masses and probably reaches 80-100 mb. over Russia. Temperature is highest in July when pressure is lowest, and lowest in January. The range of the monthly averages is about 4-6°C. except over the large land masses where it is about 9°C.

In the southern hemisphere in the regions where there is a single polar tropopause its pressure shows little variation through the year. The temperature is lowest in winter (July) and highest in summer (January) but the range of variation is difficult to assess owing to lack of data. In Australasia, in the region of two tropopauses, the variation of pressure at the polar tropopause is similar to that in the northern hemisphere with the appropriate reversal of season i.e. highest pressure in winter or spring and lowest in summer (frequently in January or February) with a range of 40-60 mb. Temperature on the other hand seems to reach its highest value in spring (around October) and its lowest in late summer or early autumn (February or March) i.e. several months earlier than would be expected on the analogy of the northern hemisphere. The range is of the same order of magnitude as that in the northern hemisphere. In the oceanic regions of the sub-tropics, away from land masses, the pressure at the tropopause probably varies little through the year.

/Tropical tropopause

Tropical tropopause

In the northern hemisphere the tropical tropopause generally shows higher mean values of both pressure and temperature in summer than in winter, the range being 15-20 mb. and 4-6°C. respectively.

In the sub-tropics of the northern hemisphere, however, at such stations as Malta and Habbaniya where two tropopauses occur frequently for a large part of the year, during the summer months when the polar tropopause ceases to exist or becomes infrequent the pressure and temperature of the tropical tropopause depart from this pattern and both fall instead of rising.

For those regions of the southern hemisphere where the tropical tropopause occurs frequently throughout the year, the few data available indicate that the annual variation of the pressure at the tropopause is less pronounced than that in the northern hemisphere. With a range of 10-15 mb. the monthly mean tropopause pressure reaches its highest value in winter or spring and lowest in summer or autumn. Temperature shows a range of 6-8°C. with highest values in spring and lowest in summer or autumn.

Bibliography

General

1. Flohn, H. — Die Mittlere Höhenlage der Tropopause über der Nordhalbkugel. Met. Rdsch., Berlin, 1, 1947, p. 26.

2. Dines, W.H. — The characteristics of the free atmosphere. Met. Office, Geophys. Mem., London, No. 13, Vol. 2, 1919.

3. Vuorela, L.A. — Synoptic aspects of tropical regions of the Atlantic Ocean, West Africa and South America. Institute of Meteorology, University of Helsinki, 1950.

4. Durandin, P., Mironovitch, V. et Viaut, A. — Structure verticale de l'atmosphère en automne entre les Açores et Bermudes. Memorial de l'O.N.M., Paris, No. 29, p. 10, 1938.

Sources of Data

Class A

Africa

5. MS. data supplied by the Directors of the respective meteorological services.

(a) Khartoum (Sudan Met. Office)
(b) Nairobi (British East Africa Met. Service)
(c) Pretoria (Union of South Africa Weather Bureau)
(d) Salisbury (Rhodesia Met. Service)

Australia

6. MS. data for Australian Stations supplied by the Director of the Commonwealth of Australia Met. Bureau.

7. Commonwealth of Australia Dept. of External Affairs. — A.N.A.R.E. Reports Series D, Meteorology, Volumes II, III and IV, 1949-51, (Heard and Macquarie Islands).

8. Loewe, F. and Radok, U. — A meridional aerological cross-section in the SW. Pacific. American Met. Soc., Journal of Meteorology, Vol. 7, No. 1, Feb. 1950, p. 58.

Canada

9. Toronto, Dept. of Transport, Met. Division. — Summaries of radio-sonde observations in Southern Canada (South of lat. 55°N.), June 1941 - Dec. 1949.

10. " " — Aerological Data for Northern Canada, Toronto, 1949.

Germany

11. London, Met. Office. — MS. data for Langenhagen & Schleswigland.

Hong Kong

12. MS. data supplied by the Director, Royal Observatory, Hong Kong.

Hungary

13. Béll, B. — Mittlere Werte der Temperatur in der freien Atmosphäre über Budapest. Kleinere Veröff. Reichsanst. Met., Budapest, Neue Reihe No. 10, 1941.

/14.

14. Wagner, A. — Klimatologie der freien Atmosphäre. Handbuch der Klimatologie, Köppen, W. & Geiger, R., Bd. I, Teil F., 1931.

India

15. Poona, India Met. Dept. — India Weather Review, 1926-27.

16. " " " " — Upper Air Data, 1928-40.

17. Krishna Rao, P.R. and Ganesan, V. — Characteristics of the upper troposphere, tropopause and lower stratosphere over Trivandrum. Indian J. Met. Geophys., Poona, 4, 1953, p. 193.

New Zealand

18. Gabites, J.F. — Temperature in the troposphere and lower stratosphere over the New Zealand region. N.Z. J. Sci. Tech., Wellington, N.Z., 1953, p. 213.

19. Hutchings, J.W. — A meridional cross-section for an oceanic region. American Met. Soc., Journal of Meteorology, Vol. 7, No. 2, 1950, p. 94.

Norway

20. — MS. data for Norwegian stations supplied by the Director of Det Norske Meteorologiske Insitutt.

Class B

Alaska

21. Washington, U.S. Weather Bureau. — Daily Series Synoptic Weather Maps, 1949-51.

British Isles

22. London, Met. Office. — MS. data for British Isles stations.

China

23. Tokyo, Central Met. Observatory. — Aerological data of Manchuria, 1942-44.

Falklands

24. London, Met. Office. — MS. data for Port Stanley.

Greenland & Iceland

25. Washington, U.S. Weather Bureau. — Daily Series Synoptic Weather Maps, 1949-51.

Japan

26. Tokyo, Central Met. Observatory. — Aerological data of Japan, 1949-52.

Mediterranean & Middle East (M.O. stations)

27. London, Met. Office. — MS. data.

Ocean Stations

28. U.S. Weather Bureau, Dept. of Commerce. — Data from microfilm.

29. Toronto, Dept. of Transport, Met. Division. — Data from microfilm.

Switzerland

30. — Annalen der Schweizerischen Meteorologischen Zentralanstalt, Zurich, 1948-51.

U.S.A. & U.S.S.R.

31. Washington, U.S. Weather Bureau. — Daily Series Synoptic Weather Maps, 1949-51.

Class C

Caribbean

32. Ratner, B.J. — Upper air average values of temperature, pressure and relative humidity over the U.S. and Alaska. Washington, D.C., Weather Bureau Tech. Paper, No. 6, 1943.

Pacific Is.

33. U.S. Weather Bureau, Dept. of Commerce. — Data from microfilm.

U.S.S.R.

34. Flohn, H. — Zur Aerologie der Polargebiete. Met. Rdsch., Berlin, 5, 1952, p. 81.

Fig. 1(a)

TROPOPAUSE PRESSURE (MB)

January MRP 874

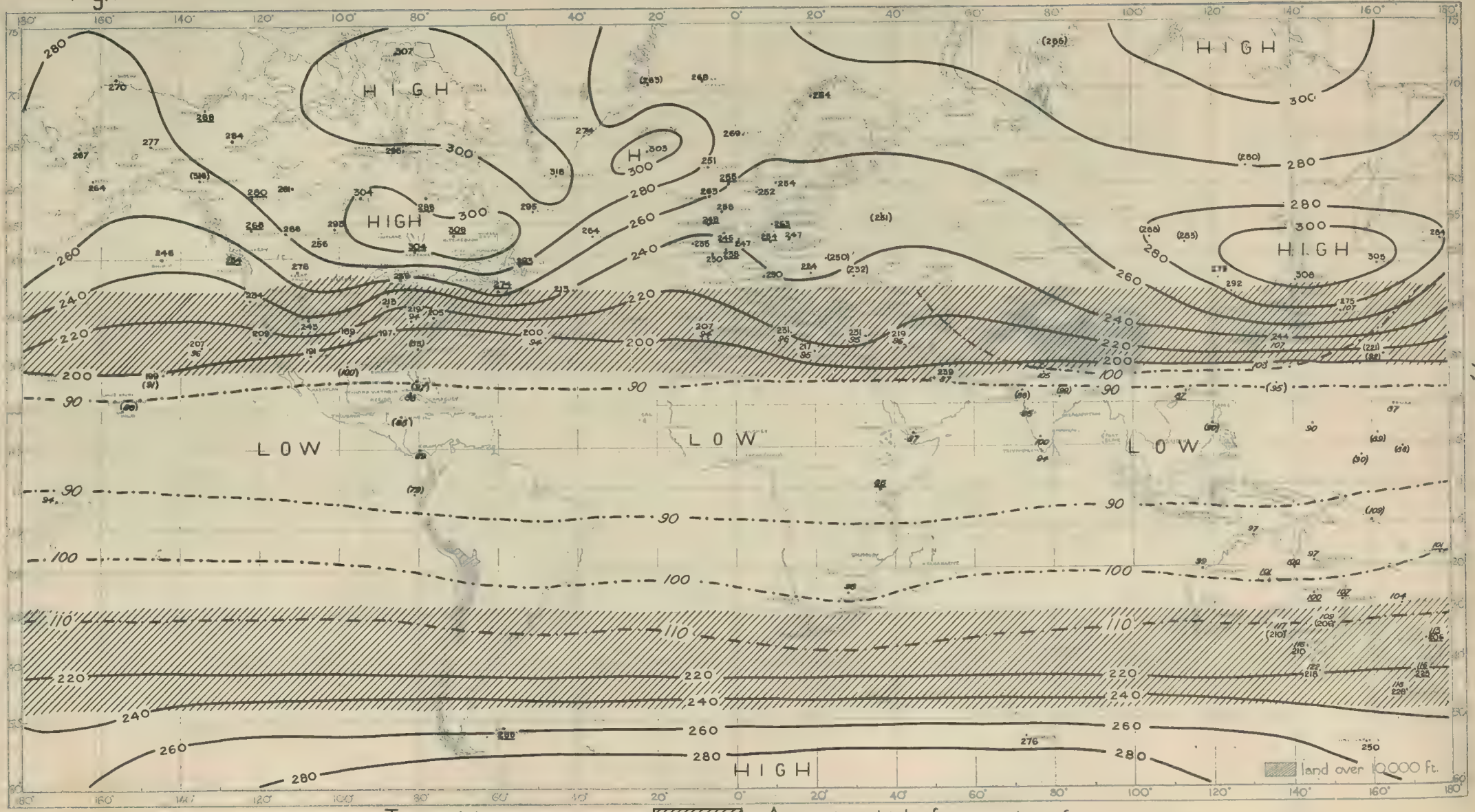

M.R.P. 874

Fig. 1(b) TROPOPAUSE PRESSURE (MB) January

Polar tropopause

Fig. 2 (a) TROPOPAUSE PRESSURE (MB) April MRP 874

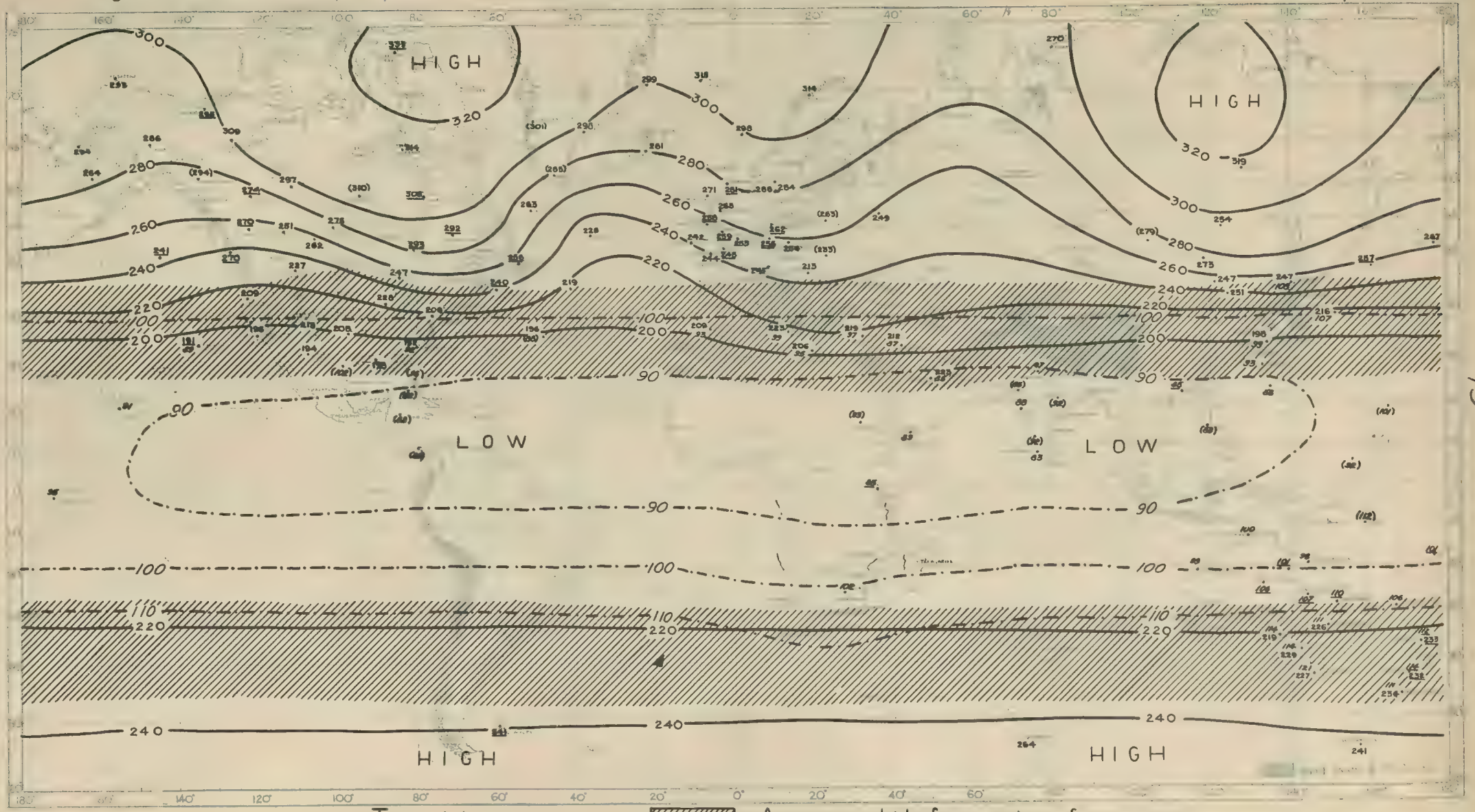

Tropical tropopause
Polar tropopause

Areas in which frequencies of occurrence of both tropopauses are greater than 10%

Fig. 2(b) TROPOPAUSE PRESSURE (MB) April

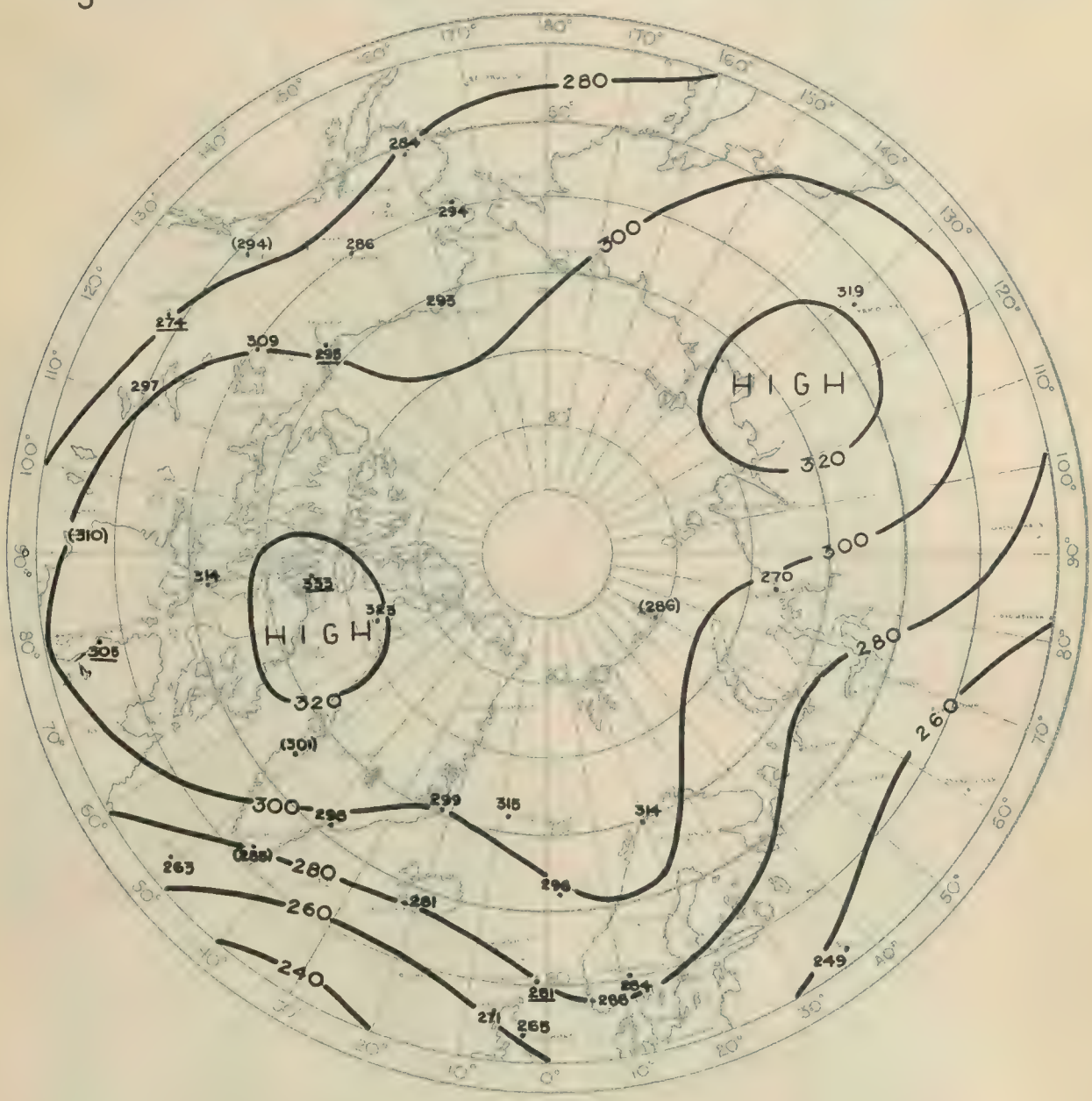

Polar tropopause

Fig. 3(a)

TROPOPAUSE PRESSURE (MB)

July M.R.P. 874

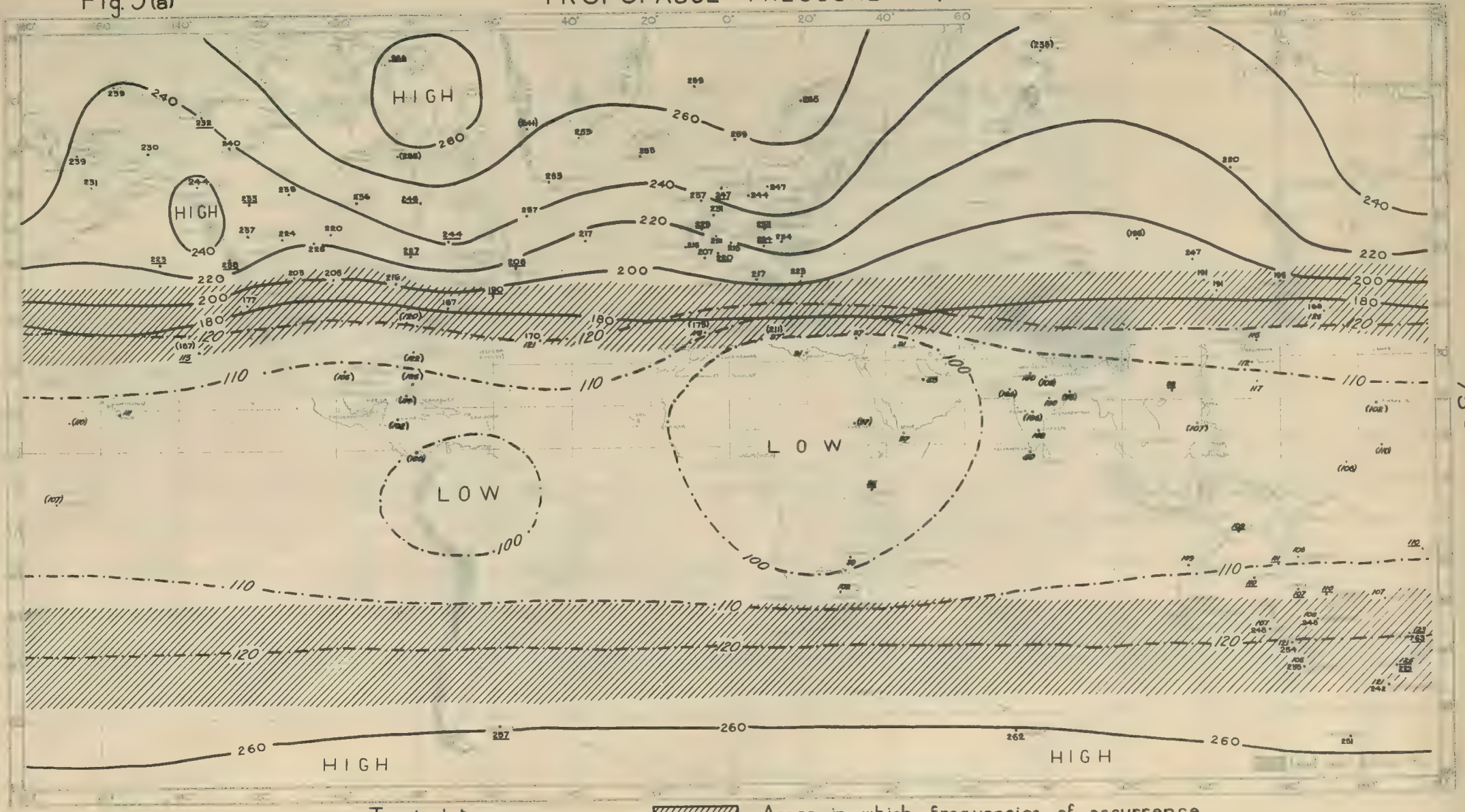

Fig.3(b) TROPOPAUSE PRESSURE (MB) July

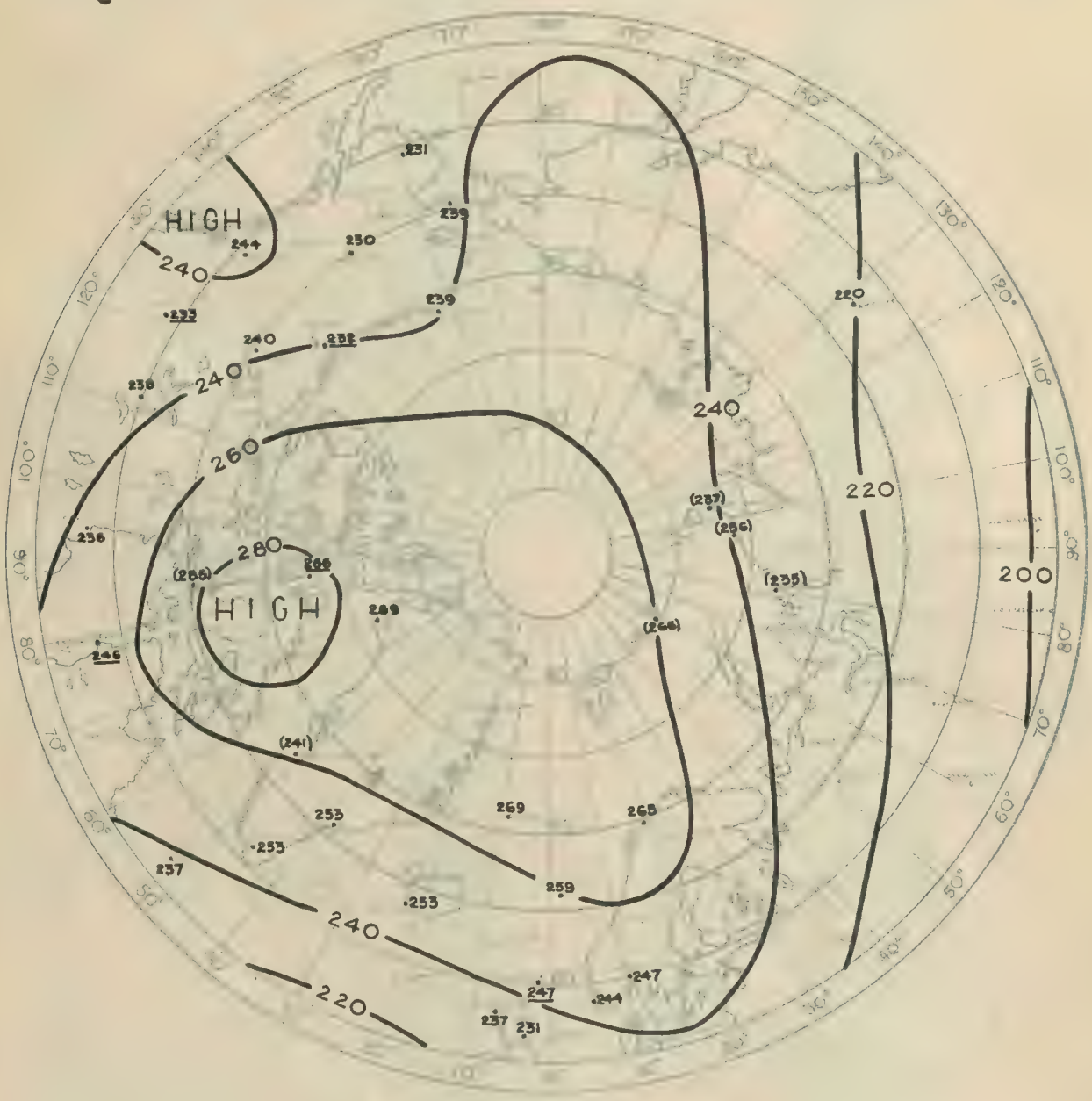

Polar tropopause

Fig. 4(a) TROPOPAUSE PRESSURE (MB) October MRP 874

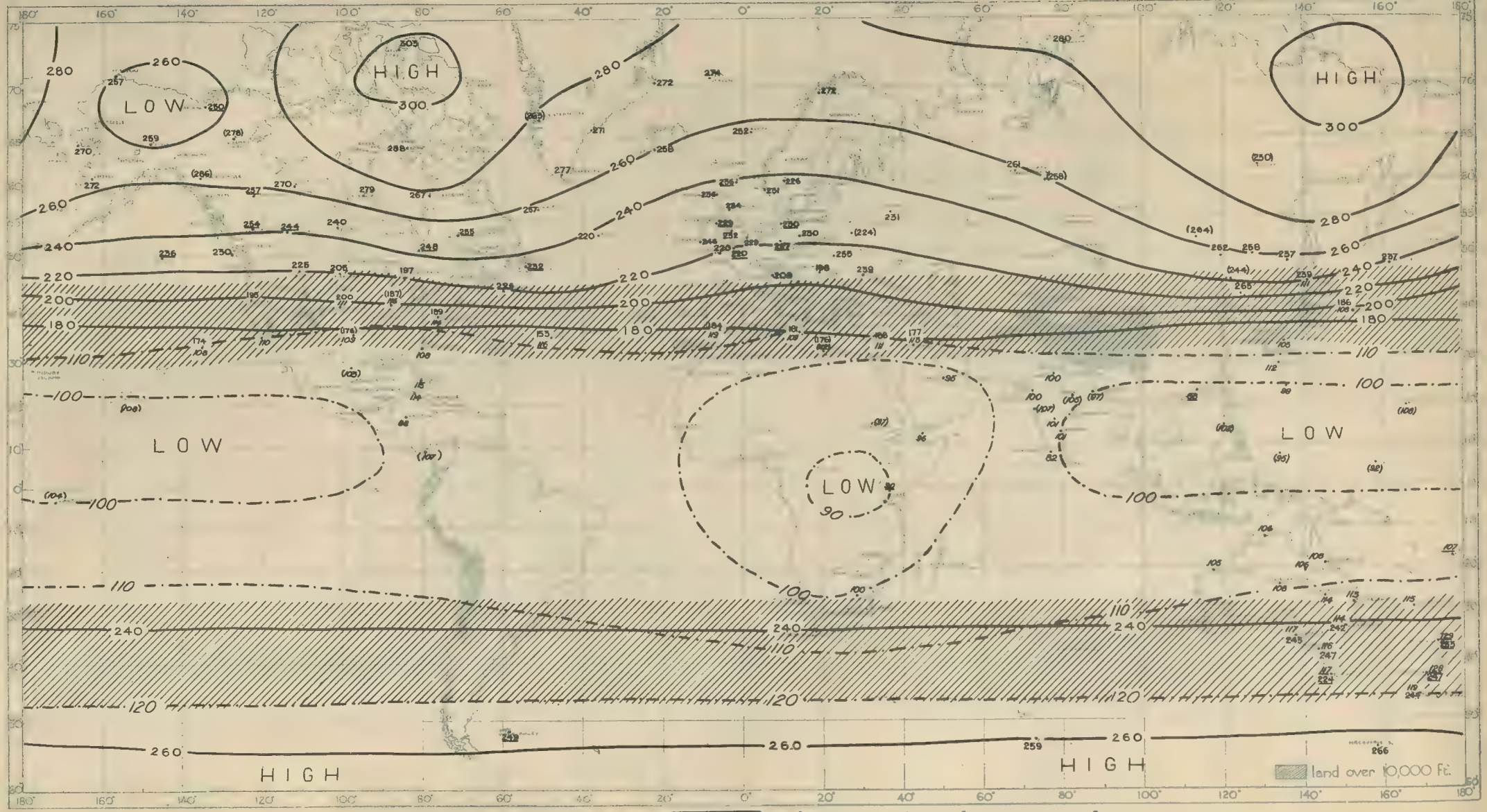

Tropical tropopause
Polar tropopause

Areas in which frequencies of occurrence of both tropopauses are greater than 10%

Fig. 4 (b) TROPOPAUSE· PRESSURE (MB) October

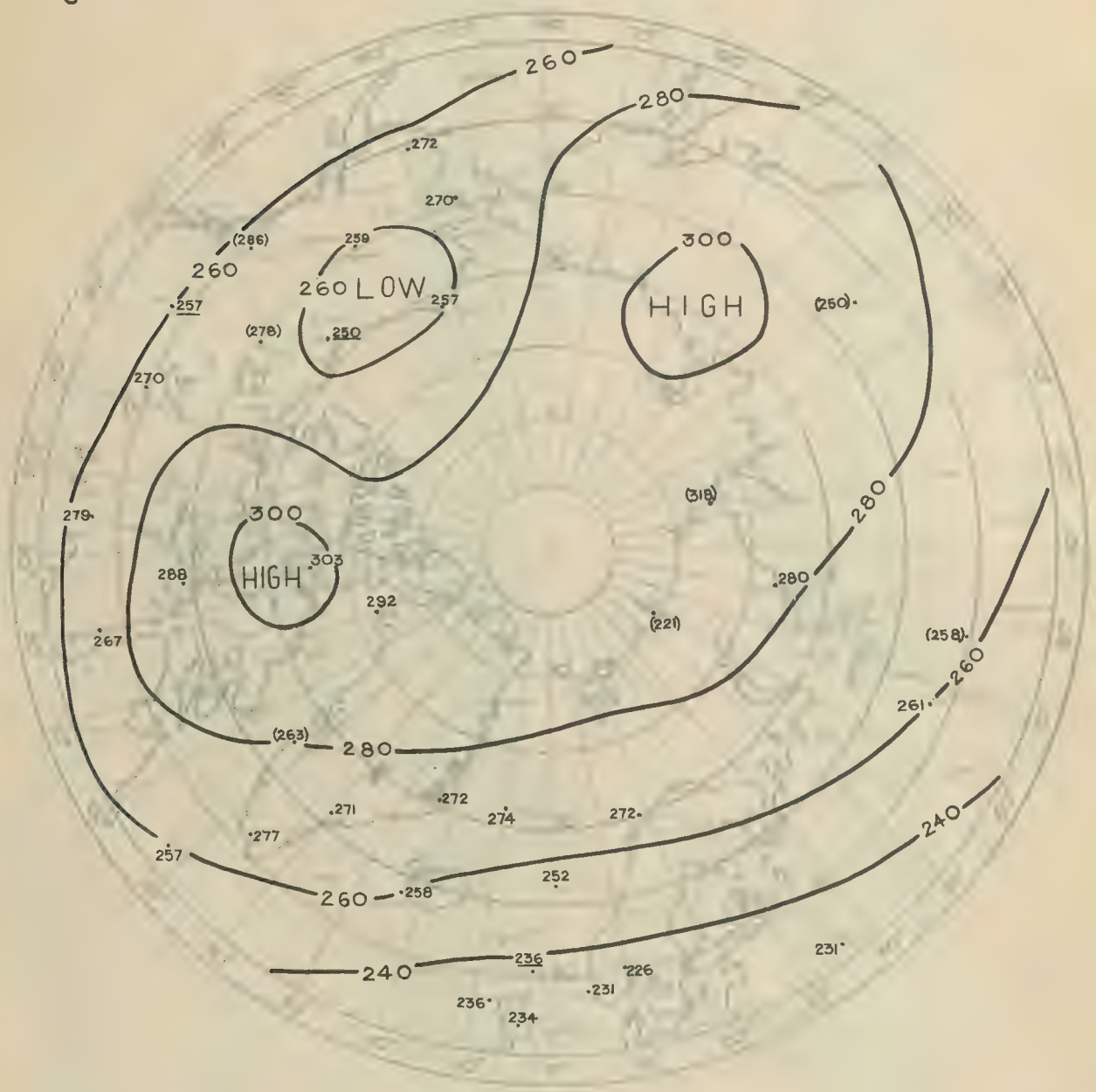

Polar tropopause

Fig. 5 (a) TROPOPAUSE TEMPERATURE (°C) January M.R.P. 874

Isopleths numbered in °A

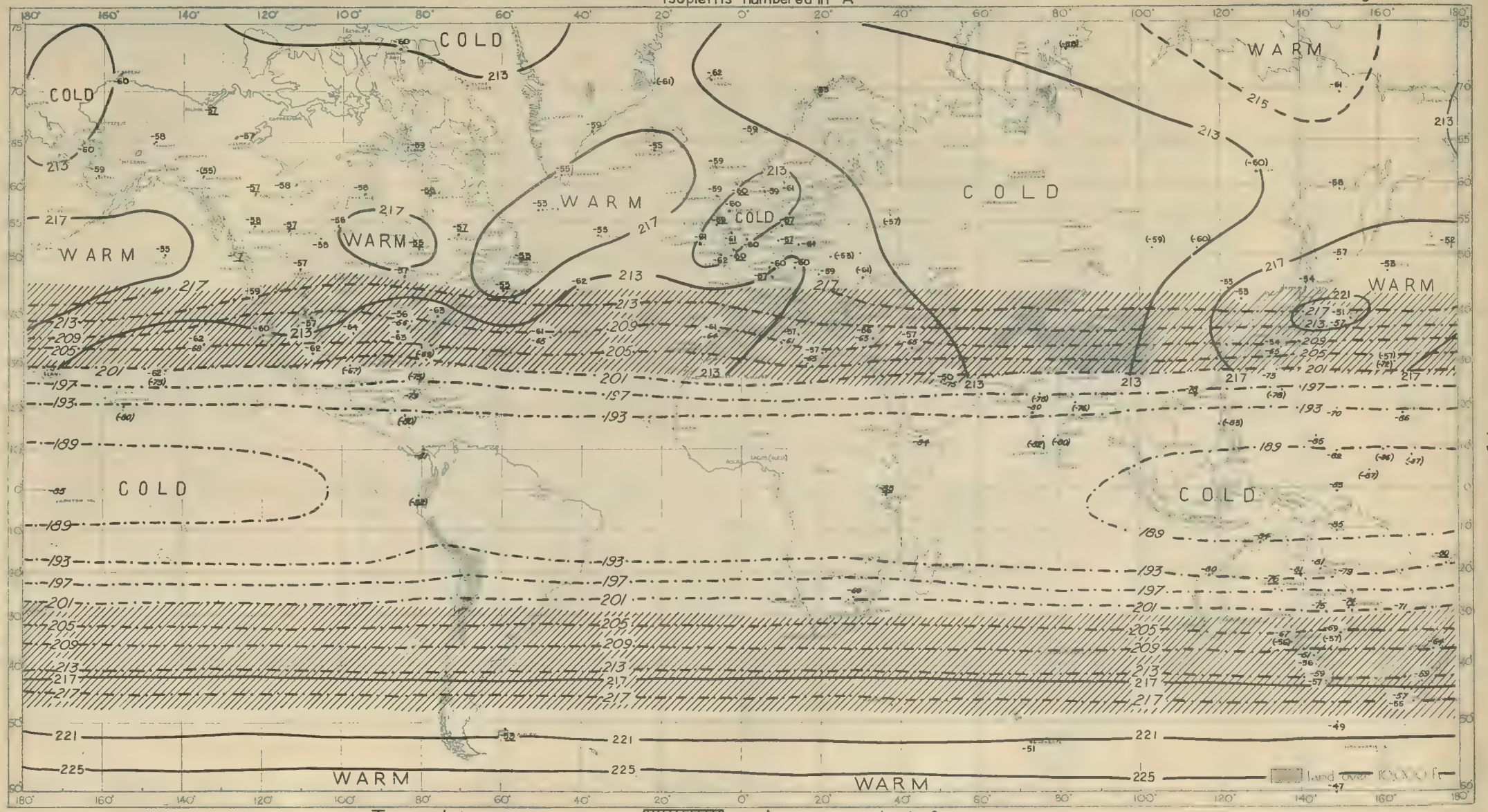

Tropical tropopause

Polar tropopause

Areas in which frequencies of occurrence of both tropopauses are greater than 10%

Fig. 5 (b) TROPOPAUSE TEMPERATURE (°C) January

Isopleths numbered in °A

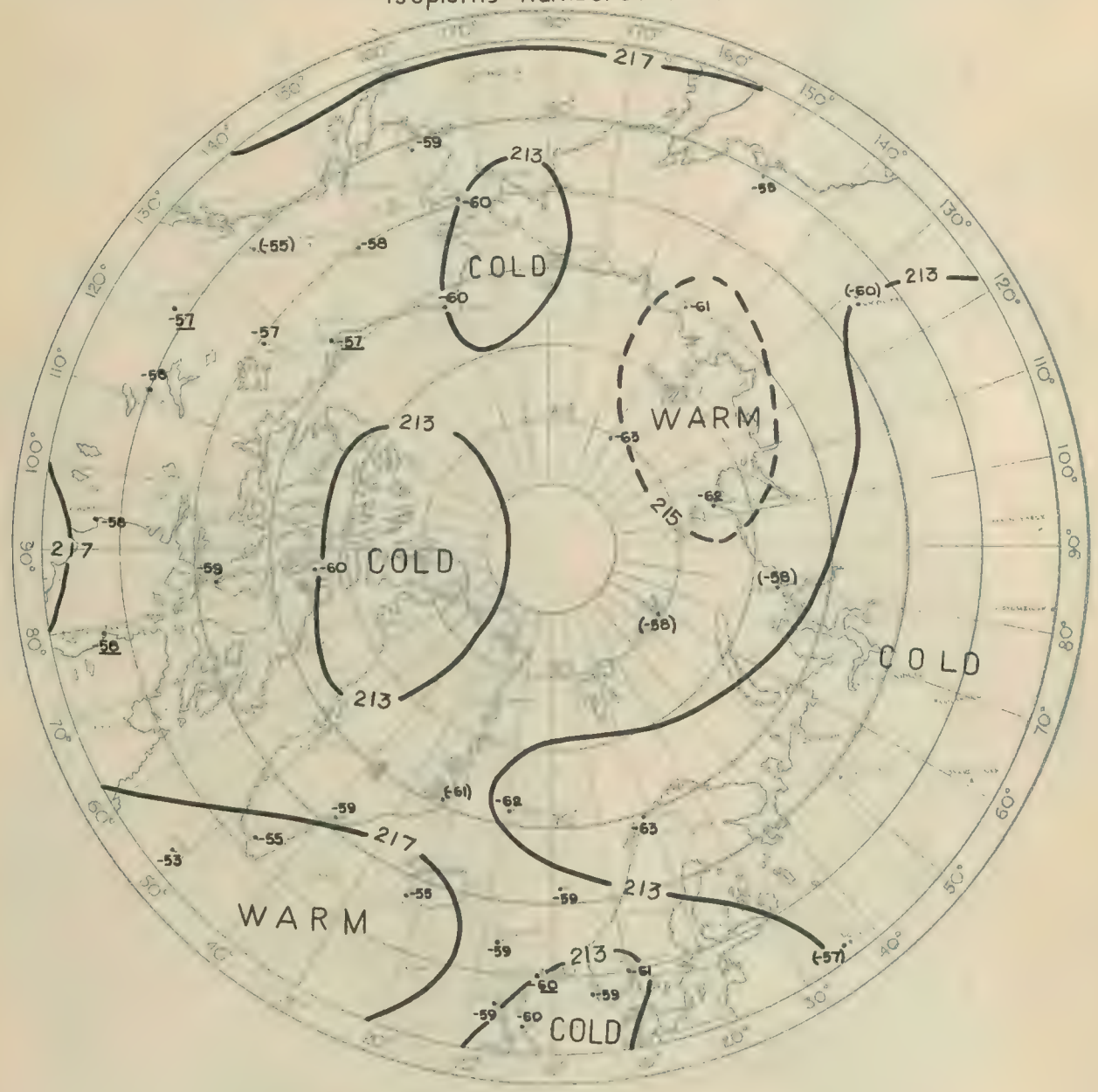

——— Polar tropopause

Fig. 6(a)

TROPOPAUSE TEMPERATURE (°C)

Isopleths numbered in °A

April MRP 874

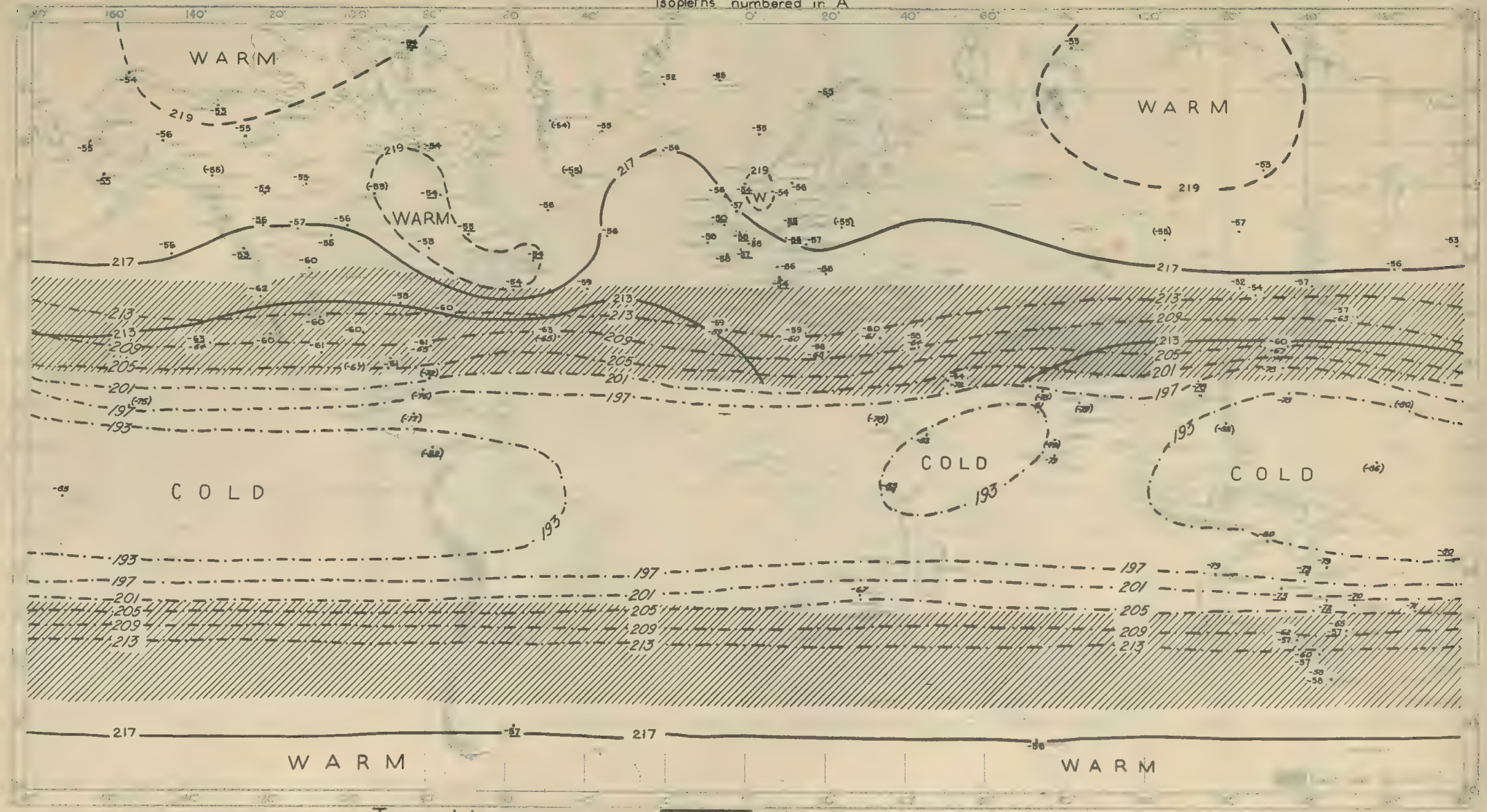

M.R.P. 874

Fig. 6(b) TROPOPAUSE TEMPERATURE (°C) April

Isopleths numbered in °A

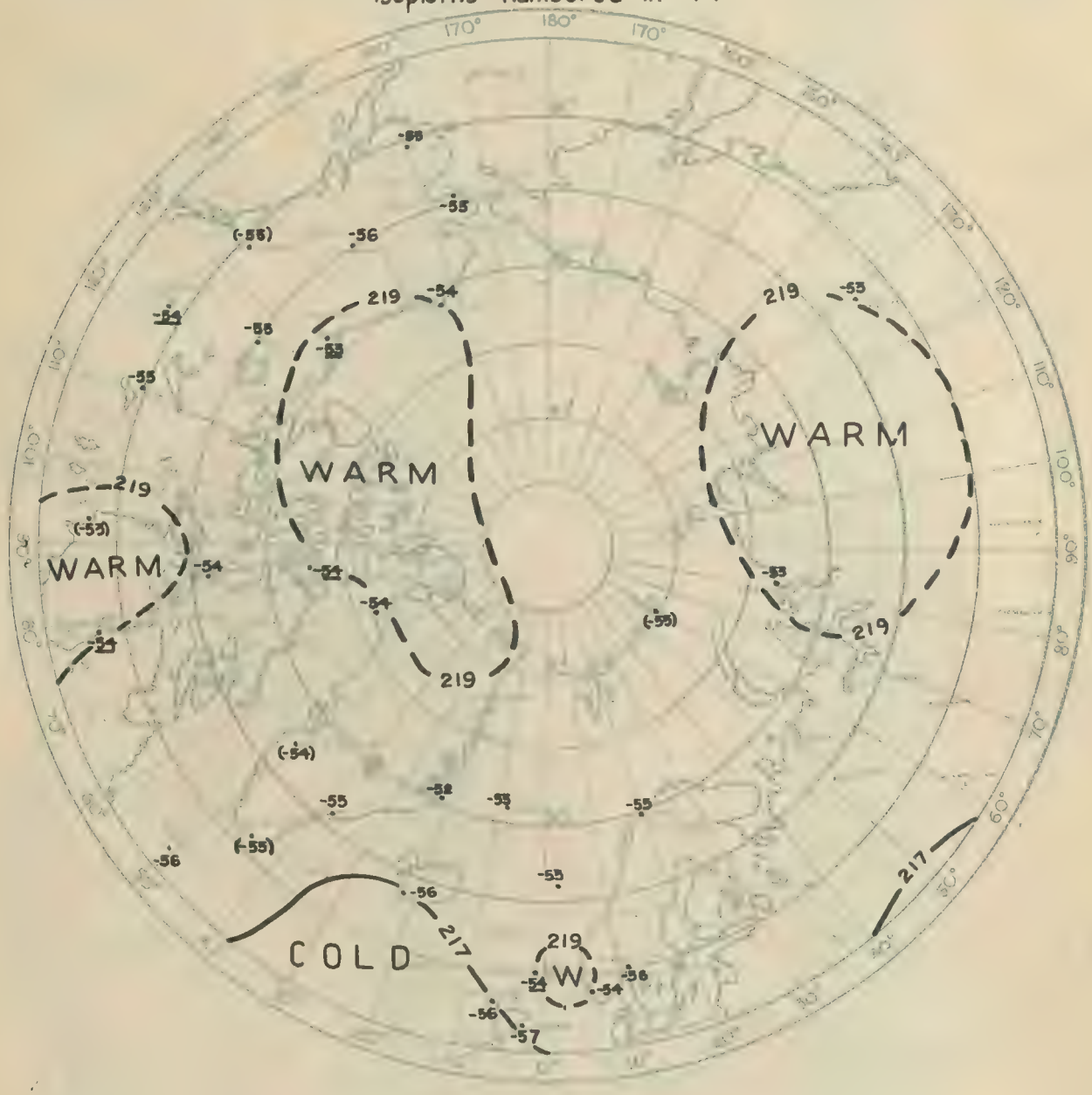

——— Polar tropopause

Fig. 7(a) TROPOPAUSE TEMPERATURE (°C) July M.R.P. 874

Isopleths numbered in °A

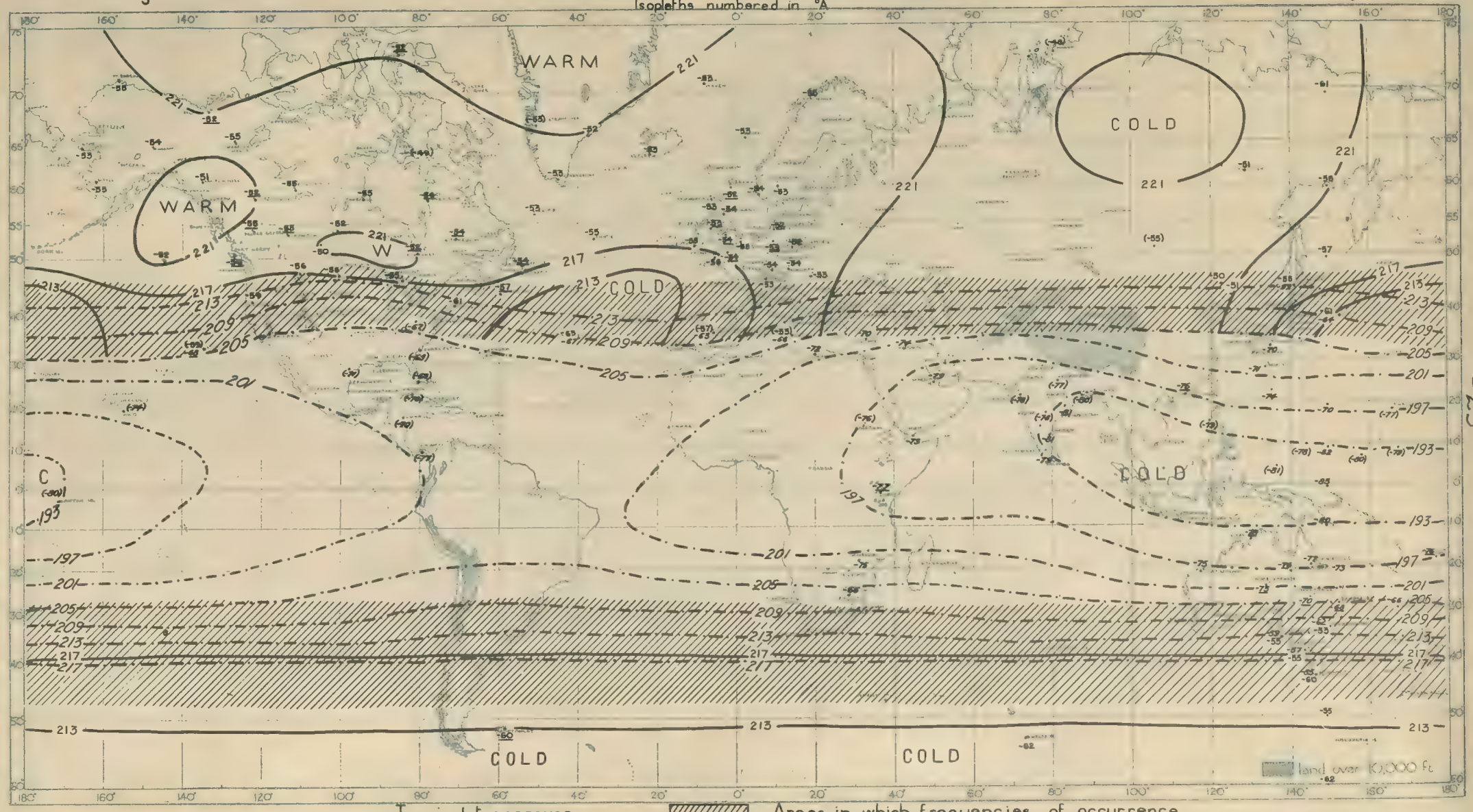

Tropical tropopause

Polar tropopause

Areas in which frequencies of occurrence of both tropopauses are greater than 10%

Fig. 7(b) TROPOPAUSE TEMPERATURE (°C) July

Isopleths numbered in °A

——— Polar tropopause

Fig. 8(a)

TROPOPAUSE TEMPERATURE (°C)

Isopleths numbered in °A

October M.R.P. 874

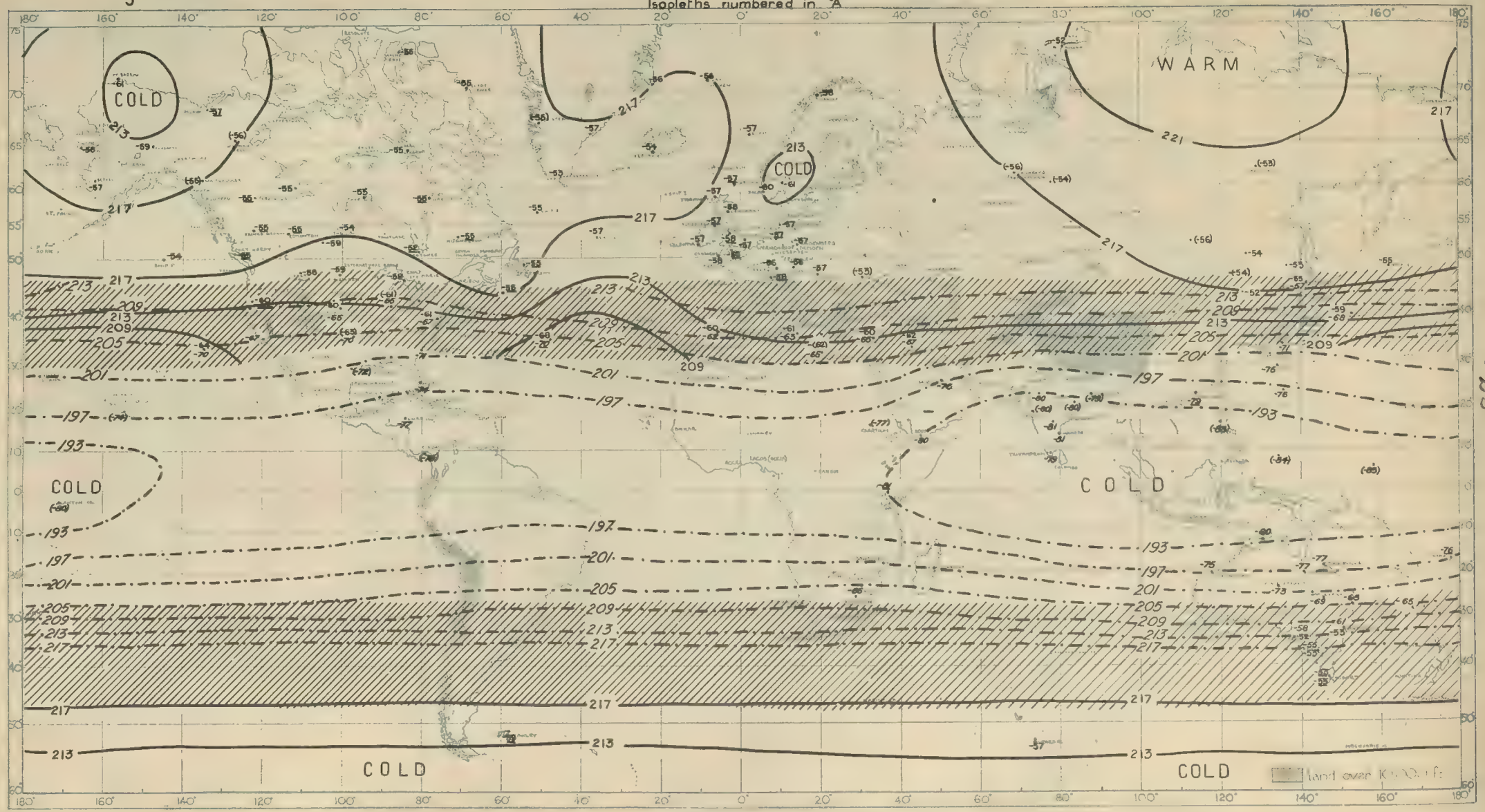

Tropical tropopause

Polar tropopause

Areas in which frequencies of occurrence of both tropopauses are greater than 10%

Fig. 8(b) TROPOPAUSE TEMPERATURE (°C) October

Isopleths numbered in °A

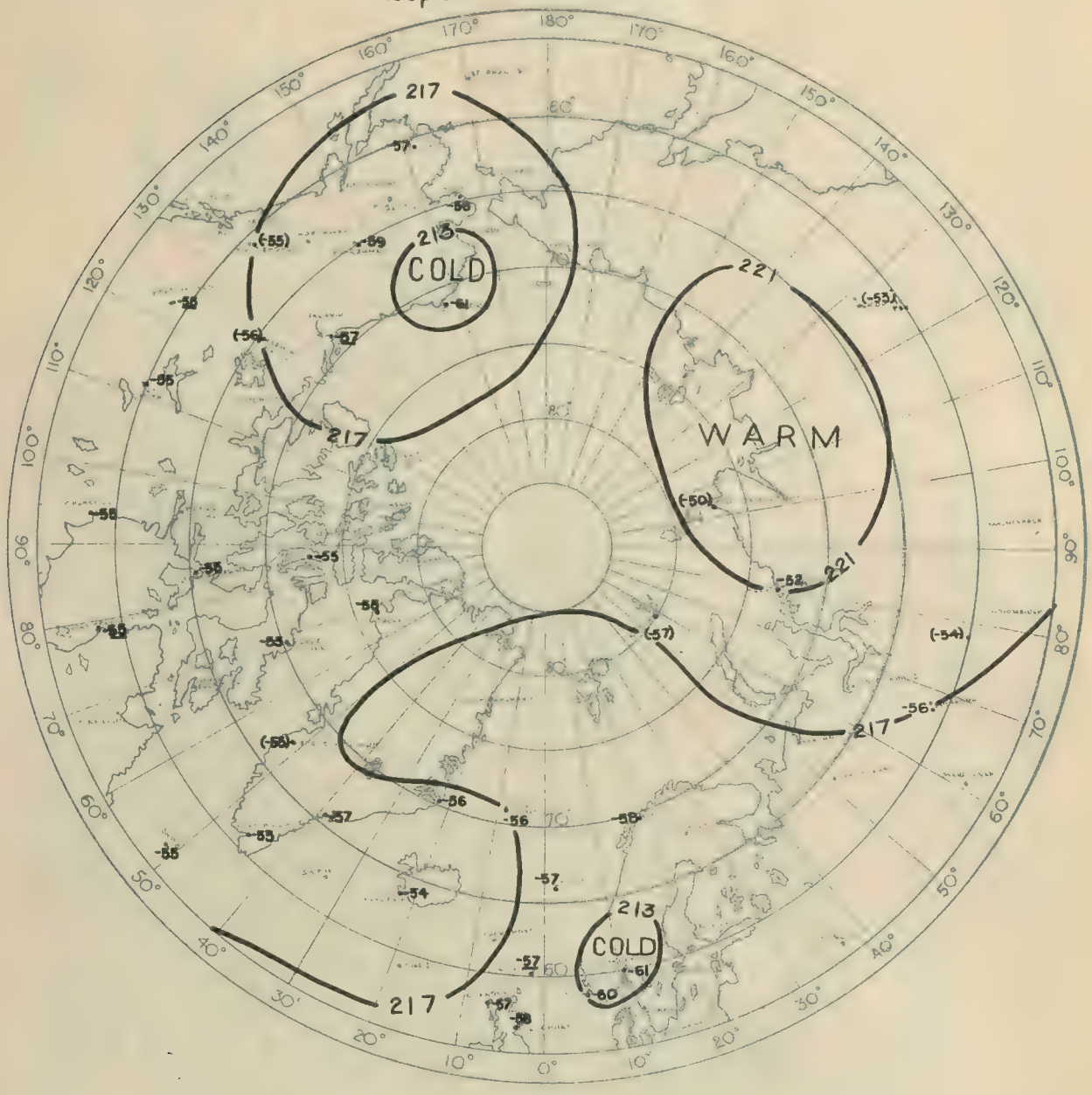

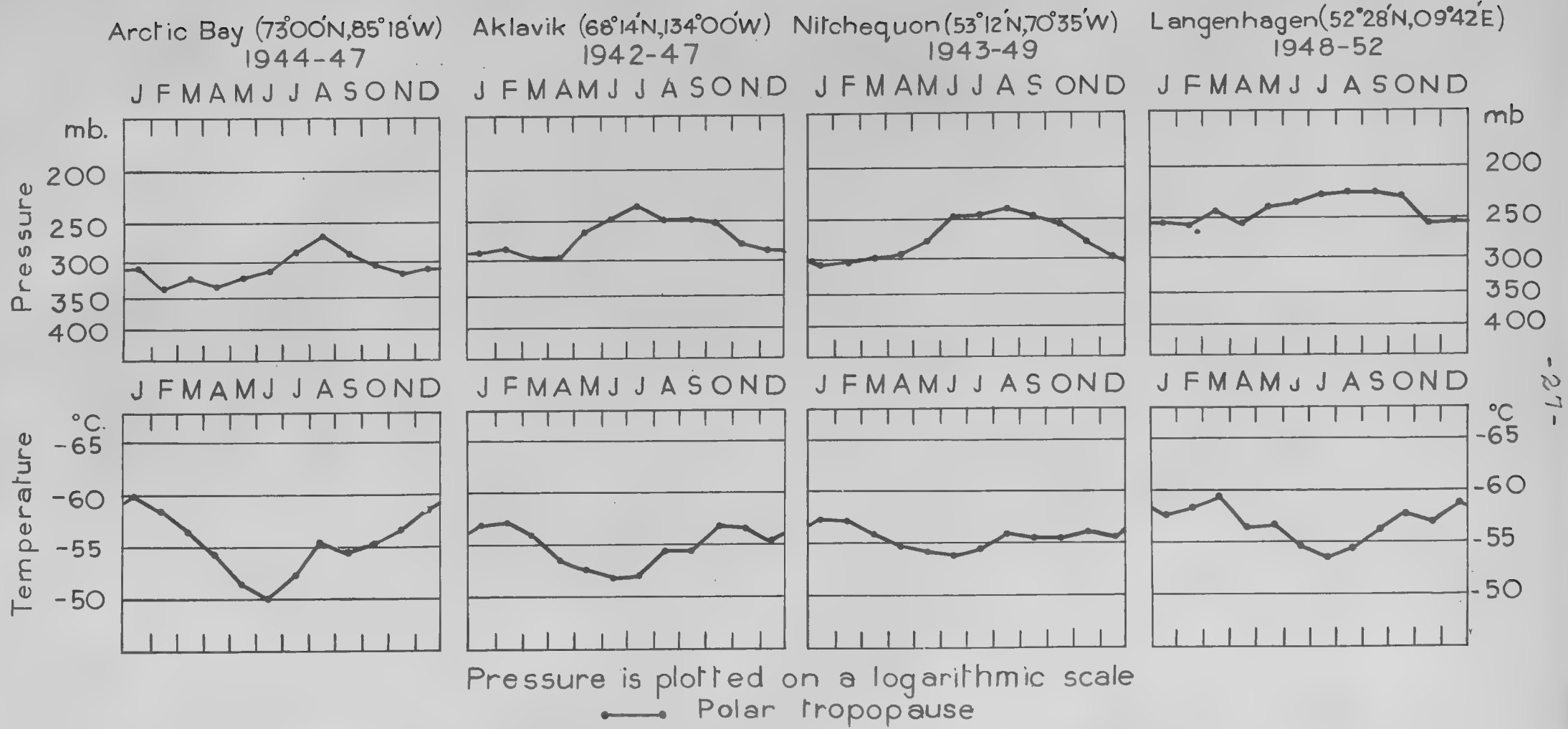

Fig.9. Annual variation of the mean monthly tropopause pressure and temperature

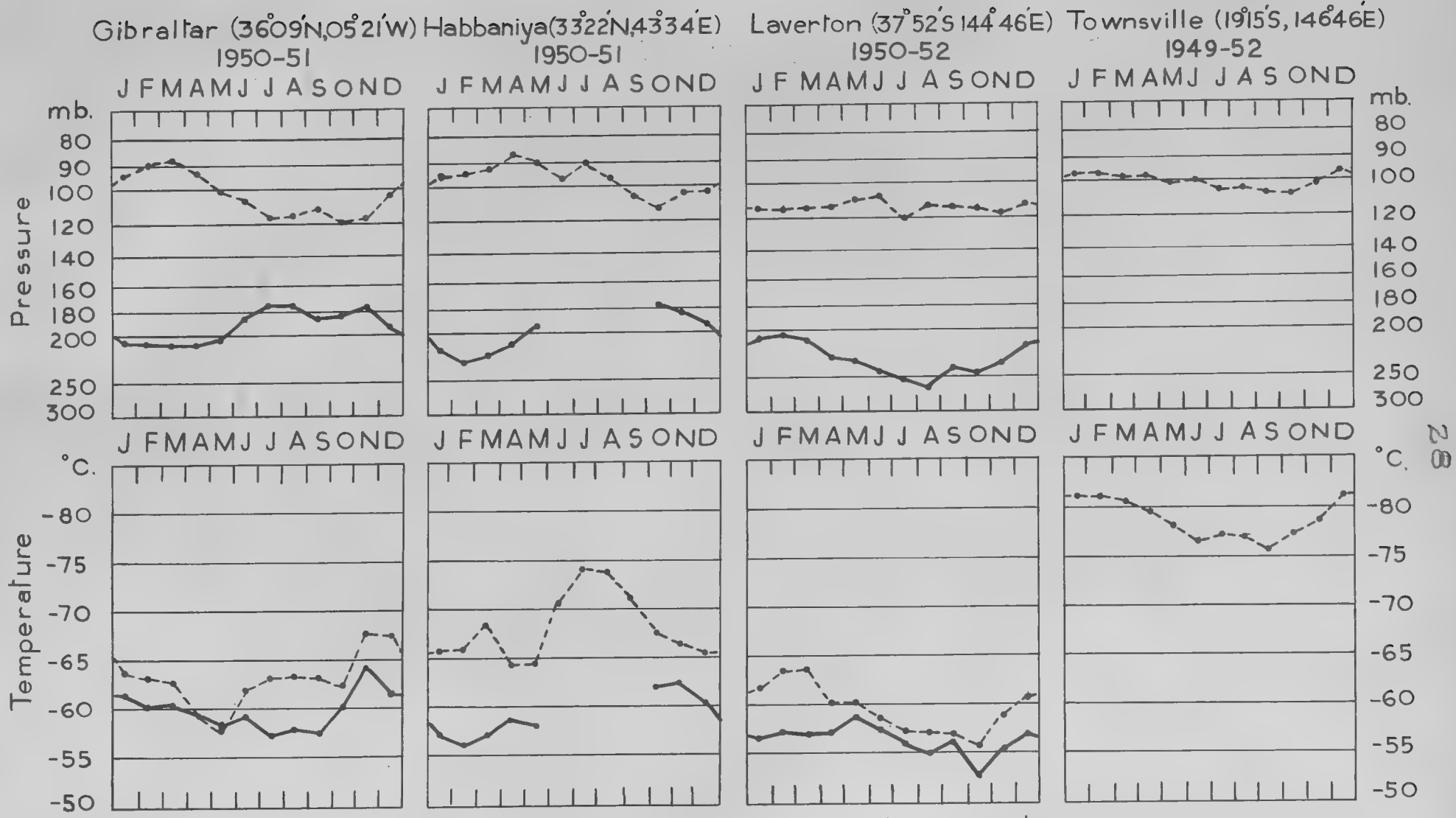

Fig.10. Annual variation of the mean monthly tropopause pressure and temperature

CSOS E.3 Agenda 10-1-07

Control Number C.D. 8055.
AD 63982

[illegible] by Dr. D.A. Samson.
A copy is available in the Library

[illegible] in the lowest 5,000 ft of the [illegible]

[illegible] 500 ft to 5,000 ft above ground and the [illegible] with some theories on thermal convection. A [illegible] to explain some of the phenomena recorded.

[illegible] statistical summary of several of the flights is given together [illegible] samples of [illegible] records obtained from the sensitive instrumen[illegible]

[illegible] hastings aircraft of the Meteorological [illegible] thermal [illegible] the air, [illegible] profile of the air [illegible] modified by transport over a cold surface. Preliminary analysis [illegible] technique of [illegible]

[illegible] Precautions [illegible] or near calm [illegible] each occasion [illegible]

At the time of issue this report has not been published. Any author desiring to quote this paper should refer to it as "A paper of the Meteorological Research Committee (London), M.R.P. No.875 by Dr. D.G. James. A copy is available in the Library of the Meteorological Office."

M.R.P. 875

S.C.III/172

31st August, 1954

AD63982

AIR MINISTRY

METEOROLOGICAL RESEARCH COMMITTEE

Fine scale characteristics of the lowest 5,000 ft of the atmosphere as observed from an aircraft

by

D.G. James (Meteorological Office)

Summary

Data derived from observations made by an aircraft of the Meteorological Research Flight of small scale disturbances in the lowest 5,000 ft of the atmosphere are discussed. Flights were made over land and sea at times when thermal convection was thought to be active over land.

Sensitive instruments were used to measure gustiness and fluctuations of temperature and dew point from 500 ft to 5,000 ft above ground, and the records obtained are compared with some theories on thermal convection. A tentative suggestion is offered to explain some of the phenomena recorded.

A short statistical summary of several of the flights is given together with some examples of the camera records obtained from the sensitive instruments.

1. Introduction

Twenty three flights were made by a Hastings aircraft of the Meteorological Research Flight between June 1952 and August 1953 at times when thermal convection was expected to be active over land. Six of these flights were carried out over the sea, when the vertical temperature profile of the air mass had been modified by transport over a cold surface. Preliminary analysis of early flight data indicated modifications necessary to the flying technique of subsequent flights in order to obtain the maximum of desirable information.

A short statistical summary of the results obtained from the flights is given, but although the histograms presented serve to illustrate the broader features of thermal convection over land, it must be emphasised that the parameters vary considerably from flight to flight.

Any investigation of thermal convection over a land area must necessarily include the effects of forced convection due to surface friction. Precautions taken to minimise these effects were (i) flights were made on calm or near calm days with approximately the same surface wind direction (ii) on each occasion the flights were made over the same area.

Table I shows the number, date and time of each flight, the instruments used and the flight procedure adopted.

2. Instruments

(a) Ultra rapid thermometer

To measure small fast fluctuations of temperature, a speedy sensitive thermometer was used the lag of which was some 5 msec. (Grant, 1950). This instrument was situated below the nose of the aircraft when in use, but could be withdrawn into a wooden fairing for protection on the ground and in cloud.

/(b)

(b) Hot wire anemometers

The gustiness of the airstream was detected and measured by two sensitive hot wire anemometers (Murgatroyd and James, 1953), the display and recording system being that of the ultra rapid thermometer. One of these anemometers, situated below the nose of the aircraft, was non-directional and measured the total airspeed fluctuations, including those of the aircraft itself.

The second anemometer, mounted 5 to 6 ft forward of the nose, was unidirectional and measured upgusts and downgusts only, the output being independent of aircraft speed.

(c) Automatic frost point hygrometer

Towards the end of the sequence of flights, an automatic hygrometer became available for use. This instrument, constructed by Dr. A.W. Brewer of the Clarendon Laboratory at Oxford, was readily adaptable to the display system of the ultra rapid thermometer and consequently continuous records of dew points could be obtained. The hygrometer has shown in extensive tests, that it followed fluctuations in dew and frost points rapidly and faithfully, the lag of the thermometer element being less than 1 sec and its accuracy better than 1.0°F at dew points around 40°F.

(d) Dobson-Brewer frost point hygrometer

The mean value of the frost or dew point was obtained in level flight by the use of a manual frost point hygrometer. This instrument was slow, a frost point being obtained every 10 sec in level flight and its accuracy was of the order of ± 1°F.

(e) Meteorological Office flat plate thermometer

Mean absolute values of temperature were obtained by use of a standard flat plate thermometer. This instrument was slow, its lag being of the order of 8 sec, but it provided an average value for any given level run, the usual corrections being applied for height and airspeed.

(f) Altimeter and airspeed indicator

Height and airspeed were recorded from standard aircraft instruments, accurate to within ± 10 ft and ± 1 kt respectively when flying straight and level below 6,000 ft. These instruments had lags of about 2 - 3 sec. For runs below 500 ft over the sea, the radio altimeter was frequently used.

(g) Accelerometer

The response of the aircraft to any turbulence encountered was recorded by a standard accelerometer. This instrument had a full scale deflection of ± 0.25 g, records being obtained on positive photographic film.

3. Operational procedure

On a convection flight a crew of six was usually taken, consisting of pilot, engineer, and four observers. Visual observations of height, airspeed, temperature as given by the Meteorological Office flat plate thermometer, dew point, amount and type of the cloud above, and nature of the ground below were made every 10 sec. Continuous time-marked records were obtained of each sensitive instrument in turn.

To reduce the effect of any forced convection, and any variation in thermal convection brought about by a change of ground surface, all flights over land were flown along a line joining two well defined land positions some seven miles apart. Over the sea, such definition was not necessary, provided that the air had a long sea track before reaching the area to be investigated. However, all runs over the sea were performed in a north-south direction over the English Channel, the northernmost point being some two miles south of Brighton.

/Two

Two types of flights were performed. At first, readings were confined to those made in level flight. On these flights several runs were made at 500 ft intervals from 500 ft above ground up to cloud base, the altimeter having been set to read directly heights above the average ground level over which the flight was executed. Although constant height, airspeed and attitude were desirable, preference was given to constant height when fluctuations of temperature were being recorded, constant airspeed for the measurement of omnidirectional gustiness, and constant attitude for the measurement of upgusts and downgusts. The mean airspeed always required was 120 kt and it is to the credit of the pilots that little variation on this figure was obtained even in the most turbulent conditions, and that the sensitive instruments rarely suffered any damage due to excessive speed. Each run at a given height usually lasted three minutes, during which the film records of the sensitive instruments were marked every minute. Calibration of the ultra rapid thermometer was carried out at the end of each run.

Towards the end of the series of flights, slow descents were performed at constant airspeed, direction and rate of descent. As before, continuous records of the sensitive instruments were obtained from 6-7,000 ft down to 500 ft, with spot readings of temperature, height, airspeed and frost point every 250 ft of height.

No special effort was made to fly at particular times of day, the flights being almost evenly divided between morning and afternoon, with one flight at night.

4. Data from flights over land

Table 2 presents data obtained from level runs on eleven flights when the ultra rapid thermometer, hot wire anemometers, and accelerometer were used. Mean values of temperature, obtained by the flat plate thermometer, at each level are given, together with the mean frost point obtained from the manual hygrometer. The mean temperature given at 1,000 ft on 31 March 1953 in Table 2 is suspect. A reading error of 5°F would give 40.6°F as the temperature at this level, though such errors are uncommon with the Meteorological Office flat plate thermometer. The average maximum variation from mean values is given under the heading of 'Span'.

Data from records of descents over land are presented in Tables 6, 7, 8, 9, 11, 14 and 15. The flights were undertaken to determine the structure of the vertical temperature distribution on convective days.

(a) Temperature

Level runs were carried out at 500 ft and at intervals up to cloud base, and occasionally above this level. From close study of the observations made on these runs, it seems that the region from ground to cloud base can be divided into three layers.

Figs. 4 and 5 are histograms of frequency per minute flying time (i.e. 12,000 ft) of the temperature excess and horizontal extent of temperature pulses recorded in level flight through these three layers.

(i) The first layer extending from ground to 800 or 1,200 ft, depending on the time of day, the cloud cover and the surface wind strength, seems to be a region of chaotic temperature fluctuations (Fig.9). The number of fluctuations in this layer is extremely large, some fifteen or twenty being encountered in a horizontal run of some 40,000 ft whilst the temperature excess varies from 0.2°F to 1.8°F (Fig. 4) though isolated examples have been observed when the temperature excess was 4.0°F. The upper surface of this layer, though well marked, is by no means flat; straight and level flight at this height results in this boundary being crossed and recrossed several times.

/The

The lapse rate in this layer is frequently super adiabatic, though the number of temperature fluctuations encountered renders an accurate estimation extremely difficult.

(ii) A second layer apparently extends from the top of this turbulent layer to some 200 to 300 ft below cloud base, this latter value being a function of the time of day, and of the vertical temperature profile of the ambient air (Fig. 10). The layer is characterised by positive temperature pulses which show a definite preference for an excess of 0.2 to 0.3°F though a preferred horizontal dimension is less apparent (Figs. 4 and 5). The average horizontal extent is 500 to 700 ft though occasional pulses have been measured with 1,500 ft diameter (Fig. 5). The slow variation in temperature of the ambient air, possibly produced by the passage through it of the warm pulses, is considerably less than in the lower turbulent layer, but increases somewhat with height. No evidence is found to indicate that the temperature pulses increase in diameter with height, the spectrum of pulse sizes being similar for all levels in this intermediate layer. It is noticeable that for two consecutive runs at the same height in this region, there is a considerable variation in the number of pulses encountered.

The lapse rate in this layer is approximately dry adiabatic, though on all descents small layers of more stable air are observed. These sub-layers, characterised by an isothermal or small temperature inversion of the order of 0.5°F are usually 100 to 200 ft thick, but are not permanent configurations of the vertical temperature profile of the air mass. Consecutive and similar descents do not indicate the presence of these more stable layers at the same heights, though on average their frequency of occurrence - some two or three per descent - remains fairly constant.

(iii) The third layer extending from cloud base down to some 200 to 400 ft below, called the "sub-cloud layer" by other authors, is characterised by an increase in stability of the vertical temperature gradient (Fig. 12). Frequently, this layer is composed of several shallow strata in which the vertical temperature gradient is either zero or slightly positive. The layer varies in depth during the day and seems to become more prominent during the afternoon. If the cloud base lifts during the day, the sub-cloud layer extends upwards and becomes more stable. If the cloud disappears, the height of the original cloud base becomes a preferred height for the formation of a more stable layer. In all cases, however, random temporary isothermals and inversions are recorded at all levels from the top of the turbulent layer to the maximum height reached during any flight.

Fig. 8 indicates the percentage of horizontal runs, (3 min at 120 kt) where the total temperature variation recorded exceeds a given value. It can be clearly seen from this figure that the amplitudes of the long-wave temperature fluctuations are quite small in the intermediate layer, but are large both in the turbulent layer and in the sub-cloud layer. At the lower levels of the sub-cloud layer, the number of warm pulses encountered decreases, but increases again just below cloud base. A feature of this layer is the presence of long-wave temperature fluctuations recorded on a level run (Fig. 11), the amplitude being of the order of 2°F near cloud base, with wavelength varying from 3,000 to 8,000 ft. Some positive temperature fluctuations are also recorded in this layer, with magnitudes of the order of 0.2°F, and horizontal extents of less than 100 ft.

(b) Gustiness, as recorded by the hot wire anemometers

The three layers described above are again evident from observations of gustiness, particularly in the records of the directional hot wire anemometer.

Figs. 6 and 7 are histograms of frequency per minute flying time (i.e. 12,000 ft) of the magnitudes and horizontal extents of gusts recorded in level flights through these three layers.

/(i)

(i) In the lower turbulent layer continuous gustiness is experienced by both anemometers (Fig. 9). The results show that the gusts are well defined, with sharp edges and occasional flat tops. Their magnitudes are in general up to 10 to 12 ft/sec, though a few of 15 to 20 ft/sec have been recorded (Fig. 6). The horizontal extents of the gusts vary from 200 to 1,500 ft, their frequencies and extents being given by Fig. 7.

A characteristic of this layer is that the number of upgusts recorded is only slightly greater than the number of downgusts. The upper boundary of the turbulent layer is clearly seen on the records of descents using the directional hot wire anemometer, being marked by a sudden increase in the number of gusts recorded.

(ii) In the intermediate layer the gusts are less frequent, more isolated, and in this respect better defined than those in the lower layer. The gust size is in general some 4 to 6 ft/sec at all heights in this region, though a few have been recorded of up to 15 ft/sec (Fig. 6). The horizontal extent of a gust in this layer is variable, the average value being 500 to 600 ft (Fig. 7). A feature of this layer is the difference in background noise in the records of the two anemometers. The directional anemometer gives a well-defined trace, with occasional well-defined and isolated upward gusts. This possibly indicates that nearly all the vertical motion in this layer is due to the upward transport of air by warm temperature pulses. The non-directional anemometer, however, has considerable background noise which extends throughout the record, and which indicates either the presence of horizontal vector gustiness in this layer, or uneveness of aircraft performance.

(iii) The third layer, near cloud base, is characterised by a decrease in frequency of the isolated gusts (Fig. 11) and in the background noise of both anemometers. The gusts recorded are in general similar to those at lower levels, the average being 5 to 8 ft/sec (Fig. 6) and are accompanied by slower long-wave changes in airspeed, usually obtained on the trace of the non-directional anemometer. This fluctuation has neither constant amplitude nor constant wave length, amplitudes of 3 to 8 ft/sec and wavelengths of 3,000 to 8,000 ft being observed. Sudden downgusts of magnitudes up to 5 ft/sec are evident in this layer on the directional anemometer trace, though the frequency of occurrence is small.

(c) Bumpiness, as recorded by an accelerometer

The boundary between the lower and middle layers is extremely well marked on the accelerometer trace, though the corresponding division between the middle and upper layers is not obvious.

(i) In the lower layer the bumps recorded are very frequent (Figs. 1 and 9) the accelerometer trace being one of continuous bumps which show a preference for sizes between 0.10g and 0.15g, though the largest recorded is greater than 0.3g. The horizontal extent of these bumps varies from 300 ft to 700 ft, the average extent being about 500 ft.

(ii) The middle layer indicates a marked decrease in the number of bumps encountered over a given time (Fig. 1) and the presence of long "quiet" periods, sometimes as great as 6,000 ft when no bumps greater than 0.10g are recorded (Fig. 10). The average size of a bump in this layer shows little variation, being 0.13g to 0.16g at the lower and 0.14g to 0.17g at the higher levels. There is a steady decrease with height in the number of bumps encountered in this region, though the average horizontal extent shows little change from 500 to 600 ft.

(iii) The records obtained in the third layer near cloud base indicate a slight increase in the frequency of occurrence of bumps, whilst there is a marked decrease in the size and number of "quiet" periods. Otherwise the average size and horizontal extent of a bump in this layer differs little from those of a bump in the middle region.

/In

In the presence of a temperature inversion, the size and frequency of bumps recorded varies considerably as the aircraft descends through the stable layer, reaching a maximum at the base of the layer.

(iv) Above cloud, the bumps recorded show not only a sharp decrease in frequency and intensity, but also differ in shape, from those at lower levels. Whereas at lower levels the bumps are generally well-defined with steep sides, above cloud they appear more as undulations.

5. Data from flights over the sea

Data are presented in Table 3 from two flights over the sea when records were obtained of temperature fluctuations, gustiness and bumpiness. In Tables 10, 12, 13 and 16, data from the records of slow descents over the sea are given. Although in four of the six flights described no convective type cloud was evident over the sea, thermal convection was active over the land. These results are presented so that a comparison may be made between phenomena observed at similar heights over land and sea. A short discussion is now given of the observations made on these flights.

(a) Temperature

There is no evidence for the formation of three well-defined layers at heights similar to those over land.

Slow descents from 6,000 ft to 100 ft above the sea frequently show the presence of a well-defined inversion at the lower levels (Fig. 16). Consecutive descents in the same area indicate a considerable change in the height and thickness of this layer, which becomes more pronounced as several hours elapse between descents (Tables 12 and 13). This inversion serves as a dividing line between two very different states of disturbance.

Below the inversion, numerous positive pulses of temperature excess are recorded, having magnitudes up to 0.8°F with horizontal extents to 600 ft in a lapse rate which is nearly isothermal (Fig. 14). Long-wave negative pulses of temperature excess are also recorded in level flight at these heights, and may be accounted for by variations in the inversion.

Above the inversion, positive pulses of temperature excess are recorded which are similar to those in the intermediate layer over land, though fewer in number (Fig. 15). The lapse rate in this region is disturbed by the presence of shallow layers of more stable air, again similar to those over land (Fig.16).

(b) Gustiness

In general, gustiness observed over the sea is small, individual gusts being mainly 2 - 3 ft/sec with occasionally a larger gust of 5 to 6 ft/sec. The frequency of occurrence of gusts falls off considerably with height, few being found above 1,500 ft.

(c) Bumpiness

In general, the majority of bumps experienced by the aircraft between 6,000 ft and 250 ft above sea level are less than 0.10g. A few individual bumps, however, are as large as 0.17g and are in association with pulses of warm air recorded by the ultra rapid thermometer.

The greatest proportion of bumps encountered occurs below 500 ft (Fig.2). The trace at this level exhibits continuous bumpiness, with a maximum on one flight of 0.15g. The frequency of the bumps falls off rapidly until at 2,000 ft few of measurable size are found.

The bumps over sea have a different character from those experienced over land, resembling smooth undulations as opposed to sharp edged pulses. Extensive regions are found on the descent where no bumps at all are recorded, extending as deep as 500 ft in the vertical, and some 12,000 ft in the horizontal.

/6.

6. Data from flights with the automatic hygrometer

Observations made on flights with the automatic hygrometer are presented in Table 4, for two flights over land and one over sea. The ultra rapid thermometer and accelerometer were usually employed on the same flight, and some comparison can be made of the excess of temperature and dew point of a thermal pulse.

Considering first the two flights, numbers 21 and 22, on 28 July 1953 over land, all levels indicate the presence of wet and dry patches, with variations of dew point of 4 - 6°F from that of the ambient air. The morning flight shows well defined pulses of the same order of dew point excess up to 1,500 ft, but at this level and up to cloud base the variations in dew point are slow. At the lower levels, the temperature pulses have an excess of up to 1.3°F at 500 ft and 0.6°F at 1,000 ft, whilst long-wave changes of 0.4 - 0.7°F amplitude are recorded at 1,500 ft and 2,000 ft with few faster fluctuations. The records of the afternoon flight indicate a warming of the air from 500 ft to 2,000 ft of some 3 - 4°F, with no significant change in mean dew points. Temperature fluctuations take the form of fast positive pulses of 0.2 - 0.4°F excess, with a slow change of 1.0°F appearing at 2,500 ft. Towards the end of the temperature traces obtained at the lower levels, there is a sharp well-defined drop of temperature, being 1.3°F at 500 ft, 1.0°F at 1,000 ft and 0.5°F at 1,500 ft, at which height the full horizontal extent of this cold patch was 5,000 ft. This change in temperature is accompanied at 500 ft by a sudden increase in dew point of 4°F - the runs are made on reciprocal headings, and the end of the patch appears as a sudden decrease in dew point - but there is little evidence of this cold wet patch on the hygrometer trace at higher levels. In general, the rapid changes of dew points recorded are some 2 - 4°F in excess of that of the ambient air, at levels up to 2,000 ft, with long-wave changes of 6°F appearing from 1,000 ft to 2,000 ft. Above this level, fluctuations of dew point occur as well marked groups of pulses with an excess of 1 - 2°F.

Flight 23, over the sea, shows very many temperature fluctuations of 0.5°F at 100 ft decreasing in number and size up to 3,000 ft. At this level and at 1,000 ft long-wave changes of 0.5°F are evident, those at the higher level having a half wavelength of 6,000 ft. The automatic hygrometer records show well-defined pulses of wet air at 100 ft and 500 ft with an excess dew point of 2 - 3°F. At 1,000 ft eight well-defined pulses are recorded of 4 - 5°F excess dew point. These are very evenly spaced, there being some 4,500 - 5,000 ft horizontal distance between them. A slow descent made on completion of the level runs (Table 16) indicates an inversion of 1.0°F between 800 ft and 900 ft, and it seems probable that the upward transport of water vapour is being limited by the inversion. Above 1,000 ft few pulses of moist air are observed, only three being evident at 2,000 ft of 2°F excess dew point. At 3,000 ft no well-defined pulses are recorded the only variation in dew point being a long-wave change of 5°F.

7. Statistical analysis of accelerometer traces

A complete statistical analysis has not been made of all the accelerometer traces obtained on these convection flights. However, the bumps greater than 0.1g obtained on some 20 level flights have been counted, and are presented in a form of histograms, for land and sea (Figs. 1 and 2). In these diagrams the total number of bumps per minute flying time (i.e. some 12,000 ft) is plotted against height. On the average, about ten runs are made at each level from 500 to 3,000 ft over land, and three runs over the sea. Cases are only considered when the cloud base was about 3,000 ft or above, or alternatively when there was no low cloud. It can be seen at once from Fig. 1 that there is a sharp decrease from 5.7 to 3.5 bumps/min between 1,000 ft and 1,500 ft with further smaller drops up to 2,500 ft. At 3,000 ft, in general near cloud base, the number of bumps per minute increases slightly. Over the sea, there is a continuous falling off with height, though in all cases the number of bumps recorded is considerably less than over land.

/On

On six flights, numbers 3 to 8, each bump recorded has been tabulated according to its magnitude, horizontal duration, and mean value. The mean value is defined as that value, which when multiplied by the horizontal extent of the bump, gives the area enclosed between the accelerometer trace and the line of no acceleration. Table 5 shows the mean value of such characteristics of the accelerometer traces for occasions when cloud base was 3,000 ft or above. The first column shows the number of bumps greater than 0.10g at heights from 500 ft to 2,500 ft. A sharp decrease can be found between 1,000 ft and 1,500 ft when the total number of bumps per minute flying time falls from 6.2 to 4.6. The second, third and fourth columns of the table show respectively the average maximum, average duration, and average mean of all bumps at each height. The fifth column shows the average area enclosed for each bump, between the accelerometer trace and the line of no acceleration. Bunker (1952) obtained a number of accelerometer traces in a series of similar flights over sea, and defined a "Turbulence Index" for any height as the average area enclosed between the accelerometer trace and the line of no acceleration over ten seconds at that height. The sixth column shows the average turbulence index for each height from 500 ft to 2,500 ft for the six flights analysed.

8. Notes on the comparison of our observations with previous ideas on convection proposed by other authors

(a) Bunker (1953) shows, by an extension of the equations of Houghton and Cramer, how under certain conditions a thermal bubble can pass through a turbulent layer and still maintain its identity. He shows a diagram of the temperature profile of such a bubble at 350 ft moving upwards at about 8 ft/sec with a temperature excess of about 1.3°F. This agrees well with our temperature observations at 500 ft, which show similar temperature pulses moving at 6 - 8 ft/sec with a temperature difference of 0.5 - 1.5°F. However, it is difficult to conceive of a turbulent region obeying his conditions at all points independent of time. Indeed this is not the case since the frequency of occurrence of pulses falls off very rapidly above 1,000 ft.

Bunker also concludes that bubbles of some 250 ft horizontal extent have a temperature excess of 0.5°F and a vertical velocity of 2 ft/sec whilst those of 1,500 ft horizontal extent have a temperature excess of about 1.0°F and a vertical velocity of 3 to 5 ft/sec. This does not agree with our observations at 500 ft which indicate little variation of temperature excess with horizontal extent.

(b) Bunker (1952) presents a diagram showing the divisions into which the first 3,000 ft or so of the atmosphere have been divided by various authors. Some of these authors suggest the three layers which are indicated by the measurements made by the Meteorological Research Flight. Fig. 3 shows a typical division made in the light of our observations, assuming a cloud base of 3,000 ft.

Bunker (1952, page 9) states that an inversion is capable of severely limiting the transport of water vapour, which agrees entirely with our observations over sea. It has been shown that positive pulses of temperature have been observed above an inversion over the sea on flights 11 and 12, whilst there was no cumulus forming. A later flight, number 23, confirmed that there was a sharp drop in dew point above the top of the inversion, although numerous wet pulses were observed in the inversion itself. It seems therefore that the warm pulses observed in flights 11 and 12 came from the top of the inversion, and hence contained much drier air than any bubble rising directly from the sea.

Bunker also comments upon "the process of destroying the original inversion and of forming a new inversion at a higher or a lower level." This agrees well with the observations between the top of the turbulent layer and cloud base, where several small inversions can be observed.

/(c)

(c) Langwell (1953) suggests that an inversion 2,000 ft above the sea oscillates about this height and can, under certain circumstances, form small cumulus clouds at the peaks. No fixed inversion has been found by the Meteorological Research Flight at the height Langwell suggests. However, on three flights, numbers 19, 20a and 23, an inversion has been observed below 1,000 ft. Above the top of the inversion a few positive pulses of temperature have been observed, whilst below the inversion these pulses are considerably more frequent. On consecutive descents, considerable variation in the thickness of the inversion has been recorded (flight 20a), which could be attributed to long-wave oscillations in the layer.

(d) In a comprehensive article on convection, Ludlam and Scorer (1953) quote Hohnsdorft as suggesting that the presence of a hill or good thermal source would send up a shower of bubbles followed by a long pause, when the cold air replacing the warm ascending air would itself warm up. This fits our observations well, since, for two successive level runs at a given height outside the friction layer, considerable variation is obtained in the number of warm pulses found for a given time.

Ludlam & Scorer (1953) suggest that below a convection bubble there is a wake which consists of a mixture of the warm air of the bubble with the surrounding air through which it has passed. It is clear that rapid temperature fluctuations as recorded by the ultra rapid thermometer can be divided into two groups, namely those consisting of well-defined sharp edged pulses, and those which seem to be small bursts of temperature. These latter are usually smaller in excess temperature than any isolated pulse at the same height, and also have greater horizontal extent. It is possible that these small bursts of fluctuation are part of the wake of a bubble, though the evidence is not sufficient to be conclusive.

It is also claimed that the horizontal extent of thermal bubbles increases with height, but this is not supported by either the temperature records or those of the accelerometer.

9. Discussion

From the above accumulation of data, it seems evident that the atmosphere from ground to cloud base may be divided into three layers, each having its own characteristics. A short discussion follows of the observations made in these regions.

(a) The turbulent ground layer

The first division may be made at a height above which the numbers of temperature pulses and their temperature excesses are considerably less than are the corresponding quantities below it. This boundary is recorded as being always above 500 ft and always below 1,500 ft though the 1,000 ft level is sometimes below and sometimes above this line. In all probability the height of the line varies from 800 ft to 1,200 ft, the exact height depending on the surface wind and the vigour of thermal convection on any particular day.

The exact method of formation of a temperature pulse on the ground is still open to conjecture, but may take the following form. A volume of air is warmed by being in contact with the ground, which for some reason, probably the constitution of the surface, is subject to some form of differential heating (Bleeker and Andre 1950). The break away of the bubble is possibly caused by the surface wind and by thermal instability and seems to take place at irregular intervals. At 500 ft a typical temperature pulse would have a measured temperature excess of 1.0 to 1.5°F, a horizontal extent of 400 to 600 ft, an excess dew point of 5 to 7°F, and would be moving at 6 to 8 ft/sec relative to the air though this velocity is not entirely vertical. These pulses are extremely numerous, with very sharp and well-defined edges, existing in a lapse rate which is frequently super-adiabatic.

/(b)

(b) The intermediate layer

Above the boundary proposed in (a) above, but below a line drawn some 200 to 400 ft below cloud base, there exists a region which we have referred to as the intermediate layer. Its lower boundary is determined by a decrease in the frequency of occurrence of temperature pulses and a sudden change in the temperature excess of such a bubble. The upper boundary is determined chiefly by the sudden occurrence of a more stable layer just below cloud. At any point within this intermediate layer, a typical pulse would have a measured temperature excess of 0.2 to 0.3°F, a horizontal extent 300 to 900 ft, an excess dew point of 3 - 5°F, and a vertical velocity of 4 - 7 ft/sec. Together with these well-defined temperature pulses, there exist in this layer small bursts of temperature fluctuations of some 0.2°F. It may be that these phenomena are produced by the turbulent wakes of warm pulses rising through this region. Successive level runs at a given height indicate the presence of small groups or showers of such pulses.

The lapse rate in the intermediate layer is extremely variable, several stable layers being evident on any descent through the layer. These more stable regions are composed generally of isothermals or small temperature inversions, some 50 to 100 ft in vertical thickness, the temperature inversion being 0.5 to 1.0°F, and seem to be situated randomly in time and space. No explanation is offered for the formation of these more stable regions.

(c) The sub-cloud layer

Extending from cloud base and down some 200 to 400 ft there exists a more stable layer, usually composed of several thin layers of differing stabilities, a typical formation being isothermal-inversion-isothermal. The magnitude of the inversion is about 1.0 to 3.0°F. This region seems to increase in thickness and stability during a day of fair weather convection, which can be associated with a rising and flattening of cloud base.

Temperature pulses recorded at the bottom and at the top of this layer show a marked change in dew point excess. A typical pulse just below this layer will have a measured temperature excess of 0.3 to 0.4°F, a horizontal extent of 500 to 600 ft, an excess dew point of 4 to 6°F and a vertical velocity of 5 to 8 ft/sec. Above this transition level, the frequency of well-defined pulses drops off considerably. A typical pulse here would have a measured excess temperature of 0.3 to 0.4°F, a horizontal extent of 600 to 700 ft, an excess dew point of 1 to 2°F and a vertical velocity of 4 to 5 ft/sec.

A level run at any height through the sub-cloud layer would reveal the presence of long-wave temperature fluctuations, with a magnitude of the order of 1.0°F. These slow variations are attributed to two causes; first to the downward movement of air near a developing cloud, and second to some form of wave motion in the stratified layers themselves. Dry patches have been observed in a descent through this layer, which seems to support the first reason, whilst a similar fluctuation in the top of an inversion over the sea suggests the second reason.

Finally, very short pulses of temperature excess 0.2 to 0.3°F with horizontal extent of 100 ft or less are occasionally recorded, and are attributed to local condensation either in a rising bubble of warm air, or to the general mixing of air with different temperatures and dew points.

(d) Above and alongside clouds

Occasionally, positive pulses of temperature are found above cloud base. A typical pulse recorded at these levels would have a measured temperature excess of 0.2 to 0.5°F, a horizontal extent of 500 to 600 ft, an excess dew point of 1 to 2°F and would be moving upwards with a velocity of 2 to 3 ft/sec. It is possible that these pulses have their origins either in the sub-cloud layer or in a more stable region sometimes found at the sides of, or above, the clouds. Again, an analogy can be drawn with positive pulses observed above an inversion over the sea.

/Flying

Flying some 400 to 500 ft directly above small developing cumulus clouds, very rapid negative pulses of temperature are recorded (Fig. 12). These pulses give a sharp drop of some 3.0 to 4.0°F with a horizontal extent of 300 to 400 ft. No effort has been made to investigate these negative pulses fully, since they appeared on one flight only, and no explanation is offered as to their formation.

The bumps experienced by the aircraft and recorded by the accelerometer at these heights show a marked difference from those recorded at levels below cloud base. The recorded bumps take the form of small undulations rather than sudden jolts, and are probably due to gradual increases in vertical velocity rather than to well-defined rising bubbles.

10. Conclusions

When thermal convection was active over land, positive pulses of temperature were recorded from 500 ft to cloud base. The magnitudes and numbers of these pulses decreased suddenly between 500 ft and 1,500 ft but showed little change from 1,500 ft to cloud base. At all heights below cloud base, little variation was found in the average horizontal extent of these warm pulses. A few small positive pulses were also recorded above cloud base, though directly above developing cumuli well-defined negative pulses of temperature were obtained.

The vertical temperature profile of the air below cloud showed a region of stable air about 200-400 ft thick directly below cloud base. Several smaller layers of stable air about 100 ft thick were recorded at all levels down to 1,000 ft, though consecutive descents indicated that these layers were not permanent features.

The records from all sensitive instruments suggested a sub-division of the cloud to ground layer into three parts (Fig. 3). The dividing line between the "turbulent layer" and the "intermediate layer" was well defined, but the lower boundary of the "sub-cloud layer" was not easily observed.

A possible mechanism of convective cloud formation suggested by the above observations would be as follows. During the morning the rise of ground temperature, with differential heating of the surface, would cause bubbles of air to ascend and, if sufficiently moist, to form cloud. The sub-cloud layer would be established at the same time. Further ascent of air would warm and deepen this layer until no more bubbles of ground origin could reach cloud base directly. However, cloud formation could proceed by air breaking away from the top of the sub-cloud layer, and could continue long after the surface temperature is past its maximum. This would produce a flattening of the cloud base during the afternoon, and an extension of cloud formation beyond the limits deduced from surface temperature observations.

Acknowledgements

I would like to express my thanks to all the members of the Meteorological Research Flight for their assistance in obtaining flight records and in particular to Flt.Lt. Baker, M.B.E., D.F.C., and Flt.Lt. Bavin for the steadiness and accuracy of their flying, in conditions which were frequently uncomfortable.

References

1. Bunker, A.F. J.Met., 10, No. 3, June, 1953.

2. Bunker, A.F. Papers in Physical Oceanography and Meteorology, XII, No. 3, Dec., 1952.

3. Grant, D.R. M.R.P. 542, 1950.

4. Langwell, Patricia A. J.Met., 10, No. 3, June, 1953.

5. Ludlam, F.H. and Scorer, R.S. Q.J. Roy. Met. Soc., 79, No. 341, July, 1953.

6. Murgatroyd, R.J. and James, D.G. M.R.P. 804, 1953.

Table 1.

Flights and instruments used

Flight Number	Date	Time	Position	INSTRUMENTS: Ultra rapid thermometer	Hot wire anemometer	Directional hot wire anemometer	Auto-hygrometer	Type of flight
1	27. 6.52	10.30-12.30	Land	/	/			Level runs
2	30. 6.52	15.00-17.30	Land	/	/			Level runs
3	25. 8.52	10.30-12.30	Land	/	/	/		Level runs
4	25. 8.52	15.00-16.45	Land	/	/	/		Level runs
5	28. 8.52	10.30-12.30	Land	/	/	/		Level runs
6	29. 8.52	10.30-12.30	Land	/	/	/		Level runs
7	7.11.52	14.15-16.00	Land		/	/		Level runs
8	11.11.52	11.00-12.15	Land	/	/	/		Level runs
9	15.12.52	15.00-16.00	Land	/				Level runs
10	2. 2.53	14.15-16.15	Sea	/				Level runs
11	12. 3.53	14.45-16.00	Sea	/	/			Level runs
12	31. 3.53	15.00-16.30	Land	/	/			Level runs
13	23. 4.53	14.30-16.30	Land	/	/	/		Level runs, and descents
14	24. 4.53	14.30-16.30	Land	/	/	/		Level runs, and descents
15	28. 4.53	21.00-22.30	Land	/	/	/		Level runs
16	6. 5.53	11.45-13.00	Land	/	/	/		Descents
17 (a)	7. 5.53	14.40-17.00	Land	/	/	/		Descents
17 (b)	7. 5.53	14.40-17.00	Sea	/		/		Descents
18	11. 5.53	11.20-12.15	Land	/				Descents
19	12. 5.53	11.15-12.30	Sea	/				Descents
20 (a)	12. 5.53	15.00-17.30	Sea	/				Descents
20 (b)	12. 5.53	15.00-17.30	Land	/				Descents
21	28. 7.53	11.00-13.00	Land	/			/	Level runs, and descents
22	28. 7.53	15.20-17.00	Land	/			/	Level runs, and descents
23	26. 8.53	14.00-16.30	Sea	/			/	Level runs, and descents

Level

Date	Time	Cloud base (ft)	Height (ft)	Mean T(°F)	Span (°F)	Mean F.P. (°F)	Span (°F)	Ultra rapid thermometer	Hot wire anemometer	Directional hot wire anemometer	Accelerometer
27. 6.52	10.30-) 12.30)	3,300	1,000	66.9	0.5	53	2	Many small fluctuations	Continuous gusts		Continuous bumps with max. of 0.25g
			1,700	63.0	0.5	51	2	Several square shaped pulses	Numerous fast gusts		Long quiet periods. Bumps to 0.20g max.
			2,400	59.4	0.4	50	2	Positive pulses	Small gusts		Long quiet periods. Bumps to 0.20g max.
30. 6.52	15.00-) 17.30)	3,400	400	69.9	1.1	62	2	Very many positive pulses up to 1.2°F with internal fluctuations of 0.5°F	Gusts up to 10ft/sec		Very many bumps up to 0.23g max.
			800	67.8	0.8	61	2	Very many positive pulses of up to 0.6°F	Gusts 5-8ft/sec		Many bumps to 0.15g
			1,200	64.6	0.6	60	1	Positive pulses 0.3-0.4°F	Gusts 5-7ft/sec		Bumps to 0.16g
			1,600	63.5	1.0	60	3	Several positive pulses of 0.3°F and one of 0.5°F	Gusts 4-5ft/sec		A few large bumps up to 0.20g
			2,000	61.3	1.1	58	2	Small bursts of positive pulses 0.2-0.3°F	A few gusts of 4-5ft/sec		
			2,400	59.0	1.0	59	1	Few small temperature fluctuations	Gusts 3-4ft/sec		
			3,500	59.1	0.6	46	2	Slow positive pulses of 0.5°F to 3.0°F	No gusts		
25. 8.52	10.30-) 12.30)	2,000 to 2,400	1,000	61.9	0.5	54	3	First part noisy with fluctuations of 0.3°F Second part has isolated pulses 0.2-0.3°F	Very many gusts up to 10ft/sec	Very many gusts up to 10ft/sec	Many bumps up to 0.17g
			1,500	59.2	0.8	52	2	Positive pulses from 0.2-0.3°F	Regions of 7-10ft/sec	Regional 7-10ft/sec	Well-defined bumpy regions up to 0.24g
			2,000	57.1	0.6	51	2	Positive pulses from 0.2-0.3°F	Well marked regions of 7-8ft/sec	Noisy 8-10ft/sec	Variable regions; bumps to 0.31g
			6,000	48.6	0.5	26	4	Slow long waves of 1.5°F	Small gusts of 1-2ft/sec	Quiet gusts 1-3ft/sec	No bumps
25. 8.52	15.00-) 16.45)	3,300	1,000	64.4	0.4	47	2	Long waves of 0.3-0.4°F. Positive pulses of 0.3°F	Continuous gusts of 4-5ft/sec	Continuous gusts, in general 4-5ft/sec but occasionally up to 8ft/sec	Continuous bumps up to 0.16g
			1,500	61.8	0.2	53	1	Long waves of 0.3°F. Positive pulses of 0.3°F	Well marked regions of 5ft/sec		Well-defined regions of bumps up to 0.20g
			2,000	59.3	0.4	54	2	Positive pulses of 0.3°F. One negative of 0.2°F	Regions of gusts up to 5ft/sec		Regions up to 0.20g
28. 8.52	10.30-) 12.30)	3,000	500	59.6	0.5	52	3	Continuous positive pulses of 0.8-1.2°F	Continuous gusts 4-5ft/sec and up to 10ft/sec	Continuous gusts of 4-5ft/sec. Some to 10ft/sec	Continuous bumps, with max. of 0.20g
			1,000	57.0	0.5	50	2	Few pulses of 0.3°F, isolated or in groups	Gusts 4-5ft/sec in regions	Well marked regions of gusts 4-5ft/sec	Regional. Up to 0.16g
			1,500	54.7	0.5	49	3	Few pulses of 0.2°F, isolated or in groups	Gusts of 3ft/sec with 4-5ft/sec at times	Regional. Gusts up to 6-7ft/sec	Regional. Up to 0.21g
			2,000	52.5	0.5	48	2	Isolated positive pulses 0.2-0.3°F	Regional gusts 4-5ft/sec		Regional. Up to 0.21g
			2,500	50.1	0.5	48	2	One slow negative of 0.4°F. Positive of 0.2-0.3°F	Regional gusts 4-5ft/sec		
			3,000	48.2	1.2	47	3	Slow negative changes of 1°F. Positive pulses of 0.4°F. Small bursts of 0.2°F	Regional 4-6ft/sec		
29. 8.52	10.30-) 12.30)	No low cloud	500	62.9	0.8	51	2	Continuous positive pulses of 0.7°F-1.0°F	Continuous gusts of up to 7ft/sec	Continuous gusts of 6-8ft/sec	Numerous bumps up to 0.16g
			1,000	60.9	0.7	52	1	Slight grouping. Positive pulses of 0.2-0.4°F	Numerous gusts 2-3ft/sec. Occasionally 5-6ft/sec	Regions of gusts 4ft/sec and also 6-7ft/sec	Slightly regional. Bumps to 0.21g
			1,300	58.3	0.7	51	1	Regions of positive pulses of 0.3°F	Continuous gusts 4-6ft/sec	Regions of gusts 5-6 ft/sec	Regional. Bumps to 0.18g
7.11.52	14.15-) 16.00)	3,800	1,000	41.6	0.4				Very many gusts 4-6ft/sec	Numerous small gusts 5ft/sec. Occasionally 6-7ft/sec	Very disturbed, with max. of 0.25g
			1,500	39.0	0.3				Generally quiet. Groups 3-4ft/sec	Regional, with gusts 4ft/sec and occasionally 6-8ft/sec	Isolated bumps of max. 0.20g
			2,000	36.5	0.4				Quiet. Sudden gusts to 5ft/sec	Quiet. Occasionally gusts 4-6ft/sec	Regional. Bumps to 0.13g
			2,500	33.9	0.4				Long-wave gusts 3-4ft/sec	Quiet. Sudden gusts 3-6ft/sec	
			3,000	30.3	0.4				Long waves of 3-4ft/sec		
11.11.52	11.00-) 12.15)	2,900	500	41.7	0.8	36		Very many positive pulses 0.6-0.8°F	Numerous fast gusts up to 6ft/sec	Numerous gusts, with max. of 8-10ft/sec	Very bumpy, up to 0.15g
			1,000	41.3	1.0	33		Small bursts of 0.2°F. Isolated pulses of 0.4°F	Numerous gusts up to 4-5ft/sec	Regional. Well-defined gusts up to 8ft/sec max.	Regional. Bumps to 0.18g
			2,800	32.0	0.8	30		Long waves of 0.5°F. Regions of 0.2°F fluctuations	Long-wave fluctuations, with occasional 2-3ft/sec gusts	Well-defined isolated gusts up to 5ft/sec	Regional. Bumps to 0.15g
15.12.52	15.00-) 16.00)	3,600	1,500	30.3				Very disturbed. Pulses 0.3-0.4°F. A few 0.6°F			Very bumpy. Bumps to 0.20g max.
			2,000	28.4				Many positive pulses of 0.4°F			A few bumps up to 0.20g
			2,500	26.2				Very quiet. A few positive pulses of 0.2°F			Regional. Some bumps to 0.20g
			2,900	24.6				Quiet. A few pulses of 0.2°F. Warm patch 0.3°F			A few bumps of 0.20g. Mainly 0.15g
			3,400	22.4				Long-wave fluctuations of up to 1.0°F. Regions of positive pulses of 0.4°F and calm			Few bumps of 0.10g. More 0.13g
			3,500	22.0				Long-wave fluctuations of 2°F, positive and negative changes. Few pulses (positive) of 0.3°F			Few bumps of 0.10g. More 0.13g
31. 3.53	15.00-) 16.30)	4,000	500	41.9	0.8			Overall change 1.6°F. Many positive pulses to 1.0°F	Very disturbed. Gusts to 8-10ft/sec		Many bumps. Some to 0.20g
			1,000	45.6	0.1			Overall change 1.4°F. Many positive pulses to 1.0°F	Very disturbed. Gusts 6-8ft/sec		Many bumps. Some to 0.20g
			1,500	38.8	0.1			Overall change 1.5°F. Few positive pulses to 0.6°F	Regional. Gusts of 6-7ft/sec		A few bumps to 0.10g
28. 4.53	21.30-) 23.00)	No low cloud	500	42.9	0.2			Very disturbed. Many positive pulses of up to 0.5°F in overall change of 0.9°F	Many gusts of 3-4ft/sec	Many gusts 2-3ft/sec	Many bumps from 0.10g-0.20g
			1,000	40.3	0.1			Numerous small pulses of 0.1°F in overall change of 0.3°F			Many bumps of 0.10g. A few to 0.20g
			2,000	36.3	0.1						Only a few bumps of about 0.10g
			3,000	31.9							Very few undulations> 0.10g

Table 3.

Observations over sea. Level flights only

Date	Time	Cloud base (ft)	Height (ft)	Mean T. (°F)	Span (°F)	Mean F.P. (°F)	Span (°F)	Ultra rapid thermometer	Hot wire anemometer	Accelerometer
2. 2.53	14.45-16.15	3,200	500	38.3	0.5	25	1	Continuous fluctuations of 0.2°F. Slower change of 0.8°F		Continuous bumps up to 0.25g
			1,000	36.0	0.4	24	2	Small fluctuations of 0.2°F. Slow long-wave changes		Many bumps up to 0.16g
			2,000	31.5	0.3	23	2	A few slow positive pulses, 0.3-0.4°F		Regions of bumps up to 0.10g
			2,500	29.1	0.6	22	2	A few fast positive pulses of 0.4°F. Long cold pulses near edge of clouds		A few bumps up to 0.10g
12. 3.53	14.45-16.00	No low cloud	500	41.1	0.0			Very small positive pulses in overall change of 0.4°F	Long-wave changes mainly, but a few gusts of 2-3 ft/sec	Very few bumps greater than 0.10g, but maximum of 0.12g
			1,000	39.0	0.3			Many positive pulses of 0.3°F in overall change of 0.8°F	Some small gusts of 2-3 ft/sec	Very few bumps, but maximum of 0.25g
			1,500	36.8	0.2			Only positive pulse of 0.3°F	A few gusts of 2-3 ft/sec	Several bumps, with a maximum of 0.18g

Table 4. Observations on flights with the automatic hygrometer

Date	Time	Place	Cloud base (ft)	Height (ft)	Mean Temp. (°F)	Span (°F)	Mean F.P. (°F)	Span (°F)	Ultra rapid thermometer	Automatic hygrometer	Accelerometer
28. 7.53	11.00-13.00	Land	2,100	500	60.2	0.6	46	3	Numerous positive pulses up to 1.3°F, over 2,000 ft	Considerable variations up to 6°F, last mainly 4°F	Continuous bumps up to 0.30g
				1,000	57.7	0.3	45	2	A few positive pulses up to 0.6°F, over 2,000 ft	Many wet patches of 5°F. Considerable pulses 1°F	Bumps up to 0.25g, with a few quiet periods
				1,500	55.0	0.5	45	3	Long waves of 0.4°F over 4,000 ft. A few pulses of 0.3°F	No sharp pulses. Long-wave fluctuations of 4°F	Isolated bumps of 0.25g in long quiet periods
				2,000	52.6	0.6	43	4	Long-wave fluctuations of 0.5-0.7°F only	Long waves of 6°F and over. A few small 1°F pulses	Long quiet periods, with smooth bumps to 0.15g
28. 7.53	15.30-17.00	Land	3,000	500	63.0	0.9	48	3	Many positive pulses of 0.3-0.5°F. Sudden drop of 1.3°F	Many wet pulses of 3-4°F excess. Sudden dry patch of 4°F	Continuous bumps up to 0.25g
				1,000	62.0	1.2	45	4	A few positive pulses of 0.2-0.3°F. Sudden drop of 1.0°F	Long waves of 6°F. Peaks of 2-3°F excess	Isolated bumps to 0.25g
				1,500	58.3	1.1	44	4	A few positive pulses of 0.2-0.3°F. Sudden drop of 0.5°F over 5,000 ft	Long waves of 6°F. Isolated pulses of 2-3°F excess	Isolated bumps to 0.17g
				2,000	55.7	0.9	44	5	Numerous positive pulses of 0.4°F over 1,200 ft	A few pulses of 6°F excess. Slow dry patches of 4°F	Isolated bumps to 0.25g
				2,500	53.4	0.9	44	5	Long wave of 1.0°F. A few positive pulses of 0.3°F over 800 ft	Well marked group of wet pulses of 1-2°F excess	Isolated bumps to 0.15g
				3,000	50.8	0.8	42	4	A few small fluctuations of 0.3°F over 1,000 ft	One group of wet pulses of 1-2°F excess. Slow dry patch of 2°F	

Date	Time	Place	Cloud base (ft)	Height (ft)	Mean Temp. (°F)	Span (°F)	Mean F.P. (°F)	Span (°F)	Ultra rapid thermometer	Automatic hygrometer	Accelerometer
26. 8.53	14.00-16.30	Sea	4,500	100	63.2	0.2	53	2	Very many fast positive pulses of 0.5°F over 100 ft	Wet pulses of 2-3°F excess. Wet patch of 2°F over 5,000 ft	
				500	62.4	0.3	50	1	A few positive pulses of 0.3-0.5°F over 100 ft	Series of wet pulses of 2°F excess, over 1,000 - 1,500 ft	
				1,000	60.0	0.7	47	3	One region of fluctuations of 0.4°F. Long waves of 0.5°F	Eight wet pulses of 4-5°F excess, with spacing of 4,500 - 5,000 ft	
				2,000	56.2	0.3	44	2	A few bursts of small fluctuations of 0.2-0.3°F	Three wet pulses of 2°F, lasting 300 ft - 2,500 ft	
				3,000	51.3	0.5	41	3	A few fluctuations of 0.2°F. Long wave of 0.5°F over 6,000 ft	No well-defined pulses. Change of 5°F in ambient F.P.	

Table 5

Height (ft)	Total bumps per min	Average maximum of all bumps (g)	Average duration of all bumps (ft)	Average mean of all bumps (g)	Average area of all bumps	Turbulence index
2,500	3.2	0.12	510	0.06	30.6	16.4
2,000	4.4	0.13	560	0.07	39.2	28.8
1,500	4.6	0.13	520	0.08	41.6	32.1
1,000	6.2	0.13	520	0.07	36.4	37.3
500	6.1	0.12	480	0.07	33.6	34.1

Table 6

23.4.53. 14.30-16.30. Flight 13. Land. No low cloud

Instruments:- Ultra Rapid Thermometer, Hot Wire Anemometer, Directional Hot Wire Anemometer, Accelerometer.

Flight details:- Level runs at 500 ft, 1,000 ft, 2,500 ft and 5,000 ft with all instruments. Slow descent from 5,000 ft to 500 ft using the Ultra Rapid Thermometer.

Height (ft)	Details from level runs	Details from descent
5,000	No temperature fluctuations or gusts recorded. Overall temperature change 0.3°F	
4,000		A few positive pulses of 0.4°F
3,500 ft		
3,000		
2,500	Well-defined regions of temperature fluctuation, up to 0.6°F in overall change of 1.1°F. Gusts of 3-4 ft/sec, giving smooth bumps up to 0.15g maximum	Considerable temperature fluctuations, with variations of up to 0.8°F
2,000		
1,500 ft		
1,000	Numerous fast positive pulses, giving gusts 6-10 ft/sec. Continuously bumpy, with bumps up to 0.25g	Many positive pulses of 0.5°F, increasing at lower levels to 1.0°F
500	Continuous temperature fluctuation, with pulses of 0.7°F in overall change of 1°F. Gusts, very numerous, from 7-10 ft/sec and continuous bumps to 0.30g	

Table 7

24.4.53. 14.30-16.30. Flight 14. Land. No low cloud

Instruments:- Ultra Rapid Thermometer, Hot Wire Anemometer, Directional Hot Wire Anemometer, Accelerometer.

Flight details:- Level runs at 500 ft, 1,000 ft, 2,000 ft, 3,000 ft, 5,000 ft, followed by a slow descent from 5,000 to 500 ft, using the Ultra Rapid Thermometer.

Height (ft)	Mean T (°F)	Details from level runs	Details from descent
5,000	38.2°F	No fast temperature fluctuations or gusts. A few slow small changes visible	Very quiet. Long wave temperature fluctuations
4,000	42.5°F		3,900 ft Turbulent region. Fluctuations of 0.5-1.0°F
3,000	46.9°F	Top of haze layer. Very few temperature fluctuations in overall change of 0.7°F, with gusts 3-4 ft/sec, bumps less than 0.1g	2,500 ft 48.5°F Isothermal layer. Temperature fluctuations of 0.3°F 2,200 ft 48.5°F
2,000	50.6°F	A few positive pulses of 0.4°F in overall change of 1.5°F. Gusts of 4-6 ft/sec, with well-defined bumps to 0.25°F	1,900 ft Some positive pulses of 0.5°F, becoming up to 1.0°F in lower levels
1,000	55.9°F	Numerous pulses of all sizes, with maximum temperature excess 0.6-0.7°F. Gusts 6-8 ft/sec, almost continuous; many bumps greater than 0.20g	
500	58.3°F	Very many pulses of 0.8°F in overall change of 1.5°F. Continuously gusting up to 8-10 ft/sec, with bumps up to 0.25g	

Table 8

6.5.53. 11.45-13.00. Flight 16. Land. Cloud base 3,250 ft - 3,400 ft

Instruments:- Ultra Rapid Thermometer, Hot Wire Anemometer, Directional Hot Wire Anemometer, Accelerometer.

Flight details:- One descent from 4,250 ft to 500 ft using the Ultra Rapid Thermometer, followed by two other descents from 5,500 ft - 500 ft using the Hot Wire Anemometer and Directional Hot Wire Anemometer in turn.

Height (ft)	Mean T (°F)	Span (°F)	Details from descents
5,500	41.7	0.3	
			A few positive temperature pulses of 0.3°F A few gusts of 3 ft/sec All bumps less than 0.10g
3,250	49.3	0.8	Cloud base
3,140			Isothermal. Long-wave fluctuations of 0.8°F. Gusts 4-5 ft/sec. All bumps less than 0.10g
			3,050 ft
3,000	50.0	0.6	Very fast inversion of 3°F. Positive pulses of 0.5°F, with 5 ft/sec gusts and bumps up to 0.10g
			2,900 ft
2,750	51.1	0.7	Isothermal. Pulses up to 0.5°F; gusts up to 5 ft/sec. Few bumps, but one up to 0.20g
			Numerous positive pulses of temperature, 0.3°F generally, but up to 0.8°F at times. Gusts isolated and well marked 4-8 ft/sec. Bumps 0.1g-0.3g. All becoming less numerous at the lower levels
1,000	59.2	0.6	
			Traces suddenly becoming very disturbed
500	61.8	0.4	

Table 9

7.5.53. 14.40-17.00. Flight 17a. Land. Trace of cloud at 3,000 ft

Instruments:- Ultra Rapid Thermometer, Directional Hot Wire Anemometer, Accelerometer.

Flight details:- Two slow descents from 5,200 ft to 500 ft, using the Ultra Rapid Thermometer and Directional Hot Wire Anemometer in turn.

Height (ft)	Mean T (°F)	Span (°F)	Details from descents
5,200	39.5	1.5	↑ A few random isolated positive pulses of up to 0.4°F, with gusts of 3 ft/sec but no bumps greater than or equal to 0.1g ↓
3,600	39.9	0.9	↑ Inversion of 4.0°F. Large positive pulses of up to 2.0°F ↓
3,200	40.0	0.6	↑ Gusts up to 10 ft/sec. Bumps 0.1g but some 0.2g
3,000	39.6	0.6	↓ Small clouds
2,750	41.4	0.1	↑ Isothermal. Numerous small temperature fluctuations of 0.3°F, gusts of up to 5-6 ft/sec, and bumps up to 0.15g ↓
			↑ Positive pulses of 0.4°F to 0.6°F. Gusts of 3-4 ft/sec in general, but occasionally one of 8-10 ft/sec. Bumps up to 0.20g, corresponding to arrival of temperature pulse or gust. All the above in regions ↓
500	52.8	0.6	

Table 10

7.5.53. 14.40-17.00. Flight 17b. Sea. No low cloud

Instruments:- Ultra Rapid Thermometer, Directional Hot Wire Anemometer, Accelerometer.

Flight details:- Two descents made from 5,000 ft to 500 ft, using the Ultra Rapid Thermometer and Directional Hot Wire Anemometer in turn.

Height (ft)	Mean T (°F)	Span (°F)	Details from descents
5,000	39.6	0.6	
4,320	41.2	0.6	↑ Small inversion of 0.3°F, with fluctuations of the same order, and gusts 3ft/sec. Bumps less than 0.1g
4,250	41.8	0.5	↑ Long slow inversion of 3°F, becoming ragged at 3,400 ft. Small positive temperature fluctuations, with little gusts, and bumps less than 0.1g
3,000	41.1	1.5	↑ A few small positive pulses of temperature. Small gusts. Bumps less than 0.1g
500	46.0	0.1	

Table 11

11.5.53. 11.20-12.15. Flight 18. Land. Trace of cloud between 4,000 ft and 4,200 ft

Instruments:- Ultra Rapid Thermometer, Accelerometer.

Flight details:- Three slow descents from 5,500 ft to 500 ft using the Ultra Rapid Thermometer, starting from the same land position, along the same heading.

Height (ft)	Mean T (°F)	Span (°F)	Details from descents
5,000	31.6	0.6	Minor inversion, where position and magnitude vary with time from 0.8 to 2.0°F
4,850 ft			A few positive pulses up to 1.0°F. Little bumpiness. Passing over the tops of clouds gives fast negative pulses of 3-4.0°F
4,200	33.7	0.6	Small clouds
			Almost isothermal lapse rate. Positive pulses of 0.3°F to 1.2°F
3,800	34.0	0.1	
			Positive pulses of temperature, in general 0.3-0.7°F, but a few of 1.0°F. Random positions in time, but usually in groups of 2 or 3. Several temporary inversions of up to 0.5°F and isothermals, whose positions and magnitudes vary with time
1,200	47.9	0.2	
			Very many positive pulses. In general 0.5°F but increasing in size towards the ground, and reaching 2 to 3°F
500	50.4	0.4	

Table 12

12.5.53. 11.15-12.30. Flight 19. Sea. No low cloud

Instruments:- Ultra Rapid Thermometer and Accelerometer.

Flight Details:- Three descents made in turn from 6,250 ft to 250 ft, using the Ultra Rapid Thermometer.

Height (ft)	Mean T (°F)	Span (°F)	Details from descents
6,200	31.2	0.2	
6,000	32.0	0.3	6,000 ft ↑ Well marked region of temperature fluctuations. Also, well-defined smooth bumps to 0.25g ↓ 5,250 ft
			5,900 ft ↑ Minor temperature fluctuations on all descents of 0.3°F, with small inversions ↓ 5,700 ft
5,800	32.6	0.4	
5,250	39.5	0.2	
			Random positive pulses of temperature of 0.4-0.5°F Minor bumps, less than 0.1g in general, but some up to 0.17g Random temporary minor isothermals and inversions of about 0.5°F, over approximately 100 ft vertical thickness
800	50.9	0.2	
500	51.4	0.4	
250	49.7	0.1	Complex inversion of 1.8°F on all descents. Very many positive pulses of temperature, up to 0.8°F below the inversion. Becoming isothermal

Table 13

12.5.53. 15.00-17.30. Flight 20a. Sea. No low cloud

Instruments:- Ultra Rapid Thermometer, Accelerometer.

Flight details:- Two descents made from 6,000 ft to 500 ft using the Ultra Rapid Thermometer.

Height (ft)	Mean T (°F)	Span (°F)	Details from descents
6,000	36.6	0.4	
5,750	36.8	0.8	5,800 ft ↑ ↓ Small inversion shown on both descents, though magnitude changes from 1°F to 1.5°F 5,600 ft
3,250	47.2	0.3	3,300 ft ↑ ↓ Small inversion of 0.4°F. Small positive pulses 3,200 ft
			A few positive pulses of 0.4°F, with bumps to 0.10g Small temporary inversions at random levels of magnitudes up to 1.0°F
750	55.0	0.0	
500	54.8	1.2	Inversion of 4.8°F, varying in thickness Large positive pulses underneath inversion, up to 0.7°F

Table 14

12.5.53. 15.00-17.30. Flight 20b. Land. Cloud base 4,000 ft

Instruments:- Ultra Rapid Thermometer and Accelerometer.

Flight details:- Two descents made from 6,500 ft to 1,000 ft using the Ultra Rapid Thermometer.

Height (ft)	Mean T (°F)	Span (°F)	Details from descents
6,500	35.6	0.6	
6,350			Isothermal. Well marked layer of temperature fluctuations, up to 0.7°F
6,070			
6,000	36.3	0.7	Well-defined region of temperature fluctuations of 0.8-1.5°F
5,500	37.6	0.6	Positive pulses of 0.3-0.5°F Isolated
4,000	44.0	0.6	Cloud base
			Pulses increasing in frequency and becoming larger with temperature excess of up to 1.0°F at lower levels
1,000	59.0	0.0	

Table 15

28.7.53. 11.00-13.00. Flight 21. Land. Cloud base 2,100 ft

Instruments:- Ultra Rapid Thermometer, Accelerometer and Automatic Hygrometer.

Flight details:- Level runs at 500 ft, 1,000 ft, 1,500 ft and 2,000 ft. Two slow descents from 2,000 ft to 500 ft using the Ultra Rapid Thermometer and Automatic Hygrometer in turn.

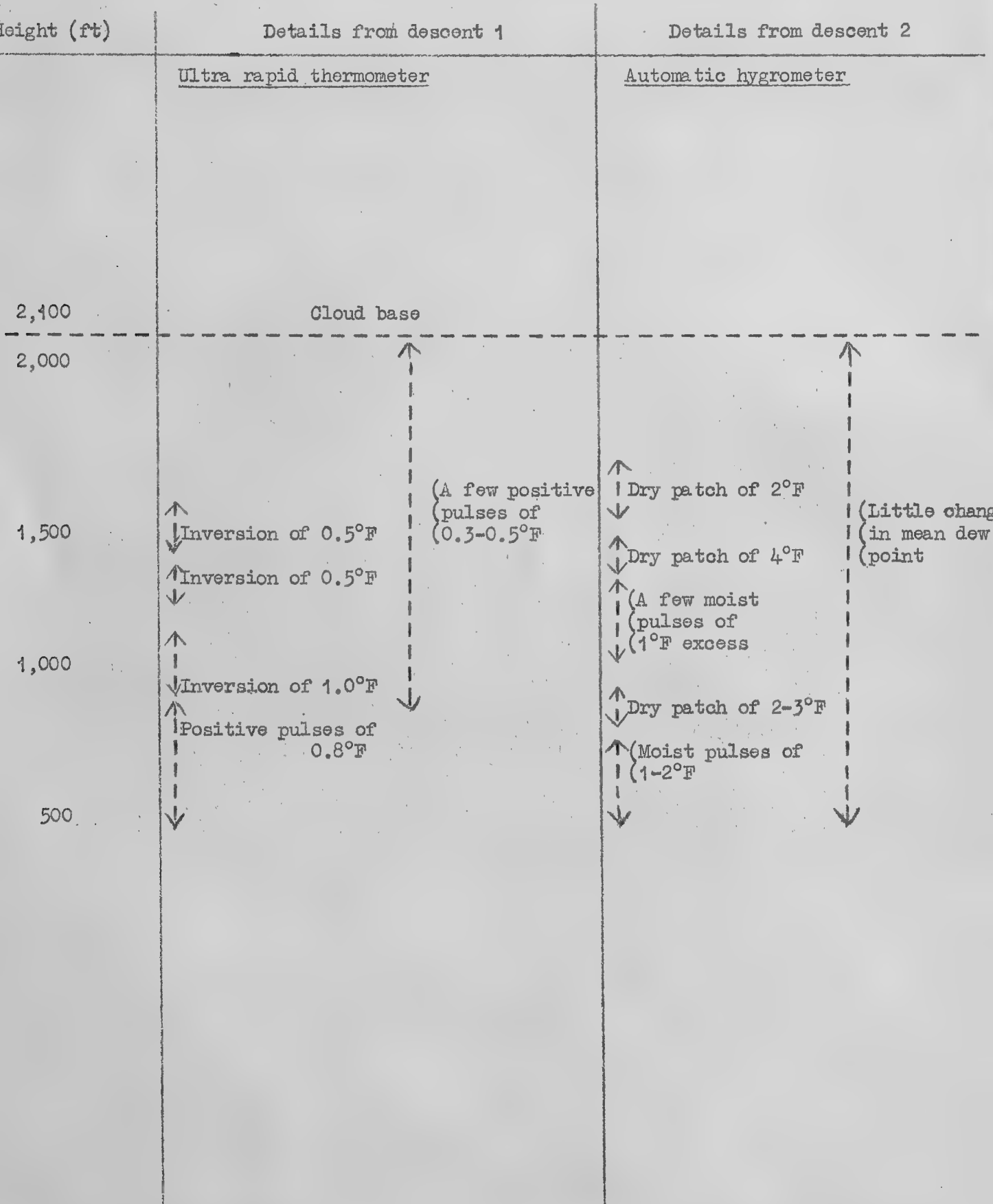

Table 16

26.8.53. 14.00-16.30. Flight 23. Sea. Cloud base 4,500 ft

Instruments:- Ultra Rapid Thermometer, Accelerometer and Automatic Hygrometer.

Flight details:- Level runs at 100 ft, 500 ft, 1,000 ft, 2,000 ft, 3,000 ft using Ultra Rapid Thermometer and Automatic Hygrometer. Slow descent from 4,000 ft to 1,000 ft using Ultra Rapid Thermometer.

Height (ft)	Details from level runs				Details from descent
	Mean T (°F)	Span (°F)	Mean F.P.(°F)	Span °F	
4,500	Cloud base				
4,000					
3,000	51.3	0.5	41	3	
	A few fluctuations of 0.2°F. Slow long-wave changes of 0.5°F over 6,000 ft No well-defined pulses. Considerable change of 5°F in ambient F.P.				(Lapse rate varying from dry adiabatic to almost isothermal. A few fluctuations seen at all heights of 0.2-0.5°F
2,000	56.2	0.3	44	2	
	A few bursts of small temperature fluctuations of 0.2-0.3°F Three wet pulses of 2°F, lasting 300 ft to 2,500 ft				
1,000	60.0	0.7	47	3	
	One region of small fluctuations of 0.3-0.4°F Long waves of 0.5°F. Eight wet pulses of 4-5°F excess, with spacing of 4,500-5,000 ft				Sudden inversion of 1.0°F at 800 ft
500	62.4	0.3	50	1	
	A few positive temperature pulses of 0.3-0.5°F over 1,000 ft. Series of wet pulses of 2°F excess, over 1,000-1,500 ft				(Very many temperature pulses of 0.3-0.6°F in dry adiabatic lapse rate
100	63.2	0.2	53	2	
	Very many fast pulses of temperature of 0.5°F over 100 ft. Moist pulses of 2-3°F excess. Wet patch of 2°F, in 5,000 ft				

Frequency of bumps recorded on occasions when cloud base was at least 3000 feet

Fig. 1 Over land

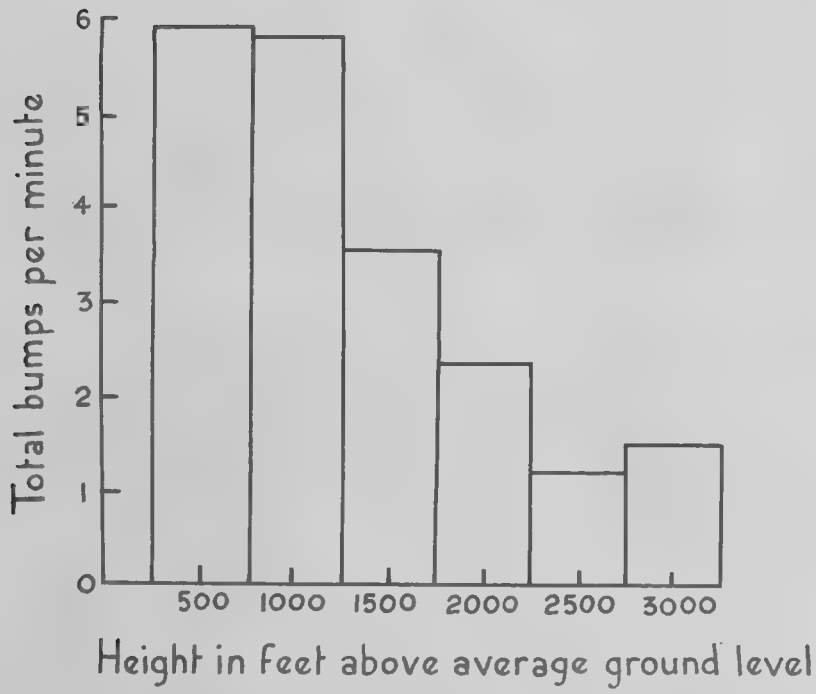

Fig. 2 Over sea

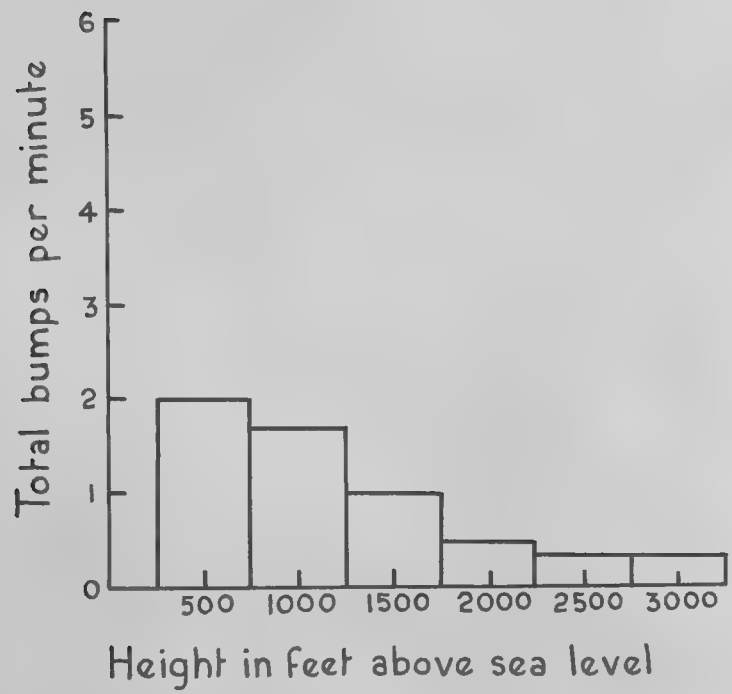

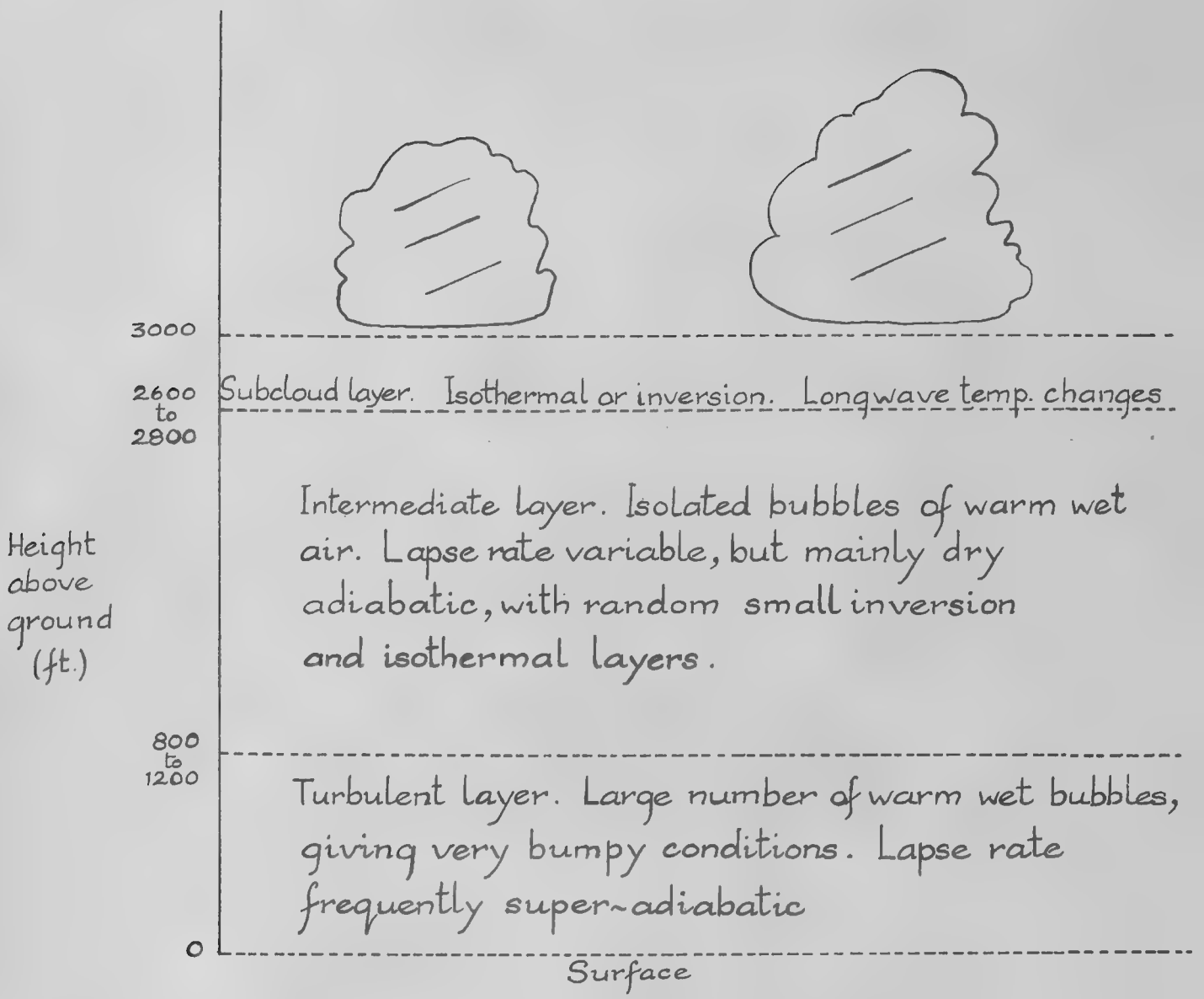

Fig. 3

Typical sub-divisions of region from ground to cloud base

Fig. 4

Frequency of temperature pulses recorded on level flights over land

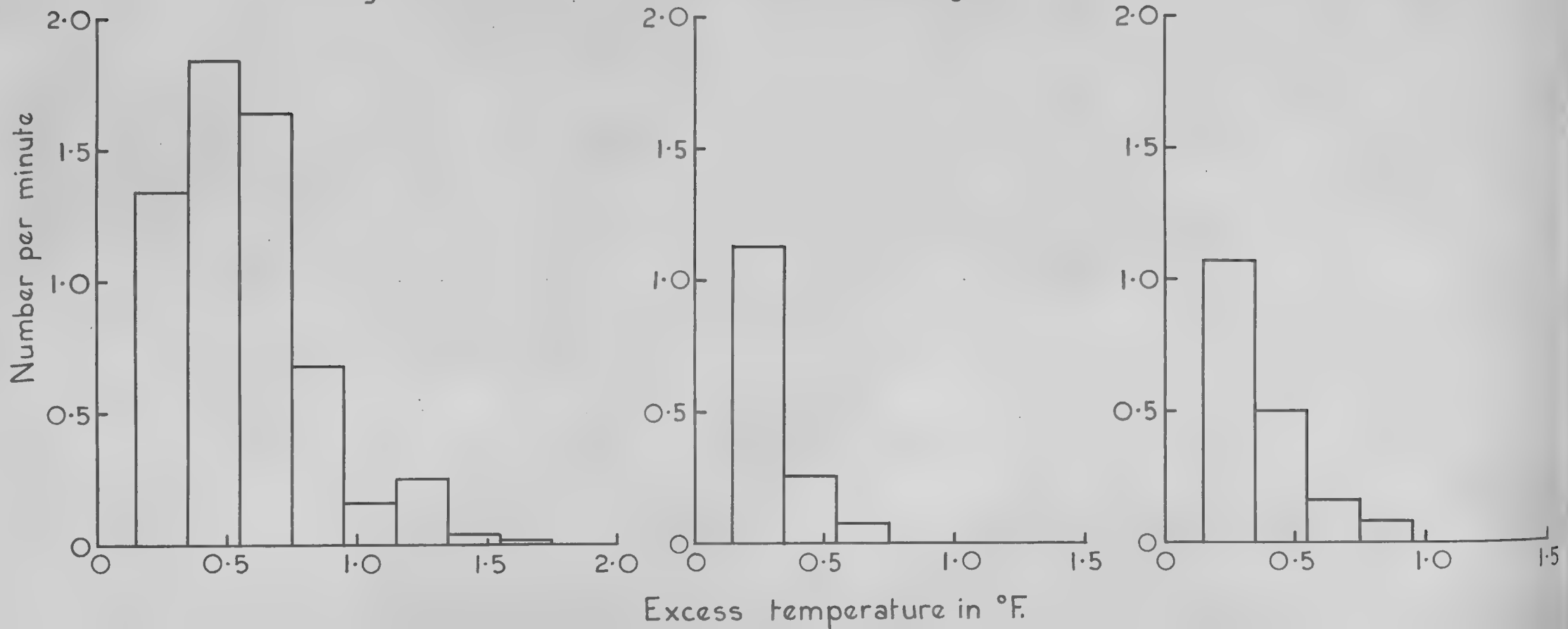

Fig. 5

Frequency of horizontal extents of temperature pulses recorded on level flights over land

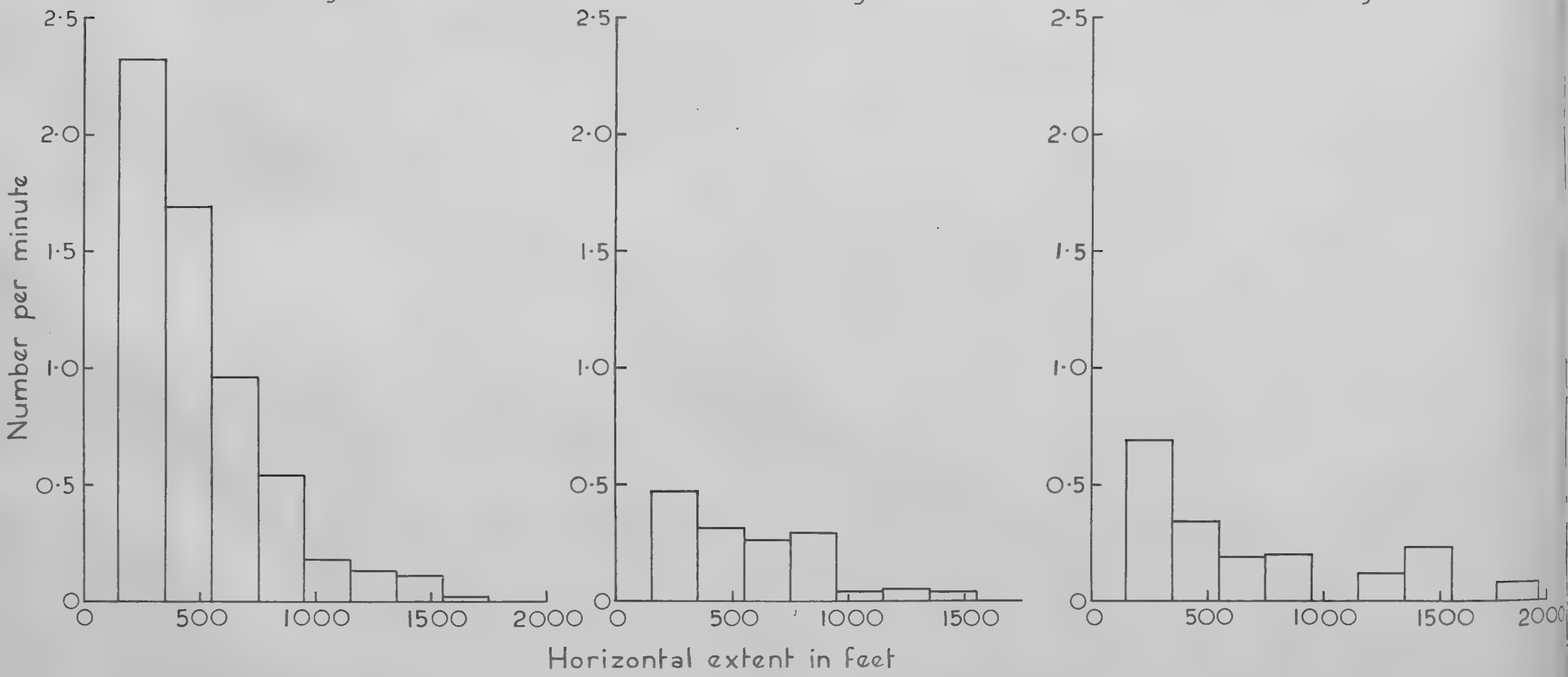

Fig. 6

Frequency of gust intensity recorded on level flights over land

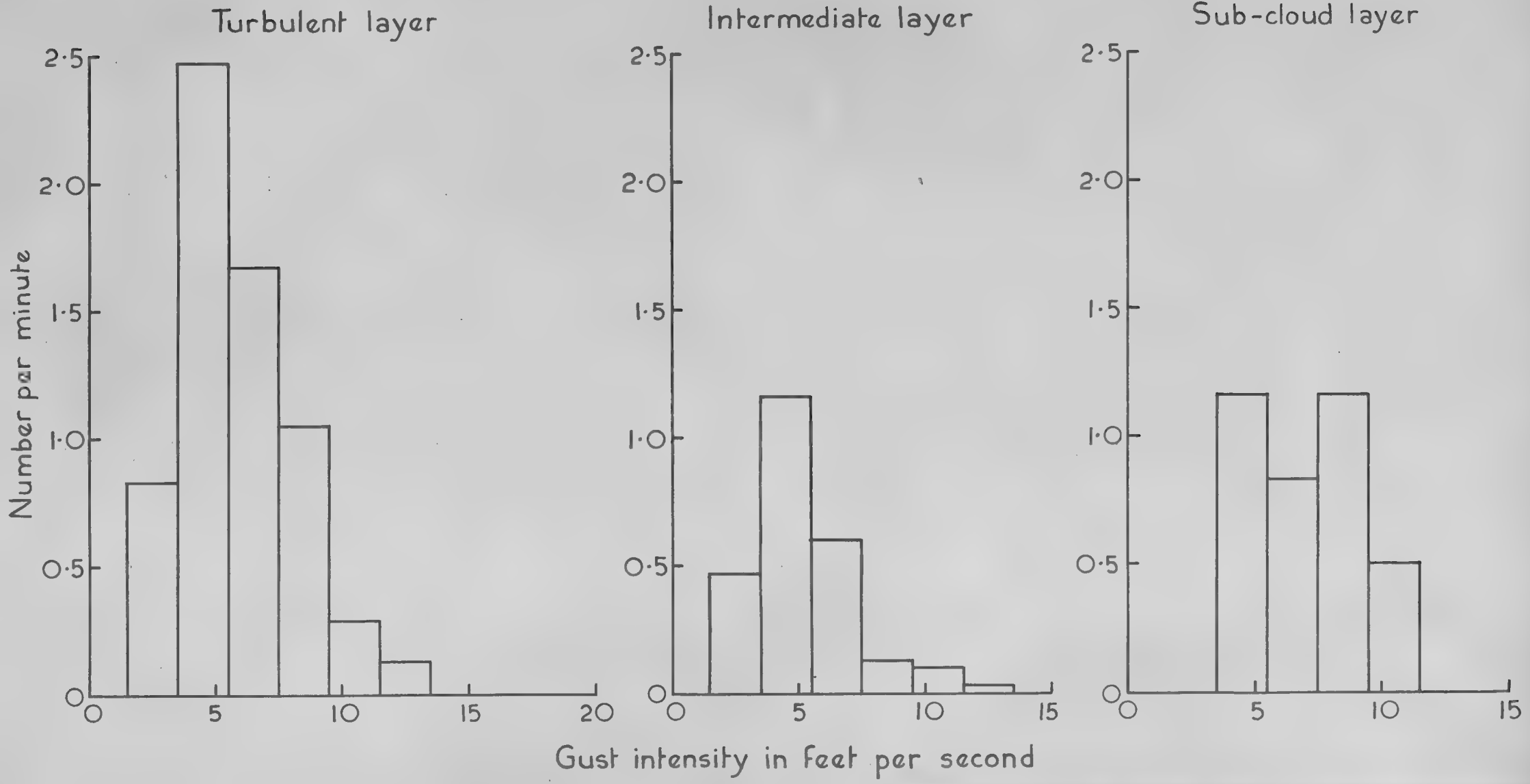

Fig. 7

Frequency of horizontal extent of gusts recorded on level flights over land

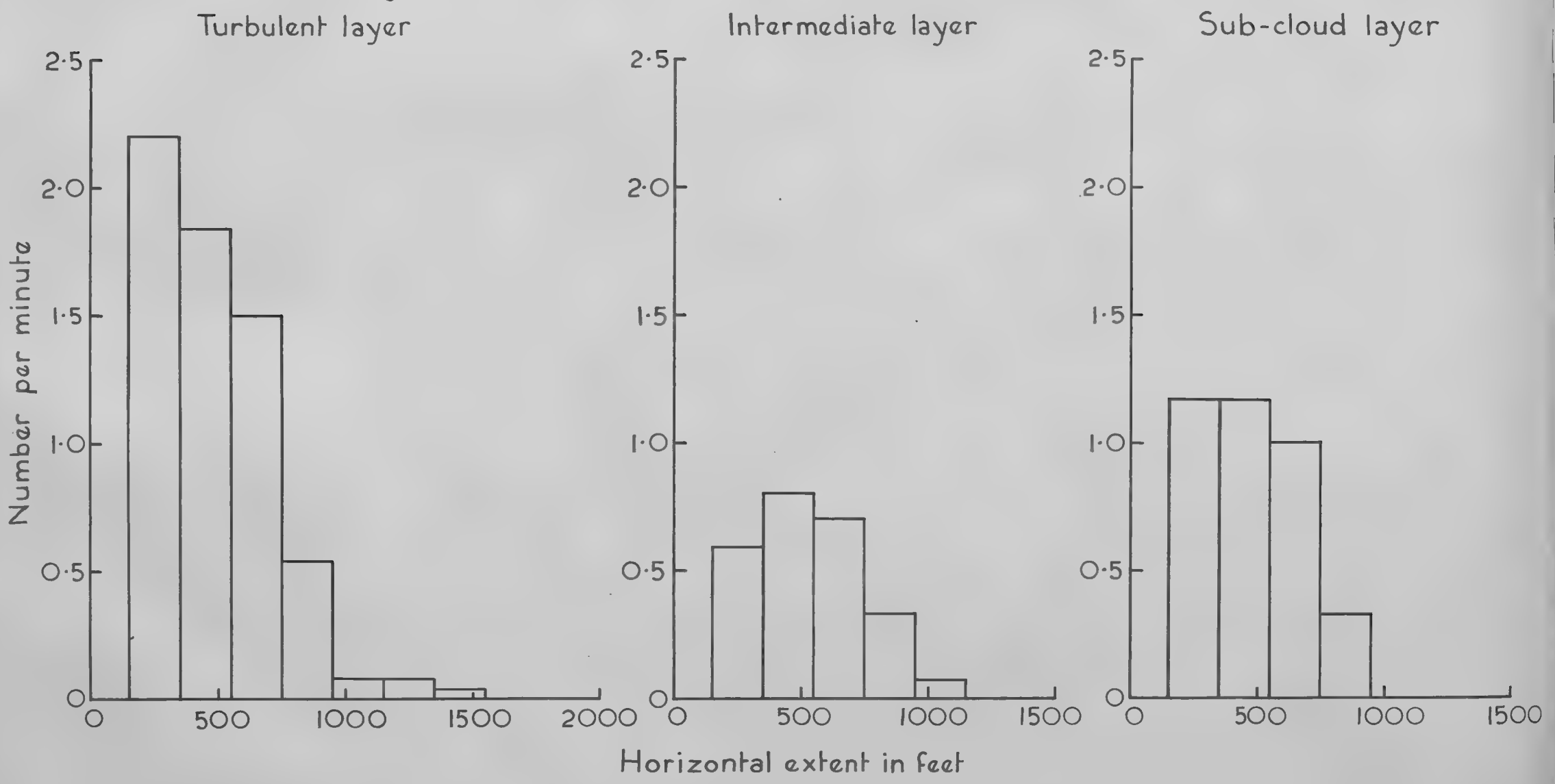

Fig. 8

Percentage of horizontal runs of 36,000 ft. where total temperature variation exceeds a given value

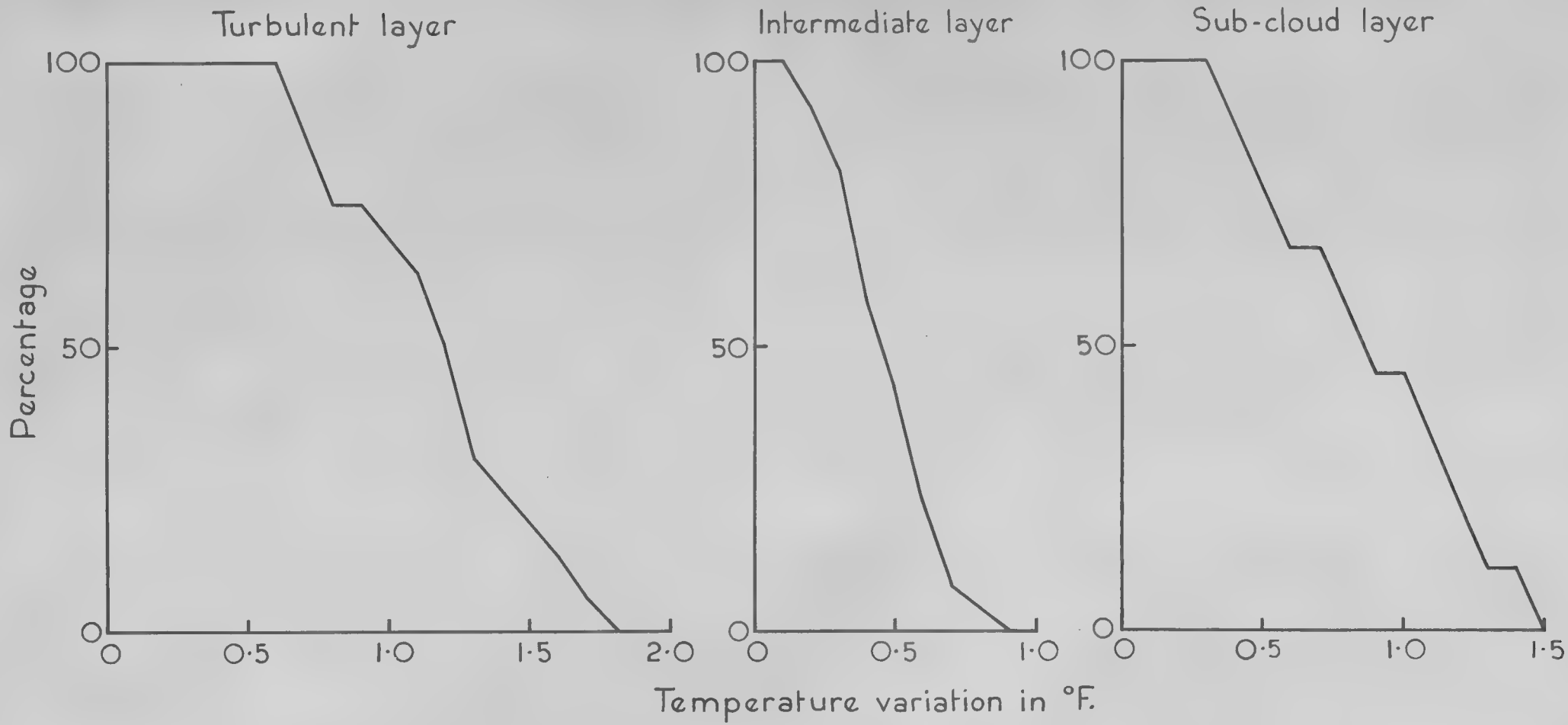

Fig. 9

TURBULENT LAYER OVER LAND

M.R.P. 875

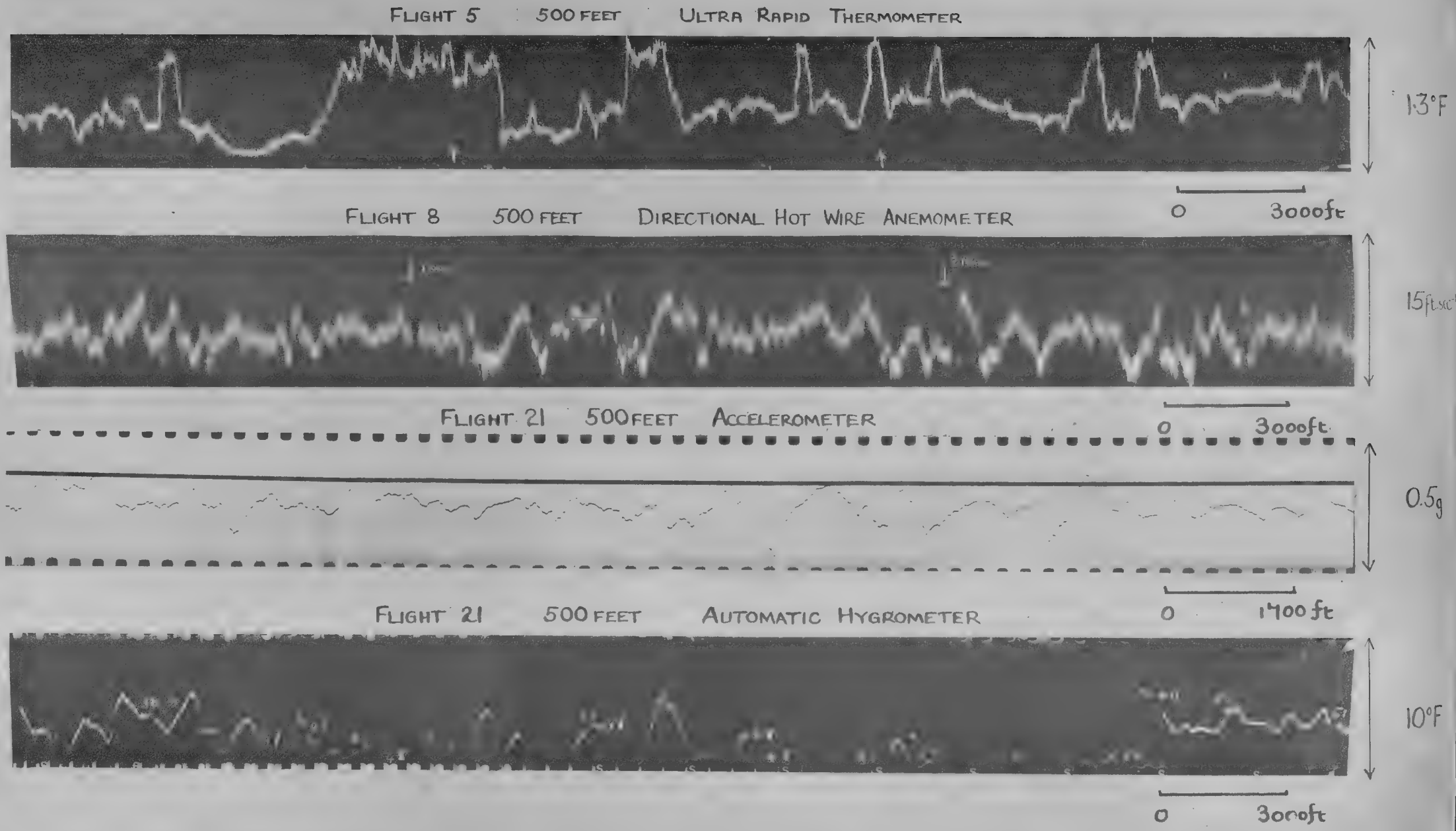

Fig. 10

INTERMEDIATE LAYER OVER LAND

M.R.P 875

FLIGHT 3 1500 FEET ULTRA RAPID THERMOMETER

0 3000ft

FLIGHT 7 1500 FEET DIRECTIONAL HOT WIRE ANEMOMETER

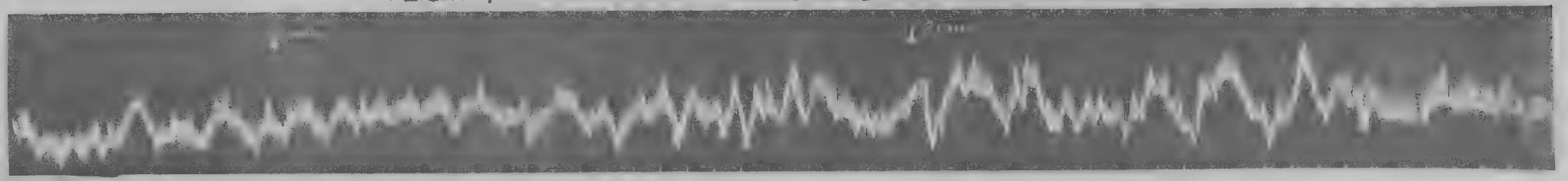

0 3000ft

FLIGHT 22 2000 FEET ACCELEROMETER

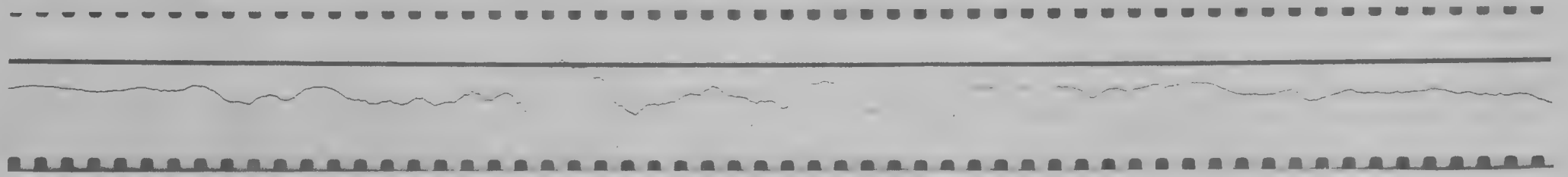

0 1400ft

FLIGHT 22 2500 FEET AUTOMATIC HYGROMETER

0 3000ft

Fig. 11

THE SUB-CLOUD LAYER OVER LAND

M.R.P. 875

FLIGHT 5 3000 FEET ULTRA RAPID THERMOMETER

FLIGHT 3 2000 FEET DIRECTIONAL HOT WIRE ANEMOMETER

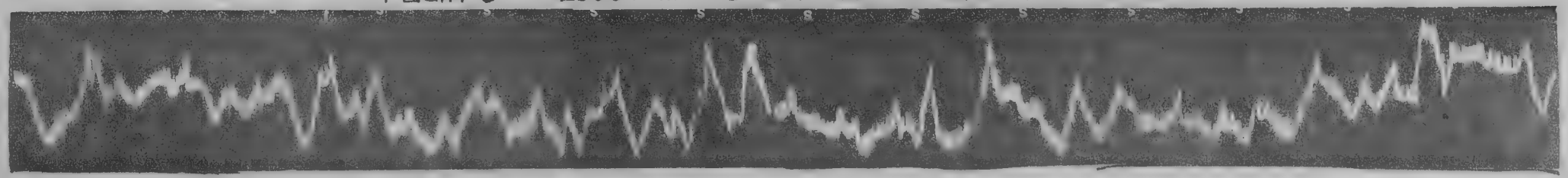

FLIGHT 21 2000 FEET ACCELEROMETER

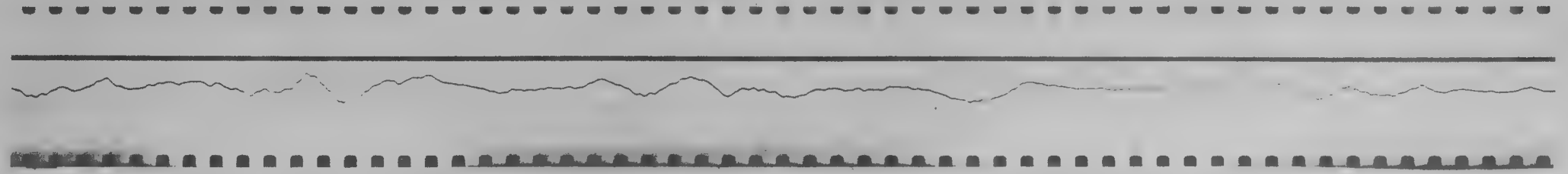

FLIGHT 22 3000 FEET AUTOMATIC HYGROMETER

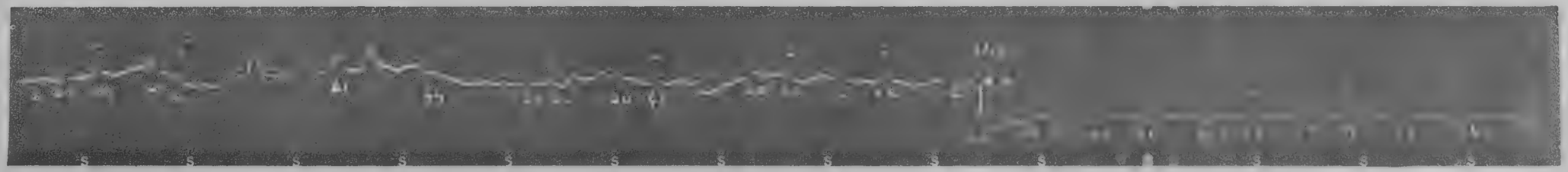

Fig. 12 SLOW DESCENTS OVER LAND USING THE ULTRA RAPID THERMOMETER

M.R.P. 875

FLIGHT 16 SHEWING SUB-CLOUD LAYER FROM 3000' TO 2800'

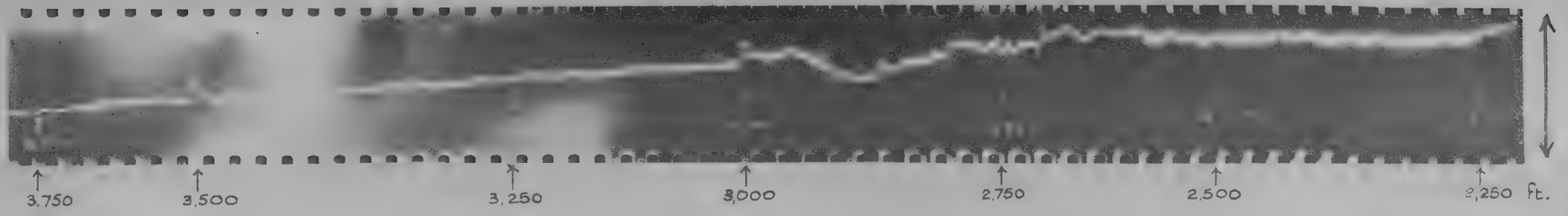

FLIGHT 18 SHEWING ONSET OF TURBULENCE AT 850 FEET

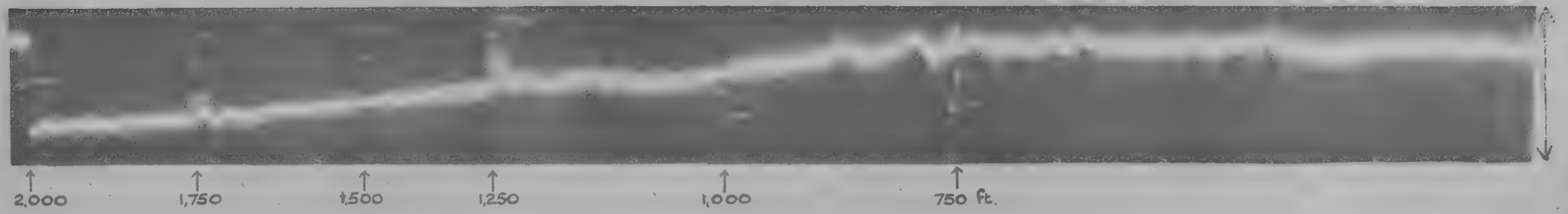

FLIGHT 18 SHEWING NEGATIVE TEMPERATURE PULSES ABOVE CLOUD

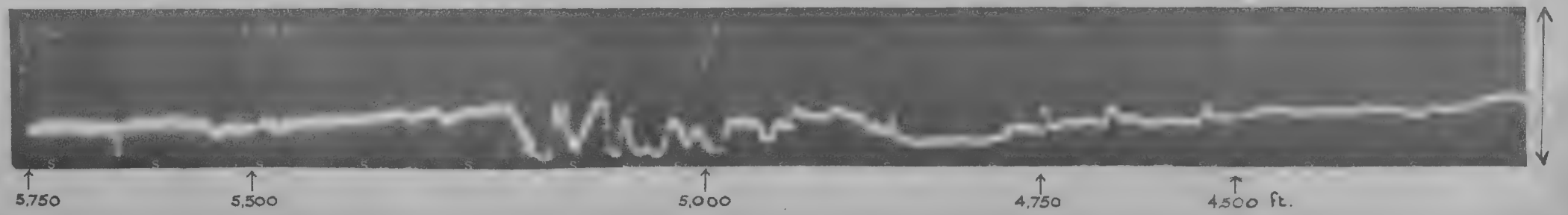

Fig. 13

SLOW DESCENTS OVER LAND

M.R.P. 875

FLIGHT 16 DIRECTIONAL HOTWIRE ANEMOMETER FROM CLOUD BASE

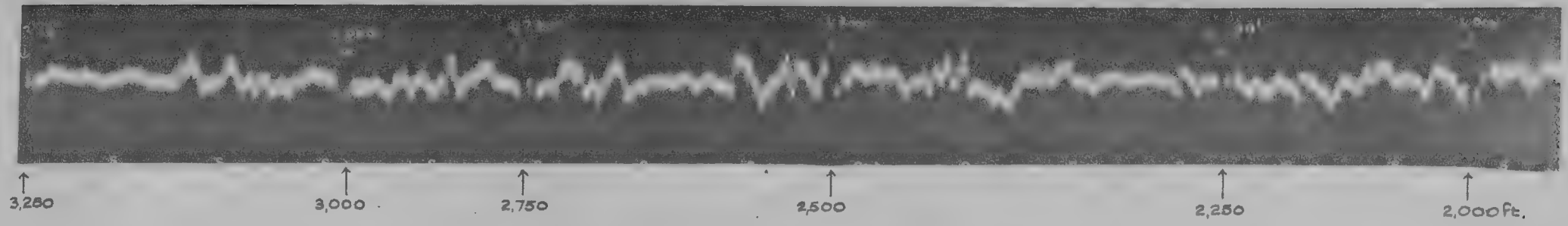

FLIGHT 21 AUTOMATIC HYGROMETER FROM CLOUD BASE

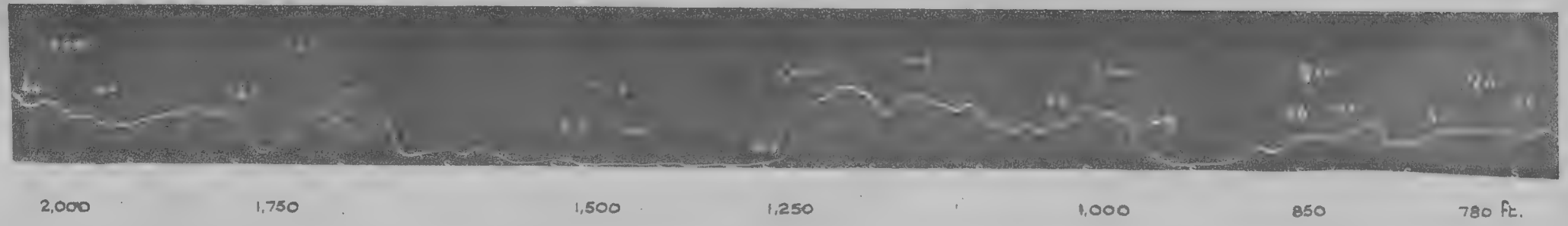

Fig. 14

BELOW INVERSION OVER SEA

M.R.P. 875

FLIGHT 23 100 FEET ULTRA RAPID THERMOMETER

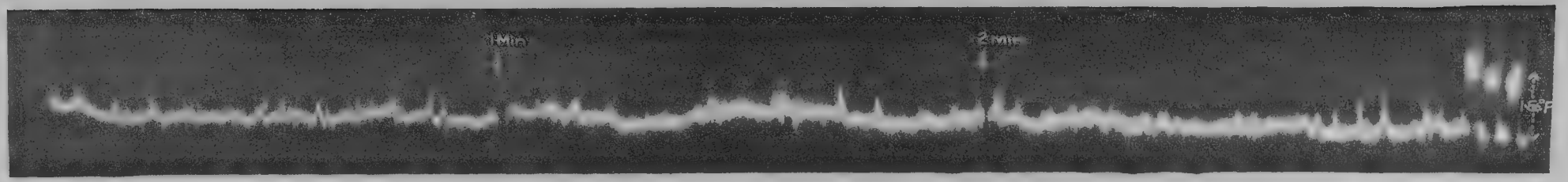

FLIGHT 10 500 FEET ACCELEROMETER

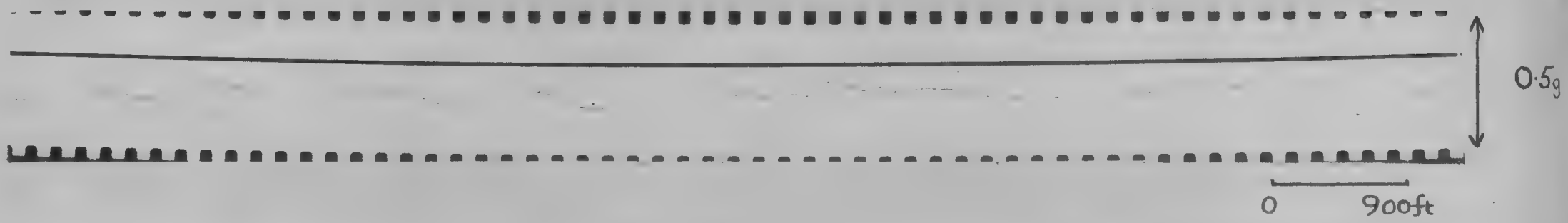

FLIGHT 23 100 FEET AUTOMATIC HYGROMETER

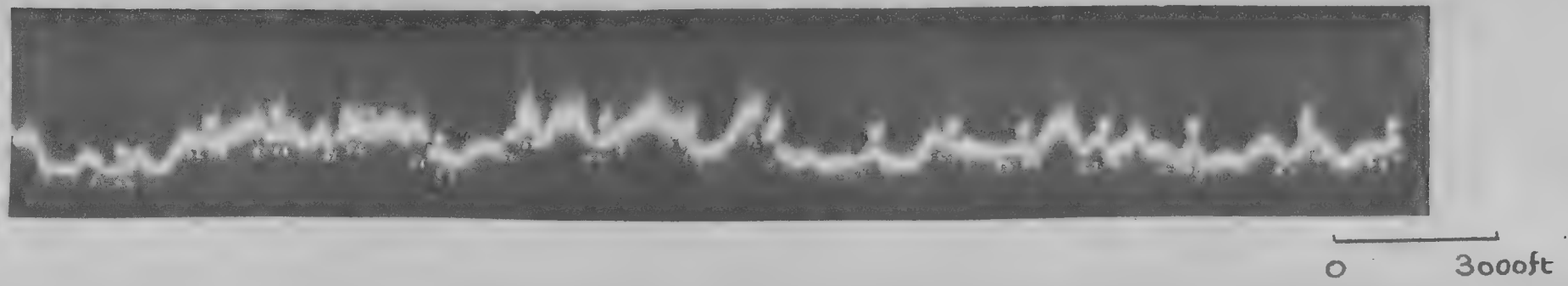

Fig. 15

ABOVE INVERSION OVER SEA

M.R.P. 875

FLIGHT 10 1000 FEET ULTRA RAPID THERMOMETER

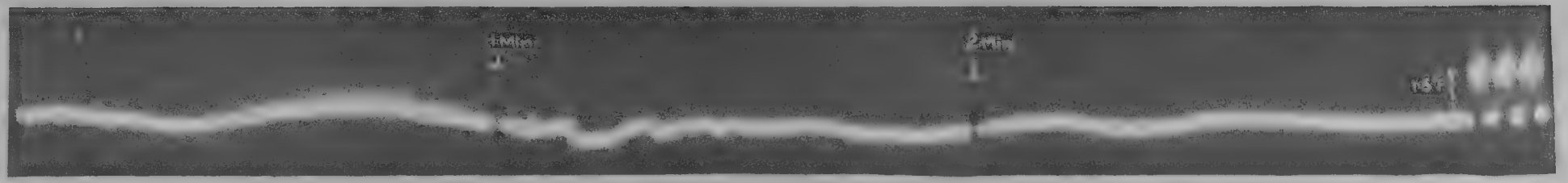

0 3000ft

FLIGHT 11 1500 FEET ACCELEROMETER

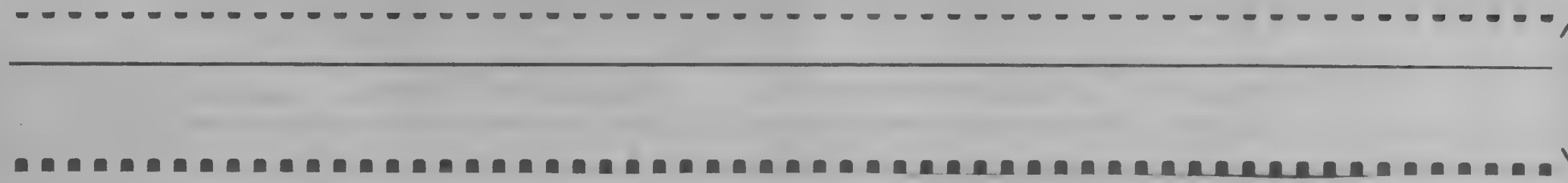

0 1300ft

FLIGHT 23 1000 FEET AUTOMATIC HYGROMETER

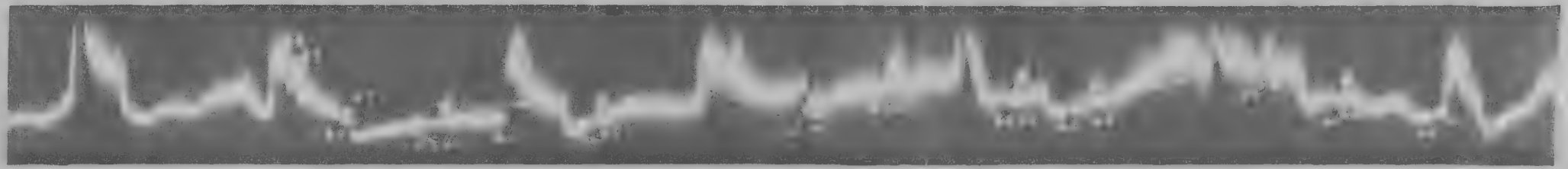

0 3000ft

Fig. 16

SLOW DESCENTS OVER SEA USING THE ULTRA RAPID THERMOMETER

M.R.P. 875

FLIGHT 20 1750 FEET TO 250 FEET, SHEWING INVERSION BELOW 600 FEET

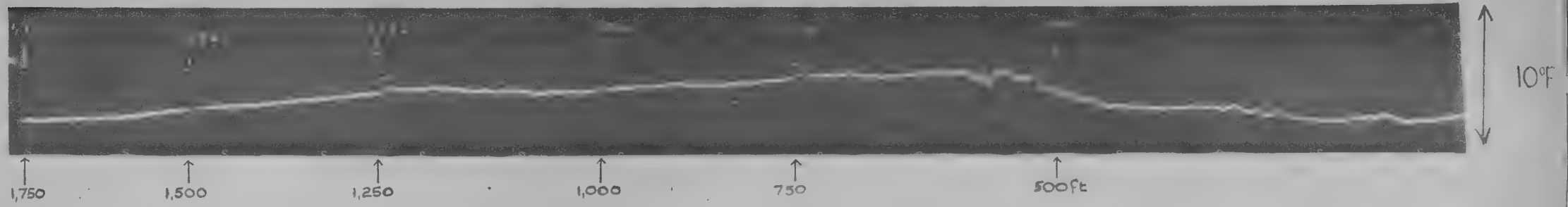

FLIGHT 20 3600 FEET TO 1750 FEET

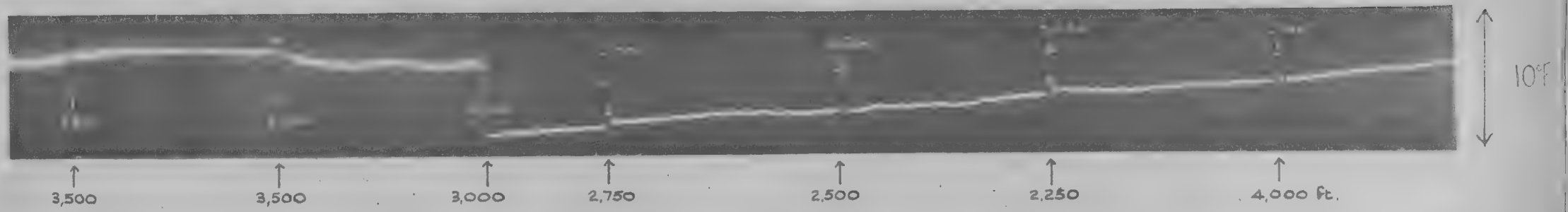

FLIGHT 20 750 FEET TO 200 FEET, SHEWING INVERSION TWENTY MINUTES LATER

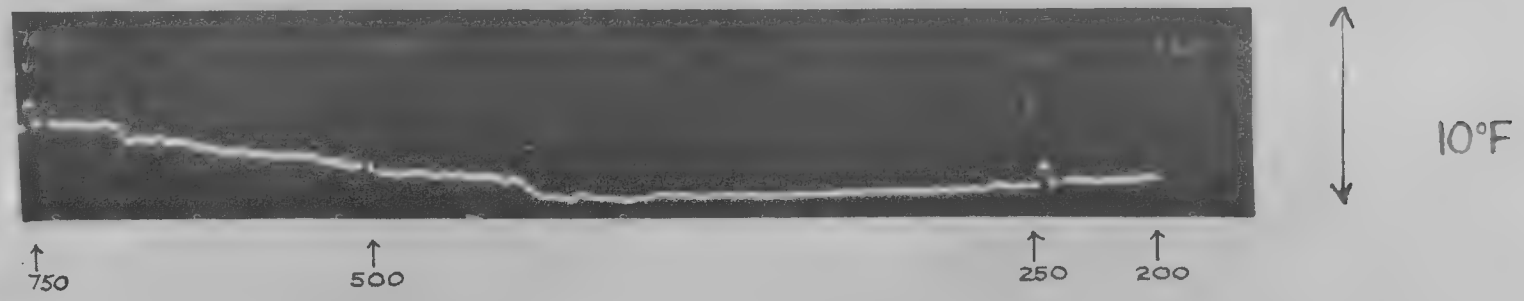

Control Number C.D. 8055

Control Number C.D. 8055.

No.877 by Messrs. R.J. Murgatroyd,

copy is available in the Library
of the Meteorological Office."

At the time of issue this report has not been published. Any author desiring to quote this paper should refer to it as "A paper of the Meteorological Research Committee (London), M.R.P. No.877 by Messrs. R.J. Murgatroyd, P. Goldsmith and W.E.H. Hollings. A copy is available in the Library of the Meteorological Office."

RAND

M.R.P. 877
S.C. III/174
S.C.I./89
9th September, 1954.

AD 63910

AIR MINISTRY
METEOROLOGICAL RESEARCH COMMITTEE

An interim report on measurements of humidity from aircraft to heights of about 50,000 feet over Southern England

by
R.J. Murgatroyd, P. Goldsmith and W.E.H. Hollings (Meteorological Office)

Summary

Results of the first 21 flights to measure humidity up to about 50,000 feet in the Meteorological Research Flight's Canberra aircraft are presented and discussed.

Introduction

The humidity measurements in the upper troposphere and lower stratosphere made by the Meteorological Research Flight at Farnborough and the High Altitude Flight at Boscombe Down, 130 ascents in all, up to June 1950 are described in Geophysical Memoir No. 88 (Ref. 1). These were limited by the operational ceiling, about 40,000 feet, of the Mosquito aircraft used and although these data have since been extended by about another 200 similar ascents it became very desirable to raise as soon as possible the ceiling to which these observations can be made. This became feasible towards the end of 1953 when the Meteorological Research Flight acquired a Canberra aircraft which now attains about 50,000 feet in regular ascents.

Instrumentation

For the first ascents a Dobson-Brewer pressurised hygrometer was installed in the normal way on the starboard side of the Canberra aircraft near the bomb-aimer's position which has now been modified for use by the Meteorological Observer. It was not known beforehand whether results could be obtained at extreme altitudes, as the frost deposits on the hygrometer thimble become progressively more difficult to recognise as the frost point decreases. It was expected that frost points of -120°F or even lower might be found between 40,000 and 50,000 feet as -110°F had been occasionally observed at lower levels, and also it was known that the deposit becomes invisible somewhere between -120° and -130°F. It turned out however that the two observers (P.G. and W.E.H.H.) who have had considerable experience at this work found that readings down to -120°F are quite possible and reasonable spans of 8° - 12°F between the "deposit increasing" and "deposit decreasing" stages can be obtained with care. One factor assisting in this is that at high altitudes a Canberra flies considerably faster than a Mosquito aircraft and thus a faster air flow is produced through the instrument.

On one occasion 11/3/54 however the observer reported that he had little confidence in his observation of an increasing deposit at -128°F and that no further increase in it was seen although he lowered the thimble temperature to -150°F or so. This is attributed to clear ice deposits forming at some temperature between -120°F and -130°F and not being seen with certainty. The nature of the deposit appears to vary from ascent to ascent and the recognition of its appearance and disappearance is very subjective so that no rules can be laid down for its recognition. Usually the readings were

made on the ascent which ensured that the observer had practice in obtaining frost points and recognising their type at higher temperatures before they lowered to the -110° to -120°F region. The factors determining deposit type - such as nature of the thimble surface, temperature and air flow - appear to require a laboratory investigation before any progress can be made in training observers quickly to do this work. The two observers however have separately obtained very similar results on all their ascents.

Nevertheless it was decided to attempt to check these observations and make them easier by using air from the engine compressor as described in M.R.P. 859 (Ref. 2). A tap was taken from the 12th stage of the starboard engine and cocks arranged so that either the outside air or air from the engine compressor could be supplied to the hygrometer. The air pressure within the hygrometer was measured with altimeters in both inlet and outlet pipes. Pressure ratios of 6 or 8 to 1 could be obtained and readings made by both methods compared on several flights. A frost point of -120°F at 50,000 feet appears as a frost point of about -90°F when the air is compressed to surface pressure. When readings were taken by both methods and the agreement was not good it was found that the value obtained from the compressed air always indicated a drier atmosphere than that of the direct reading. This discrepancy was traced to the effect of minute leaks in the joints on the inlet side of the hygrometer. A very small leak from the pressurised cabin into the hygrometer raises the measured frost point by several degrees at these low frost points. This effect is illustrated in Figs. 4a and 4b which show comparisons in which a small leak occurred in the case of Fig. 4a and not in Fig. 4b. It is interesting to observe that the effect of such a small leak only becomes important for readings at the greatest altitude. It is seen that one of the principal advantages of the compressed air system is that since the inside pressure of the hygrometer is greater than that of the cabin all leaks will be outwards. Apart from this advantage and the fact that the range of the instrument is definitely extended the increase in size of the deposit was however somewhat disappointing. This may have been due to the necessity of limiting the compressed air flow to maintain its pressure which makes the compressed air flow considerably slower than the direct flow. Some improvement may be possible here by using air from both engines.

The use of the compressed air system requires a certain amount of caution in that the hygrometer must be kept at high pressure for short periods only and the system should generally be used only at high altitudes. Otherwise it is possible for the compressed air to become hot enough and of sufficient pressure to damage the hygrometer and altimeters. On account also of this heating by compression the thermal insulation between the thimble and its surroundings must be very good to allow the thimble to be cooled efficiently. The liquid oxygen pump must also be outside the pressure seal to ensure that its operation has no effect on the internal pressure of the hygrometer. This means that the thimble itself must also be part of the pressure seal. As a result of the experience gained in these flights these features are now being incorporated in a new mark of pressurised hygrometer.

Observations

A summary of all the readings taken in the first 21 flights of the Canberra aircraft is given in Table 1 and a diagram of the frost point values of all these ascents arranged in order of tropopause height and plotted against ICAN heights is given in Fig. 1. The area covered by the flights in all cases was considerable, including most of Southern England. Each flight lasted about 2 hours during which time the aircraft covered about 1000 miles, making it impossible to obtain readings over a given position. During each reading, which takes say 2-3 minutes, the aircraft travels 20 miles or so. The ICAN heights were taken from the pilot's altimeter which is correct for pressure within about ± 200 feet. The accuracy of the frost points is believed to be ± 3°F at highest altitudes and considerably better lower

/down

down. The question of possible leaks in the normal use of the hygrometer has been mentioned above but all precautions possible were taken to avoid them. The comparatively high value at 50,000 feet of -107°F and -113°F on Flights 2 and 3 occurred between those of -121°F and -118°F of Flights 1 and 4 without any intervening adjustment of the installation and although all other readings at this height were near to -120°F we have at present no grounds for doubting them.

The air temperature was measured in each case by means of a flat plate thermometer corrected for airspeed using a speed correction coefficient of $\alpha = 1.8$ up to 750 mb decreasing to $\alpha = 1.7$ at 300 mb and above. Further work has since been done on determining these coefficients for the Canberra aircraft which indicates they are correct to ± 0.1 in α and the temperatures given usually agree to 2-3°F with the relevant radiosonde ascents.

In Table 2 and Fig. 2 the results have been presented with reference to pressure at the tropopause, and means for all ascents, ascents with low tropopauses and high tropopauses considered separately.

Fig. 3 shows the frost points at the tropopause, and at two pressure levels above plotted in date order.

Discussion of results

From Fig. 1 it can be seen that the frost point decreases with height above the tropopause and tends to approach a constant value a few thousand feet above. The lapse of frost point also decreases with height, being on the average about 11°F in the 25 mb above the tropopause but only 1°F in 25 mb at heights corresponding to 100 mb or so above the tropopause.

In Fig. 2 the mean values show that for high tropopauses the frost points are generally lower than for low tropopauses. The low tropopause values agree well with the mean curves given in Fig. 3 of G.M. 88 near the tropopause but are considerably lower above a level with a pressure 50 mb less than the tropopause pressure. It is thought that the discrepancy at higher levels may be due to the leakage effect discussed above in the Mosquito aircraft observations on which G.M. 88 is based. All the Mosquito cases at the highest levels would be for low tropopause conditions as the ceiling of this aircraft is only about 40,000 feet.

The readings in Table 2 show a range of about 30°F in frost points at the tropopause and only 8°F at 150 mb above it and it appears that there is a tendency for a constant value of frost point of about -120°F around 50,000 feet. The change from a large lapse rate of frost point near the tropopause to a smaller value at higher levels appears to be discontinuous in some cases suggesting a "humidity tropopause" a few thousand feet above the temperature tropopause. Up to the present however readings have not been taken at sufficiently small height intervals to establish whether this is usually the case. The distance from the tropopause to the region of small lapse of frost point varies between two and ten thousand feet and no relationship between it and other meteorological variables around the tropopause has yet been noticed.

The observations so far were mainly made in February and March followed by another series in June and July, with a period in April and May when no observations were possible due to a period of aircraft unserviceability. From Fig.3 it appears so far that there is little variation from late winter to early summer in the frost points at these levels. The plots of frost points at the tropopause level and at levels corresponding to 75 mb and 125 mb less than the tropopause pressure respectively show a correspondence between high and low frost point values at the tropopause and those at higher levels which becomes less marked as the height above the tropopause increases.

/The

The general picture then is of variable frost points at the tropopause with a tending to constancy of frost point at about -120°F at levels 100 mb or so above it. Values of -120°F to -130°F correspond roughly to both the values at which the deposit on the hygrometer thimble becomes glacial and also the lowest temperatures yet recorded anywhere in the world (-129°F at 60,000 feet over Nairobi is quoted in Ref. 1). The implications of this correspondence are discussed in Ref. 3. No cases of the comparatively high frost points quoted in Ref. 4 have yet been measured in this work and it appears that at 50,000 feet the air is usually extremely dry, a frost point of -120°F with an air temperature of -60°F corresponding to a relative humidity over ice of only 0.7%.

Following this preliminary report it is now hoped to make periodic ascents averaging one or two a week as a routine combined with chemical measurements of ozone as described in Ref. 5. The method of measurement will probably include the use of the automatic hygrometer described in Ref. 6 which has since been further developed up to heights of about 30,000 feet and the compressed air method at higher levels using a visual hygrometer.

References

1. Bannon, J.K., Frith, R. and Shellard, H.C. — Humidity of the upper troposphere and lower stratosphere over Southern England. Geophysical Memoirs, London, No. 88, 1952.

2. Goldsmith, P. — A method of increasing the range of the Dobson - Brewer Aircraft Frost Point Hygrometer. Air Ministry, London, M.R.P. 859, 1954.

3. Dobson, G.M.B. and Brewer, A.W. — Water vapour in the upper air. Compendium of Meteorology, p.311.

4. Barrett, E.W., Herndon, L.R. and Carter, H.J. — A preliminary note on the measurement of water vapour content in the middle stratosphere. J.Met., 6, 1949.

5. Kay, R.H. — An interim report on the measurement of the vertical distribution of atmospheric ozone by a chemical method, to heights of 12 km., from aircraft. Air Ministry, London, M.R.P. 817, 1953.

6. Palmer, H.P. — An improved automatic frost point hygrometer. Air Ministry, London, M.R.P. 774, 1952.

Summary of readings

TABLE 1

Flight No.	1		2		3		4	
Date	19/1/54		22/2/54		24/2/54		25/2/54	
ICAN Height 1000's of feet	Temp. °F	F.P. °F	Temp. °F	F.P. °F	Temp. °F	F.P. °F	Temp. °F	F.P. °F
5	46.0	-	40.0	27	31.6	21	40.0	17
7								
10	31.5	+10	30.6	12	14.6	4	9.6	-4
14								
15	15.8	-21	26.8	-14	-5.5	-19	-1.6	-52
19								
20	-4.1	-46	-9.6	-29	-26.9	-42	-22.6	-64
23								
25	-26.0	-62	-30.2	-63	-46.9	-66	-32.7	-71
26								
28								
30	-51.5	-63	-50.7	-57	-55.6	-88	-54.2	-81
32			-60.7	-66			-56.2	-87
33	-65.2	-75	-	-	-62.6	-90		
34			-68.6	-74			-60.8	-92
35			-	-				
36	-78.3	-85	-78.2	-77	-62.5	-98	-55.0	-102
38	-82.0	-90	-84.2	-87	-62.5	-102	-52.1	-108
40	-80.7	-99	-85.0	-92	-57.0	-108	-51.0	-112
41								
42	-71.2	-113	-78.3	-102	-55.6	-115	-55.2	-115
43								
44	-72.5	-124	-68.0	-105	-59.5	-115	-56.0	-117
45								
46	-72.1	-121	-63.3	-107	-57.2	-113	-56.5	-116
47								
48	-71.9	-120	-64.4	-108	-57.6	-113	-50.9	-118
49								
50	-70.8	-121	-67.6	-107	-61.7	-113	-55.0	-118
Trop. Height feet ICAN	38,000		38,000		33,000		34,000	
Method	Normal		Normal		Normal		Normal	
Obs.	P.G.		W.E.H.H.		P.G.		W.E.H.H.	

TABLE 1 (continued)

Flight No.	5		6		7		8	
Date	5/3/54		10/3/54		11/3/54		22/3/54	
ICAN Height 1000's of feet	Temp. °F	F.P. °F	Temp. °F	F.P. °F	Temp. °F	F.P. °F	Temp. °F	F.P. °F
5	36.0	+15	38.0	21			39.6	25
7					31.4	+16		
10	-	-	20.0	-25	(11)18.3	-4	29.5	-2
14			10.2	-3				
15	-11.7	-67			4.9	-28	11.8	-10
19					-11.1	-45		
20	-	-	-16.0	-41			-9.0	-19
23					-27.3	-66		
25	-49.1	-68	-36.2	-66	-	-	-27.8	-28
26					-40.4	-70		
28					-45.9	-79		
30	-61.5	-77	-52.6	-74	-51.2	-81	-52.4	-53
32			-59.4	-79	-56.1	-85	-59.5	-67
33			-	-				
34			-65.6	-83	-60.7	-91	-66.5	-73
35	-71.2	-97	-	-	-	-		
36	-	-	-69.5	-89	-61.6	-98	-69.8	-79
38	-64.0	-109	-70.6	-97	-59.6	-109	-71.2	-86
40	-	-	-66.0	-105	-57.7	-115	-70.4	-93
41	-61.5	-112						
42	-	-	-63.8	-113	-57.5	-119	-66.6	-101
43								
44	-59.0	-115	-63.7	-115	-59.2	-122	-60.2	-108
45							-58.0	-111
46	-62.0	-116	-63.3	-119	-64.2	-123	-57.2	-115
47							-56.8	-117
48	-61.7	-117	-60.5	-120	-64.3	-122	-55.0	-117
49					-64.6	-122	-59.4	-118
50	-64.0	-117	-62.3	-120	-68.0	-122	-59.0	-120
Trop. Height feet ICAN	34,000		37,000		34,000		36,000	
Method	Normal		Normal		Normal		Normal	
Obs.	P.G.		W.E.H.H.		P.G.		W.E.H.H.	

TABLE 1 (continued)

Flight No.	9		10		11		12	
Date	23/3/54		25/5/54		28/5/54		10/6/54	
ICAN Height 1000's of feet	Temp. °F	F.P. °F	Temp. °F	F.P. °F	Temp. °F	F.P. °F	Temp. °F	F.P. °F
5	32.3	-	44.9	38	53.0	40		
7								
10	24.2	-37	25.2	12	33.1	25		
14								
15	3.3	-33	10.8	13	15.4	15		
19								
20	-19.3	-54	-4.3	-9	-2.6	-3		
23								
25	-38.3	-58	-26.0	-26	-22.0	-38		
26								
28								
30	-57.9	-82	-47.0	-49	-41.2	-46	-52.1	-74
32			-56.8	-62	-49.0	-56		
33								
34			-62.5	-76	-56.2	-62		
35	-55.9	-103					-48.0	-93
36			-65.5	-86	-60.0	-81		
38			-59.5	-90	-63.5	-85		
40	-52.3	-111	-60.3	-101	-70.6	-91	-46.5	-113
41					-67.9	-98		
42	-53.2	-117	-57.0	-105	-67.7	-106		
43			-63.5	-112	-61.6	-114	-46.9	-114
44	-51.6	-119	-53.4	-114	-58.0	-112		
45	-51.4	-119	-53.0	-120	-57.5	-114		
46	-53.0	-120			-54.0	-113	-46.2	-118
47	-52.2	-121			-57.8	-117		
48	-52.5	-121			-57.1	-117	-45.8	-118
49	-53.0	-120			-57.4	-118		
50	-55.2	-120			-58.2	-119		
Trop. Height feet ICAN	32,000		36,000		40,000		30,000	
Method	Normal		Normal		Normal		Compressor	
Obs.	W.E.H.H.		W.E.H.H.		W.E.H.H.		P.G.	

TABLE 1 (continued)

Flight No.	13		14		15		16	
Date	11/6/54		16/6/54		26/6/54		28/6/54	
ICAN Height 1000's of feet	Temp. °F	F.P. °F	Temp. °F	F.P. °F	Temp. °F	F.P. °F	Temp. °F	F.P. °F
5			47.0	-1				
7								
10			35.7	+25				
14								
15			20.1	+13				
19								
20			3.5	-16				
23								
25			-22.2	-37				
26								
28								
30	-55.1	-74	-44.1	-61	-40.7	-48	-53.8	-60
32								
33								
34								
35	-52.4	-103	-67.2	-75	-60.5	-71	-54.7	-96
36								
38								
40	-44.7	-115	-56.4	-108	-76.2	-90	-43.6	-110
41								
42								
43	-47.6	-118	-59.8	-114	-64.1	-107	-45.2	-114
44								
45								
46	-49.4	-120	-61.0	-118	-59.6	-117	-48.2	-116
47								
48	-48.7	-121	-58.6	-121	-60.8	-118	-48.4	-
49								
50	-50.0	-	-	-	-61.2	-119		
Trop. Height feet ICAN	32,000		38,000		40,000		30,000	
Method	Compressor		Compressor		Compressor		Compressor	
Obs.	P.G.		P.G.		P.G.		P.G.	

TABLE 1 (continued)

Flight No.	17		18			19		
Date	29/6/54		1/7/54			5/7/54		
ICAN Height 1000's of feet	Temp. °F.	F.P. °F.	Temp. °F.	F.P. °F.	F.P. °F.	Temp. °F.	F.P. °F.	F.P. °F.
5	34.1	33						
7								
10	28.0	12						
14								
15	9.3	0						
19								
20	-9.8	-34						
23								
25	-29.6	-48						
26								
28								
30	-50.2	-62	-47.0	-41	-55	-46.3	-85	-82
32	-58.9	-68						
33								
34	-60.4	-84						
35			-61.3	-79	-79	-41.6	-104	-105
36	-53.8	-99						
38	-50.6	-107						
40	-47.6	-112	-55.3	-110	-106	-44.0	-111	-110
41								
42	-47.9	-117						
43			-53.4	-115	-113	-41.7	-115	-114
44	-49.2	-120						
45								
46	-49.0	-120	-53.6	-117	-116	-46.7	-117	-117
47								
48	-51.1	-120	-54.1	-119	-118	-50.2	-118	-118
49								
50	-50.1	-120	-50.7	-118	-119	-50.0	-	-
Trop. Height feet ICAN	34,000		38,000			30,000		
Method	Normal		Normal		Compressor	Normal		Compressor
Obs.	W.E.H.H.		P.G.			P.G.		

TABLE 1 (continued)

Flight No.	20		21	
Date	6/7/54		14/7/54	
ICAN Height 1000's of feet	Temp. °F.	F.P. °F.	Temp. °F.	F.P. °F.
5				
6	+31.4	20	22	
7				
10	15.8	-4	-4	
14				
15	-3.1	-33	-34	
19				
20	-23.9	-35	-33	
23				
25	-41.7	-59	-57	
26				
28				
30	-50.6	-83	-80	-39.5 -56
32				
33				-54.0 -58
34				
35	-42.7	-102	-101	
36				-64.9 -69
38				
39				-66.3 -96
40	-43.2	-112	-110	
41				
42				-59.2 -112
43	-43.3	-112	-112	
44				-56.1 -116
45				
46	-45.6	-113	-115	-53.7 -119
47				
48	-48.8	-116	-117	-57.7 -119
49				
50	-46.4	-117	-118	-58.1 -121
Trop. Height feet ICAN	31,000		36,000	
Method	Normal	Compressor	Compressor	
Obs.	P.G.		P.G.	

TABLE 2

Frost points at pressure levels referred to the tropopause

Flight Number	Date	Tropopause Height Ft. 10^{-3} ICAN	High or Low	Tropopause Frost Point °F.	-25 mb F.P. °F.	-50 mb F.P. °F.	-75 mb F.P. °F.	-100 mb F.P. °F.	-125 mb F.P. °F.	-150 mb F.P. °F.	-175 mb F.P. °F.
1	19/1/54	38	H	-90	-103	-122	-120	-120			
2	22/2/54	38	H	-87	-96	-105	-108	-108			
3	24/2/54	33	L	-92	-98	-104	-112	-114	-113		
4	25/2/54	34	H	-92	-102	-109	-114	-117	-118		
5	5/3/54	34	H	-90	-98	-107	-111	-114	-116		
6	10/3/54	37	H	-93	-103	-114	-119	-120			
7	11/3/54	34	H	-91	-98	-111	-118	-122	-122		
8	22/3/54	36	H	-75	-83	-93	-104	-115	-120		
9	23/3/54	32	L	-92	-102	-106	-110	-117	-119	-120	
10	25/5/54	36	H	-88	-96	-105	-111				
11	28/5/54	40	H	-90	-112	-113	-119				
12	10/6/54	30	L	-76	-84	-92	-103	-114	-115	-118	
13	11/6/54	32	L	-87	-98	-106	-112	-117	-120	-122	
14	16/6/54	38	H	-92	-98	-104	-109				
15	24/6/54	40	H	-90	-105	-117	-119				
16	28/6/54	30	L	-65	-80	-95	-102	-110	-113	-116	
17	29/6/54	34	H	-78	-94	-106	-114	-119	-120	-120	
18	1/7/54	38	H	-96	-110	-114	-118	-119			
19	5/7/54	30	L	-84	-93	-100	-109	-113	-116	-119	
20	6/7/54	31	L	-85	-92	-101	-106	-111	-112	-114	-119
21	14/7/54	36	H	-69	-94	-109	-117	-120			
Mean (all occasions)				-86.1	-97.1	-106.3	-112.2	-115.9	-117.0	-118.4	-119.0
Mean for H Tropopause				-87.4	-99.8	-109.2	-114.2	-117.4	-119.0	-120.0	-
Mean for L tropopause				-83.0	-92.4	-100.6	-107.7	-113.7	-115.6	-116.5	-119.0
Extreme range				31	30	30	18	14	10	8	
Mean F.P. lapse/25 mb					11.0	9.2	5.9	3.7	1.1	1.4	0.6

M.R.P. 877

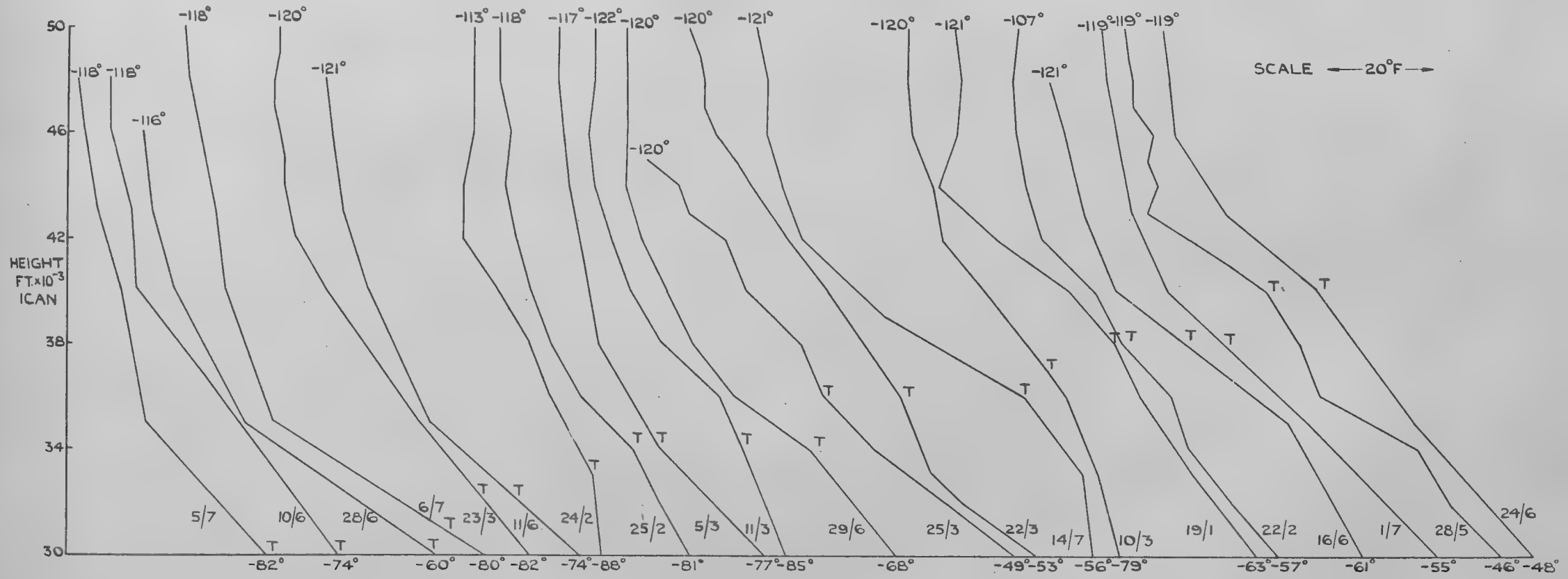

FIG. I. FROST POINTS, INDIVIDUAL FLIGHTS °F.

T DENOTES TROPOPAUSE HEIGHT (PLOTTED WITH HIGHEST VALUES OF T TO THE RIGHT.)

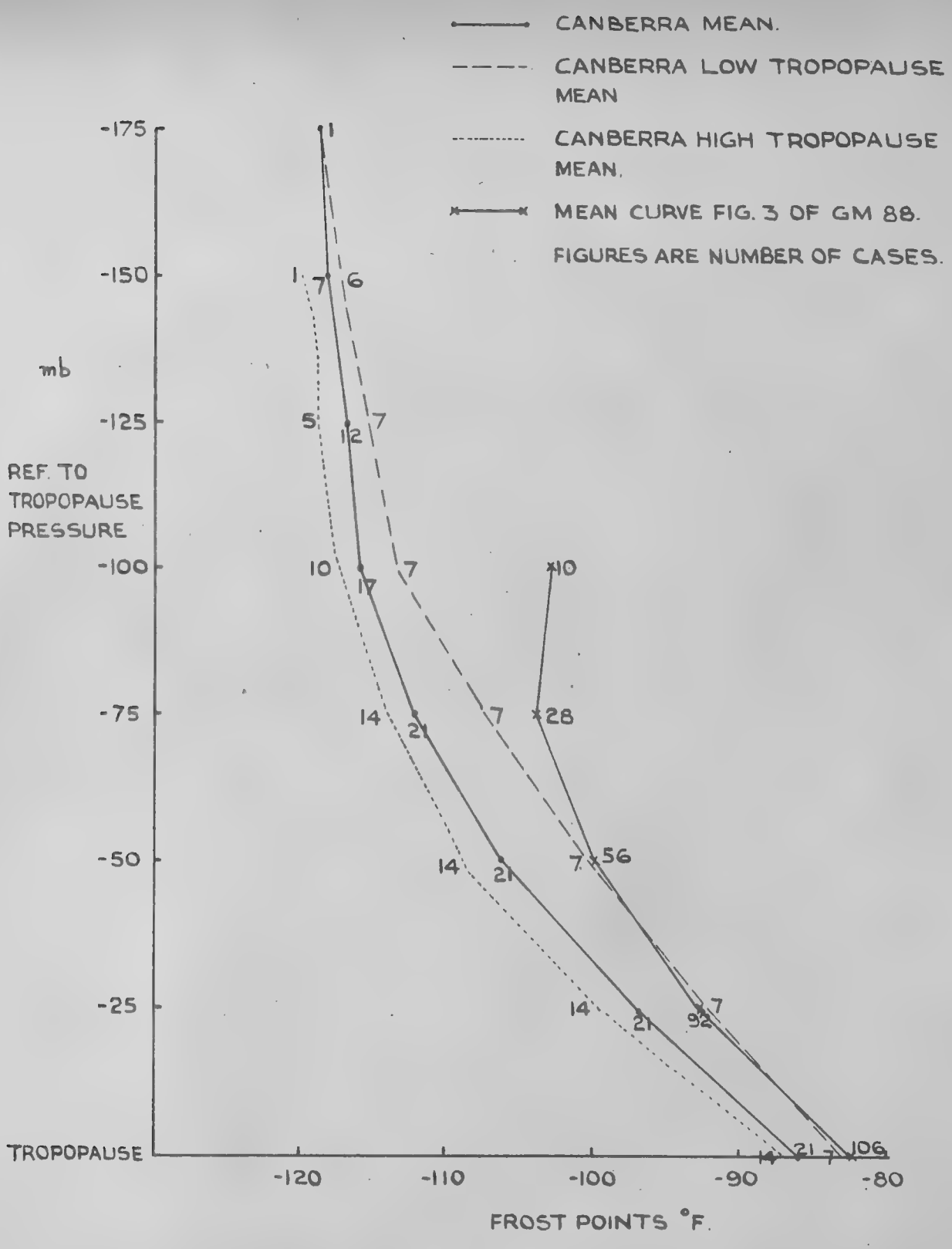

FIG. 2. MEAN FROST POINTS AT LEVELS ABOVE THE TROPOPAUSE.

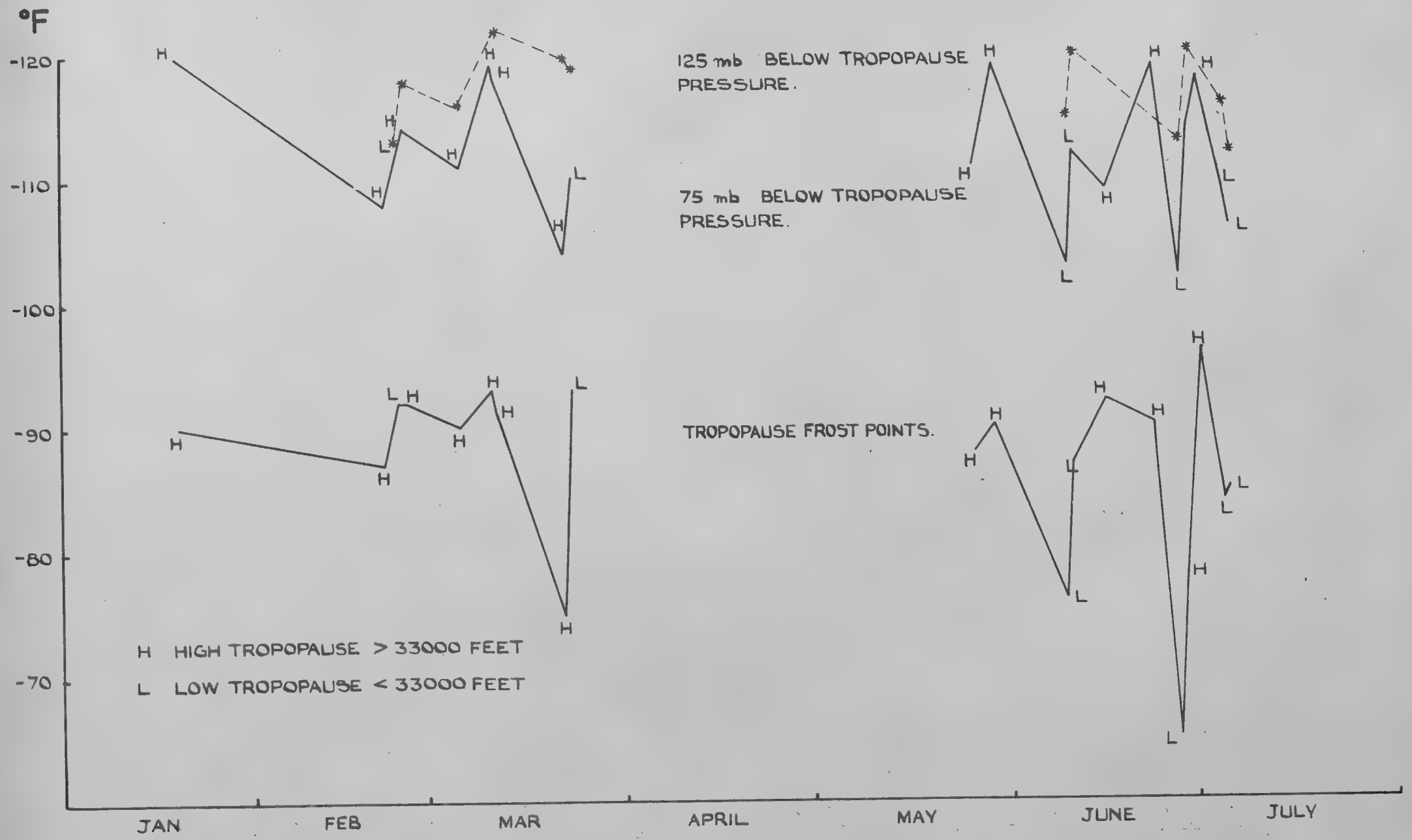

FIG. 3. VARIATION OF FROST POINTS WITH HEIGHT AND TIME.

M.R.P. 877

A Comparison of the Frost Points obtained by the Normal and Compressed Air Methods.

(a) With a probable small leak.

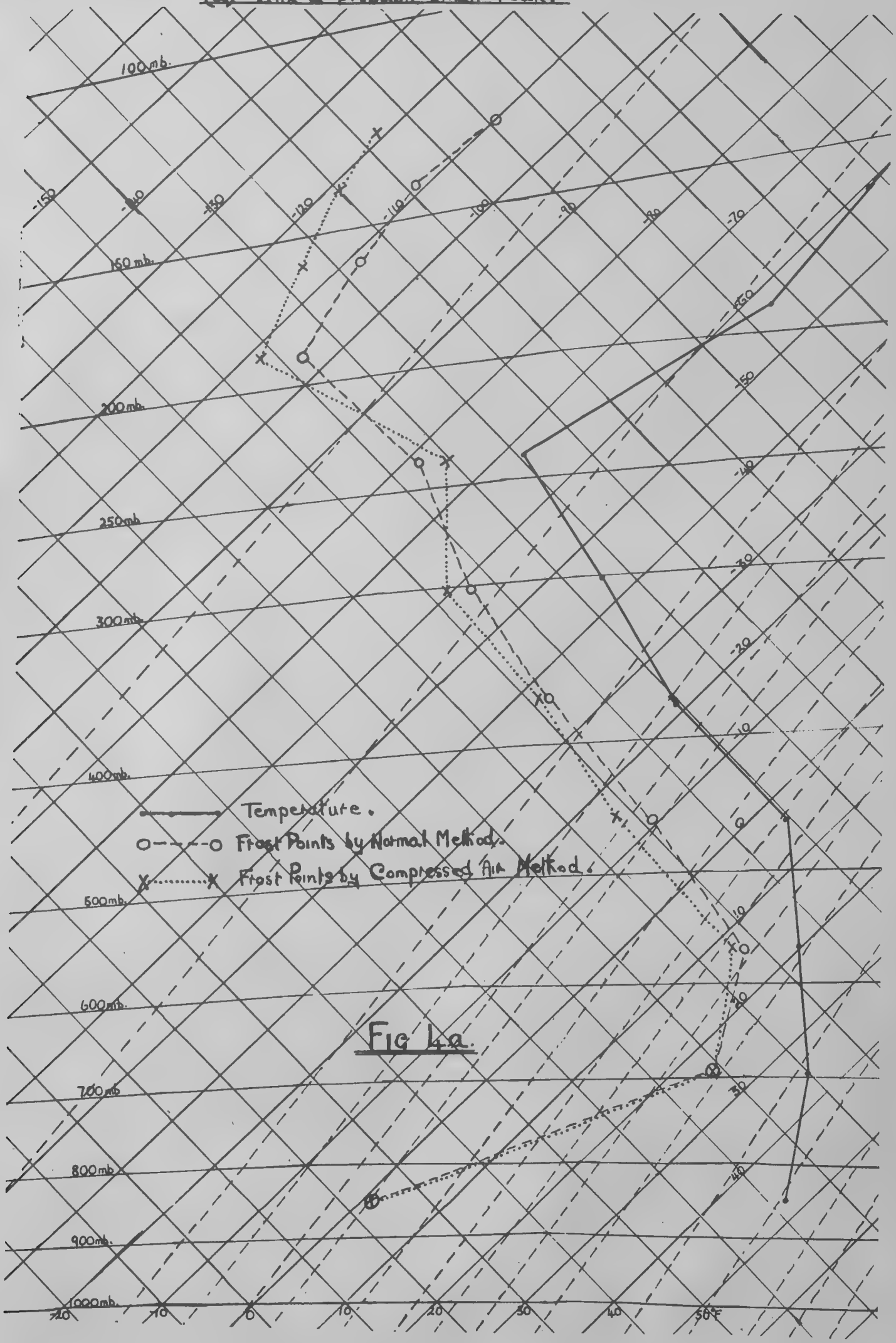

Fig 4a.

A Comparison of the Frost Points obtained by the Normal and Compressed Air Methods.

(b) With all seals satisfactory

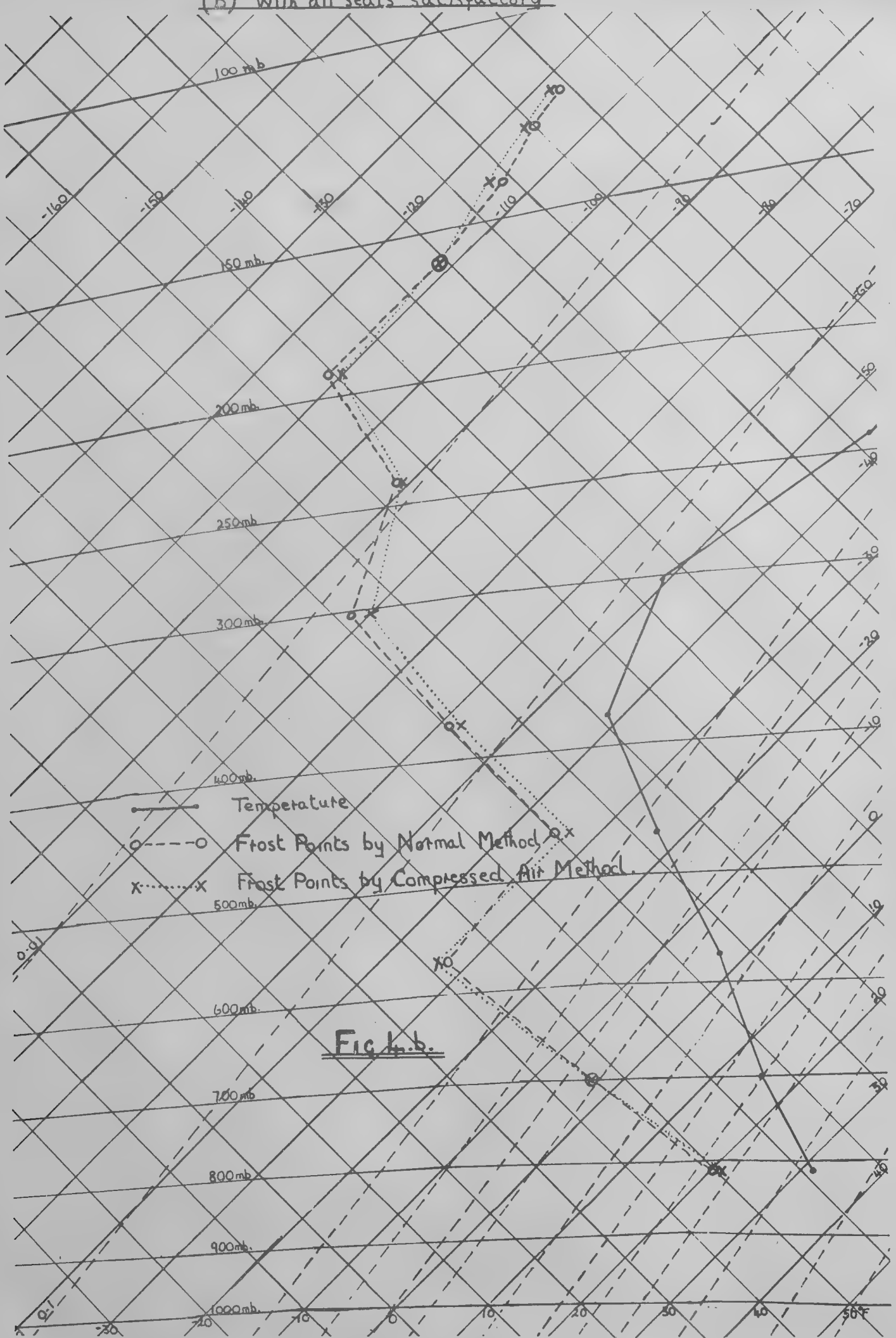

Fig 4.b.

P. No.878 by Dr. A.C. Best.
copy is available in the Library
of the Meteorological Office."

At the time of issue this report has not been published. Any author desiring to quote this paper should refer to it as "A paper of the Meteorological Research Committee (London), M.R.P. No.878 by Dr. A.C. Best. A copy is available in the Library of the Meteorological Office."

M.R.P.878
S.C.III/175
20th September, 1954.

AD 22-3076

AIR MINISTRY

METEOROLOGICAL RESEARCH COMMITTEE

Assessment of maximum concentration at ground level of gas from a heated elevated source

by

A.C. Best (Meteorological Office)

1. Introduction. The assessment of the maximum concentration at ground level of gas discharged from an elevated source, such as a tall chimney, is a matter of considerable practical importance. Many industrial chimney stacks discharge gases which are harmful to health. The gas concentration at ground level is influenced by meteorological factors and also by factors related to the stack and furnace design and it is obviously desirable that the same formula should be used in all cases for computing the maximum gas concentration likely to be experienced at ground level. The effect of a specified gas concentration varies with the individual and for this reason great accuracy in predicting the maximum concentration is not essential. The purpose of the present note is to compare three current formulae.

If the effluent has the same density as the ambient air and is discharged without significant vertical velocity there is no real difficulty. Sutton (1) has given a formula which can be used to compute ground level concentrations at various distances from the stack. If the gas experiences significant vertical movement after leaving the stack the concentration at ground level is more difficult to predict. In general the gas will be discharged into a horizontal wind and the vertical velocity of the gas will diminish as the gas gets further from the stack. The gas plume will thus be vertical at the stack exit and will then bend over in the direction of the wind and at a considerable distance from the stack the plume will be nearly horizontal. An approximate method of computing ground level concentration is thus to treat the source as a cold source emitting with zero vertical velocity but to assume that the source is raised by an amount z equal to the height of the plume above the source at a distance where the plume is "practically" horizontal. It is in the method for computing this height z that the three formulae discussed below differ.

2. Ground level concentration from a cold elevated source. Sutton (1) has shown that if the effluent has the same density as the atmosphere and is emitted without significant vertical motion the concentration at ground level increases with increasing distance from the source up to a critical distance and then decreases again. The maximum concentration at ground level is given by

$$X = \frac{2Q}{e\pi u h^2}\left(\frac{C_z}{C_y}\right) \qquad (1)$$

and occurs at a distance x given by

$$x = \left(\frac{h^2}{C_z^2}\right)^{1/(2-n)} \qquad (2)$$

where

Q = strength of source (gm/sec)

u = wind velocity

/h =

h = height of source above ground

C_y, C_z = the usual turbulence coefficients in Sutton's diffusion theory

n = a parameter which depends upon the stability of the atmosphere. Sutton suggests that with n = 0.25 equations (1) and (2) will give satisfactory results in conditions of small temperature gradient and moderate wind.

If we assume the source is raised to a height z above the top of the stack we should replace equation (1) by

$$X = \frac{A}{u(h + z)^2} \qquad (3)$$

where A ($= \frac{2Q}{e\pi} \frac{C_z}{C_y}$) is a parameter which is independent of stack design, of u and of h. It is intuitively obvious that z will decrease as u increases and it is convenient here to consider the effect of expressing z as a power of u. Suppose we put

$$z = \frac{B}{u^p} \qquad (4)$$

then X, which is already a maximum concentration with respect to distance from the stack, will be a function of u. It is easily seen that X has a maximum value with respect to u given by

$$X_{max} = \frac{A}{B^{1/p}} \quad \frac{1}{h^{2-1/p}} \quad \frac{(2p - 1)^{2-1/p}}{4p^2} \qquad (5)$$

when

$$u^p = \frac{B(2p - 1)}{h} \qquad (6)$$

$$z = \frac{h}{2p - 1} \qquad (7)$$

The distance at which this maximum concentration occurs would be of interest in a specific case but is not relevant to the general question of stack design.

3. Sutton's treatment of a heated elevated source

Sutton considers first a steady continuous point source of heat of strength Q_H (cal/sec) discharging into a completely calm atmosphere. The plume of course is vertical. He makes the following assumptions:-

(i) The potential temperature of the ambient atmosphere is uniform at all heights and the difference between the temperature in the plume and the ambient temperature is so small that density differences may be neglected.

(ii) There is no significant variation of density with height.

(iii) The rate of entrainment of ambient air into the jet (per unit area of the jet boundary surface) is proportional to the radius of the jet and the vertical gradient of the vertical velocity.

(iv) The radius of a (circular) cross-section of the jet at any height is proportional to a power of the height, i.e. $r = 1.5\ C_z^{m/2}$ where C is a generalized diffusion coefficient and m is unspecified at this stage.

Then by utilizing the principles of conservation of mass and of heat and equating the rate of dissipation of energy owing to turbulence to the rate of loss of potential energy as the air in the jet moves upwards Sutton obtains the following equation for the speed in the vertical plume

$$v = v_1\ z^{-m/6} \qquad (8)$$

/where

where

$$v_1^3 = \frac{7 Q_H g}{3 \pi c_p \rho T_a C} \qquad (9)$$

c_p is the specified heat of air, ρ the density of air and T_a the air temperature. By analogy with the rate of spread of a horizontal plume from a cold source in a steady wind Sutton then deduces that m = 1.75 so that

$$v = v_1 z^{-0.29} \qquad (10)$$

To apply these results to the practical case of a hot source emitting into a steady horizontal wind of speed u Sutton then assumes that, as a first approximation, the centre line of the plume will follow the trajectory of a particle subjected to a constant horizontal velocity u and a vertical velocity v which decays according to

$$v = v_1 s^{-1/3} \qquad (11)$$

s being the distance measured along the trajectory and the index - 1/3 being taken as an approximation to - 0.29 in order to obtain explicit equations for the trajectory. Sutton describes the trajectory by the equations

$$s = \left(\frac{v_1}{u}\right)^3 \cot^3 \psi \qquad (12)$$

$$z = \frac{3}{2}\left(\frac{v_1}{u}\right)^3 F \qquad (13)$$

$$F = \cot \psi \operatorname{cosec} \psi - \ln(\cot \psi + \operatorname{cosec} \psi) \qquad (14)$$

where ψ is the inclination of the trajectory to the horizontal. When ψ is small the plume is practically horizontal and Sutton suggests that z be computed by assuming $\psi = 10^\circ$ (this gives F = 30.3). We note that equation (13) has the same form as equation (4) and that in applying Sutton's treatment to equation (5) we put

$$B = \frac{3}{2} v_1^3 F \qquad p = 3 \qquad (15)$$

It is convenient to note here that the horizontal distance corresponding to equations (12) to (14) is given by

$$x = \left(\frac{v_1}{u}\right)^3 (\operatorname{cosec}^3 \psi + 2 - 3 \operatorname{cosec} \psi) \qquad (16)$$

4. The method of Bosanquet, Carey and Halton (2). These three authors have considered the rise of a plume of gas which emerges from the chimney stack with a temperature above that of the ambient air and with a definite issuing velocity. The detailed arguments by which they obtain their final formulae are not given in the published paper but are contained in a paper deposited in the library of the Institution of Mechanical Engineers. In brief their argument is as follows.

As the plume emerges (vertically) from the chimney it has a velocity relative to the ambient air. After emergence the ambient air mixes with the plume thereby reducing the excess temperature in the plume and also the relative velocity. The reduction of the excess temperature affects the buoyancy of the heated plume and so determines the upward motion of the gas. The governing factor is thus the rate of dilution of the plume by the ambient air. The authors attribute this dilution to three independent causes, viz. diffusion of air into the plume by eddy motion, longitudinal motion of the plume relative to the ambient air and transverse motion of the plume relative to the ambient air, and for each cause a "rate of inflow" of ambient air into the plume is calculated.

/From

From analogy with pipe flow and kinetic theory the authors assume that the diffusion coefficient which expresses the diffusion of air into the plume is given by $p \sigma u$ where p is an undetermined multiplier and σ is the r.m.s. distance of the particles in the plume above and below a horizontal plane through the axis. With the assumption of a conical distribution of gas density in a cross-section of the plume (the precise form of the density distribution does not seem to be important) it is then deduced that the effects of diffusion are equivalent to a radial inflow of air into the plume equal to 2.58 pu. From consideration of a paper by Heywood (3) the authors conclude that a reasonable value for p is 0.05 so that the radial inflow of air into the plume owing to eddy diffusion is 0.129u feet per second per square foot of surface where u is the wind speed in feet per second.

To deal with the effect of the motion of the plume relative to the air and parallel to the axis of the plume the authors appeal to laboratory results which show that when a jet of air issues from a cylindrical nozzle into stagnant air

(i) the jet spreads into a cone of semi-angle θ where $\tan \theta = 0.214$

(ii) the velocity distribution over all cross-sections is similar and approximates to the conical form

(iii) the mean velocity over a cross-section varies inversely as the cone radius.

From these laboratory results and with the assumption of constancy of momentum it is shown that the radial inflow into the plume is $0.107 \bar{V}$ where $\bar{V}$ is the mean relative velocity parallel to the axis over a cross-section of the plume.

The effect of the relative motion of the plume transverse to the axis is dealt with by considering the resistance to transverse motion of a solid cylinder of unit length. This is $\frac{1}{2} \rho V_T^2$ per unit projected area (ρ is the air density). If the solid cylinder is replaced by a cylinder of air the latter will experience the same resistance and will slow down but the decreasing velocity now results from the cylinder being diluted with ambient air which shares the original momentum of the cylinder. From these considerations the authors show that the radial inflow owing to transverse relative motion is $V_T/2\pi$.

Having obtained the rates of inflow arising from the three causes the total rate of inflow is assumed to be the root mean square of the sum. The rate of dilution of the plume by the ambient air is thus determined and thence it is a matter of mathematics to compute the rate of rise of the gas through the atmosphere.

The results obtained by Bosanquet, Carey and Halton are expressed in the following formulae.

Rise caused by exit velocity of stack gases

$$z_{max} = \left[\frac{4.77}{1 + 0.43\frac{u}{V}}\right] \left[\frac{\sqrt{Q_g V}}{u}\right] \qquad (17)$$

$$z = z_{max} \left(1 - 0.8 \frac{z_{max}}{x}\right) \text{ when } x > 2z_{max} \qquad (18)$$

Rise caused by density difference between stack gases and atmosphere

$$x = 3.57 \sqrt{\frac{Q_g V}{u}} X \qquad (19)$$

$$z = 6.37 g \frac{Q_g \Delta}{u^3 T_1} Z \qquad (20)$$

provided $u^2 > \frac{\Delta g}{T_1} \sqrt{\frac{Q_g}{V}}$ and where X and Z are related by the curve given in figure 2.

/Maximum

Maximum rise of plume above stack exit

The plume reaches a maximum height when its density becomes equal to that of the surrounding atmosphere and when the potential atmospheric temperature gradient is positive. The maximum rise owing to the exit velocity is given by equation (17). The maximum rise owing to density difference between the issuing gas and the atmosphere is given by

$$z_{max} = 6.37 g \frac{Q_g \Delta}{u^3 T_1} (\ln J^2 + \frac{2}{J} - 2) \qquad (21)$$

where

$$J = \frac{u^2}{\sqrt{Q_g g v}} \left[0.43 \sqrt{\frac{T_1}{gG}} - 0.28 \frac{v}{g} \frac{T_1}{\Delta} \right] + 1 \qquad (22)$$

In these formulae

Q_g = rate of exit of gas from stack in $ft^3 sec^{-1}$, the gas being assumed to have a temperature at which its density equals atmospheric density

v = actual gas velocity at stack exit ($ft\ sec^{-1}$)

T_1 = temperature at which density of flue gases equals that of the atmosphere (^oC abs.)

Δ = temperature difference between actual flue gas temperature and T_1 (^oC)

G = gradient of potential atmospheric temperature ($^oC\ ft^{-1}$).

5. The Oak Ridge formula. This is a purely empirical formula derived from observations of the height at which the plumes from three different stacks at Oak Ridge (Tennessee, U.S.A.) became horizontal. The formula arose from a suggestion that $uz = 1.5vd$ for each stack (u = wind speed (m.p.h.), z = height above stack exit (ft), v = stack gas exit velocity (m.p.h.) and d = stack diameter (ft)). On test it became clear that this simple formula is inadequate and, in fact, it contains no reference to the temperature of the issuing gas. The authors of the report then plotted ($uz - 1.5vd$) against Q_H and obtained the curve shown in figure 1. From this figure it is clear that a reasonably accurate approximation is given by

$$uz = 1.5vd + 3 \times 10^{-4} Q_H \qquad (23)$$

It is to be noted that the X-10P point is based upon 11 observations, the X-10SP point upon 34 observations and the WBSP point upon 93 observations. The Oak Ridge report also states that in lapse conditions uz is larger than indicated by equation (23) by 10 to 20% and smaller by a similar amount in inversion conditions. If the variables in equation (23) are measured in c.g.s. units (Q_H in cal/sec) the equation becomes

$$uz = 1.5vd + 0.4\ Q_H \qquad (24)$$

It will be noted that this equation is equivalent to equation (4) if we put

$$B = 1.5vd + 0.4\ Q_H \qquad p = 1 \qquad (25)$$

6. Comparison of the three formulae for rise of plume. Comparison of the three formulae for z is not quite straightforward since they do not contain the same parameters. Sutton's formula takes no account separately of the stack diameter, the gas temperature or the exit velocity from the stack though a combination of these three is implicit in the use of Q_H. The formula of Bosanquet et al. takes account of almost every physical variable which can affect the problem and, as a result, is somewhat cumbersome. It does not

/contain

contain Q_H explicitly but if the effluent has the physical properties of air it is clear that

$$Q_H = Q_g \rho c_p \Delta = \frac{\pi}{4} d^2 v \frac{T_1}{T_1 + \Delta} \rho c_p \Delta \qquad (26)$$

The Oak Ridge formula ignores gas temperature except insofar as it is implicit in Q_H.

In order to compare the three formulae z has been calculated for four different values of Q_H and three different values of u by each method. It was necessary to make certain assumptions about the emission. These were

(i) The exit velocity from the stack is 50 ft/sec

(ii) The effluent has the physical properties of air

(iii) The ambient and effluent temperatures are 288°A and 423°A respectively.

The rise of plume (z) computed by the three methods is given in table 1. The stack diameter d tabulated results from the assumptions listed above and equation (26).

The outstanding feature of this table is the great disparity between the values predicted by the three formulae. It must be borne in mind however that our primary interest is not in the rise of the plume but in the maximum gas concentration at ground level.

7. The maximum gas concentration at ground level. We have seen that there is an easy method of computing X_{max} if z can be represented by an equation similar to equation (4) and that in fact Sutton's formula and the Oak Ridge formula are of this form. Accordingly the total (buoyancy plus velocity) rise by the formula of Bosanquet et al. was computed for four sets of "stack conditions" and various values of u. This total rise has been plotted logarithmically against u (foot second units were employed as in the original formula) in figure 3. It is apparent that over the range u = 5 to 40 ft/sec for $Q_H = 10^5$ and over the range u = 20 to 150 ft/sec for $Q_H = 10^8$ can be represented by an equation similar to equation (4). It is necessary for the present argument that the critical velocity (equation (6)) shall fall within the range of u for which the power law for z is assumed. The conditions assumed in computing figure 3, the deduced values of B, p and d (c.g.s. units) and of the critical velocity (ft/sec) for a stack height of 100m are as follows.

In each case $T_1 = 288°C$ $\Delta = 135°C$

Q_H (cal/sec)	10^5	10^5	10^8	10^5
G (°C/1,000ft)	1	1	1	5
w (m/sec)	15.25	5.0	15.25	15.25
B (c.g.s.)	5.5×10^7	6.0×10^8	3.6×10^{10}	3.3×10^7
p	1.75	2.18	2.0	1.69
d (metres)	0.55	0.97	17.5	0.55
crit. vel. (ft/sec)	7.6	8.9	10.7	6.6

With z represented by equation (4) for all three formulae we now have a ready means of comparing the predicted maximum concentrations at ground level. When using Sutton's formula we put $c_p = 0.25$, $\rho = 1{\cdot}2\times10^{-3}$, $T_a = 288$ and $C = 0.3$ in equation (9) and equation (13) (with $F = 30.3$) then gives $z = 1{\cdot}28\times10^6 Q_H/u^3$. For the Oak Ridge formula we use $z = (1.5vd + 0.4Q_H)/u$.

/If

Table 1

Rise of plume predicted by the three formulae

Strength of heat source Q_H cal/sec		2.5×10^6			5×10^6			2.5×10^7			5×10^7		
Power station capacity M.W. (approx)		50			100			500			1,000		
Stack diameter (ft)		9.1			12.8			28.7			40.5		
Wind speed m.p.h.		6.7	10	13.3	6.7	10	13.3	6.7	10	13.3	6.7	10	13.3
Rise of plume (ft) by Sutton's formula (To 10° inclination)		3,700	1,100	460	7,400	2,200	920	37,000	11,000	4,600	74,000	22,000	9,200
Rise of plume (ft) according to Bosanquet et al. $G = 1^oC/1,000$ ft	Buoyancy	730	310	160	1,190	540	300	3,340	1,750	1,000	4,470	2,820	1,680
	Velocity	150	95	70	210	135	99	470	300	220	667	426	312
Rise of plume (ft) according to Bosanquet et al. $G = 0.5^oC/1,000$ ft)	Buoyancy	-	-	-	-	-	-	4,420	2,120	1,180	6,700	3,550	2,020
Rise of plume (ft) by Oak Ridge formula	Buoyancy	113	75	57	230	150	113	1,125	750	570	2,250	1,500	1,130
	Velocity	68	45	34	96	64	48	214	143	108	302	203	152

If we use X_G, X_B and X_R to denote the maximum concentrations at ground level according to Sutton, Bosanquet et al. and Oak Ridge respectively then table 2 gives the ratio X_R/X_S for a variety of conditions. Table 3 gives the values of X_S/A and X_B/A for various conditions, this different form of presentation being preferred in order to emphasize some of the conditions attached to the calculations.

Table 2
Ratio X_R/X_S

v	d	h	Q_H (cal/sec)			
m/sec	m	m	10^8	10^7	10^6	10^5
5	5	50	0.23	0.97	2.57	2.22
	10		0.23	0.90	1.73	1.17
15	5		0.22	0.83	1.30	0.79
	10		0.22	0.68	0.75	0.40
45	5		0.21	0.58	0.53	0.27
	10		0.20	0.40	0.28	0.13
5	5	100	0.36	1.54	4.06	3.51
	10		0.36	1.42	2.74	1.84
15	5		0.35	1.31	2.06	1.25
	10		0.35	1.08	1.18	0.63
45	5		0.33	0.91	0.83	0.43
	10		0.31	0.63	0.44	0.22
5	5	200	0.57	2.46	6.44	5.57
	10		0.57	2.26	4.34	2.92
15	5		0.56	2.09	3.28	1.98
	10		0.55	1.72	1.88	1.01
45	5		0.53	1.45	1.32	0.67
	10		0.49	1.00	0.70	0.34

Table 3
Values of $10^{13}X_B/A$ and $10^{13}X_S/A$

G	v	d	h	Q_H (cal/sec)			
				10^8		10^5	
°C/1,000ft	m/sec	m	m	$10^{13}X_B/A$	$10^{13}X_S/A$	$10^{13}X_B/A$	$10^{13}X_S/A$
1	5	0.97	50	-	-	640	556
1	15.2	0.55	50	-	-	585	556
1	15.2	17.5	50	48.5	55.6	-	-
5	15.2	0.55	50	-	-	644	556
1	5	0.97	100	-	-	219	176
1	15.2	0.55	100	-	-	222	176
1	15.2	17.5	100	17.2	17.6	-	-
5	15.2	0.55	100	-	-	243	176
1	5	0.97	200	-	-	75.1	55.6
1	15.2	0.55	200	-	-	82.6	55.6
1	15.2	17.5	200	6.1	5.56	-	-
5	15.2	0.55	200	-	-	92.4	55.6

Table 2 shows that X_R and X_S differ by a factor exceeding 3 in only 17 out of 72 cases. To simplify discussion let us assume temporarily that X_S is "correct". Then we see that, broadly, X_R underestimates X_{max} with either very large values of Q_H or very large values of v. Now when Q_H is very large X_{max} will normally be small and the underestimation is perhaps unimportant. The largest value of v dealt with in table 2 is probably unrealistic and we need not pay undue attention to the ratios for v = 45m/sec. We have not so far considered whether the critical wind velocities corresponding to X_R and X_S in table 2 are within

/normal

normal experience. If the cases for $Q_H = 10^8$ or v = 45m/sec are excluded the greatest value of B by the Oak Ridge formula is $6{\cdot}25 \times 10^6$. For a stack 50m high this would lead to a critical wind speed of 12.5 m/sec - a value well within common meteorological experience. According to Sutton's formula $B = 1{\cdot}28 \times 10^6 Q_H$. Putting $Q_H = 10^7$ cal/sec and h = 50 metres leads to a critical wind speed of 23.3 m/sec. This is rather high but is not outside experience. The critical wind speed is lower for taller stacks or smaller values for Q_H of course.

Turning now to table 3 the only worthwhile comment seems to be one of surprise that two such dissimilar formulae should give such concordant results.

8. Conclusion. In making a selection between the three methods of computing X_{max} from a hot source the following considerations seem relevant

(i) Sutton's formula for computing concentration (equation (1)) is based upon a great deal of experimental field work. His formula for the rise of a heated plume (equation (13)) is admittedly only a first approximation and has not been compared with full scale observations (but see appendix).

(ii) The formula of Bosanquet et al. (equations (21) and (22)) has given reasonable agreement with some full scale observations. The deviation however is partly dependent upon laboratory observations of the flow from a cylindrical nozzle and the resistance of a circular cylinder in a moving fluid.

(iii) The Oak Ridge formula for the rise of the plume is empirical and expresses the result of a number of full scale observations.

(iv) The differences between the results given by the three formulae are small compared with the uncertainty and variability of the effects of specified concentrations of gas on a human being. In those conditions in which the discrepancy is largest and the concentration itself is also large the Oak Ridge formula generally gives the highest value. In view of these considerations, it is recommended that the Oak Ridge formula, combined with Sutton's equation (1), be employed for computing the maximum concentration likely to be experienced at ground level from a heated elevated source. If the discrepancy between X_R and X_S for large values of Q_H is considered important the three formulae could be brought more into line by increasing the coefficient of Q_H in equation (24) to, say, 0.8. This would have little effect on table 2 at the small values of Q_H but would improve the agreement at large values. Such an "adjustment" could be regarded only as a matter of expediency however.

/Table 4

Table 4

Rise of plume (ft) at various distances from stack as observed (z) and as predicted by Bosanquet et al. (z_B) and by Sutton (z_S)

Distance from stack (feet)

Test No.	u ft/sec		100	150	200	300	400	600	800
	Plant No. 1 Q_g = 1,000 ft^3/sec v = 31ft/sec Δ = 180°C Q_H = 1·53x10^6 cal/sec								
1	14	z	60		99		156	186	
2		z_B	77		122		176	210	
		z_S	79		131		198	265	
2	33	z	29		35		52	70	84
		z_B	22.2		27.4		32.2	35.1	37.2
		z_S	35		59		90	118	143
3	26.5	z	28		40		63	80	101
		z_B	30.6		39.8		48.9	54.3	58.6
		z_S	42		69		110	147	177
4	19	z	55		75		121	165	200
		z_B	49.9		71.9		95.2	109.4	119.3
		z_S	58		94		150	199	243
	Plant No.2 Q_g = 341 ft^3/sec v = 28ft/sec Δ = 25°C Q_H = 7·24x10^4 cal/sec								
1	10	z	46	53	58	67			
		z_B	34.6	41.9	46.3	52.3			
		z_S	41	54	66	87			
2	13.3	z	36	38	41	47			
		z_B	26.4	30	32.3	35.2			
		z_S	31	41	51	66			
	Plant No. 3 Q_g = 1,245 ft^3/sec v = 35.5 ft/sec Δ = 149°C Q_H = 1·58x10^6 cal/sec								
1	20.4	z	46		66	82	92	103	
		z_B	45.0		64.9	76.9	85.4	97.7	
		z_S	54		88	117	143	190	

/Appendix

Appendix

In the appendix to their paper Bosanquet et al. quote the rise of the plume at various distances from the stacks of four different plants and with various wind speeds. They compare these observed rises with the rise predicted by their formula. Particulars of eight such tests are given. The rise of the plume referred to here is not the rise with which we have been concerned above since all the measurements were made so close to the stack that even at the greatest distance the height of the plume was still obviously increasing. The characteristics quoted for the plants are, naturally, those used in the theoretical part of their paper. In seven of the eight cases however T_1, the temperature at which the density of the flue gases equals that of the atmosphere, is given as 283°A. This is so near to normal atmospheric temperature that it seemed justifiable to regard the effluent as air with temperature $(283 + \Delta)$°A discharging into an atmosphere at temperature 283°A. Another parameter quoted for the tests was Q_g, the volume rate of discharge at atmospheric density (in cubic feet per second). Assuming air density to be 1.2gm/cm^3 and the specific heat to be 0.25 cal/gm we then get

$$Q_H = 8.5\, Q_g\, \Delta \text{ cal/sec}$$

for the strength of heat source above atmospheric temperature. We now have the necessary data with which to compare Sutton's formula for rise of plume with the observations quoted by Bosanquet et al. From equations(13) and (16) we have

$$\frac{x}{z} = \frac{2}{3}\,\frac{(\operatorname{cosec}^3\psi + 2 - 3\operatorname{cosec}\psi)}{[\cot\psi\ \operatorname{cosec}\psi - \ln(\cot\psi + \operatorname{cosec}\psi)]}$$

This ratio is a function only of ψ. The ratio xu^3/v_1^3 is also a function only of ψ. These two ratios were computed for various values of ψ and a subsidiary curve of x/z against xu^3/v_1^3 plotted.

If in equation (9) we substitute $g = 32$, $c_p = 0.25$, $\rho = 1{\cdot}2\times10^{-3}$, $T_a = 283$ and $C = 0.3$ we obtain

$$v_1^3 = 2.86 \times 10^4\, Q_H$$

Since the values of u are quoted in each test we can thus compute xu^3/v_1^3 for any specified distance, read off x/z from the subsidiary curve, and hence compute z. In table 4 the observed rise of plume above the stack exit is denoted by z, the total rise predicted by Bosanquet et al. by z_B and the rise computed as indicated above by z_S. The paper by Bosanquet et al. does not say how the rise of plume was measured but some of the values of z are so small that one may expect the error of measurement to have been, sometimes, a significant fraction of z. For this reason it has seemed preferable to tabulate z, z_B and z_S rather than ratios. It is clear that z_S is invariably greater than either z or z_B though in view of the need for estimating some of the quantities the agreement between z and z_S may be regarded as reasonably satisfactory. On the average z_S exceeds z by a factor of about 1.4.

References

1. Sutton, O.G. 1953. "Micrometeorology" McGraw Hill Book Company.

2. Bosanquet, C.H., Carey, W.F. and Halton, E.M. 1950. Proc. Inst. Mech. Eng., 162, 355.

3. Heywood, G.P. 1931. Quart. J.R. Met. Soc., 57, 433.

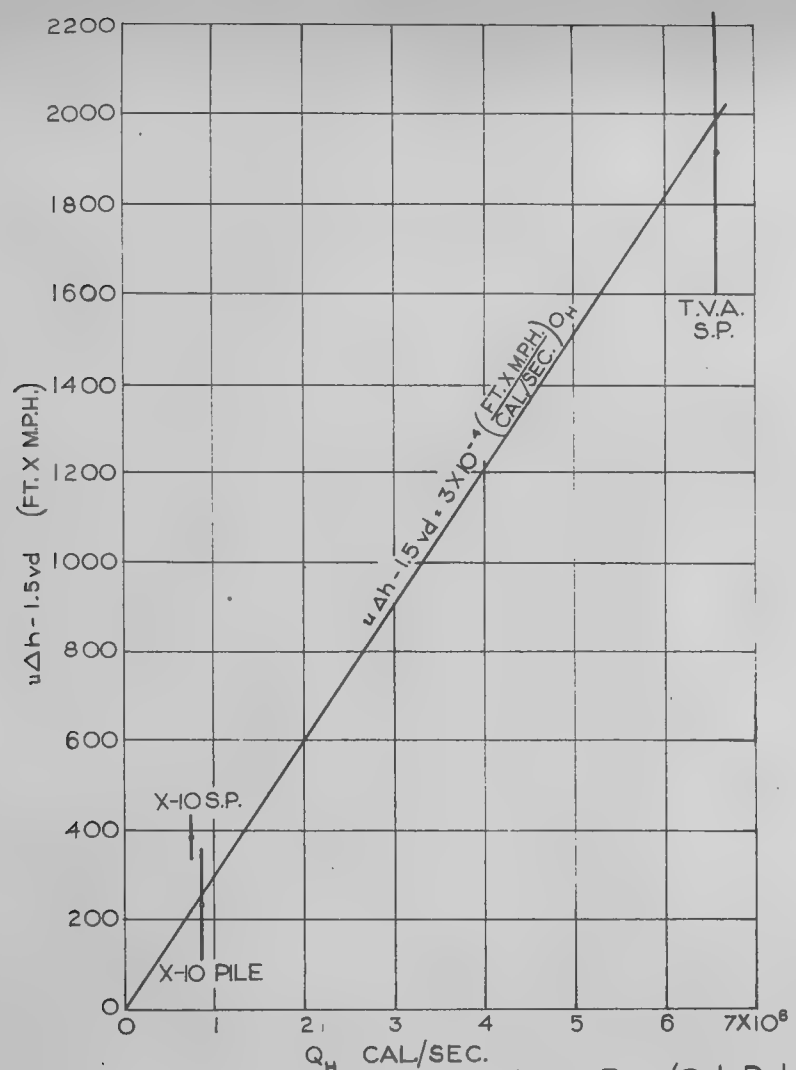

Fig.1 Thermal Component of Plume Rise (Oak Ridge)

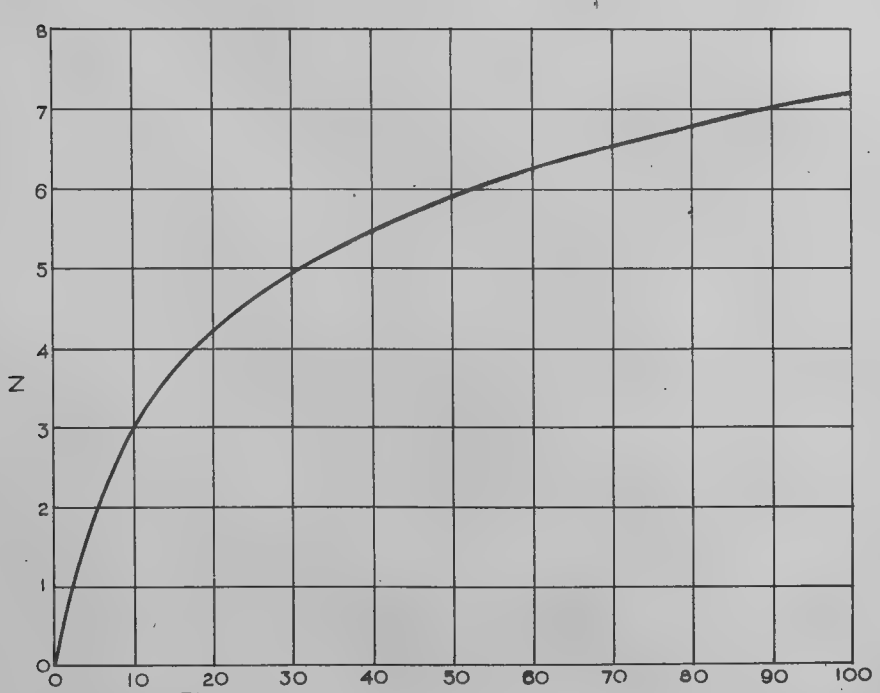

Fig. 2. Thermal Rise of a Plume

Showing relation between X and Z.

$x = 3{\cdot}57 \frac{\sqrt{Q_H v}}{u} X$ and $z = 6{\cdot}37 g \frac{Q_H}{u^3 T_1} Z$

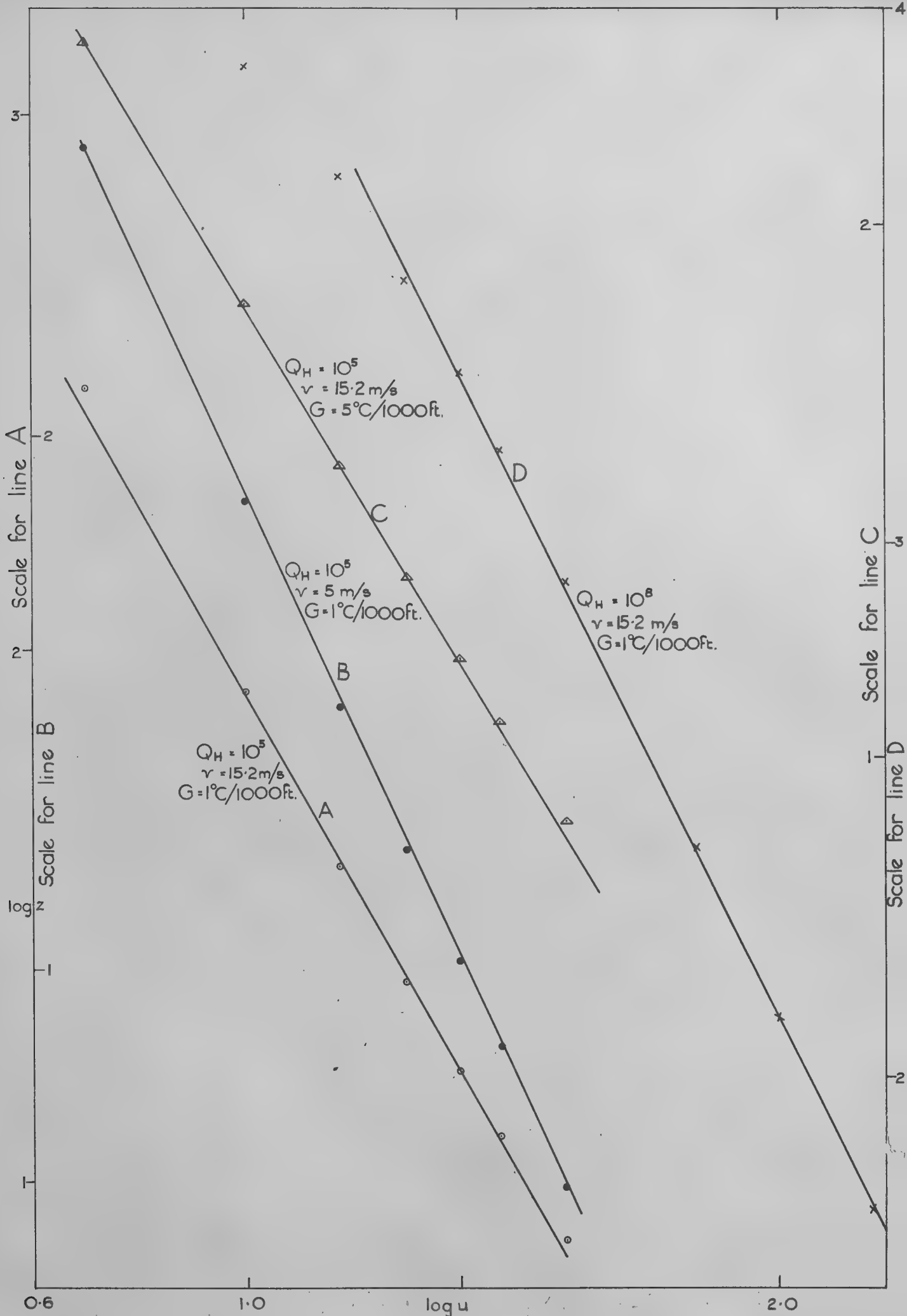

Fig.3. Rise of a plume according to Bosanquet et al as a power of wind speed.

Control Number C.D. 8033

this paper should refer to it
er of the Meteorological Research
Committee (London).
M.R.P. No. 883 by Mr. N. E. Rider
A copy is available in the Library of
the Meteorological Office."

MATS

A note on an instrument [illegible]

Introduction

[illegible] acted strength, are stuck in
[illegible] bulbs are filed to be

At the time of issue this report has not been published. Any author desiring to quote this paper should refer to it as "A paper of the Meteorological Research Committee (London).
M.R.P. No. 883 by Mr. N. E. Rider
A copy is available in the Library of the Meteorological Office."

M.R.P. 883
S.C.I./93
27th October, 1954.

MATS

AIR MINISTRY
METEOROLOGICAL RESEARCH COMMITTEE

A note on an instrument for the continuous recording of soil temperatures

by
N.E. Rider (Meteorological Office)

Introduction

The need arose at Cambridge to record soil temperatures at a number of depths below various crop surfaces. Previously such records have been obtained by using mercury in steel thermographs (see e.g. Hutchings 1952), platinum resistance thermometers (see e.g. Johnson and Davies 1927) and single thermojunctions working in conjunction with photographic galvanometer recorders (see e.g. de Villiers 1951). In siting these instruments, considerable quantities of soil have to be removed and replaced and any vegetation cover is at least severely damaged. The instrument to be described depends upon the thermo-electric principle and is a development of that used by Pasquill (1949) and others in heat balance observations for which the indications of a sensitive eye reading galvanometer at relatively infrequent intervals were sufficient. It is simple to construct, requires a minimum of attention when in operation, does not disturb the soil cover to any great extent on siting, and provides an immediately visible record at a convenient distance from the site. No power supplies other than one six volt accumulator are required.

General Construction

The thermometer as constructed enables temperatures at five depths namely, 1, 5, 10, 20 and 40 cm. to be recorded to 0.1°F over a range of approximately 60°F when working with the recording galvanometer to be described. A view of the thermometer, together with certain constructional details, is shown in Fig. 1. It consists of a Tufnol tube $1\frac{1}{2}$ in. outside diameter and $\frac{3}{4}$ in. inside diameter which is closed at one end by a brass spike and at the other by a brass cap. Copper plugs which form the thermometer bulbs are inserted through the wall of the Tufnol tube at appropriate intervals along its length and, at each depth, three bulbs are inserted 120° apart around the tube. Thus three complete sets of bulbs are provided, S_1, S_2 and S_3 of Fig. 2 which shows a schematic wiring diagram. Each set has a reference junction (R_1, R_2 and R_3, Fig.2) which is normally kept in melting ice contained in a vacuum flask. The thermojunctions are made from enamelled 28 s.w.g. constantan and 32 s.w.g. copper wire. Each bulb has a hole drilled through its centre into which a pair of the wires is soldered, each thermojunction pair being made up of the same lengths of wire and covered with P.V.C. sleeving. The bulbs are tight push fits in the Tufnol and, to give added strength, are stuck in position with Araldite D. After insertion the bulbs are filed to be flush with the wall of the tube and the instrument is covered with a coating of Araldite to insulate the copper bulbs and render the whole watertight. The thermocouple leads are brought up the centre of the tube and leave near its upper end by way of three short brass side tubes which are screwed into the Tufnol wall, the wires from one set of bulbs leaving by each tube.

/They

294

They are terminated in junction boxes where they are joined by those from the reference junctions. Between the thermometer and the junction boxes the leads are protected by P.V.C. sleeving which fits tightly over the brass side tubes at one end and over the junction boxes at the other. At these boxes the constantan leads of each of the three sets, together with that from the appropriate reference junction, are soldered together. Any excess lengths of lead are contained in these boxes. A six core cable with single 22 s.w.g. copper conductors leaves each of the three junction boxes and leads to the recorder. As constructed at Cambridge, the cables are 100 yd. long.

An Elliot six circuit, six colour recording galvanometer having a coil resistance of 35 ohms and a full scale deflection for 40 microamps is used. This recorder, as supplied by the makers, has a double pole six position rotary switch for circuit selection which is operated by an electromagnet which also actuates the colour changing mechanism. The switching interval is 2 min. and is regulated by a clock attached to the instrument. A 6 volt D.C. supply is required.

The eighteen copper leads from the thermometer are brought to a board near the recorder on which are mounted six P.O. type 3000 relays (100 ohm, 6 volt operating), the M's of Fig. 2. Each has two platinum contact pairs which are made on energising the relay. In Fig. 2 only five relays are shown, the sixth being used to provide a zero position on the galvanometer chart. They are energised in the required sequence by applying current through one side of the rotary switch in the recorder, the recorder wiring being modified for this purpose. The other side of the switch, I of Fig. 2, is used as indicated in that figure. The back e.m.f. produced on switching the relays is suppressed by the use of a condenser and resistance circuit across each relay coil and arcing at the rotary switch is avoided. Thus at each depth at which a temperature record is required, we have in effect a thermopile having three "hot" and three "cold" junctions. The output from a single thermocouple pair is insufficient to provide the necessary current to give a reasonably open scale of temperature on the recorder chart, unless the galvanometer employed has a much higher current sensitivity or D.C. amplifiers are available. The use of a more sensitive galvanometer would entail photographic recording which is never convenient on a field site and the use of D.C. amplifiers leads to well known complications.

The apparatus provides a record of the temperature at each of the five depths once in 12 min. and there is no possibility of the recording mechanism becoming out of step with the relays. Soil temperatures below freezing point can be recorded by moving the zero position of the galvanometer, which represents 32°F, and when such conditions are anticipated the galvanometer zero is set some way up the chart.

Calibration

The thermometer and its associated recorder are calibrated as a single unit. The calibration is conducted in the normal way by the use of stirred water baths. After reasonable care in construction the calibration factor is found to be the same for the circuits at all depths. However, calibration shows an increase in deflection per degree with increase in temperature, the increase amounting to a change of 4 per cent. over the temperature range 30°F to 90°F. The overall resistance of a circuit for one depth, including the galvanometer and 100 yd. of cable, is approximately 95 ohms, and one scale division of the chart represents approximately 1.4°F. No change in the calibration factor could be detected as a result of heating by the relay operating coils, the relays being mounted so that any heat generated would have the minimum effect on the contacts.

Field Use

The thermometer is driven into the soil and the cables are led away to a portable hut which houses the recorder and accumulator. The only attention

/required

required is a replenishment of the ice flask every second day in average summer conditions (lat. 52°N). One 6 volt 65 amp. hr. accumulator will operate the apparatus for one week on a single charge. Three sets of this apparatus have been exposed at Cambridge for eight months and no faults have developed in the thermometers; such loss of record that has occurred has been the result of minor mechanical faults in the recorders. In future it would be more convenient to use one cable with sufficient conductors together with one junction box in place of the three of each at present employed.

Fig. 3 shows a tracing of the record produced by the instrument on 10th May, 1954. In the original, each trace is in a distinctive colour and is much easier to identify than the black and white tracing indicates.

References

Hutchings, J.W. 1952 Proc. 7th Pacific Science Congress, Christchurch, 3.

Johnson, N.K. and Davies, E.L. 1927 Q.J. Roy. Met. Soc., 53, 221, p.45.

Pasquill, F. 1949 Proc. Roy. Soc., A 198, p.116.

de Villiers, C.D.B. 1951 Pretoria, Dept. Agr. Sci. Bull., No. 309.

G.419215/EF/10/54/40

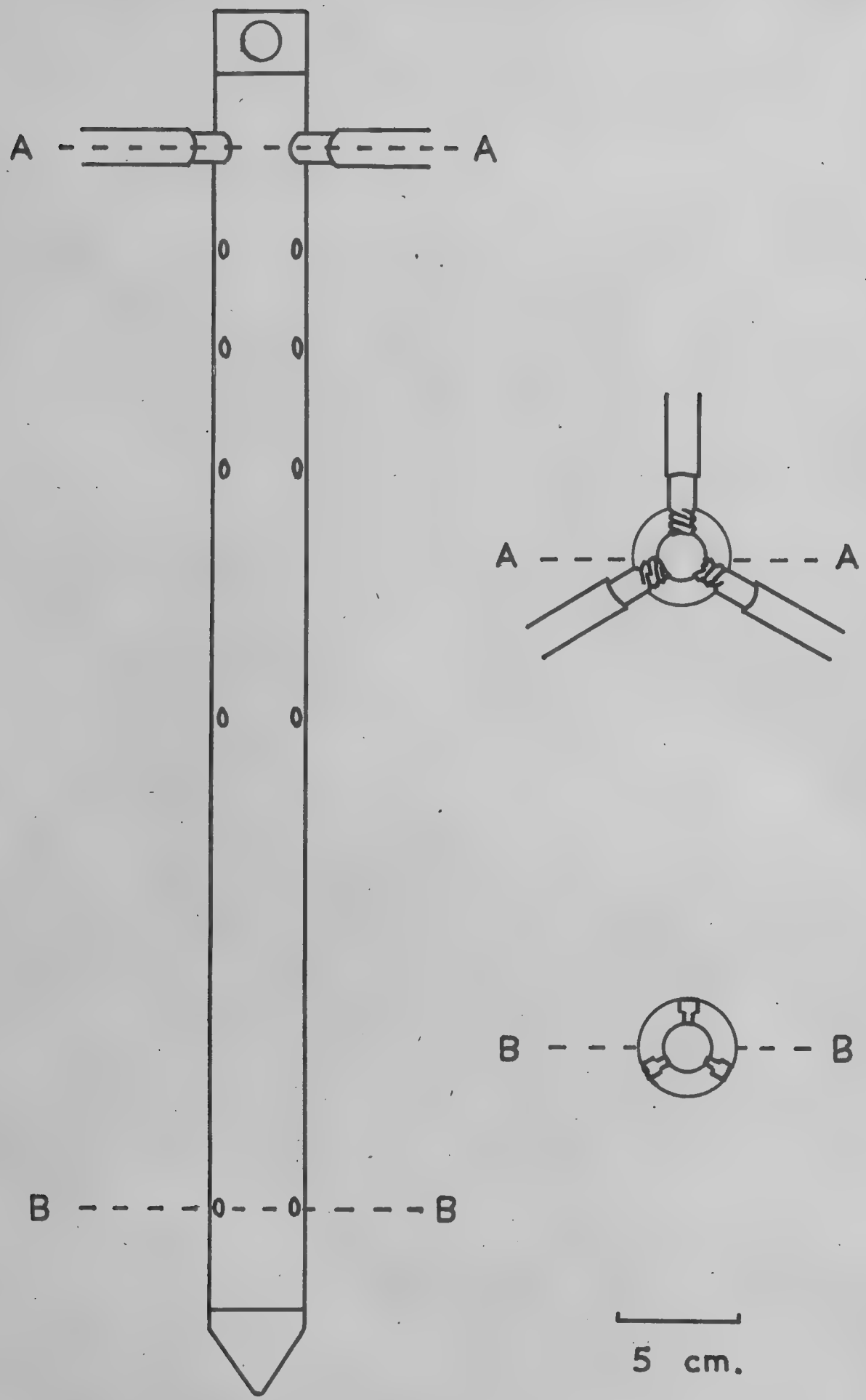

fig 1. General constructional arrangement of Thermometer.

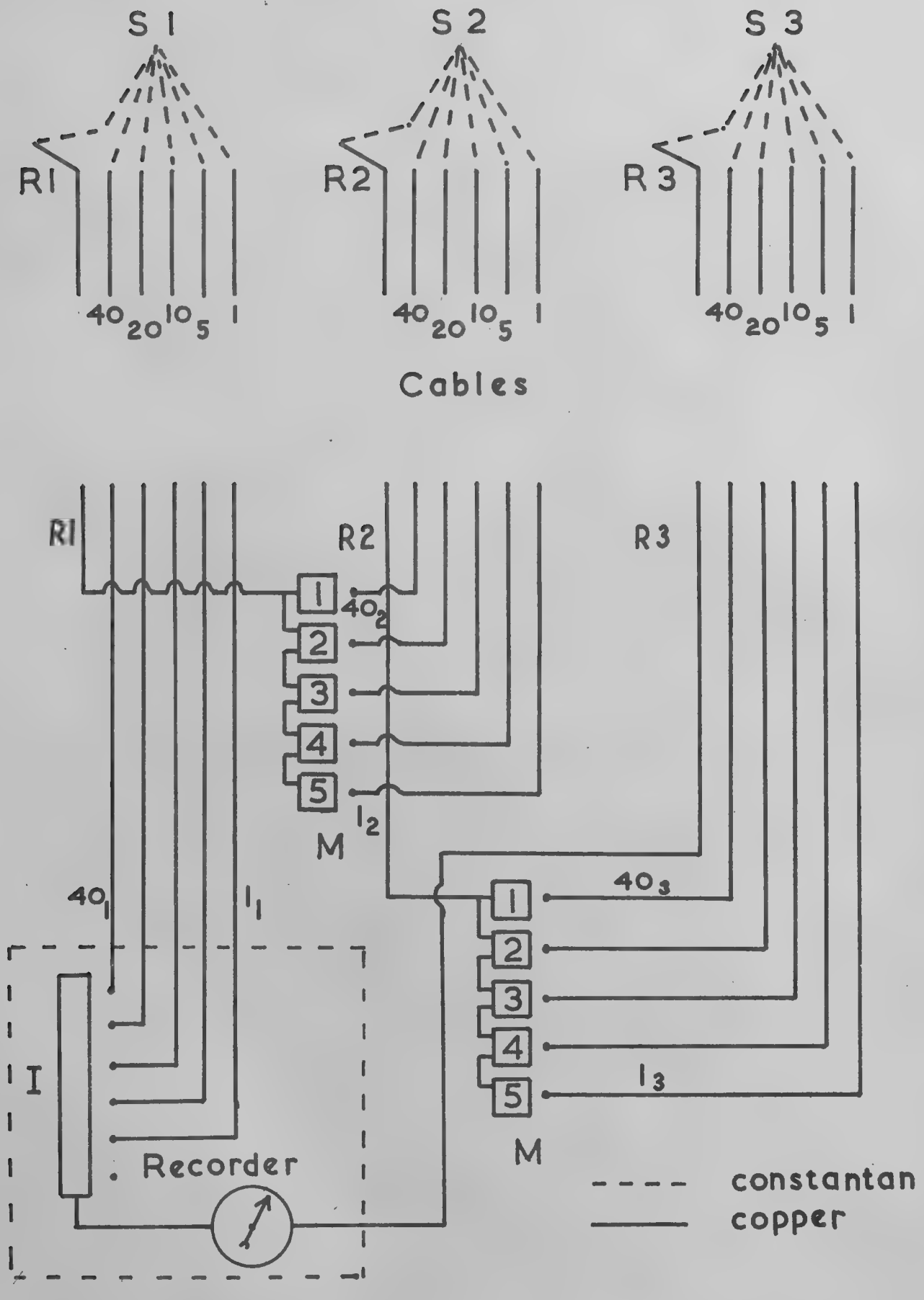

fig 2. Schematic wiring diagram of Thermometer and recording circuits.

fig 3. Tracing of temperature record under bare soil on May 10th., 1954.

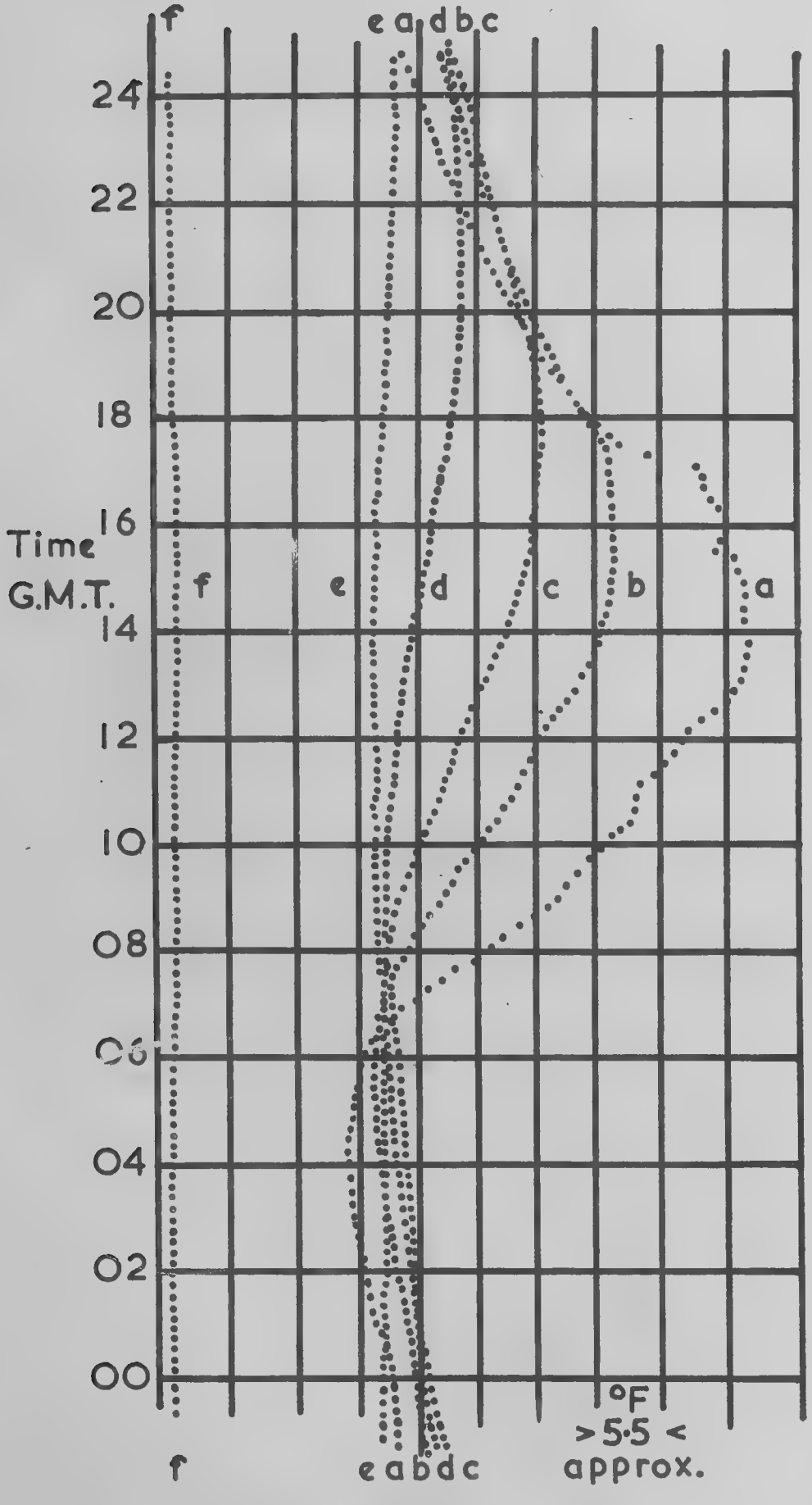

Trace a 1 cm. depth. Trace d 20 cm. depth.

" b 5 " " " e 40 " "

" c 10 " " " f zero line (32°F)

MRP's 888, 889, 894, 895, 896

At the time of issue this report has not been published. Any author desiring to quote this paper should refer to it as "A paper of the Meteorological Research Committee (London). M.R.P. No. 888 by Mr. D.H. Johnson. A copy is available in the Library of the Meteorological Office."

M.R.P. 888
S.C.I/94
S.C.II/179
12th November, 1954

AD 71765

AIR MINISTRY

METEOROLOGICAL RESEARCH COMMITTEE

Diurnal and interdiurnal variations of the measured heights of pressure surfaces

by
D.H. Johnson (Meteorological Office)

1. Introduction

It is well known that there are systematic diurnal changes, which vary with the season and become increasingly important with height, in the measured heights of pressure surfaces. At 100 mb, the diurnal variations may be up to four times as great as the average 12 hr synoptic change, and together with the random errors of measurement they have the effect of completely masking the 12 hr contour height tendencies. The random errors are partially smoothed out in the process of chart construction. To eliminate diurnal effects, the analysts either have applied approximate seasonal corrections based on experience or have considered 24 hr height tendencies only. In order to provide a basis for strict comparison with each other of heights measured at different synoptic hours, the diurnal variations appropriate to all times of the year have been computed for Larkhill (51°12'N, 1°48'W), Lerwick (60°8'N, 1°11'W), Malta (35°50'N, 14°27'E) and Nicosia (35°9'N, 33°17'E).

There has been much speculation in the past as to whether the observed diurnal changes genuinely occur in the atmosphere. Recent work by Scrase (1) leads to the conclusion that the observed variations are largely false, being due to the effect of solar radiation on the thermometer element of the radiosonde rather than on the atmosphere itself. The synoptician, however, does not need to discriminate between the real and the spurious, provided that the variations occur, as the evidence suggests they do, on the scale of tides rather than on the synoptic scale. In either case he wishes to eliminate them in order to see clearly the synoptic changes.

2. The observed variations

Upper air charts are constructed for the hours, 0300 GMT, 0900 GMT, 1500 GMT and 2100 GMT and it is customary to think of the plotted observations as referring to those times. In fact, the British ascents normally start within a few minutes of 0200 GMT, 0800 GMT, etc., and they reach the 100 mb level about 40 minutes later. Lerwick ascents are exceptional in that they normally commence at 0145 GMT, 0745 GMT, etc. Conventionally the 6 hr variations will be referred to as the 0900-0300 GMT, etc. variations, even though the actual measurements are made during the hour or so preceding 0300 GMT, 0900 GMT, etc.

The diurnal changes have been computed for the standard pressure levels: 700 mb, 500 mb, 300 mb, 200 mb and 100 mb. For Larkhill and Lerwick four-year monthly mean 6 hr variations of contour height have been calculated for the years 1948-51, and five-year monthly mean 12 hr variations have been calculated for 1948-52. The Upper Air Climatology Branch of the Meteorological Office supplied monthly totals of contour heights, for individual hours, which had been obtained by Hollerith punched card methods. These totals were used in calculating the variations at levels up to 200 mb. The 100 mb monthly mean variations were computed from chosen occasions, when 100 mb heights were given

/in

in the Daily Aerological Record at the appropriate times t and t + 6 hr or t and t + 12 hr on the same day. Apparent anomalies in the Hollerith tables were checked by reference to individual observations given in the D.A.R. and to the Upper Air Forecaster's working charts.

Upper air observations are made regularly at Malta and Nicosia at 0300 GMT and at 1500 GMT, and for these stations, only the 12 hr 1500-0300 GMT variations could be computed. These refer to the years 1948-51 in the case of Malta and 1948-52 for Nicosia. Hollerith totals were again used except for those months when less than 25 observations were made at either hour. In these latter months recourse was made to the pairing procedure described above, the individual observations being obtained from the Overseas Supplement to the Daily Weather Report or from tabulations supplied by the Upper Air Climatology Branch.

All the computed 6 hr and 12 hr variations in the measured contour heights are contained in Tables 1 and 2.

3. Smoothed values

The observed diurnal variations contain "errors" due to real random synoptic variations and due to random errors of measurement of the contour heights. The effect of these "errors" can be seen in the graphs of the annual march of the diurnal variations contained in Figures 1 and 2. These graphs, while showing clear trends, are irregular, but there is no reason to suppose that an accurate graph of the seasonal variation would not be quite smooth. Where the curve forms are approximately sinusoidal, smoothing by fitting one or two harmonics is feasible. In some cases, however, the curves are not nearly sinusoidal and it is necessary to investigate the forms which the seasonal variations should take, theoretically.

F.J. Scrase has given a method (1) by which the radiation and lag errors of the Meteorological Office radio-sonde can be estimated. Scrase's calculations suggest that a large part of the observed diurnal variation of temperature can be accounted for in terms of radiation error. Integration of these estimated temperature errors can therefore be expected to provide a good indication of the form which the annual march of the observed diurnal variation of contour height takes.

Table V of M.R.P.836 (1) gives the calculated radiation errors at a number of heights for five solar altitudes from 10° to 90°. Interpolation within this table is not sufficiently accurate for present purposes, so the radiation errors have been calculated afresh from data given in Figure 2 and Table III of M.R.P.836, at one degree intervals over the range from -5° to 0° solar altitude, at five degree intervals from 0° to 40° solar altitude and at ten degree intervals from 40° to 70° solar altitude. It was necessary to extrapolate slightly certain of the curves given in Scrase's Figure 2 in order to obtain rates of absorption of radiation, by the thermometer element and its shield, at negative solar altitudes. Lag errors have been neglected since, according to Scrase (1), these are not appreciably affected by time of day at levels up to 100 mb. Radiation emitted (as distinct from reflected) from below the instrument has also been neglected since this, too, does not contribute an appreciable amount to the diurnal variation. Following Scrase, to allow for depletion of the sun's radiation by absorption and scattering before it reaches the sonde, use has been made of a diagram prepared by Vaisala (2), which gives the radiation intensity at the radio-sonde, as a percentage of the radiation intensity at the top of the atmosphere, in terms of the true solar altitude and the height of the instrument. This diagram takes into account the refraction of the sun's rays.

For the present work, diagrams have been prepared which enable the radiation temperature errors at any level up to 20 km to be read off for true solar altitudes between -5° and 70°. These are given as Figures 4(a) and (b). The true solar altitude at any place and at any time can be calculated from the formula $\sin A = \sin\delta \sin\phi + \cos\delta \cos\phi \cos\theta$ where A is the true solar

/altitude

altitude, δ is the sun's declination, ϕ is latitude and θ is the local hour angle. Curves giving the solar altitudes, (a) at the time the sonde leaves the surface and (b) at the time the sonde reaches 100 mb, have been calculated for each of the hours of observation at Larkhill, Lerwick, Malta and Nicosia. These are contained in Figure 5.

Interpolating where necessary, the temperature errors at all levels for the routine ascents were obtained using Figures 4 and 5. The consequent errors in the measured contour heights were then calculated using a convenient derivation of the hydrostatic equation,

$$\delta h' = 122{\cdot}8 \left(\log_{10} p_1/p_2\right) \delta T$$

where δT is the temperature error in degrees Fahrenheit, p_2 and p_1 are pressures in mb at the top and the bottom of the layer whose thickness in feet is h'.

Increments in thickness of each 100 mb layer up to 300 mb and each 50 mb layer between 300 mb and 100 mb were calculated using the mean temperature error appropriate to each layer. The apparent diurnal variations of contour height which would result from these estimated radiation errors were computed for dates approximately at the beginning and centre of each month of the year. Figures 1 to 3 contain curves which show graphically the results of these calculations.

It is clear from Figures 1 and 2 that the diurnal variations computed from estimated radiation errors are mostly of similar magnitude to the variations computed from observations. Further, they illustrate the way in which a number of features of the "observed variation" curves can be explained in terms of the sun's behaviour. E.g., for most of the year at Lerwick, the sonde is affected by direct radiation from the sun at the time of the 0900 GMT observation, but at 100 mb, the sonde is also in sunlight at the time of the 0300 GMT observation for a period in the summer: in consequence the 100 mb, 0900-0300 GMT Lerwick curve (Figure 2(a)) is flat-topped. At Larkhill, on the other hand, the sonde is never affected by direct sunlight during the 0300 GMT ascent and the 100 mb, 0900-0300 GMT Larkhill curve (Figure 1(a)) therefore tends to have a sharper peak than the corresponding Lerwick curve.

Examination of the 1500-0300 GMT curves for Larkhill (Figure 1(e)) and Lerwick (Figure 2(e)) shows that the values based on estimated radiation errors underestimate the observed variations. A greater percentage underestimation occurs with the 0300-2100 GMT variations at Larkhill (Figure 1(d)) and Lerwick (Figure 2(d)). It must not be assumed that these systematic differences between the observed variations and those computed from estimated radiation errors are due to real diurnal changes in the temperature of the atmosphere. It is possible that the differences are due largely to inaccuracies in the estimated radiation errors, since a number of approximations necessarily had to be made both by Scrase, in evolving his technique for calculating radiation errors, and also by Vaisala in estimating the effect of absorption and scattering on the sun's radiation.

That the summer 0300-2100 GMT variations should be so far underestimated suggests that some factor which is particularly important at low solar altitudes has been insufficiently allowed for. One factor contributing to the discrepancy may be the neglect of the effect of radiation from the sky, as opposed to direct radiation from the sun. According to Landsberg (3), on clear days, at a solar altitude of 70 degrees, about 15% of the total radiation at ground level comes from the sky, while at a solar altitude of 10 degrees only 60% of the total radiation comes from the sun and 40% from the sky.

Figures 3(a) and 3(b) show that the observed diurnal variations are of similar magnitude at Malta and Nicosia. This is a surprising result since Nicosia is about 19 degrees farther east than Malta and, as the curves giving the variations due to estimated radiation errors show, the Malta 1500-0300 GMT variation would be expected appreciably to exceed the Nicosia variation on that account.

Whilst the estimated errors do not completely account for the observed variations, it is clear that they provide a reasonable basis for smoothing the curves computed from observations. Two methods of smoothing were tried experimentally on the 100 mb variations: (i) by relating the observed to the estimated variations by means of a regression equation; and (ii) by subtracting the estimated from the observed variations and smoothing the difference by taking weighted running means. Arguments can be advanced in favour of each of these two methods. Experiment showed that there was little difference between the smoothed curves obtained by the two methods. Method (ii) was adopted for all levels, since it is easier to apply and does not restrict the form of the curve to quite the same extent as Method (i). The smoothed curves were also adjusted slightly, (a) so as to be symmetrical about the solstices and (b) so that the sum of the 0900-0300 GMT and the 1500-0900 GMT variations should be equal and opposite to the sum of the 2100-1500 GMT and 0300-2100 GMT variations. Solar altitude varies symmetrically about the solstices and the effects of radiation on both the sonde and the atmosphere are functions of solar altitude. Moreover, in the early stages of this work, the first harmonics of the measured 1500-0300 GMT variations were calculated for Larkhill and Lerwick data. It was found that the position of the maximum of the sine curve, taking an average over all levels from 700 mb to 100 mb, occurred on the 22nd of June. Thus there is both theoretical and practical justification for adjustment (a). One effect of adjustment (b) is to remove those parts of the 6 hr variations which are due to the seasonal variation of contour height. Figure 6 contains graphs of the change of contour height in 24 hours due to the seasonal variation. After suitable smoothing these graphs would enable an analyst to allow for the seasonal variation of contour height if he wished, but at no season or level does the 24 hr change exceed 25 feet, a change which is synoptically unimportant.

The final smoothed versions of the observed diurnal variations curves are contained in Figures 7 to 9, where they may be compared with the unsmoothed observed diurnal changes. The root-mean-square difference between the observed and the final smoothed monthly values of the 6 hr variations, calculated for the Larkhill and Lerwick 100 mb data, was found to be 28.3ft. The standard errors of the December and June monthly mean 6 hr changes at Larkhill and Lerwick as deduced from the standard deviations of the individual 6 hr changes have a mean (r.m.s.) value of 31.4 ft, which suggests that the degree of smoothing attained is of the correct order.

For over half the year the sonde is in darkness at both 2100 GMT and at 0300 GMT over British stations. It will be noted from Figures 7(d) and 8(d) that during this period, there is a small negative 0300-2100 GMT variation. This corresponds to the nocturnal cooling, of about $\frac{1}{2}^{\circ}$F per 6 hr in the lower stratosphere, found by Kay (4).

4. Practical application

Figures 7, 8 and 9 enable corrections to be made to observations from Larkhill, Lerwick, Malta and Nicosia to remove the diurnal variation. For practical purposes it may be found more convenient to use a set of tables, such as Tables 3(a) to 3(e), to reduce the observations to some standard time. Tables 3(a) to 3(e) contain the amount, to the nearest ten feet, which should be subtracted from 0900 GMT, 1500 GMT and 2100 GMT observations to make them comparable with 0300 GMT observations. Linear interpolation is sufficiently accurate to give the reduction applicable to any day of the year from these tables. By suitable interpolation between the Larkhill and Lerwick values, similar tables could be constructed for any station in the British Isles.

5. The interdiurnal variation of contour height

If ϵ is the standard (random) error of measurement of the height of some pressure surface, s_{24} is the true interdiurnal variation and t_{24} is the root-mean-square 24 hr variation of the measured height of the pressure surface then we can write,

$$t_{24}^2 = s_{24}^2 + 2\epsilon^2$$

since S_{24} and ϵ are independent.

Further, if δ is the systematic variation of measured contour height over a given 12 hr period, S_{12} is the r.m.s. 12 hr variation due to random synoptic changes and ϵ_{12} is the r.m.s. variation of the measured 12 hr changes we also have,

$$\epsilon_{12}^2 = S_{12}^2 + 2\epsilon^2 + \delta^2 .$$

S_{12} and S_{24} are the variations which are synoptically important.

Figure 10 shows how S_{12} and S_{24} compare in magnitude with ϵ and δ at all levels in the winter and summer seasons. For the winter period, data relating to the three months Dec.-Feb. 1952-53 at Larkhill and Lerwick were combined. The summer variations refer to June 1948-51 at Larkhill. The 12 hr variations are for the period 1500 GMT to 0300 GMT and the 24 hr variations were calculated from 0300 GMT observations. The calculated S_{12} bear a reasonable relation to the calculated S_{24} except at 100 mb in June. The June 100 mb S_{24} however, was computed from only 39 observations. As can be seen from the diagram, the corresponding value of S_{24} calculated over a longer period from 1946-52 was smaller.

Figures 10(a) and 10(b) illustrate the peculiar difficulties which arise in the lower stratosphere, where both the random and systematic errors increase markedly with height while the true synoptic variations become smaller.

6. Summary and conclusions

The 6 hr and 12 hr apparent diurnal variations of the measured contour heights have been evaluated for levels up to 100 mb. at Larkhill, Lerwick, Malta and Nicosia. Calculated values of the apparent diurnal variation, based on estimates of the radiation errors made by Scrase, tend to underestimate the observed variation, but nevertheless provide a reasonable first approximation to the diurnal changes, except for the 0300-2100 GMT variation, when both ascents are made whilst the sun is low in the sky. Tables are given which enable contour heights computed from radio-sonde observations made by stations in the British Isles, Malta and Nicosia to be corrected for diurnal variation.

References

(1)	Scrase, F.J.	1953	Air Ministry, Met. Res. Ctee., M.R.P. No. 836.
(2)	Vaisala, V.	1948	Geophysica, Helsinki, 3, 39.
(3)	Landsberg, H.	1945	Handbook of Meteorology, McGraw-Hill Book Co. Inc., New York. Section XII, 928.
(4)	Kay, R.H.	1951	Quart. J. R. Met. Soc., 77, 427.

/TABLE 1.

TABLE 1. 6 HR VARIATIONS OF CONTOUR HEIGHT IN FEET COMPUTED FROM OBSERVATIONS (1948-51)

700 mb.

Period GMT	Station	Jan.	Feb.	Mar.	Apr.	May	June	July	Aug.	Sept.	Oct.	Nov.	Dec.
0900-	Larkhill	7	1	13	7	6	17	6	7	7	8	6	9
0300	Lerwick	-3	-3	0	15	14	9	0	-2	1	2	-5	-1
1500-	Larkhill	-1	17	12	35	37	30	31	27	25	11	1	-5
0900	Lerwick	9	23	0	24	27	31	21	24	21	2	1	2
2100-	Larkhill	14	-2	-14	-18	-16	-9	-19	-18	-13	-3	-5	-1
1500	Lerwick	11	-2	-7	-11	-18	-23	-14	-10	-8	3	4	4
0300-	Larkhill	-8	-16	-18	-24	-25	-38	-10	-16	-19	-16	-11	11
2100	Lerwick	-22	-24	0	-26	-24	-17	-7	-12	-14	-7	0	0

500 mb.

Period GMT	Station	Jan.	Feb.	Mar.	Apr.	May	June	July	Aug.	Sept.	Oct.	Nov.	Dec.
0900-	Larkhill	12	16	11	19	26	22	30	14	26	22	8	-5
0300	Lerwick	-11	3	6	35	27	35	14	24	13	13	-12	-1
1500-	Larkhill	14	10	29	49	20	58	47	50	24	11	21	0
0900	Lerwick	10	29	16	37	33	35	23	38	33	15	6	4
2100-	Larkhill	-9	-23	-24	-37	-41	-34	-56	-43	-30	-18	-4	-15
1500	Lerwick	-2	-12	-22	-37	-47	-34	-29	-40	-18	-10	-15	-8
0300-	Larkhill	-20	-3	-16	-29	-35	-46	-23	-21	-20	-15	-19	20
2100	Lerwick	-9	-11	9	-39	-30	-36	-12	-22	-28	-18	23	7

300 mb.

Period GMT	Station	Jan.	Feb.	Mar.	Apr.	May	June	July	Aug.	Sept.	Oct.	Nov.	Dec.
0900-	Larkhill	29	27	51	52	81	75	88	52	52	40	28	-7
0300	Lerwick	24	-16	19	68	81	82	67	54	35	19	-7	10
1500-	Larkhill	30	47	64	76	56	94	60	76	65	59	37	3
0900	Lerwick	18	67	40	59	53	51	40	69	60	16	11	17
2100-	Larkhill	-69	-50	-106	-100	-81	-114	-109	-119	-95	-83	-44	-21
1500	Lerwick	-25	-55	-62	-100	-85	-59	-48	-106	-72	-33	-26	-27
0300-	Larkhill	-45	-24	-14	-28	-61	-55	-43	-9	-22	-16	-21	4
2100	Lerwick	-12	6	5	-13	-60	-74	-64	-17	-23	-2	22	3

200 mb.

Period GMT	Station	Jan.	Feb.	Mar.	Apr.	May	June	July	Aug.	Sept.	Oct.	Nov.	Dec.
0900-	Larkhill	56	22	84	126	142	126	149	118	145	81	41	39
0300	Lerwick	-2	-6	68	133	113	131	105	106	85	51	4	26
1500-	Larkhill	81	84	86	71	42	121	88	88	38	80	20	35
0900	Lerwick	37	85	44	68	48	64	37	67	57	22	19	52
2100-	Larkhill	-93	-128	-162	-173	-119	-184	-179	-179	-141	-152	-67	-53
1500	Lerwick	-14	-94	-126	-145	-110	-104	-88	-147	-110	-63	-37	-50
0300-	Larkhill	-49	22	-8	-24	-71	-63	-53	-27	-42	-9	-6	5
2100	Lerwick	-48	-11	4	-21	-70	-91	-71	-26	-32	-10	22	9

100 mb.

Period GMT	Station	Jan.	Feb.	Mar.	Apr.	May	June	July	Aug.	Sept.	Oct.	Nov.	Dec.
0900-	Larkhill	109	81	194	230	302	298	305	194	247	148	200	127
0300	Lerwick	46	64	151	268	216	253	218	247	184	160	45	26
1500-	Larkhill	110	93	84	57	42	121	93	117	63	121	-15	58
0900	Lerwick	165	61	39	55	88	72	89	72	52	62	25	119
2100-	Larkhill	-177	-212	-212	-300	-274	-309	-307	-307	-265	-255	-133	-186
1500	Lerwick	-126	-181	-172	-249	-221	-231	-207	-201	-218	-151	-118	-123
0300-	Larkhill	-25	31	-41	17	-68	-88	-68	8	-31	-5	-50	-43
2100	Lerwick	-53	8	-17	-2	-80	-165	-95	-60	-9	-69	1	-41

/TABLE 2.

TABLE 2. 12 HR (1500 GMT-0300 GMT) VARIATION OF CONTOUR HEIGHT IN FEET COMPUTED FROM OBSERVATIONS

700 mb.

Station	Years	Jan.	Feb.	Mar.	Apr.	May	June	July	Aug.	Sept.	Oct.	Nov.	Dec.
Larkhill	1948-52	-2	21	27	42	43	52	34	39	27	21	10	0
Lerwick	1948-52	-2	22	4	42	40	41	20	19	34	0	-3	2
Malta	1949-52	1	20	30	27	56	45	35	41	20	6	17	-7
Nicosia	1948-52	20	16	40	40	55	59	36	52	43	21	12	8

500 mb.

Station	Years	Jan.	Feb.	Mar.	Apr.	May	June	July	Aug.	Sept.	Oct.	Nov.	Dec.
Larkhill	1948-52	26	31	35	69	74	83	68	65	43	31	32	6
Lerwick	1948-52	7	22	17	74	77	73	45	58	38	28	-4	6
Malta	1949-52	17	38	69	83	102	68	69	48	48	36	34	9
Nicosia	1948-52	33	36	57	60	89	100	76	74	61	38	23	20

300 mb.

Station	Years	Jan.	Feb.	Mar.	Apr.	May	June	July	Aug.	Sept.	Oct.	Nov.	Dec.
Larkhill	1948-52	81	74	85	133	135	175	152	134	114	92	68	11
Lerwick	1948-52	18	43	32	117	141	147	122	124	98	31	20	22
Malta	1949-52	50	86	67	87	191	123	94	101	97	74	59	20
Nicosia	1948-52	51	80	124	119	143	143	122	85	88	56	47	57

200 mb.

Station	Years	Jan.	Feb.	Mar.	Apr.	May	June	July	Aug.	Sept.	Oct.	Nov.	Dec.
Larkhill	1948-52	129	102	159	211	194	247	224	218	176	153	72	62
Lerwick	1948-52	8	95	161	188	184	214	153	189	129	84	35	41
Malta	1949-52	65	127	92	138	249	177	126	125	119	96	92	42
Nicosia	1948-52	46	64	172	139	193	201	191	111	107	68	68	45

100 mb.

Station	Years	Jan.	Feb.	Mar.	Apr.	May	June	July	Aug.	Sept.	Oct.	Nov.	Dec.
Larkhill	1948-52	172	162	248	322	364	388	404	328	294	254	224	140
Lerwick	1948-52	166	154	214	324	320	356	316	336	280	184	108	162
Malta	1949-52	161	174	230	238	370	212	211	237	203	216	138	121
Nicosia	1948-52	139	168	261	192	240	246	278	211	189	147	116	67

/TABLE 3.

TABLE 3. CORRECTIONS FOR DIURNAL VARIATION, IN TENS OF FEET, TO BE SUBTRACTED FROM OBSERVATIONS MADE AT THE STATED TIMES

(a) 700 mb.

		J.1	J.15	F.1	F.14	M.1	M.15	A.1	A.15	M.1	M.15	J.1	J.15	Jy.1	Jy.15	A.1	A.15	S.1	S.15	O.1	O.15	N.1	N.15	D.1	D.15
Lerwick	0900	0	0	0	0	0	0	1	1	1	1	1	1	1	1	1	1	1	1	0	0	0	0	0	0
	1500	0	0	0	1	1	2	2	3	3	3	3	4	4	3	3	3	3	2	2	1	1	0	0	0
	2100	1	1	1	1	1	1	1	1	2	2	1	1	1	1	2	2	1	1	1	1	1	1	1	1
Larkhill	0900	0	0	0	1	1	1	1	1	1	1	1	1	1	1	1	1	1	1	1	1	1	0	0	0
	1500	0	1	1	1	2	3	3	3	4	4	4	4	4	4	4	4	3	3	3	2	1	1	1	0
	2100	1	1	1	1	1	2	2	2	2	2	2	3	3	2	2	2	2	2	2	1	1	1	1	1
Malta	1500	0	0	1	1	2	2	3	3	4	4	4	4	4	4	4	4	3	3	2	2	1	1	0	0
Nicosia	1500	1	1	2	2	3	3	4	4	5	5	5	5	5	5	5	5	4	4	3	3	2	2	1	1

(b) 500 mb.

		J.1	J.15	F.1	F.14	M.1	M.15	A.1	A.15	M.1	M.15	J.1	J.15	Jy.1	Jy.15	A.1	A.15	S.1	S.15	O.1	O.15	N.1	N.15	D.1	D.15
Lerwick	0900	0	0	0	0	0	1	2	2	3	3	3	3	3	3	3	3	2	2	1	0	0	0	0	0
	1500	0	1	1	2	2	3	5	5	6	6	6	6	6	6	6	6	5	5	3	2	2	1	1	0
	2100	0	0	0	0	1	1	2	2	2	3	3	3	3	3	3	2	2	2	1	1	0	0	0	0
Larkhill	0900	0	1	1	1	1	1	2	2	2	3	3	3	3	3	3	2	2	2	1	1	1	1	1	0
	1500	1	2	2	3	3	4	5	6	6	7	7	7	7	7	7	6	6	5	4	3	3	2	2	1
	2100	0	1	1	1	1	2	2	2	2	3	3	3	3	3	3	2	2	2	2	1	1	1	1	0
Malta	1500	2	2	3	3	4	5	6	7	7	7	7	7	7	7	7	7	7	6	5	4	3	3	2	2
Nicosia	1500	2	3	3	3	4	5	6	7	7	8	9	9	9	9	8	7	7	6	5	4	3	3	3	2

(c) 300 mb.

		J.1	J.15	F.1	F.14	M.1	M.15	A.1	A.15	M.1	M.15	J.1	J.15	Jy.1	Jy.15	A.1	A.15	S.1	S.15	O.1	O.15	N.1	N.15	D.1	D.15
Lerwick	0900	0	0	0	1	1	2	4	5	6	7	8	8	8	8	7	6	5	4	3	1	1	0	0	0
	1500	2	2	3	4	5	7	9	11	12	13	13	13	13	13	13	12	11	9	7	5	4	3	2	2
	2100	0	0	0	0	0	0	1	2	3	5	6	6	6	6	5	3	2	1	0	0	0	0	0	0
Larkhill	0900	2	2	2	3	3	4	5	6	7	7	8	8	8	8	7	7	6	5	4	3	3	2	2	2
	1500	4	5	6	7	9	10	12	13	14	15	15	16	16	15	15	14	13	12	10	9	7	6	5	4
	2100	1	1	1	1	1	2	2	2	3	4	5	5	5	5	4	3	2	2	2	1	1	1	1	1
Malta	1500	4	5	5	6	7	8	9	10	11	11	12	12	12	12	11	11	10	9	8	7	6	5	5	4
Nicosia	1500	5	5	6	7	8	9	10	11	12	13	13	13	13	13	13	12	11	10	9	8	7	6	5	5

TABLE 3 (contd.)

(d) 200 mb.

		J.1	J.15	F.1	F.14	M.1	M.15	A.1	A.15	M.1	M.15	J.1	J.15	Jy.1	Jy.15	A.1	A.15	S.1	S.15	O.1	O.15	N.1	N.15	D.1	D.15
Lerwick	0900	0	1	2	3	5	6	8	10	11	12	12	12	12	12	12	11	10	8	6	5	3	1	1	0
	1500	4	5	6	7	9	11	14	16	17	18	18	18	18	18	18	17	16	14	11	9	7	6	5	4
	2100	1	1	1	1	1	1	2	2	4	6	7	8	8	7	6	4	2	2	1	1	1	1	1	1
Larkhill	0900	4	4	5	6	7	9	11	12	13	14	14	14	14	14	14	13	12	11	9	7	6	5	4	4
	1500	9	9	10	12	14	16	18	19	21	22	23	23	23	23	22	21	19	18	16	14	12	10	9	9
	2100	2	1	1	1	1	1	2	3	3	5	5	6	6	5	5	3	3	2	1	1	1	1	1	2
Malta	1500	6	7	8	9	10	11	12	13	15	16	16	16	16	16	16	15	13	12	11	10	9	8	7	6
Nicosia	1500	5	5	6	8	9	11	12	14	15	17	19	19	19	19	17	15	14	12	11	9	8	6	5	5

(e) 100 mb.

		J.1	J.15	F.1	F.14	M.1	M.15	A.1	A.15	M.1	M.15	J.1	J.15	Jy.1	Jy.15	A.1	A.15	S.1	S.15	O.1	O.15	N.1	N.15	D.1	D.15
Lerwick	0900	3	4	7	10	13	16	19	21	23	25	25	24	24	25	25	23	21	19	16	13	10	7	4	3
	1500	15	15	15	16	18	21	24	27	30	33	33	33	33	33	33	30	27	24	21	18	16	15	15	15
	2100	3	3	2	2	2	2	2	3	6	10	11	11	11	11	10	6	3	2	2	2	2	2	3	3
Larkhill	0900	11	11	12	13	15	17	20	23	25	28	30	30	30	30	28	25	23	20	17	15	13	12	11	11
	1500	17	18	19	20	23	25	28	31	34	36	38	39	39	38	36	34	31	28	25	23	20	19	18	17
	2100	1	1	1	1	1	1	2	2	2	4	7	9	9	7	4	2	2	2	1	1	1	1	1	1
Malta	1500	13	14	15	17	19	21	23	24	25	25	24	24	24	24	25	25	24	23	21	19	17	15	14	13
Nicosia	1500	9	11	13	15	16	19	20	22	23	24	25	26	26	25	24	23	22	20	19	16	15	13	11	9

MONTHLY MEAN 0900-0300 G.M.T. CHANGE OF CONTOUR HEIGHT FOR LARKHILL 1948-51

Fig. 1(a)

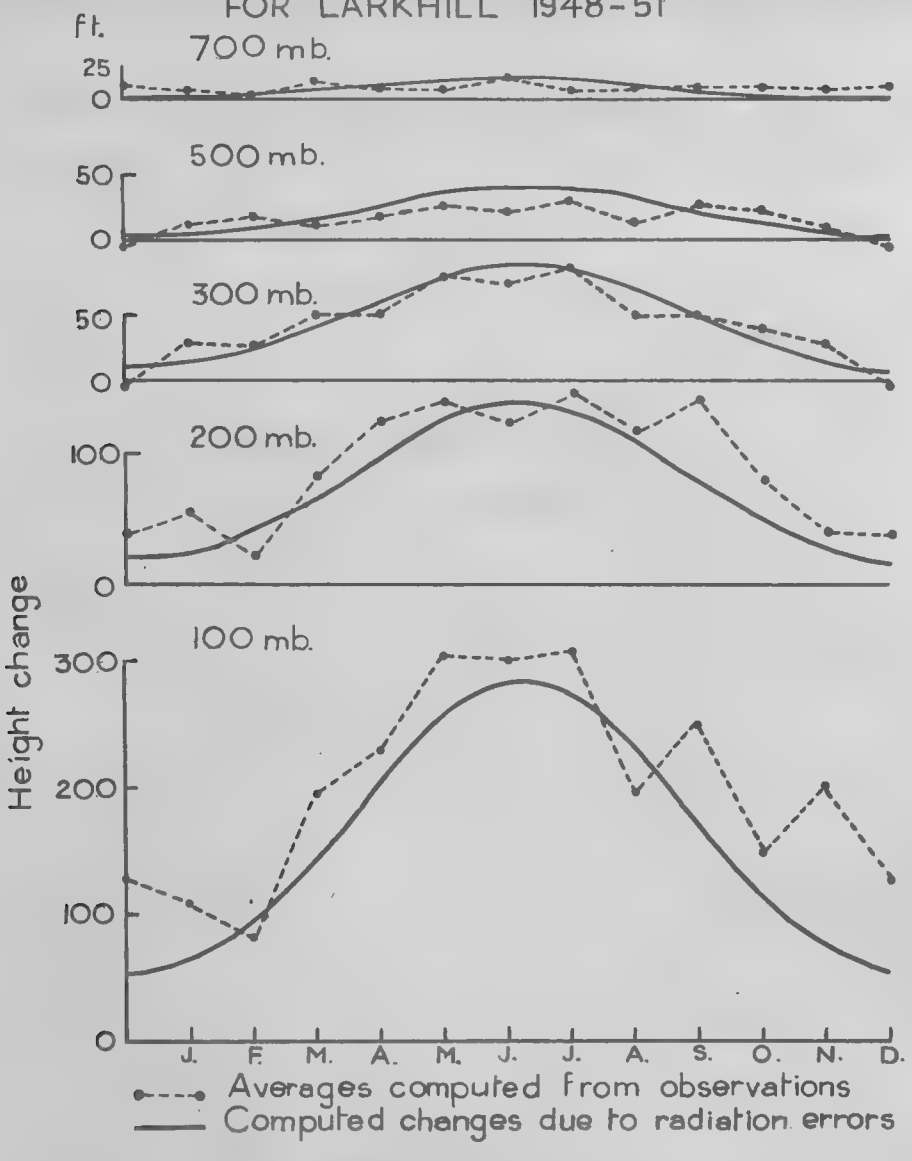

MONTHLY MEAN 1500-0900 G.M.T. CHANGE OF CONTOUR HEIGHT FOR LARKHILL 1948-51

Fig. 1(b)

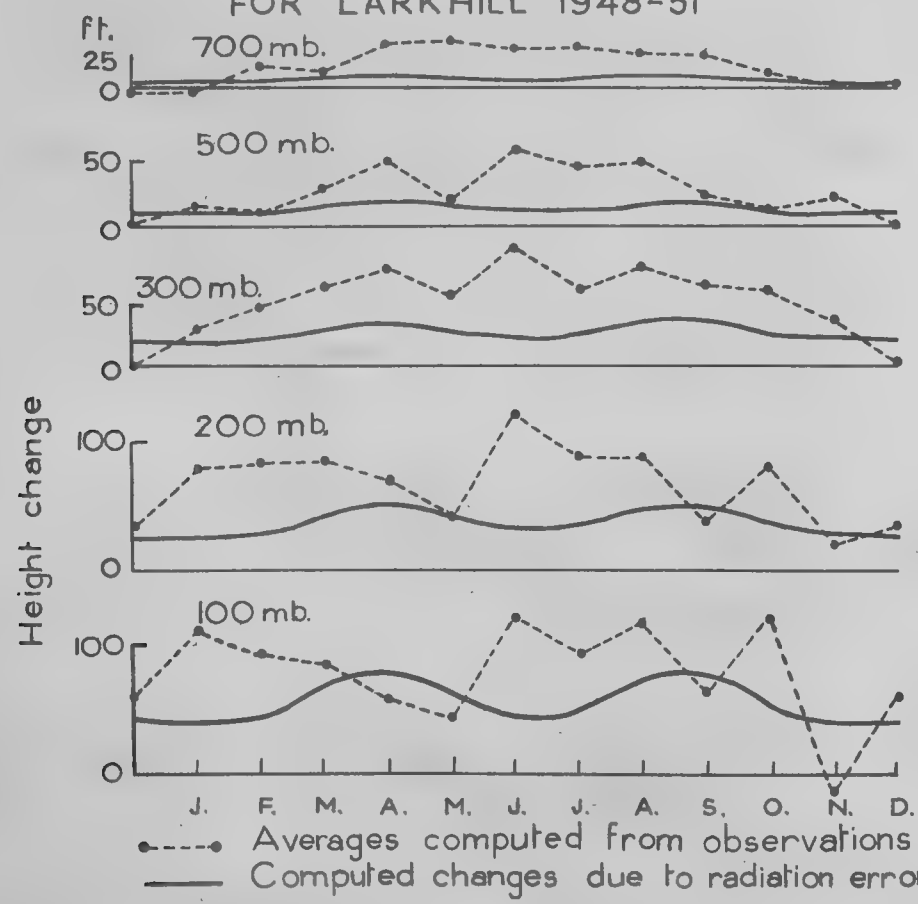

MONTHLY MEAN 2100-1500 G.M.T. CHANGE OF CONTOUR HEIGHT FOR LARKHILL 1948-51

Fig.1(c)

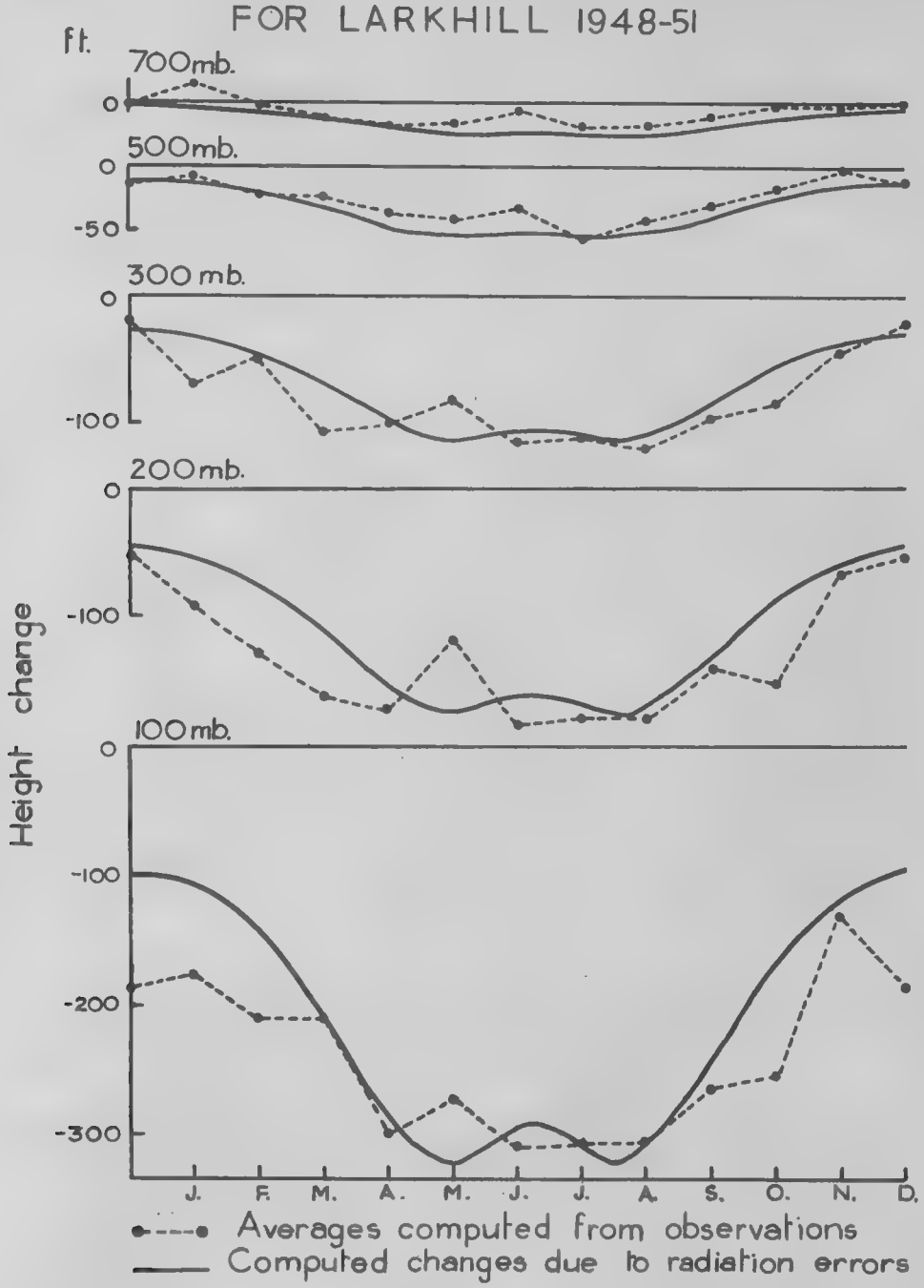

MONTHLY MEAN 0300-2100 G.M.T. CHANGE OF CONTOUR HEIGHT FOR LARKHILL 1948-51

Fig. 1 (d)

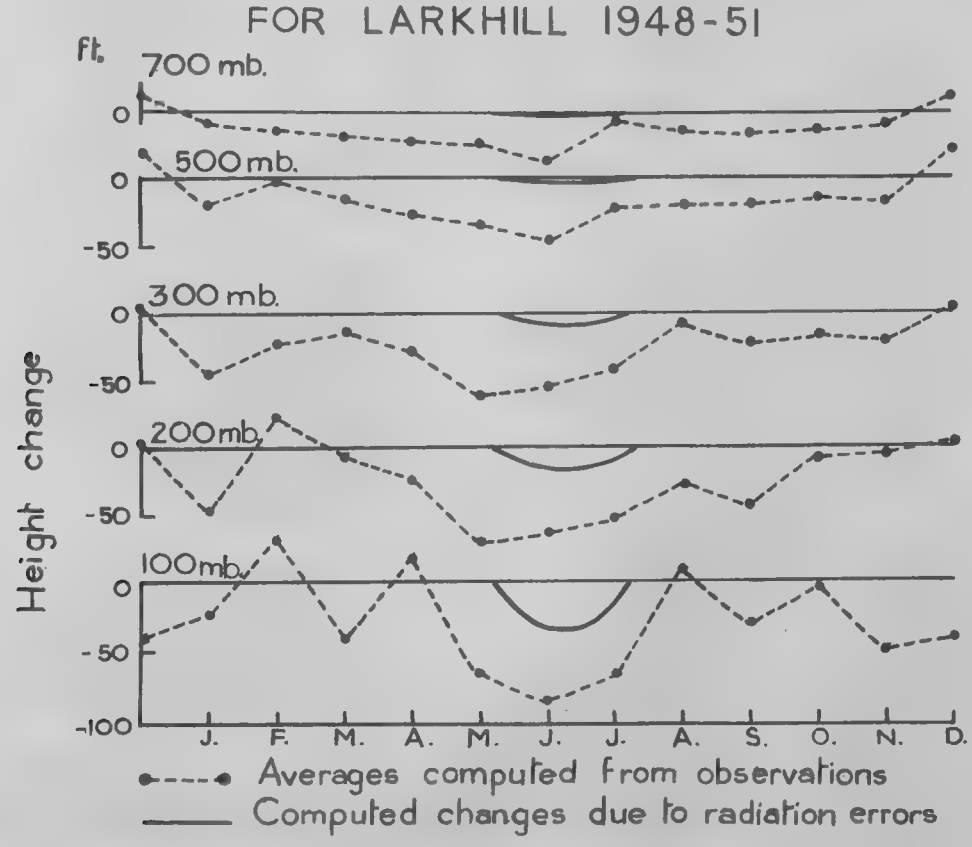

MONTHLY MEAN 1500-0300 G.M.T. CHANGE OF CONTOUR HEIGHT FOR LARKHILL 1948-52

Fig. 1(e)

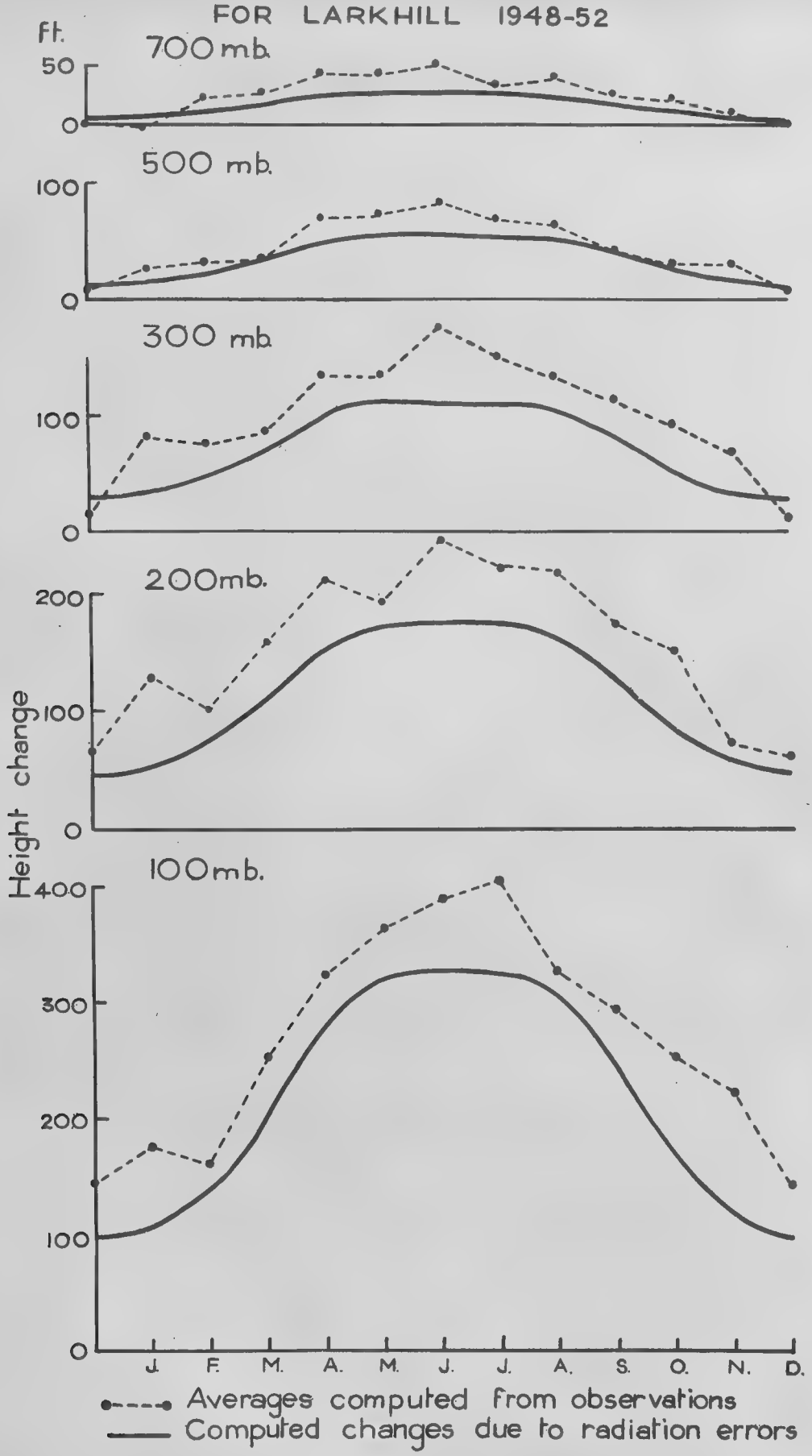

MONTHLY MEAN 0900-0300 G.M.T. CHANGE OF CONTOUR HEIGHT FOR LERWICK 1948-51

Fig. 2(a)

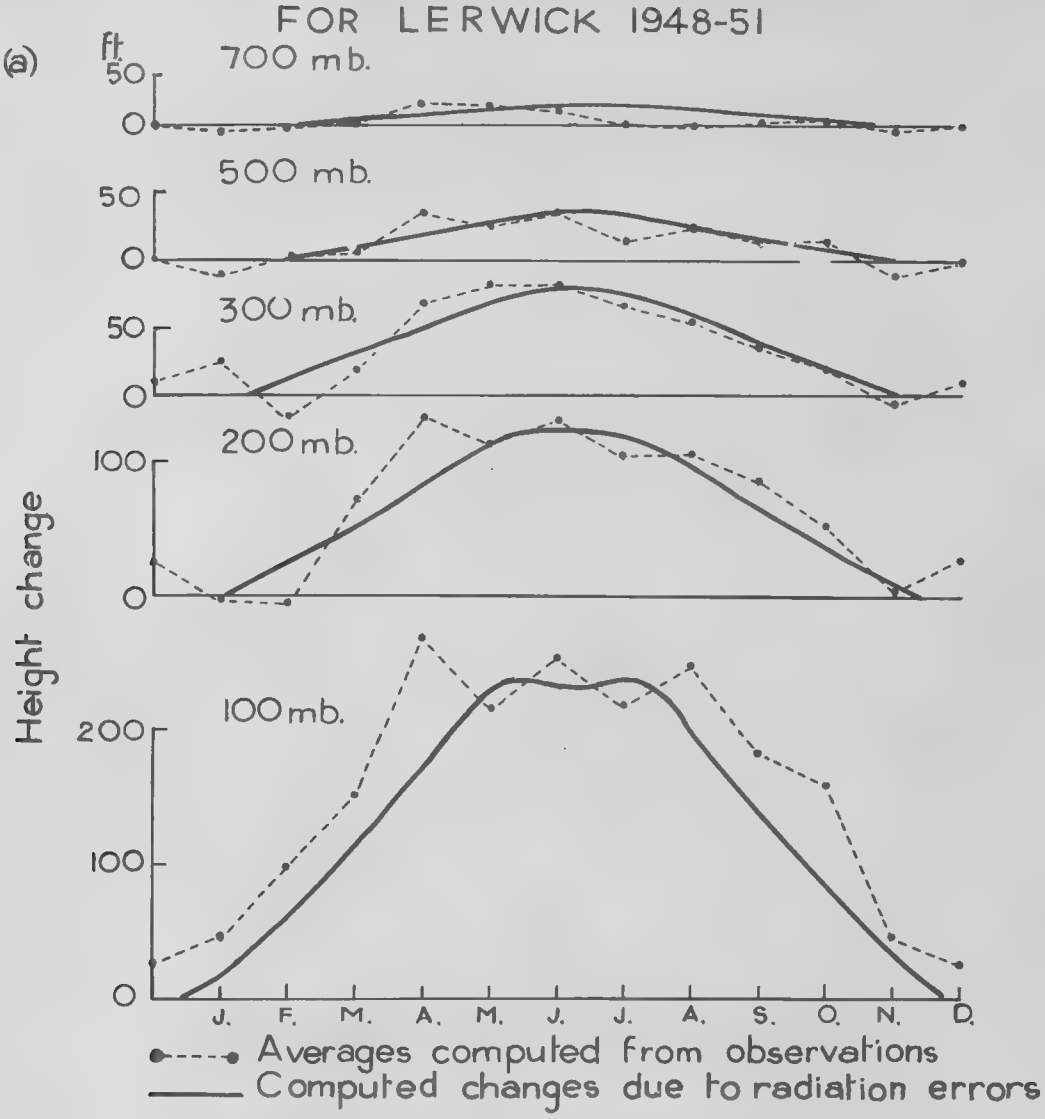

MONTHLY MEAN 1500-0900 G.M.T. CHANGE OF CONTOUR HEIGHT FOR LERWICK 1948-51

Fig. 2 (b)

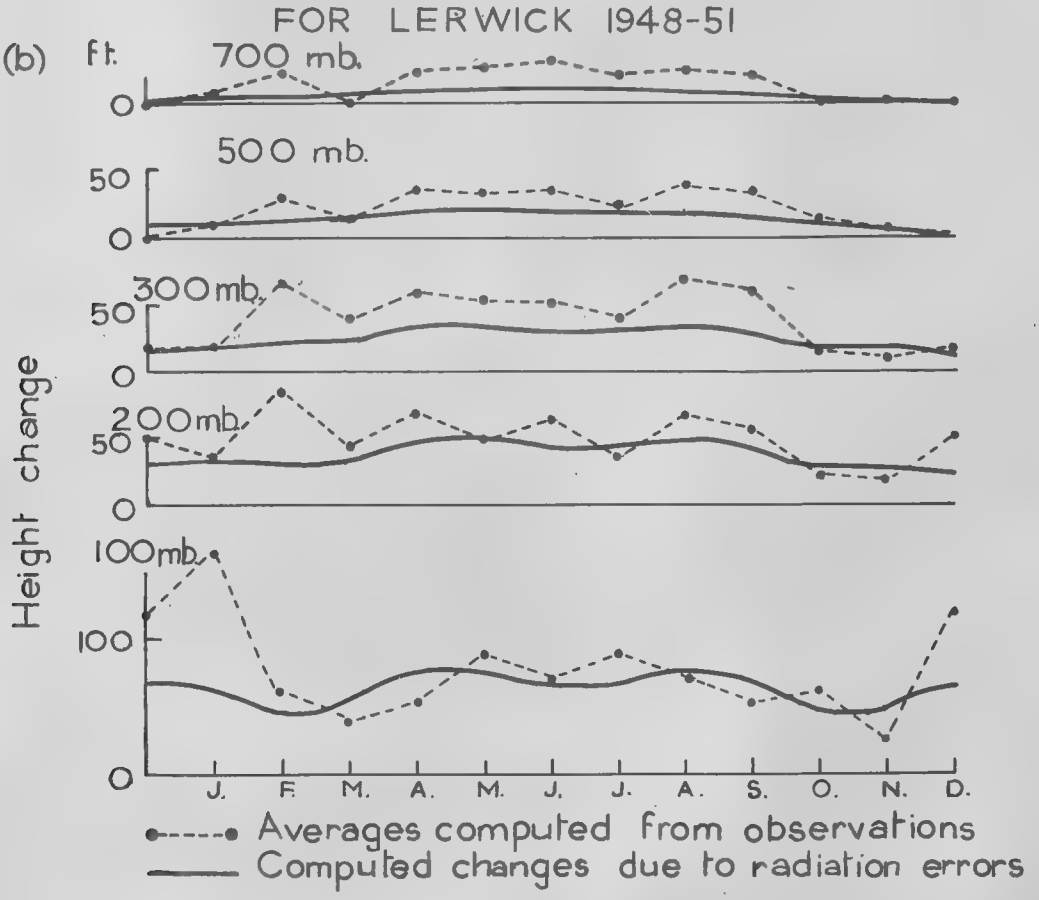

MONTHLY MEAN 2100 - 1500 G.M.T. CHANGE OF CONTOUR HEIGHT FOR LERWICK 1948-51

Fig. 2(c)

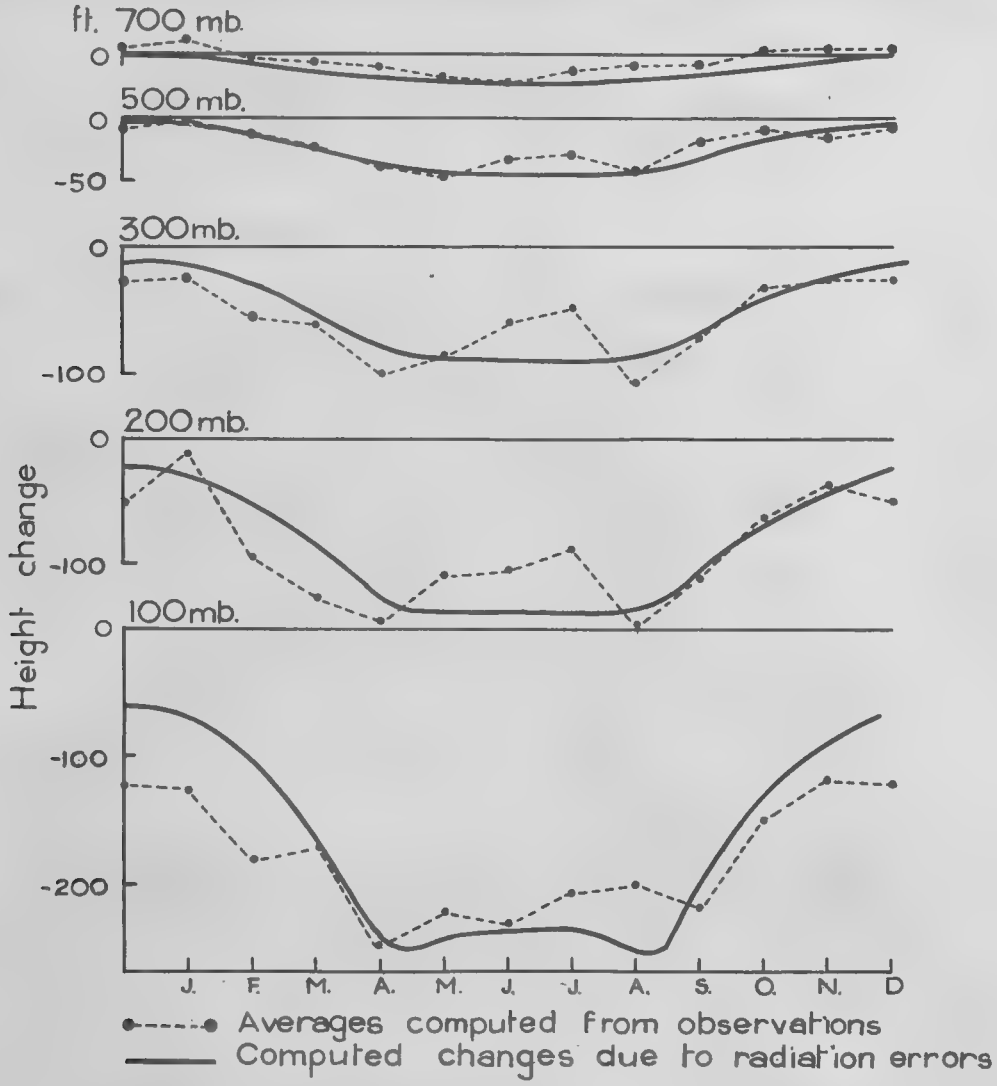

MONTHLY MEAN 0300-2100 G.M.T. CHANGE OF CONTOUR HEIGHT FOR LERWICK 1948-51

Fig. 2 (d)

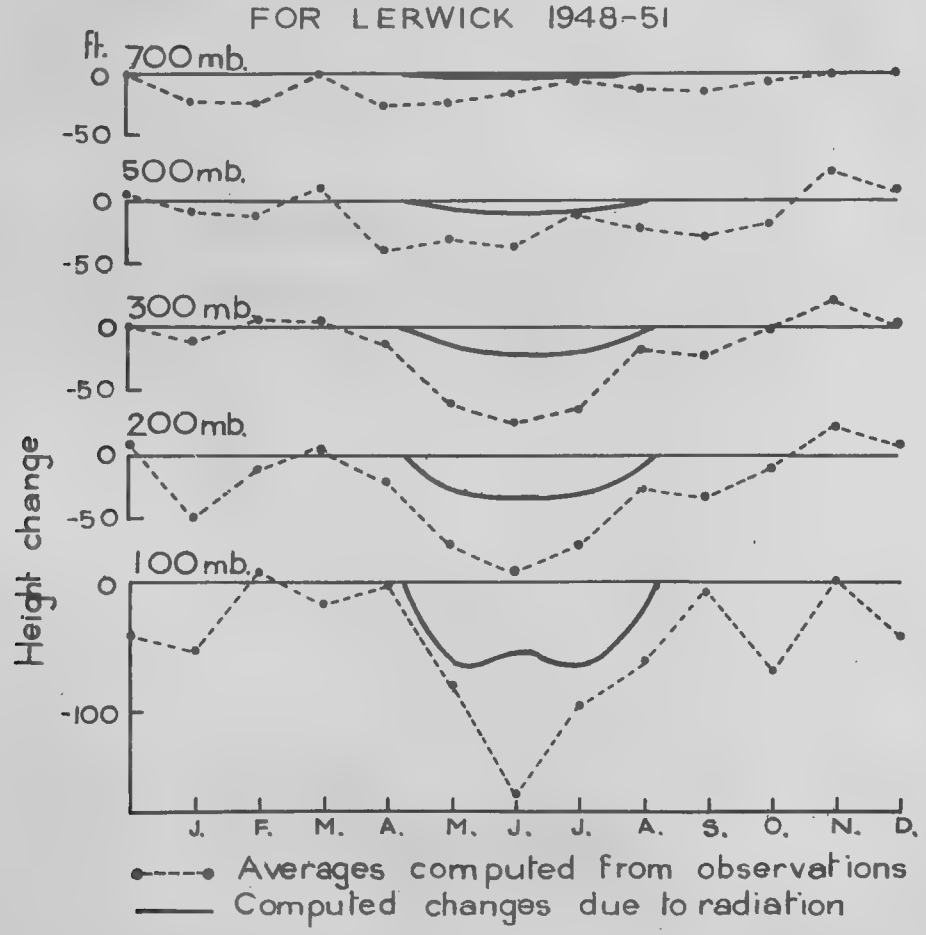

MONTHLY MEAN 1500-0300 G.M.T. CHANGE OF CONTOUR HEIGHT FOR LERWICK 1948-52

Fig.2(e)

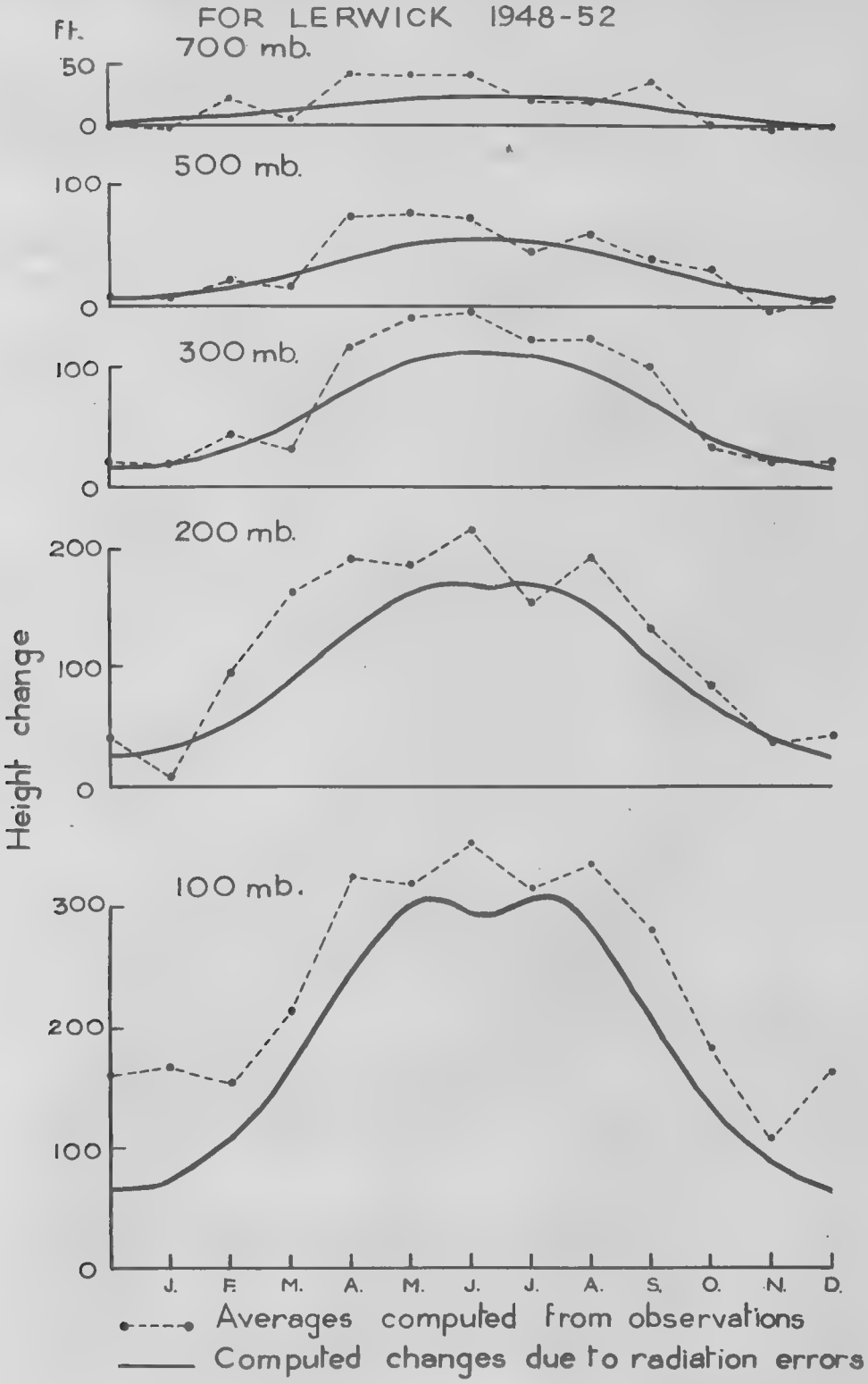

MONTHLY MEAN 1500-0300 G.M.T. CHANGE OF CONTOUR HEIGHT FOR MALTA 1949-52

Fig. 3(a)

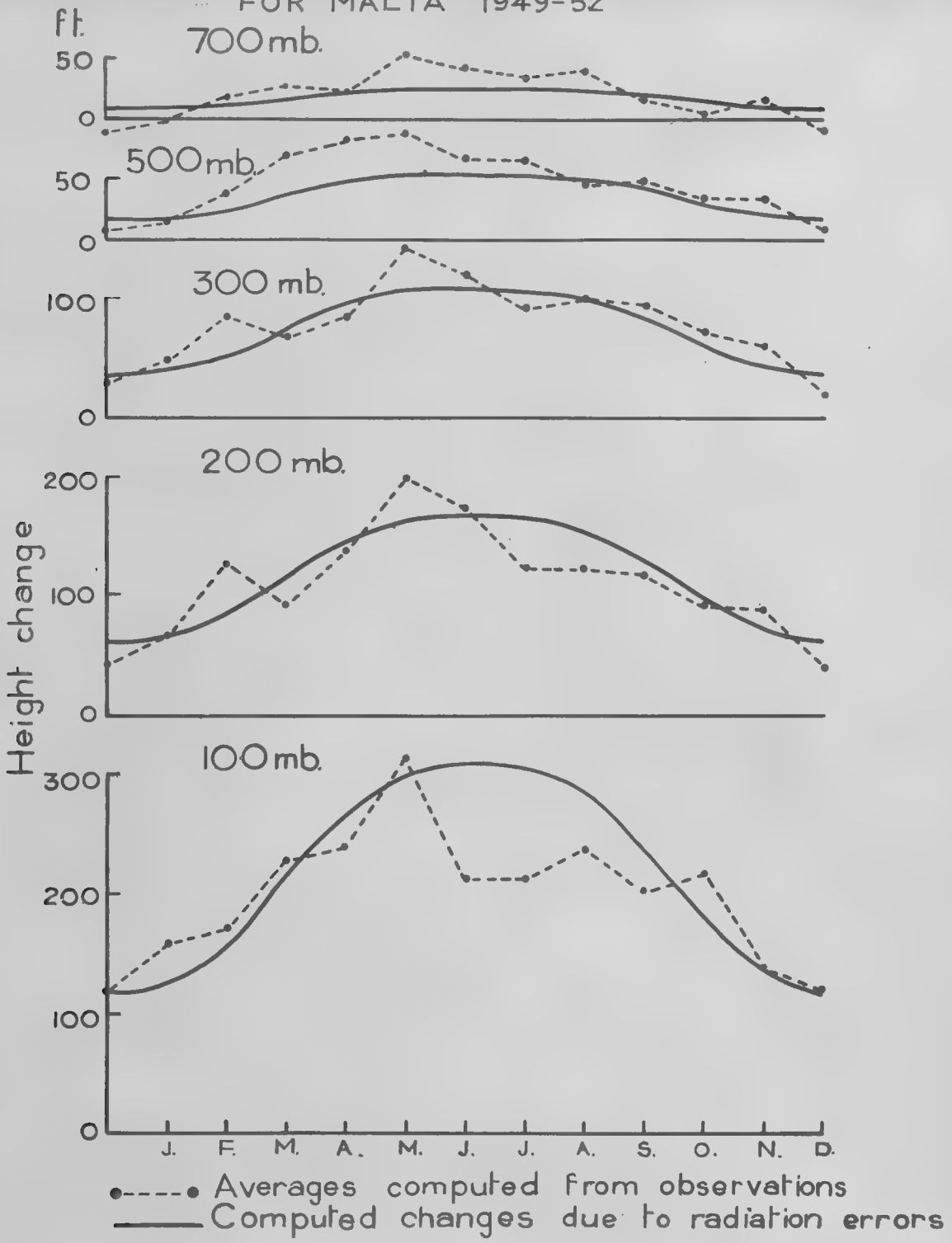

MONTHLY MEAN 1500-0300 G.M.T. CHANGE OF CONTOUR HEIGHT FOR NICOSIA 1948-52

Fig. 3(b)

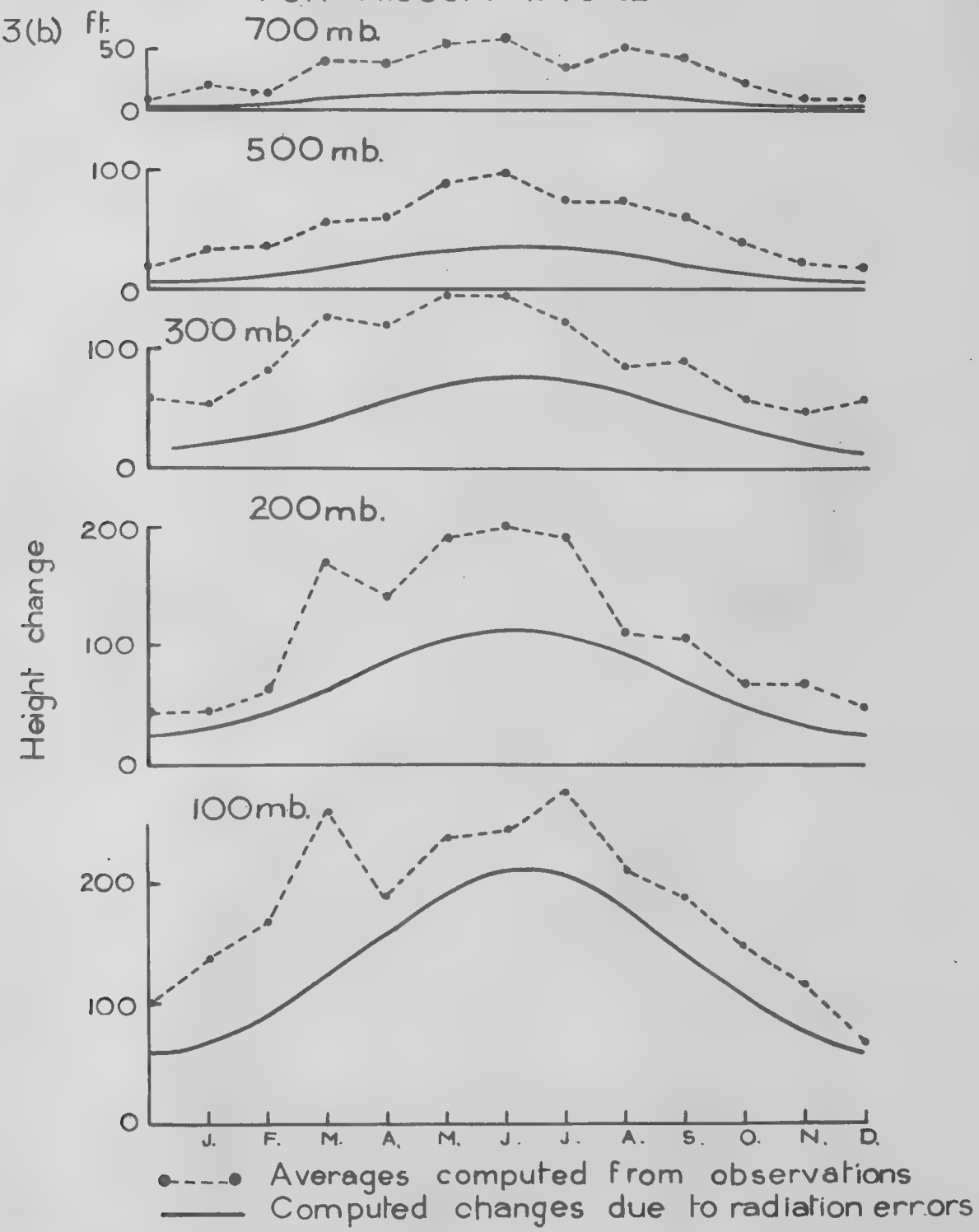

Fig.4 RADIATION ERRORS OF THE M.O. RADIO-SONDE

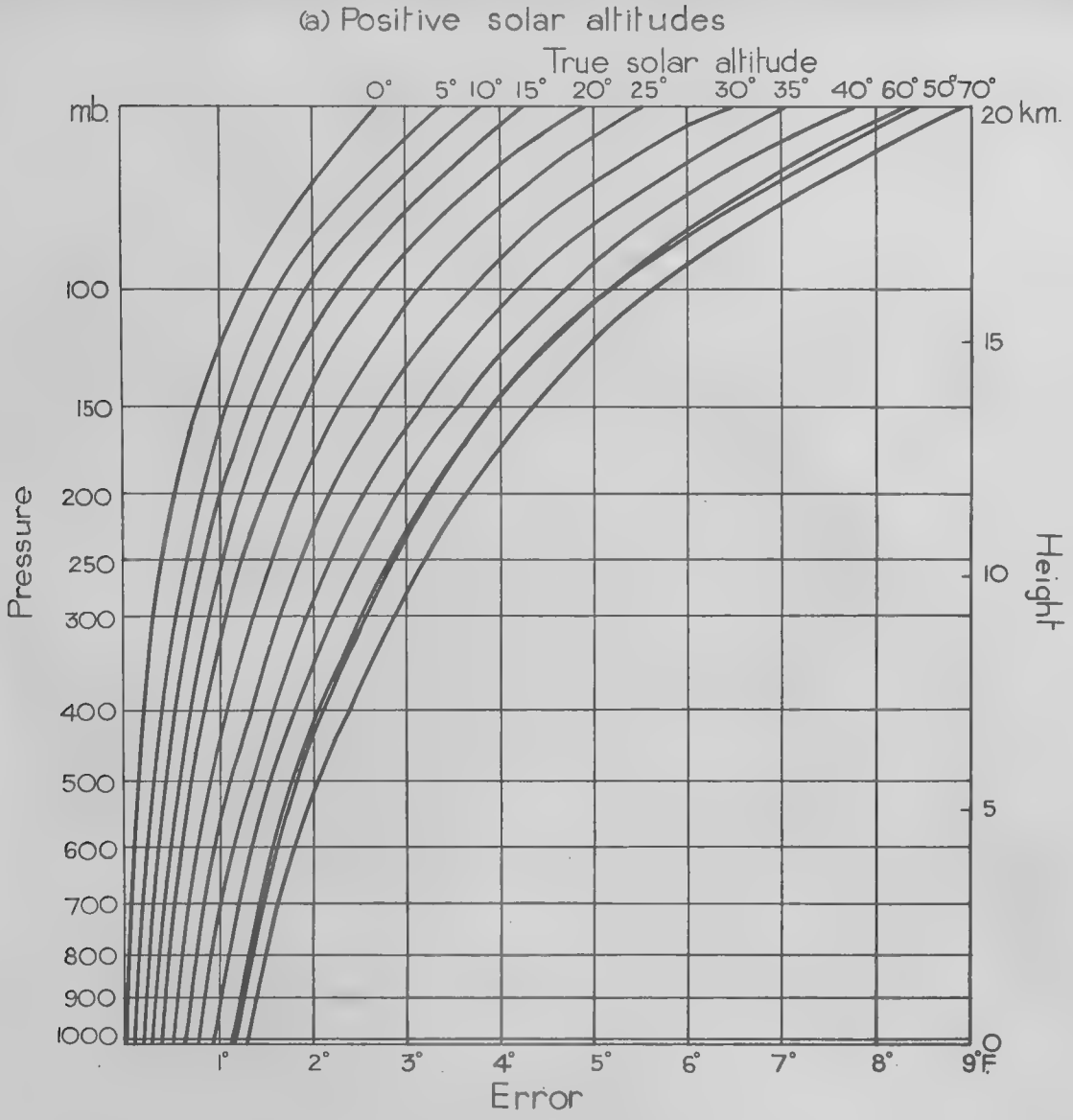

Fig.4 RADIATION ERRORS OF THE M.O. RADIO-SONDE

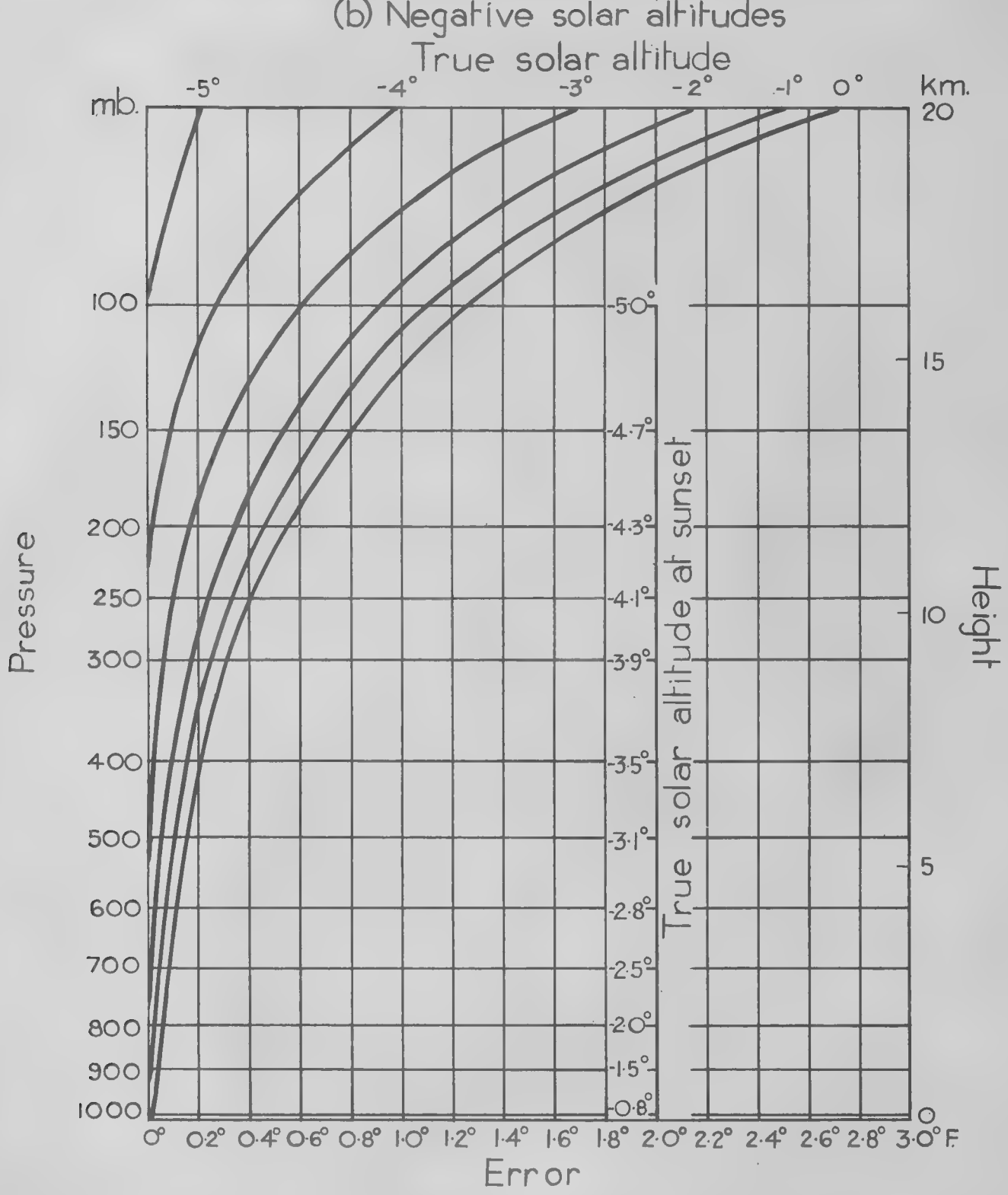

i) ANNUAL VARIATION OF SOLAR ALTITUDE AT LARKHILL (51°12'N., 1°48'W.)

(a) Sonde at surface

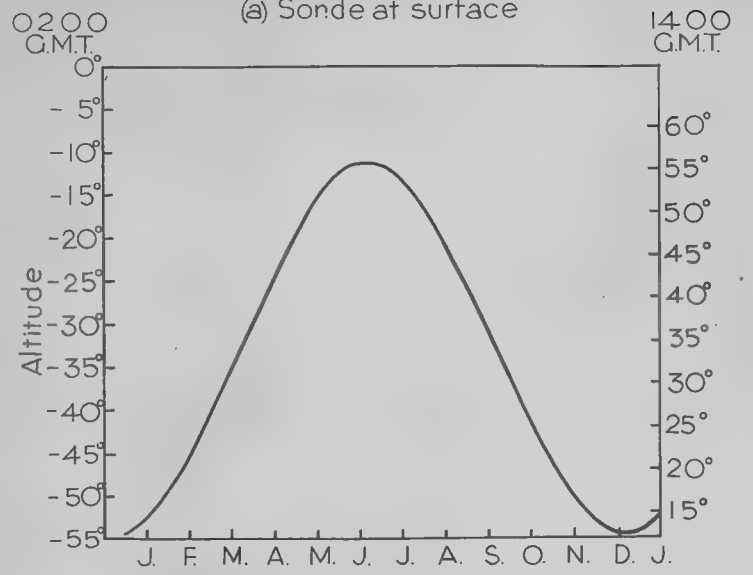

i) ANNUAL VARIATION OF SOLAR ALTITUDE AT LARKHILL (51°12'N., 1°48'W.)

(b) Sonde at 100-mb.

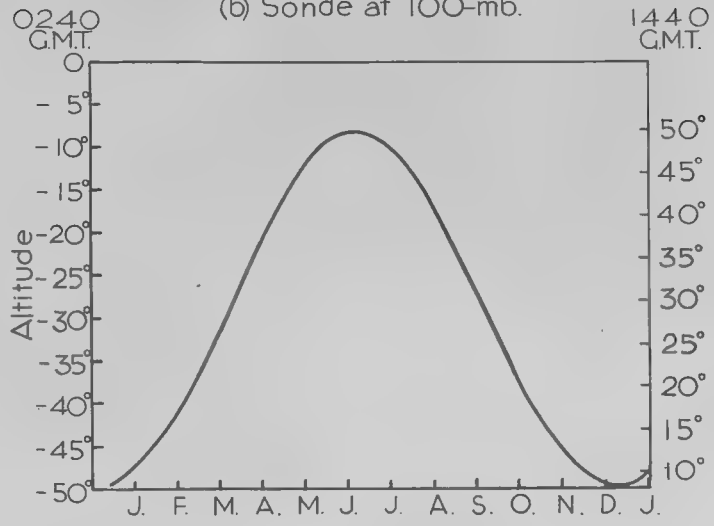

ii) ANNUAL VARIATION OF SOLAR ALTITUDE AT LERWICK (60°8'N., 1°11'W.)

(a) Sonde at surface

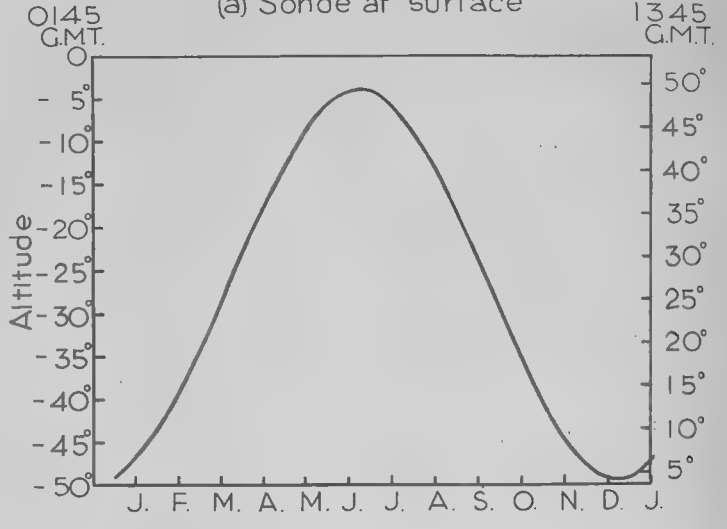

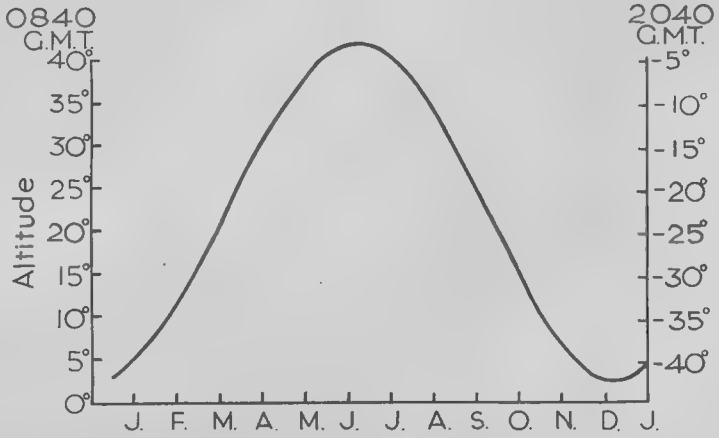

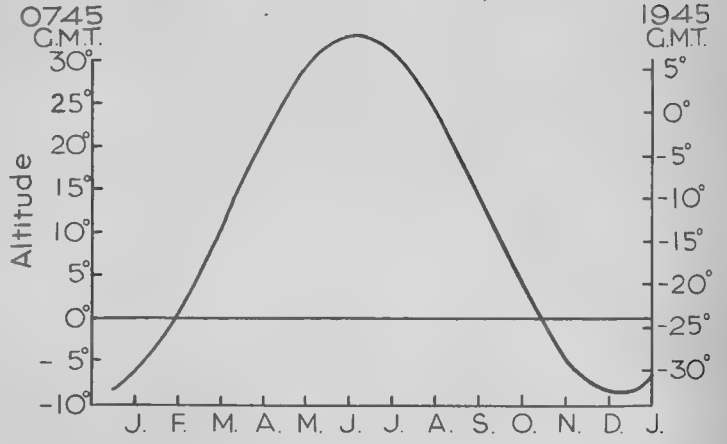

Fig. 5

(ii) ANNUAL VARIATION OF SOLAR ALTITUDE AT LERWICK (60°8'N, 1°11'W)

(b) Sonde at 100 mb.

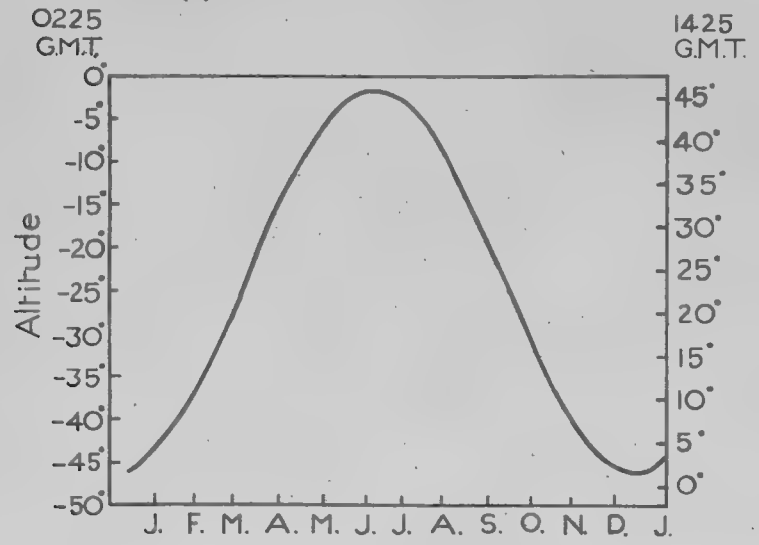

(iii) ANNUAL VARIATION OF SOLAR ALTITUDE AT MALTA (35°50'N, 14°27'E.)

(a) Sonde at surface

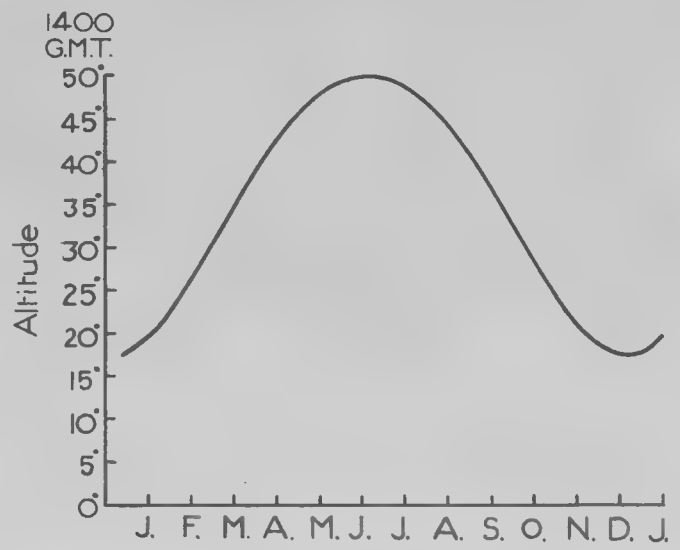

(b) Sonde at 100mb.

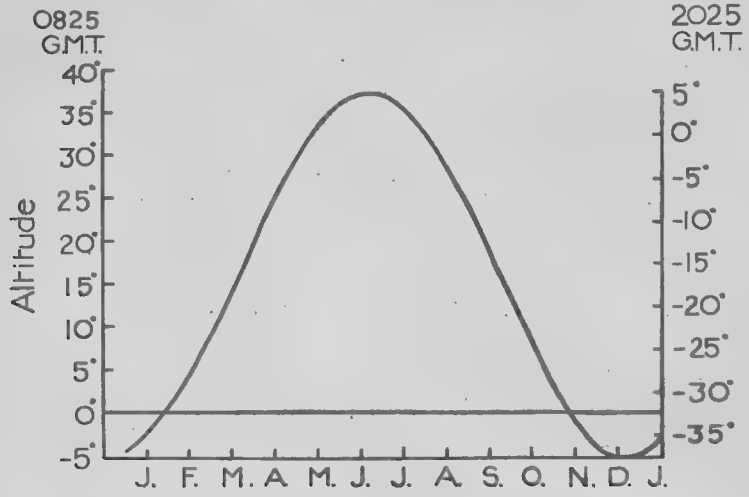

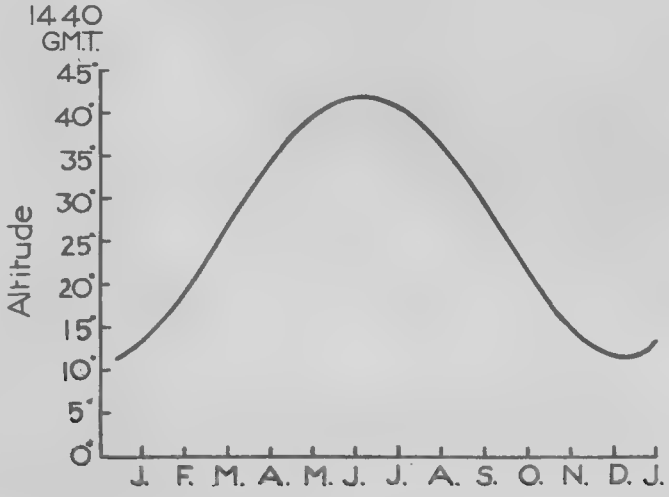

(iv) ANNUAL VARIATION OF SOLAR ALTITUDE AT NICOSIA (35°9'N, 33°17'E)

(a) Sonde at surface

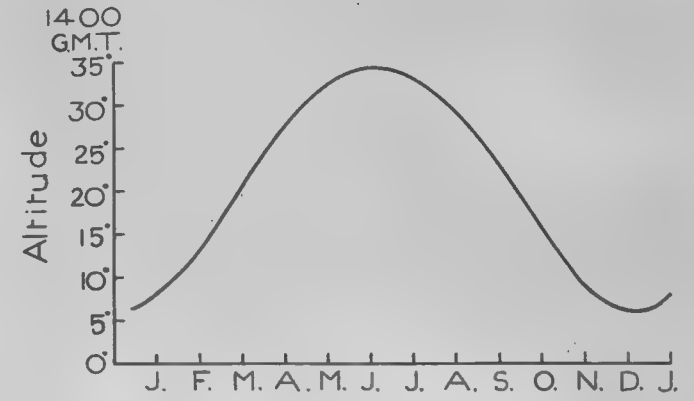

(b) Sonde at 100mb.

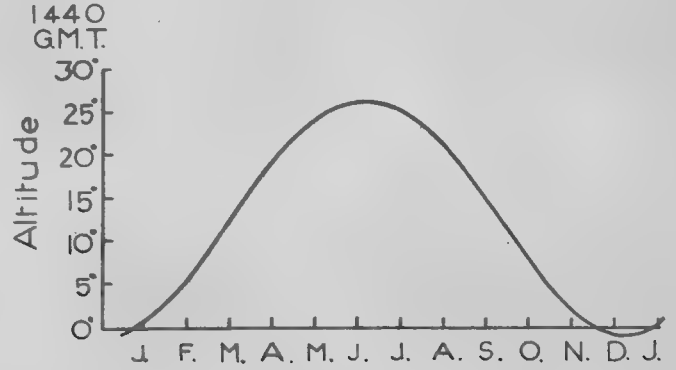

Fig.6 CHANGE IN CONTOUR HEIGHT IN 24 HOURS DUE TO THE SEASONAL VARIATION OF CONTOUR HEIGHT

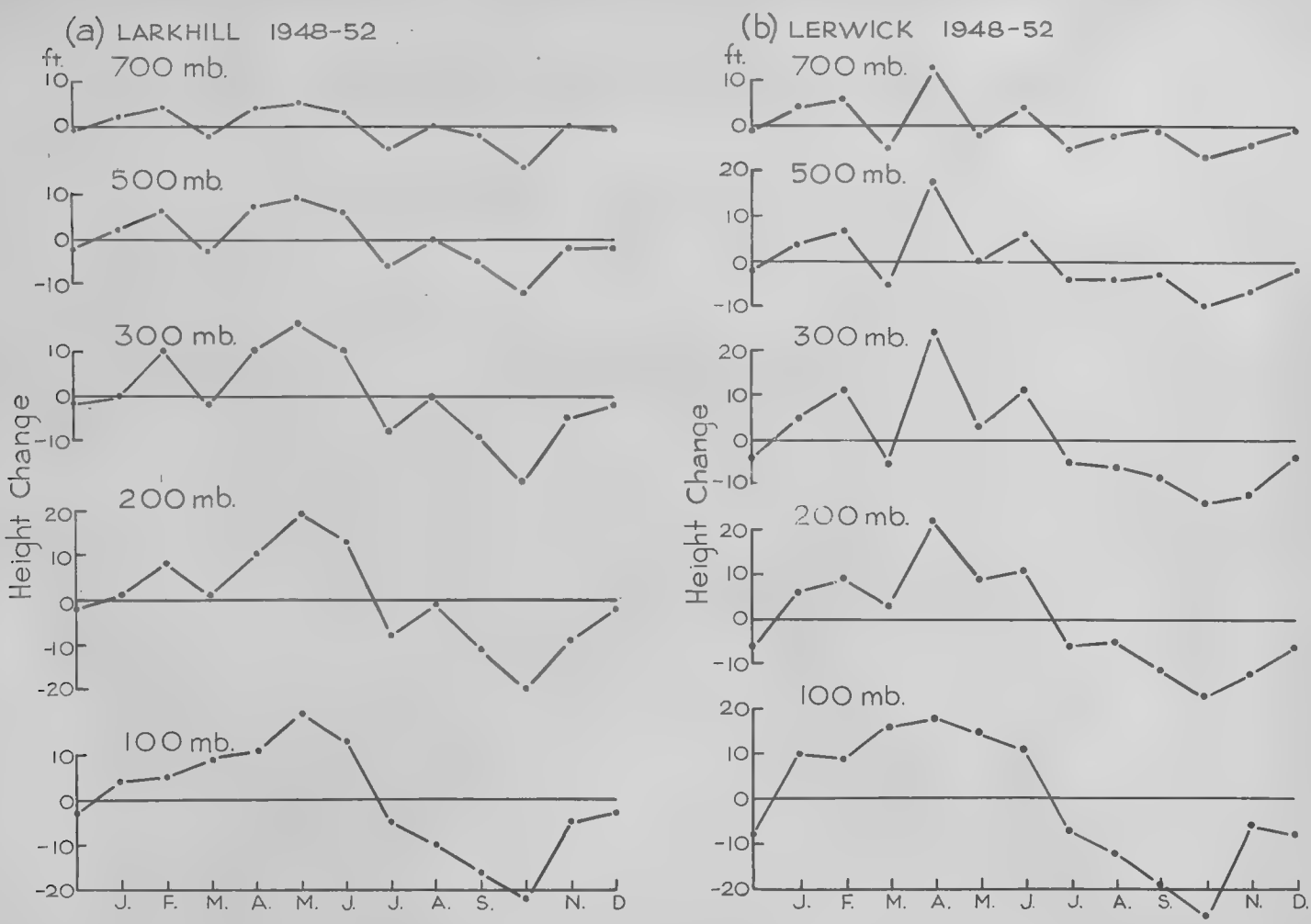

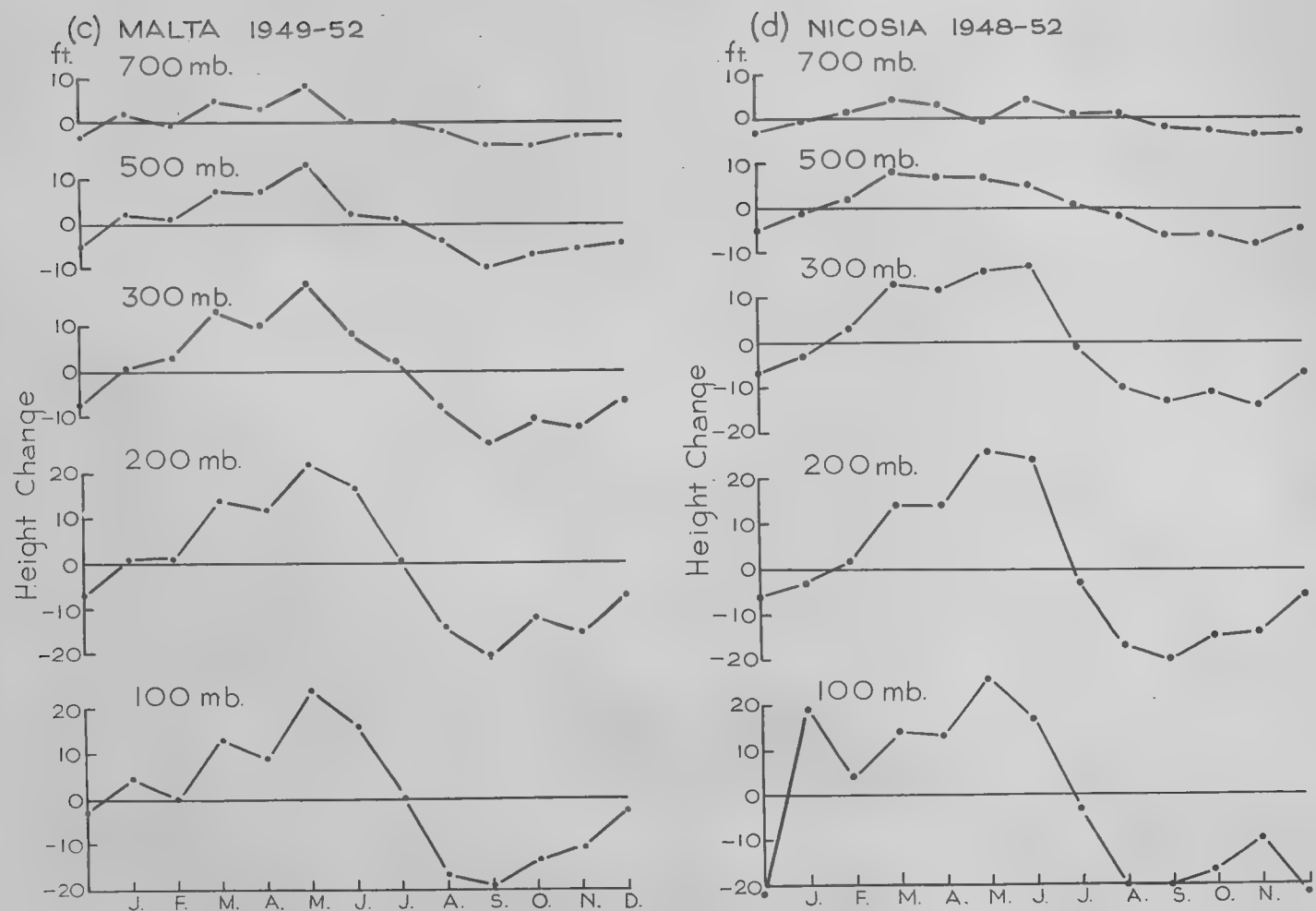

MONTHLY MEAN 0900-0300 G.M.T. CHANGE OF CONTOUR HEIGHT FOR LARKHILL 1948-51

Fig. 7(a)

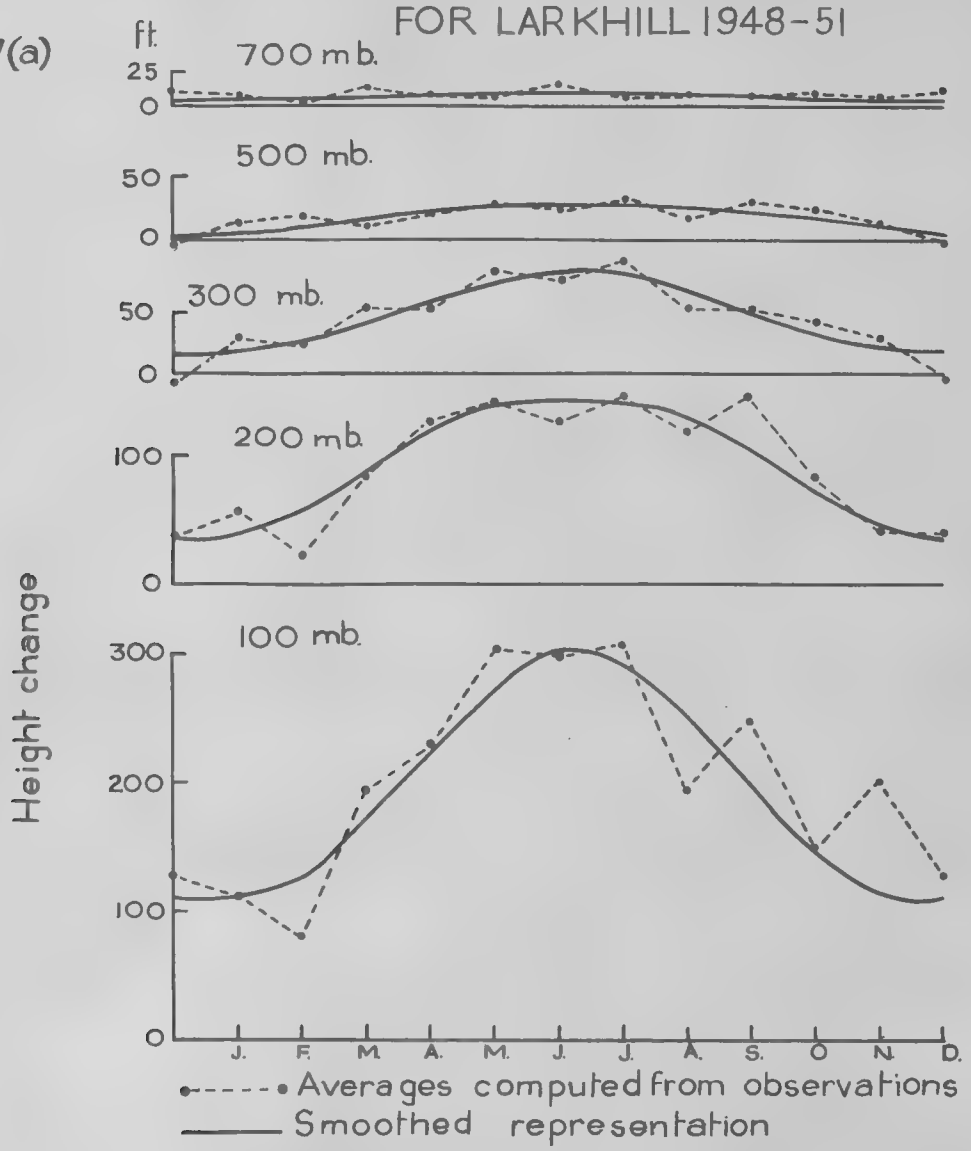

MONTHLY MEAN 1500-0900 G.M.T. CHANGE OF CONTOUR HEIGHT FOR LARKHILL 1948-51

Fig. 7(b)

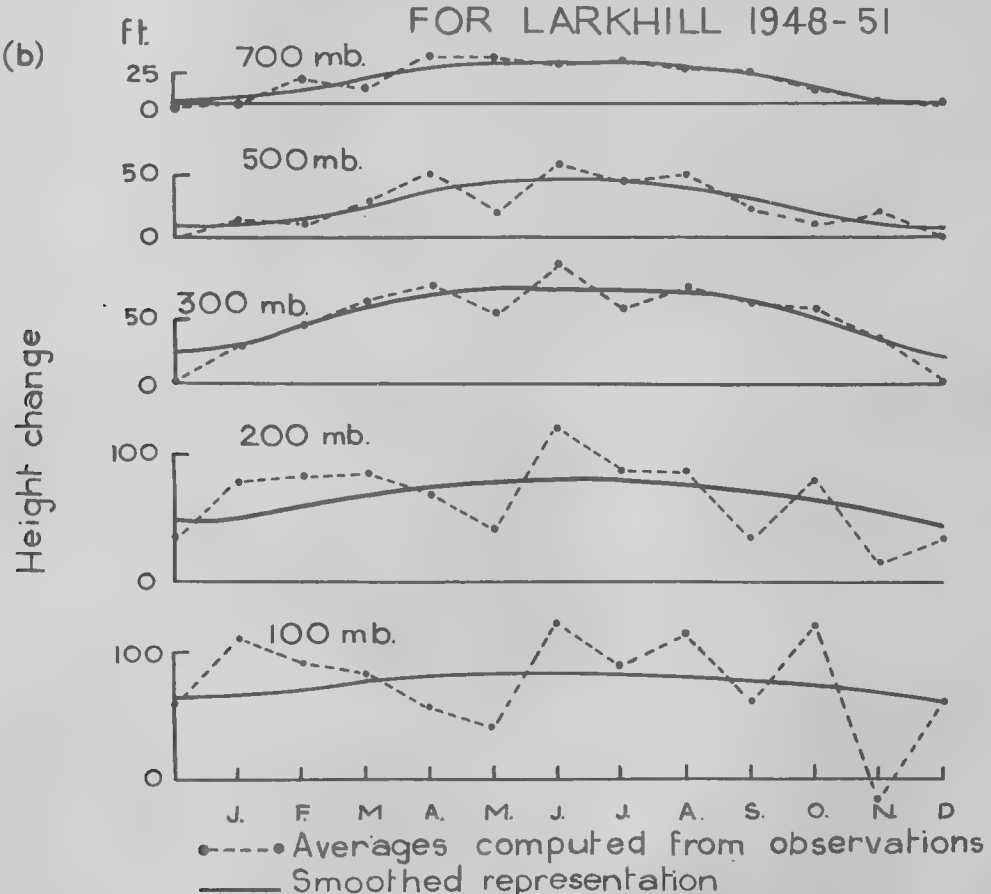

MONTHLY MEAN 2100-1500 G.M.T CHANGE OF CONTOUR HEIGHT FOR LARKHILL 1948-51

Fig. 7(c)

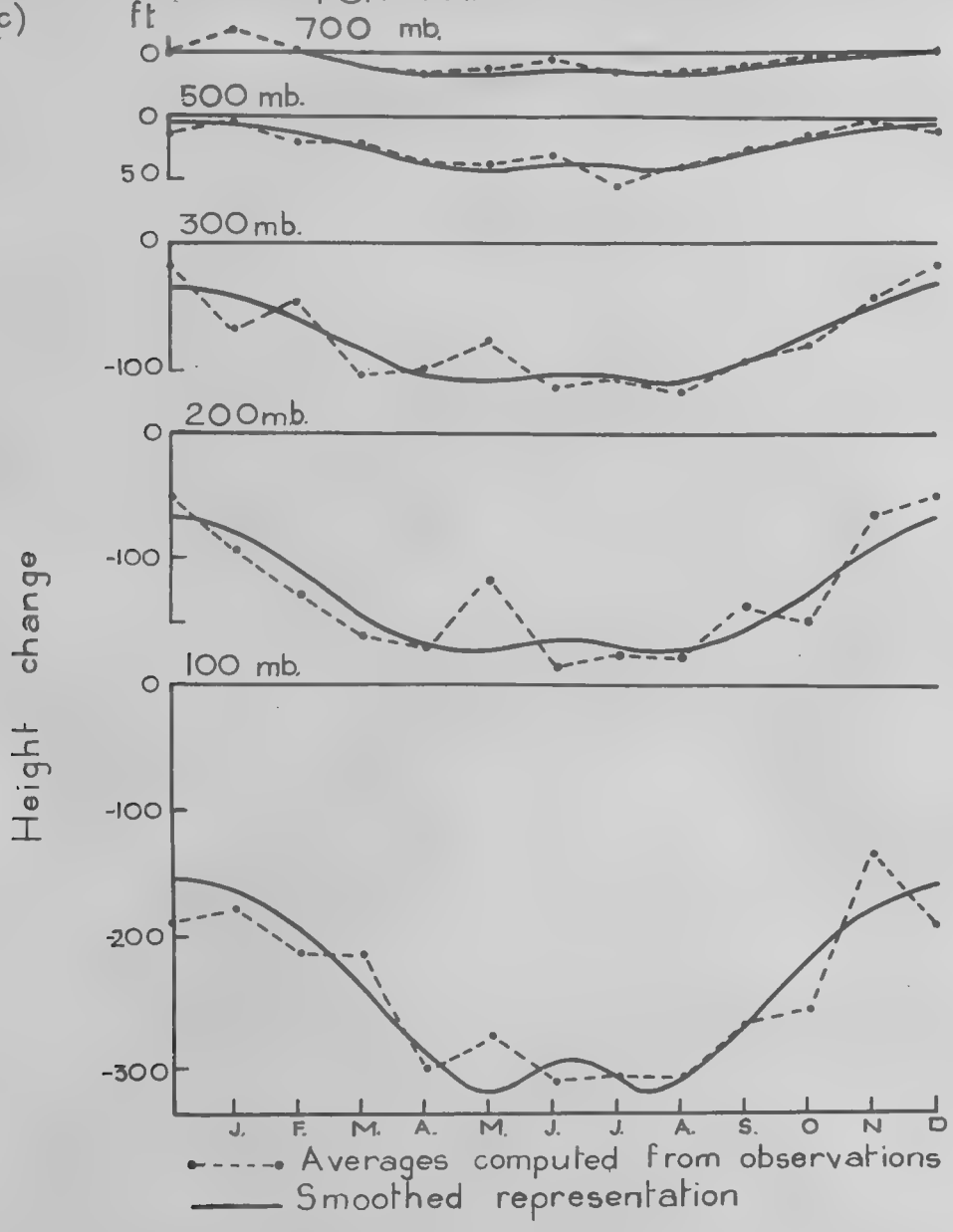

MONTHLY MEAN 0300-2100 G.M.T CHANGE OF CONTOUR HEIGHT FOR LARKHILL 1948-51

Fig. 7(d)

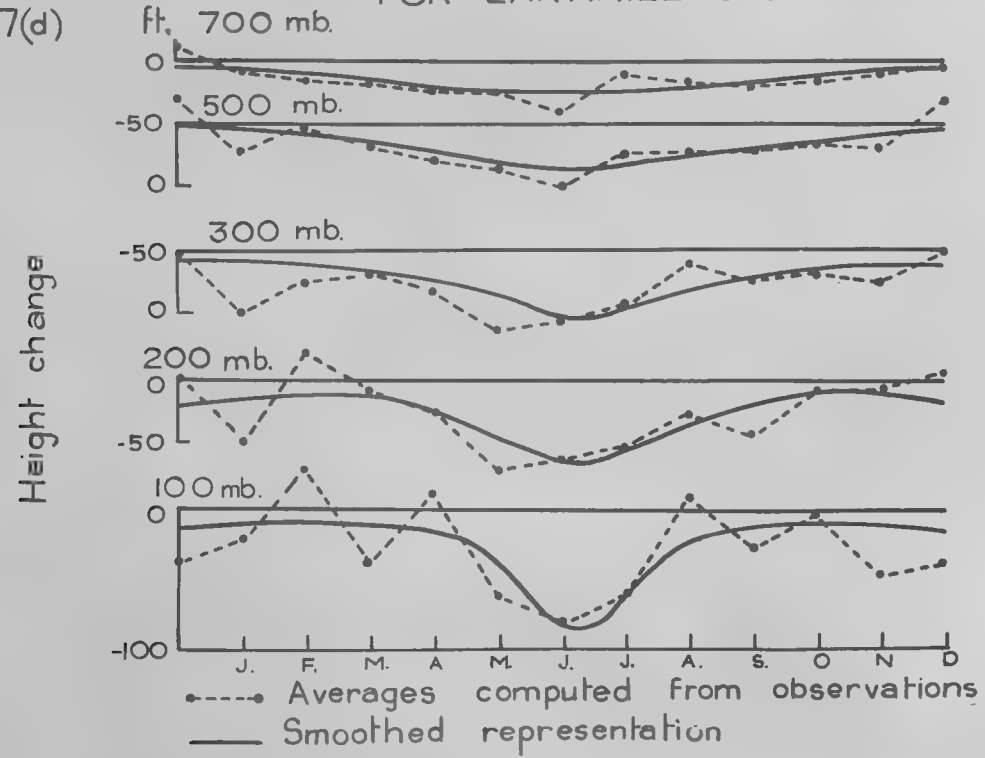

MONTHLY MEAN 1500-0300 G.M.T. CHANGE OF CONTOUR HEIGHT FOR LARKHILL 1948-52

Fig 7(e)

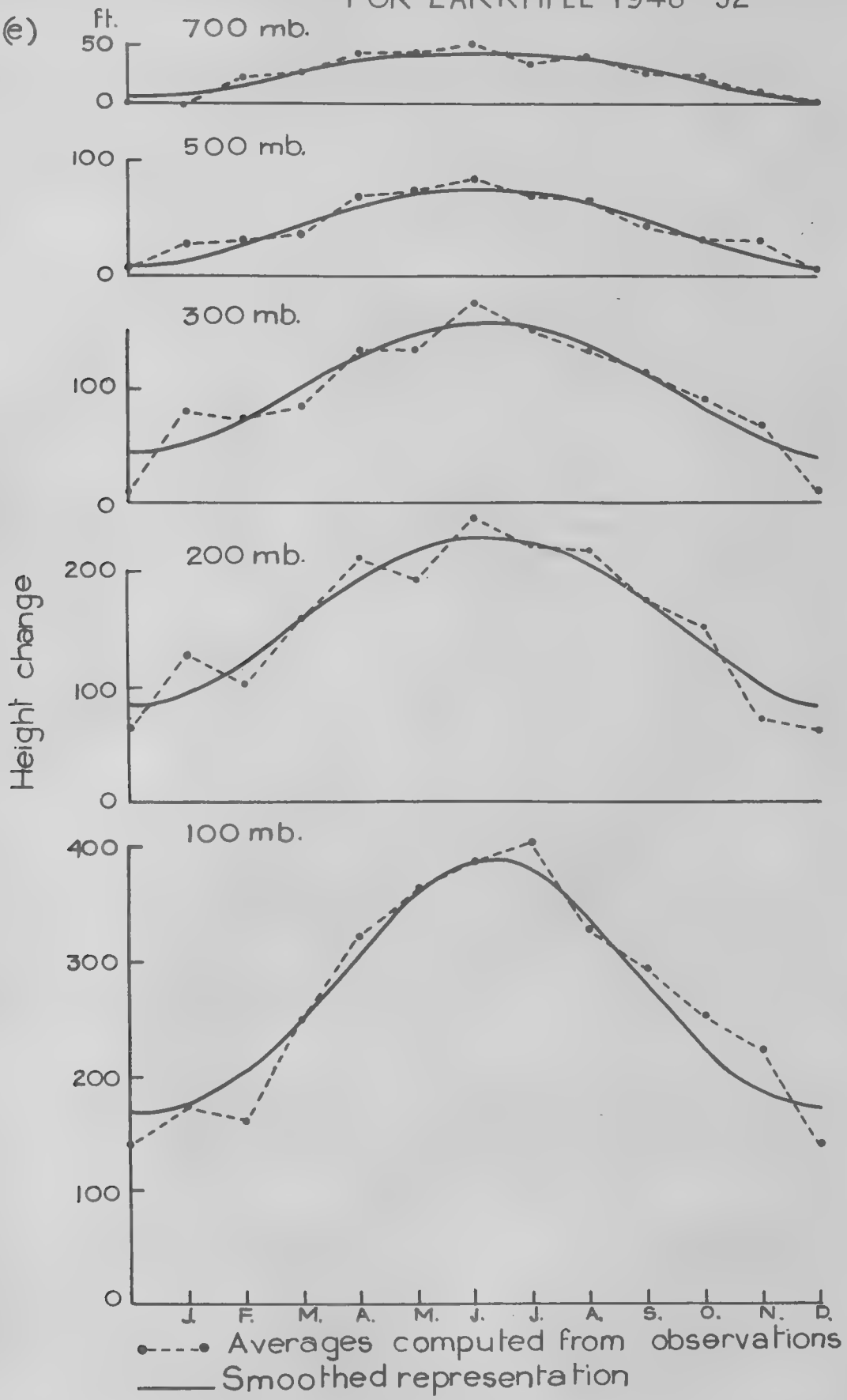

MONTHLY MEAN 0900-0300 G.M.T. CHANGE OF CONTOUR HEIGHT FOR LERWICK 1948-51

Fig. 8(a)

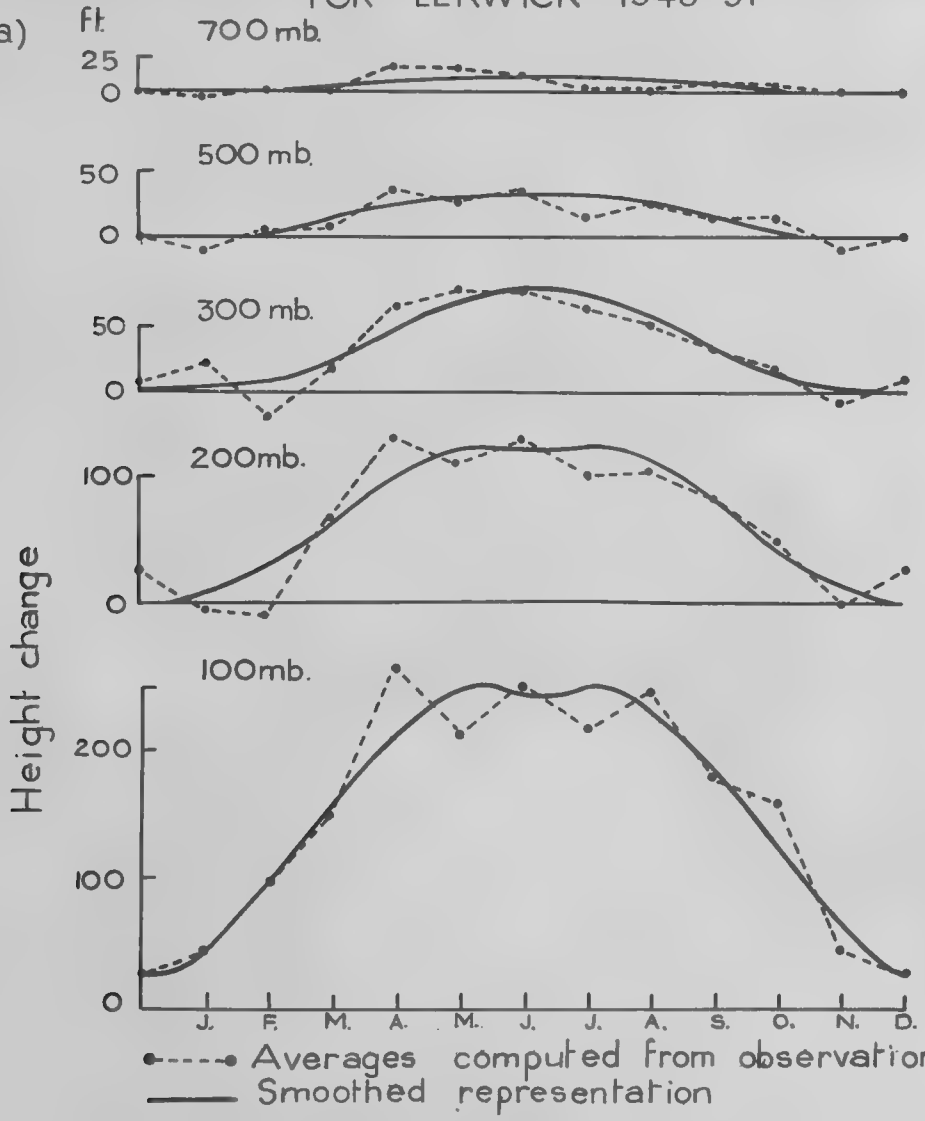

MONTHLY MEAN 1500-0900 G.M.T. CHANGE OF CONTOUR HEIGHT FOR LERWICK 1948-51

Fig. 8(b)

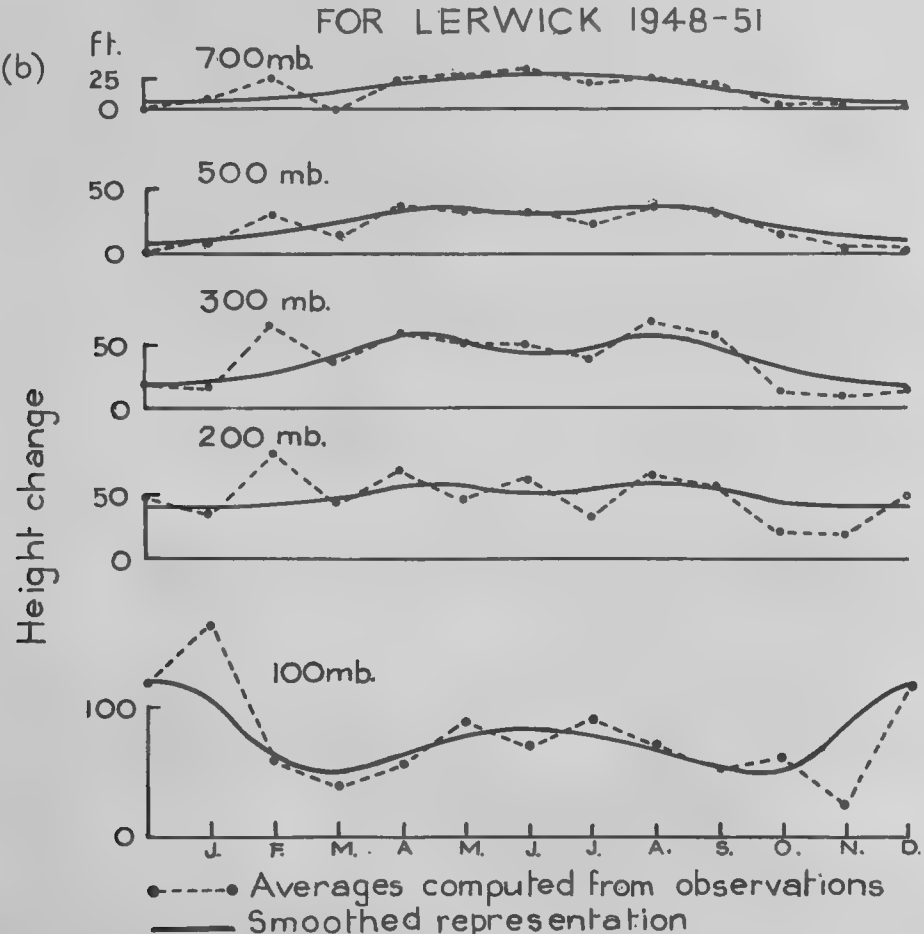

MONTHLY MEAN 2100-1500 G.M.T. CHANGE OF CONTOUR HEIGHT FOR LERWICK 1948-51

Fig. 8(c)

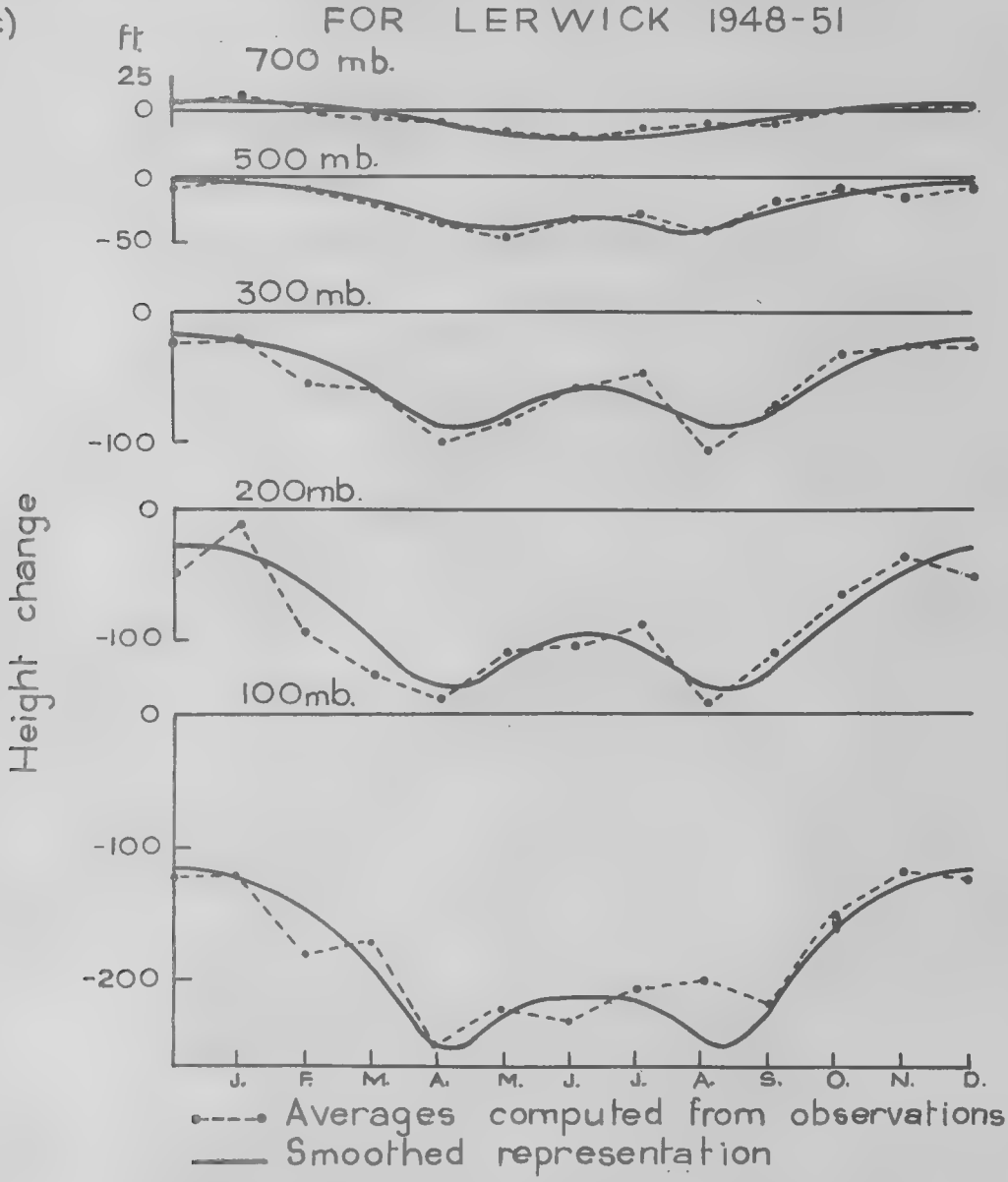

MONTHLY MEAN 0300-2100 G.M.T CHANGE OF CONTOUR HEIGHT FOR LERWICK 1948-51

Fig. 8(d)

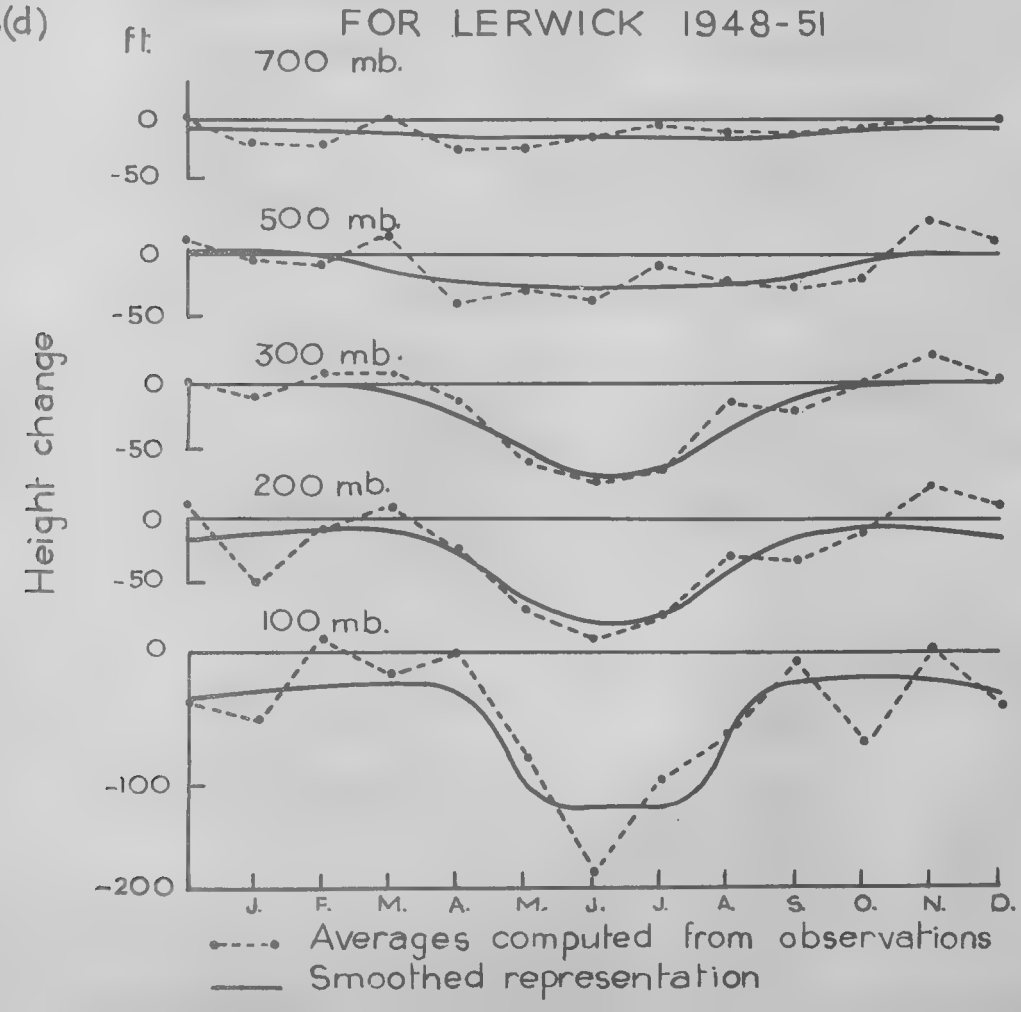

MONTHLY MEAN 1500 - 0300 G.M.T. CHANGE OF CONTOUR HEIGHT FOR LERWICK 1948-52

Fig. 8(e)

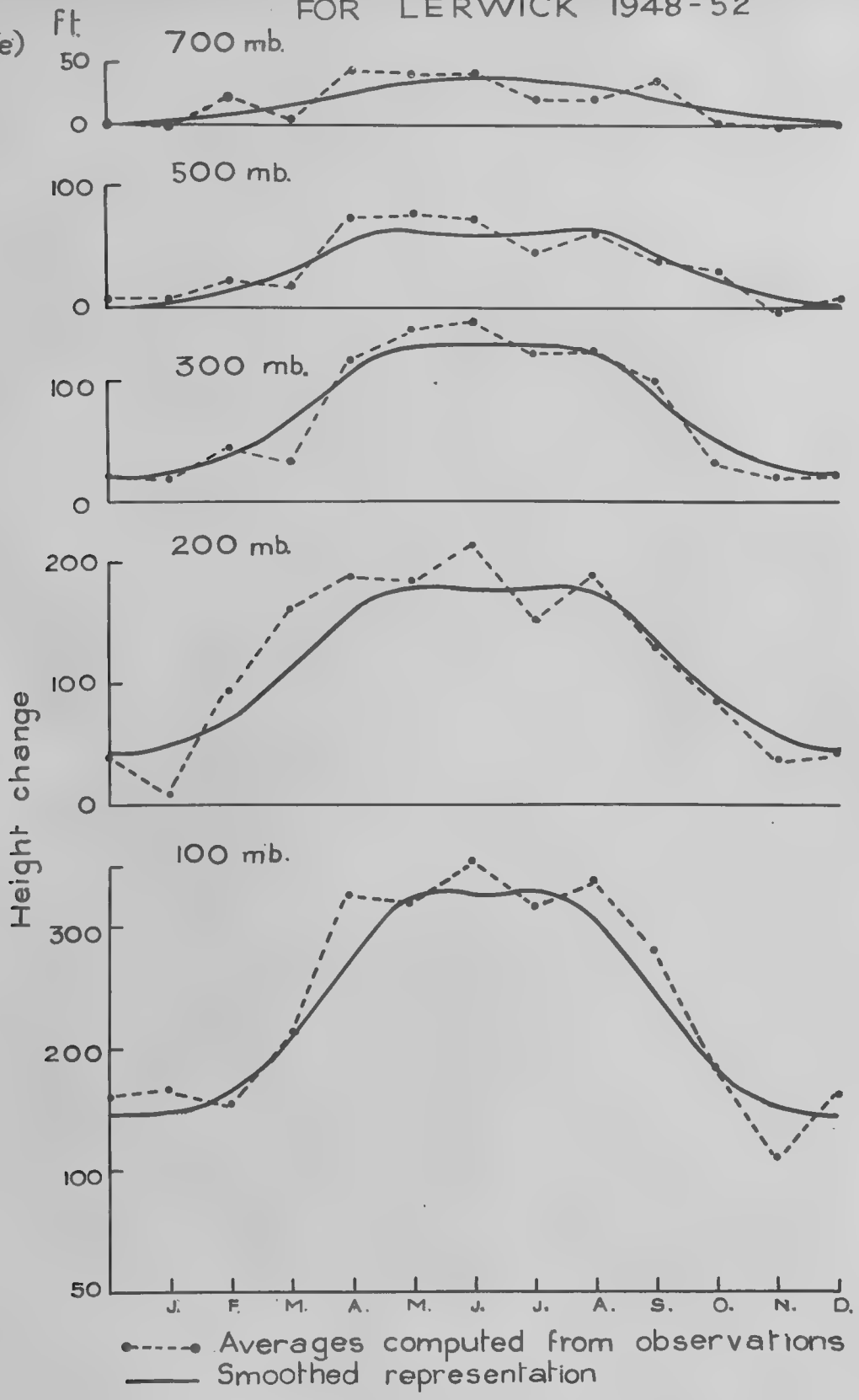

MONTHLY MEAN 1500-0300 G.M.T. CHANGE OF CONTOUR HEIGHT FOR MALTA 1949-52

Fig. 9(a)

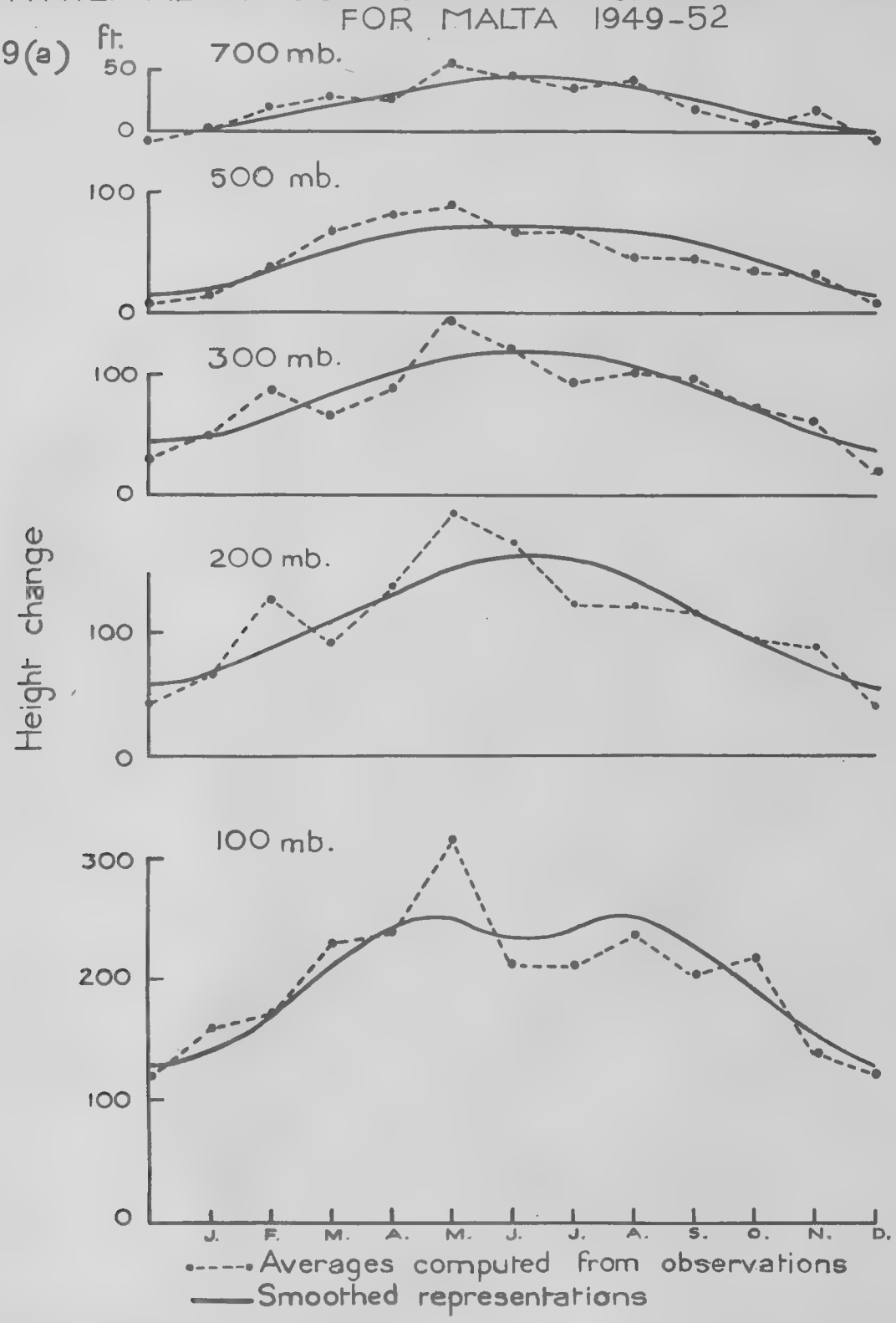

MONTHLY MEAN 1500 - 0300 G.M.T. CHANGE OF CONTOUR HEIGHT FOR NICOSIA 1948-52

Fig.9(b)

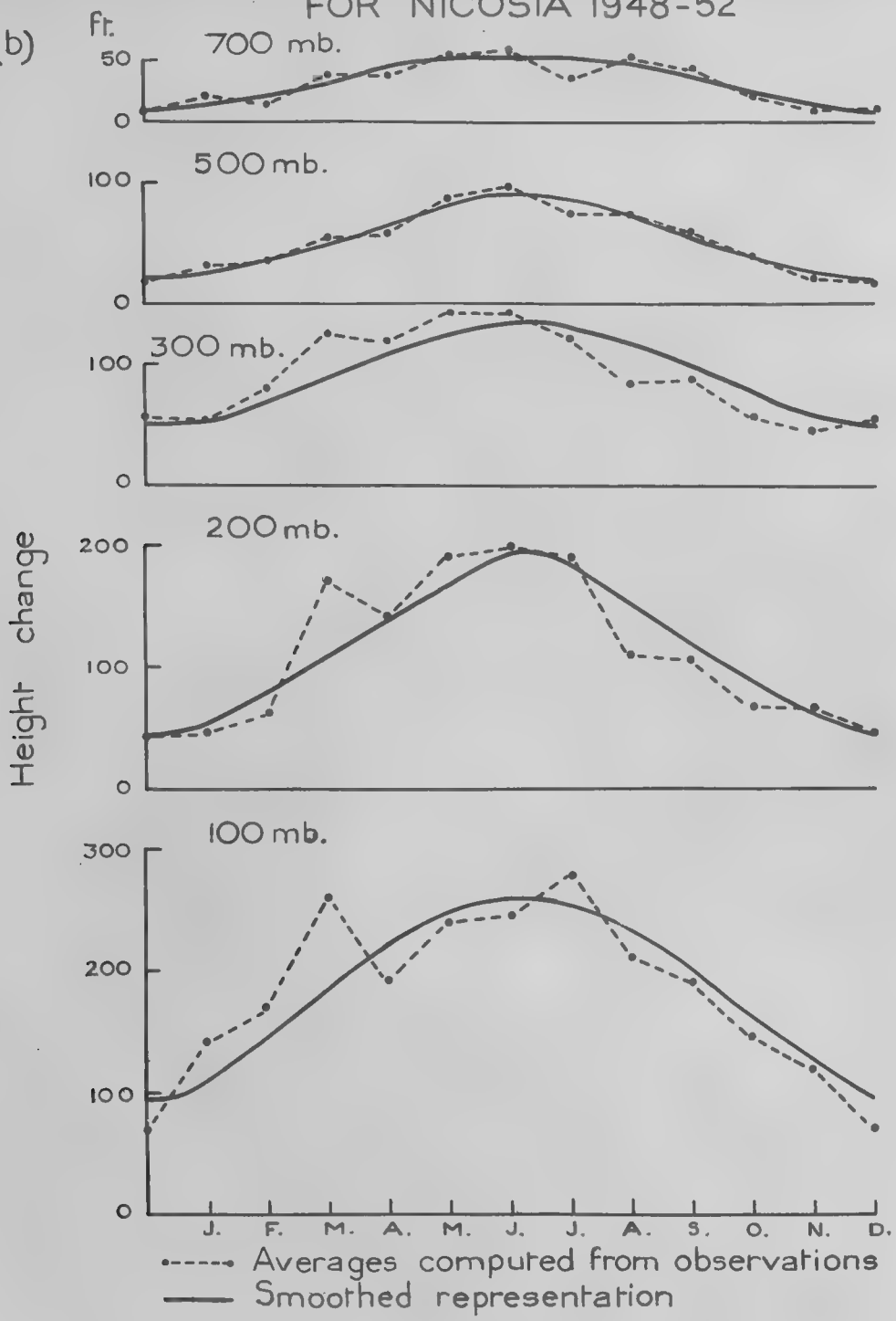

Fig.10 THE INTERDIURNAL VARIATION OF CONTOUR HEIGHT

(a) Winter (Larkhill and Lerwick combined, Dec-Feb. 1952-3)

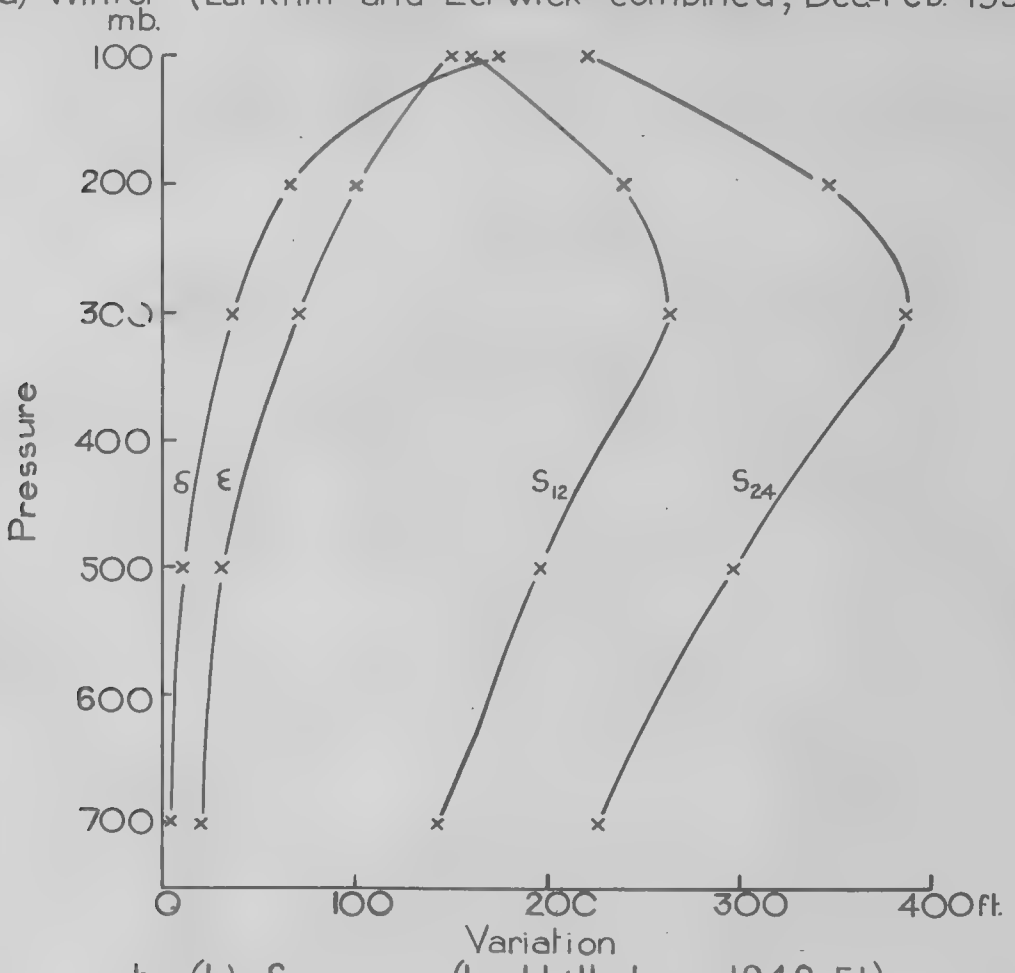

mb. (b) Summer (Larkhill, June 1948-51)

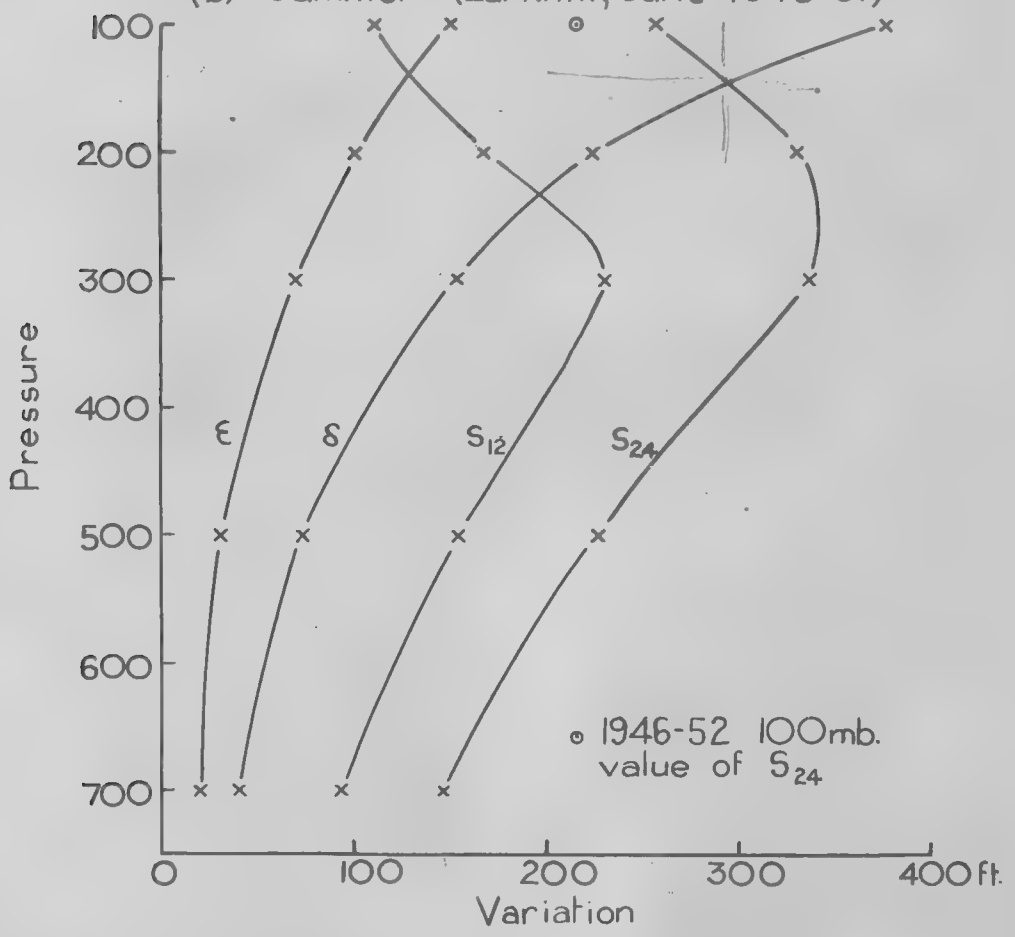

δ = Diurnal variation

ε = Standard error of measurement

S_{12} = 12hr. synoptic variation

S_{24} = 24hr. synoptic variation

Res.

[illegible]

R.P. No. 889 by Dr. F. J. Scrase
copy is available in the Library of
[illegible]

[illegible]

The radiation error of a radio sonde at any particular height and solar [illegible] of the reflecting surface below the sonde, on the [illegible] swinging of the sonde on its suspension. Some values of [illegible] radio sonde at various heights and solar altitudes are [illegible] is an expanded version of Table Vd of M.R.P. [illegible]

[illegible]	"	"	" long waves	0.18
[illegible]	[illegible]	[illegible]	[illegible]	[illegible]

mb (b) Summer

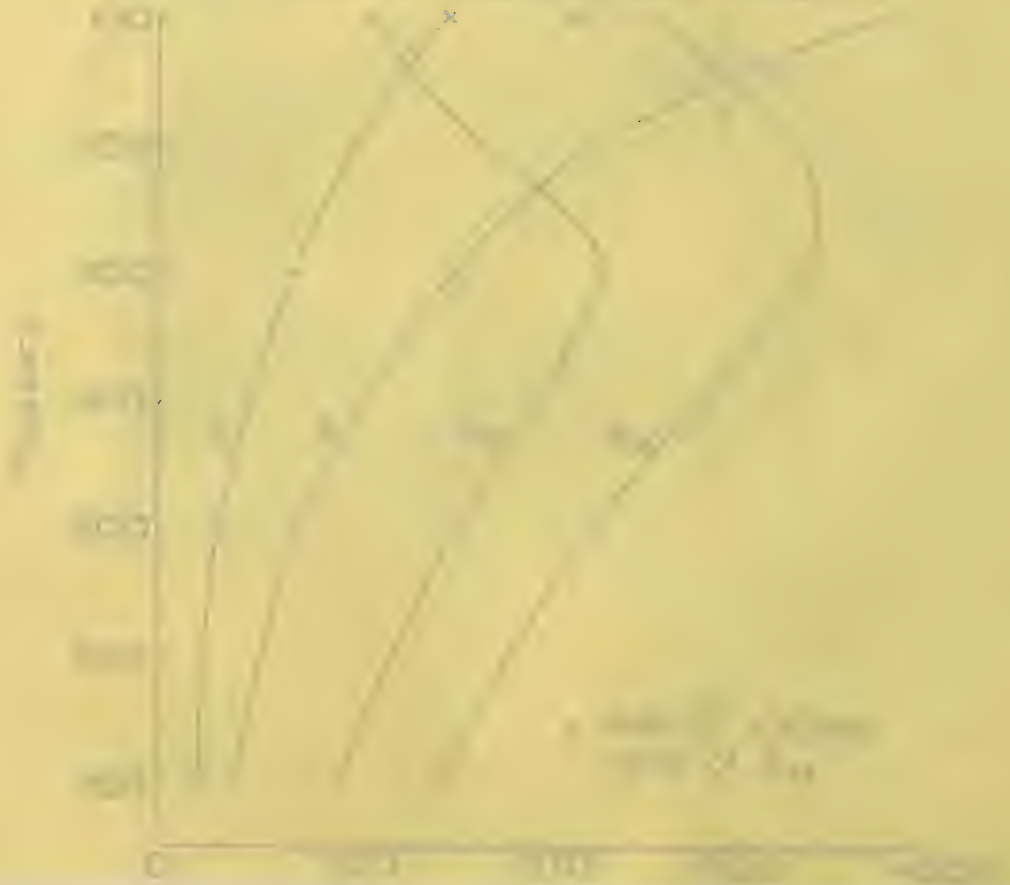

Variation

At the time of issue this report has not been published. Any author desiring to quote this paper should refer to it as "A paper of the Meteorological Research Committee (London). M.R.P. No. 889 by Dr. F. J. Scrase A copy is available in the Library of the Meteorological Office."

M.R.P. 889
S.C.I/95
S.C.II/180
19th November, 1954.

AD 23075

AIR MINISTRY

METEOROLOGICAL RESEARCH COMMITTEE

THE APPLICATION OF RADIATION AND LAG CORRECTIONS TO RADIO SONDE TEMPERATURES

by

F.J. Scrase (Meteorological Office)

Introduction

The radiation error of a radio sonde at any particular height and solar altitude depends on the absorption factors of the temperature element and its shield, on the albedo of the reflecting surface below the sonde, on the rate of ascent and on the swinging of the sonde on its suspension. Some values of the errors for the M.O. radio sonde at various heights and solar altitudes are given in Table I, which is an expanded version of Table Vd of M.R.P. 836. These values are calculated for the following conditions:

Absorption factor of element for short waves	0.67
" " " " long waves	0.18
" " shield for short waves	0.33
" " " " long waves	0.03
Albedo	0.35
Rate of ascent	6 m/sec
Maximum angle of swing	30°

Comparisons of calculated and observed radiation effects indicate that the values given in Table I are probably accurate to within 7 per cent.

We have to decide to what extent we should attempt to allow for variations in the above conditions. So long as the materials and finish of the element and shield remain unchanged their absorption factors will not differ much from the values quoted above. Variations in the swinging of the sonde would be difficult to take into account but on most occasions the assumption of a 30° angle of swing would be good enough for practical purposes.

Effect of albedo

The albedo of 0.35 is probably the best all-round value for earth surfaces with some cloud cover. Albedos for cloud appear to vary between 0.4 and 0.75, for snow and ice between 0.45 and 0.85 and for water between 0.05 and 0.45. Values ranging from 0.1 to 0.6 are, therefore, likely to be encountered in some situations. For these limits the values of the radiation errors of Table I would have to be multiplied by the following factors at all heights:

Solar altitude	10°	30°	50°	70°	90°
Albedo 0.1	0.98	0.87	0.84	0.80	0.82
Albedo 0.6	1.07	1.15	1.17	1.20	1.19

Thus, except at low solar altitudes, a change of 0.1 in the albedo alters the radiation error by about 7 per cent. In view of the difficulty which radio sonde stations would have in estimating the albedo it seems inadvisable to attempt to allow for variations from the value assumed for average conditions.

/Effect

Effect of rate of ascent

The rate of ascent of 6 m/sec (1200 ft./min.) used for Table I is about the average between 1000-400mb. but there is usually a systematic increase up to the tropopause and a decrease above that level. The change with height is roughly as follows:

Height, Km.	0	3.0	6.3	9.2	11.8	16.2	>18
mb.	1000	700	450	300	200	100	<70
Rel. rate of ascent	1.0	1.0	1.05	1.15	1.15	1.02	1.0

It would therefore be appropriate to modify Table I to take account of these systematic changes, bearing in mind that the radiation error varies inversely as the square root of the rate of ascent, except in the lower levels where the errors are, in any case, small.

The variations in rate of ascent from one sounding to another have a standard deviation of about 7 per cent. Most of these variations would, therefore, be within 20 per cent. of the average and the corresponding radiation errors within 10 per cent.

If an accuracy of 0.25°C. is aimed at, account should be taken of any large difference in the rate of ascent from normal at levels above 200 mb. with high solar altitudes and above 40 mb. with low solar altitudes. The corrections would be obtained by multiplying those given for the standard rate of ascent by the square root of the ratio of the standard rate to the actual rate.

Solar altitude

For corrections at the higher levels it is desirable to know the solar altitude to the nearest 5°. This could be obtained from Fig. 28 of the Observer's Handbook if the diagrams were extended to cover higher solar altitudes. Suitable diagrams are included in the U.S.W.B. Manual of Radio sonde Observations, Circular P. The time used for obtaining the solar altitude should be that at which the sonde reaches 200 mb. i.e. about 30 min. after the time of release.

Lag corrections

As the lag error depends directly on the lag coefficient and the rate of change of temperature of the thermometer element, the most accurate way of correcting for this error is to evaluate it from the appropriate lag coefficient and the rate of change shown on the temperature (frequency)/time graphs plotted for routine soundings. However, it should generally suffice to adopt a simpler procedure by assuming a constant lapse rate of, say, 6°C/Km in the troposphere and isothermal conditions in the stratosphere.

On this basis, and using the lag coefficients for a rate of ascent of 6 m/sec given in Table VI of M.R.P. 836, the corrections to be applied, to night as well as to day measurements, are those given in Table III. They have not been adjusted for the systematic change in rate of ascent with height since this would make no significant difference.

For the isothermal stratosphere no lag corrections are necessary at night but by day at high levels they are necessary because of the rapid change of radio sonde temperature with radiation absorption and rapidly diminishing convective heat loss. These corrections are worked out in Table II, using the rate of change of radiation error with height given in M.R.P. 836. They can, of course, be combined with the radiation corrections of Table I into a single table. It will be noted that they are hardly significant at levels below 50 mb. and they do not vary much with solar altitude.

Lapse rates differing by more than 1°C/Km from the assumed values would not alter the lag corrections by more than 0.25°C. except at levels above 40 mb.

/Recommendation

Recommendation

It is suggested that for routine reports of radio sonde temperatures Tables I and II should be combined to provide radiation corrections for day time soundings and Table III should be used to correct for lag errors in day and night soundings in the troposphere.

G.419389/PD/10/54/50

TABLE II

Lag corrections to radiation corrections

°C	0°	10°	20°	30°	40°	50°	60°	70°	80°	90°	Mean
(To be added)											
3.3	1.0	1.2	1.5	1.8	2.0	2.1	1.8	1.5	1.5	1.7	1.6
3.4	0.3	0.4	0.4	0.4	0.5	0.5	0.5	0.5	0.5	0.5	0.5
3.8	0.1	0.2	0.2	0.3	0.3	0.3	0.3	0.3	0.3	0.3	0.3
3.6	0.1	0.1	0.2	0.2	0.2	0.2	0.2	0.2	0.2	0.2	0.2
3.8	0.1	0.1	0.1	0.1	0.1	0.1	0.1	0.1	0.1	0.1	0.1
4.1	0.1	0.1	0.1	0.1	0.1	0.1	0.1	0.1	0.1	0.1	0.1
4.6	0.0	0.1	0.1	0.1	0.1	0.1	0.1	0.1	0.1	0.1	0.1
4.3	0.0	0.0	0.1	0.1	0.1	0.1	0.1	0.1	0.1	0.1	0.1
5.0	0.0	0.0	0.0	0.1	0.1	0.1	0.1	0.1	0.1	0.1	0.1
5.8	0.0	0.0	0.0	0.1	0.1	0.1	0.1	0.1	0.1	0.1	0.1
5.6	0.0	0.0	0.0	0.1	0.1	0.1	0.1	0.1	0.1	0.1	0.1
6.1	0.0	0.0	0.0	0.1	0.1	0.1	0.1	0.1	0.1	0.1	0.1
6.4	0.0	0.0	0.0	0.1	0.1	0.1	0.1	0.1	0.1	0.1	0.1
6.8	0.0	0.0	0.0	0.1	0.1	0.1	0.1	0.1	0.1	0.1	0.1
7.1	0.0	0.0	0.0	0.1	0.1	0.1	0.1	0.1	0.1	0.1	0.1
7.6	0.0	0.0	0.0	0.1	0.1	0.1	0.1	0.1	0.1	0.1	0.1
7.8	0.0	0.0	0.0	0.1	0.1	0.1	0.1	0.1	0.1	0.1	0.1
8.0	0.0	0.0	0.0	0.1	0.1	0.1	0.1	0.1	0.1	0.1	0.1
8.3	0.0	0.0	0.0	0.1	0.1	0.1	0.1	0.1	0.1	0.1	0.1
8.6	0.0	0.0	0.0	0.1	0.1	0.1	0.1	0.1	0.1	0.1	0.1
8.8	0.0	0.0	0.0	0.1	0.1	0.1	0.1	0.1	0.1	0.1	0.1
9.1	0.0	0.0	0.0	0.1	0.1	0.1	0.1	0.1	0.1	0.1	0.1
9.4	0.0	0.0	0.0	0.1	0.1	0.1	0.1	0.1	0.1	0.1	0.1
9.7	0.0	0.0	0.0	0.1	0.1	0.1	0.1	0.1	0.1	0.1	0.1
10.0	0.0	0.0	0.0	0.1	0.1	0.1	0.1	0.1	0.1	0.1	0.1
10.3	0.0	0.0	0.0	0.1	0.1	0.1	0.1	0.1	0.1	0.1	0.1
10.6	0.0	0.0	0.0	0.1	0.1	0.1	0.1	0.1	0.1	0.1	0.1
10.9	0.0	0.0	0.0	0.1	0.1	0.1	0.1	0.1	0.1	0.1	0.1
11.2	0.0	0.0	0.0	0.1	0.1	0.1	0.1	0.1	0.1	0.1	0.1
11.5	0.0	0.0	0.0	0.1	0.1	0.1	0.1	0.1	0.1	0.1	0.1
11.8	0.0	0.0	0.0	0.1	0.1	0.1	0.1	0.1	0.1	0.1	0.1
12.1	0.0	0.0	0.0	0.1	0.1	0.1	0.1	0.1	0.1	0.1	0.1
12.4	0.0	0.0	0.0	0.1	0.1	0.1	0.1	0.1	0.1	0.1	0.1
12.7	0.0	0.0	0.0	0.1	0.1	0.1	0.1	0.1	0.1	0.1	0.1
13.0	0.0	0.0	0.0	0.1	0.1	0.1	0.1	0.1	0.1	0.1	0.1
13.3	0.0	0.0	0.0	0.1	0.1	0.1	0.1	0.1	0.1	0.1	0.1
13.6	0.0	0.0	0.0	0.1	0.1	0.1	0.1	0.1	0.1	0.1	0.1
13.9	0.0	0.0	0.0	0.1	0.1	0.1	0.1	0.1	0.1	0.1	0.1
14.2	0.0	0.0	0.0	0.1	0.1	0.1	0.1	0.1	0.1	0.1	0.1
14.5	0.0	0.0	0.0	0.1	0.1	0.1	0.1	0.1	0.1	0.1	0.1
14.8	0.0	0.0	0.0	0.1	0.1	0.1	0.1	0.1	0.1	0.1	0.1
15.1	0.0	0.0	0.0	0.1	0.1	0.1	0.1	0.1	0.1	0.1	0.1
15.4	0.0	0.0	0.0	0.1	0.1	0.1	0.1	0.1	0.1	0.1	0.1
15.7	0.0	0.0	0.0	0.1	0.1	0.1	0.1	0.1	0.1	0.1	0.1
16.0	0.0	0.0	0.0	0.1	0.1	0.1	0.1	0.1	0.1	0.1	0.1
16.3	0.0	0.0	0.0	0.1	0.1	0.1	0.1	0.1	0.1	0.1	0.1
16.6	0.0	0.0	0.0	0.1	0.1	0.1	0.1	0.1	0.1	0.1	0.1
16.9	0.0	0.0	0.0	0.1	0.1	0.1	0.1	0.1	0.1	0.1	0.1

TABLE III

°C	Lag corrections for 6°C/km Subtract for lapse
3.3	3.9
3.4	2.3
3.8	1.7
3.6	1.5
3.8	1.3
4.1	1.1
4.6	1.0
4.3	0.9
5.0	0.9
5.8	0.8
5.6	0.8
6.1	0.7
6.4	0.6
6.8	0.6
7.1	0.5
7.6	0.5
7.8	0.4
8.0	0.4
8.3	0.4
8.6	0.3
8.8	0.3
9.1	0.3
9.4	0.3
9.7	0.3
10.0	0.3
10.3	0.3
10.6	0.3
10.9	0.3
11.2	0.3
11.5	0.3
11.8	0.3
12.1	0.3
12.4	0.3
12.7	0.3
13.0	0.3
13.3	0.3
13.6	0.3
13.9	0.3
14.2	0.3
14.5	0.3
14.8	0.3
15.1	0.3
15.4	0.3
15.7	0.3
16.0	0.3
16.3	0.3
16.6	0.3
16.9	0.3

of a horizontal surface, the intensity of the direct

bright sunshine, have been made at Kew Observatory

observations is demonstrated and a

vements is proposed. The additional

At the time of issue this report has not been published. Any author desiring to quote this paper should refer to it as "A paper of the Meteorological Research Committee (London), M.R.P. No.894 by Messrs. M.J. Blackwell, R.H. Eldridge and G.D. Robinson, A copy is available in the Library of the Meteorological Office."

M.R.P.894
S.C.III/178
7th December, 1954.

AD 223021

AIR MINISTRY

METEOROLOGICAL RESEARCH COMMITTEE

Estimation of the reflection and absorption of solar radiation by a cloudless atmosphere from recordings at the ground, with results for Kew Observatory

by

M.J. Blackwell, R.H. Eldridge and G.D. Robinson
(Meteorological Office)

Summary

Records of the total and diffuse solar radiation received on a horizontal surface, the illumination of a horizontal surface, the intensity of the direct solar beam for the whole spectrum and for two spectral regions defined by filters, and the duration of bright sunshine, have been made at Kew Observatory during various periods since 1946. The results are compared with those to be expected from an extraterrestrial distribution of solar radiation recently proposed by Nicolet (1951a, 1951b) and the known attenuation of an unpolluted atmosphere.

The mutual consistency of the various observations is demonstrated and a small correction to the illumination measurements is proposed. The additional absorption and scattering of the cloudless atmosphere at Kew are computed, and its albedo deduced.

1. Introduction

Continuous records of solar radiation and illumination have been maintained for some years at Kew Observatory, and the work to be reported was begun as an investigation of the mutual consistency of these records. It soon became clear that, at least as regards the means of large numbers of readings, this consistency was greater than had been expected, and that by comparison of the different elements useful results on the absorption and reflection of the atmosphere could be extracted. Whilst the precision of the results is clearly not high, a study of recent work on atmospheric albedo, particularly that of Fritz (1951) suggested that even approximate estimates would be useful, owing to wide divergence of the values accepted by different workers in the quite recent past. The atmospheric albedo for a single locality is not of itself of general interest, but the recording of various components of the solar radiation is in progress at an increasing number of stations widely distributed over the earth and a method of estimating albedo from the records of such stations would provide a valuable addition to the methods available for estimating the planetary albedo. In this report we restrict ourselves to cloudless conditions; we hope to extend some aspects of the work to average and overcast conditions at a later stage.

There is one direction in which the results obtained at Kew have a specific interest, although being at the same time of less than the normal value in the general meteorological problem of the energy balance. Kew is situated in an industrial area, with pollution sources rather sparse to the south and southwest, moderate to southeast, west, and north, and with the bulk of the London source between east of north and south of east. Some effects of smoke are almost always visible to the eye; with easterly winds they are often quite spectacular. A qualitative indication of the effect of change from light westerly to light easterly winds is given by Fig.1.

/2.

2. The material used.

(i) Available observations.

The following records, which are made on a routine basis at Kew, have been used in this investigation. The majority have been, or will shortly be, described elsewhere, and only those details essential to the present study are given. The records will be referred to by the abbreviations which are indicated in brackets.

(a) Total solar radiation on a horizontal surface (T), by Moll-Gorczynski solarimeter and recording galvanometer ("Cambridge" thread recorder) (Blackwell 1954). Records for the years 1947-1951 inclusive have been used.

(b) Diffuse solar radiation on a horizontal surface (D), by the same means as T, with the direct radiation of the sun obscured by an annular shade, mounted on a polar axis, and subtending an angle varying with time of year between about 8° and 12° at the centre of the thermopile. The reading is "corrected" for the effect of the sky obscured by this ring on the assumption (obviously erroneous) that the diffuse radiation is uniform over the sky (Blackwell 1954). Records for the years 1947-1951 inclusive have been used.

(c) Solar intensity, i.e. flux of solar radiation in the direction of the solar beam (I) by Moll thermopile with aperture limited by diaphragms, mounted on a heliostat, recording in the same way as T and D. The difficulty of specifying precisely the effective aperture of such an instrument has been discussed at length by Bossy and Pastiels (1948). For the present purpose it must suffice to say that the angle subtended at the centre of the thermopile by the diameter of the diaphragm limiting the area of sky "seen" from that point is 10°, and that there is a "penumbral" zone of about twice this diameter (Stagg 1950). Selected records in the period March 1948 to June 1949 have been used.

(d) Intensity of solar radiation transmitted by a Chance filter OY2 about 2 mm. thick (I_Y). The instrument is similar to that used for I with the addition of the filter. The transmission of the filter was determined by spectrophotometry at the N.P.L., and is shown in Fig.2. Records in the period September 1947 to September 1948 have been used. Routine recording ceased in March 1949.

(e) Intensity of solar radiation transmitted by a Chance filter O.R.1 about 2 mm. thick (I_R). The instrument was identical with that used for I_Y, being mounted on the same heliostat. The transmission of the filter, determined at the N.P.L., is shown in Fig.2. Records in the period September 1947 to June 1949 have been used. Routine recording ceased in November 1949.

(f) Total illumination of a horizontal surface (vertical luminous flux) (L), by means of a selenium photocell corrected by filter to have the response of the I.C.I. normal eye (photopic vision). Blackwell (1953) has described this instrument and discussed the adjustment of the tabulations to allow for all known systematic errors. Blackwell's tabulations for the period 1947-1951 inclusive have been used.

(g) Duration of bright sunshine (S), by Campbell-Stokes recorder exposed and read in the manner laid down in the Meteorological Observer's Handbook.

For the present purpose we required values for "cloudless" occasions only. In the case of T, D, and L these were selected in the manner indicated by Blackwell (1953), all cases occurring in the period 1947-51 being included. The main criterion of "cloudlessness" was the appearence

/of

of the record. This does not exclude cloud at some distance from the sun, but effects of this were minimised by ignoring the first and last hours of each "cloudless" spell. In the case of I, I_Y, and I_R many readings obtained during cloudless intervals of less than 1 hour have been used; if cloud is not actually covering the sun its effect is confined to the diffuse radiation.

(ii) Errors of observation.

The use of actinometric measurements to give information on scattering and absorption in the atmosphere has long been advocated by Ångström (1951), and probably the most impressive work in this connection is that of Schuepp (1949). Such work is based on comparatively few measurements made in chosen conditions with great precision. The material we have used is of an entirely different character, being the tabulations of continuously recording instruments, made as part of the Observatory routine with no one application in mind. The precision of these measurements is treated at some length by Blackwell (1953, 1954); we mention here some relevant features with a minimum of discussion.

The tabulations comprise the estimated hourly values read, necessarily rapidly, from the thread recorder charts, and we will use both single hourly readings and means of large numbers. A single reading in cloudless conditions may be in error by 3% to 5% with high sun and 10% or more with low sun, due to incorrect estimation of the mean by the tabulator. This error is known not to be systematic and is probably negligible for means of large numbers of hourly values.

The tabulations of I, I_Y, and I_R, may be low because of incorrect alignment of the heliostats in the period between inspections (at least twice daily). This error will not be present in most of the single observations, but is almost certainly present in the means of large numbers. It would probably be seen and the reading excluded from tabulation if it became more than 10% in a single hour, but smaller errors are difficult to detect and a mean might be low by about 2%. Another systematic cause of low readings is the collection of dirt on glass domes and filters, affecting all instruments. These surfaces should be cleaned at all inspections, but are no doubt neglected occasionally, and at times an appreciable deposit collects even between inspections. This error, on single readings and means, is probably less than 1%.

There is a small systematic error in the readings of I_Y and I_R which has not been removed and which acts in opposition to those just mentioned. In use the thermopile (X, Fig.3) is protected by a layer of clear glass (Y) behind the filter (Z). Incident radiation is reflected from Y and Z in the manner shown in Fig.3. Reflection from the filter at A is included in the transmission data of Fig.2 and is allowed for in use. The thermopile is standardised with Y in position and the filter removed; reflection from Y (at B) is allowed for, but not re-reflection from the filter at C. The tabulations are therefore in excess by this amount, which is about 0.7% of the incident radiation.

Errors of L due to cosine law deviations and the temperature coefficient of the instrument are quite large. They have been removed from the mean tabulated values (Blackwell 1953) but it is not possible to do this retrospectively for individual hourly values, and we have used only means of L. Blackwell estimates that these means are correct within $\pm$ 5%, including the uncertainty of standardisation (2%) discussed below. No attempt has been made to correct T and D for cosine law and temperature coefficient errors. In the main these would affect the readings in opposite directions (standardisation is normally carried out near noon in summer, and the temperature coefficient is negative), and they are in any case much smaller than the corresponding errors of L. The effect on individual values is probably small except for low solar elevations (say 15°).

/On

On the whole the systematic errors so far discussed tend to reduce the tabulated T and D below the true values. This is counteracted by an effect which, whilst not an error of measurement, has the character of one for our present purpose. D, and in consequence T, as properly defined, includes radiation which has been reflected at the earth's surface and re-reflected by the atmosphere. In what follows we shall require the total and diffuse radiation transmitted by the atmosphere without regard to surface effects. Computation of the re-reflected component is not straightforward. The total albedo of the grass-land immediately surrounding Kew Observatory is rather more than 20%, that of a wide area of the surroundings must be rather less than this. The ground albedo for radiation in the visual range is estimated as less than 10%. The ground albedo is therefore highest in the infra red, where the atmospheric albedo is low, and lowest where the atmospheric albedo is high. Anticipating results to be presented later (Section 6) we may estimate the "re-reflected" component of D and T as 1% to 2% of T, and for our purpose we must regard D and T as being systematically high by this amount. In view of all the uncertainties we have set this against the opposing errors due to dirt, cosine law deviations, and shade ring "corrections", and used the tabulated values of D and T as the diffuse and total radiation transmitted by the atmosphere. We have however applied an adjustment of about 2% for this effect to L, since other systematic errors have been removed from L by "correction".

(iii) Standardisation of the records.

The relation of the Kew sub-standard radiometer to the radiation scales in common use has been discussed by Eldridge (1952). All the records (except of course L) are standardised ultimately by reference to one of the substandard Ångstrom pyrheliometers, and the tabulations are in terms of the "uncorrected" Ångstrom scale. The precision of a single standardisation is estimated as between 1% and 2%, but the errors are not systematic and long period means of the calibration factors have been used in preparing the tabulations. The Ångstrom scale is a little low (we shall assume a value of 1%) in comparison with the radiation scale established at the N.P.L., which agrees closely with the Smithsonian scales of 1932, 1934, 1948. The other scale in common use in meterological literature, the Smithsonian scale of 1913, is about 3% high in comparison with the Ångstrom scale. There is some doubt as to the precision of these comparisons, they may be in error by $\pm$ 0.5% (see e.g. Guild 1937).

The photometric readings (L) are standardised by means of lamps standardised in their turn at the N.P.L. (Blackwell 1953). The accuracy is stated by the N.P.L. to be $\pm$ 2%, and redeterminations lie within these limits.

(iv) The extraterrestrial radiation and illumination.

The general plan which we will follow is to start with radiation outside the atmosphere and to attempt to account for all losses in transmission in order to arrive at the observed value at the ground. A knowledge of the magnitude of the extraterrestrial radiation and illumination is therefore the first essential.

After some preliminary work with the specification of extraterrestrial solar radiation given in Smithsonian Meteorological Tables 6th Edn. p.416*, we decided that more coherent results were likely to be obtained with the specification given by Nicolet (1951a, b), and we have used this throughout. Nicolet's value of the solar constant is 138 mw cm^{-2} (1.98 cal cm^{-2} min^{-1}), on the Smithsonian scale of 1932-34-48, differing considerably from the value of 1.94 cal cm^{-2} min^{-1} on the Smithsonian scale of 1913, which has been generally accepted for many years. The two specifications differ mainly in the ultra-violet and infra-red regions.

Having decided on a specification of the extraterrestrial radiation it is possible to compute the extraterrestrial luminous flux. If I_λ is the

/solar

*Footnote. This edition will be referred to below as "Smithsonian Tables".

solar intensity at wavelength λ, y_λ the relative sensitivity of the ICI standard eye at this wavelength, and K the maximum attainable luminous efficiency, we have

$$L = K\int_\lambda I_\lambda y_\lambda d\lambda \qquad (1)$$

K may be computed by appeal to the definition of the photometric standard, a black body at the temperature of freezing platinum; its value depends only on the values used for the constants in Planck's radiation formula and for the temperature of the Platinum point. We have used the figure of 680 lumens watt^{-1} given in Smithsonian Tables p.449, and combined with Nicolet's data this gives 142 kilolux as the extraterrestrial luminous flux along the solar beam at mean solar distance. (The Smithsonian solar data give 138 kl.). It is of interest to note an abstract of a paper by F.S. Johnson (1954) suggesting a value of 2.00 $\pm$ 0.04 cal cm^{-2} min^{-1} on the "Smithsonian scale as explained in 1952", and a corresponding extraterrestrial illumination of 136.7 kl. The abstract does not give sufficient detail to investigate the differences in the computed luminous flux; the solar constant is close to Nicolet's but the spectral distribution is not specified in detail. Nicolet expressed great confidence in his relative spectral variation, but says that the absolute value may be in error by as much as 5%. This uncertainty is of course repeated in the corresponding illumination but it is not increased except in so far as the constants of Planck's equation and the Platinum freezing point are in doubt, since the computation of the illumination follows from the definition of the international standard of photometry. Our radiation measurements, on the Ångström scale, are probably 0.5 to 1% low relative to the scale on which 138 mw cm^{-2} is accepted as the most probable value of the solar constant. Our illumination measurements are tied to the N.P.L. photometric standard, and the stated uncertainty of 2% presumably includes any uncertainty in the realisation there of the international standard of photometry. We will proceed to compare the Kew measurements with the assumed and computed extraterrestrial values.

3. Attenuation of radiation by the cloudless atmosphere.

The main absorbers of solar radiation, and the only ones considered here, are O_3 and H_2O, with the possibility of absorption by any particulate matter which may be present (e.g. smoke, dust, "nuclei"). The scattering agents are air molecules and particulate matter. Molecular scattering may be computed: that due to the non-polar molecules is tabulated as "Rayleigh scattering", and we have used the transmission data of Smithsonian Tables p.431 in the present work. It has been found that even in the cleanest atmospheres there is attenuation of unabsorbed radiation in excess of the Rayleigh scattering. Fowle was able to correlate this extra scattering with the amount of water vapour in the atmosphere, he referred to it as "scattering by water vapour", and it is tabulated under this heading in Smithsonian Tables p.432. There is no theoretical support for this attribution, and the spectral distribution of this scattering has a form more consistent with a particulate than a molecular source, being appropriate to a broad distribution of particle size about a mean radius of 0.25 μ. We will compute this scattering by means of the Smithsonian transmission coefficients, but will refer to it as "Fowle scattering".

To compute the depletion of the direct solar beam by the clean atmosphere we proceed as follows. Taking the extraterrestrial radiation as specified by Nicolet in bands of 0.01 μ for wavelengths less than 0.75 μ, 0.05 μ from 0.75 μ to 1.50 μ, 0.10 μ from 1.50 μ to 2.00 μ, and 0.50 μ above 2.00 μ, compute the depletion due to ozone using the absorption coefficients of the Smithsonian Tables (p.429), supplemented at wavelengths greater than 0.60 μ by those of Craig (1950, p.23). Compute in turn the Rayleigh and Fowle scattering of the beam transmitted by ozone, using the Smithsonian Tables procedure. Finally determine the water absorption by means of Kimball's coefficients (Smithsonian Tables p.437), assuming all the absorption is at wavelengths greater than 0.70 μ. The errors in neglecting the scattering prior to O_3 absorption, and in considering the radiation absorbed by H_2O

/as

as not subject to prior depletion by scattering are negligible in the present context. The transmitted luminous flux in the direct beam follows by applying (1) to the transmitted direct radiation.

This computation has been made for a model atmosphere containing 2 mm O_3 and 2 cm precipitable water, for sinh 0.8, 0.4, and 0.2, where h is the solar altitude. This was chosen in the first place as being appropriate to several days in May 1948 which formed the first case treated. In view of the considerable computation involved, and the comparatively low precision of the measurements, this model has been taken as representing average conditions, and is used as a standard atmosphere in this report.

4. Angular distribution of scattered light - a working hypothesis.

To complete the comparison of attenuation in a clean atmosphere with the observations we require a method of computing the diffuse radiation D, the downward component of the radiation scattered from the direct beam, which will depend on the sun's altitude and the angular distribution of the scattering. Fig.4 shows this distribution for red and green light for single scattering by particles of radius 0.025 μ and 0.5 μ (Hilsum 1948). The position is complicated by multiple scattering; it is reasonable to expect this to increase the backward scattering from an assembly of particles, as in the case of cloud. We recall that the present measurements of the direct beam, I, I_Y, and I_R, include radiation scattered forward within a cone of semi-angle about 5°, so that practically all the scattering from particles of radius about 1 μ or more is included in the direct rather than the diffuse radiation. Furthermore this radiation is excluded from D by the shade ring, the correction for which assumes uniform scattering over the whole sky. With this in mind we suggest, as a working hypothesis, that upward and downward components of the diffuse radiation, as measured, are equal. The hypothesis is sound (for different reasons) when applied to Rayleigh scattering and scattering by large ($r > 1\mu$) particles. In the intervening range, which presumably includes the cause of the Fowle scattering, the hypothesis fails to some extent, more seriously for high solar altitudes than for low. We suggest that the general coherence of the results shows that this failure is not serious, and is not likely to introduce discrepancies in computed D of more than about 1% of the extraterrestrial radiation. It should of course be understood that the apertures of the direct beam thermopiles and the shade ring were not chosen with this application in mind, but rather as the smallest which could conveniently be constructed and kept in alignment.

5. Procedure.

Our objects are

(a) to examine the material for internal consistency

(b) to see how far the measurements can be explained in terms of the assumptions concerning extraterrestrial radiation, transmission by the model atmosphere, and angular distribution of scattering

(c) to deduce the modifications necessary to bring the transmission properties of the model atmosphere into the closest possible agreement with observation.

We have used five independent methods of approach.

(i) Comparison of L and ($I_Y - I_R$).

The difference between I_Y and I_R gives the transmitted radiation within a band approximately bounded by $\lambda = 0.55\mu$ and $\lambda = 0.64\mu$, as may be seen from Fig.2. The maximum eye sensitivity (I.C.I. eye) lies at $\lambda = 0.555\mu$, and we may therefore expect transmission of luminous flux to be closely analogous to the transmission of ($I_Y - I_R$)

/which

which we will denote by I_X. According to our assumptions L is given by the extraterrestrial luminous flux (L ext.) less the ozone absorption (LO_3abs), less half the scattered illumination (L scat.) i.e.

$$1/2\ L\ scat. = L\ ext. - L\ O_3 abs - L \qquad (2)$$

whilst half the scattered radiation between $\lambda = 0.55\mu$ and $\lambda = 0.64\mu$ is given by

$$1/2\ I_x\ scat. = 1/2\ I_x\ ext - 1/2\ I_x\ O_3 abs - 1/2\ I_x \qquad (3)$$

Half the scattered radiation, expressed as a fraction of the extraterrestrial radiation, is according to our assumptions the albedo, if we neglect ozone absorption of the radiation scattered outwards.

This quantity, computed for the model atmosphere, is shown in Fig.5 together with the curves determined from the measurements by means of (2) and (3). More details of the experimental values are given in Table I and Appendix I. It is possible, owing to the different way in which the absorption enters (2) and (3), to explain the observed curves of Fig.5 by means of the computed curves for the model and the same additional absorption and scattering for both L and I_X. These additional values are listed in Table I. This treatment implies that the additional absorption and scattering is appreciably independent of wavelength in the region between about 0.50μ and 0.65μ, and that the scattering satisfies our assumptions regarding angular distribution. The true albedo is then to be computed from (2) and (3) having regard to any additional absorption.

(ii) Comparison of the extraterrestrial radiation on a horizontal surface (Esinh) with the sum of T, D, and the known absorption.

On our assumptions D is equal to the radiation scattered outwards from the atmosphere, so that the sum of D, T, and the absorption should be equal to Esinh. Fig.6 shows T, D, and the absorption computed for the model atmosphere, expressed as fractions of Esinh, the mean of all readings being used. The sum falls short of Esinh by a fraction which can be accounted for only by additional absorption. The additional scattering is given by the difference between the observed values of D and those computed from the model, which are also shown on Fig.6. The additional scattering and absorption derived in this way is shown in Table II. It will be seen that we have computed absorption of the direct beam only, absorption of the downward scattered radiation has been neglected. Adjustment of this might change the values of the additional absorption and scattering by 1% or 2% of Esinh but not more.

(iii) Comparison of monthly totals of I, I_Y, I_R, and D.

The attenuation of the direct beam, and of those portions passed by the filters, was computed from the model for a range of solar elevations. Monthly totals of hourly values of I, I_Y, and I_R were available and the sunshine record S gave the fraction of each hour for which the direct beam had been observed, and hence the monthly total of extraterrestrial radiation against which to compare the tabulated values. Mean values of solar altitude appropriate to the month and hour were used. Such a mean is unreliable at low solar altitude, and since the sunshine record also fails at an appreciable value of I (about 15 mw cm^{-2}) the method was not applied for hours with mean solar altitude less than 10° ($\sin h < 0.175$). Two months, May and December 1948 were treated, the readings used being set out in Table III.

Tables IV and V give, for wavelength ranges $\lambda < 0.55\mu$ (i.e. $I - I_Y$) and $\lambda < 0.64\mu$ (i.e. $I - I_R$) respectively, the monthly totals of extraterrestrial radiation in the various ranges of sin h, the observed transmitted radiation, and the attenuation computed from the model. The final columns show the radiation unaccounted for, as a fraction of E, and as a fraction of the extraterrestrial radiation in the wavelength band. It is not possible

/from

from the present data to divide this into scattered and absorbed components. Table VI shows the corresponding figures for the whole spectrum. In this case the extra attenuation may be divided approximately into scattered and absorbed components by using values of D appropriate to the month and solar altitude. D values measured on cloudless occasions during May and December 1948 are shown in Table VI; the additional scattering is twice the difference between D and half the model scattering ("computed D").

(iv) Examination of I, I_R, T and D for selected hours.

A number of occasions had been noted as "cloudless" in the original tabulations of I_Y and I_R, the implication being that a careful scrutiny had disclosed no trace of cloud, including cirrus. This rarely occurs at Kew. On several of these occasions a standardisation of some or all the thermopiles had been made, so the records could be considered more than normally reliable. Several of these occasions, to which the check equality $T = I\sin h + D$ applied within about $\pm$ 2% were examined individually in the following way. $(I - I_R)\sin h$ and $I_R \sin h$, the radiation in the direct solar beam for $\lambda < 0.64\mu$ and $\lambda > 0.64\mu$, were taken, and added to the appropriate values of absorption, and upward and downward scattering computed from the model. The additional attenuation for the two bands was obtained by taking this sum from the appropriate extraterrestrial value, and this was divided between absorption and scattering (assumed the same up and down) by adjusting the total downward scattering to give the observed D, leaving the absorption by difference. The treatment is analogous to that of para.5(iii). The results are set out in Table VII, which shows the various components of the radiation in mw cm^{-2}. It will be noted that a small adjustment has been made to the downward component of the Rayleigh and Fowle scattering, to allow for absorption in the lowest layer of the atmosphere. The two occasions in May 1948 contain the means of observations made during corresponding hours on five successive days of a settled spell of exceptionally cloud free weather; the other occasions are for individual hours.

(v) Extrapolation of $I_Y - I_R$ to zero air mass.

The radiation in the band defined by $I_Y - I_R$ is, in the model atmosphere, subject only to the small Chappuis band absorption of ozone. We may regard it as approximately monochromatic, and expect its attenuation to conform to Beer's law, so that a plot of log $(I_Y - I_R)$ against air mass (cosec h) should be linear, and should yield the extraterrestrial radiation in the wavelength band when extrapolated to zero air mass, so long as atmospheric conditions remain steady during the period of observation. The difficulty is, of course, to find periods with steady conditions. The measurements were examined and periods chosen where observations had been obtained during four or more consecutive hours, or over at least a fourfold air mass range. (These periods were not necessarily cloudless). A plot of log $(I_Y - I_R)$ against cosec h was made, and all those occasions were retained on which a straight line could be drawn without straining the imagination. Many occasions could of course be rejected even before plotting. Only twelve suitable occasions were found in an 18 months record. The choice was subjective, but we can see no way of avoiding this. The plots were extrapolated to zero air mass. (Graphically; it was thought that the precision of the measurements, with regard to systematic errors, was not such as to justify least squares computation). The results, corrected to mean solar distance, are shown in Table VIII, and a selection of the plots in Fig.7. Nicolet's value of the extraterrestrial solar energy in the band passed by the filters is 16.85 mw cm^{-2} (See Appendix I). The agreement with this value is remarkable, having regard to the fact that the measurements are on the Ångstrom scale and should be increased by about 1% for comparison, but the mean deviation, though smaller than we would expect from our knowledge of the measurements, shows that no very useful contribution has been made to the problem of the solar constant. Nevertheless the evidence is not completely negligible, and supports our assumptions. By more elaborate and precise, but fundamentally similar and not more numerous, actinometric measurements in the less variable atmosphere of Davos, Schuepp (1949) has also advanced a "high" estimate of the solar constant.

/6.

6. Discussion of results.

(i) The mutual consistency of the observations.

The additional scattering and absorption computed by the methods of Section 5 are collected in Figs.8 and 9. The division between "visual" and "infra red" for method 5(iv) is at the cut-off of the OR1 filter $\lambda = 0.64\mu$, whereas "visual" for method 5(i) refers approximately to the band $\lambda = 0.50\mu$ to $\lambda = 0.64\mu$.

The most reliable estimates may be expected from method 5(ii). This involves the greatest quantity of homogeneous material (all cloudless occasions in 5 years), and the measurements of T and D are well standardised and least subject to known systematic error. The full lines on Figs.8 and 9 have been drawn through these results. Method 5(iv) also uses the well standardised selected readings of, so far as total scattering and absorption are concerned, only two instruments. The results should be reliable but would be expected to show considerable scatter by reason of the great variability of atmospheric transmission on individual occasions. This scatter would be expected to be increased in the separate "visual" and "infra red" estimates by the employment of a third observation I_R. These expectations are confirmed by Figs.8 and 9; the individual results are entirely consistent with the mean results of method 5(ii), but show some scatter about the mean lines. Method 5(iii) has the disadvantage of using the sunshine trace S to determine the fraction of the extraterrestrial radiation employed. With high sun and broken cloud such traces notoriously overestimate the duration of bright sunshine (it is possible to interpret the standard instructions for reading the trace as a positive invitation to overestimate). With low sun and heavy pollution the card might not be burnt at a time when I and I_R are still satisfactory records and an underestimate would result. An error in S would not affect the additional scattering determined by method 5(iii) (unless it were a very serious underestimate), but would be accumulated in the additional absorption, which is determined as the residue of attenuation after other sources have been accounted for. The scattering estimates are based on D for two or three cloudless days in the month combined with I and S for the whole month; this inhomogeneity might be expected to lead to larger errors in the additional scattering estimated by this method than by methods 5(ii) and 5(iv). Examination of Figs.8 and 9 again confirms these expectations; the derived additional scattering is reasonably consistent with the other estimates, with more scatter, the additional absorption is systematically high for the May results and systematically low for December, by amounts up to 10%. The overall agreement with the other methods is certainly as good as could be expected.

The situation with regard to method 5(i), involving L, is less satisfactory. The total attenuation shown in Table I is in reasonable agreement with the total attenuation in the visible given by method 5(iv), and with the total attenuation in the regions $\lambda < 0.55\mu$ and $\lambda < 0.64\mu$, given by method 5(iii) and set out in Tables IV and V. On the other hand the attribution of this attenuation entirely to a scattering process is not in accord with the direct evidence of method 5(ii), nor with the most reasonable interpretation of the results of the other methods. It is not possible to explain the discrepancy by changes in our assumptions regarding the model atmosphere, the computed attenuation, the angular distribution of scattering, or the extraterrestrial radiation, without at the same time decreasing the agreement between the other methods. The results are however very sensitive to systematic changes in L and we have computed the result of decreasing L by 5%. The resulting additional absorption and scattering are shown in Table IX and have been plotted in Figs.8 and 9. They are now in excellent agreement with the other values.

Blackwell (1953), discussing the illumination record, estimated that the mean figures should be accurate within ±5%. They have been subjected to considerable adjustments for known errors in the original tabulations, and are clearly less reliable than any of the other records we are concerned with here.

/There

There is little external material with which to compare them, what there is suggests that they may indeed be high. Blackwell has computed the 'luminous efficiency of daylight' from them, and his figure for cloudless conditions is the highest we have seen reported. The only comparable series of measurements of which we have found a record is that of Lopukhin (1953) at Tashkent, a locality probably less subject to smoke but more subject to dust haze than Kew. His results for cloudless conditions are shown in Fig.10; they are 5% to 10% less than Blackwell's.

To summarise: our measurements and assumptions form an internally consistent scheme with the exception of the measured illumination, which falls in line with the rest if reduced by about 5%, a figure which is just within the previously estimated limits of accuracy. The scheme implies that there is considerable absorption and scattering of solar radiation by a constituent, presumably particulate, of the cloudless atmosphere at Kew, which does not figure in our model. We recall that the model is based on known gaseous causes of attenuation with the addition of the imperfectly understood scattering observed by Fowle in clear mountain atmospheres. The postulated 'additional absorption' would be reduced if our accepted value of the solar constant were to be reduced (retaining Nicolet's relative spectral distribution): our only evidence against this is contained in the results of 5(v).

(ii) The additional attenuation.

Some further comments can usefully be made on the contents of Tables IV, V, VI, VII and IX, and Figs.8 and 9. We note first that all methods suggest that the absorption is about the same in the visual and infra red, and that its variation with solar elevation is qualitatively as expected. Its mean value is probably rather less than 10%. It is interesting to compare this "grey" absorption with the "additional radiation" found by Robinson (1947, 1950) in measurements of the atmospheric radiation at Kew. This increased the computed radiation by up to 10% i.e. up to possibly 6 or 7% of the black body radiation at surface temperatures, a result entirely consistent with the present measurements if we are concerned with a true grey absorber in the lower layers of the atmosphere.

The additional scattering also appears to be approximately "grey" in character. Method 5(iv) (Figs.8 and 9) suggests rather higher scattering in the visual than the infra red, and method 5(iii) (Tables IV, V and VI) suggests a maximum in the additional attenuation between $\lambda = 0.55\mu$ and $\lambda = 0.64\mu$, but the differences are small compared with the uncertainties of measurement and interpretation. A feature of the scattering curves which deserves comment is the nature of the variation with solar altitude. We have, except very roughly in applying method 5(iv), ignored absorption of the scattered radiation, both in computing the 'model' attenuation and in examining the results. This can have little effect with high solar elevations, but is probably already an important factor for sinh = 0.2. The 'model' scattering would be overestimated, and since, in all methods except 5(i), the additional scattering is arrived at by subtracting this model scattering from D, the additional scattering would be underestimated.

It is interesting to examine the day to day variation of the additional attenuation, and the observations provide several opportunities. The most convenient arises in the computation of transmission in the band $\lambda = 0.55\mu$ to $\lambda = 0.64\mu$ which is used in method 5(i). Fig.11 shows the distribution of the fractional transmission for sinh = 0.3 to 0.4 and sinh = 0.7 to 0.8, together with the model transmission. The very wide distribution is notable, and we see that the minimum (model) transmission is rarely approached. In spite of the fact that there is quite a high probability of 5% errors in individual transmission factors only one observation of the 750 used in preparing Fig.5 fell below the model value and that by no more than 1%. We may conclude that some additional attenuation is a universal feature of the atmosphere at Kew, even with the clearest air; it is therefore almost

/certainly

certainly a normal feature of the atmosphere everywhere in this country. The low transmission "tail" of the distributions of Fig.11 is undoubtedly the dismal effect of the London pollution.

We cannot from the observations find the corresponding frequency distribution for the additional absorption alone. There is no obvious reason why this should not be similar to Fig.11, but Robinson (1947) found a different type of distribution in his measurements of the atmospheric emission. This comprised a sharp peak of about 10% of all observations very near the estimated "model" value, with a fairly uniform tail to higher values. The emission observations are however too few in number, and the "model" emission too speculative a quantity, for any great weight to be laid on the results. It seems natural to attribute the additional scattering and absorption of solar radiation and the additional emission of long wave radiation to the same cause - natural and artificial nuclei, larger particles of smoke and dust, and undetected cloud, particularly cirrus. The scattering is however postulated to be at the same time approximately grey and approximately isotropic, so it cannot be explained in terms of single scattering by dielectric spheres. Multiple scattering, as in a thin cloud layer, scattering by irregularly shaped particles, or specular reflection, must be invoked.

(iii) Estimated albedo of the cloudless atmosphere.

The fraction of the incident flux of radiation returned by the cloudless atmosphere to space without change of wavelength, the albedo, follows immediately from our assumptions and the previous results. We have collected some values in Fig.12. The most important quantity meteorologically is the total albedo; on our assumptions this is merely the diffuse radiation expressed as a fraction of the extraterrestrial. This is curve 3 of Fig.12. We will term the fraction of the extraterrestrial solar illumination returned to space the "photometric albedo", to distinguish it from the albedo for radiation in the visible wavelength band, which is termed, by Fritz and others, the "visual albedo". The photometric albedo is given by the method of 5; and on the assumption that the measured L values are high by 5% is given by curve 1 of Fig.12. As we have seen, the photometric albedo cannot be deduced from our measurements by a completely self consistent argument if the L values are correct: according to the particular inconsistency adopted values ranging between ±4% of the curve of Fig.12 can be obtained without adjustment to the measured L. Method 5(i) allows an estimate of the albedo in the range $0.55\mu \leq \lambda \leq 0.64\mu$, which is also shown in Fig.12. The albedo in the ranges $\lambda \leq 0.64\mu$ and $\lambda \geq 0.64\mu$, from the results of Table VII is also shown, the latter range gives an indication of behaviour in the infra-red. Fig.12, of course, contains no new material, it is merely a combination of the material of Fig.9 with the computed scattering of the model atmosphere.

The albedo of a cloudless atmosphere is of interest mainly as part of the material necessary for computation of the planetary albedo by methods similar to those of Fritz (1951) and Houghton (1954). The interest of the results of Fig.12 is therefore limited by the fact that they refer to the special case of the London atmosphere. The method is likely to be of more interest in showing the possibilities of routine radiation recording. The present results show an unexpectedly high additional scattering, and Lopukhin's (1953) Tashkent observations cannot yield a very different value from ours. We therefore suggest that examination of other radiation records on similar lines would be interesting and possibly rewarding.

Measurement of the direct solar radiation transmitted by filters

Except for insertion of the filters the apparatus used to measure I_Y and I_R was similar to that used for I. These notes describe only the procedure necessitated by the use of filters.

The transmission factors are shown in Fig.2. They were determined at the N.P.L. in March 1950, i.e. after completion of the observations which have been discussed. They are in close agreement with the maker's specification for new filters, and it seems clear that deterioration of the type noted by Shulman (1943) was not serious. The N.P.L. certificate remarks "The accuracy of the measurement was limited by the quality of the filters to $\pm 1\%$", which confirms that there was no gross deterioration in use.

The first step in reduction of the measurements to give I_Y and I_R is the determination of the "equivalent sharp cut-off", at a wavelength λ_o given by

$$0.90 \int_{\lambda_o}^{0.7\mu} d\lambda = \int_{o}^{0.7\mu} T_\lambda d\lambda$$

where T_λ is the fractional transmission at wavelength λ . For OY2 this cut-off is at $\lambda_o = 0.553\ \mu$, for OR1 it is at $\lambda_o = 0.641\ \mu$. For a given spectral distribution of radiation $I(\lambda)$ a factor to convert transmitted (measured) radiation into radiation in the required wavelength range incident on the filter is given by

$$\int_{\lambda_o}^{\infty} I(\lambda)d\lambda \Big/ \int_{o}^{\infty} T_\lambda I(\lambda)d\lambda$$

For an ideal filter, with a step-function transmission curve, this factor is independent of the distribution $I(\lambda)$. The two filters used have excellent properties and the factor does not vary appreciably within a reasonable range of assumed distributions $I(\lambda)$. For that proposed by Shulman (1943) - the direct solar beam after transmission through unit air mass of dry atmosphere - the factor for OY2 is 1.133 and for OR1 1.136. A factor of 1.13 has been used for both filters.

The quantity used in Section 5(i), I_X, is the difference of the energies incident on the filters in the two wavelength ranges transmitted. To obtain this from the difference of the measured energies a factor

$$\int_{0.553\mu}^{0.641\mu} I(\lambda)d\lambda \Big/ \int_{o}^{\infty} (T_Y - T_R)I(\lambda)d\lambda$$

must be employed, where $I(\lambda)$ is the distribution of incident energy. For the extraterrestrial $I(\lambda)$ this factor is 1.128, and a value of 1.13 has been used.

/TABLE I

TABLE I

Comparison of transmission for illumination and for radiation $0.55\mu < \lambda < 0.64\mu$ (Method and notation of section 5(i)). All radiation values are % extraterrestrial.

Sinh	Illumination		$0.55\mu < \lambda < 0.64\mu$		Additional absorption	Additional scattering
	$\frac{1}{2}$ L scat.	No. of observations	$\frac{1}{2}$ I_X scat.	No. of observations		
0.1 to 0.2	42.5	7	33.5	66)	7	16
0.2 to 0.3	34.5	40	31	114)		
0.3 to 0.4	34	97	28.5	118)	1	28
0.4 to 0.5	27.5	81	25.5	92)		
0.5 to 0.6	27	83	23	109)	0	26
0.6 to 0.7	22.5	67	21	95)		
0.7 to 0.8	20	77	18.5	87)	0	20
0.8 to 0.9	17.5	42	17.5	68)		

TABLE II

Additional absorption and scattering of the total solar radiation. (Method and notation of section 5(ii)). % Extraterrestrial radiation.

Sinh	0.8	0.6	0.4	0.2
Additional absorption	6	8	12	15
Additional scattering	10	10	8	4

/TABLE III

TABLE III

Observed Totals of I, I_Y, I_R (joules cm^{-2}) and S (hours).

Month	LAT.	Mean Sinh	I	I_Y	I_R	S	Direct extraterrestrial radiation during periods of bright sunshine (E x S)	I - I_Y	I - I_R
May 1948	11 - 13	0.832	8630	6460	5390	33.7	16190	2170	3240
	13 - 14								
	10 - 11	0.790	8920	6920	5740	34.8	16740	2000	3180
	14 - 15								
	9 - 10	0.713	8550	6500	5540	34.5	16580	2050	3010
	15 - 16								
	8 - 9	0.603	7580	6140	5300	34.1	16400	1440	2280
	16 - 17								
	7 - 8	0.472	7240	5740	5040	34.3	16480	1500	2200
	17 - 18								
	6 - 7	0.325	5750	4970	4360	32.5	15620	780	1390
Dec. 1948	11 - 13	0.244	2990	2620	2300	19.1	9820	370	690
	13 - 14								
	10 - 11	0.185	2170	1960	1710	15.0	7720	210	460

TABLE IV

Attenuation of direct radiation $\lambda < 0.55\mu$. Entries are % of total extraterrestrial intensity except where stated. (Method of Section 5(iii)).

Month	Mean Sinh	Model atmosphere			Observed transmission	Additional attenuation	Additional attenuation as % waveband
		Absorption	Scattering	Transmission			
May 1948	0.832	0.7	8.8	17.7	13.4	4.3	16
	0.790	0.8	8.8	17.6	12.0	5.6	21
	0.713	0.9	9.3	17.0	12.6	4.4	16
	0.603	1.0	10.2	15.6	8.8	6.8	25
	0.472	1.1	13.6	13.5	9.1	4.4	16
	0.325	1.3	15.9	10.0	5.0	5.0	18
Dec. 1948	0.244	1.6	17.9	7.7	3.6	4.1	15
	0.185	1.9	20.0	5.3	2.8	2.5	9

/TABLE V

TABLE V

Attenuation of direct radiation $\lambda < 0.64\mu$. Entries are % of total extraterrestrial intensity except where stated. (Method of Section 5(iii)).

Month	Mean Sinh	Model atmosphere			Observed transmission	Additional attenuation	Additional attenuation as % waveband.
		Absorption	Scattering	Transmission			
May 1948	0.832	1.4	10.8	28.7	20.0	8.7	21
	0.790	1.6	11.0	28.3	19.0	9.3	22
	0.713	1.7	11.7	27.5	18.2	9.3	22
	0.603	1.9	13.4	25.6	14.0	11.6	28
	0.472	2.1	16.0	24.8	13.5	11.3	27
	0.325	2.4	20.1	18.4	8.8	9.6	23
Dec. 1948	0.244	2.7	23.0	15.2	7.0	8.2	20
	0.185	3.2	25.6	12.1	6.0	6.1	15

TABLE VI

Attenuation of direct radiation. Entries are % of total extraterrestrial intensity. (Method of Section 5(iii)).

Month	Mean Sinh	Model atmosphere				Observed D	Observed transmission	Additional attenuation	Additional scattering	Additional absorption
		Absorption	Scattering	Transmission	D (= ½ scattering)					
May 1948	0.832	12.0	13.3	74.7	6.7	10.9	53.4	21.3	8.4	12.9
	0.790	12.1	13.8	74.1	6.9	11.0	53.4	20.7	8.2	12.5
	0.713	12.4	14.9	72.7	7.5	10.3	51.6	21.1	5.6	15.5
	0.603	13.0	16.9	70.1	8.5	12.0	46.3	23.8	7.0	16.8
	0.472	14.1	20.2	65.7	10.1	13.2	44.0	21.7	6.2	15.5
	0.325	16.9	26.3	56.8	13.2	13.7	36.8	20.0	1.0	19.0
Dec. 1948	0.244	16.5	31.0	52.5	15.5	19.0	30.5	22.0	7.0	15.0
	0.185	17.6	36.0	46.4	18.0	23.0	28.0	18.4	10.0	8.4

/TABLE VII

TABLE VII

Analysis of direct and diffuse radiation on a horizontal surface for selected hours (Method of Section 5(iv)). Values are hourly means in mw cm^{-2} except where stated.

Date	LAT.	Mean Sinh	Wavelength range (μ)	Extraterrestrial I sinh	Observed I sinh	Observed D	Model atmosphere					Additional			
							O_3 Absorption	H_2O Absorption	Rayleigh and Fowle Scattering		Absorption	Scattering		Absorption % Ext.	Scattering % Ext.
									up	down		up	down		
12 March 1948	12 - 13	0.565	<0.64	32.8	16.2		1.6	-	5.4	5.0	2.2	1.2	1.2	7	7
			>0.64	46.0	25.6		-	8.7	1.6	1.5	3.3	2.7	2.7	7	12
			total	78.8	41.8	10.4				6.5			3.9	7	10
12 March 1948	15 - 16	0.33	<0.64	19.1	5.8		1.2	-	4.3	3.8	2.3	0.8	0.8	12	8
			>0.64	26.9	12.1		0.1	6.2	1.2	1.1	3.3	1.4	1.4	12	10
			total	46.0	17.9	7.0				4.9			2.2	12	9
15-19 May 1948	8 - 9 / 15 - 16	0.61	<0.64	34.3	14.6		1.7	-	5.5	5.1	2.8	2.3	2.3	8	13
			>0.64	48.2	30.0		0.1	9.1	1.6	1.5	3.9	1.0	1.0	8	4
			total	82.5	44.6	9.9				6.6			3.3	8	8
15-19 May 1948	10 - 11 / 13 - 14	0.80	<0.64	43.3	23.7		1.9	-	5.7	5.4	1.5	2.5	2.5	3	11
			>0.64	63.1	42.0		0.1	10.7	1.5	1.4	2.5	2.4	2.4	4	7
			total	106.4	65.7	11.7				6.8			4.9	4	9

TABLE VII(Contd.)

Date	LAT.	Mean Sinh	Wavelength range (μ)	Extraterrestrial I sinh	Observed I sinh	Observed D	Model atmosphere					Additional			
							O_3 Absorption	H_2O Absorption	Rayleigh and Fowle Scattering		Absorption	Scattering		Absorption % Ext.	Scattering % Ext.
									up	down		up	down		
26 July 1948	08 - 09	0.62	<0.64	34.4	17.3		1.7	-	5.5	5.2	2.1	1.3	1.3	6	8
			>0.64	48.2	30.2		0.1	9.1	1.6	1.5	2.9	1.4	1.4	6	6
			total	82.6	47.5	9.3				6.7			2.7	6	7
26 July 1948	11 - 12	0.835	<0.64	46.8	26.6		2.1	-	5.7	5.2	3.7	1.8	1.8	8	8
			>0.64	65.7	42.0		0.1	11.2	1.6	1.5	5.3	2.0	2.0	8	6
			total	112.5	68.6	10.5				6.7			3.8	8	7
21 June 1949	12 - 13	0.875	<0.64	48.2	23.6		2.2	-	5.8	5.2	5.4	3.0	3.0	11	12
			>0.64	67.6	49.6		0.1	11.6	1.7	1.7	2.7	0.1	0.1	4	0
			total	115.8	73.2	9.8				6.9			3.1	7	5
21 June 1949	17 - 18	0.385	<0.64	21.3	3.3		1.3	-	4.6	3.9	3.7	2.2	2.2	15	21
			>0.64	29.9	17.1		-	6.7	1.3	1.2	2.5	0.6	0.6	8	4
			total	51.2	20.4	7.6				5.1			2.8	11	11

/TABLE VIII

TABLE VIII

Direct radiation in wavelength region λλ 0.553μ - 0.641μ (i.e. $I_Y - I_R$), extrapolated to zero air mass, in mw cm^{-2} on Angstrom scale.

Date	Extrapolated intensity	Correction to mean solar distance	Corrected intensity
12th March '48	16.7	0.990	16.55
23rd April '48	17.8	1.011	18.00
7th May '48	15.4	1.019	15.70
16th May '48	15.4	1.022	15.75
17th May '48 (a.m.)	16.1	1.023	16.45
17th May '48 (p.m.)	16.7	1.023	17.10
18th May '48	15.4	1.023	15.75
3rd June '48	14.9	1.029	15.35
7th June '48	15.4	1.031	15.85
26th July '48	17.5	1.033	18.05
27th July '48	16.6	1.033	17.15
26th Sept. '48	16.8	1.006	16.90
Mean and Mean deviation			16.55±0.7
Extraterrestrial rad.^{n} according to Nicolet (Smithsonian 1933 scale)			16.85

TABLE IX

Additional scattering and absorption (% extraterrestrial) computed by the method of Section 5; on the assumption that the tabulations of L are 5% too high.

Sinh	0.8	0.6	0.4	0.2
Additional absorption	9	9	11	18
Additional scattering	14	16	16	4

/References

References

Ångström, A.	1951	Compendium Met., pp. 50-57.
Bossy, L. and Pastiels, R.	1948	Inst. Roy. Met. Belg. Mem. No.29.
Blackwell, M.J.	1953	M.R.P. 831.
Blackwell, M.J.	1954	MS. to be submitted to M.R.C.
Craig, R.A.	1950	Met. Monog. Amer. Met. Soc., 1, No.2.
Eldridge, R.H.	1952	Q.J.R. Met. S., 78, pp. 260-264.
Fritz, S.	1951	Compendium Met. pp. 13-33.
Guild, J.	1937	O.M.I. Strahlungskommission. Protokolle der Sitzungen in Oxford. Sept. 1936. pp. 53-57.
Hilsum, C.	1948	Atmospheric Attenuation of Infra-red and Visible Radiation. ARL/R3/E600.
Houghton, H.G.	1954	J. Met., 11., pp. 1-9.
Johnson, F.S.	1954	Bull. Amer. Met. Soc., 35, p. 83.
Lopukhin, E.A.	1953	Isvest. Akad. Nauk. U.S.S.R. Ser. Geophys. 5, p. 469.
Nicolet, M.	1951a	Archiv. fur Met. Geophys. u. Bioklim. B. 3, pp. 209-219.
	1951b	Annales Astrophys., 14, pp. 249-265.
Robinson, G.D.	1947	Q.J.R. Met. S., 73, pp. 127-150.
	1950	Q.J.R. Met. S., 76, pp. 37-51.
Schuepp, W.	1949	Archiv. fur Met. Geophys. u. Bioklim. B. 1, pp. 257-346.
Shulman, E.	1943	Harvard Met. Studies, No. 7.
Stagg, J.M.	1950	Geophys. Mem., 11, No. 86.

FIG. 1 ILLUSTRATING THE EFFECT OF ATMOSPHERIC POLLUTION ON ILLUMINATION AT KEW.

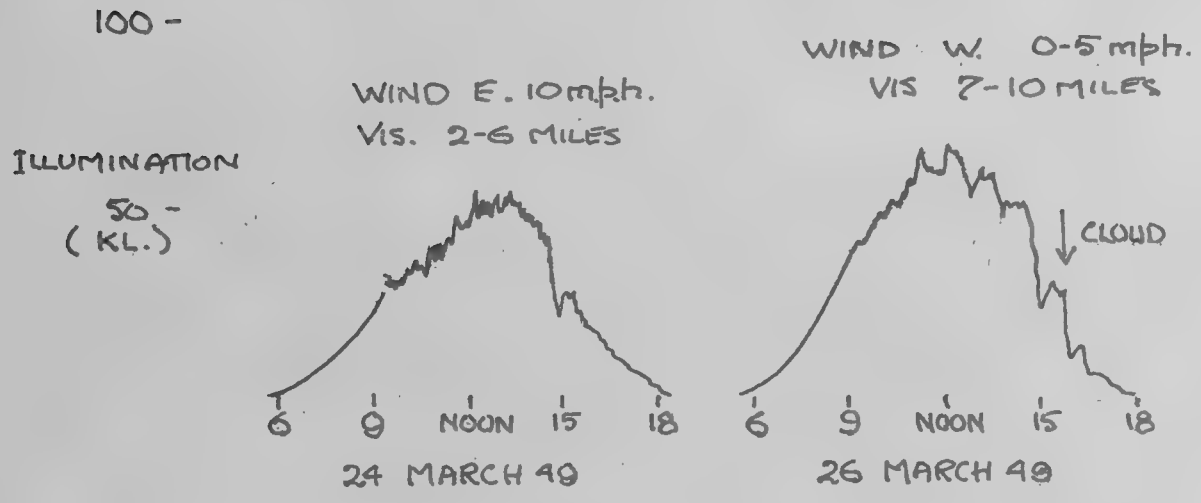

FIG 3 REFLECTION OF RADIATION FROM FILTER AND COVER GLASS.

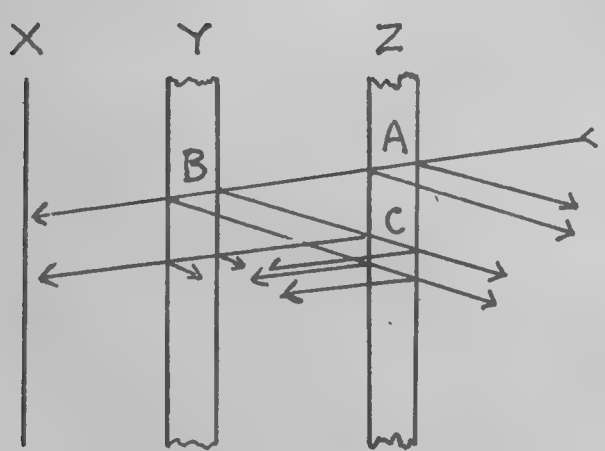

Fig 2. Transmission properties of the filters (at 20°C)

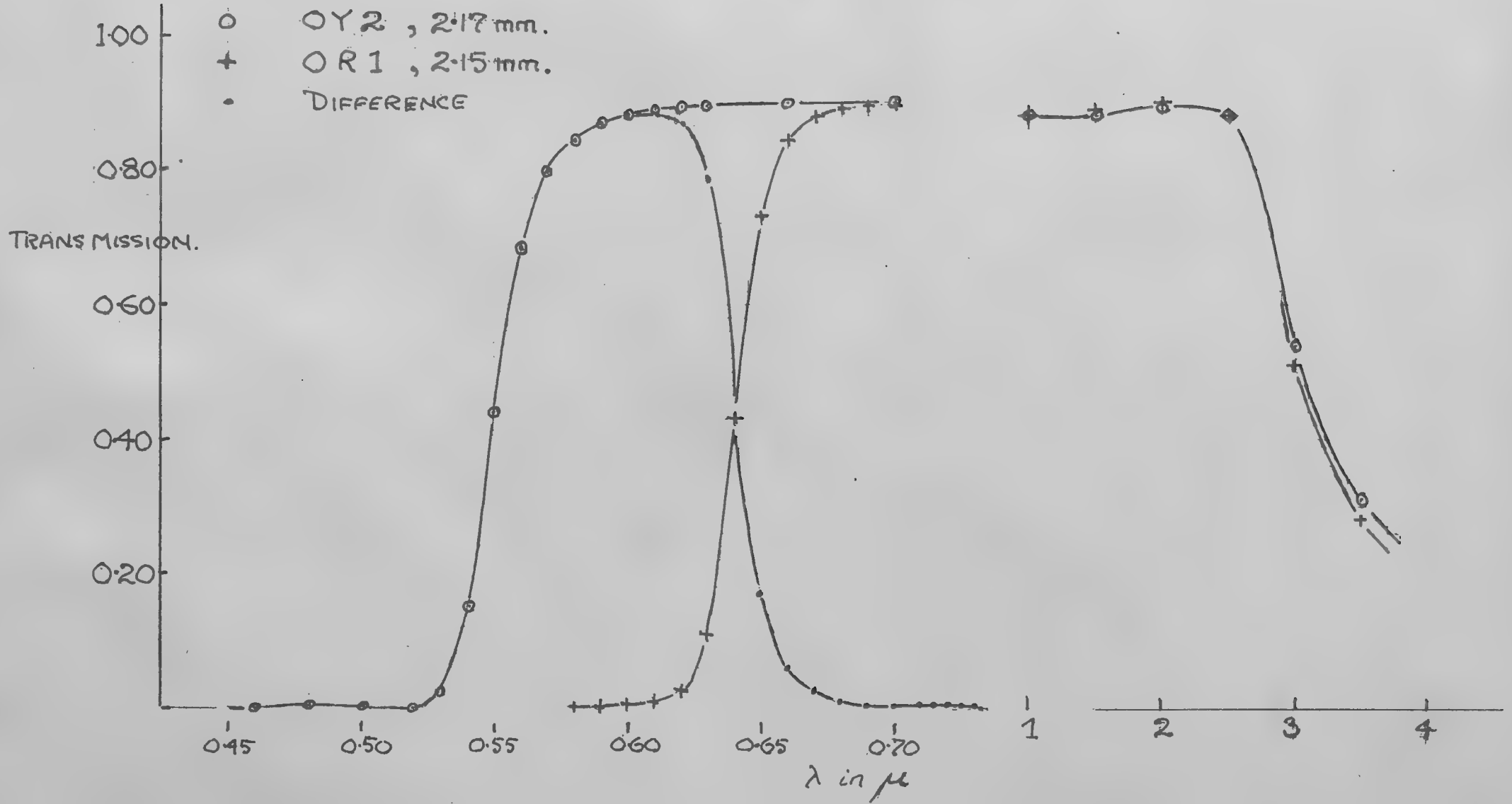

FIG 4. ANGULAR DISTRIBUTION OF LIGHT SCATTERED BY A SPHERICAL PARTICLE (HILSUM, 1948.) APERTURE OF RADIOMETER IS SHOWN.

(a). RADIUS 0·025 μ.

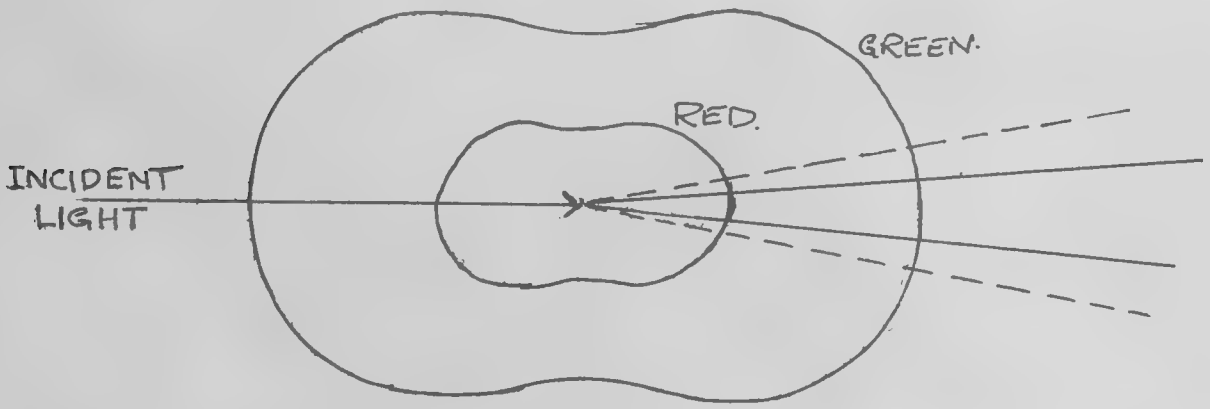

(b) RADIUS 0·5 μ.

SCALE OF (b) IS 3×10^7 x SCALE OF (a)

Fig 5 COMPARISON OF TRANSMISSION FOR ILLUMINATION AND FOR RADIATION IN RANGE $0.55\mu < \lambda < 0.64\mu$
METHOD AND NOTATION OF SECTION 5i

M.R.P. 894

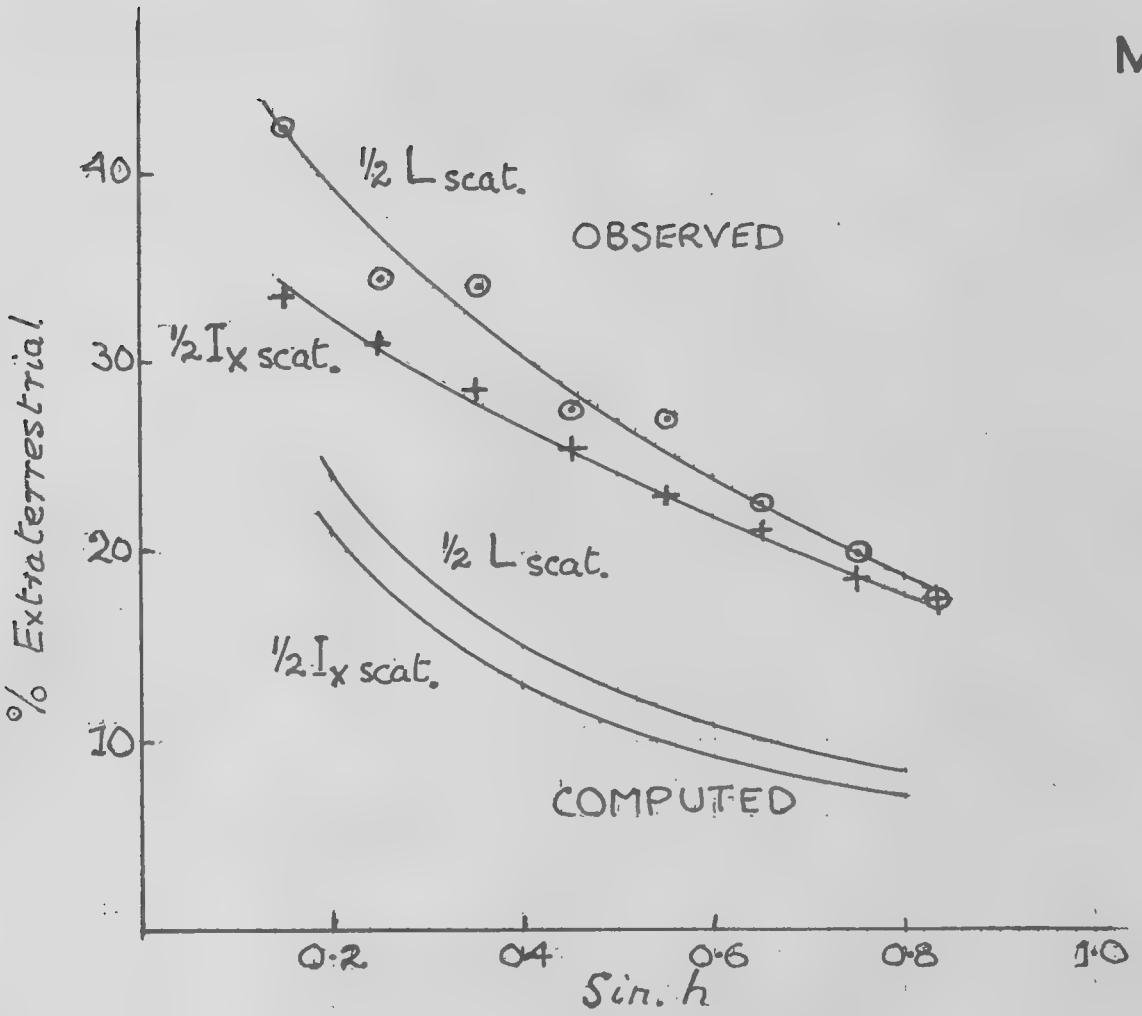

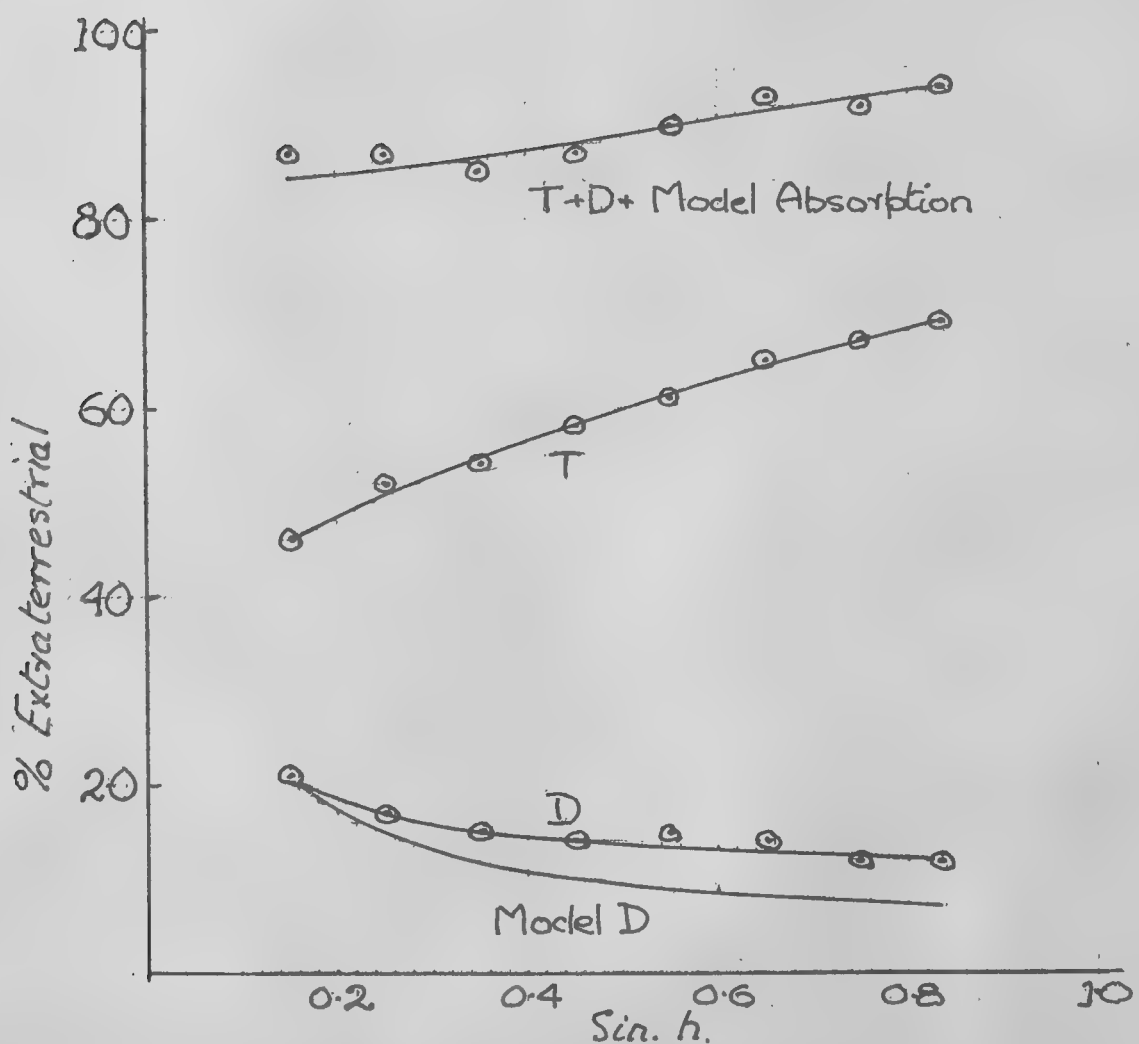

Fig. 6 ESTIMATION OF ADDITIONAL ABSORPTION AND SCATTERING. BY METHOD OF SECTION 5ii

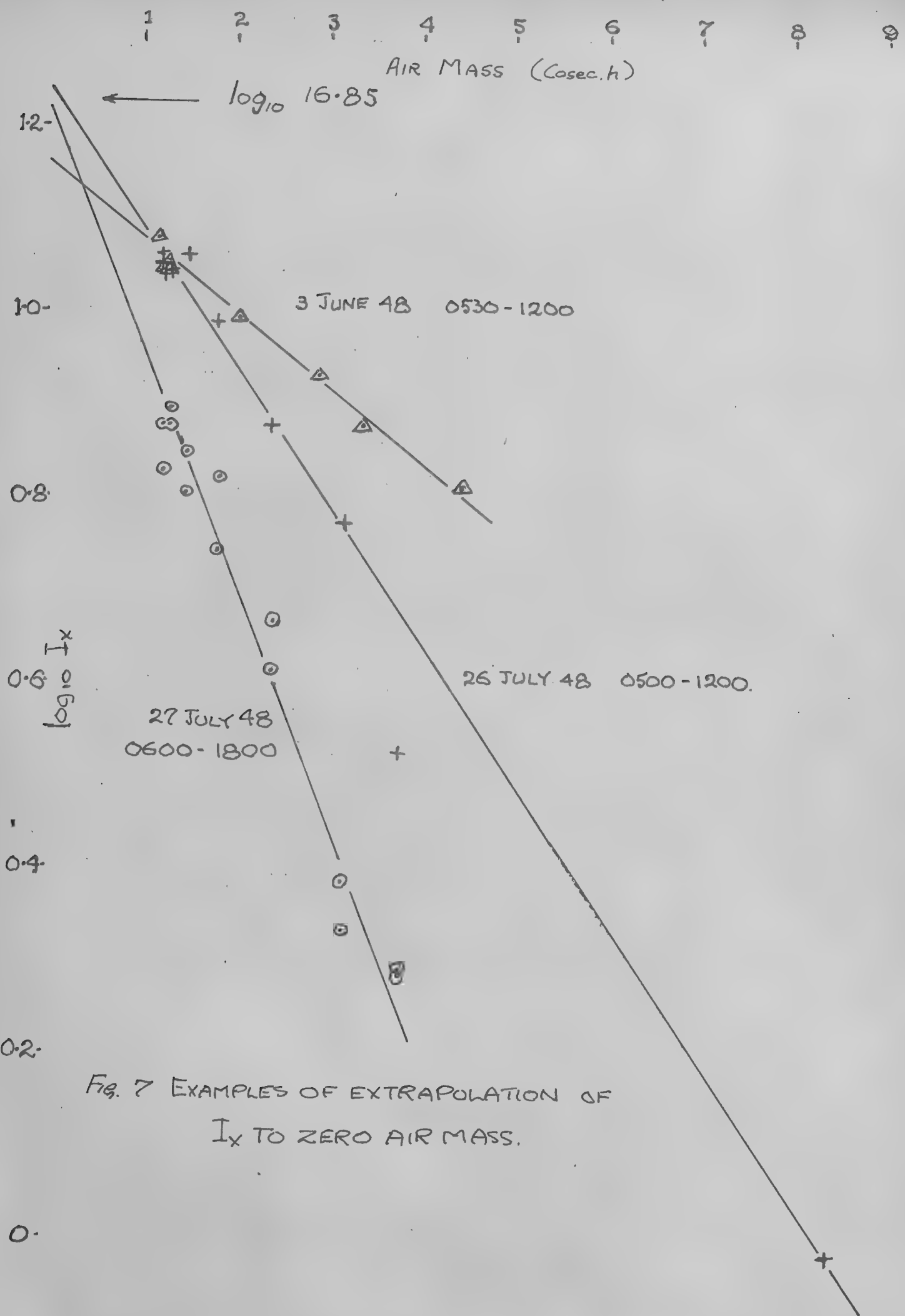

FIG. 7 EXAMPLES OF EXTRAPOLATION OF I_x TO ZERO AIR MASS.

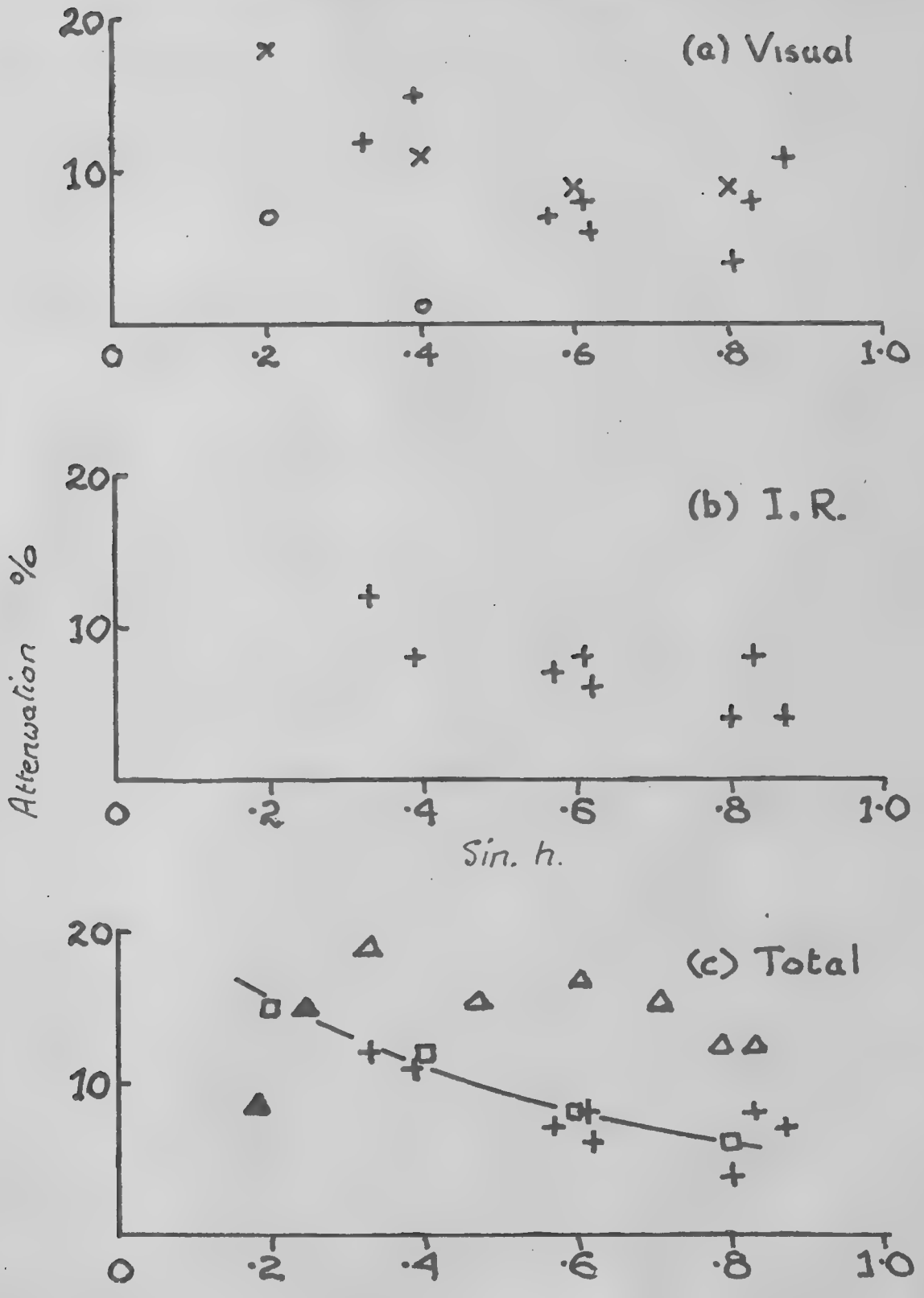

Fig. 8. The Additional Absorption

o Means of L and I_x (Method 5 i)
x Means of 0·95 L and I_x (Method 5 i)
+ Individual values of I, I_R, and D (Method 5 iv)
□ Means of T and D, 5 years (Method 5 ii)
△ Means of I and D, May 1948 (Method 5 iii)
▲ " " " " " , Dec " " "

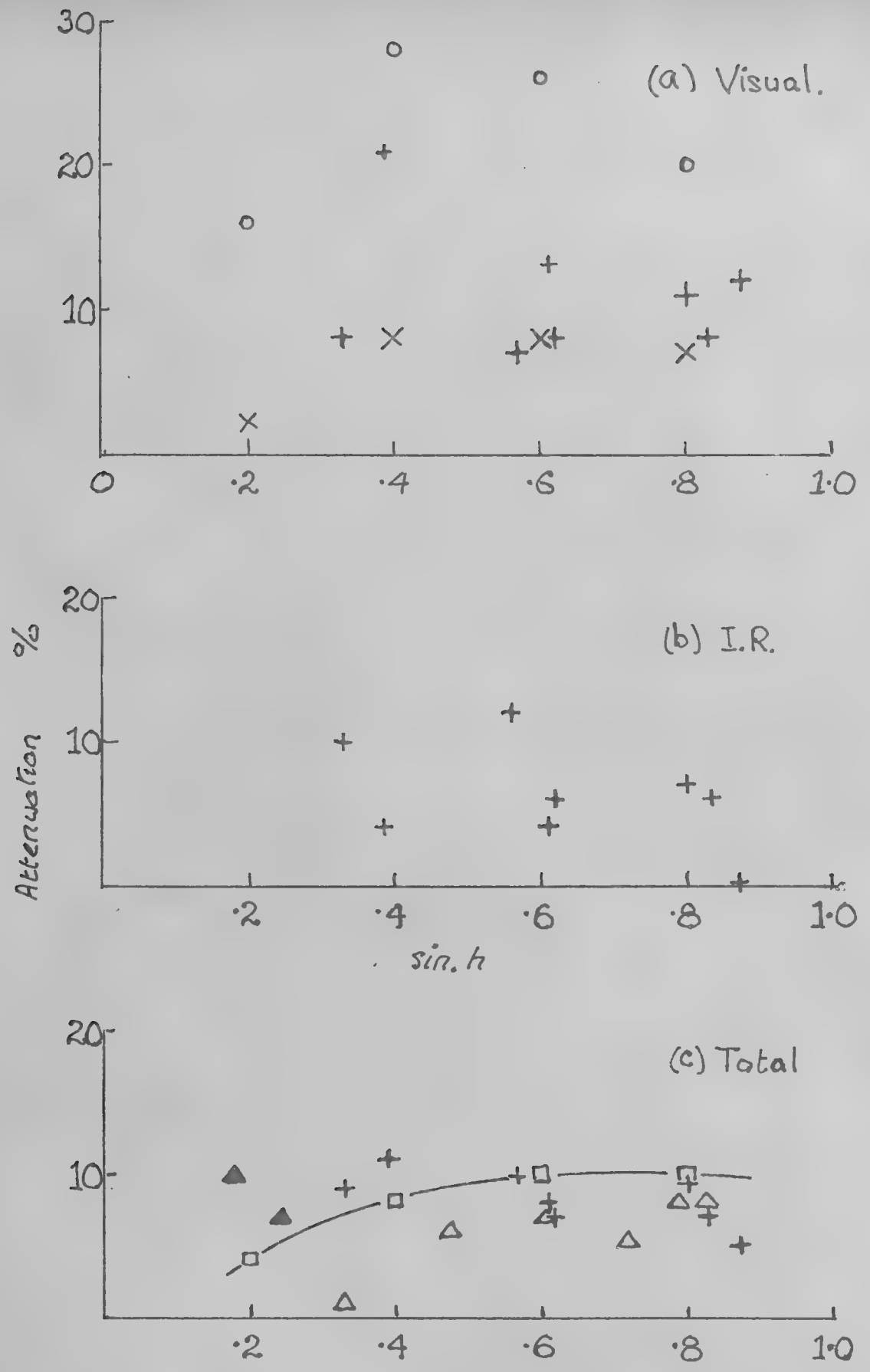

Fig. 9. The Additional Scattering

o Means of L and. I_x (Method 5i)
× Means of 0·95 L and I_x (Method 5i)
+ Individual values of I, I_R, and D (Method 5iv)
□ Means of T and D, 5 years (Method 5ii)
△ Means of I and D, May 1948 (Method 5iii)
▲ Means of I and D, Dec. 1948 (Method 5iii)

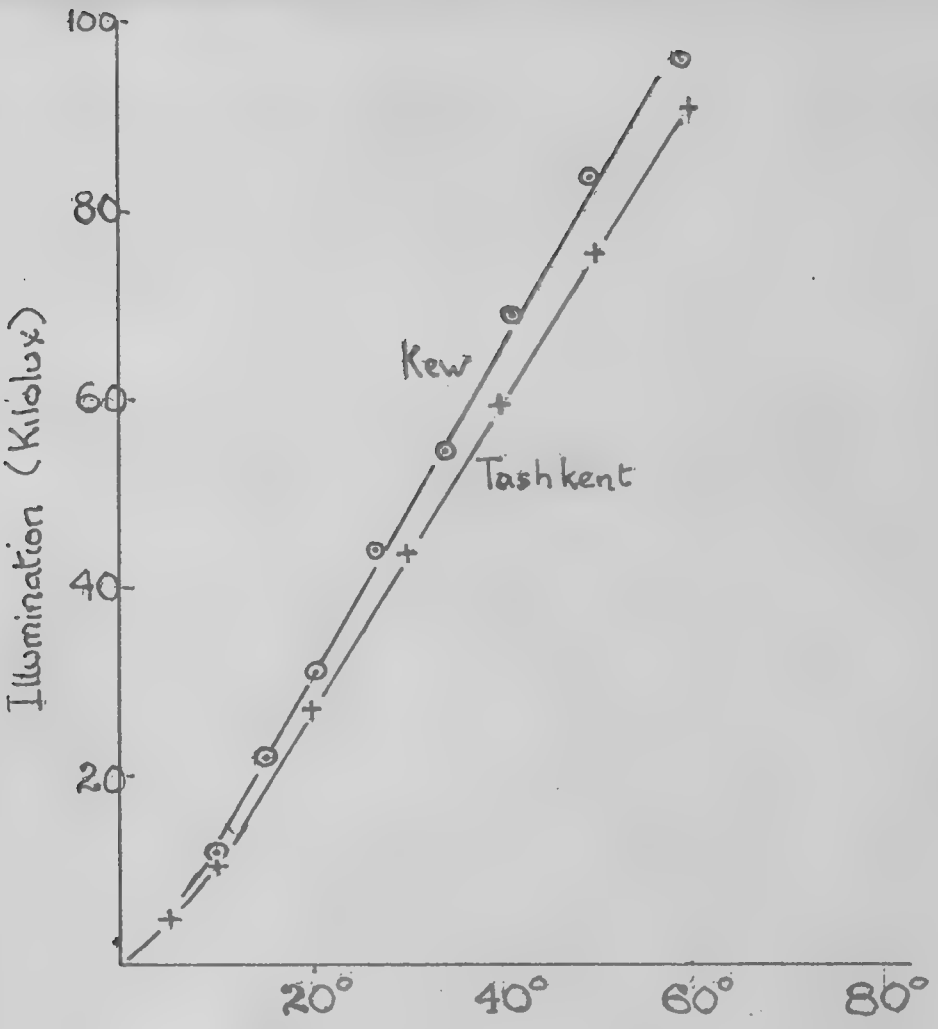

Fig. 10 Illumination of a horizontal surface under cloudless skies v. solar altitude
Kew (Blackwell) and Tashkent (Lopukhin)

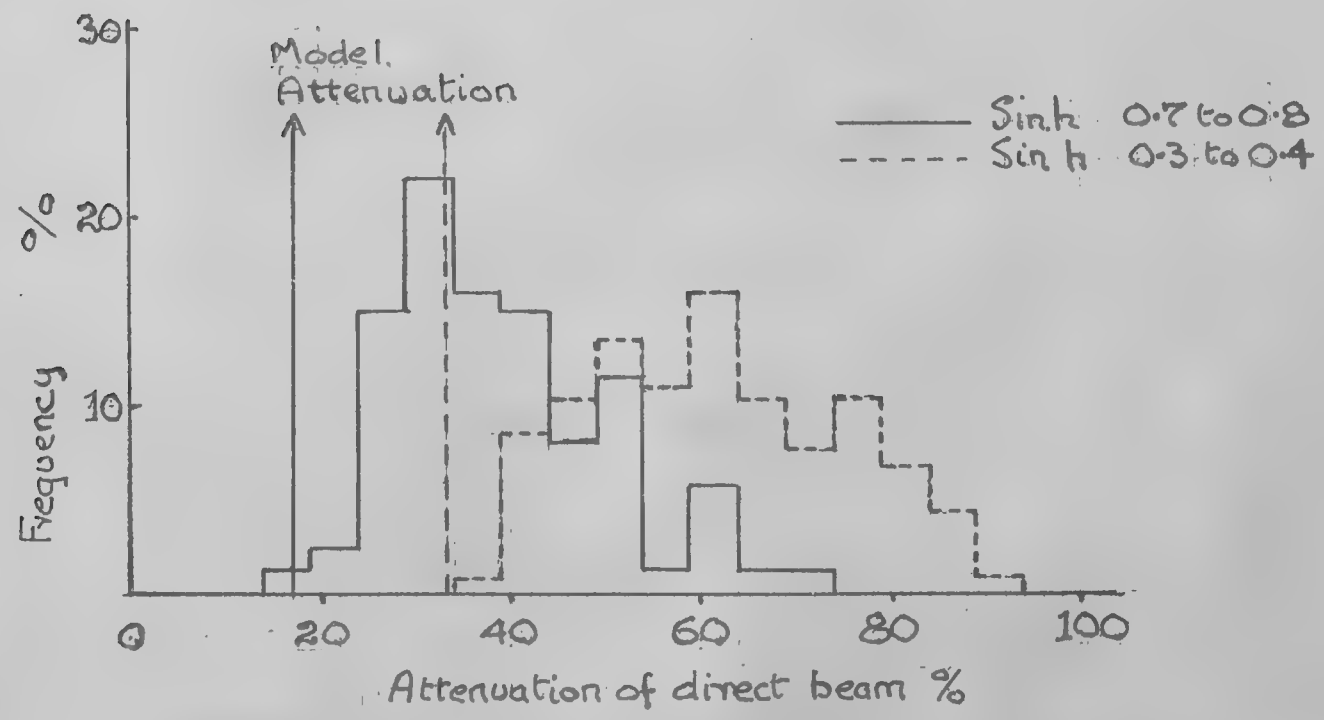

Fig. 11 Distribution of attenuation factor of direct radiation

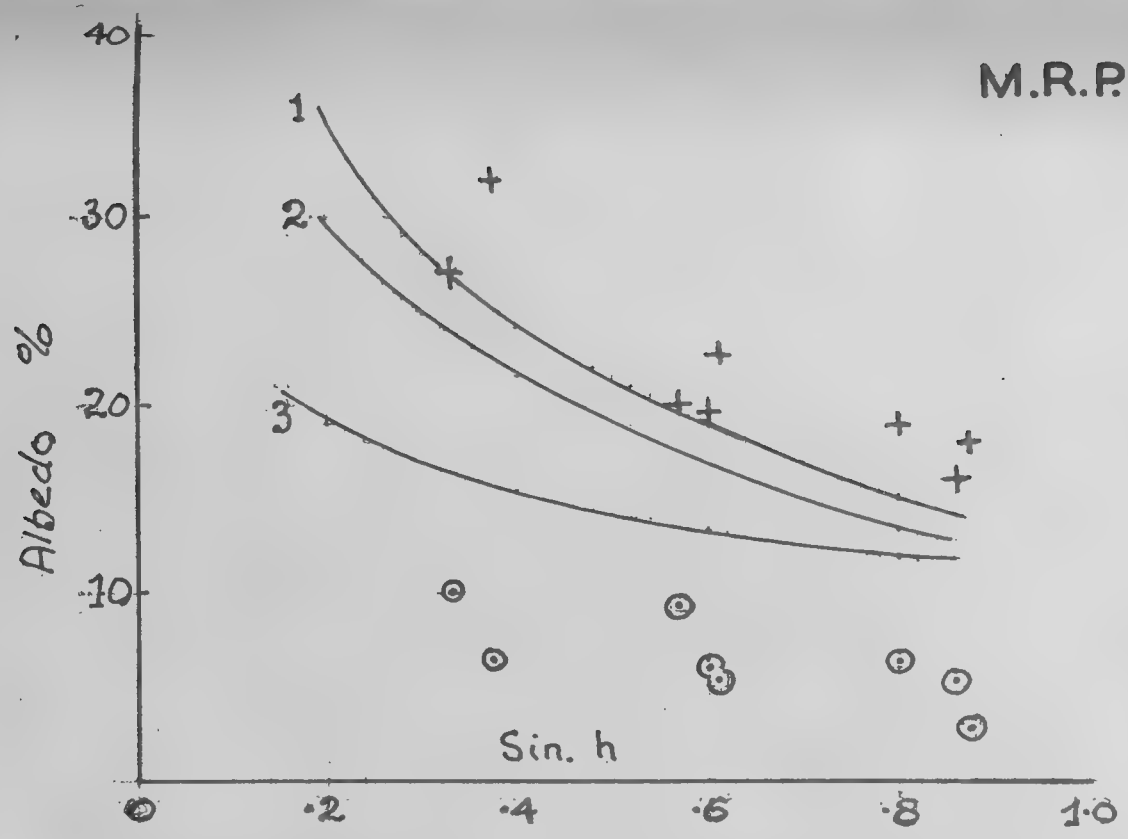

Fig 12 Albedo of the cloudless atmosphere at Kew

1 Photometric albedo

2 Albedo $0{\cdot}55\mu < \lambda < 0{\cdot}64\mu$

3 Total albedo

+ $\lambda < 0{\cdot}64\mu$ } Selected occasions

⊙ $\lambda > 0{\cdot}64\mu$ }

Control Number C.D. 8053

the Meteorological Office."

r T, D (total and diffuse radiation on a horizontal surface),
t sunshine) and I (direct radiation normal to the beam).

acy of the data is examined, and useful inter-relationships

r cloudless and overcast days (see Sec. 6). No

ematic errors due to use of provisional instrumental
nce been revised. In addition, the allowances for

n Secs. 4 and 7. Sufficient practical details are
ng corrections to be computed and applied at other

At the time of issue this report has not been published. Any author desiring to quote this paper should refer to it as "A paper of the Meteorological Research Committee (London). M.R.P. No. 895 by Mr. M.J. Blackwell A copy is available in the Library of the Meteorological Office."

M.R.P. 895

S.C.III/179

30th December, 1954

AD 223084

MHD

AIR MINISTRY

METEOROLOGICAL RESEARCH COMMITTEE

Five years continuous recording of total and diffuse solar radiation at Kew Observatory

by

M.J. Blackwell (Meteorological Office)

Summary

The first complete five years' data, obtained at Kew Observatory during 1947-51, are discussed with reference to their main systematic and random errors, the methods of correcting them, and the calibration techniques employed.

Corrected hourly means for 10-day periods are presented, after removal of all known errors, for T, D (total and diffuse radiation on a horizontal surface), S (duration of bright sunshine) and I (direct radiation normal to the beam).

The self-consistency of the data is examined, and useful inter-relationships are outlined. Diurnal variation is given for each of the four seasons, and the luminous efficiency of radiation discussed. Practical details are interposed whenever they are thought to be useful to other workers.

1. Introduction

Total and diffuse solarimeters were installed at Kew Observatory in 1946 to record the radiation received on a horizontal surface from sun and sky, and from the sky alone. Continuous recording of these components commenced in July of that year and has been maintained ever since. The data discussed in this paper are for the first complete five years of recording, namely 1947-51, but some reference will be made to selected occasions from 1952-53, when diurnal curves are constructed for cloudless and overcast days (see Sec. 8). No significant changes have been made in the installation during the period.

Provisional results based on the first fourteen months of recording (July 1946 to August 1947) have already been quoted by Stagg (1). The basic tabulations from which these were derived contained certain computational errors, and small systematic errors due to use of provisional instrumental factors which have since been revised. In addition, the allowances for incomplete exposure of the instruments were incorrect. The theory, calculations and experimental evidence for the present treatment of these obstruction corrections are given in Secs. 4 and 7. Sufficient practical details are included for corresponding corrections to be computed and applied at other observing stations.

In order that any previously published data may be related to the results found below, a conversion table is given under Table I. Since the corrections to total radiation involve a knowledge of the corresponding diffuse radiation at the time, the relations between total and diffuse radiation under various conditions, given in Sec. 8, can be used to obtain sufficiently accurate data by direct means.

The instruments used are two Moll-Gorczynski solarimeters obtained from Messrs. Kipp and Zonen. These thermopiles, having 14 thermojunctions and covered by two hemispherical glass domes, have been thoroughly discussed by Bener (2). Their purpose is to measure the short wave radiation from sun and sky. Since the glass domes transmit nearly all radiant energy in the waveband 0.3 μ to 3.0 μ , this purpose is achieved for all practical purposes. In this connection, see also Sec. 3.

55

B-40

2. Disposition of instruments and recording equipment

The instruments are mounted horizontally on the south balustrade of the Observatory. Behind them (to the north), the Observatory dome rises 14 feet above the instrumental horizon at a distance of 18 feet. Each solarimeter is surrounded by a circular guard-plate in the same plane as the sensitive surface of thermojunctions. This has two functions, firstly to prevent radiation from below the horizon reaching the thermopile after refraction at the domes, secondly to moderate the temperature variations of the case (and hence, also, the cold junctions) by shielding it from the direct rays of the sun.

For the diffuse recording thermopile, a circular metal band is mounted on a polar axis so that, with slight movements up or down the axis to allow for changing declination, the sun's direct radiation is prevented from falling on the solarimeter. From the beginning of recording until June 1951, the width of the band was 18 mm, the radius being 135 mm. After this date the band's width was increased to 29 mm to prevent loss of record due to incomplete shading, (the band is only moved along its axis on days when the sun is shining clearly enough to cast a shadow across the thermopile). * Condensation inside the domes is prevented by connecting the air-space to a tube of silica-gel.

The output from the two solarimeters is taken first to the Observatory dome, and then inside the building to a Cambridge thread-recorder in the basement. This contains three circuits which are connected in turn at minute intervals. One records the output of the total solarimeter, the second that of the diffuse solarimeter, and the third marks the baseline. The latter circuit is interrupted at the hour to give a time-mark. From the calibration factors of each instrument (see Sec. 3) suitable series resistors are included in the thermopile circuits so that under overcast skies the two traces will fall together. Apart from being a continual check on the continuity of the circuits, this method of display facilitates subsequent analysis of the data, particularly when selecting overcast periods (see Sec. 8).

3. Calibration of the records

The standard of radiation at Kew is based on readings of the Ångstrom compensation pyrheliometer, which has unshielded black strips. Radiation intensities derived from the Moll solarimeters are in effect the intensities incident on the unprotected thermopile surfaces, provided the solar radiation transmitted by the two glass domes bears a constant relation to the total radiation falling on the outer surface of the glass. Apart from the constant fraction of some 15% lost by non-selective reflection at the four glass surfaces (the additional dome was added to reduce variations of sensitivity with sun's altitude, attributed to formation of caustic curves)✓, there is only a minute fraction of the radiation lost by absorption. Consequently when factors are chosen, relating the thermopile readings to those of the Ångstrom pyrheliometer, they yield close approximations to the actual radiation intensities, under all conditions.

Two Ångstrom pyrheliometers, Nos. 24 and 100B, are used to standardise the other instruments. Based on the "uncorrected Ångstrom scale" and calibrated at Uppsala, these have recently been shown to agree within 0.3%. Investigations at the National Physical Laboratory (3) and at Kew (4) have shown that there has been no appreciable change in recent years in what may be termed the "Kew scale". The tabulated data dealt with in this paper are therefore based on the uncorrected Ångstrom scale, in which the solar constant according to Nicolet (5) is equal to 1.96 cal/cm^2/min. In accordance with current international policy, the basic data, which were tabulated in cal/cm^2/hr, are converted here into mw/cm^2. (1 cal/hr = 1.162 mw).

/During

* Footnote: a white card, with a circular hole for the glass dome, greatly facilitates the adjustment in weak winter sunshine.

✓ Footnote: it also has the practical advantage of stabilising zero drift during periods of fluctuating intensity.

During the period concerned, minor variants of calibration procedure have been adopted by successive members of the staff. These may be briefly outlined together with the method adopted at present. The most direct, though not always the most convenient, is to take a series of Angström readings on a bright cloudless day, meanwhile alternately shading and unshading the solarimeters from the direct rays of the sun. Difficulties and sources of error are numerous. Even on apparently cloudless days (or nearly cloudless, if the existing cloud is well away from the sun), there may be rapid fluctuations of direct solar intensity, due to patches of haze or invisible high cirrus. This often means that the sample of intensity measurements (by the pyrheliometer) may not always be a representative indication of the average intensity during the period of calibration. Then also, the accuracy of the method is dependent on the sky conditions being the same for both shaded and unshaded periods, since we are, in fact, equating:-

$$I \sin h \equiv T - D$$

where I is the direct intensity, h the sun's altitude, and T, D the unshaded and shaded readings respectively.

The practice at Kew has been to calibrate the records as a whole, i.e. solarimeter, leads, resistors and thread-recorder galvanometer combined. This has one disadvantage in that only one dot is marked on each trace during a three-minute period, and this sets the minimum time for shading at $3\frac{1}{2}$ mins. so as not to miss a dot. The shade used is a circular disc, of 2 inch diameter, silvered against the sun and dull black facing the instrument. It is mounted as far away as is convenient, usually some two or three feet distant from the thermopile centre. In the case of the diffuse thermopile, the shade ring is first lowered below the instrumental horizon.

Among other radiation equipment at Kew is a Moll-Gorczynski pyrheliograph which records on a second galvanometer, adjacent to the one which registers the total and diffuse components. The two galvanometers are encased within a single thread-recorder and, as a result, the dots on the two charts are made simultaneously. This allows the pyrheliograph to be used as the standard of direct beam intensity (calibration of this against the Angström instrument being a straightforward procedure) and hence the standardisation only requires the shading and unshading of the two solarimeters by one observer. Timing errors are completely removed by this technique.

Finally, as an additional check, another solarimeter, which is maintained as a secondary standard, is repeatedly compared with the Angström pyrheliometer throughout the year (its output being measured instantaneously by potentiometer). The output of this is now compared periodically with that of each of the continuous recording solarimeters, this being possible on a large number of days since the component for comparison is total (sun and sky) radiation, and periodic shading is thus not required.

4. Exposure of the instruments

(a) Errors of obstruction

The instruments are exposed on the south roof of the Observatory, at a point where some 8% of the north sky is obstructed by the Observatory dome, and a further 1% by trees along the remaining arc of the horizon. In addition, the shade-ring of the diffuse recorder obstructs a variable fraction of the sky, according to the setting of the ring, which depends on the sun's declination.

In assessing the correction for obstruction of the horizon it must be emphasised that the term to be computed is the fraction of the vertical component of the incoming flux, which is lost by obstruction, and not the fractional solid angle of the sky obscured *. To obtain an analytical expression for this fraction, we must assume an idealised model of an isotropically diffusing hemisphere, over the surface of which a quantity I of radiative energy is emitted normally from unit area in unit time.

/Fig. 1

* Footnote: the incorrect method was used at Kew during the period under investigation, and is embodied in M.O. Instrument Instruction No.225, which is being amended.

Fig. 1 shows an elementary area at P(r, θ, ϕ), part of an annular ring ABP at an elevation of θ above the horizon. The radiative energy emitted by this element in the direction PO will be $\propto I.r\cos\theta\, d\phi.r\, d\theta$. If we further assume that the receiving surface of the solarimeter is perfect (i.e. it conforms to Lambert's cosine law), then response of horizontal surface at O is:-

$$\propto Ir^2 \sin\theta \cos\theta\, d\theta\, d\phi$$

Similarly, response to whole hemispherical radiation is:-

$$\propto Ir^2 \int_0^{2\pi} d\phi \int_0^{\pi/2} \sin\theta \cos\theta\, d\theta$$

$$\propto Ir^2.2\pi.1/2 = \pi. Ir^2$$

The fraction of the vertical component, lost by obstruction of the elementary area at P, is therefore given by:-

$$\pi^{-1}\sin\theta \cos\theta\, d\theta\, d\phi.$$

In practice, we are concerned with correcting the diffuse radiation for obstruction by the shade-ring, and both diffuse and total radiation for obstruction by the Observatory dome and surrounding trees. The principle of the method in use is identical for both corrections. For obscuring objects of finite size, we write the expression:-

$$\pi^{-1}\iint \sin\theta \cos\theta\, d\theta\, d\phi \quad \text{as} \quad \pi^{-1}\sum(\overline{1/2 \sin 2\theta}.\ \Delta\theta.\ \Delta\phi).$$

The outline of any given object is mapped out on a $\theta - \phi$ diagram, θ the elevation being ordinate, and ϕ the azimuth being abscissa. In the case of buildings or trees, this is conveniently done with a theodolite. Their projections onto the $\theta - \phi$ diagram are divided into suitable component areas over which a mean value of $\frac{1}{2}\sin 2\theta$ can be assigned (allowing for the non-linear variation of this quantity). The units of area, in terms of small squares counted on graph paper, or planimeter units, are translated into $(\text{radians})^2$. For instance, the area 5° in azimuth x 5° in elevation $\equiv 25\ (\text{deg.})^2 \equiv 0.00763\ (\text{radians})^2$.

The shade-ring correction which is variable according to the sun's declination, has been checked in two ways at Kew, either of which may be used. Since the ring is adjusted almost daily, so as always to interrupt the direct beam of the sun, it is possible to formulate an analytical expression for the projection of the ring on the $\theta - \phi$ diagram, when the sun's position is known. Fig. 2 shows how the shade-ring is mounted on a polar axis, by inclining the fixture towards the north, at an angle λ to the horizontal, where λ is the latitude of the station. When the ring AB is set so as to shade the solarimeter M at a given time, then, as the earth rotates, successive arcs of the ring will continue to obstruct the direct solar radiation, since the declination δ of the sun may be considered constant over short periods. The declination is here seen to be the angle between the direct beam and the equatorial plane.

Turning to the system of orthogonal axes in Fig. 3, we have the axis of the ring in the zy plane, at an angle λ to the y-axis. The plane of the ring is distance 'a' from the solarimeter (at the origin). The equation to this plane is therefore given by:-

$$x \cos \pi/2 + y \cos\lambda + z \sin\lambda = a.$$

To transpose into spherical polar co-ordinates, we use

$$\left.\begin{aligned} x &= r \cos\theta \cos\phi \\ y &= r \cos\theta \sin\phi \\ z &= r \sin\theta \end{aligned}\right\} \quad \phi \text{ measured +ve from east through north}$$

/whence

whence $r \cos\theta \sin\phi \cos\lambda + r \sin\theta \sin\lambda = a$

and $\cos\theta \sin\phi \cos\lambda + \sin\theta \sin\lambda = a/r = \sin\delta$.

Finally since:

$$\sin\phi = \frac{\sin\delta - \sin\theta \sin\lambda}{\cos\theta \cos\lambda}$$

and δ, λ are both known, we can express ϕ in terms of a single variable θ.

The alternative method, referred to, was used as a check, because isopleths of the sun's position at Kew had already been drawn on a $\theta - \phi$ diagram, together with the time of day. This was done by using the relation:

$$\sin A = \frac{\cos\delta \sin t}{\cos\theta}$$

where A is azimuth (measured +ve from south through west) and t is the sun's hour angle. Values of θ, for given t, were also available from isopleths based on:

$$\sin\theta = \sin\lambda \sin\delta + \cos\lambda \cos\delta \cos t.$$

The $\theta - \phi$ curves for the sun's position are identical to the projection of the shade-ring on the same diagram, and can be used as guide lines to complete the projections of the two rims of the ring.

The last stage requires the analytical representation of the projection of the two rims. Returning to the equation to the plane of the ring, for which we obtained:

$$r \cos\theta \sin\phi \cos\lambda + r \sin\theta \sin\lambda = a = R \tan\delta$$

where R is the radius of the ring, and $\tan\delta = a/R$, we add the remaining conditions given by:

$$a_1 = R \tan\delta - d \qquad a_2 = R \tan\delta + d$$

where d is the half-width of the ring, (see Fig. 4).

Also: $r_1^2 = a_1^2 + R^2 = R^2 + (R \tan\delta - d)^2$

and $r_2^2 = a_2^2 + R^2 = R^2 + (R \tan\delta + d)^2$.

Thus: $r_1 \cos\theta \sin\phi \cos\lambda + r_1 \sin\theta \sin\lambda = R \tan\delta - d$

and $r_2 \cos\theta \sin\phi \cos\lambda + r_2 \sin\theta \sin\lambda = R \tan\delta + d$.

The general equation for both rims is therefore given by:-

$$\cos\theta \sin\phi \cos\lambda + \sin\theta \sin\lambda = \frac{R \tan\delta \pm d}{\sqrt{(R \tan\delta \pm d)^2 + R^2}}$$

Substitution in this equation at a series of points will complete the projection of the shade-ring for any required date. Alternatively, pairs of points can be determined near sunrise ($\theta \sim 0°$) and near midday ($\phi \sim 270°$), and "french curves" used to complete the profiles, with the curves of sun's position as guide lines. The areas obtained are split into convenient parts (say between $\theta = 0°$ and $\theta = 10°$, etc.) over which values of $\frac{1}{2} \sin 2\theta$ may be conveniently assigned, and the final correction: $\pi^{-1} \Sigma(1/2 \sin 2\theta . \Delta\theta . \Delta\phi)$ is then computed.

/(b)

(b) Effect of back reflection

The following considerations apply to the particular exposure of the Kew installation. At most other sites, it would be permissible to regard the shade-ring and permanent obstructions as cutting off the fractions of diffuse radiation as determined by the method given above. At Kew, however, lack of space has necessitated the solarimeters being placed comparatively close to the Observatory dome, which consequently subtends a large solid angle, especially in the vertical. ⁂

With such an arrangement, it was necessary to make measurements of the back-reflection from the dome under various conditions of sun and sky. For this purpose, a Linke-Feussner radiometer with glass filter was directed at various parts of the roof, and at the surrounding sky. The dome proper is a dull black; the cylindrical part being a somewhat weathered cream (see Fig. 5). This accounts qualitatively for the values shown in Fig. 6, which were obtained on a bright sunny day. The vertical axis of reference in Fig. 6 is the direction of the centre of the dome viewed from the radiometer, which was placed close to the solarimeter. From the two traverses made, (one in the horizontal, one in the vertical), mean values have been deduced for the separate parts of the dome; these are shown thus: [10.0]. Finally, integrating the contributions to obtain the fraction of the diffuse radiation gained by back reflection, we have:-

$$\frac{\sum I_n . \overline{1/2 \sin 2\theta} . \Delta\theta . \Delta\phi}{\pi I}$$

where I_n is the radiation intensity from each part of the dome emitted in the direction of the solarimeter. Also, since πI is the integrated effect of the whole hemisphere on the receiver, we can insert the measured value given by the diffuse recorder at the time the measurements were made.

Inserting the intensities found, we obtain for the percentage contribution due to the dome, the figure of 4.5%. The diffuse radiation obscured by the dome amounts to some 2.5%. Having fixed the upper limit in this way, it is now possible to estimate the mean contribution for all conditions, or the particular figure applicable to any selected occasion. ⁄

5. Instrumental errors: temperature coefficient and cosine law

There is little disagreement on the accepted value of the temperature coefficient of the solarimeters used and experiments made at Kew agree closely with the coefficient given by Bener (2) namely 0.25% per 1°C over the normal range of ambient temperatures, the sign being negative. On the question of cosine law deviations there is less accord and this is probably due partly to real differences among instruments of the same type, and partly to variations in investigational technique.

To obtain valid data on this question, the solarimeter should be in the horizontal position, since the pattern of convection within the glass domes is sufficiently affected to alter the output of the thermopile if the instrument is tilted. In this country, natural opportunities to test the

/cosine

⁂ Footnote: see Sec. 12 regarding the improved installation which has been completed recently.

⁄ Footnote: ~~the application of this correction~~ to the basic data is discussed in Sec. 7.

cosine law (when the sun is at various altitudes) are few and far between. The use of an artificial laboratory source is therefore advantageous. A 2000 W tungsten-filament projector lamp, slightly under-run for stability, is used to irradiate the solarimeter under test at various elevations above the instrumental horizon. A rigid link between the lamp support and the solarimeter ensures the constancy of their separation. Fig. 7 shows a typical response curve found at Kew, and also some data due to Bener (2) 9.

Added to the simple variation of sensitivity with elevation is the azimuthal effect, which appears to be similar for most instruments. The following data refer to two standard thermopiles, orientated so that the longer line of thermo-junctions faces the directions given, with the artificial sun assumed always to the south:

	Longer line of junctions facing:	E	S	W	N
Response (arbitrary units)	1st pile:	87	63	83	74
	2nd pile:	85	61	81	70

The elevation during this test was kept constant at 15°; at higher angles the effect diminishes rapidly. In normal recording, the amplitude of the variation is markedly reduced by the presence of the diffuse component in the case of the total solarimeter; there is a negligible effect on the diffuse instrument.

No corrections have been made to the Kew data for errors due to the azimuthal effect, but the magnitude of the variation is sufficient to warrant the recommendation that, in future installations (see Sec. 12), all thermopiles be orientated in the same direction.

Returning to consideration of the combined effect of imperfect cosine law response and temperature coefficient, it is calculated that the diffuse solarimeter will read low by $\sim$ 0.5% on the first account and will not be greatly affected by the second factor from hour to hour. Corrections have not, therefore, been applied here, though there exists a long term annual variation of $\sim$ 3%. In the case of the total solarimeter, typical magnitudes of these errors may be usefully compared. Calibrations are most often done at high solar altitudes and consequently high ambient temperatures, and it is found that there is little significant trend in the calibration factors during the year. Thus, the assessment of possible errors is to be related to departures of natural conditions from those of the ideal calibration periods. In winter, with the sun at an altitude of 15°, a cosine law error of -2.6% (Fig. 7, Bener's curve) is to be compared with the effect of a fall in ambient temperature of some 10°C below summer values, giving a compensating increase of +2.5% in the thermopile output. Again, the best approximation is to assume the mutual compensation of the two errors.

6. Tabulating errors: random and systematic

The basic tabulations, on which subsequent sections are based, are obtained by estimating the mean intensity for the hours in question by placing a graduated transparent scale over the thread-recorder charts. Considerable random errors may be introduced by this procedure, especially on days of rapidly fluctuating intensity caused by broken clouds or haze patches. A series of trials has been carried out in which many charts were measured independently by different observers. Fig. 8 shows the ogive derived from independent tabulations of charts of total daylight illumination (which are closely similar in appearance to those of total radiation). Denoting the two estimations of each hourly tabulation by L and L', then one month's data (August 1950) were analysed in the form: $\left(\frac{L - L'}{L} \times 100\right)\%$, in 5% ranges. Errors expressed in this way can amount to 50% due to rounding off to the nearest whole number at very low intensities.

/Fig. 9

9 Footnote: Bener's data refer to the instrumental response to total (sun + sky) radiation, the Kew curve only to a direct beam.

Fig. 9 shows the ogive derived from independent tabulations of total radiation indicated on different recorders by two similar solarimeters. The estimations are here denoted by T and T_1 and expressed in the same way as before, three months' data (April and May 1949, June 1950) being taken together. Considering the implications of both these ogives, we can (insofar as the errors approximate to a normal distribution) obtain a reasonable estimate of the standard deviation (6). If the abscissae corresponding to ordinates of 16% and 84% are noted, then the range between them is equal to 2σ . From Fig. 8, σ = 7% and there is a systematic error of $2\frac{1}{2}$%; from Fig. 9, $\sigma = 5\frac{1}{2}$% and the systematic error is 4%. Apart from the slightly larger systematic error in the second case (which could easily arise from a small discrepancy in one of the calibration factors in use at this period), there is no significant difference in the two trials. This implies that the tabulating errors outweigh errors due to small differences in similar instruments. Finally it should be noted that the standard deviations obtained refer to the combination of two independent sets of estimates. The probable magnitude of errors of tabulation is therefore $1/\sqrt{2}.\sigma$ or about 5%.

The problem of eliminating errors of chart measurement has recently been attacked by automatically integrating a solarimeter's output, to give daily totals (7). It is hoped to extend this method to hourly totals.

7. The corrected hourly means

To summarise briefly the treatment of the data necessary to remove all known systematic errors, we have first the obstruction corrections. Though the Observatory dome obscures 8% of the hemisphere, the resultant loss of radiant flux is computed to be only $2\frac{1}{2}$% (assuming a perfectly black dome). When back reflection is included, we have the practically determined contribution of $4\frac{1}{2}$%, (on a cloudless day). The average cloud amount at Kew is about 5/8 and hence, to the degree of accuracy required, we consider average days to have a uniform distribution of 5/8 cloud. For 5/8 of the time, the sun being obscured, the dark dome is seen against the relatively bright sky *. Under these conditions the dome is about half as bright as the surrounding sky, giving say $1\frac{1}{4}$% of the diffuse radiation. For 3/8 of the time the sun shining on the dome makes it about $1\frac{1}{2}$ times as bright as the surrounding sky (the same as before), and the contribution becomes about $3\frac{3}{4}$% of the diffuse radiation. If the dome were replaced by the sky it obscures, the contribution would be simply $2\frac{1}{2}$%. Hence, to a close approximation, the dome has no appreciable effect on average values. The only allowance made here is for cloudless days (see Sec. 8) where the greatest effect is found, namely a gain of 2% over the diffuse radiation at a perfectly exposed site.

In addition to the permanent obstructions, which affect the exposure of both instruments, the shade-ring correction must be applied to the diffuse radiation tabulations. As previously described in Sec. 4, the percentage loss of diffuse radiation (assuming isotropic scattering) is determined by the dimensions of the ring and the declination of the sun.† The original tabulations included 3% for the shade-ring and 9% for permanent obstruction in mid-winter, involving an addition of about 14% to the measured diffuse radiation. When the correct method of computing the shade-ring allowance is used, and the average permanent obstruction contribution is assumed to be zero, the revised correction is reduced to 1%. The mid-summer figures of 7% and 9%, or 19% to the measured value, are reduced to 8%. The mean difference between the two corrections is therefore 12% for most of the period concerned, and 14% after the change to a broader ring in June 1951.

/Two

---

* Footnote: it is shown in Sec. 8 that the diffuse radiation is higher for average days (5/8 cloud) than for cloudless days.

† Footnote: unlike the dome's surface, the shade-ring is dull black and produces negligible back-reflection.

Two further errors, allowed for in the corrections to previously published data given under Table I, were: the omission of the permanent obstruction correction to the diffuse radiation, during June 1947 to December 1949, although included in the total radiation tabulations; and secondly, the makers' provisional calibration factors, used during the period, were altered slightly after sufficient experimental evidence had been acquired. Table I is extended up to the present time for completeness, and because some 1952-53 data are used in the next section.

The basic tabulations, which have necessarily been corrected retrospectively, are presented in Table II (total) and Table III (diffuse) in the form of hourly means for 10-day periods. Thus June 0, 1, 2 refer to the first, second and last 10-day period in the month (i.e.: 1st to 10th, 11th to 20th, 21st to end of month). It was shown in Sec. 6 that the standard deviation of a single tabulation is of the order of 5%. The random errors in the 10-day means, representing five years' data, are therefore reduced to about 1% since each is based on 50 observations.

8. Diurnal variation of total and diffuse radiation

Stagg (1) has described the sky conditions which produce the extreme values of total radiation (T) and diffuse radiation (D), together with the variations (with cloud type and amount) of these components. To supplement these figures, data have been extracted to construct diurnal curves for cloudless and overcast days. A preliminary selection of the 1947-51 material gave an insufficient number of suitable occasions and therefore, for this section only, data for 1952-53 have been incorporated. For comparison, the average day curves derived from Tables II and III have been included.

Figs. 10 and 11 show curves of diurnal variation (all days included) for the months of March, June, September and December, in which the components are T and D respectively. There is a high degree of symmetry about noon L.A.T., with a slight tendency for the forenoon values to be a little higher than those of afternoon. How much of this may be due to temperature coefficient, and how much to the diurnal change in cloud form (small cumuliform cloud in the morning would tend to give higher intensities than the denser cumulus or cumulonimbus of afternoon), it is not possible to decide. Certainly there is little evidence for any markedly asymmetric variation. In this connection, however, it is of interest to note that whereas the diffuse radiation tends to be high in the forenoon, the direct component I sin h is correspondingly low. The result is the comparative smoothness and symmetry in the T curves.

Figs. 12 and 13 show curves of diurnal variation on cloudless days, for D and T respectively, for the same four months. These are meant to represent the average cloudless day, which may be affected to a greater or lesser degree by the smoke pollution encountered in the Greater London area. It is thought that these curves will be representative, therefore, of the actual climatic conditions in which most people live in this country.

The method of selecting the data for these curves consists of examining the original charts for the hours during which the T and D traces were smooth and well-separated. At the same time, the sunshine tabulations were required to indicate 100% sunshine, and the Gorczynski pyrheliograph to give a smooth unbroken trace. Finally, the recorded observations were required to show 1/8 cloud or less for at least three consecutive hours. In cases of doubt, the end hours of these periods were rejected. The remaining tabulations were re-tabulated under time of day and the means corrected for systematic errors. This procedure was identical to the removal of errors from the hourly means for 10-day periods, with the single exception that the D values were reduced by 2% for back-reflection from the dome.

/In

In Fig. 13 the curves for T are again smooth and regular with a suspicion of higher morning values. The D curves in Fig. 12 are given more tentatively because of the much greater variability experienced, according to the haziness of the atmosphere. Even more data are required before mean curves can be drawn objectively. There does seem, however, an indication that the March and September curves are asymmetric; the former being higher in the afternoon, the latter in the morning. Since cloud has been eliminated as a variable, we may look to the complex effects of the atmosphere's content of water and smoke pollution.

The former will have different significance in the liquid drop phase (say in early morning) and in the vapour phase (afternoon). The latter will make a variable contribution (for the same total amount) according to whether it is concentrated in a shallow layer beneath an inversion (morning) or distributed in depth by convection (afternoon). These complex factors can not be quantitatively assessed as yet.

Fig. 14, similarly, is given as a general guide to the orders of magnitude of the intensities to be expected on overcast days. The curves are less definite around midday, due to the smaller number of observations. By definition, T and D must be equal, and therefore only tabulations of T have been used to construct the curves. The method of selecting the data consists of choosing periods when the T and D traces were approximately coincident, when the sunshine tabulations indicate no sunshine, and when the Gorczynski pyrheliograph gave no deflection. Finally, the observations were required to show 7/8 cloud or more for at least three consecutive hours. In cases of doubt, the end hours of these periods were again rejected. The remaining tabulations were similarly corrected after obtaining the means for each hour, for the same four months. The values found are similar but slightly less than the corresponding curves for cloudless days (D).

9. Comparison with direct radiation

It was mentioned in Sec. 3 that the basis of calibration of the T and D solarimeters lies in the equation:

$$I \sin h \equiv T - D.$$

It is therefore of interest to examine how closely this criterion of accuracy and self-consistency is adhered to in the course of continuous recording. For this purpose, hourly means of I for 10-day periods are presented in Table IV for the same years (1947-51) as for T and D.

During this time, I was recorded by the Moll-Gorczynski pyrheliograph, which received a complete overhaul in 1945 as described in G.M. 86. Its sensitivity remained unchanged until October 1949 when the Richard recording millivoltmeter was moved from the Observatory dome down to the basement. This appears to have increased the sensitivity of the recorder by about 5%; at the same time the blacking on the thermopile gave signs of slow deterioration (about 1% by the end of 1950). The data for October 1949 to December 1950 have therefore been multiplied by the factor 0.96.

Due partly to the uncertainty of the Richard millivoltmeter sensitivity, and partly to unsatisfactory performance of the pyrheliometer heliostat at this time, data for 1951 have been obtained from the records of the twin-mounted thermopiles (referred to in G.M. 86) which were formerly used for measuring spectral components of the direct radiation. These instruments and their thread-recorders have remained unchanged since they were first used in 1947. Before the end of 1949, the filters were removed and the outputs of the two thermopiles superposed on a single chart.

Denoting the originally tabulated readings of the single pyrheliograph by I_1, and those of the twin-mounted thermopiles by I_2, it was found that I_2 was correct in 1950, when referred to the standard Ångstrom pyrheliometer. Comparisons of I_2 and I_1, on numerous occasions during this year, show that I_1

/was

was the greater by about 4%. Since the multiplying factor of 0.96 (used above to correct the I_1 data) brings the two sets of data into full agreement, there is satisfactory confirmation, both for the use of the 1950 corrected I_1 data, and for the inclusion of the 1951 I_2 data in the five year means without introducing inhomogeneity into the material. Actual standardisations during 1951 show that I_2 was still in agreement with the standard.

The most serious source of error in measurements of direct radiation arises from incorrect adjustment of the heliostat mechanism. Thus systematically low values of order 10% can frequently occur in spite of accurate standardisations, which are only done after the alignment of the instruments has been checked. Ogives were drawn, as in Sec. 7, for independent tabulations of the same direct radiation charts. For these, σ = 12% with no systematic difference. Thus the tabulation errors ($1/\sqrt{2} \cdot \sigma = 8\frac{1}{2}\%$) are slightly larger than the corresponding errors in T and D, due to the more intermittent character of the records. Further ogives were drawn for sets of routine tabulations of I_1 and I_2 recorded on different instruments. Here, σ = 18% with a systematic term of 5% (I_1 being the lower). Since the I_2 heliostat is electrically driven and the I_1 clock-driven, the increased scatter ($1/\sqrt{2} \cdot \sigma = 13\%$) is to be expected, and it is known that the clock drive was less satisfactory at the time, giving more trouble on the I_1 record.

Since there are no cosine law errors, the only remaining systematic errors are due to temperature coefficient which gives an annual variation of about 3% between summer and winter. No correction has been made for this. In Fig. 15, the hourly means for (T - D) are plotted against I sin h; the continuous line represents the state of complete self-consistency. Apart from the further emphasis on the magnitude of the routine tabulating errors, it is clear that residual systematic errors will require further attention in the future. The low values of I sin h reflect the problem of accurate alignment on the sun, and the departure from the isotropic scattering of diffuse radiation (assumed in Sec. 4) will result in the shade-ring obscuring more than the computed fraction of D, thus giving high values of (T - D).

10. Total radiation and daylight

The measurements, so far considered, concern the range of wavelengths 0.3μ to 3.0μ ; it is of interest to compare them with the illumination measurements previously reported (8). In most countries, radiation data are more numerous than daylight illumination figures. The latter could often be deduced from the former, therefore, if a sufficiently close correlation was shown to exist between them. The continuous recording of daylight at Kew offers a favourable opportunity for examining the ratio of daylight intensity: radiation intensity (in units of lumens per watt), which is known as the luminous efficiency of daylight.

Tentative values of this ratio were given in (8); these were derived from the diurnal curves of T and L (daylight) for cloudless occasions. More recent work enables a clearer picture to be drawn, and the analysis can be extended to all occasions.

In the course of an investigation on the albedo of the atmosphere (9), the cloudless and overcast periods (such as those used in Sec. 8) were analysed under ranges of solar elevation. The L.E. (luminous efficiency) for cloudless periods was found to be remarkably constant for all solar angles (125 ± 2), but increased slightly for overcast periods with higher elevations. This may have been a feature of the sample taken, however, the mean L.E. being similar to the previous value (126 ± 5). This suggests that useful results might be obtained by assuming the approximate constancy of L.E. with sky conditions, for a given time of year. When all occasions are considered together (omitting only the hours in which sin h < 0.1), the L.E. is little changed (123 ± 3). The mean deviations here refer to the scatter of the means for each sin h range: 0.1 - 0.2, 0.2 - 0.3, etc.

/Any

Any slight trends in the mean luminous efficiencies reflect the increase of winter observations in the low sin h ranges and vice versa. To test the annual variation of L.E., the midday hours (11 - 12, 12 - 13, for all occasions) were extracted for each 10-day period from Table II of this paper and Table II of reference (8). These were averaged to give the monthly means of L.E. set out below:

J	F	M	A	M	J	J	A	S	O	N	D
113	113	110	119	122	128	133	132	134	122	123	112

Again, the mean value is nearly the same as before (122 $\pm$ 7). Approximate values of daylight illumination (on a horizontal surface) can therefore be deduced by using these monthly means of L.E. irrespective of cloud amount or time of day. It must be emphasised, however, that these somewhat tentative results are only relevant to the five year period considered, to the respective instrumental methods of measurement and to the local conditions of exposure and climate.

11. Total radiation and sunshine

In the previous section, conversion factors were given by means of which daylight illumination data could be derived from available radiation data. Of much greater need and wider application is a method of using the abundant measurements of the Campbell-Stokes sunshine-duration recorders to estimate daily values of total radiation.

A well-known formula, due to Ångström, has the form: $Q = Q_o(a + bS)$ where a and b are constants such that $a + b = 1$, S is the %age possible sunshine, and Q_o is the radiation under clear skies. The equation gives approximate values of Q, the total radiation actually received, for typical average days when the cloud cover is near the normal (e.g. about 5/8 at Kew).

It is proposed to depart from this method for three reasons. In the first place, although a linear relation can be found* to fit the data for cloud amounts between half and total cover, it grossly overestimates the radiation on cloudless days. Secondly, if a is found by putting: S = 0 (overcast days), and b adjusted accordingly, then the radiation deduced for any cloud amounts near the normal value will be underestimated. This results from the fact that cloud layers which conform to the conditions selected for overcast periods are much denser than at other times, giving a low figure for the constant a. Lastly, a much more relevant and practical point is that if cloudless day values are known, there is every likelihood that there is no need to deduce radiation data from sunshine data.

The problem has therefore been approached from the standpoint of an investigator possessing only records of the Campbell-Stokes instrument, and a knowledge of the extraterrestrial radiation falling on a horizontal surface. Table V gives hourly means of extraterrestrial radiation for 10-day periods based on Nicolet's data on the solar constant (5). These were summed cross-ways to give the corresponding daily totals (which will be denoted as Q_{Ext}, and apply to any station in the same latitude as Kew: 51° 28' N).

The hourly means of sunshine duration for 10-day periods are presented in Table VI, again for the same years (1947-51). After summing these cross-ways, the daily totals were compared with the length of day (obtained from times of sunrise and sunset at Greenwich) to give the %age possible sunshine, S. For each of the year's 36 decadal periods, values of Q/Q_{Ext} were plotted against S. As shown in Fig. 16, all these points lie between values of S from 15% to 55%. To complete the diagram, the curves in Figs. 13 and 14 were integrated to give the overcast Q/Q_{Ext} for S = 0, and the cloudless Q/Q_{Ext} for S = 100. The probable trends of the ratios Q/Q_{Ext} have been sketched in for the four months March, June, September and December.

/The

* Footnote: but only if the condition that a + b = 1 is relaxed.

The final result makes it clear why no simple linear regression equation can be found to fit the observed radiation over the whole range of cloud amount.

However, reliable estimates (probable accuracy $\sim$ 10%) can be made, by using the curves indicated, provided that decadal means of daily totals are considered throughout.

12. Conclusion and suggestions for further work

By removing all known systematic errors from the basic data, and using only means of large numbers of observations, it is possible to obtain results from routine continuous radiation records which have an estimated accuracy within $\pm$ 5%. Conclusions drawn should be typical of the smoke-polluted atmosphere in which most of us live in this country.

At the present stage of the work, there come to mind several ways in which the accuracy of further measurements could be improved:-

(i) Improvement of the exposure of the instruments.

(ii) Use of a common orientation of the instruments.

(iii) Use of a more realistic assumption than that of an isotropically diffuse hemisphere.

(iv) Measurement of the instrument temperature during calibrations.

(v) Automatic integration of the solarimeter outputs, hour by hour.

(vi) Use of new heliostat drive mechanisms, with more suitable gear-ratios.

Regarding (i), a circular platform has now been constructed clear of the Observatory dome; when the instruments are resited, (ii) will be followed. New equipment has been ordered for (vi), and (v) has been successfully implemented as far as daily totals are concerned (M.R.P. 862).

13. Acknowledgements

I wish to express my gratitude to Dr. G.D. Robinson for his guidance throughout this investigation, and to Mr. D.B.B. Powell for help with the considerable numerical work and preparation of tables. Thanks are also due to Mr. J. MacDowall for help in Sec. 4(a) on exposure, and to Mr. R.H. Eldridge who planned the trials on which the errors of tabulation have been estimated in Sec. 6.

References

1. Stagg, J.M. — Geophys. Mem., London. 11. 86. 1950.
2. Bener, P. — Arch. Met. Geophys. Biokl. B.2. 188. 1950.
3. Guild, J. — Proc. Roy. Soc. A. 161. 1937.
4. Eldridge, R.H. — Quart. J. R. Met. Soc. 78. 260. 1952.
5. Nicolet, M. — Arch. Met. Geophys. Biokl. B. 3. 1951.
6. Brooks, C.E.P. and Carruthers, N. — "Handbook of Statistical Methods in Meteorology". H.M.S.O. 1953.
7. Blackwell, M.J. — M.R.P. 862. 1954.
8. Blackwell, M.J. — M.R.P. 831. 1953.
9. Blackwell, M.J., Eldridge, R.H. and Robinson, G.D. — M.R.P. 894. 1954.

TABLE I.

Corrections to previously published data

Period	Diffuse	Total
July 1946-May 47	reduce by 16%	Subtract 10% of corrected Diffuse
June 1947-Dec. 49	reduce by 6%	Subtract 9% of corrected Diffuse
Jan. 1950-Aug. 51	reduce by 16%	Subtract 10% of corrected Diffuse
Sept. 1951-Dec. 52	reduce by 18%	Subtract 10% of corrected Diffuse, increase by 1%
Jan. 1953-Mar. 53	reduce by 18%	Subtract 10% of corrected Diffuse, increase by 3%
Apr. 1953-June 53	reduce by 6%	Subtract 2% of corrected Diffuse, increase by 3%
July 1953-Dec. 53	reduce by 5%	Subtract 1% of corrected Diffuse
Jan. 1954 onwards	correct	Correct

TABLE II.

Corrected hourly means of Total Radiation (mw.cm^{-2}) for 10-day periods

		4 – 5	5 – 6	6 – 7	7 – 8	8 – 9	9 – 10	10–11	11–12	12–13	13–14	14–15	15–16	16–17	17–18	18–19	19–20
J	0				tr	1.6	5.3	8.7	10.5	10.5	8.0	4.2	1.3				
	1				tr	2.1	6.7	10.3	12.8	11.5	8.5	5.7	1.9	tr			
	2				tr	2.8	7.0	12.0	14.9	12.8	7.6	7.3	2.9	0.1			
F	0				0.7	4.2	9.1	12.3	14.1	14.2	12.6	7.6	3.6	0.5			
	1			tr	1.6	7.1	10.8	16.3	16.6	17.1	14.8	10.7	6.4	1.4	tr		
	2			tr	3.6	10.2	17.0	21.6	23.2	23.1	20.5	16.6	10.1	2.8	0.1		
M	0			0.5	5.0	11.2	15.8	23.1	26.4	26.7	22.7	17.1	10.9	4.1	0.2		
	1		tr	1.9	8.4	14.9	22.3	26.3	28.9	29.2	24.8	19.5	13.6	7.1	1.2		
	2		tr	3.3	10.3	18.5	23.1	28.0	31.7	30.9	27.5	22.9	16.7	9.4	2.8	tr	
A	0		0.7	7.0	16.8	27.0	31.4	35.9	41.5	40.0	35.0	26.6	20.1	12.7	5.3	0.3	
	1	tr	2.4	10.5	21.0	33.3	41.8	48.4	50.9	50.1	45.4	37.4	30.4	17.9	8.0	1.6	
	2	tr	3.5	12.3	23.7	36.0	45.5	48.6	50.3	49.6	46.2	42.1	29.3	20.5	9.6	2.3	tr
M	0	0.2	3.9	10.7	18.4	24.6	32.1	41.6	42.9	40.9	39.0	37.6	30.4	23.2	13.6	4.2	0.1
	1	1.0	6.2	15.0	25.2	35.7	43.6	49.5	50.1	46.2	47.4	39.1	30.9	21.0	11.7	4.9	0.5
	2	1.6	7.1	15.1	24.3	33.8	38.9	46.7	47.8	49.9	46.9	41.9	34.4	25.7	15.7	7.6	1.5
J	0	3.0	11.5	21.6	31.5	41.6	49.1	58.2	58.8	60.9	55.3	50.8	41.5	30.0	19.6	9.4	2.4
	1	2.8	9.6	21.0	30.8	39.3	44.1	48.7	50.1	50.6	48.2	44.2	38.6	31.0	19.2	10.3	2.8
	2	2.8	9.6	18.6	29.1	38.5	46.6	51.6	52.6	51.6	51.2	49.3	37.5	28.7	17.1	9.9	2.4
J	0	2.3	8.8	17.0	27.8	36.9	41.8	47.0	49.0	47.6	45.1	39.7	33.2	23.6	15.5	8.4	2.1
	1	2.0	7.9	15.8	26.3	33.2	43.7	49.1	53.7	47.2	44.6	38.8	31.0	22.5	13.9	6.4	1.6
	2	1.3	7.2	17.3	28.0	37.9	46.0	51.6	54.5	54.4	51.3	42.4	33.8	25.0	16.6	6.6	1.0
A	0	0.3	5.0	13.5	22.0	32.7	37.9	44.6	48.2	48.8	45.9	39.1	31.6	22.3	13.7	5.1	0.2
	1	tr	3.9	13.0	24.4	35.7	43.8	47.0	50.9	50.8	46.5	39.5	33.0	21.3	12.0	3.4	tr
	2	tr	2.4	9.6	19.3	32.4	41.4	43.8	47.3	47.6	43.7	35.0	27.4	18.2	9.5	2.2	
S	0		0.9	6.2	15.8	26.6	35.1	40.7	45.4	42.4	40.5	32.5	24.9	13.2	6.0	0.3	
	1		0.1	3.6	11.9	22.0	28.7	33.6	35.7	34.6	34.0	27.0	20.3	11.6	3.5	tr	
	2		tr	2.1	9.5	17.5	23.6	31.3	34.3	33.6	28.9	25.9	17.8	8.4	1.7	tr	
O	0			1.0	5.8	13.2	20.9	28.9	32.4	33.5	30.1	22.7	14.3	5.6	0.5		
	1			0.1	3.6	10.3	16.0	22.0	25.8	25.7	21.4	15.2	10.1	3.8	tr		
	2			tr	1.6	6.3	10.7	16.4	19.5	20.3	17.1	12.9	6.7	1.7	tr		
N	0				0.9	5.5	10.5	15.3	17.9	17.8	14.8	10.1	4.4	0.6			
	1				0.2	3.8	9.1	13.1	15.3	14.9	12.1	7.7	2.8	tr			
	2				tr	2.4	5.9	10.3	12.6	12.8	9.6	5.3	1.6	tr			
D	0					1.4	5.0	8.6	10.7	10.8	8.8	5.2	1.2	tr			
	1					1.0	4.2	8.3	10.2	9.4	7.1	3.9	0.8				
	2					1.3	4.1	7.3	9.3	9.5	7.1	3.7	0.9				

TABLE III.

Corrected hourly means of Diffuse Radiation (mw.cm^{-2}) for 10-day periods

		4 - 5	5 - 6	6 - 7	7 - 8	8 - 9	9 -10	10-11	11-12	12-13	13-14	14-15	15-16	16-17	17-18	18-19	19-20
J	0				-	1.2	4.2	6.1	7.3	7.8	6.1	3.6	1.1	-			
	1				tr	1.6	4.6	6.5	7.4	7.7	6.1	4.3	1.5	tr			
	2				tr	2.2	5.0	7.8	9.0	8.7	7.2	5.1	2.3	tr			
F	0				0.4	3.0	5.8	8.0	9.4	8.9	7.7	4.8	2.6	0.3			
	1				1.1	4.1	6.8	10.2	11.7	11.0	9.3	6.8	4.2	1.1	tr		
	2			tr	2.7	6.6	10.6	13.7	14.3	15.1	13.6	11.4	6.6	2.3	tr		
M	0			0.3	3.6	6.9	9.8	13.7	14.4	14.3	12.6	10.5	7.1	3.4	0.2		
	1			1.2	5.6	10.1	13.8	15.8	17.0	16.7	14.4	11.2	8.5	4.9	1.0		
	2		tr	2.2	6.4	10.5	13.0	16.2	17.4	16.8	16.3	13.6	10.4	6.1	2.1	tr	
A	0		0.5	4.2	8.7	13.6	17.1	18.0	21.1	21.6	21.2	14.6	12.4	8.4	3.5	0.3	
	1		1.7	6.1	10.9	14.7	18.0	20.1	19.5	20.7	19.7	16.0	14.3	10.4	5.4	1.2	
	2	tr	2.3	7.2	12.4	17.0	20.2	22.0	22.6	22.5	21.0	16.6	14.3	11.1	6.0	1.8	tr
M	0	0.1	2.7	6.6	10.5	12.7	16.4	21.5	23.0	22.4	21.4	18.3	16.2	11.2	7.8	3.2	0.1
	1	0.7	4.1	8.7	13.2	17.6	20.3	23.1	24.8	23.0	21.6	19.1	15.4	11.1	7.4	3.6	0.4
	2	1.1	4.5	8.8	12.8	16.5	18.4	23.3	25.5	25.5	24.4	20.4	17.4	12.0	9.4	5.5	1.2
J	0	2.1	6.5	11.2	15.4	18.1	20.2	24.0	24.8	25.0	23.3	22.1	20.0	14.4	10.4	6.1	1.8
	1	2.2	6.1	10.7	16.8	20.0	22.9	26.1	26.9	27.4	27.1	24.0	19.8	16.8	11.5	6.7	2.2
	2	1.8	6.0	10.5	16.7	20.1	23.9	26.0	28.7	26.2	26.6	24.0	19.3	14.8	9.9	5.6	1.8
J	0	1.8	5.5	9.7	15.2	18.3	22.5	24.7	24.8	23.9	23.8	21.7	18.6	15.3	10.2	5.4	1.7
	1	1.4	5.1	9.2	14.9	19.8	24.7	27.3	28.1	28.6	26.2	23.7	17.8	13.9	9.3	4.9	1.3
	2	0.9	4.7	10.2	14.5	17.5	21.4	23.5	27.2	25.7	25.6	23.7	18.5	13.4	9.3	4.5	1.0
A	0	0.3	3.5	8.1	13.4	17.9	21.6	24.4	25.7	25.8	23.7	21.5	16.7	13.3	8.0	3.6	0.2
	1	tr	2.7	7.5	11.8	14.5	17.5	21.2	22.7	20.9	19.5	18.3	15.3	11.5	7.1	2.4	tr
	2		1.7	6.2	11.2	15.6	18.5	21.6	21.2	22.5	21.1	18.7	15.1	10.5	5.8	1.6	
S	0		0.6	3.9	8.7	13.5	17.5	19.5	22.0	20.5	20.2	21.3	14.0	8.6	4.1	0.2	
	1		0.1	3.0	7.8	12.2	15.0	17.8	20.2	20.3	19.2	15.2	12.0	7.4	2.7	tr	
	2		tr	1.7	5.7	10.7	13.5	16.2	18.5	18.5	16.0	13.2	9.7	5.1	1.2	tr	
O	0			0.6	4.1	8.8	13.3	16.0	16.3	15.7	14.7	11.6	8.4	4.0	0.4		
	1			tr	2.8	6.7	10.2	13.9	15.0	15.2	13.0	9.4	6.6	2.8	tr		
	2				1.3	4.7	7.5	10.4	11.7	12.1	10.5	6.9	4.3	1.0	tr		
N	0				0.7	3.7	6.0	8.4	10.1	10.1	8.7	6.0	3.5	0.4			
	1				0.1	2.9	6.2	8.8	9.6	9.3	7.9	5.5	2.5	tr			
	2				tr	1.7	4.3	6.1	7.3	7.4	6.2	3.8	1.3	tr			
D	0					1.1	3.9	6.0	7.1	6.8	6.2	4.1	1.0	tr			
	1					1.0	3.7	5.9	6.6	6.3	5.0	3.1	0.7				
	2					0.7	3.2	4.9	5.8	6.0	5.1	3.2	0.7				

TABLE IV.

Corrected hourly means of Direct Radiation ($mw.cm^{-2}$) for 10-day periods

		4 – 5	5 – 6	6 – 7	7 – 8	8 – 9	9 –10	10–11	11–12	12–13	13–14	14–15	15–16	16–17	17–18	18–19	19–20
J	0					2.0	5.7	6.8	7.8	7.5	6.0	3.8	1.0				
	1				tr	2.3	7.3	10.2	12.3	8.6	7.1	5.6	2.1	tr			
	2				0.1	2.9	6.8	11.0	13.7	10.7	10.2	7.8	3.7	0.1			
F	0				0.7	5.3	9.4	11.5	12.0	12.7	12.8	8.9	4.5	0.8			
	1				2.3	9.1	12.4	18.6	14.2	14.5	14.3	11.8	10.1	2.7	tr		
	2			0.1	3.4	10.6	15.4	16.5	16.3	16.5	15.4	14.6	12.3	4.1	0.0		
M	0			0.3	4.9	10.6	14.5	17.6	20.1	20.8	19.2	15.9	10.9	5.3	0.2		
	1			1.3	7.5	12.2	14.5	16.3	18.1	18.9	17.0	16.6	14.3	10.1	2.2		
	2		0.0	4.5	11.1	16.5	19.3	18.2	20.5	20.2	17.5	17.5	15.0	11.0	4.2	tr	
A	0		0.9	12.0	21.8	26.7	23.8	26.8	25.4	25.2	20.2	16.5	16.7	14.4	9.5	1.4	
	1		2.7	15.6	24.0	32.3	35.4	38.0	40.4	38.2	34.0	31.7	30.4	23.0	12.8	2.7	
	2	tr	6.3	16.6	25.1	32.6	36.9	35.9	35.9	36.0	35.4	35.9	29.0	25.3	15.6	5.3	0.1
M	0	0.7	6.7	14.5	17.4	20.5	23.9	26.6	25.2	23.9	25.2	26.6	26.0	25.2	20.5	9.4	0.6
	1	1.0	9.9	17.2	23.1	28.7	31.3	35.5	31.9	30.9	32.4	30.1	25.8	22.6	17.8	9.1	1.5
	2	2.8	9.5	15.7	23.2	27.4	27.7	29.3	25.9	28.9	28.3	28.6	26.8	23.7	17.6	12.0	2.4
J	0	6.0	18.5	27.3	29.8	34.1	37.0	40.8	39.2	41.9	40.6	39.8	34.4	31.2	25.7	17.1	5.7
	1	4.8	12.2	22.5	25.0	27.4	27.6	26.9	24.3	24.4	26.2	29.1	28.7	25.9	20.1	14.9	5.6
	2	4.1	11.8	18.7	20.7	26.4	26.0	29.3	26.9	28.0	27.7	31.6	25.7	25.0	18.5	17.1	5.6
J	0	3.8	12.2	17.8	21.1	24.7	28.7	26.2	27.5	27.1	26.4	23.0	17.8	15.4	13.9	10.1	3.7
	1	2.8	10.1	17.2	18.6	18.5	25.2	23.9	28.0	21.4	20.1	21.0	20.2	16.3	11.5	7.1	2.1
	2	2.1	11.8	20.1	25.9	28.7	32.5	33.8	31.7	34.4	33.1	25.2	24.3	24.5	21.2	14.2	2.4
A	0	0.9	6.8	14.6	16.8	19.7	20.9	24.5	24.7	26.9	29.4	22.6	21.4	19.0	17.1	9.5	0.7
	1	0.2	7.4	18.2	27.4	33.9	36.9	37.0	36.1	37.0	38.0	31.3	28.0	21.7	16.1	7.2	0.1
	2	tr	3.6	11.5	19.6	26.2	31.0	30.3	34.6	32.0	28.4	23.8	22.6	21.1	15.9	4.1	tr
S	0		1.7	10.3	18.9	25.3	29.3	31.7	31.2	29.8	26.7	24.0	22.2	13.8	7.4	0.5	
	1		0.3	7.4	14.7	19.0	22.8	23.3	20.3	19.9	21.1	20.7	20.0	14.6	6.5	tr	
	2		tr	2.6	9.4	16.7	18.0	22.3	22.5	23.3	19.9	22.8	20.7	12.0	3.3		
O	0			0.7	5.7	11.7	17.6	24.1	26.2	29.3	27.7	23.5	17.5	9.1	0.7		
	1			0.2	4.9	10.8	16.1	15.8	19.4	18.6	16.4	13.7	11.0	5.0	0.0		
	2			tr	1.6	5.9	8.6	13.0	16.1	17.3	15.3	14.2	9.9	2.1	tr		
N	0				1.2	8.0	14.5	17.3	18.3	16.4	15.6	11.8	7.7	0.9			
	1				0.2	5.9	11.3	15.2	17.4	16.0	13.8	9.6	4.1	0.1			
	2				tr	4.5	9.5	14.5	17.1	16.8	13.4	8.6	3.9	0.0			
D	0					2.8	7.0	9.3	10.6	13.1	11.7	8.5	2.1				
	1					0.8	4.3	7.5	11.6	10.3	6.8	4.5	1.0				
	2					1.2	6.3	9.5	11.5	11.1	7.4	4.2	0.9				

TABLE V.

Hourly means for 10-day periods of Extra terrestrial Radiation$_o$ (mw.cm^{-2}) on a horizontal surface. Computations based on Solar Constant of 138 mw.cm^{-2} (after Nicolet), reduced by 1% to "uncorrected Angstrom scale", and adjusted for annual variation of the solar distance

		19–20 4–5	18–19 5–6	17–18 6–7	16–17 7–8	15–16 8–9	14–15 9–10	13–14 10–11	12–13 11–12
J	0					7.4	21.4	31.8	37.4
	1				1.0	9.5	24.6	35.0	40.9
	2				3.6	14.2	29.3	40.1	45.9
F	0				5.8	20.6	35.8	47.5	52.6
	1				9.1	27.0	42.6	53.5	59.4
	2			3.0	14.9	34.3	50.0	60.8	67.0
M	0			5.6	20.8	40.1	56.0	66.9	72.8
	1			9.3	28.6	47.8	63.6	74.4	80.4
	2		2.4	13.9	35.4	54.5	70.2	81.2	87.2
A	0		5.7	21.7	42.9	62.0	77.4	88.2	94.1
	1		9.1	28.4	49.3	68.2	83.6	94.0	99.9
	2	1.7	12.7	34.2	54.6	73.1	88.0	98.8	104.4
M	0	4.6	18.5	39.4	59.5	77.5	92.2	102.9	108.4
	1	6.8	23.1	43.8	63.5	81.3	95.7	106.0	111.5
	2	7.3	26.8	47.1	66.6	83.8	98.2	108.2	113.6
J	0	10.3	29.6	49.6	68.8	85.9	99.9	109.6	115.0
	1	11.9	30.8	50.7	69.8	86.8	100.7	110.3	115.7
	2	12.3	31.2	51.0	70.0	86.8	100.7	110.4	115.7
J	0	11.1	30.0	49.9	69.2	85.4	99.9	109.6	114.9
	1	8.9	27.9	48.0	67.5	84.3	98.3	108.3	113.5
	2	7.5	24.9	45.1	64.7	82.0	96.1	106.3	111.5
A	0	5.4	20.9	41.5	61.4	79.2	93.5	103.6	109.4
	1	2.5	15.2	36.2	56.5	74.3	89.1	99.4	105.0
	2		10.2	30.7	51.2	69.6	84.6	95.1	100.8
S	0		6.9	24.0	44.9	63.6	78.8	89.2	95.1
	1		5.8	16.6	37.6	56.5	71.7	82.5	88.5
	2			10.6	31.5	50.5	66.0	76.9	82.7
O	0			7.0	24.3	43.3	58.8	69.7	75.4
	1			3.4	17.1	36.3	51.4	62.3	68.2
	2			1.4	10.0	28.9	44.5	55.2	61.3
N	0				6.3	21.5	36.9	47.8	53.5
	1				3.5	15.8	30.9	41.8	47.3
	2				1.4	10.9	25.9	36.5	42.2
D	0					7.9	22.3	32.8	38.4
	1					6.6	20.1	30.6	36.2
	2					6.5	19.7	30.0	35.7

TABLE VI.

Hourly means of Duration of Bright Sunshine (hours) for 10-day periods

		4 - 5	5 - 6	6 - 7	7 - 8	8 - 9	9 -10	10-11	11-12	12-13	13-14	14-15	15-16	16-17	17-18	18-19	19-20
J	0					0.03	0.16	0.18	0.20	0.19	0.19	0.11	0.02				
	1					0.07	0.23	0.24	0.28	0.22	0.19	0.18	0.04				
	2					0.05	0.18	0.30	0.35	0.28	0.29	0.20	0.06				
F	0				0.01	0.13	0.19	0.23	0.24	0.26	0.27	0.21	0.10	0.01			
	1				0.06	0.22	0.26	0.37	0.29	0.30	0.31	0.28	0.24	0.05			
	2				0.07	0.26	0.33	0.39	0.37	0.37	0.36	0.42	0.31	0.08			
M	0				0.11	0.24	0.31	0.35	0.41	0.45	0.43	0.37	0.31	0.12			
	1			0.02	0.19	0.29	0.35	0.34	0.40	0.36	0.35	0.35	0.34	0.26	0.02		
	2			0.07	0.27	0.38	0.40	0.38	0.38	0.40	0.38	0.37	0.36	0.30	0.07		
A	0		0.01	0.28	0.46	0.53	0.50	0.46	0.52	0.48	0.42	0.34	0.35	0.34	0.24	0.01	
	1		0.04	0.39	0.53	0.63	0.67	0.71	0.71	0.68	0.63	0.62	0.61	0.53	0.34	0.03	
	2		0.13	0.35	0.52	0.62	0.62	0.62	0.62	0.61	0.62	0.59	0.53	0.52	0.40	0.13	
M	0		0.13	0.30	0.32	0.35	0.39	0.43	0.43	0.40	0.42	0.47	0.47	0.51	0.48	0.29	0.00
	1	0.02	0.25	0.39	0.47	0.55	0.56	0.57	0.55	0.52	0.56	0.50	0.42	0.42	0.40	0.25	0.04
	2	0.05	0.25	0.38	0.45	0.50	0.47	0.50	0.47	0.51	0.53	0.53	0.49	0.45	0.40	0.35	0.08
J	0	0.09	0.48	0.57	0.54	0.60	0.63	0.67	0.63	0.67	0.65	0.63	0.63	0.59	0.54	0.51	0.17
	1	0.09	0.32	0.50	0.50	0.49	0.47	0.49	0.42	0.39	0.44	0.55	0.56	0.56	0.49	0.42	0.20
	2	0.06	0.32	0.44	0.46	0.46	0.48	0.50	0.47	0.40	0.45	0.56	0.49	0.50	0.45	0.44	0.17
J	0	0.12	0.29	0.38	0.44	0.52	0.50	0.50	0.49	0.45	0.46	0.47	0.42	0.39	0.38	0.33	0.10
	1	0.03	0.26	0.39	0.42	0.41	0.49	0.51	0.53	0.45	0.46	0.46	0.42	0.37	0.37	0.25	0.06
	2	0.04	0.32	0.49	0.55	0.56	0.59	0.63	0.60	0.60	0.65	0.56	0.51	0.50	0.53	0.39	0.07
A	0	0.01	0.16	0.34	0.35	0.43	0.43	0.50	0.47	0.52	0.52	0.46	0.47	0.42	0.43	0.33	0.01
	1		0.19	0.45	0.58	0.62	0.67	0.66	0.61	0.65	0.62	0.59	0.58	0.52	0.45	0.20	0.00
	2		0.08	0.28	0.49	0.59	0.61	0.60	0.64	0.63	0.57	0.51	0.52	0.45	0.43	0.13	
S	0		0.01	0.26	0.41	0.50	0.59	0.59	0.60	0.57	0.52	0.52	0.47	0.34	0.22	0.01	
	1			0.14	0.31	0.39	0.46	0.48	0.47	0.44	0.48	0.47	0.46	0.37	0.16		
	2			0.01	0.19	0.37	0.39	0.45	0.49	0.46	0.42	0.51	0.46	0.32	0.06		
O	0			0.00	0.12	0.30	0.43	0.50	0.58	0.59	0.60	0.55	0.47	0.24	0.01		
	1				0.12	0.24	0.35	0.40	0.44	0.37	0.33	0.34	0.28	0.13			
	2				0.03	0.12	0.19	0.33	0.39	0.39	0.36	0.37	0.27	0.05			
N	0				0.01	0.22	0.31	0.35	0.38	0.40	0.35	0.30	0.21	0.00			
	1					0.14	0.28	0.33	0.35	0.34	0.31	0.24	0.06				
	2					0.10	0.20	0.30	0.36	0.33	0.32	0.22	0.05				
D	0					0.04	0.17	0.22	0.26	0.29	0.30	0.24	0.02				
	1					0.00	0.11	0.19	0.28	0.25	0.19	0.14	0.00				
	2					0.03	0.15	0.21	0.26	0.29	0.20	0.10	0.01				

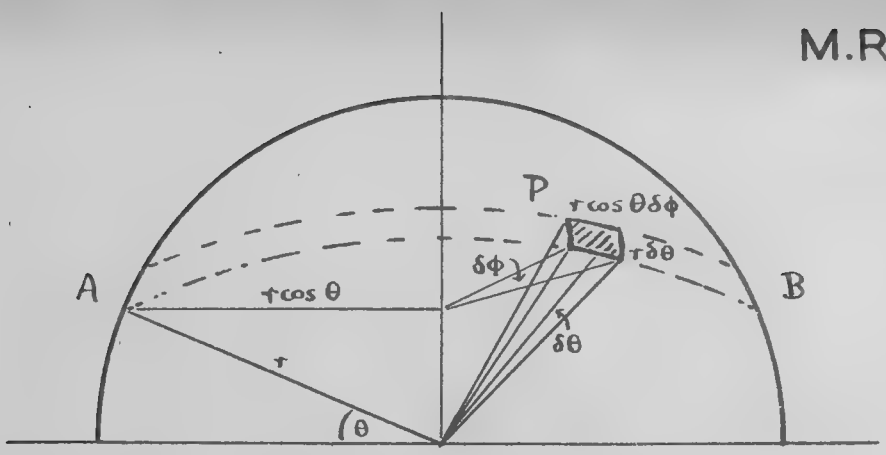

Fig. 1 - System of coordinates for obscuration calculation.

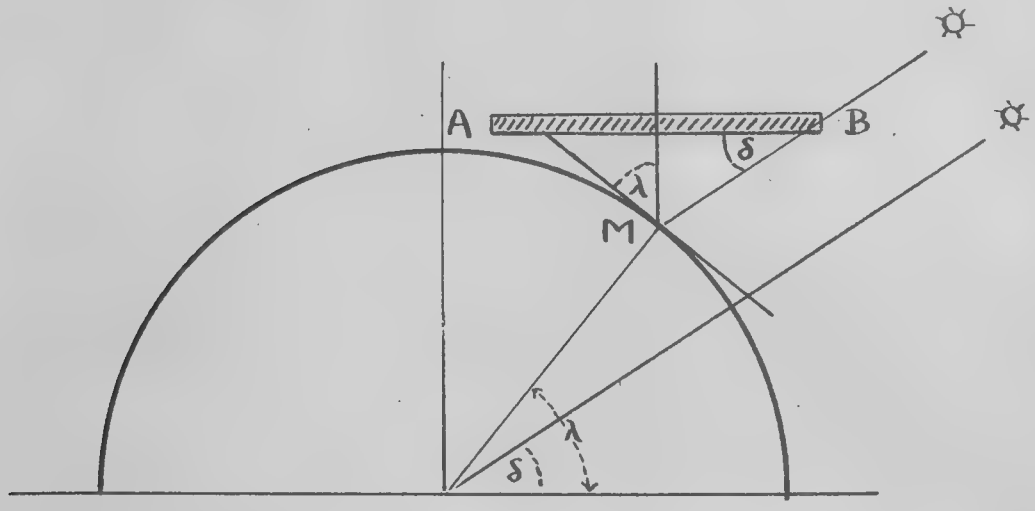

Fig. 2 - Showing the function of the shade-ring.

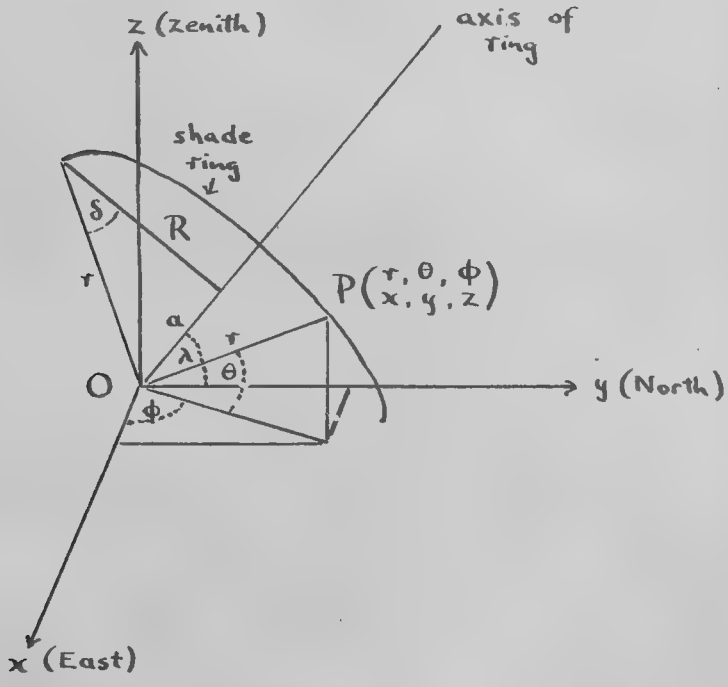

Fig. 3 - . System of coordinates for projecting centre-line of ring onto θ - φ diagram.

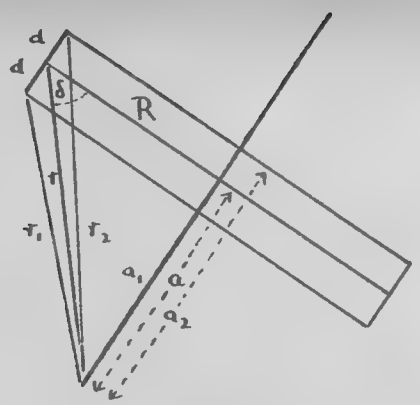

Fig. 4 - Relation between rims and centre-line of ring.

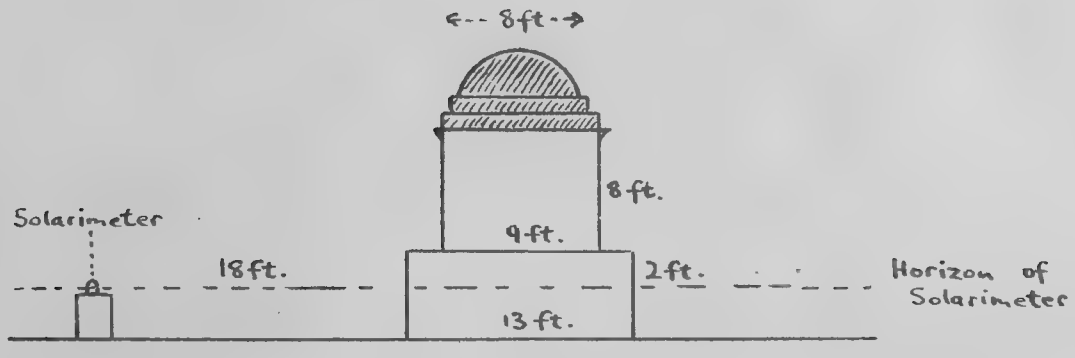

Fig. 5 - Schematic elevation of Observatory dome.

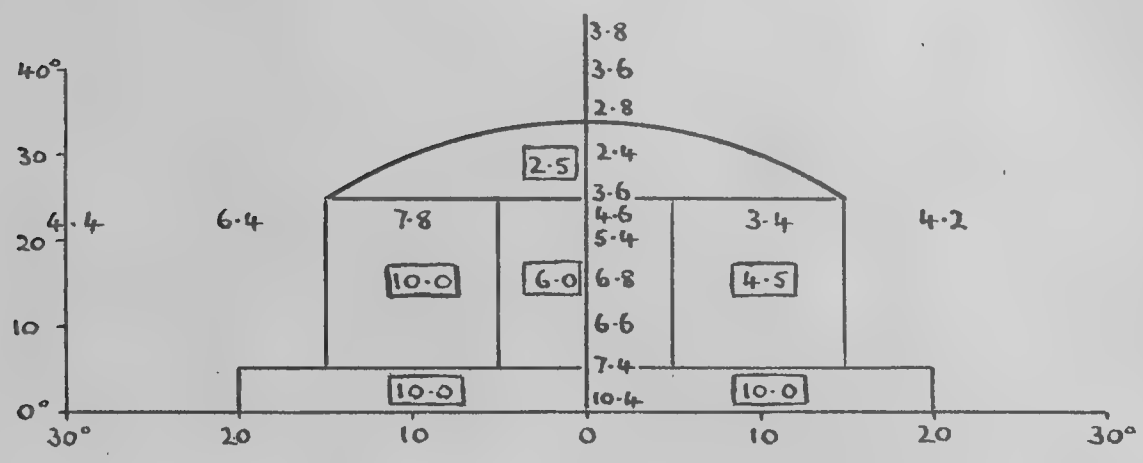

Fig. 6 - Variation of radiation intensity in vicinity of dome.

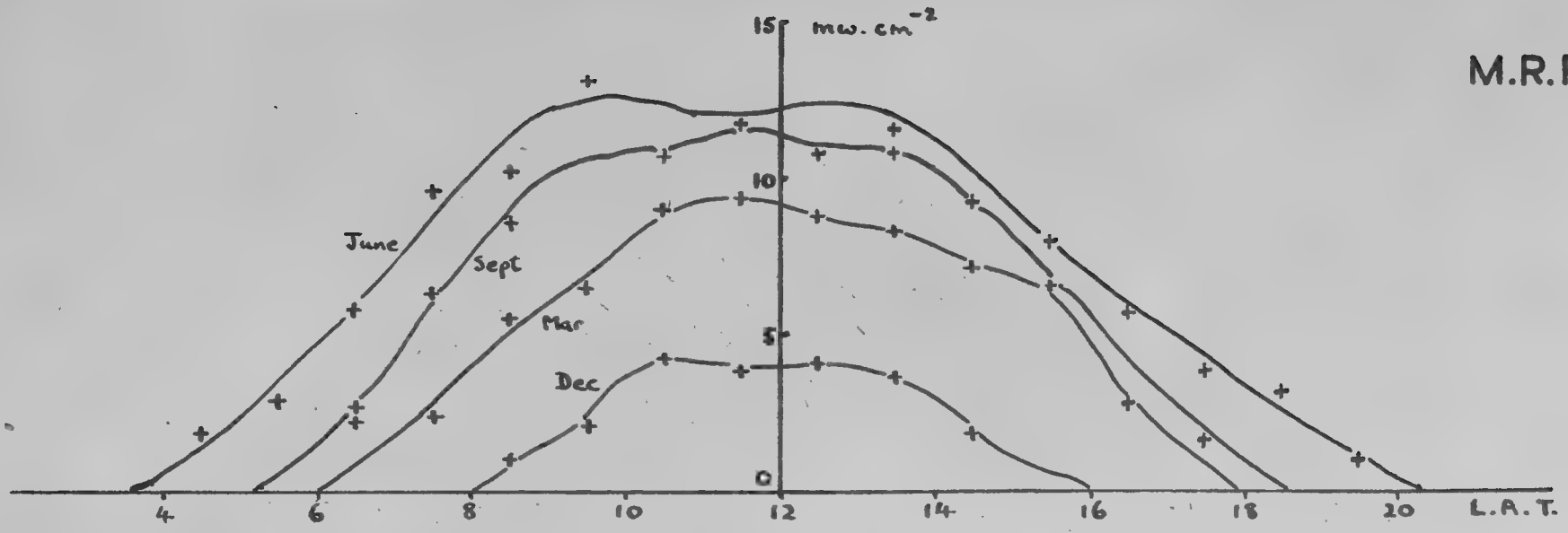

Fig. 14 - Diurnal variation of Total (= Diffuse) Radiation on overcast days.

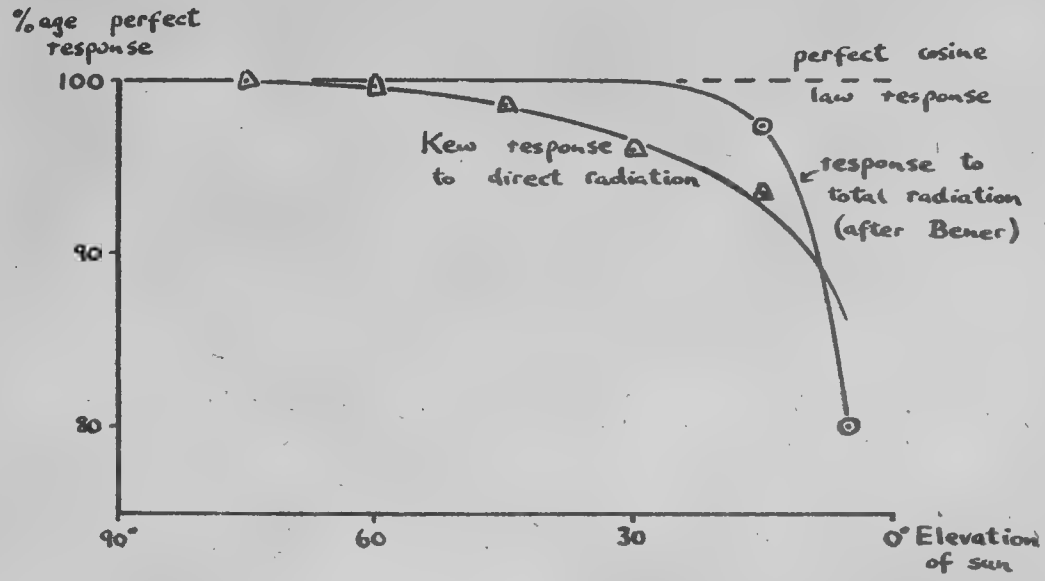

Fig. 7 - Departure of response from Cosine Law.

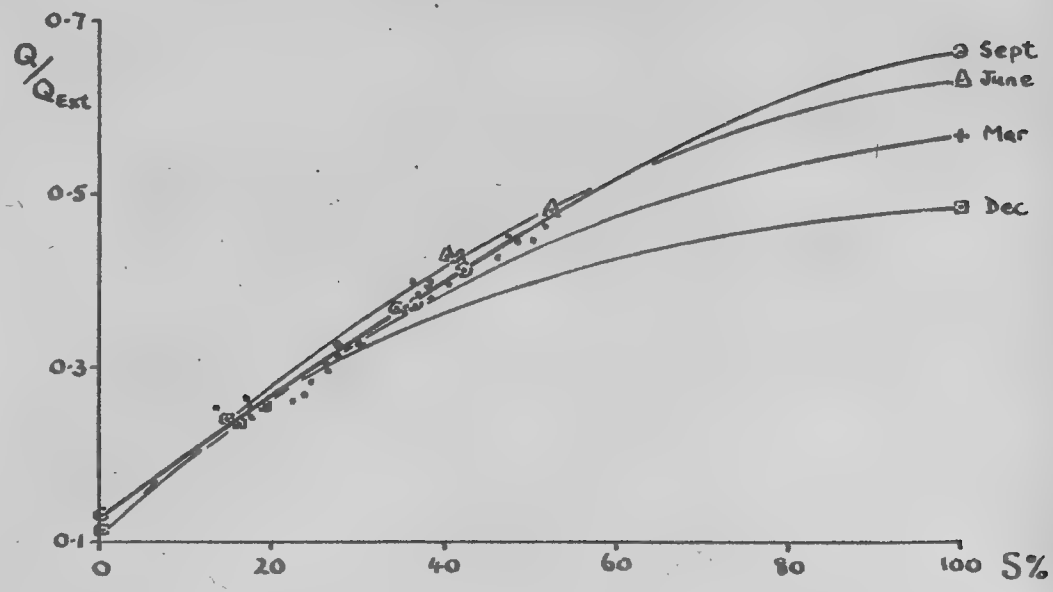

Fig. 16 - Correlation of Total Radiation and Sunshine.

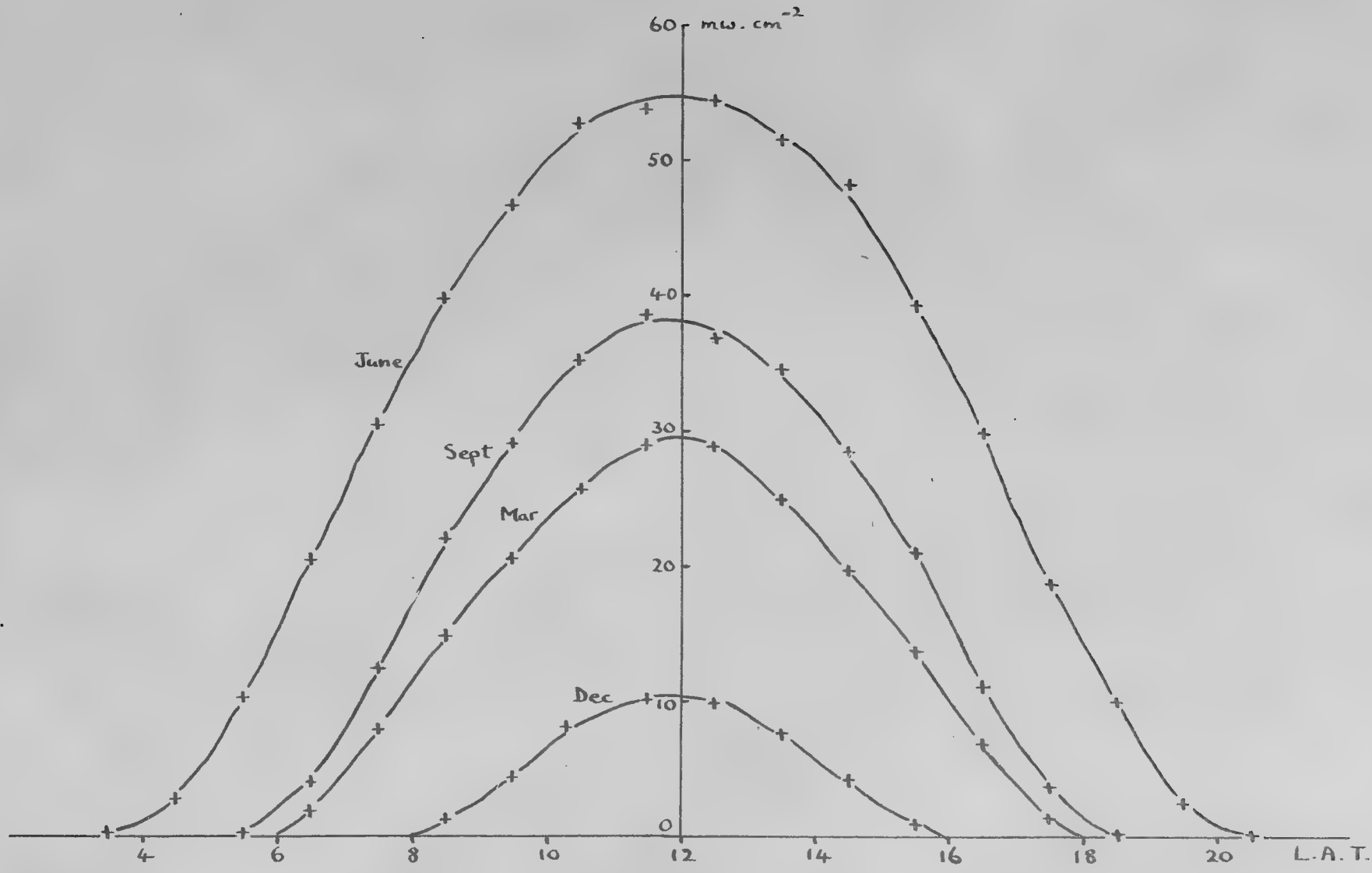

Fig. 10 - Mean diurnal curves of Total Radiation (all occasions).

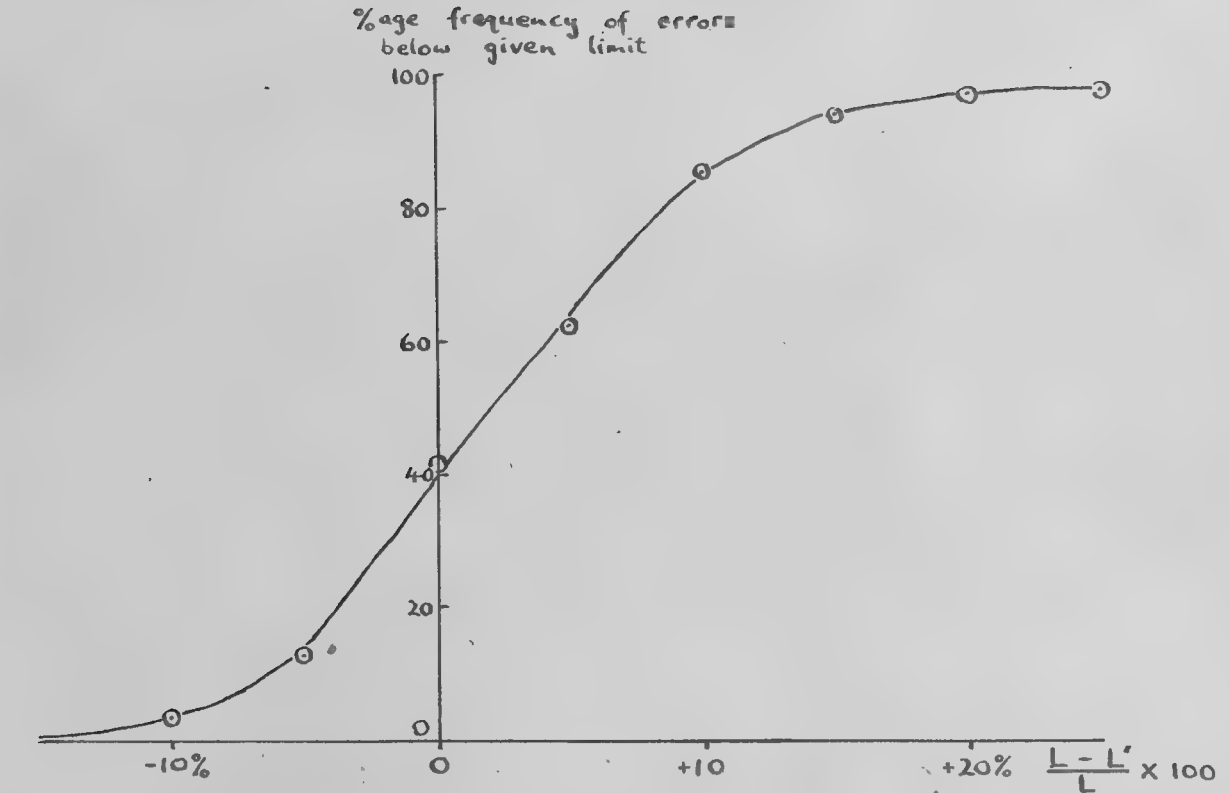

Fig. 8 - Ogive showing tabulating errors derived from independent estimations of same charts.

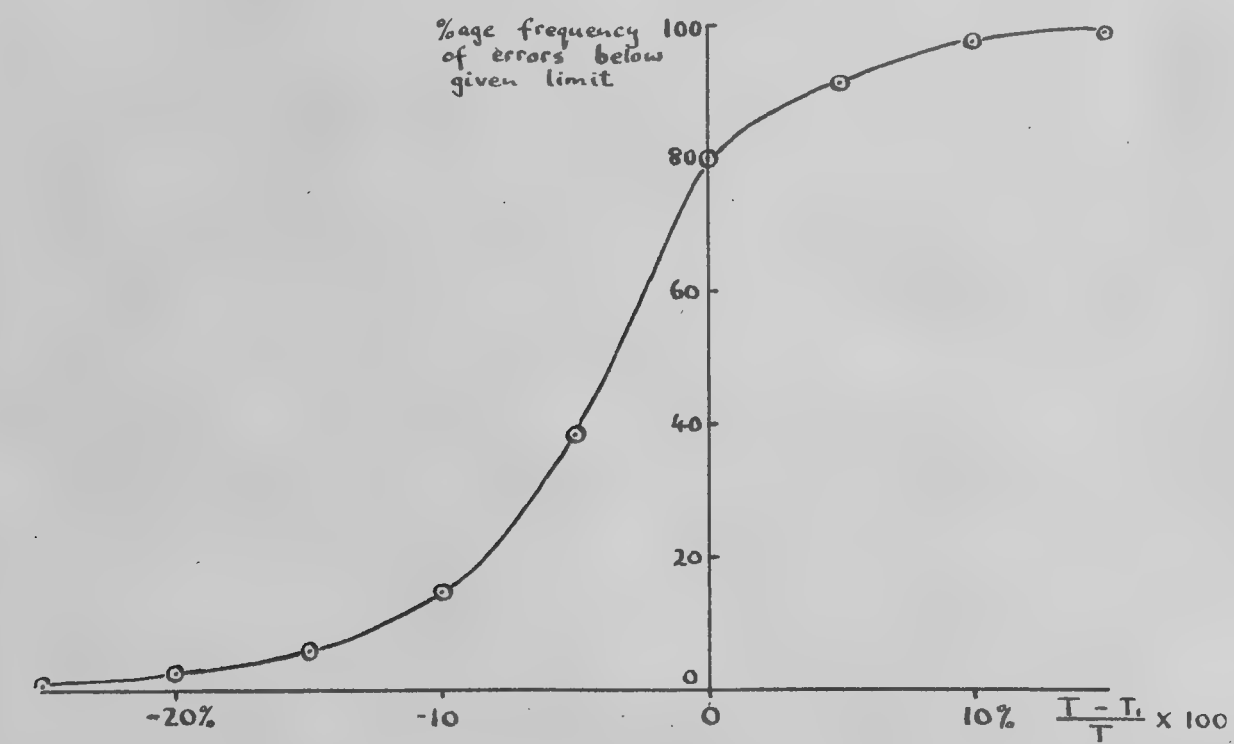

Fig. 9 - Ogive showing combined errors derived from tabulating charts of the same radiation component, but from different instruments and recorders.

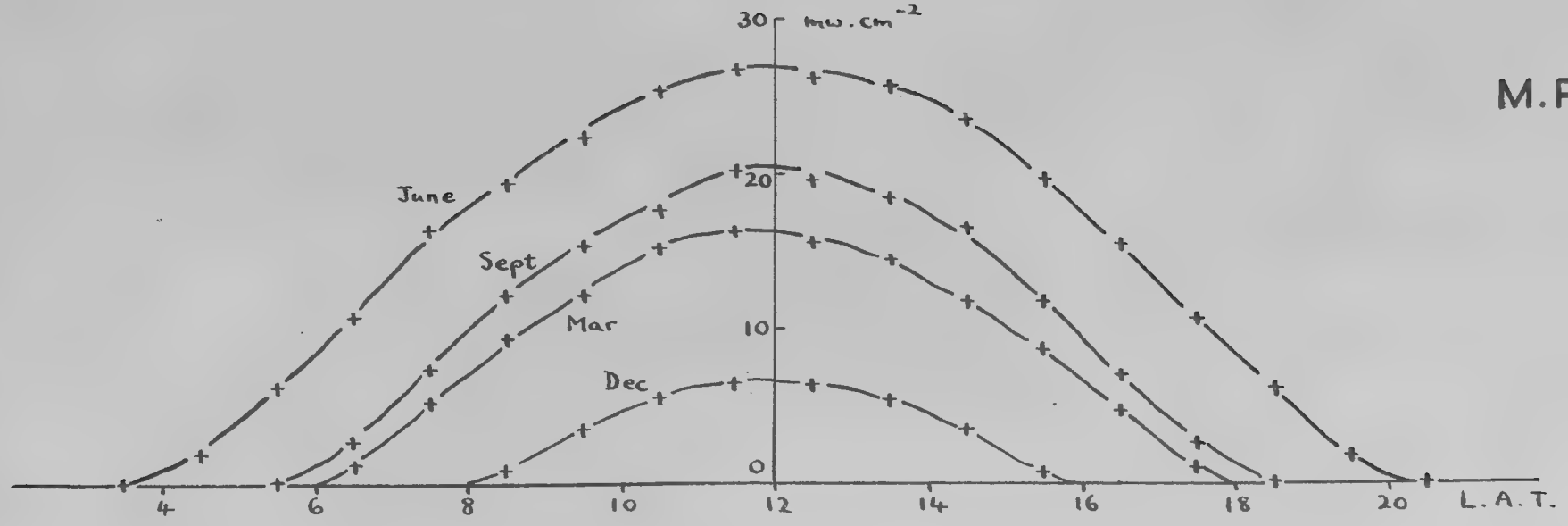

Fig. 11 - Mean diurnal curves of Diffuse Radiation (all occasions).

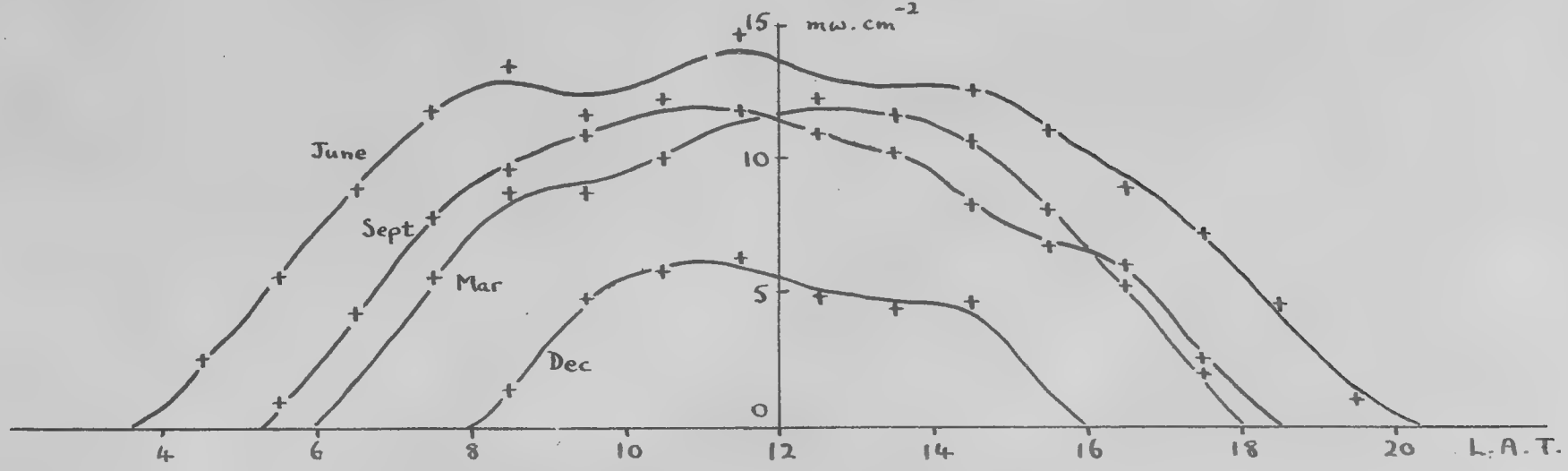

Fig. 12 - Diurnal variation of Diffuse Radiation on cloudless days.

M.R.P. 895

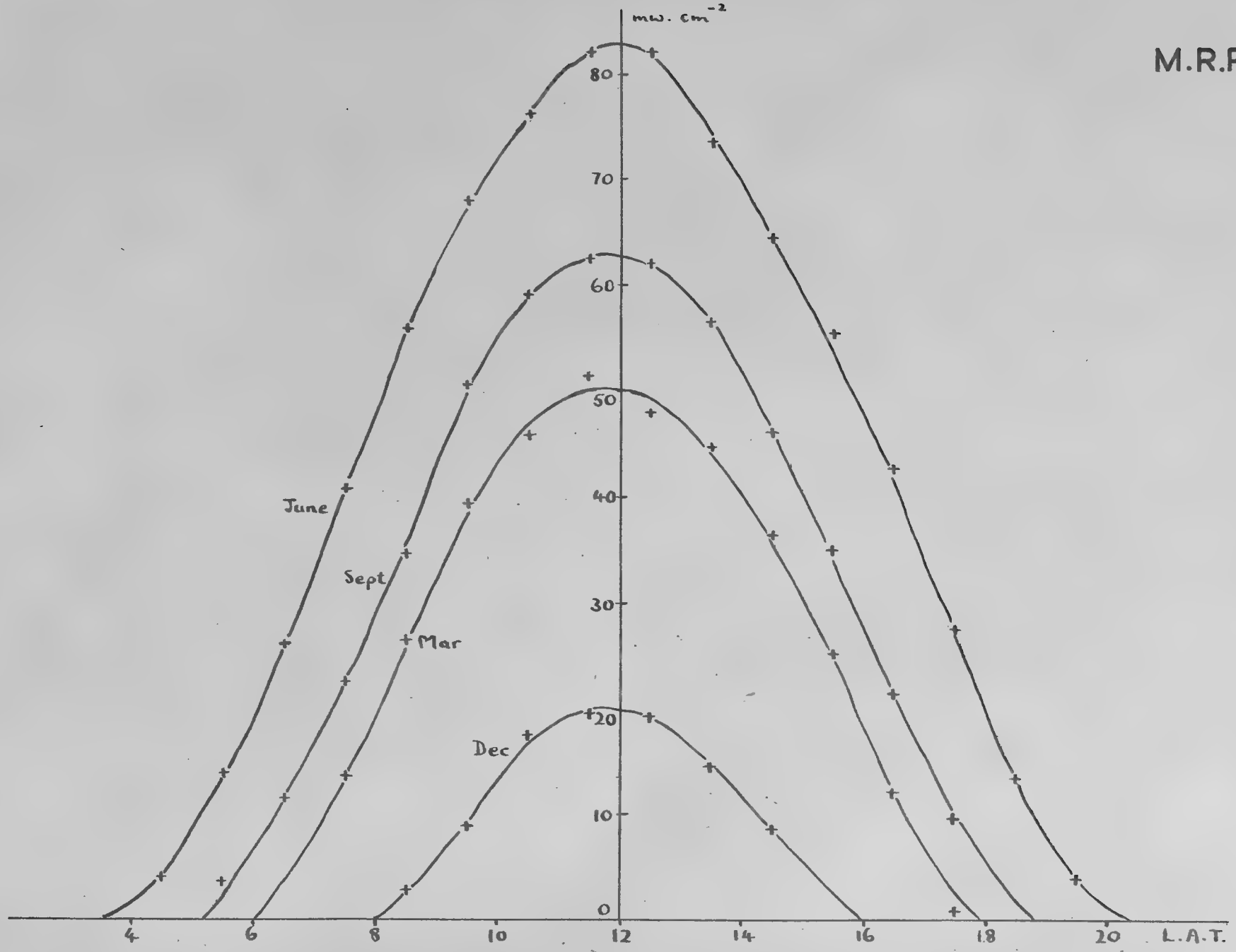

Fig. 13 - Diurnal variation of Total Radiation on cloudless days.

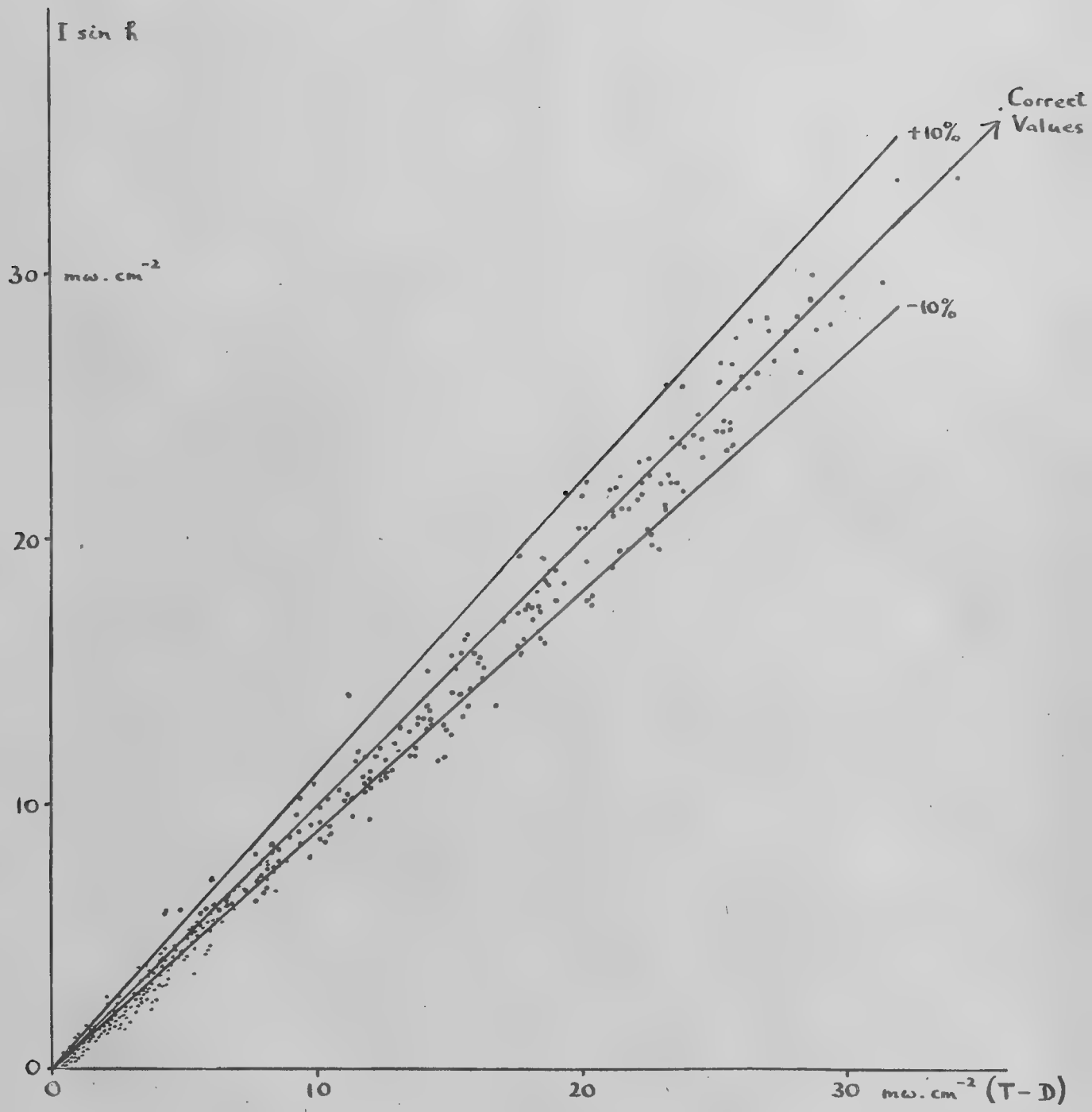

Fig. 15 - Self-consistency of the radiation measurements.

Control Number C.D. 8053

quote this paper should refer to it as "A paper of the Meteorological Research Committee (London).

A copy is available in the Library of

of fronts and their relation to frontogenesis

Although the Norwegian system of frontal analysis has been generally accepted by weather forecasters since the 1920's, no satisfactory explanation has been given for the "up-sliding" motion of the warm air to which is

in the associated field of vertical motion it is necessary to ary effects not specifically associated with the existence of the frontal zone. J.[illegible] relates the vertical velocities to zontal accelerations of the air parallel to the front and the same

of the association between fronts and rain, because

into which active confluence of air currents

vertical movements, which might be expected to destroy of a front within a day or so of its formation,

eristic features of the structure of

At the time of issue this report has not been published. Any author desiring to quote this paper should refer to it as "A paper of the Meteorological Research Committee (London). M.R.P. No.896 by Mr. J.S. Sawyer A copy is available in the Library of the Meteorological Office."

M.R.P. 896
S.C.II/183
31st December, 1954.

AD 79755
MAD

AIR MINISTRY
METEOROLOGICAL RESEARCH COMMITTEE

Some characteristics of fronts and their relation to frontogenesis

by
J.S. Sawyer (Meteorological Office)

1. Introduction

Although the Norwegian system of frontal analysis has been generally accepted by weather forecasters since the 1920's, no satisfactory explanation has been given for the "up-sliding" motion of the warm air to which is attributed the characteristic frontal cloud and rain. Simple dynamical theory shows that a sloping discontinuity between two air-masses with different density and velocity can exist without vertical movement of either air-mass, and in order to explain the associated field of vertical motion it is necessary to invoke secondary effects not specifically associated with the existence of the sloping frontal zone. J.Bjerknes (1924) relates the vertical velocities to the horizontal accelerations of the air parallel to the front and the same effect is considered in the somewhat more detailed mathematical analysis of Sawyer (1952a). Surface friction has been considered by Brunt (1941) and found inadequate to account for more than a fraction of the observed vertical motion, and turbulent mixing in the free atmosphere has been considered by Raethjen (1953). None of these explanations is entirely satisfactory as a fundamental explanation of the association between fronts and rain, because none appears to apply to all active fronts. The processes considered may however be important in modifying the structure of individual fronts.

The purpose of the present paper is to suggest that a front should not be considered so much as a stable area of strong temperature contrast between two air masses, but as an area into which active confluence of air currents of different temperature is taking place. There are several processes, friction, turbulence and vertical movements, which might be expected to destroy the sharp temperature contrast of a front within a day or so of its formation, so it would not be surprising if clearly defined fronts were found only where active frontogenesis is in progress. Some synoptic evidence for this point of view will be presented, and it will also be demonstrated that the frontogenetic process is necessarily accompanied by a vertical circulation system which can explain several characteristic features of the structure of fronts.

There is one essential difficulty which will beset any attempt to attribute the existence of fronts to any particular physical or dynamical process, namely the uncertainty as to what constitutes a front. The weather maps drawn independently by two synoptic analysts have only to be compared to show that the placing of fronts on the synoptic charts is not an objective process. With such a large uncertainty as to whether a front does or does not exist, one cannot expect to find any exact correspondence between the existence of a front on the synoptic chart and some specific physical process. On the other hand there are certain fronts which no experienced analyst would question, and there is no doubt that a systematic organisation of wind, pressure, cloud and rain occurs with them. The method adopted in the present paper is to study primarily fronts which are active and reasonably well defined and to present (in several different ways) the evidence that frontogenesis was in progress. Although a unique relationship is neither found nor expected between

/the

B-39

the existence of a front and the process of frontogenetic confluence of the horizontal flow, the evidence suggests a close association, and is believed to be adequate to show that the existence of recognisable frontal characteristics may owe much to the dynamics and kinematics of the process of frontogenesis.

2. The trajectories of air near fronts

Trajectories have been drawn of the air found in the vicinity of twenty active fronts, and serve to illustrate that the air parcels on opposite sides of the frontal zone usually have distinctly different tracks over the preceding 24 hr. The fronts, ten warm fronts and ten cold fronts, were chosen to cover a variety of synoptic situations, the sole restriction on the choice being that the front should be active and its identification reasonably unambiguous.

Air trajectories were drawn to terminate at a set of points in a vertical plane perpendicular to the front, spaced at about 100 mi intervals across the front. The trajectories were drawn separately for the 2,000 ft, 700 mb, 500 mb and 300 mb levels and covered a 24-hr period; they were based on the horizontal movement of air at these levels as deduced from appropriate measurements of geostrophic wind, supplemented by such direct wind observations as were available. Temperatures at points along the trajectories were estimated where possible by interpolation between soundings adjacent to the track, and these temperatures have been used to make some estimate of vertical motion.

Although there is evidence that vertical motion was present, such vertical movement was not sufficient to make the trajectories based on winds at one level seriously unrepresentative of the true movement of the air, and in view of the uncertainties in any drawing of air trajectories, no correction was attempted for vertical displacements.

Inspection of the air trajectories shows that air from widely different regions is frequently drawn into frontal regions. Although it is difficult in some individual cases to decide whether such a "confluent" process is present, in many cases the existence of such confluence is undeniable. A subjective assessment of the presence or absence of a marked difference in the trajectories of air on the warm and cold side of the frontal zone showed that such a difference existed in 19 cases out of 20 at the 2,000 ft level, 14 at 700 mb, 10 at 500 mb and 7 at the 300 mb levels. The single case in which no definite confluence was noted at any level was one in which the rain area was not aligned along the front and the well-defined frontal cloud system was absent.

As a rough measure of the degree of confluence the ratio of the distances between the initial and terminal points of the trajectories was calculated for trajectories terminating at points 200 to 300 mi apart enclosing the frontal zone. The mean values were 2.1, 2.7 and 3.0 for the 2,000 ft, 700 mb and 500 mb levels respectively. Values greater than unity show that the air particles were approaching one another, but some apparent confluence is inevitable from the fact that the trajectories were all drawn to terminate at points near together. As a basis for comparison 20 pairs of trajectories were also drawn to terminate at similarly spaced points in air masses away from fronts. The corresponding mean ratios of the initial and terminal distances between the air parcels namely 1.7, 1.6 and 2.1 for the 2,000 ft, 700 and 500 mb levels are definitely less than the values associated with frontal regions.

The fronts examined covered a wide variety of synoptic situations, and there was little similarity between the trajectories in different cases. It does, however, seem possible to draw a distinction between those cases in which the confluent flow pattern extended through most of the troposphere and those in which it was primarily a feature of the layer up to 700 mb. Typically, the former were associated with a well developed jet stream; in some cases they were associated with an obviously confluent pattern of stream lines at all levels but in other cases the confluence of the stream lines was not obvious

/and

and the confluence of the trajectories owes something to the movement of the stream-line pattern. A case of high-reaching confluence is illustrated by trajectories terminating at 0300 16 Aug. 1949 (Fig.1). A noteworthy feature is the fact that the line separating the two types of trajectories is displaced towards the cold air with increasing height.

An example of a front extending only to mid-troposphere with confluent flow only in the lower troposphere is given by the warm front of 3 May 1948 (Fig.2). No clear-cut confluence is found above the 700 mb level. Such cases are found mainly among fast moving warm fronts which are not clearly defined at high levels and which are not associated with the jet stream in the conventional manner. The rapid changes in the surface pressure field play an important part in bringing together air of widely different origin.

Inspection of the air temperature along the (horizontal) trajectories shows that cooling is frequent on the warm side of the frontal zone and warming on the cold side, indicative of descent of the cold air and ascent of the warm air. Fairly definite evidence of such vertical motion exists for 13 of the 20 fronts examined, in four cases the evidence is inconclusive and in three the vertical motion appears to have been slight. Table I was obtained by classifying the vertical motion of the air parcels according as the trajectory terminated in the warm, transitional or cold air mass. A change of 5°F or more in 12 hr was required before a case was classified as one of warming or cooling. The tendency at the 700 mb and 500 mb levels for cooling along the trajectory in the warm air mass and warming in the cold air mass is apparent. The temperature contrast between the air parcels moving into the frontal zone was reduced in 12 cases out of 14 at the 700 mb and 10 out of 11 at the 500 mb levels; the mean ratio of the final to the initial temperature difference being 0.74 at 700 mb, 0.71 at 500 mb and 0.77 at 300 mb.

Table I - Classification of temperature changes following horizontal air trajectories near frontal zones

Level	Warm Air			Transitional Air			Cold Air		
	Warming	Little change	Cooling	Warming	Little change	Cooling	Warming	Little change	Cooling
				(number of cases)					
700 mb	0	16	5	4	15	5	12	18	1
500 mb	0	27	6	15	2	1	4	3	3
300 mb	8	20	9	3	1	2	0	3	0

These temperature changes are consistent with a vertical air circulation upward in the warm air and downward in the cold air which tends to reduce the temperature contrast across the front; a contrast which is maintained primarily by the confluence of the air flow.

3. The field of frontogenesis in the vicinity of fronts-individual cases

The kinematics of frontogenesis have been considered by a number of writers, in particular by Bergeron (1928) and Petterssen (1935)[M].
It can be shown directly that at any point in a two-dimensional field of flow two adjacent fluid elements will approach or separate at a rate which depends on the orientation of the line joining the fluid elements as well as on the derivatives of the components of velocity u and v. The orientations

/for

Footnote[M] Throughout this paper "frontogenesis" has been taken to mean a condition of increasing horizontal temperature gradient. This is not exactly the same interpretation as that used by Petterssen who requires that a maximum rate of increase of horizontal temperature gradient should occur along a line.

for maximum expansion of the distance between the particles and for maximum contraction are mutually perpendicular; they are the axes of strain in the deformation field. Here they will be referred to as the "axis of dilatation" and "axis of contraction". In large scale meteorological systems of the size of depressions and anticyclones, and even down to the scale of fronts, a first approximation to the flow is given by the geostrophic wind field. Neglecting the variation of the Coriolis parameter with latitude, the geostrophic wind field is non-divergent, and it is readily shown that the rate of separation between two air parcels separated by a small distance S is given by

$$\frac{1}{S}\frac{\partial S}{\partial t} = \frac{1}{2}(A^2 + B^2)^{1/2} \cos 2\phi$$

where ϕ is the angle between the orientation of the line joining the fluid elements and the orientation which gives maximum contraction; following the notation of Petterssen (1953), A and B are defined by

$$A = \frac{\partial u}{\partial x} - \frac{\partial v}{\partial y} \qquad \text{and} \quad B = \frac{\partial u}{\partial y} + \frac{\partial v}{\partial x}$$

The angle, θ, between the direction for maximum contraction and the x-axis is given by

$$\cot \theta = \frac{A}{B} - \frac{1}{B}(A^2 + B^2)^{1/2}$$

(The positive sign of the square root is to be used in the preceding equations).

If geostrophic flow is assumed, A and B are readily calculated from a contour chart of an appropriate isobaric level. A simple method is to place a transparent scale of the form illustrated in Fig. 3 on the chart, and to evaluate A and B from the relations.

$$A = \frac{1}{a^2}\frac{g}{l}\left(H_D + H_H - (H_F + H_B)\right)$$

$$B = \frac{1}{a^2}\frac{g}{l}\left(H_A + H_E - (H_C + H_G)\right)$$

The symbol H_X indicates the value of the contour height at point X, g is the acceleration due to gravity, l is the Coriolis parameter and a is the radius of the circle on the scale in terms of map distance. If a corresponds to 168 nautical mi the multiplying factor g/a^2l becomes 1/10 in latitude 50°N. for values of H in units of 100 ft and values of A and B in units hr^{-1}. Such a scale has been used to evaluate A and B in the work which is described below.

It will be seen that the maximum rate of approach of any two adjacent fluid elements is proportional to $(A^2 + B^2)^{1/2}$. Thus this expression gives a measure of the maximum degree of frontogenesis in the given velocity field, and in order to realise this effect the isotherms must be orientated in the direction of the axis of dilatation. For any other orientation the rate of concentration of the temperature gradient is proportional to $(A^2 + B^2)^{1/2}\cos 2\phi$ where ϕ is the angle between the isotherms and the axis of dilatation. The velocity field will thus be frontogenetic or frontolytic according as the isotherms lie within 45° of the axis of dilatation or not.

Several charts have been drawn to show the distribution of the values of $1/2(A^2+B^2)^{1/2}$ and $1/2(A^2+B^2)^{1/2}\cos 2\phi$ in the vicinity of fronts. The charts have been calculated for the 700 mb level because although this level is within the lower troposphere and results may be related to surface fronts, the contour lines as drawn at C.F.O. are not distorted to conform to any conventional idea of the distribution of pressure in the vicinity of fronts.

Most of these charts show areas in which $\frac{1}{2}(A^2+B^2)^{1/2}\cos 2\phi$ has a maximum lying to the cold side of surface fronts. The correspondence is not perfect, but is sufficient to suggest that active frontogenesis is an important feature

/of

of the frontal organisation. An example of such a chart is provided by the cold front of 5 Nov. 1949 (Fig. 4). A well defined maximum of $\frac{1}{2}(A^2+B^2)^{1/2}$ lies parallel to the front and slightly to the cold side; it coincides closely with the position of the front at 700 mb. The axis of dilatation and the directions of the isotherms are nearly parallel in this region and the expression for the frontogenesis $\frac{1}{2}(A^2+B^2)^{1/2}\cos 2\phi$ also has a well defined maximum. The maximum of $\frac{1}{2}(A^2+B^2)^{1/2}$ in the west is less important because of the absence of any substantial thermal gradient, and because such thermal gradient as there is does not closely parallel the axis of dilatation over any significant area.

4. The field of frontogenesis in the vicinity of a series of fronts

In order to obtain some further information about the distribution of the field of frontogenesis in the vicinity of fronts, all of the active and well defined fronts occurring in the vicinity of the British Isles during January 1953 were examined. On each six-hourly chart on which such a front appeared, the values of $\frac{1}{2}(A^2+B^2)^{1/2}$ and $\frac{1}{2}(A^2+B^2)^{1/2}\cos 2\phi$ (in the notation of the preceding section) were calculated for a series of points extending at 200 mi intervals from the position of the surface front towards the cold air. These calculations were carried out separately for the 1,000 mb, 700 mb and 300 mb levels. It was found difficult to analyse the temperature field satisfactorily at 1,000 mb and 300 mb; at the former level the difficulty arose from the unrepresentative nature of surface temperatures and at the latter from the complications introduced by the tropopause. The direction of the 1,000 - 700 mb thickness lines and 500 - 300 mb thickness lines were therefore used to define a direction representative of the run of the isotherms in the lower and upper troposphere for use in determining the angle ϕ.

Histograms showing the frequency of values of $\frac{1}{2}(A^2+B^2)^{1/2}$ and $\frac{1}{2}(A^2+B^2)^{1/2}\cos 2\phi$ in various ranges are displayed in Figs. 5 and 6 for the individual points I, II, III and IV which were chosen to be 0, 200, 400 and 600 mi from the surface front respectively. The mean values are also given. Histograms are also given for the 700 mb level in respect of 22 cases of inactive fronts occurring during the first half of the month.

The important fact demonstrated by these histograms is the tendency for $\frac{1}{2}(A^2+B^2)^{1/2}\cos 2\phi$ to be positive near active fronts at the surface and 700 mb levels. From the frequency distribution the standard error of the mean is estimated to be about $0.06 \times 10^{-1}\,hr^{-1}$, so that it is clear that the mean values of $\frac{1}{2}(A^2+B^2)^{1/2}\cos 2\phi$ are significantly greater than zero for points 0, 200 and 400 mi from an active front at the surface and 0 and 200 mi from an active front at 700 mb. The mean values for inactive fronts are negative at three points and positive at one, but barely exceed twice the estimated standard error. At 300 mb the positive values at points II and III exceed twice the estimated standard error but the negative values at points I and II do not. It may be concluded that there is a definite tendency for the axis of dilatation to lie within 45° of the isotherms in an active frontal region, but not in an inactive one. The effect is particularly well-marked at 700 mb at a distance of 200 mi from the surface front where 38 out of the 42 values of $\frac{1}{2}(A^2+B^2)^{1/2}\cos 2\phi$ were positive.

The mean values of $\frac{1}{2}(A^2+B^2)^{1/2}$ do not differ significantly between active and inactive fronts, nor between the individual points at various distances from the front. This suggests that the orientation of the local axis of dilatation with respect to the isotherms is a more important factor in determining the activity of a front than the actual intensity of the deformation field.

The values of $(A^2+B^2)^{1/2}$ are greater for 300 mb than for the lower levels. This is partly an effect of the stronger winds at higher levels but may also arise in part from the greater errors of estimation at these high levels. Vuorela (1953) has pointed out that the neglect of the ageostrophic components of wind leads to an overestimate of the dilatation.

/Included

Included among the fronts of Jan. 1951 was one warm front which moved across the British Isles with very little change of form. It was active in the north and inactive in the south and it was possible to estimate the values of the dilatation on both active and inactive sections over a sequence of five charts at 6-hr intervals. The mean values of $\frac{1}{2}(A^2+B^2)^{1/2}\cos 2\phi$ so obtained are displayed in vertical section in Fig. 7, together with the axis of dilatation of the mean flow at 700 mb at several points placed with respect to the front. The axis of dilatation is seen to closely parallel the isotherms near the active section of the front leading to a well-defined maximum frontogenetic effect about 200 mi ahead of the active part of the front. This is also shown at the surface, but at 500 mb and 300 mb the maximum is split, part being 400-600 mi ahead of the surface front and part vertically above it. The values of the frontogenesis on the inactive section of the front are smaller and no clearly defined pattern is apparent.

5. Theoretical aspects of the role of confluence in fronts

Some idea of the possible role of the confluence process in the dynamics of fronts may be obtained from the consideration of a much simplified case. This is illustrated in Fig. 8 by horizontal and vertical sections. It is clear that a horizontal flow such as illustrated in Fig. 8 (a) would be expected to concentrate the temperature gradient near the central straight stream line. The flow is assumed to have the same general form at all levels, but as approximate geostrophic balance is required, the velocity in the direction of the isotherms will increase with height and the isokinetics will have the general form shown in the vertical cross-section Fig. 8(b).

As the thermal gradient increases the vertical wind shear must also increase if approximate geostrophic flow is maintained. Thus either the high level winds will be accelerated or the low level winds will be retarded and in either case a cross-isobaric flow towards the cold air aloft must be expected relative to the flow at lower levels. This arises from the well known relation between the acceleration of the air and its ageostrophic movement (see Sutcliffe 1938). A vertical circulation of the type indicated in Fig. 8(b) must result because the cross-isobaric flow will be much less at a distance from the axis of confluence than in the frontal zone because the thermal gradients are much less at a distance.

The preceding simple argument may be made the basis of mathematical calculation in order to estimate the numerical values of the vertical and cross-isobar movements. It is then possible to make some allowance for the effect of the vertical air-movement on the temperature field. Geostrophic flow will be assumed to be adequate to represent the flow parallel to the isotherms, but no such assumption will be made regarding the flow in the perpendicular direction.

We take the x axis in the direction of the isotherms in Fig. 8(a) which are assumed straight and parallel at all levels, and we use isobaric coordinates. The horizontal components of velocity are then u and v, and the vertical motion is described by $w \equiv dp/dt$. We shall assume that the large-scale field of confluence imposes an extension of fluid elements in the x-direction such that $\partial u/\partial x = F$ and that F is the same everywhere.

The equation of continuity then imposes the following condition on motion in the y, z plane.

$$\partial v/\partial y + \partial w/\partial p = -F \qquad (1)$$

In order to simplify the mathematics we shall treat the atmosphere as an incompressible frictionless fluid of specific volume α. The variations of α from place to place then represent the temperature gradients in the atmosphere. It seems likely that the essential characteristics of the motion will not be affected by this neglect of compressibility except in so far as the vertical variation of height as a function of pressure is changed.

/The

The assumption that geostrophic flow is an adequate representation of the motion in the x -direction implies that

$$lu = -g\frac{\partial h}{\partial y} \qquad (2)$$

where h is the height of an isobaric surface.

If we write u_g and v_g for the components of the geostrophic wind then

$$\frac{\partial u_g}{\partial x} = -\frac{\partial v_g}{\partial y} = \frac{-g}{l}\frac{\partial^2 h}{\partial x \partial y}$$

As we have assumed that $\partial u/\partial x = F$ and that the motion in the x -direction is adequately treated as geostrophic, it follows that $\partial v_g/\partial y = -F$ and without further loss of generality we can write $v_g = -Fy$. The x-component of the equations of motion can, therefore, be written,

$$\frac{\partial u}{\partial t} + u\frac{\partial u}{\partial x} + v\frac{\partial u}{\partial y} + w\frac{\partial u}{\partial p} = l(v + Fy) \qquad (3)$$

The hydrostatic equation gives

$$g\frac{\partial h}{\partial p} = -\alpha \qquad (4)$$

and combining with Eq. (2) we obtain the thermal wind equation $l\partial u/\partial p = \partial\alpha/\partial y$

The conservation of density requires

$$\frac{\partial \alpha}{\partial t} + v\frac{\partial \alpha}{\partial y} + w\frac{\partial \alpha}{\partial p} = 0 \qquad (5)$$

By operating on Eq. (3) with $l\,\partial/\partial p$ and on Eq. (5) by $\partial/\partial y$, subtracting and substituting from Eqs. (2) and (4), the following equation is obtained

$$l\frac{\partial v}{\partial p}\frac{\partial u}{\partial y} + l\frac{\partial w}{\partial p}\frac{\partial u}{\partial p} - \frac{\partial v}{\partial y}\frac{\partial \alpha}{\partial y} - \frac{\partial w}{\partial y}\frac{\partial \alpha}{\partial p} = l^2\frac{\partial v}{\partial p} - l\frac{\partial u}{\partial p}\frac{\partial u}{\partial x} - lu\frac{\partial^2 u}{\partial x \partial p} \qquad (6)$$

In view of the equation of continuity (1), the velocities v and w in the y,p - plane may be expressed in terms of a form of stream function by relations

$$v = \frac{\partial \theta}{\partial p} - Fy \qquad w = -\frac{\partial \theta}{\partial y} \qquad (7)$$

Substitution from (7) in Eq. (6) together with the condition $\frac{\partial u}{\partial x} = F$ then gives

$$l\left(l - \frac{\partial u}{\partial y}\right)\frac{\partial^2 \theta}{\partial p^2} + 2\frac{\partial \alpha}{\partial y}\frac{\partial^2 \theta}{\partial p \partial y} - \frac{\partial \alpha}{\partial p}\frac{\partial^2 \theta}{\partial y^2} = 2F\frac{\partial \alpha}{\partial y} \qquad (8)$$

If u and α are known functions of y and p this is a second order partial differential equation for θ which may be solved numerically given suitable boundary conditions. Such solutions have been obtained for selected density and velocity distributions and show the vertical circulation which should be expected to accompany them. Substitution of the calculated velocities into Eq. (5) gives $\partial\alpha/\partial t$ and shows how the density distribution should respond to the confluent wind field.

/It

It is natural to solve Eq. (8) over an area of the y,p plane bounded by two pressure surfaces $p = p_1$, and $p = p_2$ and two verticals $y = y_1$, and $y = y_2$ chosen to be well outside the baroclinic zone. We can assume that $w = 0$ for $p = p_1$, and $p = p_2$ and that the motion across the planes $y = y_1$, and $y = y_2$ is purely that resulting from the geostrophic confluent wind field which is the basis of the frontogenesis. The boundary conditions then become $\theta = 0$ at all boundary points.

For the purposes of numerical solution it is desirable to use units of length and pressure which permit the grid length used in solving the equation to be one unit and which give values of the coefficients of the order of magnitude of unity. It is also convenient to replace the variables y, p etc. by non-dimensional variables $y' = y/y_o$ where y_o is the selected unit of length etc.

The units which have been found convenient are

$$y_o = 50 \text{ nautical mi}, \quad p_o = 133 \text{ mb}, \quad t_o = 10 \text{ hr}$$

and $\alpha_o = 10/1.28$ gm cm^{-3} (i.e. roughly one hundredth of the normal specific volume of air near the ground).

With these units Eq. (8) becomes (in latitude 50°N.)

$$\left(1 - \frac{1}{4}\frac{\partial u'}{\partial y'}\right)\frac{\partial^2\theta'}{\partial p'^2} + 2\frac{\partial\alpha'}{\partial y'}\frac{\partial^2\theta'}{\partial p'\partial y'} - \frac{\partial\alpha'}{\partial p'}\frac{\partial^2\theta'}{\partial y'^2} = 2F'\frac{\partial\alpha'}{\partial y'} \qquad (9)$$

It is useful to recall that $\frac{\partial\alpha'}{\partial y'} = 1$ corresponds to a density gradient of 1 part in 100 in 50 nautical mi or approximately 6°C (11°F) in 100 mi. Also $\frac{\partial\alpha'}{\partial p'} = 1$ corresponds to a density gradient of 1 part in 100 in 133 mb. A corresponding lapse rate in the real atmosphere will depart by 3°C in 133 mb or roughly 2.5° C/Km from the appropriate dry or saturated adiabatic lapse rate. A reasonable representative value of $\frac{\partial\alpha'}{\partial p'}$ for an atmosphere without saturation would therefore be about 2. When saturation occurs near fronts the lapse rate in the warm air is frequently close to the moist-adiabatic and corresponding values of $\frac{\partial\alpha'}{\partial p'}$ may be less than $\frac{1}{2}$.

Eq. (8) is of the elliptic, parabolic or hyperbolic type according as the following expression is greater, equal to or less than zero.

$$1\left(1 - \frac{\partial u}{\partial y}\right)\left(-\frac{\partial\alpha}{\partial p}\right) - \left(\frac{\partial\alpha}{\partial y}\right)^2$$

The condition that Eq. (8) should be elliptic is easily shown to be equivalent to the condition obtained by Solberg (1936) for dynamic stability of a steady baroclinic current. This is often quoted in the form

$$1 - \left(\frac{\partial u}{\partial y}\right)_\alpha > 0 \qquad (10)$$

where $\left(\frac{\partial u}{\partial y}\right)_\alpha$ indicates differentiation along an isentropic surface.

If Eq. (8) is elliptic, that is if the motion is dynamically stable, a unique solution for θ can be determined if θ is known round the boundary.

If Eq. (8) is hyperbolic, that is if the motion is dynamically unstable, a unique solution is not always determined by the boundary values of θ, and it is possible to have non-zero solutions for θ without frontogenesis ($F = 0$). These correspond to the unstable circulations envisaged by perturbation theory.

/Condensation

Condensation processes may be important in determining the dynamical stability of the motion. This can be demonstrated by introducing a modification into the incompressible fluid model to correspond to the effect on the air density of the release of latent heat. We assume that instead of being governed by the requirement of constancy following the fluid motion, namely $\frac{d\alpha}{dt} = 0$, α satisfies the relation

$$\frac{d\alpha}{dt} = -\gamma w \qquad (11)$$

where $\gamma \geq 0$ in non-saturated areas and $\gamma > 0$ in areas corresponding to cloud. Eq. (8) then becomes

$$1(1 - \partial u/\partial y)\frac{\partial^2\theta}{\partial p^2} + 2\frac{\partial\alpha}{\partial y}\frac{\partial^2\theta}{\partial p \partial y} - (\partial\alpha/\partial p + \gamma)\frac{\partial^2\theta}{\partial y^2} = 2F\frac{\partial\alpha}{\partial y} \qquad (12)$$

and since the condition for dynamical instability involves γ, dynamical instability can arise in a previously stable situation solely on account of the occurrence of saturation.

Dynamic instability is unlikely to be a persistent feature of meteorological systems because the effect of friction operating within the unstable circulations would be to return the system to neutral stability. However the case of neutral dynamic stability may be a significant one and one case with neutral stability in part of the field has been included among those studied numerically.

Examination of a number of cross-sections through fronts confirms that the condition for dynamical instability is rarely, if ever, satisfied except in very limited regions, but the condition of neutral stability is frequently approached and probably reached on the upper troposphere on the warm side of the jet stream and (under saturated conditions) within the cloud mass that lies below this region.

In order to study the nature of the vertical circulation Eq. (9) has been solved for θ' by relaxation methods under a number of different conditions. The results are outlined in the following paragraphs and illustrated in Figs. 9 to 12. The solution has been carried out over a grid of points separated by unit distances of y' and p'. The grid extended from $p' = 0$ to $p' = 6$ (say from 200 to 1000 mb) and sufficiently far in the y'-direction to ensure that the solution in the central area was not materially affected by the lateral boundary conditions. In Figs. 9 to 12 the results are displayed in terms of meteorological units with a logarithmic pressure scale, in order to facilitate comparison with the atmosphere. The fields of vertical and horizontal motion normal to the front are shown together with the resulting rate of change of the field of specific volume. The assumed field of specific volume α is also shown, and these isopleths can be regarded as equivalent to isopleths of potential temperature in the atmosphere.

In all cases the value of F' has been taken to be unity corresponding to $\frac{\partial u}{\partial y} = 0.1\ \text{hr}^{-1}$ i.e. an extension of the fluid elements of ten per cent per hour in the x- direction.

Case I (Fig. 9)

The distribution of α' was assumed to be given by

$$\alpha' = -\left(\tan^{-1}\frac{y'}{2} + 2p'\right)$$

This corresponds to a vertical frontal zone with a horizontal density gradient equivalent to an air mass difference of temperature of 5°C, of which half is concentrated in a distance of 100 mi. The vertical density gradient is appropriate to a lapse rate of about $\frac{3}{4}$ of the dry adiabatic in dry air. The boundary conditions assume no motion across the isobaric surfaces at 1000 mb and 200 mb and no ageostrophic motion at 900 mi from the front.

/The

The field of vertical motion has maxima of about 3.4 mb/hr situated about 100 mi from the axis of main temperature contrast; the warm air ascends and the cold air descends. There is a slight asymmetry in the field of vertical motion with the zero isopleth inclined upward towards the warm air. Cross-isobar flow has a maximum of about 5 kt at the top and bottom of the layer considered - it is directed towards the warm air near the ground and towards the cold air aloft. The concentration of the density gradient by the confluent wind field is largely confined to the top and bottom quarter of the layer - density changes in the middle of the layer are small, the effect of the horizontal confluence being largely balanced by the vertical movements.

Case II

The distribution of α' was assumed to be

$$\alpha' = -(\tan^{-1} y'/2 + 2p')$$

This case is similar to the preceding one except that the total density contrast across the front is twice as great but is assumed spread over twice the distance (i.e. total contrast equivalent to 10°C of which half is concentrated in a distance of 200 mi). The computed patterns of vertical and horizontal motion are similar - the maxima of vertical movements being about 4.6 mb/hr and about 150 mi from the maximum temperature gradient. Maximum horizontal ageostrophic winds are about 7 kt.

Case III

Case III shows the pattern of vertical and horizontal motion that would be expected to accompany confluence at a sloping frontal zone. The distribution of specific volume is taken to be

$$\alpha' = -\tan^{-1}(y'/2 + p' - 3) - 2p'$$

and corresponds to the same horizontal temperature contrast as in case II but the frontal transition zone has a slope of about 1 in 100. The patterns of vertical and horizontal motion are similar to case II; they are inclined in the direction of the front but rather less steeply; the vertical velocities are somewhat lower than for a vertical frontal zone, but spread over a larger area. The rate of density change is dominated by the tendency of the confluent winds to increase the slope of the front, but again there is little density change in the middle of the troposphere.

Case IV (Fig. 11)

This is similar to case II but some allowance for the effect of condensation has been made. It has been arbitrarily assumed that the ascending air is saturated in the shaded area and that the vertical stability in this area has thereby been reduced to $\frac{1}{4}$ of its value elsewhere. The general patterns of vertical and horizontal motion are not greatly affected by the change in the stability although the upward velocity in the less stable area is increased to a maximum of 5.6 mb/hr. The change in the rate of density change is however more striking - the rate of warming in mid-troposphere in the "cloudy" area is twice what it was in case II and a notable tendency to increase in thermal gradient is shown along the cold side of the "cloud".

Case V

Some indication of the effect of the stratosphere has been obtained by solving Eq. (9) over a grid which contained an additional row of points along which it was assumed that the density gradient was the reverse of that at the remaining points. The additional row represented the stratosphere, and the vertical stability was taken to be twice as great ($\partial\alpha'/\partial p' = -4$) as at the remaining points which represented the troposphere.

/The

The grid was too coarse to hope that any detailed structure will be adequately portrayed. However it is probably significant that the vertical and horizontal movements in the troposphere are very little affected by the addition of the stratosphere. Slight upward motion is found in the stratosphere above the frontal zone and a small area of weak downward motion is computed about 100 mi towards the warm air mass; at greater distances from the front the circulation in the stratosphere is computed to be in the same sense as in the troposphere but vertical currents are less than 1/5 of their magnitude in the troposphere.

Case VI (Fig. 12)

As indicated in previous paragraphs the character of the solution of Eq. (9) is likely to be considerably affected if the thermal gradient becomes so great, or the vertical stability becomes so small, that the condition for dynamical instability (10) is approached. It was therefore considered desirable to carry out the solution of Eq. (9) for a case in which the condition for neutral dynamical stability was satisfied through a large part of the warm air mass. The example and solution are illustrated in Fig. 12.

The distribution of specific volume which was assumed corresponded to a sloping baroclinic zone with a slope of 133 mb in 50 mi, and to a total temperature contrast of about 15°C of which half is concentrated in a distance of 100 mi. The form used for α' was

$$\alpha' = -\frac{3}{2}\tan^{-1}(y' + p') - 2p'$$

The region above midpoint of the frontal zone was assumed to be saturated with water vapour and the value of γ in Eq. (11) was taken to be 2. This implies neutral vertical stability of the warm air at a distance from the front, but slight vertical stability in the vicinity of the front. The dynamical stability of the system depends also on the horizontal wind shear, and it is possible to specify the distribution of the component of velocity in such a way as to give neutral dynamical stability in the warm air above the frontal surface but not elsewhere.

The choice of u' to effect this was

$$u' = F(y') - 6\tan^{-1}(y' + p')$$

where $F(y') = 4y'$ for $-7/2 < y' < +7/2$

$F(y') = -14$ for $y' \leq -7/2$

$F(y') = +14$ for $y' \geq +7/2$

This distribution of u' is not unrealistic as it implies a cyclonic shear in the vicinity of the front, and an anticyclonic shear in the cold air beneath the frontal zone.

The solution of Eq. (9) for this case is illustrated in Fig. 12. Its detail must not be regarded as of much relevance to the meteorological problem because some features are largely dependent on the somewhat artificial discontinuity between the cloudy and unsaturated air along the thick sloping line. However the following features probably have a more general validity:-

(a) The upward motion is concentrated above the surface position of the front and is of much greater magnitude than computed in the cases in which dynamical instability was not approached (the maximum in Fig. 12 is 29 mb/hr).

(b) Subsidence is found in the cold air. It is spread over a larger area and the speed is less than that of the ascending current.

/(c)

(c) The density gradient between cold and warm air masses is increasing along the boundary of the cloudy region particularly near the ground, although the cold air is being appreciably warmed by subsidence at some distance from the frontal zone.

6. Interpretation of results

In sections 2, 3 and 4 evidence has been collected to show that active confluence is usually in progress in the vicinity of well-defined precipitating fronts. This confluence may extend through the troposphere but on some occasions is confined to the lower half. By considering simple theoretical models it has been shown in section 5 that such a system of confluence in a frontal belt throughout the troposphere requires a vertical circulation in which the warm air mass rises and the cold air mass sinks - a vertical circulation which is confirmed observationally in section 2. It is therefore reasonable to suppose that the characteristic distribution of cloud, rainfall and vertical motion in the vicinity of fronts is derived not solely from the existence of a horizontal temperature gradient but also from the existence of a frontogenetic wind field which tends to concentrate the temperature gradient.

Once the band of cloud and rain is established it will not disperse immediately the frontogenetic wind field is removed and it should not be surprising if fronts are drawn on the weather map without associated frontogenesis. However, such fronts appear to be less active and less well-defined than those associated with marked frontogenesis.

The theoretical discussion of section 5 gives an indication of the magnitude of the horizontal and vertical circulations which may be expected to arise from the proposed mechanism. The rate of rainfall corresponding to any distribution of vertical velocity depends on the temperature and humidity of the air column but for a saturated atmosphere with a wet bulb potential temperature near 50°F the highest values of the vertical velocity computed in any of the theoretical examples of section 5 (with the exception of case VI) correspond to rainfall rates of only 0.5 mm/hr, insufficient to be classed as "moderate" rain. In case VI, in which the density field is such as to give neutral dynamical stability over an extensive cloud mass, the maximum rate of rainfall would be between 2 and 3 mm/hr, a typical rate of steady moderate rainfall.

The various values which have been used for the temperature gradients and rate of frontogenesis etc. in the calculations of section 5 are to some extent arbitrary, but it is unlikely that they seriously underestimate the naturally occurring values. In fact the value of the frontogenesis, F, which has been assumed, namely 0.1 hr^{-1}, is likely to be an overestimate rather than an underestimate of the confluence effect (the mean value of $\frac{1}{2}(A^2+B^2)^{1/2}$ for the 700 mb level in the region of fronts obtained from the analysis of section 4 is only a little over 0.05hr^{-1}). We may therefore conclude that the vertical circulation accompanying frontogenesis is likely to result in only light rainfall unless the distribution of wind and density is such that neutral dynamical stability is approached.

It is not, however, to be expected that all of the vertical motion and rainfall which is observed in the vicinity of fronts owes its origin to characteristics of the front itself. Fronts are usually to be found within regions of cyclonic development where upward motion is to be found as a result of large-scale dynamical factors not directly connected with the front. Indeed recent numerical studies have provided calculated values of the vertical air movement of the correct order of magnitude and distribution to explain the main features of the rainfall distribution without specific consideration of the fronts. Although these calculations may take into account the frontogenetic effect considered in section 5, other dynamical factors also enter into the calculations and are generally of greater importance. It may be remarked that the particular frontogenetic effect, upon which the preceding calculations depend, was omitted from Sutcliffe's treatment of development (Sutcliffe 1947) and

/consequently

consequently was not considered in the calculations of rainfall for the two synoptic situations studied by Sawyer (1952b). Nevertheless the general features of the rainfall distribution were adequately calculated.

It is uncertain whether dynamically unstable conditions occur over sufficiently extensive areas to be important in modifying the vertical circulation, or whether extensive dynamically neutral conditions must be taken into account. However, the occasional occurrence of such conditions together with the existence of superimposed fields of vertical motion associated with the larger scale synoptic systems is probably an adequate explanation of the occurrence of heavy rainfall intensities at some fronts. Making allowance for the occurrence in some cases of near neutral dynamical stability, the theoretical model of section 5 is probably an adequate explanation of the light or moderate rainfall which is more commonly associated with fronts. To resolve the relative importance of the various factors would require a detailed study of individual fronts.

The distribution in Figs. 8 to 12 of $\partial\alpha'/\partial t$, the rate of change of specific volume shows clearly that the rate of intensification of the density gradient is much more rapid near the ground and near the tropopause than it is in mid-troposphere. This conforms with the observed fact that fronts are best defined in the lowest and highest layers of the troposphere. The gradient of $\partial\alpha'/\partial t$ found near the cold boundary of the assumed cloud mass in Figs. 11 and 12 suggests that the condensation process may be an important factor in concentrating the temperature gradient in mid-troposphere near the cold boundary of the cloud.

In Fig. 12 ageostrophic winds of 15 kt are shown blowing across the direction of the front; these values may be rather too large, but values of say 10 kt would imply a difference in the transverse velocity between lower and upper troposphere of 20 kt. Over ten hours such a shear could cause a displacement of the frontal zone in the upper troposphere of 200 mi from its surface position. This transverse circulation may be a significant factor contributing to the slope of a front although it probably is not the only one. The frontogenetic properties of the wind field are not usually as uniform as assumed in the theoretical model and may have a maximum which is displaced towards the cold air at higher levels. This is also suggested by the kinematic analysis of a depression given by Sawyer (1953).

7. Conclusions

The large scale circulation around depressions and anticyclones inevitably contains regions of confluence and when these are associated with a temperature gradient perpendicular to the axis of dilatation frontogenesis results. This frontogenesis leads to a vertical circulation which causes the ascent of the warm air and descent of the cold air and the formation of an inclined frontal zone.

Synoptic evidence suggests that such frontogenesis is in progress in association with most active fronts and it seems likely that they owe their characteristic features to it.

The theoretical discussion which has been given necessarily applies to a very much simplified model. Fronts will usually be found in areas where active cyclogenesis is in progress as a result of dynamical developments on a larger scale so that the characteristic frontal pattern of vertical motion is superimposed upon that resulting from the larger scale cyclogenesis. It is thus not to be expected that all the rainfall found in the vicinity of fronts is to be explained from the frontogenetic process, although the explanation of the characteristic frontal distribution of cloud and rain probably lies therein.

/References

References.

Bergeron, T.	1928	Geofysiske Publikasjoner, Oslo, Vol. 5, No. 6.
Bjerknes, J.	1924	Geofysiske Publikasjoner, Oslo, Vol. 3, No. 6.
Brunt, D.	1941	Physical and Dynamical Meteorology (second edition), p.353.
Petterssen, S.	1935	Geofysiske Publikasjoner, Oslo, Vol. 11, No. 6.
	1953	Tellus, Stockholm, Vol. 5, p. 231.
Raethjen, P.	1953	Dynamik der Zyklonen, Leipzig, pp.164, 165.
Sawyer, J.S.	1952(a)	Quart J. R.Met. Soc., London, Vol. 78, p. 170.
	1952(b)	Quart J. R.Met. Soc., London, Vol. 78, p.231.
	1953	Proceedings Toronto Met.Conference, p. 145.
Solberg, H.	1936	U.G.G.I., Ass.Met., Edinburgh, 1936, p. 66.
Sutcliffe, R.C.	1938	Quart.J.R. Met. Soc.,London, Vol. 64, p. 498.
	1947	Quart. J.R. Met. Soc., London, Vol. 73, p. 370.

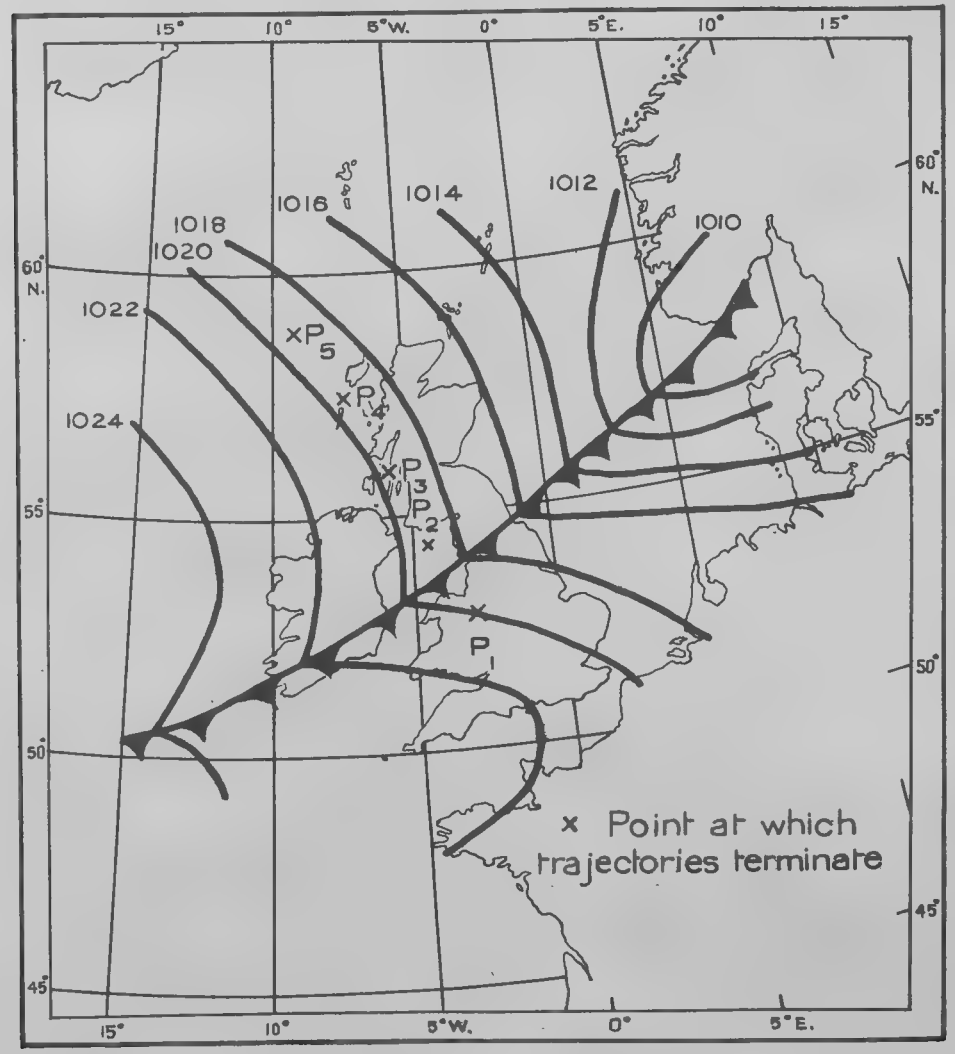

Fig.1(a) Synoptic chart 0300 G.M.T., August 16, 1949.

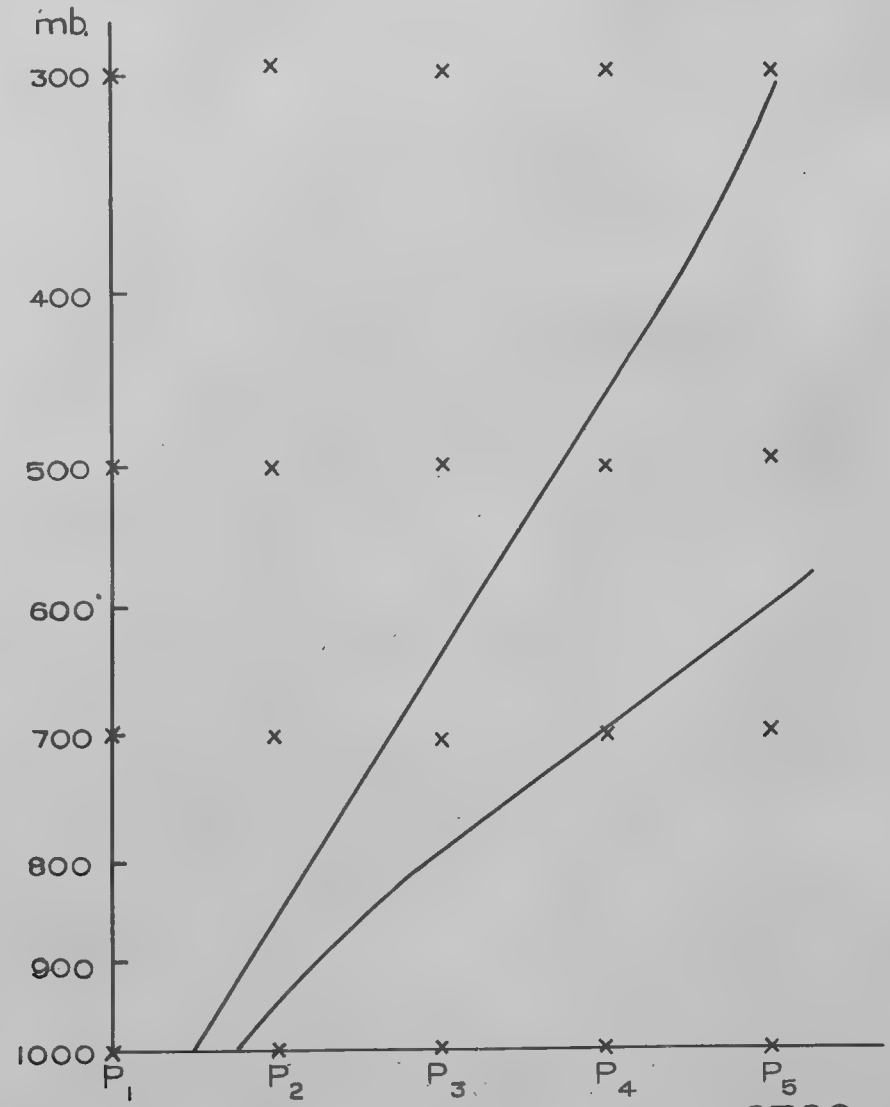

Fig.1(b) Vertical cross-section for 0300 G.M.T., August 16, 1949, showing boundaries of frontal zone along the line on which trajectories terminate.

Fig.1. (c,d,e and f) 24 hour trajectories terminating in the frontal zone over the British Isles 0300 G.M.T. August 16 1949

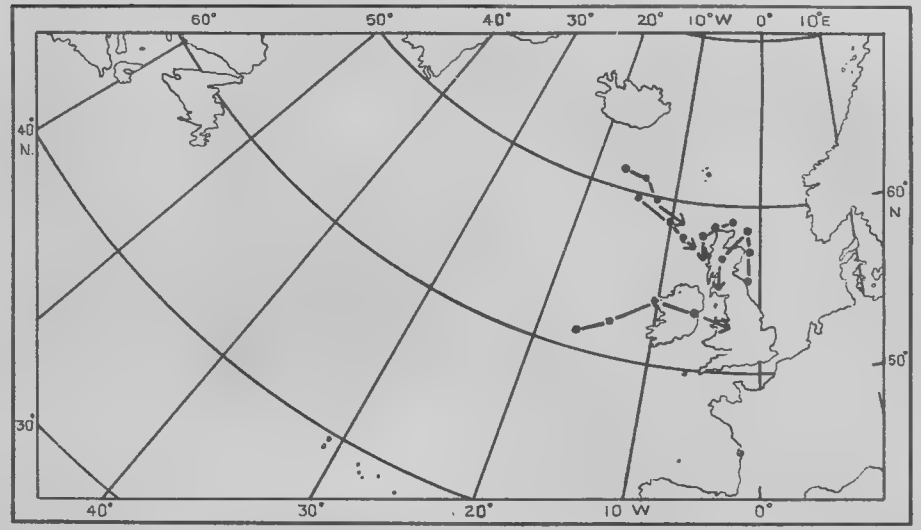

Fig.1 (c) Surface trajectories

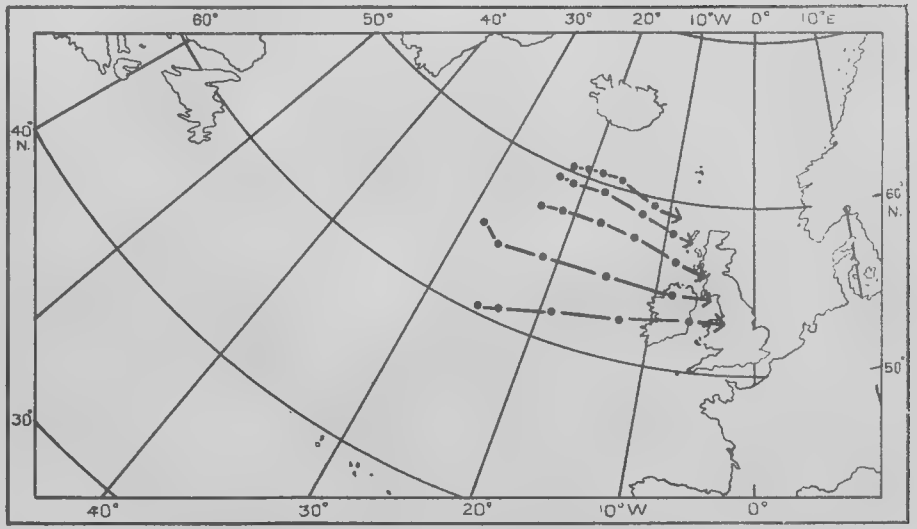

Fig.1(d) 700 mb. trajectories

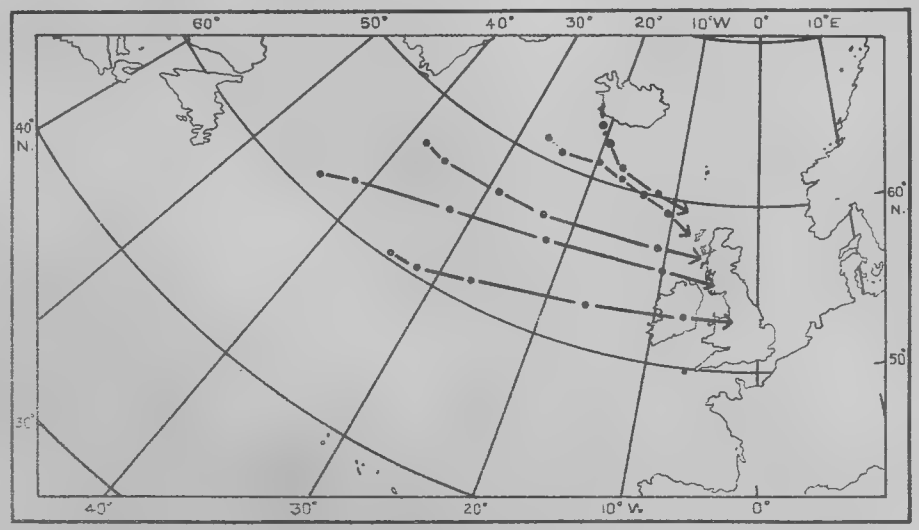

Fig.1(e) 500 mb. trajectories

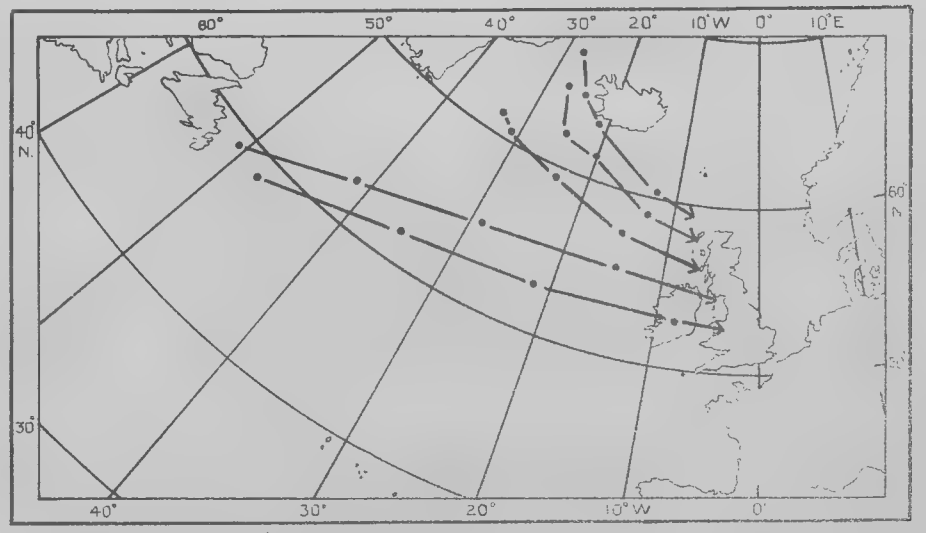

Fig.1(f) 300 mb. trajectories

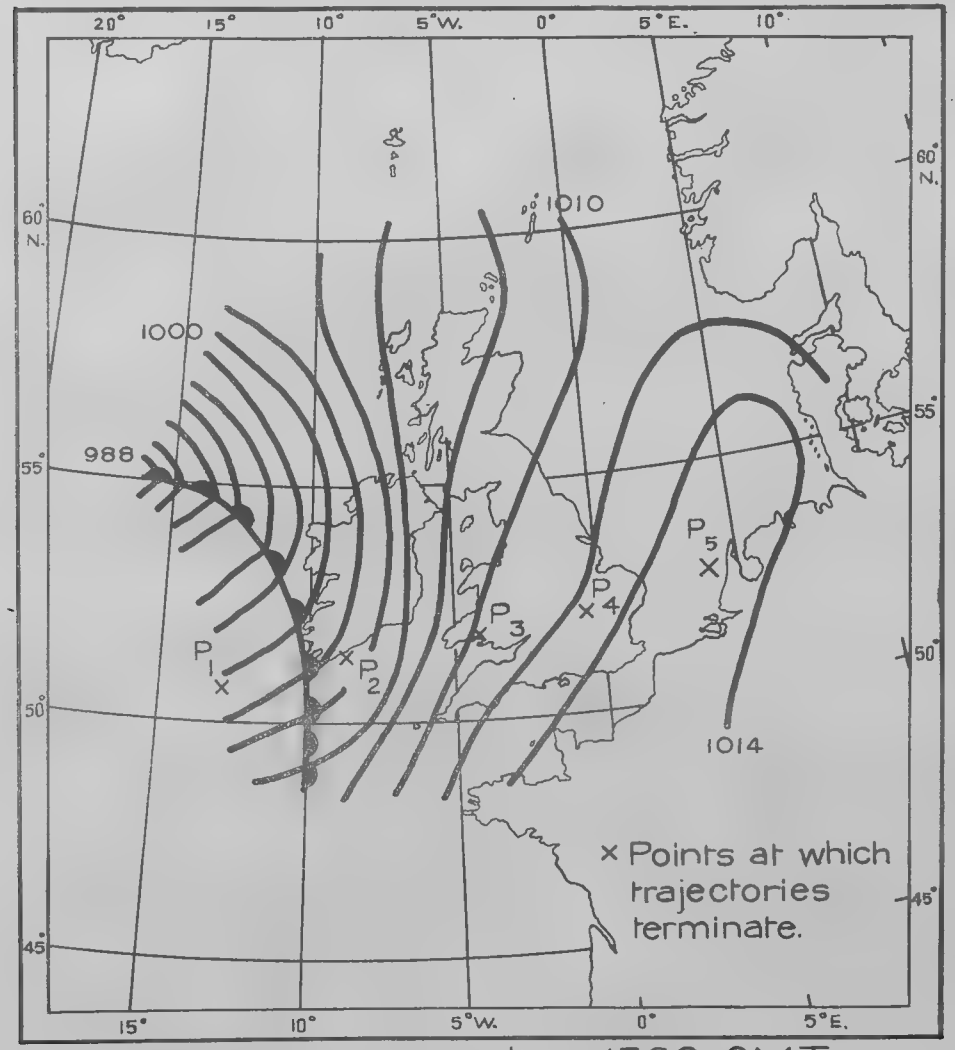

Fig. 2 (a) Synoptic chart 1500 G.M.T., May 3, 1948.

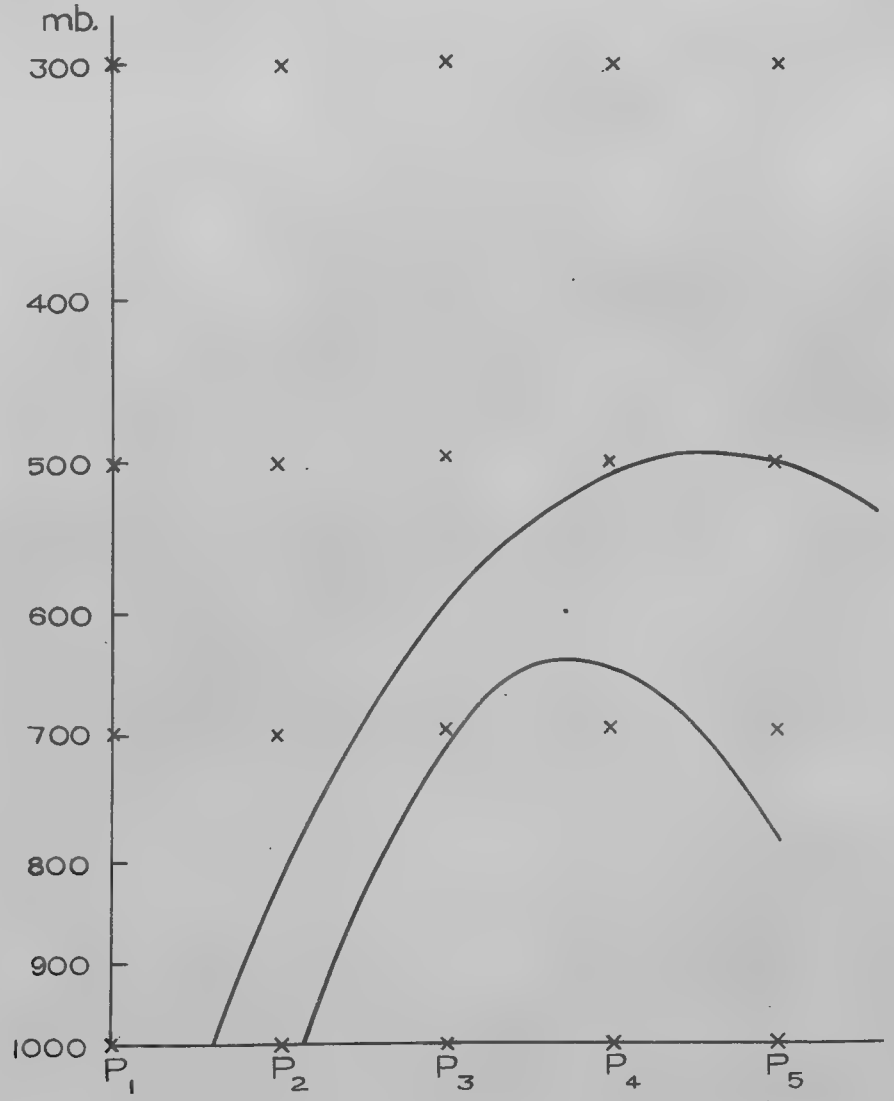

Fig. 2 (b) Vertical cross-section for 1500 G.M.T., May 3, 1948, showing boundaries of frontal zone along the line on which trajectories terminate.

Fig.2 (c,d,e and f) 24 hour trajectories terminating in the frontal zone over the British Isles at 1500 G.M.T., May 3, 1948.

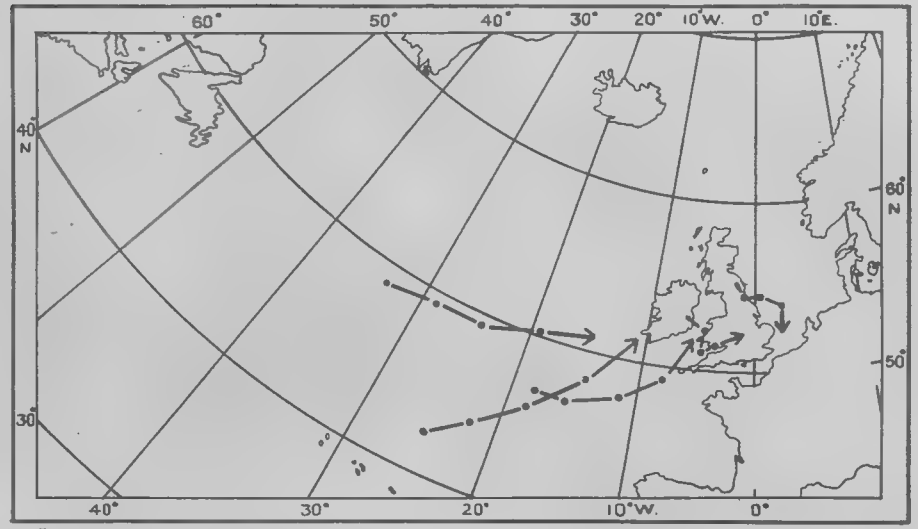

Fig.2(c) Surface trajectories

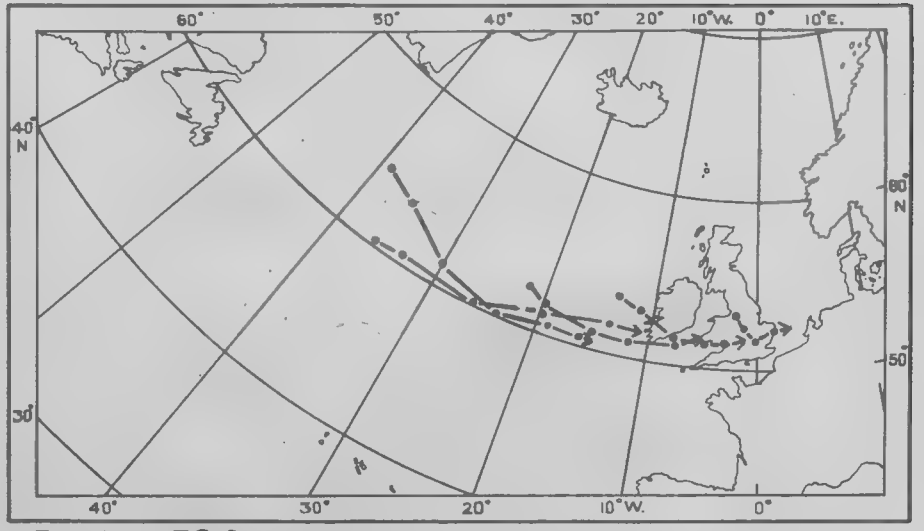

Fig.2(d) 700 mb. trajectories

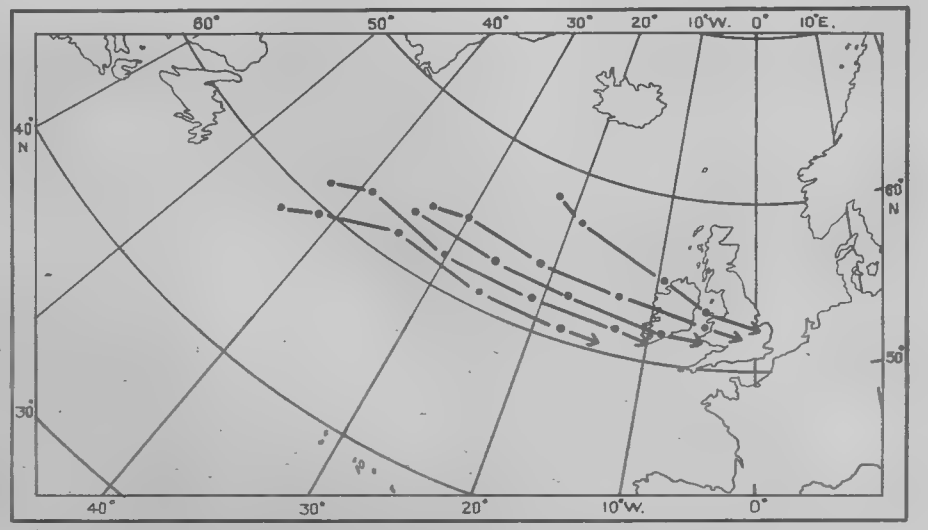

Fig.2(e) 500 mb. trajectories

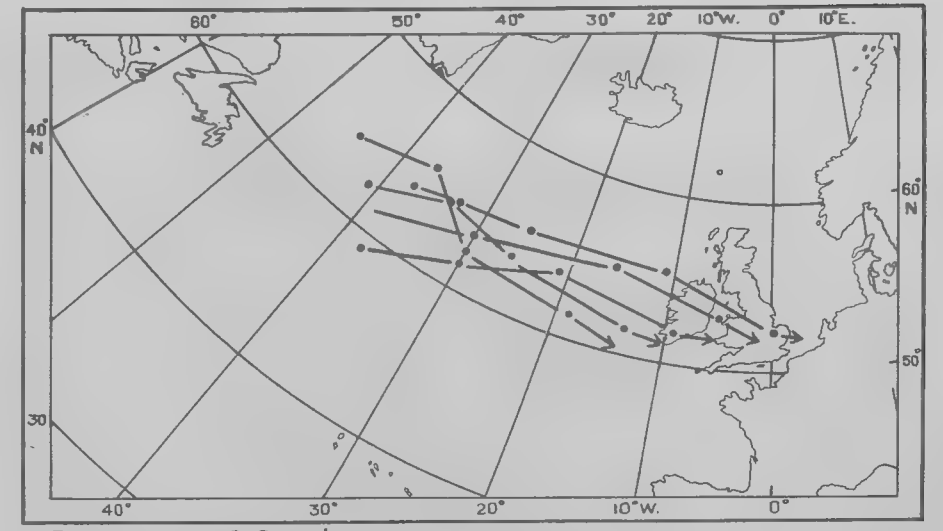

Fig.2(f) 300 mb. trajectories

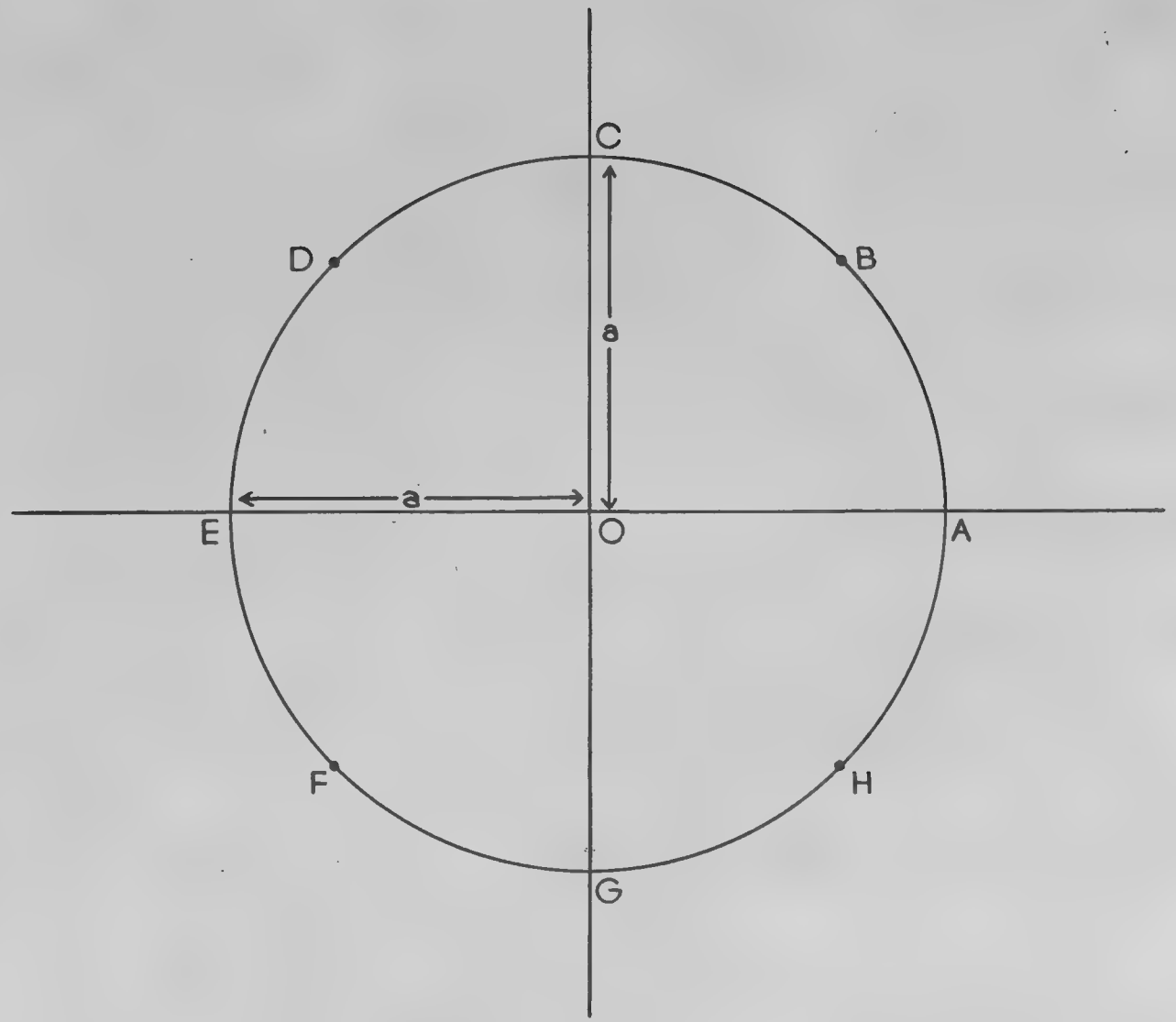

Fig. 3. Form of transparent scale used in estimating "Frontogenesis" from an isobaric chart.

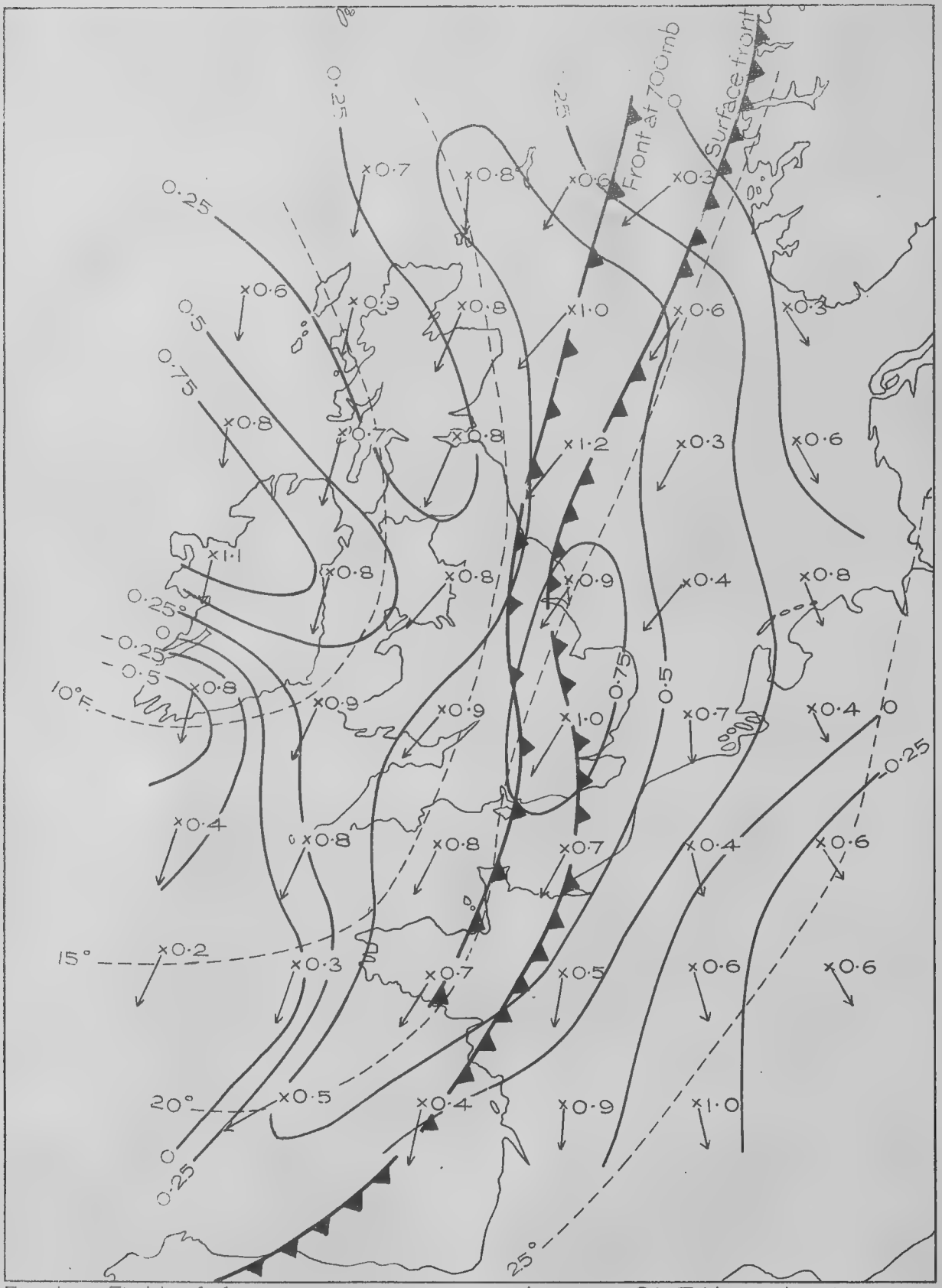

Fig.4 Field of frontogenesis at 700 mb. 1800 G.M.T. November 5, 1949

——— isopleths of $\frac{1}{2}(A^2+B^2)^{\frac{1}{2}} \cos 2\phi$

– – – – isotherms

Arrows indicate axis of dilatation and figures give value of $\frac{1}{2}(A^2+B^2)^{\frac{1}{2}}$ unit hr.$^{-1}$ $\times 10^{-1}$

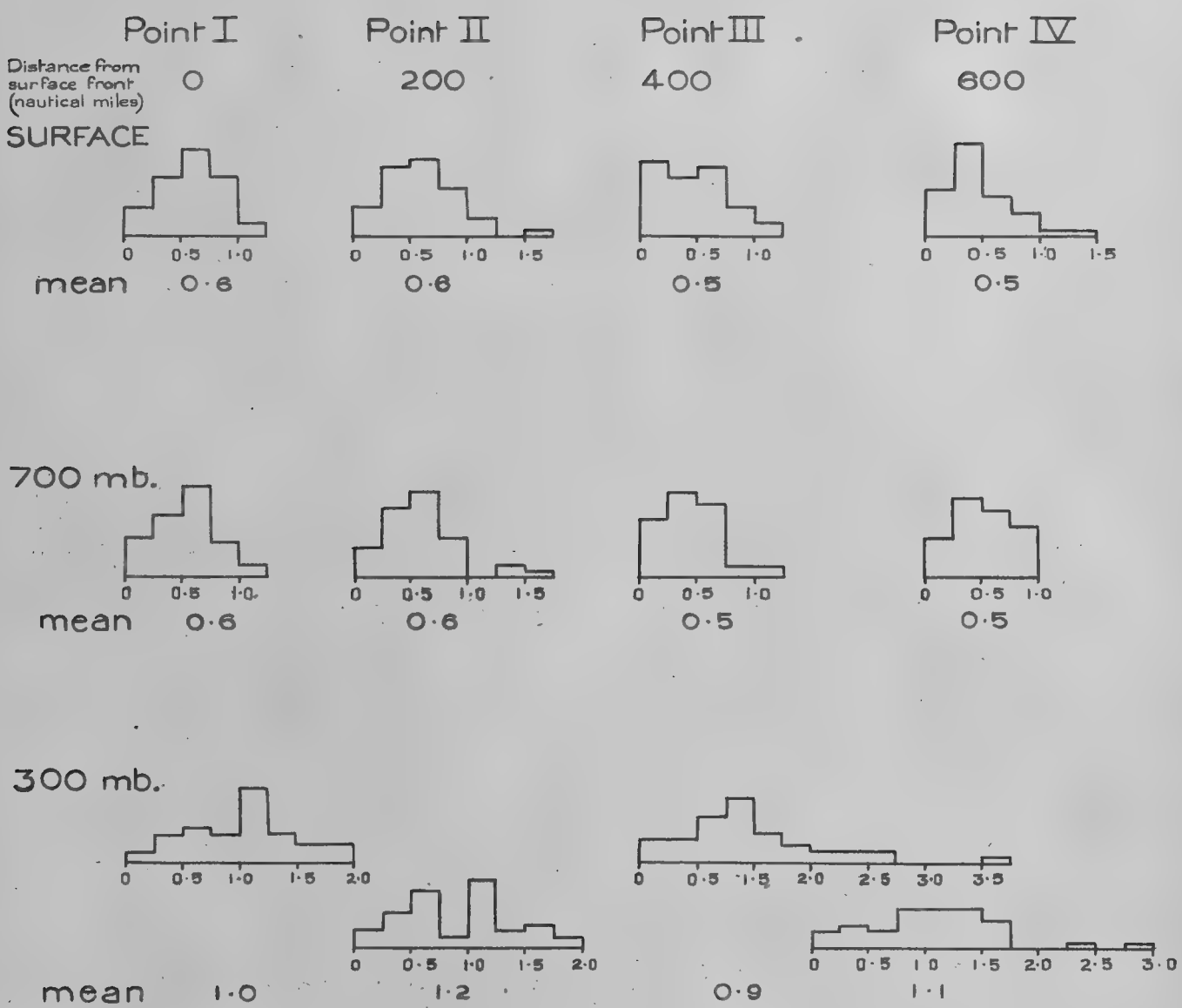

Fig.5 (a) Histograms showing the frequency of values of $\frac{1}{2}(A^2 + B^2)^{\frac{1}{2}}$ at points near active fronts (unit 10^{-1} hr^{-1})

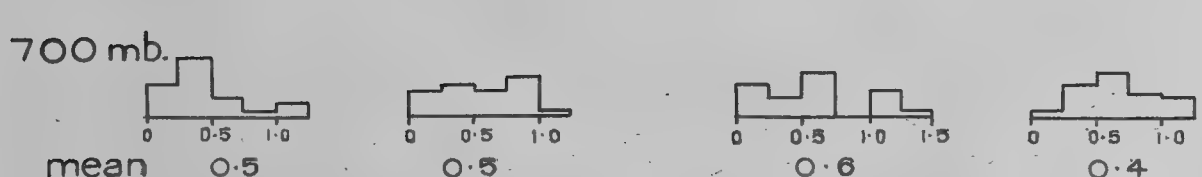

Fig.5(b) Histograms showing the frequency of values of $\frac{1}{2}(A^2 + B^2)^{\frac{1}{2}}$ at points near inactive fronts (unit 10^{-1} hr^{-1})

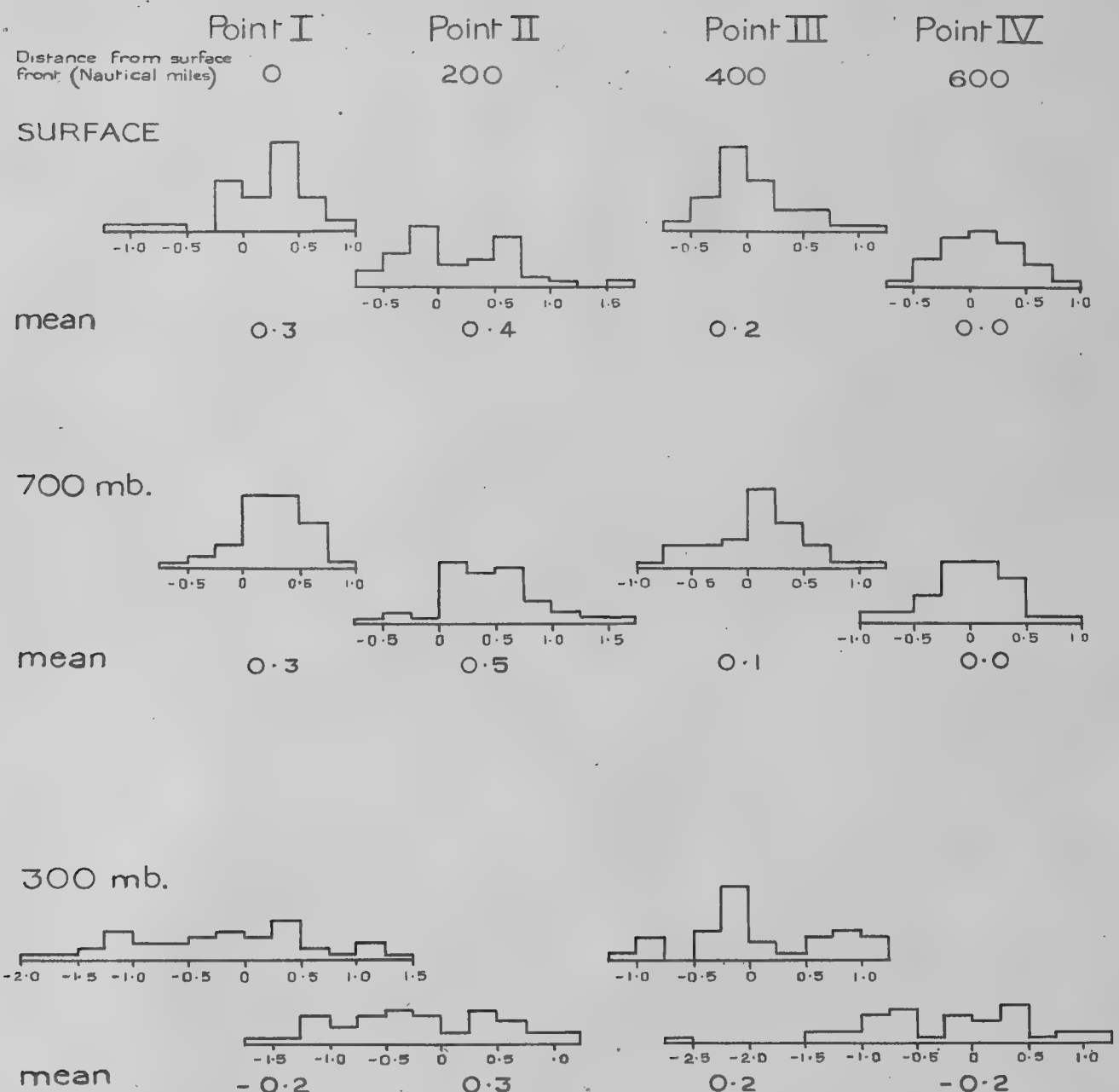

Fig.6(a) Histograms showing the frequency of values of $\frac{1}{2}(A^2 + B^2)^{\frac{1}{2}} \cos 2\phi$ at points near active fronts (unit $10^{-1} hr^{-1}$)

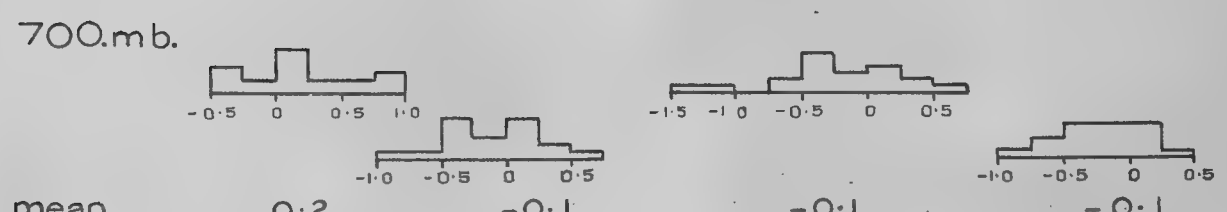

Fig.6(b) Histograms showing the frequency of values of $\frac{1}{2}(A^2 + B^2)^{\frac{1}{2}} \cos 2\phi$ at points near inactive fronts (unit $10^{-1} hr^{-1}$)

Fig. 7. Average field of frontogenesis in the vicinity of the warm front of January 16-17, 1951.
All values are averages over five charts from 0300 G.M.T. January 16 to 0300 G.M.T. January 17, 1951.

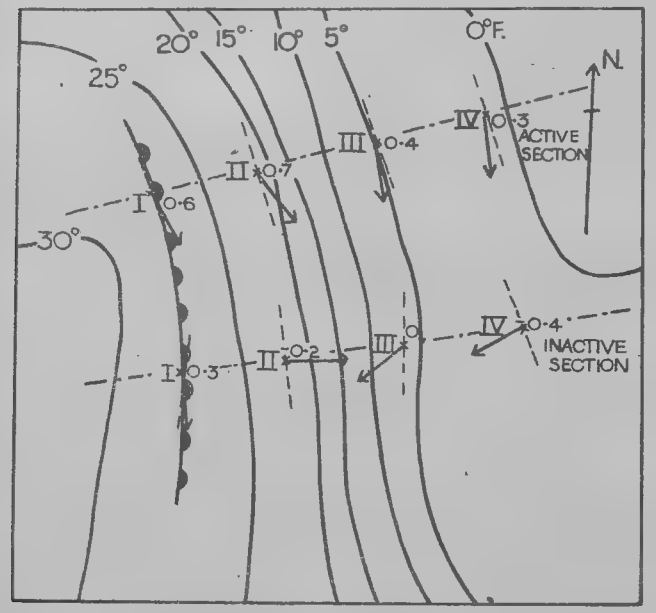

HORIZONTAL DISTRIBUTION OF TEMPERATURE AND FRONTOGENESIS AT 700 MB.

Arrows indicate axis of dilatation.

	I	II	III	IV
300mb.	0·8	0·3	1·0	0·8
500mb.	0·7	0·1	0·5	0·1
700mb.	0·6	0·7	0·4	0·3
1,000mb.	0·2	0·5	0·4	0·2

Active section of front.

	I	II	III	IV
300mb.	0·3	0·5	-0·1	-1·1
500mb.	0·5	0·3	0	-0·5
700mb.	0·3	-0·2	0	-0·4
1,000mb.	0·1	0·2	0·1	-0·1

Inactive section of front.

VERTICAL DISTRIBUTION OF FRONTOGENESIS

Numbers against each plotted point give values of $\frac{1}{2}(A^2+B^2)^{\frac{1}{2}} \cos 2\phi$ [Unit 10^{-1} hr.$^{-1}$]

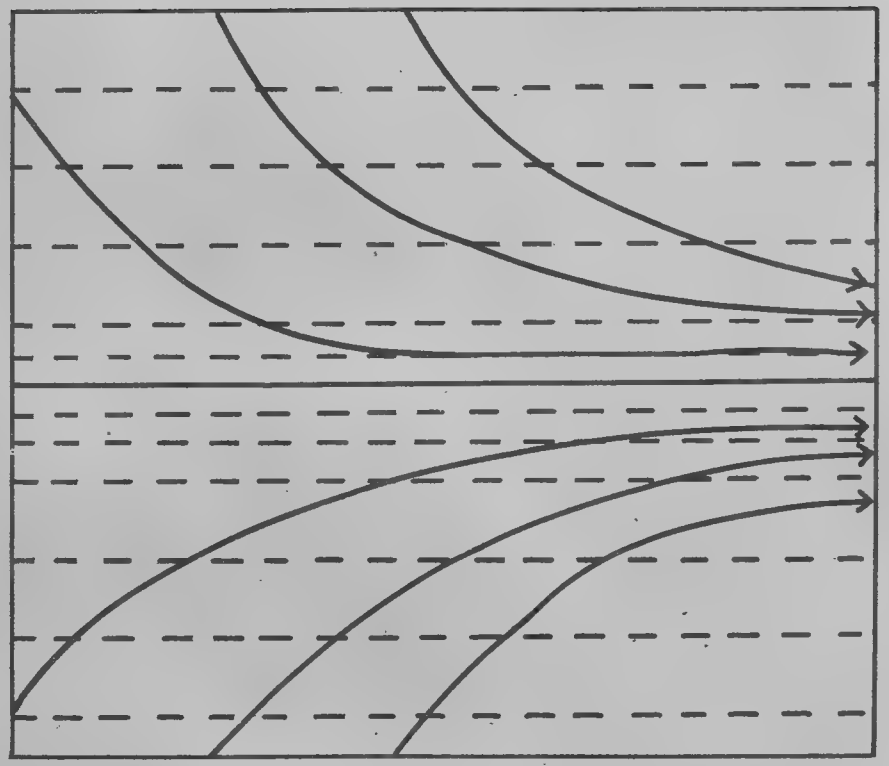

Fig 8a

Horizontal distribution of stream lines and isotherms in a frontogenetic confluence.

——— Stream lines

– – – Isotherms

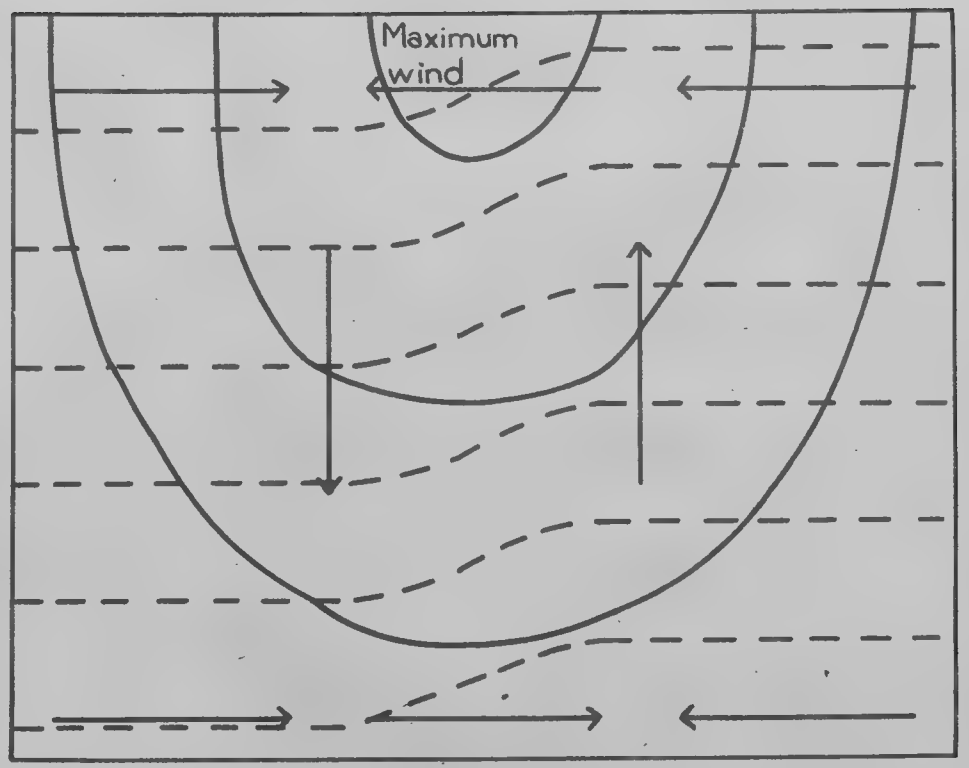

Fig 8b

Vertical section through frontogenetic confluence showing vertical circulation.

——— Isokinetics

– – – Isotherms

Fig. 9

CASE I — VERTICAL FRONTAL ZONE — DRY

Theoretical distribution of vertical and horizontal velocity and corresponding rate of change of specific volume

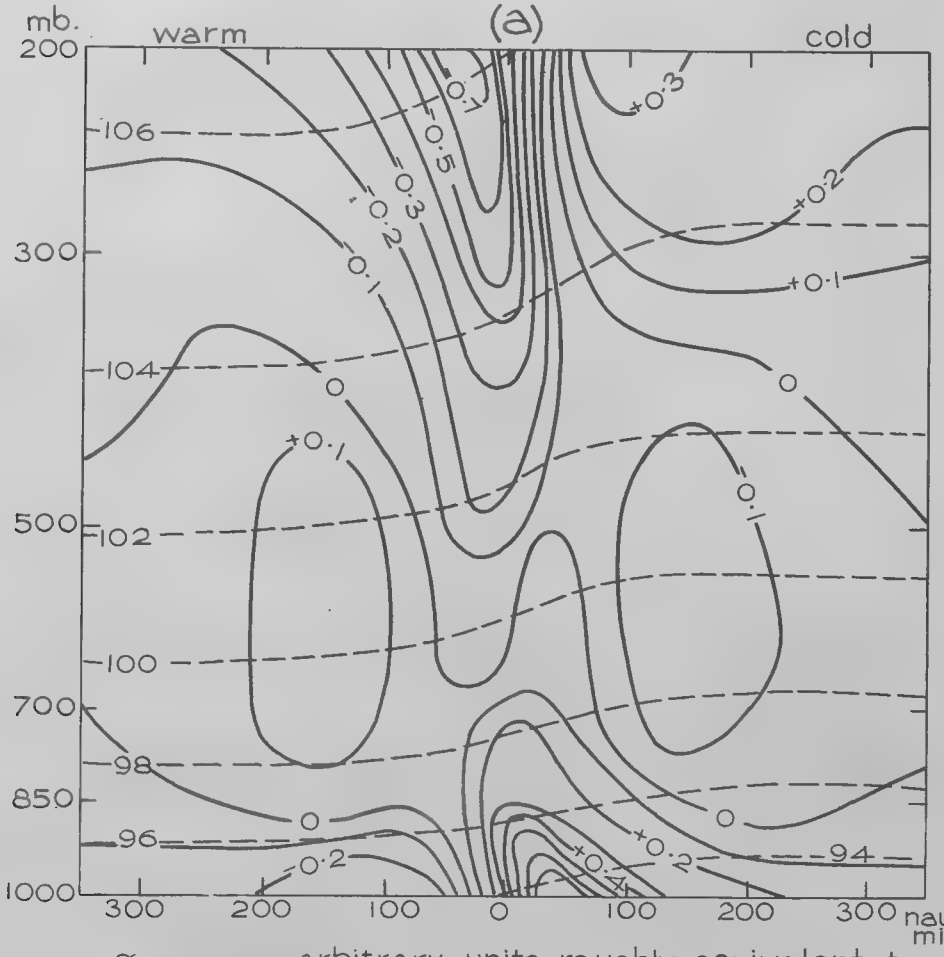

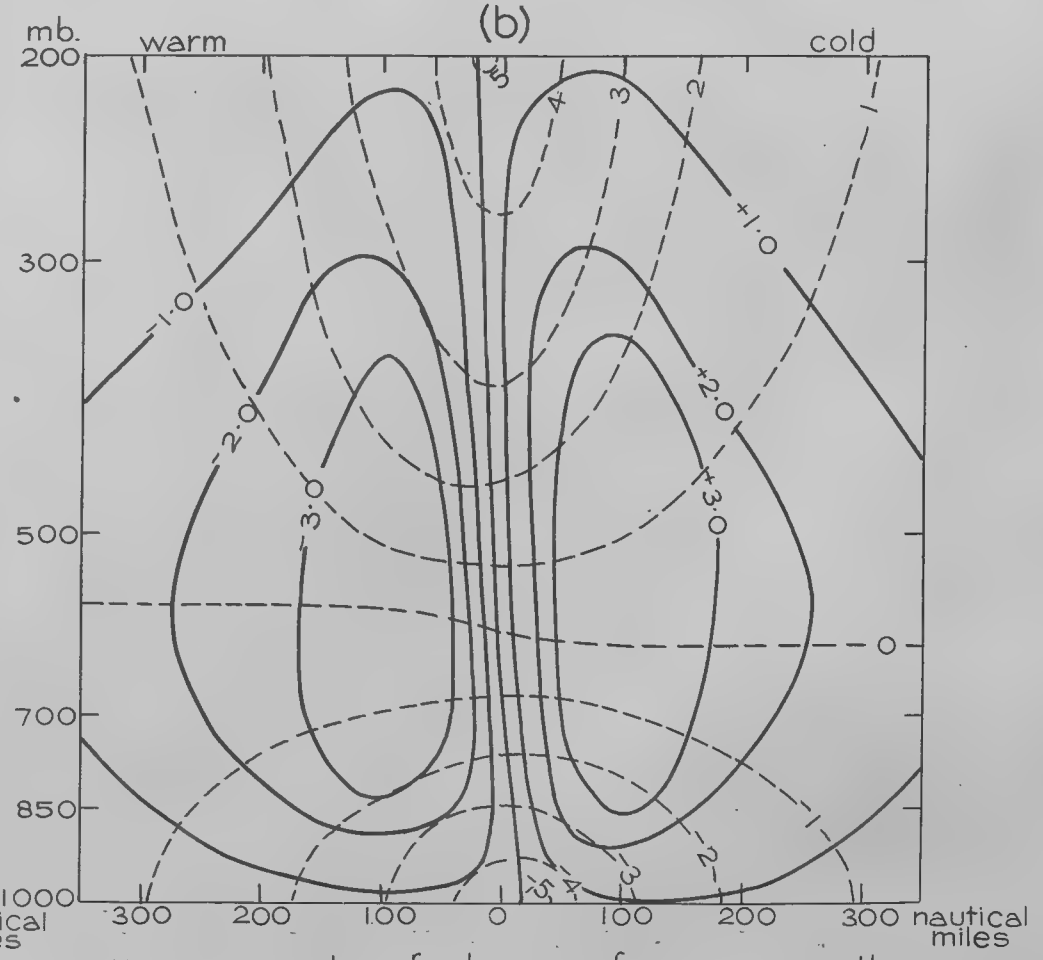

α ——— arbitrary units roughly equivalent to one hundredth of the specific volume at the ground in a standard atmosphere.

$\partial\alpha/\partial t$ ——— rate of change of α per hour

ω ——— rate of change of pressure in the moving air parcel i.e. dp/dt in mb./hr.

v_a ——— ageostrophic wind component in the y-direction in knots.

Fig. 10

CASE III — SLOPING FRONTAL ZONE — DRY

Theoretical distribution of vertical and horizontal velocity and corresponding rate of change of specific volume

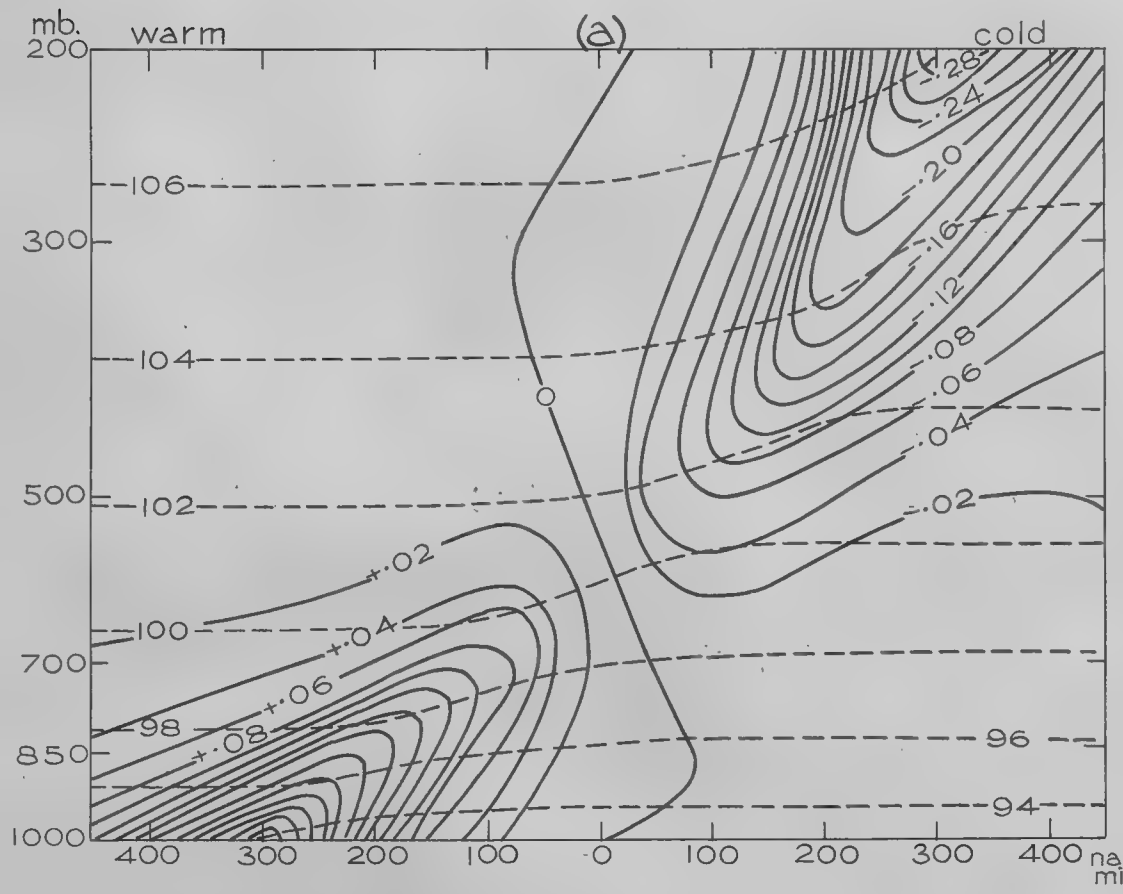

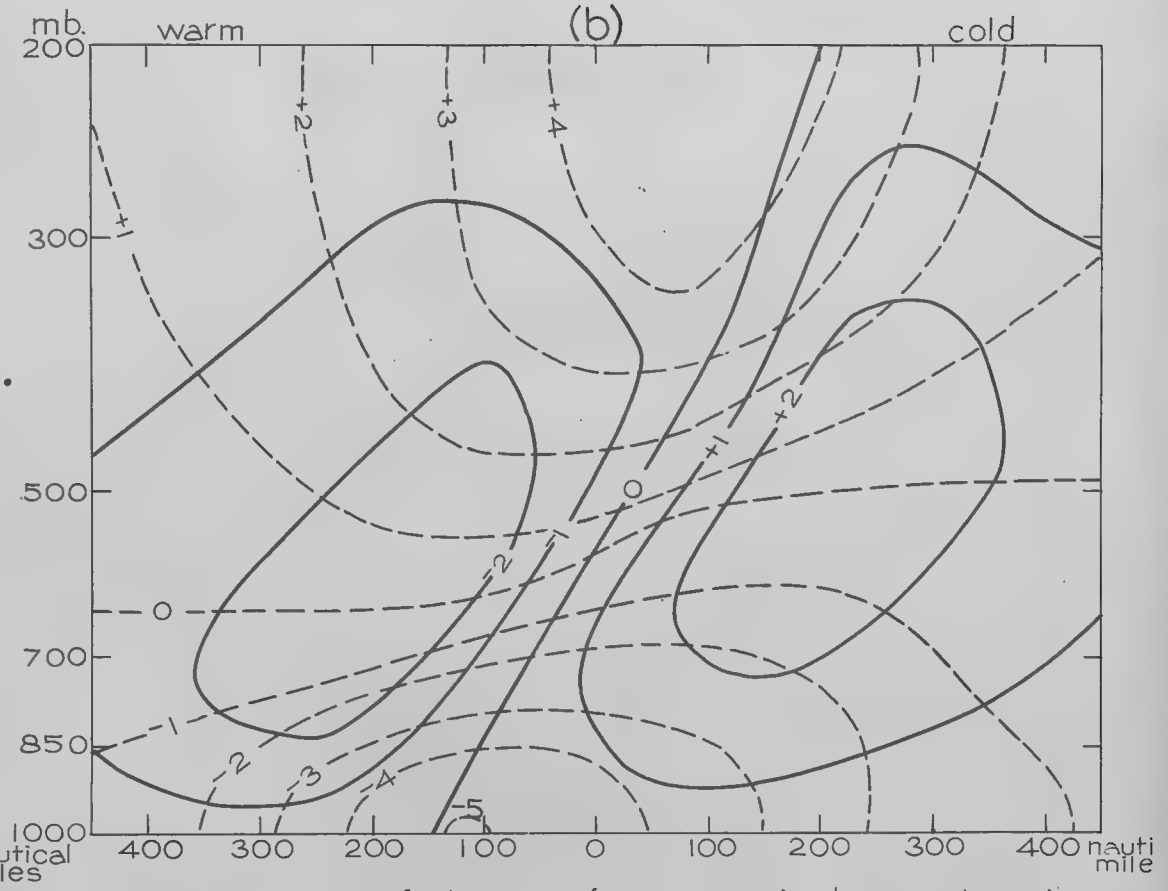

α – – – arbitrary units roughly equivalent to one hundredth of the specific volume at the ground in a standard atmosphere

$\partial\alpha/\partial t$ —— rate of change of α per hour

ω —— rate of change of pressure in the moving air parcel i.e. dp/dt in mb./hr.

v_a – – – ageostrophic wind component in the y-direction in knots

Fig. 11 CASE IV — VERTICAL FRONTAL ZONE WITH VERTICAL CLOUDS

Theoretical distribution of vertical and horizontal velocity and corresponding rate of change of specific volume

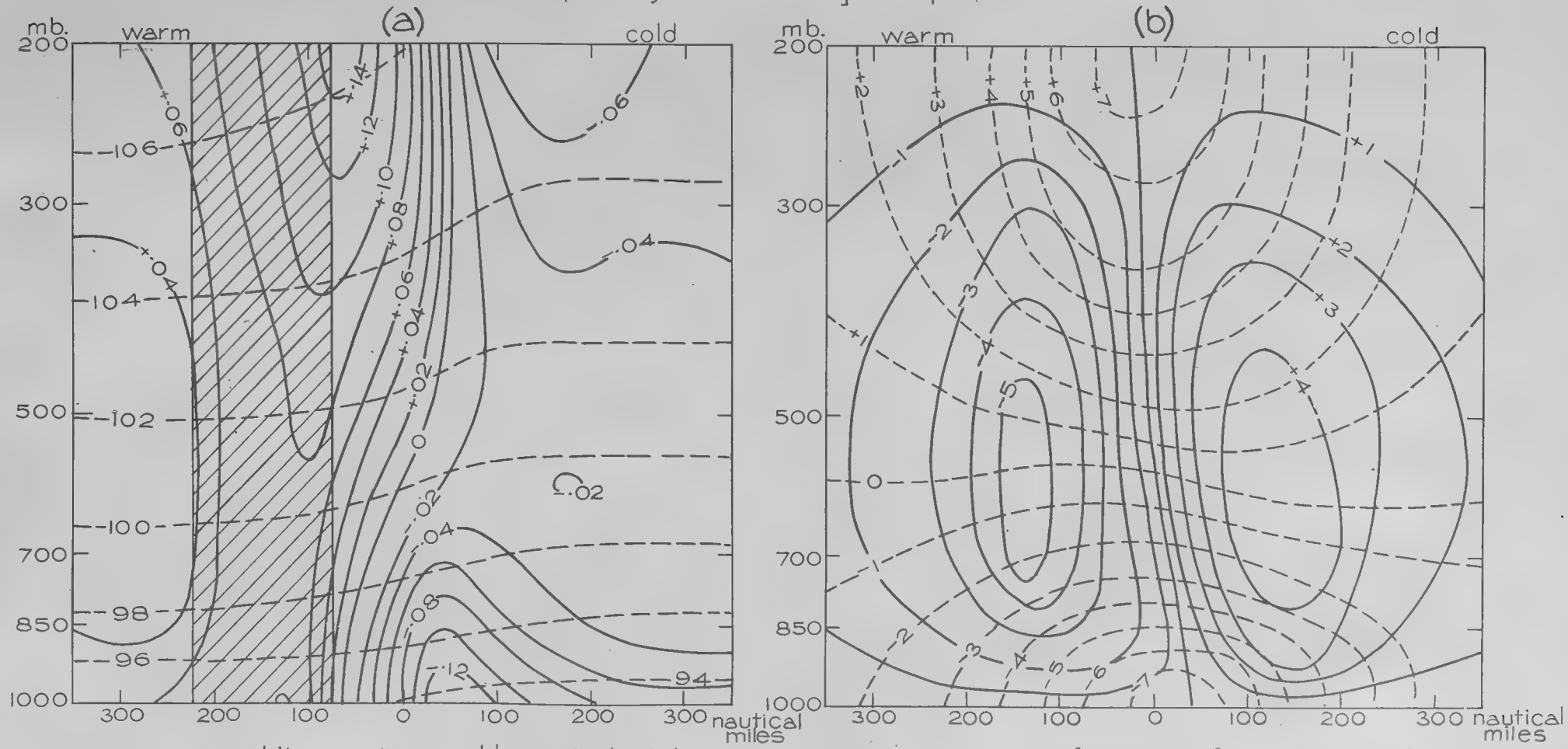

α – – – arbitrary units roughly equivalent to one hundredth of the specific volume at the ground in a standard atmosphere

$\partial\alpha/\partial t$ ——— rate of change of α per hour

▨ area assumed to be occupied by cloud

ω ——— rate of change of pressure in the moving air parcel i.e. dp/dt in mb/hr.

v_a – – – ageostrophic wind component in the y-direction in knots

Fig. 12

CASE VI — SLOPING FRONTAL ZONE WITH CLOUD

Theoretical distribution of vertical and horizontal velocity and corresponding rate of change of specific volume

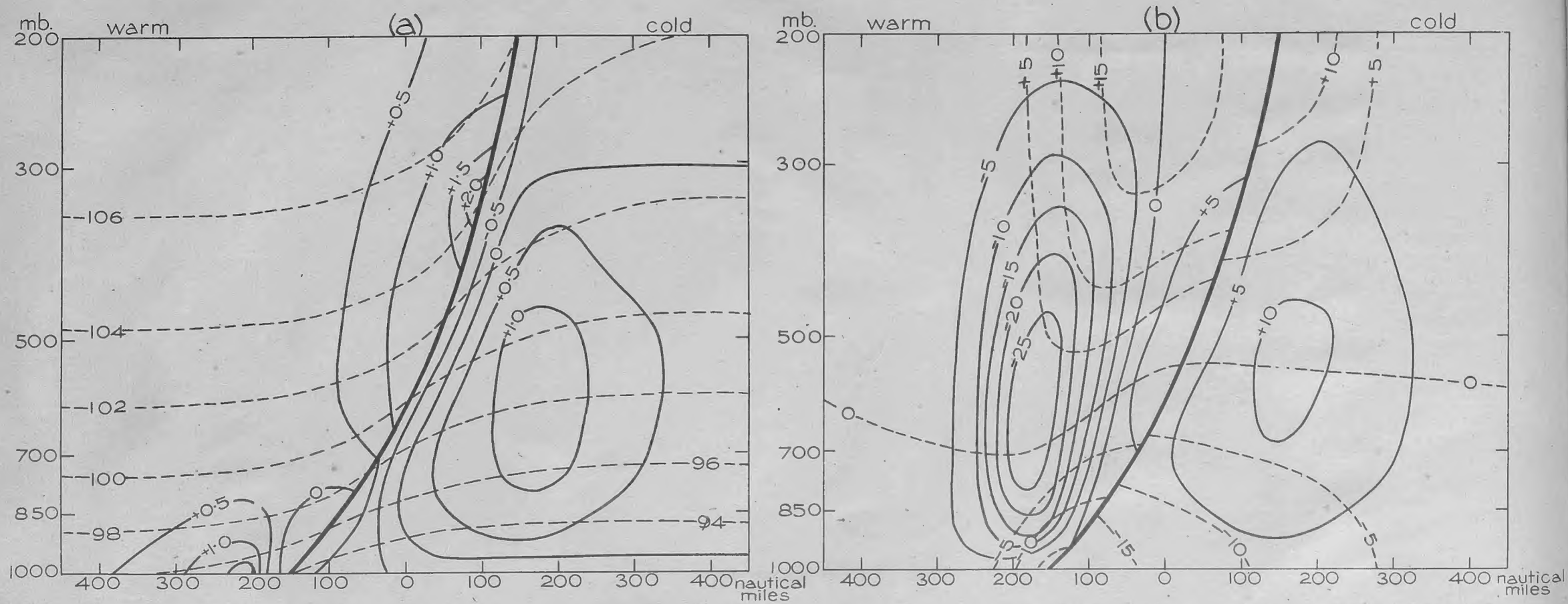

α ––– arbitrary units roughly equivalent to one hundredth of the specific volume at the ground in a standard atmosphere

$\partial\alpha/\partial t$ —— rate of change of α per hour

ω —— rate of change of pressure in the moving air parcel i.e. dp/dt in mb/hr.

v_a ––– ageostrophic wind component in the y-direction in knots

The area above and to the left of the thick sloping line is assumed to be saturated with water vapour; the remaining area is assumed dry